MEDICAL RADIOLOGY

Diagnostic Imaging

A. L. Baert
M. Knauth
K. Sartor

Imaging of Orthopedic Sports Injuries

F. M. Vanhoenacker
M. Maas
J. L. Gielen
Editors

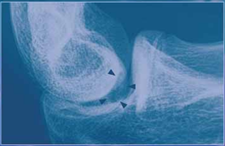

Springer

MEDICAL RADIOLOGY

Diagnostic Imaging

Editors:
A. L. Baert, Leuven
M. Knauth, Göttingen
K. Sartor, Heidelberg

F. M. Vanhoenacker · M. Maas · J. L. Gielen (Eds.)

Imaging of Orthopedic Sports Injuries

With Contributions by

G. Allen · S. E. Anderson · J. Beltran · A. Bernaerts · P. Brys · K. Chapelle
A. M. Davies · M. de Jonge · M. De Maeseneer · A. Demeyere · F. Ebrahim · P. Ehlinger
D. G. Fransen-Franken · H. R. Galloway · E Geusens · W. Geyskens · W. Gibbon
J. L. Gielen · W. C. J. Huysse · F. Kainberger · A. Karantanas · A. Kelekis · D. Kelekis
N. L. Kelekis · E. Llopis · M. Maas · E. G. McNally · S. Ostlere · M. Padron
O. Papakonstantinou · P. M. Parizel · W. C. G. Peh · B. M. Pluim · P. Robinson
E. Schilders · J. Slavotinek · A. Suhardja · A. Van der Stappen · H.-J. Van der Woude
P. Van Dyck · F. M. Vanhoenacker · R. A. W. Verhagen · K. L. Verstraete · W. J. Willems
D. J. Wilson

Foreword by A. L. Baert

Introduction by C. Faletti

With 526 Figures in 914 Separate Illustrations, 62 in Color and 23 Tables

Springer

Filip M. Vanhoenacker, MD, PhD
Department of Radiology
University Hospital Antwerp
Wilrijkstraat, 10
2650 Edegem
Belgium

Mario Maas, MD, PhD
Department of Radiology
Academic Medical Centre
Meibergdreef, 9, Suite C1-210
1105 AZ Amsterdam
The Netherlands

Jan L. Gielen, MD, PhD
Department of Radiology
University Hospital Antwerp
Wilrijkstraat, 10
2650 Edegem
Belgium

Medical Radiology · Diagnostic Imaging and Radiation Oncology
Series Editors: A. L. Baert · L. W. Brady · H.-P. Heilmann · M. Knauth · M. Molls · K. Sartor

Continuation of Handbuch der medizinischen Radiologie
Encyclopedia of Medical Radiology

Library of Congress Control Number: 2006925524

ISBN 3-540-26014-5 Springer Berlin Heidelberg New York
ISBN 978-3-540-26014-1 Springer Berlin Heidelberg New York

Springer is part of Springer Science+Business Media

http//www.springer.com

Printed in Germany

Medical Editor: Dr. Ute Heilmann, Heidelberg
Desk Editor: Ursula N. Davis, Heidelberg
Production Editor: Kurt Teichmann, Mauer
Cover-Design and Typesetting: Verlagsservice Teichmann, Mauer

Printed on acid-free paper – 21/3151xq – 5 4 3 2 1 0

Foreword

Sports activity is an important part of our modern lifestyle, among both amateurs and professionals. It makes an important contribution to our sense of well-being in today‘s society. However, it has its price in terms of orthopedic injuries.

This volume therefore addresses an important issue of everyday life and medicine. Its contents cover the entire imaging field of all orthopedic sports injuries remarkably well and in great detail.

The editors and contributing authors are all renowned experts in musculoskeletal radiology.

I congratulate them on this up-to-date, well-researched and superbly illustrated volume which covers modern radiological imaging of the whole spectrum of orthopedic sports injuries comprehensively and thoroughly.

I am convinced that this book will be a great teaching tool for radiologists in training, as well as for certified radiologists. It will also constitute a highly informative reference book for other medical disciplines.

I sincerely hope that this volume will meet with the same success as the numerous other volumes already published in the series Medical Radiology – Diagnostic Imaging.

Leuven | Albert L. Baert

Preface

Imaging of sports related injuries has always been a very popular topic and the interest of radiologists in this domain has even increased in recent years.

Competitive athletes are vulnerable to a variety of injuries and they are often very demanding in their expectations of a correct diagnosis, appropriate treatment and advice on prognosis and estimated recovery period. Working in sports imaging means team effort, whereby sports physicians, physical therapists, orthopaedic surgeons, radiologists and technicians work closely together. Radiology plays a pivotal role in this process.

Since our society is more fitness oriented than ever, a large percentage of the general population is involved in recreational sports activities, and thus prone to injuries. This underscores the impact of sports medicine in our daily practice.

Imaging of sports injuries has evolved dramatically since the introduction of MR imaging, high resolution ultrasound and multi-detector computed tomography.

Indeed, whereas imaging evaluation was almost exclusively done by plain radiography and scintigraphy in the early years, application of new techniques enables the radiologist to make a more precise diagnosis.

Before 1988, the term *"bone marrow edema"* did not exist in the radiological literature, but since the introduction of MR imaging in musculoskeletal imaging, more than 300 articles have been written on this specific item.

Several recent monographs and review articles on sports imaging concentrated on a single imaging technique, such as ultrasound or MR imaging.

This book aims to provide a comprehensive overview of all imaging techniques used in the evaluation of patients with sports injuries.

Therefore, we summarized the merit of each technique in the diagnostic setting of these injuries in a concise table in each chapter of this book.

We have been very fortunate to work with talented and outstanding experts in the field of musculoskeletal imaging.

Furthermore, we are particularly grateful to Professor Albert L. Baert for giving us the opportunity to edit this work, as well as to our previous mentors Professor Arthur M. De Schepper and the late Dr. Piet F. Dijkstra for teaching us special aspects of musculoskeletal radiology.

We are also deeply indebted to the technicians and co-workers in our respective departments for providing us high quality images.

Last but not least, we want to thank our families for their constant support while we were working on this amazing project.

We hope that this work becomes a valuable resource for those participating in the care of patients who have sustained sports-related injuries.

Antwerp — Filip M. Vanhoenacker
Amsterdam — Mario Maas
Antwerp — Jan L. Gielen

Introduction

Performing sports activities brings with it the possibility of producing alterations in muscle-tendinous structures and joints through trauma or overuse.

Both these pathologies imply that the activities are to be suspended, which often leads to the athlete, who is by definition an active individual, having to accept his/her condition, something which is not always easy to do. Therefore, the athlete and the entire sports environment surrounding him/her expect the problem to be solved in the shortest possible time.

The mandatory clinical examination, even if often able to provide precise information, must also include a diagnostic study which confirms or details the clinical data.

This means that diagnostic imaging is a fundamental step in orthopedic sports injuries. It is essential, however, that the imaging technique/s chosen for the trauma be tailored on the basis of the sensitivity and specificity of each individual technique in relation to the type of injury. Moreover, the specialist must be well versed in this particular field of pathology.

Indeed, also on the basis of my personal experience as the radiologist responsible for the diagnostic imaging of various National Italian Teams in several sports (soccer, volley-ball, basket-ball, athletics etc.), as well as for the radiological coverage of the 2006 Winter Olympic Games, I have observed that it is very important on the one hand to establish a good collaborative relationship with the clinician/s, while on the other, and more particularly, to be aware of the limitations and possibilities of each technique.

Although it is not always easy to determine the precise technique capable of demonstrating a lesion, with the aid of patient's history and clinical experience it is possible to choose the most appropriate imaging modality.

It is often difficult to differentiate the changes induced by the athletic movements (typical for each individual sport), to be considered an asymptomatic para-physiological adaptation, from the lesion itself, which lies at the basis of such alterations.

Consequently, in muscle-tendinous pathology, US and MRI are able to complement one another, as long as they are used correctly on the basis of temporal and topographic parameters. When a lesion is recent and superficial, US is able to offer a correct diagnosis, whilst MRI is more sensitive in the detection of the deeper lesion/s, or when a more panoramic view is required.

When dealing with skeletal lesions, plain radiography is surely the first examination to be performed, complemented with the CT scan for multiplanar codification and MRI for bone marrow alterations.

MRI is often the first examination for joint pathology to establish whether intra-articular alterations are present. In some cases administration of intra-articular contrast medium (MR-arthrography is required).

Imaging in the follow-up phase of sports injuries is also fundamental, so as to monitor the evolution of the lesion/s, both after surgical and/or conservative/re-educational treatment, supplying useful data so as to forecast when the athlete may return to normal sports activities again.

In conclusion, the radiologist responsible for this interesting field of activity, i.e. orthopedic sports injuries, must be able to apply his/her specialist technical knowledge in radiology to the many and varied problems involved in sports injuries, thus identifying not only the most suitable technique to be used, but also, and above all, to try to propose diagnostic protocols for each individual pathology in collaboration with the trauma team specialists. Indeed, the ultimate goal is to make a correct diagnosis, follow the evolution of the lesion and re-integrate the athlete into sports activities in as short a time as possible and in the best possible health.

Professor Carlo Faletti
Head of the Imaging Department and Interventional Radiology
Trauma Centre - Orthopaedic Hospital,
Consultant Professor   Sports Medicine University Department
Turin, Italy.

Contents

Relevant Basic Science and General Imaging Principles

The Clinician's Point of View

1

Babette M. Pluim

CONTENTS

1.1 Introduction

Over the last ten, years imaging techniques have become increasingly important as a diagnostic tool for sports injuries without replacing the traditional methods of management (Geertsma and Maas 2002; De March et al. 2005). An accurate diagnosis can often be made based on a history and physical examination alone but imaging techniques can be very helpful if there is doubt about the diagnosis. In patients who do not respond to conservative management, imaging can be especially useful to acquire a better understanding of the extent of the lesion. However, over-imaging can cause problems in high-level athletes, who have easy access to imaging modalities when travelling abroad. This is particularly so when there is lack of communication between the various treating physicians and when an understanding of the mechanism of injury is essential in order to establish the correct diagnosis.

This chapter will review a number of situations where good communication between the radiologist and sports physician can result in the correct choice of imaging technique and a greater chance of establishing the correct diagnosis. The specific demands that elite athletes and sports physicians may place on the radiologist and the radiology department are also discussed.

1.2 Role of Imaging

It should be noted that the patient population of the sports physician differs slightly from the normal population. In general, athletes tend to be highly motivated and are keen to resume sport as soon as possible. The majority of their injuries are caused by training overload yet they find it very difficult to reduce this load. There is always another match, another race, another goal to achieve. So in a situation where a 'normal' patient may be content to give his/her ankle sprain or stress fracture the required three to six weeks rest, an athlete will want to know if he/she can participate in next week's tournament. When working with athletes, time is always a pressure.

This is where imaging can play an important role for both the sports physician and the athlete. First, by establishing the correct diagnosis at the start, the correct treatment procedures can be initiated immediately with no unnecessary time lag. Second, it is

B. M. Pluim, MD, PhD
KNLTB, PO Box 1617, 3800 BP Amersfoort, The Netherlands

often very helpful to provide the athlete with visual evidence that a significant injury is present (e.g. stress fracture, muscle rupture or meniscal lesion) and thereby to convince him/her that rest is indeed essential. Hopefully this will also obviate the inclination of the athlete to get multiple opinions ("medical shopping"). Finally, it may clarify whether surgery is necessary. In cases where conservative management is indicated, imaging may also help determine the appropriate form of treatment; for example, if calcifications are present, use of Dolorclast (shock wave therapy) may be indicated. Despite the fact that corticosteroid injections are used less and less in sports medicine, there are still instances when this type of treatment is indicated and imaging can help in this choice, e.g. a tenosynovitis (trigger finger), ganglion cyst, bursitis or iliotibial tract syndrome. Ultrasound may also be used to guide the injection needle (Jacob et al. 2005).

1.3 What is Expected from the Radiologist?

When dealing with elite athletes, there are certain aspects that differentiate the general radiologist from the 'sports' radiologist.

1. Interest in sports and 'feel' for the athlete. It is very important that the radiologist has an interest in sports and is able to place himself/herself in the position of the athlete. For athletes, minor injuries can cause great distress and hamper the athlete in his or her training (e.g. a minor muscle strain in a long-distance runner). The radiologist has to be aware of this fact and needs to look for minor abnormalities that may have no clinical significance in a non-athletic patient. It is essential that the radiologist is willing to analyze the problem with the sports physician.
2. Interest in the musculoskeletal system. The radiologist needs to be knowledgeable about the musculoskeletal system, because this is where the vast majority of sporting injuries occur. Musculoskeletal imaging is still a developing field in radiology (De March et al. 2005).
3. Access to a broad network. The radiologist does not need to be an expert in every area but should have a broad network of specialist colleagues who have an interest in and/or knowledge of sports related problems.

1.4 What is Expected from the Radiology Department?

1. Expertise in ultrasound imaging. The department should have a radiologist with extensive experience in ultrasound imaging and a specific interest in the musculoskeletal system. The radiology department should have Magnetic Resonance Imaging (MRI), CT-scan and bone scanning (DEXA) facilities in addition to plain radiography. If all these modalities are not available on site, the radiologist should have alternative facilities to which the athlete can be referred.
2. Availability within 24 h to 5 days. Since there is a lot of time pressure on elite athletes, flexibility and easy access is important. It is preferable that the department has slots open for elite athletes for diagnostics within 24 h to 5 days, if required. This is not always necessary, but can be essential when the athlete is competing in a tournament, or has to travel again within a short period of time.

1.5 What is Expected from the Sports Physician?

1. To provide detailed information. The sports physician has to provide detailed information to the radiologist. For example, when referring an athlete with a high probability of a stress fracture, information regarding the nature of the activity or sport (e.g. jumping, hurdling, plyometrics) and the load on the athlete is very important in establishing the diagnosis. A detailed history, including a training history, is essential. Most radiologists should have a high level of suspicion of a fracture of the 2nd metatarsal in military recruits or athletes. However, in order to detect more uncommon stress fractures (such as a humeral stress fracture in a tennis player, a stress fracture of the lower back in a gymnast, or a stress fracture of the hip in a long distance runner), good communication between the sports physician and radiologist is essential. This is particularly important because the sensitivity of plain radiographs in the early stages of a stress fracture is very low (Kiuru et al. 2004). In athletes where there is a high probability

of a stress fracture, a normal radiograph should prompt further investigation with other imaging techniques (Tuan et al. 2004).

2. Seek advice before referring. Since the choice of the imaging modality depends on the expected type of lesion, the sports physician should be willing to seek advice from the radiologist before referring an athlete. No clearer example can be given than that the ideal imaging technique for examination of the shoulder joint (plain radiography, ultrasound, MR(-arthrography) or CT(-arthrography), bone scan) will differ along with the clinical problem (SLAP lesion, (partial) tendon rupture, bursitis, synovitis or fracture) (Sander and Miller 2005; Tirman et al. 2004).

1.6 Risks of Over-Imaging

When working with high level athletes, there are certain situations that are less likely to occur in the general population or in lower level athletes.

1. No direct relation between clinical symptoms and imaging findings. Athletes are often tempted to repeat imaging to establish if "things are improving". The diagnosis is already established and imaging has already been carried out so repeat studies should only be undertaken if symptomatic improvement is not taking place. Repeat studies often lead to confusion in the mind of the athlete and coach. He feels better, he is getting better, but that is not confirmed by MRI, which may cause anxiety. Not performing an imaging study would have been a better decision for the patient, although the hospital finance department might not agree. If the diagnosis is already known, and the treatment plan has been determined, and performing an imaging study will have no influence on this, imaging is unnecessary.
2. Non-significant abnormalities. Asymptomatic athletes may have abnormalities on plain radiographs, CT-scan or MRI which have no clinical significance. It is important to make this very clear to athletes in order not to disturb their positive body image.
3. Different reports. There is also the risk that serial imaging will produce slightly different reports. Again, this may have no clinical significance, but it is important to explain this clearly to the athlete and his coach. Ultrasound or MRI reports are not always black and white, so if the reporting radiologist focuses on slightly different areas than the previous radiologist, this may lead to a confused athlete. For example, when examining a shoulder with ultrasound, there may be a thickening of the supraspinatus tendon, some fluid in the bursa, and small calcifications present. If the (non-significant) calcifications were not mentioned the first time, this may put doubt in the athlete's mind that the injury is getting worse instead of better. The same may happen with an MRI of the lower back after a herniated disc. Clinical symptoms do not always coincide with MRI images, and one clinician may call the herniation "small" whereas the next report may mention a "significant" herniation. It is always recommended that copies of the previous films and reports are available when repeat imaging is being carried out.

1.7 The Travelling Athlete

An extra challenge may be encountered when dealing with elite athletes who are travelling regularly or have just returned from travelling. Their documentation may be incomplete and the athlete may not know or remember whether they had a partial medial or lateral meniscectomy. Even the referring sports physician may not know the answer and this can make it very difficult for the radiologist who has to perform an MRI because of residual or recurrent symptoms. This problem has been recognised at the international level, but has not yet led to a unified approach. Three options are available to tackle this problem:

1. The athlete carries his/her own 'medical passport' and takes it with him/her when they visit a doctor. This requires the athlete to be efficient and carry the passport at all times. The feasibility of a "hematologic passport" for endurance athletes has already been studied (Malcovati et al. 2003).
2. The injuries are registered in an electronic database that is hosted by the international federation of the athlete's sport. The governing bodies in tennis (Association of Tennis Professionals, Women's Tennis Association and the International Tennis Federation) are currently looking into the possibilities of having a joint web-based database

for all international players. The data need to be stored in a highly secure environment, whereby access is carefully controlled to ensure that data is available to relevant parties only. For example, tournament physicians will only have access to the data on players at their tournament during the tournament week. The principle of the system will be comparable to the Anti-Doping Administration & Management System (ADAMS) that is currently in use by the World Anti-Doping Agency (WADA-AMA Org 2005).

3. The information is sent from the previous doctor to the current doctor by internet or by fax. This requires that the name of the previous doctor and hospital are known, that they can be traced, and that they are able to send this information very quickly. However, not all hospitals have a good electronic database that is able to store radiographs, MR images and other images in a reduced format.

1.8 Conclusions

The use of imaging techniques is an important tool for the sports physician in establishing the correct diagnosis and choosing the appropriate treatment procedures. In addition, imaging techniques can be useful for the evaluation and monitoring of the healing process and the early identification of complications.

Good communication between the radiologist and the sports physician is essential. The information the sports physician provides to the radiologist regarding the history of injury, athlete's training program and physical examination will help the radiologist choose the correct imaging technique. The sports physician should also share his/her knowledge of the special demands of the sport involved and the effects that this has on the musculoskeletal system of the athlete.

The radiologist should have an interest in sport and be willing to spend some extra time with the athlete for a detailed history and to communicate with the referring sports physician. The department should be flexible enough to examine athlete within 24 h to 5 days, if warranted. Detailed feedback from the radiologist to the sports physician will help the latter to make the correct interpretation of any abnormalities and direct him/her towards the appropriate form of treatment.

It is only as a result of teamwork between the sports physician and the radiologist that an optimal outcome can be achieved.

Things to Remember

1. The radiologist should have an interest in sport and be willing to spend some extra time with the athlete for a detailed history and to communicate with the referring sports physician.

2. The use of imaging techniques is an important tool for the sports physician in establishing the correct diagnosis and choosing the appropriate treatment procedures. It is only as a result of teamwork between the sports physician and the radiologist that an optimal outcome can be achieved.

References

De March A, Robba T, Ferrarese E et al. (2005) Imaging in musculoskeletal injuries: state of the art. Radiol Med 110:15–131

Geertsma T, Maas M (2002) Beeldvormende diagnostiek in de sportgeneeskunde. Geneesk Sport 35:12–16

Jacob D, Cyteval C, Moinard M (2005) Interventional sonograhy. J Radiol 86:1911–1923

Kiuru MJ, Pihlajamaki HK, Ahovuo JA (2004) Bone stress injuries. Acta Radiol 45:317–326

Malcovati L, Pascutto C, Cazzola M (2003) Hematologic passport for athletes competing in endurance sports: a feasibility study. Haematologica 88:570–581

Sander TG, Miller MD (2005) A systematic approach to magnetic resonance imaging interpretation of sports medicine injuries of the shoulder. Am J Sports Med 33:1088–1105

Tirman PF, Smith ED, Stoller DW et al. (2004) Shoulder imaging in athletes. Semin Musculoskelet Radiol 8:29–40

Tuan K, Wu S, Sennett B (2004) Stress fractures in athletes: risk factors, diagnosis, and management. Orthopedics 27:583–591

WADA-AMA Org. (2005) http://www.wada-ama.org/en/dynamic.ch2?pageCategory.id=265, accessed 29 November 2005

Imaging Techniques and Procedures in Sports Injuries

2

Pieter Van Dyck, Jan L. Gielen, and Filip M. Vanhoenacker

CONTENTS

2.1 Introduction

Sports medicine is one of the most rapidly growing subspecialties in orthopedics. It has been estimated that 25% of patients seen by primary care physicians complain of musculoskeletal problems, many of which are sports- or activity-related (Johnson 2000). Symptoms and clinical findings in sports injuries are often non-specific and further imaging investigations may be required for accurate diagnosis and optimal treatment planning.

The choice of which imaging modality is used depends on the clinicians' and radiologists' comfort and experience with those modalities, the financial costs, and availability and invasiveness of each technique balanced against the diagnostic award. The "optimal imaging pathway" that meets all these criteria probably does not exist and, in many cases, the imaging pathway to be followed should be tailored to individual cases. For a more in-depth discussion of the clinician's point of view, we refer to Chap. 1.

This chapter reviews the imaging strategies that can be employed to diagnose and grade sports injuries. The role of each imaging technique, with its specific advantages and limitations, will be highlighted. The reader will find some practical guidelines for the evaluation of sports injuries that, in our opinion, may be useful in daily clinical practice.

P. Van Dyck, MD
J. L. Gielen, MD, PhD
Department of Radiology, University Hospital Antwerp, Wilrijkstraat 10, 2650 Edegem, Belgium
F. M. Vanhoenacker, MD, PhD
Department of Radiology, AZ St-Maarten, Duffel/Mechelen, Belgium
and
Department of Radiology, University Hospital Antwerp, Wilrijkstraat 10, 2650 Edegem, Belgium

2.2 Imaging Modalities

2.2.1 Plain Radiography and Conventional Arthrography

Radiographs in two projections perpendicular to each other are general the first and often the only diagnostic images needed for the evaluation of sports injuries, most commonly to detect or exclude fracture. The lack of soft tissue contrast-resolution is a well-recognized limitation of plain radiography, but when present, soft tissue changes can be used as indirect signs of osseous pathology. Furthermore, the presence of loose bodies or degenerative joint

changes can easily be assessed with plain radiography.

Although oblique (¾) views may be helpful, e.g., to demonstrate fractures of the radial head or for detection of bone spurs in anterior ankle impingement, they are not commonly used in daily clinical practice and have largely been replaced by cross-sectional imaging.

Stress views may provide indirect evidence of ligamentous injury. However, recent studies have questioned the value of stress radiographs. For example, in chronic ankle pain, it has been shown that there is significant overlap between stable and unstable ankles, according to the guidelines of the American College of Radiology (2005).

Radiographs are mandatory to confirm the results after internal or external fixation with reduction of dislocations and alignment of displaced fracture fragments, for monitoring the progress of fracture healing with callus formation or detection of soft tissue calcification after severe muscle trauma (e.g., myositis ossificans).

When complications of the healing process occur, such as infection or avascular necrosis, the role of plain radiography may be limited and other imaging techniques, such as bone scintigraphy and/or MRI, may be useful for confirming the diagnosis.

For decades, conventional arthrography (after sterile preparation and injection of intra-articular contrast medium) was used for investigating intra-articular pathology. This imaging modality has now been largely replaced by cross-sectional imaging techniques and is only performed as part of CT- or MR-arthrography.

2.2.2 Ultrasound

Since approximately 30% of sports injuries deal with muscle and tendon injuries, ultrasound (US) plays a major role in sports traumatology, helping the clinician to decide whether the athlete should or should not return to training and competition (Peterson and Renstrom 1986).

Due to the excellence of spatial resolution and definition of muscle structure, US keeps its leading edge when dealing with muscle pathology, both in the initial phase for recognition of a lesion, but also for follow-up of lesions and search for healing problems such as fibrosis, muscle cysts, hernias or myositis ossificans.

High-frequency (13.5 MHz) linear-array probes are used to perform musculoskeletal US examinations. Transverse and longitudinal slices are mandatory. US palpation is a very valuable tool, trying to find the point of maximal tenderness, during the examination by a gentle but firm compression of the probe on the skin (Peetrons 2002). Dynamic US study may be very helpful to the correct diagnosis, e.g., to search for muscle hernia (during muscle contraction) or to evaluate the snapping hip syndrome (during hip flexion and lateral rotation). To avoid artefacts or pitfalls, comparison with the contralateral side is necessary.

Major advantages of US are its low cost, availability at short notice, ease of examination, short examination times and lack of radiation exposure.

The recent addition of color-power Doppler imaging to US has allowed for the non-invasive study of blood flow and vascularity within anatomic structures and lesions. In patients with tendinosis, increased vascularity in the tendon may be correlated with clinical symptoms (Weinberg et al. 1998; Zanetti et al. 2003).

Furthermore, US provides image guidance for interventional procedures such as drainage of fluid collections and cysts (Peetrons 2002). Recently, US guided sclerosis of neovascularity in painful chronic tendinosis has been described as an effective treatment with significant reduction of pain during activity (Öhberg and Alfredson 2002).

The trade-off for high-frequency, linear, musculoskeletal transducers is their limited depth of penetration and the small, static scan field. This is a disadvantage if the structure to be visualized is large (e.g., large intramuscular hematoma) or deeply localized (e.g., hip joint). Extended field of view ultrasonography (EFOVS) overcomes this disadvantage by generating a panoramic image. With this technique, sequential registration of images along a broad examination region and their subsequent combination into an image of larger dimension and format is obtained (Weng et al. 1997). EFOVS does not add much in diagnosis but is, however, easily interpretable by the novice and improves cross-specialty communication.

For better evaluating deeply localized structures, such as the hip joint in an obese patient, other (cross-sectional) imaging modalities are often required.

Other disadvantages of ultrasound include operator dependency, selective and often incomprehensible documentation and the inability to penetrate osseous structures.

2.2.3 Multidetector Spiral CT Scan

2.2.3.1 Technique

CT imaging, by virtue of its excellent multiplanar capability and submillimeter spatial resolution due to the development of the spiral acquisition mode and current multidetector row technology, is a valuable imaging tool for the evaluation of all kinds of sports injuries (Berland and Smith 1998). Very fast image-acquisition times of large volumes with submillimeter section thickness have become the norm.

It has proved to be an effective method of documenting injuries particularly in complex bony structures such as the wrist and pelvis, and may often show post-traumatic changes not shown by radiography.

For most musculoskeletal studies, slice thickness is 0.75 mm, reconstructed to 1 mm images with increment of 0.5 mm. The images should be assessed using both bone and soft tissue window settings.

From the three-dimensional data set, images can be reformatted in other planes (2-D technique) and be used for volume rendering (3-D technique).

The 2-D reformatting of sagittal and coronal images from axial images can highlight longitudinal fracture lines and can make it easier to evaluate horizontal interfaces, such as the acetabular roof.

The 3-D rendering allows different displays of the volume data. Surface rendering by thresholding, which, in contrast to volume rendering, incorporates only a portion of the data into the 3-D image, is the most widely used technique. By adding a virtual light source, a shaded surface display (SSD) can be achieved, which enhances the 3-D understanding of the image. However, it may provide an inadequate display of undisplaced and intra-articular fragments and, in comparison to axial imaging, surface rendering does not increase the detection rate of fractures and should only be supplementary to plain films and axial CT scan in the evaluation of comminuted fractures. Volume rendering, incorporating all the data into the 3-D image, requires more computer manipulation.

All reconstruction methods offer a more effective display of complex anatomic and pathologic structures. It may be helpful for the assessment of comminuted fractures, improving visualization of the fracture's extent and location, shape and position of the fracture fragments and the condition of articular surfaces (Bohndorf et al. 2001).

2.2.3.2 CT Arthrography

Intra-articular injection of iodinated contrast material mixed with 1 ml of a 0.1% solution of epinephrine is performed under fluoroscopic observation (Newberg et al. 1985). The volume of contrast medium injected depends on which joint is studied: shoulder: 10–15 ml; wrist: 5 ml; hip: 10 ml; knee: 20 ml; ankle: 6–12 ml. After injection of contrast material, patients are asked to perform full-range mobilisation of the joint. Anteroposterior, lateral and oblique views are routinely obtained to image the entire articular cavity. Subsequently, multidetector CT is performed.

The major advantage of CTA for the assessment of the cartilage is the excellent conspicuity of focal morphologic cartilage lesions that results from the high spatial resolution and the high attenuation difference between the cartilage substance and the joint contrast filling the lesion. Vande Berg et al. (2002) found, in a study with spiral CTA of cadaver knees, a better correlation for grading articular surfaces between macroscopic examination and spiral CTA than with MR imaging.

Other potential advantages of spiral CTA with respect to MR imaging are the short examination time, the availability at short notice (short waiting list) and the low sensitivity and limited degree of imaging artefacts related to the presence of microscopic metallic debris which may hinder MR imaging studies.

Limitations of CTA include its invasiveness, possible allergic reaction, use of ionizing radiation and poor soft tissue contrast resolution. Another major limitation of CTA imaging of the cartilage is its complete insensitivity to alterations of the deep layers of the cartilage.

2.2.4 Magnetic Resonance Imaging

2.2.4.1 Technique

Equipment and techniques for MRI vary widely, and although it is generally accepted that high field strength magnets provide the highest quality images, there has been considerable advancement in the technology of low field strength systems over the past few years, greatly improving their image quality.

Although appropriate selection of imaging planes will depend on the location and desired coverage of the anatomical region to be examined and the pathology to be expected, a complete MR examination requires that images be obtained in the axial, coronal and sagittal planes. Of utmost importance is to respect the anatomical orthogonal planes since, with excessive rotation of a limb, inappropriate positioning of imaging planes may result in images which are difficult to interpret. Oblique planes may also be useful, e.g. in the shoulder (paracoronal and parasagittal images).

The number of pulse sequences and combinations (‘hybrid techniques’) is almost infinitive: in musculoskeletal MR, the most commonly used sequences include conventional spin echo (SE) for T1-weighting, turbo SE (TSE) sequences for T2- weighting and gradient echo (GRE) sequences.

SE T1-WI is used for anatomic detail, and as an adjunct in the evaluation of the osseous structures.

TSE sequence has replaced conventional SE for T2-weighting (due to its relatively long acquisition times). However, because of image blurring, TSE sequences are not recommended for proton density imaging. Blurring can be reduced by increasing TE, decreasing inter-echo time, echo train length (ETL), and by increasing matrix. TSE sequences are less susceptible to field inhomogeneity than SE sequences. Therefore, when metallic artefacts are present, such as in post-surgical patients, TSE sequences are preferred over SE and GRE.

GRE sequences are used for the evaluation of articular cartilage and for dynamic contrast-enhanced imaging. They are also used in a limited number of T2* protocols (glenoid labrum, meniscus of the knee).

When using short TE in T1-weighted or PD images, one should take the magic angle phenomenon into account, a source of false positive MR findings.

Furthermore, a pulse sequence is always a compromise between acquisition time, contrast, detail or signal-to-noise ratio (SNR). SNR is highest in TSE and decreases respectively in SE and GRE sequences.

Concerning the different fat suppression (FS) techniques, in our institution, we prefer the spectral FS technique because of its better SNR and spatial resolution compared to the inversion recovery fat suppression techniques (Fleckenstein et al. 1991). Both T2-WI with (spectral) FS and STIR images are most sensitive to bone marrow and soft tissue edema or joint effusion. This item is discussed more in detail in Chap. 6. For good detection of fluid with preservation of anatomical detail and good differentiation between joint fluid and hyaline cartilage, we include an FS TSE intermediate weighted sequence (TR/TE=75/30–35 msec) in at least one imaging plane in our standard protocols.

Cartilage specific sequences have been developed, and are discussed more in detail in Chap. 4 (Disler et al. 2000).

The musculoskeletal system, especially in the extremities, is not influenced by motion, and, as a consequence, motion artefacts are rare. Infolding artefacts can be avoided by selecting an appropriate imaging matrix, saturating anatomical areas outside the region of interest, and off-center imaging. Artefacts due to distortions of the local magnetic field are attributable to ferromagnetic and, to a lesser degree, nonferromagnetic orthopaedic devices. The use of surface coils will improve the SNR; smaller slice thickness and larger matrices are essential for soft tissue imaging. The choice of small “field-of-view” (FOV) without changing the matrix size will increase the spatial resolution. Sometimes, imaging of the contra-lateral side may be useful, requiring a larger FOV and the use of a body coil.

Contrast-enhanced MR studies lead to a prolonged examination time and high costs, and therefore, the use of intravenous contrast agents is not indicated when evaluating a sports lesion. It should be reserved for cases in which the results would influence patient care (Kransdorf and Murphey 2000). Application of intravenous gadolinium is indicated when dealing with a tumoral or pseudotumoral mass (see also Chap. 8) to detect neovascularization and intralesional necrosis (which is a major parameter for malignancy), in cases of inflammation or as part of indirect arthrography. For detection of subtle areas of contrast enhancement, we use subtraction images (SE T1-WI with FS after minus SE T1-WI with FS before gadolinium) (static MR imaging). After i.v. administration of gadolinium, STIR type sequences should not be used, since not only fat but also enhancing tissue will be shown with a reduced signal intensity.

Recently, diffusion tensor imaging (DTI) has been used to study muscle architecture and structure. In future, DTI may become a useful tool for monitoring subtle changes in skeletal muscle, which may be a consequence of age, atrophy or disease (Galban et al. 2004). Furthemore, important information about muscle biomechanics, muscle energetics, and joint function may be obtained with unique MRI contrast such as T2-mapping, spectroscopy, blood-oxygenation-level-dependent (BOLD) imaging, and molecular imaging. These new techniques hold the promise for a more complete and functional examination of the musculoskeletal system (Gold 2003).

The clinical MR imaging protocol will be greatly influenced by local preferences, time constraints and MR system available (field strength, local coil). For an in-depth discussion of the different MR imaging protocols, the reader is referred to subsequent chapters.

MRI has the disadvantage of not always being well accepted by patients, of being incompatible with dynamic manoeuvres and of not always being possible in emergency conditions. Furthermore, it provides the evaluation of an entire anatomical area – bone structures included – but is only good for the study of a limited part of the skeleton. This is in contrast to scintigraphy, with which the whole skeleton can be evaluated at once. Otherwise, MRI helps to elucidate the true nature of highly nonspecific hotspots on scintigraphy. For a discussion of the value of nuclear medicine techniques used in sports lesions, we refer to the following chapters.

2.2.4.2 Direct and Indirect Arthrography

MR arthrography is a technique which is mainly used in the shoulder, wrist, ankle, knee and hip joint. Two different techniques are described – direct and indirect MR arthrography.

Direct Technique

The contrast medium is a 2 mmol/l solution of Gd-DTPA in 0.9% NaCl. Eventually add 1–5 ml 1% Lidocaine. Fluoroscopy is used to bring the needle-tip into a correct intra-articular position. To assure the correct position, 1–2 ml of 60% non-ionic contrast medium is injected. The amount of the MR-contrast medium injected depends on the selected joint. MR imaging (with FS SE T1-WI) is initiated within 30 min after injection to minimize the absorption of contrast solution and the loss of capsular distension.

Indirect Technique

Intravenous administration of 10–20 ml 0.1 mmol Gd-DTPA/kg body-weight. Synovial excretion of contrast medium occurs in the minutes after injection to shorten the relaxation time of the synovial fluid, and is heightened by rigorous exercise (joint movements) for about 10 min. MR imaging (with FS SE T1-WI) is initiated within 30 min after injection, when maximal enhancement is reached blanc line.

The clinical and radiological importance of the direct technique for the assessment of chondral and ligamentous lesions is well established. A major disadvantage of the direct technique is its invasiveness. An additional drawback of the direct technique is that in many European countries, intra-articular injection of gadolinium is not permitted. The indirect technique has the advantage of not requiring direct access to the joint but lacks the advantages of joint distension.

2.3 General Principles and Indications

As a general rule, MRI and US are most accurate for grading soft tissue injuries while bone injury can be assessed with conventional radiography and MRI. For internal derangements of joints, we prefer MRI because of its non-invasive character. In our institution, CT is used for better evaluation of fracture or fracture healing or for biometric views (e.g., anteversion femoral neck, Q-angle). We recommend that conventional radiography should always be the first diagnostic modality performed to depict (associated) skeletal or joint abnormalities.

Radiographic assessment of a stress fracture, an entity frequently encountered in sportsmen, can be insensitive, especially in the early stage of the condition and follow-up films may demonstrate abnormalities in only 50% (Spitz and Newberg 2002). Bone scintigraphy has a high sensitivity but low specificity and lacks spatial resolution and has been largely superseded by MRI, providing excellent sensitivity and specificity, as it can also identify alternative sources of pain, such as muscle tears or joint degeneration (Anderson and Greenspan 1996). Moreover, MRI is useful for follow up of stress injury, with a return of normal bone marrow signal on T2-WI at three months compared to scintigraphy, which may show abnormal uptake for up to ten months (Slocum et al. 1997).

Conventional arthrography has now been replaced by cross-sectional imaging techniques and is only performed as part of CT- or MR-arthrography.

For the diagnosis of muscle and tendon lesions, US is considered the best imaging modality, both in the initial phase for recognition of a lesion, but also for the assessment of the various changes it undergoes until complete healing has been achieved. In most cases, MRI adds no additional diagnostic information. Well-established indications for US are summarized in Table 2.1.

If plain radiographs and/or US are negative or reveal unequivocal findings and clinical symptoms persist, MR imaging must be performed.

MR examinations most frequently requested are of the knee and shoulder. Well-established indications for MRI are summarized in Table 2.2.

Due to the recent developments in CT technology, multidetector CTA has become a valuable alternative to MR imaging for the assessment of internal derangement of joints and has proved to be an accurate technique to detect articular cartilage lesions. A major drawback of spiral CTA, however, is its invasive character.

The choice between multidetector CTA and MR imaging for assessment of internal joint derangement is offered to the referring clinician, depending on the clinical situation. In general, children and young patients, patients with allergy to iodinated contrast, patients with suspicion of ligamentous lesions and patients with recent trauma (and hemarthrosis) are imaged with MR imaging. Multidetector CTA is favored in patients with chronic symptoms, suspected cartilage lesions, or in patients with recurrent symptoms after surgery (e.g., post-operative meniscus).

Table 2.1. Well-established indications for US

Foot/ankle	Achilles tendinosis, plantar fasciitis, ligamentous injury
Shoulder	Rotator cuff disease, biceps tendon (dynamic evaluation), spinoglenoid cyst
Elbow	Common extensor, flexor and triceps brachii tendinosis
Wrist/hand	Tenosynovitis, synovial cyst
Hip/pelvis	Inguinal hernia, snapping hip, bursitis, avulsion injury
Knee	Collateral ligaments, patellar and quadriceps tendon, bursitis, meniscal cyst

Table 2.2. Well-established indications for MRI

Foot/ankle	Osteochondral lesion
Shoulder	Labral abnormalities, suprascapular nerve entrapment, quadrilateral space syndrome, Parsonage-Turner
Elbow	Osteochondral lesion, ligamentous injury, instability
Wrist/hand	TFCC, AVN, distal radioulnar joint (DRUJ)
Hip/pelvis	Osteitis pubis, adductor strain, labral abnormalities, AVN
Knee	Meniscus, osteochondral lesion, cruciate ligaments, posterolateral corner

2.4 Optimal Moment of Investigation

The ideal time for the US examination of fresh traumatic muscle lesions is between 2 and 48 h after trauma. Before 2 h, the hematoma is still in formation. After 48 h, the hematoma can be spread outside of the muscle (Peetrons 2002). However, with some muscles it can stay for much longer. It is recommended that for lesions in the hamstrings the US examination be done as soon as possible after the 2-h delay. For rectus femoris and gastrocnemius lesions, the examination can be postponed for as long as two or three days, or even longer sometimes (Brandser et al. 1995).

2.5 Safety, Availability and Economic Aspects

Because all ionizing radiation is harmful and there is no safe lower threshold of radiation, consideration must be given to the radiation dose to the patient when plain radiography or a CT examination is requested. Examinations on children require an even higher level of justification since they are at greater risk from radiation than are adults. Therefore, when clinically appropriate, the alternative use of safer non-ionizing techniques (such as ultrasound and MRI) or of low dose radiography/CT techniques must always be considered (see also Chap. 26).

The number of sport participants, both amateur and professional athletes, has increased dramatically over recent decades. The benefits to health are debated but are generally accepted. However, more participation has led to more sports-related injuries. The increase has been in both acute and, even more, in overuse injuries (Garrick and Requa 2003). Although some researchers and policy makers have expressed concern about the lack of high quality evidence regarding the cost-effectiveness and efficiency of MRI, it was demonstrated that, in most diagnostic categories, MRI findings may have a significant impact on diagnosis and treatment planning (Hollingworth et al. 2000). For example, several studies have documented that MR imaging can be an accurate, cost-effective means of assessing injuries in the knee, preventing patients from undergoing unnecessary arthroscopy. Appropri-

ate selection of patients will probably yield similar results in other anatomic locations. The advancements in MRI technology may expand the range of usefulness of this modality, leading to even greater utilization of MR imaging in patients with sports injuries, and, eventually, to reduced costs and greater availability.

2.6 Conclusion

The diagnosis of sports injuries can be difficult owing to the degree of overlap of symptoms between different injuries, necessitating further imaging evaluation. Different imaging techniques, with their specific advantages and limitations, can be used to diagnose and grade such injuries. The correct use of these imaging modalities will lead to an early and accurate diagnosis preventing the development of chronic pain or other complications and thus, avoiding waste of limited financial resources. The specific merit of each imaging modality in the evaluation of sports related lesions will be further high-lighted in the next chapters and summarized in schematic boxes.

Things to Remember

1. The imaging requirements for sports medicine physicians should begin with conventional radiography.
2. Ultrasound is considered the imaging technique of first choice for the diagnosis of muscle lesions. The examination must be performed between 2 and 48 h after the muscle trauma to assess the extension of the hematoma and hence predict a grading of muscle lesions.
3. MR imaging has become the dominant imaging modality in the assessment of sports-related injury, because sports medicine and high-quality imaging are inextricably linked. There are, however, many findings on MRI that may not represent clinically significant disorders. Therefore, optimization of image acquisition and interpretation requires correlation with clinical findings.
4. Multidetector CT arthrography is a valuable alternative to MR imaging for the assessment of internal derangement of joints. In daily, clinical practice, the choice between the two imaging modalities is offered to the referring clinician, depending on the clinical situation.

References

American College of Radiology (2005) Expert Panel on Musculoskeletal Imaging. Chronic ankle pain. www.guideline.govn, National Guideline Clearinghouse

Anderson MW, Greenspan A (1996) Stress fractures. Radiology 199:1–12

Berland LL, Smith JK (1998) Once again, technology creates new opportunities. Radiology 209:327–329

Bohndorf K, Imhof H, Pope TL Jr (2001) Musculoskeletal Imaging. Thieme. Stuttgart, New York. First Edition

Brandser EA, El-Khoury GY, Kathol MH et al. (1995) Hamstring injuries: radiographic, conventional tomographic, CT and MR imaging characteristics. Radiology 197:257–262

Disler DG, Recht MP, McCauley TR (2000) MR imaging of articular cartilage. Skeletal Radiol 29:367–377

Fleckenstein JL, Archer BT, Barker BA et al. (1991) Fast short-tau inversion-recovery MRI. Radiology 179:499–504

Galban CJ, Maderwald S, Uffmann K et al. (2004) Diffusive sensitivity to muscle architecture: a magnetic resonance diffusion tensor imaging study of the human calf. Eur J Appl Physiol 93:253–262

Garrick JG, Requa RK (2003) Sports and fitness activities: the negative consequences. J Am Acad Orthop Surg 11:439–443

Gold GE (2003) Dynamic and functional imaging of the musculoskeletal system. Semin Musculoskeletal Radiol 7:245–248

Hollingworth W, Todd CJ, Bell MI (2000) The diagnostic and therapeutic impact of MRI: an observational multi-centre study. Clin Radiol 55:825–831

Johnson R (2000) Sports Medicine in primary care. Philadelphia, Pa: Saunders

Kransdorf MJ, Murphey MD (2000) Radiologic evaluation of soft tissue masses: a current perspective. AJR Am J Roentgenol 175:575–587

Newberg AH, Munn CS, Robbins AH (1985) Complications of arthrography. Radiology 155:605–606

Öhberg L, Alfredson H (2002) Ultrasound guided sclerosis of neovessels in painful chronic Achilles tendinosis: pilot study of a new treatment. Br J Sports Med 36:173–175

Peetrons P (2002) Ultrasound of muscles. Eur Radiol 12:35–43

Peterson L, Renstrom P (1986) Trauma in sport. Nurs RSA 1:20–23

Slocum KA, Gorman JD, Puckett ML et al. (1997) Resolution of abnormal MR signal intensity in patients with stress fractures of the femoral neck. AJR Am J Roentgenol 168:1295–9

Spitz D, Newberg A (2002) Imaging of stress fracture in the athlete. Radiol Clin N Am 40:313–331

Vande Berg BC, Lecouvet FE, Poilvache P et al. (2002) Spiral CT arthrography of the knee: technique and value in the assessment of internal derangement of the knee. Eur Radiol 12:1800–1810

Weinberg EP, Adams MJ, Hollenberg GM (1998) Color Doppler sonography of patellar tendinosis. AJR Am J Roentgenol 171:743–4

Weng L, Tirumalai AP, Lowery CM et al. (1997) Ultrasound extended-field-of-view imaging technology. Radiology 203:877–880

Zanetti M, Metzdorf A, Kundert H-P et al.(2003) Achilles tendons: clinical relevance of neovascularization diagnosed on power doppler US. Radiology 227:556–60

Muscle Injuries

3

Jan L. Gielen, Philip Robinson, Pieter Van Dyck, Anja Van der Stappen, and Filip M. Vanhoenacker

CONTENTS

Box 3.1. US

- Best technique for diagnosis of strain and contusion
- Evaluation of the muscular ultrastructure provides a good assessment of tear
- Best technique for follow up of strain

Box 3.2. MRI

- Best technique for detection of edema
- Time dependent presentation of blood degradation products

Box 3.3. Standard radiography

- Main role is evaluation of maturity of myositis ossificans and avulsion fractures
- Characteristic in calcific myonecrosis

3.1 Introduction

Skeletal muscle comprises the largest tissue mass in the body, accounting for 40–45% of body mass (Best and Garret 1994; Garrett and Best 1994). The muscle-tendon unit (MTU) is, in essence, a mechanical system, that enables locomotion. Muscles are subject to traumatic processes that can compromise their function. Muscle trauma is common in athletes, it can lead to changes that may be observed on US and MRI, and that may manifest as abnormalities of muscle reflectivity respectively intensity and (ultra)structure as well as volume alterations. Muscles were difficult to image with early techniques (radiographs, computerized tomography (CT) and low resolution

J. L. Gielen, MD, PhD
Associate Professor, Department of Radiology, University Hospital Antwerp, Wilrijkstraat 10, 2650 Edegem, Belgium
P. Robinson, FRCR
Consultant Musculoskeletal Radiologist, Department of Radiology, Musculoskeletal Centre, Chapel Allerton Hospital, Leeds Teaching Hospitals, Leeds LS7 4SA, UK
P. Van Dyck, MD
A. Van der Stappen, MD
F. M. Vanhoenacker, MD, PhD
Department of Radiology, University Hospital Antwerp, Wilrijkstraat 10, 2650 Edegem, Belgium

ultrasound) because of low soft tissue contrast. With the advent of high resolution ultrasound (US) and magnetic resonance imaging (MRI) it became much easier to diagnose injuries primarily affecting the soft tissues. Currently more attention is paid to traumatic lesions of the MTU in radiological literature (Campbell and Wood 2002; El-Khoury et al. 2004). US grading of muscle injury can be performed, and follow-up studies can assess repair of muscle tissue and identify complications of the healing process. Some features such as vascularity and intralesional calcification may be more easily appreciated on ultrasound than MRI.

This chapter reviews to the imaging relevant anatomy, ultrastructure and (patho)physiology of muscle as well as the radiological characteristics of normal and injured muscle as seen on ultrasound and MRI with emphasis on its clinical relevance.

3.2 Anatomy, Ultrastructure and (Patho)physiology with Imaging Correlation

The muscle fibre is the basic structural element of skeletal muscle; the sarcomere is the smallest contractile unit of muscle fibre. The muscle fibre is a long cell connected to the tendon or bone on which it acts. The contractile filaments, myosin and actin filaments, are interswitched with a minimum overlap. Greater overlap of these filaments produces muscle shortening-contraction (Fig. 3.1). There are no end to end connections between muscle fibres. Muscles originate from and insert on bone or dense connective tissue either directly or via a tendon. A layer of fibrous connective tissue, the *endomysium*, surrounds each individual muscle fibre. These fibres are bundled into fascicles, which themselves are surrounded by perimysium. The *perimysium* is easily recognized on longitudinal ultrasound as linear reflective lines separating the hyposonant contractile fascicles (Peetrons 2002) (Fig. 3.2a, Fig 3.3a, b, d, f, g (left)). Transversely they appear as dotted reflective areas. Thicker reflective septa may occasionally be seen within the muscle belly, resulting in a reticular or honeycomb pattern on transverse images (Fornage 1995) (Fig. 3.2b, Fig. 3.3c, e, g (right)). On MRI this fascicular structure is not well appreciated. Muscular tissue produces a homogeneous intermediate SI on T1- and T2-weighted MR images (WI) with intermediate to slightly long T1 relaxation time and short T2 relaxation time. The fat along fascial and subcutaneous tissue planes allows identification of individual muscles. The axial plane is particularly helpful for outlining specific muscle contours to determine location of lesions and to compare atrophy or expansion of muscle. Including the opposite side for comparison may be helpful (Kathol et al. 1990). The outer thicker layer or *epimysium* (muscle fascia) that surrounds the entire muscle belly is also reflective on US. This thick fascia may produce a low SI cocoon around the muscle belly on T1- and T2-WI MR images.

These layers of connective tissue within the muscle belly are called the connective tissue skeleton of the muscle (endo-, peri-, and epimysium). At the myotendinous junction the contractile elements end and the connective tissue skeleton of the muscle belly continues in endo-, peri- and epitendineum of the tendons of attachment. This transition site of connection between the contractile muscle cells and the tendon is known as the myotendinous junction (Noonan and Garrett 1992). It is a specialized region of highly folded membranes at the muscle-tendon interface. The folding increases the junctional surface area by 10–20 times, decreasing the stress per unit area.

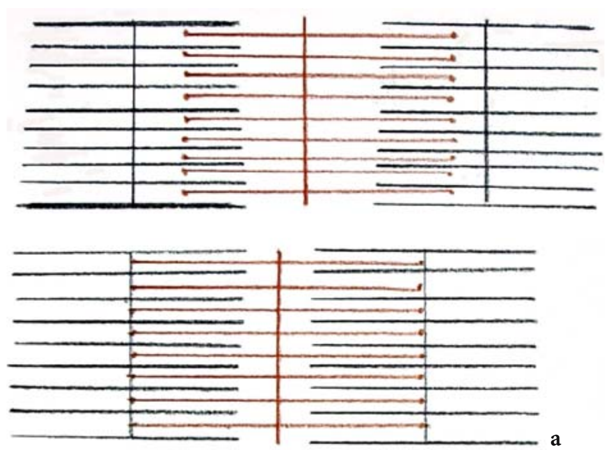
a

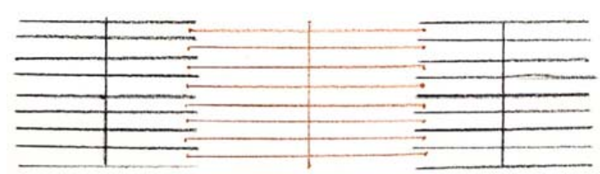
b

Fig. 3.1a,b. Schematic drawing of muscle filament orientation. **a** Normal actin and myosin filament orientation during rest (*top*), and maximum contraction (*bottom*). **b** Filament elongation after strain injury grade 1

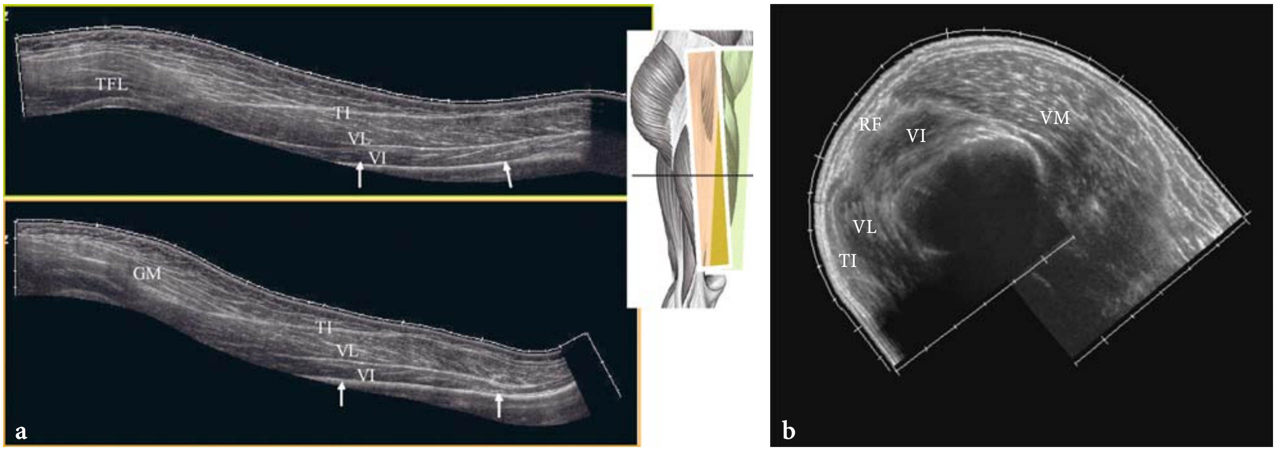

Fig. 3.2a,b. Thigh muscles and tractus iliotibialis. Lateral longitudinal (**a**) and transverse (**b**) extended field of view ultrasound images of the thigh muscles. Longitudinal posterior and anterior view with a total length of 40 cm on *top and bottom* respectively. The gluteus maximus (*GM*), vastus lateralis (*VL*) and vastus intermedius (*VI*) muscles and the tractus iliotibialis (*TI*) can be identified on longitudinal images. The four quadriceps heads including vastus medialis (*VM*) and rectus femoris (*RF*) can be identified on the transverse image. The reflective linear lines of the perimysium are best appreciated in the localized longitudinal ultrasound images. The reflective line between muscles corresponds to the epimysium (muscle fascia). The deep reflective line (*arrows*) is formed by the cortical lining of the femur diaphysis and distal metaphysis

The orientation of reflective layers of perimysium on ultrasound depends on the orientation of the muscle fibre. Unipennate (e.g. gastrocnemius muscles) and bipennate (e.g. rectus femoris muscle) muscles have muscle fibres obliquely oriented to the epimysium and myotendinous junction (Fig. 3.3a–f). In these cases, the myotendinous junction is often quite large, extending a long distance into the muscle belly. This configuration allows for a large number of short muscle fibres in a given cross-sectional area (CSA), producing powerful muscles that resist elongation. The angle of the muscle fibres in relation to the tendon or aponeurosis in pennate muscle types is easily appreciated on ultrasound; it grows in hypertrophied muscles as is the case in athletes, especially in body builders (Fig. 3.3a). It is believed that resultant force vector parallel to the tendon diminishes in angulations over 45° resulting in lower muscle strength. In a parallel or fusiform configuration, the muscle fibres are oriented with the long axis of the muscle, with a smaller number of longer muscle fibres in the same CSA. This allows a greater range of movement and maximum velocity of shortening, but less power.

Research in muscle biology has proved the existence of different types of muscle fibres with distinctly different structural, physiological, and biochemical characteristics. Differences in fibre type are related to performance characteristics of certain muscles which reflect the speed of contraction and endurance of the muscle (Garrett et al. 1984). The type I (slow twitch) fibre has slow contraction and relaxation times; it is, however, resistant to fatigue and has more mitochondria and capillaries per fibre. Muscles active in postural activities are rich in type I fibres. The type II (fast twitch) fibre is divided into subtypes but generally the type II fibre has lower mitochondrial content, functions glycolytically and is better adapted to intense movement activities of short duration. More tension can developed in type II fibres than in the type I fibres. The amount of active tension that a muscle produces has been shown to be proportional to the fibre type content, so that muscles with higher proportion of type II fibres are able to generate more force. Low intensity exercise selectively involves type I fibres, while more type II fibres are recruited as exercise intensity increases. Muscle biopsies from sprinters are more likely to show a predominance of type II fibres, as compared with long distance runners where type I fibres predominate. It is not certain if these fibre distributions are genetically determined or are a response to training (Garrett 1990).

Most muscles cross one joint but some cross two or more joints. Those muscles that cross only one joint are located more deeply and are usually involved in postural activities (type 1 fibres), with greater strength and slow speeds of contraction. Muscles

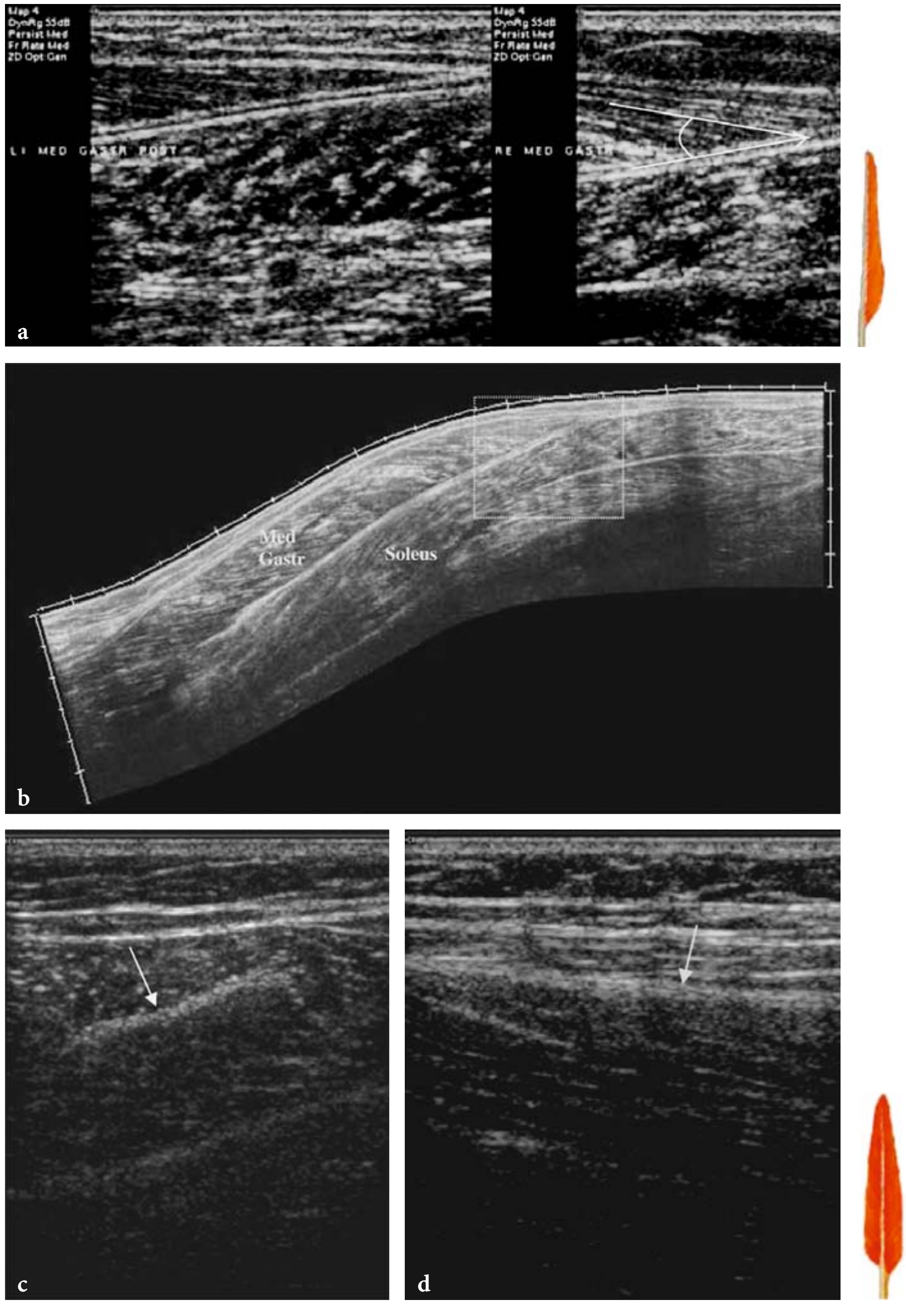

Fig. 3.3a–g. Ultrasound and diagram illustrating the arrangement of muscle fibres. **a,b** Unipennate medial gastrocnemius muscle. A distal third of left and right muscle and B extended field of view (left=proximal). The angulation of the muscle fibres relative to the tendon (aponeurosis) is measured at 20° (white angle on **a**). Extended field of view image (**b**) from the popliteal fossa (left side) to the Achilles tendon (right side). **a** is the part at the *dotted box* in **b**. **c–f** Circumpennate adductor longus muscle (**c** transverse and **d** longitudinal imaging plane at the proximal third, **e** and **f** extended field of view). The central reflective structure represents the tendon (*arrow*) that is surrounded by hypo-echoic contractile elements, the reflective dots and lines in between the contractile elements represent perimysium. Superficial thick reflective line is epimysium or superficial muscle fascia. **g** Parallel or fusiform muscle type, musculus biceps brachii. (*Left*: longitudinal plane. *Right* transverse US plane). The larger number of muscle fibres in a given cross-sectional area in the unipennate and bipennate muscle types allows for greater muscle strength, but less ▷

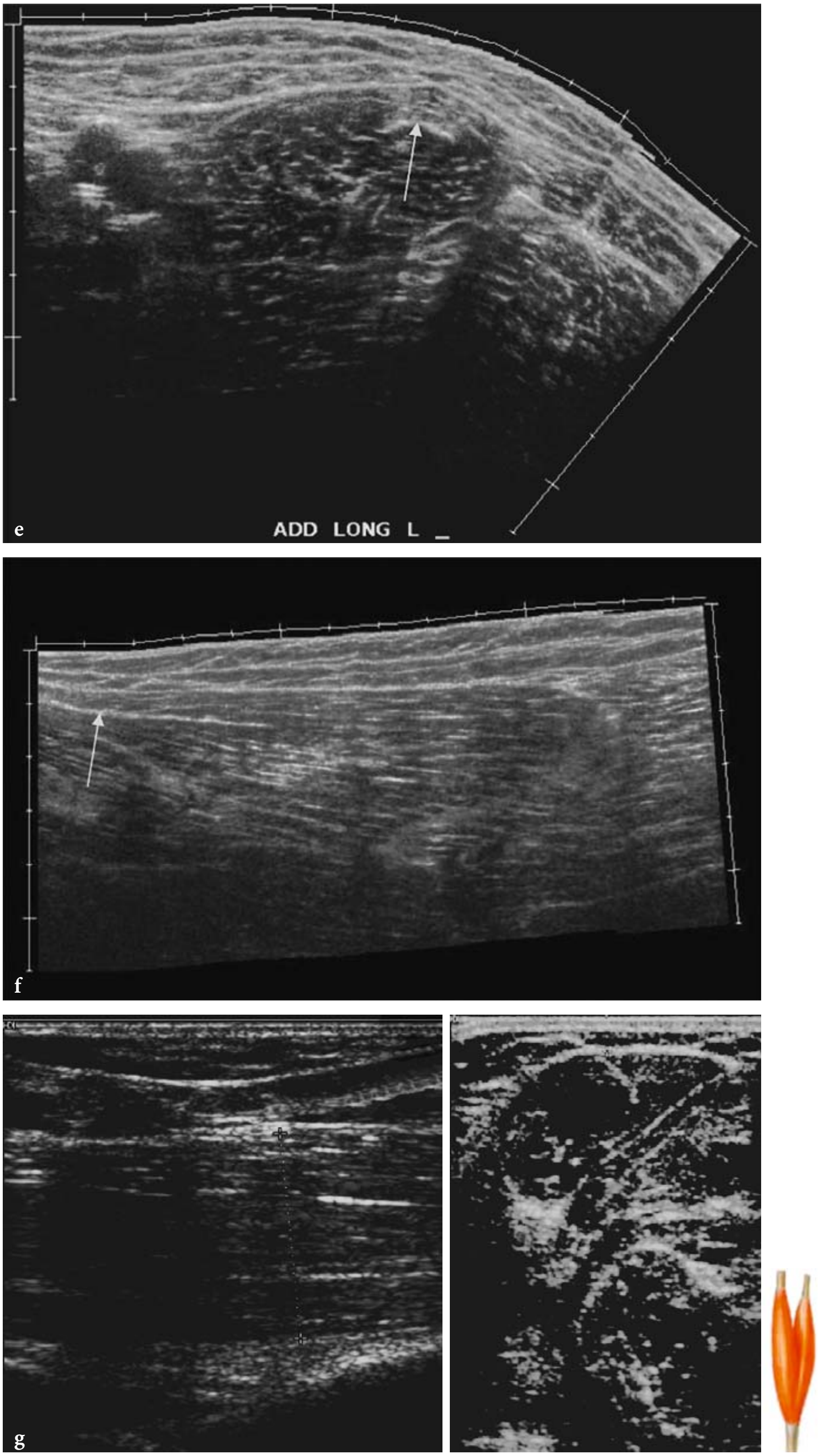

capacity for muscle shortening than in the parallel muscle type. Dynamic ultrasound during active muscle contraction demonstrates the change in muscle shape and fibre orientation in the longitudinal plane

that cross more than one joint produce higher speeds of contraction and a greater shortening index, but produce less tension over the full range of movement (type 2 fibres).

Muscles that are located deeply, i.e. adjacent to bony structures, are more prone to crush (direct) trauma. Muscles that span more than one joint are more prone to distraction (indirect) injury.

Skeletal muscles are controlled by motor nerves. A motor unit is made up of a single nerve axon and all the muscle fibres it supplies. Muscle fibres in a motor unit have the same contractile and metabolic properties.

Muscle activation generates force within the muscle. If the resisting load is less than the force generated by the muscle, then the muscle will shorten; this is referred to as concentric contraction. When the resisting force is greater than that generated by the muscle, the muscle will elongate; this is referred to as eccentric elongation. A large portion of muscle activity occurs in an eccentric fashion. Eccentric muscle activation can produce more force or tension within the muscle than when it is activated concentrically, making it more susceptible to rupture or tearing. Dynamic US in a longitudinal plane during active muscle contraction demonstrates changes in muscle volume, and fibre orientation.

A tear in the muscle-tendon unit will occur when the tension in the unit exceeds the strength of the weakest structural element. From an imaging standpoint, the myotendinous junction is an important region, because injuries involving the muscle belly tend to occur near, but not precisely at the true histological muscle-tendon junction.

3.3 Muscle Trauma

A large segment of the population participates in sports activities resulting in injuries to a variety of muscles. The majority of muscle injuries are self-limited and imaging is rarely indicated. US and MRI may be employed for the assessment of (professional) sports injuries involving muscles. In the evaluation of muscle injury US may be performed in the acute setting and during rehabilitation to grade the injury, identify the muscle groups involved, help predict rehabilitation time, monitor the healing response and evaluate complications. Monitoring and natural history of muscle trauma will be discussed in Chap. 29. This chapter will focus on the initial diagnosis of muscle trauma.

3.3.1 Acute Muscle Injuries

Acute muscle injury occurs as a result of two mechanisms. Direct crush trauma or compressive injury results in contusions and haematomas. Over-elongation of muscle fibres, during active contraction or passive stretching, leads to muscle strains and ruptures.

3.3.1.1 Muscle Strain

3.3.1.1.1 Biomechanical Basis

Muscle functions to initiate skeletal movement, but also resists and modifies other movements by transmitting forces to the skeleton through the tendons (Herzog 1996; Brinckmann et al. 2002).

Indirect muscle injuries, or muscle strains, are frequently encountered following athletic activities; they represent a major reason for time lost from sports (Shellock et al. 1994). Muscle injuries occur during powerful eccentric contraction because more tension is generated within muscles during eccentric contraction than during concentric contraction.

Muscle and tendon injury occur at zones of anatomical or functional transition as these sites generate the greatest concentrations of intrinsic forces (Garrett et al. 1987; Nordin and Frankel 2001). Experimentally, muscle-tendon units stretched to failure, consistently disrupt near the myotendinous junction. Indeed, already more than 60 years ago, McMaster (1933) showed experimentally that a tendon does not rupture when a normal muscle-tendon unit is subjected to powerful strain. This is also true clinically and has been shown repeatedly on US and MRI studies, in adults muscles subjected to forceful eccentric contraction consistently disrupt at the muscular side near and not at the muscle-tendon junction or near the bone-tendon junction (Fig 3.4).

At the microscopic level initially haemorrhage is found. Twenty four to 48 h after the injury, a pronounced inflammatory response is seen with fiber necrosis, capillary ingrowth, and a proliferation of disorganized fibroblasts (Nikolaou et al. 1987). The

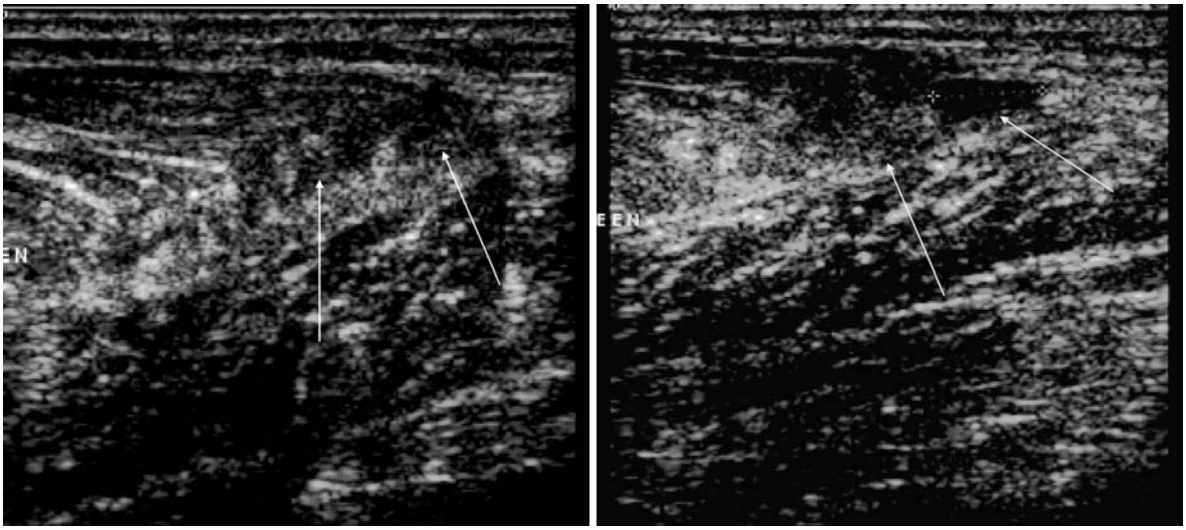

Fig. 3.4. Acute grade 2 injury of the medial gastrocnemius on longitudinal US. Unipennate muscle type. Typical example of "tennis leg". A small low reflective focal haematoma (*arrows*) with a few internal echoes, replaces the retracted fibres at the distal musculotendinous junction. The soleus muscle lies immediately deep to the haematoma and is normal. Compare with Fig. **3.2a** demonstrating the normal musculotendinous junction

edema and inflammatory response is resolved after one to two weeks. After 72 h collagen synthesis may be found that, together with myotube, bridges the injury site. Stress produces secondary remodelling of the muscle that goes on for months. It is obvious that the imaging aspect of muscle tears largely depends on the time interval to the injury. Imaging aspect of muscle tears also depends on the grade of strain injury. Correlative imaging and histopathologic studies to grade muscle strain lesions have not been published yet. We propose the following hypothetic mechanism of distraction injury that is based on long-lasting ultrasound practice on acute and chronic lesions at different grades and stages. In a first grade of injury the myosin and actin filaments are distracted above their level of maximum physiologic elongation without being torn apart, thus no filament or muscle fibre rupture is present (Fig. 3.1b). Capillary vessels at the contractile apparatus and at the surrounding endomysium probably are injured and this may result in diffuse bleeding (haemorrhage). At this grade not tissue loss but swelling may be clinically apparent (Fig. 3.5a,b, US low grade 1 strain). Ongoing distraction forces will cause contractile fibres and endomysium discontinuity, and may tear perimysium apart (grade 2). On ultrasound, fibre discontinuity and local bleeding is seen. There is some destruction of the connective tissue skeleton of the muscle. The location of muscle strain injury will vary along with the type of muscle. In unipennate muscles the musculotendinous junction is located superficially and in these circumstances, epimysium (fascial) injury may be present in low grade injury. The commonest example of this is "tennis leg", occurring at the distal medial gastrocnemius muscle (Fig. 3.4). Some authors describe this particular variation of muscle rupture at the myotendinous junction as a muscle–aponeurosis avulsion. Injury to the epimysium causes perimuscular fluid or bleeding and is often followed by scarring. In contrast, in parallel or circumpennate muscles the tears are more frequently located centrally.

Grade 3 injury corresponds to complete muscle rupture with injury of the epimysium. In grade 2 and grade 3, clinically, tissue loss with a gap is often felt at the rupture site. Occasionally a subcutaneous ecchymosis can occur but this usually develops 12–24 h later (Peterson and Renstrom 1986). This ecchymosis is probably only found in cases of epimysium tear. It is located typically distally to the tear where the fascial planes abut the subcutis and gravitation brings it to the surface. Major haematoma is not often found in distraction injury, as larger vessels are not involved. Clinical examination may be confusing in rare cases of extensive hematoma as it fills in the gap and may eventually give the impression of a swelling.

The forces experienced can be exacerbated by concurrent injury, fatigue and the severity of external forces as well as their speed of application (Mair et al. 1996; Brinckmann et al. 2002). Weakened or fatigued

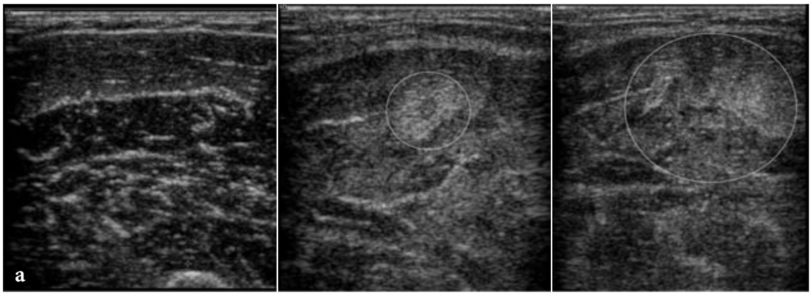

Figure 3.5a,b. Hyperacute grade 1 injury. **a** Transverse US images of the biceps brachii muscle. Parallel muscle type. *Left image* represents normal right muscle, *middle and right images* represent side of the injury (left). Several small areas of low and high reflectivity adjacent to one of the intramuscular septae are seen in the long axis of the left muscle belly (*dotted circles*). **b** Longitudinal ultrasound image of the of long head of biceps femoris muscle with diffuse reflective infiltration due to diffuse bleeding with central small hematoma

muscles absorb less energy and therefore are more likely to be injured. Muscles containing predominantly type II fibres and muscles that cross more than one joint are at increased risk of strains.

The majority of athletes are skeletally mature with little tendon degeneration. In this setting excessive tensile forces across the musculoskeletal unit typically lead to failure near the myotendinous junction (Mink 1992; Taylor et al. 1993). This is in contrast to skeletally immature athletes in which the apophysis is the most sensible link (Chap. 26) and athletes with tendinosis where the diseased tendon can fail rather than the myotendinous junction (Chap. 27) (Mink 1992; Taylor et al. 1993).

3.3.1.1.2 Clinical Presentation

Clinically, muscle strain is characterised by immediate focal pain and decreased function that can be due to muscle disruption or associated reactive spasm in adjoining muscles (Nicholas and Hershman 1986; Peterson and Renstrom 1986; Speer et al. 1993; Noonan and Garrett 1999). Muscle strains are clinically classified as either complete or partial based on whether the muscle-tendon unit is grossly disrupted or not (Zarins and Ciullo 1983). The most established clinical grading system has three components but it is recognised that differentiation of clinical grades can be difficult (O'Donoghue 1984). Grade one injury is less than 5% loss of function with mild evidence of a haematoma or edema (O'Donoghue 1984). Grade two injury is more severe but with some function preserved. Grade three strains are complete muscle tears with no objective function and occasionally a palpable gap in the muscle belly.

Most muscle strains occur in the lower extremities with the *rectus femoris, biceps femoris* and *medial gastrocnemius* muscle being most commonly affected; they are followed by the *semitendinosus*, adductor, vastus medialis and soleus muscles (Greco et al. 1991). The muscles in *italics* span more than one joint.

Previous incomplete injury, without total recovery of tensile strength, predisposes to more serious strains.

3.3.1.1.3 Imaging

In experienced hands and with modern equipment MR imaging and ultrasound are both accurate techniques for the evaluation of lower limb muscle strain (Steinbach et al. 1998; Van Holsbeeck and Introcasco 2001; Connell et al. 2004; Cross et al. 2004; Robinson 2004). When symptoms are localised, acute muscle injury is best evaluated with ultrasound. In comparison to MR imaging it is fast and allows dynamic stressing which can be useful for differentiating large grade 2 from grade 3 tears (Van Holsbeeck and Introcasco 2001; Robinson 2004).

However, the large muscle bulk often present in athletes means that the depth of resolution and field of view offered by ultrasound can be limiting especially in the pelvis and proximal thigh. Therefore, MR imaging can be more accurate in these anatomical areas or when symptoms are diffuse and, ideally, the radiologist should be familiar with both techniques.

The main imaging classification has been described in an attempt to correlate with clinical evaluation and is also graded 1–3 (Takebayashi et al. 1995) using a US system varying from normal to complete muscle tears with retraction (Table 3.1). In clinical practice, the most important aim is to identify the presence of significant muscle bundle tears and bleeding. In the very acute stage within 2 h after the injury, haemorrhage and haematoma has a reflective aspect, in this stage the lesion is underestimated. After 48–72 h the lesion is correctly graded due to the anechoic aspect of the haematoma.

Table 3.1. US grading system of muscle trauma

Grade 1	Elongation injury: no abnormalities or diffuse bleeding with or without focal fibre rupture (less than 5% of the muscle involved)
Grade 2	Partial rupture: focal fibre rupture more than 5% of the muscle involved, with or without fascial injury
Grade 3	Complete muscle rupture with retraction, fascial injury is present

MRI may also be used to assess muscle injury, but evaluation can be difficult as ultra-structure of muscles is not discriminated, and thus even minor elongation injuries can produce quite dramatic appearances that can be overestimated in their severity. All acute muscle injuries have associated edema and haemorrhage which cause prolongation of the T1 and T2 relaxation times of the injured tissue. Occasionally an added sequence utilizing fat suppression may be required. T2-weighted MR images are ideal for the delineation of muscle tears; the bright signal from high water content stands out against the relatively low signal of muscle and intermediate signal of fat on T2-weighted MR images. T1-weighted MR images are less sensitive in depicting soft tissue abnormalities because most pathologic processes have long T1-relaxation times similar to muscle; the contrast between muscle and haemorrhage or between muscle and edema may be imperceptible on T1-weighted MR images. T1-weighted MR imaging may be useful, however, in providing specificity in regard to the presence of haemorrhage or fat (Deutsch and Mink 1989).

Grade 1

Minor elongation injuries, also called *claquage,* will either appear on US as normal, or as small areas of low reflective cavities in the case of grade 1 injuries (Fig. 3.5), in which no or a minority of muscle fibres are ruptured (less than 5% of the muscle volume). A normal US with clinical history of a sharp stabbing pain that increases by muscle contraction is diagnostic for a grade 1 muscle tear or elongation (Mink 1992; Van Holsbeeck and Introcasco 2001; Robinson 2004). Occasionally MRI also may have a normal appearance or may present as a (small) area of edema that presents as a diffuse area with prolonged T2-relaxation time (high SI).

In this grade of injury MR imaging can be superior to ultrasound (Fig. 3.6 MRI) (Gibbs et al. 2004). However, in daily clinical practice, a normal ultra-

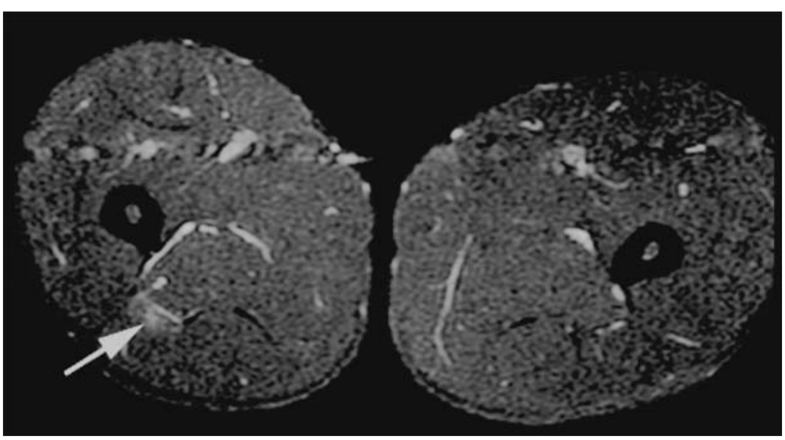

Fig. 3.6. Professional footballer with acute onset thigh pain. Axial fat suppressed T2 weighted MR image shows minor area of edema (*arrow*) within the long head of biceps femoris (grade 1 injury) (for further discussion see Chap. 21)

sound is sufficient in most cases to exclude higher grade injury (Gibbs et al. 2004; Robinson 2004). Grade 1 injuries usually heal quickly within one to two weeks.

Grade 2

More serious elongation injuries result in partial or complete ruptures, and are evident by the discontinuity of muscle fibres and bundles, and by the presence of haematomas (Fig. 3.4 US). Grade 2 injuries correspond to a partial tear with haematoma and muscle fibre disruption (over 5%) but not affecting the whole muscle belly. This is an area where both clinical and imaging classifications can be misleading as a grade 2 injury can describe a 10% or 90% thickness tear yet these two injuries will have significantly different rehabilitation times (Fig. 3.7 MRI and US, and Fig. 3.8 US, Fig. 3.9 MRI and US). Therefore when describing a grade 2 tear it is important to convey also the percentage volume of muscle disrupted and the length of injury (Verrall et al. 2001, 2003; Slavotinek et al. 2002; Connell et al. 2004; Cross et al. 2004; Gibbs et al. 2004). As these parameters increase the severity of injury also increases, implying the need for longer rehabilitation. Ultrasound can visualize the torn ends of the muscle bundles, and retracted muscle tissue may be highlighted by the presence of refractile shadowing. In some cases of partial or complete rupture, the torn ends of the muscle can be seen floating within the haematoma («clapper in the bell» sign) (Fig. 3.8). It may also be helpful to ask the patient to contract the muscle actively, which will accentuate the retraction of muscle tissue facilitating the identification and sizing of the muscle tear.

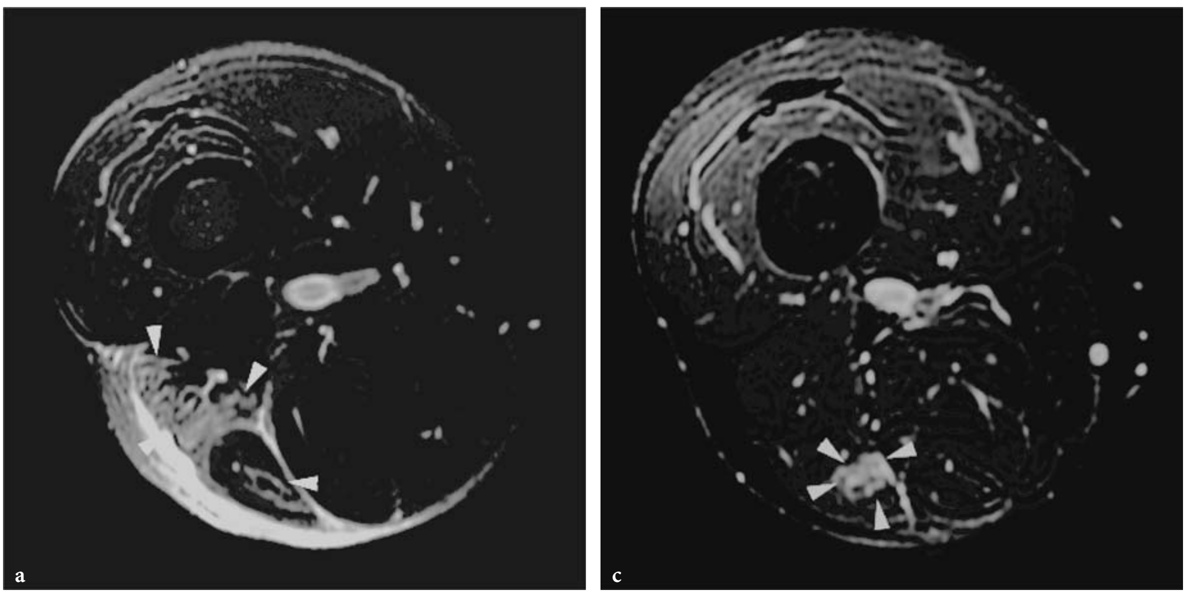

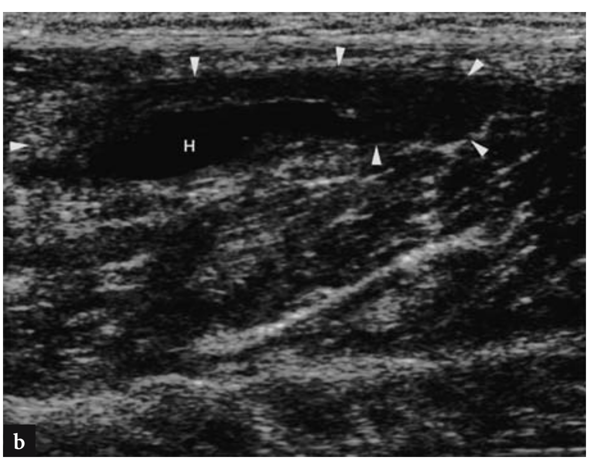

Fig. 3.7a–c. Professional footballer with recurrent hamstring injuries. **a** Axial fat-suppressed T2 weighted MR image from 2002 shows an acute grade 2 injury involving the long head of biceps femoris (*small arrowheads*). **b** Corresponding longitudinal ultrasound image one week later shows a hypoechoic haematoma (H) with an area (*arrowheads*) occupying 10–20% of the muscle diameter (grade 2 injury). **c** Axial fat suppressed T2 weighted MR image from new injury in 2005 shows marked edema involving the myotendinous junction of the short and long heads (*arrowheads*) of biceps femoris (for further discussion see also Chap. 21)

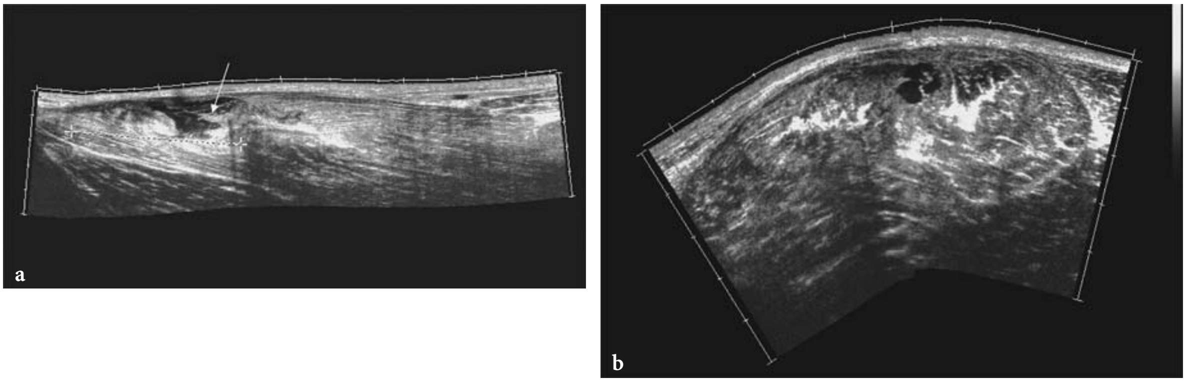

Fig. 3.8. Grade 2 injury of the adductor longus muscle, circumpennate muscle type. A longitudinal US imaging plane, B axial US imaging plane. There is a subacute partial tear at the muscle proximal at the myotendinous junction (grade 2), with organizing hematoma. The torn end is evident by the presence of retracted muscle fibres surrounded by fluid (clapper bell sign, *arrow*). Perimysium tear with extramuscular fluid is evident

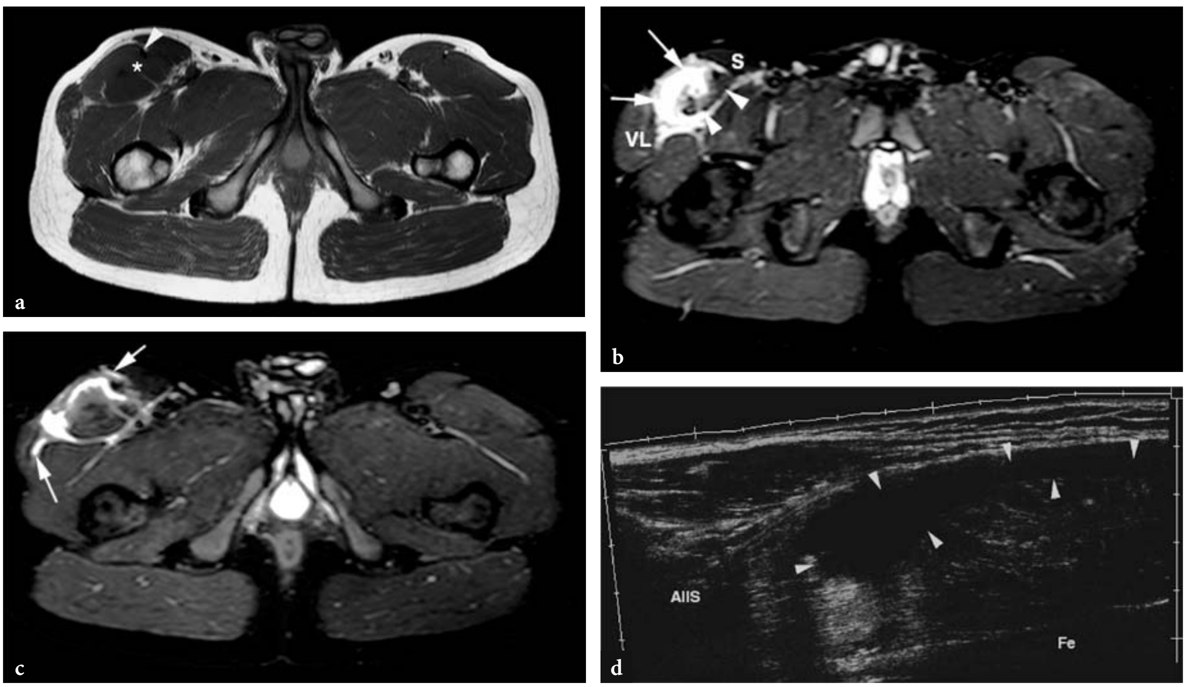

Fig. 3.9a–d. Professional footballer with severe acute proximal thigh pain. Axial (**a**) fat suppressed T1 and (**b**) T2 weighted MR images show a swollen and edematous proximal right rectus femoris (*), extensive perifascial fluid (*arrows*) and intact low signal tendon (*arrowhead*). (**c**) Axial fat suppressed T2 weighted MR image above the level of the previous images show more extensive muscle edema and fluid (*arrows*) extending towards vastus lateralis (*VL*) and overlying sartorius (*S*). A small remnant of muscle is seen intact (*arrowheads*). (**d**) Longitudinal extended field of view ultrasound image confirms grade 2 injury (*arrowheads*) just distal to the origin from the anterior inferior iliac spine (*AIIS*). The muscle deep to the area and adjacent to the femur (Fe) appears intact (*arrows*) (for further discussion see also Chap. 21)

Grade 3

Grade 3 injuries are complete muscle tears with loss of muscle continuity and marginal distraction. Blood and edema within the tear and surrounding fascial planes can also be seen. Differentiating acute high grade 2 injuries from grade 3 tears can sometimes be problematic on T2 weighted MR images as it can be difficult to distinguish edematous muscle from fluid within the tear. Occasionally this can be resolved by correlation with T1 weighted MR images or post-gadolinium images where the edematous muscles enhance but fluid should not. In this situation it may also be better to perform ultrasound evaluation as it is usually easier to distinguish edematous muscle from haematoma during static and dynamic imaging (Fig. 3.10) (Van Holsbeeck and Introcasco 2001; Robinson 2004). A defect is detected at the site of the tear, and a mass which is isointense with normal muscle is detected due to retraction of the torn muscle.

Muscle ruptures (grade 2 and 3) are more serious injuries and often require longer periods of rehabilitation, from several weeks to months, depending on the magnitude of muscle involvement.

Haematomas and haemorrhage are a key sign of muscle rupture. Haematomas typically appear as circumscribed areas of low or absent reflectivity, and, as cellular elements separate out, fluid-fluid levels may be seen. However, in the very early stages of a tear, the haemorrhage and haematoma may appear diffuse and hyper-reflective (Fig. 3.5) (Takebayashi et al. 1995), or cause an increase in the separation of the reflective layers of perimysium. If the epimysium or aponeurosis is also torn, then the haematoma may extend beyond the boundaries of the muscle and may appear diffuse and indistinct (Figs. 3.7–3.10). Perifascial fluid is relatively common for all grades of injury as any breach of the muscle aponeurosis allows blood to track along the fascial planes (Jarvinen et al. 2005).

MRI findings in muscle strains not only depend on whether the tear is complete or incomplete but also on the duration of the tear. In the acute incomplete tear, blood and edema may infiltrate between the muscle bundles, especially in the region of the

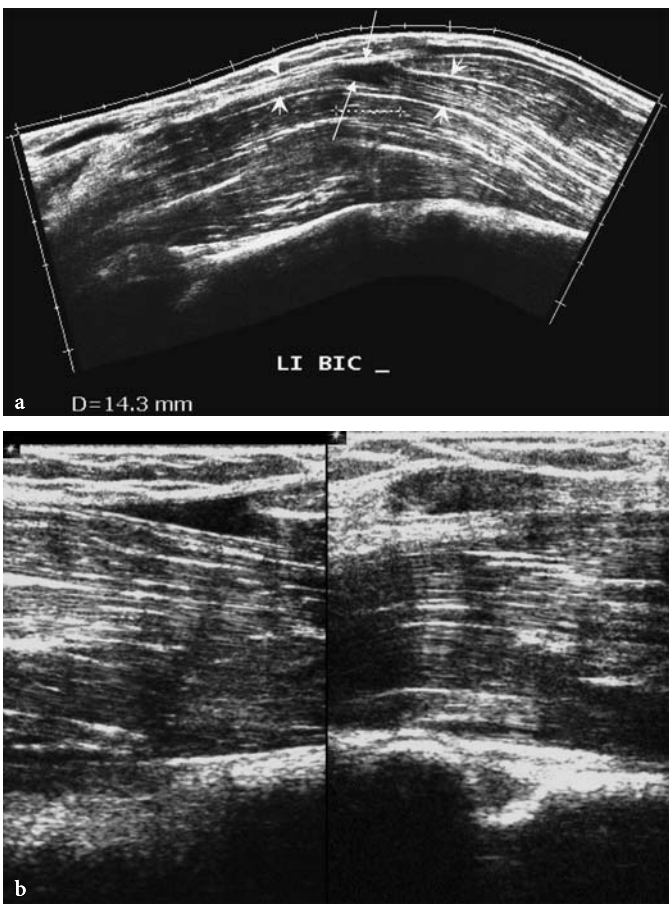

Fig. 3.10a,b. Early (age 24 h) biceps brachii strain grade 3 at the lacertus fibrosus myotendinous junction (*short arrows*). Parallel muscle fibre type. **a** Longitudinal panoramic US image illustrating an ill defined and hypo-reflective haematoma (*arrows*). **b** Haematoma at the myotendinous junction of the muscle is seen as hypo-reflective area on respectively longitudinal (*left*) and axial (*right*) US planes

myotendinous junction, giving a feathery appearance. Blood and edema may also insinuate between the fascial planes (Fleckenstein et al. 1989). Perifascial fluid accumulations are commonly seen as high signal intensity rimming the muscle on T2-weighted images (Figs. 3.7a and 3.9b,c). Acutely, a mass may be detected at the site of the injury; the mass is usually associated with abnormal signals from bleeding and edema as well as muscle retraction (DeSmet 1993).

3.3.1.2 Crush Trauma

Muscle trauma resulting from direct trauma represents a crush injury of the muscle fibres. It causes predominant muscular haemorrhage and haematoma and less muscle fibre disruption. This usually results from muscle being compressed against bone but can also occur when superficial muscle is compressed against a contracted underlying muscle (Jarvinen et al. 2005). Anatomical boundary may be absent and multiple muscles may be involved. Muscle crush trauma is commonly seen in contact sports. It is a clinical diagnosis obtained from patient history, muscle function is relatively normal given the degree of pain (Jackson and Feagin 1973; Zarins and Ciullo 1983; Armstrong 1984; Stauber 1988; Jarvinen et al. 2005).

In a similar manner to muscle strain, MR imaging or ultrasound can be used. The difficulty for either imaging modality is defining if there is muscle distraction especially if the clinical history is unclear.

Crush trauma may bring about Morel-Lavallée effusions. They are the result of the skin and subcutaneous fatty tissue abruptly separating from the underlying fascia, a traumatic lesion pattern that has been termed "closed degloving injury".

3.3.1.2.1 Muscle Contusion

Initially and in minor cases, interstitial bleeding or haemorrhage results in ill defined areas of increased ultrasound reflectivity within the muscle belly, which become better defined and poorly reflective over time (Fig. 3.11). Depending on the timing of the ultrasound these lesions may be difficult to detect, and an appreciation of the overall increase in muscle size compared with the normal side may be the only ultrasound finding. An acute contusion (0–48 h) appears ill defined with irregular margins and marked echogenic swelling of the fascicles and entire muscle (Fig. 3.12) (Aspelin et al. 1992). MR imaging also demonstrates edema and mixed intrinsic signal as the blood products develop. In snapping hip an intrinsic cause of muscle contusion edema at the psoas may be found (Fig. 3.12).

3.3.1.2.2 Muscle Haematoma

Intramuscular haematoma, is a frequent finding in patients with athletic crush muscle injures. Haematomas are usually identifiable on ultrasound within a few hours of injury, or sooner in some cases. The

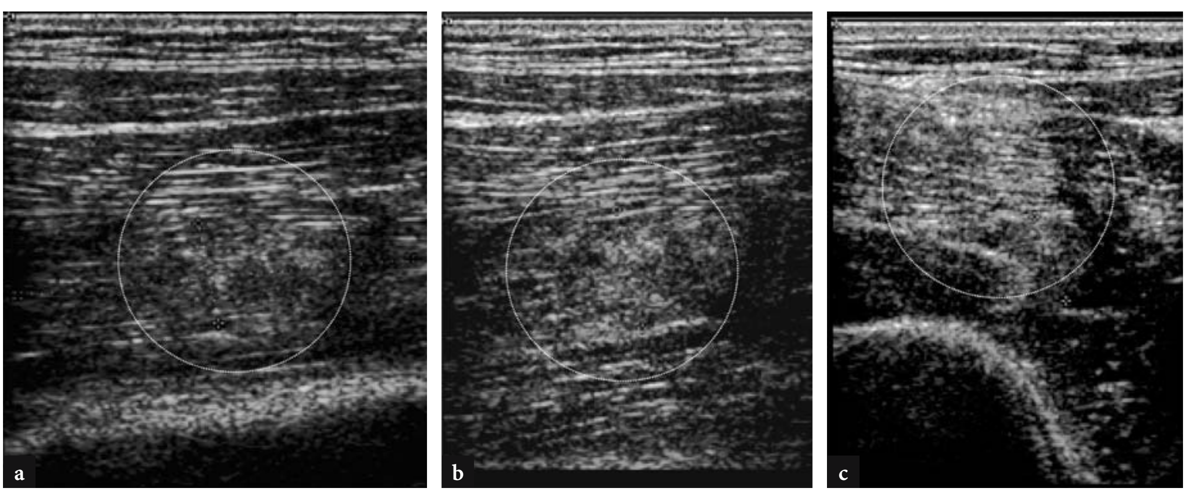

Fig. 3.11a–c. Crush trauma,. Hyperacute haemorrhage at the vastus medialis muscle. **a,b** Longitudinal ultrasound image, **c** Axial ultrasound image. Diffuse hyper-reflective area with unsharp margins and without shadowing (*dotted circle*)

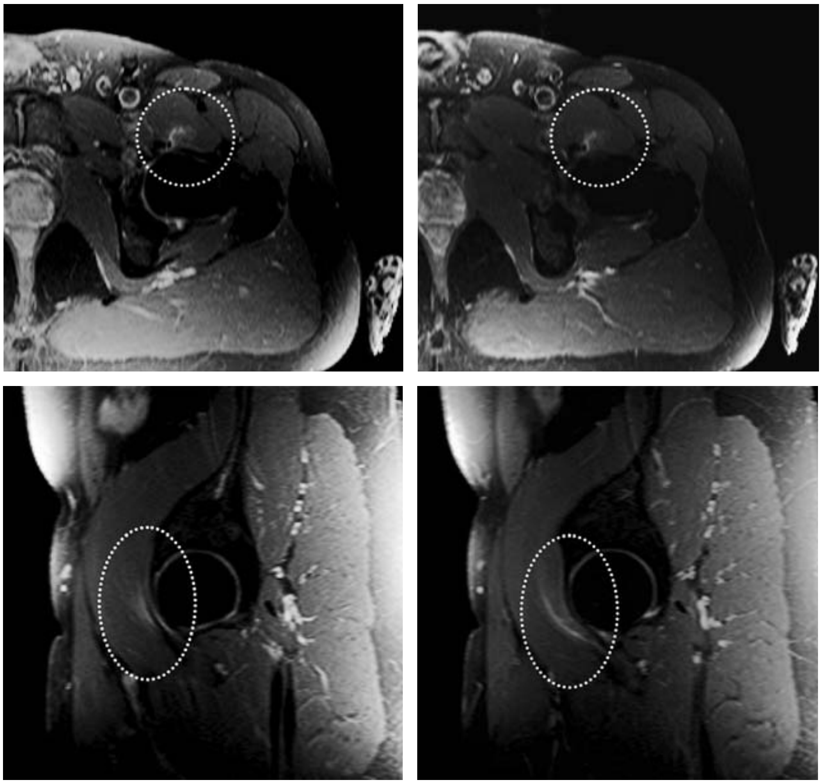

a b c d

Fig. 3.12a–d. Snapping hip. **a,b** Axial fat suppressed TSE T2-WI. **c,d** Sagittal fat suppressed TSE T2-WI. Prolonged T2-releaxation time due to edema at the musculotendinous junction of the psoas muscle (region of the lacuna musculorum (*dotted circles*))

timing of ultrasound examination of muscle injury is ideally between 2 and 48 h after trauma. More serious compressive injuries result in typical haematoma formation, a confined collection of blood; this wedges the muscle fibres away and gives the clinical impression of a mass; fibre rupture is not predominant in crush trauma (Figs. 3.13 and 3.14). It may cross aponeurotic boundaries representing the demarcation of the impact (Van Holsbeeck and Introcasco 2001; Robinson 2004). Dynamic ultrasound imaging confirms that a major tear is not present and documents the extent of muscle damage. At 48–72 h ultrasound appearances become better defined with the haematoma appearing hypoechoic and a clearer echogenic margin which expands centrally as the muscle repairs (Van Holsbeeck and Introcasco 2001; Robinson 2004). MR imaging also demonstrates these changes although the degree of adjacent muscle and soft tissue edema can persist for some time.

MRI criteria for diagnosing intramuscular blood, whether haematoma or infiltrating haemorrhage, have been confusing. Blood degrades with time, resulting in changed signal characteristics. Thus the age of a blood collection determines its signal characteristics on MRI. Signal characteristics also vary with field strength. All haemoglobin compounds occurring in a muscular haematoma are paramagnetic except oxyhaemoglobin. Methaemoglobin is the only haemoglobin breakdown product encountered in a haematoma which is capable of significant T1 shortening by this mechanism. Hemosiderin, intracellular deoxyhaemoglobin, and intracellular methaemoglobin all cause T2 shortening. In the case of intracellular deoxyhaemoglobin and intracellular methaemoglobin, this effect is of importance only at high field strengths. The simultaneous presence of many haemoglobin breakdown products in a haematoma can result in very complex-appearing masses on MRI, but the recognition of the T1 shortening of methaemoglobin and/or the T2 shortening of hemosiderin can often suggest the diagnosis (Bush 2000).

Typically an intramuscular haematoma resorbs spontaneously over a period of six to eight weeks, but on rare occasions it may persist for a long time as a seroma or cystic haematoma (Figs. 3.13 and 3.14).

3.3.1.2.3
Morel Lavallée Effusions

Morel Lavallée effusions are the result of the skin and subcutaneous fatty tissue abruptly separating from the underlying fascia. They are particularly

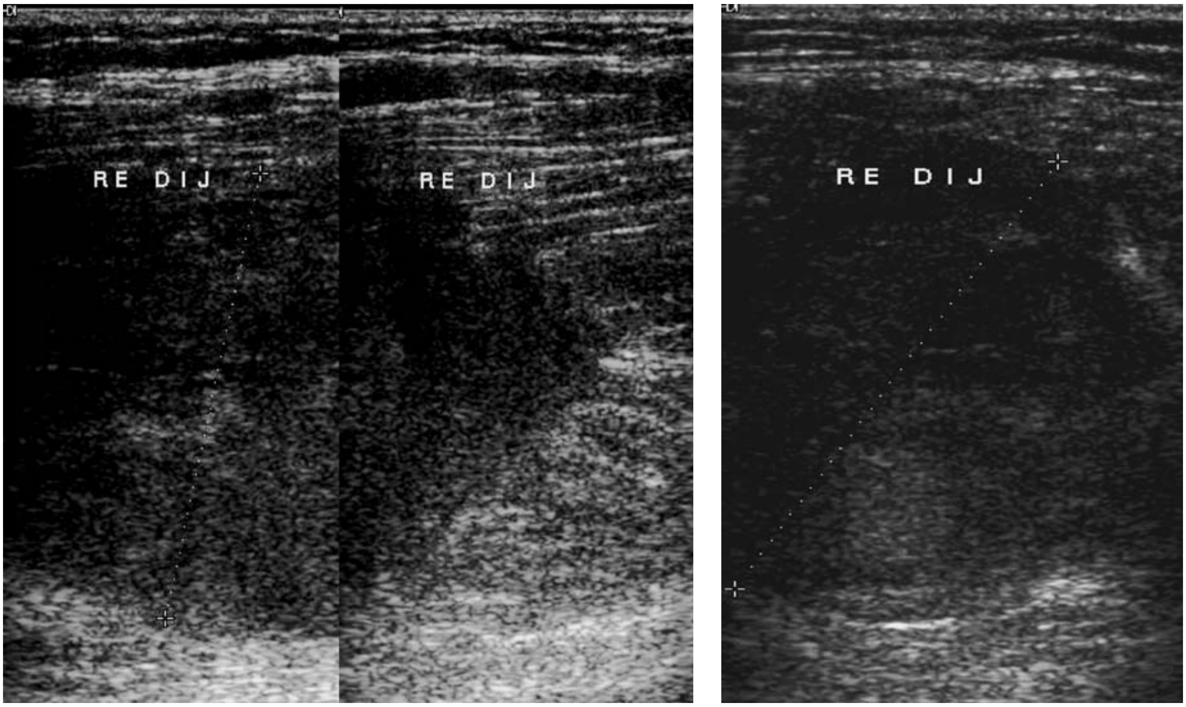

a b

Fig. 3.13a,b. Right gluteal hematoma, subacute phase. **a** Longitudinal ultrasound image of the buttock shows hypoechoic haematoma (*arrowheads*) predominantly involving the gluteus maximus with . **b** Axial imaging plane

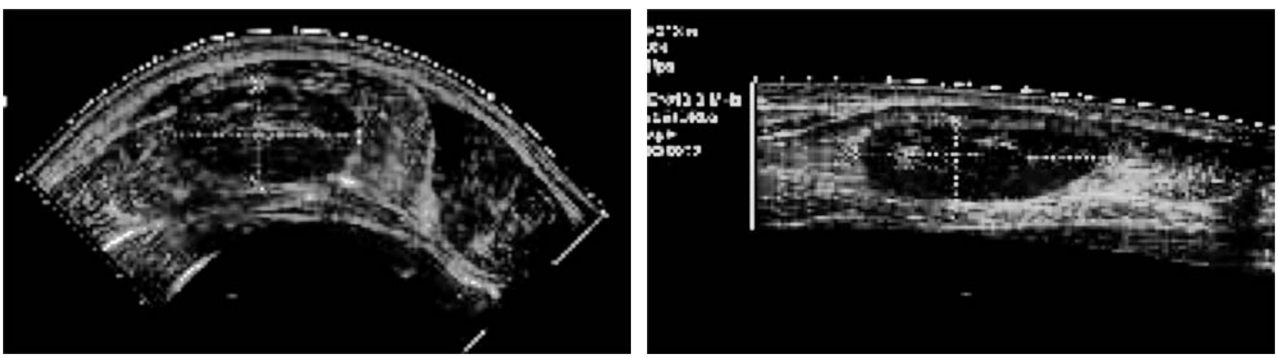

a b

Fig. 3.14a,b. Subacute hematoma at the vastus medialis of the quadriceps. Axial (**a**) and longitudinal (**b**) extended field of view US. Hypo-echoic sharply delineated area wedging away muscle fibres. No ruptured muscle fibres are visualised

common in the trochanteric region and proximal thigh, where they have been specifically referred to as Morel-Lavallée lesions. In this region, the dermis contains a rich vascular plexus that pierces the fascia lata. The disrupted capillaries and/or lymph vessels may continuously drain into the perifascial plane, filling up the virtual cavity with blood, lymph, and debris. An inflammatory reaction commonly creates a peripheral capsule, which may account for the self-perpetuation and occasional slow growth of the process (Mellado et al. 2004).

Three different MR presentations of Morel-Lavallée effusions are discriminated. They may present with cyst-like, hematoma-like at the methemoglobin degradation phase and hematoma-like with hemosiderotic wall and capillary ingrowth. Long-standing Morel-Lavallée lesions may present cyst-like MRI signal characteristics correlated with encapsulated serosanguinous fluid or seroma. The lesions appear homogeneously hypointense on T1-weighted MR sequences, hyperintense on T2-weighted MR sequences and are partially surrounded by a periph-

eral ring that appears hypointense on all pulse sequences.

Morel-Lavallée lesions may also show homogeneous hyperintensity on both T1- and T2-weighted MR sequences and appear surrounded by a hypointense peripheral ring (Fig. 3.15a,b). This T1 signal-intensity behaviour is probably related to the existence of methemoglobin, characteristic of subacute hematomas. Methemoglobin is first observed on the periphery of subacute hematomas and produces a "concentric ring" sign. As the hematoma evolves, it becomes progressively encapsulated and homogeneously hyperintense on T1-weighted MR sequences (Fig. 3.15a).

Long-standing Morel-Lavallée lesions may also show a third MRI pattern that includes variable signal intensity on T1-weighted MR images, heterogeneous hyperintensity on T2-weighted MR sequences, and a hypointense peripheral ring. Patchy internal enhancement and peripheral enhancement may also be present. The heterogeneous hyperintensity on T2-weighted MR sequences correlates with the existence of hemosiderin deposition, granulation tissue, necrotic debris, fibrin, and blood clots characteristic of chronic organizing hematoma. The hypointense peripheral ring has been found to represent a hemosiderin-laden fibrous capsule with mild inflammatory infiltrate. The internal enhancement after gadolinium administration on MRI and power Doppler signal is probably related to the capillary formation in the lesion. Differentiation of these lesions with soft tissue neoplasm with bleeding is difficult on MRI and US. In cases without a history of trauma specific attention is needed to avoid misdiagnosis of neoplasm with bleeding, i.e. synovial sarcoma, leiomyosarcoma and malignant peripheral nerve sheath tumour. Also clear cell sarcoma may present with high SI on T1-weighted MR due to the presence of melanin. Every "haematoma" that grows with time or that does not diminishes over a few weeks is suspect; it is examined by MRI and eventually biopsied prior to resection (Mellado et al. 2004).

3.3.2 Complications of Muscle Injury

Occasionally intramuscular haematomas fail to resolve, and form chronic cysts. These are manifest as discrete areas of absent reflectivity with posterior acoustic enhancement. They can persist for several years and may be responsible for continued muscle pain (Fig. 3.13, Fig. 3.14 and Fig 3.16.a).

Acute compartment syndrome may result from a single traumatic event, due to the presence of a large haematoma with mass effect. This can compromise vessels and nerves and lead to ischaemic necrosis. In particular the anterior and deep posterior compartment of the lower leg are at risk. Diffuse increased reflectivity of the muscles in the involved compartment may be seen in conjunction with an overall increase in muscle dimension. In later stages, areas of necrosis will develop that appear identical to rhabdomyolysis. Therefore prompt evacuation of haematoma is indicated in patients with increased compartment pressure.

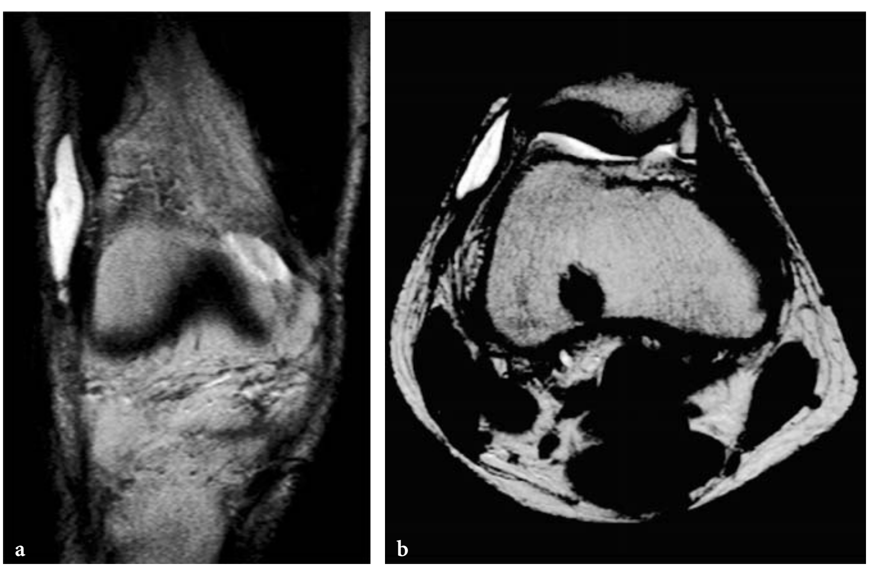

Fig. 3.15 Morel-Lavallée perifascial fluid located at the right vastus lateralis near its myotendinous junction. Coronal (*top*) and axial (*bottom*) SE T1-WI and TSE T2-WI MR sequence respectively. Fusiform mass with high signal intensity externally adjacent to muscle fascia

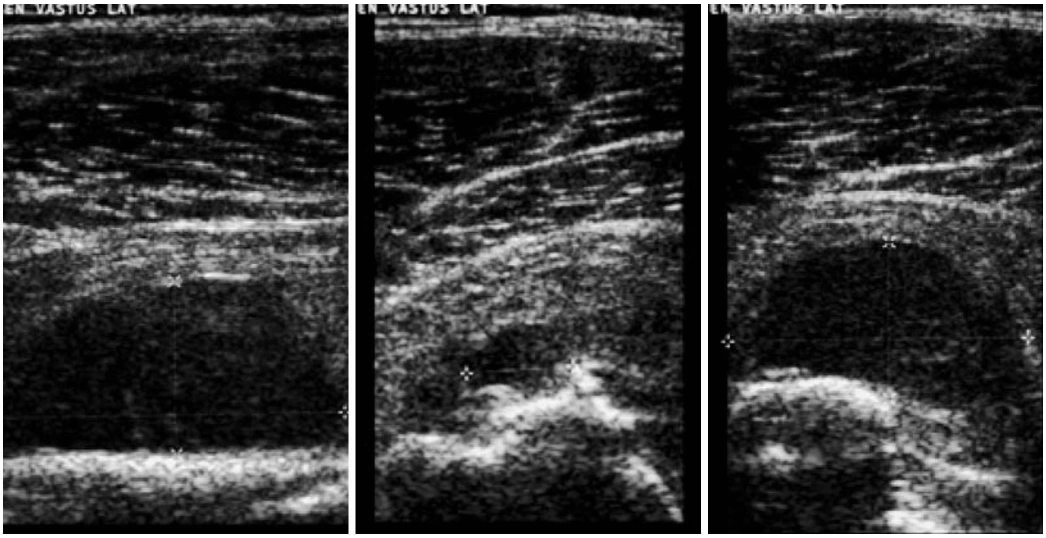

a

b

Fig. 3.16.a Late crush trauma with myositis ossificans and cyst. Four months after crush trauma at the left upper leg. Longitudinal (*left*) and axial (*middle and right*) US images of the thigh. Focus of calcification and posterior acoustic shadowing, which corresponded to a palpable soft tissue mass at the vastus intermedius muscle adjacent to the femur diaphysis. Seroma or cyst formation adjacent to the ossifying nidus is represented by the hyporeflective well demarcated area (between *crosses*) that wedges away muscle fibres. **b**. Radiograph obtained on the same day demonstrates a massive focus of mature ossification. These appearances are compatible with late myositis ossificans

Percutaneous needle aspiration of haematomas is possible. However, there is risk of infection in incompletely aspirated collections of blood, which provide a good medium for bacteria. Aspiration may be used if there is severe pain, or in an attempt to promote early healing. Ultrasound provides a useful means of evaluating haematoma to identify features that might result in failed or incomplete aspiration, such as extensive loculation of the haematoma during organization.

An other major complication of muscle injury is the development of myositis ossificans. A tumour-like mass develops within muscle, which undergoes calcification followed by ossification. The relationship to an actual traumatic event is often not recalled by the patient. It is more frequent in crush trauma than muscle strain. In our own experience the proximal musculotendinous junction of the rectus femoris is the most frequent site of myositis ossificans in muscle strain. The calcification becomes apparent sooner on ultrasound than on radiographs and quickly develops typical acoustic shadowing (Fig. 3.16a,b) (Fornage and Eftekhari 1989). The calcification may develop along the plane of

the muscle bundles (Peck and Metreweli 1988), or may be more irregular (Kramer et al. 1979). At early stages of development the appearances may mimic a soft tissue sarcoma, and although the typical distribution of calcification at the periphery of myositis is different to the central calcification noted in tumours, it may be extremely difficult to make this distinction. Histological diagnosis is also fraught with difficulty and an erroneous diagnosis of sarcoma is possible. If the diagnosis is unclear, the most appropriate course of action is to repeat radiographs after an interval of a few weeks when myositis will demonstrate maturation of the calcifying/ossifying process. In some instances large symptomatic lesions may be removed surgically; this is only done in cases that show mature bone.

Muscle hernias are the result of tears of the epimysium and result in masses, which appear on active contraction of the muscle. Although usually clinically apparent, ultrasound can demonstrate the muscle bulge and defect in the fascia. The hernia may sometimes be reduced by pressure with the ultrasound probe (Fig. 3.17a,b) (See also section 3.9).

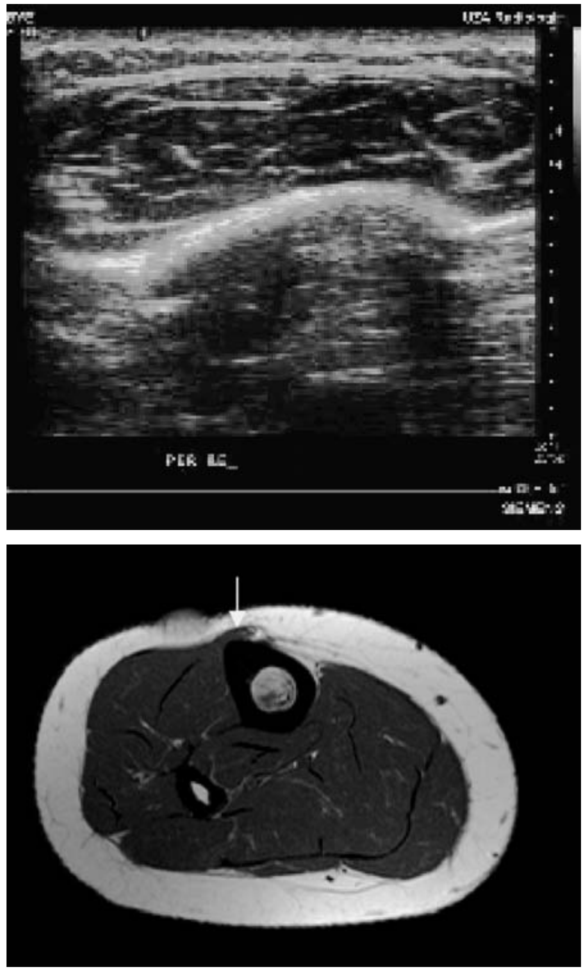

a

b

Fig. 3.17a,b. Muscle hernia. **a** Longitudinal dynamic US of muscle herniation at the anterior tibial muscle. Bulging of muscular tissue toward the subcutaneous tissue is obvious during muscular contraction. **b** Axial SE T1-weighted imaging. Bulging of anterior tibial muscle in front of tibial diaphysis representing muscle hernia (*arrow*)

3.4 Delayed Onset Muscular Soreness (DOMS)

Delayed Onset Muscular Soreness (DOMS), a common ailment, is another form of muscle injury. At the turn of the last century, Hough described the phenomenon of DOMS and his ideas are still valid today (Armstrong 1984). Regardless of a person's general level of fitness, nearly every healthy adult has experienced DOMS. Following unaccustomed muscular exertion, patients develop DOMS and experience a sensation of discomfort and pain in their skeletal muscles. For example, after prolonged downhill running (eccentric muscle activity) in an experimental setting, athletes experienced pain in all the extensor and flexor muscles groups around the hip, thigh and leg. Structural abnormalities in the Z band and a rise in the serum creatine kinase have been described by Nurenberg et al. (1992). Pain increases in intensity for the first 24 h after exercise, peaks between 24 and 72 h, and then subsides in 5 to 7 days. Temporary loss of strength, up to 50%, can be present. The diminished performance results from reduced voluntary effort due to pain as well as reduced capacity of the muscle to produce force. The soreness is believed to be due to reversible structural damage at the cellular level. There is no associated long-term damage or reduced function in the muscles. Some authorities believe that the clinical syndrome of exertional rhabdomyolysis may represent a severe form of DOMS. US demonstrates no obvious abnormalities in either stage of DOMS.

MR imaging of DOMS is very rarely required. Experimental studies by Shellock et al. (1991) showed that DOMS follows a consistent pattern where signal intensity on T2-weighted images increases gradually over few days after initial eccentric exercises, peaks after several days, and gradually returns to normal over as long as 80 days. There is a high correlation between the increase in signal intensity on

MR and the ultrastructural injury demonstrated in the Z bands. Because DOMS is not associated with bleeding, it is assumed that the MRI changes are primarily due to edema. Muscle strain and DOMS frequently have similar appearance, and the two clinical conditions are difficult to differentiate on the basis on the imaging findings alone (Fleckenstein and Shellock 1991). Muscle strain often appears on MRI less extensive or uniform in its distribution within a muscle than DOMS.

3.5 Chronic Exertional Compartment Syndrome

3.5.1 Definition, Clinical Presentation and Diagnosis

Compartment syndrome is defined as increased interstitial pressure within an anatomically confined compartment that interferes with neurovascular function. Normal pressures within a muscle compartment are 0–4 mmHg and can peak above 60 mmHg on exercise but quickly dissipate on cessation. However if this pressure is sustained above 15 mmHg blood flow is compromised and muscle ischaemia can occur (Zabetakis 1986).

Chronic exertional compartment syndrome commonly affects the anterior and deep posterior calf lower leg musculature (Martens et al. 1984; Peterson and Renstrom 1986; Zabetakis 1986). It is thought that chronic traction on the muscle fascia alters its compliance and subsequent ability to accommodate volume change on exercise (Nicholas and Hershman 1986; Peterson and Renstrom 1986). The athlete usually presents with crescendo pain and paraesthesia after exercise which eases on ceasing activity and unlike popliteal artery syndrome is not posture dependant (Martens et al. 1984; Nicholas and Hershman 1986). There may also be muscle swelling and it is important to rule out an underlying muscle hernia. The diagnosis can sometimes be made with history alone but compartmental pressure measurements may be necessary. Pressure pre exercise of greater than 15 mmHg, or post exercise pressure greater than 30 mmHg at 1 min, or greater than 20 mmHg at 5 min confirm the diagnosis (Pedowitz et al. 1990).

3.5.2 Imaging

Appearances on imaging can be non-specific and are not always reliable in confirming the diagnosis (Edwards et al. 2005).

On ultrasound the muscle can appear echogenic with relative sparing of periseptal areas which are still receiving sufficient blood flow from the adjacent fascia (Van Holsbeeck and Introcasco 2001). Studies evaluating muscle cross sectional area on ultrasound both before and after exercise describe two different patterns in symptomatic patients. In one group the muscle compartment cannot expand with a relatively rigid fascia compared to normal subjects (where muscle volume can increase by 10–15%). In the other symptomatic group, although the muscle compartment does expand during exercise, there is a slow reduction in volume post exercise compared to normal subjects (Van Holsbeeck and Introcasco 2001).

Post exercise MR imaging can show edema in the clinically affected muscles confirming the diagnosis (Fig. 3.18). However, like ultrasound, this technique is not completely sensitive or specific with edema being

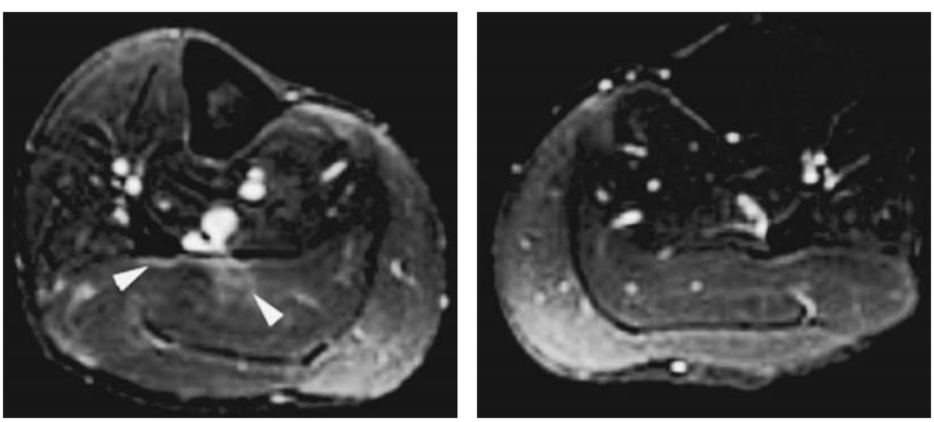

Fig. 3.18. Compartment syndrome. Running athlete with chronic exertional right leg pain. Axial T2 weighted fat suppressed MR image post exercise shows persisting soleus edema (*arrowheads*). The athlete underwent fasciotomy

found in asymptomatic athletes and normal muscle appearances occurring in athletes with objective clinical features (Fleckenstein and Shellock 1991).

The initial treatment of chronic exertional compartment syndrome includes training modifications and assessment for orthotics; however if symptoms persist fasciotomy of the muscle compartment is performed. Morbidity can potentially result if there is subsequent muscle herniation or scarring (Van Holsbeeck and Introcasco 2001).

3.6 Muscle Atrophy

Muscle atrophy may be secondary to disuse, muscle denervation, e.g. compressive neuropathy, muscle rupture or a consequence of a primary muscle disorder, e.g. muscular dystrophy. Varying degrees of atrophy exist and, where possible, comparison with normal muscle aids diagnosis as differences may be subtle. Discrepancies in muscle bulk may be easier to detect near the myotendinous junction. Atrophic muscle appears characteristically hyper-reflective owing to the replacement of muscle fibres by fat (Hide et al. 1999). It may also be possible to detect a relative decrease in vascularity on Doppler ultrasound, especially after exercise. In cases of compressive neuropathy, ultrasound can be a useful means of identifying compressive lesions and may help in demonstrating the pattern of involved muscle groups. Function loss of the motor nerve leads to muscle paralysis that is easily demonstrated on dynamic US investigation by the absence of motion at the muscle fibres during voluntary activation.

A specific cause of muscle atrophy is suprascapular nerve lesion resulting in weakness of the supraspinatus or infraspinatus muscle. It is found idiopathically in athletes and in relation to paralabral cyst with compression of the nerve at the level of the suprascapular notch.

Early phases of denervation present as diffuse muscle edema, in chronic phases atrophy with lipomatous infiltration is found; these are demonstrated as high SI on T2-weighted MR imaging and T1-weighted MR imaging respectively (Fig. 3.19).

For further discussion of muscle atrophy, see also Chaps. 17 and 29.

a

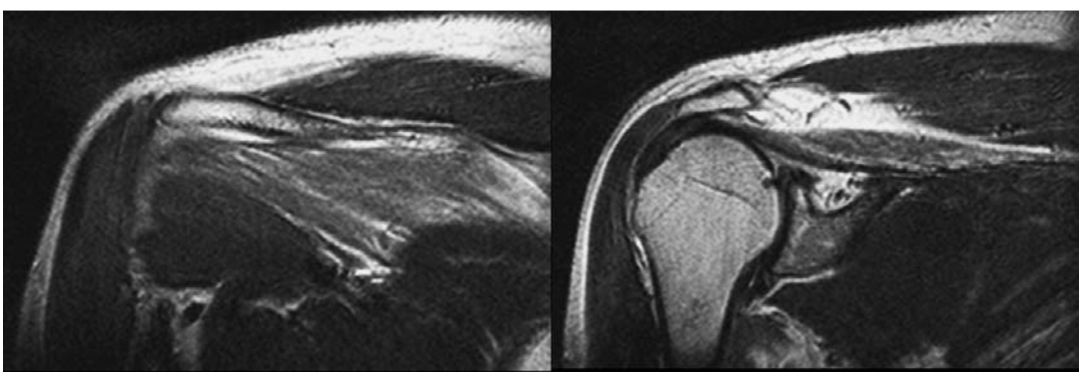

b

Fig. 3.19a,b. Eighteen-year-old track and field athlete with infraspinate muscle weakness due to idiopathic infraspinate denervation. Subacute stage. Ultrasound and MRI examination after one month of symptoms. Hyperreflective aspect of the infraspinate muscle on US (**a**). Diffuse high SI on T2 WI due to edema on MRI (**b**, *left*). No tendon lesion is present. No paralabral cyst is detected (**b**, *right*)

3.7 Rhabdomyolysis

Rhabdomyolysis is a condition that results in necrosis of skeletal muscle. The causes include primary muscle injury, diabetes, burns, hypoxia secondary to peripheral vascular disease, infection, inflammation and drugs and toxins. Early diagnosis is important as complications include acute renal failure, hyperkalaemia and disseminated intravascular coagulation.

Ultrasound usually demonstrates a heterogeneous echo pattern within affected muscles (Lamminen et al. 1989; Fornage and Nerot 1986). The muscle often appears diffusely enlarged with loss of normal fibrillar architecture and thickening of the layers of perimysium. A hypo-reflective inflammatory exudate engulfs necrotic muscle cells. Hyper-reflective areas are due to gas within necrotic tissue. The aspiration of clear serous fluid under ultrasound guidance supports the diagnosis of uncomplicated rhabdomyolysis.

Ultrasound appearances must be interpreted in conjunction with clinical and haematological findings as similar features may be seen at ultrasound in cases of acute haematoma and pyomyositis.

3.8 Calcific Myonecrosis

Calcific myonecrosis is a rare, (very) late sequel of trauma with myonecrosis occurring almost exclusively in the lower extremity (anterior and posterior tibial compartment) which may be confused with an aggressive primary neoplasm. The platelike mineralization pattern seen on radiographs is characteristic but not widely recognized by clinicians (Fig. 3.20c,d) (Holobinko et al. 2003). US shows diffuse calcifications encompassing a complete muscle or muscle compartment that is avascular on power Doppler color duplex US (Fig. 3.20a,b). On MRI a tumorlike

Fig. 3.20a–d. Calcific myonecrosis of the right anterior tibial compartment detected 15 years after blunt trauma with the development of drop foot. Painless, soft swelling at the anterior tibial compartment for two months. Axial (**a**) and longitudinal (**b**) extended field of view US images and radiographs (**c**,**d**, anteroposterior and lateral view respectively). Mass lesion with amorphous calcifications with characteristic platelike aspect on radiographs. No ossified parts are seen

avascular mass with bleeding components and fibrosis is found (Fig. 3.21).

3.9 Muscle Herniation

Muscle herniation is a relative rare condition which is often diagnosed clinically, although occasionally the symptomatology is confusing and MRI or ultrasound may offer an unequivocal diagnosis by demonstration of the fascial rent and characterization of the protruding mass as being muscle tissue (Zeiss et al. 1989). Blunt trauma can produce a rent in the fascia, allowing the underlying muscle to protrude, it is usually seen in the leg, particularly over the anterior tibial compartment. It may be helpful to perform the ultrasound and MR scanning with the herniated muscle both relaxed and contracted in order to demonstrate a change in size of the herniated portion (Fig. 3.17a,b) (Bianchi et al. 1995). Muscle herniation will be discussed more in detail in Chaps. 21 and 29.

3.10 Conclusion

The ability of ultrasound, to study muscle tissue through a dynamic range of movements, to compare with normal structures in the contralateral limb, and

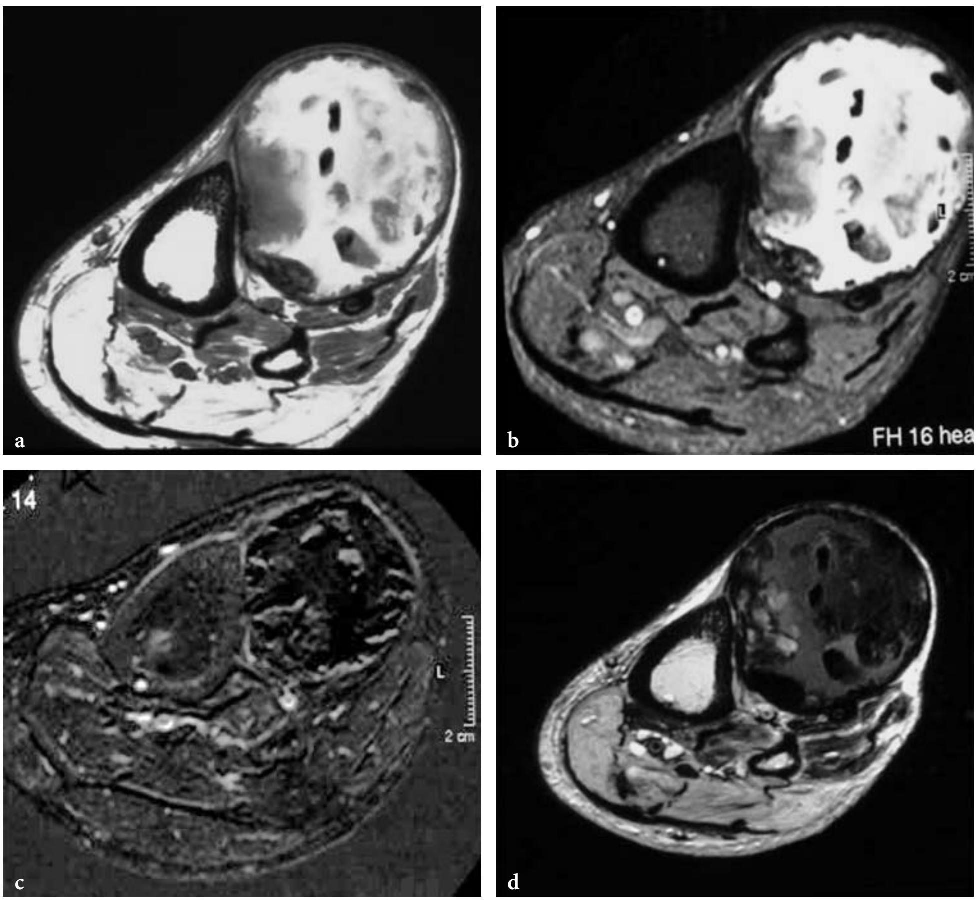

Fig. 3.21.a Calcific myonecrosis of the left anterior tibial compartment. Axial SE T1-weighted MR image. **b** Axial fat suppressed SE T1-weighted image. **c** Axial subtraction of T1 weighted image after and before gadolinium administration. **d** Axial TSE T2 weighted image. Calcifications and fibrosis of low SI on all sequences. Methemoglobin degradation product are of high SI on T1-weighted images with and without fat suppression. No enhancement at the mass lesion. Necrosis of all the muscles at the anterior tibial compartment. (Courtesy of Dr. Mattelaer AZ. St.-Lucas Brugge, Belgium)

follow lesions through time, make it a very versatile tool in clinical practice. MRI represents the main alternative radiological modality for the study of muscle trauma; however, despite the better soft tissue contrast of MRI, US is the first choice because of better spatial resolution with evaluation of muscular ultrastructure and the still poor availability of MRI.

Although many muscle abnormalities share similar ultrasound and MRI features, imaging can provide an accurate diagnosis in many instances, when clinical findings are taken into account. Ultrasound can help confirm or exclude abnormality. A "dynamic" evaluation of muscle can be performed with ultrasound, which may detect abnormalities not appreciated on MRI.

Because the majority of muscle injuries are self limiting US investigation is limited to delineate the extent of the muscle injury in high performance athletes and to evaluate lesions prone to complications in elongation trauma. This is the case in "tennis leg" and in crush trauma. It can be valuable for determining which patients will benefit from aspiration or surgery and which can be treated conservatively. It is used to provide a prompt diagnosis when rapid initiation of proper therapy is crucial and to evaluate obscure muscle pain, such as intermittent muscle herniation through a fascial rent. The use of MRI is limited to the evaluation of deeply located muscles and to assess the severity of DOMS or rhabdomyolysis.

Plain radiographs are only indicated for assessment of bony avulsions and to depict myositis ossificans and gas bubbles in myositis.

Things to Remember

1. Many muscle abnormalities share similar ultrasound and MRI features, and therefore clinical findings have to be taken into account to obtain an accurate diagnosis.

2. US and MRI are excellent tools to evaluate muscle strain in high performance athletes. US is preferred because of its dynamic characteristics. A negative US examination with typical clinical presentation of strain injury is diagnostic for grade 1 strain or claquage.

3. US is the imaging modality of choice to evaluate specific locations of muscle strain prone to complications, i.e. tennis leg and rectus femoris strain.

4. Muscle contusion is studied by a combination of US and radiographs to exclude complications, i.e. myositis ossificans and cyst formation.

5. In suspect cases hydrostatic pressure measurement is the only way to exclude early acute compartment syndrome.

References

Armstrong RB (1984) Mechanisms of exercise-induced delayed onset muscular soreness: a brief review. Med Sci Sports Exerc 16:529–538

Aspelin P, Ekberg O, Thorsson O et al (1992) Ultrasound examination of soft tissue injury of the lower limb in athletes. Am J Sports Med 20:601–603

Best TM, Garrett WE (1994) Muscle and tendon. In: DeLee JC, Drez D (eds) Orthopaedic sports medicine. W B Saunders, Philadelphia PA, pp 1–45

Bianchi S, Abdelwahab IF, Mazzola CG et al. (1995) Sonographic examination of muscle herniation. J Ultrasound Med 14:357–360

Brinckmann P, Frobin F, Leivseth et al. (2002) Musculoskeletal biomechanics. Thieme, New York

Bush C (2000) The magnetic resonance imaging of musculoskeletal hemorrhage. Skeletal Radiol 29:1–9

Campbell RS, Wood J (2002) Ultrasound of muscle. Imaging 14:229–240

Connell DA, Schneider-Kolsky ME, Hoving JL et al. (2004) Longitudinal study comparing sonographic and MRI assessments of acute and healing hamstring injuries. Am J Roentgenol 183:975–984

Cross TM, Gibbs N, Houang MT et al. (2004) Acute quadriceps muscle strains: magnetic resonance imaging features and prognosis. Am J Sports Med 32:710–719

DeSmet AA (1993) Magnetic resonance findings in skeletal muscle tears. Skeletal Radiol 22:479–484

Deutsch AL, Mink JH (1989) Magnetic resonance imaging of musculoskeletal injuries. Radiol Clin North Am 27:983–1002

Edwards PH Jr, Wright ML, Hartman JF (2005) A practical approach for the differential diagnosis of chronic leg pain in the athlete. Am J Sports Med 33:1241–1249

El-Khoury G, Brandser EA, Kathol MH et al. (2004) Imaging of muscle injuries. Springer, Berlin Heidelberg New York

Fleckenstein JL, Shellock FG (1991) Exertional muscle injuries: magnetic resonance imaging evaluation. Top Magn Reson Imaging 3:50–70

Fleckenstein JL, Weatherall PT, Parkey PW et al. (1989) Sports-related muscle injuries: evaluation with MR imaging. Radiology 172:793–798

Fornage B (1995) Muscular trauma. In: Fornage B (ed) Mus-

culoskeletal ultrasound. Churchill Livingstone, New York NY, pp 1–19
Fornage BD, Eftekhari F (1989) Sonographic diagnosis of myositis ossificans. J Ultrasound Med 8:463–466
Fornage BD, Nerot C (1986) Sonographic diagnosis of rhabdomyolysis. J Clin Ultrasound 14:389–392
Garrett WE Jr (1990) Muscle strain injuries: clinical and basic aspects. Med Sci Sports Exerc 22:436–443
Garrett WE Jr, Best TM (1994) Anatomy, physiology, and mechanics of skeletal muscle. In: Simon SR (ed) Orthopaedic basic science. American Academy of Orthopaedic Surgeons, Rosemont IL, pp 89–126
Garrett WE Jr, Califf JC, Bassett FH III (1984) Histochemical correlates of hamstring injuries. Am J Sports Med 12:98–103
Garrett WE Jr, Safran MR, Seaber AV et al. (1987) Biomechanical comparison of stimulated and nonstimulated skeletal muscle pulled to failure. Am J Sports Med 15:448–454
Gibbs NJ, Cross TM, Cameron M et al. (2004) The accuracy of MRI in predicting recovery and recurrence of acute grade one hamstring muscle strains within the same season in Australian Rules football players. J Sci Med Sport 7:248–258
Greco A, McNamara MT, Escher RMB et al. (1991) Spin-echo and STIR MR imaging of sports-related muscle injuries at 1.5T. J Comput Assist Tomogr 15:994–999
Herzog W (1996) Muscle function in movement and sports. Am J Sports Med 24:S14–19
Hide IG, Grainger AJ, Naisby GP et al. (1999) Sonographic findings in the anterior interosseous nerve syndrome. J Clin Ultrasound 27:459–464
Holobinko JN, Damron TA, Scerpella PR et al. (2003) Calcific myonecrosis: keys to early recognition. Skeletal Radiol. 32:35–40
Jackson DW, Feagin JA (1973) Quadriceps contusions in young athletes. Relation of severity of injury to treatment and prognosis. J Bone Joint Surg Am 55:95–105
Jarvinen TA, Jarvinen TL, Kaariainen M et al. (2005) Muscle injuries: biology and treatment. Am J Sports Med 33:745–764
Kathol MH, Moore TE, El-Khoury GY et al. (1990) Magnetic resonance imaging of athletic soft tissue injuries. Iowa Orthopaed J 9:44–50
Kramer FL, Kurtz AB, Rubin C et al. (1979) Ultrasound appearance of myositis ossificans. Skeletal Radiol 4:19–20
Lamminen AE, Hekali PE, Tiula E et al. (1989) Acute rhabdomyolysis: evaluation with magnetic resonance imaging compared with computed tomography and ultrasonography. Br J Radiol 62:326–330
Mair SD, Seaber AV et al. (1996) The role of fatigue in susceptibility to acute muscle strain injury. Am J Sports Med 24:137–43
Martens MA, Backaert M, Vermaut G et al. (1984) Chronic leg pain in athletes due to a recurrent compartment syndrome. Am J Sports Med 12:148-151
McMaster PE (1933) Tendon and muscle ruptures. J Bone J Surg 15:705–722
Mellado JM, Perez del Palomar L, Diaz L et al. (2004) Long-standing Morel-Lavallee lesions of the trochanteric region and proximal thigh: MRI features in five patients. AJR Am J Roentgenol 182:1289–1294
Mink JH (1992) Muscle injuries. In: Deutsch A, Mink JH, Kerr R (eds) MRI of the foot and ankle. Raven Press, New York, pp 281–312
Nicholas J, Hershman E (1986) The lower extremity and spine in sports medicine. Mosby, St Louis
Nikolaou PK, Macdonald BL, Glisson RR et al. (1987) Biomechanical and histological evaluation of muscle after controlled strain injury. Am J Sports Med 15:9–14
Noonan TJ, Garrett WE Jr (1992) Injuries at the myotendinous junction. Clin Sports Med 11:783–806
Noonan TJ, Garrett WE Jr (1999) Muscle strain injury: diagnosis and treatment. J Am Acad Orthop Surg. 7:262–269
Nordin M, Frankel VH (2001) Biomechanics of skeletal muscle. In: Nordin M, Frankel VH (eds) Basic biomechanics of the musculoskeletal system. Lippincott Williams and Wilkins, Philadelphia, pp 149–174
Nurenberg P, Giddings CJ, Stray-Gundersen J et al. (1992) MR imaging-guided muscle biopsy for correlation of increased signal intensity with ultrastructural change and delayed-onset muscle soreness after exercise. Radiology 184:865–869
O’Donoghue D (1984) Principles in the management of specific injuries. In: O’Donoghue D (ed) Treatment of injuries to athletes. WB Saunders, Philadelphia, pp 39–91
Peck RJ, Metreweli C (1988) Early myositis ossificans: a new echographic sign. Clin Radiol 39:586–588
Pedowitz RA, Hargens AR, Mubarak SJ et al. (1990) Modified criteria for the objective diagnosis of chronic compartment syndrome of the leg. Am J Sports Med 18:35–40
Peetrons P (2002) Ultrasound of muscles. Eur Radiol 12:35–43
Peterson L, Renstrom P (1986) Sports injuries. Year Book Medical, Chicago
Robinson P (2004) Ultrasound of muscle injury. In: McNally E (ed) Practical musculoskeletal ultrasound. Churchill Livingston, London
Shellock FG, Fukunaga T, Mink JH et al. (1991) Exertional muscle injury: evaluation of concentric versus eccentric actions with serial MR imaging. Radiology 179:659–664
Shellock FG, Mink J, Deutsch AL (1994) MR imaging of muscle injuries. Appl Radiol Feb:11–16
Slavotinek JP, Verrall GM, Fon GT (2002) Hamstring injury in athletes: using MR imaging measurements to compare extent of muscle injury with amount of time lost from competition. AJR Am J Roentgenol 179:1621–1628
Speer KP, Lohnes J, Garrett WE Jr (1993) Radiographic imaging of muscle strain injury. Am J Sports Med 21:89–95;discussion 96
Stauber W (1988) Eccentric action of muscles: physiology, injury, and adaption. In: Stauber W (ed) Exercise and sports sciences reviews. Franklin Institute, Philadelphia, pp 158–185
Steinbach L, Fleckenstein J, Mink J (1998) MR imaging of muscle injuries. Semin Musculoskeletal Radiol 1:128–141
Takebayashi S, Takasawa H, Banzai Y et al. (1995) Sonographic findings in muscle strain injury: clinical and MR imaging correlation. J Ultrasound Med 14:899–905
Taylor DC, Dalton JD Jr, Seaber AV et al. (1993) Experimental muscle strain injury. Early functional and structural deficits and the increased risk for reinjury. Am J Sports Med 21:190–194
Van Holsbeeck MT, Introcaso JH (2001) Sonography of muscle. In: Van Holsbeeck MT, Introcaso JH (eds) Musculoskeletal ultrasound, 2nd edn. Mosby, St Louis MI, pp 23–75
Verrall GM, Slavotinek JP, Barnes PG et al. (2001) Clinical risk factors for hamstring muscle strain injury: a prospective

study with correlation of injury by magnetic resonance imaging. Br J Sports Med 35:435–439; discussion 440

Verrall GM, Slavotinek JP, Barnes PG et al. (2003) Diagnostic and prognostic value of clinical findings in 83 athletes with posterior thigh injury: comparison of clinical findings with magnetic resonance imaging documentation of hamstring muscle strain. Am J Sports Med 31:969–973

Weng L, Tirumalai AP, Lowery CM et al. (1997) US extended-field-of-view imaging technology. Radiology 203:877–880

Wootton JR, Cross MJ, Holt KWG (1990) Avulsion of the ischial apophysis. J Bone Joint Surg [Br] 72-B:625–627

Zabetakis P (1986) Muscle soreness and rhabdomyolysis. In: Nicholas J, Hershman E (eds) The lower extremity and spine in sports medicine. Mosby, St Louis, pp 59–81

Zarins B, Ciullo JV (1983) Acute muscle and tendon injuries in athletes. Clin Sports Med 2:167–182

Zeiss J, Ebraheim NA, Woldenberg LS (1989) Magnetic resonance imaging in the diagnosis of anterior tibialis muscle herniation. Clin Orthop 244:249–253

Cartilage Trauma

4

Wouter C. J. Huysse and Koenraad L. Verstraete

CONTENTS

Box 4.1. Plain radiography

- Adequately displays advanced cartilage loss
- Evaluation of joint space width
- Special views may be needed
- Arthrography without subsequent CT or MR imaging is obsolete to evaluate cartilage

Box 4.2. CT arthrography

- Equals MR imaging for cartilage
- Bone marrow edema invisible
- Invasive (radiation and contrast medium injection)

Box 4.3. MR imaging

- Best method for cartilage imaging
- Three imaging sequences allow good morphologic evaluation of cartilage
- Bone marrow edema well displayed

Box 4.4. MR arthrography

- Improved visualisation in smaller joints
- Stable vs unstable osteochondral lesions
- Direct vs indirect technique

W. C. J. Huysse, MD
K. L. Verstraete, MD, PhD
Ghent University, De Pintelaan 185, 9000 Gent, Belgium

4.1 Basic Science

4.1.1 Composition, Organisation and Function of Normal Articular Cartilage

4.1.1.1 Introduction

The articular surface of diarthrodal joints is covered by hyaline cartilage, a fibrous tissue made up of chondrocytes lying within an extracellular matrix. This matrix is composed of tissue fluid containing dissolved electrolytes, gases, small proteins and metabolites on the one hand and macromolecules such as collagens, proteoglycans and noncollagenous proteins on the other. The type of molecules and their distribution differ depending on the joint and the location within the joint (Gurr et al. 1985; Huber et al. 2000). They also change with age (Bayliss and Ali 1981; Meachim 1969; Huber et al. 2000; Eyre et al. 1991).

4.1.1.2 The Structure of Articular Cartilage

Articular cartilage can be divided into four or five layers (Fig. 4.1) depending on the differentiation of the superficial layer in one or two compartments (Imhof et al. 2002). These two layers are the lamina splendens, composed of tightly packed bundles of collagen arranged parallel to each other and a second layer, made of collagen fibres perpendicular to the surface (Huber et al. 2000). The chondrocytes in the superficial region are flattened and tangential to the articular surface (Martinek 2003). There is a high water and low proteoglycan content.

The middle zone or the transitional zone contains more rounded chondrocytes and the collagen fibres are oriented randomly and are of larger diameter. Proteoglycan content is higher than in the superficial zone. In the deep or radial region chondrocytes are grouped in columns and proteoglycan content is highest. This region has the lowest density of cells. The diameter of collagen fibrils is maximal in this region (Poole 1997). The collagen fibres have an overall orientation towards the surface and are arranged in large bundles approximately 55 µm in diameter (Minns and Steven 1977). The water content in these three layers is a mirror image of the proteoglycan concentration with high water content in the superficial region and low water content in the deep region (Huber et al. 2000).

Underneath the radial region there is the calcified region, constituting approximately 5% of the total cartilage volume (Peterfy 2000). The two are separated by the tide mark, a wavy line representing the mineralized front of the calcified cartilage.

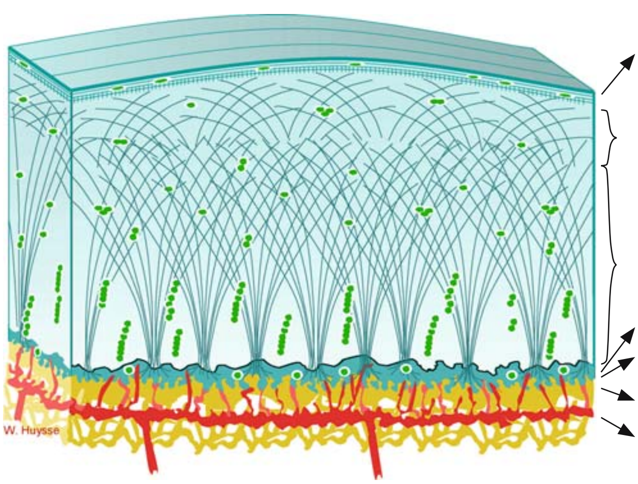

Fig. 4.1. Schematic representation of the different layers within articular cartilage. Hyaline cartilage is a fibrous tissue made up of chondrocytes lying within an extracellular matrix composed of tissue fluid containing dissolved electrolytes and macromolecules such as collagen II and proteoglycans. It is secured to the bony endplate in a jigsaw like manner. Collagen fibrils are anchored in the calcified cartilage, have a largely vertical orientation in the radial zone and a more random orientation in the transitional zone. The top layer consists of densely packed collagen bundles parallel tot the cartilage surface. Water content decreases towards the deeper regions and proteoglycan (PG) content increases, with the exception of the calcified cartilage, where no PG is found

The calcified zone is characterized by rounded chondrocytes surrounded by uncalcified lacunae (Huber et al. 2000). These chondrocytes have hardly any metabolic activity (Martinek 2003). There are no proteoglycans in the calcified zone (Huber et al. 2000). The collagen fibres run perpendicular to the articular surface and are anchored in a calcified matrix. This layer serves as a bridge between the upper layers of the cartilage and the subchondral bone.

Articular cartilage is closely connected to the subchondral bone plate, also called the cortical end plate or the articular bone plate. It penetrates into the recesses of the highly irregular bone plate, somewhat like the pieces of a jigsaw puzzle. The subchondral bone is situated underneath the endplate and contains fatty bone marrow and trabecular bone. In this subchondral region underneath the end plate many terminal arterial branches are found that end in a transverse sinus, located just below the end plate and formed by multiple venous branches (Imhof et al. 2000). The end plate is penetrated by small vascular branches originating from the subchondral bone region. These invade the calcified cartilage up to the tide mark. The distribution of these branches and the bony channels they run in is related to compressive forces acting on the cartilage and the subchondral bone (Imhof et al. 2000). This vascularisation also varies with age, individually and within joints. At least 50% of the oxygen and glucose required by the cartilage is supplied by these vessels (Imhof et al. 2000).

4.1.1.3 Function of Cartilage

In combination with synovial fluid, the smooth (Bloebaum and Radley 1995) surface of articular cartilage serves as a gliding surface with very low resistance. The elasticity of cartilage has only a limited role in cushioning compressive forces. The majority of load forces (30%) are taken up by the subchondral bone. Hyaline cartilage absorbs only 1–3% of compressive forces. The main function of cartilage in weight bearing is dissipating the loading forces to a larger area (Imhof et al. 2002).

4.1.2 Composition and Function of Fibrocartilage

Although hyaline cartilage provides a frictionless surface in the diarthrodal joint, many joints also contain fibrocartilagenous structures. These structures include the meniscus in the temporomandibular joint, the labrum in shoulder and hip joints, the triangular fibrocartilage in the wrist and both menisci in the knee. Occasionally a meniscus can be found in the acromioclavicular joint. These structures have an important stabilizing function (Rath and Richmond 2000): a labrum significantly increases the surface area of the joint and adds to the depth of the joint socket (Parentis et al. 2002); menisci compensate joint congruency and aid in transmitting the load. The menisci in the knee have also been shown to improve lubrication and nutrition of the articular cartilage.

Like hyaline cartilage, a fibrocartilagenous structure relies on diffusion from the synovial fluid for an important part of its nutrition (Rijk 2004). Most vascular branches end in the peripheral rim and are connected to vessels in the periosteum or the joint capsule.

Fibrocartilage is made up of about 75% water, 20% collagen and a small amount of proteoglycan, elastin and cells. Type I collagen accounts for more than 90% of the total collagen present, but types II, III, V, and VI have also been shown to be present in small amounts(McDevitt and Webber 1990; Rijk 2004).

Most collagen fibres in a labrum or meniscus are arranged in a circumferential direction and woven together by smaller, radially oriented fibres. Due to this configuration, most tears tend to progress more or less tangentially to the free edge (Rath and Richmond 2000). For a more detailed description of the pathological conditions of fibrocartilage we refer to Chaps. 9 (shoulder labrum), 15 (hip labrum) and 16 (meniscus of the knee)

4.1.3 Mechanical Injury of Articular Cartilage: Mechanisms and Staging

4.1.3.1 Introduction

Articular cartilage injury is a common finding during arthroscopy (Curl et al. 1997). In the knee most of these injuries are associated with other problems, such as meniscal lesions and anterior cruciate ligament injury.

As there are an unknown number of people who sustain chondral lesions without seeking treatment, it is extremely difficult to uncover the natural progression of an untreated cartilage lesion. According to a

number of investigators, many of these lesions, and especially the partial thickness injuries, are non-progressive (Fuller and Ghadially 1972; Ghadially et al. 1977a, b; Mankin 1982; Gillogly and Myers 2005; Thompson 1975).

4.1.3.2
Mechanism of Injury

Loading of articular surfaces causes movement of fluid within the cartilage matrix that dampens and distributes the load within the cartilage and to the subchondral bone (Buckwalter 2002). If the force is great enough, the framework is ruptured, chondrocytes are damaged and, in extreme cases, the subchondral bone is fractured. Acute and repetitive blunt joint trauma can result in damage to the subchondral bone and the deeper regions of the cartilage without visual disruption of the surface (Buckwalter 2002). This damage will result in subchondral bone marrow edema with or without associated microfractures (Fig. 4.2).

Healing of these fractures will lead to microcallus formation and focal subchondral sclerosis (Fig. 4.3).

Severe overloading leads to changes in uncalcified cartilage, such as fibrillation and production of abnormal matrix proteins. This initiates swelling in the deepest regions of the cartilage and can result in delamination of the articular surface if (repetitive) overloading persists (Imhof et al. 2000).

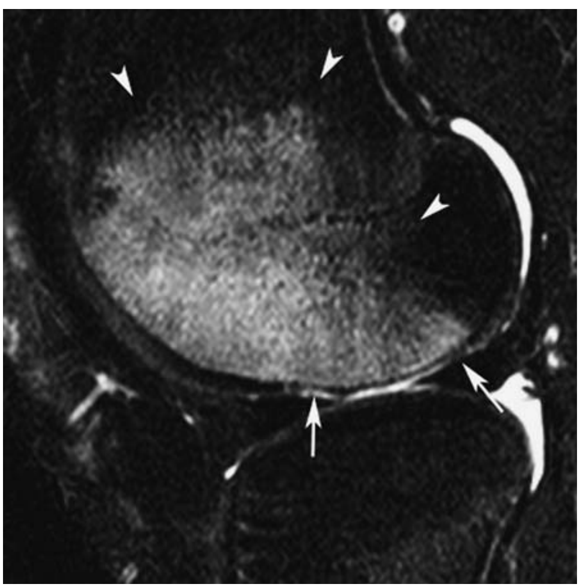

Fig. 4.2. Grade III–IV cartilage defect. Sagittal fat suppressed T2-weighted MR image. Cartilage injury (*arrow*) with extensive bone marrow edema (*arrowheads*)

Fig. 4.3. Grade V cartilage defect. Coronal DESS 3D MR image. Full thickness cartilage lesion with subjacent sclerosis and slight flattening of the condyle secondary to healed osteochondral trauma with subchondral microfractures

Repetitive microinjuries to subchondral bone and calcified cartilage may result in the activation of repair mechanisms. Increased activity of osteoblasts, osteoclasts and fibrovascular tissue, results in the formation of subchondral sclerosis and establishment of one or more new tide marks (Imhof et al. 2000, 2002).

4.1.3.3
Staging of Cartilage Lesions

The most well known arthroscopic staging method for articular cartilage is that proposed by Outerbridge in 1961 (Outerbridge 2001) and modified by Shahriaree (Shahriaree 1985). Other systems to grade cartilage, osteoarthritis and cartilage repair procedures with imaging methods were developed, but most of these systems were proven to have only a moderate reproducibility (O'Driscoll et al. 1988; Mankin et al. 1971; Ostergaard et al. 1997, 1999; van der Sluijs et al. 1992; Biswal et al. 2002; Cameron et al. 2003).

A practical classification system, based on systems used by Disler, Recht and Verstraete (Disler et al. 1994, 1995; Recht et al. 1996; Verstraete et al. 2004; Kramer and Recht 2002) uses four grades of chondromalacia:

- 0: normal cartilage
- I: slight swelling (not adequately assessable on routine MR and CT imaging)

- II: fissuring or cartilage defects less than 50% of cartilage thickness (Fig. 4.4)
- III: fissuring or cartilage defects more than 50% but less than 100% of cartilage thickness (Fig. 4.5)
- IV: cartilage defects and erosion with exposure of subchondral bone (Fig. 4.6)

A final grade V could be added to allow for differentiation between full thickness lesions with intact subchondral bone or with penetration of the bony endplate (Fig. 4.7). These grade V lesions are often associated with focal areas of bone marrow edema.

Limitations of this classification are the inability of CT and MR imaging to demonstrate reliably early

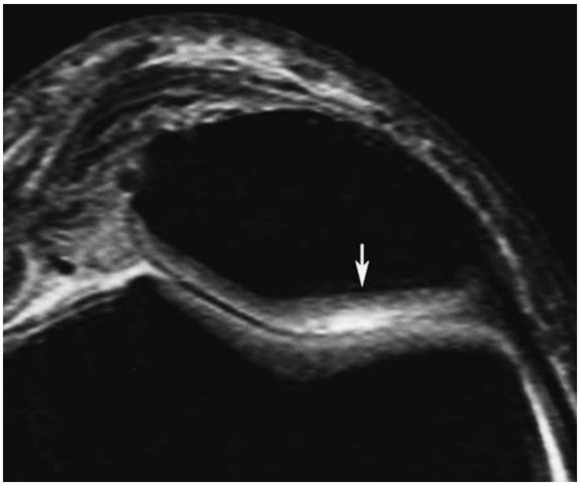

Fig. 4.4. Grade II cartilage defect. Axial fat suppressed T2-weighted MR image. Partial thickness defect of less than 50% of the cartilage width

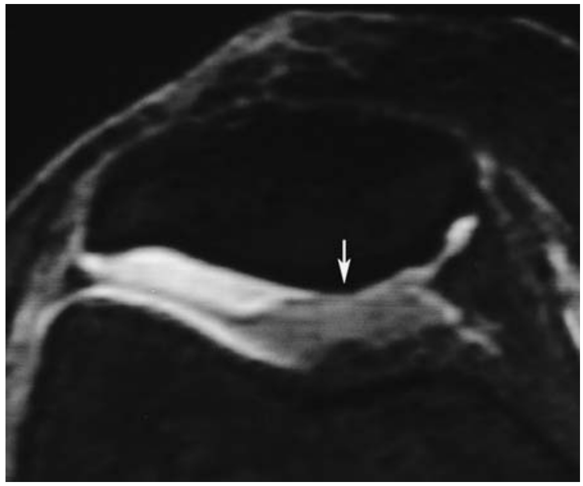

Fig. 4.6. Chronic cartilage defect. Axial 3D SPGRwe MR image. Extensive cartilage loss on the medial facet of the patella with a grade IV cartilage lesion on the crista (*arrow*)

Fig. 4.5. Recent cartilage defect. Sagittal 3D SPGR MR image. Acute grade III cartilage lesion: more than 50% but less than 100%. Note the residual basal layer of cartilage in the defect. There is also an intra-cartilaginous tear posterior to the defect and an area of bone contusion anterior in the proximal tibia (*asterisk*)

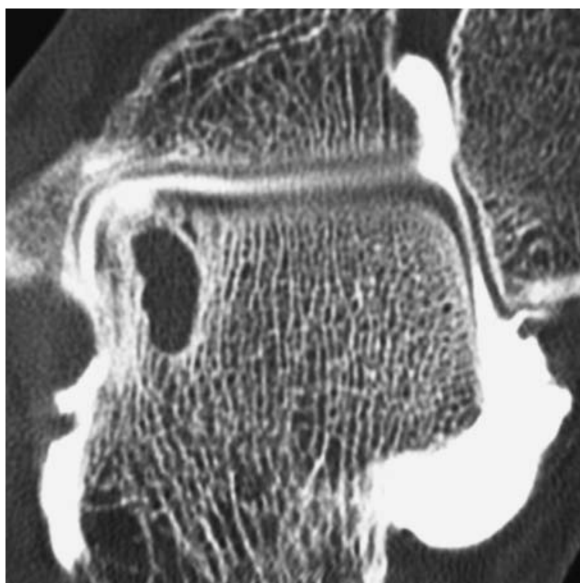

Fig. 4.7. Osteochondral lesion of the talus. Coronal CT arthrography. Grade V cartilage defect with indentation of the articular endplate. Note the large degenerative cyst underneath the defect

degenerative changes (Peterfy 2000). Moreover, the size of a lesion is not taken into account in this classification as it is difficult to measure the diameter of an often irregular lesion.

A comparison between the arthroscopic and MR classification of lesions of the articular cartilage is given in Table 4.1.

A similar arthroscopic grading system was proposed by the members of the International Cartilage Repair Society (Brittberg et al. 2005a) and can be found on the ICRS website (http://www.cartilage.org).

Table 4.1. Arthroscopic and MR classification system to grade cartilage lesions

Arthroscopic classification	
Grade 0	Normal
Grade 1	Softening or swelling
Grade 2	Shallow fibrillation, cartilage defects (<50% of cartilagethickness) and blister like swelling
Grade 3	Surface irregularities and areas of thinning (>50% of cartilage thickness)
Grade 4	Cartilage defects and exposure of subchondral bone
MR classification	
Grade 0	Normal
Grade 1	Normal contour±abnormal signal
Grade 2	Superficial fraying; erosion or cartilage defects of less than 50%
Grade 3	Partial-thickness defect of more than 50% but less than 100%
Grade 4	Full-thickness cartilage loss
Grade 5	Full thickness lesions with penetration of the bony endplate

4.2 Imaging

4.2.1 Imaging Articular Cartilage

4.2.1.1 Conventional Radiography and Arthrography

The overall status of the articular cartilage in a joint can be measured by the width of joint space. For the lower limbs this is best evaluated in weight bearing position. For many joints a normal range of width has been established (Keats and Sistrom 2001) and specific views have been developed to allow a better evaluation of the joint space.

Conventional X-ray images are very well suited for the evaluation of moderate or severe osteoarthritis, clearly depicting joint space narrowing, osteophytes and the presence of degenerative cysts (Figs. 4.8 and 4.9).

Fig. 4.8. Coxarthrosis. Standard radiography shows an osteophyte at the acetabular roof (*hollow arrow*), a small degenerative cyst (*white arrow*), and joint space narrowing (*arrowheads*)

Indications for conventional arthrography have diminished significantly in recent years due to the higher availability and accuracy of other diagnostic methods, particularly MR imaging. For imaging articular cartilage, arthrography without subsequent CT or MR imaging in no longer indicated (Resnick 2002). Arthrography is often combined with CT (CT arthrography) because this technique is not impeded by superposition and allows displaying the lesions in several planes (multiplanar reconstruction; MPR).

4.2.1.2 CT-Arthrography

After intra-articular administration of water-soluble iodine containing contrast agents (preferably non-ionic and of low osmolality) CT has a sensitivity and specificity comparable to MR imaging for detecting articular cartilage defects (Nishii et al. 2005; Waldt et al. 2005).

a b

Fig. 4.9a,b. Gonarthrosis. Standard (**a**) AP and (**b**) PA radiographs. The PA radiograph with 30° flexion or "schuss" position of the knee is used to evaluate the posterior third of the weight bearing part of the femoral condyles. In this case there is marked thinning of the articular cartilage in this region, not visible on regular AP images

CT-Arthrography very well depicts surface lesions of cartilage (grades II–IV) in different imaging planes (Fig. 4.10).

In patients with osteochondritis dissecans the integrity of the cartilage and the attachment of the osteochondral lesion to the surrounding bone can be assessed with high accuracy (Fig. 4.11).

A major drawback of CT is its inability to visualise associated subchondral bone marrow edema, which may be the cause of the patient's pain. Loose (cartilaginous) bodies on the other hand are more easily seen on a CT arthrography.

Other disadvantages of CT arthrography compared to MR imaging are the radiation dose and the very rare potential complications associated with arthrography, such as septic arthritis and allergic reactions to iodine containing contrast media (Dupas et al. 2005).

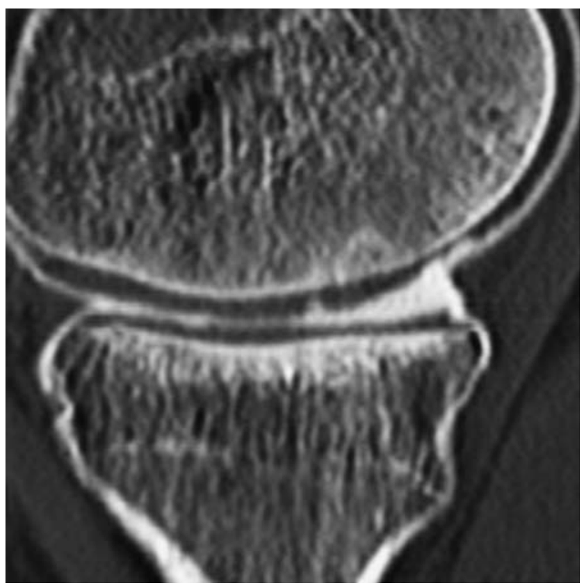

Fig. 4.10. Cartilage defect. Sagittal CT arthrography of the knee. Cartilage lesion starting with a full thickness fissure anteriorly, followed by a grade II region which progresses to grade III posteriorly

4.2.1.3
MR Imaging

The ideal MR imaging sequence for the evaluation of articular cartilage should be able to:

1. Show changes in the subchondral bone plate and display the exact thickness of the subchondral bone plate without magnetic susceptibility
2. Detect bone marrow edema, subchondral cysts and granulation tissue
3. Detect changes in the internal structure (disruption of the collagen framework) and biochemi-

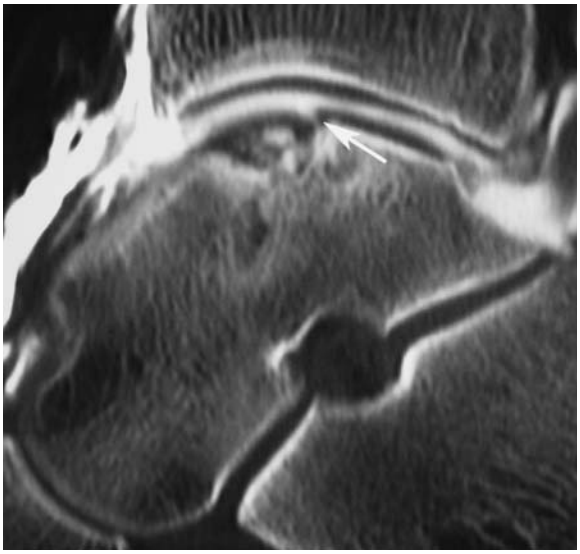

Fig. 4.11. Osteochondral defect of the talus. Sagittal CT arthrography of the ankle. Fissure in the cartilage overlying an osteochondral defect. The contrast medium infiltrates between the lesion and the surrounding subchondral bone over o short distance

cal composition of articular cartilage (mainly depletion of proteoglycans and increase of water content), with high contrast between normal and abnormal cartilage, both in deep and superficial layers
4. Sharply delineate superficial and deep defects in the articular cartilage
5. Display cartilage with an optimal contrast resolution, high spatial resolution and/or allow segmentation, volume calculation and three-dimensional (3D) display

Currently, three imaging sequences allow good morphologic evaluation of cartilage and chondral abnormalities. The proton-density and T2-weighted fast spin-echo (FSE) sequence, the fat-suppressed, T1-weighted, 3D spoiled gradient-echo (GRE) sequence and the 3D double echo steady state (3D-DESS) sequence have demonstrated excellent sensitivity for detection of grades 2, 3 and 4 chondral lesions (Verstraete et al. 2004).

Both proton-density and T2-weighted FSE images with or without fat suppression have been shown to be accurate in the detection of chondral abnormalities, with a sensitivity of 73–87% and a specificity of 79–94% (Potter et al. 1998; Sonin et al. 2002; Lang et al. 2005; Broderick et al. 1994; Bredella et al. 1999). In these sequences, articular cartilage shows an intermediate signal intensity(SI) compared to the high SI of the adjacent joint fluid and the low SI of the subchondral bone (Fig. 4.12).

Even in the absence of fluid, the borders of the cartilage are readily visible (Lang et al. 2005; Sonin et al. 2002). Moreover, these images can be obtained in a short acquisition time (4–5 min) with high resolution, and also allow simultaneous evaluation of other structures in the knee, such as menisci, ligaments and tendons. Therefore, in routine clinical practice, proton density and T2-weighted FSE images are usually sufficient. Without fat suppression, the soft tissues, like menisci, tendons and ligaments, are well displayed, in contrast to fat-suppressed FSE images, which are better for detection of bone marrow edema (Fig. 4.2).

As the deepest cartilage layers are not displayed well, overestimation of the depth of a cartilage lesion may occur. Therefore more time consuming high-resolution 3D techniques have to be performed whenever deep cartilage lesions are detected on the FSE images. In our experience, for detection of grade 2 lesions, fat-suppressed FSE sequences have equal sensitivity to the 3D sequences and are slightly better than FSE sequences without fat suppression.

Thin-partitioned, fat-suppressed 3D-spoiled GRE images, either using selective fat suppression (e.g. fat-suppressed 3D-SPGR) or selective water excitation (we) (e.g. FLASH-3Dwe; DESS-3Dwe), provide higher spatial and contrast resolution, but require

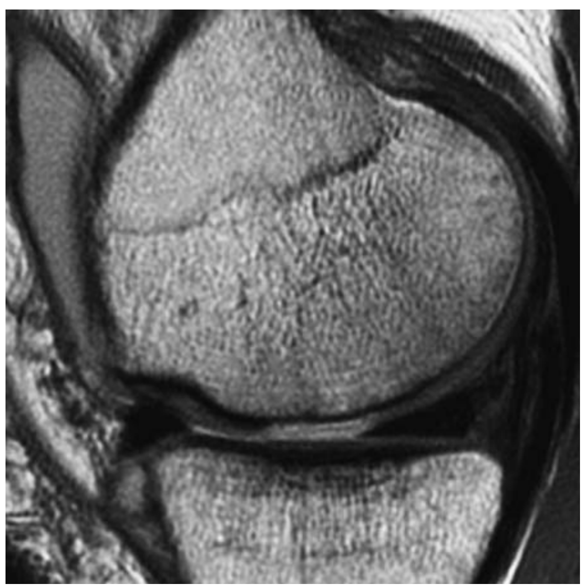

Fig. 4.12. Grade IV cartilage defect. Sagittal proton density-weighted FSE MR image. Long standing full thickness cartilage lesion with slightly irregular but intact bony endplate

longer acquisition times (7–10 min) and are more vulnerable to magnetic susceptibility and metallic artefacts.

In fat-suppressed 3D-SPGR and FLASH-3Dwe, articular cartilage has very high signal intensity, joint fluid has an intermediate to low signal intensity, and subchondral bone and bone marrow are dark. Reported sensitivity and specificity for detection of cartilage lesions are 75–85% and 95–97%, respectively (Disler et al. 1996; Recht et al. 1996; Trattnig et al. 2000; Ruehm et al. 1998). Deep cartilage layers and focal loss of trabecular bone is much better appreciated on 3D-fat-suppressed GRE images than on FSE images. These two fat-suppressed 3D sequences allow high-quality multiplanar reconstructions (MPR), which are useful for evaluating the patellar, trochlear or condylar surfaces with images perpendicular to the curved articular surface (Fig. 4.13).

Moreover, thin-section volume acquisitions allow segmentation and accurate 3D reconstructions of articular cartilage (Fig. 4.14).

However, quantification of cartilage volume by summing the voxels containing cartilage using 3D imaging techniques is relatively time-consuming. Automated methods for segmentation are being developed to make this tool valuable in routine daily practice.

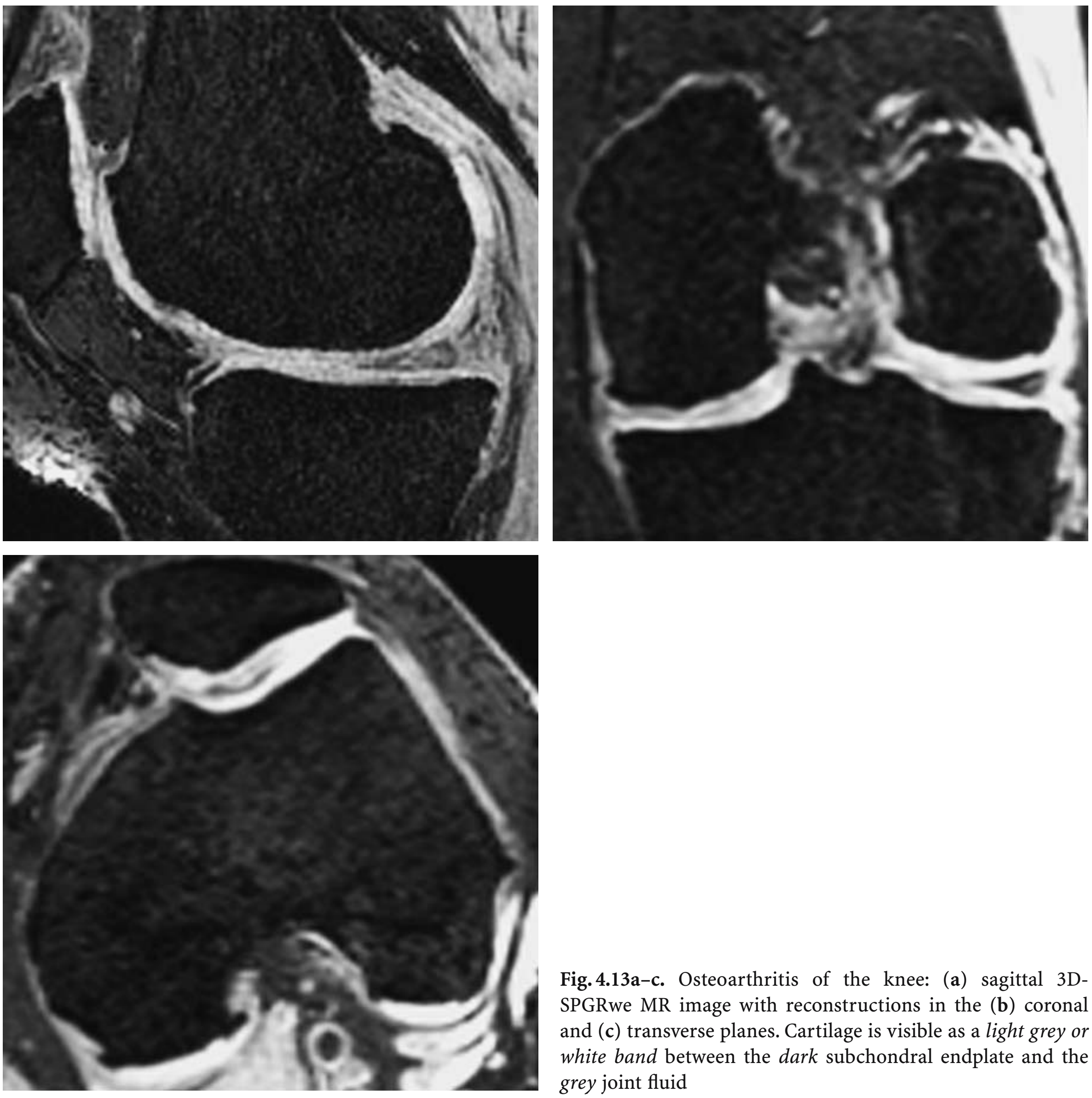

Fig. 4.13a–c. Osteoarthritis of the knee: (**a**) sagittal 3D-SPGRwe MR image with reconstructions in the (**b**) coronal and (**c**) transverse planes. Cartilage is visible as a *light grey or white band* between the *dark* subchondral endplate and the *grey* joint fluid

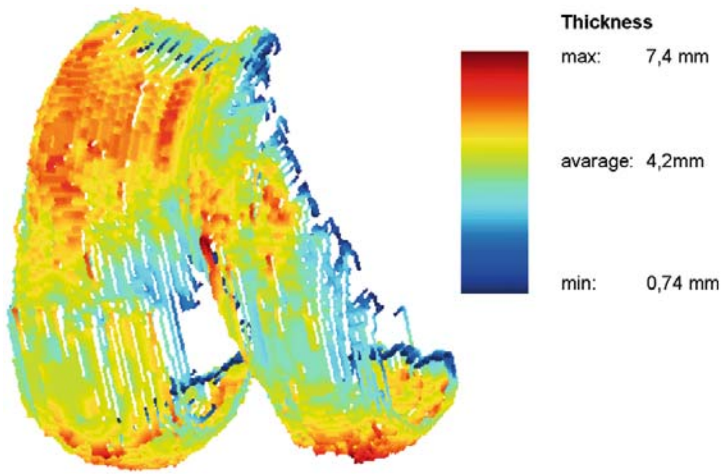

Fig. 4.14. Cartilage thickness map of femoral condyle, displaying thickness of cartilage in a 3D-image with a colour-encoded thickness scale. This image was created by semi-automated segmentation and extraction of high signal intensity voxels of cartilage from a thin section volume acquisition (fat-suppressed 3D-SPGR MR image) using selective water excitation (we) (FLASH-3Dwe; 128 slices of 1 mm)

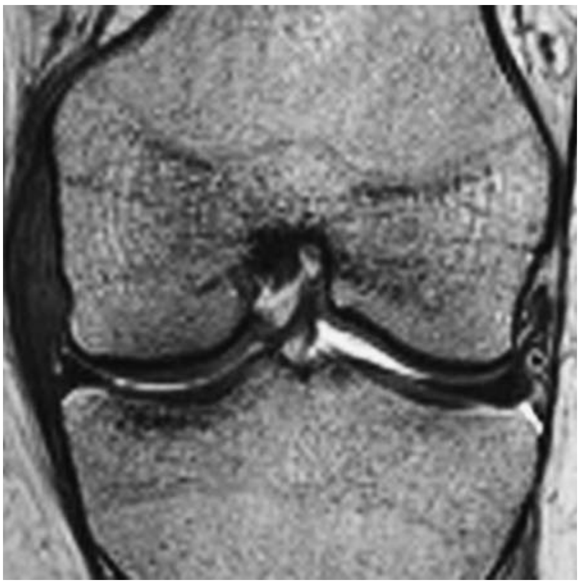

Fig. 4.15. Normal knee joint. Coronal DESS 3D MR image. Cartilage is visible as a *thin grey layer* between the *black* bony endplate and *white* joint fluid. The medial collateral ligament is thickened after a recent blunt trauma to the knee

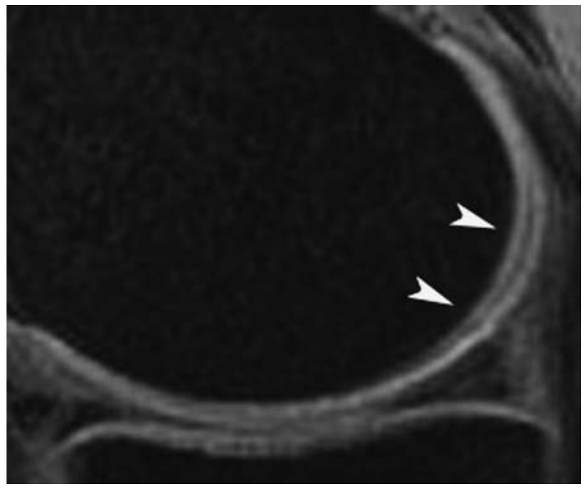

Fig. 4.16. Artefacts in cartilage imaging. Sagittal 3D SPGRwe MR image. Trilaminar appearance of the cartilage due to truncation artefact. The artefact is visible as a *dark line* at half distance between the surface and the bony endplate

In the 3D-DESS sequence without fat suppression or water excitation (Fig. 4.15), the cartilage has intermediate signal intensity, but is well delineated because joint fluid exhibits very high signal intensity.

If there is not enough fluid present within the joint, delineation of cartilage may become problematic. Due to the intermediate signal intensity of cartilage, segmentation for volume measurements is not possible. The 3D-DESS sequence allows high-quality multiplanar reconstructions (MPR) and provides T1 contrast in the soft tissues. Therefore, it allows better visualization of menisci, muscles, ligaments and tendons than fat-suppressed 3D-SPGR (FLASH-3Dwe; DESS-3Dwe) that can only be used to evaluate the cartilage, because all other tissues are dark and contrast is low.

Another drawback of the 3D-SPGR sequences are the significant image artefacts, which are much more pronounced than those on FSE images and tend to result in overestimation of cartilage disease and failure of automated cartilage segmentation (Lang et al. 2005). Truncation artefacts may create one or more thin, central bands of low signal intensity in the cartilage, and are commonly seen in 3D-SPGR images with fat suppression or water excitation (Erickson et al. 1996) (Fig. 4.16).

Table 4.2. MR methods for evaluation of cartilage

Pulse sequences for routine clinical MR imaging of cartilage		
Pulse sequence	**Signal of articular cartilage and fluid**	**Remarks**
Proton density-and T2-weighted fast spin-echo ± fat suppression	Articular cartilage has a lower SI than fluid	Other joint structures readily visible
Fat-suppressed T1-weighted spoiled gradient echo; fat-suppressed 3D-spoiled gradient echo/FLASH-3D we/3D-T1-FFE WATSc	Articular cartilage has a very high SI; fluid has low SI	High resolution and contrast; MPR possible; assessment of other joint structures not possible
DESS-3D	Cartilage has intermediate SI; joint fluid has a very high SI	High resolution and contrast; MPR possible; other joint structures readily visible
DESS-3Dwe	Cartilage has intermediate SI; joint fluid has a very high SI	High resolution and contrast; MPR possible; assessment of other joint structures possible

An overview of the properties of these different imaging sequences is summarized in Table 4.2.

Early cartilage degeneration (grade 1) cannot be reliably demonstrated using any of these sequences, and therefore novel MR imaging techniques that are sensitive to subtle structural and biochemical changes occurring early in the course of articular cartilage degeneration are being developed (Peterfy 2000).

4.2.1.4
MR Arthrography

In small joint and joints with thinner cartilage like the hip, 3D SPGR sequences, even with fat suppression or water excitation, do not achieve the same specificity and sensitivity as in the knee (Keeney et al. 2004). MR arthrography allows a better delineation of the articular cartilage surface and the detection of small cartilage lesions (Cerezal et al. 2005). As the joint distends after the intra-articular administration of gadolinium solution, opposing cartilage surfaces become separated and more easily evaluated. The cartilage is also separated from surrounding tissues such as the synovium and meniscal structures (Fig. 4.17).

In osteochondral lesions, MR arthrography can be performed to differentiate more accurately between stable and unstable lesions.

MR arthrography can be performed in a direct or indirect manner. Direct arthrography implies the intra-articular injection of contrast solution under fluoroscopic visualization. Indirect MR arthrography takes advantage of the diffusion of contrast material from the blood vessels in the synovium into the synovial fluid. After 5–10 minutes of exercise, the concentration of gadolinium-base contrast agents in the synovial fluid is high enough to shorten markedly the T1-relaxation time of the fluid. Indirect arthrography in osteochondral lesions has the advantage that contrast is able to enter the bone-lesion interface as opacified synovial fluid or trough diffusion from hypervascular granulation tissue lining the interface. Both situations indicate instability. Another advantage is the enhancement of the extra-articular soft tissues and of possible hyperaemic sites underneath areas of cartilage contu-

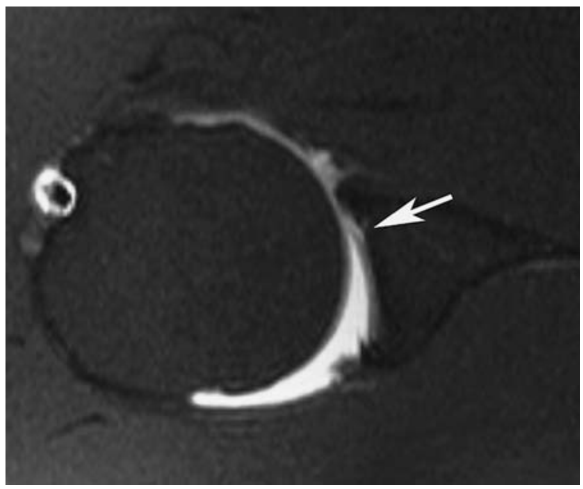

Fig. 4.17. Grade II–III cartilage defect. Transverse fat suppressed T1-weighted MR image after intra-articular contrast administration. A small tear in the glenoidal cartilage seen on direct MR arthrography could easily have been missed on unenhanced MR imaging

sion (Kramer et al. 1992, 1994; Kramer and Recht 2002; Recht and Kramer 2002).

The main drawback of indirect MR arthrography is the lack of joint distension.

4.2.2 Imaging of Cartilage Trauma

4.2.2.1 Chondral Defects

Large defects diminish joint space width but conventional radiography is not accurate. MR imaging, CT and MR arthrography reliably show chondromalacia and acute chondral defects but all are incapable of demonstrating grade I lesions.

The outline of a cartilage lesion, best seen after direct or indirect arthrography but also appreciable on unenhanced MR imaging, allows to differentiate between acute and more chronic lesions. In general, if the edges are sharp (Fig. 4.18) and the cartilaginous lesion is accompanied by bone marrow edema in the subjacent bone, an acute lesion must be suspected. A shallow lesion with wide margins, a more gradual slope to its edges and sclerosis of the subchondral bone suggest a chronic, degenerative lesion (Fig. 4.19).

Fig. 4.18. Recent cartilage defect. Sagittal CT arthrography. Traumatic grade IV cartilage defect (*arrow*) showing straight edges. Bone marrow edema is not visible on CT imaging

Fig. 4.19. Chronic cartilage defect. Sagittal T2-weighted FSE MR image. The gradual slope of the margins of the cartilage lesion and the subchondral sclerosis are suggestive for a chronic grade V lesion

4.2.2.2 Osteochondritis Dissecans and Osteochondral Lesions

Preferential places for osteochondral lesions and osteochondritis dissecans are the femoral condyles, talar dome and capitulum of humerus.

Possible etiologies for osteochondral lesions in the knee are osteochondritis dissecans, post-traumatic osteochondral fractures or insufficiency fractures of an osteonecrotic area. Mechanically, these lesions are caused by repetitive and prolonged overloading or a sudden compressive stress of the articular surface and subchondral bone. These lesions can be classified in four stages.

Stage I lesions are stable, show no discontinuity between the lesion and the surrounding bone and are covered by intact cartilage. Stage II lesions are partially detached but stable. Stage III lesions are completely detached and considered unstable but not dislocated. In stage IV lesions, the fragment is displaced or loose within its bed (Bobic 2000). A summary of the stages is given in Table 4.3.

Table 4.3. Stages of osteochondritis dissecans

Stage I	No discontinuity of bone and cartilage; covered by intact cartilage
Stage II	Partially detached osteochondral lesion but stable
Stage III	Completely detached osteochondral lesion but not dislocated
Stage IV	Displaced or loose osteochondral lesion within its bed

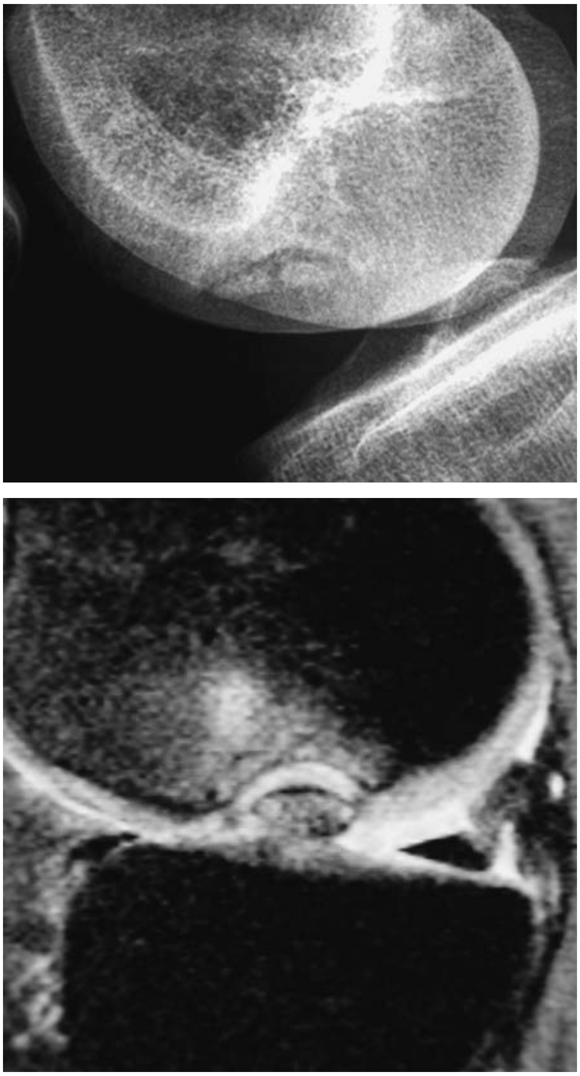

a

b

Fig. 4.20a,b. Osteochondritis dissecans or the knee. Radiograph, lateral view (**a**), and sagittal fat suppressed T2-weighted FSE MR image (**b**). Both images show typical unstable osteochondral lesions of the femoral condyle. The radiograph shows a radiolucent defect with sclerotic margins containing at least two loose bodies. The MR image shows an osteochondral lesion with a high signal intensity rim and the absence of cartilage covering the lesion. Note bone marrow edema in the unstable osteochondral lesion and in the surrounding femoral condyle

The role of imaging is first to identify the lesion and secondly to differentiate between stable and unstable lesions (Fig. 4.20). MR imaging has proven most accurate in doing this (Chung et al. 2005). MR findings indicating an unstable lesion are a linear high signal deep to the lesion on T2-weighted images (which is the most important finding), an articular fracture indicated by a high signal passing through the endplate, a focal osteochondral defect and a fluid-filled cyst more than 5 mm in diameter (Chung et al. 2005; De Smet et al. 1990). The presence of intra-articular gadolinium contrast clearly improves the diagnostic accuracy of MR as the contrast solution outlines the (osteo)chondral defect from the surrounding bone.

At the talar dome "*osteochondral lesion of the talus*" is the common term for lesions like osteochondritis dissecans, osteochondral fractures and talar dome fractures. These lesions are caused by impaction of the dome during an inversion trauma and are preferentially located on the medial or lateral edge of the talar dome, depending on whether the impaction occurred during inversion combined with plantar flexion and external rotation of the tibia or inversion and dorsiflexion of the foot (Cerezal et al. 2005). The most widely accepted classification of the lesions is that of Berndt and Harty (Berndt and Harty 1959; Beltran and Shankman 2001). It is similar to the classification of osteochondritis dissecans with an added grade (IIa) representing cystic degeneration of the lesion. Like in osteochondritis dissecans, it is important to distinguish between stable and unstable lesions. A linear high signal on T2-weighted

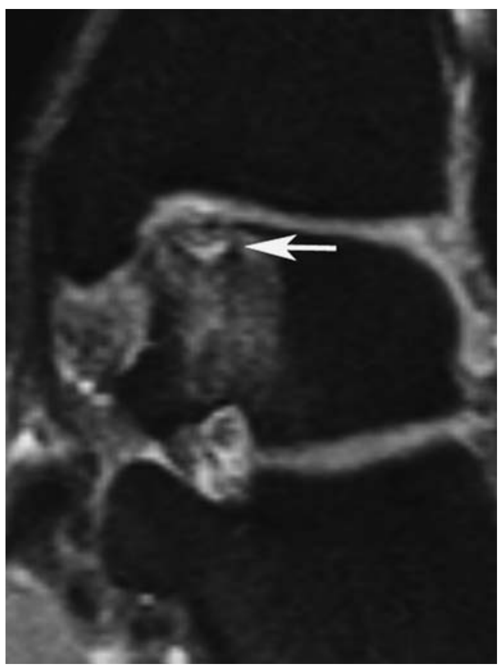

Fig. 4.21. Osteochondral lesion of the talus. Coronal 3D SPGRwe MR image. A linear area of high signal intensity underneath an osteochondral lesion of the talus indicating fluid or fibrovascular tissue

images between the lesion and native bone represents fluid or granulation tissue (Fig. 4.21). When this area of bone resorption surrounding the osteochondral lesion abuts the cartilage, the lesion is classified as unstable. A linear signal of moderate intensity may represent fibrovascular tissue.

This is also considered as an unstable lesion but healing can occur spontaneously or after a period of non-weight bearing. Another criterion of instability is the presence of cystic degeneration larger than 5 mm.

In the capitulum of the humerus, osteochondral lesions are located at the anterolateral part and are typically seen in young baseball players and other throwing sports with valgus stress on the elbow (see Chap. 12). Etiology, imaging findings and differentiation between stable and unstable lesions are the same as in osteochondral lesions of the talus and the femoral condyle (Fig. 4.22). Unstable osteochondritis dissecans lesions have a peripheral rim of high signal intensity or an underlying fluid filled cyst on T2-weighted images (Fig. 4.23). The main pitfall in MR imaging of the elbow is the pseudodefect at the posterior rim of the capitulum. This is caused by the abrupt transition between the postero-inferior articular surface of the capitulum and the nonarticulating surface of the lateral epicondyle. This pseudodefect is a normal finding and should not be mistaken for osteochondritis-like lesions found more anteriorly within the capitulum (Kijowski and De Smet 2005; Nakagawa et al. 2001).

Fig. 4.23. Osteochondritis dissecans of the elbow. Coronal T1-weighted SE MR image. Large, unstable osteochondral lesion in the capitulum, with fragmentation

Fig. 4.22. Osteochondritis dissecans. Standard AP radiograph of the right elbow. Plain radiograph readily demonstrates the subcortical radiolucent area with sclerotic margin, typical for osteochondritis dissecans

4.2.3 Modalities for Cartilage Repair

As no stem cells are found within hyaline cartilage, intrinsic repair capabilities of cartilage are limited. No meaningful repair of the cartilage occurs in partial thickness defects. Spontaneous repair is initiated if the subchondral bone plate is damaged and there is communication with the subchondral marrow cavity (Shapiro et al. 1993). Given the poor intrinsic repair capabilities of adult articular cartilage, many different surgical repair techniques have been developed. These can be divided into three groups: the palliative (débridement or stabilization of loose articular cartilage), reparative (stimulation of repair from the subchondral bone) and restorative procedures (replacement of damaged cartilage) (Redman et al. 2005; Shelbourne et al. 2003; Verstraete et al.

2004). The palliative procedures are lavage, débridement and shaving. None of these procedures, however, induce repair and relief, therefore, is usually temporary (Newman 1998; Paar et al. 1986; Redman et al. 2005; Smith et al. 2005).

Reparative procedures take advantage of the intrinsic repair response after opening the subchondral plate and. This introduces all the vascular-mediated elements necessary for the classic healing response, such as fibrin clot, blood and marrow cells, cytokines, growth factors, and vascular invasion (Newman 1998; Redman et al. 2005; Smith et al. 2005). The most well known is microfracturing (Fig. 4.24), introduced by Steadman et al. in 1997 (Blevins et al. 1998; Newman 1998; Steadman et al. 1999). In most all cases the defect is filled with collagen I rich fibrocartilage which does not resist compression and shear loads as predictably as hyaline cartilage does and is likely less durable over time.

The ideal patient for this type of repair procedure is young, has small, stage III or IV articular surface lesion and a well-defined history of trauma. He or she is compliant with the postoperative rehabilitation protocols and does not have mechanical axis malalignment.

Other reparative procedures are Pridie (Pridie 1959) drilling and abrasion arthroplasty (Johnson et al. 1998; Johnston 1997). The effects and results of these are similar to those of microfracturing.

The restorative procedures are more numerous and more diverse. They can be divided into several subgroups. First there are the soft tissue transplants. During these procedures perichondrium or periosteum is transferred to the defect after removal residual cartilage in the defect to create a full thickness lesion and of 2–3 mm of subchondral bone. Periosteum is more widely used because it is more readily available.

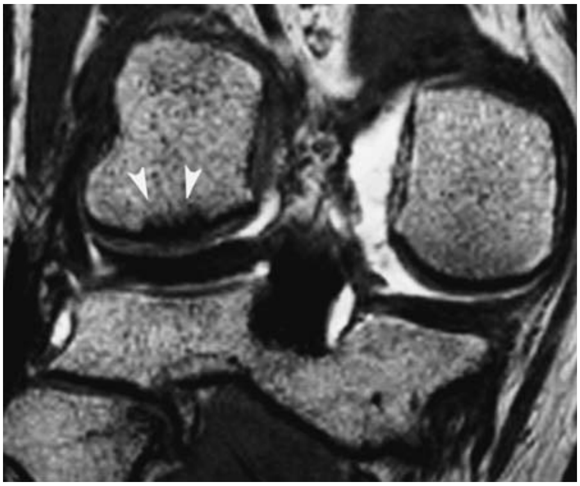

Fig. 4.24. Pridie microfracturing at the knee. Coronal DESS 3D MR image. A grade IV cartilage lesion on the weight-bearing part of the lateral femoral condyle was treated with microfracturing. Note the irregular aspect of the subchondral bone plate

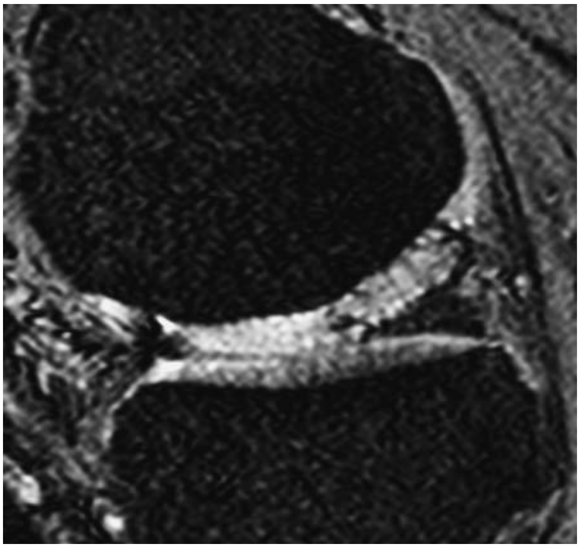

Fig. 4.25. Autologus chondrocyte implantation (ACI) at the knee. Sagittal 3D-SPGRwe MR image. Slight hypertrophy of the repair tissue after ACI. The repair tissue is surrounded by micrometallic artefacts caused by iron particles embedded in the covering periosteum

Although preliminary results were encouraging, with one group reporting repair tissue with a collagen II content of 74% (Homminga et al. 1990), few other groups have pursued this further.

A second group encompasses all cell transplantation based repair. This includes autologous chondrocyte implantation (ACI) (Fig. 4.25), allogenic chondrocyte transplantation (ACT) and auto- or allogenic stem cell transplantation. Autologous chondrocyte transplantation results in a durable repair for the majority of patients.

If there is failure of the repair tissue, this occurs almost always in the first two years (Peterson et al. 2002). In vivo, only hyaline-like repair tissue has been formed, without the structural or mechanical properties of mature cartilage (Redman et al. 2005).

A third subgroup includes the autogenous or allogenous osteochondral transfers. These techniques are most often used for the repair of large osteochondral defects. Autologous osteochondral plug transfer (AOT) (Fig. 4.26) is most effective in small to medium sized full thickness defects. For larger lesions several

Fig. 4.26. Autologous osteochondral plug transfer (AOT) of the knee. Sagittal 3D SPGR MR image. The lateral side of the graft has a small step-off. The rim of high signal intensity around the osseous part of the graft corresponds to bone turnover during the integration process

osteochondral plugs can be fitted in the defect. The gaps between the plugs are filled with fibrocartilage, reducing the durability of the repair.

4.2.4 Imaging Cartilage Repair

MR Imaging is a good technique to evaluate cartilage repair by displaying thickness, edge integration, surface, subchondral bone plate and marrow.

After surgical cartilage repair, the repair tissue should ideally have the same thickness and signal intensity as the surrounding cartilage. Furthermore, it should have a smooth surface and the margins should be continuous with the native cartilage. Ideally, the subchondral bone plate beneath the repair tissue should be smooth and continuous with the adjacent endplate although small differences are not clinically

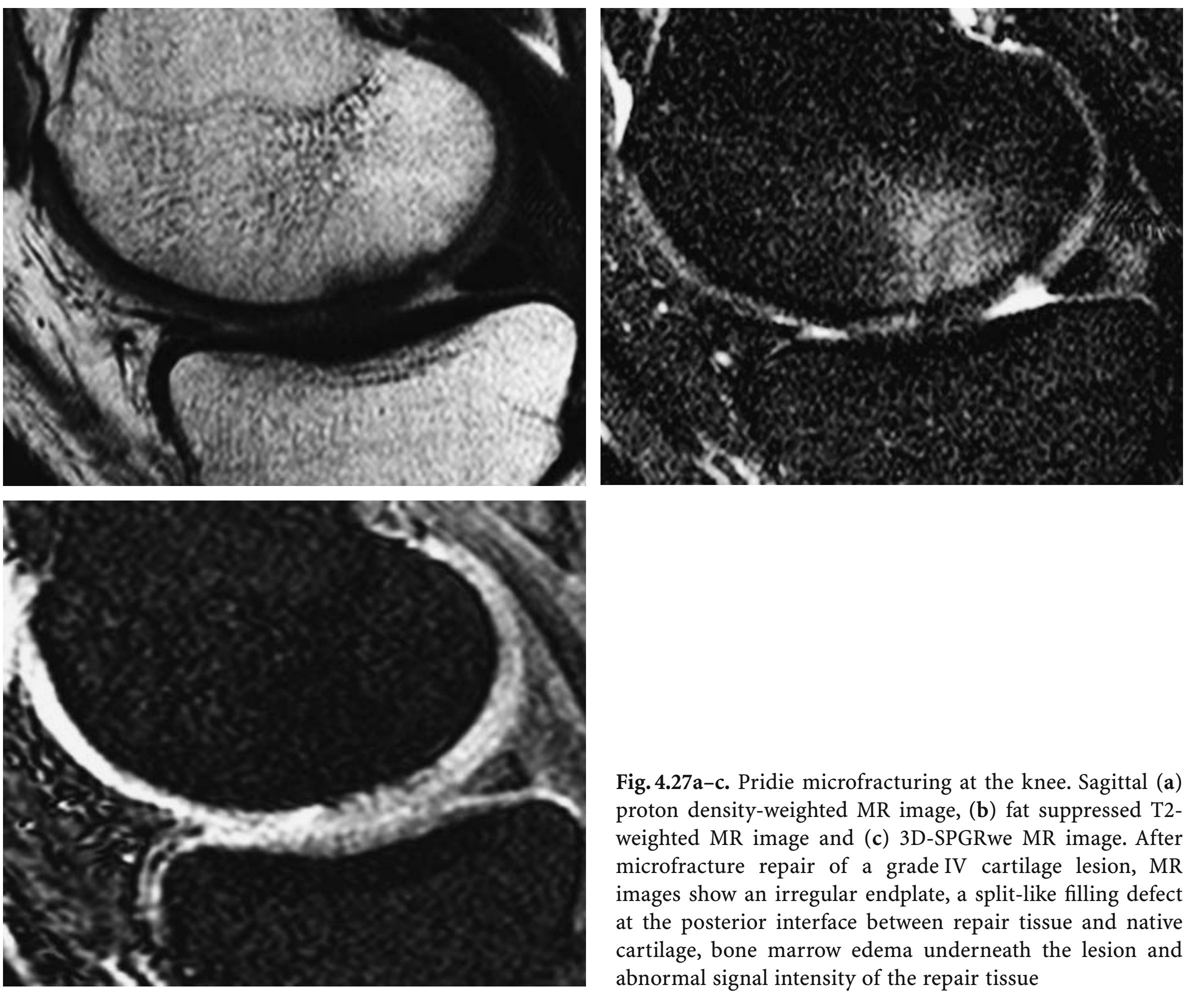

a b c

Fig. 4.27a–c. Pridie microfracturing at the knee. Sagittal (**a**) proton density-weighted MR image, (**b**) fat suppressed T2-weighted MR image and (**c**) 3D-SPGRwe MR image. After microfracture repair of a grade IV cartilage lesion, MR images show an irregular endplate, a split-like filling defect at the posterior interface between repair tissue and native cartilage, bone marrow edema underneath the lesion and abnormal signal intensity of the repair tissue

significant. There should be no abnormal signal in the underlying bone marrow. Other valuable information is location and size of the repair site as this is not always easy to assess particularly during arthroscopic procedures. Magnetic resonance imaging (Fig. 4.27) is ideally suited to evaluate these variables (Marlovits et al. 2004; Brittberg and Winalski 2003; Brittberg et al. 2005b).

When evaluating the filling of a defect, the result is best recorded as a percentage of the thickness of the surrounding, native cartilage. This can exceed 100% if the repair tissue is hypertrophic, which is often noted in the first months (Brown et al. 2004; Winalski and Minas 2000; Alparslan et al. 2001). If the repaired lesion had an osseous component, separate evaluation of bone and cartilage repair should be done.

In a majority of patients, the interface between native and repair cartilage is visible and can be seen as an interface between two regions of different signal intensity or as a fluid filled fissure. When a clear gap is seen between repair and native cartilage in ACI, thorough assessment of the integration with subchondral bone is needed, as failure of the repair often occurs in both locations.

MR arthrography is helpful in evaluating detachment of the graft (Brown et al. 2004).

When osteochondral plug transfer is performed, integration and integrity of the osseous component should also be assessed.

The subchondral bone plate can display irregularities, subchondral cysts, especially located underneath the interface of native and repaired cartilage, and outright defects. In the early post-operative period, bone marrow edema is a common finding. This should resolve with progressive osseous incorporation, which takes between 6 and 14 weeks (Marlovits et al. 2004). Persistence of this abnormal signal after 6–12 months may indicate graft failure and is associated with pain complaints. The extent of this edema should be compared to the size of the lesion.

An overview of the most important criteria associated with graft failure is given in Table 4.4 (Marlovits et al. 2004; Plank et al. 2005; Trattnig et al. 2006).

4.3 Conclusion

For evaluating sports related traumatic chondral and osteochondral lesions or assessing the quality of cartilage repair, MR imaging has long since become the most important diagnostic tool. In the future, this will become even more the case as experimental imaging sequences are integrated in routine clinical examinations. The only other imaging modality that can adequately depict the articular surface is CT-arthrography. This technique is, however, unable to demonstrate bone marrow edema, an imaging finding with high clinical significance.

Things to Remember

1. Conventional radiographs show only late degenerative cartilage changes but are valuable in the detection of osteochondral lesions.
2. CT arthrography is excellent for detecting grade II, III and IV lesions.
3. MR allows good evaluation of articular cartilage and is the only imaging technique that demonstrates bone marrow edema.
4. MR-arthrography has no added value for the evaluation of articular cartilage but MR arthrography and CT arthrography demonstrate the degree of separation of a fragment in osteochondritis dissecans.

Table 4.4. Signs of graft failure

Subchondral bone	Cartilage
Persistent bone marrow edema after 8 to 12 months	Thickness of repair tissue less than 50% of native cartilage
Subchondral cyst formation	Delamination or dislocation of repair tissue
Extensive subchondral sclerosis	Extensive surface damage with loss of more than 50% of cartilage thickness
Collapse of the bony endplate	

References

Alparslan L, Minas T, Winalski C (2001) Magnetic resonance imaging of autologous chondrocyte implantation. Semin Ultrasound CT MR 22:341–351

Bayliss MT, Ali SY (1981) Age-related-changes in human articularcartilage proteoglycans. Semin Arthritis Rheum 11:20–21

Beltran J, Shankman S (2001) MR imaging of bone lesions of the ankle and foot. Magn Reson Imaging Clin N Am 9:553–566

Berndt A, Harty M (1959) Transchondral fractures (osteochondritis dissecans) of the talus. J Bone Joint Surg Am 41A:988–1020

Biswal S, Hastie T, Andriacchi TP et al. (2002) Risk factors for progressive cartilage loss in the knee. Arthritis Rheum 46:2884–2892

Blevins FT, Steadman JR, Rodrigo JJ et al. (1998) Treatment of articular cartilage defects in athletes: an analysis of functional outcome and lesion appearance. Orthopedics 21:761–768

Bloebaum RD, Radley KM (1995) 3-Dimensional surface-analysis of young-adult human articular-cartilage. J Anat 187:293–301

Bobic V (2000). ICRS MR Imaging protocol for knee articular cartilage. In ICRS Standards Workshop 2000, p 12

Bredella MA, Tirman PFJ, Peterfy CG et al. (1999) Accuracy of T2-weighted fast spin-echo MR imaging with fat saturation in detecting cartilage defects in the knee: comparison with arthroscopy in 130 patients. AJR Am J Roentgenol 172:1073–1080

Brittberg M, Winalski CS (2003) Evaluation of cartilage injuries and repair. J Bone Joint Surg Am 85A:58–69

Brittberg,M, Aglietti,P, Gambardella,R et al. (2005a). International Cartilage Repair Society ICRS. ICRS [On-line]. Available: http://www.cartilage.org

Brittberg M, Sjogren-Jansson E, Thornemo M et al. (2005b) Clonal growth of human articular cartilage and the functional role of the periosteum in chondrogenesis. Osteoarthritis Cartilage 13:146–153

Broderick LS, Turner DA, Renfrew DL et al. (1994) Severity of articular-cartilage abnormality in patients with osteoarthritis – evaluation with fast spin-echo MR vs arthroscopy. AJR Am J Roentgenol 162:99–103

Brown WE, Potter HG, Marx RG et al. (2004) Magnetic resonance imaging appearance of cartilage repair in the knee. Clin Orthop Relat Res 422:214–223

Buckwalter JA (2002) Articular cartilage injuries. Clin Orthop Relat Res 402:21–37

Cameron ML, Briggs KK, Steadman JR (2003) Reproducibility and reliability of the outerbridge classification for grading chondral lesions of the knee arthroscopically. Am J Sports Med 31:83–86

Cerezal L, Abascal F, Garcia-Valtuille R et al. (2005) Ankle MR arthrography: how, why, when. Radiol Clin North Am 43:693–707

Chung CB, Isaza IL, Angulo M et al. (2005) MR arthrography of the knee: how, why, when. Radiol Clin North Am 43:733–746

Curl WW, Krome J, Gordon ES et al. (1997) Cartilage injuries: a review of 31,516 knee arthroscopies. Arthroscopy 13:456–460

De Smet A, Fisher D, Graf B et al. (1990) Osteochondritis dissecans of the knee: value of MR imaging in determining lesion stability and the presence of articular cartilage defects. AJR Am J Roentgenol 155:549–553

Disler DG, Peters TL, Muscoreil SJ et al. (1994) Fat-suppressed spoiled GRASS imaging of knee hyaline cartilage: technique optimization and comparison with conventional MR imaging. AJR Am J Roentgenol 163:887–892

Disler DG, McCauley TR, Wirth CR et al. (1995) Detection of knee hyaline cartilage defects using fat-suppressed three-dimensional spoiled gradient-echo MR imaging: comparison with standard MR imaging and correlation with arthroscopy. AJR Am J Roentgenol 165:377–382

Disler D, McCauley T, Kelman C et al. (1996) Fat-suppressed three-dimensional spoiled gradient-echo MR imaging of hyaline cartilage defects in the knee: comparison with standard MR imaging and arthroscopy. AJR Am J Roentgenol 167:127–132

Dupas B, Frampas E, Leaute F et al. (2005) Complications of fluoroscopy-, ultrasound-, and CT-guided percutaneous interventional procedures. J Radiol 86:586–598

Erickson SJ, Waldschmidt JG, Czervionke LF et al. (1996) Hyaline cartilage: truncation artifact as a cause of trilaminar appearance with fat-suppressed three-dimensional spoiled gradient- recalled sequences. Radiology 201:260–264

Eyre DR, Wu JJ, Woods PE (1991) The cartilage collagens – structural and metabolic studies. J Rheumatol 18:49–51

Fuller JA, Ghadially FN (1972) Ultrastructural observations on surgically produced partial-thickness defects in articular-cartilage. Clin Orthop Relat Res 86:193–205

Ghadially FN, Thomas I, Oryschak AF et al. (1977a) Long-term results of superficial defects in articular-cartilage – scanning electron-microscope study. J Pathol 121:213–217

Ghadially JA, Ghadially R, Ghadially FN (1977b) Long-term results of deep defects in articular-cartilage – scanning electron-microscope study. Virchows Arch B Cell Pathol Incl Mol Pathol 25:125–136

Gillogly SD, Myers TH (2005) Treatment of full-thickness chondral defect with autologous chondrocyte implantation. Orthop Clin North Am 36:433–446

Gurr E, Mohr W, Pallasch G (1985) Proteoglycans from human articular cartilage: the effect of joint location on the structure. J Clin Chem Clin Biochem 23:811–819

Homminga GN, Bulstra SK, Bouwmeester PS et al. (1990) Perichondral grafting for cartilage lesions of the knee. J Bone Joint Surg Br 72B:1003–1007

Huber M, Trattning S, Lintner F (2000) Anatomy, biochemistry and physiology of articular cartilage. Invest Radiol 35:573–580

Imhof H, Sulzbacher I, Grampp S et al. (2000) Subchondral bone and cartilage disease – a rediscovered functional unit. Invest Radiol 35:581–588

Imhof H, Nobauer-Huhmann IM, Krestan C et al. (2002) MRI of the cartilage. Eur Radiol 12:2781–2793

Johnson D, Urban W, Caborn D et al. (1998) Articular cartilage changes seen with magnetic resonance imaging-detected bone bruises associated with acute anterior cruciate ligament rupture. Am J Sports Med 26:409–414

Johnston SA (1997) Osteoarthritis – joint anatomy, physiology, and pathobiology. Vet Clin North Am Small Anim Pract 27:699–723

Keats T, Sistrom C (2001) Atlas of radiologic measurement, 7th edn. C.V. Mosby, St Louis, MO

Keeney JA, Peelle MW, Jackson J et al. (2004) Magnetic resonance arthrography versus arthroscopy in the evaluation of articular hip pathology. Clin Orthop Relat Res 429:163–169
Kijowski R, De Smet A (2005) MRI findings of osteochondritis dissecans of the capitellum with surgical correlation. AJR Am J Roentgenol 185:1453–1459
Kramer J, Recht MP (2002) MR arthrography of the lower extremity. Radiol Clin North Am 40:1121–1132
Kramer J, Stiglbauer R, Engel A et al. (1992) MR contrast arthrography (MRA) in osteochondrosis dissecans. J Comput Assist Tomogr 16:254–260
Kramer J, Recht MP, Imhof H et al. (1994) Postcontrast MR arthrography in assessment of cartilage lesions. J Comput Assist Tomogr 18:218–224
Lang P, Farima N, Hiroshi Y (2005) MR imaging of articular cartilage: current state and recent developments. Radiol Clin North Am 43:629–639
Mankin HJ (1982) The response of articular-cartilage to mechanical injury. J Bone Joint Surg Am 64A:460–466
Mankin HJ, Dorfman H, Lippiello L et al. (1971) Biochemical and metabolic abnormalities in articular cartilage from osteo-arthritic human hips. II. Correlation of morphology with biochemical and metabolic data. J Bone Joint Surg Am 53A:523–537
Marlovits S, Striessnig G, Resinger CT et al. (2004) Definition of pertinent parameters for the evaluation of articular cartilage repair tissue with high-resolution magnetic resonance imaging. Eur J Radiol 52:310–319
Martinek V (2003) Anatomy and pathophysiology of articular cartilage. Dtsch Z Sportmed 54:166–170
McDevitt CA, Webber RJ (1990) The ultrastructure and biochemistry of meniscal cartilage. Clin Orthop Relat Res 252:8–18
Meachim G (1969) Age changes in articular cartilage. Clin Orthop Relat Res 69:33–44
Minns RJ, Steven FS (1977) Collagen fibril organization in human articular-cartilage. J Anat 123:437–457
Nakagawa Y, Matsusue Y, Ikeda N et al. (2001) Osteochondral grafting and arthroplasty for end-stage osteochondritis dissecans of the capitellum: a case report and review of the literature. Am J Sports Med 29:650–655
Newman A (1998) Articular cartilage repair. Am J Sports Med 26:309–324
Nishii T, Tanaka H, Nakanishi K et al. (2005) Fat-suppressed 3D spoiled gradient-echo MRI and MDCT arthrography of articular cartilage in patients with hip dysplasia. AJR Am J Roentgenol 185:379–385
O'Driscoll SW, Keeley FW, Salter RB (1988) Durability of regenerated articular-cartilage produced by free autogenous periosteal grafts in major full-thickness defects in joint surfaces under the influence of continuous passive motion - a follow-up report at one year. J Bone Joint Surg Am 70A:595–606
Ostergaard K, Petersen J, Andersen CB et al. (1997) Histologic/histochemical grading system for osteoarthritic articular cartilage: reproducibility and validity. Arthritis Rheum 40:1766–1771
Ostergaard K, Andersen CB, Petersen J et al. (1999) Validity of histopathological grading of articular cartilage from osteoarthritic knee joints. Ann Rheum Dis 58:208–213
Outerbridge RE (2001) The etiology of chondromalacia patellae (Reprinted from Outerdridge RE: The etiology of chondromalacia patella, vol 43B, pp 752–757, 1961). Clin Orthop Relat Res 389:6–8
Paar O, Lippert MJ, Bernett P (1986) Measurement of femoropatellar pressure and surface-contact – cartilage shaving either alone or in combination with other methods in chondromalacia of the normal and malformed oatella – an experimental-study. Unfallchirurg 89:555–562
Parentis MA, Mohr KJ, El Attrache NS (2002) Disorders of the superior labrum: review and treatment guidelines. Clin Orthop Relat Res 400:77–87
Peterfy CG (2000) Scratching the surface: articular cartilage disorders in the knee. Magn Reson Imaging Clin N Am 8:409–430
Peterson L, Brittberg M, Kiviranta I et al. (2002) Autologous chondrocyte transplantation: biomechanics and long-term durability. Am J Sports Med 30:2–12
Plank CM, Kubin K, Weber M et al. (2005) Contrast-enhanced high-resolution magnetic resonance imaging of autologous cartilage implants of the knee joint. Magn Reson Imaging 23:739–744
Poole CA (1997) Articular cartilage chondrons: form, function and failure. J Anat 191:1–13
Potter HG, Linklater JM, Allen AA et al. (1998) Magnetic resonance imaging of articular cartilage in the knee – an evaluation with use of fast-spin-echo imaging. J Bone Joint Surg Am 80A:1276–1284
Pridie K (1959) A method of resurfacing osteoarthritic knee joints. J Bone Joint Surg Am 41A:618–619
Rath E, Richmond JC (2000) The menisci: basic science and advances in treatment. Br J Sports Med 34:252–257
Recht MP, Kramer J (2002) MR Imaging of the postoperative knee: a pictorial essay. Radiographics 22:765–774
Recht MP, Piraino DW, Paletta GA et al. (1996) Accuracy of fat-suppressed three-dimensional spoiled gradient-echo FLASH MR imaging in the detection of patellofemoral articular cartilage abnormalities. Radiology 198:209–212
Redman SN, Oldfield SF, Archer CW (2005) Current strategies for articular cartilage repair. Eur Cell Mater 9:23–32
Resnick D (2002) Arthrography, tenography, and bursography. In: Resnick D (ed) Diagnosis of bone and joint disorders, 4th edn. W.B. Saunders, Philadelphia,PA, pp 193–318
Rijk PC (2004) Meniscal allograft transplantation – part I: background, results, graft selection and preservation, and surgical considerations. Arthroscopy 20:728–743
Ruehm S, Zanetti M, Romero J et al. (1998) MRI of patellar articular cartilage: evaluation of an optimized gradient-echo sequence (3D-DESS). J Magn Reson Imaging 8:1246–1251
Shahriaree H (1985) Chondromalacia. Contemp Orthop 11:27–39
Shapiro F, Koide S, Glimcher MJ (1993) Cell origin and differentiation in the repair of full-thickness defects of articular-cartilage. J Bone Joint Surg Am 75A:532–553
Shelbourne KD, Jari S, Gray T (2003) Outcome of untreated traumatic articular cartilage defects of the knee: a natural history study. J Bone Joint Surg Am 85A:8–16
Smith GD, Knutsen G, Richardson JB (2005) A clinical review of cartilage repair techniques. J Bone Joint Surg Br 87B:445–449
Sonin AH, Pensy RA, Mulligan ME et al. (2002) Grading articular cartilage of the knee using fast spin-echo proton density-weighted MR imaging without fat suppression. AJR Am J Roentgenol 179:1159–1166

Steadman JR, Rodkey WG, Briggs KK et al. (1999) The microfracture technique to treat full thickness articular cartilage defects of the knee. Orthopade 28:26–32

Thompson RC (1975) Experimental study of surface injury to articular-cartilage and enzyme responses within joint. Clin Orthop Relat Res 107:239–248

Trattnig S, Mlynarik V, Huber M et al. (2000) Magnetic resonance imaging of articular cartilage and evaluation of cartilage disease. Invest Radiol 35:595–601

Trattnig S, Pinker K, Krestan C et al. (2006) Matrix-based autologous chondrocyte implantation for cartilage repair with HyalograftC: two-year follow-up by magnetic resonance imaging. Eur J Radiol 57:9–15

van der Sluijs JA, Geesink RG, van der Linden AJ et al. (1992) The reliability of the Mankin score for osteoarthritis. J Orthop Res 10:58–61

Verstraete KL, Almqvist F, Verdonk P et al. (2004) Magnetic resonance imaging of cartilage and cartilage repair. Clin Radiol 59:674–689

Waldt S, Bruegel M, Ganter K et al. (2005) Comparison of multislice CT arthrography and MR arthrography for the detection of articular cartilage lesions of the elbow. Eur Radiol 15:784–791

Winalski CS, Minas T (2000) Evaluation of chondral injuries by magnetic resonance imaging: repair assessments. Oper Tech Sports Med 8:108–119

Tendon and Ligamentous Trauma

5

Gina M. Allen

CONTENTS

G. M. Allen, DCH, MRCP, FRCR
The Royal Orthopaedic Hospitals NS Trust, Bristol Road South, Northfield, Birmingham, B31 2AP, UK

Box 5.1. Ultrasound

- Best spatial resolution and assessment of internal architecture
- Imaging technique of choice for superficial tendons and ligaments
- Dynamic examination
- Comparison with normal side
- Colour Doppler may assess neovascularity
- Calcifications are better seen than on MRI

Box 5.2. MR Imaging

- Best contrast resolution
- Imaging technique of choice for deep lying tendons and intra-articular ligaments
- Fat suppressed T2-weighted imaging useful for assessment of paratenonitis
- Demonstrates intra-articular lesions and bone injury

5.1 Introduction

To appreciate the effects of trauma on a ligament and tendon, it is important to review the basic function and anatomy of these structures. It is also necessary to understand some of the biomechanical properties of tendons and ligaments. In this chapter, these issues will be discussed to help understand the concepts that support diagnostic imaging.

5.2 The Microstructure

5.2.1 Composition of Tendons and Ligaments

The first division of tendons and ligaments is the fascicle; this is then broken down systematically into progressively smaller units. The fascicle is made up of fibrils, which are the essential building blocks of tendons and ligaments. The fibril is divided into sub-fibrils, which are composed of micro-fibrils and finally tropocollagen (Fig. 5.1) (Kastelic et al. 1978). The mechanical behaviour of the ligaments and tendons depends largely on collagen, as this is the principal tensile constituent. Collagen is a fibrous protein which is made up of three polypeptide chains. These amino-acid residue chains consist of a left-handed *helix* named an alpha-chain. Three of these alpha-chains are then arranged in a right-handed helix (named the gamma-chain) which makes up a molecule of collagen. The collagen molecules are then arranged with overlapping regions within the microfibril (Robinson et al. 2004).

Depending on the variation of amino-acids within the alpha-chains, the collagen is divided into different types. The principal element in adult ligaments and tendons is type 1 and this is important in providing tensile strength. Type 3 collagen is found in immature and healing ligaments. Type 3 collagen is always found in association with type 1 and the proportion of type 1 increases as ageing or healing occurs. Type 3 collagen is therefore thought to be an intermediate material. Other types of collagen are found in cartilage and muscle and synovial membrane (Cooke 1989).

The collagen in ligaments is more elastic than in tendons, as more flexibility is necessary for their function.

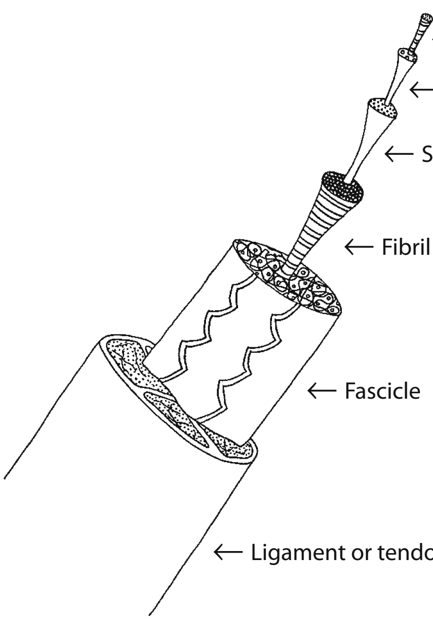

Fig. 5.1. Line diagram of the hierarchical structure of tendons and ligaments

5.2.2 Tendon Anatomy and Imaging Correlation

The collagen is arranged in a longitudinal orientation building up through microfibrils and subfibrils to eventually make up a fibril. The overlap of the collagen fibres is approximately one-quarter of the length of its neighbour and this is stabilised by covalent bonds forming crosslinks (Robinson et al. 2004). The fibrils are the smallest element of the tendon that can be seen by imaging. Only high resolution ultrasound is capable of visualising these elements (Figs. 5.2 and 5.3). A linear fibrillar arrangement results from the highly oriented nature of extracellular collagen in tendons (Adler 2005). This fibrillar pattern is not visible with MR imaging.

Tendons are highly reflective because of the strong reflection of the US beam. Because of the arrangement of extracellular collagen, tendon echogenicity is dependent on the angle of incidence of the US beam. Rocking the transducer by as little as 5–10° can make the tendon appear hypoechoic, a phenomenon which is better known as anisotropy (Adler 2005).

Scarcity of mobile protons causes normal tendons to have a low signal intensity on all MR pulse sequences. Care must be taken to avoid misinterpreting all increased signal within a tendon as abnormal. There are two major causes for increased signal within a normal tendon. If multiple tendon slips are converging to form a single tendon, as seen in the quadriceps tendon, longitudinal striations of intermediate signal may be seen within the tendon substance (Zeiss et al. 1992). Tendon alignment relative to the magnetic field can also result in increased signal intensity caused by the so-called "magic angle phenomenon" (Erickson et al. 1991).

The fibrils of tendons range in diameter depending on their maturity. In immature tissues they are smaller. The fibrils then make up the fascicles by mingling between fibroblast and ground substance.

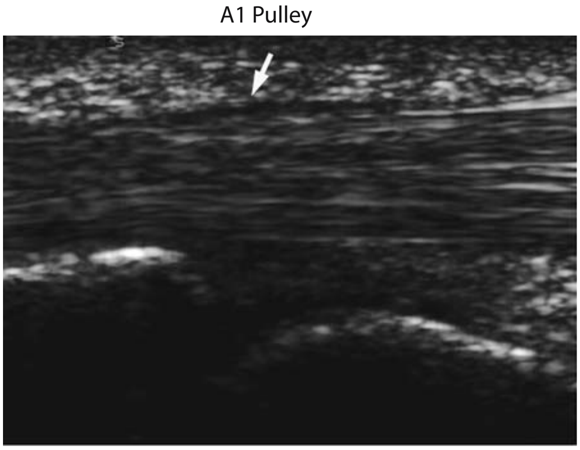

Fig. 5.2. Normal flexor tendon shown on ultrasound. This shows the fibrillary structure of the flexor tendon at the metacarpal-phalangeal joint and the A1 pulley attaching the tendon to bone

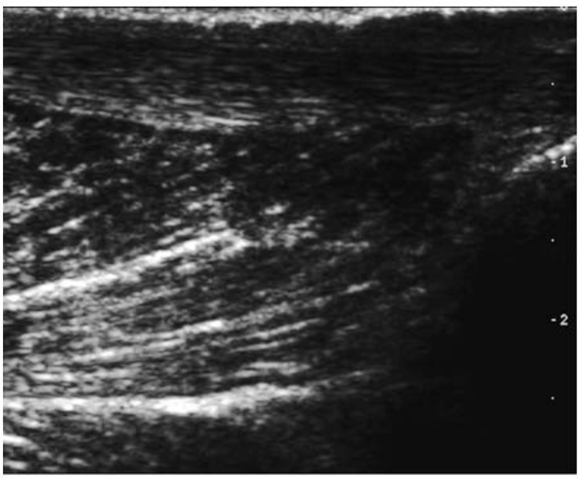

Fig. 5.3. Normal Achilles tendon. This ultrasound shows the normal Achilles tendon at its attachment into the calcaneum. Incidental note is made of a low lying insertion of the soleus muscle in this ballet dancer – an accessory soleus

Again they are arranged in a parallel longitudinal position. The fascicles are then enclosed within a reticular membrane that separates them from the surrounding tissue.

Tendons attach a muscle to bone and often cross joints. Some tendons are therefore named contentiously, for example the patellar tendon which joins the patella to the tibial tuberosity (Webb and Bulstrode 2004).

There are two types of tendon. Those that have a synovial sheath which provides a cover to reduce friction as they cross joints, bone or where they pass through fibro-osseous tunnels. These have a covering of connective tissue that is the visceral synovium and are joined to a second cover, the parietal synovium by a mesotenon. There is a thin layer of fluid, the synovial fluid, that lies between these layers and this reduces friction. The neurovascular supply of the tendon enters via the mesotenon. Some tendons need to be kept close to bone as they cross joints for example the finger flexor tendons are held down by pulleys. The osseous tunnels are formed by fibrous bands crossing the roof such as the carpal tunnel (Fig. 5.2).

The other types are tendons without a synovial sheath. In these tendons the epitendineum, a dense connective tissue layer is tightly bound to the tendon. On ultrasound images, the epitendineum is seen as a reflective line surrounding the tendon (Fornage 1986). Connective tissue fibres permeate the fascicles, causing the epitendineum to adhere to the tendon. Blood vessels and nerves enter the tendon along these fibres. Loose connective tissue, the paratenon, envelops the epitendineum (Van Holsbeeck and Introcaso 2001).

This again is broadly formed of two layers that are loosely held together (Valle et al. 2005). The Achilles tendon is an example of such a tendon (Fig. 5.3).

At the insertion of the tendon to bone, a narrow band of avascular fibrocartilage is present. This part of the tendon is hypoechoic on ultrasound examination. This effect may be the result of the cartilage in its substance or the anisotropic characteristics of the curved fibres in the tendinous attachment (Van Holsbeeck and Introcaso 2001). On MRI, similar increased intratendinous signal intensity on proton density MR images has been described. This may be related either to intratendinous fibrocartilage and/or magic angle phenomenon seen in the curved fibres (Defaut et al. 2003).

5.2.3 Ligament Anatomy and Imaging Correlation

Ligaments join bones together.

Ligaments are composed of dense, regular connective tissue similar to that of tendons. Their structure differs from that of tendons in that there is more interweaving of collagen fibres giving them a less regular histological and sonographic appearance (Bloom and Fawcett 1980).

Ultrasound and MRI are the only diagnostic methods suited for examination of ligaments. CT has

insufficient contrast resolution to define ligaments (Van Holsbeeck and Introcaso 2001).

The advantages of ultrasound examination over MRI are its excellent near field resolution, the short examination time, the ability to perform a dynamic examination and the ease of comparison with the normal side.

Although ultrasound examination is a valuable technique for the study of extra-articular ligaments, it is of little use in the assessment of intra-articular ligaments, such as the cruciate ligaments of the knee. MRI is the preferred method for the study of intra-articular ligaments (see Chap. 17).

Using MR imaging, normal ligaments have a variable appearance dependent on their location. Although most ligaments are hypointense on all pulse sequences, some may show a mixed signal intensity due to the presence of internal fibro-fatty tissue (e.g. the deep layer of the deltoid ligament and the anterior cruciate ligament). MR is technically more demanding as ligaments may be small and scan planes have to be exact. This means that it is difficult to orientate an MR section along the course of a specific ligament. If the sections cross the ligament it may erroneously cause it to appear absent or deficient. The slice thickness must be small to avoid volume averaging artefacts and to study these thin structures. Poor examination technique commonly leads to errors on the part of the inexperienced interpreter. Detailed discussion of this variability is beyond the scope of this chapter (see specific topographic chapters in this book).

Using ultrasound ligaments appear as reflective bands joining bone surfaces. They vary in size; the anterior tibiofibular ligament is one to two millimetres thick whilst the calcaneofibular ligament is much more substantial being up to 5 mm in depth. The alignments of ligaments vary considerable between individuals. When using ultrasound it is easier for the examiner to rotate the probe to align with the expected course of the ligament as this plane can be adjusted to fit the subtle normal variations in bone shape.

Absence or deficiency of a ligament, especially the thinner ones, is more reliably determined using ultrasound.

5.3 Biomechanical Properties of Ligaments and Tendons

Longitudinal forces applied across the ligament and tendon lead to a non-linear load extension curve. As the load is increased the ligament stiffens and this continues until subsequent rupture. The shape of the load extension curve changes, however, with external factors such as orientation of the load and temperature and the rate at which the load is applied. Once a load exceeds a certain point, the ligament or tendon becomes permanently deformed and this is when a failure occurs (Kastelic and Baer 1980; Towers et al. 2003). Repeated loading on a cyclical basis can train the ligament and tendon to take on more load, this is shown in vitro as a pre-conditioning of the tendon and ligament, but in vivo shows the importance of an athlete warming up prior to an event (Kannus et al. 1997) (Fig. 5.4).

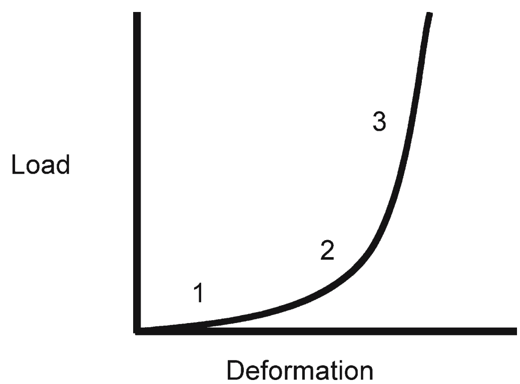

Fig. 5.4. The characteristic load/deformation plot for collagenous tissues. Initially a small load produces a relatively large extension of the collagen (region 1). As the load is increased, the ligament or tendon stiffens (region 2) until a constant linear relationship is reached (region 3) This continues until yield and subsequent rupture occurs

Ligaments and tendons rupture at the weakest point. The most vulnerable location depends on the age of the patient (Fig. 5.5).

For example in the adult the musculotendinous junction is weakest point (O'Connor and Groves 2005).

In the child, the bone is the most vulnerable and therefore tendon injuries are extremely uncommon.

In the adolescent, injuries to muscle often occur at the site of the apophysis so that bone avulsion

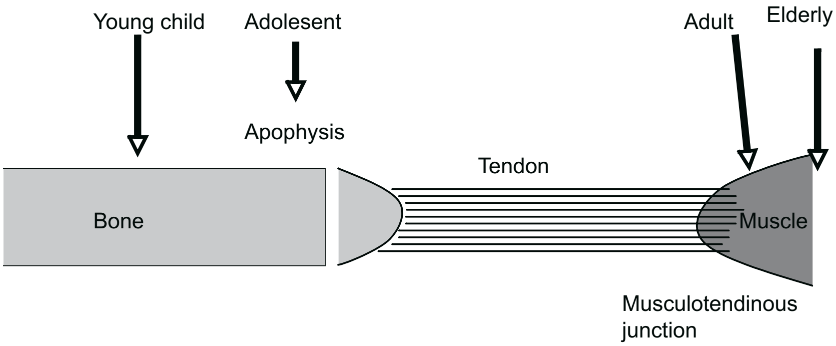

Fig. 5.5. Muscle–tendon–apophysis–bone (diagram). This depicts the area of weakness in the tendon–bone chain according to the age of the patient

injuries are the most common in this age group (see Chap. 26).

As for tendons, ligaments are stronger than the metaphyseal growth plate in youth, and therefore trauma to children's joints often results in injury to the growth plate (see Chap. 26) (Salter-Harris epiphyseal fractures). In the adult athlete, the ligaments are more vulnerable than the adjacent bone.

5.4 Imaging of Tendon Disease

5.4.1 Tendon Disorders

The tendon and adjacent structures can react in a number of ways to (repetitive) trauma.

5.4.1.1 Tendinosis and Insertion Tendonopathy

Repetitive injury and a high level of athletic activity leads to degeneration or tendinosis of the tendon (Wang et al. 2006). Loss of cross-linking between collagen fibres, edema, myxoid degeneration, vascular proliferation (angiofibroblastic hyperplasia) and reparative phenomena (collagenous type 3 matrix production) are seen on histologic examination. Neovascularity is a specific sign of disease and attempted repair. There is associated ingrowth of nerve endings that explains the increased pain in most of these patients. Rarely calcium deposits may occur within the tendons as a result of hypoxia. These histological changes will result in changes in morphology and internal architecture on imaging. They will be exhibited as swelling due to edema and matrix production (hypoechogenicity on US examination, raised signal intensity on T2-weighted MR studies), loss of fibrillar structure and calcium deposits.

Insertion tendonopathy occurs commonly in athletes. It is limited to the fibro-cartilaginous insertion of the tendon to bone. Differentiation from tendinosis is very important because there is no indication for surgery for insertion tendonopathy (Van Holsbeeck and Introcaso 2001).

5.4.1.2 Tenosynovitis, Paratenonitis and Tendinobursitis

The involvement of structures surrounding the tendon can result in different disease entities, dependent on the affected region.

In tendon with a synovial sheath, fluid may surround the tendon. Tenosynovitis (or tenovaginitis) is swelling and abnormality of the synovium within the tendon sheath, which is often associated with increased fluid in that sheath. In acute tenosynovitis, the tendon itself is of normal thickness, whereas in subacute tenosynovitis, the tendon may be thickened. In chronic forms, there is frequently no increase in synovial fluid and comparison with the normal side is required to make the diagnosis.

In tendons without a synovial sheath, the epitendineum and surrounding paratenon can be involved resulting in a paratenonitis. Edema and swelling is present in the paratenon surrounding the tendon. This is seen as a hypoechoic appearance on ultrasound and high signal on T2-weighted MR imaging. It is a much more conspicuous sign on fat suppressed T2-weighted MRI than when seen as hypoechogenicity using ultrasound (Fig. 5.6). The tendon itself is not always affected. The involvement of one of the peritendinous bursae may be described as tendinobursitis (Fig. 5.6).

Acute tenovaginitis or paratenonitis often precede tendinous lesions. They are associated with inflammatory infiltration and can be treated with antiflo-

Fig. 5.6. Achilles tendinobursitis and paratenonitis. Sagittal fat suppressed T2-weighted MR image. The distal Achilles tendon is enlarged, with internal linear areas of intermediate signal. Note associated deep retrocalcaneal bursitis and paratenonitis

gistic therapy (NSAID or corticosteroids). In contradistinction, inflammation is not found in tendinosis; the tendon itself will not benefit from antiflogistic therapy.

5.4.1.3
Tendon Rupture

A sudden explosive force can lead to rupture of the tendon – whether partial or complete. Tears are more common in older patients as the tendon is less flexible and has a poorer blood supply. In addition pre-existing tendinosis may result in internal splits and tears, which may predispose to complete rupture.

5.4.1.4
Tendon Dislocation or Subluxation

Displacement of tendons from their proper location may occur in athletes, often as a result of chronic trauma. Dislocation of the peroneal tendons may be seen in American footballers, soccer players and gymnasts (Van Holsbeeck and Introcaso 2001). Dislocation of the long head of the biceps tendon may be combined with tears of the rotator cuff that involve the subscapularis tendon.

Grading of tendon injury has little value. It is very dependent on the method of imaging employed and bears little relationship to the symptoms that will result. The primary role of imaging is to locate the problem and to determine if the tendon is abnormal. It is of less use in defining the severity of the problem.

5.4.2
Imaging of Tendon Disease

5.4.2.1
Plain Radiographs

Radiographs will not show tendon damage unless there is a massive loss of the normal tissue planes as is seen in some cases of rupture of the quadriceps tendon. Radiographs may, more importantly, show an associated fracture at the tendon insertion. For example, avulsion on the dorsum and at the base of the distal phalanx in an extensor tendon rupture of the hand (mallet finger) (Fig. 5.7). Occasionally calcification in a tendon may be observed. Unfor-

a

b

Fig. 5.7a,b. Avulsion of flexor digitorum profundus while playing volleyball. **a** Plain radiograph showing an avulsion fracture from the base of the distal phalanx that has moved proximally up the finger (*arrows*). **b** Ultrasound showing the same avulsion fracture and the attached flexor tendon (*oval*) that has been pulled proximally with the fracture fragment

tunately plain radiographs are not very sensitive because many tendons are injured without any bony injury.

5.4.2.2 Computed Tomography

CT is useful if there has been bony trauma. It may be particularly helpful for detection and assessment of subtle fractures, which are not seen on plain films. Before the advent of MRI, CT arthrography was used to image tendons indirectly. It can still be useful in patients who are unable to tolerate an MR scan or have cardiac pacemakers.

5.4.2.3 MR Imaging

MR imaging has become the main imaging technique for assessing both soft tissue and bones in one examination. Twenty percent of the population are claustrophobic and therefore in these patients MRI is a frightening experience. The introduction of more open MR scanners may help although some will remain intolerant to the method.

MRI can identify fluid in the tendon sheath and can start to appreciate internal change within a tendon (Figs. 5.6 and 5.8). Fat suppressed T2-weighted images are very effective in demonstrating paratenonitis (Fig. 5.6). MRI cannot identify the distinction between synovitis and fluid within a tendon sheath without the use of intravenous contrast. Whilst MRI contrast agents are fairly safe they still carry a very small risk of adverse reaction including death.

The microfracturing that often accompanies tendon injuries can be detected by MRI which is much more common than the fractures seen on CT or plain films. Certain patterns of microfracturing help the clinician to assess the mechanism of injury and increase awareness of accompanying injuries to soft tissue (see Chap. 6).

MRI is unfortunately not currently a dynamic method of imaging and therefore in chronic injury abnormalities may be missed. Although MRI will usually demonstrate full thickness tears with retraction, partial tears or tears without retraction may be very difficult to detect. Finding calcification within an injured tendon can be difficult as can fibrosis and scarring when using MRI alone (Adler and Finzel 2005).

5.4.2.4 Ultrasound

Ultrasound is the microscope of tendon and ligament disease. With the latest high resolution of ultrasound machines the fibrils can be visualised and more subtle abnormalities appreciated (Fig. 5.9). The intrinsic line pair resolution of US well exceeds that of commercially available MR systems and the detail seen within tendons is much greater using US. The influx of neovascularisation (angiofibrous hyperplasia) can also be appreciated by using Colour or Power Doppler without the need for contrast injections (Fig. 5.10). This can help detect subtle injuries.

If the patient has pain at a particular site that coincides with new vessels, this will confirm the origin of the symptoms. This can be useful in assessing response to treatment, when the vessels are shown to decrease in number at follow up examinations (Ohberg and Alfredson 2002).

The examination can be directed at the site of the sportsman's painful area. Ultrasound is extremely useful when the patient can point to an area of pain.

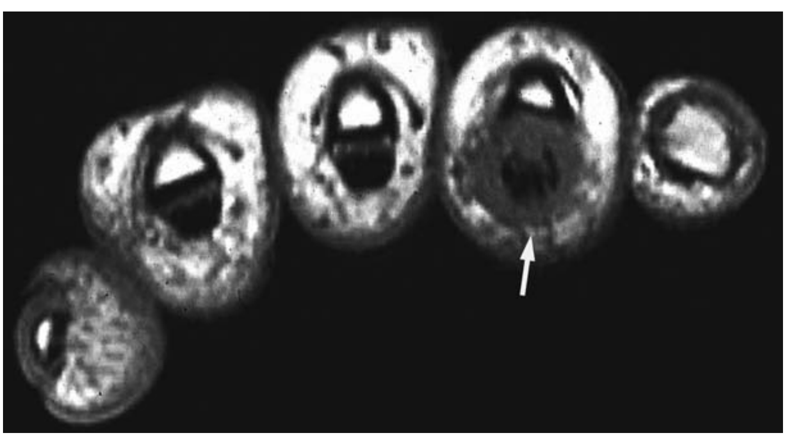

Fig. 5.8. Flexor tendinosis in a rower. Axial SE T1-weighted MR image showing thickening and signal changes within the flexor tendon of the fourth finger (*arrow*)

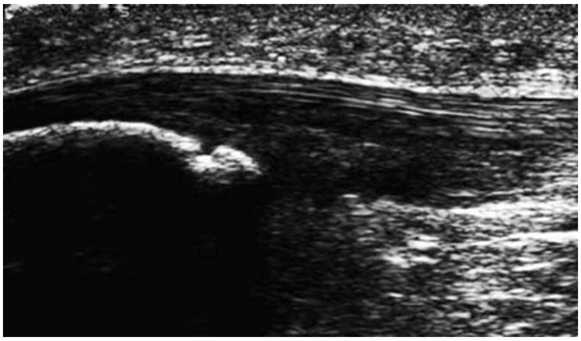

Fig. 5.9. Proximal patellar tendinosis in an elite goalkeeper. Longitudinal ultrasound. There is thickening, loss of fibrillar structure and hypoechogenicity at the proximal patellar tendon affecting the central patellar tendon most marked posteriorly

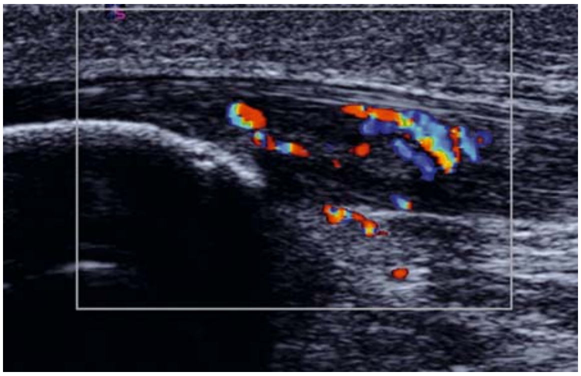

Fig. 5.10. Proximal patellar tendinosis in an elite goalkeeper. *Colour* Doppler shows marked neovascularity in the proximal patellar tendon

If the area is extensive and ill defined then MR may be a better way to image in the first instance.

Fluid and synovitis in tendon sheaths can be identified as separate entities without the need for contrast injections. Ultrasound is an excellent means of differentiating fluid from solid matter.

US can detect small areas of calcification and scar tissue. Dynamic movement can assess the full extent of tendon rupture. Moving the tendon actively (muscle contraction) or passively (the operator moves the limb) may give different information as these actions apply force to different ends of the tendon. Stressing the tendon can make a tear more obvious and allow assessment of a gap in the tendon (Fig. 5.11). This separation can be measured assisting the surgeon in planning their repair. Movement will differentiate between full and partial thickness tears. Partial tears may open under load when they are difficult to identify on static imaging but they will not separate or show paradoxical movement of the tendon ends.

Ultrasound is becoming easier for the clinician to interpret since the advent of extended field of view images. These can demonstrate a whole limb to the surgeon who needs to know the site of rupture of a tendon. Electronic recording and display provides a composite image of an area many times the width of the ultrasound probe so that the full length of a tendon and its muscle can be visualised on one image (Fig. 5.12).

Dynamic examination with stress manoeuvres is mandatory to assess tendon dislocation or subluxation (e.g. dorsiflexion and eversion stress for evaluation of peroneal tendon subluxation)

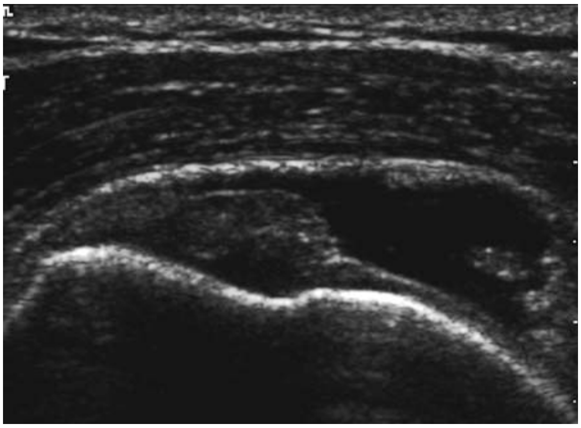

Fig. 5.11. Full thickness tear of the supraspinatus tendon in a weekend tennis player. Longitudinal ultrasound shows a fluid filled gap within the supraspinatus tendon

Fig. 5.12. Complete Achilles rupture in non-professional footballer. Extended field of view ultrasound image showing a tendon gap within the Achilles tendon

5.5 Imaging of Ligament Disease

5.5.1 Intra-Articular Ligaments

Although some investigators have been successful in demonstrating tears of intra-articular ligaments of the knee and the wrist, the examination for injuries to intra-articular ligaments is best performed using MRI (Van Holsbeeck and Introcaso 2001).

5.5.2 Extra-Articular Ligaments

Ultrasound provides a reliable means of assessing acute ligament injury, in cases when clinical examination is made difficult by pain and swelling (Van Holsbeeck and Introcaso 2001). Some argue that ultrasound is only required in a limited number of athletes with equivocal clinical findings, especially when surgery is being considered (Van Dijk et al. 1996). Others would hold that prognosis and reassurance are important factors in management and a test that is non-invasive and safe like ultrasound examination has a useful supportive role.

5.5.2.1 Acute Ligament Injury

Ligaments respond to injury by either complete rupture or partial rupture (spraining).

In case of partial rupture, the involved area of the ligament appears markedly thickened and decreased in echogenicity on ultrasound examination. Complete ruptures are demonstrated as a discontinuity of the ligament and the free ends may be separated by a haematoma. The fluid occupying the gap will appear hyperechoic or of reduced echogenicity, depending on how long after the injury imaging is performed. The diagnosis tends to be made most easily when imaging occurs as soon after injury as possible although in the first few minutes the appearances may be confusing. Some retraction of the ends of ligament may result in a slightly rounded appearance (Van Holsbeeck and Introcaso 2001). Avulsion fractures at the insertion of the ligaments may be detected using ultrasound (Fig. 5.13) and may not all be seen by standard radiography.

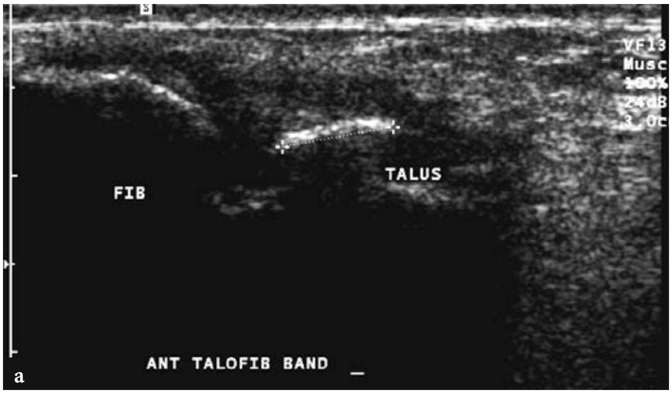

Fig. 5.13a,b. Avulsion fracture at the distal insertion of the anterior talofibular ligament. **a** Ultrasound. The avulsed fragment is seen as a linear reflection, representing cortical bone from the talus. **b** The corresponding plain radiograph confirms the avulsion fracture

Ultrasound is particularly valuable for assessment of stability of a joint, because dynamic examination can be performed, putting stress on the ligament and opening the bone gap.

MR imaging is rarely performed for assessment of acute ligament disorders. It can however detect associated microfracturing (bone bruise, see Chap. 6) (Figs. 5.14 and 5.15). The main indication for MR imaging is to detect associated intra-articular abnormality, such as meniscal lesions or injuries of intra-articular ligaments. For simple medial collateral ligament lesions of the knee, a three-grade MR staging system has been developed which correlates well with clinical staging (see Chap. 17).

a

b

Fig. 5.14a,b. Ligament rupture on MRI: knee ligaments. **a** Sagittal fat suppressed proton density MR image. Note ruptures of the ACL and PCL with microfracturing. **b** Coronal fat suppressed proton density MR image. Note rupture of the LCL with a fracture of the proximal fibula

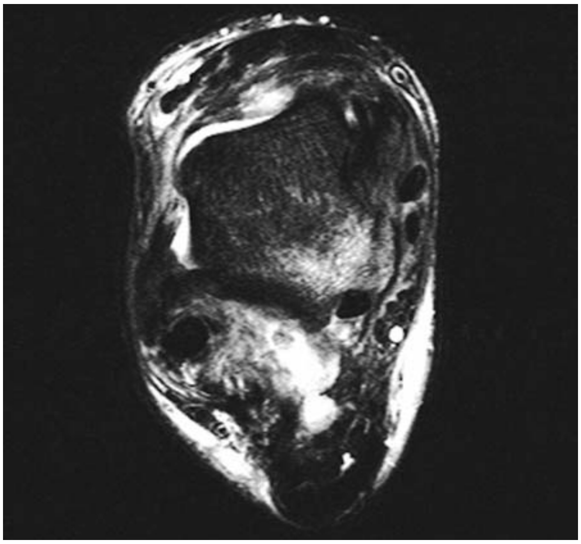

Fig. 5.15. Ligament rupture on MRI: ankle ligaments. Axial oblique fat suppressed FSE T2 weighted MR image. Note a rupture of the anterior talofibular ligament in an elite athlete with microfracturing of the postero-medial talus

5.5.2.2 Chronic Ligament Injury

With suitable treatment, partial ruptures heal completely within two months, whilst complete ruptures can take six months to recover.

Inappropriate or delayed treatment may result in ligamentous non union. Persisting ligament interruption occurs in a minority of patients (10%), and this can be demonstrated using both US or MR imaging as a residual gap or focal thinning of the ligament.

Hypertrophic non-union is a more frequent complication of untreated partial ligament ruptures that result in excessive formation of granulation tissue and mucoid degeneration.

Clinically, pain and tenderness is present over the lesion. This type of non-union may be seen at different locations, including the ankle ligaments, sinus tarsi, coracoacromial ligament (common in impingement syndrome in tennis players), plantar fascia (long distance runners) and the medial collateral ligament of the knee (soccer, football, basketball, hockey...). It is characterised by thickening seen both on ultrasound and MRI examination. Ultrasound may demonstrate few internal reflections within a hypoechoic mass. In repair stages granulation tissue and reactive synovitis may lead to new blood vessels which can be identified using power Doppler imaging. Internal calcifications may be observed (Van Holsbeeck and Introcaso 2001).

As with tendon disease, ultrasound will show calcification better than MRI (Fig. 5.16).

Pelligrini-Stieda disease is perhaps part of the spectrum of hypertrophic non-union of the MCL of the knee although the location of the calcification is

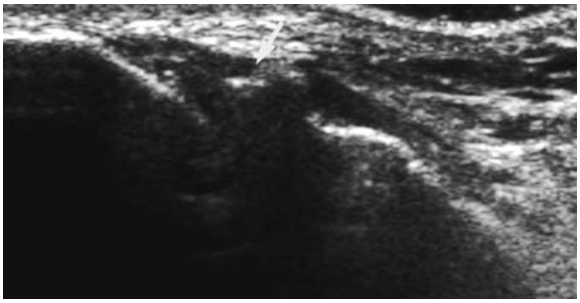

Fig. 5.16. Ligament rupture on ultrasound: ankle ligaments. Ultrasound shows calcification (*arrow*) at the site of a previously ruptured anterior talofibular ligament in an elite athlete

sometimes more proximal and may reflect associated damage to the distal adductor muscles.

5.6 Conclusion

Ligaments and tendons are complex collagenous soft tissue elements that respond to injury in a number of ways according to the age group of the patient and the mechanism of injury.

They can be imaged in a number of ways but MRI and ultrasound are the most informative techniques for assessing these structures.

Things to Remember

1. Tendons respond to injury in a number of ways, dependent on the patients' age.
2. Ultrasound is the best way of imaging superficial tendons and ligaments as it best demonstrates their microstructure.
3. MR Imaging is the preferred method of assessing associated injuries, especially those in bone. It can also assess ligament and tendon damage. This combination is especially useful in the knee.
4. Imaging is an important adjunct to the clinician who should first take a good history and perform a clinical examination. The imaging findings must fit the clinical picture, otherwise further investigation is mandatory.

References

Adler RS, Finzel KC (2005) The complementary roles of MR imaging and ultrasound of tendons. Radiol Clin N Am 43:771–807

Bloom W, Fawcett DW (1980) A textbook of histology, 11th edn. WB Sauders, Philadelphia

Cooke P (1989) The effects of mechanical characteristics of ligaments upon joint function and degeneration. Bristol, p 20

Delfaut EM, Demondion X, Bieganski A et al. (2003) The fibrocartilaginous sesamoid: a cause of size and signal variation in the normal distal posterior tibial tendon. Eur Radiol 13:2642–2649

Erickson SJ, Cox IH, Hyde JS et al. (1991) Effect of tendon orientation on MR imaging signal intensity: a manifestation of the «magic angle» phenomenon. Radiology 181:389

Fornage B (1986) Achilles tendon: US examination. Radiology 159:759–764

Kannus P, Jozsa L, Natri A et al. (1997) Effects of training, immobilization and remobilization on tendons. Scand J Med Sci Sports 7:67–71

Kastelic J, Baer E (1980) Deformation in tendon collagen. Symp Soc Exp Biol 34:397–435

Kastelic J, Galeski A, Baer E (1978) The multicomposite structure of tendon. Connect Tissue Res 6:11–23

O'Connor PJ, Groves C (2005) Trauma and sports-related injuries. In: Wilson D (ed) Paediatric musculoskeletal disease with an emphasis on ultrasound. Springer, Berlin Heidelberg New York, pp 19–38

Ohberg L, Alfredson H (2002) Ultrasound guided sclerosis of neovessels in painful chronic Achilles tendinosis: pilot study of a new treatment. Br J Sports Med 36:173–175; discussion 176–177

Robinson P, Barron DA, Parsons W et al. (2004) Adductor-related groin pain in athletes: correlation of MR imaging with clinical findings. Skeletal Radiol 33:451–457

Towers JD, Russ EV, Golla SK (2003) Biomechanics of tendons and tendon failure. Semin Musculoskelet Radiol 7:59–65

Valle M, Toma P, Martinoli C (2005) Ultrasonography of tendons and ligaments. Springer, Berlin Heidelberg New York

Van Dijk CN, Moll BW, Lim LS (1996) Diagnosis of ligament rupture of the ankle joint. Physical examination, arthrography, stress radiography and sonography compared in 16 patients after inversion trauma. Acta Orthop Scand 67:566–570

Van Holsbeeck MT, Introcaso JH (2001).Musculoskeletal ultrasound, 2nd edn. Mosby, St Louis

Wang JH, Iosifidis MI, Fu FH (2006) Biomechanical basis for tendinopathy. Clin Orthop Relat Res 443:320–332

Webb JM, Bulstrode CK (2004) Sports medicine and biomechnics. In: Russell RC, Williams NS, Bulstrode CJ (eds) Bailey and Love's short practice of surgery, 24th edn. Arnold, London, pp 506–517

Zeiss J, Saddemi SR, Ebraheim NA (1992) MR imaging of the quadriceps tendon: normal layered configuration and its importance in cases of tendon rupture. AJR Am J Roentgenol 159:1031–1034

6

Bone Marrow Edema in Sports Injuries: General Concept

Filip M. Vanhoenacker, Pieter Van Dyck, Jan L. Gielen, and Wim Geyskens

CONTENTS

F. M. Vanhoenacker, MD, PhD
P. Van Dyck, MD
J. L. Gielen, MD, PhD
Department of Radiology, University Hospital Antwerp, Wilrijkstraat 10, 2650 Edegem, Belgium
W. Geyskens, MD
Algemeen Ziekenhuis Maria Middelares, Hospitaalstraat 17, 9100 Sint-Niklaas, Belgium

Box 6.1. MRI

- Gold standard for evaluation of traumatic bone marrow edema
- May reveal associated soft tissue lesions or intra-articular pathology
- Fat suppression techniques are most valuable

Box 6.2. Standard radiography / (multidetector)-CT

- No role for depiction of bone marrow edema
- Main role is detection of (subtle) avulsion fractures

6.1 Introduction

Macroscopically, living bone consists of compact bone and cancellous bone.

Cancellous bone, also designated as trabecular or spongy bone is a honeycomb of large cavities with an internal latticework of bars and plates (trabeculae).

Compact bone is usually limited to the cortices of mature bones (cortical bone) and is most important in providing the strength of bone.

Cancellous bone lies in the inner part of the bone, and particularly, in case of the long bones, within their expanded ends (metaphyses and epiphyses). Cancellous bone gives additional strength to cortical bone and supports the bone marrow (Soames 1995).

Before the advent of Magnetic Resonance Imaging (MRI), trauma to the trabecular bone was difficult to assess on radiological examinations, because

the overlying cortex is often intact (Mandalia et al. 2005). This chapter will review bone marrow edema due to sports injuries, with special emphasis on the mechanisms of trauma, clinical significance and natural evolution.

6.2 Definition and Classification

'Bone bruise' was described for the first time in the knee by Yao and Lee in 1988. The term "bruise" indicates the traumatic origin of these bone marrow changes. It was defined as region of T2-hyperintensity in the absence of frank osseous fracture or subchondral cysts. MRI examination showed intraosseous areas, hyperintense on T2-weighted/STIR images and (to a lesser degree) hypo-intense on T1-images, in acutely injured joints with no abnormalities on plain radiographs. The use of an intermediate TE in FS T2-weighted images has an additional value in demonstrating underlying cartilage lesions. Since then bone bruise, bone contusion and occult fracture have been used interchangeably. Most authors use the term occult when standard radiograph shows no abnormalities but with the advent of multidetector CT with submillimetric multiplanar reconstructions we will probably have to redefine 'occult'. In radiologically overt fractures one can speak of accompanying bruise in the surrounding cancellous bone.

Several classification systems have been proposed. Most authors agree on differentiation between reticular and geographic/demarcated pattern. Others stress the importance of the location (subchondral versus at distance of joint space). Costa-Paz et al. (2001) proposes the following classification: type I: diffuse, often reticular, alterations of the medullary component, distant from the subjacent articular surface; type II (a and b) localized/geographic signal (mostly convex margins towards normal marrow) with contiguity to articular surface; type III: (slight) disruption or depression of the normal contour of the cortical surface/ subchondral lamella, often associated with type II lesion (small osteochondral compression fractures).

In a type II lesion compared to type I, the impact is more focally concentrated. Some authors describe subchondral impaction fractures as an additionally marked hypo-intense area on T1-WI directly beneath the subchondral lamella, representing focal cancellous impaction (possible patterns are geographic, crescent and linear). Those lesions can be designated as type IIb lesions.

Multidetector CT will of course pick up the focal depressions / osteochondral fractures (III) and probably also the subchondral impactions (IIb).

6.3 Pathogenesis of Bone Marrow Edema in Sports Injuries

Traumatic bone marrow edema (bruise) is most frequent and the underlying mechanism may be either acute or chronic.

Variable incidences have been published but edema is often encountered in acute trauma (published incidences vary from 27% to 72%).

A minority of the studies of acute injuries (knee and ankle) will show bruising only without associated injuries.

6.3.1 Acute Traumatic Lesions

Bone marrow edema is frequently encountered on MRI after an injury to the musculoskeletal system (Sanders et al. 2000). These osseous injuries may result from several forces acting on the joint. In general, compressive forces vs traction forces will influence the extent of BME edema around the joint (Hayes et al. 2000).

6.3.1.1 Impaction Injuries

Focal bruise may result from direct trauma to the bone (Fig. 6.1), but often a specific pattern of bone marrow changes on adjacent bones occurs due to impaction of one bone on another.

Impaction type of BME is extensive and will involve a broad surface of the involved bony structures.

6.3.1.2 Avulsive Injuries

Distraction injuries are usually due to valgus, varus or rotational stress on a joint, resulting in a small

Fig. 6.1. Bone marrow edema (BME) due to a direct blow (impaction type BME). Sagittal fat suppressed FSE T2-weighted image of the knee shows extensive BME at the anterior aspect of the distal femur

avulsion fracture related to a tendinous, ligamentous or capsular attachment on the bone.

Because the cortical bone is involved rather than the trabecular bone, the resulting "avulsion BME pattern" is much less extensive than in impaction injuries.

Moreover, the avulsed bone fragment may be very difficult to detect on MRI (Fig. 6.2a). In most instances, a small avulsion is far better demonstrated on conventional radiographs (Fig. 6.2b) or CT.

6.3.1.3 Complex Patterns

In most clinical situations, this rigorous distinction between *"pure impaction type injuries"* and "*avulsive type injuries*" is artificial, because both types will be seen in a single joint after acute traumatic injuries. Generally, the impaction type of bone marrow edema will be encountered on the *entry site* of the force acting on a joint, whereas a distraction type of bone marrow edema will be seen on the *exit site* of the force. Although avulsive type bone marrow edema is less extensive than the impaction type, the

a b

Fig. 6.2a,b. Typical example of an avulsion fracture and associated BME (avulsion type BME). **a** Coronal fat suppressed FSE T2-weighted image of the right knee shows only minor focal BME at the lateral aspect of the tibia. The bony avulsion fracture is barely visible. **b** Standard radiograph (AP spot view) clearly shows an avulsion fracture (Segond fracture)

former is usually the witness of underlying ligamentous sprain.

These soft tissue lesions are often less conspicuous than the bruises, though they are more important, at least in the short term follow-up, for stability reasons.

Indeed, sprain of the supporting structures of the joint may cause instability, if not recognised and appropriately treated.

Moreover, bone marrow edema around a joint is usually the result of a combination of multiple forces (and not of a single force), which all have a certain amplitude and direction. The impact of these forces may differ with the position of the joint at the moment of the trauma (e.g. degree of flexion, varus, valgus....).

Certain combinations of forces are known to cause a specific injury.

Systematic analysis of the BME-pattern, together with the associated soft tissue changes can often reveal the specific mechanism of injury.

In this regard, the pattern and distribution of BME represents a 'footprint' of the mechanism of acute trauma (Sanders et al. 2000).

In the knee for example, classic patterns which are encountered in sports injuries are the pivot shift injury (Figs. 6.3 and 6.4), the hyperextension injury (Fig. 6.5), the clip injury (Fig. 6.6), dashboard injury (Fig. 6.7) and (transient) lateral patellar dislocation (Fig. 6.8).

Pivot shift injury which occurs when valgus load is applied to the knee in various states of flexion, combined with external rotation of the tibia or internal rotation of the femur, will result in disruption of ACL. Resultant anterior subluxation of the tibia will cause impaction of the lateral femoral condyle against the posterolateral margin of the lateral tibial plateau. Therefore, BME will be present in the posterior aspect of the lateral tibial plateau and the middle portion of the lateral femoral condyle. Associated bone bruising at the posterior lip of the medial tibial plateau may be the result of contrecoup forces due to valgus forces (Kaplan et al. 1999). According to others this medial-sided bone bruise is attributed to avulsion at the semimembranosus attachment (Chan et al. 1999). Concomitant soft tissue injuries of the pivot shift injury are medial collateral ligament (MCL) lesions, lesion of the posterior horn of the lateral and medial meniscus or a tear at the posterior joint capsule.

Hyperextension injury results in a kissing contusion pattern in the anterior aspect of the distal femur and proximal tibia. Associated soft tissue lesions may include ACL or PCL tears or meniscal lesions.

The classic bone contusion pattern seen after lateral patellar dislocation includes involvement of the anterolateral aspect of the lateral femoral condyle and the inferomedial aspect of the patella.

Associated soft tissue injuries include sprain or disruption of the medial soft tissue restraints (medial

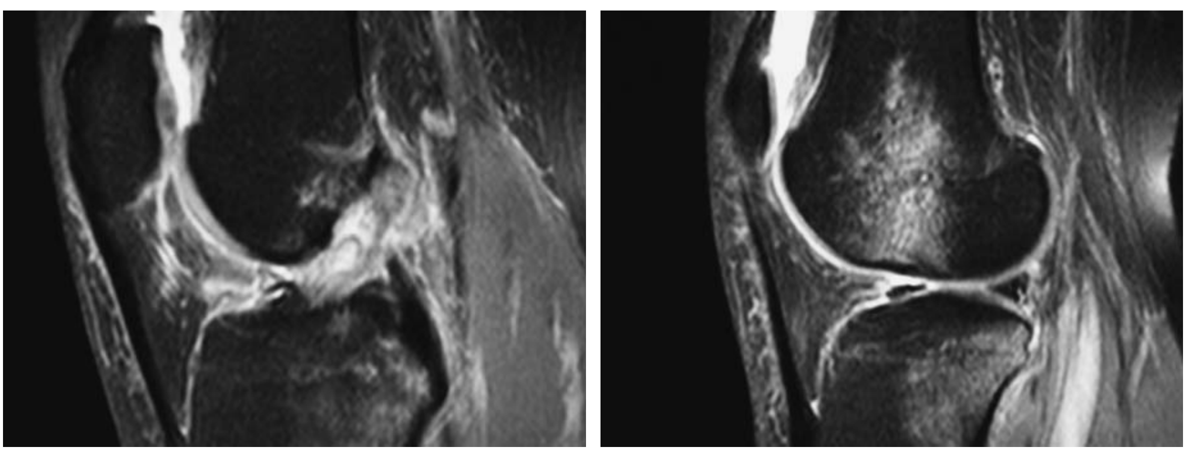

a b

Fig. 6.3a,b. Pivot shift injury due to a combination of external rotation of the tibia, valgus stress and flexion in a skier. These manoevers stress the anterior cruciate ligament (ACL), which is prone to rupture. **a** Midsagittal fat suppressed FSE T2-weighted image of the right knee shows complete disruption of the ACL. **b** Sagittal fat suppressed FSE T2-weighted image of the right knee. Due to anterior subluxation of the tibia relative to the femur, impaction occurs between the posterolateral margin of the lateral tibial plateau and the lateral femoral condyle, resulting in extensive impaction type BME

a b c

Fig. 6.4a–c. Another pivot shift injury in a soccer player with associated BME at the posteromedial corner of the knee. **a** Sagittal fat suppressed FSE T2-weighted image of the lateral aspect of the right knee. BME at the posterolateral aspect of the tibia and corresponding BME at the middle part of the lateral femur condyle (with associated focal cortical depression). **b** Midsagittal fat suppressed FSE T2-weighted image of the right knee shows complete disruption of the ACL. **c** Sagittal fat suppressed FSE T2-weighted image of the medial aspect of the right knee. Note also BME at the posteromedial aspect of the tibia near the distal of the semimembranosus tendon. According to some authors, this lesion represents a contre-coup impaction lesion. According to others, however, this lesion represents a traction injury at the posteromedial corner of the knee due to external rotation of the knee

retinaculum, medial patellofemoral ligament and the medial patellotibial ligament).

Clip injury occurs when pure valgus stress is applied to the knee while the knee is in mild flexion. BME is most prominent in the lateral femoral condyle due to impaction forces, whereas a second smaller area of edema may be present in the medial femoral condyle secondary to avulsive forces at the insertion of the MCL.

Dashboard injury occurs when a posteriorly directed force is applied to the anterior aspect of the proximal tibia while the knee is in a flexed position. This will result in BME at the anterior aspect of the tibia and occasionally at the posterior surface of the patella. Associated soft tissue injuries are disruption of the posterior cruciate ligament and posterior joint capsule.

Failure of this pattern approach revealing the underlying mechanism of trauma may be due to several factors, including insufficient trauma, massive injury, or pre-existing osteoarthritis associated with BME (Felson et al. 2001; Vanhoenacker et al.

Fig. 6.5. Hyperextension trauma in a soccer player. Midsagittal fat suppressed FSE T2-weighted image of the right knee. Severe hyperextension of the knee can result in the impaction of the anterior aspect of the femoral condyle against the anterior aspect of the tibial plateau. At the posterior aspect of the knee (distraction site), there is rupture of the posterior cruciate ligament and indistinct outline of the posterior joint capsule

Fig. 6.6. Clip injury in a soccer player. Coronal fat suppressed FSE T2 weighted image of the left knee shows a large area of BME involving the lateral femoral condyle. Minimal edema is noted within the medial femoral condyle near the proximal attachment of the MCL. There is partial disruption of the MCL

a

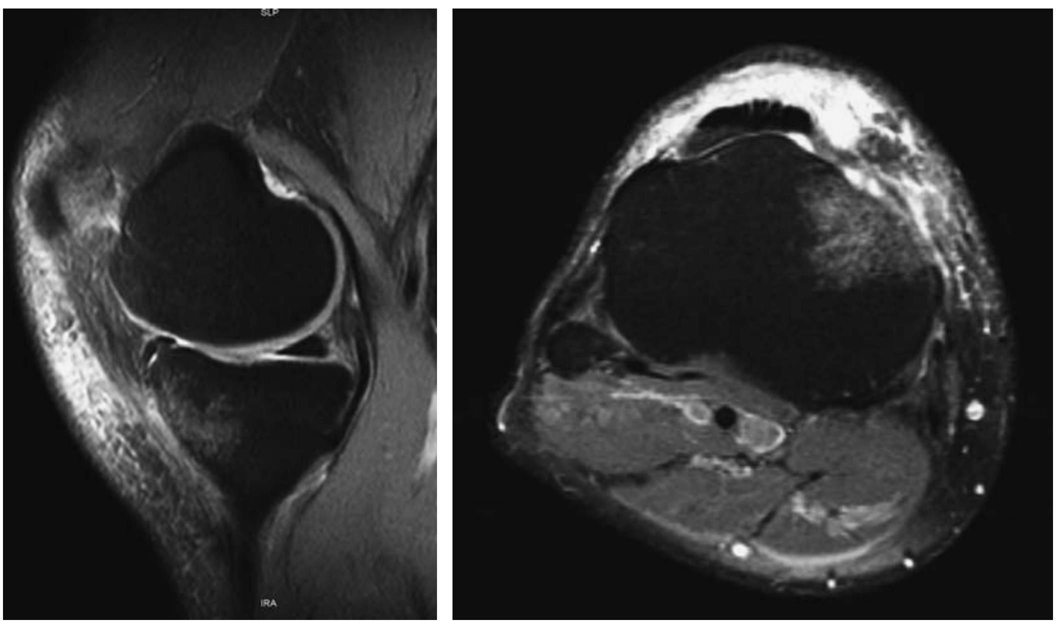

b

Fig. 6.7a,b. Dashboard injury. **a** Sagittal fat suppressed FSE T2-weighted image showing BME at the proximal tibia. **b** Axial fat suppressed FSE T2-weighted image demonstrating focal BME at the proximal tibia as well as an associated superficial infrapatellar bursitis

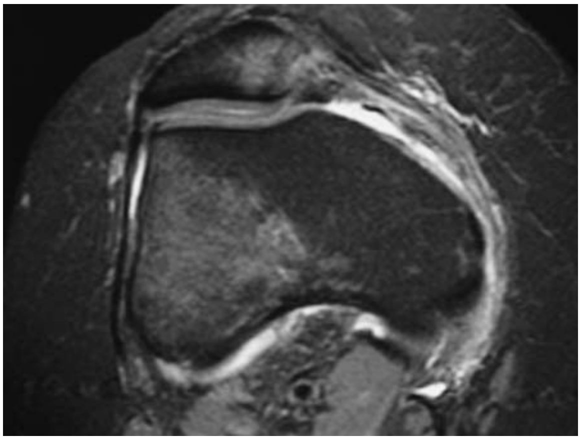

Fig. 6.8. Impaction type bone marrow edema, associated with lateral patellar dislocation in a soccer player. An axial fat suppressed FSE T2-weighted image of the right knee demonstrates BME involving the medial patellar facet and the anterior aspect of the lateral femoral condyle. Associated distraction at the medial patellar retinaculum will result in thickening and extensive hyperintensity due to partial disruption

2005), usually encountered in older sporters. Moreover, accelerated osteoarthritis is more prevalent in sporters than in the general population, due to previous repetitive trauma.

6.3.2 Chronic Traumatic Lesions (Repetitive Trauma)

Besides pure acute traumatic causes of BME, BME may result from repetitive or chronic trauma in sports activities.

6.3.2.1 Fatigue Fractures

Chronic stress on a normally mineralized bone may result in a spectrum of MRI findings ranging from periosteal edema over severe marrow edema to a hypo-intense fracture line in cancellous or cortical bone. This item will be described more in detail in Chap. 7.

6.3.2.2 Chronic Avulsive Injuries

Typical examples of chronic avulsive injuries include shin splints (traction periostitis of the calf muscles along the posteromedial tibia), thigh splints (distal adductor insertion avulsion syndrome) and adductor/gracilis syndrome.

Apart from periostal edema, MRI may also reveal BME and cortical signal abnormalities.

6.3.2.3 Altered Biomechanics and BME

Altered biomechanics due to certain sports activities (jogging, golf, etc.) may induce physiologic bone response to repeated stress. MRI may reveal bone marrow edema in these cases, which may not necessarily correspond with severe trauma (Grampp et al. 1998; Yochum and Barry 1997).

The potential role of limb malalignment and bone marrow edema was described by Felson et al. (2003). Medial bone marrow lesions can be seen in athletes with varus limb, whereas lateral lesions are associated with valgus limbs.

The importance of alignment is experimentally demonstrated by Libicher et al. (2005) in an in vivo MRI demonstration of the Pond-Nuki animal model for the evaluation of osteoarthritis. In this experimental study, 24 beagle dogs underwent transsection of the anterior cruciate ligament of the left leg (modified Pond-Nuki model). The first sign on MRI was the appearance of subchondral bone marrow edema at the posteromedial aspect of the tibia followed by progressive cartilage degeneration, meniscus degeneration and osteophytosis.

6.3.3 Lesions of Unknown Pathogenesis

Bone marrow edema syndromes without any history of trauma are increasingly recognized on MRI (Mandalia et al. 2005).

Distinction between bone bruising and marrow edema syndromes is primarily based on the clinical history of the patient.

6.3.3.1 Bone Marrow Edema Syndrome

Transient bone marrow edema syndrome (BMES) is an unusual but distinct selflimiting syndrome located at the weight bearing joints of the lower limbs (Toms et al. 2005). It usually affects middle-aged men and women in the last trimester of pregnancy, but association with sports activities has been reported (Miltner et al. 2003).

BMES usually affects only one bone, predominantly the proximal femur. The tarsal bones and the knee joint are involved less frequently (Radke et al. 2001).

Three distinct clinical phases have been described (Schapira 1992). In the first phase, pain is rapidly aggravated, with functional disability lasting approximately one month. The second phase, lasting one or two months, the pain reaches a plateau phase. The third phase is characterized by regression of symptoms. This period lasts approximately four months.

Imaging features consist of BME without associated findings on MRI (Hayes et al. 1993).

In the second phase of the disease, osteopenia may be present on the plain radiographs, whereas the third phase is characterized by reconstitution of bone density (Fig. 6.9).

Regional migratory Bone Marrow Edema Syndrome is a special form of BMES, characterized by migration between the weight-bearing joints. The lower limbs are most frequently involved (Hofmann 1999).

6.3.3.2 Bone Marrow Edema in Long Distance Runners

Bone marrow edema can be seen in recreational athletes one to eight weeks after sports running (Krampla et al. 2001; Trappeniers et al. 2003). The affected bones included the knee and the tarsal and metatarsal bones. STIR or T2-WI with spectral fat suppression are most sensitive to detect these edema patterns.

6.3.3.3 Subchondral Insufficiency Fracture

The concept of subchondral insufficiency fracture and its relationship with spontaneous osteonecrosis (SONK) and rapidly destructive osteoarthritis will be discussed briefly in Chap. 7 with regard to "overuse trauma and stress fractures".

6.4 Histopathological Correlation

A variety of histologic studies of patients with BME have been described with different results. Some studies revealed necrosis of cellular elements in the subchondral bone, trabecular microfractures and hemorrhage and edema (Johnson et al. 1998; Rangger et al. 1998; Ryu et al. 2000), whereas others demonstrated only edema with displacement of cel-

a b

Fig. 6.9a,b. Bone Marrow Edema Syndrome of the right foot two months after onset of symptoms at the foot. **a** Sagittal fat suppressed FSE T2-weighted image showing multifocal BME at the tarsal bones. **b** Plain radiograph demonstrating the presence of patchy osteopenia of the foot

lular elements, but absence of necrosis (Escalas and Curell 1994).

Review of the different histologic studies suggests that differing degrees and severity of injury may determine the differing histological patterns. Relatively less severe trauma causes marrow edema without obvious injury to the cellular element, whereas with increasing severity of trauma microfractures and hemorrhage are seen within the trabecular bone (Mandalia et al. 2005).

6.5 Clinical Significance

The clinical significance of bone marrow edema has been an issue of discussion even since the first reports on bone bruise.

It is very difficult to identify clinical signs and symptoms directly attributable to the underlying bone bruising, because there are usually associated soft tissue changes (Mandalia et al. 2005).

In a prospective study of 95 patients with inversion injuries of the ankle and no fracture on plain radiographs, Alanen et al. (1998) found an incidence of bone bruises of 27%. Most of the bruises were located in the talus, typically in the medial part.

The authors found no statistical difference in the time to return to work, limitation in walking or physical activity and clinical outcome at three months in two groups with and without BME. These findings were in line with a previous study by Zanetti et al. (1997).

Vincken et al. (2005) evaluated the clinical consequences of bone bruise on MRI around the knee in 664 consecutive patients with subacute knee complaints. They evaluated the relation between bone bruise and (peri-)articular derangement and the impact of bone bruise at the time of MRI and six months thereafter.

Bone bruises were diagnosed in 18.7% of patients.

They concluded that bone bruise is no predictor for the presence of intra-articular pathology. Indeed, prevalence of bone bruise was not significantly different between patients with (21%) and those without (16%) intra-articular pathology. Bone bruise was particularly associated with tears in anterior cruciate ligaments, collateral ligaments and lateral meniscus, whereas the medial meniscus tears (although representing the most common knee lesion) were not associated with bone bruise.

On the other hand, patients presenting with bone bruise at the time of MRI had a significant higher level of symptoms, functional deficit and decrease in activity.

In particular, the presence of bone bruise and MCL tear has the most impact on function and symptoms at the time of MRI.

However, bone bruise did not have any effect on function, symptoms and activity at six months.

Future long-term prospective studies are required to answer the question related to the clinical significance of BME.

6.6 Natural Evolution

6.6.1 Follow-up of Acute Traumatic Bone Marrow Edema

The reported time for the resolution of bone bruising is variable, ranging from as early as three weeks to two years (Mandalia et al. 2005; Roemer and Bohndorf 2002). This variability may be attributed to several factors, such as the severity of injury, extent of bone bruising and other associated internal knee derangement. Future large prospective studies are required to validate those factors affecting the radiological evolution of bone bruising (Mandalia et al. 2005).

Two patterns of bruise resolution have been described by Davies et al. (2004). The *centripetal* pattern is the most frequent (Fig. 6.10.), whilst other lesions (mostly types IIb and III) tend to resolve *towards the joint margin* (see also Chap. 28). The latter generally resolve more slowly and probably require longer rehabilitation because of higher risk of premature osteo-arthritis.

The natural history of bruises is not well known as well as whether they predispose to premature osteoarthritis.

Many studies have shown that bone bruising may have a deleterious effect on the overlying articular cartilage, although this concept is not generally accepted (Mandalia et al. 2005). The pathophysiological mechanisms by which the cartilage can undergo this degenerative process may be multifactorial. The initial blunt trauma might exceed a supraphysiological threshold and lead to progressive chondral damage

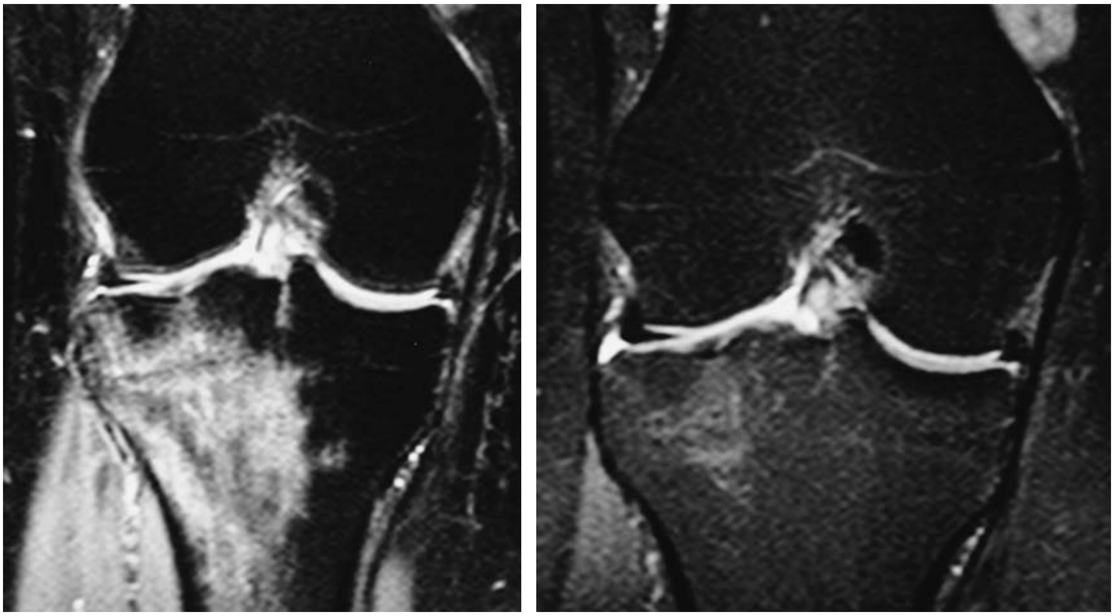

Fig. 6.10a,b. Resolution pattern of BME. Coronal fat suppressed FSE T2 weighted image of the right knee at the moment of a direct trauma at the knee (**a**) and after three months follow-up (**b**). **a** Extensive impaction BME at the proximal tibia. **b** There is centripetal resolution of BME, with some residual BME at the center of the original lesion

(Mankin 1982). Additionally, the osseous lesion might heal into a stiffer construction than the previous normal bone. The decreased compliance might then generate greater loads in the articular cartilage, leading to a progressive cartilage degeneration.

6.6.2 Follow-up of Chronic Traumatic Lesions

This item will be described more in detail in Chap. 28 on "Monitoring and Natural History of Fractures and Microfractures".

6.6.3 Follow-up of BMES

In BMES, the mean interval from the onset of symptoms until complete clinical resolution ranges from 4 to 24 months, with an average of 6 months. All patients with BMES recover completely without intervention. Therefore, the term transient BMES can be used. Recovery, however, can be speeded up with vasodilatators (Aigner et al. 2002).

6.7 Conclusion

BME is a relatively recently recognized entity. MRI has proved to be the most powerful tool to assess BME, as conventional imaging techniques are insensitive for detection of trabecular injuries.

The pathogenesis of BME is variable and may be due to acute or chronic trauma or even causes without any history of obvious trauma.

Distinction between traumatic and non-traumatic bone marrow edema in sports injuries is primarily based on a clinical history of trauma, as imaging features are mostly indistinguishable.

In traumatic cases, the pattern of bone marrow edema, however, may reveal the mechanism of underlying trauma and is often a secondary sign for detecting associated abnormalities.

The clinical significance of BME is still a matter of debate, and long-term follow-up studies are required for further evaluation of this item.

Things to Remember

1. MRI is the imaging modality of choice to detect bone marrow lesions in sports injuries. Fat-suppressed T2-weighted images or (S)TIR sequences are the most sensitive-ones.
2. Mostly BME in itself is benign/self limited. Longer follow-up studies are needed to determine the clinical importance of the osteochondral sequelae and to evaluate the possible evolution towards premature degeneration. Isolated bruise can be the cause of pain.
3. Moreover, a systematic analysis of the BME-pattern often reveals a specific underlying trauma-mechanism. This can help to detect the associated soft tissue lesions, which are often less conspicuous.
4. Residual indications for conventional radiography (and/or CT) are (subtle) avulsion fractures and some stress fractures.

References

Aigner N, Petje G, Schneider W et al. (2002) Juvenile bone marrow oedema of the acetabulum treated by iloprost. J Bone Joint Surg Br 84:1050–1052

Alanen V, Taimela S, Kinnunen J et al. (1998) Incidence and clinical significance of bone bruises after supination injury of the ankle. A double-blind prospective study. J Bone Joint Surg Br 80:513–515

Chan KK, Resnick D, Goodwin D et al. (1999). Posteromedial tibial plateau injury including avulsion fracture of the semimembranosus tendon insertion site: ancillary sign of anterior cruciate liagment tear at MR imaging. Radiology 211:754–758

Costa-Paz M, Musculo DL, Ayerza M et al. (2001) Magnetic resonance imaging follow-up study of bone bruises associated with anterior cruciate ligament ruptures. Arthroscopy 17:445–449

Davies NH, Niall D, King LJ et al. (2004) Magnetic resonance of bone bruising in the acutely injured knee-short-term outcome. Clin Radiol 59:439–445

Escalas F, Curell R (1994) Occult posttraumatic bone injury. Knee Surg Sports Traumatol Arthrosc 2:147–149

Felson DT, Chaisson CE, Hill CL et al. (2001) The association of bone marrow lesions with pain in knee osteoarthritis. Ann Intern Med 134:541–549

Felson DT, McLaughlin S, Goggins J et al. (2003) Bone marrow edema and its relation to progression of knee osteoarthritis. Ann Intern Med 139:330–336

Grampp S, Henk CB, Mostbeck GH (1998) Overuse edema in the bone marrow of the hand: demonstration with MRI. J Comput Assist Tomogr 22:25–27

Hayes CW, Conway WF, Daniel WW (1993) MR imaging of bone marrow edema pattern: transient osteoporosis, transient bone marrow edema syndrome, or osteonecrosis. Radiographics 13:1001–1011

Hayes CW, Brigido MK, Jamadar DA et al. (2000) Mechanism-based pattern approach to classification of complex injuries of the knee depicted at MR imaging. Radiographics 20:S121–134

Hofmann S (1999) Bone marrow edema in transient osteoporosis, reflex sympathetic dystrophy and osteonecrosis. In: Jocob RP, Fulford P, Horan F (eds) European instructional course lectures. The British Editorial Society of Bone and Joint Surgery, London, pp 138–151

Johnson DL, Urban WP Jr, Caborn DNM et al. (1998) Articular cartilage changes seen with magnetic resonance imaging-detected bone bruises associated with acute anterior cruciate ligament rupture. Am J Sports Med 26:409–414

Kaplan PA, Gehl RH, Dussault RG et al. (1999). Bone contusions of the posterior lip of the medial tibial plateau (contrecoup injury) and associated internal derangement of the knee at MR imaging. Radiology 211:747–753

Krampla W, Mayrhofer R, Malcher J et al. (2001) MR imaging of the knee in marathon runners before and after competition. Skeletal Radiol 30:72–76

Libicher M, Ivancic M, Hoffmann M et al. (2005) Early changes in experimental osteoarthritis using the Pond-Nuki dog model: technical procedure and initial results of in vivo MR imaging. Eur Radiol 15:390–394

Mandalia V, Fogg AJB, Chari R et al. (2005) Bone bruising of the knee. Clin Radiol 60:627–636

Mankin HJ (1982) The response of articular cartilage to mechanical injury. J Bone Joint Surg Am 65:951–957

Miltner O, Niedhart C, Piroth W et al. (2003) Transient osteoporosis of the navicular bone in a runner. Arch Orthop Trauma 124:646–647

Radke S, Vispo-Seara J, Walther M et al. (2001) Transient bone marrow edema of the foot. Int Orthop 25:263–267

Rangger C, Kathrein A, Freund MC et al. (1998) Bone bruise of the knee: histology and cryosections in 5 cases. Acta Orthop Scand 69:291–294

Roemer FW, Bohndorf K (2002) Long-term osseous sequelae after acute trauma of the knee joint evaluated by MRI. Skeletal Radiol 31:615–623

Ryu KM, Jin W, Ko YT et al. (2000) Bone bruises: MR characteristics and histological correlation in the young pig. J Clin Imaging 24:371–380

Sanders TG, Medynski MA, Feller JF et al. (2000) Bone contusion patterns of the knee at MR Imaging: footprint of mechanism of injury. Radiographics 20:S135–S151

Schapira D (1992) Transient osteoporosis of the hip. Semin Arthritis Rheum 22:98–105

Soames RW (1995) Skeletal system. In: Williams PL (ed) Gray's anatomy. Churchill Livingstone, New York, pp 425–736
Toms AP, Marshall TJ, Becker E et al. (2005) Regional migratory osteoporosis: a review illustrated by five cases. Clin Radiol 60:425–438
Trappeniers L, De Maeseneer M, De Ridder F et al. (2003) Can bone marrow edema be seen on STIR images of the ankle and foot after 1 week of running. Eur J Radiol 47:25–28
Vanhoenacker FM, Snoeckx A, Vandaele L et al. (2005) Bone marrow changes in sports injuries. JBR-BTR 88:332–335
Vincken PW, Ter Braak BP, van Erkel AR et al. (2005) Clinical consequences of bone bruise around the knee. Eur Radiol, DOI 10.1007/s00330-005-2735-8
Yao L, Lee JK (1988) Occult intraosseous fracture: detection with MR imaging. Radiology 167:749–751
Yochum TR, Barry MS (1997) Bone marrow edema caused by altered pedal biomechanics. J Manipulative Physiol Ther 20:56–59
Zanetti M, De Simoni C, Wetz HH et al. (1997) Magnetic resonance imaging of injuries to the ankle joint: can it predict clinical outcome? Skeletal Radiol 26:82–88

Overuse Bone Trauma and Stress Fractures

7

Annick Demeyere and Filip M. Vanhoenacker

CONTENTS

A. Demeyere, MD
Department of Radiology, Imelda Hospital, Imeldalaan 9, 2820 Bonheiden, Belgium
F. M. Vanhoenacker, MD, PhD
Department of Radiology, University Hospital Antwerp, Wilrijkstraat 10, 2650 Edegem, Belgium

Box 7.1. Plain films

- Always the initial first imaging modality
- First signs of stress fractures in cortical bone are gray cortex sign, cortical striations and periosteal new bone formation
- Early signs in cancellous bone are subtle and include blurring and faint sclerotic radiopaque areas

Box 7.2. Bone scintigraphy

- Very sensitive but lacks specificity
- Particularly useful for demonstration of multiple stress fractures, and distinguishing bipartite bones from stress fractures
- Too sensitive for stress reactions and subclinical bone remodeling
- Not useful for follow-up the healing

Box 7.3. CT scan

- Less sensitive
- Specific indication are complex anatomical sites, longitudinal stress fractures and differential diagnosis with tumoral lesions

Box 7.4. MR imaging

- Comparable sensitivity and higher specificity than scintigraphy distinguishing bone involvement from soft-tissue injuries
- More accurate in grading the stage of stress fractures and predicting the time of recovery
- No radiation exposure, non-invasive

7.1 Introduction

Stress related bone injuries are common in athletes and account for up to 10% of cases in sports medicine practice. Stress fractures have been classified into two types: fatigue and insufficiency. The fatigue fracture is caused by an abnormal stress to a normally elastic bone. Fatigue fractures are thought to occur in different sites depending on the age, sex and activity of the athlete. Insufficiency fractures arise from the application of a normal stress on a bone that is mineral deficient or abnormally inelastic. Insufficiency fractures are most prevalent in nutrient-deficient (osteomalacia) and older populations in whom osteoporosis and rheumatoid arthritis are more common (Romani et al. 2002; Anderson and Greenspan 1996). The focus of this chapter is sports-related injuries and so this latter will not be further discussed.

Stress fractures are common injuries frequently seen in athletes and military recruits. Although the reported incidence of stress fractures in the general athletic population is less than 1%, the incidence in runners may be as high as 20%. But with the increasing emphasis on exercise for the elderly and the recreational athletic population, stress fractures should not be overlooked in this population.

Although stress fractures have been described in nearly every bone, they are most common in the weight-bearing bones of the lower extremities. Specific anatomic sites for stress fractures may be associated with individual sports, such as the humerus in throwing sports, the ribs in golf and rowing, the spine in gymnastics, the lower extremities in running activities, and the foot in gymnastics (Bennell and Brukner 1997). In a review of 370 athletes with stress fractures, the tibia was the most commonly involved bone (49.1% of cases), followed by the tarsals (25.3%), the metatarsals (8.8%) (Boden and Osbahr 2000) and pelvis. Bilateral stress fractures occurred in 17% of cases.

Pain in the lower leg brought on by exercise but relieved by rest is a common complaint. Stress injuries involving the tibia account for up to 75% of exertional leg pain, and encompass several clinical syndromes such as medial tibial syndrome (shin splints), chronic compartment syndrome, soleus syndrome, and stress fracture (Bhatt et al. 2000).

Accurate diagnosis of a stress lesion is essential in the early phase after the onset of pain to apply specific treatment and to insure an early return to sports activity.

7.2 Pathophysiology

7.2.1 Anatomy of Bone

Bone has both cortical and cancellous components (Fig. 7.1). Cortical bone is dense and highly organized and withstands stress in compression better than in tension. Cancellous (trabecular) bone is an irregularly shaped meshwork and withstands stress according to the alignment of the fiber matrix. The outer shafts of long bones are mainly cortical, with

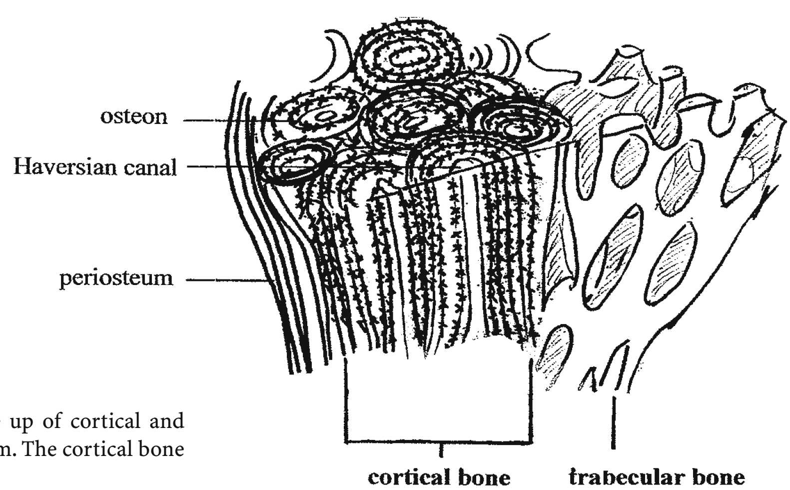

Fig. 7.1. Anatomy of bone. Bone is made up of cortical and trabecular bone surrounded by periosteum. The cortical bone unit is the osteon

a large percentage of cancellous bone making up the ends of the bone and the central portion of the shaft. Short and flat bones such as the tarsals and pelvis have a higher amount of cancellous bone.

The fundamental unit of cortical bone is the osteon (Fig. 7.2). In the osteon, concentric layers of lamellar bone surround small channels called Haversian canals. These canals house nerves and blood vessels. On the outside of the lamellae are small cavities, known as lacunae. Each lacuna contains a single bone cell, or osteocyte. Canaliculi form a transport system between the lacunae and the Haversian canals which are responsible for the nutrition and metabolic transport system within the bone.

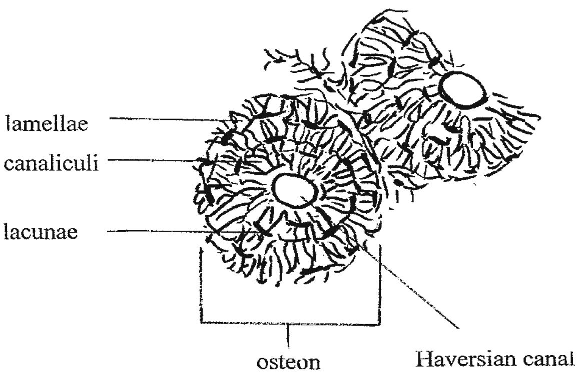

Fig. 7.2. Anatomy of an osteon. An osteon is made up of concentric lamellae and lacunae (containing an osteocyte) and include a central Haversian canal. The canaliculi form the transport system between the lacunae and the Haversian canals

The outer surface of long bones is surrounded by a highly vascular outer coating called the periosteum. The periosteum is responsible for providing nutrition to the outer portion of the cortex and enlarges during remodeling to provide support to the cortex. On the inner portion of the cortex, medullary canals allow the vascular passage for nutrients and blood vessels to the inner two-thirds of the cortex (Romani et al. 2002).

7.2.2 Remodeling of Bone

Bone constantly remodels in order to endure external forces (Mori and Burr 1993). According to the column law, the magnitude of stress is greatest on the surface of a column and decreases to zero at the center. Therefore, most of the remodeling in long bones takes place in the outer cortex. Remodeling consists of both resorption of existing bone by osteoclasts and formation of new bone cells by osteoblasts. Participating in regular activity promotes bone strength through proper perfusion of nutrients to the osteocytes and normal bone remodeling. Conversely, a sedentary lifestyle contributes to bony atrophy (Mori and Burr 1993).

Activation of osteoclasts is required for the start of the remodeling process. The piezoelectric effect is one mechanism implicated in the activation of bone remodeling. Tension forces create a relative electropositivity on the convex, or the tension side, of the bone. Thus, as bending produces repeated distraction forces at a focal point of a bone, the electropositive charge may stimulate osteoclastic resorption (Romani et al. 2002).

The streaming effect is the movement of extracellular fluids in the Haversian canals and canaliculi during deformation. If the surface charge on the Haversian canal or canaliculi walls is positive, negative ions in the fluid are attracted to the outside of the fluid stream, creating a positively charged current in the middle. As bone is bent, the positive stream is forced toward the open or distracted surface of bone. This electropositive stream may, in turn, stimulate osteoclastic activity. Other possible activators are bone 'sensors' that recognize increased and decreased mechanical strains, hormones, decreased venous flow and decreased oxygen.

Upon activation, osteoclastic cells form a cone and begin to secrete proteolytic enzymes to cut longitudinal tunnels through the bone. This tunnels correspond to the striations, which are seen on all imaging modalities (see below). These new Haversian canals are aligned with the stresses placed on the bone. Each osteoclast cone can resorb nearly three times its volume in burrowing a canal 3–10 mm deep. The new Haversian canals are filled with osteoblasts that create a mineralized matrix supporting the walls of the new channel. The remaining space of the channel is then filled with immature lamellar bone.

Haversian canal formation and osteoblast support with lamellar bone begins 10–14 days after the onset of remodeling. The conversion of lamellar bone into mature osteocytes cells lags behind resorption by about a week and may continue for as long as 20–90 days. The result is a temporarily weakened bone due to the new, hollow Haversian canals. The inflammation of periosteum is designed to bolster the weakened area of bone until it can

mature. However, the periosteum does not mature until about 20 days after the remodeling process begins. This six- to ten-day lag between the deposit of immature lamellar bone and periosteal maturity leaves the bone temporarily weakened at the point of stress during the third week of remodeling. Continued stress applied to remodeling bone during the 'weak third week' may lead to an accelerated breakdown of the cortex. It is at this time that a stress fracture is most likely to develop.

7.2.3 Pathophysiology of Stress Fractures

Until recently, the cause of stress fractures was thought to be due to the breakdown of bone after repetitive loading. It has been estimated that, at normal physiologic levels of strain, it would require 10^8 cycles of loading to produce failure of a weight-bearing bone such as the tibia. This level of loading is not easily attained, and stress fractures commonly occur soon after the onset of a stressful activity. The rapid onset of symptoms and bone remodeling (sometimes within the first seven days) consistent with stress fracture suggest that mechanical stress cannot be the only cause.

Recently, several studies demonstrate that impaired bone perfusion may be the most important factor in the pathogenesis of stress fractures.

Otter et al. (1999) proposed that the perfusion and reperfusion of bone after a repetitive load causes a temporary oxygen debt to the area of bone being stressed. This ischemia, in turn, facilitates bone remodeling and subsequent bone weakness and stress fracture. When a bone is loaded to normal physiologic levels, the small blood vessels that supply the cortex are squeezed. In most cases, this pressure is necessary for proper movement of the blood. When the load is higher, the blood flow may be temporarily cut off. The result is a brief period of ischemia in the cells that would normally be perfused by the compressed medullary vessels. Repeated loads over a prolonged period of an activity, such as a long run, cut off the oxygen during that period as well. This decrease in oxygen to the bone is believed to trigger the remodeling process.

Restriction of venous flow without any mechanical loading is another mechanism for stimulation of bone remodeling (Romani et al. 2002).

Repeated pressure to the capillaries is also believed to cause microdamage to the vessels. As neutrophils respond to plug the damaged capillaries, the blood flow through the vessels is further restricted. In addition, small leaks in the vessels allow fluid flow into the surrounding tissue during reperfusion, further restricting the perfusion of oxygen into the cells. This leaking increases with subsequent bouts of loading, worsening ischemia and triggering a further increase in remodeling. The repetition of this cycle causes an increase in remodeling, a breakdown in the cortex, a weakening of the bone, and potentially a stress fracture (Romani et al. 2002; Otter et al. 1999).

Direct damage to the extracellular matrix may also initiate angiogenesis (Globus et al. 1989). Cultured platelets have recently been shown to stimulate osteogenic activity by releasing growth factors (Slater et al. 1995). Clearly, bone remodeling and angiogenesis are intimately related, and the major stimulus initiating each process may be altered bone perfusion, rather than an altered strain environment by itself.

7.3 Mechanisms of Injury

A stress fracture is a partial or incomplete fracture caused by the accumulation of stress forces to a localized area of bone. Stress fractures are not the result of a single insult. Instead, they arise as the result of repetitive applications of stresses that are lower than the stress required to fracture the bone in a single loading (Romani et al. 2002).

Bone endures a stress whenever a force is loaded upon it. Whether the stress comes from the pull of a muscle or the shock of a weight-bearing extremity contacting the ground, it is defined as the force applied per unit area of the loadbearing bone. Low levels of these forces cause bone to deform, which is known as strain. The stress-strain response of bone depends on the direction of the load; the geometry, microarchitecture, and density of bone; and the influence of surrounding muscular contractions.

In most activities of daily living, when the force is removed, the bone elastically rebounds to its original position. The force that a bone can endure and still rebound back to its original state without damage is within the elastic range. Forces that exceed a critical level above the elastic range are in the plastic range. Once forces reach the plastic range, a lower

load causes greater deformation; it is at this level that forces accumulate to cause permanent damage to bone.

Forces can be applied to bone through compression, tension, bending, torsion or shear. Compression forces are generally seen in cancellous bones, such as the calcaneus and femoral neck. Tension forces result in bone pulling away from bone, as is common in compact bones such as the tibia en femur. As the load is applied to the bony shaft through a bend; a tension strain is placed upon the convex surface of the shaft and compressive forces act on the concave side.

Several theories have been established to explain the development of stress fractures and it is likely a combination of the following factors that ultimately results in bone fatigue and fracture (Haverstock 2001; Spitz and Newberg 2002; Anderson and Greenspan 1996).

7.3.1 Muscle Fatigue Theory

One of the major roles of muscle is to minimize the tensile stress on bone (Spitz and Newberg 2002). The muscles decrease bending or tensile forces in bone and increase compressive forces. Because bone is more resistant to force in compression than tension, the supporting muscles help prevent fatigue fractures. When the supporting structures fatigue, the tensile forces increase, rendering bone failure more likely (Ross 1993). The muscles also have a shock absorption function by dissipating forces away from bone (Haverstock 2001; Anderson and Greenspan 1996). Accordingly, fatigue of muscles in the poorly conditioned athlete creates increased tensile stress on bone and decreased shock-absorbing capacity, resulting in stress fracture.

7.3.2 Overload or Increased Muscle Strength Theory

Another explanation of stress fractures relates to increased muscle strength. Under normal conditions, when a new stress is applied, muscle tone is achieved more quickly than bone strengthening. This results in a mechanical imbalance, with muscle exerting an excess of load on bone, resulting in bone fatigue (Spits and Newberg 2002; Haverstock 2001; Anderson and Greenspan 1996; Ross 1993).

7.3.3 Remodeling Theory

The physiologic response of bone to stress is also important in the pathophysiology of stress injury. Bone is a dynamic tissue that requires stress for normal development, and it undergoes constant remodeling in response to changing environmental forces. Initially, osseous remodeling manifests as osteoclastic activity and resorption of lamellar bone. This is subsequently replaced by denser, stronger osteonal bone. In repetitive stress overload, however the accelerated remodeling results in an imbalance between bone resorption and bone replacement, leading to weakening of the bone. Continued stress results in further imbalance, leading to bone fatigue, injury, and fracture. Osseous stress injury is not an all-or-none phenomenon, but a physiologic continuum ranging from normal osseous remodeling, to accelerated remodeling with fatigue and early injury, to frank stress fracture (Spits and Newberg 2002; Haverstock 2001; Ross 1993).

7.4 Risk Factors

7.4.1 Training Factors

7.4.1.1 Alteration of Training

Stress fractures often result from participation in a new activity or from an alteration in a training program such as an increase in intensity, duration, or frequency of training in a short time span. Stress fractures related to a single training session have been described as well (Haverstock 2001).

7.4.1.2 Footwear and Training Surfaces

Inadequate footwear that has lost its shock absorptive properties does not provide sufficient cushioning increasing the risk for fatigue fracture.

A hard running surface also can be a factor, particularly if the runner’s footwear is inadequate or he/she is running in a state of fatigue when the skeletal structure is absorbing the impact of the running surface (Haverstock 2001).

7.4.2 Lower Extremity Biomechanics

7.4.2.1 Pronated Foot

The pronated foot with a rearfoot valgus position produces increased stress on the lateral malleolus. When the foot pronates through the midstance phase of gait into the toe-off phase, the first metatarsal is hypermobile and dorsiflexes, resulting in an increased pressure load on the second metatarsal. If the second metatarsal is short, then increased load is transferred to the third metatarsal (Haverstock 2001).

7.4.2.2 Cavus Foot

The cavus foot is generally rigid in nature and the shock absorptive properties are poor. The plantarflexed forefoot results in increased pressure on the metatarsals. A rigidly plantarflexed first metatarsal is placed under increased stress, which places the sesamoid complex at risk of stress fracture. A long or plantarflexed lesser metatarsal is exposed to a greater load and is subjected to fatigue failure. Limited subtalar joint motion produces increased pressure on the calcaneus and renders it susceptible to a stress fracture (Haverstock 2001).

7.4.2.3 Varus Alignment

Varus alignment such as genu varum, tibia vara, subtalar varus and forefoot varus is associated with lower extremity stress fractures, 49% of which are located at the tibia. The resulting excessive pronation increases the eccentric work that must be done by the medial aspect of the soleus muscle and enforces the strain on the posteromedial side of the tibia (Krivickas 1997).

7.4.2.4 Limb Length Discrepancy

Limb length discrepancy is a relatively common skeletal malalignment with predisposition to stress fractures. It has been reported that runners with a leg length discrepancy experienced stress fractures more often than runners without. During running, the short leg rotates externally to increase stability and overstriding may occur. The foot on the short side is subjected to greater force over a short period of time (Haverstock 2001).

7.4.3 Systemic Factors

7.4.3.1 Bone Mineral Density (BMD)

The BMD increases with age, up to about the age of 35 years, and slowly decreases thereafter. Especially in the premenarcheal years, the increase in BMD and exercise-induced bone modeling is most significant (Morris et al. 1997).

Lauder et al. (2000) found a strong positive association between the body mass index and the BMD and the probability of stress fractures. Low body weight is a well-known risk factor associated with low BMD in women, especially female athletes.

Although exercise has been reported to increase BMD, it is well established that stress fractures occur more frequently in subjects who exercise intensely. Consistent with these findings, Lauder et al. (2000) described a gradual increase in BMD as the hours of exercise per week increased. At the same time, the percent of women with stress fractures increased from 12% among those performing 5 h or less of exercise per week to 50% among those exercising 10 h or more per week.

Other factors causing a low BMD are Caucasian race, any condition that results in altered gait or an ipsilateral joint prosthesis and systemic factors (Cohn et al. 1977; Anderson and Greenspan 1996; Hester 2001; Romani et al. 2002). These are summarized in Table 7.1. As most of these factors are not seen in sports medicine, further discussion is beyond the scope of this chapter.

7.4.3.2 Female Sex

A high incidence of stress fractures has been reported in women (Boden and Osbahr 2000; Anderson and Greenspan 1996; Romani et al. 2002; Bennell and Brukner 1997). They seem to occur more commonly in the sacrum, pelvis and femoral neck. Therefore, it is especially important to investigate intrinsic factors in female athletes. The term ‘female athlete triad’ refers to the combination of an eating disorder, amenorrhea, and osteoporosis. In an effort to minimize body fat and maintain high athletic perfor-

Table 7.1. Systemic factors that influence the development of (insufficiency) stress fractures

Metabolic disorders
- Osteoporosis
- Osteomalacia
- Hyperparathyroidism, Cushing's syndrome, hypothyroidism, renal insufficiency
- Rickets
- Scurvy
Inflammatory conditions
- Rheumatoid arthritis
- Osteomyelitis
Bone dysplasias
- Osteogenesis imperfecta
Neurological disorders
- Neurotrophic diseases
- Poliomyelitis
Paget's disease
Pharmacological
- Corticosteroids
- Diuretics
- Anticonvulsants
Nutritional deficiencies
Sleep deprivation
Smoking

mance, many young women develop eating disorders during puberty. Amenorrhea and oligomenorrhea are common findings in competitive female distance runners. The resultant estrogen-deficient state leads to decreased bone mineral density and an increased risk of stress fractures.

Bennell et al. (1996) showed in his study that age of menarche and calf girth were the best independent predictors of stress fractures in women. Their bivariate model correctly assigned 80% of the female athletes into their respective stress fracture or nonstress fracture groups. Their results suggest that it may be possible to identify female athletes most at risk for this overuse bone injury.

7.5 Diagnostic Imaging

Bone response to stress is evaluated on a dynamic continuum between early remodeling and periostitis to a cortical stress fracture. It is important to note that these bony changes reflect a wide spectrum of physical findings and radiographic presentations.

7.5.1 Radiography

Plain radiography plays an important role in the initial work-up of a suspected stress fracture. They can be used to confirm the diagnosis at a relatively low cost. Unfortunately, initial radiographs are often normal, which is not surprising given the degree of microscopic remodeling that occurs in the early stages of stress injury. The sensitivity of early radiographs can be as low as 15%, and follow up radiographs will demonstrate diagnostic findings in only 50% of cases (Nielsen et al. 1991). The lag time between manifestation of initial symptoms and detection of radiographic findings ranges from one week to several months, and cessation of physical activity may impede the development of typical plain radiographic findings (Fig. 7.3) (Anderson and Greenspan 1996; Spitz and Newberg 2002).

In addition to the time course, radiographic changes are dependent on the type of bone involved (Table 7.2).

Initial changes in the cortical bone are the so called "gray cortex" sign seen as a subtle ill definition of the cortex (Mulligan 1995) or faint intracortical radiolucent striations, which are presumably related to the osteoclastic tunneling found early in the remodeling process (Muthukumar et al. 2005; Daffner and Pavlov 1992). These changes may be easily overlooked until periosteal new bone formation and/or endosteal thickening develops in an apparent attempt to buttress the temporarily weakened cortex. As damage increases, a true fracture line may appear. These injuries typically involve the shaft of a long bone and are common in the posterior portion of the tibia in runners (Fig. 7.4).

Stress injuries in cancellous bone are notoriously difficult to detect. Subtle blurring of trabec-

Fig. 7.3a–c. Metatarsal stress fractures on radiography. **a** Subtle faint periosteal reaction on the lateral aspect of the diaphysis of the second metatarsal in a 42-year-old patient (stress fracture grade 2). **b** The plain film of the same patient one month later shows obvious more periosteal new bone formation (stress fracture grade 3). **c** Stress fracture of the second metatarsal from another patient (30-year-old) with a true fracture line and periosteal new bone formation (grade 4)

Table 7.2. Radiologic grading system for stress injuries: the correlation between histology, radiography, bone scintigraphy and MR imaging

	Stress reaction	Grade 1	Grade 2	Grade 3	Grade 4
Histology	-	Periosteal bone and cortical tunneling	Cortical resorption more than periosteal reaction	Extensive cortical tunneling and periosteal reaction	Trabecular microfractures, granulation tissue and necrotic areas
Radiography: Cortical bone	-	-	Cortical striations, gray cortex sign	Periosteal and endosteal new bone formation	True fracture line
Radiography: Cancellous bone	-	-	Blurring of trabecular margins, faint sclerotic densities	Sclerotic band	True fracture line
Scintigraphy	Amorphous lesion in the bone marrow	Small, ill-defined lesion with mildly increased activity in the cortical region	Larger well-defined, elongated lesion with moderately increased cortical activity	Wide fusiform lesion with highly increased activity in the corticomedullary region	Wide extensive lesion with intensely increased activity in the transcorticomedullary region
MR imaging	Ill-defined zone of bone marrow edema (only on T2W)	Mild periosteal edema, without bone marrow edema (only on T2W)	Moderate to severe periosteal edema and bone marrow edema (only on T2W)	Moderate to severe periosteal edema and bone marrow edema (on both T1W and T2W)	Moderate to severe periosteal edema and bone marrow edema, 'low signal' fracture line (on both T1W an T2W)

ular margins and faint sclerotic radiopaque areas may be seen secondary to peritrabecular callus, but a 50% change in bone capacity is required for these changes to be radiographically detectable. With progression, a readily apparent sclerotic band will be seen. Common sites for cancellous lesions include the calcaneus (Fig. 7.5), proximal tibia, distal tibia and fibula, pelvis and femoral neck (Fig. 7.6) (Anderson and Greenspan 1996; Spitz and Newberg 2002).

Sometimes stress fractures may mimic tumor and tumorlike conditions (see Chap. 8).

Fig. 7.4. Radiograph of a stress fracture of the tibia shows a sclerotic band perpendicular to the trabeculae

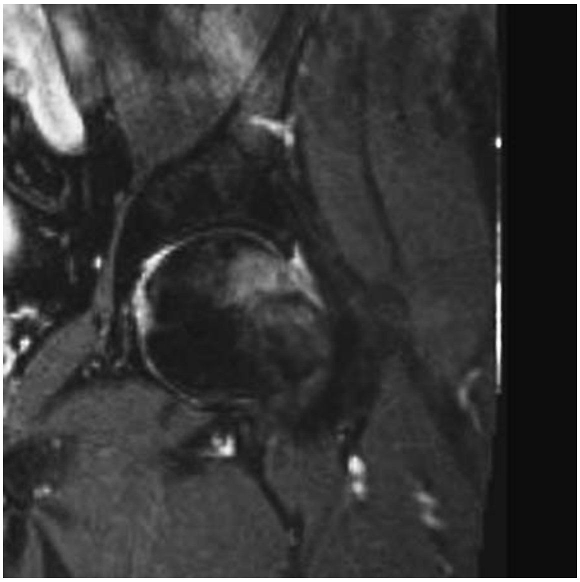

Fig. 7.6. Example of a tensile stress fracture of the femoral neck on a coronal T2-weighted MR image with fat suppression

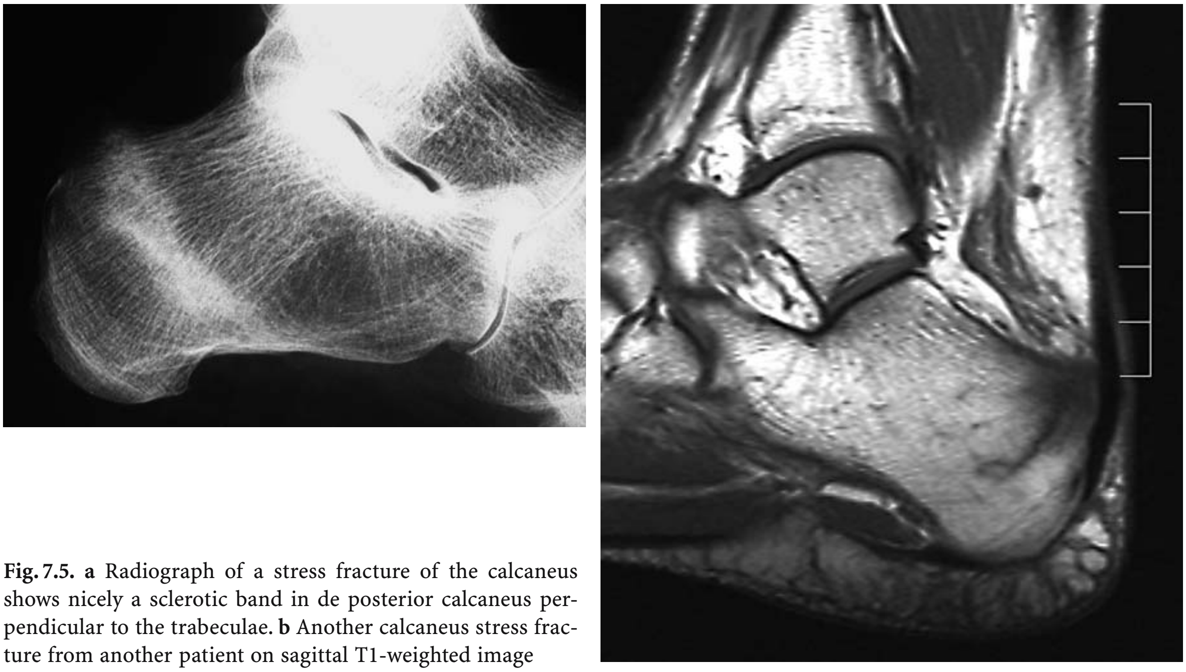

a

b

Fig. 7.5. a Radiograph of a stress fracture of the calcaneus shows nicely a sclerotic band in de posterior calcaneus perpendicular to the trabeculae. **b** Another calcaneus stress fracture from another patient on sagittal T1-weighted image

7.5.2 Bone Scintigraphy

Bone scintigraphy is an effective modality in the evaluation of athletes with clinically suspected osseous stress injuries. Before the advent of MR imaging it had been the gold standard for evaluating stress fractures (Zwas et al. 1987).

Bone scintigraphy demonstrates abnormal findings early in the continuum of the stress response in bone, by detecting the increased bone metabolism and osteoblastic activity associated with osseous remodeling.

Scintigraphy is typically abnormal one to two weeks or more before the radiographic changes appear.

Bone scintigraphy should optimally be performed using a three-phase technique. The most widely used radiopharmaceuticals for skeletal imaging are the technetium-99m phosphate analogues; these are taken up at sites of bone turnover. The degree of uptake depends primarily on the rate of bone turnover and local blood flow, and abnormal uptake may be seen within 6–72 h of injury (Anderson and Greenspan 1996).

The three-phase technique can help differentiate between soft tissue injury and osseous injury (Spitz and Newberg 2002). In the first phase, the blood flow phase, imaging is performed by acquiring dynamic 2- to 5-s images over the area of clinical concern for 60 s after the bolus intravenous injection. In the second phase, the blood pool or soft tissue phase, imaging is acquired after 5 min. The final phase of imaging is the delayed skeletal phase. These images should be acquired approximately 2–4 h after injection to maximize clearance of the radiopharmaceutical from the overlying soft tissues.

Zwas et al. (1987) described a scintigraphic classification of stress fractures ranging from grade 1 (mild) to grade 4 (severe) according to size, extent, and tracer concentration in the lesions (see Table 7.2.) (Fig. 7.7).

Despite its high sensitivity, the specificity of scintigraphy is slightly lower than that of radiography because other conditions such as tumors, infection, bone infarction, and shin splints or periostitis can produce similar findings (Fig. 7.8). This can be improved by using the three-phase technique. The localisation and distribution of the tracer accumulation and the timing can help in the differentiation (Nielsen et al. 1991; Zwas et al. 1987). For example, stress fractures are hot within all phases and have a more focal or fusiform morphology, whereas tracer uptake in shin splints is limited to the delayed phase and has a linear aspect.

On the other hand, bone scintigraphy is more sensitive than magnetic resonance, especially in evaluating suspected lesions in the spine or pelvis, identifying multiple stress fractures, and distinguishing bipartite bones from stress fractures.

However, scintigraphy may be too sensitive; as many as 50% of scintigraphically positive findings can occur at asymptomatic sites. Areas of increased uptake may represent subclinical sites of bone remodeling or stress reactions.

Although bone scanning is good for detection of stress fractures, it is not useful for follow-up of healing, because the intensity of activity decreases over 3–18 months as the bone remodels and often lagging behind clinical resolution of symptoms (Boden and Osbahr 2000). Since these entities are usually treated differently, CT or MR imaging can be helpful for better delineation.

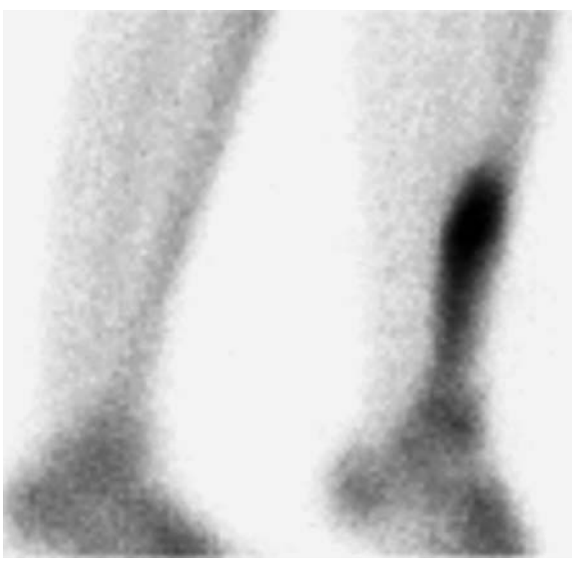

Fig. 7.7. Longitudinal stress fracture grade 4 with a wide transcorticomedullary increased activity on scintigraphy

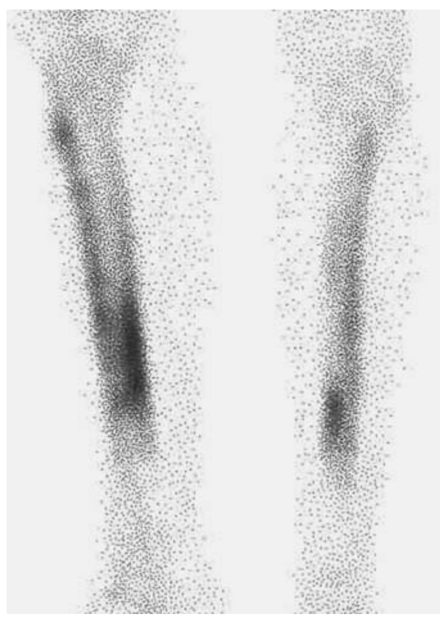

Fig. 7.8. Bone scintigraphy of shin splints demonstrates faint linear hot spots on the posteromedial aspect of both tibiae

7.5.3 CT Scan

CT is limited in its ability to detect early osseous stress injuries, and is less sensitive than bone scintigraphy and MR imaging. It does, however, have a role in more advanced injuries and injuries in specific anatomic locations where radiography fails to detect early changes due to superposition of adjacent structures. CT is particularly well suited for stress fractures of the tarsal bones (Fig. 7.9), longitudinal stress fracture of the tibia (Fig. 7.10), pars interarticularis stress fractures (spondylolysis), and stress fractures in the sacrum.

Whether the fracture is actually seen at CT may depend on orientation and the stage in evolution of the injury. A fracture that courses longitudinally may be particularly well demonstrated with CT in comparison to one coursing transversely to the long axis of the bone. This drawback of axial CT scanning may be overcome by multidetector CT with appropriate reformatting.

Gaeta et al. (2005) demonstrated that CT had the best performance in the identification of cortical abnormalities. Early CT changes consist of osteopenia, resorption cavities and striations within the cortical bone. They believe that these changes may precede formation of a cortical fracture.

CT findings in stress fracture are sometimes nonspecific, but findings of endosteal and periosteal reaction surrounding a thin cortical translucency are diagnostic of stress fracture. In longitudinally stress

Fig. 7.9a–d. Navicular stress fracture with a true fracture and diastasis on CT and MR-imaging in a 31-year-old women. Note the parallel orientation of the fracture line with the bone trabeculae. **a** Axial CT image. **b** Axial T1- weighted MR image. **c** Axial T2-weighted MR image with fat saturation. **d** Coronal CT image

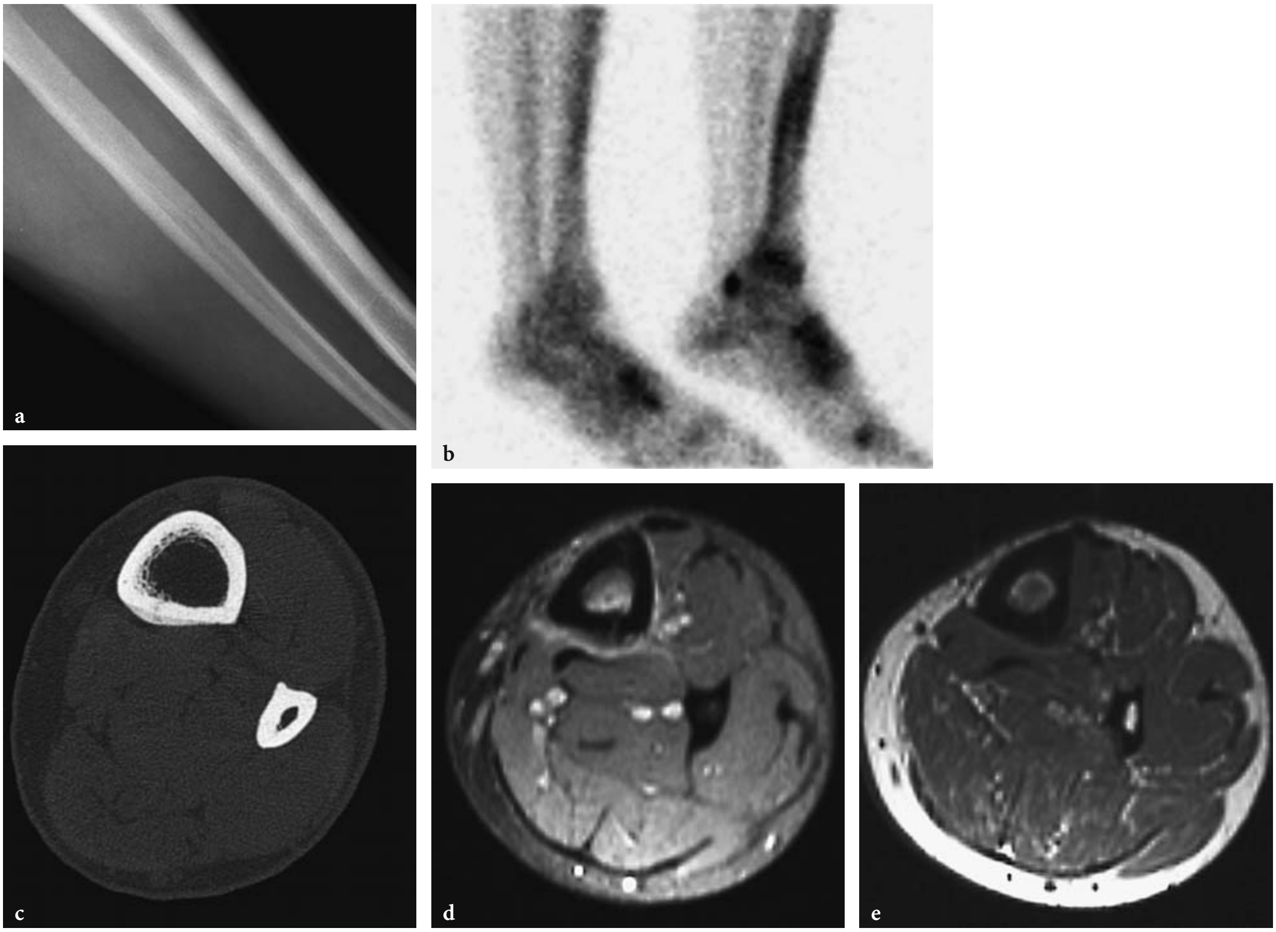

Fig. 7.10a–e. Longitudinal stress fracture of the tibia in a 41-year-old man. **a** Radiograph demonstrates periosteal new bone formation on the posterior aspect of the tibia diaphysis without a clearly lucent fracture line. **b** Scintigraphy shows an extensive long linear increased activity with a transcorticomedullary extension. **c** Axial CT-image shows nicely the vertical oriented true fracture line and the periosteal new bone formation. **d** Axial T2-weighted MR image with fat suppression shows a hyperintense transcortical line on the posterior aspect of the tibia with periosteal edema and hypointense new bone formation. **e** Hyperintense transcortical fracture line and hypointense new bone formation on an axial T1-weighted MR image

fractures CT has a particular interest in demonstrating a fracture line that extends along the axis of the bone (Allen 1988).

Additionally, CT may be problem solving when findings are equivocal on radiographs, MR imaging or scintigraphy. The value of CT in this regard lies in the detection of a discrete lucent or sclerotic fracture line or periosteal reaction. CT is also extremely helpful in differentiating between stress fracture and osteoid osteoma, because both entities may be hot on bone scan, show bone marrow edema at MR imaging, and demonstrate sclerosis on radiographs. The presence of a radiolucent nidus – however – is diagnostic for osteoid osteoma.

CT has also proven its value in the diagnosis of pediatric stress fractures. Initial radiographs may demonstrate marked periosteal bone formation, which may mimic tumor. Demonstration of endosteal bone formation on CT often leads to the correct diagnosis (Anderson and Greenspan 1996).

7.5.4 Ultrasound

Ultrasound is not reliable in the diagnosis of stress fractures and therefore is not recommended as the imaging technique of choice. Literature available

about the use of ultrasound is scarce. Ultrasound findings consist of a thickened hypoechogenic periosteum (Fig. 7.11), hyperechogenic cortical irregularities compatible with new bone formation (Fig. 7.12) or cortical discontinuity compatible with a fracture (Van Holsbeeck and Introcaso 1991). According to Boam et al. (1996), a sensitivity of 43% and a specificity of 49% was reported.

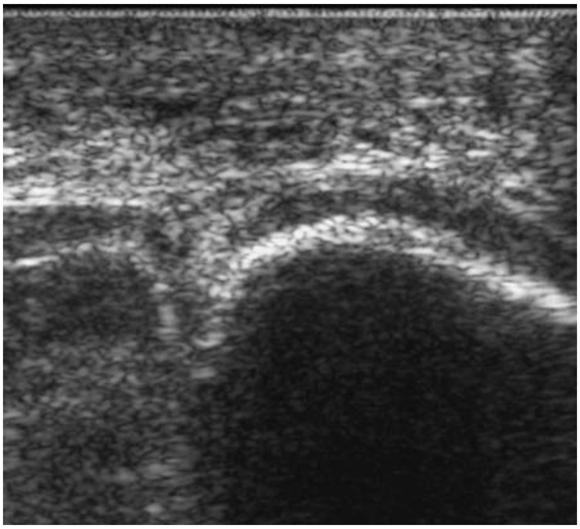

Fig. 7.11. Ultrasound in shin splints demonstrates a hypoechoic thickened periosteum on the anterior aspect of the tibia

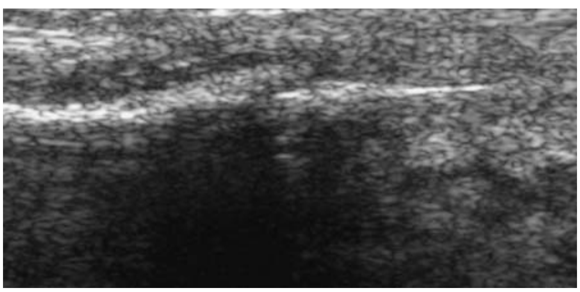

Fig. 7.12. The hyperechoic cortical irregularity on ultrasound corresponds to the new bone formation in a healing fracture

7.5.5 MR Imaging

Magnetic resonance imaging is a valuable tool in identifying stress fractures in case of high index of suspicion. MR has a comparable sensitivity and higher specificity than scintigraphy in distinguishing bone involvement from soft-tissue injuries. Moreover, MR imaging is helpful in grading the stage of certain stress fractures (Table 7.2) and, therefore, predicting the time to recovery. In addition, MR imaging avoids radiation exposure, is non-invasive and requires less time than three-phase bone scintigraphy (Boden and Osbahr 2000).

The MR imaging sequences necessary for evaluating stress injuries are summarized in Table 7.3. MR-imaging should also be performed in multiple orthogonal planes (Anderson and Greenspan 1996).

Table 7.3. Recommended MR-sequences for stress injury

Sequence	Characteristic detection
T1-weighted sequence	Anatomy and more advanced stress-related findings
Edema-sensitive sequence: - Short tau inversion recovery (STIR) - T2-weighted with fat suppression	Detection of the earliest changes of stress reaction, such as periosteal, muscle or bone marrow edema

MR imaging findings will differ along with the stage of the lesion and the sequences used. The MR grading system, developed by Fredericson et al. (1995) corresponds very well with the scintigraphic grading system of Zwas et al. (1987).

As discussed earlier, both resorption and replacement of bone constitute the most early histological changes of stress injury to bone. This stress reaction is accompanied by local hyperemia and edema, which is easily depicted by signal changes on MRI, especially on fluid sensitive sequences. This is why MR can be regarded as an excellent modality for the detection of early stress injury (Table 7.2) (Zanetti et al. 2002).

Indeed, MR can detect subtle cortical abnormalities like on CT on both T2-weighted and fast STIR images. The resorption cavity appears as a round or oval area of high signal intensity, and striation or cortical tunneling appears as a slightly hyperintense line extending through only a part of the cortical thickness. Usually, multiple parallel striations can be seen within the cortex. Osteopenia appears as an area of intermediate signal intensity. Irregularity of subperiosteal bone can be seen as well.

The appearance of resorption cavities and striations within the cortex may correlate with osteoclastic proliferation. High signal intensity depicted on T2-weighted MR images within striations and resorption cavities may be well explained by cell accumulation (osteoclasts, osteoblasts, and fibroblastic cells), increased amount of blood vessels, and production of

connective tissue and osteoid matrix, which all occur in osteoporotic bone (Gaeta et al. 2005).

MR also allows depiction of periosteal and endosteal marrow edema, which are believed to be useful ancillary markers for stress injury (Schweitzer and White 1996; Fredericson et al. 1995).

Especially in cancellous bone, stress injuries result in non-specific bone marrow alterations similar to those described in patients with bone marrow edema syndrome of bone bruise (Anderson and Greenspan 1996) (see Chap. 6).

The most common pattern of a frank fatigue-type fracture is a fracture line that has a low signal on all pulse sequences, surrounded by a larger, ill-defined zone of edema. The fracture line is continuous with the cortex and extends into the intramedullary space oriented perpendicular to the cortex and the major weight-bearing trabeculae.

Fredericson et al. (1995) also concluded that MR imaging is more accurate than bone scan in correlating the degree of bone involvement with clinical symptoms, allowing for more accurate recommendations for rehabilitation and return to activity (Fig. 7.13).

The term shin splints has been used to describe the clinical entity of activity related lower leg pain, typically associated with diffuse tenderness along the posteromedial tibia. A similar entity in the upper leg has been described as thigh splints or adductor insertion avulsion syndrome (Anderson et al. 2001; Van de Perre et al. 2003). Recent MR imaging studies have suggested that shin splints are a part of the continuum of fatigue damage in bone (Anderson et al. 1997; Fredericson et al. 1995). On T2-weighted images, a linear abnormal high signal is seen along the posteromedial surface of the tibia representing subperiosteal edema (Fig. 7.14). This implies that one cause of shin splints may be traction periostitis along the insertion of the soleus fascia and tibialis posterior. It can also appear as a linear high signal along the subcortical aspect of the bone marrow. This is considered to be secondary to edema or hemorrhage related to microdamage and the associated reparative response (Aoki et al. 2004). In thigh splints the periosteal reaction is located at the proximal third of the medial femoral shaft near the insertions of the adductor brevis and longus muscles (Anderson et al. 2001).

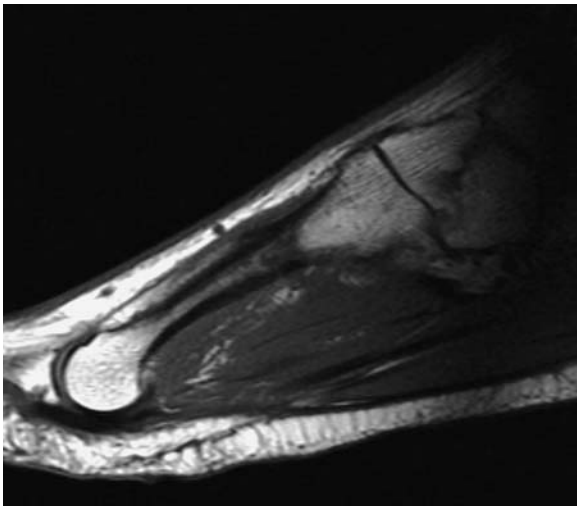

Fig. 7.13. Example of a grade 4 stress fracture of the second metatarsal on a sagittal T1-weighted MR image

7.6 Sites of Injury and Relationship to Specific Mechanism of Trauma

7.6.1 Location

Although most common in the lower extremity, stress injury to bone and stress fractures have been reported in nearly every bone in the body. This possible sites of stress injury are summarized in Table 7.4 (Resnick 1996).

7.6.2 Compressive vs Tensile Type of Stress Fracture

There are different types of stress fractures. The vast majority of stress fractures are perpendicular to the trabeculae, in cortical bone as well as in cancellous bone (Fig. 7.5). This type can be at the compressive side or at the tensile side, as seen in the femoral neck or tibial shaft (Fig. 7.15).

In the more common compression stress fractures of the femoral neck, that is more frequent in younger patients; the injury begins at the inferior cortex of the femoral neck. The lateral or tensile stress fracture, more common in older patients, starts in the superior cortex of the femoral neck and may advance across the femoral neck as a fracture line perpendicular to the axis of the femoral neck (Fig. 7.6) (Spitz and Newberg 2002; Boden and Osbahr 2000; Resnick 1996).

The tibial shaft is the most common location of stress fractures in athletes. Depending on the patient

Fig. 7.14a–c. Shin splints. **a** Axial T2-weighted MR image with fat saturation demonstrates a discrete hyperintense signal on the posteromedial aspect of the tibia representing subperiosteal edema in shin splints in a 28-year-old man. **b** Axial T2-weighted MR image with fat suppression from the tibia in another patient shows minimal subperiosteal edema with subcortical bone marrow edema. **c** Radiograph of the same women demonstrates no "gray cortex" sign or periosteal reaction

Table 7.4. Possible sites of stress injuries

Upper extremity: – Phalangeal tufts – Carpal bones: hook of hamate – Ulna: coronoid, olecranon process, diaphysis – Humerus: distal diaphysis – Scapula: coracoid, inferior edge of glenoid fossa
Lower extremity: – Sesamoids – Metatarsals – Navicular – Talus – Calcaneus – Tibia: mid and distal diaphysis, proximal shaft, medial malleolus – Fibula: distal and proximal diaphysis – Patella – Femur: diaphysis, neck – Pelvis: obturator ring, pubic rami, sacrum
Spine: – Lumbar vertebra: pars interarticularis – Lower cervical, upper thoracic spinous process
Thorax: – Ribs – Clavicle – Sternum

population, the incidence may range from 20% to 75% of all stress fractures. Tibial stress fractures may occur at any site along the shaft of the bone, but are most frequently encountered in the posteromedial cortex (compression side), in either the proximal of the distal third of the shaft (Fig. 7.16). A less common tibial stress fracture occurs on the tension side of the bone or anterior cortex of the midshaft of the tibia (Krivickas 1997).

7.6.3 Subchondral Insufficiency Fracture, SONK and Rapid Destructive Joint Disease

A more special form to be mentioned is the spontaneous osteonecrosis of the knee (SONK), mostly occurring in the area of maximum weight-bearing of the

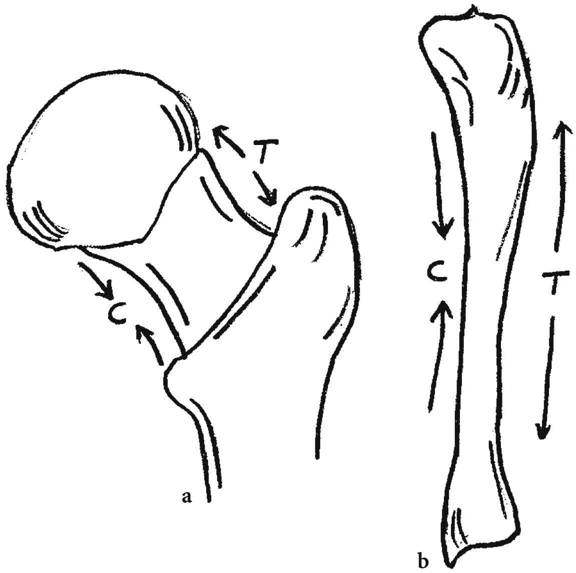

Fig. 7.15a,b. Forces along the femur (**a**) and tibia (**b**). Compressive forces (*C*) along the medial side of the femoral neck and the posteromedial side of the tibia result in compressive fractures. Tensile forces (*T*) along the lateral side of the femoral neck and the anterior side of the tibia result in distraction fractures

Fig. 7.16. Sagittal T1-weighted MR image with fat suppression after Gadolinium demonstrates a typical stress fracture of the proximal tibia on the posterior side. Note the cortical thickening, periosteal new bone formation and the bone marrow edema

(medial) femurcondyle and tibial plateau. Narvaez et al. (2000) believe that entity has a strong correlation with the subchondral insufficiency fracture(SIF), because of the usual sudden onset of symptoms. This is supported by the similarity in MRI appearance between SONK and stress fractures. This lesions can be seen in younger people with meniscal injuries and after meniscal surgery (Fig. 7.17). Meniscal pathology, however, is not the exclusive factor in the pathogenesis, because some patients have no evidence of a meniscal pathology and they appear mostly in middle-aged and elderly patients. Furthermore, SIF has been described in the hip.

Fig. 7.17. Sagittal T1-weighted MR image of the knee showing subchondral osteonecrosis of the knee (SONK). Note the subchondral insufficiency fracture of the medial tibial plateau in correlation with a medial meniscal tear

Altered biomechanics due to the subchondral fracture or resorption of the avascular segment may induce abnormal stress on the articular surfaces. Resulting destructive changes of the joint may ultimately result in rapid destructive osteoarthritis (Greyson et al. 1982).

7.6.4 Longitudinal Stress Fracture

The vast majority of tibial stress fractures are transverse in orientation, but longitudinal stress fractures

have also been reported (Fig. 7.10) (Allen 1988; Umans and Kaye 1996; Pozderac 2002; Anderson and Greenspan 1996; Gaeta et al. 2005; Boden and Osbahr 2000). Longitudinal stress fractures often have an atypical presentation, often necessitating MR or CT imaging for diagnosis.

Another relatively uncommon site for stress fractures is the medial malleolus. Repetitive impingement of the talus on the medial malleolus during ankle dorsiflexion and tibial rotation may result in a longitudinal orientated medial malleolar stress fracture.

Another longitudinal type of stress fracture is the navicular stress fracture, occurring in elite athletes including runners, gymnasts, basketball and football players. This fracture occurs in the sagittal plane in the middle third or at the junction of the central and lateral thirds of the navicular bone (Fig. 7.9) (Spitz and Newberg 2002; Boden and Osbahr 2000).This site corresponds to the zone of maximum shear stress on the navicular from the surrounding bones during plantar flexion combined with pronation. The lesion begins at the proximal dorsal articular surface and propagates in a distal and plantar direction, resulting in a partial or complete injury. Microangiographic studies have demonstrated that the navicular bone is supplied by peripheral, medial, and lateral vessels, leaving the central third relatively avascular. The diagnosis of navicular stress fracture is often missed on routine radiographs and therefore CT is usually required for demonstration of this type of fracture.

Things to Remember

1. Two types of stress fractures can be recognized: fatigue fracture caused by an abnormal stress to normal bone and insufficiency fracture caused by a normal stress to abnormal bone.
2. Stress fractures are often the result of an alteration in training.
3. The diagnosis of stress fractures starts always with plain films.
4. The gold standard for diagnosis of stress fractures is MR-imaging.
5. Stress injuries involve most frequently the lower leg, mostly the tibia.

References

Allen GJ (1988) Longitudinal stress fractures of the tibia: diagnosis with CT. Radiology 167:799–801

Anderson MW, Greenspan A (1996) Stress fractures. Radiology 199:1–12

Anderson MW, Ugalde V, Batt M et al. (1997) Shin splints: MR appearance in a preliminary study. Radiology 204:177–180

Anderson MW, Kaplan PA, Dussault RG (2001) Adductor insertion avulsion syndrome (thigh splints). Am J Roentgenol 177:673–675

Aoki Y, Yasuda K, Tohyama H et al. (2004) Magnetic resonance imaging in stress fractures and shin splints. Clin Orthop Relat Res 421:260–267

Bennell KL, Brukner PD (1997) Epidemiology and site specificity of stress fractures. Clin Sports Med 16:179–196

Bennell KL, Malcolm SA, Thomas SA et al. (1996) Risk factors for stress fractures in track and field athletes. A twelve-month prospective study. Am J Sports Med 24:810–818

Bhatt R, Lauder I, Finlay DB et al. (2000) Correlation of bone scintigraphy and histological findings in medial tibial syndrome. Br J Sports Med 34:49–53

Boam WD, Miser WF, Yuill SC et al. (1996) Comparison of ultrasound examination with bone scintiscan in the diagnosis of stress fractures. J Am Board Fam Pract 9:414–417

Boden BP, Osbahr DC (2000) High-risk stress fractures: evaluation and treatment. J Am Acad Orthop Surg 8:344–353

Brukner P, Bradshaw C, Khan KM et al. (1996) Stress fractures: a review of 180 cases. Clin J Sport Med 6:85–89

Cohn SH, Abesamis C, Yasumura S et al. (1977) Comparative skeletal mass and radial bone mineral content in black and white women. Metabolism 26:171–178

Daffner RH, Pavlov H (1992) Stress fractures: current concepts. Am J Roentgenol 159:245–252

Fredericson M, Bergman G, Hoffman KL et al. (1995) Tibial stress reaction in runners: correlation of clinical symptoms and scintigraphy with a new magnetic resonance imaging grading system. Am J Sports Med 23:472–481

Gaeta M, Minutoli F, Scribano E et al. (2005) CT and MR imaging findings in athletes with early tibial stress injuries: comparison with bone scintigraphy findings and emphasis on cortical abnormalities. Radiology 235:553–561

Globus RK, Plouet J, Gospodarowicz D (1989) Cultured bovine bone cells synthesize basic fibroblast growth factor and store it in their extracellular matrix. Endocrinology 124:1539–1547

Greyson ND, Lotem MM, Gross AE et al. (1982) Radionuclide evaluation of spontaneous femoral osteonecrosis. Radiology 142:729–735

Haverstock BD (2001) Stress fractures of the foot and ankle. Clin Podiatr Med Surg 18:273–284

Hester JT (2001) Diagnostic approach to chronic exercise-induced leg pain. Clin Podiatr Med Surg 18:285–306

Krivickas LS (1997) Anatomical factors associated with overuse sports injuries. Sports Med 24:132–146

Lauder TD, Dixit S, Pezzin LE et al. (2000) The relation between stress fractures and bone mineral density: evidence from active-duty army women. Arch Phys Med Rehabil 81:73–79

Mori S, Burr DB (1993) Increased intracortical remodeling following fatigue damage. Bone 14:103–109

Morris FL, Naughton GA, Gibbs JL et al. (1997) Prospective ten-month exercise intervention in premenarcheal girls;

positive effects on bone and lean mass. J Bone Miner Res 12:1453–1462
Mulligan MF (1995) The "gray cortex": an early sign of stress fracture. Skeletal Radiol 24:201–203
Muthukumar T, Butt SH, Cassar-Pullicino VN (2005) Stress fractures and related disorders in foot and ankle: plain films, scintigraphy, CT and MR imaging. Semin Musculoskelet Radiol 9:210–26
Narváez J, Narváez A, Rodriquez-Morena J et al. (2000) Osteonecrosis of the knee; differences among idiopathic and secondary types. Rheumatol 39:982–989
Nielsen MB, Hansen K, Holmer P et al. (1991) Tibial periosteal reactions in soldiers. Acta Orthop Scand 62:531–534
Otter MW, Qin YX, Rubin CT et al. (1999) Does bone perfusion/reperfusion initiate bone remodeling and the stress fracture syndrome? Med hypotheses 53:363–368
Pozderac RV (2002) Longitudinal tibial fatigue fracture. An uncommon stress fracture with characteristic features. Clin Nucl Med 27:475–478
Resnick D (1996) Bone and joint imaging, 2nd edn. W.B. Saunders Company, pp 717–738
Romani WA, Gieck JH, Perrin DH et al. (2002) Mechanisms and management of stress fractures in physically active persons. J Athl Train 37:306–314
Ross J (1993) A review of lower limb overuse injuries during basic military training. Part 1: types of overuse injuries. Milit Med 158:410–415
Schweitzer ME, White LM (1996) Does altered biomechanics cause marrow edema? Radiology 198:851–853
Slater M, Patava J, Kingham K et al. (1995) Involvement of platelets in stimulating osteogenic activity. J Orthop Res 13:655–663
Spitz DJ, Newberg AH (2002) Imaging of stress fractures in the athlete. Radiol Clin N Am 40:313–331
Umans HR, Kaye JJ (1996) Longitudinal stress fractures of the tibia: diagnosis by magnetic resonance imaging. Skelet Radiol 25:319–324
Van de Perre S, Vanhoenacker FM, De Schepper AM (2003) Thigh splints in a skeletally immature boy. Rofo 175:1582–1584
Van Holsbeeck M, Introcaso JH (1991) Musculoskeletal ultrasound, Mosby Year Book, pp 212–213
Zanetti M, Christian LS, Burkhardt S et al. (2002) Clinical outcome of edema-like bone marrow abnormalities of the foot. Radiology 222:184–188
Zwas ST, Elkanovitch R, Frank G (1987) Interpretation and classification of bone scintigraphic findings in stress fractures. J Nucl Med 28:452–457

8

Pseudotumors in Sports

Suzanne E. Anderson and A. Mark Davies

CONTENTS

S. E. Anderson, PhD
Institute of Diagnostic, Interventional and Pediatric Radiology, University Hospital, Inselspital, Freiburgstrasse, 3010 Bern, Switzerland
A. M. Davies, MD
Consultant Radiologist, The MRI Centre, Royal Orthopedic Hospital NHS Trust, Bristol Road, Birmingham, B31 2AP, UK

Box 8.1. Plain radiography/CT

Imaging technique of choice for evaluation of:

- (Mature) myositis ossificans
- Calcifications
- Radiopake foreign bodies
- Evaluation of acute or chronic avulsion fractures

Box 8.2. MR Imaging

- Imaging in three planes required
- Imaging protocol should include at least T1-WI and STIR or fat suppressed T2-WI
- Gradient echo imaging: useful to detect hemosiderin, metallic foreign bodies and gas
- Should always be correlated with clinical history and plain films/CT

8.1 Introduction

In many instances it will be clear that an apparent clinical mass is directly due to a specific sporting injury, such as a thigh hematoma after direct impaction during football. Commonly the sports person is fully aware of the injury and relationship with the development of the mass or abnormal region and many sports activities are associated with specific injuries and findings. However sports injuries may

be minor and forgotten and not immediately perceived as being related to the current clinical problem, or if acute maybe be associated with unusual radiological findings confusing the diagnosis or be related to chronic overuse. This insult may then be complicated by secondary infection. Contributory features include the presence of normal variants with overuse syndromes, body habitus and inappropriate training and equipment or overwork. In other cases, characteristic locations and patient age may be suggestive of the diagnosis, such as elastofibroma dorsi of the infra-scapular posterior thoracic wall.

Musculoskeletal pseudotumors on MRI are not infrequent and may be due to an increased availability of MRI and expanding clinical referral basis. A large variety of MRI pseudotumors exist.

There are two types of pseudotumors. First, clinical ones, i.e. those patients who present with findings of a mass or swelling suggestive of a tumor. Second, an apparent tumor evident on imaging in which patients present with imaging findings mistaken for a tumor. Pseudotumors are far more common than true tumors. They can be classified either anatomically or by etiology. All anatomical structures may be involved.

8.2 Imaging Principles

All modalities are involved in pseudotumor imaging. Often the radiologist does not have a choice, as imaging has already been performed before the patient presents. When radiology can influence the simple imaging choices, remaining with basic principles is always prudent. Radiographs in two planes are helpful – to review for example any calcification, zoning phenomena, fracture, or for the presence of normal variants or overuse such as advanced degenerative joint disease ill fitting with age. Computed tomography can help with clarifying the above and MRI is a main stay with sports pseudotumors given its multiplanar capability, regional anatomical review, and capacity to review all anatomical structures. Regarding MRI, routine sequences in three planes are important. Ensure T1 and T2-weighting and STIR (Short Tau Inversion Recovery) in at least one plane. Gradient echo sequences may be useful to enhance a "blooming" artefact associated with hemosiderin deposition, metallic foreign bodies and gas. Though contrast administration may not necessarily change the diagnosis, it may increase conspicuity of findings, differentiate between solid and cystic masses and has been shown to be of use with professional athletes where muscle strains may be negative on T2-weighting.

Improved MRI diagnosis for pseudotumor is possible with increased awareness by the radiologist to the imaging appearances of commoner types of pseudotumors, by correlation with radiographs and by obtaining an appropriate clinical history. Either with the use of a small questionnaire before MRI or quick check by the reporting radiologist with brief review of the patient's clinical history and clinical appearance, the MRI diagnosis may be quite specific. Often this diagnosis may be a surprise to the referring clinician.

Correlation with conventional radiographs is extremely important as many masses or focal abnormalities on MRI simulating neoplasms may have characteristic radiographic appearances and be easily diagnosed (Jelinek and Kransdorf 1995; Kransdorf and Murphey 1997). Examples include the peripheral calcific rim of myositis ossificans, retained radio-opaque foreign bodies, stress fracture of bone and hydroxyapatite deposition within tendons.

Fat necrosis, muscle hematoma and myositis ossificans of muscle may give rise to MRI pseudotumors. Fat necrosis after minor trauma may result in a clinically palpable mass. Only one quarter of children with an MRI fat necrosis pseudotumor recalled a history of trauma (Tsai et al. 1997). On MRI there was linear signal intensity within the subcutaneous tissues of either the anterior tibia or of the buttock region, an absence of a mass, though there was commonly a volume plus of the subcutaneous region (Tsai et al. 1997).

On MRI if there is an absence of a true mass, and a finding associated with a large reactive soft tissue component or hemorrhage, and there has been a history of sports injury, trauma or overuse, then at least an MRI pseudotumor should be included in the differential diagnosis. If after review of the imaging appearances, particularly with MRI and radiographs, attention is paid to the clinical and history details, then sometimes a biopsy may not be needed. It is always prudent to have routine clinical and imaging follow-up after suggesting a pseudotumor diagnosis particularly when early on the learning curve for these abnormalities. It will decrease the surprise element.

8.3 Keys to Differential Diagnosis and True Tumors

Typically true musculoskeletal tumors of either bone or soft tissues present with an increasing mass effect and relatively minor pain compared to the mass size, unless there has been a history of bleeding, biopsy or accident. Radiologically with a true tumor there is commonly a mass lesion, which is displacing or invading local anatomy. Usually with pseudotumors, there is an absence of a genuine mass lesion, with more often a lack of an anatomical structure, making comparison with the contralateral side helpful and also imperative in some circumstances. Pseudotumors are very commonly associated with a marked adjacent tissue reaction, as classically seen with myositis ossificans. Adjacent marked reactive soft tissue change or hemorrhage is extremely unusual with a true tumor unless there has been a history of direct trauma, bleeding or biopsy.

8.4 Myositis Ossificans

Localized myositis ossificans is a common MRI pseudotumor (Fig. 8.1) (Boutin et al. 2002). Usually the heterotopic formation of bone occurs within muscle and in approximately one quarter of cases due to an identified trauma. It may rarely occur in association with other structures such as tendons and fascia. During the active initial phase the mass-like

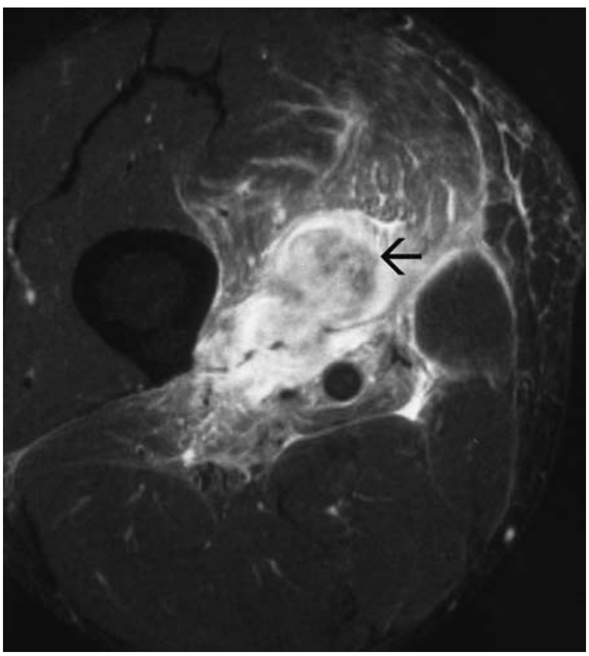
a

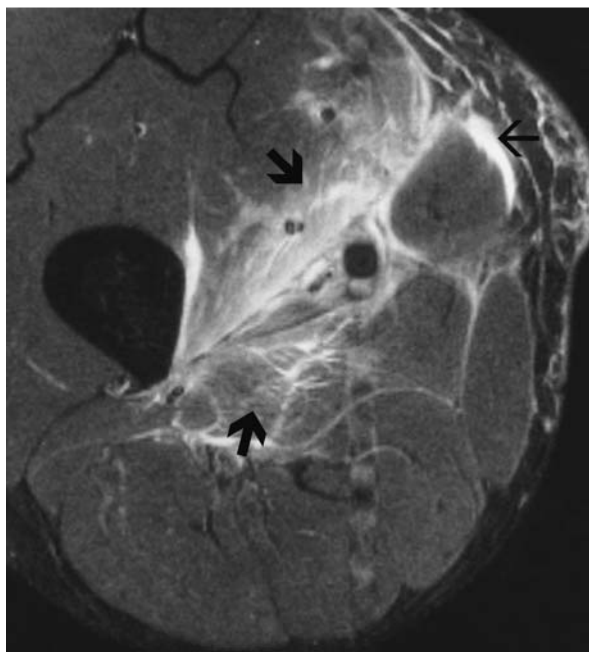
b

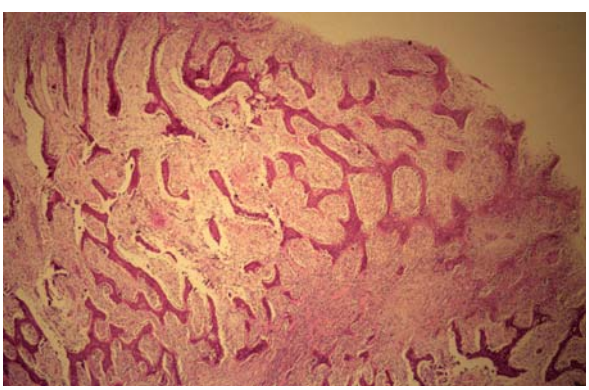
c

Fig. 8.1a–c. Sixty-year-old male with lower limb mass – intermediate phase of myositis ossificans. **a** Axial T-1 weighted fat suppressed post contrast enhanced MR image with "tide mark sign" (*arrow*) representing the beginning of the peripheral rim of calcification. **b** Adjacent axial image, shows marked soft tissue reaction (*thick arrows*) and perifascial fluid (*thin black arrow*) commonly associated with myositis ossificans, which would be most unlikely to be seen with a true tumor unless after trauma or biopsy with hemorrhage. **c** Hematoxylin and eosin stained histology showing peripheral zone ossification, typical for myositis ossificans. (Pathology courtesy of Edouard Stauffer)

region may be clinically warm, painful and woody in consistency. Biopsy during the early phase of development may give a false osteosarcoma diagnosis, as there is florid osteoblastic activity. Serial radiographs demonstrate the development of a peripheral rim of calcification of the mass at usually six to eight weeks after injury and that the calcification is separate from bone. If the trauma involves deep muscle injury in some cases there may be an associated periosteal reaction of the adjacent bone, referred to as periostitis ossificans. The appearances on MRI reflect the phase of development of the myositis ossificans and the zone phenomenon of the histology. In the early phase before ossification the lesion is usually isointense to muscle on T1-weighting with no distinct borders and increased in signal intensity on T2-weighting centrally (De Smet et al. 1992), with marked adjacent soft tissue edema. At this stage there may or may not be a subtle peripheral rim, like a tidemark. In subacute lesions with early peripheral calcification there is a low signal intensity rim, like a tidemark on the beach when the wave is residing, reflecting this calcification. The center of the lesion may be isointense to muscle or slightly increased in signal intensity on T1-weighting. On T2-weighting the central portion of the lesion is very high in signal intensity and the rim's decreased signal is more clearly evident (Jelinek and Kransdorf 1995; De Smet et al. 1992). At this subacute stage the adjacent edema of soft tissues may be very prominent. A common feature to myositis ossificans in the acute and subacute phases is the marked adjacent soft tissue reaction, which is very unusual in primary malignant tumors, which have not been previously biopsied or undergone intratumoral hemorrhage (Jelinek and Kransdorf 1995). In the chronic phase, the central portion of the lesion is slowly ossifying, so eventually the signal intensity is similar on T1- and T2-weighting to that of fatty marrow of bone (De Smet et al. 1992). It should be stressed that maturation on radiographs and CT is a good discriminator of this condition from mineralising real soft tissue sarcomas such as synovial sarcoma and soft tissue osteosarcoma. Though less common, multiple muscles and the regions between muscles may be involved. A variant of myositis ossificans occurring in the fingers and less commonly in the toes is fibro-osseous pseudotumor of the digits or florid reactive periostitis.

8.5 Inflammatory Myopathies

Inflammatory myopathies are most usually diffuse in nature, commonly bilateral in the thighs or calves and associated with weakness or tiredness, though quite rare some forms may be focal such as nodular myositis, sarcoid associated myopathy (Fujimoto et al. 2002) and diabetic muscle infarction. They may occur in sporting individuals and are often finally diagnosed with histology.

8.6 Nodular Fasciitis or Pseudosarcomatous Fasciitis

Nodular fasciitis or pseudosarcomatous fasciitis commonly occurs in 20–35 year old athletic patients presenting with a focal clinical mass with pain. There are three forms: subcutaneous the commonest, intramuscular which may appear as a focal mass and MRI pseudotumor, and fascial which usually spreads along superficial fascial planes. Early lesions typically have a high T2 signal intensity reflecting the myxoid histology (Jelinek and Kransdorf 1995; Kransdorf and Murphey 1997) and older lesions may have more decreased signal intensity on T2-weighting reflecting the more predominantly fibrous histology (Jelinek and Kransdorf 1995). Overall the MRI appearance is non-specific.

8.7 Tears and Overuse of Ligaments and Muscles

Tears and overuse of ligaments and muscles, both acute and chronic, may cause MRI pseudotumors. Partial avulsion of the adductor muscles of the thigh from the femoral diaphysis in children due to sports injuries or overuse may cause an MRI pseudotumor, which may simulate a malignant sarcoma (Anderson et al. 2001). In five young patients, who presented with a provisional clinical and radiological diagnosis of femoral sarcoma, review of MRI from three patients showed a periosteal reaction on the posteromedial aspect of

the femur centered on the muscle-bone interface of the vastus medialis and intermedius and adductor muscle insertions on the femoral shaft (Charkes et al. 1987). There was widespread intramedullary edema and an absence of bone or soft tissue mass. Stress fractures lines were excluded. This condition has been studied using bone scans in adults, in army training and called "adductor insertion avulsion syndrome" or "thigh splints". The cause is thought to be due to excessive adductor contraction with stripping of the femoral periosteum posteromedially. Knowledge, particularly of the MRI findings with an appropriate clinical setting can help physicians to make the correct diagnosis and eliminate unnecessary biopsy. Proximal adductor avulsions near the symphysis pubis (Schneider et al. 1976) and intramuscular strains (Yoshioka et al. 1994) have been described in adults. Chronic muscle avulsive injuries in a variety of lower limb sites in children have been described (Donnelly et al. 1999; Anderson et al. 2004a). Overuse with excessive prolonged carrying of large babies may rarely lead to masses of the wrist, found to be due to de Quervains tenosynovitis.

Fig. 8.2. Young male soccer player with left sided symphyseal stress reaction (*arrow*) and adductor strain on an axial STIR image

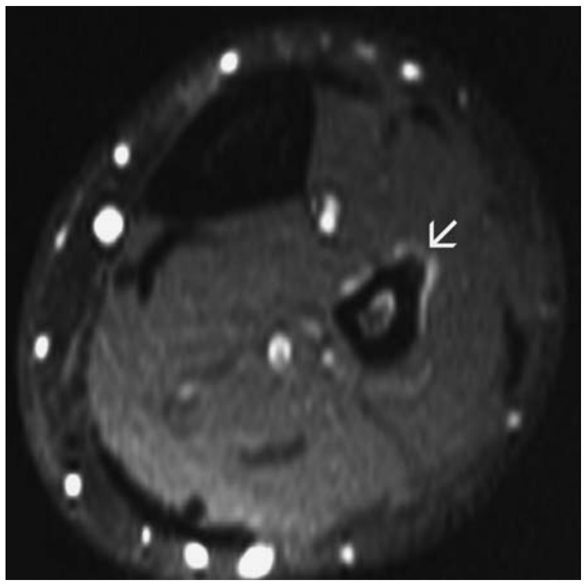

Fig. 8.3. Young female professional snow boarder with distal fibular stress reaction (*arrow*) on axial T1-weighted fat suppressed MR image after contrast administration, performed as part of a routine tumor work-up MR protocol

8.8 Stress Reactions and Fractures

Post-traumatic bony abnormalities such as stress reactions and fractures may cause MRI pseudotumors. Many sporting activities are associated with common sites and patterns (Figs. 8.2 and 8.3) (Pavlov 1995), such as junction of pelvis and ischium in long distance runners, and hook of hamate in golf and tennis players. In the clinical history review for altered or excessive training and changed equipment may be helpful. Excessive training with suboptimal shoes in figure ice skaters and professional snow boarders may cause MRI pseudotumors of soft tissues around the ankle associated with the shoe rim (Anderson et al. 2004b). Some sites for stress fractures are practically pathognomonic for specific sports such as spinal pars defects of the thoracic and lower lumbar spine in cricketers particularly in fast spin bowlers with unilateral defects often involving the side opposite to the bowling arm (Fig. 8.4) (Hardcastle et al. 1992). Fortunately these are now rare due to awareness and change of training. Any periosteal reaction associated with muscle hypertrophy in a sports person should prompt review of type of training and accurate history of pain, as the MRI findings may be due to overuse. Radiographic correlation and follow-up are important. Any linear low signal intensity on T1-weighting associated with increased signal intensity of T2-weighting (Fig. 8.5), which becomes more obvious with contrast enhancement and fat suppression should prompt a diagnosis of stress fracture. Radiographic and clinical correlation and follow-up are important.

Stress reactions and fractures is the largest area where stress/trauma-related lesions on imaging are mistaken for sarcomas. Stress fractures in the immature skeleton are frequently mistaken for sarcomas

on imaging (particularly the proximal tibia and distal femur). If the correct diagnosis is not made on conventional radiographs, and the clinical problem is followed with imaging modalities, notably MRI, a large number of pseudotumor appearances may be displayed, and compounds the diagnostic error. This may lead to unnecessary biopsies and also to errors in pathology results.

Fig. 8.4.a Fast spin bowler in action after a hat trick, representing Australia against Pakistan. **b** Sagittal T1-weighted fat suppressed MR image depicting L3 and L4 left sided pars interarticularis stress reaction (*arrows*). (Case and images courtesy of Anthony Stuart)

Acute or chronic stress avulsion injuries in the immature skeleton, particularly acute-on-chronic traumatic avulsions (Fig. 8.6), not uncommonly may simulate bone forming surface lesion tumors or intraosseous sarcomas. These are a particular problem around the pelvis and may be compounded by the presence of normal variation in synchondroses Donnelly et al. 1999).

8.9 Muscle Abnormalities, Partial and Full Thickness Tears and Hematomas

Muscle abnormalities and tears (Fig. 8.7) (May et al. 2000), soft tissue hematomas, abscess formation and ischemic-compression syndromes are common MRI pseudotumors. Superficial soft tissue hematomas may be associated with minimal trauma and the event little thought of at the time of presentation to MRI. Whereas deep muscle hematomas are more commonly associated with more obvious trauma, coagulation disorders such as hemophilia or diffi-

a 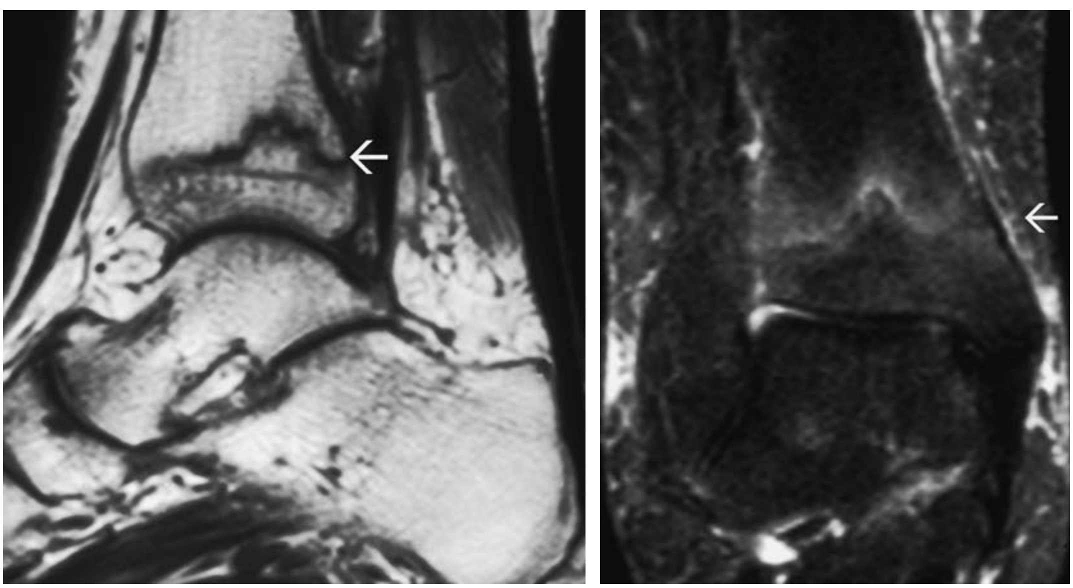 b

Fig. 8.5a,b. Sixty-year-old female with known osteoporosis, and ankle pain after increasing exercise fitness programme. **a** Sagittal T1-weighted MR image with stress fracture evident (*arrow*). **b** Coronal T2-weighted fat suppressed MR image with stress fracture (*arrow*)

a

b

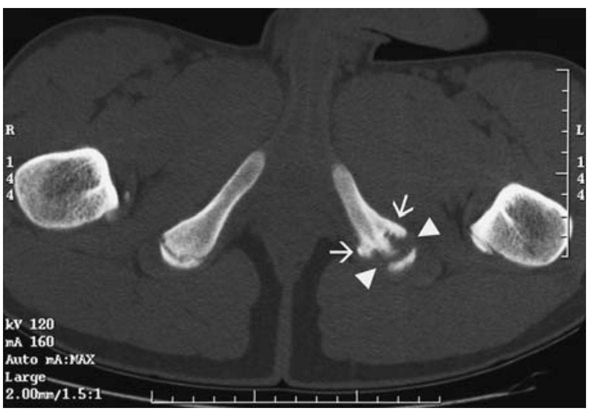

c

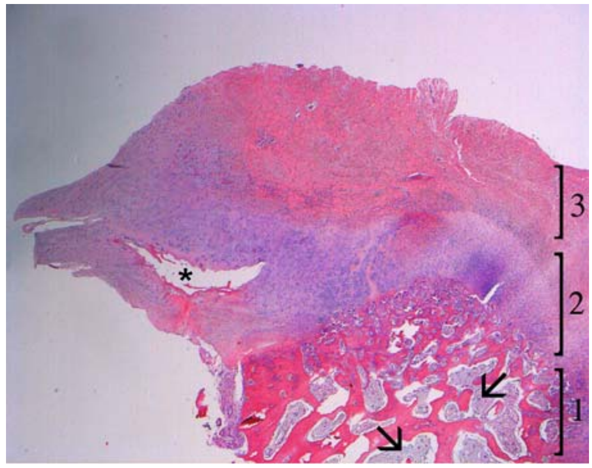

d

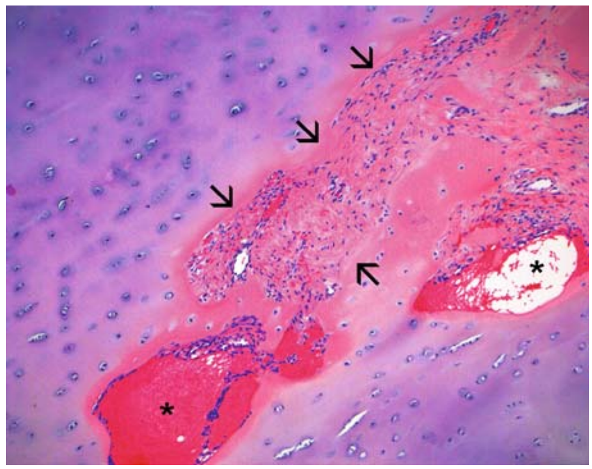

e

Fig. 8.6a–e. Fifteen-year-old male ice hockey player with pelvic pain and concern for Ewing's sarcoma of ischium-pseudotumor: chronic apophyseal avulsion. **a** Coronal STIR sequence with increased marrow signal within posterior acetabulum (*), inferior ischium (*arrowhead*), and widening of the ischial synchondrosis (*white arrow*). **b** AP Radiograph of the pelvis shows widening of the ischium (*) and associated periosteal reaction medially (*arrow*) and inferiorly (*arrowheads*). **c** CT axial image shows asymmetrically widening ischial synchondrosis (*arrowheads*) and periosteal reaction (*arrows*). **d** Despite pseudotumor diagnosis, family insisted on biopsy. Hematoxylin and eosin histology, original magnification 2.5×, shows the central cleft (*) within the distal apophyseal cartilage and chronic granulation tissue within bone (*arrows*) and depicts the zones of reaction: 1. underlying normal bone, 2. synchondrosis cartilage reactive changes, 3. superficial component of the hamstring tendon. **e** Hematoxylin and eosin histology, original magnification 10×, shows reactive connective tissue with neovascularisation (*) and surrounding inflammatory cells (*arrows*) within normal cartilage tissue. (Case courtesy of Chris Loupatatzis, Klaus A. Siebenrock, and pathology from Edouard Stauffer)

culties with acute or chronic anticoagulation therapy can also cause such hematomas. Often the MRI appearances may be complex as there is repeated hemorrhage within soft tissues and muscle movement. The MRI appearances of hematoma depends on the state of the hemoglobin molecule, whether it is intra- or extracellular in nature (Kransdorf and Murphey 1997; Dooms et al. 1985; Gomori et al. 1985; Rubin et al. 1987). In the hyper acute phase blood is isointense on T1-weighting and decreased on T2-weighting, reflecting the earliest phase of oxygenated hemoglobin to deoxyhemoglobin. With cell lysis, in the subacute phase (one week to three months old), the hemoglobin molecule becomes extracellular methemoglobin and is characteristically increased in signal intensity on T1- and T2-weighting. Weeks to

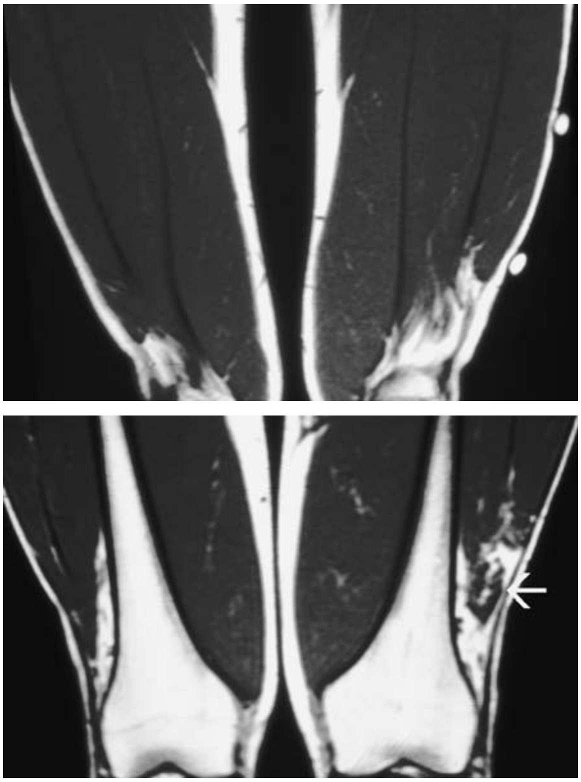

a

b

Fig. 8.7a,b. Nineteen-year-old soccer player presenting with a clinical mass. **a** Coronal T1-weighted MR image with vitamin capsules demarcates the mass. **b** Further coronal T1-weighted MR image shows focal muscle atrophy (*arrow*), within vastus lateralis chronic muscle tear

months later the methemoglobin breaks down into hemosiderin (Fig. 8.8) with decreased signal intensity on T1- and T2-weighting. Breakdown of blood products in the hematoma is not uniform with accelerated peripheral breakdown reflecting a low signal rim and centrally there is more inhomogeneous signal intensity. It may sometimes be difficult to distinguish simple hematoma from a large hemorrhage into a malignant mass (Jelinek and Kransdorf 1995). A tumor nodule or rim of irregular tumor, or contrast enhancement within an irregular nodule may be helpful to distinguish the two (Jelinek and Kransdorf 1995). Hematomas may become secondarily infected and present a more complex MRI appearance with more peripheral and surrounding soft tissue reaction.

8.10 Infection

Pyomyositis may occur in healthy sporty individuals (Fig. 8.9); however the clinical picture prior to MRI strongly suggests infection with reddened skin, anatomy that is extremely painful and often systemic features such as fever. However patients with immunosuppression may present to MRI with a mass that

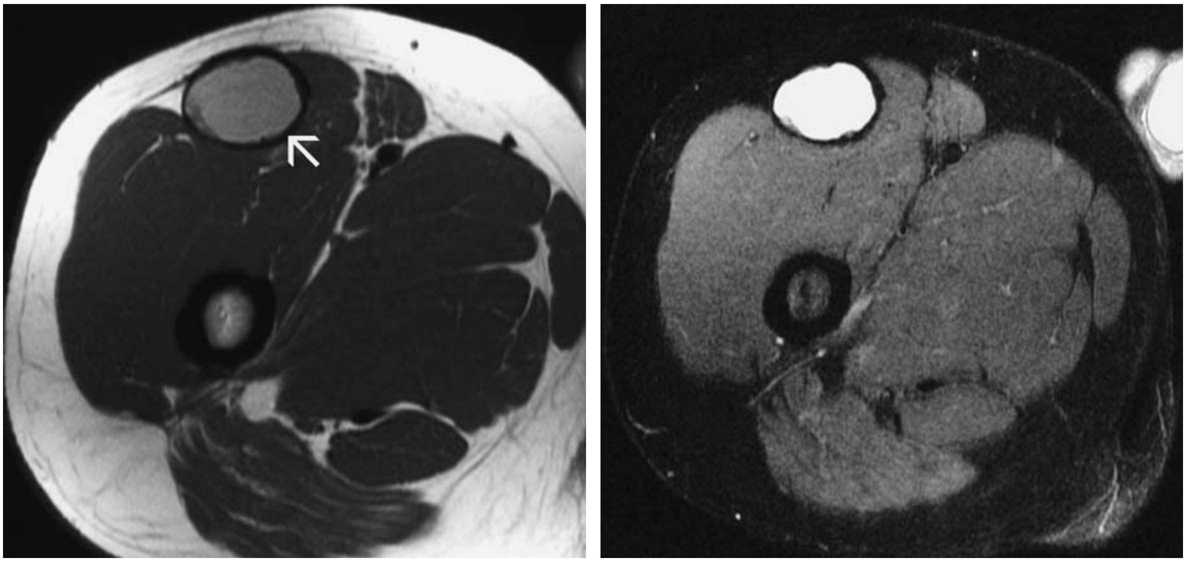

a

b

Fig. 8.8a,b. Twenty-eight-year-old male soccer player with mass. Enquiring after additional history, revealed a sports injury two years ago with "corked thigh". **a** Axial T1-weighted MR image shows a focal fluid collection with rectus femoris muscle with increased central signal intensity and a decreased signal intensity wall (*arrow*), consistent with hematoma formation and hemosiderin deposition within the wall. **b** Corresponding axial T2-weighted MR image with fat suppressed depicts the hematoma

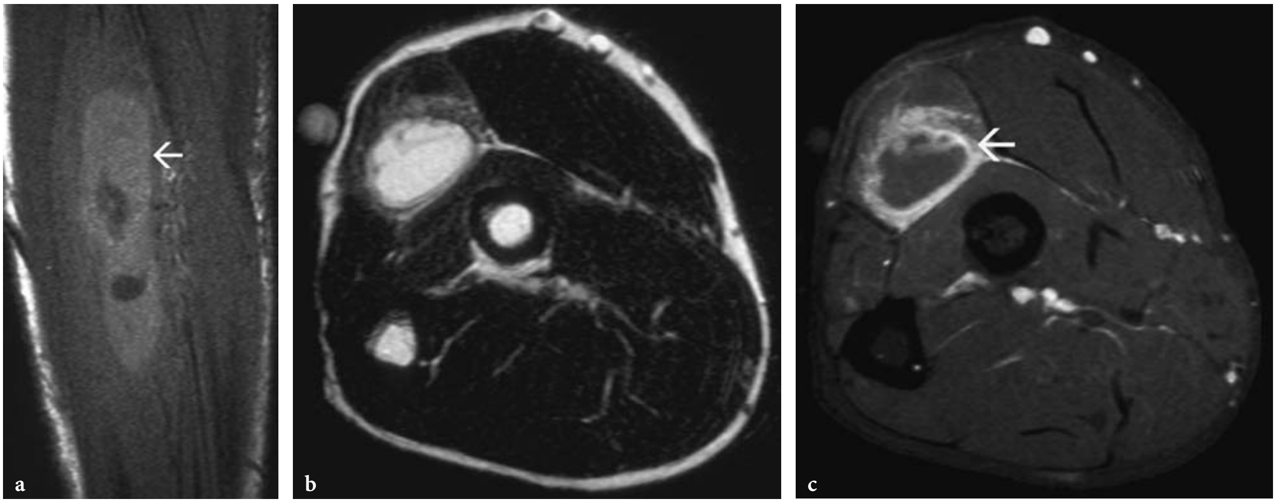

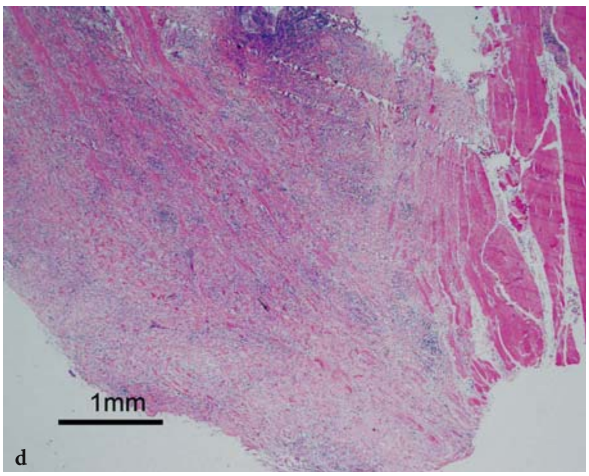

Fig. 8.9a–d. Fifty-year-old female skier with forearm mass. Further history obtained suggested mass occurred at site of minor trauma with ski poles. **a** Oblique coronal T1-weighted MR image with abscess wall sign: increased signal intensity on T1-weighting (*arrow*). **b** Axial T2-weighted MR image shows focal high signal intensity region, consistent with a fluid collection. A vitamin capsule demarcating the clinical mass region is evident. **c** Axial T1-weighted fat suppressed MR image after administration of contrast agent shows contrast within thickened abscess wall and in adjacent soft tissues (*arrow*). Presumably there was secondary infection of a hematoma. **d** Hematoxylin and eosin histology shows a thickened irregular abscess wall. (Pathology courtesy of Edouard Stauffer)

is confusing both clinically and radiologically as the usual signs are not present. MRI features (Soler et al. 1996, 2000; Ogilvie et al. 2001; Abdelwahab et al. 2003) suggesting an abscess include a thickened peripheral rim on T1- and T2-weighting, which may be increased in signal intensity on T1-weighting and demonstrates marked contrast enhancement. Immunosuppressed patients commonly have an absence of marked adjacent soft tissue and subcutaneous edema. Fortunately atypical organisms may rarely cause abscess formation with a mass like appearance on MRI such as cysticercosis, *Echinococcus granulosus* in hydatid disease and *Coccidioides immitius* in Coccidioidomycosis (Jelinek and Kransdorf 1995). In human immunosufficiency patients, *Bartonella henselae*, a Gram-negative bacillus, may rarely cause bacillary angiomatosis-focal infection in soft tissues, which is highly vascularized, and may erode and involve adjacent bone, mimicking a sarcoma (Biviji et al. 2002). This organism may also be involved in 'cat scratch disease' (Dong et al. 1995), as the carrier is usually a cat and is usually associated with single lymph node enlargement.

8.11 Normal Variants

Normal variants and their overuse may present as MRI pseudotumors. Normal bone marrow may occasionally cause concern for tumors; however use of T1-, and T2-weighting and STIR sequences usually excludes real pathology (Fig. 8.10). Supernumerary bones (styloid bone, accessory ossification centers for scaphoid tuberosity) (Capelastegui et al. 1999), tarsal coalition, accessory soleus muscle, and extensor digitorum manu brevis muscle (Capelastegui et al. 1999) are some targets. Occasionally tarsal coali-

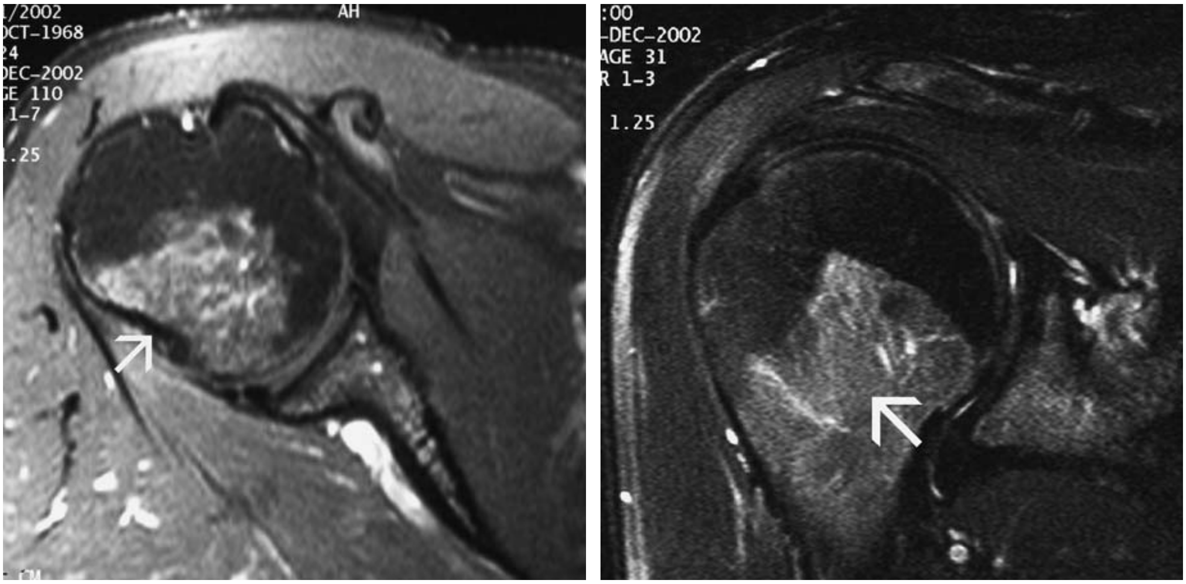

a b

c

Fig. 8.10a–c. Twenty-six-year-old female with sports related shoulder overuse, presents to MRI for clinical review and with STIR sequences only. **a** Axial STIR image shows red marrow signal intensity (*arrow*), in error diagnosed as a bone sarcoma of the proximal humerus. **b** Coronal STIR sequence again shows the falsely interpreted normal red marrow (*arrow*). **c** Coronal T-weighted MR image shows the normal red marrow signal intensity (*arrow*) can be diagnosed as a normal variant of marrow

tion and calcaneal spurs associated with peroneal tendon inflammation and partial tear may be associated with a marked synovial reaction and tenosynovitis, prompting a pseudotumor (Fig. 8.11). Awareness of these syndromes and review of the radiographs usually allows correct diagnosis, such as with the distal femoral avulsive cortical irregularity/periosteal desmoid, which is a normal variant around the medial aspect of the knee, frequently mistaken for a sarcoma. Schmorl's nodes may rarely present as giant cystic-like lesions of the vertebral bodies in young patients (Hauger et al. 2001). Additional computer tomography may confirm these diagnoses. Ruptured Baker's cysts with perifascial fluid medial to the medial calf muscles, may appear as a mass on MRI, however extension to the posteromedial knee joint should allow for the correct diagnosis.

8.12 Calcium Deposition Disorders

Hydroxyapatite, gout and calcium pyrophosphate dehydrate crystal deposition disorders with calcium deposition in tendons, ligaments and bursae may create MRI pseudotumors. Patients with a

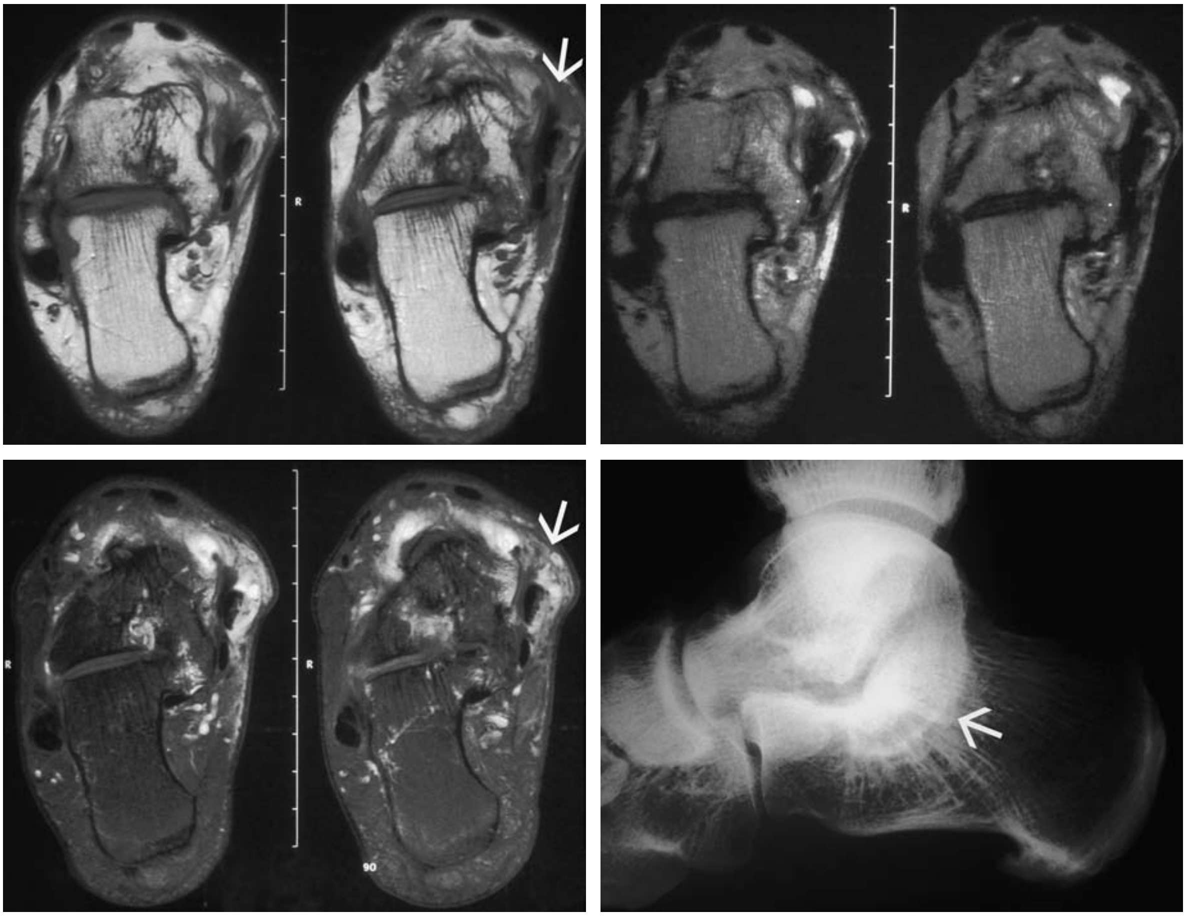

Fig. 8.11a–d. Young female weekend athlete tries to increase her fitness, with increasing ankle swelling. Outside MRI initially interpreted as synovial sarcoma for staging. **a** Oblique short axis T1-weighted MR image shows medial soft tissue swelling (*arrow*). **b** Corresponding T2-weighted MR image shows some evidence of tenosynovitis. **c** Corresponding T1-weighted fat suppressed MR image after intravenous contrast enhancement (*arrow*) shows active synovitis. **d** Review of lateral radiograph shows evidence of tarsal coalition (*arrow*) with reversed "c" sign

provisional clinical diagnosis of tumor associated with ligament calcification may be referred for MRI (Anderson et al. 2003a). Focal thickening of the lateral collateral ligament associated with adjacent marked soft tissue reaction with intravenous gadolinium contrast enhancement, which on review of the radiographs correlated to soft tissue calcifications. With its acute clinical onset and dissipation on follow-up radiographs, this entity is presumed to be due to hydroxyapatite deposition. Review of radiographs at the time of MRI reporting and awareness of this entity and others like it, is critical for correct MRI diagnosis of pseudotumor. It is more characteristic within the rotator cuff tendons of the shoulder.

8.13 Metabolic Disorders

Metabolic disorders may be associated with MRI pseudotumors such as amyloid deposition and hyperparathyroidism, though are most unusual in sporting individuals. Secondary amyloidosis is the commonest of this unusual group, usually seen in association with chronic renal failure. It is due to the deposition of beta-2 microglobulins within joint capsules and tendon sheaths and may rarely be associated with pseudotumors near joints. Characteristically there is a decreased signal intensity on T2-weighting, which appears to reflect the collagen-like nature of the amy-

loid (Kransdorf and Murphey 1997). Primary, or now more commonly, secondary hyperparathyroidism may be associated with brown tumors of bone which are non-specific on MRI. The most common clinical setting is chronic renal failure and laboratory results are diagnostic with high serum calcium, low serum phosphorus and a high parathormone level. Idiopathic tumoral calcinosis may present as an MRI pseudotumor with large septated regions of variable signal intensity in periarticular regions on both T1- and T2-weighting (Steinbach et al 1995), however review of the radiographs allows for this diagnosis.

8.14 Foreign Body Reactions

Foreign body reactions due to trauma or as a consequence of trauma such as retained surgical swabs (“cottonballoma”) (Fig. 8.12) (Kalbermatten et al. 2001) are fortunately less common, though should be considered in the appropriate clinical setting. Close inspection for traces of intramedullary screws, subtle metallic artifacts or direct evidence of retained foreign bodies, such as glass (Fig. 8.13), should be sought.

8.15 Vascular Pseudoaneurysms

Less common MRI pseudotumors include hand pseudoaneurysms (Anderson et al. 2003b). Of 25 cases, 10 presented clinically as soft tissue masses without other symptoms. These are usually caused by acute trauma with direct arterial injury; however they may be due to chronic repetitive trauma and the hypothenar hammer syndrome (Conn et al. 1970; McCue 1986). This syndrome describes signs and symptoms associated with ischemia of the hand and fingers secondary to blunt repetitive injury of the ulnar artery and superficial volar arch against the hook of hamate. Arterial wall damage may lead to pseudoaneurysm formation and or vessel thrombosis, micro emboli formation (Glichenstein et al. 1988) and compression of the sensory branch of the ulnar nerve (Glichenstein et al. 1988). Usually described in men of working age with industrial occupations involving repetitive blunt trauma to the hands (Newmeyer 1993; Little and Ferguson 1972) it has also been described in sports-related injuries in handball players and baseball catchers (Glichenstein et al. 1988; Newmeyer 1993; Little and Ferguson 1972). The thenar hammer syndrome (Janevski in Green et al. 1979) involves acute or chronic compression of the radial artery between the first and second metacarpal where the artery is more superficial in location and covered only by the muscle of flexor pollicis brevis and subcutaneous fat. The commonest pseudoaneurysms involve the popliteal artery, and if due to arteriosclerosis they will be bilateral in up to 75% of cases (Kransdorf and Murphey 1997). Adding an MR angiography sequence may give the diagnosis here.

8.16 Post Treatment/Intervention and Others

Though rare in sporting individuals, post therapy including post radiation MRI appearances may be associated with an MRI pseudotumor. Radiotherapy MRI findings of altered soft tissue and bone marrow signal intensities may be suspicious, however on close review there is usually no real mass and review of the radiotherapy details and port positioning usually allow a correct diagnosis (Richardson et al. 1996). Usually the history is apparent.

8.17 Rheumatological or Degenerative Joint Disease

Young sports people may also first present with mono-articular joint disease or due to overuse with advanced degenerative joint disease. Laboratory screens are helpful here.

8.18 AVN and Transient Osteoporosis

Avascular necrosis may occasionally mimic a cartilage lesion on radiographs, but the presence of the

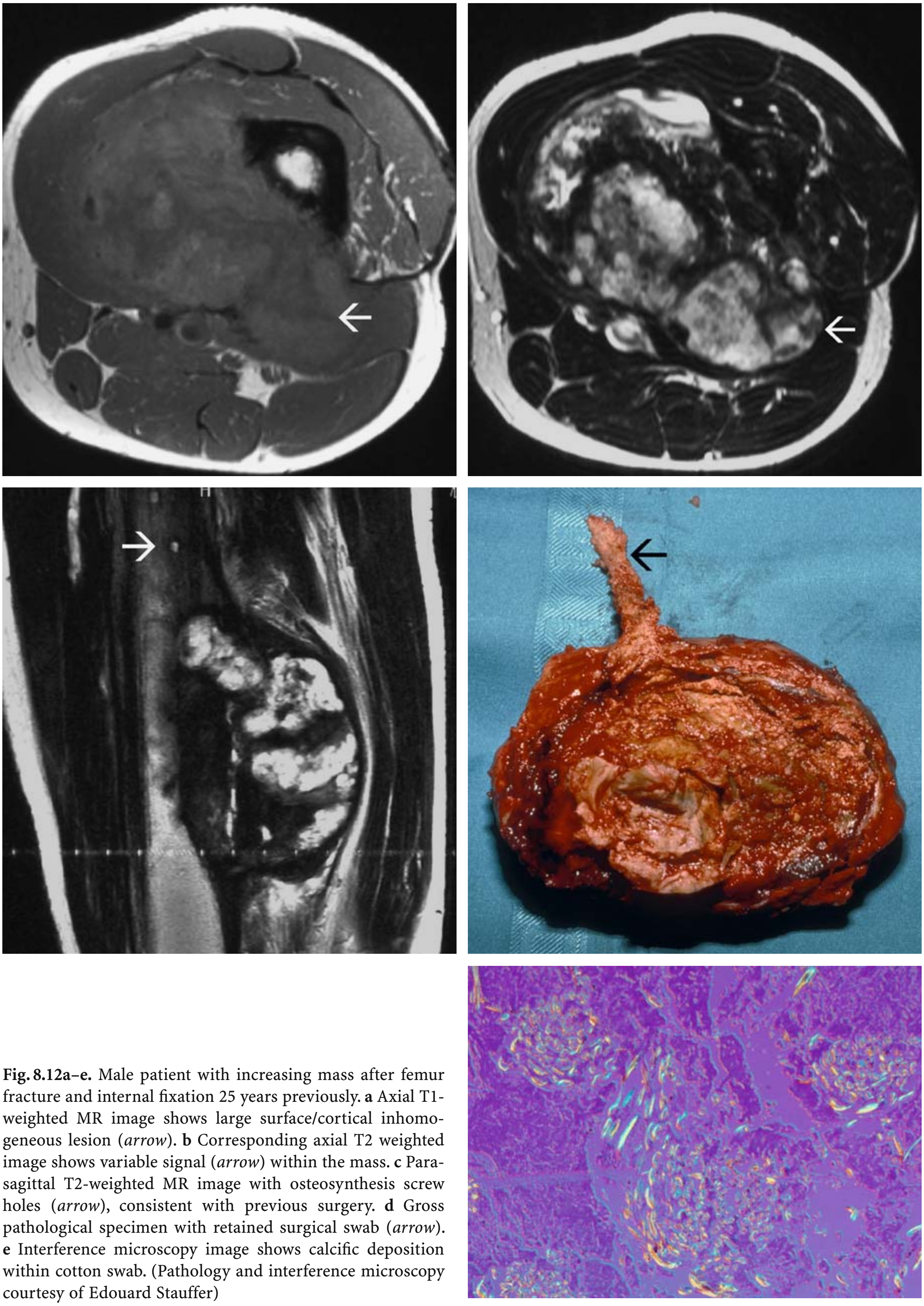

Fig. 8.12a–e. Male patient with increasing mass after femur fracture and internal fixation 25 years previously. **a** Axial T1-weighted MR image shows large surface/cortical inhomogeneous lesion (*arrow*). **b** Corresponding axial T2 weighted image shows variable signal (*arrow*) within the mass. **c** Parasagittal T2-weighted MR image with osteosynthesis screw holes (*arrow*), consistent with previous surgery. **d** Gross pathological specimen with retained surgical swab (*arrow*). **e** Interference microscopy image shows calcific deposition within cotton swab. (Pathology and interference microscopy courtesy of Edouard Stauffer)

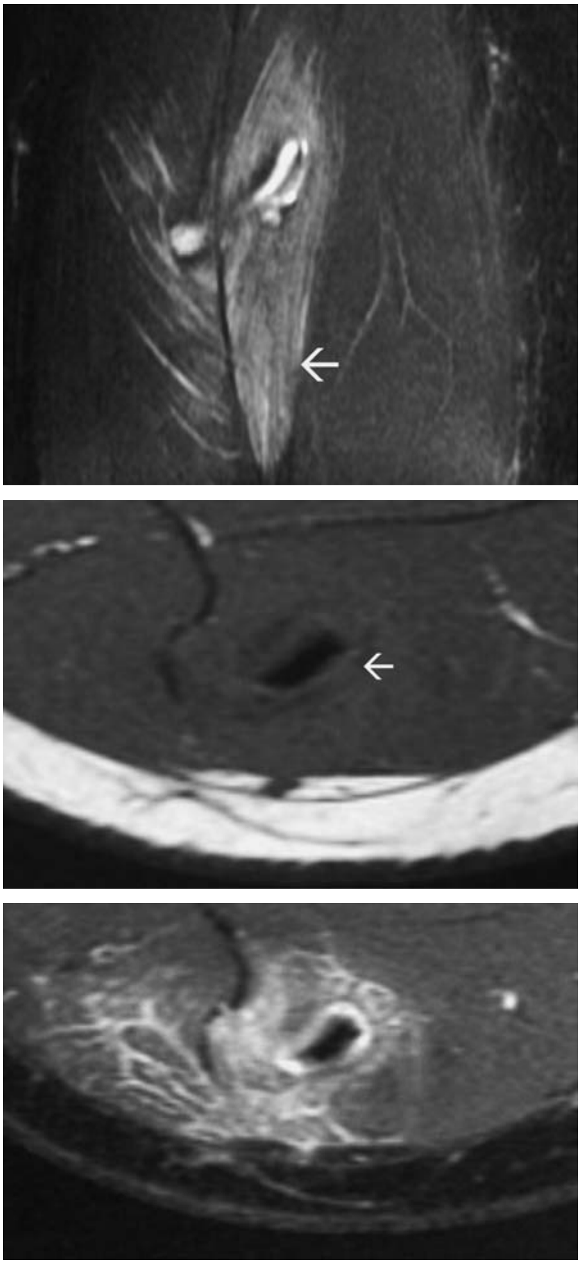

Fig. 8.13a–c. Eighteen-year-old jogger with swelling after minor trauma. **a** Coronal STIR shows subtle muscle altered signal intensity (*arrow*). **b** Axial T1-weighted MR image shows a small retained foreign body (*arrow*). **c** Corresponding axial T2-weighted MR image with fat suppressed shows the glass fragment

classical double geographic line sign should make this diagnosis obvious on MRI. Transient osteoporosis of bone may rarely mimic a tumor, with altered bone marrow signal intensity initially described within the proximal femur and also knee joint region, however there is a lack of a real mass and the pain and marrow signal subside.

8.19 Muscle Denervation

Post-surgical denervation muscle finding at MRI may mimic a tumor, particularly in the acute phase where this swelling and edema within muscle, however there is an absence of a mass. This may occur around the knee after minor sports related trauma, with common peroneal nerve injury (Fig. 8.14).

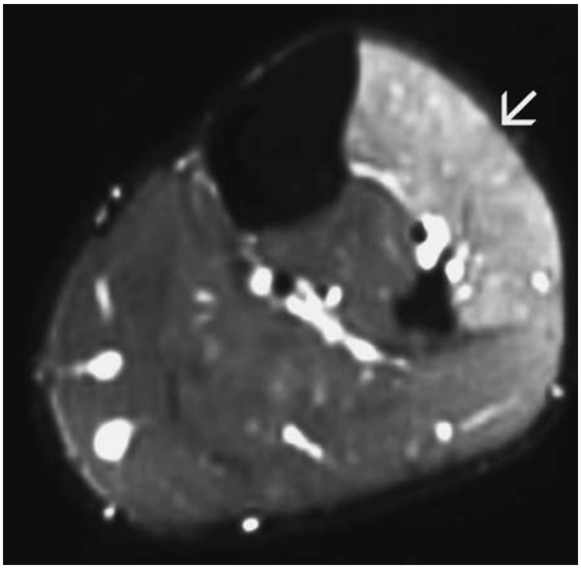

Fig. 8.14. Young male jogger presents with lower limb subtle swelling after minor trauma. Axial STIR shows subtle anterior compartment altered muscle signal intensity (*arrow*) consistent with peroneal nerve acute denervation atrophy. Further images excluded a mass around the knee joint

Things to Remember

1. Check for history of trauma – think myositis ossificans.
2. Review history for specific sport and repetitive activity – think overuse/tears of ligaments, muscles and stress reactions or fractures.
3. Ascertain whether a true focal mass is present.
4. Always correlate MRI with radiographs and/CT.
5. In case of superficial lesion – think hematoma/fat necrosis
6. In case of intra-muscular lesion – think hematoma / infection / myositis ossificans (tide mark sign).
7. Remember age specific lesions.
8. Aging population – more osteoporosis and insufficiency fractures.
9. Check risk factors for AVN.
10. Adolescents – stress reactions and fractures chronic avulsion fractures may mimic neoplastic lesion.
11. Joint lesions – remember systemic disorders may first present in one joint.
12. Marked irregular synovitis – think rheumatological disorder or infection.
13. Abscess wall sign – increased signal on T1-weighting within thickened wall.
14. Ensure T1-weighting to review for normal marrow signal.
15. Exclude normal variants with overuse – check radiographs.

References

Abdelwahab IF, Klein MJ, Hermann G (2003) Solitary cysticercosis of the biceps bracchi in a vegetarian: a rare and unusual pseudotumor. Skeletal Radiol 32:424–428
Anderson SE, Johnston JO, ODonnel R et al. (2001) MR imaging of sports related pseudotumor in children: mid femoral diaphyseal periosteitis at insertion site of adductor musculature. AJR Am J Roentgenol 176:1227–1231
Anderson SE, Bosshard C, Steinbach LS et al. (2003a) Calcification of the lateral collateral ligament of the knee: a rare pathology and cause of lateral knee pain shown by MR imaging. AJR Am J Roentgenol 181(1):199–202
Anderson SE, De Monaco D, Buechler U et al. (2003b) Imaging features of pseudoaneurysms of the hand in children and sdults. AJR Am J Roentgenol 180:659–664
Anderson SE, Steinbach LS, De Monaco D et al. (2004a) The baby wrist: MRI of an overuse syndrome of mothers. AJR Am J Roentgenol 182:719–724
Anderson SE, Weber M, Steinbach LS et al. (2004b) Shoe rim and shoe buckle pseudotumor of the ankle in elite and professional ice figure skaters and snow boarders: MR imaging findings. Skeletal Radiol 33:325-329. Epub 2004 May 6
Biviji AA, Paiement GD, Steinbach LS (2002) Musculoskeletal manifestations of the human immunodeficiency virus infection. J Am Acad Orthop Surg 10:312–320
Boutin RD, Fritz RC, Steinbach LS (2002) MRI of muscle injury. Radiol Clin N Am 40:333–362
Capelastegui A, Astigarraga E, Fernandez-Canton G et al. (1999) Masses and pseudomasses of the hand and wrist: MR findings in 134 cases. Skeletal Radiol 28:498–507
Charkes ND, Siddhivarn N, Schneck CD (1987) Bone scanning in the adductor insertion avulsion syndrome ("thigh splints"). J Nucl Med 28:1835–1838
Conn J Jr, Bergan JJ, Bell J (1970) Hypothenar hammer syndrome: posttraumatic digital ischaemia. Surgery 68:1122–1128
De Smet AA, Noris MA, Fisher DR (1992) Magnetic resonance imaging of myositis ossificans: analysis of seven cases. Skeletal Radiol 21:503–507
Dong PR, Seeger LL, Yao L et al. (1995) Uncomplicated cat-scratch disease: findings at CT, MR imaging, and radiography. Radiology 195:837–839
Donnelly LF, Bisset GS, Helms CA et al. (1999) Chronic avulsive injuries of childhood. Skeletal Radiol 28:138–144
Dooms GC, Fisher MR, Hricak H et al. (1985) MR imaging of intra-muscular hemorrhage. J Comput Assist Tomogr 9:908–913
Fujimoto H, Ikeda M, Shimofusa R et al. (2002) Sarcoidosis breaching the fascia and mimicking a sarcoma. Skeletal Radiol 31:706–708
Glichenstein J, Ohana J, Leclercq C (1988) Tumors of the hand. Springer, Berlin Heidelberg New York, pp 147–150
Gomori JM, Grossman RI, Golberg HI et al. (1985) High field magnetic resonance imaging of intracranial hematomas. Radiology 157:87–93
Hardcastle P, Annear P, Foster DH et al. (1992) Spinal abnormalities in young fast bowlers. J Bone Joint Surg Br 74-B:421–425
Hauger O, Cotten A, Chateil JF et al. (2001) Giant cystic Schmorls nodes: imaging findings in six patients. AJR Am J Roentgenol 176:969–972

Janevski BK (1979) Angiography of the upper extremity. In: Greep JN, Lemmens HAJ, Roos DB et al. (eds). Pain in the shoulder and arm. Nijhoff M, The Hague Boston London, pp 25–48

Jelinek J, Kransdorf MJ (1995) MR imaging of soft-tissue masses. Mass-like lesions that simulate neoplasms. Magn Reson Imaging Clin N Am 4:727–741

Kalbermatten DF, Kabermatten NT, Hertel R (2001) Cotton-induced pseudotumor of the femur. Skeletal Radiol 30:415–417

Kransdorf M, Murphey M (1997) Masses that may mimic soft tissue tumors. In: Kransdorf M (ed) Imaging of soft tissue tumors. WB Saunders, Philadelphia, pp 373–420

Little JM, Ferguson DA (1972) The incidence of Hypothenar hammer syndrome. Arch Surg 105:684–685

May DA, Disler DG, Jones EA et al. (2000) Abnormal signal intensity in skeletal muscle at MR imaging: patterns, pearls and pitfalls. Radiographics 20:S295–315

McCue FC (1986) Soft tissue injuries to the hand. In: Pettrone F (ed) American Academy of Orthopedic Surgeons, Symposium on the Upper extremity injuries in athletes. Mosby, Washington, pp 79–94

Newmeyer W (1993) Vascular disorders. In: Green D (ed) Operative hand surgery, 3rd edn. Churchill Livingstone, New York, pp 2251–2299

Ogilvie CM, Kasten P, Rovinsky D et al. (2001) Cysticercosis of the triceps – an unusual pseudotumor. Clin Orthop Relat Res 382:217–221

Pavlov H (1995) Physical injuries: sports related abnormalities. In: Resnick D (ed) Diagnosis of bone and joint disorders, 3rd edn. WB Saunders, Philadelphia, pp 3229–3263

Richardson ML, Zink-Brody GC, Patten RM et al. (1996) MR characterization of post-irradiation soft tissue edema. Skeletal Radiol 25:537–543

Rubin JI, Gomori JM, Grossman RI et al. (1987) High-field MR imaging of extracranial hematomas. AJR Am J Roentgenol 148:813–817

Schneider R, Kaye JJ, Ghelman B (1976) Adductor avulsive injuries near the symphysis pubis. Radiology 120:567–569

Soler R, Castro JM, Rodriguez E (1996) Value of MR findings in predicting the nature of soft tissue lesions: benign, malignant or undetermined lesion? Comput Med Imaging Graph 20:163–169

Soler R, Rodriguez E, Aguilera C et al. (2000) Magnetic resonance imaging of pyomyositis in 43 cases. Eur J Radiol 35:59–64

Steinbach LS, Johnston JO, Tepper EF et al. (1995) Tumoral calcinosis: radiologic-pathologic correlation. Skeletal Radiol 24:573–578

Tsai TS, Evans HA, Donnelly LF et al. (1997) Fat necrosis after trauma: a benign cause of palpable lumps in children. AJR Am J Roentgenol 169:1623–1626

Yoshioka H, Anno I, Niitsu M et al. (1994) MRI of muscle strain injuries. J Comput Assist Tomogr 18:454–460

Topographic Discussion

Shoulder Instability

9

Javier Beltran and Agustinus Suhardja

CONTENTS

J. Beltran, MD, FACR
A. Suhardja, MD
Department of Radiology, Maimonides Medical Center, 4802 Tenth Avenue, Brooklyn, New York 11219, USA

9.1 Introduction

The complex anatomy of the glenohumeral joint allows the greatest range of mobility compared with any other joint in the body (over 180 in several planes). This presents a higher risk for dislocation and development of chronic instability. The stability of the glenohumeral joint is maintained by active and passive mechanisms depending on the presence or absence of energy expenditure. Active mechanisms include the long head of the bicipital tendon (LBT) and the rotator cuff muscles and tendons. Passive mechanisms include the size and shape of the glenoid fossa, the labrum, adhesion and cohesion of the articular surfaces, the joint capsule and the superior, middle and inferior glenohumeral ligaments. In this chapter, the normal anatomy, variants, basic biomechanics and pathology of the glenohumeral joint are discussed, with focus on the labrum, the capsuloligamentous complex and the LBT.

Plain film radiography is essential for the initial evaluation of patients with acute shoulder dislocation, for proper assessment of adequate reduction and evaluation of associated bony lesions such as Hill Sachs lesion, reverse Hill Sachs lesion, avulsion fracture of the anterior inferior glenoid labrum (bony Bankart lesion) and avulsion fracture of the humeral insertion of the anterior band of the inferior glenohumeral ligament.

Unenhanced computed tomography provides the same information but it has the main advantage of multiplanar reconstruction and surface rendering capabilities. Additionally provides some information regarding the soft tissues such as the presence of hematoma or joint effusion or other fluid collections.

CT arthrography allows additional assessment of the intracapsular structures including labrum, inner capsule and articular cartilage but it requires intra-articular injection of contrast material.

Ultrasonography has limited value in the evaluation of patients with glenohumeral instability due to its lim-

Box 9.1. Plain Film Radiography

- Evaluate acute dislocation
- Asses proper reduction and residual or associated bone lesions (Hill-Sachs lesion, bony Bankart)
- Advantages: Easily accessible

Box 9.2. Ultrasonography

- Limited use in glenohumeral instability
- Only to asses associated rotator cuff lesions

Box 9.3. Computed Tomography

- Same as Plain Film Radiography
- Additional but limited soft tissue information
- Advantages: Multiplanar and surface rendering reconstruction

Box 9.4. CT Arthrography

- Intra-articular injection of iodine contrast material allows better visualization of the internal capsular anatomy and pathology
- Main indication: Assessment of suspected labral tears
- Indicated when there is a contraindication to MRI or in patients with claustrophobia
- Advantages
  - Excellent depiction of osseous structures and calcified tissues
  - Multiplanar and surface rendering capabilities
  - Non-claustrophobic
  - Availability

Box 9.5. MRI

- Visualization and assessment of soft tissue anatomy and pathology including labrum, capsule, ligaments, rotator cuff, capsulolabral and neurovascular structures and osseous pathology
- Advantages
  - Multiplanar , non-ionizing

Box 9.6. Direct MR Arthrography

- Very accurate assessment of lesions associated with glenohumeral instability due to excellent depiction of intracapsular anatomy including labrum and capsuloligamentous complex
- Preferred examination in young athletic population

Box 9.7. Indirect MR Arthrography

- Similar indications as direct MR arthrography, but less invasive
- Limited capsular distension unless preexisting joint effusion. Therefore, subtle lesions may be missed

ited visualization of the joint. It may have a role in the assessment of associated lesions of the rotator cuff.

Unenhanced MRI provides excellent, multiplanar evaluation of the bones capsule, labrum and extracapsular soft tissue structures and it is considered the more appropriate modality for evaluation of patients with glenohumeral pathology, especially when used with intra-articular or intravenous injection of gadolinium (direct or indirect MR arthrography). Indirect MR arthrography offers the advantage of less invasiveness but its main disadvantage is the lack of significant capsular distension, unless a preexisting effusion is present. Direct MR arthrography is more invasive, since it requires the intra-articular injection of contrast material but it is considered the most accurate modality to evaluate patients with glenohumeral joint instability. In this chapter, emphasis is placed on MR imaging of glenohumeral instability in the athletic population.

9.2 Normal Anatomy and Variants

9.2.1 Osseous Anatomy

The osseous structures forming the shoulder joint include the scapula, clavicle and proximal humerus. The articular surface of the glenoid articulates with the humeral head. The acromion process along with

the coracoid process and coracoacromial (CA) ligament form the acromial arch. A portion of the rotator cuff (the supraspinatus and infraspinatus muscles and tendons) glides between the acromial arch and the humeral head.

The inherent instability about the shoulder is in part, related to the shallow depth of the glenoid cavity. Though a fibrocartilaginous labrum attached to the rim adds depth to the fossa, there is variability in the contour. From a deep socket to a flat surface, the contour of the fossa is as variable as the shape of the articulating humeral head. Two important tendons have attachments to the bony glenoid. The LBT arises from the supraglenoid tubercle and the infraglenoid tubercle gives rise to the long head of the triceps muscle.

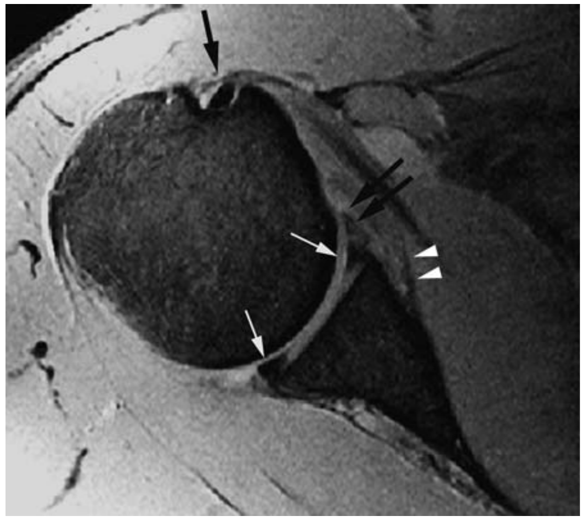

Fig. 9.1. Normal glenoid labrum. Axial GRE. The anterior and posterior segments of the glenoid labrum (*white arrows*) are identified as hypointense triangular structures. Note the MGHL (*short white arrows*) adjacent to the anterior labrum. The anterior capsular insertion in the glenoid is located about 1 cm medial to the glenoid margin (Type III). The LBT is identified as a low signal intensity structure within the bicipital grove (*long black arrow*)

9.2.2 Labrum

The labrum is a fibrous/fibrocartilaginous structure surrounding the edge of the osseous glenoid which increases the depth of the glenoid fossa and hence the stability of the glenohumeral joint. However, its more important function is to serve as the anchoring structure for the glenohumeral ligaments and the LBT, superiorly. The normal glenoid labrum on the standard MR examination is best evaluated by a combination of axial, sagittal and coronal projections. The axial plane best demonstrates the anterior and posterior labrum, while the oblique coronal plane illustrates the superior and inferior portions (Figs. 9.1 and 9.2). The classic morphology is described as smooth, with triangular anterior and posterior wedges as seen on the axial images, although occasionally, the edge of the labrum may be blunted. In the elderly population the labrum may become smaller and irregular due to degeneration. Signal intensity should be low on all pulse sequences. However, using low TE pulse sequences, parts of the labrum can become hyperintense when are oriented at 55° with the main magnetic field. The posterior portion of the labrum is generally smaller than its anterior counterpart. The normal labrum is firmly attached to the glenoid margin of the scapula and the scapular periosteum. Not infrequently the anterior superior labrum is partially detached, creating a space between the glenoid and the labrum called the sublabral foramen or sublabral hole (Fig. 9.3). This is a normal variant and should not be confused with an anterior superior labral tear when performing arthroscopy or MRI.

Fig. 9.2. Normal glenoid labrum. Coronal fat suppressed T1-weighted direct MR arthrogram. Note the hypointense triangular structures (*white arrows*) representing the fibrocartilaginous segments of the superior and inferior glenoid labrum. Observe the continuity of the labrum with the intermediate signal intensity articular cartilage

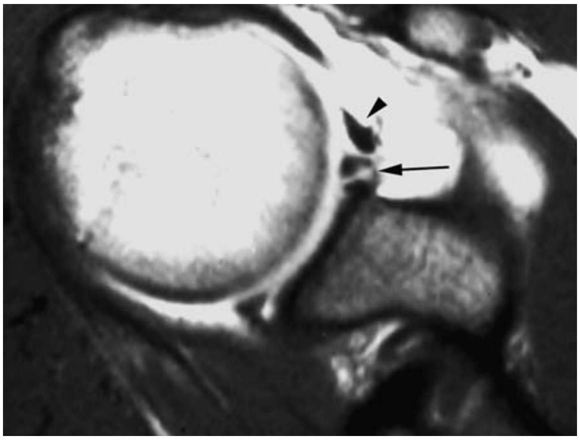

Fig. 9.3. Sublabral foramen. Axial fat suppressed T1-weighted direct MR arthrogram. Note the contrast-filled space (*arrow*) between the anterior glenoid labrum and the glenoid margin. The MGHL is thickened (*arrowhead*)

The junction of the LBT and the superior labrum also represents an area of potential normal variants. A space or recess between the superior labrum and glenoid, termed the sublabral recess may be confused with a superior labral tear (Beltran et al. 1997). Three types of junction between the LBT and the superior labrum may be seen: In type I the junction between the two structures is smooth and no indentation or recess is present. In type II a small recess is seen, reaching about 50% of the vertical thickness of the labrum, and in type III the recess is almost complete (Fig. 9.4). Fortunately, the orientation of the sublabral recess is medially, towards the head of the patient, whereas a superior labral tear points towards the shoulder of the patient. The inferior labrum is continuous with the articular cartilage and detachment in this region is considered an abnormal finding.

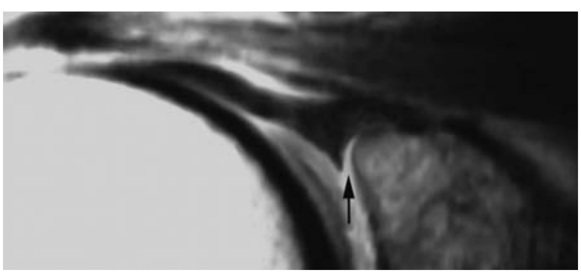

Fig. 9.4. Sublabral recess. Coronal fat suppressed T1-weighted direct MR arthrogram demonstrating a partially contrast-filled space (*arrow*) between the superior labrum and the glenoid margin. The LBT originates from the superior labrum

The insertion of the LBT may be in a broad base or in a thin area. It may have a predominant anterior or predominant posterior insertion. The predominant posterior insertion is prone to superior labral tears with posterior extension of the tear in the throwing athlete.

9.2.3 The Ligaments

The superior (SGHL), middle (MGHL) and inferior (IGHL) glenohumeral ligaments reinforce the joint capsule anteriorly (Fig. 9.5). The glenohumeral ligaments are infoldings of the capsule and each one contributes to a different degree to the stability of the glenohumeral joint, depending on the position of the arm. Significant variability exists as to the number of glenohumeral ligaments and even the relative size of the ligaments when present.

The SGHL usually arises from the shoulder capsule just anterior to the insertion of the LBT. The SGHL can have a common origin with the LBT or with the MGHL (Fig. 9.6). It inserts into the fovea

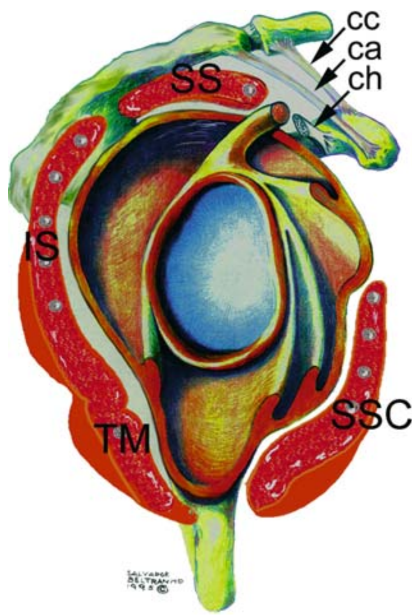

Fig. 9.5. Capsuloligamentous structures. Schematic drawing illustrating the glenoid fossa surrounded by the labrum. Note the infoldings of the capsule representing the glenohumeral ligaments. Outside of the capsule note the rotator cuff muscles and their corresponding tendons: *SS*: Supraspinatus; *IS*: Infraspinatus; *TM*: Teres minor; *SSC*: Subscapularis. The coracoid ligaments are also depicted: *cc*: Coracoclavicular; *ca*: Coracoacromial; *ch*: Coracohumeral

capitis, a line just superior to the lesser tuberosity. In this region, the SGHL is subjacent to the coraco-humeral (CH), a structure located superior to the LBT. The relationship between these three structures changes from medial to lateral. Medially, near the origin of the SGHL, the CH is located superior to the LBT and the SGHL anterior. More peripherally, at the level of the rotator cuff interval, the SGHL is located inferior to the LBT while the CH covers the LBT (Fig. 9.7).

The MGHL has been described arthroscopically as being attached to the anterior surface of the scapula, medial to the articular margin. It then lies in the oblique plane, posterior to the superior margin of the subscapularis muscle and blends with the anterior capsule. Distally the MGHL is attached to the anterior aspect of the proximal humerus, below the attachment of the SGHL (Caspari and Geissler 1993; Chandnani et al. 1995). Using MR arthrography, the scapular insertion of the MGHL is seen more

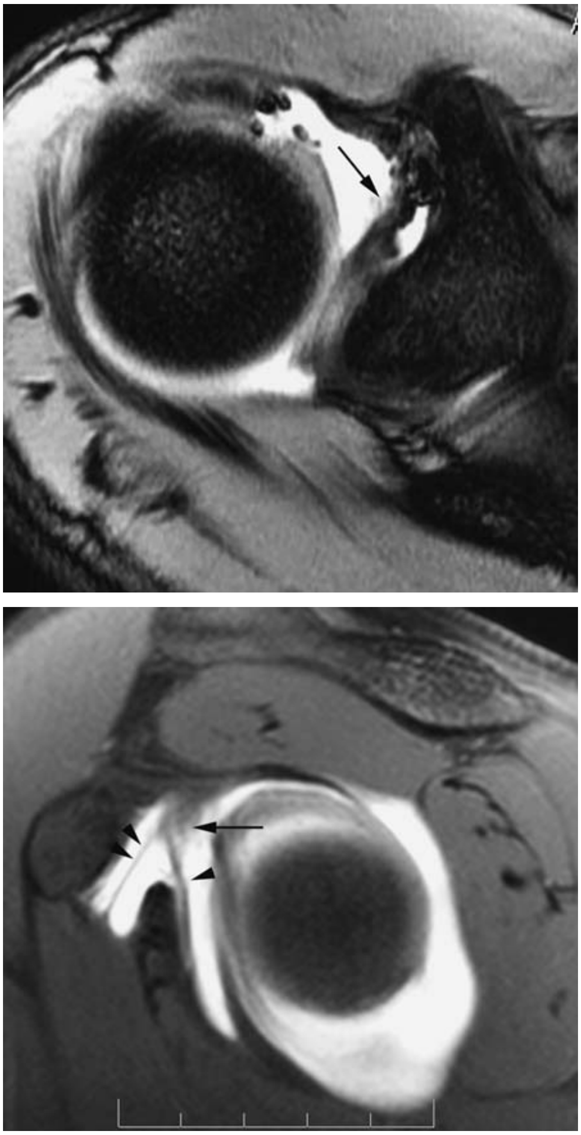

a

b

Fig. 9.6a,b. Superior glenohumeral ligament. **a** Axial GRE direct MR arthrogram. **b** Oblique sagittal fat suppressed T1-weighted direct MR arthrogram. On the axial plane (**a**), the SGHL (*arrow*) is identified as a hypointense structure concentric with the lateral cortex of the coracoid process. On the oblique sagittal plane (**b**) it is seen as a hypointense line (*double arrowhead*) adjacent to the coracoid process. In this particular case, the SGHL and the MGHL (*arrowhead*) have a common origin (*arrow*), a frequent normal variant

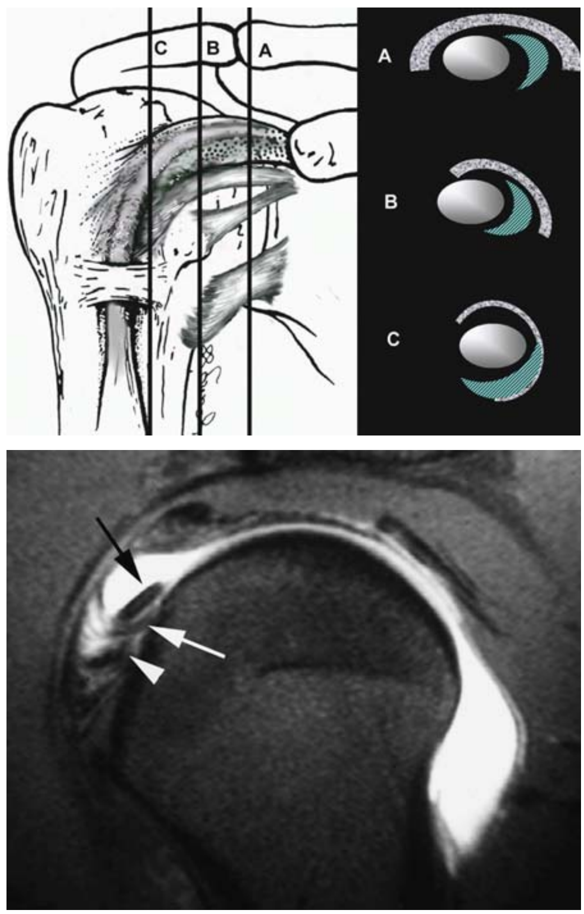

a

b

Fig. 9.7a,b. Relationship between the LBT, CH and SGHL. **a** Corona line drawing illustrating the position of the CH and the SGHL in relationship to the LBT. A medial section on the sagittal plane (section *A*) depicts the CH in top of the LBT and the SGHL anterior to it. In a more lateral section *B*, the SGHL is located partially under the LBT. In a further lateral section (*C*) the SGHL is located inferior to the LBT. **b** Sagittal fat suppressed T1-weighted direct MR arthrogram demonstrates the LBT (*black arrow*) and the fibers of the SGHL (*white arrow*). Note the CH (*arrowhead*) in a more anterior position

often at the level of the superior anterior labrum than at the level of the scapula, as it was originally suggested arthroscopically (Caspari and Geissler 1993; Chandnani et al. 1995) (Fig. 9.8).

The MGHL presents the largest multiplicity of normal variants. In one anatomic study, the ligament was absent in 30% of the specimens (Moseley and Overgaard 1962). In Chandnani's series (Chandnani et al. 1995), the MGHL was identified with MR arthrography in 85% of their cases. Other frequent variants include a common origin of the MGHL with the SGHL (Fig. 9.6); common origin with the SGHL and LBT; a common origin with the IGHL; cord-like thickening, with or without associated absence of the anterior superior portion of the labrum (Buford complex) (Fig. 9.9); and a split or duplicate ligament (Tirman et al. 1996; Williams et al. 1994; Yeh et al. 1998; Matsen et al. 1990).

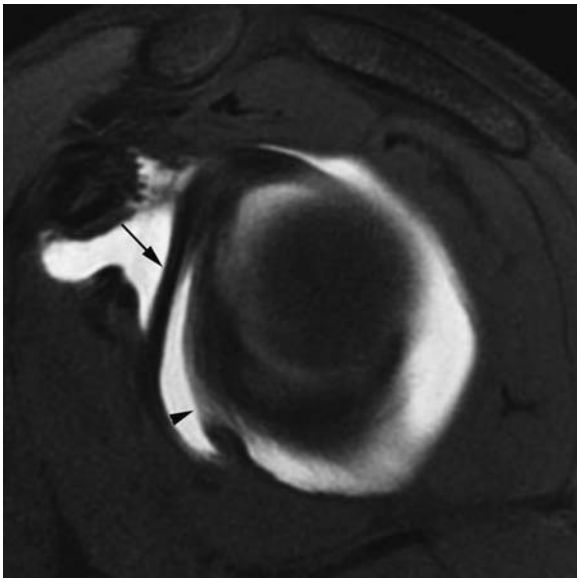

Fig. 9.8. MGHL. Oblique sagittal fat suppressed T1-weighted direct MR arthrogram demonstrating the MGHL (*arrow*) and the anterior band of the IGHL (*arrowhead*)

The IGHL is composed of an anterior band, a posterior band and the axillary recess of the capsule located in between the two bands (Figs. 9.5 and 9.10). It inserts in a collar-like fashion in the inferior aspect of the anatomic neck of the humerus. The anterior band is better assessed on MRI with the arm in the abduction and external rotation position (ABER position).

The ligaments related to the coracoid process include the coracohumeral, the coracoclavicular (CC) and the CA ligaments. These are important structures contributing to the normal biomechanics of the joint. The CH functions to maintain the stability of the LBT within the bicipital groove, and to resist superior translation of the humeral head (Fig. 9.11). The CA forms a strong band, which functions as a portion of the fibro-osseous roof of the glenohumeral joint called the coracoacromial arch (Fig. 9.12). This roof is also termed the coracoacromial arch. Its unyielding substance has been implicated in impingement syndromes of adjacent soft tissue structures. The coraco-

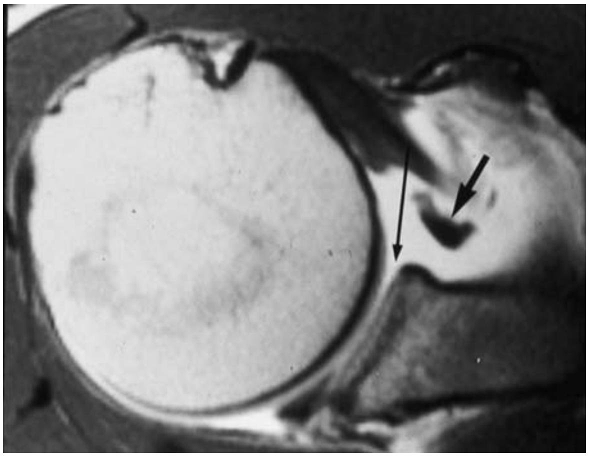

a

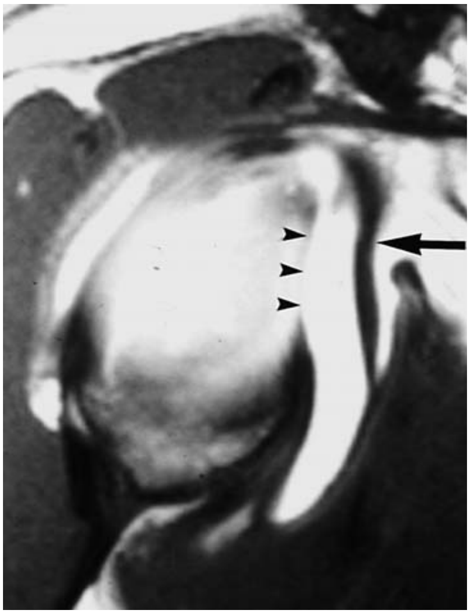

b

Fig. 9.9a,b. Buford complex. Axial (**a**) and oblique (**b**) sagittal T1-weighted direct MR arthrogram demonstrates the absence of the anterior superior labrum (*long arrow* in **a**, *arrowheads* in **b**) and the thick MGHL (*short black arrows* in **a**, **b**

a b c

Fig. 9.10a,b. IGHL. Axial (**a**), oblique sagittal fat suppressed T1-weighted direct MR arthrogram (**b**) and (**c**) fat suppressed T1-weighted direct MR arthrogram in ABER position (**c**). Note the anterior band of the IGHL (*triple arrow* in **a**, *double arrow* in **b** and **c**). The MGHL (*single arrow* in **b**) and SGHL (*arrowhead* in **b**) are also shown

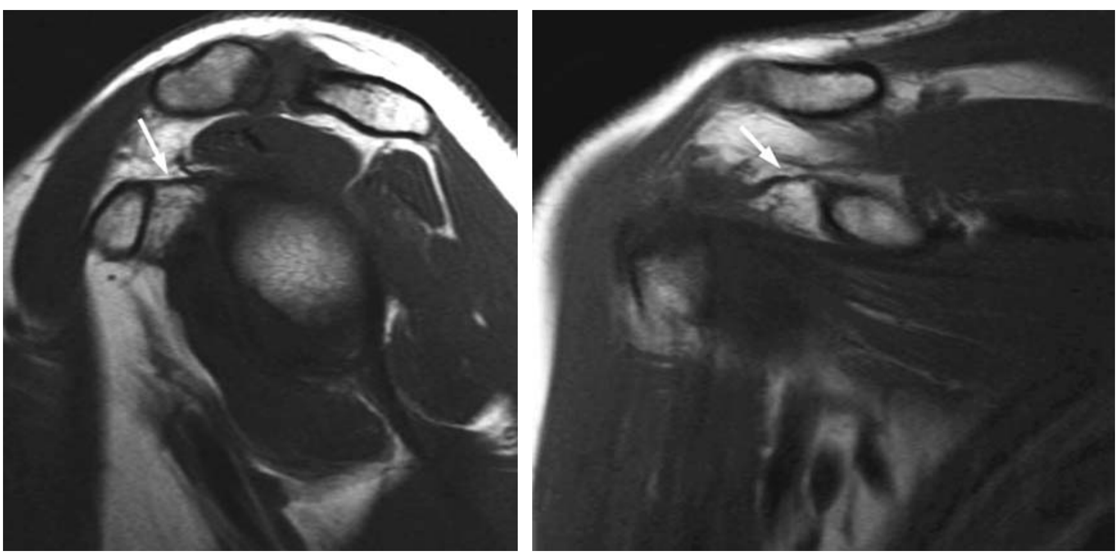

a b

Fig. 9.11a,b. CH ligament. Sagittal oblique (**a**) and coronal oblique (**b**) T1-weighted MR demonstrating the CH (*arrow*) as it extends from its origin in the base of the coracoid process towards the humeral head

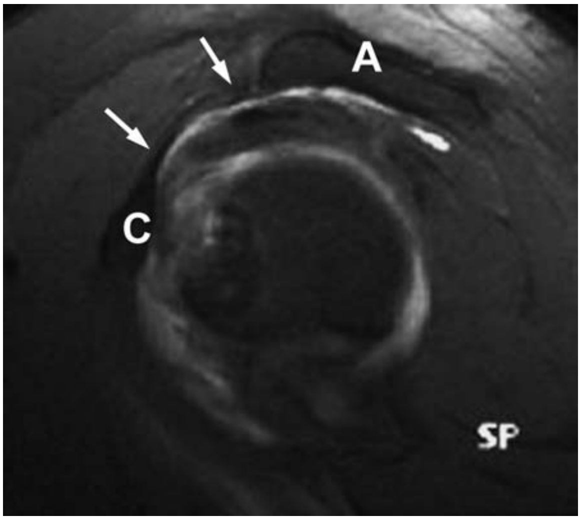

Fig. 9.12. Coracoacromial arch. Oblique sagittal fat suppressed T1-weighted direct MR arthrogram demonstrating the coracoid process (*C*), the CA ligament (*arrows*) and the acromion (*A*) forming an arch concentric with the humeral head. The rotator cuff is noted between the coracoacromial arch and the humeral head

clavicular ligament has two portions, the conoid and the trapezoid ligaments which function is to maintain vertical stability (see Chap. 11).

9.2.4 Muscular Anatomy

The four muscular components of the rotator cuff serve to stabilize the glenohumeral joint by preventing excessive motion at the joint (Fig. 9.5). In addition to their contribution to joint motion, their tendons reinforce the joint capsule. The tendon slips of the subscapularis muscle, which occupies the region of the medial portion of the subscapularis fossa on the ventral aspect of the scapula, reinforce the capsule anteriorly. Superior to the spine of the scapula the supraspinatus muscle takes its origin and extends to insert on the anterior, horizontal portion of the greater tuberosity. Inferior to the spine of the scapula the infraspinatus muscle originates from the infraspinatus fossa and extends laterally to insert posteriorly on the middle facet of the greater tuberosity. Together the infraspinatus and supraspinatus tendons reinforce the joint capsule superiorly. The teres minor muscle takes origin from the mid portion of the lateral aspect of scapula as well as the fascia of the infraspinatus muscle. Upon joining the posterior inferior portion of the joint capsule, it inserts onto the inferior facet of the greater tuberosity.

The rotator cuff interval, a space that is located in the anterosuperior aspect of the rotator cuff, represents an important intersection providing stability and direction to the structures that comprise this area (Fig. 9.7). The roof of this triangular shaped space is bound by the coracoid process superiorly, anteriorly the subscapularis tendon and posteriorly the supraspinatus tendon. The SGHL is an important structure traversing this area. It blends with the joint capsule to insert into the borders of the subscapularis and supraspinatus tendons. This provides a network of stabilizing fibers in this region. The CH ligament appears to provide additional reinforcement to the anterior aspect of the rotator cuff interval and may prevent inferior translation of the humeral head. The LBT traverses this area and is discussed in more detail below.

The biceps brachii muscle is composed of two heads; the long head arises from the supraglenoid tubercle and is continuous with the superior portion of the labrum. Its short head arises from the tip of the coracoid process. The LBT has an intracapsular portion and an extracapsular portion. The intracapsular portion extends from its insertion into the superior labrum to the bicipital groove, surrounded by the CH superiorly and the SGHL anteriorly and inferiorly. The morphology of the tendon insertion is variable with either a narrow or broad base of attachment. The normal MR appearance of the LBT includes low signal on all pulse sequences (Figs. 9.1 and 9.13). However, when using short TE pulse sequences, magic angle artifact can occur as the LBT turns around the humeral head and reaches a 55° angle with the magnetic field, exhibiting high signal intensity, not to be confused with tendinosis. The LBT may be followed on multiple sequences from its intra-articular position namely the origin from the supraglenoid tubercle through the intertubercular sulcus (the bicipital groove). At the level of the bicipital groove, the LBT and its synovial sheath leave the joint space to the myotendinous junction.

9.2.5 Glenohumeral Joint Capsule

The capsular mechanism provides the most important contribution to the stabilization of the glenohumeral joint. The anterior capsular mechanism includes the fibrous capsule, the glenohumeral liga-

a

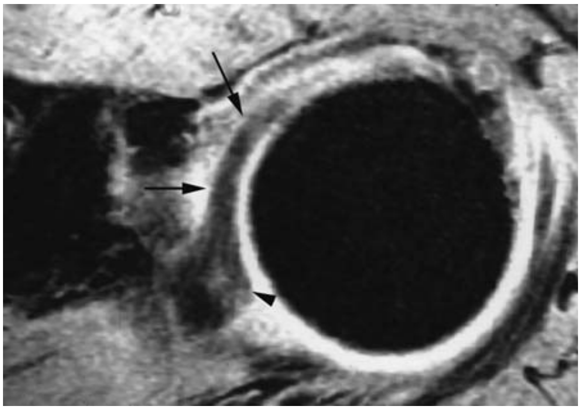

b

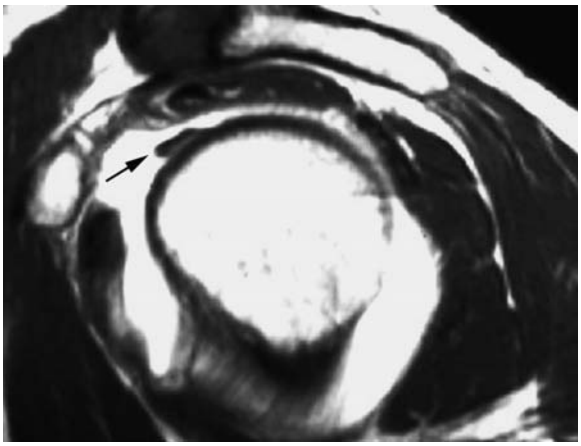

Fig. 9.13a,b. LBT, intracapsular portion. Axial GRE (**a**) and oblique sagittal T1-weighted direct MR arthrogram (**b**) showing the LBT (*arrows*) adjacent to the humeral head. Note the origin of the LBT in the superior labrum (*arrowhead* in **a**)

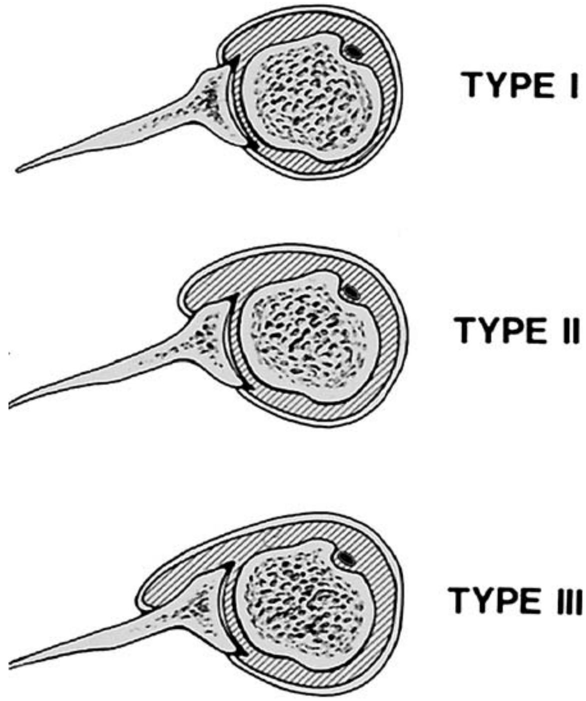

Fig. 9.14. Types of anterior capsular insertion. Type III, the more medial insertion is prone to anterior glenohumeral instability

ments, the synovial membrane and its recesses, the fibrous glenoid labrum, the subscapularis muscle and tendon, and the scapular periosteum. The anterior capsular origin can be divided into three types depending on the proximity of the capsular origin to the glenoid margin (Fig. 9.14) (Zlatkin et al. 1988). In general, the further the anterior capsular origin is from the glenoid margin (type III), more unstable the glenohumeral joint will be.

The posterior capsular mechanism (Rafii et al. 1986) is formed by the posterior capsule, the synovial membrane, the glenoid labrum and periosteum, and the posterosuperior tendinous cuff and associated muscles (supraspinatus, infraspinatus, and teres minor). The LBT originating in the superior aspect of the labrum and the long head of the triceps tendon originating in the infraglenoid tubercle inferiorly constitute additional supportive structures of the glenohumeral joint.

The joint capsule originates in the glenoid margin of the scapula and in the anatomical neck of the humerus. There are two main recesses of the capsule: the subscapularis recess and the axillary recess. The subscapularis recess is located between the coracoid process superiorly and the superior margin of the subscapularis tendon. The entrance to the subscapularis recess from the joint is termed the upper foramen of Weitbecht. The axillary recess is located between the anterior and posterior bands of the IGHL. A smaller recess can occasionally be present between the MGHL and the anterior band of the IGHL. The entrance to this recess from the joint is termed the lower foramen of Rouviere.

9.3 Normal Biomechanics

The function of the shoulder requires the coordinated motion of four joints: the scapuloclavicular, acromioclavicular, glenohumeral and scapulothoracic joints. Almost 30 muscles contribute to the motion of this joint complex. Most of the motion occurs at the level

of the glenohumeral and scapulothoracic joints. The glenohumeral joint is the joint of the human body with the greatest range of motion: 0–180° in elevation, internal and external rotation of 150° and anterior and posterior rotation in the horizontal plane of approximately 170°.

The relatively large articular surface of the humeral head compared with the small articular surface of the glenoid cavity explains the extended mobility of the joint. Because of its wide range of motion, the glenohumeral joint is also more susceptible to dislocations, subluxations, and lesions related to chronic stress in the surrounding soft tissues.

9.3.1 The Overhead Throwing Mechanism

The overhead throwing action places high stress loads on the capsulolabral complex and rotator cuff and even minor degrees of injury to these structures can become symptomatic and produce significant functional impairment. Joint laxity may develop as a consequence of the injury to the tissues, leading to even more damage and further instability. It is now understood that in the throwing athlete these injuries are not the consequence of a single event of dislocation but are the result of multiple episodes of microtrauma producing gradual increase of shoulder pain at some point in the throwing position.

In order to understand the pathophysiology of the glenohumeral instability in the throwing athlete is important to know the normal joint motion during the action of throwing. With minor differences, overhead throwing, the volleyball spike, the golf swing, and the tennis serve all have similar throwing mechanics (Meister 2000; Pink et al. 1990). There are six phases in the overhead throwing motion (Fig. 9.15): wind-up, early cocking, late cocking, acceleration, deceleration and follow-through (Matsen et al. 1991).

During the wind-up phase, there is minimal stress loading and muscular activity of the shoulder. At the end of this phase the shoulder is in minimal internal rotation and slight abduction (Positions 1 and 2, Fig. 9.15).

During the second phase of early cocking the shoulder reaches 90° of abduction and 15° of horizontal abduction (elbow posterior to the coronal plane of the torso) (Position 3, Fig. 9.15). During this phase there is early activation of the deltoid muscle and late activation of the rotator cuff muscles with the exception of the subscapularis muscle. With the arm at 90° of abduction, a normal range of 90–110° of internal and rotation is easily achieved in the normal individual.

During the third phase of late cocking the shoulder ends in maximum external rotation of 170° to 180° maintaining 90° to 100° of abduction. The 15° of horizontal abduction changes to 15° of horizontal adduction (Position 4, Fig. 9.15). The scapula retracts to facilitate this position and provide a stable base for the humeral head. The combination of abduction and external rotation forces posterior translation of the humeral head on the glenoid. The activity of the deltoid muscle decreases, while the rotator cuff muscles reach their peak. During the terminal portion of the late cocking phase, the subscapularis, latissimus dorsi, pectoralis major and serratus anterior muscles increase their activity.

During the early and late cocking phase, with the arm in about 90° of abduction, while moving from internal to the external rotation positions, the humeral head rotates centered in the middle of the glenoid fossa (the bare area) and the greater tuberosity describes a concentric arc from anterior to posterior as the humerus rotates (Fig. 9.16).

During the fourth phase of acceleration abduction is maintained while the shoulder rotates to the ball release (Position 5, Fig. 9.15). The scapula protracts

Fig. 9.15. The six phases of the throwing action (see text)

Fig. 9.16. Center of rotation. Sagittal depiction of the glenoid fossa and cut capsule. The yellow dot represents the center of rotation of the humeral head in abduction, during the external rotation. The curved yellow arrow represents the path and direction of the greater tuberosity as the arm externally rotates

as the body moves forward and the humeral head re-centers in the glenoid fossa, decreasing the stress on the anterior capsule. During the early acceleration phase the triceps muscle shows marked activity, while the latissimus dorsi, pectoralis major and serratus anterior muscles increase their activity during the late acceleration phase.

During the fifth phase of deceleration, the energy not imparted to the ball is dissipated. It begins at the moment of ball release and it ends with cessation of humeral rotation to 0°. Abduction is maintained at 100° and horizontal adduction increases to 35°. All muscle groups contract violently, with eccentric contraction, allowing the arm to slow down. During this phase joint loads are very high posteriorly and inferiorly, as well as compressive forces, through strong contraction of the biceps muscle.

During the sixth phase of follow-though, the body moves forward with the arm until the motion ceases. Shoulder rotation decreases to 30°, horizontal adduction increases to 60° and abduction is maintained at 100° while joint loads decrease, ending in adduction (Position 6, Fig. 9.15).

9.3.2 Joint Stability

As indicated earlier, the stability of the glenohumeral joint is maintained by the presence of active and passive mechanisms depending on whether or not muscle energy is used. Active mechanisms include the biceps tendon and the rotator cuff muscles and tendons. Passive mechanisms include the labrum, the joint capsule and the superior, middle and inferior glenohumeral ligaments which reinforce the joint capsule anteriorly.

The relative contribution of each individual glenohumeral ligaments to joint stability has been the subject of debate. Matsen et al. (Matsen et al. 1991) and Caspari and Geissler (Caspari and Geissler 1993) indicated that the SGHL and MGHL are absent in a high percentage of individuals; therefore they must not be important structures in maintaining joint stability. Turkel et al. (Turkel et al. 1981) studied the contribution of each one of the glenohumeral ligaments by means of selectively cutting these structures in cadavers and then assessing the stability of the join at different degrees of abduction and external rotation. They concluded that the IGHL is the most important structure in the prevention of dislocation with the arm at 90° of abduction and external rotation.

In another classic experiment, O'Connell et al. (O'Connell et al. 1990) measured the tension of the glenohumeral ligaments in cadavers after application of a controlled external torque. They concluded that at 90° of arm abduction, the IGHL and the MGHL developed the most strain, whereas with the arm at 45° of abduction, the most strain was also developed by the IGHL and MGHL, but some strain also occurred at the SGHL.

The IGHL is considered the most important stabilizer of the glenohumeral joint. The complex attachment of the IGHL, with its anterior and posterior bands and the axillary recess allows the greatest distribution of stress in different degrees of rotation. For example, in the throwing position of abduction and external rotation, the anterior band is under greater tension than the posterior band. Conversely, if the arm is placed in abduction and internal rotation, the posterior band experiences greater tension. The humeral head is supported by the "hammock" of the axillary recess, reinforced anteriorly and posteriorly by the anterior and the posterior bands (the reciprocal cable model described by O'Brien et al.) (O'Brien et al. 1990).

The LBT, the CH and CA ligaments are also important structures contributing in different ways to the normal biomechanics of the joint. The CH helps in maintaining the stability of the LBT and the acromio humeral ligament is an important part of the acromial arch. The LBT has an intracapsular portion and an extracapsular portion. The intracapsular portion extends from its insertion into the superior labrum to the bicipital groove. The insertion of the tendon may be in a broad base or in a thin area.

The muscles around the shoulder are important contributors to the stability of the shoulder joint. The rotator cuff muscles provide internal and external rotation and some degree of abduction and, along the LBT provide dynamic compression of the humeral head into the glenoid fossa, centering the humeral head and countering the oblique translational forces generated during the act of throwing (Itoi et al. 1993; Pagnani et al. 1996). It has been demonstrated by Warner et al. (Warner et al. 1999) that this concavity-compression mechanism provides greater stability to the glenohumeral joint in the inferior direction than negative intra-articular pressure or ligament tension in all degrees of abduction and rotation.

Another significant factor contributing to the stability of the glenohumeral joint is the scapulothoracic coordination during throwing. This is achieved mainly through synchronization with the latissimus dorsi, pectoralis major and serratus anterior muscles (Meister 2000). There is 2:1 ratio of glenohumeral to scapulothoracic motion during abduction. More recent studies indicate that this ratio is even higher and it is more significant during the early degrees of abduction (Pink et al. 1990). Failure of the scapulothoracic coordination may place additional stress on the capsulolabral complex, hence increasing the risk for soft tissue damage. It has been shown that patients with shoulder instability have increased scapulothoracic asymmetry.

9.4 Glenohumeral Instability

Pathologic movement of the humeral head with respect to the glenoid fossa characterizes the entity of glenohumeral joint instability. The direction of instability combined with an assessment of the etiology and chronicity allow the clinician to characterize the lesion. This entity represents the final common pathway for a host of lesions for which advanced imaging techniques, such as direct and indirect arthrography, have been employed in the problem solving armamentarium.

Classically, non-enhanced MRI of the shoulder for the detection of lesions associated with glenohumeral instability has been reported to have variable results by different researchers (Garneau et al. 1991; Chandnani et al. 1993). Different types of surface coils, field strengths and imaging parameters contribute to the variability. More recently, MR arthrography, following intra-articular injection of contrast material has gained popularity because of its ability to depict small intracapsular structures when the joint capsule is distended with contrast. In addition, greater knowledge of the anatomy and normal variants also contributes to improved accuracy (Shankman et al. 1999).

Glenohumeral instability can be categorized along a spectrum from minimal translation of the humeral head (microinstability) to shoulder dislocation. Glenohumeral instability can be unidirectional or multidirectional.

To categorize glenohumeral instability on the basis of pathogenesis, namely traumatic or atraumatic etiologies, mnemonics have been developed which may help on making clinical determinations (surgical vs. conservative management). TUBS refer to patients with ***t***raumatic instability, with ***u***nilateral involvement, commonly involving a ***B***ankart lesion and often requiring ***s***urgery. AMBRI refers to ***a***traumatic instability, which may be ***m***ultidirectional, commonly ***b***ilateral and treated with either ***r***ehabilitation or an ***i***nferior capsular shift. A third type known as AIOS refers to the ***a***cquired ***i***nstability from ***o***verstress (microinstability), usually treated with ***s***urgery.

Most frequently, a single event instigates a constellation of lesions leading to other episodes of dislocation or subluxation. The capsule and glenohumeral ligaments (GHL) provide resistance to the anterior translation of the humeral head as indicated above. The labrum is torn as part of the avulsion forces produced by the GHL at the time of the injury. Anteroinferior dislocation of the humeral head to the subcoracoid location is the most frequent cause of anterior glenohumeral instability. The associated lesions that may take place during an anteroinferior dislocation include anteroinferior labral tear (the Bankart lesion) with tear of the IGHL and / or capsular-periosteal stripping; fracture of the anteroinferior glenoid margin (the bony Bankart lesion); and compression fracture of the superolateral aspect of the humeral head (Hill-Sachs lesion) (Fig. 9.17).

Fig. 9.17a–d. Anteroinferior glenohumeral dislocation, bony Bankart lesion, Hill Sachs Lesion and classic Bankart lesion. Plain radiograph (**a**) demonstrates an anteroinferior glenohumeral dislocation associated with a fracture of the anteroinferior glenoid labrum (bony Bankart) (*arrow* in a). Plain film radiograph following reduction of a glenohumeral dislocation in another patient (**b**) demonstrates a prominent Hill Sachs lesion (*arrow* in b). CT surface rendering (**c**) demonstrates a Hill Sachs lesion (*arrows*). Axial (**d**) fat suppressed T1-weighted direct MR arthrogram in another patient. Note the torn and displaced labrum (*single arrow*), the torn periosteum (*short arrows*) and the stripped capsule (*double long arrows*)

Persistent shoulder pain in young athletes may be caused by posterior instability due to repeated episodes of microtrauma without frank dislocation. Abduction, flexion and internal rotation are the mechanisms involved in these cases (swimming, throwing and punching) and can be associated with posterior capsular laxity. Associated lesions of posterior instability include posterior labral tears, posterior capsular stripping or laxity, fractures, erosions, sclerosis and ectopic bone formation of the posterior glenoid (the Bennett lesion) (Fig. 9.18) and vertical impaction fractures of the anterior aspect of the humeral head (reverse Hill-Sachs, McLaughlin fracture). Posterior shoulder dislocation more often occurs as a result of a violent muscle contraction, particularly in the setting of seizures or electrical shock or after an anterior blow to the shoulder in football players. Following the acute episode of dislocation, the arm frequently remains locked in adduction and internal rotation.

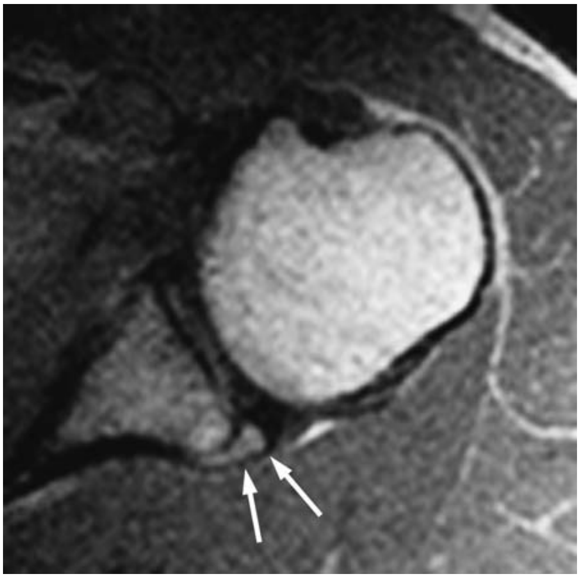

Fig. 9.18. Bennett lesion. Axial PD image demonstrating the spur like formation in the aposterior glenoid margin (*arrows*)

9.4.1 Labral Pathology

Using non-enhanced conventional MRI, the main finding in patients with anterior instability is the Bankart lesion, with labral tear (Fig. 9.17). The low signal intensity of the fibrous labrum contrasts with the adjacent articular cartilage and allows detection of labral tears. However, unless the capsule is distended by native fluid, associated lesions of the glenohumeral ligaments or small, non-displaced labral tears may be difficult to detect. The classic Bankart lesion is the combination of an anterior labral tear and capsuloperiosteal stripping. On arthroscopy, the Bankart lesion is seen as a fragment of labrum attached to the anterior band of the IGHL and to the ruptured scapular periosteum, "floating" in the anteroinferior aspect of the glenohumeral joint. Extensive bone and soft tissue damage and persistent instability may lead to multidirectional instability, resulting in episodes of posterior dislocation (Novotny et al. 1998; Mizuno et al. 1993; Wolf et al. 1995; Mallon and Speer 1995; Schenk and Brems 1998; Legan et al. 1991).

A number of variants of anterior labral tears have been described. The ***a***nterior ***l***abroligamentous ***p***eriosteal ***s***leeve ***a***vulsion (ALPSA) refers to a tear of the anteroinferior labrum, with associated capsuloperiosteal stripping. The torn labrum is rotated medially and a small cleft or separation can be seen between the glenoid margin and the labrum (Fig. 9.19). Contrary to the Bankart lesion, the ALPSA lesion can heal (synovialization), leaving a deformed and patulous labrum (Fig. 9.19). The ***g***lenoid ***l***abral ***a***rticular ***d***isruption (GLAD) represents a tear of the anteroinferior labrum, attached to a fragment of articular cartilage, without associated capsuloperiosteal stripping (Fig. 9.20) (Neviaser 1993a, b).

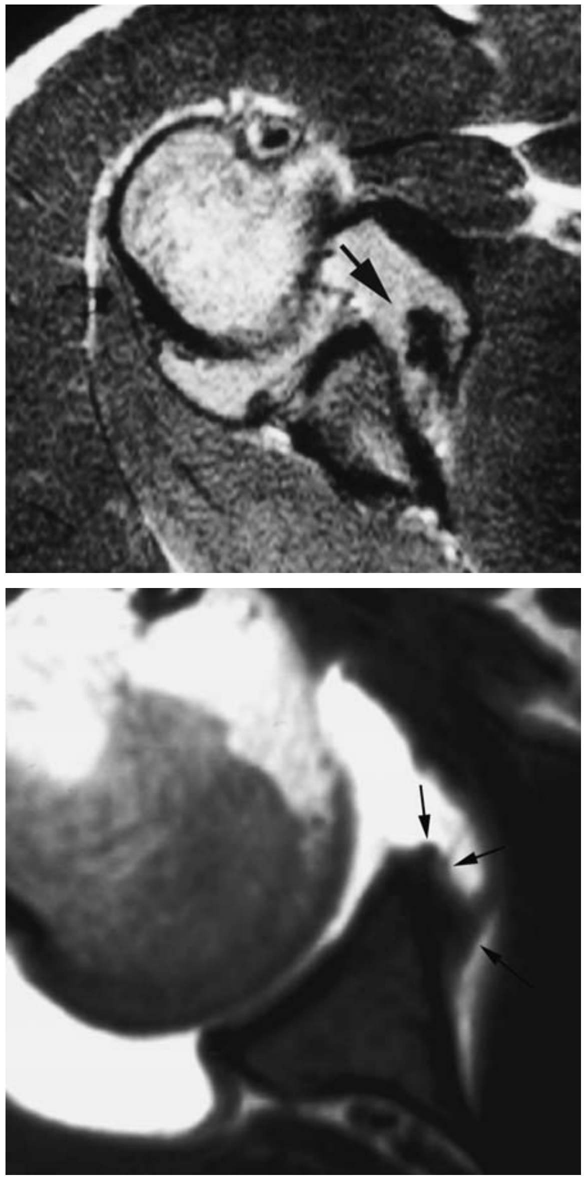

a

b

Fig. 9.19a,b. ALPSA. Axial T2-weighted image (**a**) demonstrates a torn and medially displaced labrum (*arrow*), representing an acute ALPSA lesion. Axial fat suppressed T1-weighted direct MR arthrogram (**b**) demonstrates in another patient a chronic ALPSA lesion with thickening of the capsuloperiosteal junction and the labrum (*arrows*), due to synovialization

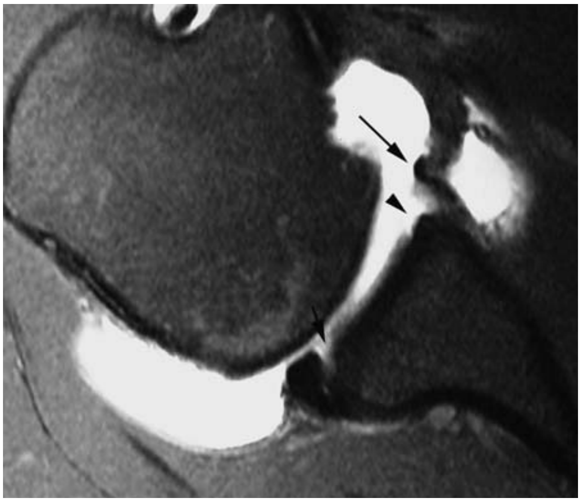

Fig. 9.20. GLAD lesion. Axial fat suppressed T1-weighted direct MR arthrogram demonstrating a torn labrum (*long arrow*) with an attached cartilage fragment separated from its normal position in the glenoid fossa (*arrowhead*). Note the presence of a posterior labral tear (*short arrow*)

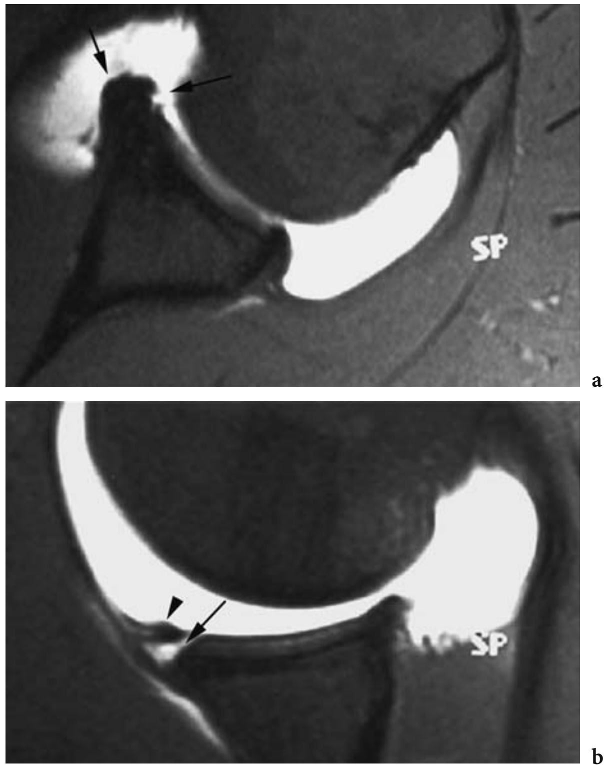

Fig. 9.21a,b. Perthes lesion. Axial (**a**) and ABER (**b**) fat suppressed T1-weighted direct MR arthrogram. The lesion of the anterior labrum is poorly visualized on the axial plane. There is irregularity and thickening of the anteroinferior labrum (*arrows* in **a**). The ABER position (**b**) demonstrated separation of the labrum (*arrowhead*) from the glenoid margin due to the traction of the labrum by the anterior band of the IGHL. Note the contrast material between the base of the labrum and the glenoid margin (*arrow*)

The Perthes lesion, another variation on the Bankart lesion, occurs when there is avulsion of the anterior labrum from the glenoid but remains partially attached medially to the scapula by an intact periosteum (Wischer et al. 2002). At arthroscopy these lesions may go undetected as there may be no or minimal displacement of the torn labrum. In their study, Wischer (Wischer et al. 2002) found that the ABER position increased the sensitivity of detecting a Perthes lesion from five lesions based on only axial MR images to seven lesions when the ABER position was utilized. This represents a 20% increase in their ability to detect the lesion in the ten cases of arthroscopically proven Perthes tears (Fig. 9.21).

Humeral failure should be suspected in the older patient with anterior glenohumeral instability in whom a Bankart lesion is not present. ***H***umeral ***a***vulsion of the ***g***lenohumeral ***l***igament (HAGL) represents tearing of the anterior humeral neck attachment of the IGL (Fig. 9.22). Associated lesions may include tears of the subscapularis tendon and recurrent anterior glenohumeral instability. If a humeral avulsion is present, the term BHAGL, ***b***ony ***h***umeral *a*vulsion of the ***g***lenohumeral ***l***igament is used (Fig. 9.22). If failure occurs on both the humeral and glenoid sides of the joint a "floating" AIGHL results where there is ***a***vulsion of the anterior band of the ***IGHL*** at the humeral as well as the labral attachments.

Posterior labral lesions are less frequently seen and their diagnosis may be elusive. These lesions originate from a posterior glenohumeral dislocation, from a direct anterior shoulder trauma or from seizures. An anterior impacted fracture of the humeral head (reverse Hill Sachs lesion, McLaughlin lesion) may result (Fig. 9.23). The MRI signs are the same as for anterior or superior lesions: detachment of the labrum, absence, or abnormal position (Fig. 9.23). A variant of the posterior labral tear is the ***po***sterior ***l***abrum ***p***eriosteal ***s***leeve ***a***vulsion or ***POLPSA***, with the posterior labrum displaced posterior and medially to the glenoid margin, similar to the anterior counterpart, the ALPSA lesion.

A frequent location of labral lesions involves the anterior aspect of the labrum extending from the base of the LBT insertion to the insertion of the IGHL, involving also the insertions of the SGHL and MGHL. In a series of 45 patients, Palmer et al. reported 9 out of 27 labral tears having this distribution (Palmer et al. 1994).

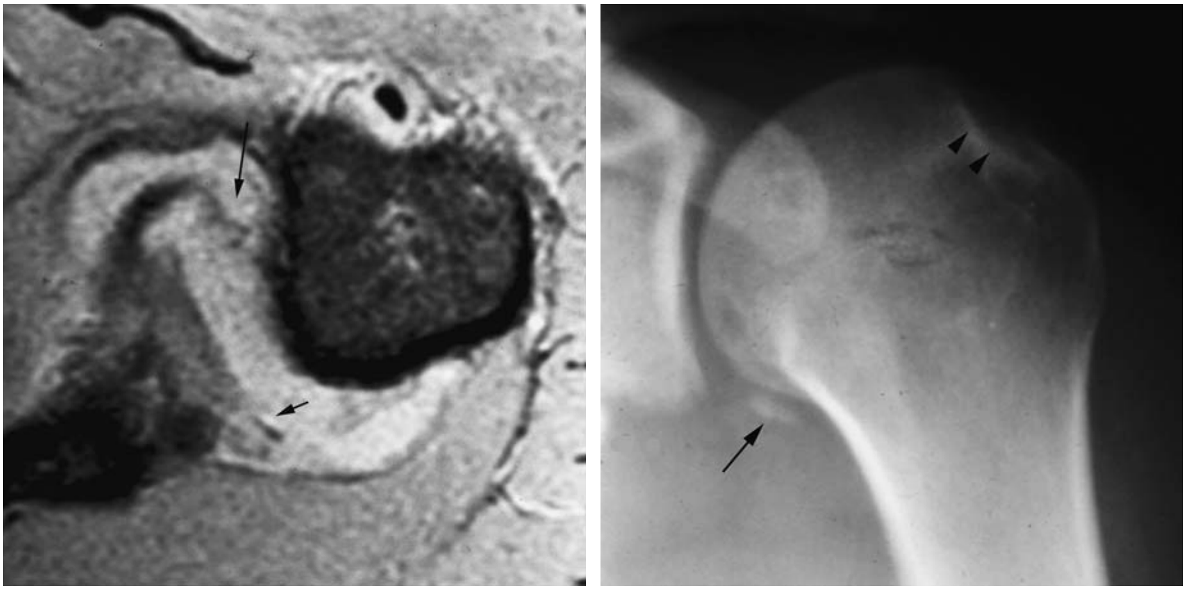

a b

Fig. 9.22a,b. HAGHL lesion and bony HAGHL (BAGHL). Axial GRE image (**a**) demonstrates a tear of the humeral insertion of the anterior band of the IGHL (*long arrow*). There is a joint effusion and a tear of the posterior labrum (*short arrow*). Plain film radiograph in another patient (**b**) demonstrates a bony avulsion of the humeral insertion of the IGHL (*arrow* in **b**) and a Hill Sachs lesion (*arrowheads* in **b**)

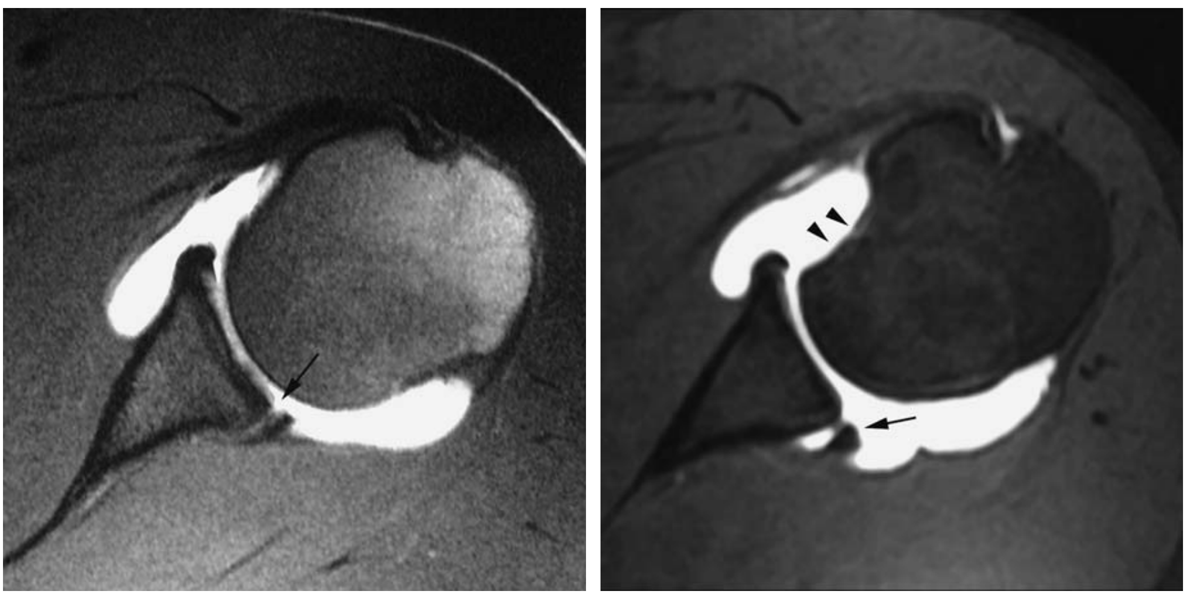

a b

Fig. 9.23a,b. Posterior labral tear (**a**). Axial fat suppressed T1-weighted direct MR arthrogram demonstrates a tear of the posterior labrum (*arrow* in **b**). Posterior labral tear displaced posteromedialy (POLPSA Lesion) (**b**). Note the posterior labral tear in a more medial posterior location that in **a**) (*arrow* in **b**). Note also a reversed Hill-Sachs lesion (*arrowheads* in **b**)

Superior labral anterior to posterior lesions (SLAP lesions) were initially considered rare (3.9% of patients undergoing arthroscopy), although more frequent use of MR arthrography has lead to higher rates of diagnosis of this lesion and probably are more frequent than previously believed. Increased awareness of the existence of tears involving the superior aspect of the labrum (SLAP lesions) allows radiologists to make the diagnosis of these lesions on a non-enhanced MRI (Cartland et al. 1992; Monu

et al. 1994; Bencardino et al. 2000). These lesions involve the superior part of the labrum with varying degrees of LBT involvement. Pain, clicking, and occasional instability in a young patient are the typical clinical manifestations. Not all SLAP lesions produce glenohumeral instability. In general, those SLAP lesions extending into the anterior inferior aspect of the labrum or involving the MGHL may produce instability. Four types of SLAP lesions were originally described based on arthroscopic findings (Fig. 9.24) (Cartland et al. 1992; Monu et al. 1994; Hodler et al. 1992). Type I is a partial tear of the superior part of the labrum with fibrillation of the LBT (Fig. 9.25). Type II is an avulsion with tear of the anterior and posterior labrum (Fig. 9.26). Type II SLAP lesions can be subdivided into type IIA (anterior extension), type IIB (posterior extension) and type IIC (anterior and posterior extension). Type III is a bucket-handle tear of the labrum (Fig. 9.27) and type IV is a bucket-handle tear of the labrum with longitudinal extension of the tear into the LBT (Fig. 9.28). More recently, multiple additional types have been described, representing a combination of superior labral tears with extension into different areas of the labrum and glenohumeral ligaments. However, for practical descriptive purposes only lesions I–IX are described, (Shankman et al. 1999) (Figs. 9.29–9.33) (See Table 9.1).

Paralabral cysts are almost invariably associated with labral tears. Their presence should incite the search for a labral tear if not apparent on initial inspection. The cyst arises from loss of the integrity of the joint through labral tears, degeneration or tears of the capsule. The imaging features include a cystic appearing mass adjacent to labrum or capsule with increased signal on the T2 weighted sequences (Fig. 9.34). They can be single or multiple. The presence of a chronic cyst may lead to a variety of denervation syndromes depending on their location. For example, if the paralabral cyst is in the posterosuperior location, in the suprascapular notch or the spinoglenoid notch, impingement of the suprascapular nerve or its branches may result. Signs of atrophy from denervation are usually late sequelae of these nerve compression syndromes. Another cause of denervation is the anteroinferior dislocation with damage to the axillary nerve or its branches within the quadrilateral space, leading to atrophy of the teres minor muscle. (Fig. 9.35)

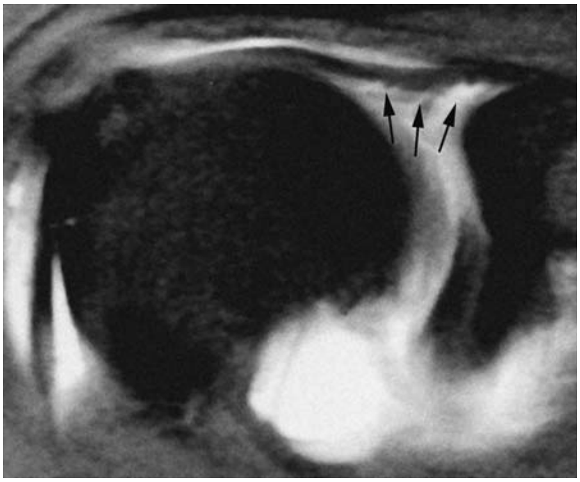

Fig. 9.25. SLAP type I. Oblique coronal fat suppressed T1-weighted direct MR arthrogram demonstrating irregularity of the inferior margin of the superior labrum extending into the LBT (*arrows*)

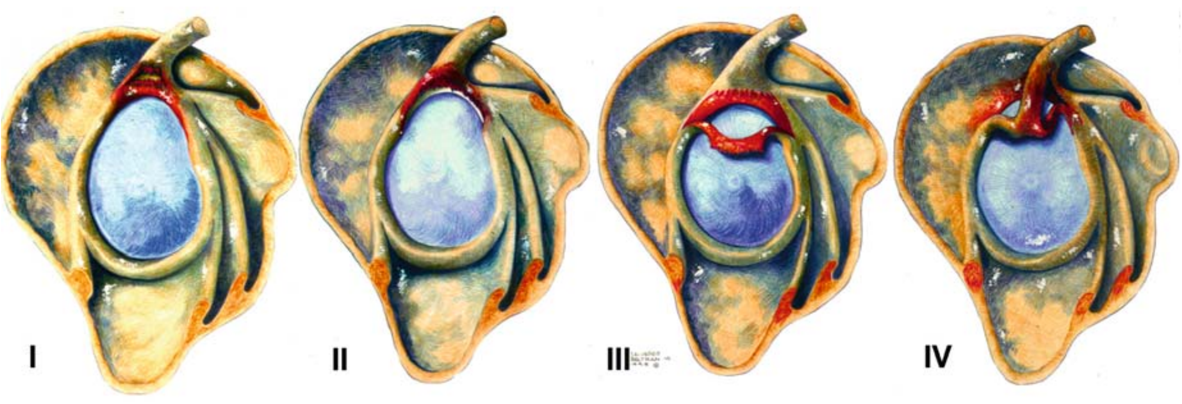

Fig. 9.24. The schematic drawings illustrate the classic four types of SLAP lesion as originally described (see text)

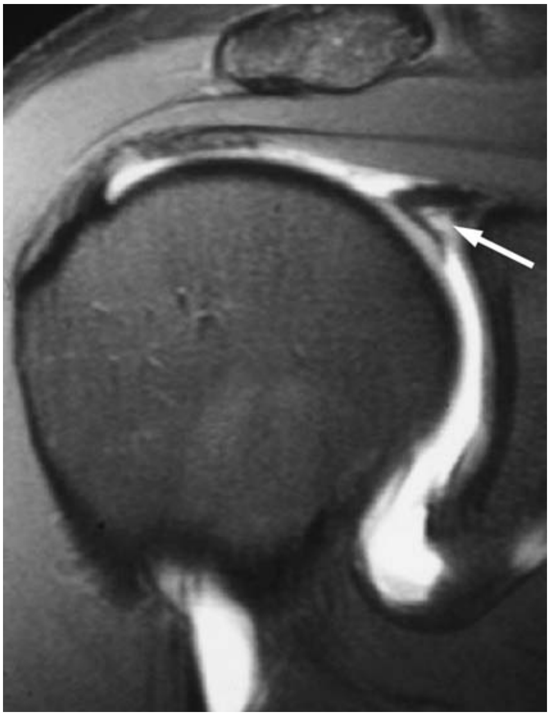

Fig. 9.26. SLAP type II lesion. Oblique coronal fat suppressed T1-weighted direct MR arthrogram demonstrating a tear of the superior labrum (*arrow*) without complete separation

Fig. 9.27. SLAP type III lesion. Oblique coronal fat suppressed T1-weighted direct MR arthrogram demonstrates a fragment of the superior labrum separated and inferiorly displaced (*arrow*)

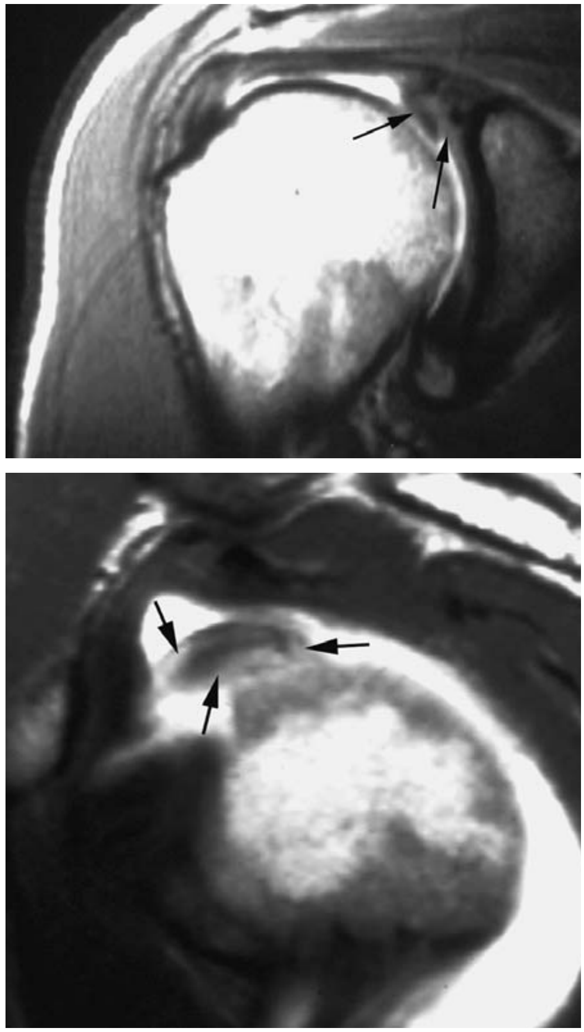

a

b

Fig. 9.28a,b. SLAP type IV lesion. Oblique coronal (**a**) and oblique sagittal (**b**) T1-weighted direct MR arthrograms demonstrating the superior labral tear (*arrows* in **a**) and the extension of the tear into the LBT (*arrows* in **b**)

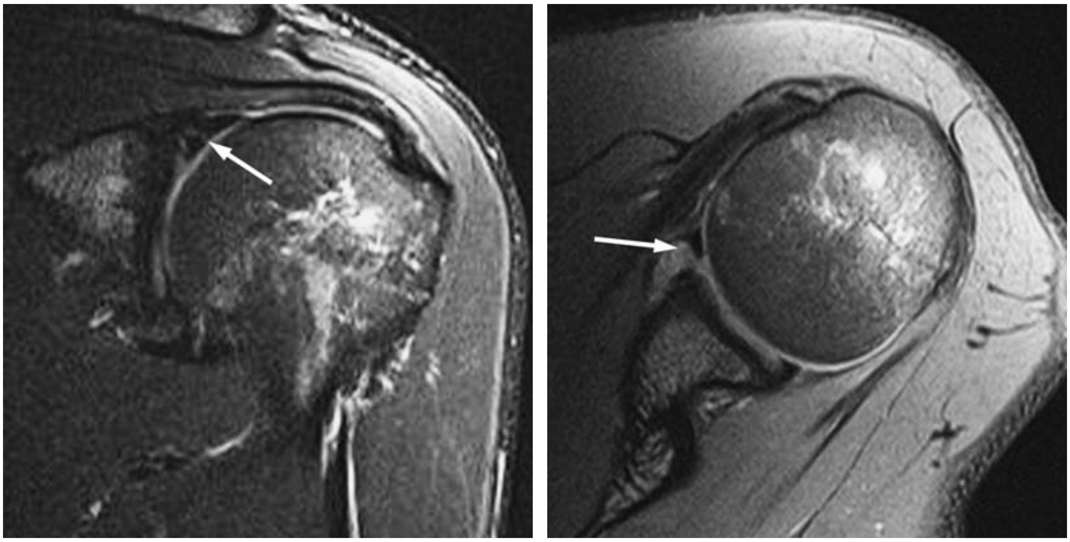

a b

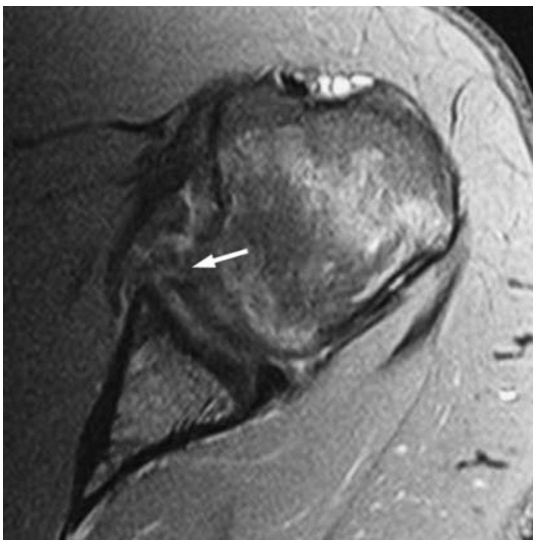

c

Fig. 9.29a–c. SLAP type V lesion. Oblique coronal fat suppressed T2-weighted image (**a**), and axial fat suppressed GRE proximal (**b**) and distal (**c**). This lesion extends from the superior labrum (*arrow* in a) anteriorly (*arrow* in **b**) and to the anteroinferior labrum (*arrow* in **c**)

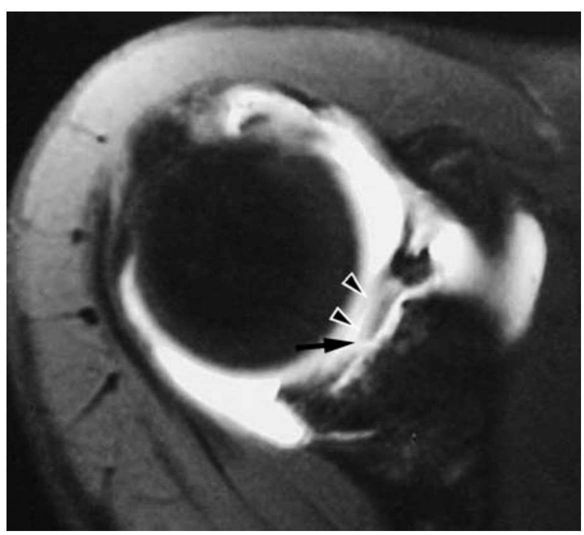

Fig. 9.30. SLAP type VI lesion. Axial fat suppressed T1-weighted direct MR arthrogram demonstrating a radial tear of the superior labrum (*arrow*) extending anteriorly, producing a flap of labral tissue (*arrowheads*). Note also a short posterior extension

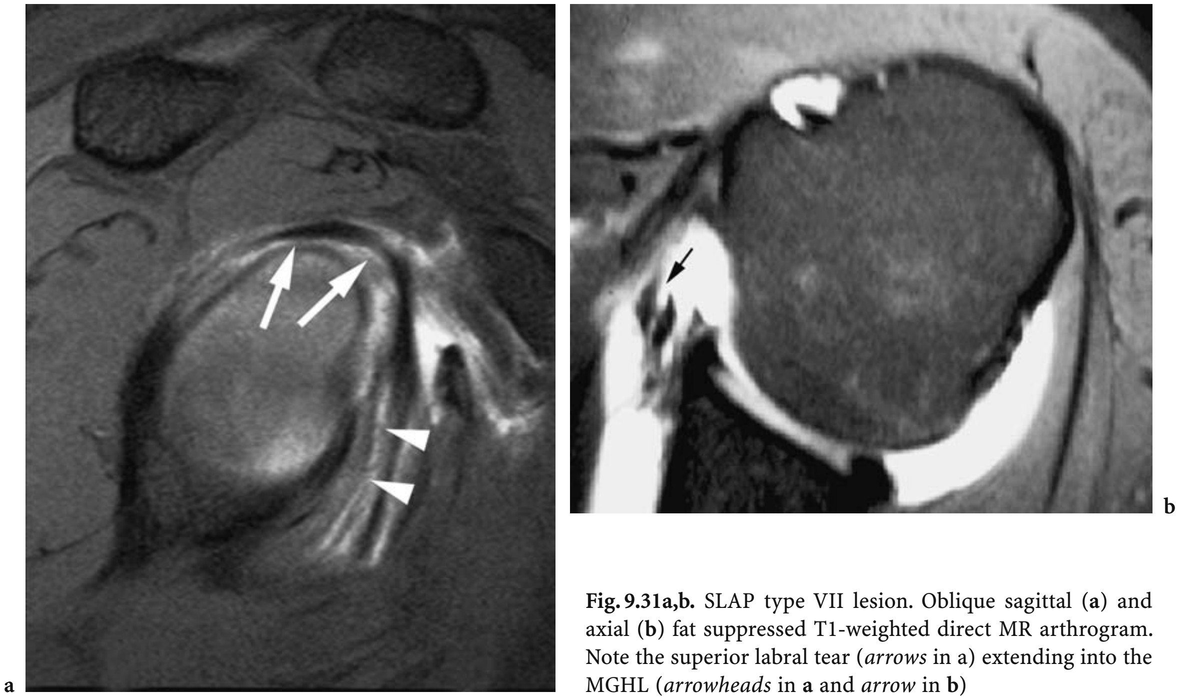

Fig. 9.31a,b. SLAP type VII lesion. Oblique sagittal (**a**) and axial (**b**) fat suppressed T1-weighted direct MR arthrogram. Note the superior labral tear (*arrows* in a) extending into the MGHL (*arrowheads* in **a** and *arrow* in **b**)

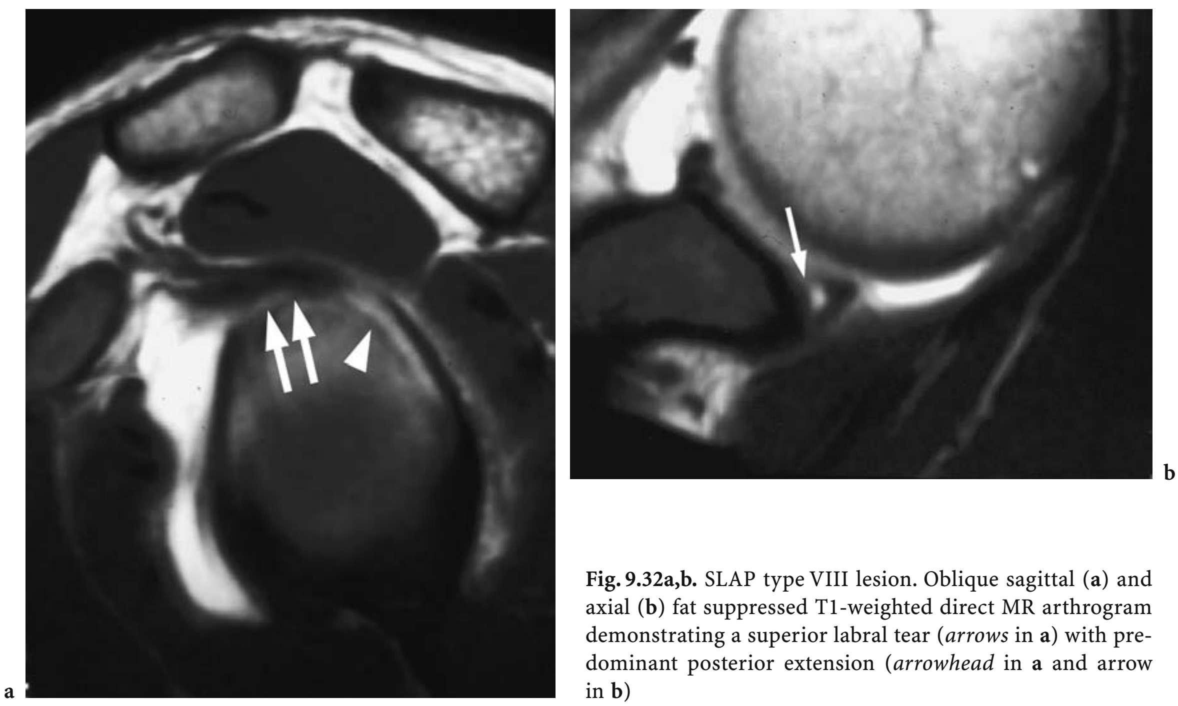

Fig. 9.32a,b. SLAP type VIII lesion. Oblique sagittal (**a**) and axial (**b**) fat suppressed T1-weighted direct MR arthrogram demonstrating a superior labral tear (*arrows* in **a**) with predominant posterior extension (*arrowhead* in **a** and arrow in **b**)

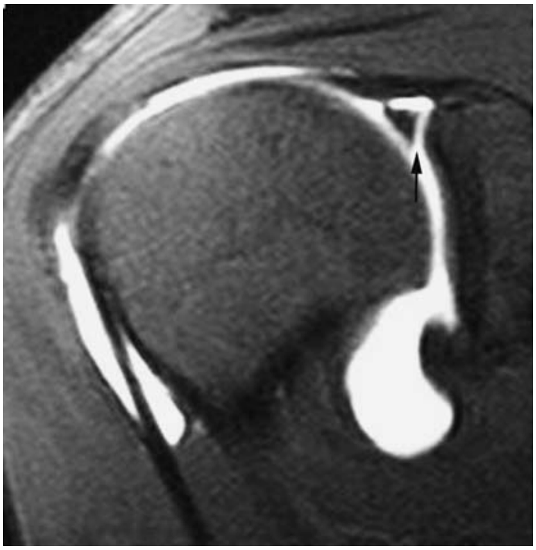
a


b

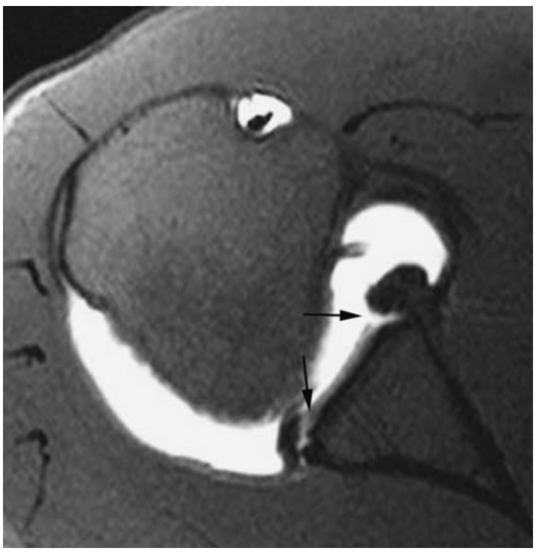
c

Fig. 9.33a–c. SLAP type IX lesion. Oblique coronal (**a**), proximal axial (**b**) and distal axial (**c**) fat suppressed T1-weighted direct MR arthrogram. Note the superior labral tear (*arrow* in **a**) with circumferential extension with involvement of the entire anterior and posterior labrum (*arrows* in **b** and **c**)

Table 9.1. SLAP Lesions

SLAP Lesion Type	Description
SLAP I	Irregularity of the superior biceps tendon / labrum
SLAP II A	Superior tear with predominant anterior extension
SLAP II B	Superior tear with predominant posterior extension
SLAP II C	Superior tear with anterior and posterior extensions
SLAP III	Superior tear with displaced fragment
SLAP IV	Superior tear with involvement of the long biceps tendon
SLAP V	Superior lesion with extension to the anterior inferior labrum
SLAP VI	Superior lesion with a displaced flap of tissue
SLAP VII	Superior lesion extending into the MGHL
SLAP VIII	Superior lesion extending into the posterior inferior labrum
SLAP IX	Circumferential labral tear

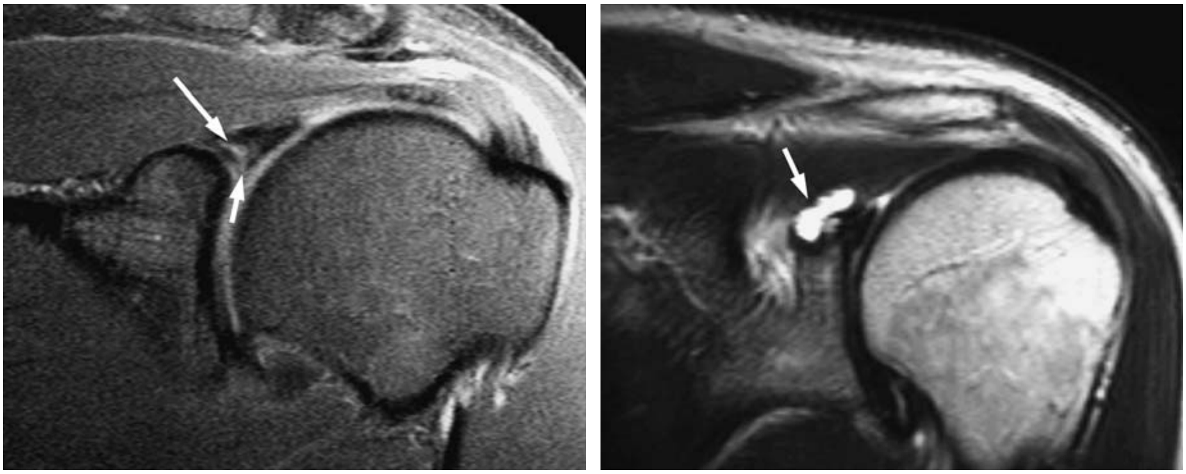

Fig. 9.34a,b. SLAP lesion with paralabral cyst. Oblique coronal fat suppressed T1-weighted indirect MR arthrogram (**a**) and oblique coronal T2-weighted image (**b**) demonstrate a superior labral tear (*arrows* in **a**) with an adjacent paralabral cyst (*arrow* in **b**)

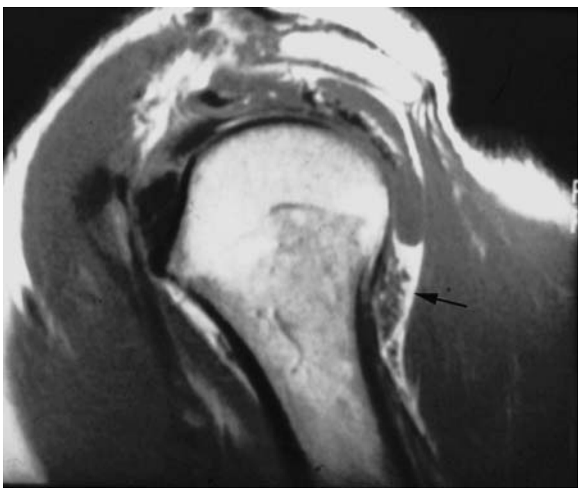

Fig. 9.35. Teres minor denervation atrophy. Oblique sagittal T1-weighted image demonstrates atrophy of the teres minor (*arrow*) secondary to axillary nerve damage following an anteroinferior glenohumeral dislocation

9.4.2 Internal Impingement Syndromes

Internal impingements have raised the interest of medical community due to its potentially producing career-ending ailment among overhead throwing athletes (Burkhart et al. 2003). These internal syndromes are related to some degree of capsuloligamentous failure that leads to microinstability. A variety of internal impingements have been described in the medical literature which include the posterosuperior, the anterosuperior and the anterior impingement syndromes (Jobe et al. 1990; Gerber and Sebester 2000).

9.4.2.1 Posterosuperior Impingement Syndrome

Although posterosuperior internal impingement is mostly described in baseball pitchers who suffered from severe pain in the posterior shoulder during the late cocking phase of throwing, it is also found in the follow through phase of batting, in forklift drivers who drive in reverse looking over the opposite shoulder and injury involving sudden overhead throwing of the arms above the head (Jobe 1996). In addition, this condition can also be seen in other activity such as volleyball spike, the golf swing or tennis serve (Meister 2000; Pink et al. 1990). The proposed pathomechanics includes maximal abduction and external rotation. This activity, however, is also seen in normal individuals that do not involve in vigorous sport activity. This has lead to the proposition that there are at least two mechanisms by which posterior superior impingement may develop in overhead throwing athletes.

The first proposed mechanism was put forward by Jobe (Jobe 1996) and subsequently by Walch et al. (Walch et al. 1992) who indicated that posterior superior impingement develops due to the laxity of the anterior IGHL. This laxity allows translation of the humeral head anteroinferior allowing non-physiologic contact between the greater tuberosity of the

humerus with posterior superior aspect of the glenoid rim and the inferior surface of the rotator cuff, eventually producing a rotator cuff tear. Decreased scapulothoracic motion and muscle weakness can also contribute to the production of the rotator cuff lesions. Stiffness of soft tissue around the scapula may produce resistance to scapular movement. Weakness of muscles that rotate the scapula may also lead to increased contact between the rotator cuff and posterosuperior glenoid labrum.

The second proposed mechanism for posterosuperior impingement syndrome was developed by Burkhart et al. (Burkhart et al. 2003) These authors proposed that the primary pathologic entity is the tightness of the posterior inferior capsule with secondary pseudolaxity of the anterior capsular structure, based on arthroscopic observations and the fact that posteroinferior capsulotomy may lead to increased of internal rotation and decreased of pain (Schenk and Brems 1998). These authors also noted that decreased internal rotation of the shoulder with the arm in abduction (***G***lenohumeral ***I***nternal ***R***otation ***D***eficit, GIRD) was a common clinical manifestation. They also observed an increased incidence of SLAP type II B lesions associated with rotator cuff pathology in these patients.

Hence, Burkhart et al. (Burkhart et al. 2003) proposed that patients with GIRD develop the ability to increase the external rotation of the arm in the late cocking phase, necessary to produce high velocity of throwing. This hyper external rotation leads to a torsion force of the intracapsular portion of the LBT that may result in peeling away of the superior labrum from the bony glenoid margin, resulting in a SLAP IIB lesion ("peel back" mechanism). At this point the athlete looses its ability to throw the ball with the necessary speed and precision, developing the so called "dead arm" which may be the end of a professional career (Burkhart et al. 2003).

Burkhart et al. (Burkhart et al. 2003; Jobe et al. 1990) also proposed that the rotator cuff tear is due to torsional and shear stress during repeated internal and external rotation. The author noted that maximum hyper twisting of the rotator cuff is located at the articular surface of the muscle which is also the most common lesion of the rotator cuff tear in throwers (Burkhart et al. 2003).

Meister et al. (Meister et al. 1999) proposed that the presence of exostosis in the posterior glenoid labrum further supports traction hypothesis as the cause of labral injury. The authors proposed that the traction of the biceps tendon during the follow-through phase of throwing may lead to the fraying of the glenoid labrum as opposed to the "peel back" mechanism indicated by Burkhart et al. (Burkhart et al. 2003). The presence of exostosis may further lead to impingement of the undersurface of the rotator cuff (Walch et al. 1992).

MRI manifestations of the posterosuperior impingement syndrome include irregularity and thickening of the anterior IGHL reflecting the capsular laxity, microfractures of the posterosuperior glenoid rim and greater tuberosity of the humerus and tears of the posterior superior labrum (SLAP IIB lesion). These lesions can be better appreciated with MR arthrography in the ABER position (Fig. 9.36). In this position, the supraspinatus tendon can be seen impinged between the greater tuberosity of the humerus and the posterosuperior glenoid rim (Fig. 9.37). In the late stages, irregularity and partial tearing of the rotator cuff may be observed. Patients with GIRD may exhibit thickening of the inferior capsule, partial or complete rotator cuff tears and SLAP II lesions (Fig. 9.38).

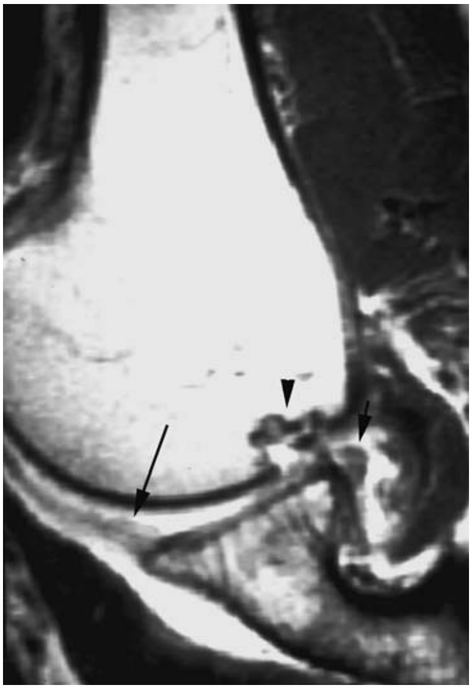

Fig. 9.36. Posterosuperior impingement syndrome. T1-weighted direct MR arthrogram in ABER position demonstrates increased signal intensity and irregularity of the anterior band of the IGHL (*long arrow*), impacted fracture of the greater tuberosity (*arrowhead*) and an irregular tear of the posterior superior labrum (*short arrow*)

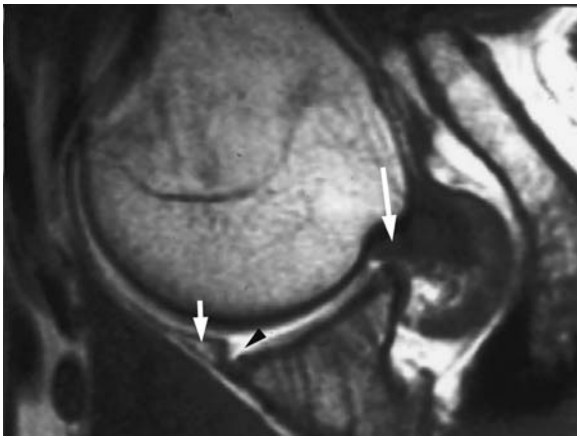

Fig. 9.37. Posterosuperior impingement syndrome. Fat suppressed T1-weighted direct MR arthrogram in ABER position demonstrates increased signal intensity within the anterior band of the IGHL (*short arrow*). Note the supraspinatus tendon impinged between the greater tuberosity of the humerus and the posterosuperior labrum (*long arrow*)

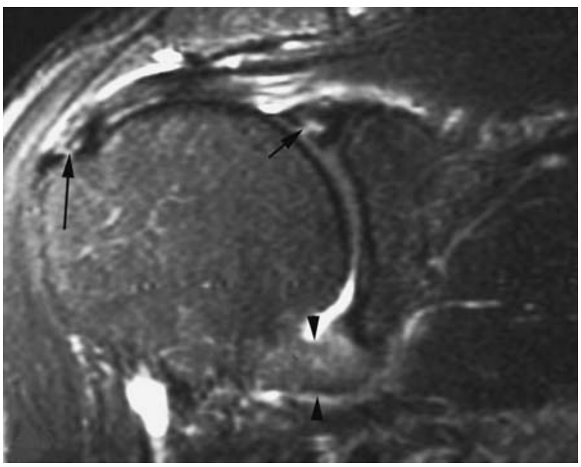

Fig. 9.38. Posterosuperior impingement syndrome. Oblique coronal fat suppressed T2-weighted image demonstrating a superior labral tear (*long arrow*), superior labral tear (*short arrow*) and thickening of the inferior capsule (*arrowheads*)

9.4.2.2
Anterosuperior Impingement Syndrome

While both posterosuperior and anterosuperior internal impingements are associated with repetitive overhead movements, anterosuperior internal impingement is more likely to be related to pain during the follow-through phase of throwing as opposed to late-cocking phase of throwing seen more commonly in posterosuperior internal impingement (Gerber and Sebester 2000). The difference in the clinical manifestations of these two shoulder internal impingement syndromes may be related to the different pathomechanics involved. While posterosuperior impingement syndrome is linked to abduction and external rotation of the shoulder, anterosuperior impingement syndrome has been proposed to involve flexion and internal rotation of the shoulder (Gerber and Sebester 2000).

The different pathomechanics proposed to occur during the development of the posterosuperior and anterosuperior internal impingements are manifested with different structures involved in anterosuperior impingement. While undersurface of the rotator cuff is almost universally involved in posterosuperior impingement syndrome, anterosuperior impingement is mostly related to the tear of the subscapularis tendon (Meister et al. 1999). Anterosuperior impingement is most commonly associated with anterosuperior labral tearing (SLAP IIA) while the posterosuperior impingement is more commonly related to posterosuperior labral fraying or SLAP IIB.

Although both posterosuperior impingements and anterosuperior impingements have been proposed to involve the anterior translation of the humeral head, anterosuperior impingement syndrome more commonly involves the SGHL as well as the rest of the pulley system. In addition, lesions of the LBT are more commonly seen in anterosuperior impingement syndrome.

The subscapularis tendon is almost invariably torn in anterosuperior impingement. Gerber and Sebesta (Gerber and Sebester 2000) reviewed 16 patients with anterior shoulder pain who underwent arthroscopic evaluation for their pain. The authors found subscapularis tendon tear in 13 of the 16 patients. The authors observed that tear of the subscapularis tendon frequently occurred in the deep surface, superior border adjacent to its insertion at the lesser. In addition, they observed mechanical contact between undersurface of the subscapularis muscle and anterior superior glenoid labrum when the shoulder is put in 90° flexion and internal rotation and concluded that the tear of the undersurface of the subscapularis tendon is due to direct impingement of the humeral head and the anterosuperior glenoid labrum.

Another pathomechanics of subscapularis tendon tear in anterosuperior internal impingement was proposed by Habermeyer et al. (Habermeyer et al. 2004). These investigators reviewed 89 patients with pulley lesions observed during arthroscopic procedure and

noted the presence of partial undersurface tear of the subscapularis tendon in 42 of the 89 patients. The authors concluded that pulley lesions leads to the medial subluxation of the LBT at it entrance at the bicipital groove. The subluxed LBT displaced medially which leads to the development of the undersurface tear of the subscapularis tendon (Habermeyer et al. 2004). Habermeyer et al. (Habermeyer et al. 2004) developed a classification system base on the combination of lesions observed in patients with anterosuperior impingement syndrome. Type I: there is an isolated lesion of the SGHL. Type II: there is a lesion of the SGHL associated with a partial articular side supraspinatus tendon tear. Type III: there is a lesion of the SGHL associated with partial subscapularis tendon tear. Type IV: there is a lesion of the SGHL associated with a partial subscapularis tendon tear and a partial supraspinatus tendon tear. The common feature in this combination of lesions was the presence of long bicipital pathology, including tenosynovitis, dislocation, subluxation or tear.

Gerber and Sebesta (Gerber and Sebester 2000) observed SLAP lesions in 10 of 16 cases of anterior shoulder pain which underwent arthroscopic evaluation. In 8 of these 10 patients with SLAP lesions, subscapularis tendon tear was seen. The authors ascribed these findings on direct impingement of the anterior superior glenoid labrum since impingement of the anterosuperior glenoid labrum is invariably seen on modified impingement test (Gerber and Sebesta 2000). Interestingly, in the Habermeyer series (Habermeyer et al. 2004) none of their patients suffered SLAP II or higher grade SLAP lesions.

Another hypothesis concerning the pathogenesis of the fraying of the anterosuperior glenoid labrum was proposed by Budoff et al. (Budoff et al. 2003). The authors argue that anterosuperior glenoid labrum is more susceptible to labral fraying and tear than the posterosuperior labrum because of its preponderance to degenerative changes (Budoff et al. 2003). The rotator cuff dysfunction, which is thought to be the primary lesion, may cause the instability and anterosuperior displacement of the humeral head which impinges upon the anterosuperior glenoid labrum. In addition, the fact that the anterosuperior glenoid labrum has poorer blood supply makes it more likely to undergo degeneration, fraying and tear (Budoff et al. 2003; Cooper et al. 1992).

The MRI manifestations of anterosuperior impingement syndrome reflect the arthroscopic findings noted by Habermeyer et al. (Habermeyer et al. 2004) and include lesions of the LBT, partial tears of the subscapularis tendon, partial tears of the supraspinatus tendon and tears of the SGHL (Fig. 9.39). These findings have a resemblance with those noted in rotator cuff interval tears. The relationship between anterosuperior impingement syndrome and rotator cuff interval lesions is yet to be ascertained.

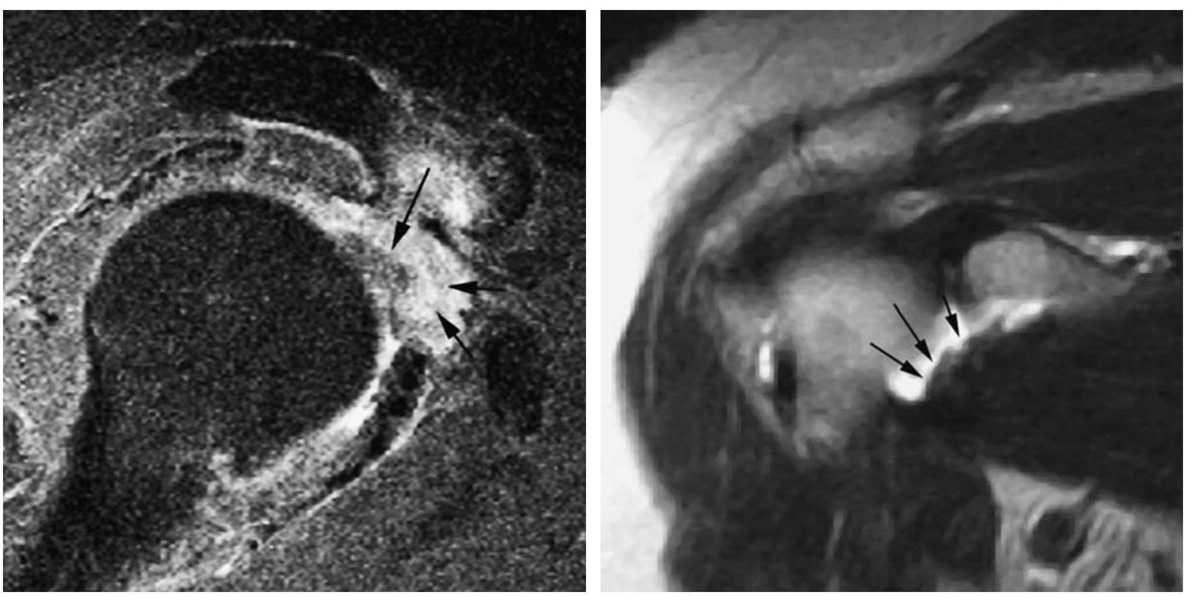

a b

Fig. 9.39a,b. Anterosuperior impingement syndrome. Oblique sagittal fat suppressed T1-weighted indirect MR arthrogram (**a**) and oblique coronal T2-weighted MR image (**b**) demonstrate severe tendinosis of the intracapsular LBT (*long arrow* in **a**), tears of the CH and SGHL (*short arrows* in **a**) and partial tear of the superior margin of the subscapularis muscle (*arrows* in **b**)

9.4.2.3 Anterior Internal Impingement Syndrome

Struhl described impingement in the anterior labrum which more likely involves labral fraying as well as undersurface tear of the rotator cuff as compared to anterosuperior impingement. SGHL and subscapularis muscle are unlikely to be involved in anterior internal impingement (Struhl 2002). Direct arthroscopic observation revealed that there is direct contact between the humeral head and the anterior glenoid labrum anterior to the attachment of the LBT in internal rotation and flexion (Struhl 2002).

It is interesting to note that the clinical presentation of patients with anterior internal impingement is similar with the clinical presentation of patients with subacromial impingement (Struhl 2002). The average age of the patients with anterior impingement, however, is significantly younger than patients with subacromial impingement. Pre-operative diagnosis of this condition, however, is very challenging due to the fact that this condition only detected by MRI in only 20% of cases (Struhl 2002). This difficulty is compounded by the fact that subacromial impingement is sometimes coexistent with anterior internal impingement.

9.5 Conclusion

Shoulder instability is an increasing entity among throwing athletes and proper preoperative assessment is sometimes difficult to obtain based on history and physical examination alone. Shoulder MRI with or without contrast enhancement has been proven a very valuable diagnostic modality for the detection of subtle lesions involving the capsule, labrum and ligaments. Recent and changing new concepts on the etiology of some of the instability patterns, especially microinstability, in these patients makes MRI even more valuable to determine if a particular surgical approach may be successful. Further understanding of the early capsular lesions that lead eventually to severe impairment of joint function will be followed undoubtedly by the need for further refinement of the accuracy of the MRI technique and diagnostic skills of the interpreting radiologist.

References

Beltran J, Bencardino J, Mellado J et al. (1997) MR arthrography of the shoulder: variations and pitfalls. Radiographics 17:1403–1412
Bencardino J, Beltran J, Rosenberg ZR et al. (2000) Superior labrum anterior and posterior lesions: MR arthrography of the shoulder. Radiology 214:267–271
Budoff JE, Nirschl RP, Ilahi OA et al. (2003) Internal impingement in the etiology of rotator cuff tendinosis revisited. Arthroscopy 19:810–814
Burkhart SS, Morgan CD, Kibler WB (2003) The disabled throwing shoulder: spectrum of pathology. Part I: Pathoanatomy and biomechanics. Arthroscopy 4:404–420
Cartland JP, Crues JP, Stauffer A et al. (1992) MR Imaging in the evaluation of SLAP injuries of the shoulder: findings in 10 patients. AJR 159:787–792
Caspari RB, Geissler WB (1993) Arthroscopic manifestations of shoulder subluxation and dislocation. Clin Orthop Rel Res 291:54–66
Chandnani VP, Yeager TD, DeBerardino T et al. (1993) Glenoid labral tears: prospective evaluation with MR imaging, MR arthrography, and CT arthrography. AJR 161:1229–1235
Chandnani VP, Gagliardi JA, Murnane TG et al. (1995) Glenohumeral ligaments and shoulder capsular mechanism: evaluation with MR arthrography. Radiology 196:27–32
Cooper DE, Arnoczky SP, O'Brien SJ et al. (1992) Anatomy, histology, and vascularity of the glenoid labrum. An anatomical study. J Bone Joint Surg Am 74:46–52
Garneau RA, Renfrew DL, Moore TE et al. (1991) Evaluation with MR imaging. Radiology 179:519–522
Gerber C, Sebesta A (2000) Impingement of the deep surface of the subscapularis tendon and the reflection pulley on the anterosuperior glenoid rim: a preliminary report. J Shoulder Elbow Surg 9:483–490
Habermeyer P, Magosch P, Pritsch M et al. (2004) Anterosuperior impingement of the shoulder as a result of pulley lesions: a prospective arthroscopic study. J Shoulder Elbow Surg 13:5–12
Hodler J, Kursunoglu-Brahme S, Flannigan B, Snyder et al. (1992) Injuries of the superior portion of the glenoid labrum involving the insertion of the biceps tendon: AJR 159:565–568
Itoi E, Keuchle DK, Newman SR et al. (1993) Stabilizing function of the biceps in stable and unstable shoulders. J Bone Joint Surg Br 75:546–550
Jobe CM (1996) Superior glenoid impingement. Clin Orthop Related Res 330:98–107
Jobe FW, Tibone JE, Jobe CM et al. (1990) The shoulder in sports. In: Rockwood CA, Matsen FA (eds) The shoulder. Vol 2. Philadelphia, WB Saunders, pp 961–990
Legan JM, Burkhard TK, Goff WB et al. (1991) Tears of the glenoid labrum: MR imaging of 88 arthroscopically confirmed cases. Radiology 179:241–246
Mallon WJ, Speer KP (1995) Multidirectional instability: current concepts. J Shoulder Elbow Surg 4:54–64
Matsen FA III, Thomas SC, Rockwood CA Jr (1990) Anterior glenohumeral instability. In: Rockwood CA, Matsen FA III (eds) The shoulder. Saunders, Philadelphia, pp 526–622
Matsen FA, Harryman DT, Sidles JA (1991) Mechanics of glenohumeral instability. Clin SportsMed 10:783–788

Meister K (2000) Injuries to the shoulder in the throwing athlete. Part one: biomechanics/pathophysiology/classification. Am J Sports Med 2:265–275

Meister K, Andrews JR, Batts J et al. (1999) Symptomatic thrower's exostosis. Arthroscopic evaluation and treatment. Am J Sports Med 27:133–136

Mizuno K, Nabeshima Y, Hirohata K (1993) Analysis of Bankart lesion in the recurrent dislocation or subluxation of the shoulder. Clin Orthop 288:158–165

Monu JUV, Pope TL, Chabon SJ et al. (1994) MR diagnosis of superior labral anterior poster (SLAP) injuries of the glenoid labrum: value of routine imaging without intrarticular injection of contrast material. AJR 163:1425–1429

Moseley HF, Overgaard B (1962) The anterior capsular mechanism in recurrent anterior dislocation of the shoulder. J Bone Joint Surg 44:913–927

Neviaser TJ (1993a) The anterior labroligamentous periosteal sleeve avulsion: a cause of anterior instability of the shoulder. Arthroscopy 9:17–21

Neviaser TJ (1993b) The GLAD lesion: another cause of anterior shoulder pain. Arthroscopy 9:22–23

Novotny JE, Nichols CE, Beynnon BD (1998) Kinematics of the glenohumeral joint with Bankart lesion and repair. J Orthop Res 16(1):116–121

O'Brien SJ, Neves MC, Arnoczky SP et al. (1990) The anatomy and histology of the inferior glenohumeral ligament complex of the shoulder. Am J Sports Med 18:449–456

O'Connell PW, Nuber GW, Mileski RA et al. (1990) The contribution of the glenohumeral ligaments to anterior stability of the shoulder joint. Am J Sports Med 18:579–584

Pagnani MJ, Deng XH, Warren RF et al. (1996) Role of the long head of the biceps brachii in glenohumeral stability: a biomechanical study in cadavera. J Shoulder Elbow Surg 5:255–262

Palmer WE, Brown JH, Rosenthal DJ (1994) Labral-ligamentous complex of the shoulder: evaluation with MR arthrography. Radiology 190:654–651

Pink M, Jobe FW, Perry J (1990) Electromyographic analysis of the shoulder during the golf swing. Am J Sports Med 8:137–140

Rafii M, Firooznia H, Golimbu C et al. (1986) CT arthrography of capsular structures of the shoulder. AJR 146:361–367

Schenk TJ, Brems JJ (1998) Multidirectional instability of the shoulder: patho-physiology, diagnosis, and management. J Am Acad Orthop Surg 6(1):65–72

Shankman S, Beltran J, Bencardino J (1999) MR Arthrography of the shoulder: glenohumeral instability. Skeletal Radiol 28:365–382

Struhl S (2002) Anterior internal impingement: an arthroscopic observation. Arthroscopy 18:2–7

Tirman PFJ, Feller JF, Palmer WE et al. (1996) The Buford complex. A variation of normal shoulder anatomy: MR arthrographic imaging features. AJR 166:869–873

Turkel SJ, Panio MW, Marshall JL et al. (1981) Stabilizing mechanisms preventing anterior dislocations of the glenohumeral joint. J Bone Joint Surg 63:1208–1217

Walch G, Boileau P, Noel E et al. (1992) Impingement of the deep surface of the supraspinatus tendon on the posterosuperior glenoid rim: an arthroscopic study. J Shoulder Elbow Surg 1:238–245

Warner J, Bowen M, Deng X et al. (1999) Effect of joint compression on inferior stability of the glenohumeral joint. J Shoulder Elbow Surg 8:31–36

Weishaupt D, Zanetti M, Tanner A et al. (1999) Lesions of the reflection pulley of the long biceps tendon. MR arthrographic findings. Invest Radiol 34:463–469

Williams MM, Snyder SJ, Buford D (1994) The Buford complex-the cordlike MGHL and absent anterosuperior labrum complex: a normal anatomic capsulolabral variant. Arthroscopy 10:241–247

Wischer TK, Bredella MA, Genant HK et al. (2002) Perthes lesion (a variant of the Bankart lesion): MR imaging and MR arthrographic findings with surgical correlation. AJR 178:233–237

Wolf EM, Cheng JC, Dickson K (1995) Humeral avulsion of glenohumeral ligaments as a cause of anterior shoulder instability. Arthroscopy 11(5):600–607

Yeh LR, Kwak S, Kim YS et al. (1998) Anterior labroligamentous structures of the glenohumeral joint: correlation of MR arthrography and anatomic dissection in cadavers. AJR 171:1229–1236

Zlatkin MB, Bjorkengren AG, Gylys-Morin V et al. (1988) Cross-sectional imaging of the capsular mechanism of the glenohumeral joint. AJR 150:151–158

Rotator Cuff and Impingement

10

Henk-Jan Van der Woude, Diana G. Franssen-Franken, and W. Jaap Willems

CONTENTS

H.-J. Van der Woude, MD, PhD
D. G. Franssen-Franken, MD
Department of Radiology, Onze Lieve Vrouwe Gasthuis, PO Box 95500, 1090 HM Amsterdam, The Netherlands
W. J. Willems, MD
Dept. of Orthopedic Surgery, Onze Lieve Vrouwe Gasthuis, PO Box 95500, 1090 HM Amsterdam, The Netherlands

10.1 Introduction

Shoulder pain is a common sports-related clinical complaint, both in the recreational and professional setting, that may be caused by many disorders including abnormalities of the rotator cuff and osseous acromial outlet, the biceps-labrum complex, and various other pathologic conditions, based on repetitive stress but also on torsional forces (Fritz 2002). One should be aware that cuff and biceps-labral lesions secondary to trauma or overuse may coexist, making physical examination difficult and findings inconclusive. The role of accurate (preoperative) imaging is thus pivotal, particularly when uncertainty exists regarding the primary cause of the pain (Helms 2002; Sanders and Miller 2005; Tirman et al. 2004). In professional sports the income interests are enormous, and athletes may return to sports activities earlier than medical justified. Insight into the right diagnosis thus has important consequences for timing and type of treatment with subsequent outcome. Because magnetic resonance (MR) imaging and ultrasonography (US) are non-invasive examinations, both imaging tools are touted for establishing rotator cuff disease and cuff-related abnormalities.

MR imaging, and MR arthrography in particular, is nowadays the preoperative imaging tool of choice for many sports medicine surgeons (Fritz 2002; Helms 2002; Magee et al. 2004; Palmer et al. 1993). MR imaging is superior for the visualization of even delicate soft-tissue structures involved in the clinical syndrome of impingement but, because of the multiplanar capabilities, is also optimal for the detection of anatomical variations of the osseous outlet that may contribute to impingement (Fritz 2002; Sanders and Miller 2005) (Box 10.1). MR arthrography, performed after intra-articular injection of diluted contrast medium, improves the diagnostic accuracy in individuals with shoulder pain with regard to the detection of (partial) rotator cuff lesions and lesions of the glenoid labrum, capsule and glenohumeral lig-

Box 10.1. Privileges MRI in imaging shoulder

- Non-invasive and multidimensional
- High soft-tissue contrast
- Depiction of anatomical variants of (osseous) outlet

Box 10.2. Privileges of MR arthrography in shoulder imaging

- Depiction of even small partial-thickness rotator cuff tears
- Optimal depiction of labroligamentous lesions

Box 10.3. Privileges of ultrasonography in shoulder imaging

- Non-invasive and highly available
- Interaction with patient
- Dynamic capabilities and comparison with contralateral shoulder
- Imaging-guided interventions

Box 10.4. Shoulder MR imaging protocol

- Combination of axial, oblique coronal and oblique sagittal sequences
- Combination of T1 or proton-density and T2-weighted TSE sequences with and without fat-saturation
- MR arthrography: add axial, oblique coronal and sagittal T1-weighted fat-saturated series and abduction-exorotation (ABER) sequence

Box 10.5. MR spectrum of rotator cuff abnormalities

- Tendinosis: normal or increased SI on PD/T2, normal or thickened tendon
- Partial thickness tear: partial defect with water-like SI on bursal or articular side, thinning or thickening of tendon
- Full-thickness tear: gap with water-like SI through entire thickness of tendon, with or without retraction and/or atrophy and/or bursal fluid

Box 10.6. Ultrasonographic criteria for cuff abnormalities

- Tendinosis: ill-defined heterogeneous hypo- and hyperechoic area with or without increased tendon size
- Partial-thickness tear: hypoechoic, anechoic or mixed hypo- and hyperechoic area and/partial discontinuity of fibrillar pattern
- Full-thickness tear: non-visualization of tendon substance, fluid-filled gap, fluid in joint and/or bursa

aments. Young athletes with chronic injuries or instability seem to benefit most from direct MR arthrography because they tend to have smaller labral tears and in addition partial rotator cuff pathology tend to occur more frequently and in atypical locations (Jbara et al. 2005; Magee et al. 2004; Tuite 2003) (Box 10.2).

Ultrasonography has substantial privileges for shoulder examination because of its non-invasive and non-ionizing capabilities. Moreover, it is highly available and non-expensive, and the painful shoulder can be easily compared with the asymptomatic side (Box 10.3). Another advantage of US is the dynamic evaluation capability which can be helpful in assessment of subluxated tendons. Besides diagnostic imaging, US can also be used as guidance for interventional procedures, including aspiration of fluid or

needle aspiration of calcific deposits, and biopsies, or injections for therapeutic reasons. Despite the limitation of intra- and interobserver variability, US is a strong non-invasive tool in the examination of shoulder pain (Brenneke and Morgan 1992; Hodler et al. 1988; O'Connor et al. 2005; Teefey et al. 2000, 2004; van Holsbeeck et al. 1995; Wiener and Seitz 1993).

10.2 MR Imaging Technique

Imaging of the shoulder can be performed on both high and mid-field strength MR systems. Low-field systems are adequate for evaluation of rotator cuff and osseous structures, but may be insufficient for secure evaluation of the labroligamentous structures. In any system, a dedicated surface coil is essential for acquiring optimal details. Patients should be placed in a comfortable supine position with the arm at the side in neutral or slight external rotation. Field of views chosen should be kept as small as possible, still enclosing the entire shoulder. Slice thickness should be in the range of 3–4 mm (Sanders and Miller 2005). In the literature, different imaging protocols are recommended (Fritz 2002; Jbara et al. 2005; Jost et al. 2005; Meister et al. 2003; Miniaci et al. 2002). A standard conventional MR protocol typically includes sequences in the axial, oblique coronal and oblique sagittal plane (Box 10.4). The axial images extend from the (complete) acromion through the glenoid. The oblique coronal images are prescribed from the axial images and should be directed parallel to the supraspinatus tendon. The oblique sagittal images are also prescribed from the axial series and aligned perpendicular to the coronal images. Sagittal images extend from the scapular neck and distal clavicle through the lateral aspect of the greater tuberosity. T2- and proton-density weighted images with or without fat-suppression in the axial, oblique coronal and sagittal planes are the working horses for evaluation of the painful shoulder. These sequences in all dimensions optimally reflect pathology of bones, rotator cuff, capsule and labrum, by identifying fluid and edema related to bursae, muscles and tendons, joints and paralabral cysts (Jbara et al. 2005; Sanders and Miller 2005).

T1-weighted sequences can be included for further anatomical information of the rotator cuff and osseous structures and to determine signs of fatty atrophy of the cuff (Jbara et al. 2005; Jost et al. 2005; Miniaci et al. 2002; Sanders and Miller 2005).

A non-enhanced MR imaging study in three directions is usually sufficient in patients with clinical symptoms of impingement and/or suspected rotator cuff abnormalities. At least full-thickness tears can be demonstrated accurately (Fig. 10.1.). However,

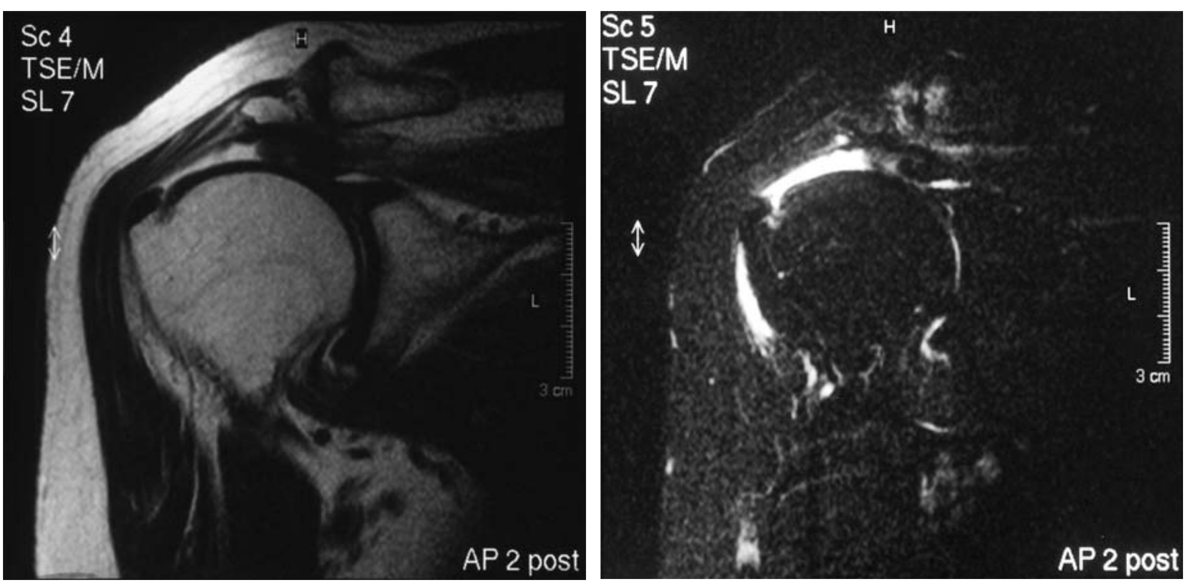

a b

Fig. 10.1a,b. Large full-thickness tear of supraspinatus tendon. Coronal T2-weighted TSE MR image (**a**) and T2-weighted fat-saturated TSE image (**b**) display tear as high SI defect equal to water. There is retraction of proximal tendon part

although conventional MRI is accurate for detection of rotator cuff tears in the elderly patient, accuracy is considered less in young athletic individuals (Tirman et al. 1994a,b; Tuite 2003). In the latter group, partial thickness tears are most frequently encountered. In our view, and that of others, these partial tears, particularly articular surface tears, can be detected more accurately when intra-articular dilute gadolinium is administered. Using MR arthrography, T1-weighted fast spin-echo sequences are performed with fat suppression in the axial, oblique coronal and oblique sagittal direction after intraarticular injection of approximately 15 ml of a 0.1 mmol/kg solution of gadopentetate dimeglumine (Vanhoenacker et al. 2000). Adding abduction and exorotation stress imaging (ABER) to this protocol is also very useful for detecting small partial tears on the articular side, besides the improved appreciation of (non-displaced) antero-inferior labral tears (Fig. 10.2) (Jbara et al. 2005; Meister et al. 2003; Sanders and Miller 2005). Delayed indirect MR arthrography after intravenous administration of gadolinium allows visualization of synovial tissue lining the bursae, joint capsule and tendon sheaths in the early phase and may enhance (partial) cuff tears in the later phase after diffusion of the contrast medium into the joint space (Fig. 10.3).

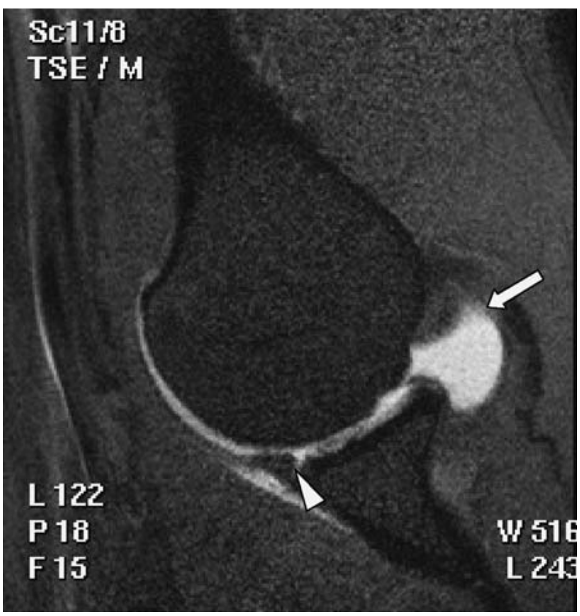

Fig. 10.2. Anteroinferior labral tear with intact spinatus tendons. T1-weighted fat-saturated MR arthrogram in ABER view. Articular undersurface of supraspinatus tendon is completely normal (*arrow*). Inferior glenohumeral ligament is under stress in this view accentuating subtle anteroinferior labral tear (*arrowhead*)

Fig. 10.3. Full-thickness supraspinatus tear. Coronal T1-weighted fat-saturated TSE MR image after delayed i.v. contrast administration (indirect arthrogram). Gap representing tear (*arrow*) is filled with contrast medium after transsynovial diffusion into the joint

10.3 Ultrasonography: Normal Appearance of the Shoulder

Over the last few decades, significant improvements of shoulder US have been achieved by the introduction of linear-array, high-frequency transducers. Initially, 5 MHz sector and curved-array transducers with diverging ultrasonic beam were used, with anisotropy as result. Nowadays, 7.5–13 MHz linear-array transducers are used, allowing section thicknesses of 0.5–1 mm and in-plane spatial resolution in the range of 200–400 μm. Using these high frequencies, the spatial resolution with US is higher than acquired with MR imaging.

Information concerning clinical complaints and plain radiographs should ideally be present prior to US examination. Performance of the shoulder US investigation has been eminently reported by Teefey et al. (1999). Most imagers prefer a seated position of the patient with the examiner facing the patient or standing position behind the patient. The rotator cuff tendons must always be carefully evaluated in both coronal (longitudinal) and transversal dimensions to verify its continuity. Moreover, extending the examination dynamically with passive motion is a

prerequisite. The tendon must be strained during the investigation by rotating and extending the arm in the direction which is contrary to the function of that muscle. Hypoechoic appearance and a non-stretched buckled tendon can erroneously be mistaken for a torn tendon.

From inside out, cortical bone, hyaline cartilage, rotator cuff tendons and muscles, subacromial/subdeltoid bursa, peribursal fat, deltoid muscle and subcutis are normally appreciated with US (Fig. 10.4). The appearance of the cortical bone is hyperechoic with posterior acoustic shadowing. Hyaline cartilage is hypoechoic in contrast with the echogenicity of bone. Hodler et al. established an average depth of cartilage of 1.23 mm with MR imaging (Hodler et al. 1995) confirmed by Seibold et al. (Seibold et al. 1999) based on US. At the bare area, the posterolateral part of the humeral head, lack of hyaline cartilage is detected as a normal finding. The echogenicity of the tendons is substantially dependent on probe position. When the ingoing ultrasonic beam is not perpendicular to the tendon, the appearance of the tendon can modify from hyperechoic, hypoechoic to even anechoic referred to as anisotropy (Crass et al. 1988b). Perpendicular direction of the beam will result in a hyperechoic appearance of the tendon with a echogenic fibrillar echotexture (Fig. 10.4) (Martinoli et al. 1993). Rotator cuff muscle texture appears isoechoic. The subacromial-subdeltoid bursa, which is interposed between the rotator cuff and the acromion and deltoid muscle, is a two-layered hyperechoic compartment in which very little fluid can be seen. This fluid visually disappears by compression. The deltoid muscle itself has a less echogenic appearance compared with the rotator cuff tendons.

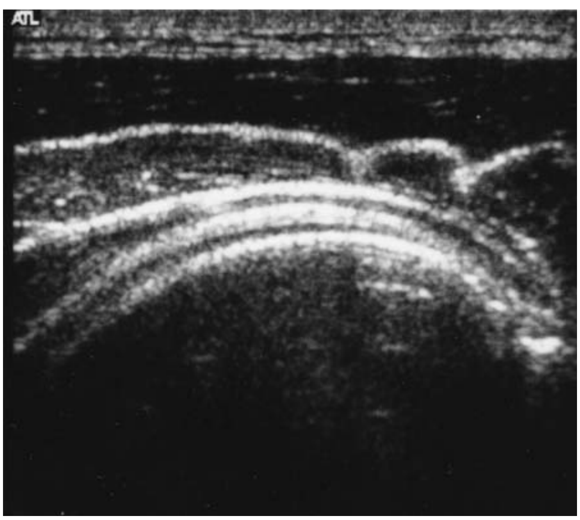

Fig. 10.4. Normal appearance of rotator cuff. Axial ultrasonographic image reveals from inside out hyperechoic cortical bone, hypoechoic cartilage, hyperechoic appearance of rotator cuff tendon, hypoechoic peribursal fat and hyperechoic subacromial/subdeltoid bursa beneath deltoid muscle

10.4 Shoulder Impingement Syndrome

Impingement reflects a clinical condition in which the subacromial soft tissues (supraspinatus tendon, biceps tendon, bursa) are compressed between the humeral head and (components of) the coracoacromial arch. Mechanical impingement may lead to a compromise of tensile integrity and eventually rotator cuff tears. Several types of impingement can be distinguished when discussing sports trauma to the rotator cuff: primary (extrinsic) impingement, secondary impingement from instability and posterosuperior (internal) impingement, particularly in throwing athletes. Another rare form of impingement is coracohumeral impingement, which involves anterior soft tissues, particularly the subscapularis muscle and tendon.

MR imaging and MR arthrography are important tools in establishing the form of impingement with significant relevance for subsequent therapy.

10.4.1 Primary Extrinsic Impingement

The arch that surrounds the rotator cuff is composed of the acromion, the acromioclavicular joint, the coracoid process and the coracoacromial ligament. Anatomical variants and reactive degenerative irregularities of this osseous outlet may result in primary extrinsic impingement of the underlying cuff tendons and adjacent bursa with subsequent clinical impingement (Fritz 2002). Although rotator cuff degeneration and tearing may be due to intrinsic factors, such as diminished vascularity and overuse, it has been proposed that the vast majority of cuff tears are secondary to chronic impingement between the humeral head and coracoacromial arch. It should be noticed, however, that primary impingement is fairly uncommon in young (athletic) individuals (Tuite 2003). The pain is believed to be caused primarily by compression of the well-innervated subacromial

bursa between cuff and arch. In this respect, the shape and aspect of the anterior acromion, assessed on the oblique sagittal and coronal MR images have been found to be of critical importance (Peh et al. 1995). The shape of the undersurface of the anterolateral acromion can be classified as flat (I), curved (II), anteriorly hooked (III) or convex (IV); however, variability among observers can be significant. Types II and III in particular are associated with higher incidence of impingement and rotator cuff abnormalities (Farley et al. 1994; Peh et al. 1995) (Fig. 10.5). Downsloping of the acromion, either anteriorly (determined on sagittal images, immediately lateral to the A–C joint) or laterally (on coronal images) may result in narrowing of the outlet and impingement of the distal part of the supraspinatus tendon (Fritz 2002) (Fig. 10.6). Another factor causing impingement may be the presence of bony spurs on the inferior surface of the acromion (Farley et al. 1994). Incidentally, a non-fused os acromiale may lead to osteophytic lipping at the acromial gap and as such impingement of the rotator cuff, tendinopathy and tearing of the supraspinatus (Park et al. 1994). The non-fused ossification center of the acromion is best appreciated on axial MR images, the subsequent effects on the rotator cuff are best visible on the oblique coronal and sagittal images.

Osteoarthritic changes of the A–C joint are frequently encountered after the age of 40. This may result in spur formation and synovial and capsular hypertrophy with scarring. Although these factors may influence the rotator cuff, it is usually less critical compared with changes of the anterior acromion (Sanders and Miller 2005). Separation or instability of the A–C joint may result in a low lying acromion that may contribute to impingement (Tirman et al. 1994a, 2004). In the young athlete, posttraumatic A–C separation and/or lysis of the distal clavicle is not uncommon (see Chap. 11). This may occur after acute moderate trauma or secondary to repetitive microtraumata caused by repetitive stress to the joint. In the early phase marrow edema of the distal clavicle can be seen on T2-weighted fat-suppressed images with some effusion, mild synovial hypertrophy and soft-tissue edema. Later on, joint widening can be found with irregularity of the cortex and subchondral sclerosis (Tirman et al. 1994a, 2004). Bone marrow edema in the acromion and/or distal clavicle can be found in a clinical picture of impingement without cuff abnormalities, but may also be appreciated in asymptomatic subjects (Fig. 10.7).

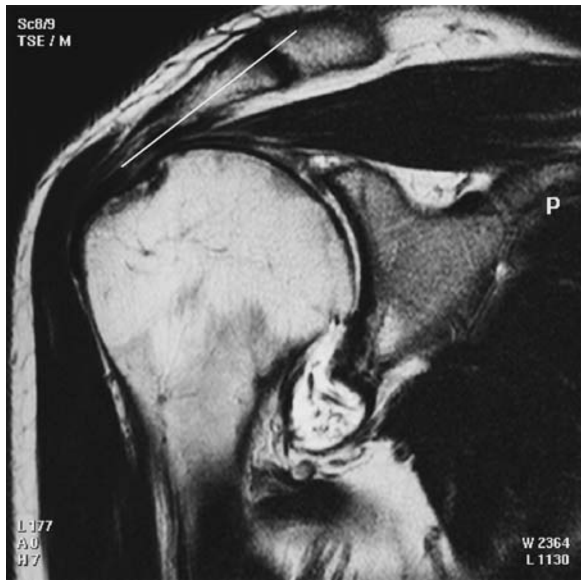

Fig. 10.6. Downsloping of acromion. Coronal T2-weighted MR arthrogram shows lateral downsloping of acromion (*white line*) contributing to impingement of subacromial soft tissues. There is also synovitis within axillary recessus

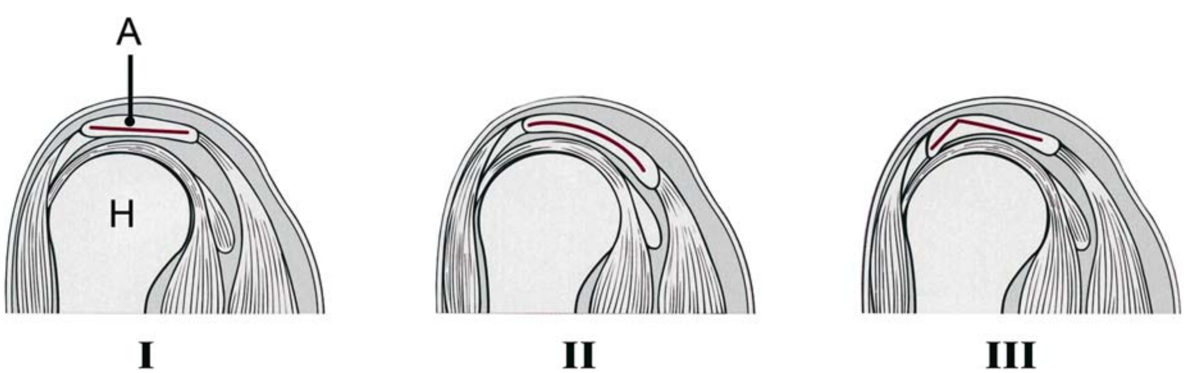

Fig. 10.5. Schematic drawing of most common anterolateral acromion types. Type I: flat undersurface, type II: smoothly curved undersurface, type III: anteriorly hooked acromion (*A*, acromion, *H*, humerus). Type IV (not shown) represents convex undersurface of acromion

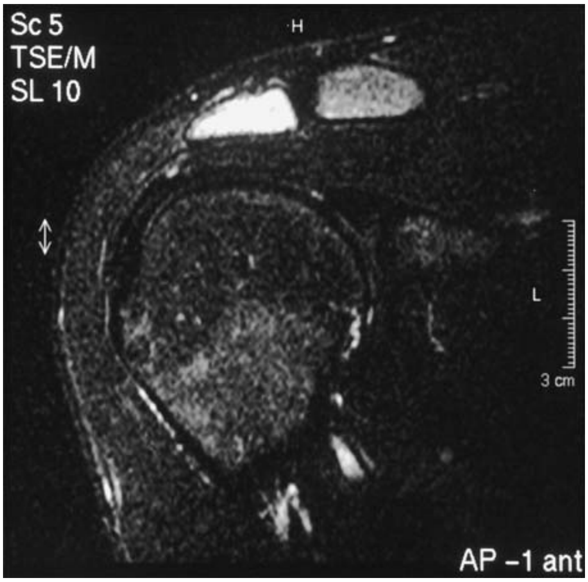

a

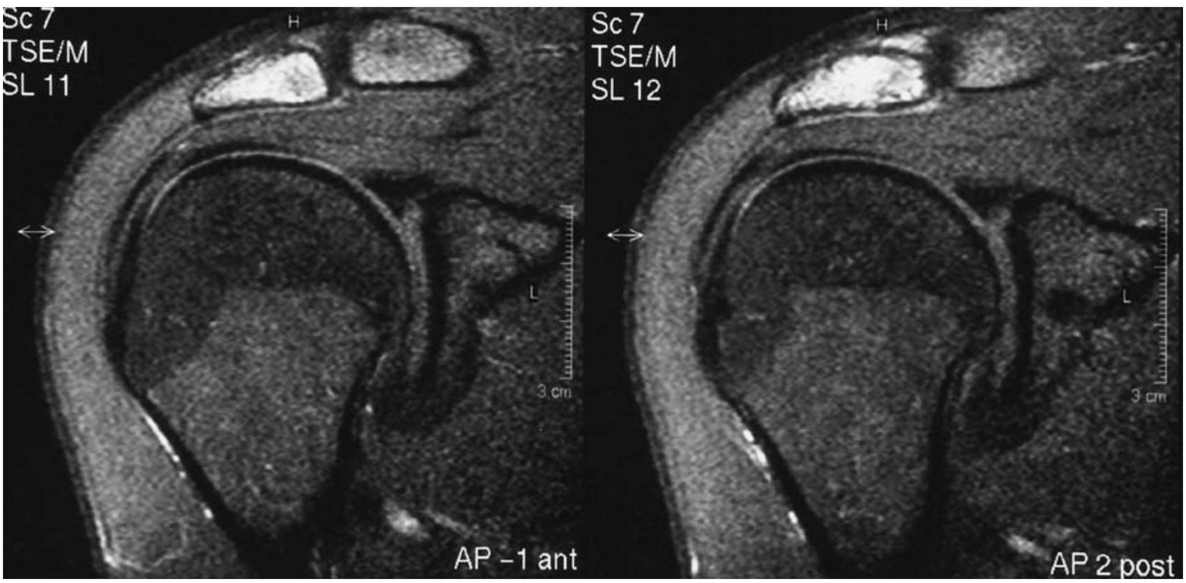

b

Fig. 10.7a,b. Young table tennis player with complaints of impingement, no trauma. Coronal T2-weighted fat-saturated TSE (**a**) and T1-weighted contrast-enhanced fat-saturated TSE (**b**) MR images show diffuse high SI of acromion with enhancement and a completely normal underlying cuff

The coracoacromial ligament (CAL) is another component of the osseous outlet. This ligament is best appreciated on the oblique sagittal MR images, as it extends from the coracoid process anteriorly to the acromion more posteriorly, covering the anterior fibers of the supraspinatus tendon and the rotator cuff interval. The thickness of the normal ligament measures about 2–3 mm. The CAL can be congenitally thickened and incidentally be a source of primary impingement (Tuite 2003), or thickening can be reactive due to chronic pressure exerted by subacromial structures during arm abduction. Incidentally, and almost exclusive in athletes, hypertrophy of the supraspinatus may cause clinical symptoms. In this case, the enlargement of the soft tissues is the cause of impingement rather than (osseous) narrowing of the acromiohumeral space.

10.4.2 Secondary Extrinsic Impingement

Secondary extrinsic impingement refers to instability of the glenohumeral joint that results in dynamic narrowing of the coracoacromial outlet (Fritz 2002). The outlet itself can be morphologically normal. This secondary impingement is considered the most common cause of impingement pain in the athlete (Tirman

et al. 2004). Usually, stability of the shoulder joint is provided by the static effects of the capsule, ligaments and labrum on one hand and by dynamic stabilizers including rotator cuff muscles and biceps tendon on the other hand. Repetitive microtraumata and weakening of the anterior capsule is quite commonly seen in overhead throwing athletes. The instability itself is usually minor and by itself asymptomatic and may result from a lax capsule or stretched glenohumeral ligaments that develop over time. This injury of the static stabilizers may influence and overload the dynamic stabilizers (cuff muscles). Due to superior translation of the humeral head in these throwers, there is dynamic impingement of the rotator cuff in the coracoacromial outlet, resulting in tendinosis and tearing (Tirman et al. 1994a, 1994b, 2004).

Accurate assessment of the cause of impingement has critical consequences for further treatment: in the primary form of extrinsic impingement, open or arthroscopic surgery is warranted to remove osseous irregularities, whereas secondary impingement may be best treated by physical therapy aiming at strengthening of the cuff and avoidance of activities causing instability. Various surgical procedures are available to decrease the many factors that contribute to mechanical impingement of the rotator cuff, particularly the supraspinatus tendon: these include resection of a thickened coracoacromial ligament, anterior acromioplasty, resection of the distal clavicle and resection of inferior osteophytes. Partial-thickness tears will be treated by arthroscopic debridement, whereas full-thickness tears should be repaired.

10.4.3 Internal Impingement

Internal impingement, also referred to as posterosuperior glenoid impingement, is a condition which is also encountered in athletes performing repetitive overhead throwing. Impingement occurs of the undersurface of the posterior rotator cuff between the humeral head and the posterosuperior labrum and osseous glenoid (Fritz 2002; Jobe et al. 1989; Walch et al. 1992) (Fig. 10.8). This position occurs during the late cocking phase of throwing with the arm in extreme abduction and exorotation. This may result in degeneration and partial cuff tears, particularly infraspinatus and posterior supraspinatus, fraying of the posterosuperior labrum and quite large subcortical cystic changes of the humeral head in the posterior greater tuberosity, due to repetitive impaction. Moreover, posterior capsular thickening and ossification (Bennet lesion) may occur under these circumstances (Ferrari et al. 1994). These changes at this particular site are optimally appreciated on MR arthrograms in abduction-exorotation position (Fritz 2002; Tirman et al. 1994a, 1994b, 2004; Tuite 2003) and crucial in making the diagnosis prior to arthroscopy.

10.4.4 Coracohumeral Impingement

An usual form of impingement is coracohumeral impingement, in which the coracohumeral distance is narrowed (less than the normal 11 mm) on axial images, for instance due to developmental enlargement of the coracoid process or posttraumatic changes of the coracoid process or lesser tuberosity. This may result in entrapment of the subscapularis tendon between the humeral head and coracoid process comparable to the classic impingement syndrome of the supraspinatus tendon (Sanders and Miller 2005).

10.5 MR Imaging and Rotator Cuff Injuries

The most common MR finding in the athlete with complaints of mild impingement pain is a normal cuff (Tuite 2003). Conversely, abnormal MR imaging findings are frequently encountered in shoulders of throwing athletes, due to highly repetitive stress and loads of the joints; however these findings do not necessarily indicate pathologic symptoms. In a study among professional handball players, abnormal findings were encountered in 93% but only 37% were symptomatic (Jost et al. 2005). Only players with simultaneous MRI abnormalities of all three cuff tendons were more frequently symptomatic. Partial rotator cuff lesions, posterosuperior glenoid impingement and superolateral osteochondral defects with cyst formation and edema were most frequently identified in throwing shoulders (Connor et al. 2003; Jost et al. 2005; Miniaci et al. 2002). Knowledge of these signal changes of the rotator cuff in athletes may assist in differentiation between pathologic and non-pathologic findings, but corre-

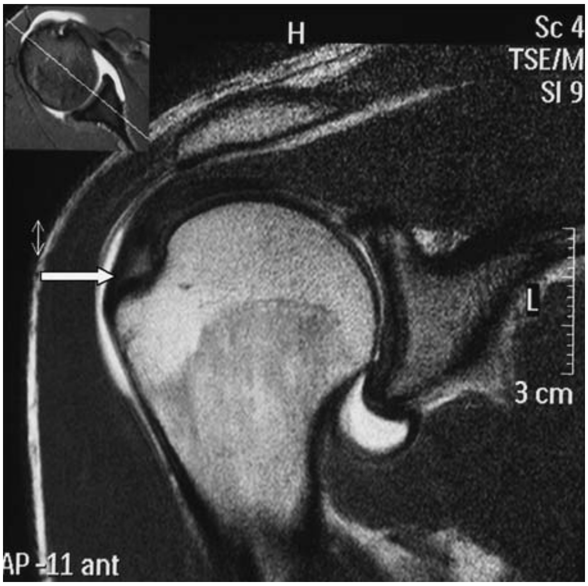

a

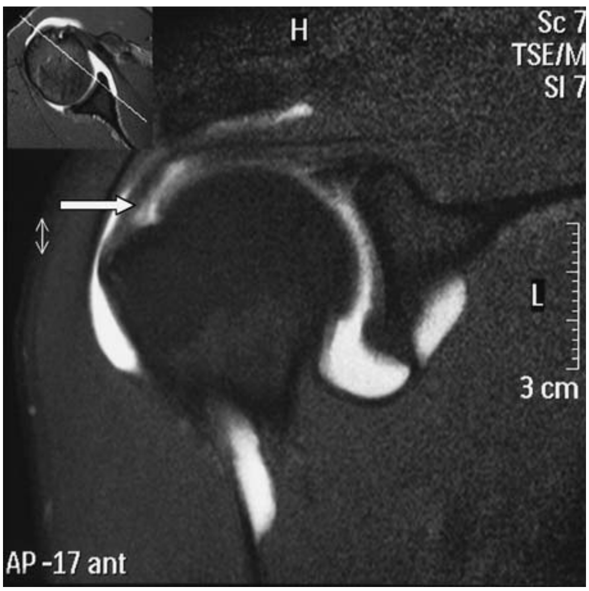

b

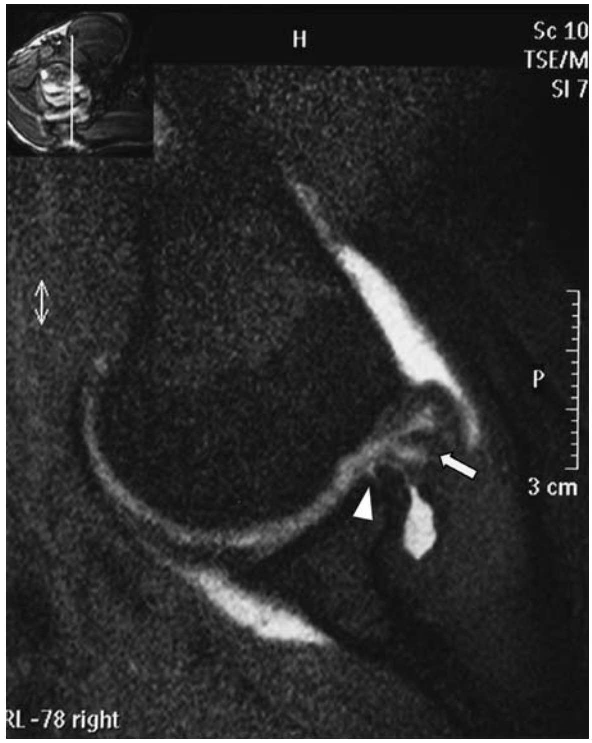

c

Fig. 10.8a–c. Internal impingement in 27-year-old American football player. Coronal proton-density-weighted TSE MR arthrogram (**a**) reveals increased SI at insertion site of supraspinatus tendon, consistent with tendinosis (*arrow*). Coronal T1-weighted TSE fat-saturated MR arthrogram (**b**) shows disruption of articular sided posterior supraspinatus tendon with contrast imbibition (*arrow*). ABER view (**c**) also shows branching extension of contrast medium within tendon (*arrow*) and subtle abnormality of posterior labrum (*arrowhead*)

lation with physical examination is always pivotal (Connor et al. 2003; Jost et al. 2005). In another study no significant signal differences were found in supra- and infraspinatus tendons between throwing and non-throwing athletes (Miniaci et al. 2002). Moreover, abnormal MRI signals can also be found in up to 30% of asymptomatic non-athletic shoulders, with an increase of incidence with age (Miniaci et al. 2002; Sanders and Miller 2005).

In the spectrum of cuff abnormalities, tendinopathy or tendinosis is defined as presence of intermediate to high signal intensity not equal to that of water within the otherwise low SI substance of the tendon, frequently but not always accompanied with mild to moderate thickening of the tendon (Fritz 2002) (Fig. 10.9). Degeneration of the rotator cuff becomes more common with age and may be primarily caused by intrinsic factors, such as diminished vascularity, overuse and failure of the normal healing response within the tendon. Tendinosis is common in the supraspinatus tendon near the humeral attachment of the tendon. When the tendon is morphologically normal, it may not be possible to differentiate tendinosis from signal alterations due to magic angle effect or partial volume averaging of signal from adjacent soft tissues on short echo time (TE) images. Persistence of abnormal signal on long TE images is a stronger indicator for tendino-

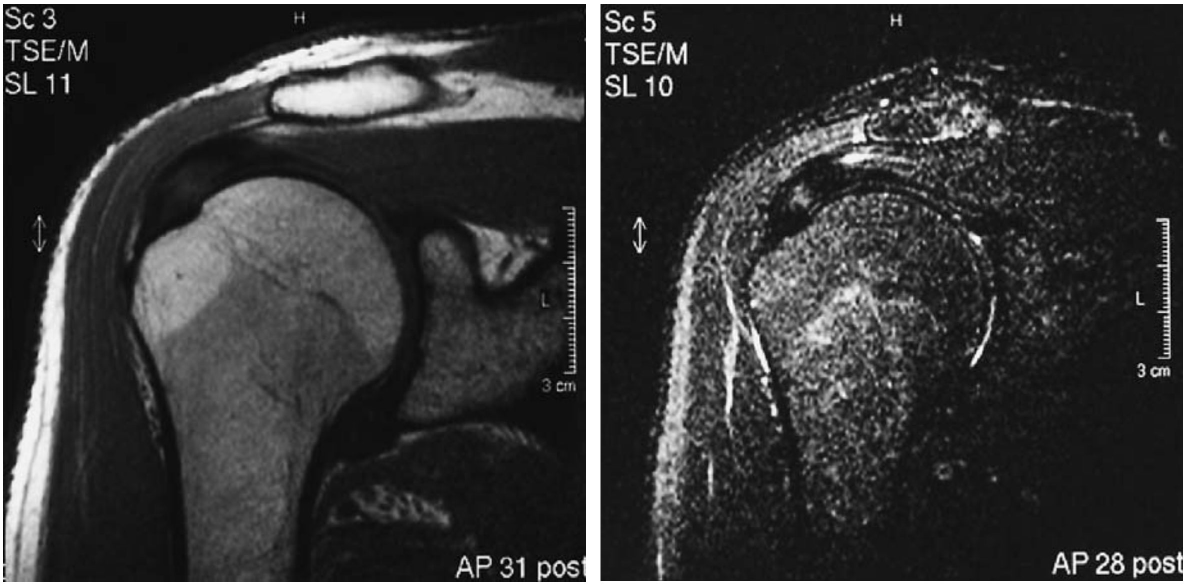

Fig. 10.9a,b. Tendinosis of supraspinatus tendon. Coronal proton-density weighted TSE (**a**) and T2-weighted fat-saturated TSE (**b**) MR images display thickened supraspinatus tendon with increased intrasubstantial SI, not equal to water

sis (Fritz 2002). In the more severe cases, fissures, edema and myxoid changes may develop within the tendon substance with associated MR findings including fluid-signal fissures, intrinsic high signal intensity not equal to water within the cuff and/or swelling of the cuff.

In calcifying tendinosis calcific deposits can be found either within the rotator cuff or in the bursa or periarticular ligaments. These calcifications are best seen either on plain radiographs or by US (Fig. 10.10). On MR imaging, the calcific deposits demonstrate as foci of low SI on both T1- and T2-weighted sequences (Fig. 10.11), and are most conspicuous on gradient-echo T2*-weighted images. Calcific tendinosis most commonly affects the supraspinatus tendon. Commonly, there is associated thickening of the tendon and reactive inflammation of the bursal soft tissues. It should be noticed that increased signal intensity changes on T2-weighted images of the peribursal fat plane may also be present in the normal asymptomatic population. Superimposed tears of the rotator cuff are not typically appreciated.

Fig. 10.10. Calcifying tendinosis. Ultrasonographic image of distal supraspinatus tendon shows hyperechoic linear focus (between *marks*) reflecting calcific deposit

In general, sensitivity and specificity numbers of MR imaging in the detection of rotator cuff tears are in the range of 88%–100% (Hodler et al. 1992; Meister et al. 2003; Quinn et al. 1995). Correct identification of rotator cuff tearing in the young athletic individual by conventional MRI can be difficult since these tears are usually small and shallow and may not appear as the classic fluid-filled high SI defects on T2-weighted images. Moreover, tears can be found in more atypical locations (Tuite 2003).

Partial thickness tears extend by definition partially through the thickness of the tendon in the superior-inferior direction, either on the articular or bursal surface. Moreover, interstitial partial tears can

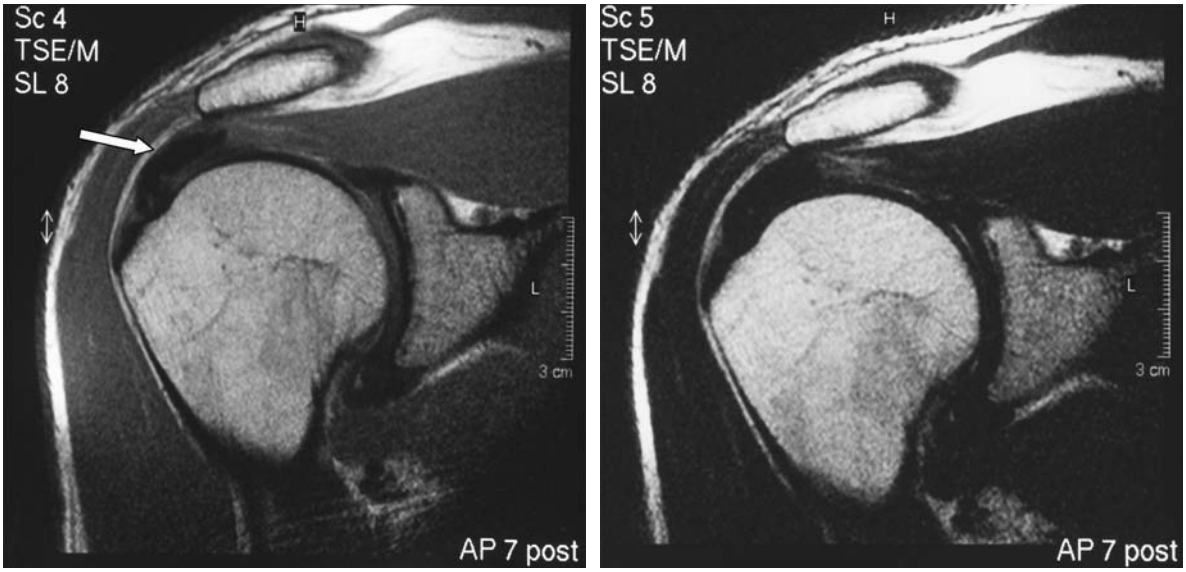

a b

Fig. 10.11a,b. Calcifying tendinosis. Coronal proton-density (**a**) and T2-weighted (**b**) TSE MR images reveal foci of decreased SI representing calcific deposits in distal supraspinatus tendon (*arrow*). Due to low SI these are easily overlooked on T2-weighted images

be encountered. Irregularity and thinning or thickening of the tendon are other findings suggestive of a partial thickness tear. In the group of athletes, these types of tears are most frequently encountered (Tirman et al. 2004). The high tensile strength of the tendons in young athletes make the cuff resistant to extensive tearing. On T2-weighted images, the partial-thickness tear is represented by high SI, equal to that of water, which is the hallmark of a rotator cuff tear. Fluid that extends in a discrete defect of the bursal surface is found in bursal surface partial tears. However, the most frequent locations of rotator cuff tears in athletes are the critical zone in the anterior half of the supraspinatus tendon at 0.5–1 cm from the insertion, the undersurface area of the cuff attachment to the humerus (referred to as rim-rent tears), and posterosuperior tears at 0.5–1 cm from the insertion site, particularly in overhead throwing athletes (Tirman et al. 2004; Tuite 2003). The higher incidence of articular surface tears compared with bursal side tears is related to the eccentric forces on the cuff that are greater on the articular side in athletes. Moreover, the articular side fibers are weaker and healing after injury is diminished due to less vascularization. On native MR images, partial tears are best demonstrated on oblique coronal images, in particular on combined proton-density and T2 weighted images with and without fat suppression.

MR arthrography with fat-suppression including coronal sequence (Fig. 10.12) and images in the abduction-exorotation stress position (ABER) allows detection of even small partial tears and delamination on the articular surface of the spinatus tendons and is strongly advocated by many authors (Hodler et al. 1992; Magee et al. 2004; Meister et al. 2003; Palmer et al. 1993; Sanders and Miller 2005; Tirman et al. 1994b; Tuite 2003) (Fig. 10.13). In the ABER position, the posterosuperior cuff is relaxed whereas simultaneously the anteroinferior labroligamentous complex is stressed. Analysis of the ABER images in (throwing) athletes should be focused on the posterosuperior articular surface side, which is a predilection site for small partial thickness tears. Both the vertical and horizontal (interstitial) component of a tear can be evaluated (Lee and Lee 2002). Folds that may appear when the cuff is not under tension should not be misinterpreted as tears (Fig. 10.14).Tears of the posterosuperior glenoid labrum are not uncommonly demonstrated in association with articular surface partial tears at the junction of the supra- and infraspinatus tendon. Partial-thickness tears, if untreated, can evolve to full-thickness tears and finally to complete tears. Therefore, although treatment of impingement pain usually starts with physical therapy, athletes with small partial tears may benefit from arthroscopic debridement to become pain free (Fig. 10.15) (Payne et al. 1997).

Full thickness tears are lesions that extend through the entire thickness of the tendon in superior-infe-

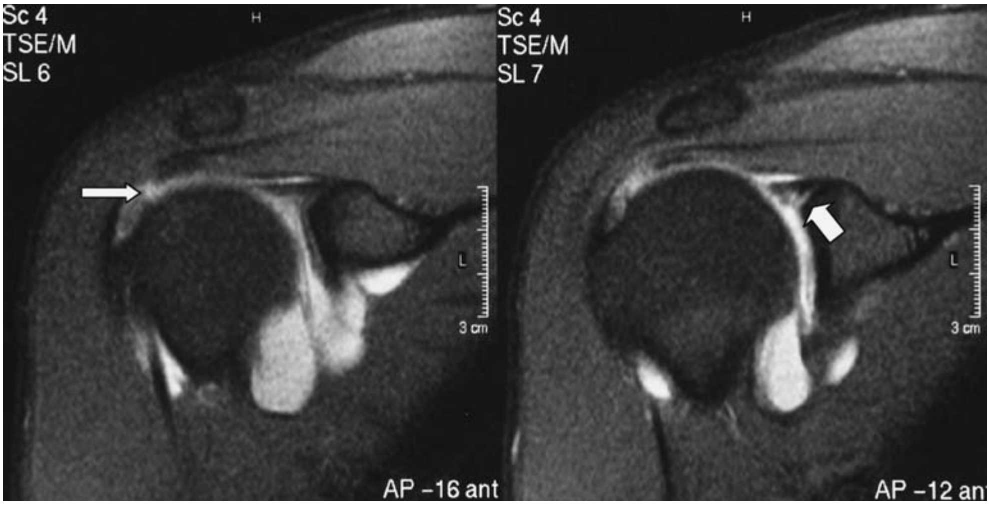

Fig. 10.12. Partial cuff tear in 27-year-old professional soccer goal keeper. Coronal T1-weighted fat-saturated TSE MR arthrogram demonstrates partial cuff tear on articular side of supraspinatus tendon (*arrow*), which was not detected on proton-density and T2-weighted images. Notice also irregular appearance of superior labrum, consistent with SLAP lesion (*short arrow*)

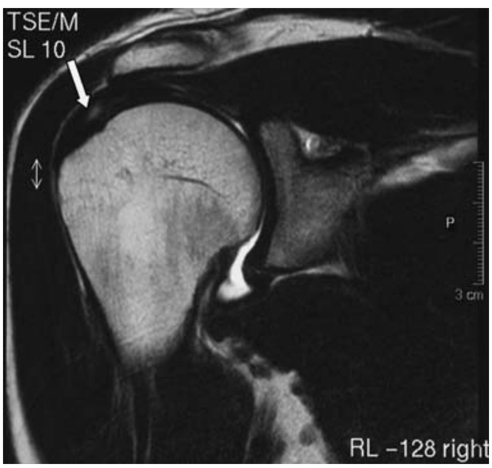

a

Fig. 10.13a,b. Partial thickness cuff tear in 22-year-old female tennis player with clinical picture of impingement. Coronal T2-weighted TSE (**a**) MR arthrogram reveals focal intrasubstantial increased signal within slightly thickened supraspinatus tendon (*arrow*).T1-weighted fat-saturated ABER MR arthrograms (**b**) show delamination of tendon fibres through partial-thickness tear with horizontal and vertical extension (*arrow*)

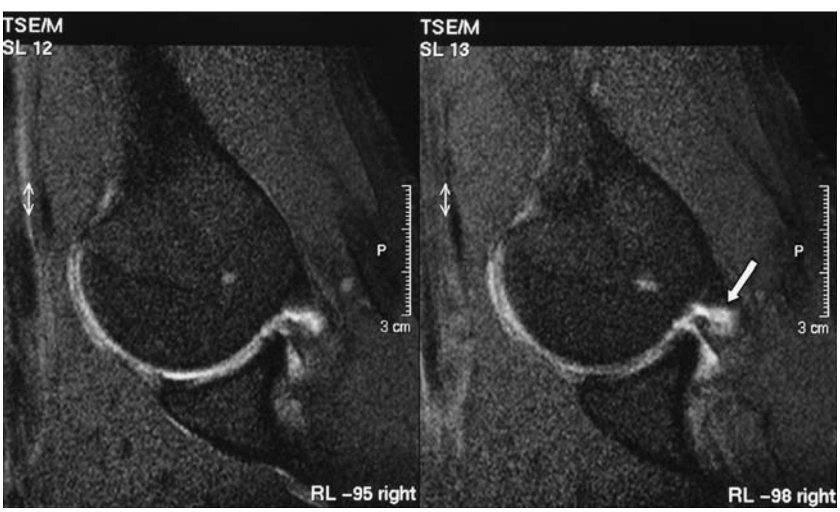

b

Fig. 10.14. Relaxation of supraspinatus tendon. T1-weighted fat-suppressed MR arthrogram, ABER view, shows relaxation of posterosuperior supraspinatus tendon (*arrow*), which should not be misinterpreted as a partial tear

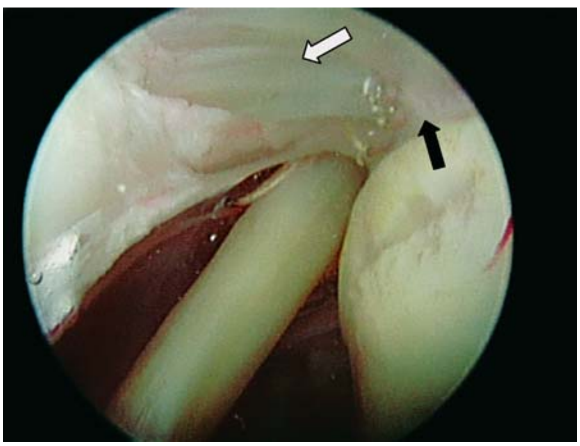

Fig. 10.15. Partial thickness rotator cuff tear. Arthroscopic image of right shoulder demonstrates partial thickness undersurface tear (*arrow*) of supraspinatus tendon, posterior to biceps tendon, leaving a small area of the footprint uncovered (*black arrow*)

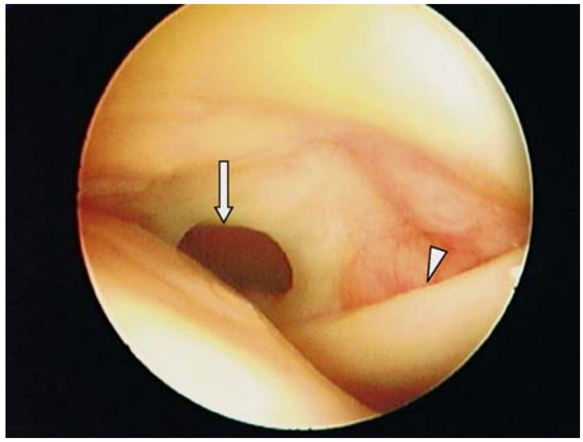

Fig. 10.16. Full-thickness rotator cuff tear. Arthroscopic image of left shoulder displays small full-thickness tear of supraspinatus tendon, adjacent to biceps tendon (*arrowhead*). On the left side humeral head is appreciated

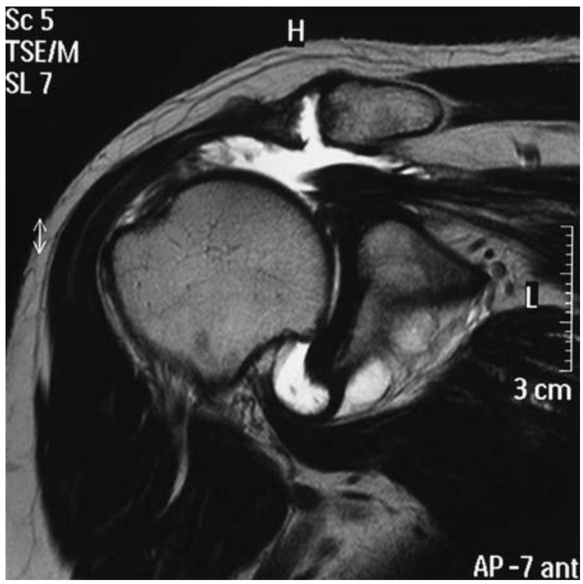

Fig. 10.17. Full-thickness rotator cuff tear. Coronal T2 weighted TSE MR arthrogram shows full-thickness rupture of supraspinatus tendon with retraction, fluid extension into AC-joint and fatty streaks within muscle due to (mild) atrophy

rior direction (Fig. 10.16). In case of a complete tear, there is also full extension in the anterior-posterior direction. Oblique coronal T2-weighted images may reveal a gap filled with high SI of fluid and there may be attraction of the involved tendon (Fig. 10.17). Some tears do not show fluid signal intensity due to tendon debris or granulation tissue. In equivocal cases, when a typical fluid-filled gap is not present, additional MR arthrography can be useful (Fig. 10.18). Full thickness tears can be characterized on the basis of location and size. The latter factor, expressed in both the antero-posterior and mediolateral dimensions, appears to have the highest clinical significance regarding outcome and prognosis (Gartsman and Milne 1995). MR reports should thus ideally include the exact site and extension of the tear, the estimated size of the

a b

Fig. 10.18a,b. Articular sided partial cuff and full-thickness tear. Proton-density weighted MR arthrogram (**a**) shows areas of increased signal within supraspinatus tendon. Articular sided partial cuff tear and full-thickness tear in supraspinatus tendon seen as increased signal on proton-density weighted MR arthrogram (**a**), even better appreciated on T1-weighted fat-saturated TSE image (**b**)

gap, involvement of different tendons and rotator cuff interval and secondary characteristics such as retraction of the tendon, muscle atrophy and fatty infiltration. The rate of fatty atrophy of the rotator cuff muscles can be scored on sagittal images and graded using a modified classification based on CT (Goutallier et al. 1994): minor: streaks of fat within the muscle, moderate: more remnant muscle tissue than fat and marked: more fat than muscle (Box 10.5).

Full-thickness tears are most commonly appreciated in the distal anterior part of the supraspinatus tendon. Larger tears may extend posteriorly to involve the entire attachment of the supraspinatus and further extension may involve the infraspinatus tendon posteriorly or the rotator cuff interval capsule with the long head of the biceps tendon and subscapularis tendon anteriorly. Isolated tears of the infraspinatus tendon are unusual, but may be encountered in young overhead throwing athletes (Tirman et al. 1994a, 2004) or in view of a posterosuperior impingement syndrome. The teres minor is typically spared in an otherwise complete ruptured rotator cuff. Incidentally, teres minor tears can be shown after posterior dislocation with injury of the posterior capsule. Isolated tears of the subscapularis are also uncommon, but can be seen after acute abduction and exorotation trauma (Fig. 10.19) (Deutsch et al. 1997). Axial and oblique sagittal MR images are optimal to assess partial and complete subscapularis tears, and also to determine or exclude injury or (sub)luxation of the biceps tendon, which is quite often seen in association with subscapularis tears (Fig. 10.20). Involvement of both the supra- and infraspinatus as well as (portions of) the subscapularis may lead to a high-riding humeral head within the glenohumeral joint, in close relation to the undersurface of the acromion.

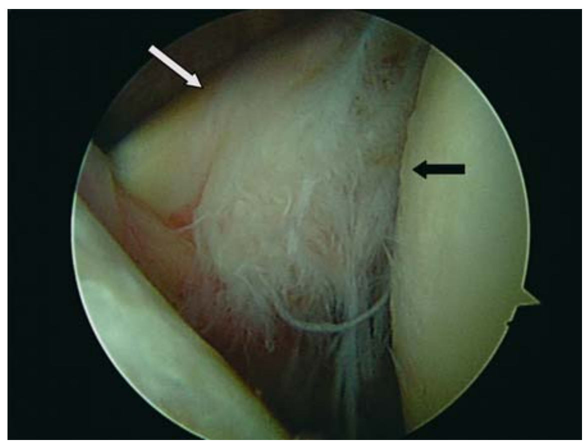

Fig. 10.19. Partial tear of subscapularis tendon. Arthroscopic image of right shoulder demonstrates intra-articular part of subscapularis tendon (*white arrow*) which is partly detached from insertion at humeral head (*black arrow*). On the left, glenoid surface is appreciated

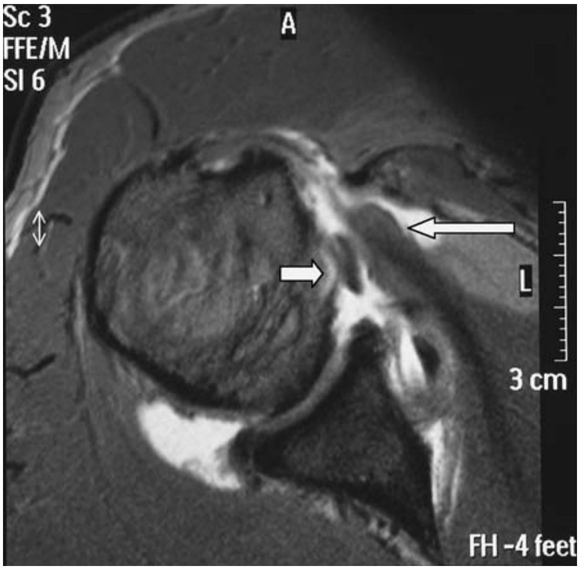

Fig. 10.20. Tear of subscapularis tendon. Axial T1-weighted fat-saturated TSE MR arthrogram shows disruption of subscapularis tendon with retraction (*long arrow*), combined with intra-articular dislocation of biceps tendon (*short arrow*). Notice empty bicipital groove

10.6 Ultrasonography and Rotator Cuff Injuries

The ultrasonographic appearance of tendinosis is a focal or diffuse heterogeneous, ill-defined hypoechoic (sometimes hyperechoic) tendon with increased size (Fig. 10.21) (Bachmann et al. 1997; Jacobson et al. 2004). Sometimes in tendinosis the size of the tendon may be unaltered, but will show increased signal on T2-weighted MR images, which makes MR more sensitive for assessment of tendinosis.

In calcifying tendinosis, hydroxyapatite crystal depositions can be appreciated as hyperechoic foci within the rotator cuff, most commonly the supraspinatus tendon.

The established criteria of a partial-thickness tear using US are a hypoechoic, anechoic or a mixed hypo- and hyperechoic area and/or discontinuity of the fibrillar pattern (Fig. 10.22). The hypoechogenicity of the tear is based upon filling of the tear with fluid or edema. Some larger partial-thickness tears of the bursal surface may demonstrate flattening under compression. Tiny tears can be easily overlooked, whereas on the other hand an extensive partial-thickness tear can be mistaken for a complete full-thickness tear without retraction.

The sensitivity and specificity figures for detection of partial tears using US are operator dependent and vary from respectively 41% to 93% and from 76% to 94% (Brenneke and Morgan 1992; Farin and Jaroma 1995; Read and Perko 1998; Teefey et al. 2000; van Holsbeeck et al. 1995; Wiener and Seitz 1993). The highest accuracy rates for detection of partial cuff tears, although dependent on tear size, were obtained in studies with experienced examiners (Teefey et al. 2004, 2005; van Holsbeeck et al. 1995; Winter et al. 2001).

Secondary findings that may be encountered with partial thickness tears include arthrotic signs in up

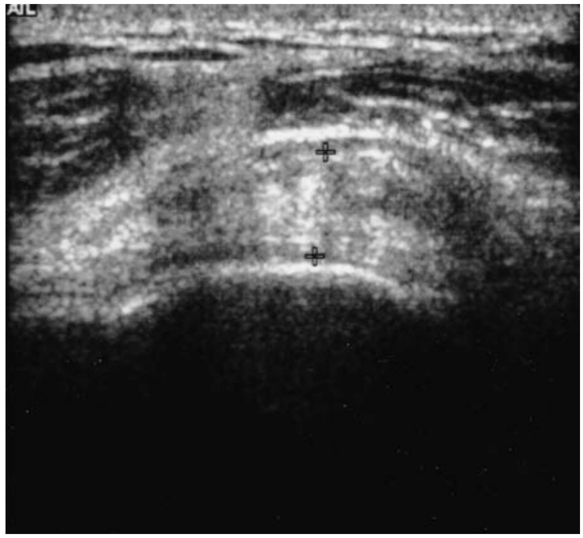

Fig. 10.21. Rotator cuff tendinosis. Ultrasonographic image of supraspinatus tendon reveals ill-defined diffuse heterogeneous hypo-and hyperechoic area with increased tendon size

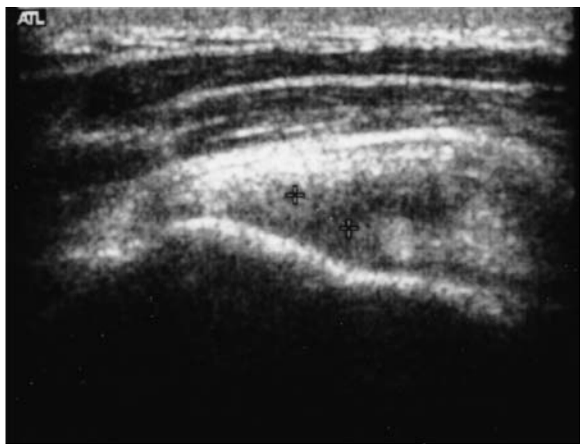

Fig. 10.22. Partial thickness rotator cuff tear. Axial ultrasonographic image of supraspinatus tendon reveals partial-thickness tear, shown as anechoic area at articular surface extending into tendon substance, with partial discontinuity of fibrillar pattern

to 50%–71% of patients, joint effusion in 13%–19% but reserved to articular sided partial-thickness tears, and subacromial-subdeltoid bursal effusion in 20% of patients (established as an amount of fluid greater than 2 mm) (Arslan et al. 1999; Hollister et al. 1995; Jacobson et al. 2004; van Holsbeeck and Strouse 1993; van Holsbeeck et al. 1995). Moreover, Jacobson et al. established subacromial-subdeltoid bursal effusion in more symptomatic patients without presence of a tear than with a partial-thickness tear (Jacobson et al. 2004).

The highest sensitivity and positive predictive values were observed for focal hypoechoic abnormalities within the tendon. The highest specificity, negative predictive values, and accuracy were established for nonvisualization of the tendon since this finding is exclusively correlated with full-thickness tears.

US has been reported to have high accuracy for the detection of full-thickness tears, even in non-experienced hands (Moosmayer and Smith 2005) with sensitivity and specificity values ranging from 57% to 100% and 76% to 100%, respectively (Bachmann et al. 1997; Brenneke and Morgan 1992; Crass et al. 1988a; Hodler et al. 1988; Miller et al. 1989; Paavolainen and Ahovuo 1994; Read and Perko 1998; Teefey et al. 2004; Vick and Bell 1990; Wiener and Seitz 1993). The appearance of such tears can be variable: non-visualization of tendon substance based on full retraction in 24%–50%, abnormal tendon echogenicity in 25%–56% of patients, and tendon flattening in 71% of patients (Bachmann et al. 1997; Jacobson et al. 2004; Teefey et al. 1999, 2005; Wiener and Seitz 1993) (Fig. 10.23). To increase the efficacy of US, the transducer should be compressed on the shoulder structures. The deltoid muscle or the peribursal fat may be compressed within the defect or flatten the supraspinatus. Both ends of the torn but non-retracted tendon will separate and this facilitates visualization of the tear. Fully retracted tendon and the cartilage interface sign (seen as a small linear hyperechoic part lying over the hypoechoic cartilage) are findings exclusively observed in full-thickness tear (Jacobson et al. 2004).

Secondary findings that are frequently observed in full-thickness tears include arthrotic signs in 86% of patients, joint effusion in 65% of patients and subacromial-subdeltoid bursal effusion in 68% of patients (Arslan et al. 1999; Farin et al. 1990; Jacobson et al. 2004; Teefey et al. 1999; van Holsbeeck and Strouse 1993; van Holsbeeck et al. 1994). Combined fluid in joint and subacromial-subdeltoid bursa raises the probability of a rotator cuff tear up to 95% (Hollister et al. 1995) (Box 10.6). Finding of a normal greater tuberosity was associated with absence of a rotator cuff tear in 96% (Wohlwend et al. 1998). The highest sensitivity, negative predictive value, and accuracy values were respectively observed for cortex irregularity (86%), bursal to articular surface abnormality (82%), and joint fluid (80%).

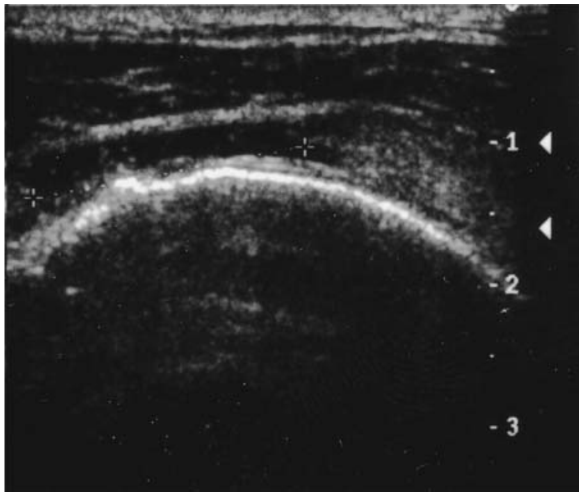

Fig. 10.23. Full-thickness rotator cuff tear. Axial ultrasonographic image shows large anechoic area of non-visualized supraspinatus tendon as a result of full-thickness tear

In patients in a seated position, joint fluid will surround the long head of the biceps brachii tendon, since this is the lowest part of the articular joint. Effusion in the biceps sheath is not a specific finding for a torn tendon, as this may also be observed in patients with synovitis and adhesive capsulitis. Dislocation or subluxation of the long head of the biceps brachii may return into normal position and therefore be undetected by MR imaging in contrast to dynamic US imaging. Disruption of the transverse humeral ligament may lead to subluxation or complete dislocation of the biceps tendon medially, even slide outside the biceps groove and shift beneath the subscapularis tendon. The latter condition can only exist in case of complete subscapularis tendon disruption. Subscapularis tears may occur due to forced exorotation and abduction or in patients with recurrent anterior shoulder luxation but the incidence is significantly lower compared with supraspinatus tears. Small circumference subscapularis tears (less than 5 mm) or limited external rotation of the shoulder during examination may contribute to failure of interpretation. Diagnosis of a subscapularis tear is important because of the altered surgical approach (Teefey et al. 2005)

10.7 Rotator Cuff Interval and Biceps Tendon Injuries

The rotator cuff interval is the anatomic space along the anterosuperior aspect of the shoulder between the supraspinatus and subscapularis prior to their fusion. Oblique sagittal MR images are the most important in analyzing the interval (Ho 1999). The interval is bridged by the rotator cuff interval capsule and also the coracohumeral ligament (CHL) contributes to the interval as it extends from the coracoid posteriorly and laterally and merges with the capsule. The fused capsule and CHL further merge with the anterior margin and superficial and deep fascial fibres of the supraspinatus. The capsule and ligament together serve as roof over the intraarticular course of the biceps tendon (Fig. 10.24). As such, the CHL together with the superior glenohumeral ligament, which is a focal thickening of the glenohumeral capsule, contribute to the stability of the long biceps tendon within the sulcus.

The many structures that are involved with and course through the rotator cuff interval can be injured together. The interval and biceps tendon are stressed in the athlete who uses repetitive and/or forceful overhead motions. Also a fall on the outstretched hand may sprain or tear the rotator cuff interval. The normal CHL should show thin and smooth with low SI on oblique sagittal images. As a result of acute injuries such as traumatic tearing, the rotator cuff interval and CHL may show thickening and irregularity with heterogeneous higher SI. With more chronic derangement, such as in repetitive overuse situations, irregular scarring of the rotator cuff interval capsule and CHL may be seen (Ho 1999).

Fig. 10.24. Rotator cuff interval. Oblique sagittal T2-weighted TSE MR arthrogram showing the relationship of the CHL (*short arrow*) to the intraarticular course of the biceps tendon (*arrowhead*), rotator cuff interval capsule and SGHL (*arrow*)

Prominent scarring of the CHL has also been thought to play a role in the clinical picture of an adhesive capsulitis. Besides thickening on the oblique sagittal images, one should be aware of synovitis within the rotator cuff interval. Frequently, however, no specific MR abnormalities are noticed in patients with clinical symptoms of adhesive capsulitis (Sanders and Miller 2005).

The long tendon of the biceps extends from the superior glenoid tubercle or superior labrum, through the glenohumeral joint and rotator cuff interval and exits the joint anteriorly. Extra-articularly, the tendon is located within the intertubercular sulcus. The biceps tendon together with the superior labrum attribute to prevention of superior dislocation of the humeral head.

Serious injuries of those structures may result in a pseudo-impingement syndrome, as impingement of the rotator cuff may occur between the high-riding humeral head and the acromial arch. The spectrum of biceps tendon injuries includes tendinopathy, partial thickness tear, complete disruption, and subluxation or dislocation of the extra-articular portion of the tendon (Sanders and Miller 2005). The extra-articular appearance of the biceps tendon is best evaluated on axial MR images. Tears of the long head of the biceps tendon are usually a complication of a supraspinatus injury. Clinically, it can be difficult to differentiate partial biceps tendon tears from partial-thickness anterior supraspinatus tendon tears or tendinosis. In partial thickness biceps tendon tears, fluid signal is appreciated within the tendon substance. Presence of two rather than one tendon slips, which is a normal variant, should not be misinterpreted as partial tearing. In complete tears, the tendon is absent or there is complete discontinuity.

Tearing most frequently occurs in the lateral intra-articular portion. In complete tears, the tendon is no longer visualized within the bicipital groove due to distal retraction of the muscle. A small proximal remnant at the biceps-labral anchor is frequently seen. Severe degeneration with thinning of the long biceps tendon may give rise to an apparently empty interval. An empty sulcus on the other hand can also exist without complete tear of the tendon, in case of medial dislocation. Intra-articular biceps tendon dislocation is usually associated

with a full-thickness tear of the subscapularis tendon or rotator cuff interval injury, whereas extra-articular dislocation is associated with a partial thickness tear of the subscapularis or tear of the transverse ligament (Sanders and Miller 2005) (Fig. 10.25).

10.8 Miscellaneous Conditions that May Mimic Rotator Cuff Pathology

MR imaging is also very useful to identify abnormalities that may mimic cuff lesions or labroligamentous lesions, including, among others, Parsonage-Turner syndrome, quadrilateral space syndrome and spinoglenoid notch cyst (Helms 2002; Helms et al. 1998). Parsonage-Turner syndrome (acute brachial neuritis) is a self-limiting disorder, which presents with sudden onset of shoulder pain, sometimes bilateral, and accompanying weakness. MR imaging usually shows characteristic edema of rotator cuff muscles and deltoid muscle. In quadrilateral space syndrome, patients present with pain that may simulate cuff pathology, presumably due to (posttraumatic) scar tissue and fibrous band in the quadrilateral space that may cause impingement on the axillary nerve. Again, MR is rather typical demonstrating fatty atrophy of the teres minor muscle. A cyst in the spinoglenoid notch is usually associated with tearing of the posterior labrum (Fritz et al. 1992). The cyst or ganglion cannot be detected with arthroscopy which stresses the role of MRI or US. Due to compression on the suprascapular nerve, edema and atrophy of the infraspinatus muscle can be appreciated on fat-saturated T2-weighted MR images or US (see Chap. 11).

10.9 Conclusion

Shoulder pain due to trauma or overuse is a common complaint in the populations of athletes in general, with a variety of causes that are frequently difficult to differentiate by physical examination alone.

MR imaging and ultrasonography are optimal and complementary tools to discriminate different forms of impingement and to localize and classify rotator cuff injuries. A native MR imaging protocol including axial, oblique sagittal and oblique coronal sequences is in general suitable for patients presenting with symptoms of impingement, and to assess full-thickness tears.

Partial thickness rotator cuff tears are most commonly encountered in (overhead throwing) athletes, particularly on the articular side, which are best appreciated using MR arthrography including abduction-exorotation views.

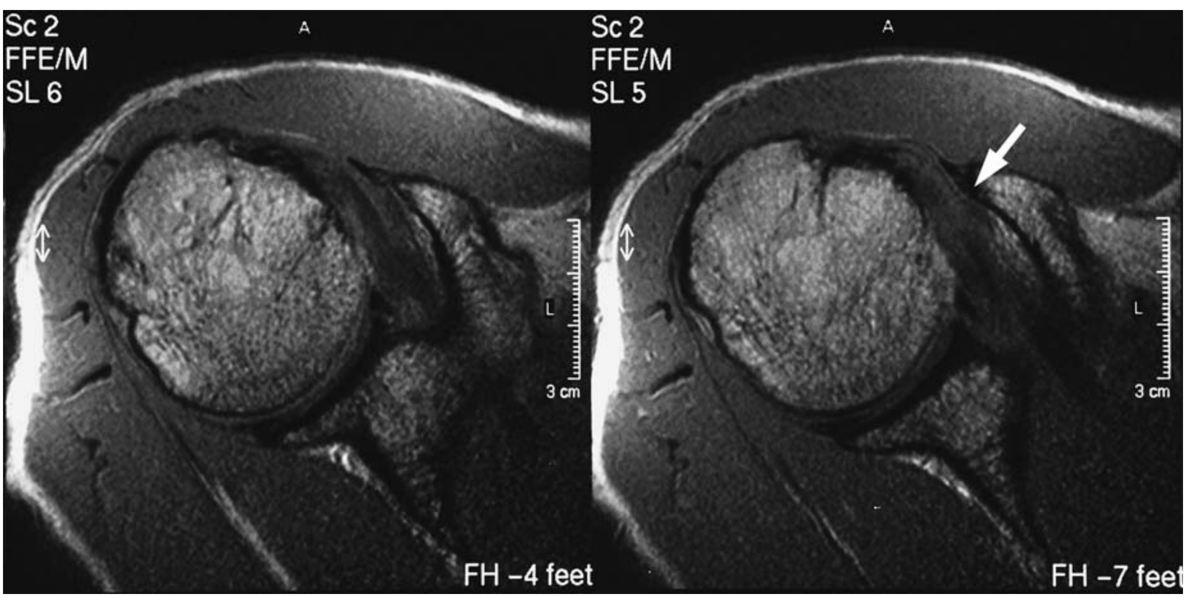

Fig. 10.25. Partial tear of subscapularis tendon. Subsequent axial T1-weighted gradient-echo images show irregularly thickened subscapularis tendon with increased SI consistent with partial tear which was confirmed with arthroscopy

Things to Remember

1. Cuff and biceps-labral lesions secondary to trauma or overuse may be encountered simultaneously in athletes.

2. ABER views in an MR arthrography protocol are very helpful to detect small partial cuff tears on the articular side, besides the identification of non-displaced labroligamentous tears.

3. Most frequent locations of rotator cuff tears in athletes are the anterior half of the supraspinatus tendon at 0.5–1 cm from the insertion, the undersurface area of the cuff attachment to the humerus and posterosuperior tears at 0.5–1 cm from the insertion site.

4. Secondary extrinsic impingement is frequently encountered in throwing athletes. Usually, instability is minor and the coracoacromial outlet is morphologically normal.

References

Arslan G, Apaydin A, Kabaalioglu A et al. (1999) Sonographically detected subacromial/subdeltoid bursal effusion and biceps tendon sheath fluid: reliable signs of rotator cuff tear? J Clin Ultrasound 27:335–339

Bachmann GF, Melzer C, Heinrichs CM et al. (1997) Diagnosis of rotator cuff lesions: comparison of US and MRI on 38 joint specimens. Eur Radiol 7(2):192–197

Brenneke SL, Morgan CJ (1992) Evaluation of ultrasonography as a diagnostic technique in the assessment of rotator cuff tendon tears. Am J Sports Med 20:287–289

Connor PM, Banks DM, Tyson AB et al. (2003) Magnetic resonance imaging of the asymptomatic shoulder of overhead athletes: a 5-year follow-up study. Am J Sports Med 31:724–727

Crass JR, Craig EV, Feinberg SB (1988a) Ultrasonography of rotator cuff tears: a review of 500 diagnostic studies. J Clin Ultrasound.16(5):313–327

Crass JR, van de Vegte GL, Harkavy LA (1988b) Tendon echogenicity: ex vivo study. Radiology 167(2):499–501

Deutsch A, Altchek DW, Veltri DM et al. (1997) Traumatic tears of the subscapularis tendon: clinical diagnosis, magnetic resonance imaging findings, and operative treatment. Am J Sports Med 25:13–22

Farin PU, Jaroma H, Harju A et al. (1990) Shoulder impingement syndrome: sonographic evaluation. Radiology 176(3):845–9

Farin PU, Jaroma H (1995) Acute traumatic tears of the rotator cuff: value of sonography. Radiology 197(1):269–273

Farley F, Neumann C, Steinbach L et al. (1994) The coracoacromial arch: MR evaluation and correlation with rotator cuff pathology. Skeletal Radiol 23:641–645

Ferrari JD, Ferrari DA, Courmas J et al. (1994) Posterior ossification of the shoulder: the Bennett lesion. Etiology, diagnosis and treatment. Am J Sports Med 22:171–176

Fritz RC (2002) Magnetic resonance imaging of sports-related injuries to the shoulder: impingement and rotator cuff. Radiol Clin N Am 40:217–234

Fritz RC, Helms CA, Steinbach LS et al. (1992) Suprascapular nerve entrapment: evaluation with MR imaging. Radiology 182:437

Gartsman GM, Milne JC (1995) Articular surface partial thickness tears of the rotator cuff. J Shoulder Elbow Surg 4:409–415

Goutallier D, Postel J, Bernageau J et al. (1994) Fatty muscle degeneration in cuff ruptures: pre- and postoperative evaluation by CT scan. Clin Orthop Relat Res 304:78–83

Helms CA (2002) The impact of MR imaging in sports medicine. Radiology 224:631

Helms CA, Martinez S, Speer KP (1998) Acute brachial neuritis (Parsonage-Turner syndrome): MR imaging appearance-report of three cases. Radiology 207:255

Ho CP (1999) MR imaging of rotator interval, long biceps, and associated injuries in the overhead-throwing athlete. Magn Reson Imaging Clin N Am 7;23–37

Hodler J, Fretz CJ, Terrier F et al. (1988) Rotator cuff tears: correlation of sonographic and surgical findings. Radiology 169:791–794

Hodler J, Kursunoglu-Brahme S, Snyder S et al. (1992) Rotator cuff disease: assessment with MR arthrography versus standard MR imaging in 36 patients with arthroscopic confirmation. Radiology 182:431–436

Hodler J, Loredo RA, Longo C et al. (1995) Assessment of articular cartilage thickness of the humeral head: MR-anatomic correlation in cadavers. AJR Am J Roentgenol 165(3):615–620

Hollister MS, Mack LA, Patten RM et al. (1995) Association of sonographically detected subacromial/subdeltoid bursal effusion and intraarticular fluid with rotator cuff tear. AJR Am J Roentgenol 165(3):605–608

Jacobson JA, Lancaster S, Prasad A et al. (2004) Full-thickness and partial-thickness supraspinatus tendon tears: value of US signs in diagnosis. Radiology 230(1):234–242

Jbara M, Chen Q, Marten P et al. (2005) Shoulder MR arthrography: how, why, when. Radiol Clin N Am 43(4):693–709

Jobe FW, Kvitne RS, Giangarra CE (1989) Shoulder pain in the overhand or throwing athlete: the relationship of anterior instability and rotator cuff impingement. Orthop Rev 18:963–975

Jost B, Zumstein M, Pfirrmann CW et al. (2005) MRI findings in throwing shoulders – abnormalities in professional handball players. Clin Orth Rel Res 434:130–137

Lee SY, Lee JK (2002) Horizontal component of partial-thickness tears of rotatot cuff: imaging characteristics and comparison of ABER view with oblique coronal view at MR arthrography. Radiology 224:470–476

Magee T, Williams D, Mani N (2004) Shoulder MR arthrography: which patient group benefits most? AJR Am J Roentgenol 183:969–974

Martinoli C, Derchi LE, Pastorino C et al. (1993) Analysis of echotexture of tendons with US. Radiology 186(3):839–843

Meister K, Thesing J, Montgomery W et al. (2003) MR arthrography of partial thickness tears of the undersurface of the rotator cuff: an arthroscopic correlation. Skeletal Radiol 33:136–141

Miller CL, Karasick D, Kurtz AB et al. (1989) Limited sensitivity of ultrasound for the detection of rotator cuff tears. Skeletal Radiol 18(3):179–183

Miniaci A, Mascia AT, Salonen DC et al. (2002) Magnetic resonance imaging of the shoulder in asymptomatic professional baseball pitchers. Am J Sports Med 30:66–73

Moosmayer S, Smith HJ (2005) Diagnostic ultrasound of the shoulder – a method for experts only? Results from an orthopedic surgeon with relative inexpensive compared to operative findings. Acta Orthop 76:503–508

O'Connor PJ, Rankine J, Gibbon WW et al. (2005) Interobserver variation in sonography of the painful shoulder. J Clin Ultrasound 33:53–56

Paavolainen P, Ahovuo J (1994) Ultrasonography and arthrography in the diagnosis of tears of the rotator cuff. J Bone Joint Surg Am 76:335–340

Palmer WE, Brown JH, Rosenthal DI (1993) Rotator cuff: evaluation with fat-suppressed MR arthrography. Radiology 188:683–687

Park JG, Lee JK, Phelps CT (1994) Os acromiale associated with rotator cuff impingement: MR imaging of the shoulder. Radiology 193:255–257

Payne LZ, Altcheck DW, Craig EV et al. (1997) Arthroscopic treatment of partial rotator cuff tears in young athletes. Am J Sports Med 25:299–305

Peh W, Farmer T, Totty W (1995) Acromial arch shape: assessment with MR imaging. Radiology 195:501–505

Quinn SF, Sheley RC, Demlow TA et al. (1995) Rotator cuff tendon tears: evaluation with fat-suppressed MR imaging with arthroscopic correlation in 100 patients. Radiology 195:497–500

Read JW, Perko M (1998) Shoulder ultrasound: diagnostic accuracy for impingement syndrome, rotator cuff tear, and biceps tendon pathology. J Shoulder Elbow Surg 7(3):264–271

Sanders TG, Miller MD (2005) A systematic approach to magnetic resonance imaging interpretation of sports medicine injuries of the shoulder. Am J Sports Med 33:1088–1105

Seibold CJ, Mallisee TA, Erickson SJ et al. (1999) Rotator cuff: evaluation with US and MR imaging. Radiographics 19(3):685–705

Teefey SA, Middleton WD, Yamaguchi K (1999) Shoulder sonography. State of the art. Radiol Clin N Am 37(4):767–785

Teefey SA, Hasan SA, Middleton WD et al. (2000) Ultrasonography of the rotator cuff. A comparison of ultrasonographic and arthroscopic findings in one hundred consecutive cases. J Bone Joint Surg Am 82:498–504

Teefey SA, Rubin DA, Middleton WD et al. (2004) Detection and quantification of rotator cuff tears. Comparison of ultrasonographic, magnetic resonance imaging, and arthroscopic findings in seventy-one consecutive cases. J Bone Joint Surg Am 86(4):708–716

Teefey SA, Middleton WD, Payne WT et al. (2005) Detection and measurement of rotator cuff tears with sonography: analysis of diagnostic errors. AJR Am J Roentgenol 184(6):1768–1773

Tirman PF, Bost FW, Garvin GJ et al. (1994a) Posterosuperior glenoid impingement of the shoulder: findings at MR imaging and MR arthrography with arthroscopic correlation. Radiology 193:431–436

Tirman PF, Bost FW, Steinbach LS et al. (1994b) MR arthrographic depiction of tears of the rotator cuff: benefit of abduction and external rotation of the arm. Radiology 192:851–856

Tirman PF, Smith ED, Stoller DW et al. (2004) Shoulder imaging in athletes. Semin Musculoskel Radiol 8:29–40

Tuite MJ (2003) MR imaging of sports injuries to the rotator cuff. Magn Reson Imaging Clin N Am 11:207–219

Vanhoenacker FM, Vanhoenacker P, Crevits I et al. (2000) MR imaging of the shoulder: imaging techniques and anatomy. JBR-BTR 83:309–312

van Holsbeeck M, Strouse PJ (1993) Sonography of the shoulder: evaluation of the subacromial-subdeltoid bursa. AJR Am J Roentgenol 160(1):561–564

van Holsbeeck M, Introcaso JH, Kolowich PA (1994) Sonography of tendons: patterns of disease. Instr Course Lect 43:475–481

van Holsbeeck MT, Kolowich PA, Eyler WR et al. (1995) US depiction of partial-thickness tear of the rotator cuff. Radiology 197:443–446

Vick CW, Bell SA (1990) Rotator cuff tears: diagnosis with sonography. AJR Am J Roentgenol 154(1):121–123

Walch G, Boileau P, Noel E et al. (1992) Impingement of the deep surface of the supraspinatus tendon on the posterosuperior glenoid rim: an arthroscopic study. J Shoulder Elbow Surg 1:238–245

Wiener SN, Seitz WH Jr (1993) Sonography of the shoulder in patients with tears of the rotator cuff: accuracy and value for selecting surgical options. AJR Am J Roentgenol 160:103–107

Winter TC III, Teefey SA, Middleton WD (2001) Musculoskeletal ultrasound: an update. Radiol Clinics North Am 465–483

Wohlwend JR, van Holsbeeck M, Craig J et al. (1998) The association between irregular greater tuberosities and rotator cuff tears: a sonographic study. AJR Am J Roentgenol 171(1):229–233

Scapular, Clavicular, Acromioclavicular and Sternoclavicular Joint Injuries

11

Peter Brys and Eric Geusens

CONTENTS

P. Brys, MD
E. Geusens, MD
Dept. of Radiology, University Hospitals Leuven, Herestraat 49, 3000 Leuven, Belgium

11.1 Introduction

11.1.1 Scapula

The scapula is a flat bone with three prominences, the spine and acromion, the glenoid, and the coracoid process. Medial to the base of the coracoid process is the scapular notch arched by the superior transverse scapular ligament. The spinoglenoid notch arched by the inferior transverse scapular ligament is situated between the lateral margin of the base of the scapular spine and the dorsal side of the glenoid. Both notches are important fixation points along the course of the suprascapular nerve.

11.1.2 Clavicle

The growth plates of the medial and lateral clavicular epiphyses do not fuse until the age of 25 years. The deltoid, trapezius, and pectoralis major muscles have important attachments to the clavicle. The deltoid muscle inserts onto the anterior surface of the lateral third of the clavicle, and the trapezius muscle onto the posterior aspect. The pectoralis major muscle inserts onto the anterior surface of the medial two thirds.

11.1.3 Acromioclavicular Joint

The synovium-lined AC joint has interposed between its fibrocartilaginous joint surfaces a fibrocartilaginous disc of variable size which is frequently completely absent (Wickiewicz 1983). The joint has a thin capsule, reinforced by the AC ligaments of which the superior one is continuous with the deltoid and trapezius aponeuroses. The lateral clavicle is anchored to the coracoid process by the coracoclavicular liga-

Box 11.1. Plain radiography

- Initial modality in osseous or articular disease
- Tailored approach and good quality essential
- Only AC stress views when therapeutical consequences
- No special SC views when CT available
- Low sensitivity for early stress fracture or LCO

Box 11.2. CT

- Second stage evaluation of fractures or SC dislocation
- If plain radiography negative and bone scan positive

Box 11.3. Ultrasound

- Limited role in AC joint
  - AC sprain: type 1 or muscular status
  - AC joint: joint distension? Arthrosynovial cyst?
- Limited role in SC joint: distension?
- Posterior shoulder pain/weakness: paralabral cyst?
- Soft tissue trauma

Box 11.4. MRI

- No clear role in sprain or isolated disease of AC joint
- Limited role in SC sprain
- Soft tissue trauma
- Posterior shoulder pain: muscle denervation? paralabral cyst?

Box 11.5. Scintigraphy

- When plain radiography is negative
- Suspected active osseous disease
  - Occult fracture
  - Stress fracture
  - Growth plate injury or apophysitis
  - Arthritis or osteoarthritis
  - Lateral clavicular osteolysis

ment, composed of the lateral trapezoid and medial conoid parts (Fig. 11.1). The static joint stabilizers are the AC ligaments, controlling the horizontal stability, and the CC ligament controlling the vertical stability. The dynamic stabilizers are the deltoid and trapezius muscles. The trapezius muscle attaches at the dorsal aspect of the acromion, part of the anterior deltoid muscle inserts on the clavicle medial to the AC joint. Their force vectors prevent excessive superior migration of the distal clavicle after disruption of the AC and CC ligaments alone (Wulker 1998).

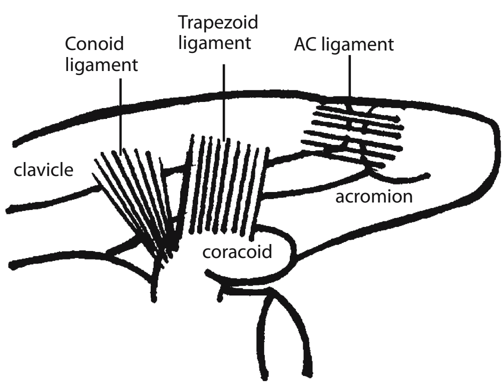

Fig. 11.1. Normal anatomy: the acromioclavicular and coracoclavicular ligament, the latter with its medial conoid and lateral trapezoid parts

11.1.4 Sternoclavicular Joint

The synovium-lined SC joint is formed by the medial clavicle, the clavicular notch of the manubrium, and the cartilage of the first rib (Fig. 11.2). Interposed between the fibrocartilaginous joint surfaces is a usually complete fibrocartilaginous disc, which acts to reduce the incongruities between the articulating

joint surfaces, and as a shock absorber against medial translation of the clavicle. The anterior and posterior SC ligaments are thickenings of the joint capsule. The interclavicular ligament connects the clavicles with the capsular ligaments and the upper sternum. The costoclavicular or rhomboid ligament runs from the first rib to the rhomboid fossa at the inferior side of the medial clavicular metaphysis. This fossa should not be mistaken for a tumor when seen on radiographs. The SC joint is freely movable and functions almost like a ball-and-socket joint with motion in almost all planes, including rotation (Lucas 1973). The ligamentous support is so strong that it is one of the least commonly dislocated joints in the body (Wirth and Rockwood 1996).

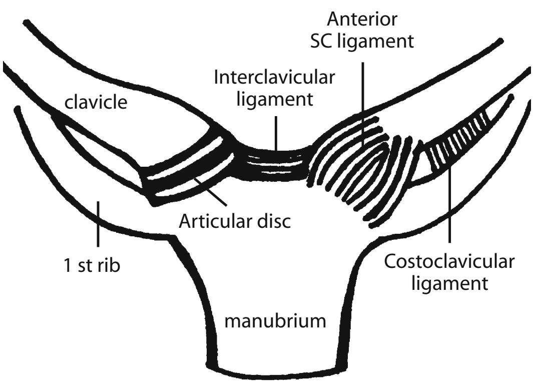

Fig. 11.2. Normal anatomy: the sternoclavicular joint

11.2 Imaging

11.2.1 Plain Radiography

Diagnostic plain films are tailored to the clinical findings and should be of impeccable quality.

11.2.1.1 Scapula

Routine views of the scapula include the *AP view* abducting the arm 90° and the lateral view or scapular Y. The axillary view, which requires abduction of the arm, gives an excellent view on the anterior acromion, the glenoid, and the coracoid process. In case of a fractured coracoid process, the patient's pain usually precludes abduction. The fracture may be demonstrated with the so-called modified axillary view (Wallace and Hellier 1983).

11.2.1.2 Clavicle

The Zanca view, an anteroposterior projection with 15° of cephalic angulation, projects the lateral and most of the middle third of the clavicle free of overlying adjacent bones (Zanca 1971). Although not required on a routine basis, visualisation of the medial third of the clavicle is accomplished with 40° cephalic angulation (Rockwood and Wirth 1996).

11.2.1.3 AC-Joint

The best view of the AC-joint is the Zanca view. In case of an AC-trauma it is recommended to obtain an upright view without the patient allowed to support his elbow with the opposite hand, which might reduce any dislocation (Neer and Rockwood 1975). Stress or weighted views may be required after an AC-joint injury to allow more accurate differentiation between type 2 and 3 AC-sprains. An axillary view can be helpful to determine the position of the clavicle with respect to the acromion.

11.2.1.4 SC Joint

Standard radiographic views of the SC joint include posteroanterior and oblique views. However, they are often inadequate due to overlap of the medial clavicle with the sternum, the first rib, and the spine. Special projections have been described to aid in the evaluation. Unless done by an experienced technologist these special views can be technically difficult to perform and interpret, limiting their utility and reproducibility (Brossman et al. 1996).

- The Rockwood projection, also called the 'serendipity view, is an anteroposterior projection obtained with a 40° cephalic tilt, centered on the manubrium. The cassette is placed under the upper part of the shoulders and neck so that the clavicle is projected in the middle of the film. In an anterior dislocation, the affected clavicle is projected superior to the normal clavicle, and with

posterior dislocation it is projected inferior to it (Fig. 11.3) (Rockwood and Wirth 1996). Other special views, such as the Hobbs view and Heinig view (Hobbs 1968; Heinig 1968) are rarely performed today and are currently replaced by multidetector CT.

- Stress maneuver: a reducible or intermittent SC dislocation can look misleadingly normal on a routine radiograph. A stress maneuver helps to avoid this problem. This maneuver is performed by bringing the ipsilateral arm across the chest and pulling against the contralateral elbow (Cope 1993).

Fig. 11.3. Anterior subluxation of the right sternoclavicular joint. Rockwood view showing a slightly more cranial projection of the right clavicle compared to the left (*black arrows*), consistent with an anterior subluxation. An AP view (not shown) revealed no abnormalities

11.2.2 Ultrasound

11.2.2.1 AC Joint

In a trauma setting, US can be used to confirm a grade 1 sprain, or in the assessment of the status of the surrounding musculature. In chronic disease, US allows the evaluation of capsular distension and presence of soft tissue lesions like arthrosynovial cysts.

11.2.2.2 SC Joint

The role of US of the SC joint is limited. It can be used for the assessment of capsular bulging or the position of the joint surfaces in suspected dislocation, the latter if CT is not readily available.

11.2.3 CT

11.2.3.1 Scapula and Clavicle

With its excellent bony detail and its multiplanar and 3D reconstruction capabilities, modern multi-detector CT equipment is the imaging technique of choice in the evaluation of fractures and stress fractures.

11.2.3.2 SC Joint

CT is particularly valuable if an SC joint dislocation is suspected. Advantages are the short procedure time, wide availability, and the quality of 3D-reformating with MDCT in the assessment of the direction and degree of a (sub)luxation and evaluation of fractures. It is recommended to image both sides, as comparison is often helpful in assessing the degree of abnormality. CT can be acquired in a neutral position alone or with the stress maneuver as described in the plain film section, which increases the sensitivity (Burnstein and Pozniak 1990; Cope 1993). If there is strong suspicion of secondary vascular compromise or impingement by a posterior dislocation, the study can be performed with IV contrast to allow optimal visualization of the adjacent vessels.

11.2.4 MRI

11.2.4.1 AC Joint

The role of MRI in isolated AC pathology is not well established. In addition to the findings visible on standard radiographs, soft tissue abnormalities (capsular hypertrophy, joint effusion, CC ligaments, muscular attachments) and subchondral bone marrow edema may be demonstrated. The coronal oblique plane best demonstrates the AC joint. The parasagittal plane roughly corresponds to the radiographic supraspinatus outlet view.

11.2.4.2 SC Joint

MRI is far superior to CT in its ability to define bone marrow abnormalities, disc- and cartilage injury,

joint effusion, and to evaluate the extra-articular soft-tissues (Fig. 11.4). To allow appropriate evaluation of all involved structures, imaging in three orthogonal planes is recommended (Klein et al. 1997; Brossman et al. 1996). There may be difficulty in obtaining good quality MR images of the SC joint: the small joint is poorly imaged with the body coil. In surface coil imaging both the applied coil and the SC joint move with patient breathing, causing severe artifact. Vascular pulsations and swallow also cause artifacts. This difficulty in imaging, combined with most radiologist's limited experience with SC joint imaging, and the availability of CT has prevented the emergence of MRI of the SC joint (Klein et al. 1997).

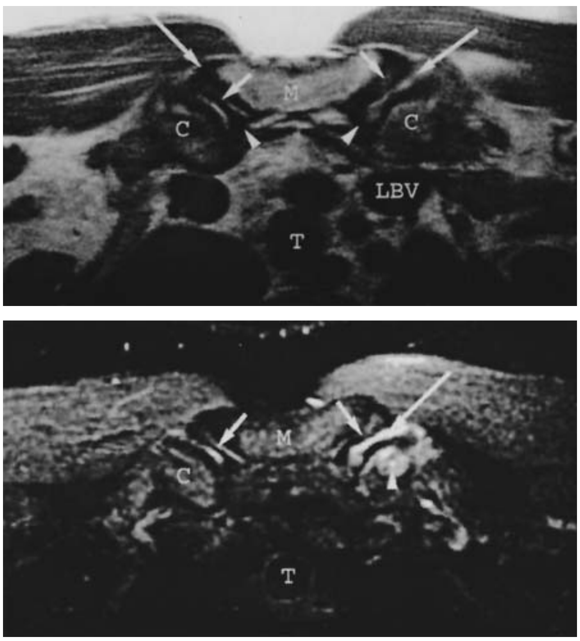

a b

Fig. 11.4a,b. A 19-year-old male. Trauma to the left SC joint resulting in a Salter II fracture of the left clavicular head. **a** Axial MR image (4000/34) shows right normal and left torn: anterior SC ligaments (*long arrows*), articular discs (*short arrows*), and posterior SC ligaments (*arrowheads*). **b** Axial MR STIR image shows left joint effusion (*long arrow*), right normal and left torn discs (*short arrows*), and bone marrow edema within the epiphysis of the left clavicular head (*arrowhead*). *LBV*, left brachiocephalic vein; *C*, clavicle; *T*, trachea; *M*, manubrium. [Reprinted from Benitez et al. (2004) with permission]

11.2.5 Scintigraphy

Bone scintigraphy is a very sensitive technique for detection of early changes related to osseous injuries. In the workup of patients with posttraumatic pain due to sports injuries, which is suspected to be of osseous origin, it is a useful next diagnostic step when plain films are negative. Examples of injury in which bone scintigraphy may be helpful are occult fractures, stress fractures or other stress-related injury, lateral clavicular osteolysis, and symptomatic AC or SC osteoarthritis.

11.3 Specific Overuse Trauma

11.3.1 Scapula

11.3.1.1 Fractures

Scapular fractures are usually the result of a direct blow to the scapular area. Fractures of the scapular body are rare in athletes. Glenoid fractures are associated with glenohumeral dislocations although an avulsion fracture of the infraglenoid tubercle may occur due to forceful contraction of the triceps. Fractures of the acromion most frequently are caused by a direct blow. An avulsion of the anterior acromion may result from deltoid muscle forces. Coracoid process fractures result from direct trauma or avulsion. Avulsion is possible with contraction of the short head of the biceps or the coracobrachialis muscle, or as a result of traction from the coracoclavicular ligament in association with a sprain of the AC joint. The latter may be seen as an apophyseal avulsion in adolescents before closure of the growth plate between 15 and 18 years of age, since the ligament is often stronger than the growth plate (Salter and Harris 1963).

11.3.1.2 Lateral Acromial Apophysitis

Repetitive contraction of muscles attaching on an apophysis can produce microfractures or apophyseal irritation, also called traction apophysitis. When apophyses begin to ossify, they are susceptible to overstress injuries. In throwing movements the deltoid muscle undergoes repeated vigorous contraction. The acromial apophysis is the weakest part in the wide origin of the deltoid muscle and the central

portion, the strongest belly attaches at this region (Morisawa et al. 1996). An apophysitis at the tip of the coracoid process from the pull of the short head of the biceps and the coracobrachialis is also described (Gregg and Torg 1988). Plain radiography typically shows fragmentation, irregularity, and sclerosis of the ossification centre (Fig. 11.5). The process resolves without complication.

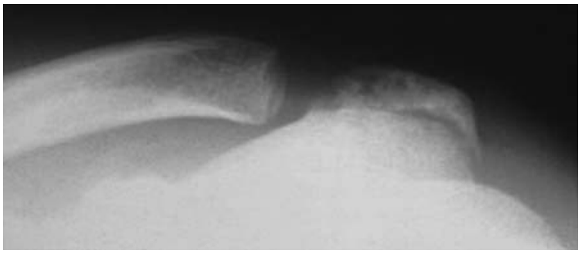

Fig. 11.5. Lateral acromial apophysitis at the left side. AP view showing a mixed lytic-sclerotic, and slightly flattened aspect of the acromial apophysis. [Reprinted from Anderson et al. (1998) with permission]

11.3.1.3 Stress-related Growth Plate Injury of the Coracoid Process

Injuries of the coracoid process physis are rare and commonly associated with AC joint sprain. A chronic, stress-related injury to this physis is described in archery caused by the considerable amount of energy load and shots required in training and tournaments. Plain radiography demonstrated persistence of the growth plate at the base of the coracoid process (Naraen et al. 1999).

11.3.1.4 Stress Fractures

Sports-related stress fractures of the scapula and clavicle are rare. Consequently the index of suspicion for these lesions is low, which may delay diagnosis and appropriate treatment. Low suspicion of a stress fracture in these bones may lead to an erroneous diagnosis of a tumoral or infectious lesion. A detailed occupational history may overcome the problem. These stress fractures can occur either as a result of repetitive loading at the point of muscular attachments to bone or as a result of impact loading (Brukner 1998).

There are isolated reports of scapular stress fractures in a variety of sports:

- American football: two similar cases at the junction of the acromion with the scapular spine. Both occurred in offensive linemen whose training included intensive weight-lifting (Schils et al. 1990; Ward et al. 1994).
- Cricket: in a fast bowler at the lateral border of the scapula, most likely at the origin of the teres minor muscle (De Villiers et al. 2005).
- Golf: at the left side in a right-handed female player at the base of the acromion, extending into the spine, probably induced by contraction of the posterior fibres of the deltoid as the head of the golf club swings forward to strike the ball (Hall and Calvert 1995).
- Jogging with hand-held weights: at the medial site of the supraspinatus fossa due to overuse of the supraspinatus muscle stabilizing the humeral head (Veluvolu et al. 1988).
- Tennis: in a female elite player between the ventral and middle third of the acromion 2 years after adequate subacromial decompression. The lesion most likely occurred due to repetitive vigorous bending stress (Rupp et al. 1998).
- Trapshooting: two reports of probably the same female athlete describe a stress fracture of the coracoid process, resulting from repeated direct trauma by the recoil of the butt of the rifle (Boyer 1975; Sandrock 1975).

Plain radiography continues to be the primary method for diagnosis, but its limitations in the early detection of these injuries are well known. MRI has a comparative sensitivity to bone scan with the additional advantage of depicting the lesion, especially the surrounding bone marrow and soft tissue edema. MDCT is excellent in depicting the presence and extension of the fracture line and callus formation.

11.3.1.5 Suprascapular Nerve Entrapment (SSNE)

The suprascapular nerve is a mixed motor and sensory nerve providing motor supply to the supraspinatus and infraspinatus muscle. Causes of suprascapular nerve injury are anatomical variants of the suprascapular or spinoglenoid notch, compressive mass lesions, which most frequently are paralabral cysts at the level of the spinoglenoid notch (Ticker et al. 1998), direct trauma such as a fracture of the scapula, direct blow to the shoulder, or traction on the nerve through a pull on the upper extremity, and dynamic entrapment.

Dynamic nerve entrapment occurs at the suprascapular or spinoglenoid notch during violent or repeated scapular motion. In athletes this appears more frequently at the spinoglenoid notch, whereas in the general population it occurs mainly at the suprascapular notch (Montagna and Colonna 1993;Ferretti et al. 1998). In the majority of cases sports-related dynamic entrapment occurs in overhead sports such as baseball, tennis, and weightlifting. Most frequently affected by entrapment at the spinoglenoid notch are professional volleyball players. Several mechanisms have been proposed but excessive traction or stretching of the nerve is the most plausible mechanism of trauma.

The diagnosis is based primarily on clinical findings, confirmed by EMG. Imaging studies may demonstrate an etiological diagnosis. US and MRI may identify a paralabral cyst. In addition MRI is able to identify signs of muscular denervation, including edema in an early stage, and fatty infiltration and atrophy in later stages (Ludig et al. 2001). Entrapment at the suprascapular notch will result in denervation of both supra- and infraspinatus muscles, entrapment at the spinoglenoid notch in isolated infraspinatus denervation.

11.3.1.6 Long Thoracic Neuropathy

The long thoracic nerve, the sole innervation to the serratus anterior muscle, courses downward and laterally along the outer surface of the muscle which arises from the first eight to nine ribs and inserts on the costal surface of the scapula along its medial border. It serves to protract the scapula and maintain the medial border of the scapula against the thorax. Isolated paralysis of the serratus anterior is a well-recognized clinical entity accounting for the characteristic scapular winging seen with weakness of this muscle, most pronounced at the inferior margin of the scapula. Many traumatic and nontraumatic causes have been reported. This injury has been reported to occur in almost every sport. However, the most common sport reported to cause the injury is tennis, especially the act of serving. The common theme in sports-related cases is that the injury occurred when the ipsilateral arm was in an outstretched an unusually overhead position, suggesting the nerve was subjected to traction (Gregg et al. 1979). This paralysis is usually apparent on clinical examination and confirmed by EMG. CT and MRI usually are not necessary unless other disease such as cervical disc herniation is suspected.

11.3.2 Clavicle

11.3.2.1 Fractures

Fractures of the clavicle are common. As many as 90% occur as the result of a fall directly on the shoulder, a small number after direct blow, and rarely a fall on an outstretched hand. The middle third is involved in 65%–80%, the lateral in 15%–30%, and the medial in 5%.

11.3.2.2 Lateral Clavicular Osteolysis (LCO)

LCO is an uncommon, self-limiting condition with uncertain pathogenesis characterized by progressive resorption of the lateral end of the clavicle (Cahill 1982; Matthews et al. 1993). Two types are described with the same radiological imaging and pathologic features:

- Posttraumatic: after a single or repeated episodes of local trauma which can be a fracture or AC dislocation. However, usually the trauma is relatively minor. The osteolytic process begins as early as 2–3 weeks and as late as several years after the injury.
- Stress-induced*:* overuse injury caused by repetitive microtrauma, most commonly seen in adult weightlifters (Scavenius and Iversen 1992) and athletes who are engaged in strenuous physical exercise involving use of the upper extremities. It is caused by repetitive compression of the distal clavicle at the AC joint encountered during lifting activities, particularly the bench press (Haupt 2001). A higher incidence of bilateral involvement is noted in this type.

Plain radiographs are not sensitive to the early stage of the disease. Initial findings often are subtle, including osteopenia of the distal clavicle, and loss of the clavicular subarticular cortex (Levine et al. 1976; Kaplan and Resnick 1986). However, early recognition and treatment with immobilisation can shorten the course of the process. The condition progresses into a lytic phase in which cystic areas, irregularity of the articular cortex, periarticular erosions, osteolysis, and soft tissue swelling can be seen. It may be associated with osteopenia and erosion of the acromion (Levine et al. 1976). If untreated this lytic phase may last 12–18 months and osteolysis may progress to include the

distal 0.5–3 cm of the clavicle, resulting in an increased AC joint space (Kaplan and Resnick 1986).

Once the lytic phase has stabilized, reparative changes occur over a period of 4–6 months, resulting in either complete reconstitution or partial reformation with a permanently widened AC joint space (Fig. 11.6) (Kaplan and Resnick 1986).

The role of MRI and its features of LCO are not well documented. Although not very specific, the most constant finding is edema in the distal clavicle (Yu et al. 2000; Patten 1995; De la Puenta et al. 1999). Other frequent findings are clavicular subchondral cortical thinning, subchondral cysts, peri-articular soft tissue swelling and joint space widening.

11.3.2.3 Stress Fractures

Sports-related stress fractures of the clavicle are rare, almost invariably occurring in the medial part of the diaphysis. From a biomechanical point of view, the clavicle may be considered a lever with is axis of rotation close to the sternoclavicular joint. It is pulled down by the pectoralis major muscle, subclavius muscle, and deltoid musculature, counterbalanced by the cranial pull of the sternocleidomastoideus and trapezius muscles. The point of maximum stress is immediately lateral to the strongly anchoring costoclavicular and sternoclavicular attachments (Calvo et al. 1995).

As in the scapula, there are isolated reports of clavicular stress fractures in several sports:

- Baseball: at the medial side in a professional third baseman with high demands on his throwing shoulder (Wu and Chen 1998).
- Gymnastics: in a 10-year-old gymnast through a deep rhomboid fossa, possibly caused by the pull of sternocleidomastoideus and pectoralis major inserting on the medial aspect of the clavicle (Fallon and Fricker 2001).
- Human tower construction: in this traditional Catalan sport the medial clavicle is pushed down

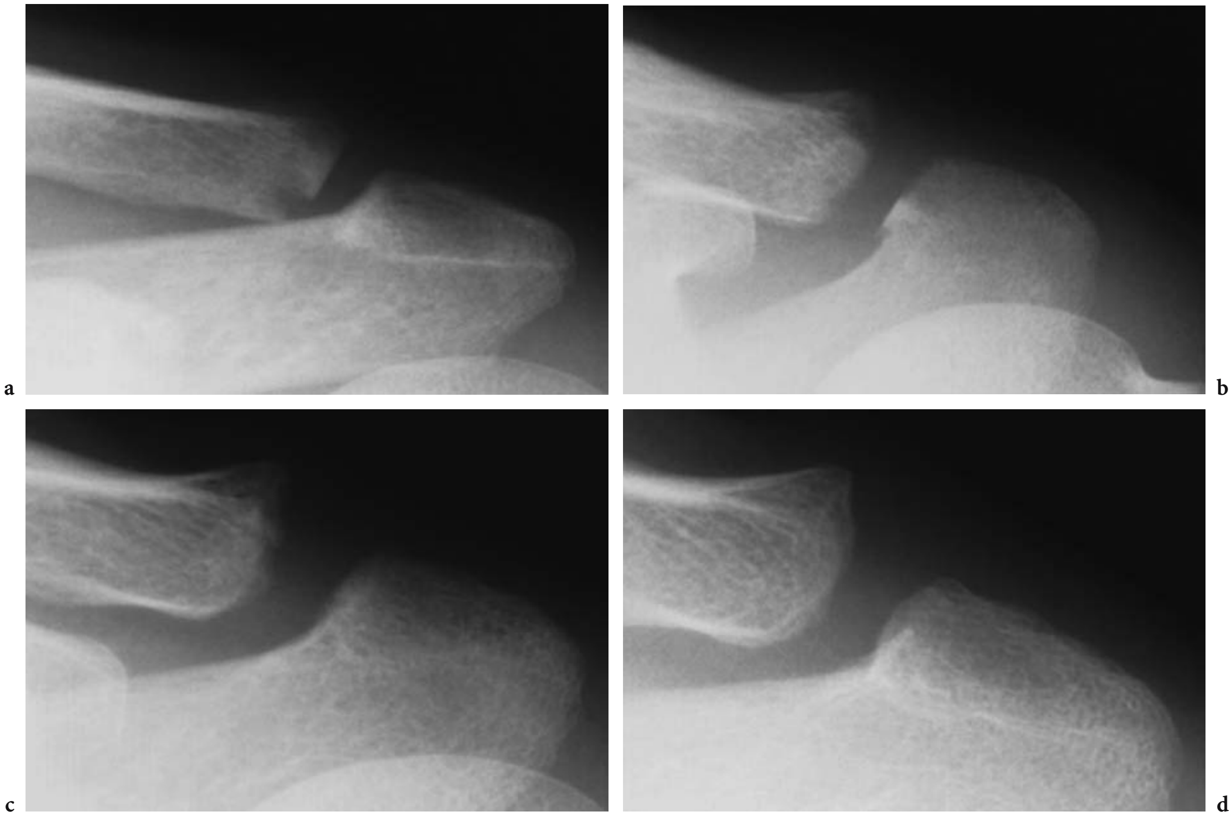

Fig. 11.6a–d. Lateral clavicular osteolysis in a judo athlete. **a** Unsharply marginated subchondral erosion at the inferior margin of the lateral end of the clavicle. Normal width of the AC joint space. **b** At 8 weeks later: widening of the AC joint space with ill-defined resorption of the lateral clavicle, and loss of the subchondral bone plate in the proximal part at the acromial side. **c** At 8 months later: further resorption of the lateral clavicle and increased width of the joint space. The margins are less ill-defined. **d** Control after 15 months: partial reconstitution of the joint space width and now sharply marginated lateral end of the clavicle

by the weight of other athletes while the surrounding muscles are pulled upon (Roset-Llobet and Salo-Orfila 1998).

- Javelin throwing: in an elite athlete, caused by repeated stress from the contraction of the clavicular portion of the deltoid and pectoralis major muscles (Adolfsson and Lysholm 1990).
- Rowing: in a lightweight sculler, occurring at 1 cm lateral to the SC joint, most likely resulting from cyclic scapular protraction and retraction (Abbot and Hannafin 2001).
- Springboard diving: in a male diver, resulting from transmission of stress from his hands to the midportion of the clavicle on entry in the water (Waninger 1997).
- Weightlifting: the only described stress fracture of the lateral clavicle occurred in a female athlete at 1 cm from the AC joint due to structural fatigue (Shellhaas et al. 2004).

11.3.3 AC Joint

11.3.3.1 Sprain/Dislocation

AC sprains are common during athletic activities, most frequently occurring directly by a blow to the acromion (a fall or other contact) with an adducted humerus driving the acromion medially and inferiorly, or indirectly by a fall on the outstretched hand or elbow with a superiorly directed force.

AC-sprains are frequent in contact sports: in American football quarterbacks 40% of all shoulder injuries are AC sprains, resulting from a contact injury while being tackled or during collision with another player or the ground (Kelly et al. 2004) In ice hockey AC sprains, caused by collisions with an opponent or the boards, are the third most common lesions (Flik et al. 2005). In wrestling the most commonly injured area is the shoulder in which 19% are AC joint separations resulting from a direct blow to the shoulder against the mat during the so-called take down (Pasque and Hewett 2000). Other sports with frequent AC sprains are alpine skiing and snowboarding due to falls or collisions with other skiers or trees (Kocher and Feagin 1996), and bicycling in which a common injury pattern involves a lateral clavicle fracture or AC separation from landing on the shoulder when thrown from the bicycle.

Initially injuries to the AC joint were graded I to III as proposed by *TOSSY* according only to the degree of injury to the AC and CC ligaments (Tossy et al. 1963). Rockwood (1984) added three additional types, all subsets of Tossy type III (Fig. 11.7, Table 11.1).

The grading of AC injuries is typically based on plain film analysis:

Table 11.1. Rockwood classification of AC injuries

Type 1	Sprain AC ligaments and intact CC ligament
Type 2	Subluxation with rupture AC ligaments and sprain CC ligament
Type 3	Dislocation with rupture AC ligaments and CC ligament
Type 4	Dislocation with posterior dislocation of the clavicle
Type 5	Dislocation with severe upward displacement of clavicle into the subcutis
Type 6	Dislocation of the clavicle inferiorly, locked under the coracoid process

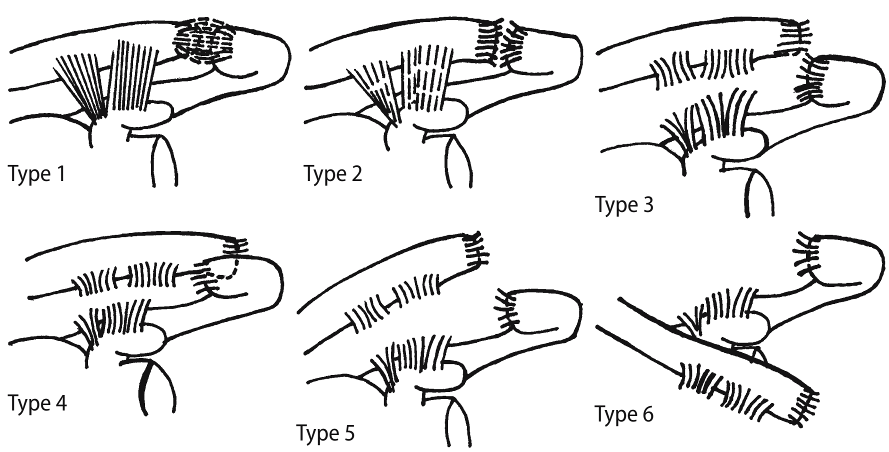

Fig. 11.7. Rockwood classification of acromioclavicular joint injuries

- In type 1 plain films are normal.
- A type 2 is characterised by widening of the joint space and slight upward displacement of the lateral clavicle, less than the width of the acromion. The width of the joint space is pathologic if more than 7 mm in men, more than 6 mm in women, or with a difference of more than 2 mm compared to the uninjured side (Petersson and Redlund-Johnell 1983). The assessment of upward displacement of the clavicle relative to the acromion should be based on the alignment of the inferior margins.
- In type 3 there is an upward dislocation of the clavicle, more than the width of the acromion. Rupture of the CC ligament is very likely if there is a difference of 5 mm or more between the two sides (Neer and Rockwood 1975). The normal coracoclavicular distance is 11–13 mm.
- To disclose the posterior dislocation of the clavicle in type 4, an axillary or modified axillary view may be required.
- A severely upward displaced clavicle, more than 100% of the CC distance, is the hallmark of a type 5 injury.

Since treatment for type 3 injuries is less clear and controversial (Phillips et al. 1998), weighted views are only required when their diagnosis may alter the treatment strategy of the local surgeon.

While in adults dislocation of the AC joint accounts for 12% of all dislocations of the shoulder (Rowe 1968), a true AC dislocation is very rare before the age of 16. Usually the trauma results in a physeal separation of the lateral clavicle. While the clavicular epiphysis remains intact in the periosteal tube, the lateral clavicle shows upward displacement through a tear in the thick periosteal tube, also called a pseudodislocation (Kocher et al. 2000).

The role of ultrasound in AC sprains is not well established. US is sensitive in the detection of type 1 sprains: findings are distension of the joint space, tenderness to sonographic palpation, and stripping of the periosteum from the medial clavicular head. Since treatment for type 3 injuries is less clear and controversial (Phillips et al. 1998), US may be valuable in differentiation between type 3 lesions based on the presence or absence of detachment of muscle insertions, the dynamic joint stabilizers (Heers and Hedtmann 2005). In the same way, MRI might be a valuable tool to decide between conservative and operative treatment based on the associated soft tissue damage.

11.3.3.2 Osteoarthritis (OA)

OA occurs early and frequently because the adult AC joint (ACJ) cannot compensate for the incongruity of the joint surfaces (Petersson 1987). OA is the most common cause of AC-related pain (Shaffer 1999). Causes of OA related to sports activity are AC sprains and chronic repetitive loading. With ruptured AC ligaments, the CC ligament is unable to control adequately anteroposterior translation, or rotation of the distal clavicle (Debski et al. 2001). Chronic repetitive loading is typically seen in overhead athletes, weight lifters, and golf players. In overhead athletes rotation of the distal clavicle, shear forces and high compressive forces from the deltoid, are believed to contribute to AC degeneration (Renfree and Wright 2003). Examples of sports with increased prevalence of OA are swimming, baseball, and handball (Turnbull 1998; JOST et al. 2005). In weightlifting the ACJ becomes a weight-bearing joint with high compressive forces. In golf injuries to the shoulder are mainly restricted to the lead shoulder (left shoulder in right-handed players) and most frequently related to the ACJ (Mallon and Colosimo 1995). Maximal forces about the ACJ in golf are attained at the top of the back swing and at the end of the follow-through, which is repeated several hundred times per day (Bell et al. 1993; Mallon and Colosimo 1995).

On routine radiography the ACJ is not loaded in compression. Consequently, the joint space does not depict the thickness of the cartilage. A loaded view, obtained by forced adduction of the humerus by pulling the elbow with the opposite hand, may demonstrate an additional 27% of OA (Stenlund et al. 1992). However, the role of this view is not well-established. Since OA may also be present on plain films in patients without symptoms (Zanca 1971; Bonsell et al. 2000), the prevalence of OA on MRIs of asymptomatic subjects has been reported to be as high as 48% and 82% (Needell et al. 1996; Shubin Stein 2001 et al.), and no real correlation was found between MRI and clinical findings in the ACJ (Jordan et al. 2002), imaging findings should always be correlated with symptoms.

11.3.4 SC Joint

11.3.4.1 Sprain/Dislocation

No more than 2%–3% of all dislocations involving the pectoral girdle occur at the SC joint. SC dislocations are classified as either anterior or posterior, the anterior one being far more common. In nearly 150 traumatic SC dislocations a sports-related injury accounted for 21% (Wirth and Rockwood 1996). Two types of injury may result in a SC dislocation: The most common is an indirect blow to the shoulder, which may be seen in contact athletes.

Subsequently the clavicle acts as a lever through the fulcrum of the costoclavicular ligament (Rogers 1983). An anterolateral blow results in anterior, a posterolateral blow in posterior dislocation (Fig. 11.8). Contact sports (especially martial arts, American football, and rugby) and motorcycle injuries are the commonest causes of posterior dislocation. Typically a blow to the posterolateral aspect of the shoulder with the arm adducted and flexed occurs during a piling-on injury in American football when a player holds the ball and tries to avoid his opponents (Wirth and Rockwood 1996). In American football quarterbacks, the frequency of SC sprain was reported as 3.4% (Kelly et al. 2004). A posterior dislocation may also result from a direct blow to the anterior medial portion of the clavicle. Typical situations are an athlete getting the knee of an opponent or a kick directly to the front of the medial clavicle.

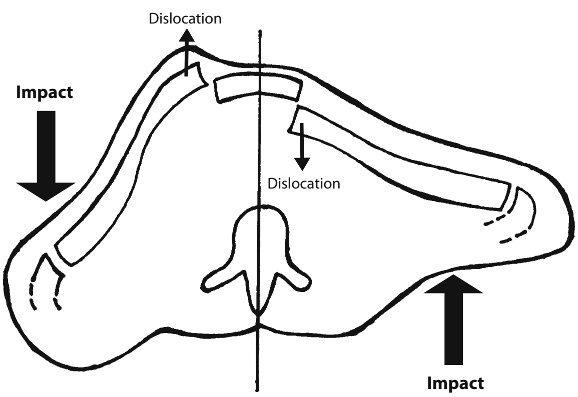

Fig. 11.8. Mechanism of sternoclavicular dislocations caused by an indirect blow to the shoulder. *Right*: anterolateral blow resulting in an anterior sternoclavicular dislocation. *Left*: posterolateral blow resulting in a posterior sternoclavicular dislocation

Approximately *25%* of posterior dislocations are associated with some form of complication as the medial clavicle can impinge on vital mediastinal structures (Neer and Rockwood 1975). They consist of pneumothorax, laceration of the superior vena cava, compression of the venous structures of the neck, compression or rupture of the trachea, rupture of the esophagus, occlusion or compression of the subclavian or carotid artery, and changes in voice caused by compression of the recurrent laryngeal nerve. A high index of suspicion is required to determine the presence of these serious complications, which may manifest insidiously.

In patients younger than 25 years all SCJ dislocations consist primarily of physeal separations, mimicking SC dislocations (Wirth and Rockwood 1996). The epiphysis stays attached to the sternum via the sternoclavicular ligaments and the medial clavicular shaft displaces anteriorly or posteriorly. Although rare, true posterior dislocations in children exist and warrant surgical reduction.

Injuries to the SC joint are graded I to III according to Allmann (1967) (Table 11.2).

Table 11.2. Allmann classification of SC injuries

Type 1	Mild sprain with intact ligaments and a stable joint
Type 2	Moderate sprain with subluxation and possible partial rupture of the ligaments
Type 3	Dislocation with complete disruption of the supporting ligaments

Dislocations of the SC joint are notoriously difficult to characterize on plain radiography. The diagnosis is usually evident on CT scan, and one should directly proceed to CT instead of focusing on special plain film projections (Fig. 11.9). US can be used to make the diagnosis if CT is not readily available. On MRI of 41 patients imaged with complaints related to a SC trauma, the most common sites of SC joint soft tissue injury were the articular disc (80%), the anterior SC ligament (73%), and the posterior SC ligament (39%). Injuries to the interclavicular and costoclavicular ligaments were rare (Benitez et al. 2004).

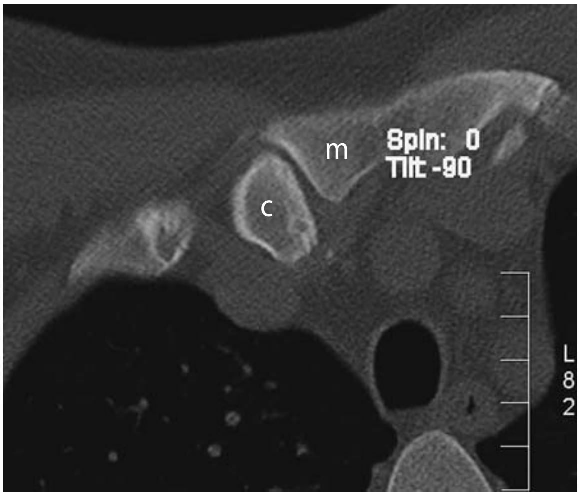

Fig. 11.9. Posterior subluxation of the right sternoclavicular joint. Axial CT slice showing a step-off at the level of the right sternoclavicular joint with asymmetrical width of the joint space and slight posterior displacement of the medial end of the clavicle (*c*) relative to the sternal manubrium (*m*)

Things to Remember

1. In sports lesions plain films tailored to the clinical findings and of impeccable quality will significantly increase diagnostic performance.
2. Because of their low prevalence and low index of suspicion, sports-related stress fractures of the scapula and clavicle may be mistaken for a tumoral or infectious lesion unless a detailed occupational history is taken.
3. In sports-related AC joint or posterior shoulder pain, radiologists respectively should also consider a possible lateral clavicular osteolysis or a suprascapular nerve entrapment syndrome.
4. In sternoclavicular joint dislocation one should immediately proceed to CT instead of focusing on special plain film projections.
5. Complications of a posterior sternoclavicular dislocation may be serious and eventually life threatening.

References

Abbot AE, Hannafin JA (2001) Stress fracture of the clavicle in a female lightweight rower. Am J Sports Med 29:370–372

Adolfsson L, Lysholm J (1990) Case report: clavicular stress fracture in a javelin thrower. Clin Sports Med 2:41–45

Allmann FI (1967) Fractures and ligamentous injuries of the clavicle and its articulations. J Bone Joint Surg Am 49:774–784

Anderson J, Read JW, Steinweg J (eds) (1998) Atlas of imaging in sports medicine. McGraw-Hill Book Company, Australia, p 125

Bell R, Acus R, Noe D (1993) A study of acromioclavicular joint forces (abstract). J Shoulder Elbow Surg 2(suppl 1–2):S24

Benitez CL, Mintz DN, Potter HG (2004) Magnetic resonance imaging of the sternoclavicular joint following trauma. J Clin Imaging 28:59–63

Bonsell S, Persall AW, Heitman RJ et al. (2000) The relationship of age, gender, and degenerative changes observed on radiographs of the shoulder in asymptomatic individuals. J Bone Joint Surg Br 82:1135–1139

Boyer D Jr (1975) Trapshooter's shoulder: stress fracture of the coracoid process. J Bone Joint Surg Am 57:862

Brossmann J, Stabler A, Preidler KW et al. (1996) Sternoclavicular joint; MR imaging-anatomic correlation. Radiology 198:193–198

Brukner P (1998) Stress fractures of the upper limb. Sports Med 26:415–424

Burnstein MI, Pozniak MA (1990) Computed tomography with stress maneuver to demonstrate sternoclavicular joint dislocation. J Comput Assist Tomogr 14(1):159–160

Cahill B (1982) Osteolysis of the distal part of the clavicle in male athletes. J Bone Joint Surg Am 64A:1053–1058

Calvo E, Fernandez-Yruegas D, Alvarez L et al. (1995) Bilateral stress fracture of the clavicle. Skeletal Radiol 24:613–616

Cope R (1993) Dislocations of the sternoclavicular joint. Skeletal Radiol 22:233–238

De la Puente R, Boutin R, Theodorou D et al. (1999) Post-traumatic and stress-induced osteolysis of the distal clavicle: MR findings in 17 patients. Skeletal Radiol 28:202–208

de Villiers R, Pritchard M, de Beer J et al. (2005) Scapular stress fracture in a professional cricketer and a review of the literature. S Afr Med J 95(5):312–317

Debski RE, Parsons IM, Woo SL-Y et al. (2001) Effects of capsular injury on the acromioclavicular joint mechanics. J Bone Joint Surg Am 83:1344–1351

Fallon KE, Fricker PA (2001) Stress fracture of the clavicle in a young female gymnast. Br J Sports Med 35:448–449

Ferretti A, de Carli A, Fontana M (1998) Injury of the suprascapular nerve at the spinoglenoid notch. The natural history of infraspinatus atrophy in volleyball players. Am J Sports Med 26:759–763

Flik K, Lyman S, Marx RG (2005) American collegiate men's ice hockey. An analysis of injuries. Am J Sports Med 33(2):183–187

Gregg J, Torg E (1988) Upper extremity injuries in adolescent tennis players. Clin Sports Med 7:371–385

Gregg JR, Labosky D, Harty M et al. (1979) Serratus anterior paralysis in the young athlete. J Bone Joint Surg Am 61:825–832

Hall R, Calvert P (1995) Stress fracture of the acromion: an unusual mechanism and review of the literature. J Bone Joint Surg Br 77:153–154

Haupt HA (2001) Upper extremity injuries associated with strength training. Clin Sports Med 20:481–490
Heers G, Hedtmann A (2005) Correlation of ultrasonographic findings to Tossy's and Rockwood's classification of acromioclavicular joint injuries. Ultrasound Med Biol 31(6):725–732
Heinig CF (1968) Retrosternal dislocation of the clavicle. Early recognition, X-ray diagnosis, and management. J Bone Joint Surg Am 50:830
Hobbs DW (1968) Sternoclavicular joint: a new axial radiographic view. Radiology 90:801
Jordan LK, Kenter K, Griffiths HL (2002) Relationship between MRI and clinical findings in the acromioclavicular joint. Skeletal Radiol 31:516–521
Jost B, Zumstein M, Pfirmann C et al. (2005) MRI findings in throwing shoulders. Abnormalities in professional handball players. Clin Orthop Rel Res 434:130–137
Kaplan P, Resnick D (1986) Stress-induced osteolysis of the clavicle. Radiology 158:139–140
Kelly BT, Barnes RP, Powelle JW et al. (2004) Shoulder injuries to quarterbacks in the National Football League. Am J Sports Med 32(2):328–331
Klein MA, Spreitzer AM, Miro PA et al. (1997) MR imaging of the abnormal sternoclavicular joint – a pictorial essay. Clin Imaging 21:138–143
Kocher MS, Feagin JA (1996) Shoulder injuries during alpine skiing. Am J Sports Med 24(5) 665–669
Kocher MS, Waters PM, Micheli LJ (2000) Upper extremity injuries in the paediatric athlete. Sports Med 30(2):117–135
Levine AH, Pais MJ, Schwartz EE (1976) Posttraumatic osteolysis of the distal clavicle with emphasis on early radiologic changes. Am J Roentgenol 127:781–784
Lucas DB (1973) Biomechanics of the shoulder joint. Arch Surg 107:425–432
Ludig T, Walter F, Chapuis D et al. (2001) MR imaging evaluation of suprascapular nerve entrapment. Eur Radiol 11:2161–2169
Mallon WJ, Colosimo AJ (1995) Acromioclavicular joint injury in competitive golfers. J South Orthop Assoc 4(4):277–282
Matthews LS, Simonson BG, Wolock BS (1993) Osteolysis in the distal clavicle in a female body builder. Am J Sports Med 21:150–152
Montagna P, Colonna S (1993) Suprascapular neuropathy restricted to the infraspinatus muscle in volleyball players. Acta Neurol Scand 87:248–250
Morisawa K, Umemura A, Kitamura T et al. (1996) Apophysitis of the acromion. J Shoulder Elbow Surg 5:153–156
Naraen A, Giannikas K, Livesley P (1999) Overuse epiphyseal injury of the coracoid process as a result of archery. Int J Sports Med 20:53–55
Needell SD, Zlatkin MB, Sher JS et al. (1996) MR imaging of the rotator cuff: peritendinous and bone abnormalities in an asymptomatic population. Am J Roentgenol 166:863–867
Neer CS, Rockwood CA Jr (1975) Fractures and dislocations of the shoulder. In: Rockwood CA Jr, Green DP (eds) Fractures. Lippincott Co, Philadelphia, p 585
Pasque CB, Hewett TE (2000) A prospective study of high school wrestling injuries. Am J Sports Med 28(4):509–515
Patten RM (1995) Atraumatic osteolysis of the distal clavicle: MR findings. J Comput Assist Tomogr 19:92–95
Petersson CJ (1987) The acromioclavicular joint in rheumatoid arthritis. Clin Orthop 223:86–93
Petersson CJ, Redlund-Johnell I (1983) Radiographic joint space in normal acromioclavicular joints. Acta Orthop Scand 54:431–433
Phillips AM, Smart C, Gromm AFG (1998) Acromioclavicular dislocation. Conservative or operative therapy. Clin Orthop 353:10–17
Renfree KJ, Wright TW (2003) Anatomy and biomechanics of the acromioclavicular and sternoclavicular joints. Clin Sports Med 22:219–238
Rockwood CA Jr (1984) Subluxations and dislocations about the shoulder. In: Rockwood CA Jr (ed) Fractures in adults. J.B. Lippincott, Philadelphia, p 722
Rockwood CA Jr, Wirth MA (1996) Injuries to the sternoclavicular joint. In: Rockwood CA Jr, Green DP, Bucholz RW et al. (eds) Rockwood and Green's Fractures in adults. Lippincott-Raven, Philadelphia, pp 1415–1471
Rogers LF (1983) The radiology of sports injuries. Curr Probl Diagn Radiol 12:1
Roset-Llobet J, Salo-Orfila JM (1998) Sports-related stress fracture of the clavicle: a case report. Int Orthop 22:266–268
Rowe CR (1968) An atlas of anatomy and treatment of midclavicular fractures. Clin Orthop Relat Res 58:29–42
Rupp S, Seil R, Kohn D (1998) Surgical reconstruction of a stress fracture of the acromion after arthroscopic subacromial decompression in an elite tennis player. Arthroscopy 14:106–108
Salter RB, Harris WR (1963) Injuries involving the epiphyseal plate. J Bone Joint Surg Am 45:587–622
Sandrock A (1975) Another sports fatigue fracture. Stress fracture of the coracoid process of the scapula. Radiology 117:274
Scavenius M, Iversen BF (1992) Nontraumatic clavicular osteolysis in weight lifters. Am J Sports Med 20:463–467
Schils JP, Freed HA, Richmond BJ et al. (1990) Stress fracture of the acromion. Am J Roentgenol 155(5):1140–1141
Shaffer BS (1999) Painful conditions of the acromioclavicular joint. J Am Acad Orthop Surg 7:176–188
Shellhaas JS, Glaser DL, Drezner JA (2004) Distal clavicular stress fracture in a female weight lifter. Am J Sports Med 32(7):1755–1758
Shubin Stein BE, Wiater M, Pfaff C et al. (2001) Detection of acromioclavicular joint pathology in asymptomatic shoulders with magnetic resonance imaging. J Shoulder Elbow Surg 10(3):204–208
Stenlund B, Goldie I, Marions O (1992) Diminished space in the acromioclavicular joint in forced arm adduction as a radiographic sign of degeneration and osteoarthrosis. Skeletal Radiol 21:529–533
Ticker JB, Djurasovic M, Strauch RJ et al. (1998) The incidence of ganglion cysts and other variations in anatomy along the course of the suprascapular nerve. J. Shoulder Elbow Surg 7:472–478
Tossy JD, Mead NC, Sigmond HM (1963) Acromioclavicular separations: useful and practical classification for treatment. Clin Orthop 28:111–119
Turnbull JR (1998) Acromioclavicular joint disorders. Med Sci Sports Exerc 30(4):S26–32
Veluvolu P, Kohn HS, Guten GN et al. (1988) Unusual stress fracture of the scapula in a jogger. Clin Nucl Med 13(7):531–532
Wallace WA, Hellier M (1983) Improving radiographs of the injured shoulder. Radiography 49:229–233
Waninger KN (1997) Stress fracture of the clavicle in a collegiate diver. Clin J Sport Med 7:66–68

Ward WG, Bergfeld JA, Carson WG (1994) Stress fracture of the base of the acromial process. Am J Sports Med 22(1):146–147

Wickiewicz TL (1983) Acromioclavicular and sternoclavicular joint injuries. Clin Sports Med 2(2):429–438

Wirth MA, Rockwood CA Jr (1996) Acute and chronic traumatic injuries of the sternoclavicular joint. J Am Acad Orthop Surg 4:268–278

Wu CD, Chen YC (1998) Stress fracture of the clavicle in a professional baseball player. J Shoulder Elbow Surg 7:164–167

Wulker N (1998) Applied biomechanics. In: Fu FH, Ticker JB, Imhoff AB (eds) Atlas of shoulder surgery. Appleton and Lange, Stanford (CT), pp 30–52

Yu JS, Dardani M, RA Fischer (2000) MR observations of post-traumatic osteolysis of the distal clavicle after traumatic separation of the acromioclavicular joint. J Comp Assist Tomogr 24(1):159–164

Zanca P (1971) Shoulder pain: involvement of the acromioclavicular joint – analysis of 1000 cases. Am J Roentgenol 112:493–506

Imaging of Sports Injuries of the Elbow

12

Milko C. de Jonge and Mario Maas

CONTENTS

12.1 Introduction

Elbow injuries in athletes are relatively uncommon. Particularly, acute traumatic elbow injuries, resulting in fractures, dislocations or musculotendineous structures are rarely seen (Gerbino 2003) (Fig. 12.1). They are summarized in Table 12.1. Most injuries and complaints of pain can be attributed to chronic overuse injuries. Sports activities that are prone to elbow injuries involve those with extensive use of the arm in throwing (e.g., baseball pitching, javelin), those in which the arm is used as a lever with swinging and/or hitting (e.g., golf, tennis, racquetball) and those in which the arm is turned into a weight bearing joint

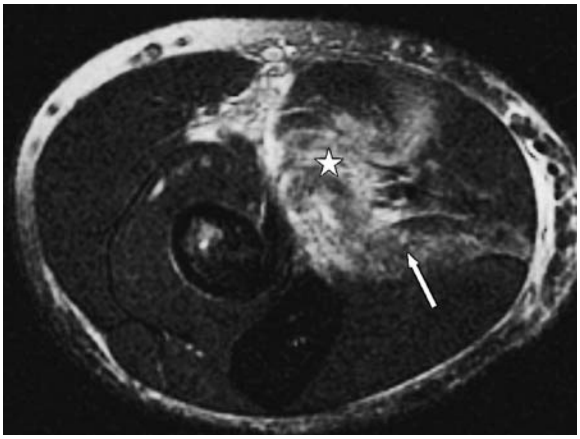

Fig. 12.1. A 23-year-old female gymnast sustained a fall on the left elbow while training on the balance beam. Axial T2-WI FS image of the left elbow at the level of the tuberositas radii. Extensive muscle edema and partial rupture of the pronator teres muscle (*asterisk*), muscle edema in the superficial flexor digitorum muscle (*arrow*) and extensive fluid in the fascial planes and subcutaneously

M. C. de Jonge, MD
M. Maas MD, PhD
Dept. of Radiology, Academic Medical Centre, PO Box 22660, Suite G1-210, 1105 AZ Amsterdam, The Netherlands

Box 12.1. Standard radiography

- Initial survey, especially in acute injuries
- Evaluation of osseous structures, avulsion injuries and calcifications
- Cheap and fast
- AP and Lateral views will usually suffice
- Reversed axial projection and stress views can be helpful

Box 12.2. Ultrasound

- Evaluation of soft tissues
- Higher sensitivity for avulsions and calcifications compared to MRI
- Very high spatial resolution compared to MRI
- Available and cheap
- Detection of loose intra-articular bodies best with joint effusion

Box 12.3. MRI

- Evaluation of soft tissues and osseous structures
- Superior contrast resolution compared to US
- Low sensitivity for small avulsions and calcifications
- Difficult especially in painful lesions
- Low sensitivity for intra-articular loose bodies in absence of joint effusion

Box 12.4. CT

- Evaluation of predominantly osseous structures
- High sensitivity for avulsions, calcifications and intra-articular loose bodies
- Available and short examination time
- High radiation dose
- Often complementary to MRI

Table 12.1. Classic traumatologic injuries of the elbow

Adult	Child/adolescent
Fracture/dislocation	**Fracture/dislocation**

- Radial head/neck fracture
- Olecranon fracture
- Elbow dislocation
  - Posterior
  - Anterior (less common)
- Supracondylar humerus Fracture
- Coronoid process fracture
- Epicondyle fracture (rare)
- Galleazzi/Monteggia Fracture-dislocation (rare)
	- Radial head dislocation (‚pulled elbow‘)
	- Supracondylar humerus fracture
	- Elbow dislocation
	  - Posterior
	  - Anterior (rare)
	- Epicondyle fracture
	- Galleazzi/Monteggia fracture-dislocation
	- Radial head and olecranon fractures (rare)

Soft tissue injury	**Soft tissue injury**
- Distal biceps tendon rupture - Triceps tendon rupture	Rare

(e.g., gymnastics, weightlifting). In addition sports activities in which the arm is used to block goal fired shots are prone to elbow injuries (e.g., goalkeepers in handball and soccer).

There are several factors that contribute to injuries of the elbow in sports activities. They can basically be divided into intrinsic and extrinsic factors (Wilder and Sethi 2004; Gissane et al. 2001). Intrinsic factors are athlete related, such as joint stability, muscle strength, skeletal maturity and history of previous injuries. Extrinsic factors are sports related such as biomechanics of the game, equipment used, training hours and coaching. Particularly game biomechanics seems to be the most important extrinsic factor. In overhead throwing athletes the amount of valgus stress at the elbow is significant even in adequately trained, non-injured, professional athletes with proper throwing techniques (Fleisig et al. 1995; Loftice et al. 2004; Werner et al. 2002). These forces are inherent to the movements the arm makes to accelerate balls. Knowledge of specific game dynamics is a prerequisite for a thorough understanding of specific sports related elbow lesions.

This chapter aims to give an overview of the dynamics of the most frequent sports related injuries of the elbow (Table 12.2). The merits of the different imaging modalities (standard radiography, ultrasound, computed tomography and magnetic resonance imaging) in the diagnostic algorithm will be emphasized and are summarized in Boxes 12.1–12.4.

Table 12.2. Common injuries in selected sports

Sport	Injury	Common name
Baseball	Ulnar collateral ligament	„Pitchers elbow“
Baseball - child/adolescent	Medial epicondyle apophysitis	„Little League elbow“
Tennis	Lateral epicondylitis	„Tennis elbow“
Golf	Medial Epicondylitis	„Golfers elbow“
Handball and soccer	Intra-articular loose bodies	„Goalkeepers elbow“
Gymnastics	Osteochondral lesions	-

12.2 Anatomy

The elbow has a central position in the shoulder-hand kinetic chain. It consists of three articulations joined in a common synovial compartment known as the humero-ulnar, the capitello-radial and the (proximal) radio-ulnar joint. To allow a combination of flexion-extension (humero-ulnar), pro- supination (radio-ulnar) and stability of the elbow joint, a specific congruent design of the humero-ulnar articular surfaces is needed. A triangular shaped fortification of the medial capsular structures is the medial or ulnar collateral ligament (UCL), the origin or top of the triangle is located at the medial epicondyle and the broad base is located at the ulna (anterior to the processus coronoideus and posterior to the olecranon). On the lateral side a capsular fortification arises from the lateral epicondyle and forms the radial ligamentous complex (RLC) (Alcid et al. 2004; Kijowski et al. 2004). The UCL consists of three separate structures, the anterior bundle, the posterior bundle and the transverse bundle (Fig. 12.2). The anterior bundle is the most important valgus stress stabilizer of the elbow joint, and can be further divided into anterior and posterior bands that alternate in tautness in extended and flexed position, respectively. Since the transverse bundle does not cross the elbow joint itself it does not contribute much to the stability (Alcid et al. 2004; Chung and Kim 2003; Kijowski et al. 2004; Thornton et al. 2003). The RLC is composed of four different ligaments and protects the elbow against varus stress and posterolateral instability. It is much less prone to injury than the UCL (Alcid et al. 2004; Chung and Kim 2003; Kijowski et al. 2004; Thornton et al. 2003). The most important osseous landmarks are the medial and lateral epicondyle of the humerus, the olecranon, the coronoid process of the ulna anterior and the radial head. The most important musculotendinous structures are, arising from the lateral epicondyle, the common extensor tendon including the lower arm, hand and wrist extensors, and the common flexor tendon or pronator-flexor complex which arises from the medial epicondyle (Alcid et al. 2004). The ulnar nerve, which is the most often compromised nerve around the elbow in athletes, runs in a fibro-osseous groove at the medial humeral epicondyle, close to the origin of the UCL (Fig. 12.10).

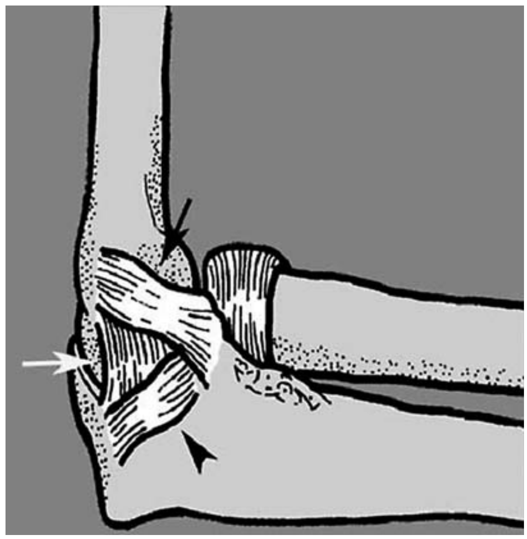

Fig. 12.2. Normal anatomy of the ulnar collateral ligament. It consists of three separate bundles: the anterior bundle (*black arrow*), the posterior bundle (*white arrow*) and the transverse bundle (*arrowhead*). Reprinted with permission from Kijowski et al. (2004)

12.3 Biomechanics

12.3.1 Introduction

Biomechanically the elbow joint acts as a combination of a hinge joint (ulno-humeral and radio-humeral) and a more pivot joint (radio-humeral and proximal radio-ulnar) allowing not only flexion-extension but also pronation-supination movements. The main stability of the elbow results from the highly congruent ulno-humeral joint surfaces and the collateral ligaments, preventing hyperextension and hyperflexion, and varus and valgus, respectively (Alcid et al. 2004; Loftice et al. 2004).

12.3.2 Baseball (and Other Overhead Throwing Sports)

In baseball, elbow injuries most commonly originate due to pitching, hence the term "pitcher's elbow" which actually most often refers to an injury of the UCL. The pitch, a very complicated movement, is commonly divided into six phases: windup, stride, cocking, acceleration, deceleration and follow through (Alcid et al. 2004; Fleisig et al. 1995; Loftice et al. 2004; Werner et al. 1993, 2002). These different phases are well described in the literature and apply more or less to other overhead throwing athletes. Essentially, the elbow moves during these phases from a flexed to an extended position, The greatest forces occur during the cocking and acceleration phases when maximum valgus and extension forces are applied to the UCL that acts as the primary valgus stabilizer (Loftice et al. 2004; Werner et al. 1993; Chen et al. 2001). This can result in acute and chronic injuries of the UCL and/or the pronator-flexor complex that acts as the secondary medial stabilizing structure (Alcid et al. 2004; Cain et al. 2003; Chen et al. 2001). The stability of the osteochondral structure itself, more specifically the olecranon in the fossa olecrani and the radio-capitellar joint, increases when the elbow moves towards extension leading to torque forces and shearing of the olecranon in its fossa and to posterior osteophyte formation resulting in what is called "valgus extension overload syndrome" (VEO) (Ahmad and ElAttrache 2004). The compressive forces that are generated in the lateral elbow can lead to cartilage damage or bone lesions of the radial head and/or capitellum (e.g., osteochondral lesions) (Bojanic et al. 2005; Cain et al. 2003; Gerbino 2003; Loftice et al. 2004; Kijowski et al. 2004).

The term '"little league elbow" usually refers to athletic injuries in the immature skeleton, probably due to improper throwing techniques. Originally described as a medial epicondyle fracture (Brogdon and Crow 1960), the term is actually reserved to describe medial epicondyle traction apophysitis or medial apophyseal avulsion.

Although javelin and American football involve overhead throwing similar to the baseball pitch, injuries to the elbow are much less frequent. It is suggested that in football this is probably due to lower forces and less torque in the elbow during the throw (Loftice et al. 2004). Although several studies have been published on the specific biomechanics of the throw in javelin (which also involves powerful flexion from maximal extended position) (Bartlett and Rent 1988; Morris and Bartlett 1996), there is lack of large studies on elbow injuries in this sports discipline.

12.3.3 Tennis

"Tennis elbow" or lateral epicondylitis is associated with excessive overuse of the hand and wrist extensor muscles (Loftice et al. 2004; Roetert et al. 1995). The tendon most commonly involved is the extensor carpi radialis brevis (ECRB) (Levin et al. 2005; Miller et al. 2002; Roetert et al. 1995). Injuries seem to be predominantly associated with improper backhand use, leading to excessive forces at the level of the common extensor origin. Despite the fact that studies have shown that in all major strokes at tennis the wrist extensors are highly involved, only improper backhand use is predominantly associated with tendinosis and paratenonitis of the origin of the ECRB (Loftice et al. 2004; Roetert et al. 1995). Other factors that have been incriminated consist of improper hand/wrist positioning (over-pronation and hyperflexion), eccentric location of impact of the ball on the racket and the amount of force impact/transfer from the ball to the racket (Roetert et al. 1995).

12.3.4 Golf

For a non-throwing sport, golf places enormous strains on the different components of the kinetic shoulder-elbow-wrist chain. An injury to the elbow in golfers is

almost always swing related or due to improper technique. Whereas the backswing is relatively harmless for the elbow, it is the downswing and impact which causes the problems (Loftice et al. 2004; McCarrol 2001). The medial epicondylitis or so called "golfer's elbow", is an overuse injury of the common pronator-flexor origin and occurs typically in the elbow of the dominant arm (the right arm in a right-handed golf player). Not only improper technique contributes biomechanically but also abrupt trauma when the player hits the ground in front of or behind the ball. It is the violent deceleration on impact that strains the medial compartment, and that raises forceful contractions at the medial and lateral lower arm musculature to stabilize the elbow and the club that lead to the condition (McCarrol 2001; Thériault and Lachance 1998). Therefore, lateral epicondylitis is also a common problem at the non-dominant arm or lead arm in golf players (Loftice et al. 2004; McCarrol 1996; McCarrol 2001; Thériault and Lachance 1998). Forceful overuse of the common extensor muscles leading to lateral epicondylitis is more frequent when the grip of the golf club is too tight. The frequency of medial and lateral injuries is more or less equal in golf players (McCarrol 1996).

12.3.5 Handball and Soccer (European Football)

Although biomechanically there is a great difference between handball and soccer players, with regards to elbow injuries the goalkeeper's in both sports share a common injury pattern of the elbow, which is called the "goalkeeper's elbow". Two mechanisms are involved: the first is the injury pattern as seen in many overhead throwing athletes. Therefore, similar elbow lesions as in overhead throwing athletes are found (Popovic and Lemaire 2002; Popovic et al. 2001). The second (which is more typical for goalkeepers) is repeated hyperextension of the elbow due to the blockage of shots fired at the goal. This hyperextension trauma leads to repetitive abutment of the olecranon in its fossa leading to cartilage damage, osteophyte formation and intra-articular loose bodies.

12.3.6 Gymnastics

Participants in gymnastics are traditionally and increasingly younger in age. This puts them at a particular risk for injuries to the growing skeleton which are different compared to injury patterns encountered in adults. Osteochondral lesions are frequently seen in gymnasts, because they use their elbow as a weight bearing joint (Bojanic et al. 2005; Jackson et al. 1989). It is predominantly an overuse injury caused by repetitive microtrauma to the immature cartilage. A similar pattern is seen in weightlifters.

12.4 Imaging the Elbow

12.4.1 Introduction

In the authors opinion, standard radiography should be the first imaging modality of choice. Apart from a so-called reversed axial projection which allows better visualisation of the olecranon and the trochlea (Fig. 12.3), additional views in many different directions are usually not helpful. The value of stress radiographs is discussed elsewhere.

Ultrasound is a fast and cheap way to evaluate the elbow. To study the anterior recess the arm is partially flexed and supinated while the posterior recess is best evaluated in elbow extension. Lateral and medial visualisation is optimal in extension or 90° flexion semi-pronated or a slightly flexed elbow exorotated, respectively. The posterior elbow soft tissues are most easily examined in flexion with the palm of the hand flat on the table (fingers directed towards patient) (Ferrara and Marcelis 1997).

In MRI the positioning of the elbow is considered to be one of the most important factors which can be either fully supinated and extended (besides supine body) or in an overhead pronated and extended position (body prone) ('Superman's position') in which case the elbow is more in the center of the magnet which improves image quality. All imaging planes can be useful but one has to make sure that the coronal plane is parallel to the middle of both humeral condyles (Fig. 12.4), although a coronal oblique plane is also proposed, especially for the collateral ligaments (Cotten et al. 1997). The role of MR arthrography is controversial, but there is no evidence that routinely MR-arthrography is more accurate than conventional MRI.

Helical High Resolution CT (HRCT) with 0.6 or 0.5 mm slice thickness can have its advantages over

Fig. 12.3. Reversed axial projection of the right elbow allows better visualization of the posterior elbow, in particular the olecranon and the posterior part of the humero-ulnar joint

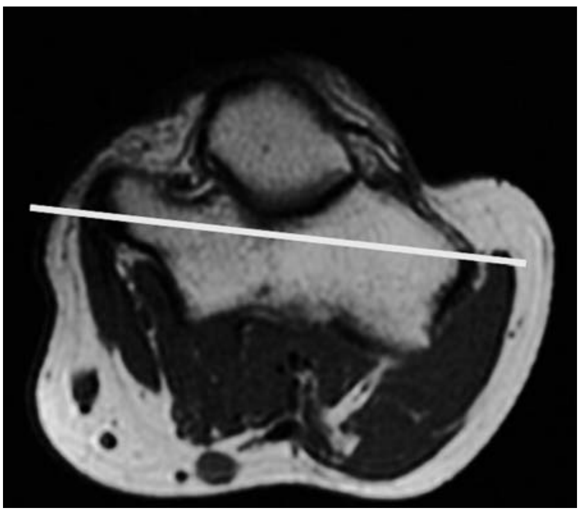

Fig. 12.4. Coronal MRI (or CT MPR) plane is planned on an axial image and runs parallel to the condyles of the distal humerus

MRI due to the superior spatial resolution in which the osseous structures are visualized. Examining the elbow with HRCT takes a considerable shorter time compared to a MRI investigation which can be of significant importance in a painful patient.

The role of bone scintigraphy is declining since the introduction of MRI. It is not the high sensitivity of scintigraphy for bony abnormalities but the low specificity and blindness to soft tissue lesions that limits its use (Vanderwal et al. 2001).

12.4.2 Baseball and Overhead Throwing Sports

12.4.2.1 Standard Radiographs

Standard radiographs of the elbow, in case of suspicion of UCL injury, aims to exclude small avulsions at its proximal attachment at the medial epicondyle of the humerus (Fig. 12.5) or at its distal insertion at the sublime tubercle, which is the medial aspect of the coronoid process of the ulna. Osteophytes are more difficult to appreciate, for these are most common at the postero-medial olecranon in case of chronic UCL injury or "valgus extension overload syndrome". There are several studies that describe the value of stress radiography of the elbow in which AP views of the elbow are made while valgus stress is applied to the elbow (Lee et al. 1998; Rijke et al. 1994; Eygendaal et al. 2000). Rijke et al. (1994) differentiates partial (grade 2) from complete (grade 3) UCL tears using this technique. Lee et al. (1998) recognized the value of stress radiography in valgus instability, with comparative views of the uninjured elbow to differentiate instability from non-traumatic joint laxity.

Medial apophysitis, in skeletally immature throwers, may produce subtle abnormalities on plain films. Slight widening of the apophysis or fragmentation of the ossification centre can be seen (Chen et al. 2005; Hang et al. 2004; Klingele and Kocher 2002).

Fig. 12.5. A 20-year-old baseball player with pain in the region of the UCL for several months. AP radiograph of the left arm. A faint calcification is seen at the region of the proximal attachment of the UCL (*arrow*)

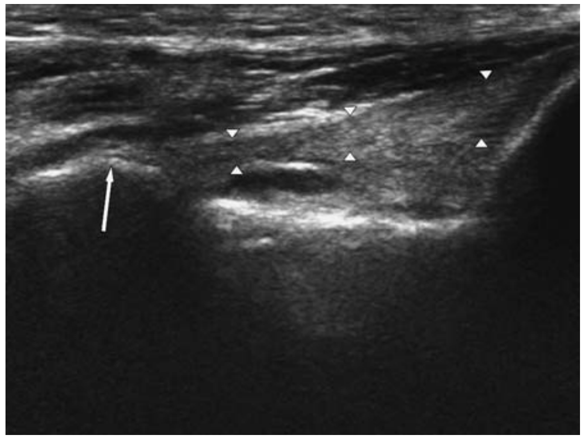

Fig. 12.6. Longitudinal ultrasound view of a normal UCL (*arrowheads*). The normal UCL is hyperechoic and has a fan-like shape proximally. Distally its insertion is at the sublime tubercle of the proximal ulna (*arrow*)

12.4.2.2
Ultrasound

The role of ultrasound in the evaluation of UCL injury remains unclear; it has been discussed in only a few papers (De Smet et al. 2002; Jacobson et al. 2003; Miller et al. 2004; Nazarian et al. 2003; Ward et al. 2003). Although the possibility of US identification of the UCL is well demonstrated on cadavers and/or compared with MRI, there are no large studies including US, clinical findings and/or MRI in athletes. Ward et al. (2003) described the ultrasonographic appearance of the UCL and correlated these findings in cadavers. Baseline parameters for the evaluation of the ligament were defined that may be helpful to determine injured from non-injured ligaments. The normal anterior bundle of the UCL is hyperechoic (compared to surrounding muscle) with a fibrillar pattern and a fanlike shape (Fig. 12.6). Miller et al. (2004) studied the UCL using US in eight baseball pitchers with clinical suspicion of UCL injury. Although the US findings were only confirmed with MRI in six patients and with surgery in three patients they described the abnormalities that can be seen in UCL, e.g., non-visualization of the ligament or alterations in morphology (hypo-echoic areas within the ligament). Jacobson et al. (2003) described in a very small population the variable appearance of the proximal part of the UCL. Nazarian et al. (2003) reported on dynamic US of the anterior band of the UCL in which he looked at the UCL and the width of the ulnohumeral joint with valgus stress, which is an ultrasonographic equivalent to the valgus stress radiography. They concluded that in pitching arms the anterior band of the UCL is thicker and contains statistically significant more calcifications and hypo-echoic foci. In addition, as we know from stress radiographs, they found an increase in width of the ulnohumeral joint when valgus stress was applied. Although populations in these studies are small it is likely that US can play a role in the evaluation of the anterior bundle of the UCL.

12.4.2.3
CT

The use of CT as a secondary imaging modality (after standard radiography) to evaluate elbow injuries in overhead throwing athletes is almost exclusively reserved for acute bony trauma (fractures). Chronic osseous injuries like stress fractures of the olecranon are relatively uncommon in overhead throwers but have been described in baseball players and javelin throwers and can be visualized with CT, especially the type III and IV fractures (classification by Arendt/Griffiths) (Iwamoto and Takeda 2003; Arendt and Griffiths 1997). If, on standard radiographs, a bony avulsion is suspected in case of an UCL injury, CT will

yield better results than MRI in describing the exact size and location of the fragment (Fig. 12.7). In case of "valgus extension overload syndrome", CT can depict the exact size and location of the osteophytes at the posterior olecranon better than standard radiography. An additional advantage of CT is that in case of absence of intra-articular fluid an intra-articular osseous loose fragment will be picked up more easily than with MRI.

Fig. 12.7. Coronal CT MPR of the same patient as in Fig. 12.5. A small avulsion at the origin of the UCL is very well appreciated on CT (*arrow*)

12.4.2.4
MRI

The anterior bundle of the UCL is the most important structure to visualize in an overhead throwing athlete with medial elbow pain. It is the only part of the medial complex that is seen in the coronal plane in which it should appear as a thin continuous linear structure with a low signal intensity on all sequences (Kijowski et al. 2005) (Fig. 12.8). A small amount of fat can be seen deep and/or superficial to the ligament (Jacobson et al. 2003). Complete rupture is demonstrated through non-visualization of the ligament or focal complete disruption at the ulnar or humeral attachment (Fig. 12.9). Other signs of rupture, either partial or compete, includes laxity, thickening, irregularities and poor definition of the ligament as well

Fig. 12.8. Normal left elbow. Coronal T1-WI. The ulnar collateral ligament (*arrowheads*) has a normal thin appearance, it is sharply outlined and of overall low signal intensity. There is a relatively broad origin below the undersurface of the medial epicondyle which is considered normal. The faint hyperintense appearance of the ligament in this area is probably due to interspersed fat

Fig. 12.9. An 18-year-old baseball pitcher with chronic ulnar sided elbow pain. Coronal T2*-weighted image. There is a complete disruption of the origin of the UCL at the level of the medial epicondyle (*arrow*) with fluid surrounding the ligament that is slackened, somewhat irregular and blurred

as abnormal signal intensity in or around the ligament (Kijowski et al. 2005; Nakanishi et al. 1996; Sonin and Fitzgerald 1996; Thornton et al. 2003). Complete ruptures are easier to diagnose than partial ruptures. A sensitivity and specificity of as high as 100% has been described for complete ruptures, for partial rupture a sensitivity of only 57% is reported (Timmerman et al. 1994). Partial ruptures are more easily seen if surrounded by fluid. This explains the preference of some radiologists to perform MR-arthrography in which there is extravasation of fluid or gadolinium extra-articular into or beyond the ligament (Munshi et al. 2004; Nakanishi et al. 1996; Timmerman et al. 1994; Thornton et al. 2003). Whatever technique used, we have to be careful in diagnosing partial tears since several studies showed that the UCL can have a variable appearance not only at its distal insertion at the sublime tubercle but also at its proximal attachment at the humeral epicondyle (Jacobson et al. 2003; Munshi et al. 2004).

In "valgus extension overload syndrome" MRI is used to evaluate the UCL, the joint cartilage and the olecranon to look for osteophytes and loose bodies. The UCL is expected to be thickened and irregular and predominantly hypo-intense on T1-weighted and T2-weighted sequences reflecting fibrosis as part of repair of microtears. Bone marrow edema can be seen in the olecranon representing repetitive bony stress. Particular attention has to be paid to the ulnar nerve since ulnar neuropathy can accompany VEO syndrome (Fig. 12.10). The ulnar nerve may be thickened with high signal intensity on PD or T2-weighted images and/or can be subluxed from the ulnar groove

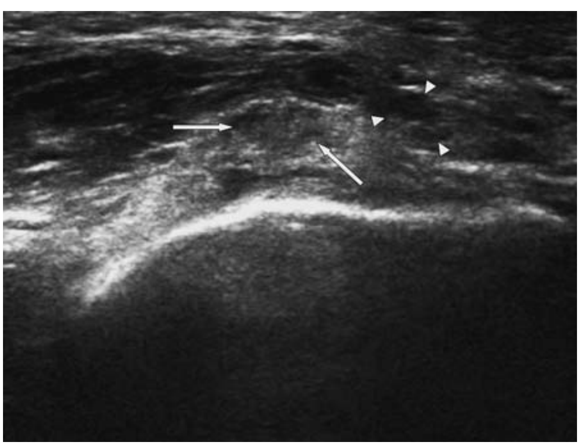

Fig. 12.10. Transverse US image of the elbow showing the UCL (*arrows*). Note the close proximity of the ulnar nerve (*arrowheads*) which is often compromised in cases of UCL injuries

(Cain et al. 2003; Field and Savoie 1998; Gerbino 2003; Kijowski et al. 2005; Thornton et al. 2003).

In the immature skeleton the apophysis of the medial epicondyle is particularly vulnerable to repetitive stress (Klingele and Kocker. 2002). The role of MRI in the evaluation of little league elbow is still unclear. The epiphyseal growth plate usually has high signal intensity on T2-weighted and STIR images which makes the differentiation with bone marrow edema not obvious. This is also true if there is fragmentation of the apophysis which is better seen on plain radiographs.

12.4.3 Golf

12.4.3.1 Standard Radiography

Standard radiography is of little value in golfer's elbow. Nonspecific findings such as soft tissue swelling, loss of normal fat planes adjacent to the medial epicondyle, small calcifications or subtle cortical irregularities at the origin of the common flexor tendon, can be seen (Chen et al. 2003; Kijowski et al. 2005). A bony avulsed fragment at the common flexor tendon origin or the UCL is another possible finding.

12.4.3.2 Ultrasound

Ultrasound is the imaging modality of choice in medial epicondylitis. The common flexor tendon will be thickened and irregularly delineated with a heterogeneous echoarchitecture. Linear hypo-echoic intratendinous fissures or small calcifications can be seen. Moreover, fluid can be identified at the extra-articular aspect of the UCL as well as focal synovitis at the medial aspect of the joint (Ferrara and Marcelis 1997). Interindividual variability with a short common flexor tendon makes ultrasonographic evaluation more difficult. In these cases, comparison with the uninjured arm is then useful.

12.4.3.3 MRI

MRI in medial epicondylitis can reveal a spectrum of abnormalities depending upon the duration and severity of the symptoms. The more acute phase

of tendinosis with paratenonitis is characterized by increased signal respectively in and around the tendon on T1 and T2-WI as well as on STIR images (Kijowski et al. 2005). This increased signal can vary between faint hyperintensity on fluid-sensitive sequences to areas with frank fluid signal. Thickening of the tendon can be seen in more chronic cases, which will most often be referred to as tendinosis. Although tendinosis and tendinitis are confusingly interchangeably used in the literature to describe overuse and degenerative pathology, the correct terminology from the histopathological point of view is tendinosis. Intratendinous inflammation is not predominantly present on pathological specimens. Inflammatory infiltration may be present at the tendon sheath or paratenon and thus is referred to as tenovaginitis and paratenonitis, respectively. It is obvious that only the "-itis" disorders respond to anti-inflammatory drugs (Khan et al. 1999; Puddu et al. 1976). In case of a rupture of the common flexor tendon, thinning or disruption with a fluid filled gap at the level of the tear is seen (Thornton et al. 2003). Bone marrow edema in the medial epicondyle and in the surrounding muscles has been described (Thornton et al. 2003). Abnormalities are most frequent at the flexor carpi radialis and pronator teres part of the common flexor tendon (Kijowski et al. 2005; Thornton et al. 2003). The ulnar nerve is compromised in up to 60% of patients (Jobe and Cicotti 1994); neuritis will show thickening of the ulnar nerve with an increased signal on T2-weighted images in the nerve and the surrounding tissues.

Fig. 12.11. Patient with chronic lateral epicondylitis. AP radiograph showing calcifications at the level of the insertion of the common extensor tendon (*arrow*)

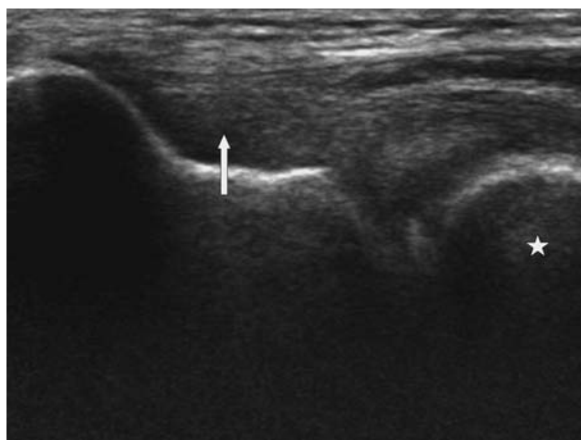

Fig. 12.12. Longitudinal US view of the normal common extensor tendon origin (*arrow*). Radial head (*asterisk*)

12.4.4 Tennis

12.4.4.1 Standard Radiography

Findings on standard radiology in cases of "tennis elbow" or lateral epicondylitis are similar to those seen in cases of medial epicondylitis, conventional films in both conditions will usually be normal or not relevant (Fig. 12.11).

12.4.4.2 Ultrasound

The ultrasound appearance of the common extensor tendinosis (Fig. 12.12) is basically similar to the findings in common flexor tendon overuse. They include: linear intrasubstance tears, thickening of the tendon, calcifications as well as enthesophytes, bone irregularities, focal hypo-echoic areas, peritendinous fluid and diffuse tendon heterogeneity (Connell et al. 2001; Levin et al. 2005; Miller et al. 2002) (Fig. 12.13). Studies by Levin et al. (2005) and Miller et al. (2002) showed a good US sensitivity for lateral epicondylitis ranging from 64% to 88% but relatively poor specificity, compared to a better sensitivity and specificity by MRI of 90%–100% and

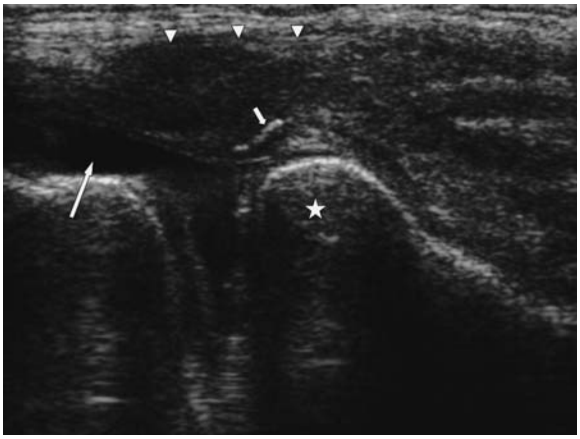

Fig. 12.13. A 26-year-old tennis player with longstanding pain at the lateral epicondyle. Longitudinal US view of the common extensor tendon. A severe tendinosis with a thickened inhomogeneous appearance of the tendon (*arrowheads*) is demonstrated. There is fluid in the joint extending between the origin of the tendon and the humerus (*long white arrow*). A calcification is seen (*short white arrow*). Radial head (*asterisk*)

83%–100%, respectively. The value of power Doppler application in the evaluation of the common extensor and flexor tendon and paratenon at the elbow has not been studied yet.

12.4.4.3
MRI

A very high sensitivity is repeatedly reported for MRI in the evaluation of lateral epicondylitis, although a meta-analysis in 2001 concluded that the assessment of MRI findings in epicondylitis is questionable due to small sample sizes and methodological shortcomings (Pasternack et al. 2001). Fluid sensitive sequences are mandatory (STIR or T2-Fat Sat); the axial and coronal planes are the most helpful in the evaluation of the common extensor tendon. The ECRB is most often involved, not rarely with secondary involvement of the extensor digitorum communis (EDC) (Nirschl 1992). Findings depend upon chronicity of the condition and are thickening or thinning of the tendon and increased signal on the fluid sensitive sequences and/or the T1-weighted sequences (Fig. 12.14). These findings can however also be found in non-symptomatic high-performance athletes (Martin and Schweitzer 1998). Furthermore, the radiologist has to be informed if any treatment has been applied (e.g., local corticosteroid injection, shock wave therapy, etc.) prior to MRI. In the coronal plane the RLC is assessed because injuries to this ligament are not uncommon in patients with lateral epicondylitis (Bredella et al. 1999). Bone marrow edema at the lateral humeral epicondyle can occur (Martin and Schweitzer 1998) as well as T2-weighted hyperintense signal in the surrounding soft tissues (e.g., anconeus muscle) (Coel et al. 1993).

a

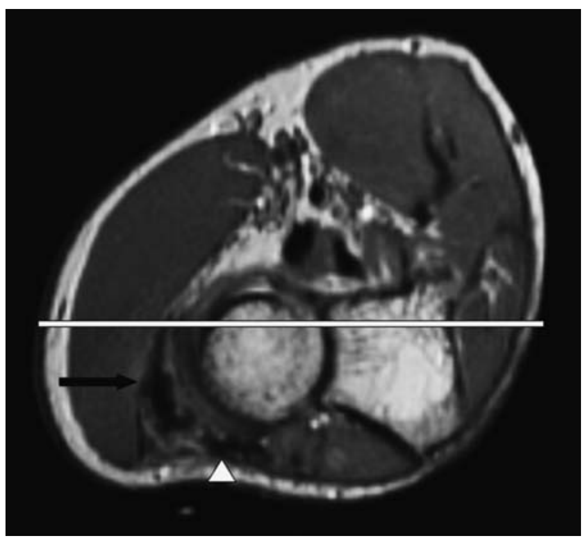

b

Fig. 12.14a,b. A 30-year-old tennis player with clinically lateral epicondylitis on the right side. Oblique coronal STIR (**a**) (imaging plane represented by *white line* in image **b**) and axial PD-MR image of the right elbow (**b**). There is hyperintense signal in and around the common extensor tendon (*white arrow*), fluid in the joint (*arrowhead* in **a**) and irregular and non-homogeneous tendon (*black arrow*). There is accompanying anconeus tendinopathy (*arrowhead* in **b**)

12.4.5 Handball and Soccer

12.4.5.1 Standard Radiography

Although not commonly demonstrated the main indication for standard radiography in "goalkeepers elbow" are intra-articular loose bodies. There are no studies describing the accuracy of plain films for the detection of loose bodies in the elbow joint. Particular attention has to be paid to the olecranon fossa and the anterior aspect of the elbow near the coronoid process of the ulna (Fig. 12.15). Sometimes a reverse axial projection can be helpful to better evaluate the posterior elbow (Chen et al. 2003).

In handball and baseball players a generalized bony hypertrophy of the humerus of the dominant arm is reported. This is manifested by an increased humeral diameter and cortical hypertrophy of the humeral shaft, regardless of any complaints (Popovic et al. 2001; Gore et al. 1980). Stress radiography usually reveals laxity of the medial elbow structures (as in baseball players) demonstrated as increase in ulno-humeral distance if valgus stress is applied to the elbow (Popovic and Lemaire 2002; Popovic et al. 2001).

Fig. 12.15. Professional 28-year-old soccer goalkeeper with recurrent right elbow pain. Lateral radiograph of the right elbow. A small ossicle is seen in the fossa olecrani (*arrow*) which can represent an accessory ossicle or intraarticular loose body. No other loose bodies are identified

12.4.5.2 Ultrasound

US is useful in the detection of loose bodies in the elbow joint (Popovic and Lemaire 2002; Popovic et al. 2001; Ferrara and Marcelis 1997). This is especially true if there is an associated joint effusion which is often present due to secondary synovitis. Calcified loose intra-articular bodies present as focal echogenic structures separate from cortical bone, the larger one's with posterior shadowing. Loose bodies as small as 1 mm can be detected especially in the presence of joint effusion (Marcelis et al. 1996). The most common locations include the olecranon fossa and the coronoid fossa (O'Driscoll 1992).

Physiologic and pathologic thickening of the various tendons surrounding the elbow joint is described in handball goalkeepers (Popovic et al. 2001).

12.4.5.3 MRI

MRI can be used to detect intra-articular loose bodies especially when there is an associated effusion (Quinn et al. 1994). The signal intensity is variable depending upon the amount of calcification and bone marrow if ossification is present. Particularly T2-weighted and gradient echo sequences are useful to detect loose bodies, the latter sequence can also be particularly helpful to evaluate a potential donor site, e.g., chondral defects. In the absence of an effusion the accuracy of MRI is far less with a sensitivity of 50% and a specificity of 60% (Miller 1999). In these cases, injection of saline or gadolinium into the joint improves accuracy but one has to be careful not to inject air bubbles into the joint for these can easily be mistaken for loose bodies. Osteophytes and synovial proliferations can be mistaken for loose bodies.

12.4.5.4 CT

In the authors opinion, CT of the elbow is superior to MRI and US in the detection of calcified loose bodies but also for the detection of osteophytes. Our high resolution CT (HRCT) protocol includes axial plane imaging with 0.5 or 0.6 mm slice thickness and two-dimensional multi planar reformatting in any desired plane. The position of the elbow is relatively unimportant and can range form fully supine to fully prone. Even in the absence of fluid, the small calcifications can be detected in any part of the joint (Fig. 12.16).

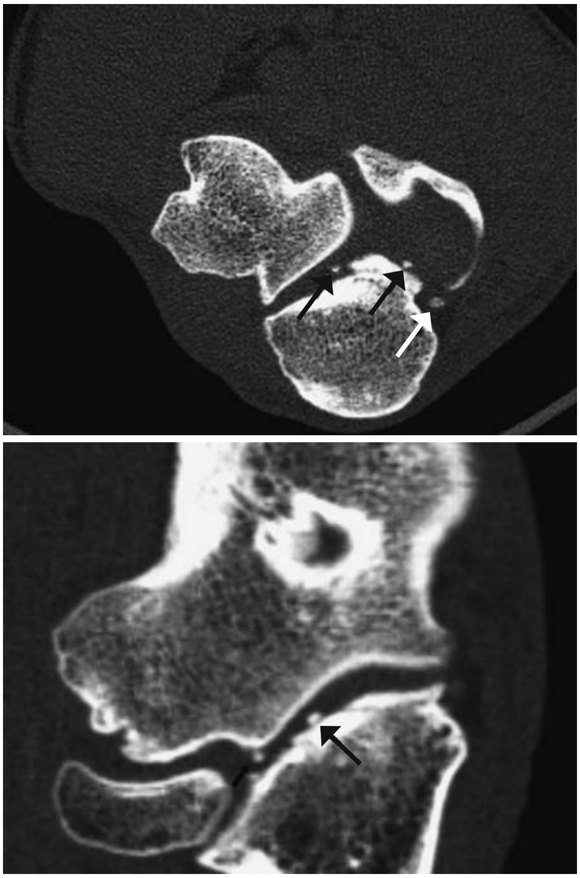

Fig. 12.16. Same patient as in Fig. 12.15. MDCT MRP reconstructions in the axial and coronal plane demonstrating multiple small intra-articular loose bodies (*arrows*) in the right elbow joint which are not appreciated on plain films

The cartilage layer itself cannot be evaluated without intra-articular iodine contrast, but for the detection of osteochondral lesions CT probably has an accuracy as high as MRI, as is demonstrated in the ankle joint (Verhagen et al. 2005). A potential pitfall is the pseudodefect of the capitellum (see Sect. 12.4.6.3).

12.4.6 Gymnastics

12.4.6.1 Standard Radiography

Osteochondral lesions in the elbow are for the most part located at the capitellum most often anterior to central. The second most frequent location is the radial head. Usually a radiolucent area is seen surrounded by more or less sclerosis depending upon the age of the lesion (Fig. 12.17). Subtle irregularities of the subchondral bone lamella may precede flattening of the contour of the involved bone. A 'displaced fat pad' sign results from joint effusion, loose bodies may be identified. A distinction has to be made between osteochondral lesions (osteochondritis dissecans, OD) and Panner's disease, which is not always easy. The latter is considered to be an osteochondrosis of the capitellum. It is most common in young prepubescent males. On radiographs the entire capitellum can be involved with sclerosis, irregularities and lucencies. It is however, a benign self-limiting disorder in which the capitellum will regain a normal appearance.

Fig. 12.17. A 15-year-old gymnast with right elbow pain. AP and lateral radiographs of the right elbow. On the lateral view the lucency in the capitellum (*arrowheads*) is compatible with an osteochondral defect. The lesion is much more difficult to appreciate on the AP view, it is discriminated because of the surrounding faint sclerosis (*black arrows*)

12.4.6.2
Ultrasound

In cases of suspicion of osteochondral lesions ultrasound is only helpful to detect joint effusion, intra-articular loose bodies or other additional findings e.g., tendinosis or UCL injuries.

12.4.6.3
MRI

The MRI appearance of osteochondral lesions in the elbow joint varies. Different patterns are described. Early OD may demonstrate focal low signal intensity on T1-WI without changes on T2- or T2*-weighted sequences (Kijowski et al. 2004; Banks et al. 2005) (Fig. 12.18). Later on, lesions will display two different signal intensity patterns (Bowen et al. 2001). The first pattern consists of focal low signal intensity on T1-weighted images accompanied by high signal intensity on corresponding T2-weighted images. The second pattern is more complex with a focal intermediate signal intensity surrounded by a low signal intensity ring on T1-weighted images, the innermost portion of the latter being high in signal intensity on corresponding T2-weighted images (Bowen et al. 2001). The clinical relevance of these different findings is unknown. In advanced stages the lesion can appear of low SI on all sequences in case of a chronic (possible necrotic) fragment. Grading osteochondral lesions is not easy and the clinical use of grading is uncertain. It is not clear whether grading or not changes treatment options and outcome (Bowen et al. 2005). An "in situ"

a b c

Fig. 12.18a–c. A 10-year-old professional female gymnast with increasing pain at the left elbow for 3 months. Sagittal CT MPR image (**a**), coronal T1-weighted MR image (**b**) and sagittal gradient-echo T2*-WI MR image (**c**) of the left elbow. There is a small hypo-intense area at the capitellum slightly anterior (*arrow* in **b**) compatible with a very early osteochondral lesion. The corresponding cartilage image (**c**) shows no abnormalities to the overlying cartilage. On CT no loose fragments were seen. The early OD lesion is seen as a small area of sclerosis with intact cortex (*arrow* in **a**)

dissecans fragment is considered unstable if it is surrounded by fluid like cysts or a complete T2-weighted high signal intensity ring (De Smet et al. 1996). On MR arthrography, the in situ fragments which are surrounded by contrast are considered unstable (Kramer et al. 1992).

A pitfall in diagnosing OD lesions is the so-called pseudo-defect of the capitellum. This is found at the junction of the inferior capitellum with the posterior non articular surface of the lateral epicondyle (Rosenberg et al. 1994) (Fig. 12.19).

Fig. 12.19. Sagittal T2-weighted MR image of the elbow showing an irregular area (*arrow*) in the posterior capitellum compatible with a pseudo-defect

12.4.6.4
CT

Imaging of osteochondral lesions in the elbow is most often performed with MRI. There are no studies to compare CT and MRI in the detection of OD elbow. In the authors opinion CT is very useful for the detection of osteochondral lesions in either the capitellum or radial head provided HRCT is performed. Osteochondral lesions will present as (subtle) subchondral bone lamella irregularities, subchondral cystic changes, subchondral density changes and/or defects at the subchondral lamella (Fig. 12.20). The joint space width will usually be normal. The cartilage itself cannot be assessed without intra-articular contrast. There is no literature on the role of CT arthrography vs non-contrast CT or vs non-contrast MRI.

a

b

Fig. 12.20a,b. A 16-year-old female gymnast with an osteochondral lesion of the radial head. Sagittal CT (**a**) and coronal gradient-echo T2*-WI MR image (**b**) of the elbow. The OD lesion with the cortical defect (*black arrow*, **a**, *white arrow*, **b**) and the small loose fragments are better appreciated on the CT than on the MRI

12.5 Conclusions

Elbow injuries in athletes are relatively uncommon, especially acute injuries. Most injuries are contributed to overuse. Throwing, using the arm as a lever or as a weight bearing joint and stopping goal fired shots are the mechanisms in which injuries most often occur. Ulnar collateral ligament injuries, lateral and medial epicondylitis, medial epicondyle apophysitis, osteochondral lesions and intraarticular loose bodies are the most common encountered injuries. Standard radiography should be the initial imaging modality but in general MRI is the most useful imaging modality to use. In certain selected cases however US and CT can replace MRI or add valuable information.

Things to Remember

1. AP and lateral radiographs of the elbow are usually sufficient to evaluate the osseous structures of the elbow. In selected cases (valgus extension overload) a reversed axial projection can be helpful.
2. Ultrasound has a very high sensitivity and specificity to diagnose lateral and medial epicondylitis and usually confirms the diagnosis.
3. In medial epicondylitis and ulnar collateral ligament injuries particular attention has to be paid to the ulnar nerve which is often compromised in these conditions.
4. Ulnar collateral ligament injuries are best assessed using MRI. There is no evidence to support that MR arthrography is superior to non-enhanced MRI.
5. CT has a better sensitivity compared to MRI for intraarticular loose bodies especially in the absence of joint effusion.
6. CT and MRI are comparable for demonstrating osteochondral lesions.

References

Ahmad CS, ElAttrache NS (2004) Valgus extension overload syndrome and stress injury of the olecranon. Clin Sports Med 23:665–676

Alcid JG, Ahmad CS, Lee TQ (2004) Elbow anatomy and structural biomechanics. Clin Sports Med 23:503–517

Arendt EA, Griffiths HJ (1997) The use of MR imaging in the assessment and clinical management of stress reactions of bone in high-performance athletes. Clin Sports Med 16:291–306

Banks KP, Ly JQ, Beall DP et al. (2005) Overuse injuries of the upper extremity in the competitive athlete: magnetic resonance imaging findings associated with repetitive trauma. Curr Probl Diagn Radiol 34:127–142

Bartlett RM, Rent RJ (1988) The biomechanics of javelin throwing. J Sports Sci 6:1–38

Bojanic I, Ivkovic A, Boric I (2005) Arthroscopy and micro fracture technique in the treatment of osteochondritis dissecans of the humeral capitellum: report of three adolescent gymnasts. Knee Surg Sports Traumatol Arthrosc Oct 11; [Epub ahead of print]

Bowen R, Otsuku N, Yoon S et al. (2001) Osteochondral lesions of the capitellum in pediatric patients: role of magnetic resonance imaging. J Pediatr Orthop 21:298–301

Bredella MA, Tirman PF, Fritz RC et al. (1999) MR imaging findings of lateral ulnar collateral ligament abnormalities in patients with lateral epicondylitis. Am J Roentgenol 193: 1379–1382

Brogdon BG, Crow NE (1960) Little leaguer's elbow. Am J Roentgenol 83:671–675

Cain EL Jr, Dugas JR, Wolf RS et al. (2003) Elbow injuries in throwing athletes: a current concepts review. Am J Sports Med 31:621–635

Chen FS, Rokito AS, Jobe FW (2001) Medial elbow problems in the overhead-throwing athlete. J Am Acad Orthop Surg 9:99–113

Chen AL, Youm T, Ong BC et al. (2003) Imaging of the elbow in the overhead throwing athlete. Am J Sports Med 31:466–473

Chen FS, Diaz VA, Loebenberg M et al. (2005) Shoulder and elbow injuries in the skeletally immature athlete. J Am Acad Orthop Surg 13:172–185

Chung CB, Kim HJ (2003) Sports injuries of the elbow. Magn Reson Imaging Clin N Am 11:239–253

Coel M, Yamada CY, Ko J (1993) MR imaging of patients with lateral epicondylitis of the elbow (tennis elbow): importance of increased signal of the anconeus muscle. Am J Roentgenol 161:1019–1021

Connell D, Burke F, Coombes P et al. (2001) Sonographic examination of lateral epicondylitis. Am J Roentgenol 176:777–782

Cotten A, Jacobson J, Brossmann J et al. (1997) Collateral ligaments of the elbow: conventional MR imaging and MR arthrography with coronal oblique plane and elbow flexion. Radiology 204:806–812

De Smet AA, Ilahi O, Graf B (1996) Reassessment of the MR criteria for the stability of osteochondritis dissecans in the knee and ankle. Skeletal Radiol 25:159–163

De Smet AA, Winter TC, Best TM et al. (2002) Dynamic sonography with valgus stress to assess elbow ulnar collateral ligament injury in baseball pitchers. Skeletal Radiol 31:671–676

Eygendaal D, Heijboer MP, Obermann WR et al. (2000) Medial instability of the elbow. Findings on valgus load radiography and MRI in 16 athletes. Acta Orthop Scand 71:480–483

Ferrara MA, Marcelis S (1997) Continuing education – ultrasound of the elbow. JBR-BTR 80:122–123

Field LD, Savoie FH (1998) Common elbow injuries in sport. Sports Med 26:193–205

Fleisig GS, Andrews JR, Dillman CJ et al. (1995) Kinetics of baseball pitching with implications about injury mechanisms. Am J Sports Med 23:233–239

Gerbino PG (2003) Elbow disorders in throwing athletes. Orthop Clin North Am 34:417–426

Gissane C, White J, Kerr K et al. (2001) An operational model to investigate contact sports injuries. Med Sci Sports Exerc 33:1999–2003

Gore RM, Rogers LF, Bowerman J et al. (1980) Osseous manifestations of elbow stress associated with sports activities. Am J Roentgenol 134:971–977

Hang DW, Chao CM, Hang YS (2004) A clinical and roentgenographic study of Little League elbow. Am J Sports Med 32:79–84

Iwamoto J, Takeda T (2003) Stress fractures in athletes; review of 196 cases. J Orthop Sci 8:273–278

Jackson DW, Silvino N, Reiman P (1989) Osteochondritis dissecans in the female gymnast's elbow. Arthroscopy 5:129–136

Jacobson JA, Propeck T, Jamadar DA et al. (2003) US of the anterior bundle of the ulnar collateral ligament: findings in five cadaver elbows with MR arthrographic and anatomic comparison– – initial observations. Radiology 227:561–566

Jobe FW, Cicotti MG (1994) Lateral and medial epicondylitis of the elbow. J Am Acad Orthop Surg 2:1–8

Khan KM, Cook JL, Bonar F et al. (1999) Histopathology of common tendinopathies. Update and implications for clinical management. Sports Med 27:393–408

Kijowski R, Tuite M, Sanford M (2004) Magnetic resonance imaging of the elbow. Part I: normal anatomy, imaging technique, and osseous abnormalities. Skeletal Radiol 33:685–697

Kijowski R, Tuite M, Sanford M (2005) Magnetic resonance imaging of the elbow. Part II: abnormalities of the ligaments, tendons, and nerves. Skeletal Radiol 34:1–18

Kijowski R, De Smet AA (2005) Magnetic resonance imaging findings in patients with medial epicondylitis. Skeletal Radiol. 34:196–202

Klingele KE, Kocher MS (2002) Little league elbow. Valgus overload injury in the pediatric athlete. Sports Med 32:1005–1015

Kramer J, Stiglbauer R, Engel A (1992) MR contrast in osteochondritis dissecans. J Comput Assist Tomogr 16:254–260

Lee GA, Katz SD, Lazarus MD (1998) Elbow valgus stress radiography in an uninjured population. Am J Sports Med 26:425–427

Levin D, Nazarian LN, Miller TT et al. (2005) Lateral epicondylitis of the elbow: US findings. Radiology 237:230–234

Loftice J, Fleisig GS, Zheng N et al. (2004) Biomechanics of the elbow in sports. Clin Sports Med 23:519–530

Marcelis S, Daenen B, Ferrara MA (1996) Peripheral musculoskeletal ultrasound atlas. Thieme, Stuttgart, pp 79–89

Martin CE, Schweitzer ME (1998) MR imaging of epicondylitis. Skeletal Radiol 27: 133–138

McCarroll JR (1996) The frequency of golf injuries. Clin Sports Med 15:1–7

McCarroll JR (2001) Overuse injuries of the upper extremity in golf. Clin Sports Med 20:469–479

Miller TT (1999) Imaging of elbow disorders. Orthop Clin North Am 30:21–36

Miller TT, Shapiro MA, Schultz E et al. (2002) Comparison of sonography and MRI for diagnosing epicondylitis. J Clin Ultrasound 30:193–202

Miller TT, Adler RS, Friedman L (2004) Sonography of injury of the ulnar collateral ligament of the elbow-initial experience. Skeletal Radiol 33:386–391

Morris C, Bartlett RM (1996) Biomechanical factors critical for performance in the men's javelin throw. Sports Med 21:438–446

Munshi M, Pretterklieber ML, Chung CB et al. (2004) Anterior bundle of ulnar collateral ligament: evaluation of anatomic relationships by using MR imaging, MR arthrography, and gross anatomic and histologic analysis. Radiology 231:797–803

Nakanishi K, Masatomi T, Ochi T et al. (1996) MR arthrography of elbow: evaluation of the ulnar collateral ligament of elbow. Skeletal Radiol 25:629–634

Nazarian LN, McShane JM, Ciccotti MG et al. (2003) Dynamic US of the anterior band of the ulnar collateral ligament of the elbow in asymptomatic major league baseball pitchers. Radiology 227:149–154

Nirschl RP (1992) Elbow tendinosis/tennis elbow. Clin Sports Med 11:851–870

O'Driscoll SW (1992) Elbow arthroscopy for loose bodies. Orthopedics 15(7):855–859

Pasternack I, Tuovinen EM, Lohman M et al. (2001) MR findings in humeral epicondylitis. Acta Radiol 42:434–440

Popovic N, Lemaire R (2002) Hyperextension trauma to the elbow; radiological and ultrasonographic evaluation in handball goalkeepers. Br J Sports Med 36:452–456

Popovic N, Ferrara MA, Daenen B et al. (2001) Imaging overuse injury of the elbow in professional team handball players: a bilateral comparison using plain films, stress radiography, ultrasound and magnetic resonance imaging. Int J Sports Med 22:60–67

Puddu G, Ippolito E, Postacchini F (1976) A classification of Achilles tendon disease. Am J Sports Med 4:145–150

Quinn SF, Haberman JJ, Fitzgerald SW et al. (1994) Evaluation of loose bodies in the elbow with MR imaging. J Magn Reson Imaging 4:169–172

Rijke AM, Goitz HT, McCue FC (1994) Stress radiography of the medial elbow ligaments. Radiology 191:213–216

Roetert EP, Brody H, Dillman CJ et al. (1995) The biomechanics of tennis elbow. Clin Sports Med 14:47–57

Rosenberg ZS, Beltran J, Cheung YY (1994) Pseudodefect of the capitellum: potential MR imaging pitfall. Radiology 191:821–823

Sonin AH, Fitzgerald SW (1996) MR imaging of sports injuries in the adult elbow: a tailored approach. Am J Roentgenol 167:325–331

Thériault G, Lachance P (1998) Golf injuries. An overview. Sports Med 26:43–57

Thornton R, Riley GM, Steinbach LS (2003) Magnetic resonance imaging of sports injuries of the elbow. Top Magn Reson Imaging 14:69–86

Timmerman LA, Schwartz ML, Andrews JR (1994) Preoperative evaluation of the ulnar collateral ligament by magnetic

resonance imaging and computed tomography arthrography. Am J Sports Med 22:26–32
Van der Wall H, Storey G, Frater C et al. (2001) Importance of positioning and technical factors in anatomic localization of sporting injuries in scintigraphic imaging. Semin Nucl Med 31:17–27
Verhagen RA, Maas M, Dijkgraaf MG et al. (2005) Prospective study on diagnostic strategies in osteochondral lesions of the talus. Is MRI superior to helical CT? J Bone Joint Surg Br 87-B:41–46
Ward SI, Teefey SA, Paletta GA Jr et al. (2003) Sonography of the medial collateral ligament of the elbow: a study of cadavers and healthy adult male volunteers. Am J Roentgenol 180:389–394
Werner SL, Fleisig GS, Dillman CJ et al. (1993) Biomechanics of the elbow during baseball pitching. J Orthop Sports Phys Ther 17:274–278
Werner SL, Murray TA, Hawkins RJ et al. (2002) Relationship between throwing mechanics and elbow valgus in professional baseball pitchers. J Shoulder Elbow Surg 11:151–155
Wilder RP, Sethi S (2004) Overuse injuries: tendinopathies, stress fractures, compartment syndrome, and shin splints. Clin Sports Med 23:55–81, vi

Imaging of Wrist Injuries

13

Wilfred C. G. Peh and Howard R. Galloway

CONTENTS

W. C. G. Peh, MD, MBBS, FRCPE, FRCPG, FRCR
Clinical Professor and Senior Consultant Radiologist, Singapore Health Services, 7 Hospital Drive, #02-09, Singapore 169611, Republic of Singapore
H. R. Galloway, BMBS, FRANZCR
Clinical Associate Professor, Department of Radiology, Australian National University, The Canberra Hospital, Yamba Drive, Garran, ACT 2605, Australia

13.1 Introduction

The benefits of sports are well- recognized but many sports-related activities carry a specific injury risk. Injuries to the wrist and hand occur with a frequency of between 3% and 9% (Geissler 2001). This injury incidence will obviously be higher in those sports utilizing the hand and wrist, and where the potential for trauma during sporting activity is present. Trauma to the wrist may cause bone or soft tissue injury, which may sometimes be difficult to diagnose. Symptoms vary, according to the structure involved or nature of injury, but pain and limited joint function are the usual complaints. Physical examination may be difficult due to the proximity of many small bony and soft tissue structures, as well as small articulations.

The wide spectrum of sporting activities places demands of different magnitudes, orientations, and degrees of repetitions on the wrist. These injuries may result from a single debilitating or repetitive traumatic episodes. Proper diagnosis of injuries in this region therefore requires a basic knowledge of the anatomy and biomechanics of the wrist (Halikis and Taleisnik 1996). Many sporting activities are associated with a specific injury pattern related to the actions and stresses associated with that particular activity. Knowledge of the sport or recreational activity therefore aids in the diagnosis of these injuries. Early diagnosis of the injury and proper referral of these patients can help prevent complications, including prolonged pain and discomfort, surgery, and lost time from sports participation. Failure to diagnose sports injuries may lead to permanent disability (McCue et al. 1979).

It is important for athletes to be educated about how to recognize wrist injuries promptly. Seeking early medical attention for wrist injuries should be emphasized to athletes. Specific care to wrist-supporting ligaments and muscles is necessary to prevent overuse injuries during the recovery period and return of function. For pre-adolescent and adolescent athletes, injury

Box 13.1. Radiography

- Standard frontal and lateral radiographs are the initial imaging investigation for detection of fractures and malalignment
- Classification of distal radial fractures are made on radiographs
- Special projections may be needed for scaphoid, hamate hook and other carpal fractures
- Stress radiographs or videofluoroscopy may be required to show dynamic carpal instability

Box 13.2. Computed Tomography

- Useful in supplementing normal or equivocal radiographs in clinically-suspected injury
- Accurate for diagnosis of hook of hamate fractures and DRUJ subluxation/ dislocation
- Helpful in assessment of healing and post-traumatic deformity

Box 13.3. Bone Scintigraphy

- Useful only while bone is still remodelling
- Helpful in radiographically-occult trauma

Box 13.4. Arthrography

- Useful for diagnosis of ligament and TFCC tears
- Single versus triple compartment injection technique
- Single radiocarpal injection followed by either CT or MR imaging is now commonly practised

Box 13.5. Ultrasonography

- Provides answers to very specific diagnostic questions for superficial lesions such as tendon abnormalities
- Cheaper and time-saving compared to MR imaging
- Highly operator-dependent with long learning curve
- Availability of high-frequency transducer is essential

Box 13.6. Magnetic Resonance Imaging

- Provides a comprehensive overview of injuries to both bone and soft tissue structures such as muscle, tendon, tendon sheath, nerve and vessels
- May be performed following arthrography
- MR arthrography is useful for TFCC and SL and LT tears

to a growing wrist requires a more gradual return to full sporting activity than a non-growing wrist. Wrist injuries may potentially be prevented by implementing proper technique, maintaining good strength and flexibility and if the particular sports permit, using wrist guards. The use of wrist guards may help protect from fractures and skin scrapes if one falls or slides in sports such as rollerblading, or hockey. Proper stretching is especially useful for sports that involve a lot of upper extremity bodywork, such as racquet sports.

13.2 Sports Injuries in Children

Hand and wrist injuries are more common in preadolescent and adolescent athletes than in adults (Geissler 2001). It is particularly important to recognize wrist injuries that occur in the immature skeleton, such as gymnast's wrist (Fig. 13.1), as continued sports participation in affected children may result in

growth arrest and other long-term problems. Injured children should therefore abstain from the sport until the symptoms disappear and the wrist has healed completely (Morgan and Slowman 2001). Worldwide, an increasing number of children are involved in competitive and organized sports. The frequency and severity of both acute and overuse injuries are continuing to rise (Flynn et al. 2002).

Sprains (34%), contusions (30%) and fractures (25%) are the most common injury types (Damore et al. 2003). The six most common sports causing injuries in children are basketball (19.5%), football (17.1%), baseball/softball (14.9%), soccer (14.2%), rollerblading/skating (5.7%), and hockey (4.6%). Sprains/strains (32.0%), fractures (29.4%), contusions/abrasions (19.3%), and lacerations (9.7%) account for 90% of injury types. The most common injury location is the wrist/hand (28%). Contact with another person or object is the mechanism for more than 50% of the sports-related injuries (Taylor and Attia 2000).

Most ball-related injuries occur during soccer and rugby (86%), while the majority of fractures occurring during wheel sports are in cycling (63%). The radius/ulna is the most frequent fracture location (36%) (Lyons et al. 1999). Hassan and Dorani (2001) found that soccer, rollerblading, cycling and netball injuries are the most frequent causes of the fractures. Soccer and rollerblading are the commonest cause of fractures among boys, while rollerblading and netball injuries are most frequent cause among girls. Brudvik and Hove (2003) found that scaphoid fracture, an infrequent fracture in children, is seen in 9% of all fractures due to rollerblading/skating, with a doubled risk of fracture in boys aged 13–15 years compared with girls.

Fig. 13.1. Female adolescent gymnast. PA radiograph shows stress changes of the distal radius, with sclerosis adjacent to the irregularly-marginated growth plates

13.3 Anatomy

The wrist is a complex joint that is comprised of bones and soft tissue structures. The bones consist of the distal radius and ulna, eight carpal bones, and the proximal metacarpal bones. The eight carpal bones are arranged in two rows to form a compact unit. The proximal carpal row is formed by the scaphoid, lunate, triquetrum and pisiform, and articulates with the distal end of the radius and the triangular fibrocartilaginous complex (TFCC). The distal carpal row is formed by the trapezium, trapezoid, capitate and hamate, and articulates with the proximal surfaces of the metacarpal bones. The ulna does not articulate directly with the carpus. The wrist is composed of a series of articulations that are separated into several major joint compartments, including: the radiocarpal, distal radioulnar, pisiform-triquetral, midcarpal, first carpometacarpal, and intermetacarpal joints.

The carpal bones are held together by a complex set of ligaments, including the intrinsic (or interosseous) and extrinsic ligaments. These strong ligamentous attachments help stabilize the wrist. The dorsal ligaments are weaker than the volar ligaments, resulting in dorsal dislocation being more common. Intrinsic (or interosseous) ligaments connect pairs of carpal bones. In the proximal carpal row, the scapholunate and lunotriquetral ligaments join the proximal, dorsal and volar margins of these carpal bones, and separate the radiocarpal from the midcarpal compartments. The extrinsic ligaments are formed by thickenings of the inner surface of the joint capsule, and are located dorsally and volarly. The main dorsal extrinsic ligaments are the radiotriquetral, triquetrotrapezial and

triquetroscaphoid ligaments. The main volar extrinsic ligaments are the radioscapholunate, and the long radiolunate and short radiolunate ligaments.

The TFCC is an important stabilizer of the wrist. Its main component is the triangular fibrocartilage (TFC) disc, which separates the radiocarpal compartment from the distal radioulnar joint (DRUJ). The TFC disc is anchored to the articular cartilage of the ulnar side of the distal radius, and attaches to the ulnar styloid through fibrous bands. The central and radial aspects of the TFC disc are avascular, while the peripheral and ulnar aspects have a blood supply. The latter regions hence have the potential to heal, either spontaneously or after surgical repair, following injury (Bednar et al. 1991). Other components of the TFCC are the dorsal and volar radioulnar ligaments, prestyloid recess, the meniscal homologue (a fibrostyloid fold that extends into the prestyloid recess), ulnar collateral ligament, subsynovial sheath of the extensor carpi ulnaris tendon sheath, and volar ulnotriquetral and ulnolunate ligaments.

The DRUJ consists of an articular surface that covers two-thirds of the circumference of the distal ulna, which in turn articulates with the sigmoid notch of the distal radius. This joint configuration allows supination and pronation of the forearm. The DRUJ is stabilized intrinsically by the TFCC and extrinsically by the interosseous membrane, extensor carpi radialis, flexor carpi ulnaris, and the pronator quadratus.

The muscles of the hand originate primarily in the forearm and pass over the wrist. The flexor carpi ulnaris, which inserts into the pisiform bone, is the only muscle that inserts into one of the wrist bones. The dorsal aspect of the wrist consists of six compartments, each containing one or more extensor tendons within a synovial sheath. The two compartments in the volar aspect of the wrist are the carpal tunnel and Guyon's canal. The carpal tunnel is bounded superficially by the transverse carpal ligament, and contains nine flexor tendons and the median nerve. The median nerve lies between the flexor carpi radialis and palmaris longus tendons within the carpal tunnel. Guyon's canal lies superficial and radial to the hook of hamate, and contains the ulnar nerve and artery. The ulnar nerve runs deep to the flexor carpi ulnaris tendon in Guyon's canal. Blood supply is via the radial and ulnar arteries which form the dorsal palmar arch. The scaphoid bone receives its blood supply from the distal part of this arch.

13.4 Biomechanics of Sports Injuries

13.4.1 Overview

The wrist is a complex joint that biomechanically transmits forces generated at the hand through to the forearm. The carpal bones serve as a link between the hands and the upper body, with much of the motion at the wrist joint occurring between the radius and carpal bones. Its size, position, and relation to the radius and surrounding carpal bones make the wrist joint vulnerable to injury. A great deal of force is transmitted through these structures for certain types of sports. The radial side of the wrist carries 80% of the axial load, and the ulnar side the remaining 20%. Wrist injuries can be divided into four categories, namely: traumatic, overuse, neurovascular, and weight-bearing injuries (Howse 1994).

Traumatic injuries are the most common. They are due either to a fall onto the hand, a direct blow to the wrist, or a combination of a rotatory and torsional force (Howse 1994). These acute wrist injuries are often caused by accident and are hard to prevent (Fig. 13.2). Fractures, dislocations, strains (injury to muscle near the musculotendinous junction due to forceful contraction of the muscle), contusions, hematomas, and sprains (ligamentous injuries) are types of these injuries. Examples of common acute traumatic injuries are: distal radius fracture (often intra-articular in athletes), scaphoid fracture, wrist joint sprain, and intercarpal ligament sprain or tear. Less common injuries include: fracture of the hook of hamate, TFCC tear, DRUJ instability, and scapholunate dissociation. Important acute injuries that should not to be missed are: lunate dislocation, perilunate dislocation, any type of carpal dislocation, and traumatic arterial thrombosis.

Overuse injuries are common in sports involving the hand and wrist, such as racquet sports, netball, and volleyball (Howse 1994). In this form of injury, pain usually develops gradually. They are the result of repetitive application of submaximal stresses to otherwise normal tissues. This causes sufficient structural disruption to overcome the tissue's adaptive ability, and thus produces injuries without necessarily causing complete loss of function (Fig. 13.3). The common pathway is most likely to be microdamage to tissue collagen, combined with a direct or indirect effect on the microvasculature, with subsequent

Fig. 13.2. Male adolescent gymnast who fell from the gymnastic apparatus. PA radiograph shows a transverse fracture of the distal ulnar shaft. Note stress changes of the distal radius and, to a lesser extent, of the distal ulna, adjacent to the growth plates

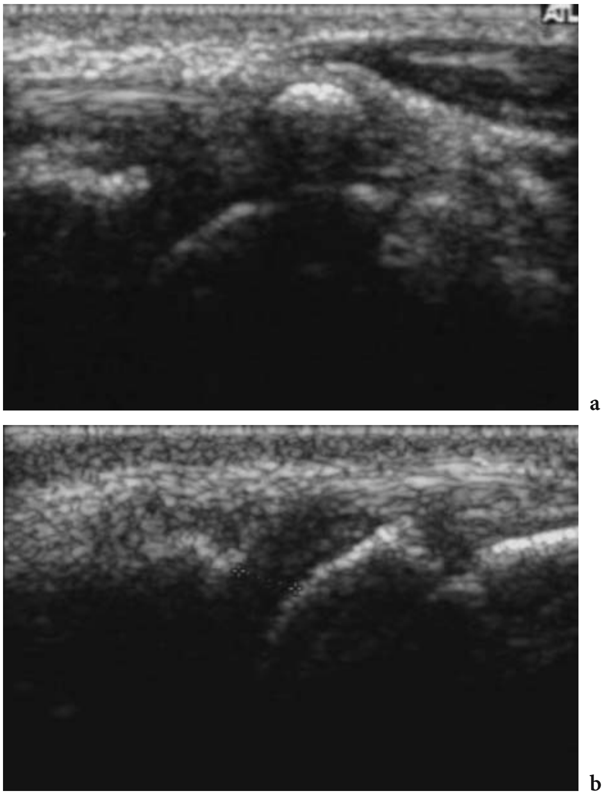

Fig. 13.3a,b. Male boxer who sustained repetitive trauma to the knuckles. Transverse (**a**) and longitudinal (**b**) US images show marked synovial thickening of the 2nd MCP joint, consistent with active synovitis

oxygen deprivation (Pitner 1990). Stress fractures, periostitis, tendinitis, and growth plate injuries in children are examples of overuse injuries. Common overuse injuries of the tendon include de Quervain's syndrome, subluxation of the extensor carpi ulnaris, and the common dorsal carpal impingement syndrome (Rettig 2004). Other overuse injuries in athletes include Kienbock's syndrome, pisotriquetral syndrome, ligamentous injuries such as scapholunate, lunotriquetral and midcarpal instability injuries, and injuries to the DRUJ and TFCC (Rettig 1998).

Nerve injuries are more commonly compressive neuropathies, and are seen in cyclists in whom there may be compression of the ulnar nerve in Guyon's canal. *Vascular injuries* are uncommon and usually result from high velocity impact from balls. *Weight-bearing injuries* are more specific to gymnasts, and they result from excessive compressive and rotational forces across the wrist (Howse 1994).

Sports-specific biomechanical injury depends on the unique characteristics that place a particular structure at risk for injury during a sporting activity. In carpal bone injury for example, a fall on outstretched hand during rollerblading or skating or a hand plant during a gymnastics move may directly result in a fracture. The chronic use and movements in racquet sports, golf and baseball require the carpus to resist torque stress. Depending on the strength of the weakest link, the hyperpronation-supination activity in the modern golf swing can result in either an acute or chronic injury.

13.4.2 Fractures

Wrist fractures are common in sports, usually occurring during a fall on the outstretched hand. Depending on the patient's age, bone density and reaction time, this type of fall can result in different injuries, such as fractured scaphoid, scapholunate dislocation or distal radius fracture. Fractures may also be caused by direct trauma, e.g. impact with a helmet during American football. The angle at which the wrist hits

the ground may also determine the type of injury. The more dorsiflexed the wrist is, the more likely the scaphoid bone will break. With less wrist dorsiflexion, it is more likely that the radius will break.

13.4.2.1 Radial Fractures

Fractures to the distal end of radius are typically caused by a fall on the pronated dorsiflexed hand. On striking a hard surface, the hand becomes fixed while the momentum of the body produces two forces, namely: a twisting force causing excessive supination of the forearm, and a compression force which acts vertically through the carpus to the radius. The type of fracture is also dependent on whether the hand is in radial or ulnar flexion at the moment of impact (Masciocchi et al. 2001). Distal radial fractures are often associated with ulnar fractures. Distal radial fractures may be extra- or intra-articular, and displaced or undisplaced (Fig. 13.4).

13.4.2.2 Scaphoid Fractures

Stress fractures of the scaphoid have been reported to be due to repetitive loading of the wrist in dorsiflexion, occurring to sportsmen such as gymnasts and shot-putters (Hanks et al. 1989). On magnetic resonance (MR) imaging, the presence of edema without a visible fracture line may represent a bone bruise or a stress reaction (Fig. 13.5).

13.4.2.3 Hamate Fractures

Hamate fractures are relatively common in athletes. They may be either isolated or associated with more widespread injury such as carpometacarpal dislocation or pisiform fracture. These fractures are most commonly classified into hook or body of hamate fractures. Isolated fracture to the body of the hamate is less common. It is due to a direct force such as a punch- press injury, falling on a hyperdorsiflexed and ulnar- deviated wrist, or posterior dislocation or subluxation of the fourth and/or fifth metacarpal.

A fractured hook of hamate is less common compared to the scaphoid fracture. It is often not diagnosed because it is not apparent on standard radiographic views. This is commonly an isolated injury and is the most common type of hamate fracture. It may occur when a patient falls while holding objects, and the object lands between the ground and ulnar side of palm. Falling on an outstretched hand that

Fig. 13.4a–c. Extra-articular distal radial fracture. **a** 3D CT image shows a displaced extra-articular radial fracture that was immobilized in a plaster cast. **b,c** CT image manipulation allowed virtual removal of the cast and rotation of images to better show the fracture

a b

Fig. 13.5a,b. Rower who fell onto her outstretched hand and had persistent wrist pain. **a** PA radiograph shows obliteration of the fat stripe adjacent to the scaphoid but no fracture is seen. **b** Coronal T2-W MR image shows hyperintense signal within the scaphoid. Similar changes of marrow edema are present in the radial styloid tip. These changes represent bone bruises. Midcarpal joint effusion is also seen. Follow-up radiograph did not reveal a fracture

impacts the ulnar side of the wrist may also result in fracture of the hamate hook, as a result of direct trauma. This injury occurs in individuals who are involved in a sport involving a bat, club or racquet.

In baseball batters, golfers and tennis players, this fracture is caused by the impact of the handle of the bat, club or racquet against the hook of the hamate. The fracture occurs when a bat hits a ball, when a golf club catches the ground, or when a racquet is swung (Futami et al. 1993). There is some controversy as to whether these fractures result from shear forces transmitted through ligamentous insertions as the wrist is forcibly hyperextended while gripping an object (Stark et al. 1977). In sports such as baseball, hockey and golf, hamate fractures usually occur in the non-dominant hand. In racquet sports, fractures affect the dominant hand.

13.4.2.4 Lunate Fractures

The lunate, being the fulcrum of the proximal carpal row, is frequently exposed to traumatic forces to the wrist. Kienbock's syndrome or osteonecrosis of the lunate is thought to be due to repetitive microtrauma and is associated with negative ulnar variance. Lunate fractures are uncommon. When occurring through the body, they are caused by compressive action between the radius and capitate. When occurring through one of the horns, they are due to ligamentous avulsion. (Masciocchi et al. 2001).

13.4.3 Wrist Instability

Injuries to the ligaments can alter the wrist kinematics, leading to instability and early post-traumatic degenerative arthritis. These injuries are usually the result of a single traumatic event. Physical findings are often equivocal. Imaging is important as diagnosis of a significant ligamentous injury will dictate treatment. Partial ligamentous injury is treated by cast immobilization, while complete disruptions may require early surgery to prevent long-term degenerative arthritis (Schlegel et al. 1999).

Wrist instability most commonly results from ligamentous disruption between bones of the proximal carpal row. Scapholunate (SL) and lunotriquetral (LT) dissociations are forms of this instability pattern, with SL instability being the most common. Patients with these injuries have a high degree of pain, even

though the initial radiographs may appear normal. A gap exceeding 3 mm in the scapholunate joint is considered abnormal. This injury should be suspected in patients with wrist effusion and pain that is seemingly out of proportion to the injury (Gilula and Yin 1996).

Patients with LT injuries typically present with ulnar-sided wrist pain after high-energy impaction to the wrist (Fig. 13.6). LT stability is most dependent on the following structures: palmar portion of the LT interosseous ligament, dorsal radiocarpal ligament, and dorsal intercarpal ligament. LT injuries without instability respond well to immobilization. Acute LT injuries with instability and chronic LT injuries can be treated arthroscopically (Weiss et al. 2000). Carpal instability can also occur due to loss of the normal ligamentous restraints between the carpal row, for example, ulnar midcarpal instability. Treatment depends on the specific type and degree of carpal disruption and the presence or absence of degenerative changes (Cohen MS 1998).

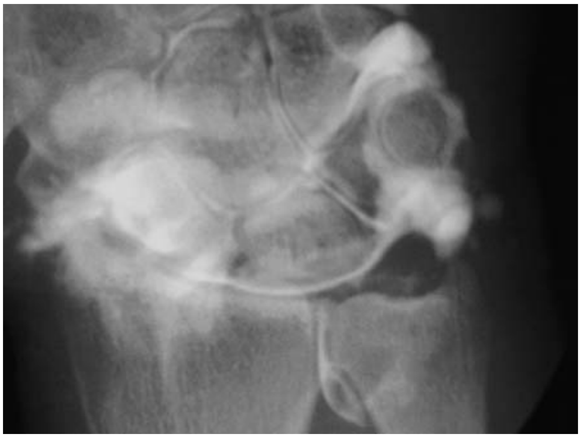

Fig. 13.6. Conventional arthrogram using a single radiocarpal injection shows a class 1A TFCC tear as well as a LT tear, with contrast leakage into the midcarpal compartment

13.4.4 Post-traumatic Deformity Patterns

Post-traumatic deformity patterns cause the lunate to lose its linear relationship with the capitate and to tilt dorsally or volarly, resulting in a collapse deformity. The most common collapse deformity is caused by the lunate dorsiflexing on the radius. This is compensated by the capitate flexing volarly, and is known as dorsiflexed intercalated segment instability pattern (DISI). DISI normally occurs in unrecognized scaphoid subluxations or scaphoid fractures. Volar intercalated segment instability pattern (VISI) can be seen in healthy patients with lax ligaments but post-traumatically, it is due to the lunate flexing volarly on the radius as the capitate tilts dorsally (Linscheid et al. 1972; Lichtman and Alexander 1997). VISI is a sign of midcarpal instability or lunotriquetral injury.

13.4.5 TFCC Injuries

TFCC injuries are quite common in athletes because of the high loads placed on the ulnar side of the wrist, especially in patients with ulnar-neutral and ulnar-positive variance. Lesions of the TFCC may be confined to the TRC disc, or involve one or more components of the TFCC. There may also be associated DRUJ instability. Injuries to the TFCC can occur during acute trauma or repetitive stress. Acute tears may be due to axial loading of the distal radius, such as a fall onto the outstretched hand, leading to proximal radial shift and tearing of the TFCC over the ulnar head. Sudden excessive pronation or supination may also cause TFCC disruption.

TFCC tears should be suspected in patients with ulnar-sided wrist pain and tenderness (Fig. 13.7).

Fig. 13.7. Boxer who developed sudden ulnar-sided wrist pain following a punch. He also had limited pronation-supination and joint line tenderness. Coronal GRE MR image shows a complex tear of the TFCC

On physical examination, there may be localised tenderness over the TFCC, with pain on pronation and supination. With rotation of the forearm, a palpable or audible click may be present. The Palmer classification of TFCC tears divides TFCC tears into traumatic (classes 1A–D) and degenerative (classes 2A–E) types (Palmer 1989). Traumatic tears are usually linear and occur at the edges of the TFCC at either the soft tissue attachments or attachment to the distal radius. Degenerative tears generally occur in ulnar impaction syndrome, in older people, and in the midportion of the TFC disc.

13.4.6 Tendon Injuries

De Quervain's tenosynovitis (or De Quervain's disease) is a common injury in racquet sport and in athletes who use a lot of wrist motion, especially repetitive rotating and gripping. Overuse of the hand in these sports may eventually result in irritation or swelling of the tendons found along the thumb side (1st dorsal compartment) of the wrist, with resultant tenosynovitis. Releasing an object with a sudden twist-and-snap action will trigger tendinitis, e.g., in bowling, weightlifting and rowing. Most closed tendon injuries, if seen acutely, can be treated successfully with nonoperative management. Those that are undiagnosed and untreated may result in permanent instability (Aronowitz and Leddy 1998). Extensor carpi ulnaris tendinosis is the second most common type of sports-related closed tendon injury. Extensor carpi ulnaris tendinosis is most commonly seen in basketball players and those playing racquet sports. Inflammation of tendons is the most frequent abnormality found on US of the wrist. Tenosynovitis involves mainly the peritendinous synovial sheath covering the tendons. Hypertrophic-exudative tenosynovitis is seen as thickening of the tendon sheath that is distended by a hypoechoic effusion (Fig. 13.8). Tendon rupture and its severity can also be detected on US.

13.4.7 Neurovascular Injuries

Neurovascular syndromes in the wrist are uncommon occurrences in athletes (Rettig 1990). Most sports-related peripheral neuropathies in the distal upper limb are compressive in nature. These result from overuse or overload superimposed on normal or variant anatomy. Nerve damage is often caused by external pressure from handles of racquets, sticks and bats, or by pressure from leaning on bicycle handlebars. Neurologic syndromes are usually incomplete, and patients typically have subjective complaints of pain or vague sensory disturbances (Weinstein and Herring 1992). Carpal tunnel syndrome is a neuropathy that is encountered in sports and is caused by median nerve compression in the carpal tunnel. Paralysis of the ulnar nerve at the wrist is seen among cyclists, usually as a result of poor bicycle set-up, causing weakness of grip and numbness of the ulnar 1.5 digits (Lorei and Hershman 1993). Timely recognition, diagnosis, and appropriate treatment of neurovascular injuries are vital in order to avoid potential risk for permanent injury (Nuber et al. 1998).

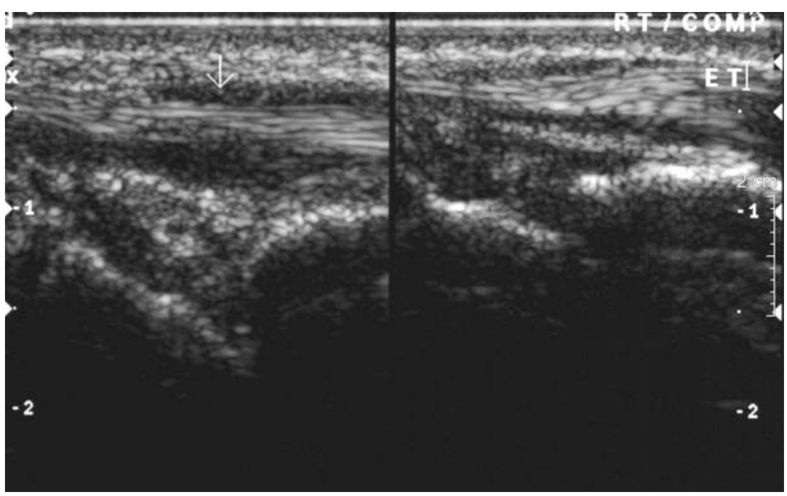

Fig. 13.8. Male gymnast presenting with pain over the dorsal aspect of his wrist on extension. Longitudinal US image shows synovial thickening of the common sheath of the extensor tendons of the index, middle and ring fingers, as well as effusion, consistent with tenosynovitis

13.5 Specific Types of Sports Injuries

Many sporting activities produce a specific injury pattern related to the actions and stresses peculiar to that particular activity. Knowledge of the sport or recreational activity can therefore aid in the diagnosis and management of injury patterns. We have highlighted some popular and emerging sports, and attempted to group sports injuries of the wrist according to their common mechanisms of injury. Knowledge of the biomechanics behind a particular sporting activity is useful for understanding the pathophysiology of wrist injury and helps explain the findings seen at imaging (Jacobson et al. 2005).

13.5.1 Golf, Baseball and Racquet Sports

Wrist injuries that are common to golf, baseball and racquet sports include hook of hamate fractures, ulnar neuropathies, and tendon injuries. All these sports entail gripping an implement such as a bat, club or racquet to strike a ball. When a bat hits a ball, a racquet makes contact with a ball or hard surface, or a golf club catches the ground, the hypothenar eminence of the palm is forcefully struck. This may result in a hook of hamate fracture (Fig. 13.9). In baseball and golf, the hamate fractures usually occur in the non-dominant hand, while fractures to the dominant hand tend to occur in racquet sports such as tennis and squash.

Among golfers, the wrist is one of the most commonly injured anatomic locations and can affect average golfers as well as high-level professionals. A study of 225 professional golfers showed a 34% incidence of wrist and hand injuries involving the soft tissue, cartilage, bone, nerve and vascular structures (McCarroll 1986). Hand and wrist injuries are more common among professionals, compared to amateurs, and are frequent in both male and female professional golfers (Batt 1992, 1993; McCarroll 1996; Gosheger et al. 2003; Wiesler and Lumsden 2005).

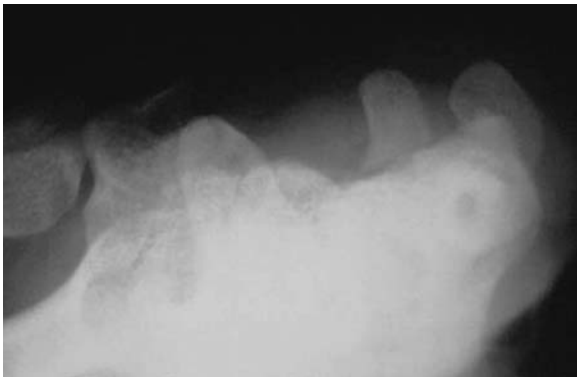

Fig. 13.9. Carpal tunnel radiographic projection shows a transverse fracture of the hook of hamate

When they occur, wrist injuries can be devastating for the avid golfer, as the hand and wrist are integral to this game. The majority of golf injuries are overuse injuries of the wrist flexor or extensor tendons. The left wrist in the right-handed golfer is the most common location. Excessive motion of the left wrist, along with a catapulting action, accounts for the vulnerability of the left wrist to injury. Hyperextension and radial deviation of the right wrist may cause an impingement syndrome. Injury may also be sustained during impact of the swing phase (Murray and Cooney 1996).

Professional and weekend golfers, although showing a similar overall anatomic distribution of injuries by body segment, tend to have differences in the ranking of injury occurrence by anatomic site. These differences can be explained by their playing habits and the biomechanical characteristics of their golf swings (Theriault and Lachance 1998). Golfing injuries are usually the result of overuse due to excessive practice, poor conditioning, excessive play, or poor swing mechanics that put the wrist at risk. Increased risk factors include previous injury, advancing age and anatomic abnormalities. In addition to producing new injuries, golf may also cause re-ignite old injuries and exacerbate pre-existing degenerative disease (Batt 1992, 1993; Wiesler and Lumsden 2005). TFCC injuries may also be seen in golfers. Increased motion of the wrist that occurs in golfers makes this structure prone to tearing.

Soft tissue injuries in racquet sports include those due to direct impact of the handle, as well as repetitive stretching that occurs as the wrist is forcefully whipped into extremes of position. Although all the tendons can be affected, tendinosis is most common in the first dorsal compartment, flexor carpi ulnaris, flexor carpi radialis, and extensor carpi ulnaris. Ligamentous tears can result in instability patterns which if untreated, may become chronic. Neurovascular structures may be compromised by repetitive blunt trauma to these structures or by entrapment by surrounding structures (Osterman et al. 1988).

Tennis is a popular racquet sport, with players frequently beginning to play in childhood and continuing into late adulthood. Most wrist injuries in tennis are due to chronic overuse rather than acute direct trauma (Rettig 1994) (Fig. 13.10). The most common types of injury in tennis players of all ages are muscle sprains and ligament sprains secondary to overuse. These are a particular problem in the adolescent age group because these athletes generally play at a lower level of physical conditioning. Fortunately, injuries in younger players are usually not longstanding and the chronic overuse problems seen in older players are less common in younger players (Bylak and Hutchinson 1998).

Young tennis players should aim at prevention of overuse injuries. Principles of a gradual, progressive increase in the intensity of tennis practice, the slow introduction of new court surfaces, and a staged progression in the teaching of tennis skills can help to reduce the incidence of injury in young tennis players (Bylak and Hutchinson 1998). The goal of early recognition and treatment of wrist injuries is to restore the wrist to a pain-free stable unit with a normal range of motion, so as to allow early return to athletic activity and prevent development of chronic discomfort or permanent disability (Rettig 1994; Osterman et al. 1988).

Ulnar-side wrist pain can be disabling in sports such as golf and tennis due to limitation of pronation-supination. Erosion of the floor of the sixth dorsal space should be considered as a possible cause of unresponsive ulnar-side wrist pain and should be suspected when severe ulnar-sided pain persists in athletes after the usual methods of treatment (Carneiro et al. 2005).

13.5.2 Gymnastics

Gymnastics places high demands on the upper extremity, and is unique in that it requires the athlete to use the upper extremities repetitively as weight-bearing structures, such that high impact loads are distributed through the elbow and wrist joints. Chronic overuse injury may therefore occur in the physis of skeletally-immature gymnasts (Gabel 1998). In gymnasts, the wrist is a frequent site of symptoms and injury, both acute and chronic. The gymnast may present with wrist pain secondary to repetitive hyperextension and overuse (Fig. 13.11). The gymnast wrist pain syndrome may present as a difficult diagnostic and therapeutic challenge. It is debilitating, resulting in a reduction in training and performance, and may be due to a response to repetitive trauma during the period of growth and development. The risk of gymnastic injuries is proportional to the competitive level of the athletes. The higher the level, the more hours are spent in practice, with a greater exposure time. With the increased risk in gymnastics, the incidence of acute injuries also increases. As the skill level increases, the load during workouts also increases, providing more opportunity for chronic injuries (Dobyns and Gabel 1990; Meeusen and Borms 1992).

Fig. 13.10a–c. Ulnar impaction syndrome in a tennis player. **a** PA radiograph shows positive ulnar variance. **b** Coronal STIR MR image shows a small focus of hyperintense signal in the ulnar aspect of the proximal lunate, due to ulno-lunate impaction. **c** Coronal GRE MR image shows an ulnar-sided TFCC tear

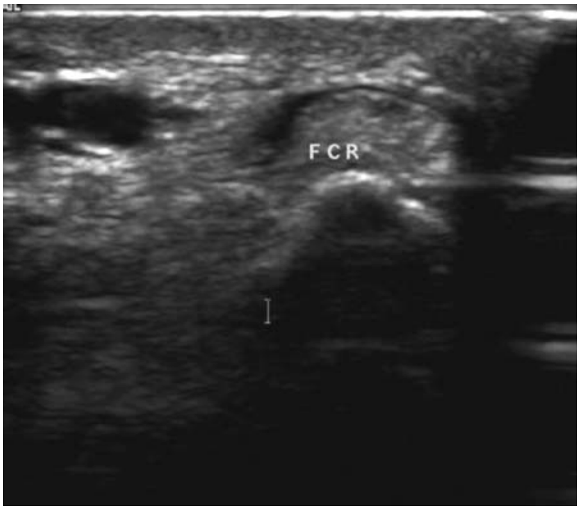

Fig. 13.11. Overuse injury in a male gymnast with left wrist pain. Transverse US image shows mild thickening of the common sheath of the extensors and flexor carpi radialis, consistent with tenosynovitis

An extensive review of the literature of gymnastic injury in the pediatric population revealed that the incidence and severity of injuries is relatively high, particularly among advanced-level female gymnasts. Overuse and non-specific pain conditions of the wrist occurred frequently among these gymnasts. Factors associated with an increased injury risk among female gymnasts included greater body size and body fat, periods of rapid growth, and increased life stress (Caine and Nassar 2005). A cross-sectional survey of 52 non-elite gymnasts (32 girls, 20 boys; average age 11.8 years) showed that wrist pain was common, occurring in 73% of gymnasts. Gymnasts with wrist pain were older, trained more hours per week, trained at a higher skill level, and began training at an older age (DiFiori et al. 1996) (Fig. 13.12).

A three-year prospective epidemiologic study of 178 competitive female gymnasts revealed an injury rate was 30/100 gymnasts/year and 52 injuries/1000 h. Injury rates excluding risk exposure increased with competitive level, but the top- level gymnasts had the lowest rate per 1000 h of practice. Fractures of the wrist, fingers and toes were most common, with nearly 40% of the sudden-onset injuries occurring in the floor event. "Missed move" was most frequently cited as the injury mechanism, while somersaults and handsprings were the most frequent injury-producing moves (Fig. 13.13). Most injuries happened with moves that were basic or moderately difficult and well-established. There was an increased chance of

Fig. 13.12. Elite gymnast with ulnar-sided wrist pain. PA radiograph shows a well-corticated bony fragment at the tip of the ulnar styloid process due to previous trauma. There is bony overgrowth, causing ulnar-sided mechanical problems

Fig. 13.13. Male gymnast who missed his landing and developed soreness over the radial aspect of his wrist. Radiographs were normal (not shown). Coronal T2-W MR image shows diffuse hyperintense signal in the scaphoid but no fracture line is seen, consistent with a bone bruise

injury when the gymnast had been on the apparatus for an extended period of time; hence loss of concentration was regarded as a major source of injury (Lindner and Caine 1990).

To determine the frequency and characteristics of wrist pain in young, non-elite gymnasts and to describe the effects of chronic wrist upon gymnastics training, a prospective cohort study of 47 non-elite female and male gymnasts between 5 and 16 years of age was performed. Wrist pain was reported by 57% (27/47) of subjects at the study onset. Both at the study onset and one year later, 89% (24/27) reported wrist pain. The floor exercise, the pommel horse, and the balance beam were most frequently associated with wrist pain symptoms. Of subjects with wrist pain at each survey, 42% reported that the symptoms interfered with training. Adolescent gymnasts between 10 and 14 years of age training at non-elite level were found to be more likely to have wrist pain (DiFiori et al. 2002a).

Gymnast's wrist injury results from repetitive and excessive loading on the joint, leading to premature closure of the growth plates and other growth disturbances. Repeated stresses affect the distal radial growth plate, causing undergrowth of the radius, and a resultant ulnar-plus variance, which may become symptomatic (Fig. 13.14). Radiographs show physeal irregularities and bony sclerosis. If untreated, radial deformity and shortening may occur, leading to permanent deformity. De Smet et al. (1993) presented six new cases, all of whom had an ulnar-plus variance and an increased sagittal angle of the distal radial epiphysis. Five of the gymnasts elected to stop their sports careers, while one was successfully treated with an arthroscopic TFCC debridement. Epiphysiodesis of the distal radial and ulnar growth plates has been used to surgically treat a skeletally- immature gymnast in order to prevent Madelung's deformity (Bak and Boeckstyns 1997).

The radiographic appearances of chronic stress injury to the wrist joint consist of bilateral, asymmetrical widening and irregularity of the distal radial growth plates, with ill-defined cystic areas, sclerosis and flaring of the metaphyses. Similar but less marked changes are seen in the distal ulnar growth plates (Fig. 13.15). The etiology is thought to be a Salter-Harris type I stress fracture of the growth plate due to chronic repetitive shear forces applied to the hyperextended wrist joint. Rapid healing of the stress fracture occurs with cessation of the sporting activity but continued strenuous use of the wrist results in further widening and irregularity of the growth plate

a

b

Fig. 13.14a,b. Female gymnast with left wrist pain and tenderness at the DRUJ on dorsiflexion. **a** PA radiograph shows stress changes adjacent to the distal radial and ulnar growth plates. **b** Coronal GRE MR image shows a central perforation of the TFCC. Positive ulnar variance is better seen on the MR image

a b

Fig. 13.15a,b. Female adolescent gymnast with stress changes to both distal forearm bones. PA radiographs of the (**a**) right and (**b**) left wrists show sclerosis and patchy cystic areas adjacent to the distal radial growth plates. Similar but milder changes are present in the distal ulna

(Carter et al. 1988). On MR imaging, fractures and stress fractures are identified as hypointense fracture lines, surrounded by patchy areas of T1-hypointensity and T2-hyperintensity representing edema (Peh et al. 1996; Breitenseher et al. 1997). The presence of edema without a visible fracture line may represent a bone bruise or a stress reaction. Stress injuries related to growth plates of the distal radius and ulna may be seen in adolescent gymnasts (Shih et al. 1995) (Fig. 13.16).

In a follow-up study of 21 young, high-performance gymnasts with stress changes related to the distal radial epiphysis, 11 of the gymnasts who presented with radiographic changes of the distal radial epiphysis took at least 3 months to recover. In comparison, 10 gymnasts who had similar symptoms but no radiographic changes recovered within an average of 4 weeks. The radiographic changes were considered to represent stress changes, possibly stress fractures, of the distal radial epiphysis (Roy et al. 1985).

A radiographic survey to determine skeletal age and the nature and prevalence of stress-related changes affecting the distal radial growth plate in 60 young competitive gymnasts (39 females, 21 males) revealed a significant delay in maturation for girls. It was found that the widening and irregularities of the distal radial physis appear to be the first in a spectrum of abnormal changes secondary to overuse, and probably represented a stress fracture of the distal radial growth plate. The authors concluded that the radiographic changes associated with this injury were not the normal adaptive changes seen in young, competitive gymnasts. More serious long-term abnormality may result even though the injury may initially resemble a Salter-Harris type I or II stress fracture. Long-term complications may include symmetrical or asymmetrical retardation or halted growth at the affected site, positive ulnar variance, and associated pathoanatomic sequelae (Caine et al. 1992).

Albanese et al. (1989) reported three cases in which wrist pain developed in skeletally-immature competitive gymnasts. In all three cases, there was radiographic evidence of premature growth plate closure, resulting in shortening of the radius and alterations in the normal distal radioulnar articulation. Repetitive compressive loading of the distal growth plate of the radius was proposed as potential etiology of this condition. Vender and Watson (1988) described bilateral closure of the ulnar side of the distal radius epiphyseal plate in a patient with a history of high-level gymnastic training. Cumulative microtrauma to the ulnar side of the distal radius epiphyseal plate may cause premature closure, leading to a Madelung-like deformity.

A cross-sectional study of 59 gymnasts (28 girls and 31 boys; average age 9.3 years) revealed that wrist pain was reported by 56% (33/59) of the gymnasts, with 45% (15/33) describing pain of at least 6 months duration. Factors significantly associated with wrist pain included higher skill level, older age, and more years

Fig. 13.16. Predominant ulnar stress changes in an elite female gymnast with wrist pain. Coronal STIR MR image shows prominent areas of hyperintense signal at the distal radius and ulna, more marked in the ulna. Midcarpal joint effusion is also present

of training. A total of 51% (30/59) of the gymnasts had findings of stress injury to the distal radial physis, and 7% had frank widening of the growth plate. Wrist pain prevalence was significantly related to the grade of radiographic injury. Mean ulnar variance was significantly more positive than established norms. Ulnar variance was not associated with wrist pain or radiographic injury of the distal radial physis. The authors concluded that radiographic findings of distal radial physeal injury are associated with wrist pain among young non-elite gymnasts (DiFiori et al. 2002b).

In a study undertaken to define and characterize factors contributing to the causes and development of gymnast wrist pain and to establish an effective means of systematic and comprehensive evaluation and treatment, 75% of 38 collegiate gymnasts were found to have wrist pain for at least 4 months. The males averaged 2.82±1.94 mm positive ulnar variance and the females averaged 1.44±1.88 mm positive ulnar variance; with all of the gymnasts having significantly greater variance than the controls, who averaged –0.52 mm. The pommel horse routine was consistently responsible for wrist pain among the males. Anatomical and histological correlation of cryosections with MR imaging performed to establish the usefulness of MR imaging in the diagnosis of wrist pain showed that MR imaging was able to differentiate the complex transitions between cortical and trabecular bone, articular surfaces, the ligaments, and the TFCC of the wrist joint (Figs. 13.13, 13.14 and 13.16). Arthroscopic findings correlated well with those of MR imaging and arthrography, with arthroscopic surgery being a successful mode of treatment (Mandelbaum et al. 1989).

To determine the prevalence of chronic wrist injuries among adolescent gymnasts and the consequences of repetitive stress, students of a Chinese opera school underwent radiography of both wrists and answered a questionnaire. They were separated into study (261) and control (63) groups, according to participation in or abstinence from exercise training, respectively, and were further separated into fused and unfused physis subgroups. An increase in both mean ulnar variance and frequency of ulnar-plus variance was noted in the study subgroups, with 8.2% (14/170) of wrists of the fused physis study subgroup having an exceedingly large ulnar-plus variance. A total of 17.3% (61/352) of wrists had abnormal morphology of the distal radius in the unfused physis study subgroup. Widening of the physis was the most common finding. The authors concluded that chronic, repetitive stress in the wrists of adolescent gymnasts results in a localized growth disturbance of the distal radius with resultant ulnar-plus variance (Chang et al. 1995).

To assess the prevalence of stress injury to the distal radial growth plate and of positive ulnar variance in a non-elite gymnast population, a radiographic survey was performed in 44 skeletally-immature non-elite gymnasts consisting of 27 girls and 17 boys. Radiographic findings consistent with stress injury of the distal radial physis were found in 25% (11/44) of participants. Ulnar variance was found to be more positive in the gymnasts when compared with age-predicted norms, with an average side-to-side difference in ulnar variance of 0.9 mm. Radiographic findings of stress injury to the growth plate and the amount of ulnar variance were not associated with age, sex, training intensity, wrist pain, height, or weight. There was also no significant relationship between ulnar variance and radiographic findings. It also appears that ulnar variance is more positive than would otherwise be predicted, suggesting growth inhibition of the distal radius, a growth stimulation of the ulna, or a combination of both (DiFiori et al. 1997). Tolat et al. (1992) described five teenage female gymnasts who had symptomatic acquired positive ulnar variance occurring due to premature physeal closure of

the growth plate. All cases demonstrated ulnocarpal impingement, and arthroscopic assessment of the wrist allowed assessment of the integrity of the TFCC and helped decide on the most appropriate surgery such as distal ulna resection and shaving for a TFCC perforation.

The ulnar variance in female gymnasts attending the 1987 Artistic Gymnastics World Championship was measured, showing a marked increase in the ulnar length in adult as well as immature gymnasts, compared with non-athletes. The changes in relative ulnar length were correlated to weight, height, and skeletal age of the athletes. In 10% of the gymnasts' wrists, stress-related changes of the distal physis of the radius were noted. The authors concluded that repetitive injury and compression of the wrist lead to a premature closure of the distal radial growth plate resulting in secondary ulnar overgrowth (De Smet et al. 1994). Interestingly, contradictory results appeared in another study using the PA radiographs of 201 female participants of the 1987 Artistic Gymnastics World Championships. This study showed that female gymnasts who demonstrated ulnar overgrowth were skeletally more advanced in maturity status of the entire hand-wrist compared with gymnasts who did not show ulnar overgrowth. The authors concluded that ulnar overgrowth was not associated with advanced maturity of the distal radial epiphysis as defined in protocols for assessing skeletal maturity and did not lead to premature epiphyseal closure of the distal radius (Beunen et al. 1999).

13.5.3 Rowing/Canoeing, Volleyball and Basketball

Overuse of the hand in sports such as rowing, volleyball and basketball may eventually result in irritation or swelling of the tendons of the wrist, with resultant tenosynovitis.

Rowing has gained considerable popularity in recent years. Rowers hail from a wide spectrum of age groups. Rowing is an endurance activity with no sudden accelerations or ballistic impact forces. It is associated with several injuries that are so typical that they are easily recognized and in many cases, do not require imaging. Injuries of the forearm and wrist are common in rowing. These include wrist tenosynovitis and the intersection syndrome (Fig. 13.17). Knowledge of the basic rowing physiology and equipment, the mechanics of the rowing stroke, and training habits will make those involved in patient management better equipped to diagnose, treat and prevent injuries in rowers (McNally et al. 2005; Rumball et al. 2005).

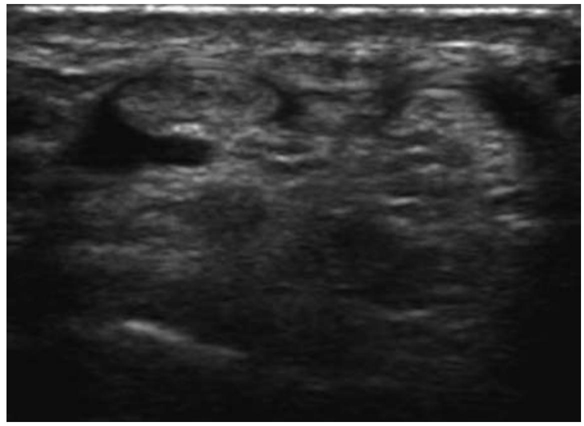

Fig. 13.17. Rower with painful right-sided intersection syndrome . Transverse US image shows increased fluid within the combined tendon sheath of the abductor pollicis longus and extensor pollicis brevis, as well the tendon sheath to the extensor carpi radialis longus. The tendons themselves are normal. Findings are consistent with tenosynovitis

Du Toit et al. (1999) investigated the incidence and causes of acute tenosynovitis in long-distance canoeists, and found that an average of 23% of competitors in each race developed this condition. The incidence was significantly higher in the dominant than in the non-dominant hand but was unrelated to the type of canoe and the angle of the paddle blades. Canoeists who covered more than 100 km a week for eight weeks preceding the race had a significantly lower incidence of tenosynovitis than those who trained less. Environmental conditions during racing, including fast flowing water, high winds, and choppy waters, and the paddling techniques, especially hyperextension of the wrist during the pushing phase of the stroke, were both related to the incidence of tenosynovitis. The study suggested that development of tenosynovitis is not related to the equipment used, but is probably caused by difficult paddling conditions, in particular uneven surface conditions, which may cause an altered paddling style. The athlete's level of fitness and the ability to balance a less stable canoe, thereby maintaining optimum paddling style without repeated eccentric loading of the forearm tendons to limit hyperextension of the wrist, appear to be important factors (Du Toit et al. 1999).

Volleyball players are subjected to application of limited multiple trauma to the dorsal radial portion of the wrist. Rossi et al. (2005) studied 45 volleyball players with the diagnosis of de Quervain‘s stenos-

ing tenosynovitis and showed that increased training time and consequent microtrauma may increase the likelihood of this injury. Volleyball players commonly complain of pain in the hypothenar area. Fatigue fracture of the pisiform bone has been suggested as a cause of this incapacity, and can be demonstrated on oblique and carpal tunnel view radiographs of the wrist (Israeli et al. 1982).

Acute basketball injuries often involve the hand and wrist. Extensor carpi ulnaris tendinosis is commonly seen in basketball players (Cohen and Metzl 2000). Tehranzadeh and Labosky (1984) reported using double-contrast wrist arthrography to detect loose intraarticular osteochondral fracture fragments caused by basketball injury. These were subsequently removed surgically.

13.5.4 Cycling/Wheelchair Athletes

Distal peripheral neuropathies have been identified in cyclists because of prolonged grip pressures on handlebars. The so-called cyclist palsy has been postulated to be an entrapment neuropathy of the ulnar nerve in Guyon's canal of the wrist. Wheelchair athletes are also prone to developing hand pain and numbness, due to extremity peripheral nerve entrapment related to prolonged gripping of the wheelchair wheels. Ulnar neuropathy, characterised by tingling, numbness and weakness in the hands is common in serious cyclists, especially following several days of riding (Mellion 1991; Richmond 1994).

Chan et al. (1991) studied the 14 national level competitive cyclists and found that the prevalence of median nerve lesions at the wrist, although usually mild, was found to substantially higher than expected. Electrodiagnosis was recommended as a sensitive detector for neuropathy, even at a subclinical stage. Fracture of the trapezium is a rare injury associated with cycling and may need a special radiographic projection (Bett's oblique view) for visualization (Lilley et al. 2000).

Wheelchair athletes commonly experience hand pain and numbness due to extremity peripheral nerve entrapment. The most common electrodiagnostic dysfunction was of the median nerve at the carpal tunnel (46%), and the portion of the nerve within the proximal carpal tunnel was most frequently affected. Ulnar neuropathy was the second most common entrapment electrodiagnostically (39%) (Burnham and Steadward 1994).

13.5.5 American Football, Horse Riding/Rodeo, Roller-Skating/Rollerblading/Skateboarding

Sporting activities that involve hand contact with a fast-moving heavy ball have potential for injury to athletes. Examples include soccer (as goalkeeper), basketball, netball, volleyball, cricket and rugby (MacGregor 2003). Ball games have been to found to account for the largest number of sports injuries among children in Hong Kong (Maffuli et al. 1996). Fractures and dislocations to the wrist may result from direct blow to hand/wrist (e.g., American football, boxing, rugby) or falls (e.g., horseriding, motocross, soccer, skating, snowboarding, track and field) (Fig. 13.18).

13.5.5.1 American Football

An analysis of injuries from American football clubs in Colorado revealed an incidence of upper extremity injuries that range from 15 to 25%. There were both traumatic and overuse injuries, with involvement of

Fig. 13.18. Male track athlete who sustained a fall. Oblique PA radiograph shows a minimally-displaced fracture of the tuberosity of the scaphoid

the distal forearm and carpus being common in this contact sports. Injuries encountered include distal radial and scaphoid fractures, ligamentous injuries, and TFCC tears (Schlegel et al. 1999). Ellsasser and Stein (1979) reviewed hand injuries in a professional American football team over a 15-year period. A total of 38 players from one professional football team suffered 46 major hand and wrist injuries. The injuries included fractures, dislocations, fracture dislocations, and soft tissue injuries of the phalanges, metacarpals, carpals (particularly the scaphoid), and distal radius/ulna, including intra-articular injuries. Twelve surgical procedures were performed, allowing the players to return to active participation with a minimum loss of practice time.

In a retrospective study of lunate and perilunate carpal dislocations in professional football players in the US National Football League over a five-year period, Raab et al. (1994) reported seven lunate and three perilunate dislocations in ten players. The mechanism of injury was hyperextension in nine of ten players. The study demonstrated that lunate and perilunate carpal dislocations were not career-ending injuries in professional football, although a minimum loss of four weeks of playing time was expected. Treatments varied but none was clearly superior or detrimental, although four of the five players who returned to play in the same season were treated by closed reduction with percutaneous pinning.

13.5.5.2 Horse Riding/Rodeo

Moss et al. (2002) found that upper limb injuries accounted for 29.2% of all horse riding injuries, the majority (85.5%) of whom sustained the injury falling from the horse. The commonest upper limb fractures were distal radial fractures, with scaphoid fractures also being reported. The authors noted that the incidence of upper limb injuries among horse riders appears to be increasing.

Rodeo is regarded as a non-traditional sporting activity that is high-collision in nature. In a radiographic study of 25 male rodeo riders, also known as roughstock athletes, 82 upper limb abnormalities were found. This comprised 24 fractures of the hand and wrist, including 5 non-unions, involving bones such as the scaphoid. There were 14 cases of degenerative joint disease (e.g., radioscaphoid, scapholunate and TFCC), joint calcification, dorsal instability, and scapholunate dissociation (Meyer et al. 2003). Inexperienced competitors have a greater rate of injury to areas such as the hand and wrist (Butterwick and Meeuwisse 2002).

13.5.5.3 Roller-Skating/Rollerblading/Skateboarding

Roller-skating, rollerblading (also known as wheels-in-line skating), skateboarding and scooter-riding are popular recreational and sporting activities among children and adolescents, but have attendant risks and can be associated with skeletal injury (Inkelis 1988). All these activities, being conducted on wheels moving along hard surfaces, involve movement at high speeds and potential for attempts at extreme manoeuvers. Most of these injuries result from falls, with fractures to the distal radius and ulna being common.

Zalavras et al. (2005), in a study of patients who presented to the pediatric fracture clinic of the level I trauma center over a one-year period after sustaining fractures due to skateboarding, roller-skating, and scooter-riding, identified 325 fractures (13.7%) among a total of 2371 fractures. Mean age of patients ranged from 9.7 to 13 years, with a male predominance. The forearm was fractured most often, composing 48.2% of skateboarding fractures, 63.1% of roller-skating fractures and 50.7% of fractures due to scooter-riding. 94% of forearm fractures were located in the distal third. Schieber et al. (1994) found that of approximately 30,863 persons treated for rollerblading injuries, for every rollerblading injury, approximately 3.3 rollerskating and 1.2 skateboarding injuries occurred. The median age of those injured in these three sports was 15, 12, and 13 years, respectively, with wrist fractures and/or dislocations being a common injury.

Powell and Tanz (1996) studied persons with injuries associated with the use of rollerblades or roller-skates reported to the United States Consumer Product Safety Commission (USCPSC) National Electronic Injury Surveillance System in 1992 and 1993. An estimated 66,465 injuries were associated with rollerblades, with the incidence of injury being highest in children aged 11 and 12 years old. There were an estimated 147,928 roller-skating injuries among young people less than 20 years old, with a mean age of 10.5 years. In 1993, the injury rate among children for rollerblades was 31/100,000, and the injury rate for roller-skates was 95/100,000. Distal forearm fractures were the most common injuries related to both rollerblade and roller-skate use.

Orenstein (1996) prospectively studied the types of injuries sustained during the use of rollerblades and compared them with injuries sustained during

the use of roller-skates and skateboards. Minor injuries (sprains, bruises, lacerations) were more common than fractures, and there was no statistical difference in the types of injury between the skate groups. The most common serious injury was fracture of the distal arm, which occurred in each of the three skater groups (43%). Injuries occurred more commonly because the skater was going too fast (35%), because the skater struck an object in the pavement (20%), or because the skater was unable to brake (19%). The authors concluded that injuries sustained by rollerbladers were similar to those sustained by roller skaters and skateboarders, and that the risk of wrist or elbow fracture was greater when wrist guards were not worn.

The most common injury in the increasingly popular recreational activity of rollerblading is a fracture of the distal radius, which comprises 50% of all fractures. Reasons for the increasing number of serious injuries in rollerblading include the fact that the majority of skaters do not wear proper protective equipment and many users cannot handle their in-line skates in dangerous situations (Ellis et al. 1995; Jerosch and Heck 2005). Studies on rollerblading injuries from Europe, Australia and the USA produced similar findings in that majority of victims were male, aged 10–14 years, had fallen, and sustained wrist injuries (Calle and Eaton 1993; Heller et al. 1996; Young et al. 1998; Nguyen and Letts 2001; Mulder and Hutten 2002).

Skateboarding has experienced intermittent periods of popularity since the 1960s. Skateboarding injuries have increased with the rise in popularity of the sport, and the changes to the injury pattern could be expected with the development of both skateboard tricks and the materials used for skateboard construction. Most documented cases occur in boys aged from 10 to 14 years, with injuries ranging from minor cuts and abrasions to multiple fractures and, in some cases, even death (Fountain and Meyers 1996). Forsman and Eriksson (2001) studied 139 people injured in skateboarding accidents, and found that most were children with a mean age of 16 years, with the most common fractures involving the ankle and wrist. Kyle et al. (2002) also found that the most frequent injuries in skateboarding were ankle strain/sprain, followed by wrist fracture.

In a prospective survey of 111 cases of roller-skating injuries, Tse et al. (1987) reported that males were more commonly injured, with the wrist (23%) being the most common region involved. Collision with other skaters and loss of control were the main factors leading to injury. Kvidera and Frankel (1983) studied 35 fractures secondary to roller-skating accidents and found that 28 involved the wrist and elbow. Of the patients, 63% were female, with the 20- to 34-year-old age group the most commonly involved. Most people were either first-time skaters or had not skated since childhood.

Wrist fractures are the most common type of injury in roller-skating, rollerblading and skateboarding. The use of industrially-tested equipment and wearing of protective gear, particularly wrist and forearm guards, are needed. If skaters do not protect themselves adequately, injuries are expected to increase with a rise in the sport's popularity (Kvidera and Frankel 1983; Calle and Eaton 1993; Schieber et al. 1994; Ellis et al. 1995; Powell and Tanz 1996). The American Academy of Pediatrics recommends that children under 5 years of age should not be allowed to ride skateboards. At an early age, injuries may occur due to reasons such as high centre of mass, immature skeletal development, an undeveloped neuromuscular system, and simply poor judgement (Fountain and Meyers 1996).

13.5.6 Snowboarding and Skiing

Alpine skiing and snowboarding are two of the most popular winter sports in the world, and both have a reputation for an inherently high risk of injury.

Snowboarding involves riding a single board down a ski slope or on a half-pipe snow ramp. The injury profile in snowboarding differs from that of traditional alpine skiing. Compared with injuries resulting from skiing, snowboarding injuries occur more frequently in the upper extremities and ankles, and less frequently in the knees. Snowboarders typically sustain wrist injuries (Young and Niedfeldt 1999; Bladin et al. 2004; Boutin and Fritz 2005) (Fig. 13.19).

In a comparative study of snowboarders and skiers, Matsumoto et al. (2002) found that upper extremity injuries were much more common in snowboarders than in skiers, with upper extremity fractures being three times more common in snowboarders. Wrist fractures were the most common fractures among snowboarders, comprising 62% of all fractures, and were found to have a different underlying cause compared with other upper extremity fractures. Matsumoto et al. (2004) found that the most common events leading to injury were falling (59.6%) and jumping (36.1%).

Different types of snowboard equipment, rider stance and snowboarding activity result in different

a b

Fig. 13.19a,b. Male adult snowboarder who fell while snowboarding. **a** PA radiograph shows disruption of all the carpal arcs. The lunate has an abnormal triangular shape, with overlapping of the LT and capitolunate articular surfaces. **b** Lateral radiographs show that the lunate is dislocated volarly and is rotated such that its distal articular surface faces volarly. Appearances are typical of a lunate dislocation. [Courtesy of Professor Shigeru Ehara, Iwate University, Morioka, Japan]

types of injury. The risk of injury may be lowered by using protective equipment, such as wrist guards, particularly for beginners. Wrist guards have been found to decrease the incidence of wrist injuries in snowboarding (Young and Niedfeldt 1999; Machold et al. 2002; Matsumoto et al. 2002; O'Neill 2003; Made and Elmqvist 2004). O'Neill (2003) tested the protective value during snowboarding of an off-the-shelf wrist guard originally designed for rollerblading, and found it to be effective.

Further information on imaging techniques: (Gilula 1979; Egawa and Asai 1983; Wechsler et al. 1987; Desser et al. 1990; Peh and Gilula 1996; Peh et al. 1996; Breitenseher et al. 1997; Potter et al. 1997; Jacobsen 1999; Scheck et al. 1997; Bottinelli and Campani 2001; Bencardino 2004; Zlatkin and Rosner 2004; Kumar et al. 2005; Schmid et al. 2005).

13.6 Conclusion

Many sporting activities produce a specific injury pattern related to the risks, actions and stresses peculiar to that particular activity. Knowledge of the sport or recreational activity aids in the diagnosis and management of injury patterns (Fig. 13.20). This chapter highlights some popular and emerging sports, and attempts to group sports injuries of the wrist according to their common mechanisms of injury. Imaging has an important role in the evaluation and diagnosis of the range of bone and soft tissue injuries due to various sports. Knowledge of the biomechanics behind a particular sporting activity is useful for understanding the pathophysiology of wrist injury and helps explain the findings seen at imaging.

Things to Remember

1. Many anatomical structures in the wrist may be injured in a wide variety of ways during participation in sports.
2. Many of these sporting activities, whether competitive or recreational, are associated with specific injury patterns related to the actions and stresses associated with that particular sport.
3. Knowledge of the sport biomechanics and imaging features aids in the early diagnosis, identification and prevention of potential complications, management and follow-up of these injuries.
4. It is particularly important to recognize wrist injuries in the immature skeleton of pre-adolescent and adolescent athletes, as continued sporting activity may result in growth arrest and other long-term problems.

a

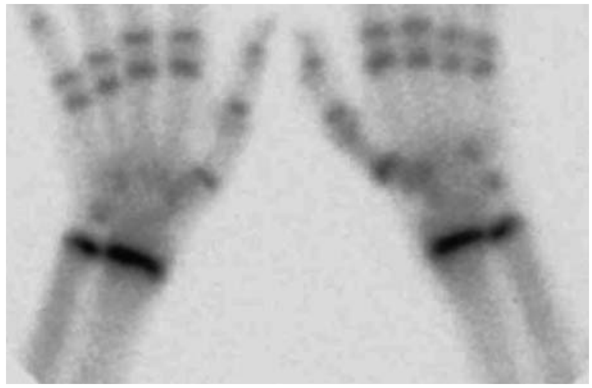

b

Fig. 13.20a,b. Male gymnast with stress changes of the distal radius and ulna bilaterally. **a** PA radiograph of the left wrist shows mild growth plate widening and adjacent sclerotic changes. **b** Bone scintiscan shows increased linear uptake at the distal ends of the radius and ulna bilaterally

References

Albanese SA, Palmer AK, Kerr DR et al. (1989) Wrist pain and distal growth plate closure of the radius in gymnasts. J Pediatr Orthop 9:23–28

Aronowitz ER, Leddy JP (1998) Closed tendon injuries of the hand and wrist in athletes. Clin Sports Med 17:449–467

Bak K, Boeckstyns M (1997) Epiphysiodesis for bilateral irregular closure of the distal radial physis in a gymnast. Scand J Med Sci Sports 7:363–366

Batt ME (1992) A survey of golf injuries in amateur golfers. Br J Sports Med 26:63–65

Batt ME (1993) Golfing injuries. An overview. Sports Med 16:64–71

Bednar MS, Arnoczky SP, Weiland AJ (1991) The microvasculature of the triangular fibrocartilaginous complex: its clinical significance. J Hand Surg Am 16:1101–1105

Bencardino JT (2004) MR imaging of tendon lesions of the hand and wrist. MRI Clin N Am 12:333–347

Beunen G, Malina RM, Claessens AL et al. (1999) Ulnar variance and skeletal maturity of radius and ulna in female gymnasts. Med Sci Sports Exerc 31:653–657

Bladin C, McCrory P, Pogorzelski A (2004) Snowboarding injuries: current trends and future directions. Sports Med 34:133–139

Bottinelli O, Campani R (2001) Ultrasound of the hand. In: Guglielmi G, Van Kuijk C, Genant HK (eds) Fundamentals of hand and wrist imaging. Springer, Berlin Heidelberg New York, pp 63–74

Boutin RD, Fritz RC (2005) MRI of snow skiing and snowboarding injuries. Semin Musculoskeletal Radiol 9:360–378

Breitenseher MJ, Metz VM, Gilula LA et al. (1997) Radiographically occult scaphoid fractures: value of MR imaging in detection. Radiology 203:245–250

Brudvik C, Hove LM (2003) Childhood fractures in Bergen, Norway: identifying high-risk groups and activities. J Pediatr Orthop 23:629–634

Burnham RS, Steadward RD (1994) Upper extremity peripheral nerve entrapments among wheelchir athletes: prevalence, location, and risk factors. Arch Phys Med Rehabil 75:519–524

Butterwick DJ, Meeuwisse WH (2002) Effect of experience on rodeo injury. Clin J Sport Med 12:30–35

Bylak J, Hutchinson MR (1998) Common sports injuries in young tennis players. Sports Med 26:119–132

Caine DJ, Nassar L (2005) Gymnastics injuries. Med Sports Sci 48:18–58

Caine D, Roy S, Singer KM et al. (1992) Stress changes of the distal radial growth plate. A radiographic survey and review of the literature. Am J Sports Med 20:290–298

Calle SC, Eaton RG (1993) Wheels-in-line roller skating injuries. J Trauma 35:946–951

Carneiro RS, Fontana R, Mazzer N (2005) Ulnar wrist pain in athletes caused by erosion of the floor of the sixth dorsal compartment: a case series. Am J Sports Med 33:1910–1913

Carter SR, Aldridge MJ, Fitzgerald R et al. (1988) Stress changes of the wrists in adolescent gymnasts. Br J Radiol 61:109–112

Chan RC, Chiu JW, Chou CL et al. (1991) Median nerve lesions at wrist in cyclists. Zhonghua Yi Xue Za Zhi (Taipei) 48:121–124

Chang CY, Shih C, Penn IW et al. (1995) Wrist injuries in adolescent gymnasts of a Chinese opera school: radiographic survey. Radiology 195:861–864
Cohen AR, Metzl JD (2000) Sports-specific concerns in the young athlete: basketball. Pediatr Emerg Care 16:462–468
Cohen MS (1998) Ligamentous injuries of the wrist in the athlete. Clin Sports Med 17:533–552
Damore DT, Metzl JD, Ramundo M et al. (2003) Patterns in childhood sports injury. Pediatr Emerg Care 19:65–67
De Smet L, Claessens A, Fabry G (1993) Gymnast wrist. Acta Orthop Belg 59:377–380
De Smet L, Claessens A, Lefevre J et al. (1994) Gymnast wrist: an epidemiologic survey of ulnar variance and stress changes of the radial physis in elite female gymnasts. Am J Sports Med 22:846–850
Desser TS, McCarthy S, Trumble T (1990) Scaphoid fracture and Kienbock's disease of the lunate: MR imaging with histopathologic correlation. Magn Reson Imag 8:357–361
DiFiori JP, Puffer JC, Mandelbaum BR et al. (1996) Factors associated with wrist pain in the young gymnast. Am J Sports Med 24:9–14
DiFiori JP, Puffer JC, Mandelbaum BR et al. (1997) Distal radial growth plate injury and positive ulnar variance in nonelite gymnasts. Am J Sports Med 25:763–768
DiFiori JP, Puffer JC, Aish B et al. (2002a) Wrist pain in young gymnasts: frequency and effects upon training over 1 year. Clin J Sport Med 12:348–353
DiFiori JP, Puffer JC, Aish B et al. (2002b) Wrist pain, distal radial physeal injury, and ulnar variance in young gymnasts: does a relationship exist? Am J Sports Med 30:879–885
Dobyns JH, Gabel GT (1990) Gymnast's wrist. Hand Clin 6:493–505
Du Toit P, Sole G, Bowerbank P et al. (1999) Incidence and causes of tenosynovitis of the wrist extensors in long distance canoeists. Br J Sports Med 33:105–109
Egawa M, Asai T (1983) Fractures of the hook of the hamate: report of six cases and the suitability of computerised tomography. J Hand Surg 8:393
Ellis JA, Kierulf JC, Klassen TP (1995) Injuries associated with in-line skating from the Canadian hospitals injury reporting and prevention program database. Can J Public Health 86:133–136
Ellsasser JC, Stein AH (1979) Management of hand injuries in a professional football team. Review of 15 years of experience with one team. Am J Sports Med 7:178–182
Flynn JM, Lou JE, Ganley TJ (2002) Prevention of sports injuries in children. Curr Opin Pediatr 14:719–722
Forsman L, Eriksson A (2001) Skatingboarding injuries of today. Br J Sports Med 35:325–328
Fountain JL. Meyers MC (1996) Skateboarding injuries. Sports Med 22:360–366
Futami T, Aoki K, Tsukamoto Y (1993) Fractures of the hook of the hamate in athletes. 8 cases followed for 6 years. Acta Orthop Scand 64:469–471
Gabel GT (1998) Gymnastic wrist injuries. Clin Sports Med 17:611–621
Geissler WB (2001) Carpal fractures in athletes. Clin Sports Med 20:167–188
Gilula LA (1979) Carpal injuries: analytic approach and case exercises. AJR 133:503–517
Gilula LA, Yin Y (1996) Imaging of the wrist. WB Saunders, Philadelphia London Toronto
Gosheger G, Liem D, Ludwig K et al. (2003) Injuries and overuse syndromes in golf. Am J Sports Med 31:438–443
Halikis MN, Taleisnik J (1996) Soft-tissue injuries of the wrist. Clin Sports Med 15:235–259
Hanks GA, Kalenak A, Bowman LS et al. (1989) Stress fractures of the carpal scaphoid. J Bone Joint Surg Am 71:938–941
Hassan I, Dorani BJ (2001) Sports related fractures in children in north east England. Emerg Med J 18:167–171
Heller DR, Routley V, Chambers S (1996) Rollerblading injuries in young people. J Paediatr Child Health 32:35–38
Howse C (1994) Wrist injuries in sport. Sports Med 17:163–175
Inkelis SH, Stroberg AJ, Keller EL et al. (1988) Roller skating injuries in children. Pediatr Emerg Care 4:127–132
Israeli A, Engel J, Ganel A (1982) Possible fatigue fracture of the pisiform bone in volleyball players. Int J Sports Med 3:56–57
Jacobsen JA (1999) Musculoskeletal sonography and MR imaging. A role for both imaging methods. Radiol Clin North Am 37:713–735
Jacobson JA, Miller BS, Morag Y (2005) Golf and racquet sports injuries. Semin Musculoskeletal Radiol 9:346–359
Jerosch J, Heck C (2005) Injury patterns and prophylaxis in inline skating. Orthopade 34:441–447
Kumar S, O'Coonor A, Despois M, Galloway H (2005) Use of early magnetic resonance imaging in the diagnosis of occult scaphoid fractures: the CAST study (Canberra Area Scaphoid Trial). NZ Med J 118:U1296
Kvidera DJ, Frankel VH (1983) Trauma on eight wheels. A study of roller skating injuries in Seattle. Am J Sports Med 11:38–41
Kyle SB, Nance ML, Rutherford GW Jr et al. (2002) Skateboard-associated injuries: participation-based estimates and injury characteristics. J Trauma 53:686–690
Lichtman DM, Alexander AH (1997) The wrist and its disorders. WB Saunders, Philadephia
Lilley J, Halikis M, Taleisnik J (2000) Fractures of the carpal bones. In: Weinzweig J (ed) Hand and wrist surgery secrets. Hanley and Blefus, Philadephia, pp 197–203
Lindner KJ, Caine DJ (1990) Injury patterns of female competitive club gymnasts. Can J Sport Sci 15:254–261
Linscheid RL, Dobyns JH, Beabout JW (1972) Traumatic instability of the wrist. Diagnosis, classification, and pathomechanics. J Bone Joint Surg Am 54:1612–1632
Lorei MP, Hershman EB (1993) Peripheral nerve injuries in athletes. Treatment and prevention. Sports Med 16:130–147
Lyons RA, Delahunty AM, Kraus D et al. (1999) Children's fractures: a population based study. Inj Prev 5:129–132
MacGregor DM (2003) Don't save the ball! Br J Sports Med 37:351–353
Machold W, Kwasny O, Eisenhardt P et al. (2002) Reduction of severe wrist injuries in snowboarding by an optimized wrist protection device: a prospective randomized trial. J Trauma 52:517–520
Made C, Elmqvist LG (2004) A 10-year study of snowboard injuries in Lapland Sweden. Scand J Med Sci Sports 14:128–133
Maffuli N, Bundoc RC, Chan KM et al. (1996) Paediatric sports injuries in Hong Kong: a seven year survey. Br J Sports Med 30:218–221
Mandelbaum BR, Bartolozzi AR, Davis CA et al. (1989) Wrist pain syndrome in the gymnast. Pathogenetic, diagnostic,

and therapeutic considerations. Am J Sports Med 17:305–317

Masciocchi C, Catalucci A, Barile A et al. (2001) Trauma of the hand and wrist. In: Guglielmi G, Van Kuijk C, Genant HK (eds) Fundamentals of hand and wrist imaging. Springer, Berlin Heidelberg New York, pp 97–421

Matsumoto K, Miyamoto K, Sumi H et al. (2002) Upper extremity injuries in snowboarding and skiing: a comparative study. Clin J Sports Med 12:354–359

Matsumoto K, Sumi H, Sumi Y et al. (2004) Wrist fractures from snowboarding: a prospective study for 3 seasons from 1998 to 2001. Clin J Sports Med 14:64–71

McCarroll JR (1986) Golf: common injuries from a supposedly benign activity. J Musculoskeletal Med 3:9–16

McCarroll JR (1996) The frequency of golf injuries. Clin Sports Med 15:1–7

McCue FC III, Baugher WH, Kulund DN et al. (1979) Hand and wrist injuries in the athlete. Am J Sports Med 7:275–286

McNally E, Wilson D, Seiler S (2005) Rowing injuries. Semin Musculoskeletal Radiol 9:379–396

Meeusen R, Borms J (1992) Gymnastic injuries. Sports Med 13:337–356

Mellion MB (1991) Common cycling injuries. Management and prevention. Sports Med 11:52–70

Meyer MC, Sterling JC, Souryal TO (2003) Radiographic findings of the upper extremity in collegiate rodeo athletes. Med Sci Sports Exerc 35:543–547

Morgan WJ, Slowman LS (2001) Acute hand and wrist injuries in the athlete require individualized management, depending on athlete's age, sport, and level of competition. J Am Acad Orthop Surg 9:389–400

Moss PS, Wan A, Whitlock MR (2002) A changing pattern of injuries to horse riders. Emerg Med J 19:412–414

Mulder S, Hutten A (2002) Injuries associated with inline skating in the European region. Accid Anal Prev 34:65–70

Murray PM, Cooney WP (1996) Golf-induced injuries of the wrist. Clin Sports Med 15:85–109

Nguyen D, Letts M (2001) In-line skating injuries in children: a 10-year review. J Pediatr Orthop 21:613–618

Nuber GW, Assenmacher J, Bowen MK (1998) Neurovascular problems in the forearm, wrist, and hand. Clin Sports Med 17:585–610

O'Neill DF (2003) Wrist injuries in guarded versus unguarded first time snowboarders. Clin Orthop Relat Res 409:91–95

Orenstein JB (1996) Injuries and small-wheel skates. Ann Emerg Med 27:204–209

Osterman AL, Moskow L, Low DW (1988) Soft-tissue injuries of the hand and wrist in racquet sports. Clin Sports Med 7:329–348

Palmer AK (1989) Triangular fibrocartilage lesions: a classification. J Hand Surg Am 14:594–606

Peh WCG, Gilula LA (1996) Normal disruption of carpal arcs. J Hand Surg Am 21:561–566

Peh WCG, Gilula LA, Wilson AJ (1996) Detection of occult wrist fractures by magnetic resonance imaging. Clin Radiol 51:285–292

Pitner MA (1990) Pathophysiology of overuse injuries in the hand and wrist. Hand Clin 6:355–364

Potter HG, Asnis-Ernberg L, Weiland AJ et al. (1997) The utility of high-resolution magnetic resonance imaging in the evaluation of the triangular fibrocartilage complex of the wrist. J Bone Joint Surg Am 79:1675–1684

Powell EC, Tanz RR (1996) In-line skate and rollerskate injuries in childhood. Pediatr Emerg Care 12:259–262

Raab DJ, Fischer DA, Quick DC (1994) Lunate and perilunate dislocations in professional football players. A five-year retrospective analysis. Am J Sports Med 22:841–845

Rettig AC (1990) Neurovascular injuries in the wrists and hands of athletes. Clin Sports Med 9:389–417

Rettig AC (1994) Wrist problems in the tennis player. Med Sci Sports Exerc 26:1207–1212

Rettig AC (1998) Elbow, forearm and wrist injuries in the athlete. Sports Med 25:115–130

Rettig AC (2004). Athletic injuries of the wrist and hand: part II: overuse injuries of the wrist and traumatic injuries to the hand. Am J Sports Med 32:262–273

Richmond DR (1994) Handlebar problems in bicycling. Clin Sports Med 13:165–173

Rossi C, Cellocco P, Margaritondo E et al (2005) De Quervain disease in volleyball players. Am J Sports Med 33:424–427

Roy S, Caine D, Singer KM (1985) Stress changes of the distal radial epiphysis in young gymnasts. A report of twenty-one cases and a review of the literature. Am J Sports Med 13:301–308

Rumball JS, Lebrun CM, Di Ciacca SR et al. (2005) Rowing injuries. Sports Med 35:537–555

Scheck RJ, Kubitzek C, Hierner R et al. (1997) The scapholunate interosseous ligament in MR arthrography of the wrist: correlation with nonenhanced MRI and wrist arthroscopy. Skeletal Radiol 26:263–271

Schieber RA, Branche-Dorsey CM, Ryan GW (1994) Comparison of in-line skating injuries with rollerskating and skateboarding injuries. JAMA 15:1856–1858

Schlegel TF, Boublik M, Ho CP et al. (1999) Role of MR imaging in the management of injuries in professional football players. MRI Clin North Am 7:175–190

Schmid MR, Schertler T, Pfirrmann CW et al. (2005) Interosseous ligament tears of the wrist: comparison of multidetector row CT arthrography and MR imaging. Radiology 237:1008–1013

Shih C, Chang CY, Penn IW et al. (1995) Chronically stressed wrists in adolescent gymnasts: MR imaging appearance. Radiology 195:855–859

Stark HH, Jobe FW, Boyes JH et al. (1977) Fracture of the hook of the hamate in athletes. J Bone Joint Surg Am 59:575–582

Taylor BL, Attia MW (2000) Sports-related injuries in children. Acad Emerg Med 7:1376–1382

Tehranzadeh J, Labosky DA (1984) Detection of intraarticular loose osteochondral fragments by double-contrast wrist arthrography. A case report of a basketball injury. Am J Sports Med 12:77–79

Theriault G, Lachance P (1998) Golf injuries. An overview. Sports Med 26:43–57

Tolat AR, Sanderson PL, De Smet L et al. (1992) The gymnast's wrist: acquired positive ulnar variance following chronic epiphyseal injury. J Hand Surg Br 17:678–681

Tse PY, Shen WY, Chan KM et al. (1987) Roller skating- is it a dangerous sports? Br J Sports Med 21:125–126

Vender MI, Watson HK (1988) Acquired Madelung-like deformity in a gymnast. J Hand Surg Am 13:19–21

Wechsler RJ, Wehbe MA, Rifkin MD et al. (1987) Computed tomography diagnosis of distal radioulnar subluxation. Skeletal Radiol 25:1–5

Weinstein SM, Herring SA (1992) Nerve problems and compartment syndromes in the hand, wrists, and forearm. Clin Sports Med 11:161–188

Wiesler ER, Lumsden B (2005) Golf injuries of the upper extremity. J Surg Orthop Adv 14:1–7

Weiss LE, Taras JS, Sweet S et al. (2000) Lunotriquetral injuries in the athlete. Hand Clin 16:433–438

Young CC, Niedfeldt MW (1999) Snowboarding injuries. Am Fam Physician 59:131–136,141

Young CC, Seth A, Mark DH (1998) In-line skating: use of protective equipment, falling patterns, and injuries. Clin J Sports Med 8:111–114

Zalavras C, Nikolopoulou G, Essin D et al. (2005) Pediatric fractures during skateboarding, roller skating, and scooter riding. Am J Sports Med 33:568–573

Zlatkin MB, Rosner J (2004) MR imaging of ligaments and triangular fibrocartilage complex of the wrist. MRI Clin N Am 12:301–331

Finger and Hand

14

Michel De Maeseneer and Farhad Ebrahim

CONTENTS

Box 14.1. Radiography

- Of value if bony injury or change in bony alignment
- Normal if bone changes are absent

Box 14.2. Ultrasound

- Excellent for fine hand soft tissue structures
- Quick, and inexpensive
- Requires excellent knowledge of anatomy and ultrasound approach
- Dynamic examination possible
- Competitive with MRI for hand soft tissue injury

Box 14.3. MRI

- Excellent for soft tissue and bone marrow changes
- Good system and technique mandatory for hand imaging
- May be time consuming and expensive

14.1 Introduction and Technical Considerations

With technical advances in imaging systems, injuries of hand and fingers can be accurately evaluated with ultrasound and magnetic resonance. Although such injuries can be assessed by expert clinical examination, additional information obtained from imaging can help in optimizing treatment planning.

For ultrasound, linear or dedicated hand transducers can be used. High resolution is essential. As a rough guideline, transducers of 12 MHz or higher are ideal. Frequency ranges above 12 MHz are offered by many vendors.

For magnetic resonance, high resolution images can be obtained with dedicated finger coils. A drawback of these coils is the very small field of view offered. Wrist coils or circular coils also give excellent results. Meticulous attention to patient immobilization, choice of the smallest field of view obtainable, and optimizing signal to noise ratio by carefully selecting imaging parameters will yield

M. De Maeseneer, MD, PhD
Division of Radiologic Sciences, Wake Forest University Hospital, Medical Center Boulevard,Winston-Salem, North Carolina, NC 27157, USA
F. Ebrahim, MD
University of Michigan Hospitals, Ann Arbor, Michigan, USA

the best results. Choice of imaging parameters may vary among systems. The same is true for the imaging sequences, although these should include "anatomical" and "fluid-sensitive" sequences. Anatomical images will consist of either spin echo T1 weighted images or spin echo proton density weighted images. These sequences offer high detail, however, excellent knowledge of normal anatomy is essential to assess pathological changes. "Fluid-sensitive" sequences will consist of STIR weighted images or T2 fat saturated images and will emphasize high signal intensity changes. These sequences offer less imaging detail in the fingers due to the small field of view. Gradient echo sequences are an alternative to spin echo sequences, but susceptibility artefacts related to bone-soft tissue interfaces, and chemical shift artifact related to muscle-fat interfaces, adversely affect image quality in the hands.

14.2 Extensor Tendon Rupture

The extensor tendon system has a distal insertion terminating on the base of the distal phalanx and a proximal insertion terminating on the base of the middle phalanx (Figs. 14.1 and 14.2.). The extensor system receives contributions from the interosseus muscles as well as from the lumbrical muscles (Landsmeer 1949). A rupture of the distal insertion is designated "mallet finger" or "baseball finger" and typically results in pain and swelling, and inability to extend the distal phalanx (Kleinbaum 2005) flexion deformity is present at the DIP joint. The diagnosis is usually made clinically. Ultrasound may be performed to establish the degree of retraction, diagnose associated collections or tiny avulsion fractures which may be underestimated clinically (Fig. 14.3). Ruptures of the central insertion are more commonly recognized in the setting of inflammatory conditions but may also relate to trauma. A rupture of the central slip insertion typically leads to boutonnière deformity. This usually results from sudden DIP extension, and leads to hyperextension at the MCP, flexion at the PIP, and hyperextension at the DIP joints. Diagnosis of tendon rupture is straightforward with ultrasound. Ultrasound can show the tendon rupture dynamically, as well as demonstrate the extensor fibers that slide to the side of the PIP joint (Fig. 14.4). More proximal ruptures of the extensor system over the midhand can also occur (Fig. 14.5). MR may also be employed to diagnose extensor rupture, but lacks the dynamic capability and imaging detail of ultrasound.

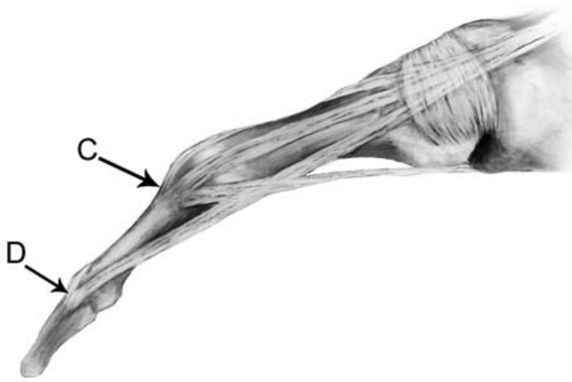

Fig. 14.1. Extensor system. Line drawing shows lateral aspect of finger. Extensor tendon combines with interosseus tendons to terminate in central insertion (*arrow*, *C*), and distal insertion (*arrow*, *D*)

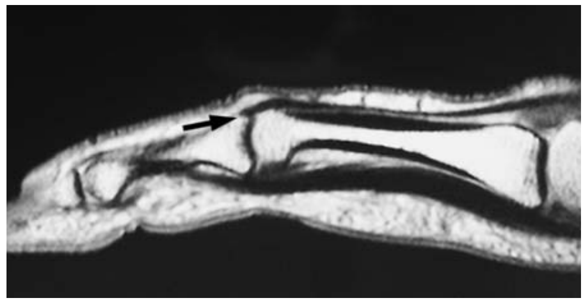

Fig. 14.2. Central extensor insertion. Sagittal proton density weighted MR image. Termination of the central insertion is shown (*arrow*)

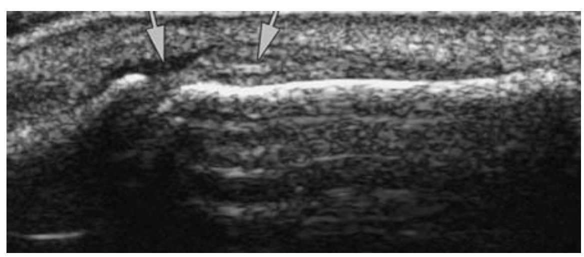

Fig. 14.3. Mallet finger. Sagittal ultrasound image. Note complete tear of distal insertion (Mallet finger) appearing hypoechoic, and retracted tendon end (*arrows*)

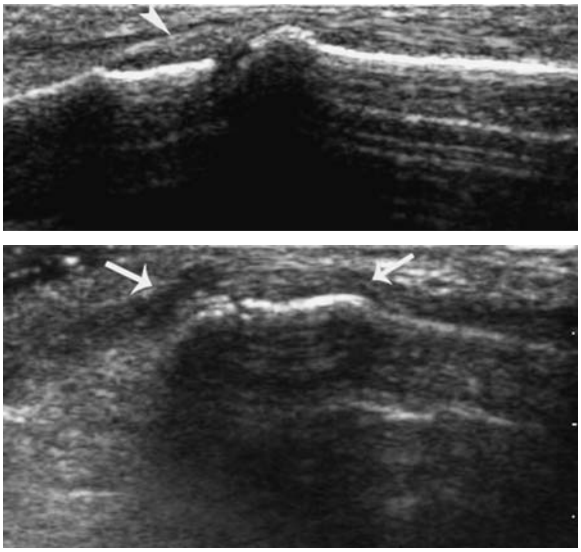

a

b

Fig. 14.4a,b. Boutonniere deformity. **a** Sagittal ultrasound image. Note avulsion of fibers at insertion of central slip (*arrowhead*). **b** Coronal ultrasound image at lateral aspect of finger shows laterally located components (*arrows*) of extensor system that are thickened and scarred down adjacent to the bone

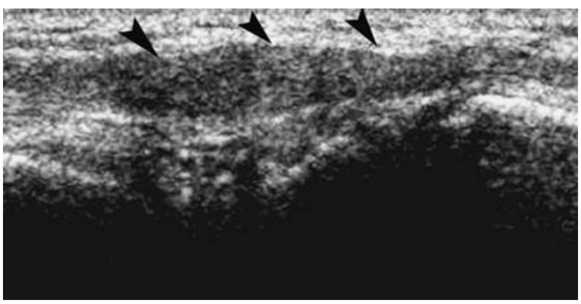

Fig. 14.5. Extensor rupture. Sagittal ultrasound image shows proximal rupture of extensor tendon over midhand (*arrowheads*)

14.3 Dorsal Hood Rupture

At the level of the metacarpophalangeal joint the extensor tendon is kept in place by dorsal reinforcements designated dorsal hoods (Fig. 14.6). The dorsal hood consists of lateral bands attaching to and covering the extensor tendons at the metacarpal head level. Ruptures of the sagittal bands leads to displacement of the extensor tendons from their central positions over the metacarpal heads (Fig. 14.7). Usually the second and third digits are involved secondary to direct trauma such as in boxing. On ultrasound the tendon can be shown dynamically to displace from its normal central position. A hypoechoic cleft also may be apparent in the normal location of the sagittal bands. At MR disruption of the sagittal bands may be depicted as a hyperintense signal intensity area adjacent to the tendons.

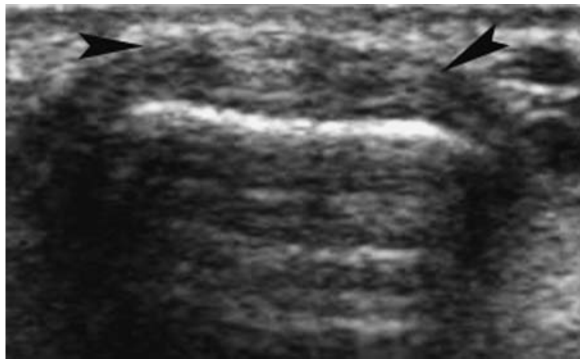

Fig. 14.6. Dorsal hood. Transverse ultrasound image shows triangular sagittal bands (*arrowheads*) at both sides of extensor tendon

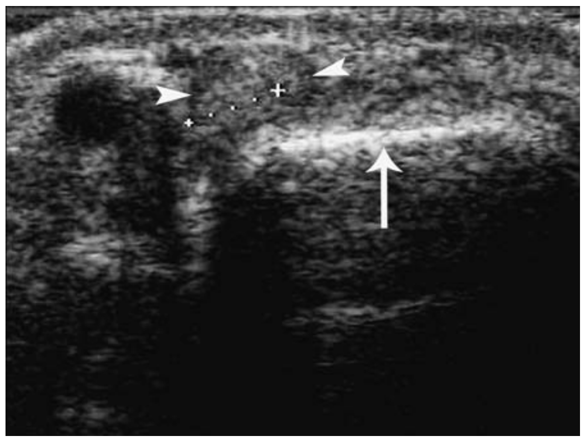

Fig. 14. 7. Dorsal hood injury. Transverse ultrasound shows displacement of extensor tendon (*arrowheads*) relative to central position over metacarpal head (*arrow*)

14.4 Flexor Tendon Rupture

At midhand level the flexor tendons are easily depicted. The flexor superficialis tendon is located more ventrally (Fig. 14.8). On the radial side of the

tendons the muscular belly of the lumbricalis muscle is attached. The lumbrical muscle bellies are located at the radial side of the flexor system in the hand (Figs. 14.9 and 14.10). The lumbricals are located on the radial side of the flexor system. Their tendons move from ventrally in a dorsal direction to attach to the extensor system. Tears of the lumbricals have been described in rock climbers leading to rupture and hematoma in the muscle belly (Schweizer 2003). Such muscle tears are most easily demonstrated with ultrasound (Fig. 14.11). "Fluid sensitive" magnetic resonance sequences also may show muscle tears as hyperintense areas.

The relationship of the flexor superficialis tendon and the flexor profundus tendon varies considerably throughout the finger. The flexor profundus tendon passes through an opening in the flexor superficialis tendon and continues to insert onto the base of the distal phalanx. The flexor superficialis tendon inserts at the level of the middle aspect of the middle phalanx (Fig. 14.12). Flexor tendon disruption may be related to transsection. Avulsive injuries in blunt trauma typically involve the distal insertion (flexor profundus) and this condition is also designated rugger jersey finger (Fig. 14.13) (Cohen et al. 2004). Tendon ruptures can be demonstrated both by ultrasound and magnetic resonance.

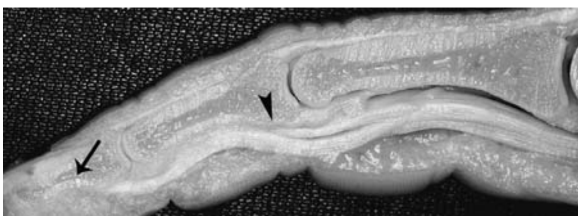

Fig. 14. 8. Flexor tendons. Sagittal anatomical slice shows insertion of flexor profundus (*arrow*) and of flexor superficialis (*arrowhead*)

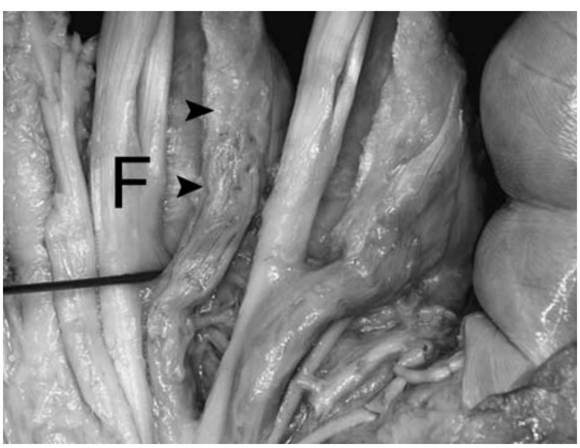

Fig. 14. 9. Lumbricals. Anatomical dissection shows lumbricalis muscle (*arrowheads*) adjacent to radial side of flexor tendons (*F*)

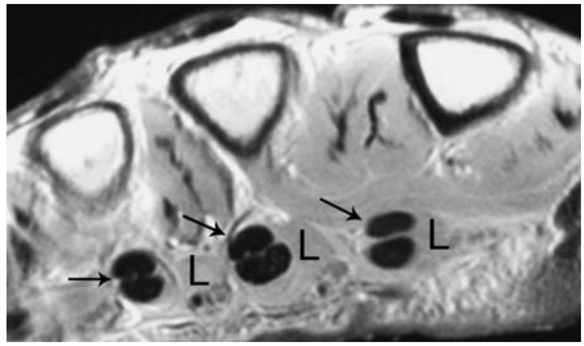

Fig. 14. 10. Lumbricals. Transverse proton density MR image shows lumbricals (*L*) at radial aspect of flexor tendons (*arrows*)

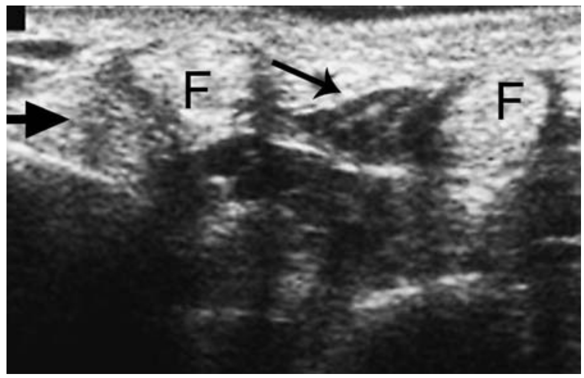

Fig. 14.11. Lumbrical tear. Transverse ultrasound image. Normal flexor tendons are seen (*F*). Normal hypoechoic lumbrical (*thin arrow*) is seen, as well as hyperechoic lumbrical (*thick arrow*) corresponding to recent tear

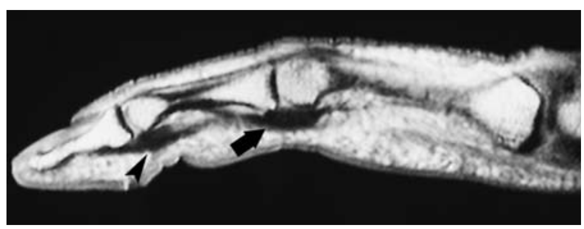

Fig. 14. 12. Flexor tendons. Sagittal proton density MR. Normal insertion of flexor profundus tendon (*arrowhead*), and flexor superficialis tendon (*bold arrow*) is seen

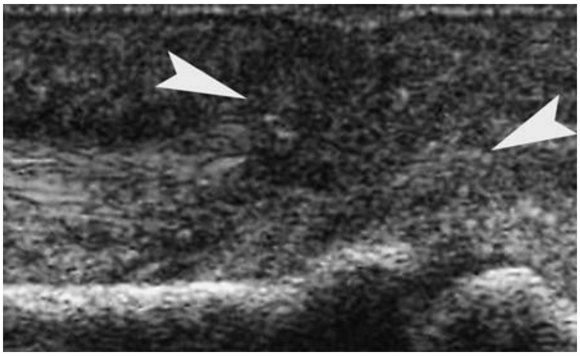

Fig. 14.13. Flexor rupture. Sagittal ultrasound image. Hypoechoic cleft corresponding to avulsion of flexor profundus (*arrowheads*) is seen

14.5 Annular Pulley Rupture

The flexor tendons are covered by fibrous reinforcements that are termed annular or cruciform pulleys (Fig. 14.14) (Parellada 1996; Kovacs 2002).The cruciform reinforcements are less important and are even difficult to recognize on anatomic dissection. The annular reinforcements are strong bands easily recognizable at dissection . They are classified as five different bands, termed the A1 to the A5 pulleys. Usually, when an injury occurs, it extends from proximal to distal involving the A1 pulley first, and then continuing distally involving the A2 pulley. The A3 pulley is located in regard of the proximal interphalangeal joint. The A4 pulley is located at the middle aspect of the middle phalanx, and the A5 pulley is located in regard of the distal interphalangeal joint. The purpose of the annular pulleys is to keep the tendon in close contact with the bone during flexion of the finger. The pulleys cannot be seen consistently using US, but may occasionally be evident as hypoechoic interfaces at the superficial aspect of the tendons. Annular pulley rupture has typically been described in rock climbers. Dynamic ultrasound shows the increased distance of the tendon to the bone in comparison to the normal side (Fig. 14.15). This displacement, also designated "bowstring deformity" may also be shown using magnetic resonance.

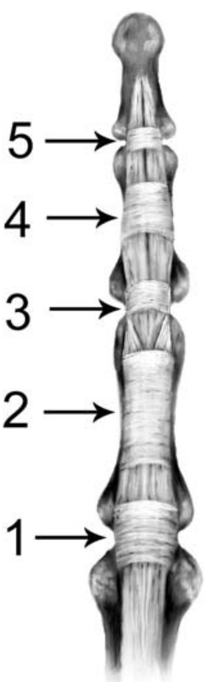

Fig. 14.14. Annular pulleys. Line drawing shows ventrally located annular pulleys A1 to A5 (*arrows*)

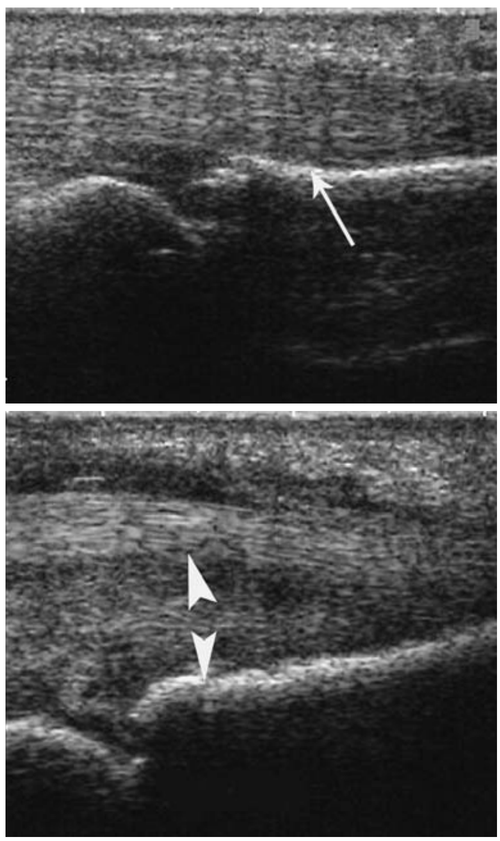

Fig. 14.15. Pulley rupture. Composite image of sagittal ultrasound images. A flexor system in close proximity to bone (*long arrow*), above. *A* pulley tear with bowstring appearance; flexor system is displaced from adjacent bone (*arrowheads*), below

14.6 Volar Plate and Collateral Ligament Injury

At the level of the joints the flexor tendons are at a slight distance from the bone. This is related to the shape of the head of a phalanx, but also to the presence of thick volar plates at the level of the interphalangeal and metacarpophalangeal joints (Figs. 14.16 and 14.17). The volar plates are fibrous structures attached to the distal phalanx and extending proximally (Nance et al. 1979). The oblique bands of the collateral ligaments of the joint connect to the volar plates. Hence, volar plate injuries are often associated with injuries of the collateral ligaments. Volar plate injuries can occur as a consequence of hyperextension but also medial or lateral deviation. Ultrasound can show the disrupted volar plate, bony avulsion or associated small collections (Figs. 14.18–14.21). Magnetic resonance may show thickening of the volar plates and collateral ligaments.

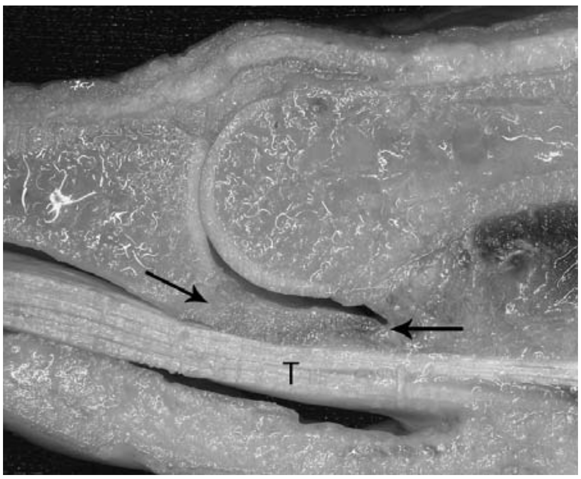

Fig. 14.16. Volar plate. Sagittal anatomic slice shows flexor tendons (*F*), superficial to volar plate (*arrows*)

Fig. 14.18. Volar plate avulsion. Lateral radiographs shows avulsion (arrowhead) of ventral aspect of base of phalanx, typical of volar plate avulsive injury

Fig. 14.17. Volar plate. Sagittal ultrasound image shows hyperechoic volar plate (*arrow*)

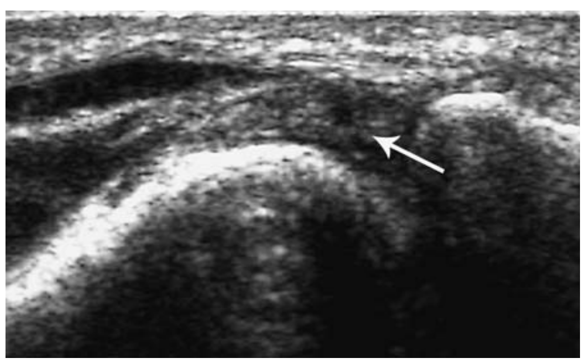

Fig. 14.19. Volar plate tear. Sagittal ultrasound image shows hypoechoic cleft (*arrow*) in thickened volar plate corresponding to tear

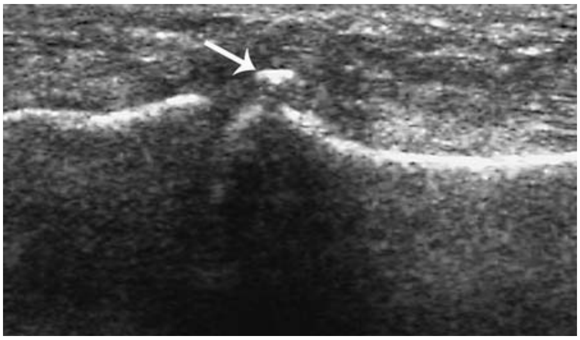

Fig. 14.20. Volar plate injury. Sagittal ultrasound image shows hyperechoic bone fragment (*arrow*), in the setting of volar plate avulsion

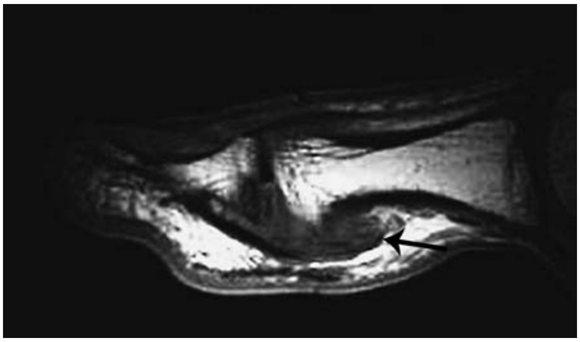

Fig. 14.21. Volar plate injury. Sagittal proton density MR image shows thickened volar plate (*arrow*) of increased intensity corresponding to tear

14.7 Ulnar Collateral Ligament of the Thumb

The metacarpophalangeal area of the thumb is vulnerable to a spectrum of injuries, sometimes designated ski thumb, or gamekeepers thumb. Such injury may occur by thumb hyperextension or radial deviation. Injuries of the ligament may result in loss of grasp function between thumb and index finger (Figs. 14.22 and 14.23). The ulnar collateral ligament may show partial or complete tears (Fig. 14.24). Plain radiographs may show an avulsion fracture at the base of the proximal phalanx (Fig. 14.25). A specific complication occurs when the ulnar collateral ligament retracts and becomes located superficially to the adductor pollicis aponeurosis. This complication is designated "Stener lesion" (O'Callaghan et al. 1994).

Fig. 14.23. Ulnar collateral ligament of thumb. Coronal MR image shows hypointense adductor aponeurosis and deeper ulnar collateral ligament (*arrow*)

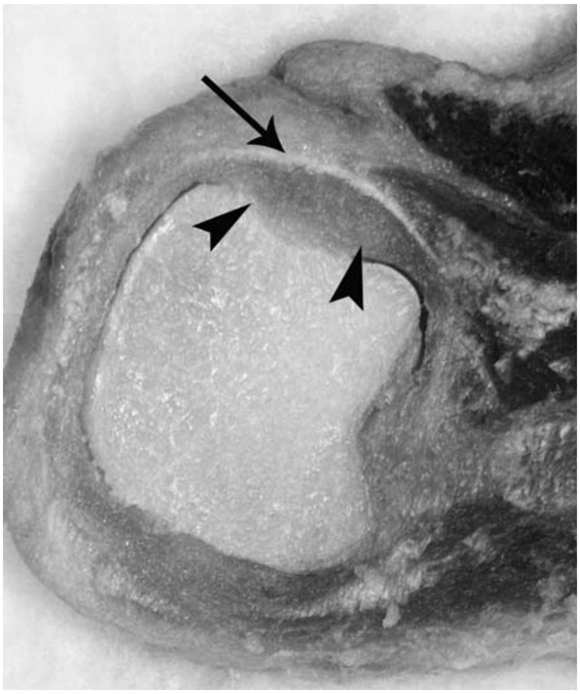

Fig. 14.22. Ulnar collateral ligament of thumb. Transverse anatomical slice shows adductor aponeurosis (*arrow*) overlying ulnar collateral ligament of thumb (*arrowheads*)

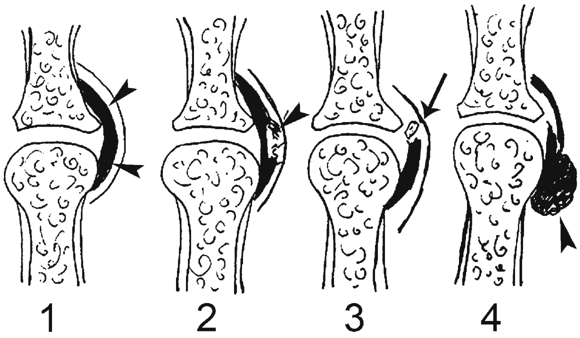

Fig. 14.24. Ulnar collateral ligament of thumb injury. Line drawing shows spectrum of injury. In 1, sprain of the ligament is seen (*arrowheads*). In 2, a partial tear (*arrowhead*) is illustrated. In 3, a complete tear and a small bony avulsion is seen (*arrow*). In 4, proximal retraction and displacement superficial to the adductor aponeurosis, corresponding to Stener lesion, is shown (*arrowhead*)

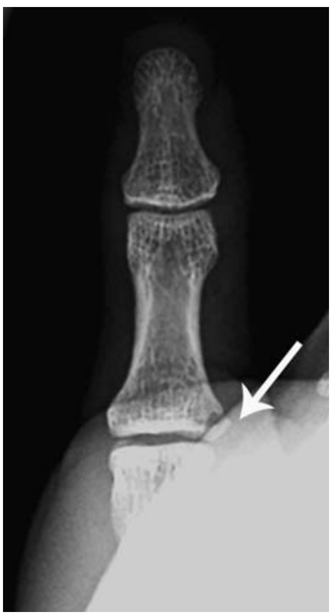

Fig. 14.25. Gamekeepers thumb. AP radiograph shows avulsion (*arrow*) at base of proximal phalanx corresponding to gamekeepers thumb

Diagnosis of different stages of UCL tear and Stener lesion can be accomplished by ultrasound (Fig. 14.26). Magnetic resonance can also differentiate between ulnar collateral ligament tear and Stener lesion. In Stener lesion a proximally located soft tissue nodule is apparent which has been designated the "jojo" sign.

14.8 De Quervain Tendons

The de Quervain tendons consist of the abductor pollicis longus and the extensor pollicis brevis (De Quervain 2005). Inflammation results in tendon thickening, synovial sheath and retinaculum thickening. It may be caused by overuse such as in racquet sports, or sports requiring repetitive rotating of the wrist. Diagnosis can be made either by ultrasound or magnetic resonance (Fig. 14.27).

14.9 Other Sport Related Injuries of the Hand

In a study of 100 consecutive hand injuries in boxing, Noble (1987) found that 35% of the injuries occurred at the base of the 2nd to 5th metacarpals, including the wrist joint. Mechanism of injury was forced flexion of the wrist. Other boxing injuries affecting the hand occurred in the thumb area (39%) and the phalanges and the rest of the metacarpals (Fig. 14.28), excluding the bases (26%). Other soft tissue structures of the wrist may also be traumatized.

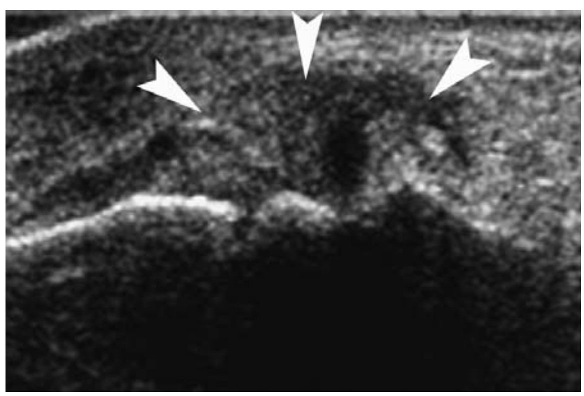

Fig. 14.26. Stener lesion. Coronal ultrasound image shows lobulated and swollen appearance of proximal aspect of torn ulnar collateral ligament of thumb, typical of Stener lesion (*arrowheads*)

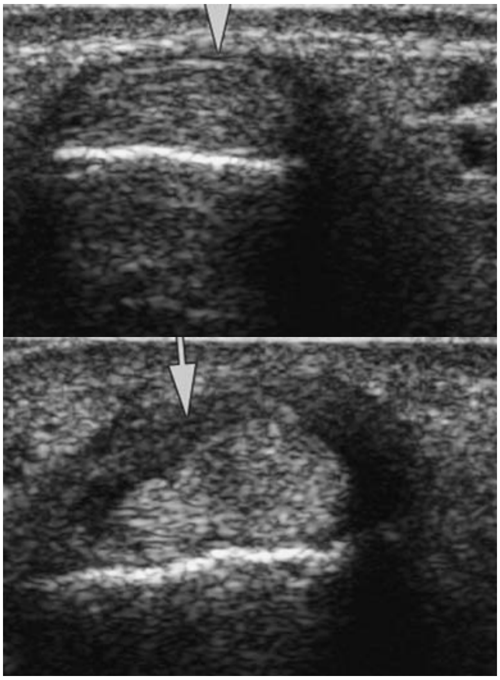

Fig. 14.27. de Quervains tenosynovitis. Composite transverse ultrasound image. A normal first extensor group is seen above. Note thickened aspect of tendons, synovium and retinaculum on abnormal side, below (*arrows*)

Fig. 14.28. Spiral fracture of the third metacarpal shaft in a boxer, as seen on a PA radiograph of the hand (Courtesy of W. Peh)

14.10 Conclusion

Ultrasound and MRI are important tools for diagnosing sports related injuries of the ligaments and tendons of the hand. Important injuries may involve the flexor and extensor tendons, collateral ligaments, annular pulleys, volar plate, and dorsal hood.

Things to Remember

1. Rupture of central extensor insertion can lead to "boutonniere", distal insertion to "mallet" finger.
2. With dorsal hood injury extensor tendons can be displaced from their central position over the MCP heads.
3. Flexor avulsion typically involves the flexor profundus and is designated rugger jersey finger.
4. With rupture of the pulleys, bowstring deformity can occur.
5. Volar plate and collateral ligament injuries are often associated.
6. When the proximal portion of the UCL of the thumb becomes located superficial to the adductor aponeurosis, Stener lesion is diagnosed.
7. Racquet sports may be a risk factor for developing De Quervain tenosynovitis.

References

Cohen SB, Chabra AB, Anderson MW et al. (2004) Use of ultrasound in determining treatment for avulsion of the flexor digitorum profundus (rugger jersey finger): a case report. Am J Orthop 33:546–549

De Quervain F (2005) On the nature and treatment of stenosing tendovaginitis on the styloid process of the radius. (Translated article: Muenchener Medizinische Wochenschrift 1912, 59, 5–6). J Hand Surg 30:392–394

Kleinbaum Y, Heyman Z, Ganel A et al. (2005) Sonographic imaging of mallet finger. Ultraschall Med 26:223–226

Kovacs P, Bodner G (2002) High resolution ultrasound diagnosis of the annular tendon system of the hand. Orthopade 31:284–287

Landsmeer JM (1949). The anatomy of the dorsal aponeurosis of the human finger and the functional significance. Anat Rec 104:31–44

Nance EP Jr, Kaye JJ, Milek MA (1979) Volar plate fractures. Radiology 133:61–64

Noble C (1987). Hand injuries in boxing. Am J Sports Med 15:342–346

O'Callaghan BI, Kohut G, Hoogewoud HM (1994) Gamekeeper thumb: identification of the Stener lesion with US. Radiology 192:477–480

Parellada JA, Balkisson AR, Hayes CW, Conway WF (1996) Bowstring injury of the flexor tendon pulley system: MR imaging. AJR Am J Roentgenol. 167:347–349

Schweizer A (2003) Lumbrical tears in rock climbers. J Hand Surg 28:187–189

Pelvis, Hip and Groin

15

Wayne Gibbon and Ernest Schilders

CONTENTS

Box 15.1. Magnetic resonance imaging

- This is probably the first line investigation for most causes of pelvic, hip and groin pain in athletes due to its high anatomical detail and ability to demonstrate a wide range of osseous and soft-tissue pathologies
- Conventional MR imaging acts as a "water map" for demonstrating bone marrow and soft-tissue edema whereas fat-suppressed contrast enhanced studies demonstrate hyperaemia and therefore acts as a surrogate market for inflammation
- Intra-articular contrast may be helpful in demonstrating conditions such as hip labral tears

Box 15.2. Conventional radiography

- The value of conventional radiographs resides is their ability to rapidly, simply and inexpensively demonstrate acute bony injury, late stress injury to bone, arthropathy and coincidental osseous condition e.g. primary and secondary bone tumours and skeletal infection
- Stress radiographs are of limited value for assessing pelvic instability

Box 15.3. Computed tomography

- The indications for CT in athletes with pelvic, hip and groin pain are limited but include bony abnormalities at complex anatomical sites such as the sacroiliac joints, diagnostic confirmation of specific local conditions e.g., myositis ossificans circumscripta and causes of referred pain to region e.g., lumbar spondylolysis

Box 15.4. Ultrasound

- Sonography is able to demonstrate acute and chronic tendon injury, define the extent of muscle tears and correlate imaging abnormalities with site of anatomical tenderness
- Ultrasound is also useful in studies requiring a dynamic component e.g., Valsalva Manoeuvre for functionally assessing hernias, conditions where Colour or Power Doppler imaging may be helpful e.g., hip synovitis and for guiding a range of percutaneous diagnostic and therapeutic procedures

W. Gibbon, MD, PhD, Professor
E. Schilders, MD
18th Seventh Ave, St. Lucia, Brisbane Q 4067, Australia

15.1 Introduction

Chronic hip, groin and pelvic pain are major causes of morbidity in professional and elite athletes and these problems are often inter-related. Groin injuries are the commonest cause of chronic injury in a wide range of sports, especially football. Depending on which published data is chosen they constitute up to 27% of injuries in soccer (Ekstrand and Gillquist 1983), 12% in American Football (Moretz et al. 1978), 11.3% in rugby (Hornof and Napravnik 1969) and 6.6% in Australian-rules football (Seward et al. 1993). In soccer players, groin injuries tend to be associated with a prolonged recovery and 50% of players with groin pain will have symptoms that persist for more than 20 weeks after initial injury (Nielsen and Yde 1989). Therefore, as they constitute 55% of overuse injuries, the impact on a team's performance is great (Fifa 1992).

Great diagnostic difficulties exist reflecting the fact that the causes of groin pain are protean (Table 15.1) and also possibly reflecting clinical prejudice. In one study reviewing the case-notes of 189 athletes with chronic groin pain, 27% were found to have multiple pathologies (Lovell 1995). One possible explanation for the diagnostic confusion could be that there may indeed be more than one diagnosis in many athletes. However, this confusion could also be due to the fact that many of the diagnoses are anatomically and/or biomechanically linked. Consequently, adequate treatment requires the addressing of more than one of these clinical conditions (Holmich et al. 1999) and, therefore, medical imaging has a most important role in patient management, i.e. in defining as precisely as possible the underlying injury and disease processes.

The problem of groin pain in athletes is not a new one. Pierson (1929) was probably the first to describe chronic stress injury to the symphysis pubis or "osteitis pubis" in 1929. He termed the condition osteochondritis of the symphysis pubis which indeed better reflects the articular nature of the injury. Spinelli described osteitis pubis in athletes as early as 1932 (Spinelli 1932). This condition has also been termed dynamic osteopathy (Losada and Saldias 1968) and tenosteochondrosis of the pubis, reflecting the dynamic nature of the condition and the interrelationship of bone, joint and tendon aetiological components (Rosenklint and Anderson 1969). Subchondral trabecular fracture as a cause for groin pain in athletes was reported by Williams in 1978.

Table 15.1. The differential diagnosis of groin pain

1. Muscle tear
   - a) Adductor group – adductor longus
     – adductor brevis
     – gracilis
   - b) Rectus femoris
   - c) Rectus abdominis
   - d) Oblique/tranversalis (inferior portions)
   - d) Hamstring group
   - e) Sartorius
   - f) Ilio-psoas
2. Tendinitis or tear
   - a) Adductor origin – adductor longus
     – adductor brevis
     – gracilis
   - b) Rectus femoris
   - c) Ilio-psoas
3. Bone or apophysis avulsion
   - a) Adductor origin
   - b) Anterior inferior iliac spine/apophysis
   - c) Ischial apophysis
   - d) Anterior superior iliac spine/apophysis
   - e) Lesser trochanter/apophysis
4. Bursitis
   - a) Ilio-pectineal
   - b) Ilio-psoas
5. Pubic symphysitis/osteitis pubis
6. Pubic osteomyelitis
7. Stress fracture
   - a) Inferior pubic ramus
   - b) Parasymphyseal
   - c) Femoral neck
8. Entrapment neuropathy
   - a) Ilio-inguinal nerve neuralgia
   - b) Obturator neuralgia
   - c) Genito-femoral causalgia
9. Hip pathology
   - a) Osteoarthrosis
   - b) Slipped capital femoral epiphysis
10. Inguinal lymphadenitis
11. Hernia
    - a) Direct inguinal
    - b) Indirect inguinal
    - c) Femoral
    - d) Obturator
    - e) Spigelian
12. Genito-urinary
    - a) Orchitis
    - b) Prostititis
    - c) Scrotal trauma/haematocele
    - d) Low renal calculus
13. Haematoma
    - a) Direct blow
    - b) Tear of inferior epigastric artery (Rectus sheath)
14. Referred pain
    - a) Spine – spondylolysis
      – Scheuermann's disease
      – high lumbar disc prolapse
    - b) Sacro-iliac joint – instability
      – sacro-iliitis
      – osteoarthrosis
15. Acute abdominal/pelvic viscus inflammation
16. Idiopathic

Pubic symphyseal osteomyelitis was first described in an athlete in Adams and Chandler (1953) and the differentiation between inflammatory osteitis pubis and low grade pubic osteomyelitis has remained a diagnostic problem in athletes ever since.

Probably the first description of adductor muscle injuries in athletes was in ten-pin bowlers in Hoon (1959). Wiley was the first investigator in the English literature to associate traumatic osteitis pubis with abnormalities of the gracilis tendon origin in 1983. This single case report described the significant histopathological findings seen in the excised tissue at the gracilis enthesis. These included a mixture of viable and non-viable bone fragments, extensive fibrosis and an absence of infection, suggesting a chronic traction phenomenon at the osseotendinous junction inferior margin of the symphysis pubis. Although this was the first record of the condition in the English literature, it had been described 20 years earlier in the German literature (Schneider 1963). Wiley in his report also commented on the fact that avulsion of the gracilis tendon origin is associated with concurrent avulsion of the ligamentous support of the inferior region of the symphysis and avulsion of bony fragments at the edge of the pubis (Wiley 1983). This infers a relationship between the stability of the symphysis and tendinous avulsion. Pelvic adductor syndrome as a cause of groin pain in footballers was first postulated in Reideberger et al. (1967), rectus abdominis tendinopathy in Martens et al. (1987) and adductor longus tendinopathy in Akermark and Johansson (1992).

Carnevale (1954) described a condition, he termed inguinocrural pain in footballers, which was probably an early description of the "sportsman's hernia", i.e. an imminent, but non-palpable, direct inguinal hernia. This has subsequently been thought to be a common cause of unexplained chronic groin pain in athletes especially in the UK. Ashby (1994) found inflammation of the inguinal ligament at its pubic insertion to be a cause of obscure chronic groin pain. This and the above pubic adductor tendon and rectus abdominis insertional problems are all probable descriptions of enthesopathy as the primary cause of chronic groin pain. The large muscle bulk of the hip adductor relative to their pubic insertion cross-sectional area means that a large force is generated per unit area at their entheseal attachments potentially resulting in an entheseal overuse phenomenon.

Physician bias may also affect the eventual clinical diagnosis. Ekberg et al. (1988) compared the diagnoses made by 5 specialists (general surgeon, orthopaedic surgeon, urologist, nuclear medicine physician and radiologist), in 21 athletes complaining of unexplained chronic groin pain. These investigators found that in 90% of cases more than one diagnosis was made and in 14% of cases the specialists made four or more different diagnoses for each patient. The authors concluded that "the final diagnosis (and treatment) often reflects the specialty of the doctor and as a result alternative causes of groin pain are overlooked". Further clinical investigation in athletes, who are not cured by hernia repair, will produce an alternative treatable diagnosis in more than 80% of cases, most of which are subsequently cured by addressing the more latterly diagnosed condition. Conversely, adductor origin symptoms often subside following hernia repair. Therefore, the mechanism for adductor origin injury appears to be linked in some way to that of the "pre-hernia complex". It could be implied from these results that the actual diagnosis made in athletes with groin pain reflects clinical prejudice (Fredberg and Kissmeyer-Nielsen 1996) and that greater recognition of the interlinked nature of the different conditions is required.

15.2 Anatomical Considerations

There are a significant number of errors is the classical description of the soft tissue attachments to the pubic bodies (Fig. 15.1). In only 3% of groins does a conjoint tendon representing the fused inferomedial aponeuroses of internal oblique and transversus abdominis actually insert into the pubic tubercle and adjacent pubic crest as is classically described. In 97% of cases, these tendinous aponeuroses are separate structures with 74% inserting separately into the rectus sheath at least 5 mm above the pubic tubercle.

The gorilla's rectus abdominis (RA) muscle inserts onto the anterolateral pubic margin immediately medial to the longer gracilis origin (Gregory 1950). It does so more distally than is usually described in humans. It is possible that man's more erect posture has resulted in developmental proximal migration of the RA insertion with its vestige remaining as pyramidalis muscle and with the anterior rectus sheath interdigitating with the more distal adductor tendon aponeuroses and gracilis fascia (Fig. 15.2).

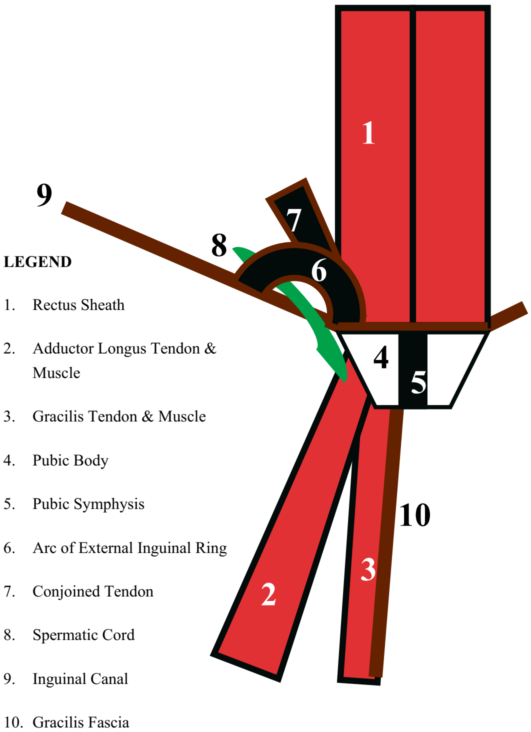

Fig. 15.1. Illustration of the frontal view of the pubic symphyseal region – classical description

Human anatomical and MR imaging studies show that the posterior symphyseal margin is only covered by a thin (<2 mm) sheet of soft tissue consisting of a condensation of the anterior pelvic peritoneum. The tight adherence of the deep surface of the rectus sheath to the superior pubic bone surface and symphysis constitutes a superior symphyseal ligament (SSL). The tendons of gracilis and adductor brevis are themselves fused to a variable extent as they arise from the same ridge of bone (ventral arc of the pubis) and the fibres of the ventral pubic ligament which are attached to its medial border (Budinoff and Tague 1990). The RA and the above “common adductor origin” (CAO) form a conjoined aponeurosis tightly which adheres to the central portion of the anterior pubic surfaces and also to the antero-lateral public margin. A condensation of the adductor tendon origins extends inferiorly and slightly medially from the anterolateral pubic margin of the inferior radial ligament and fuses with the strong inferior pubic arch ligament. These findings mean that direction of least resistance for pubic symphyseal extrusion is posteriorly. Posterior symphyseal extrusion progresses to form the posterior pubic eminence by ossicle formation within the extruded fibrous tissue (Fig. 15.3).

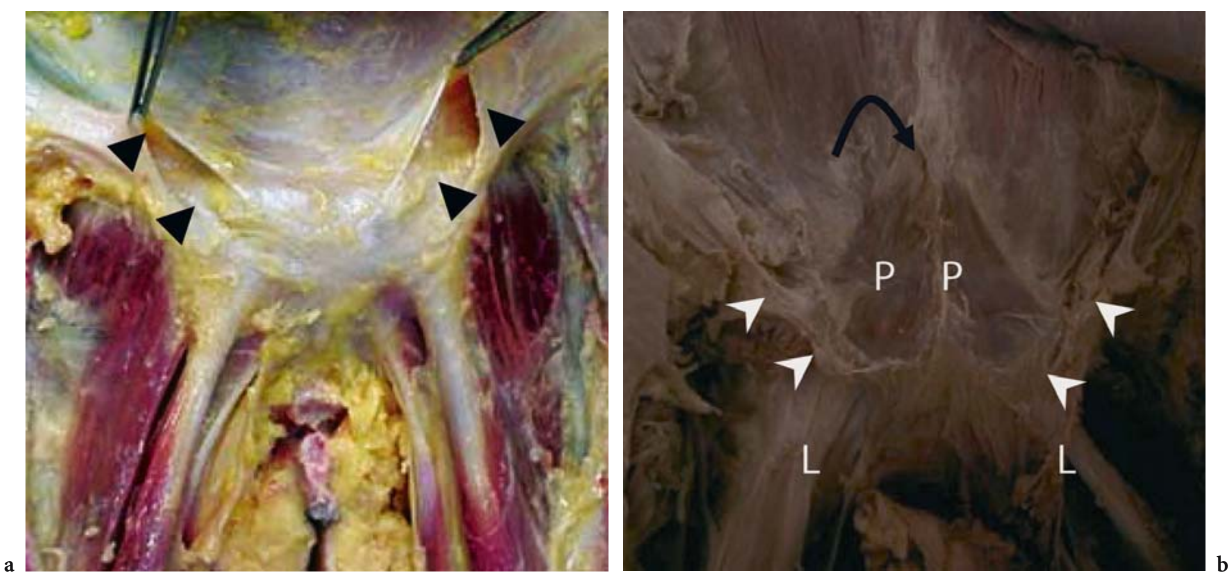

Fig. 15.2a,b. Rectus abdominis-common adductor origin functional unit. **a** A fresh female cadaveric specimen showing a pair of forceps retracting the superior portions of the external inguinal rings. The medial portions of these rings are inseparable from the anterior rectus sheath whilst infero-laterally the lateral borders of these inguinal rings fuse with the inguinal ligaments (*arrowheads*). **b** A formalin-fixed female cadaveric specimen showing the median raphé (*curved arrow*) of the rectus sheath passing through the midline of the rectus abdominis musculature separating the two halves of pyramidalis muscle (*P*). These latter muscles appear to be in continuity with the adductor longus insertions (*L*) separated by the inguinal ligaments (*arrowheads*). These dissections show how the inguinal ligaments, rectus sheath, rectus abdominis/pyramidalis muscle and adductor longus muscles are anatomically interlinked

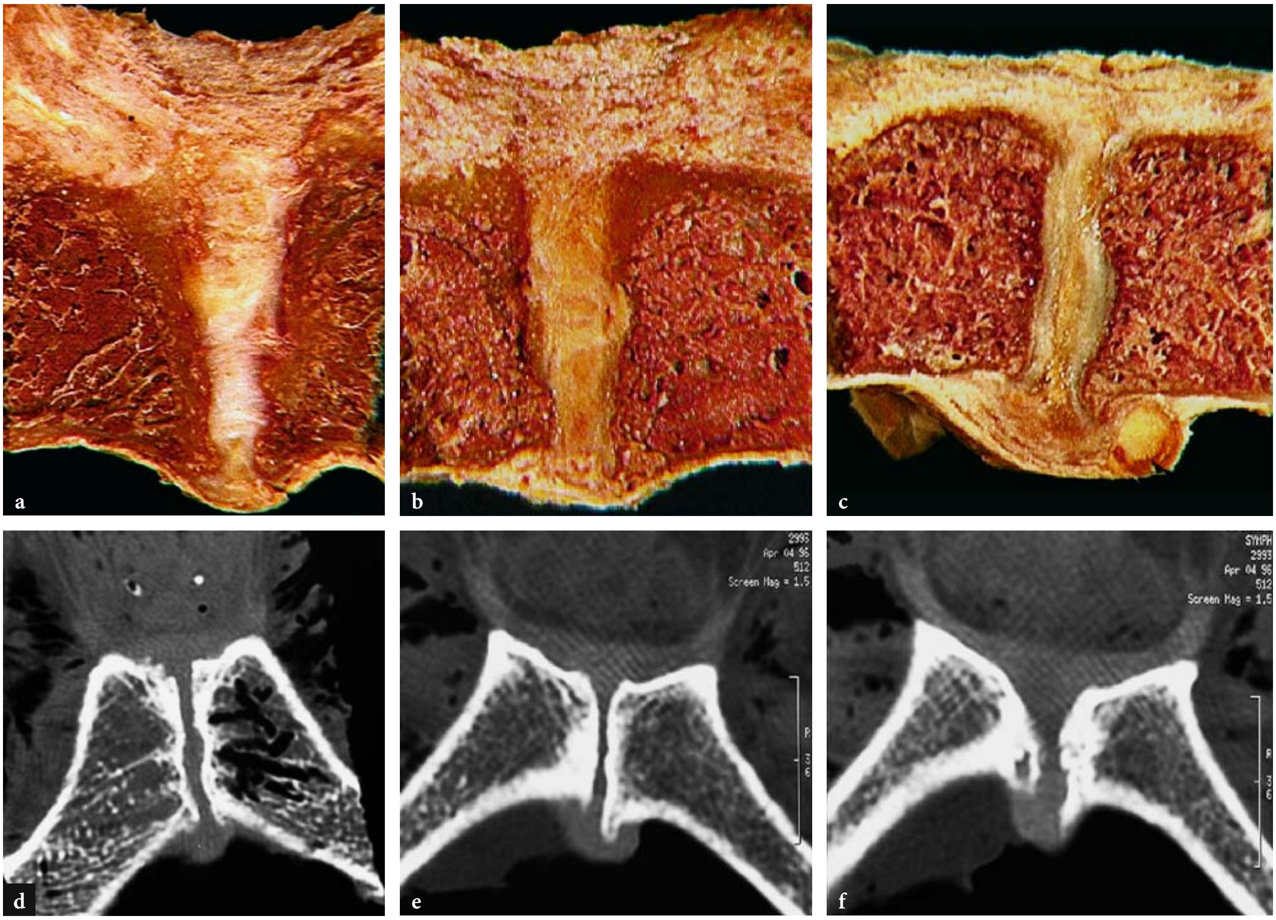

Fig. 15.3a–f. Progression of posterior symphyseal extrusion and posterior symphyseal osteophyte formation. **a–c** Transverse sections have been taken from three different cadaveric specimens and show increasing changes. **a** A bulge is seen at the posterior symphyseal margin reflecting early posterior extrusion. **b** Increasing posterior symphyseal extrusion is seen with asymmetric extension to the left and there is a suggestion of early changes of ossification. **c** Progressive posterior symphyseal extrusion with an ossicle within the laterally extruding fibrocartilaginous disc on the left. **d–f** Transverse axial CT scan images of three different cadavers again showing progressive development of buttress osteophyte formation adjacent to the posteriorly extruded pubic symphysis. In this series these changes are again asymmetrical more prominent on the left

The RA muscle and rectus sheath in man, as in other members of the ape family (Ackerman and Spencer 1992), does not terminate at the SSL but extends anteriorly to cover the anterior aspect of the pubic bones and the pubic symphysis. Inferiorly it interdigitates with the common adductor tendon origins of gracilis, adductor brevis and adductor longus (i.e. the common adductor origin or CAO) to form a functional and structural unit (RA-CAO unit). They also show that the inguinal ligament does not terminate at the pubic tubercle but extends obliquely over the anterior surfaces of the pubic bones, i.e. as a pre-pubic inguinal ligament extension (ILE), forming an incomplete V-shaped configuration (Fig. 15.4). The "V" is incomplete as the ligament terminates just short of the anterior surface of the pubic symphysis. Here they fuse with the presymphyseal connective tissue in the majority of cases adhering tightly to the anterior portion of the symphyseal fibrocartilage. It is this layer which apparently limits the anterior symphyseal migration.

The lateral half of the RA can be muscular or tendinous and inserts onto the anterosuperior pubis and corresponding ILE. The adductor longus (AL) originates from the anterior surface of the pubic bone and corresponding ILE. The AL tendon and pyramidalis muscles form a continuous line separated only by the ILE (Fig. 15.5). Injury to one link of this functional chain may affect one of the other links resulting in clinical diagnostic confusion. This confusion is perhaps reduced if the *actual* anatomy is recognised rather than just the classical description (Fig. 15.6).

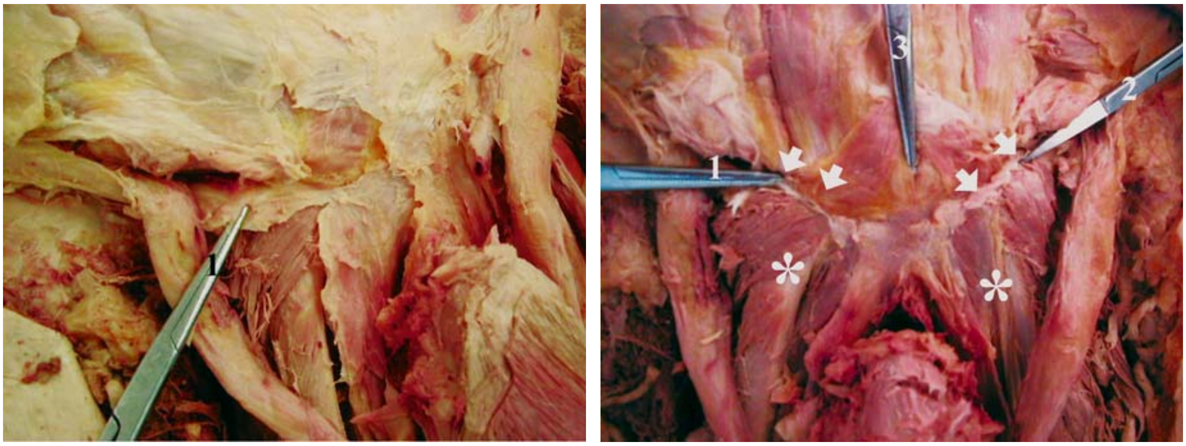

a b

Fig. 15.4a,b. The anterior pubic extension of the inguinal ligament. **a** The external oblique aponeurosis has been incised transversely and extended medially into the anterior rectus sheath in a male patient. A pair of forceps (*1*) is reflecting the inferior border of this extension inferiorly and lies in the region of the right pubic tubercle. **b** The external oblique aponeurosis and rectus sheath has been excised whilst the forceps from (**a**) continues to lie at the pubic tubercle. A pair of scissors tips (*2*) marks the corresponding left pubic tubercle. A second pair of forceps (*3*) is lying at the apex of the pyramidalis muscle. This dissection illustrates how the inguinal ligament does not terminate at the pubic tubercle but continues as a V-shaped structure over the anterior pubic bodies (*arrowheads*). Pyramidalis inserts into its superior border whilst the adductor muscles (*) insert into this inguinal ligament extension at its inferior margin

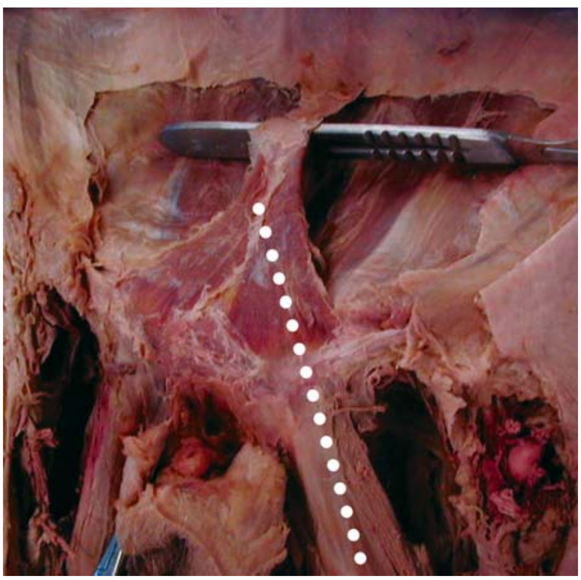

Fig. 15.5. Common alignment of pyramidalis and adductor longus. A scalpel blade is elevating the pyramidalis muscles away from the underlying rectus abdominis muscle. Once elevated there appears to be a common alignment (*broken line*)

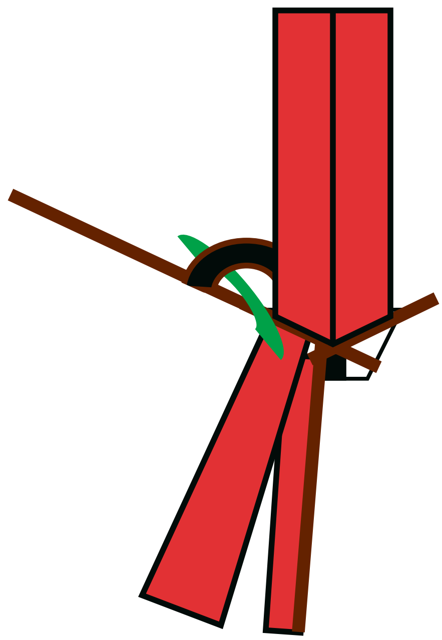

Fig. 15.6. Illustration of the frontal view of the pubic symphyseal region – actual anatomy

In sagittal cross-section a triangular condensation of fibrocartilage lies between the muscular adductor brevis pubic origin, the AL and RA representing their common ILE origin (Figs. 15.7 and 15.8). It can be seen from the above anatomical studies that the RA-CAO aponeurosis attaches to the anterior pubic bodies at their antero-lateral margin and the inguinal ligament at its insertion into the pubic tubercle and its pre-pubic extension. It is possible that this is analogous to the pre-pubic tendon seen in other mammals which can be similarly avulsed from its bony pubic origin (Sturesson et al. 1989). A shear or avulsion

Fig. 15.7. Triangular pre-pubic fibrocartilaginous condensations. Sagittal sections through six different pubic bodies in all of these specimens different variations in form are seen but with the common theme that some form of triangular cross-section fibrocartilaginous condensation appears to exist (*)

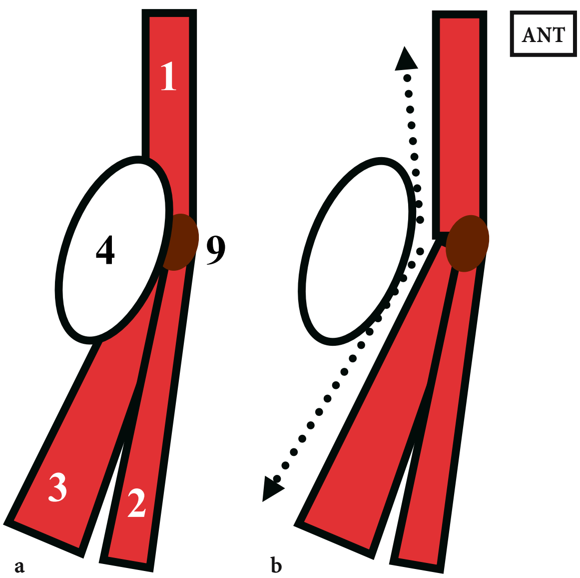

Fig. 15.8a,b. Illustration of the sagittal section through the upper pubic bodies showing: **a** Normal anatomical arrangement; **b** Separation of the pre-pubic soft-tissues due to shearing forces – *arrows* (From RA Pull (*above*) or CAO Pull (*below*). For figure legend; see also Fig 15.1

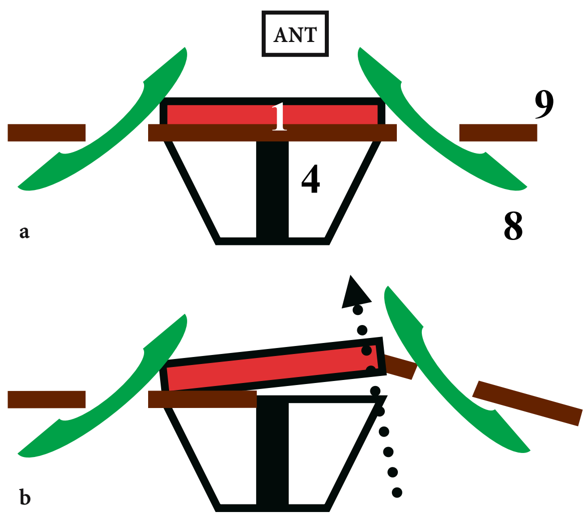

Fig. 15.9.a Illustration of the axial section through the upper pubic bodies. **b** Illustration of the axial section through the upper pubic bodies with separation of the supero-lateral soft-tissues due to shearing forces – (*arrow*) (or raised intra-abdominal pressure). The result of the shearing injury is a defunctioning of the external inguinal ring and formation of a "pre-hernia" complex. For figure legend; see also Fig 15.1

injury to the conjoint RA-CAO aponeurosis where it attaches to the anterolateral pubic margin potentially will also shear-off the inguinal ligament at the pubic tubercle. Therefore, an injury to the RA-CAO at its pubic insertion will potentially weaken the posterior wall of the inguinal canal at the level of the external inguinal ring, i.e. it may predispose to a "sportsman's hernia, or vice versa (Fig. 15.9).

The medial half of each of the bellies of rectus abdominis can continue distally as a ligament running over the anterior symphysis, partially decussating so as to interdigitate distally with the gracilis origin and fascia bilaterally (recto-gracilis ligament; Fig. 15.10). This again may cause difficulty in localising symptoms and exacerbate any clinical diagnostic confusion.

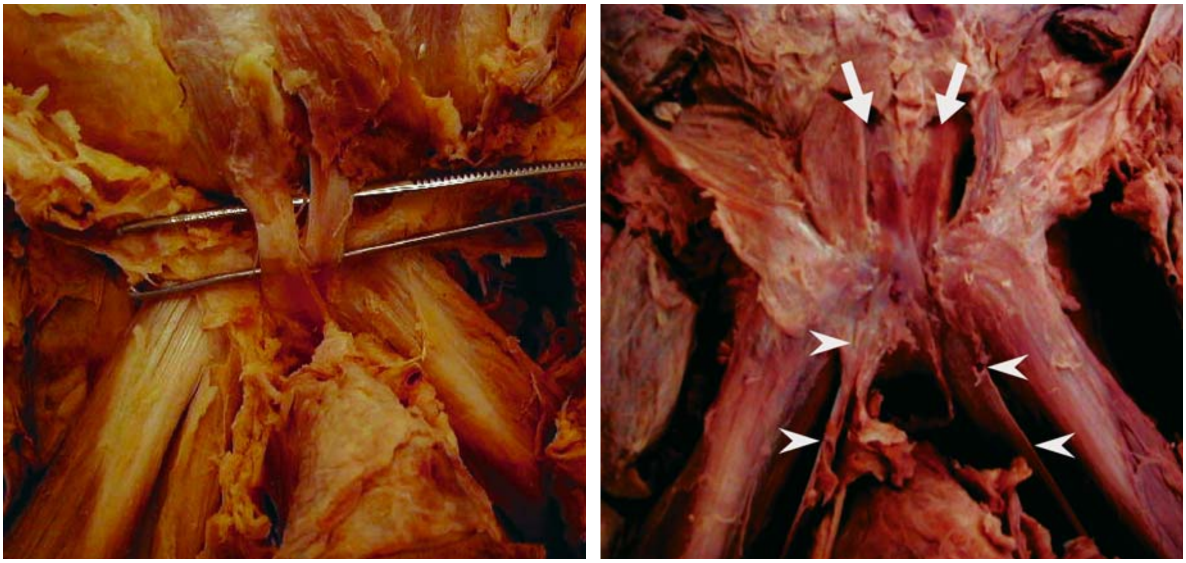

Fig. 15.10a,b. The recto-gracilis ligament. Two male cadaver dissections showing the thin bilateral extensions of the rectus abdominis. **a** A pair of dissection forceps is lying between these ligaments and the pubic symphyseal region. **b** A window has been cut through the more superficial pyramidalis muscle to expose the underlying ligaments. It can be seen that at the proximal end there appears to be a rudimentary muscular component (*arrows*). At the distal end these ligaments partially decussate to fuse with both ipsilateral and contralateral gracilis fasciae (*arrowheads*)

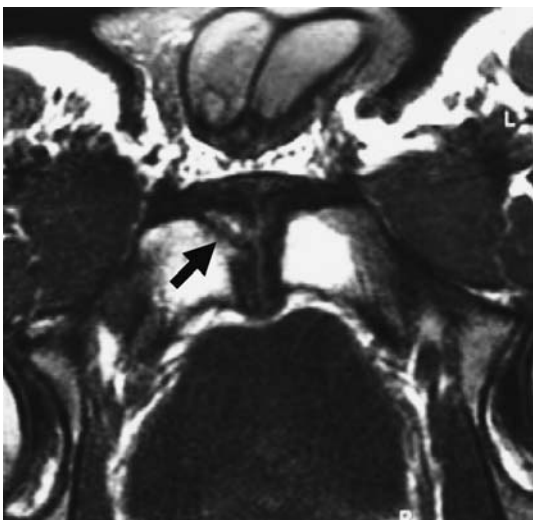

Fig. 15.11. Pubic growth retardation secondary to chronic soccer-related adolescent injury. The T1-weighted transverse sections both show features of symphyseal degeneration with posterior osteophyte formation subchondral sclerosis and cyst formation and loss of joint space. In addition there is failure of normal fusion of the right pubic apophysis to the pubic body (*arrow*)

Excessive forces at entheseal sites predispose to a subsequent parasymphyseal stress injury to bone. Such a link between the RA insertion, pubic apophysis and CAO may also explain the apparent injury to the apophyses seen either unilaterally or bilaterally in young athletes and subsequent apophyseal developmental retardation (Fig. 15.11).

15.3 Osteitis Pubis

Osteitis pubis, as described in the literature, essentially reflects two distinctly separate conditions:

1. Symphyseal Stress Injury/Symphyseal Degeneration/Mechanical Osteitis Pubis: a stress phenomenon involving the symphyseal region often with coexisting associated degenerative changes.
2. Inflammatory "True" Osteitis Pubis: a true inflammatory "osteitis" representing a non-suppurative condition which is clinically (and radiologically) very similar to parasymphyseal osteomyelitis except for it being self-limiting and less destructive.

15.3.1 Symphyseal Stress Injury

In spinal intervertebral disc degeneration there is loss of disc height, vertebral body end-plate sclerosis

and marginal osteophyte formation on conventional radiographs and disc desiccation with end-plate fatty infiltration or sclerosis (Modic types 2 and 3 changes) on MR imaging (Modic et al. 1988). A mechanical discitis may also occur with fluid signal within the central nuclear cleft, edema within the end-plates (Modic type 1 change) and adjacent perivertebral soft tissue edema. In severe cases, differentiation of a mechanical discitis from an infective discitis may be extremely difficult requiring biopsy for microbiological assessment. Personal experience of MR imaging of athletes with groin pain suggested that the pubic symphysis may be considered analogous to the intervertebral discs of the spine, only lying in a sagittal rather than a horizontal plane (recognising this concept formed in part the original stimulus for embarking on the current body of work).

On both conventional radiography and MR imaging the appearances of pubic symphyseal degeneration and pubic "symphysitis" are remarkably similar to those changes seen in intervertebral disc degeneration and mechanical discitis. MR imaging, in particular, is able to demonstrate pubic bone marrow changes analogous to the Modic types 1–3 changes seen in the spine (Figs. 15.12–15.14). These spinal changes can be centred around the disc and the vertebral end plates or at the site of entheseal attachment, i.e. the anterior and posterior longitudinal ligaments. In the symphyseal region these changes may be seen to be related to the subchondral plate or at the insertion of the inguinal ligament, rectus abdominis and

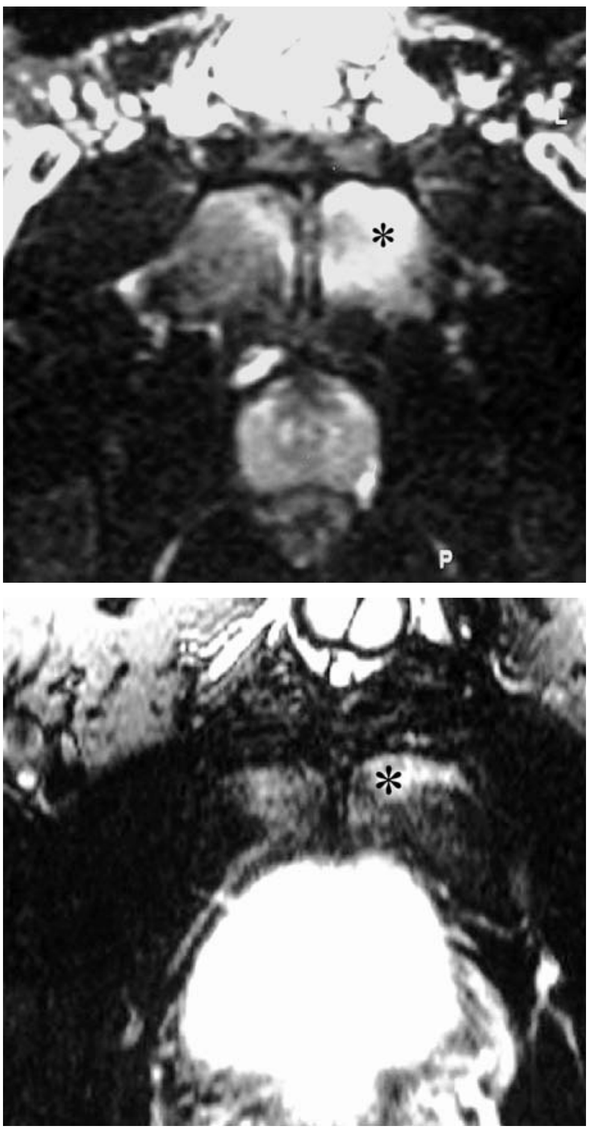

a

b

c

Fig. 15.12a–c. Modic type 1-equivalent changes. T2-weighted fat-suppressed transverse section images though the mid-pubic symphysis in two different professional soccer players showing two different distributions of bone marrow edema(*). In both cases these changes are more marked on the left side. **a** Subarticular – adjacent to the symphysis pubis. **b** Subentheseal – at the site of insertion of the anterior pubic soft tissue. **c** T1-weighted sagittal image through the lower lumbar spine showing typical Modic type 1 end-plate changes adjacent to the L3/4 intervertebral disk

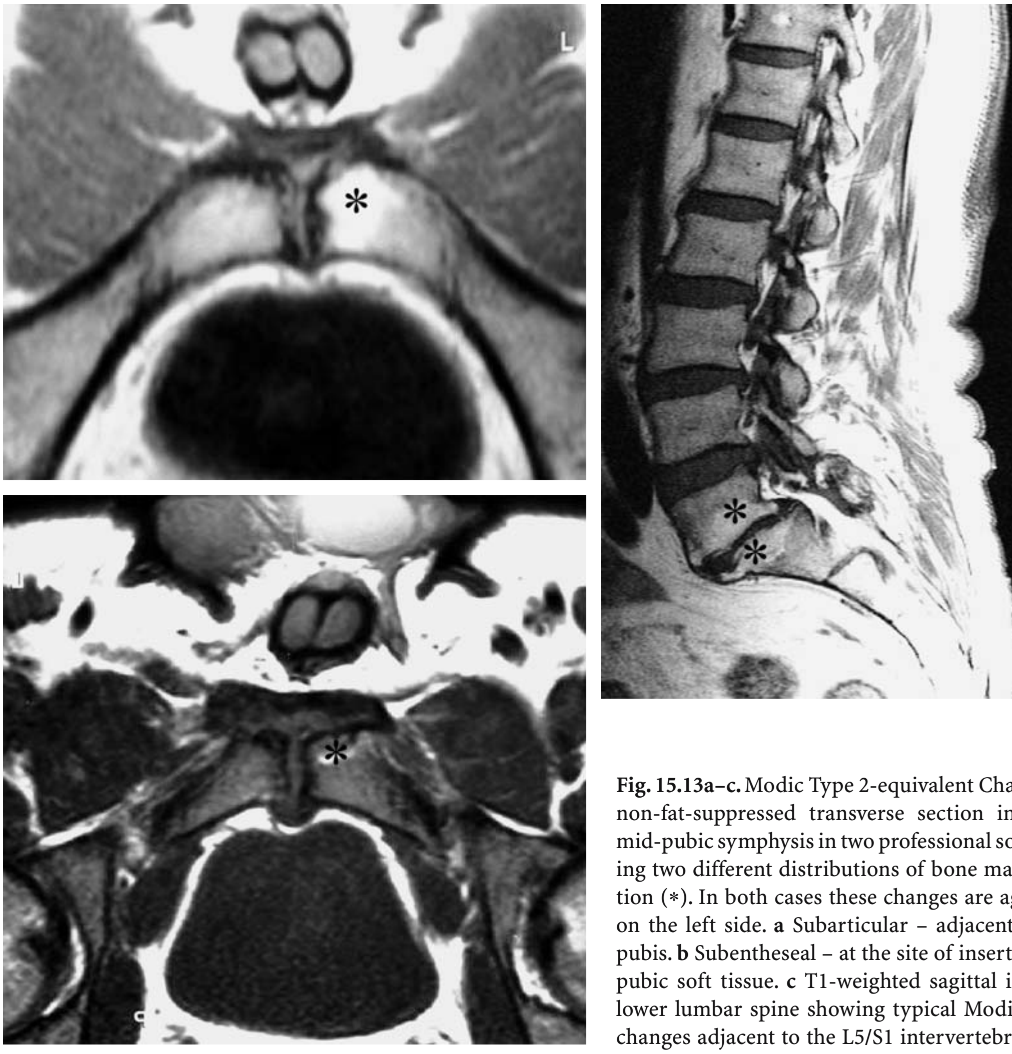

a

b

c

Fig. 15.13a–c. Modic Type 2-equivalent Changes. T1-weighted non-fat-suppressed transverse section images though the mid-pubic symphysis in two professional soccer players showing two different distributions of bone marrow fatty infiltration (∗). In both cases these changes are again more marked on the left side. **a** Subarticular – adjacent to the symphysis pubis. **b** Subentheseal – at the site of insertion of the anterior pubic soft tissue. **c** T1-weighted sagittal image through the lower lumbar spine showing typical Modic type 2 end-plate changes adjacent to the L5/S1 intervertebral disk

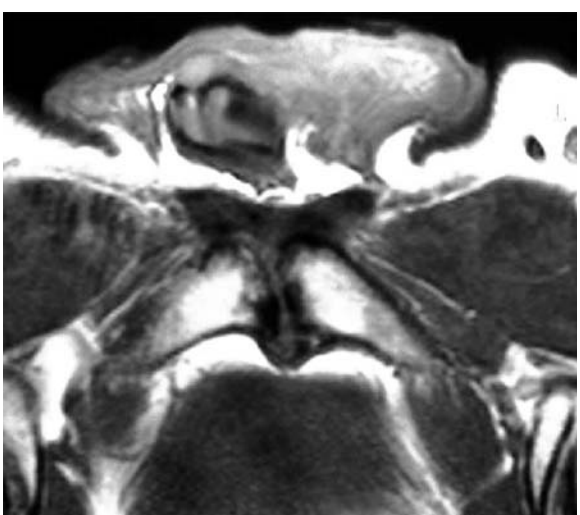

Fig. 15.14. Modic type 3-equivalent changes. T1-weighted non-fat-suppressed transverse section images though the mid-pubic symphysis in a professional soccer players showing two different distributions of subcortical/subchondral bone sclerosis bilaterally, i.e. these changes are present both in a sub-articular position posteriorly adjacent to the symphysis pubis and also in a sub-entheseal position at the site of insertion of the anterior pubic soft tissue

anterior adductor tendons, again showing the analogous nature of these anatomical sites and their corresponding chronic injury processes.

Therefore, the condition traditionally considered to be "osteitis pubis" appears to be structurally and pathophysiologically akin to intervertebral disc degeneration reflecting excessive wear from physical activity and as such is unlikely to be a *major* cause of groin symptoms in athletes.

MR imaging is able to show "mechanical" changes of parasymphyseal subchondral sclerosis, posterior-superior pubic symphyseal extrusion with buttressing osteophyte formation, subchondral cyst formation (and para-sacroiliac joint sclerosis), i.e. MR-equivalent changes to those thought to represent "osteitis pubis" on conventional radiographs (Fig. 15.15).

The prominence of anterior and posterior symphyseal extrusion is likely to reflect the repeated high-impact lateral compression forces being applied. The iliac pubic bones represent a long lever arm with the sacroiliac joints as fulcrum. The medial compression forces at these sacroiliac joints are greatest anterior to the point of ligamentous attachment. As the stronger ligaments are posteriorly placed (Ogden 1980) then logic would seem to state that any compression force is likely to be greatest at the anterior margin of the joint. Also, as the sacrum is relatively fixed compared to the pubic bones during bipedal gait, any subse-

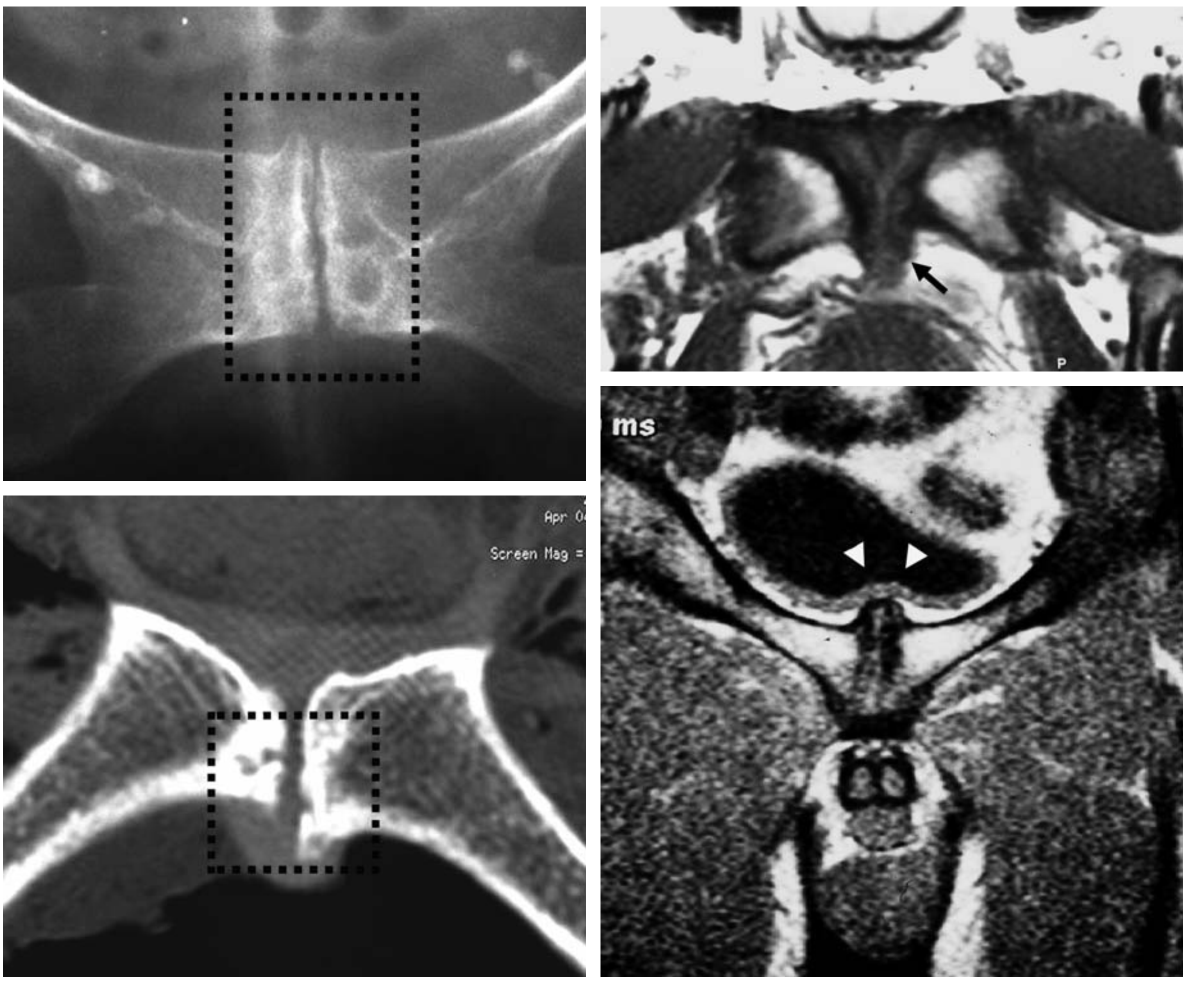

a b c d

Fig. 15.15a–d. Symphyseal degenerative changes – "Osteitis Pubis". **a** Frontal pelvic radiograph showing superior marginal osteophyte formation, subchondral cysts and subarticular sclerosis. **b** Axial CT scan demonstrating posterior marginal osteophyte formation, subchondral cysts and subarticular sclerosis (*Box*). **c** T1-weighted axial MR image showing marked posterior symphyseal extrusion in 16-year-old "apprentice" soccer player (*arrow*). **d** Coronal T1-weighted image showing apparent superior symphyseal extrusion indenting the bladder bas (*arrowheads*)

quent stress-related changes would be expected to be more on the pelvic, rather than sacral, side of the sacroiliac joints. The physical laws governing a bone adaptive response to mechanical stresses are poorly understood but have become known as Wolff's Law (Numaguchi 1971). This law basically states that bone formation will increase in areas of compression and decrease in areas of tension. The primary bone trabeculae remodel and orientate themselves along stress lines and eventually form the secondary trabeculae. These latter trabeculae act as internal struts or tie beams to support a bone's integrity against deforming forces. Therefore, any bone changes due to these compressive forces at the sacro-iliac joints should be greatest at the anterior sacroiliac joint margin of the ilium. If this concept is correct then in accordance with Wolff's Law there should be an increase in trabeculae in a triangular configuration at the anterior border of the ilium adjacent to the sacro-iliac joints (Cochrane 1971). In MR imaging terms this would appear as a triangular area of signal void. These are the typical appearances of hyperostosis triangulare ilii seen in professional soccer players. This would seem to explain significant increase in such appearances in professional soccer players compared to non-athletes and amateur players. Although lateral pelvic compression forces appear to be much higher in professional footballers generally they do not, however, appear to directly reflect symptomatology.

Any changes at the sacroiliac joints are likely to be greatly magnified at the symphysis pubis due to the moments of force generated via the long pelvic bone "lever". This could explain the pubic trabecular bone configuration seen in the pubic region where the denser trabecular pattern is greatest in the subarticular region and forms a triangular configuration broadest anteriorly. Lateral compression forces applied to the pubic symphyseal fibrocartilaginous disc should produce loss of disc height/joint space and circumferential bulging of its periphery (Fig. 15.15). However, such bulging will only take place where the surrounding soft tissues permit the disc to do so. In the pubic region there is only minimal soft tissue support at the posterior margin of the pubic symphysis. Therefore, there is little to oppose posterior symphyseal bulging and progressive posterior extrusion explaining the posterior symphyseal eminence noted with aging. In order to obtain biomechanical neutrality when such a process occurs anywhere in the body a rim of buttressing osteophytes is formed in an attempt to support the otherwise unsupported fibrocartilage and as the first stages of bone remodelling.

15.3.2 "True" Osteitis Pubis

An acute inflammatory condition akin to a spinal "mechanical" (non-infective) discitis can occur in the pubic symphyseal region with fluid within the pubic symphysis and symphyseal cleft and edema in the sub-chondral bone as well as below the attached anterior tendons and the bladder base. This condition is a "true osteitis pubis" or "symphysitis" and like spinal discitis may be the cause of quite severe symptoms (Fig. 15.16).

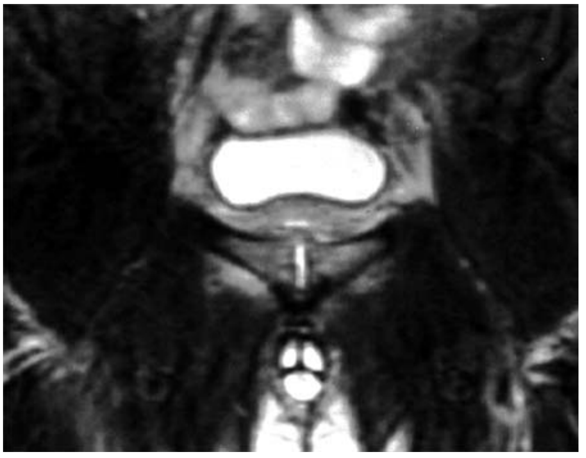

Fig. 15.16. "True" osteitis pubis. Coronal STIR image showing fluid within the symphysis pubis, bilateral parasymphyseal bone marrow edema and edema in the adjacent soft tissues at the bladder base and adductor muscles bilaterally. The patient was a professional soccer player with severe symphyseal pain and bilateral groin pain. The condition was completely resolved with rest and non-steroidal oral anti-inflammatory agents

Athletes with "true" osteitis pubis have bilateral severe adductor pain, exacerbated by symphyseal compression. It has been suggested that the chronic behaviour of osteitis pubis may be promoted by poor vascular supply that often exists to the periosteal and subperiosteal regions of the pubic bones. MR imaging shows profound bilateral para-symphyseal bone marrow edema, with edema at both adductor origins, fluid within the symphyseal cleft and often edema around the bladder base. The raised intra-osseous pressure related to this bone marrow edema may in part be instrumental in the production of the severe pain. Injection of steroids into the symphyseal cleft often produces dramatic benefit in such patients presumably by reducing the effects of the regional edema (Fig. 15.17). Greater care, however, must be taken to

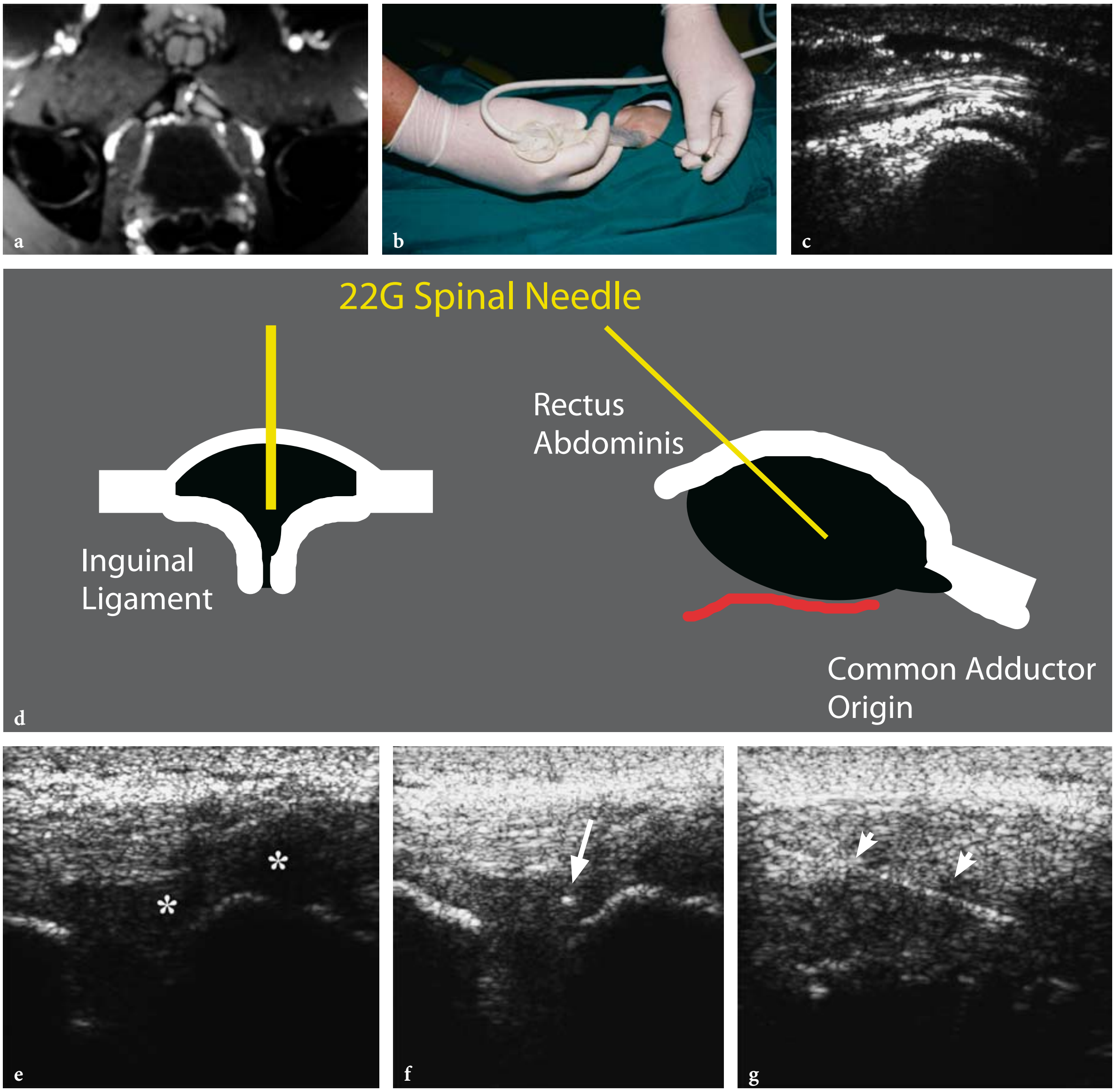

Fig. 15.17a–g. Technique for ultrasound-guided pubic symphyseal steroid injection. **a** MR imaging was initially performed to ensure correct diagnosis. **b** Under aseptic condition and local anaesthesia using a 5–10 Mhz linear-array ultrasound transducer for guidance; a 22 G spinal needle is inserted into the symphyseal cleft. **c** Microbubbles in the triamcinolone (40 mg in 1 ml) are clearly seen as reverberation artefact. **d** Diagram of needle placement. **e** Transverse ultrasound image in similar plane to MR image in a shows a hypoechoic band of granulation tissue within an area of osseo-tendinous separation of left common adductor origin (*). **f** Same as e but with echogenic needle tip now visible to left side of pubic symphysis (*arrow*). **g** Longitudinal view of same needle (*arrowheads*)

avoid steroid injections if there is anything to suggest an infective cause as this is likely to be seriously exacerbated by local corticosteroid effects.

It is interesting that an injection of local steroid into the symphyseal region has been shown to produce dramatic effect in patients with osteitis pubis, which appears to be degenerative rather than primarily inflammatory in origin (Koch and Jackson 1981). If apparent pubic symphyseal symptoms are actually related to an adjacent entheseal injury and not the symphyseal degenerative process itself, then perhaps it would not be surprising to find that steroids infiltrated below the pre-pubic soft tissues should produce dramatic results (as is the case in patients with an inflammatory arthritis-related enthesitis). In distance runners an association appears to exist between

strenuous conditioning of the rectus abdominis and adductor muscles and the production of this condition (Koch and Jackson 1981). In a different study, eight intercollegiate athletes with refractory osteitis pubis (who on analysis of the article would appear to have symphyseal stress changes) all had significant symptomatic benefit from subsequent injection of corticosteroid into their symphysis pubis (Holt et al. 1995).

The differentiation between pubic osteomyelitis and "True" Osteitis Pubis is important, as the majority of cases of pubic osteomyelitis require surgical debridement and curettage for adequate control of the infective process. The clinical course of osteomyelitis is usually progressive in contrast to the osteitis pubis which is self limiting and generally produces less bone destruction. The eventual clinical course of osteomyelitis of the pubis is, therefore, sufficiently different from that of osteitis pubis to justify considering it as a separate entity. The spectra of these conditions, however, tend to overlap, and it is in this overlapping area that diagnostic difficulties arise (Rosenthal et al. 1982). Occasionally a traumatised parasymphyseal area may act as a focus for bloodbourne infection especially in the immunocompromised (a state which may occur in athletes due to the effects of "over-training"), making differentiation from pubic osteomyelitis even more difficult.

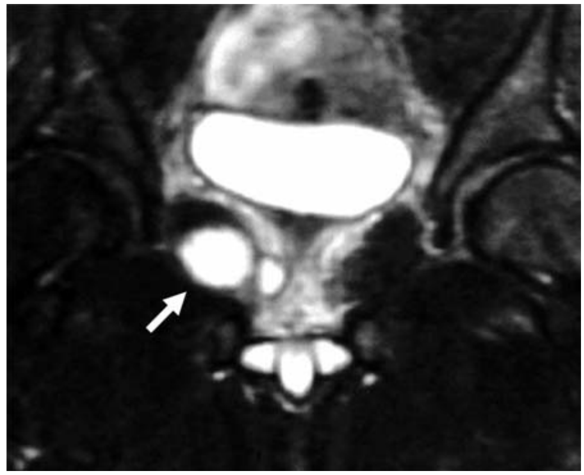

a

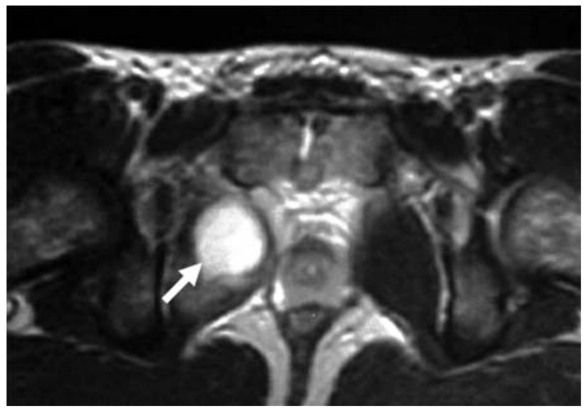

b

Fig. 15.18a,b. Pubic osteomyelitis: **a** coronal; **b** transverse axial STIR images through the pubic regions showing a discrete abscess cavity within the right obturator internus muscle (*arrows*), with fluid within the symphysis and edema within the parasymphyseal bone marrow and adjacent soft tissues. The patient was a professional footballer with pubic symphysitis and a pelvic abscess following an episode of acute prostatitis which subsequently resolved following intravenous antibiotic therapy

15.4 Pubic Osteomyelitis

Osteomyelitis of the pubic symphyseal region is rare, accounting for less than 1% of all cases of osteomyelitis produced by haematogenous spread (Heldrich and Harris 1979). Unfortunately, athletes are not immune to pubic osteomyelitis and indeed as stated above, the combination of their tendency to immunosuppression and minor trauma to the region may even increase the risk. When conventional radiography has been performed in athletes with pubic symphyseal osteomyelitis there has usually been symmetrical bone destruction of the pubic symphysis with apparent widening of the symphyseal region (Bouza et al. 1978; Patterson and Yovanovich 1975). Even on MR imaging it can be extremely difficult to distinguish between pubic osteomyelitis and non-infective osteitis pubis particularly in their early stages before discrete abscess formation occurs (Fig. 15.18).

Bacteriologically proven staphylococcus aureus osteomyelitis of the symphysis pubis can be completely asymptomatic (Evans et al. 1985). Needle biopsy may be inadequate and even open biopsy is not always able to isolate organisms which are often sparse within the infected subchondral bone in patients with parasymphyseal osteomyelitis. Indeed, in patients with known infection who undergo such curettage, a causative organism is only isolated in approximately 50% of cases, emphasising the difficulty in making the definitive diagnosis of pubic osteomyelitis, particularly in its early stages. That being said, it may be the only certain way of distinguishing between early osteomyelitis and osteitis pubis as initially both on clinical examination and imaging investigations, they may appear to be identical (Sexton et al. 1993).

15.5 Stress Fractures

These high forces at the adductor origins are reflected in the prominent primary trabeculae in the parasymphyseal pubic bones. Such a phenomenon reflects trabecular micro-fracture and repair along the line of deforming forces which in this case is the line of pull of the adductor tendons in accordance with Wolff's Law (Fig. 15.19). This process provides a degree of protection against the applied forces. Such a phenomenon results in intra-osseous marrow edema at the site of entheseal attachments.

If the rate of trabecular injury exceeds the speed with which the body can repair these microfractures then a macrofracture will occur, i.e. a stress fracture. In the osteoporotic skeleton such stress fractures may occur with relatively low or normal level of cyclical loading (parasymphyseal insufficiency fracture, Fig. 15.20) (Casey et al. 1984; Goergen et al. 1978). In the skeleton of a young athlete where there is excessive cyclical loading of normal or even "supernormal" bone, overuse fractures may result (Orava et al. 1978).

At an earlier stage, before actual stress fracture formation, the marrow edema produced by the reparative response could presumably cause some degree of discomfort due to the associated raised intra-osseous pressure. The triangular configuration of the area of increased trabecular bone density reflects the site of greatest entheseal surface area and the line of applied traction forces (in accordance with Wolff's Law). The pattern of the trabeculae seen demonstrates the direction of the greatest forces applied to the pubic bones. The greatest areas of trabecular bone density were the subchondral and subentheseal regions. The former reflects the transverse compression forces across the

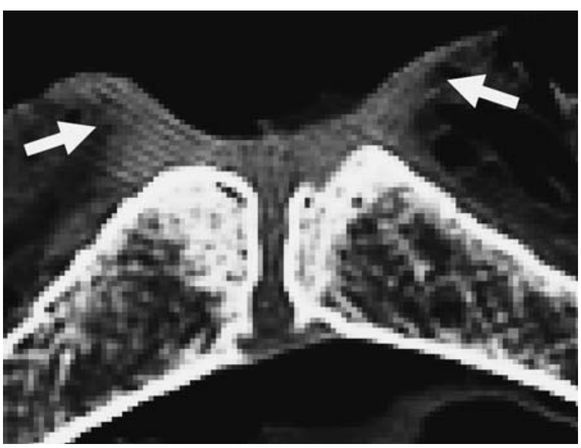

Fig. 15.19. Parasymphyseal trabecular bone pattern (macroscopic appearance). Transverse axial CT image demonstrating a triangular area of increased trabecular bone density either side of the pubic symphysis. The oblique lateral border with "normal" trabecular density appears to be in line with the attached insertion of the inferior radial ligament formed by combination of adductor longus and gracilis tendons (*arrows*)

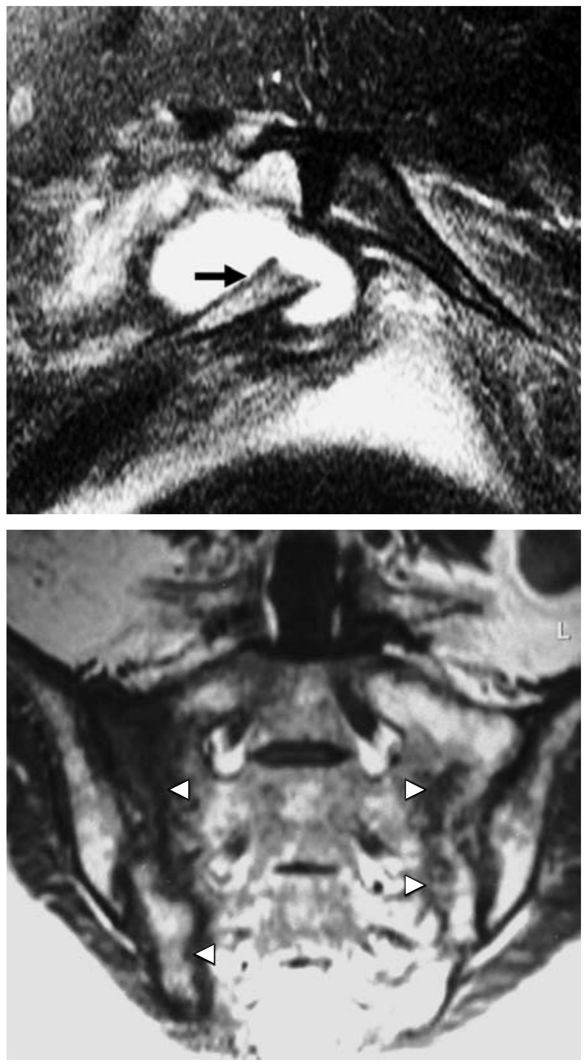

a

b

Fig. 15.20a,b. Pubic stress injury. **a** T2-weighted fat-suppressed transverse image through the mid pubic symphyseal region. **b** T1-weighted coronal images through the sacrum. There is (**a**) a right parasymphyseal stress fracture which has become medially displaced due to lateral compression forces (*arrow*), and (**b**) there are bilateral lines of decreased signal parallel to the sacro-iliac joints (*arrowheads*) reflecting the fact that the stress forces are acting on both anterior and posterior sections of the pelvic ring

pubic symphysis resulting in anterior, or more commonly, posterior symphyseal extrusion. The triangular area of higher trabecular density anterolaterally in the superior portion of the pubis corresponded to the site of entheses. The phenomenon of parasymphyseal stress changes has been previously termed osteitis condensans pubis (Jajic and Jajic 1998). Such a description is not unreasonable, reflecting it being analogous to the anterior parasacroiliac changes seen. The same appearances in the inferior portion of the pubic bodies corresponded with the origin of the gracilis tendons and gracilis fascia.

The anterior pubis, inferior ischial ramus and iliac crest have been previously shown to be the anatomical sites of the innominate bones with the lowest average calcium-equivalent densities particularly the area of the pubic tubercles and crest using dual-energy quantitative computed tomography (Dalstra et al. 1993).

These recorded figures relate to subjects 72–87 years of age and are consistent with the sites of insufficiency fractures of the pelvis. There is a boundary between the dense and less dense trabecular bone regions which could result in a "fault-line", i.e. these entheseal forces may predispose to parasymphysael stress injury.

Excessive cyclical loading of the parasymphyseal region may lead to a stress injury. Parasymphyseal stress fractures, however, are rare in athletes being more common as insufficiency rather than overuse fractures. With regards to "True" Osteitis Pubis the

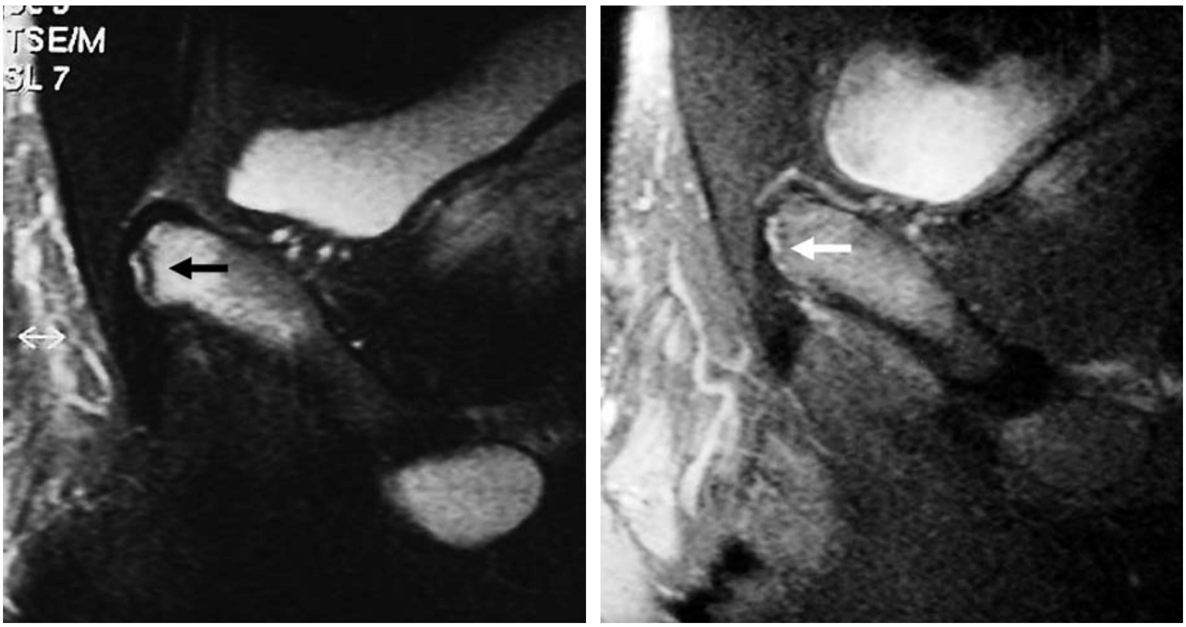

a b

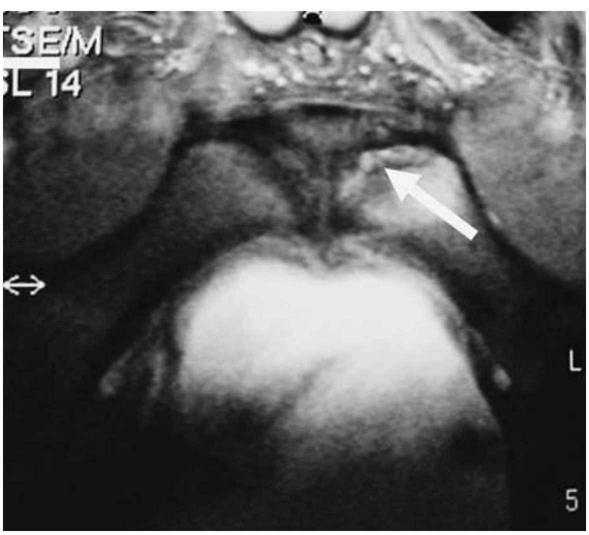

c

Fig. 15.21a–c. Subentheseal pubic bone stress injury. **a** Fat-suppressed T2-weighted sagittal image through the left pubic body. **b** Corresponding contrast-enhanced fat-suppressed sagittal and (**c**) transverse section through the mid pubis. There is a line of signal void parallel to the site of insertion of the rectus abdominis and adductor pubic origins (*arrows*) with surrounding bone and soft tissue edema consistent with stress injury to bone

MR imaging appearances would tend to agree with the concept of trabecular microfracture stress injury as the main underlying pathological process. There would appear to be a correlation between MR imaging Modic type I change and increased uptake on Technetium 99m MDP isotope bone scan studies in such cases (Fig. 15.21).

15.6 Hip Joint Dysfunction

Restriction of hip rotation may increase the shear stresses applied to the ipsilateral hemi-pelvis in the anteroposterior plane (Williams 1978). It has also been suggested that "mechanical" Osteitis Pubis may be a stress phenomenon related at least in part, to a limitation of hip movement (Williams 1978). That hip problems can affect the biomechanical forces across the pelvic ring is evidenced by the fact that para-symphyseal insufficiency fractures may have associated hip osteoarthritis (OA) and approximately 30% have associated rheumatoid arthritis (Nicholas et al. 1989). Conversely, stress fracture of the hip has been reported after sacral fusion in an adult with scoliosis (Morcuende et al. 2000).

In patients with a degenerative symphysitis there is loss of hip internal rotation and to a lesser extent external rotation, possibly relating to a very minor degree of prior slipped capital femoral epiphysis during adolescence. In a retrospective review of 59 patients with a clinical diagnosis of sports-related osteitis pubis radiographic analysis showed an increased femoral head ratio in 7% of cases suggesting adolescent or childhood epiphysiolysis to be a possible underlying aetiological factor (Fricker et al. 1991). There appears to be an increased tilt deformity in 83% of athletes with osteitis pubis as compared to 25% of athletes overall. It has also been noted that there is an increased incidence of symphyseal stress phenomena following hip arthrodesis (Breitenfelder et al. 1975). These observations would tend to support the concept that minor limitation of hip movement, due to adolescent injury to the proximal femoral physeal plate, can predispose to later pubic symphyseal problems.

This association with hip pathology is made particularly important by the fact that injuries to the hip itself are not uncommon in athletes (Weaver 2002) and anterior acetabular labral tear with adjacent chondral damage is now becoming increasingly recognised as a cause of groin pain in footballers with the wider use of hip arthroscopy (Saw and Villar 2004; Mitchell et al. 2003). Conventional MRI and ultrasound imaging are relatively insensitive at demonstrating labral tears and although MR-arthrography may be more sensitive, it is still probably inferior to hip arthroscopy in diagnosing these injuries (Fig. 15.22). There may also be accelerated hip joint

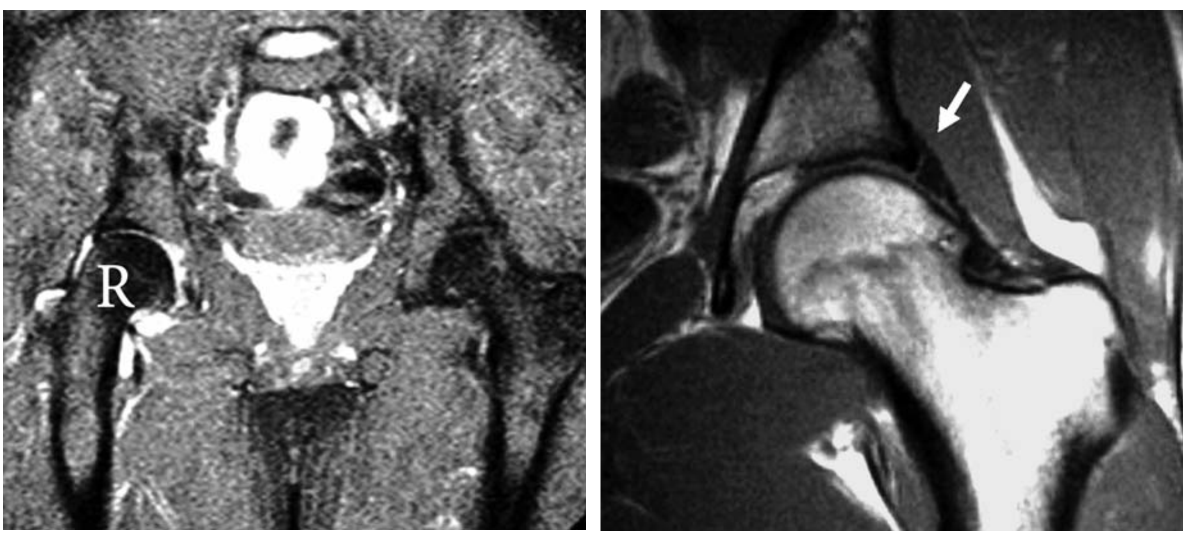

a b

Fig. 15.22a,b. Hip joint osteoarthritis and labral tear. Two different professional soccer players, both in their mid-twenties and both with groin pain related to hip joint OA. **a** Coronal STIR image showing a mildly deformed right femoral head (*R*) and profound hip joint effusion. **b** Non-fat suppressed T1-weighted image from a MR arthrogram showing a rim of femoral head osteophytes. There is also a high signal band between the joint capsule and lateral acetabular margin (*arrow*) reflecting an associated labral tear

degeneration in the older soccer player which may present as groin pain. Symptomatic hip osteoarthritis (OA) will usually exhibit increased enhancement with intravenous Gadolinium-DTPA due to an associated synovitis which may benefit, at least temporarily, from ultrasound-guided intra-articular injection of steroids.

This impingement may take two different forms. First, the pincer type where the femoral head-neck junction contacts the acetabular rim, typically as a result of an underlying acetabular abnormality. Second, the CAM type, which is probably the more common in athletes, where at MR arthrography there is a triad of abnormal morphology of the anterior femoral head-neck junction (abnormal α angle), anterosuperior labral tear and anterosuperior cartilage lesion (Kassarjian et al. 2005; Lebrun et al. 2005).

15.7 Sacroiliac Joint Dysfunction

It has been previously suggested that symphyseal degenerative changes are often associated with concurrent sacroiliac joint (SIJ) dysfunction (Harris and Murray 1974). In one radiographic study of professional footballers with symptoms at time of investigation, there was evidence of overt symphyseal instability in one third of players, marginal irregularity in three quarters and reactive sclerosis adjacent to the symphysis in two thirds of players. There were abnormalities in the region of the gracilis origin in a further two thirds and evidence of stress sclerosis in the iliac component of one or both sacroiliac joints in just over half of these professional soccer players. In this study there was good overall correlation between radiological SIJ abnormality and a past history of groin or lower abdominal pain (Harris and Murray 1974).

15.8 Entheseal Injury

This same balance of micro-injury and repair also occurs in tendons again in response to applied deforming forces (Gibbon et al. 2000). It can be seen that if the pubic symphyseal cleft propagates anterolaterally then this common aponeurosis may be sheared off its pubic attachment. However, a traction injury mechanism is also possible. Repetitive minor injury to a tendon may result in microtears. These may in turn accumulate at the site of excessive mechanical loading, sufficiently weakening the tendon's tensile strength so that it results in a spectrum of tendinosis which in its severest form reflects intrasubstance tear or even tendon avulsion (Gibbon et al. 1999). If the generation of tendon micro-tears exceeds the rate of repair then the tensile strength of the tendon may be sufficiently decreased as to result in partial rupture or even tendon avulsion (Figs. 15.23 and 15.24) (Gibbon 1998).

In myotendinous units anywhere in the body there is a tendency for them to fail acutely at their musculotendinous junctions and chronically at their osseo-tendinous junctions resulting in an enthesopathy. Occasionally tendons may apparently spontaneously rupture. There is, however, sufficient evidence to suggest that in humans at least there is insufficient force generated to create a breaking strain, i.e. a force sufficient to produce a truly spontaneous rupture. Such ruptures probably occur as a spontaneous event in a sub-clinically degenerate tendon. A repetitive traction injury to adductor origins, as is common in sports such as soccer, will potentially result in an avulsion of the CAO from the underlying pubic bone. MR imaging in such individuals exhibits sub-entheseal bone marrow edema at an early stage (Fig. 15.25) and entheseal and perientheseal edema and intravenous-contrast-enhancing granulation tissue at a later stage (Figs. 15.26 and 15.27).

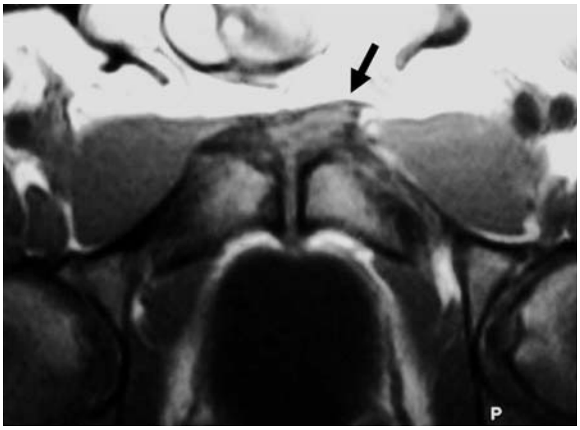

Fig. 15.23. Left adductor longus origin avulsion. The left tendon origin (*arrow*) is exhibiting a grossly abnormal signal and has been incompletely separated from the underlying pubis

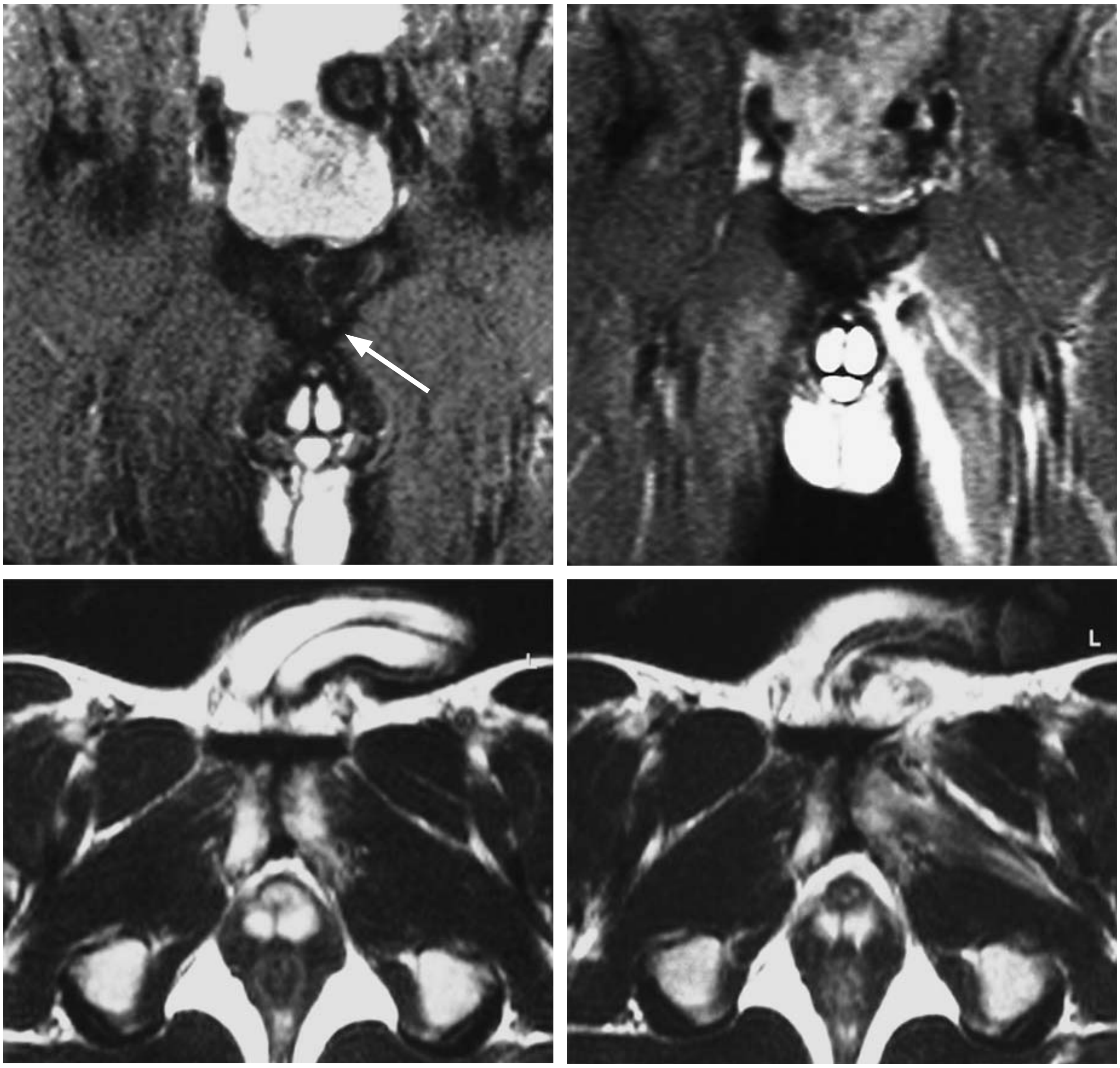

a c b d

Fig. 15.24a–d. Acute-on-chronic left gracilis origin avulsion: (**a**) STIR coronal and (**b**) T2-weighted transverse sections through the pubic region performed on a professional soccer player complaining of chronic left groin pain; (**c**) coronal, and (**d**) T2-weighted transverse sections through the pubic region performed on the same player 48 h later having come off the field after 20 min of play with sudden severe left groin pain. The small focus of subentheseal high signal in **a** (*arrow*) can be seen to be the site of weakness resulting in the subsequent "acute" gracilis tendon avulsion seen in **c** and **d**

Tendons themselves do not have much in the way of pain fibres. In cases where there is chronic entheseal injury, pain may be due either to a more acute inflammatory process in the paratenon or, where it exists, tendon sheath. The only tendon in the groin region to have such a sheath is the iliopsoas tendon and this certainly can become inflamed. All of the other tendons have a paratenon. Pain can also be due to subentheseal marrow edema resulting in raised intra-osseous pressure. Finally, it can occur at the site of tendon insertion into bone, i.e. at the Sharpey-Shaffer fibres analogous to the site of inflammation in patients with spondyloarthopathies such as ankylosing spondylitis. The treatment for recalcitrant chronic entheseal tendinopathies of mechanical origin at other site such as the plantar aponeurosis (fascia) and common extensor origin of the elbow, is tenotomy. Spontaneous rupture is in effect an "auto-tenotomy". This is the reason why acute tendon rupture in athletes with chronic groin pain may result

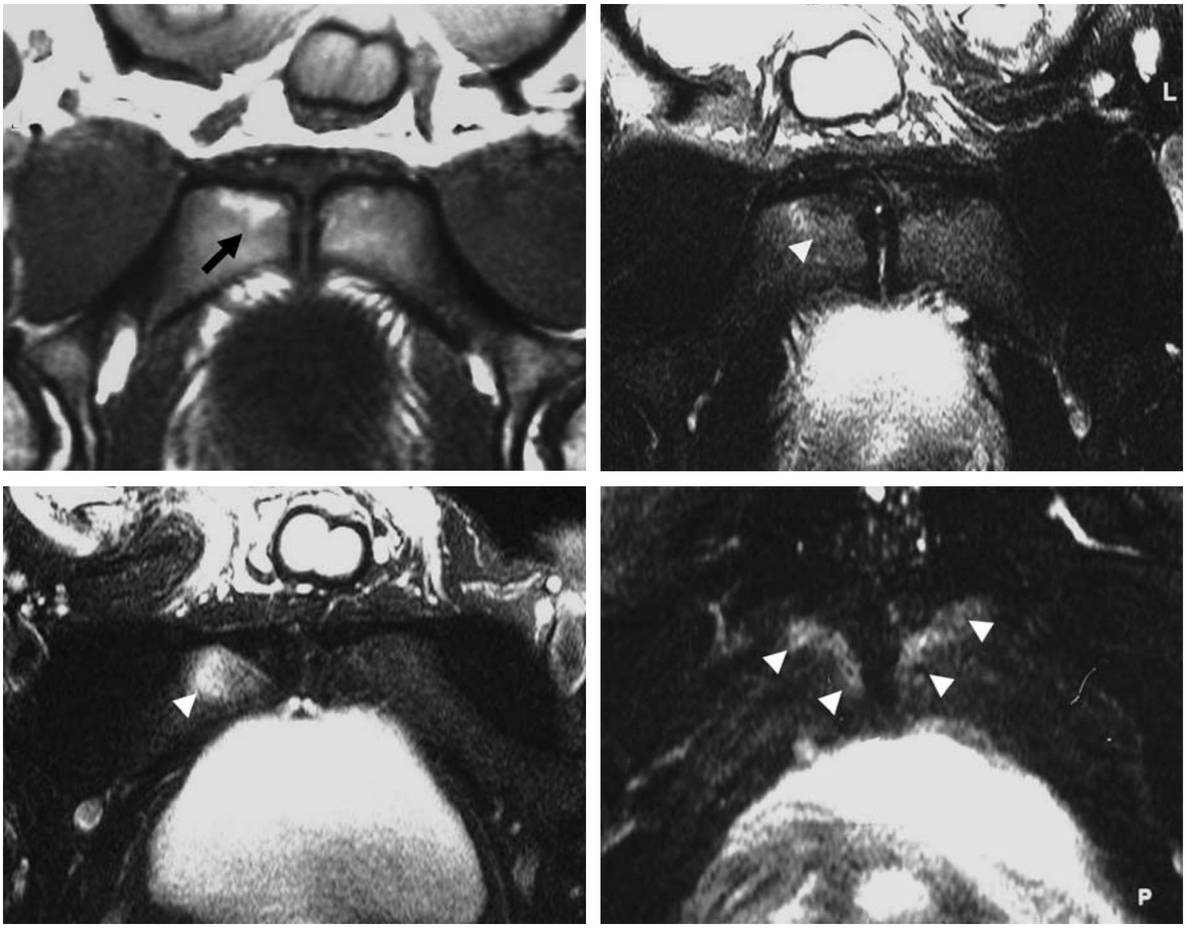

Fig. 15.25a–d. Subentheseal pubic bone marrow change. Transverse section images through the upper pubic bodies at the level of the rectus abdominis/inguinal ligament insertions. (**a**) T1-weighted sequence. High signal fatty infiltration can be seen in the right pubic body (*arrow*) below the broad area of soft tissue insertion. Lesser changes are present on the left. The appearances are consistent with Modic type 2 change. **b**–**d** T2-weighted fat suppressed images showing variations in the anatomical site of marrow edema i.e. Modic type 1 change (*arrowheads*). In (**b**) it is slightly more medially placed at the entheseal origins than in (**c**) reflecting the former being at the rectus abdominis insertion and the latter at the inguinal ligament attachment. In (**d**) the edema is more extensive and also has a prominent subarticular component

in long-term symptomatic relief after initial symptoms related to haematoma formation have subsided (assuming there is sufficient tendon retraction of the adductor tendons to avoid the tendon reuniting).

Whether due to shearing injury from below or traction injury from above, the overall effect is separation of the RA-CAO anatomical and functional unit from the underlying pubic bone (Fig. 15.28). This linkage could result in a high shearing force across the pre-pubic soft tissues due to their forced contraction and an entheseal shearing injury with repetitive use. Such an overuse injury is possible during the action of kicking or rapid turning and trunk rotation as regularly occurs in soccer.

Balanced micro-injury and subsequent repair normally occurs in tendons in response to applied deforming forces (Gibbon et al. 1999, 2000; Gibbon 1998). If the generation of tendon micro-tears exceeds the rate of repair then the tensile strength of the tendon may be sufficiently reduced as to result in partial rupture or even adductor tendon origin avulsion. Their large muscle bulk relative to their pubic insertional cross-sectional area means that a large force per unit area is generated at their entheseal attachments, potentially resulting in an entheseal overuse phenomenon. At other anatomical sites where powerful muscles act via long lever-arms through small surface area entheseal attachments, (e.g., common extensor origin at the elbow,

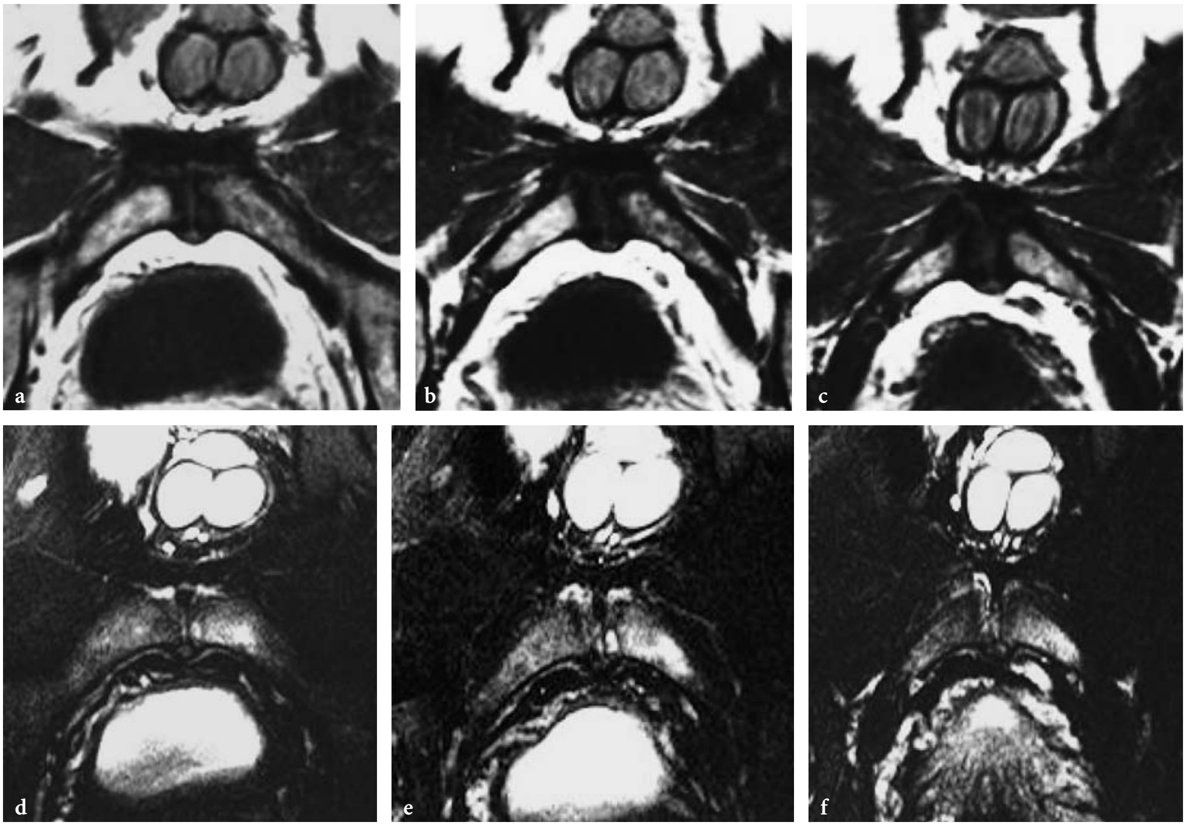

Fig. 15.26a–f. "Typical" parasymphyseal changes of a professional soccer player. **a**, **c**, **e** are T1-weighted images through the upper, middle and lower thirds of the same pubic region and **b**, **d**, **f** are the respective corresponding fat suppressed T2-weighted transverse sections. These images show symphyseal and subchondral degeneration, bilateral entheseal granulation tissue at rectus abdominis, adductor longus and gracilis insertions right > left, and possible gracilis avulsion developing on the right and pubic stress injury developing on the left

a 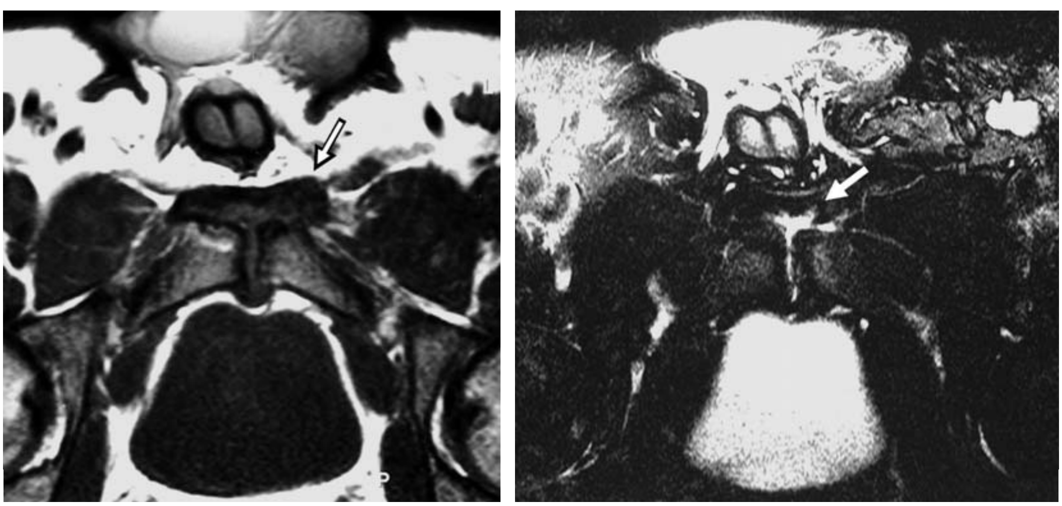 b

Fig. 15.27a,b. Bilateral adductor longus tendon origin enthesopathy: (**a**) T1-weighted and (**b**) T2-weighted fat-suppressed transverse axial images through the mid-pubic region showing an area of abnormality. This is but not typical fluid signal being high signal on T1- and high signal on T2-weighted consistent with granulation tissue at the junction between the left anterior pubis and the overlying adductor longus (*arrows*). This is bordering on frank avulsion at its lateral margin. There are lesser adductor longus tendon changes with subtle Modic type 2 changes at the corresponding entheseal insertion on the right

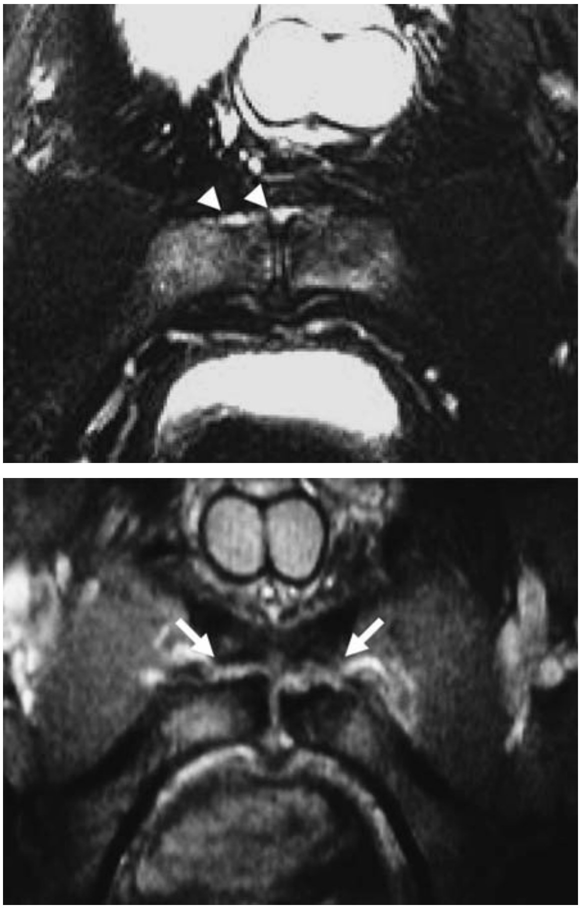

Fig. 15.28a,b. Rectus abdominis insertion entheseal injury. **a** Contrast-enhanced fat suppressed T1-weighted transverse section through the upper pubis at the level of the rectus abdominis insertion showing enhancing granulation tissue at the entheses (*arrowheads*). **b** A similar sequence in another patient at slightly lower level showing extensive enhancement at both rectus abdominis / adductor longus entheses (*arrows*). Appearances are those of granulation tissue consistent with early unilateral (**a**) and severe bilateral (**b**) chronic entheseal injury which in the latter is bordering on true entheseal avulsion

plantar aponeurotic origin at the calcaneum), excessive repetitive cyclical activity will result in focal tendon degeneration (tendinosis) or insertional inflammation (enthesitis). In this respect adductor origin tendinopathy may be considered to be akin to "tennis elbow". Also these muscles extend a long way down the thigh before inserting broadly into the femoral shaft or, in the case of gracilis, the tibial plateau. Accordingly they have a longer effective lever-arm. The longer lever-arm plus the greater muscle bulk and relatively smaller entheseal surface area in males compared to females may explain, at least in part, the higher incidence of chronic adductor problems in male athletes.

15.9 "Sportsman's Hernia"

This condition is not a true hernia and is perhaps more accurately referred to as the inguinal "pre-hernia" complex (Fig. 15.29). In one study of 65 consecutive professional footballers undergoing surgery for groin pain due to a "pre-hernia", 25 players (39%) also had pain in the adductor origin region (Gilmore 1993). There was a return to full sporting activity ten weeks after surgery in 97% of these professional footballers, regardless of the fact that any associated adductor injury was not specifically addressed by the surgery. Presumably, therefore, the adductor origin symptoms subsided following hernia repair.

Conversely, the reported symptomatic cure rates for herniorrhaphy in sportsman's hernia range between 63% and 94%, compared to greater than 99% for many studies of herniorrhaphy for conventional inguinal herniae (Marsden 1962), i.e. the poorer success rate in athletes may reflect failure to attend to any associated adductor problem. Further clinical investigation in athletes who are not cured by herniorrhaphy produced an alternative treatable diagnosis in more than 80% of cases, most of which are cured by addressing the more latterly diagnosed condition (Gregory 1950).

For further discussion of "sportman's hernia", we refer to Chap 25.

15.10 Parasymphyseal Muscle Tears

Any of the muscles in the groin region may be torn in athletes although clinically it is well recognised that the adductor muscles are particularly vulnerable in soccer players (Keller et al. 1987). Chronic tears may produce a diffuse muscle swelling with symptoms due to mass effect. These tears may markedly enhance with intravenous Gadolinium-DTPA. On MR imaging these combined features mean that such tears are liable to be confused as being due to more ominous pathology (Fig. 15.30). It is interesting that once such an adductor muscle tear occurs (or if the tendinous origin is completely avulsed) then chronic symptoms may disappear due to defunctioning of the causative overload process.

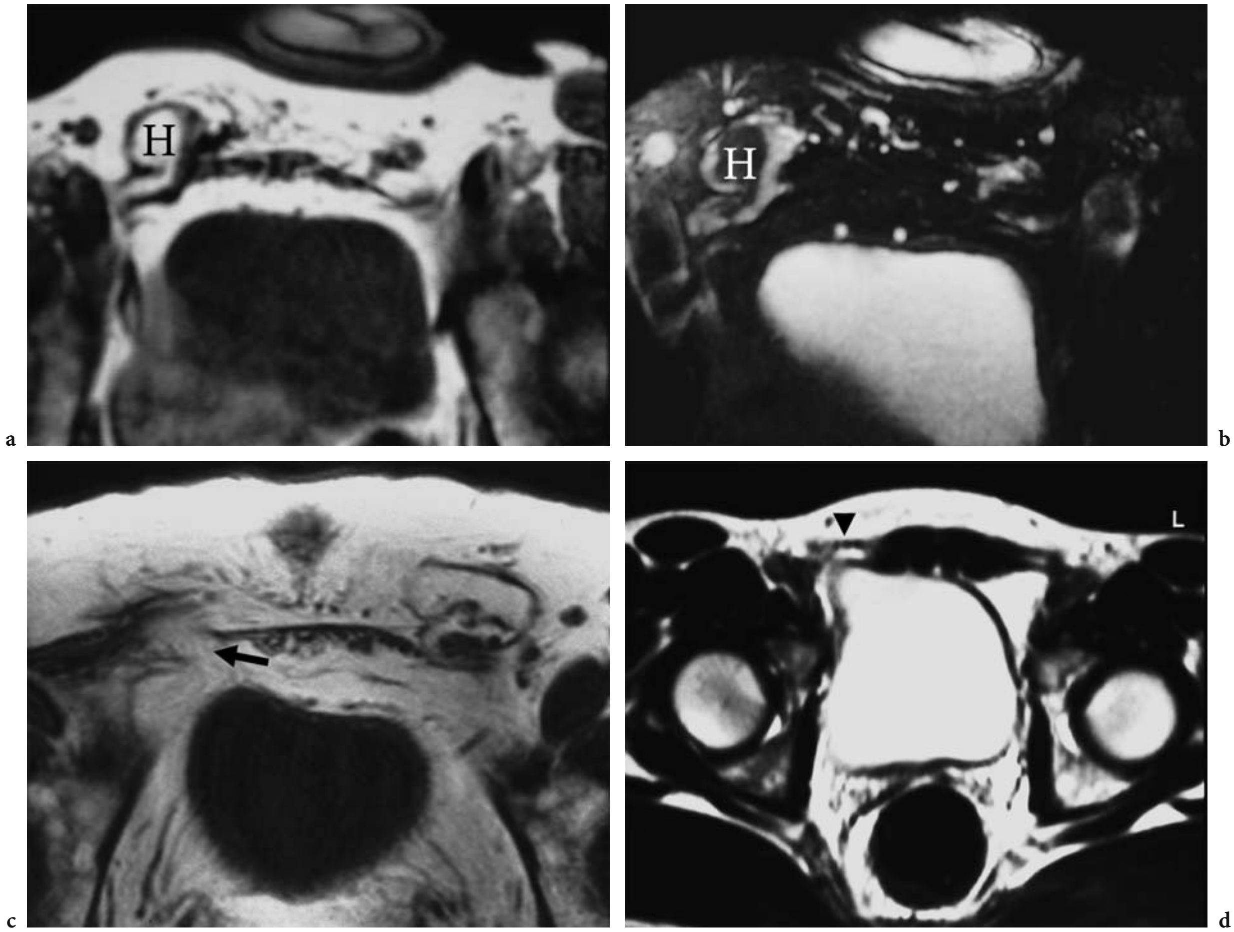

Fig. 15.29a–d. Hernia formation. Transverse axial images through the groin in patients complaining of groin pain: **a,b** indirect hernia (*H*) with an edematous surrounding tunica vaginalis; **c** direct hernia (*arrow*); **d** pre-hernia complex with bulging/weakness of the anterior abdominal wall at the level of the external inguinal ring (*arrowhead*)

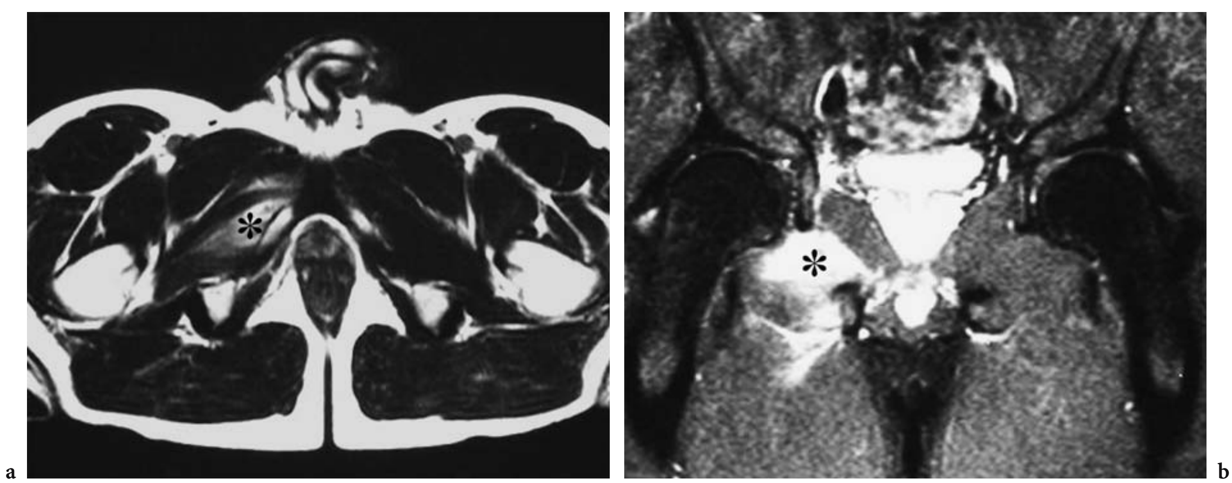

Fig. 15.30a,b. Acute muscle tear (obturator externus): (**a**) transverse axial T2-weighted and (**b**) coronal STIR images showing high signal intramuscular haematoma within the right obturator externus muscle (*)

15.11 Iliopsoas Tendinopathy

This usually reflects a tenosynovitis (Fig. 15.31) rather than tendinitis and not uncommonly there is associated "snapping" of the iliopsoas tendon over the anterior capsule/acetabular margin of the underlying hip (Fig. 15.32). Alternatively such an overuse phenomenon may reflect the iliopsoas muscle functioning as a hip flexor particularly in kicking sports a process which again could be exacerbated by limita-

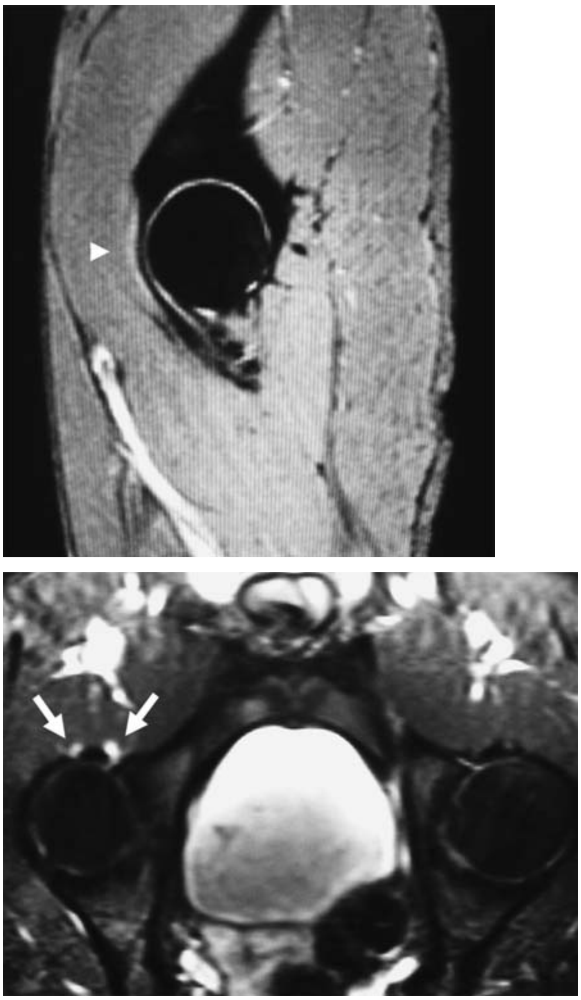

a b

Fig. 15.31a,b. Iliopsoas tenosynovitis ("snapping hip"). **a** Sagittal T2* image through the right hip showing high signal surrounding the iliopsoas tendon due to it repeatedly "snapping" over the anterior acetabular margin (*arrowhead*). **b** T1-weighted fat-suppressed transverse axial image following administration of intravenous Gadolinium-DTPA. There is marked enhancement of the iliopsoas tendon sheath (*arrows*)

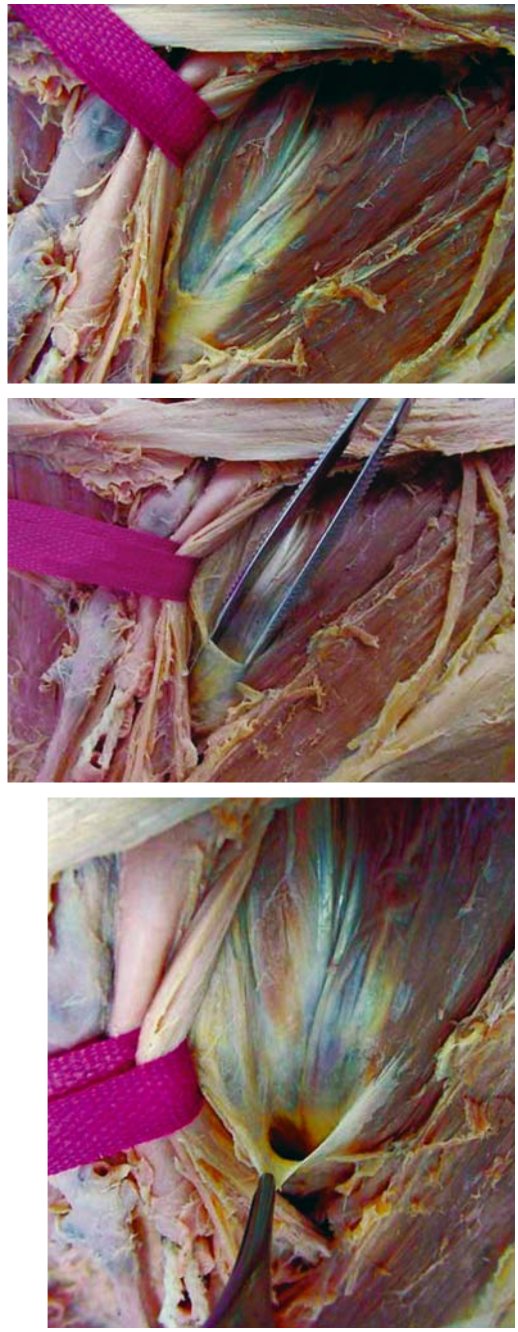

a b c

Fig. 15.32a–c. The anatomical basis for the "snapping" iliopsoas tendon. Three photographs of a dissected male left groin. The tape is retracting the femoral neurovascular bundle medially. **a** The myotendinous region of the iliopsoas tendon has been exposed. **b** A pair of dissection forceps has been passed down a funnel-shaped facial opening through which the tendon passes to reach its insertion into the lesser trochanter of femur. **c** The funnel shaped tunnel has been opened up. The tendon is lying on its posterior wall. This dissection suggests that the snapping can occur at two points – the iliopsoas tendon may "snap" within this tunnel or the whole tunnel containing the tendon "snaps" over the underlying hip

tions in hip movement. Symptomatic athletes often benefit from ultrasound-guided steroid infiltration reflecting the inflammatory nature of the tenosynovitis.

15.12 Nerve Entrapment

Thickening of the fascial plane overlying the anterior division of the obturator nerve, and deep to the adductor longus and pectineus muscles can result in entrapment of this nerve (Albert 1983). The close proximity of the adductor longus tendon at this point means that an adductor tendinopathy and associated scarring of the intervening fascia may result in obturator nerve entrapment and, therefore, produce "neurogenic" medial groin pain (Fig. 15.33). The characteristic clinical pattern in athletes is that they complain of medial thigh pain commencing in the region of the adductor muscle origin and radiating distally along the medial thigh with sporting activity. Needle electromyography demonstrates denervation of the anterior adductor muscles and surgical decompression produces symptomatic relief (Bradshaw et al. 1997). Injury to neurovascular bundles containing terminal branches of the iliohypogastric nerve as it passes through a tear in the external oblique aponeurosis has also been noted at the time of surgical exploration in 25 male athletes presenting with groin pain (Ziprin et al. 1999). All had improved function following repair of the aponeurotic tear and nerve decompression. Such tears can be expected to occur in some athletes as part of the proposed RA-CAO combinational injury. A similar injury has been described as the "hockey groin syndrome," which relates to the tearing of the external oblique aponeurosis and entrapment of the ilioinguinal nerve (Albert 1983; Irshad et al. 2001). Dissection studies have demonstrated four distinct distributions of the ilioinguinal nerve (Irshad et al. 2001). Normally there is a dominance of the genitofemoral nerve in the sensory supply to the scrotal/labial and the ventromedial thigh region. However, in type C and D the ilioinguinal nerve has sensory branches to the mons pubis and inguinal crease together with an anterior, proximal part of the root of the penis or labia majora. The nerve was found to share a branch with the iliohypogastric nerve. This would explain the similar results for studies where iliohypogastric and iliohypogastric nerves have both been implicated and also why there may be apparent perineal symptoms related to chronic groin injuries. In addition to the cutaneous branches from the ilioinguinal nerve, cutaneous branches originating from the genital branches of the genitofemoral nerve have been found in the inguinal region in 35% of subjects (Akita et al. 1999). In a further 13% the genital branch and the ilioinguinal nerve unite in the inguinal canal. In 11% the genital branch pierces the inguinal ligament to enter the inguinal canal and in 5% the genital branch pierced the border between the ligament and the aponeurosis of the obliquus externus muscle to be distributed to the inguinal region.

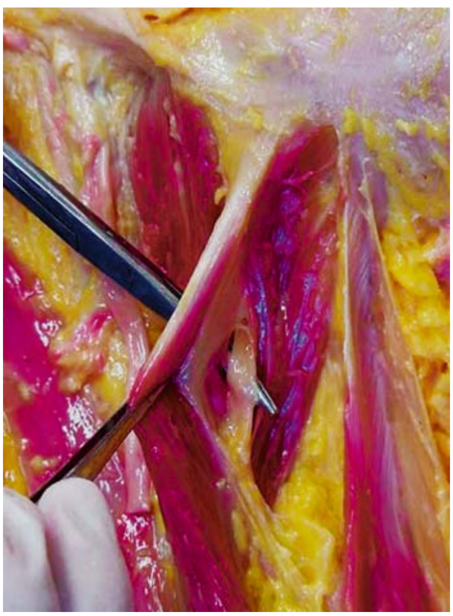

Fig. 15.33. Relationship between obturator nerve and adductor longus origin. Dissection of the right groin in a fresh cadaveric specimen with the right adductor tendon retracted laterally by a pair of forceps to show the obturator nerve. The tip of a pair of scissors is lying between the nerve and the underlying pectineus and adductor brevis muscles

The symphysis itself is innervated by numerous branches from the pudendal and genitofemoral nerves. Therefore, entrapment by the ligament may be a reasonable candidate for the cause of chronic groin pain. This entrapment could presumably occur with entheseal swelling due to repetitive minor injury or swelling, deformity and scarring related to soft tissue separation in the inguinal/pubic region injury.

In groin pain of neural origin the exact nerve involved can be narrowed down clinically by realising that symptoms can be referred to regions other than the groin (Lee and Dellon 2000):

- Iliohypogastric nerve also provides sensory fibres to the pelvic viscera
- Lateral femoral cutaneous nerve also provides sensory fibres to the knee
- Genitofemoral nerve also provides sensory fibres to the testicle

Although there has been much recent interest in possible neurogenic causes for groin pain it is also interesting to note that in 1984 (Leno et al. 1984) bilateral obturator neuralgia was described secondary to osteitis of the pubis. If due to "true" osteitis this could reflect the associated marked peri-pubic soft tissue inflammation/edema.

The role of imaging in such nerve entrapment syndromes is unclear at the present time.

15.13 A Unifying Concept for Groin Pain in Athletes

MR imaging is able to shows that a RA-CAO injury can occur either involving the whole or part of this linkage. On MR imaging there is evidence of a rectus abdominis pubic insertion injury, common adductor origin injury or both in 91% of professional soccer players with groin pain and a significant association exists between symptoms and these appearances. Although, an entheseal injury was also seen at these sites in 26% of the asymptomatic contralateral sides in footballers with unilateral symptoms, almost all of these groins will develop symptoms within three years. When considering groins exhibiting a direct inguinal hernia or "pre-hernia complex" 79% also exhibit features of a rectus abdominis shear injury whilst another 50% exhibit a CAO shear injury. Conversely, in the present study, there was no evidence of a residual/recurrent inguinal hernia in symptomatic players following hernia repair, i.e. the repairs had been surgically "successful" even though symptoms remained. Therefore, if a "sportsman's hernia" is associated with groin pain it does not appear to be the sole contributing factor.

The concept of an anatomical and functional relationship between the RA and CAO provides a unifying concept for groin injuries in athletes. It explains why the surgical procedures of herniorrhaphy (Hackney 1993), rectusplasty (Martens et al. 1987) and adductor tenotomy (Akermark and Johansson 1992) have all been shown to produce symptomatic relief. The presence of an underlying entheseal traction phenomenon and tendinitis would explain why infiltration of the entheses by lignocaine (2%) and triamcinolone (1%) produces symptomatic cure of unexplained groin pain in 25% and symptomatic reduction in 30% of groins (Ashby 1994). It would also explain why 6.6% of patients with a palpable and surgically proven direct inguinal hernia exhibit symptomatic relief by local entheseal injection (Ashby 1994). Should the entheseal bone be weaker than the attached tendons then a stress injury may occur to the parasymphyseal bone, this possibly explaining the configuration of parasymphyseal stress fractures (Fink-Bennett and Benson 1984). The presence of an underlying RA-CAO unit dysfunction would also explain why correcting the muscle imbalance between abdominal and adductor musculature has been shown to be beneficial (Holmich et al. 1999). If the pubic attachment of the conjoint rectus abdominis-common adductor aponeurosis is subjected to repeated excessive traction forces it seems reasonable to expect that it may become "sheared off" its osseous attachment. The attachment is a major stabiliser of the pubic symphysis and, therefore, its detachment results in potential pelvic instability to para-sagittal pelvic rotatory forces. The configuration of the pubic symphysis and the loss of symphyseal joint space may exacerbate this pelvic instability. The inguinal ligament is inseparable from the superolateral attachment of the above common aponeurosis and therefore it is likely to be "sheared off" its osseous attachment to the pubis in this same region therefore pre-disposing to the inguinal pre-hernia complex.

The pubic symphyseal region can be considered analogous to the spine/intervertebral discs both in terms of the anatomy and any associated injury and disease processes. The features typically ascribed to "Osteitis Pubis" are due to a premature degenerative phenomenon and are not themselves major cause of groin pain in athletes. Imaging can demonstrated subclinical entheseal injury and can help differentiate a range of aetiological conditions producing groin pain in athletes. Central anterior, posterior and superior symphyseal extrusion, increased symphyseal signal and all types of para-symphyseal or para-sacroiliac marrow change although abnormal in non-athletes must be considered to be "normal" in professional soccer (and rugby) players. Therefore, a mechanical osteitis pubis reflects excessive physical activity and cannot be assumed to be the cause of groin pain per se.

A "true" osteitis pubis is an unusual condition (and can be very difficult to differentiate from pubic osteomyelitis). The MR imaging findings suggest that in footballers, changes within the symphysis pubis and adjacent subchondral bone (Albers et al. 2001), often mistakenly termed "osteitis pubis", are simply an accelerated degenerative phenomenon and have no correlation with symptoms, i.e. they reflect the pelvic stress forces existing in professional players, by virtue of their sport, rather than a cause of symptoms. However, based on the prior gross anatomical studies, MR imaging is able to demonstrate entheseal changes which do appear to be associated with symptoms. These entheseal changes are similar to those seen in primary inflammatory arthritis (McGonagle et al. 1998; Tan et al. 2004). The bone marrow edema and corresponding raised intraosseous pressure may in part be the cause of diffuse pubic pain seen in these footballers and if excessive would be compatible with the MRI appearances seen in a true "osteitis pubis" i.e. a severe but self-limiting inflammatory process akin to a "sterile" pubic osteomyelitis.

Ultrasound-guided symphyseal cleft corticosteroid injection can significantly help reduce symptoms in certain professional soccer players, i.e. the ones where an inflammatory process predominates due to enthesitis or "true" osteitis pubis. Ultrasound-guided pubic symphyseal corticosteroid infiltration avoids surgery and full sporting activity in 56% of symptomatic players.

Allowing for elastic recoil there is a marked repetitive change in axial loading of the posterior pelvis during sprinting with resulting significant sagittal torsion force on the pelvis and shear force across the sacroiliac joints (Walheim and Selvik 1984). Also, when the lumbar spine is flexed, lateral compression forces are exerted on the pelvis (Walheim and Selvik 1984). There is only a thin connective tissue layer over the back of the symphysis pubis and it would not be surprising for these compression forces to result in posterior symphyseal extrusion and buttressing osteophyte formation. The overall effect is a decrease in the width of the disc space with time. This loss of joint space may then allow further increased movement at the symphysis which in-turn would result in increased movement and parallel stress changes at the sacroiliac joints reflecting pelvic instability. This movement would increase the shearing forces on the anterior pubic soft tissues. If the adductors and rectus sheath are then sheared-off the pubis, this would further exacerbate the effects of the pelvic torsional forces. Involvement of adjacent nerves by tearing, scarring or adjacent soft tissue edema may exacerbate symptoms and further cloud the diagnostic picture.

15.14 Conclusion

Medical imaging has an extremely valuable role in the differentiation between the wide range of potential causes of hip and groin pain in athletes. Without such differentiation effective treatment is difficult to achieve especially where considering overuse injuries which may even be exacerbated by treatment based on diagnostic inaccuracy.

Understanding the anatomy of the anterior pubic soft tissues allows correlation with MR imaging pathoanatomical appearances and therefore a better understanding of the pathomechanism of groin pain in athletes on which to base subsequent treatment.

Things to Remember

1. Groin injuries are the commonest cause of chronic injury in a wide range of sports, especially football. Great diagnostic difficulties exist reflecting the fact that the causes of groin pain are protean and also possibly reflecting clinical prejudice.
2. There are a significant number of errors in the classical description of the soft tissue attachments to the pubic bodies.
3. The pubic symphysis may be considered analogous to the intervertebral discs of the spine. The condition traditionally considered to be "osteitis pubis" appears to be structurally and pathophysiologically akin to intervertebral disc degeneration reflecting excessive wear from physical activity and as such is unlikely to be a major cause of groin symptoms in athletes. An acute inflammatory condition akin to a spinal "mechanical" (non-infective) discitis can occur in the pubic symphyseal region and this condition is, therefore, a "true osteitis pubis" or "symphysitis".

4. A repetitive traction injury to adductor origins, as is common in sports such as soccer, will potentially result in an avulsion of the common extensor origin from the underlying pubic bone. The concept of an anatomical and functional relationship between the rectus abdominis and common extensor origin provides a unifying concept for groin injuries in athletes. The inguinal ligament is inseparable from the superolateral attachment of the above common aponeurosis and therefore it is likely to be "sheared off" its osseous attachment to the pubis in this same region therefore pre-disposing to the inguinal pre-hernia complex.

References

Ackerman N, Spencer CP (1992) What is your diagnosis? Prepubic tendon injury, with avulsion fracture of the left pubis. J Am Vet Med Assoc 200(5):721–722

Adams RJ, Chandler FA (1953) Osteitis pubis of traumatic etiology. J Bone Joint Surg (Am) 35(3):685–696

Akermark C, Johansson C (1992) Tenotomy of the adductor longus tendon in the treatment of chronic groin pain in athletes. Am J Sports Med 20:640–643

Akita K, Niga S, Yamato Y et al. (1999) Anatomic basis of chronic groin pain with special reference to sports hernia. Surg Radiol Anat 21(1):1–5

Albers SL, Spritzer CE, Garrett WE Jr et al. (2001) MR findings in athletes with pubalgia. Skeletal Radiol 30(5):270–277

Albert M (1983) Descriptive Three Year Data Study of Outdoor and Indoor Professional Soccer Injuries. Athletic Train; 18:218–220

Ashby EC (1994) Chronic obscure groin pain is commonly caused by enthesopathy - "tennis elbow" of the groin. Br J Surg 81:1632–1634

Bouza E, Winston DJ, Hewitt WL (1978) Infectious osteitis pubis. Urology 12:663–669

Bradshaw C, McCrory P, Bell S et al. (1997) Obturator nerve entrapment. A cause of groin pain in athletes. Am J Sports Med 25(3):402–408

Breitenfelder J, Huke B, Wolf N (1975) The problem of stress of the symphysis following hip arthrodesis (German). Archiv Orthopad Unfall-Chirurgie 81(2):119–124

Budinoff LC, Tague RG (1990). Anatomical and developmental bases for the ventral arc of the human pubis. Am J Phys Anthropol 82(1):73–79

Carnevale V (1954) La Denominada 'Inguiocruralgia Traumatic de los Jugadores de Futbol'. Prensa Med Argent 41(5):355–357

Casey D, Mirra J, Staple TW (1984) Parasymphyseal insufficiency fractures of the os pubis. Am J Roentgenol 142:581–586

Cochrane GM (1971) Osteitis pubis in athletes. Br J Sports Med 5:233–235

Dalstra M, Huiskes R, Odgaards A et al. (1993) Mechanical and textural properties of pelvic trabecular bone. J Biomech 26:523–535

Ekberg O, Persson NH, Abrahamsson PA et al. (1988) Long-standing groin pain in athletes. A multidisciplinary approach. Sports Med 6:56–61

Ekstrand J, Gillquist J (1983) The avoidability of soccer injuries. Int J Sports Med 4:124–128

Evans TW, Eveley RS, Morcos SK (1985) Asymptomatic osteomyelitis of the symphysis pubis. Postgrad Med J 61:267–268

Fink-Bennett DM, Benson MT (1984) Unusual exercise related stress fractures - two case reports. Clin Nucl Med 9:430–434

Fredberg U, Kissmeyer-Nielsen P (1996) The sportsman's hernia - fact or fiction? Scand J Med Sci Sports 6:201–204

Fricker PA, Taunton JE, Ammann W (1991) Osteitis pubis in athletes. Infection, inflammation or injury? Sports Med 12(4):266–279

Gibbon WW (1998) Are Achilles tendon ruptures ever spontaneous? Br J Sports Med 32(3):266

Gibbon WW, Cooper JR, Radcliffe GS (1999) Sonographic incidence of tendon microtears in athletes with chronic Achilles tendinosis. Br J Sports Med 33(2):129–130

Gibbon WW, Cooper JR, Radcliffe GS (2000) Distribution of sonographically detected tendon abnormalities in patients with a clinical diagnosis of chronic Achilles tendinosis. J Clin Ultrasound 28(2):61–66

Gilmore OJA (1993) "Gilmore's groin": a previously unsolved problem in sportsmen. In: Mcleod DA, Maughan RJ, Williams C, Madeley CR, Sharp JMC, Nutton RW et al. (eds) Intermittent high intensity exercise; preparation, stresses and damage limitation. Chapman and Hall, London, pp 477–486

Goergen TG, Resnick D, Riley RR (1978) Post-traumatic abnormalities of the pubic bone simulating malignancy. Radiology 126(1):85–87

Gregory WK (1950) The anatomy of the gorilla; Henry Cushior Memorial Volume. Gregory WK (ed) New York, Columbia University Press, pp 150–151

Hackney RG (1993) The sports hernia: a cause of chronic groin pain. Br J Sports Med 27:58–62

Harris NH, Murray RO (1974) Lesions of the symphysis in athletes. Br Med J 4:211–214

Heldrich F, Harris V (1979) Osteomyelitis of the pubis. Acta Paediatr Scand 68:39–41

Holmich P, Uhrskou P, Ulnits L et al. (1999) Effectiveness of active physical training as treatment for long-standing adductor-related groin pain in athletes: randomised trial. Lancet 6; 353:439–443

Holt MA, Keene JS, Graf BK et al. (1995) Treatment of osteitis pubis in athletes. Results of corticosteroid injections. Am J Sports Med 23(5):601–606

Hoon JR (1959) Adductor muscle injuries in bowlers. JAMA 171:2087–2089

Hornof Z, Napravnik C (1969) Analysis of various accident rate factors in ice hockey. Med Sci Sports 5:283–286

Irshad K, Feldman LS, Lavoie C et al. (2001) Operative management of "hockey groin syndrome": 12 years of experience in National Hockey League players. Surgery 130(4):759–764

Jajic Z, Jajic I (1998) Condensing osteitis of the pubic bone. Reumatizam 46(1):51–53

Kassarjian A, Yoon LS, Belzile E et al. (2005) Triad of MR arthrographic findings in patients with cam-type femoro-acetabular impingement. Radiology 236:588–592

Keller CS, Noyes FR, Buncher CR (1987) The medical aspects of soccer injury epidemiology. Am J Sports Med 15(3):105–112

Koch RA, Jackson DW (1981) Pubic symphysitis in runners - a report of two cases. Am J Sports Med 8(1):62–63

Lebrun C, Vanhoenacker FM, Willemen D (2005) Anterior femoro-acetabular impingement of the CAM type. Radiological documents (2):15

Lee CH, Dellon AL (2000) Surgical ,anagement of groin pain of neural origin. J Am Coll Surg 191(2):137–142

Leno C, Combarros O, Polo JM et al. (1984) Bilateral obturator neuralgia secondary to osteitis of the pubis. Arch Neurobiol (Madr) 47(6):347–352

Losada A, Saldias E (1968) Osteopatia dinamica del pubis. Revista Med 96:110–113

Lovell G (1995) The diagnosis of chronic groin pain in athletes: a review of 189 cases. Aust J Sci Med Sport 27(3):76–79

Marsden AJ (1962) Inguinal hernia: a three year review of two thousand cases. Br J Surg 49:384–394

Martens MA, Hansen L, Mulier JC (1987) Adductor tendinitis and musculus rectus abdominis tendopathy. Am J Sports Med 15:353–356

McGonagle D, Gibbon W, O‘Connor P et al. (1998) Characteristic magnetic resonance imaging entheseal changes of knee synovitis in spondylarthropathy. Arthritis Rheum 41(4):694–700

Mitchell B, McCrory P, Brukner P et al. (2003) Hip joint pathology: clinical presentation and correlation between magnetic resonance arthrography, ultrasound, and arthroscopic findings in 25 consecutive cases. Clin J Sport Med 13(3):152–156

Modic MT, Steinberg PM, Ross JS et al. (1988) Degenerative disk disease: assessment of changes in vertebral body marrow with MR imaging. Radiology 166(1):193–199

Morcuende JA, Arauz S, Weinstein SL (2000) Stress fracture of the hip and pubic rami after fusion to the sacrum in an adult with scoliosis: a case report. Iowa Orthop J 20:79–84

Moretz A, Rashkin A, Grana WA (1978) Oklahoma high school football injury study: a preliminary report. J Okla State Med Assoc 71:85–86

Nicholas JJ, Haidet E, Helfrich D et al. (1989) Groin and hip pain due to fractures at or near the pubic symphysis. Arch Phys Med Rehabil 70(9):696–698

Nielsen AB, Yde J (1989) Epidemiology and traumatology of injuries in soccer. Am J Sports Med 17(6):803–807

Numaguchi Y (1971) Osteitis condensans ilii, including its resolution. Radiology 98:1

Ogden JA (1980). Chondro-osseous development and growth. In: Urist MR (ed) Fundamental and clinical bone physiology. JB Lippincott Company, Philadelphia, pp 108–171

Orava S, Puranen J, Ala-Ketola L (1978). Stress fractures caused by physical exercise. Acta Orthop Scand 49:19–27

Patterson FP, Yovanovich R (1975) Pubic osteomyelitis and septic arthritis of the symphysis pubis. In: Proceedings of the Canadian Orthopaedic Association. J Bone Joint Surg (Br) 57(4):531–532

Pierson EL (1929) Osteochondritis of the symphysis pubis. Surg Gynecol Obstet 49:834–838

Reideberger Von J, Luschnitz E, Bauchspeiss (1967) The pubic adductor syndrome in footballers. Zentralblatt Chirugie 92:2655–2657

Rosenklint A, Anderson RB (1969) Tenosteochondrosis of the pubis. Acta Rheum Scand 15:262–270

Rosenthal RE, Spickard WA, Markham RD et al. (1982) Osteomyelitis of the symphysis pubis: a separate disease from osteitis pubis. J Bone Joint Surg (Am) 64(1):123–128

Saw T, Villar R (2004) Footballer‘s hip: a report of six cases. J Bone Joint Surg (Br) 86(5):655–658

Schneider PG (1963) Das Grazilissyndrom. Z Orthop 93:43–46

Seward H, Orchard J, Hazard H, Collinson D et al. (1993) Football injuries in Australia at the elite level. Med J Aust 159:298–301

Sexton DJ, Keskestad L, Lambeth WR et al. (1993) Postoperative pubic osteomyelitis misdiagnosed as osteitis pubis: report of four cases and review. Clin Infect Dis 17(4):695–700

Spinelli A (1932) Nuova Malattia Sportive: La Pubialgia Degli Schernitori. Ortopedia E Trauma Apparato Motore 4:111–127

FIFA (1992) Statistics on the 186 Affiliated National Associations of FIFA, FIFA, Zurich, Switzerland

Sturesson B, Selvik G, Uden A (1989) Movements of the sacroiliac joints. A Roentgen stereophotogrammetric analysis. Spine 14(2):162–165

Tan AL, Marzo-Ortega H, O‘Connor P et al. (2004) Efficacy of anakinra in active ankylosing spondylitis: a clinical and magnetic resonance imaging study. Ann Rheum Dis 63(9):1041–1045

Walheim GG, Selvik G (1984) Mobility of the pubic symphysis - in vivo measurements with an electromechanic method and a Roentgen stereophotogrammetric method. Clin Orthop 191:129–135

Weaver CJ, Major NM, Garrett WE et al. (2002) Femoral head osteochondral lesions in painful hips of athletes: MR imaging findings. Am J Roentgenol 178(4):973–977

Wiley JJ (1983) Traumatic osteitis pubis: the Gracilis syndrome. Am J Sports Med 11(5):360–363

Williams JGP (1978) Limitation of hip joint movement as a factor of traumatic osteitis pubis. Br J Sports Med 12(3):129–133

Ziprin P, Williams P, Foster ME (1999) External oblique aponeurosis nerve entrapment as a cause of groin pain in the athlete. Br J Surg 86(4):566–568

Sports-related Meniscal Injury

16

Pieter Van Dyck, Jan L. Gielen, and Filip M. Vanhoenacker

CONTENTS

Box 16.1. Plain Radiography and Conventional Arthography

- Have been replaced by other (cross-sectional) imaging techniques for the evaluation of meniscal injury

P. Van Dyck, MD
J. L. Gielen, MD, PhD, Associate Professor
F. M. Vanhoenacker, MD, PhD
Department of Radiology, University Hospital Antwerp, Wilrijkstraat 10, 2650 Edegem, Belgium

Box 16.2. Ultrasound

- No significant role for the detection of meniscal tears

Box 16.3. MR Arthrography and CT Arthrography

- High accuracy for the evaluation of meniscal injury
- Invasive
- May be useful for the evaluation of the post-operative meniscus

Box 16.4. Standard MRI

- Non-invasive
- The dominant imaging technique for the assessment of meniscal lesions
  Because both asymptomatic grade 3 and symptomatic grade 2 lesions exist, MRI findings need to be correlated with clinical symptoms in order to plan treatment optimally.

16.1 Introduction

Meniscal injuries are very common among professional and amateur athletes and are a major cause of functional impairment of the knee. It is the most common indication for arthroscopic surgery of the knee. For athletes, unnecessary treatment or intervention may be as damaging to a competitive future as failure to diagnose a clinically significant injury. Therefore, rapid and accurate evaluation of possible injuries in this group is crucial (Ludman et al. 1999).

Acquisition of a precise history of the injury mechanism may be difficult, as is performance of an accurate physical examination in the setting of an acute injury (Karachalios et al. 2005).

Magnetic Resonance Imaging (MRI) is performed more commonly on the knee than on any other joint, and it is an excellent diagnostic tool that can aid in the evaluation of a host of sports-related injuries involving the ligaments, tendons, menisci, osseous structures, and articular surfaces. It has currently become the most widely used noninvasive imaging method for detecting meniscal injuries, with a reported diagnostic accuracy of as high as 98%, compared to arthroscopy, remaining the gold standard for confirming the diagnosis of meniscal tear. MRI is a valuable, cost-effective tool for the preoperative evaluation of the menisci, and proved useful, on the basis of its high negative predictive value, to exclude patients from unnecessary arthroscopy, and, thus, avoiding unnecessary hospitalization, morbidity, and waste of limited financial and manpower resources (Karachalios et al. 2005; Elvenes et al. 2000).

However, radiologists must be aware of numerous imaging pitfalls and artefacts simulating a tear and leading to an erroneous diagnosis. Moreover, it must be kept in mind that "silent" meniscal abnormalities in athletes exist and knowledge of these MR appearances is important in order to avoid attributing a greater significance to these than is clinically justified.

For many years, the meniscus was treated with disrespect as an unnecessary appendage that could be sacrificed with the first hint of malfunction. As long term results after major meniscectomy were disappointing, a conservative approach to the management of meniscal tears has developed over the past two decades, with emphasis on meniscal preservation (Rath and Richmond 2000).

16.2 Anatomy and Function

To evaluate and treat meniscal injuries adequately, understanding of meniscal anatomy and function is necessary. From a gross anatomic perspective, the menisci are C-shaped fibrocartilaginous structures, firmly attached to the anterior and posterior aspects of the tibial plateau by the so-called 'root ligaments'. Conventionally, they are described as having three segments: anterior horn, body, and posterior horn. Each meniscus measures approximately 5 mm in height along its periphery and tapers to a thin inner edge such that it demonstrates a triangular shape in cross section. The outer rims of the menisci are convex and attached to the fibrous joint capsule and through it to the edges of the articular surfaces of the tibia. The inner edges are concave, thin and free. Their superior surfaces are slightly concave for reception of the femoral condyles, whereas their inferior surfaces that rest on the tibial condyles are flatter (Fig. 16.1).

The *medial meniscus* is C-shaped and occupies 50% of the articular contact area of the medial compartment (Fig. 16.2). Its posterior horn is wider than the anterior horn. Although anatomic variations in meniscal morphology and attachments exist, the anterior horn of the medial meniscus has a firm bony attachment to the tibia anterior to the anterior cruciate ligament (ACL). The posterior horn is attached immediately in front of the attachment of the posterior cruciate ligament (PCL). The outer border of the medial meniscus is firmly attached to the knee joint capsule. The meniscotibial and meniscofemoral ligament attach the meniscus to the tibia and femur, respectively, and is referred to as the deep medial collateral ligament (Fig. 16.3).

The *lateral meniscus* is more uniform in width and semicircular, covering 70% of the lateral tibial plateau (Fig. 16.2). The anterior horns of the medial and lateral menisci are attached to each other through the transverse ligament. The posterior horn of the lateral

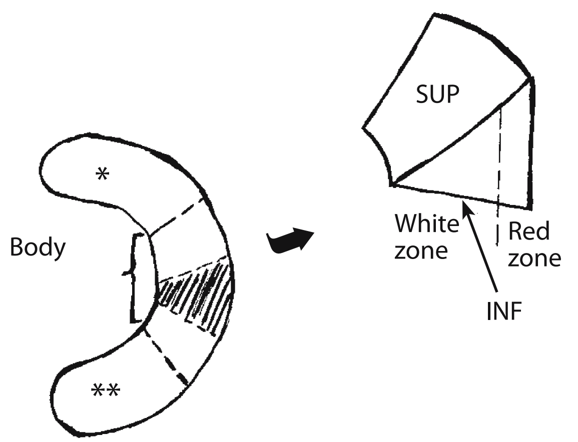

Fig. 16.1 Meniscal anatomy. Each meniscus is arbitrarily divided into anterior horn (*), body and posterior horn (**) segments. A cross-section to the body illustrates the superior (*SUP*) and inferior (*INF*) articular surfaces, and the more vascularized periphery of the meniscus (*red zone*), and the relatively avascular inner two thirds of the meniscus (*white zone*)

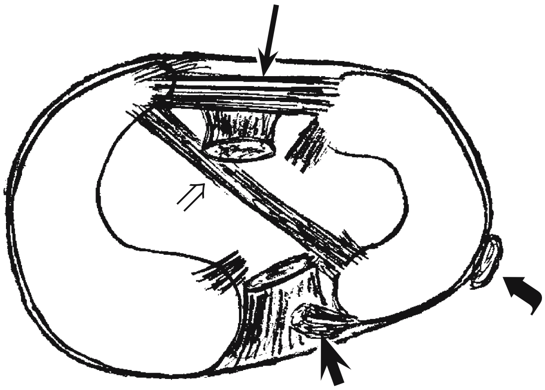

Fig. 16.2. Diagram of the menisci (seen from above). Note the transverse intermeniscal ligament anteriorly (*small arrow*), the meniscofemoral ligament attaching to the posterior horn of the lateral meniscus (*large arrow*), an oblique meniscomeniscal ligament (*open arrow*) and the popliteus tendon (*curved arrow*)

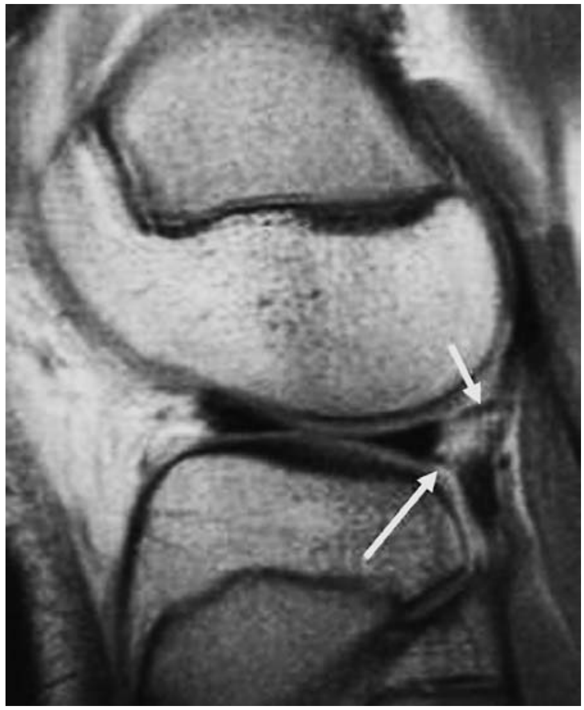

Fig. 16.4. Popliteal meniscal fascicles. Sagittal PD-WI. The superior (*small arrow*) and inferior (*large arrow*) popliteal meniscal fascicles are seen, running from the peripheral margin of the meniscus, around the popliteus tendon, to the joint capsule

Fig. 16.3. The “deep medial collateral ligament”. Coronal fat suppressed PD-WI. The meniscofemoral (*small arrow*) and meniscotibial (coronary) ligament (*large arrow*) attach the meniscus to the femur and tibia, respectively, and is referred to as “the deep medial collateral ligament”

meniscus is attached to the medial femoral condyle through the posterior meniscal-femoral (Wrisberg) and anterior meniscal-femoral (Humphrey) ligament. Therefore, during rotation, the motion of the lateral meniscus is coupled with that of the femoral condyle. The lateral meniscus has loose attachments to the joint capsule and is separated from it by the popliteus tendon posterolaterally where it courses through a meniscocapsular tunnel. In this region, the superior and inferior popliteal meniscal fascicles are seen, running from the peripheral margin of the meniscus, around the popliteus tendon, to the joint capsule (Fig. 16.4). The lateral meniscus is more mobile and is not anchored to the lateral collateral ligament. In flexion and internal rotation, the popliteal tendon retracts the posterior horn, thus reducing entrapment of the lateral meniscus between the femur and the tibia. It is therefore less likely to be injured than the relatively immobile medial meniscus (Rath and Richmond 2000).

The *microanatomy of the menisci* may explain injury patterns (Fig. 16.5). A network of type I collagen fibers arranged in a circumferential direction

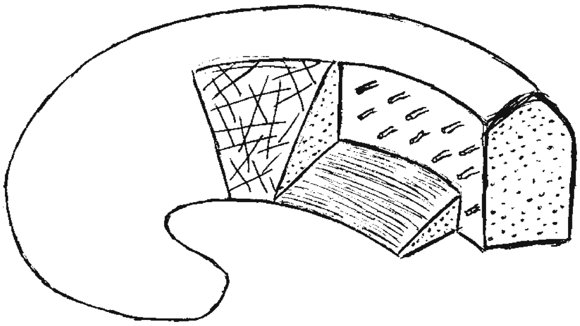

Fig. 16.5. Micro-anatomy of the meniscus. Most collagen bundles course in a circumferential direction with fewer radially oriented fibers, resisting longitudinal splitting

is the dominant morphological pattern, allowing dispersion of compressive loads and the development of "hoop stresses". Radial oriented fibers ("tie fibers") may function to restrain motion between circumferential fibers and resist longitudinal splitting. At the surface of the meniscus, fiber orientation is more of a random configuration (Greis et al. 2002).

The *blood supply to the menisci* originates from the lateral and medial superior and inferior genicular arteries. These vessels reach the periphery of the meniscus through the synovial covering of the anterior and posterior horn attachments. Vessels are present throughout the substance of the fetal menisci. Beginning at birth, there is a progressive decrease in vascularity proceeding from the inner to the outer regions of the meniscus. The adult meniscus is avascular in the inner two thirds ("*white zone*") and vessels are most prominent in the peripheral one third of the menisci and in the adjacent coronary and capsular ligaments ("*red zone*") (Fig. 16.1) (Rath and Richmond 2000).

The menisci are important in many aspects of knee function, with the main functions being tibiofemoral load transmission and shock absorption (Greis et al. 2002). The menisci compensate for significant incongruity between the femoral and tibial articulating surfaces and increase tibiofemoral contact area, with subsequent reduction in joint contact stresses. The menisci transmit at least 50–70% of the load when the knee is in extension. This increases to 85–90% with 90° of knee flexion. These loads are well distributed when the menisci are intact (Greis et al. 2002). After meniscectomy, tibiofemoral contact area may decrease by 50–70%, leading to a proportional increase in contact and shear stresses across the joint. These changes will lead eventually to joint degeneration. Furthermore, several studies have demonstrated that meniscal tissue is approximately one half as stiff as articular cartilage. The shock absorption capacity of the normal knee is reduced by 20% after meniscectomy (Voloshin and Wosk 1983).

It is important to remember that the menisci are not stationary structures. With flexion and extension of the knee, the medial meniscus translates about 2 to 5 mm on the tibia, and the lateral meniscus translates about 9 to 11 mm (Greis et al. 2002).

The menisci play a key role in enhancing joint stability, largely as secondary soft tissue restraints which prevent anterior tibial displacement (Rath and Richmond 2000). The body of the meniscus prevents the femur from gliding too far off the tibia. Shoemaker and Markolf (1986) demonstrated that the posterior horn of the medial meniscus is the most important structure resisting an applied anterior tibial force in an ACL deficient knee. Patients who tear the posterior meniscal horn may feel instability – even if their ACL is intact – because this stabilizing effect is lost.

Finally, the menisci contribute significantly to joint lubrication, probably by fluid exudation across their surfaces. Compression squeezes the liquid out into the joint space, to allow smoother gliding of the joint surfaces. This also helps to distribute synovial fluid throughout the joint and aids the nutrition of the articular cartilage (Rath and Richmond 2000).

16.3 Imaging Modalities in Meniscal Injuries

Although meniscal injuries are extremely common, the clinical history and mechanism of injury are usually non-specific, and must be regarded as of little value in determining the diagnosis. Mechanical symptoms of popping, catching, locking or buckling along with joint line pain are suggestive, but not conclusive, of meniscal pathology, and other types of intra- and extra-articular pathology may confound the clinical picture.

Numerous specialized tests have been described that may aid in making the diagnosis of meniscal tear. These include joint line palpation, McMurray test, the Apley grind test, and many others. Although conflicting results regarding the diagnostic accuracy of the various meniscal tests have been reported, no specific examination maneuver has impressive test performance characteristics, with the exception of the

joint-line tenderness test, which showed an acceptable diagnostic accuracy (Karachalios 2005).

16.3.1 Plain Radiography and Conventional Arthrography

The imaging evaluation of the patient presenting with suspected meniscal pathology should always start with plain radiography. A standard series will include a 30° or 45° posteroanterior flexion weight-bearing view of both knees, a true lateral radiograph, and a skyline view. The radiographs are inspected for associated skeletal injury or fracture, presence of loose bodies, or degenerative changes.

For decades, conventional fluoroscopic arthrography (after sterile preparation and injection of intra-articular contrast medium), was the radiological technique for investigating meniscal injury. Conventional arthrography has the merit of allowing dynamic examination of the knee with application of varus and valgus forces, helping to displace the apposed edges of a meniscal tear which may not otherwise be apparent. This may be useful when evaluating the postoperative meniscus. Although it may be an alternative for patients with a cardiac pace-maker or claustrophobic symptoms, this imaging modality has now been replaced by cross-sectional imaging techniques.

16.3.2 Magnetic Resonance Imaging

Because of its exquisite contrast resolution and ability simultaneously to display the osseous and soft tissue structures of the knee in virtually any plane, MRI has currently become the most widely used non-invasive imaging method that can aid in the evaluation of the entire spectrum of internal derangements of the knee.

16.3.2.1 Technique

Equipment and techniques for MRI vary widely. A circumferential surface coil is mandatory to ensure uniform signal-to-noise across the entire image and provide better spatial resolution. Complete assessment of the knee requires that images be obtained in the sagittal, coronal and axial planes.

Sequences that use a short echo time (TE<20 ms), such as T1, proton density (PD) and gradient echo T2*-weighted images, are most sensitive for identifying meniscal tears (Fig. 16.6). Long echo-time (T2) sequences are less sensitive but more specific. Conventional spin-echo sequences are more sensitive to meniscal pathology than fast spin-echo sequences. If a fast spin-echo technique, which offers the advantage of faster data acquisition, is used, the echo train

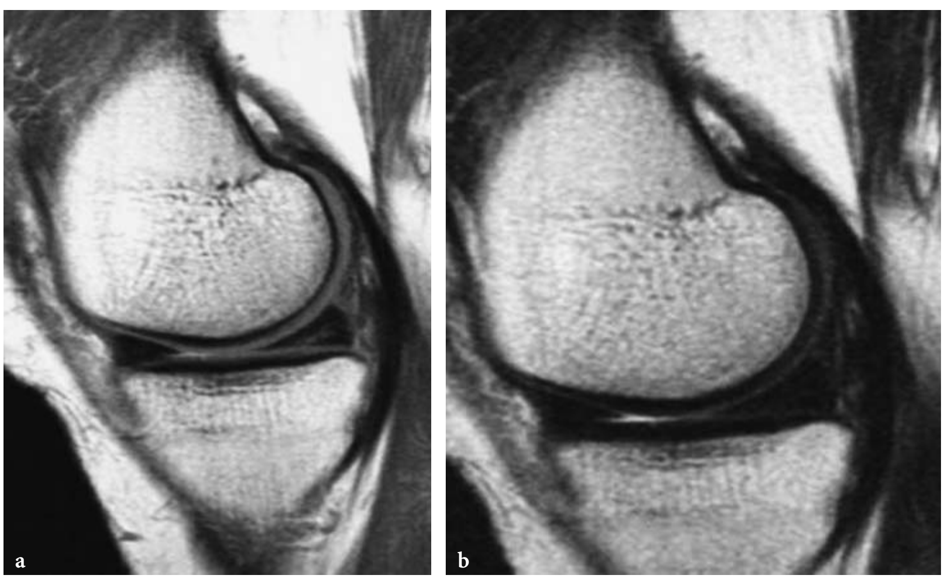

Fig. 16.6a,b. Proton density vs T2-weighted imaging. Fifty-six-year-old male with knee pain at the medial joint line during running since several weeks. **a** Sagittal PD-WI shows equivocal grade 3 signal in the posterior horn of the medial meniscus. **b** These findings are not well demonstrated on the sagittal T2-WI

length (ETL) should be kept below four to five and the interecho spacing minimized to reduce blurring effect inherent to this technique that can obscure a meniscal tear. Although useful for the evaluation of the morphology of the meniscus (in complex tears or postoperative partial meniscectomies), fast spin-echo sequences are not recommended for the primary diagnosis of meniscal tears (Rubin et al. 1994). T2-weighted images using either fast spin-echo techniques with spectral fat saturation (FS) or short inversion time inversion recovery (STIR) can be performed in conjunction to enhance the detection of bone marrow edema or contusion.

16.3.2.2
Normal MR Anatomy

The normal menisci demonstrate diffusely low signal intensity on all MRI pulse sequences because of their fibrocartilaginous structure. Menisci must be evaluated on both the sagittal and coronal images. Recently, Tarhan et al. (2004) have demonstrated the value of the axial imaging plane for the detection and characterization of meniscal tears in standard knee examinations, especially when disease existed in the periphery of the meniscus. Also, small radial tears of the free edge of the meniscus have been reported to be better visualized in the axial plane (Tarhan et al. 2004).

The most peripheral images of the sagittal plane demonstrate a "bow tie" appearance of the meniscus. The normal meniscus should have 1.5 to 2 bow ties (5–13 mm) on 4–5 mm thick images. Broad and disk shaped menisci (>13 mm) with three to four or more bow ties are called "discoid" and are more prone to meniscal tears. The normal meniscus measures 3 to 5 mm in height. The medial meniscus varies in width from 6 mm at the anterior horn to 12 mm at the posterior horn. The lateral meniscus is approximately 10 mm in width throughout its length.

More centrally, the normal meniscus becomes triangular in appearance. The anterior and posterior horns of the lateral meniscus are nearly equal in size, whereas the posterior horn of the medial meniscus is nearly twice the size of the anterior horn.

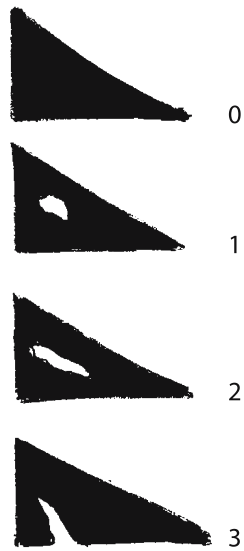

Fig. 16.7. Grading of intrameniscal signal as seen on MRI. Grade 0, normal; grade 1, intrasubstance globular-appearing signal not extending to the articular surface; grade 2, linear increased signal patterns not extending to the articular surface; grade 3, the abnormal signal extends to the articular surface. Only grade 3 signal represents meniscal tear

16.3.2.3
Classification of Meniscal Tears

To understand the significance of increased signal intensity in meniscal abnormalities, an MR grading system has been developed and correlated with a histopathologic model (Fig. 16.7) (Stoller et al. 1987): *grade 1*, intrasubstance globular-appearing signal not extending to the articular surface; *grade 2*, linear increased signal patterns not extending to the articular surface; *grade 3*, the abnormal signal extends to the articular surface. The clinical importance of grade 2 signal abnormality in the meniscus, as seen on MRI and not visualized arthroscopically, is still not well understood. Grades 1 and 2 represent intrasubstance mucinous degeneration in an adult or prominent vascularity in a child and have no surgical significance. Grade 3 is visible by arthroscopy and represents a meniscal tear.

In addition to observing increased signal intensity within tears, the morphology of the meniscus should be assessed when evaluating meniscal lesions.

The "*direct*" signs (De Smet et al. 2001) associated with meniscal tears on MRI (Fig. 16.8) include:

1. Unequivocal grade 3 signal
2. Abnormal meniscal morphology with displaced or missing meniscal tissue
   - Absent bow tie sign (1 or fewer): either postsurgical or displaced tear
   - Double PCL sign: displaced bucket-handle tear of the medial meniscus
   - Large anterior horn sign: displaced bucket-handle tear of the meniscus with flipped fragment
3. Meniscocapsular separation

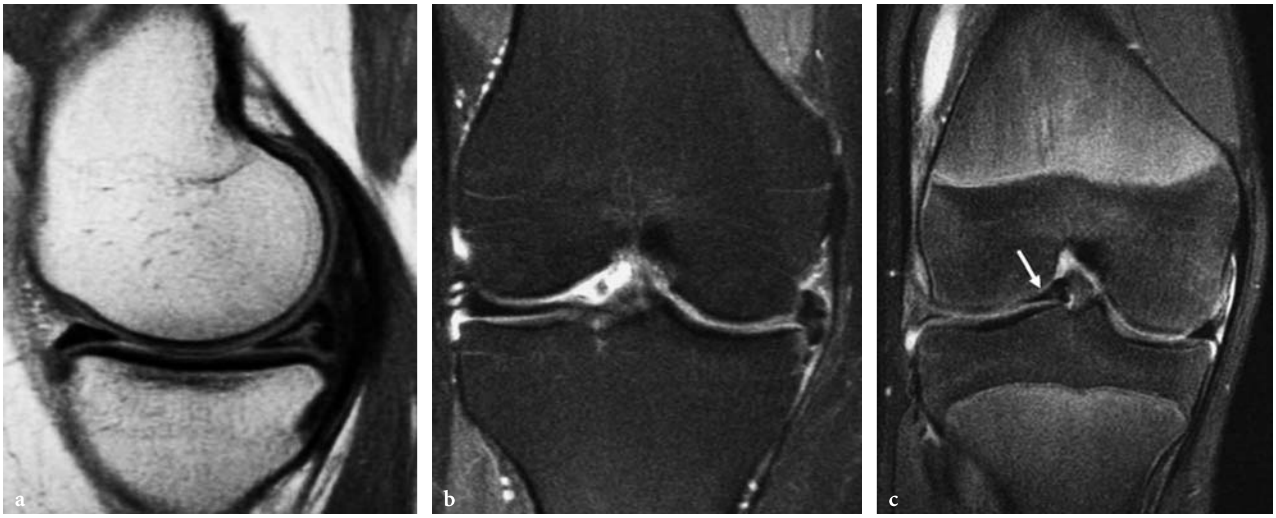

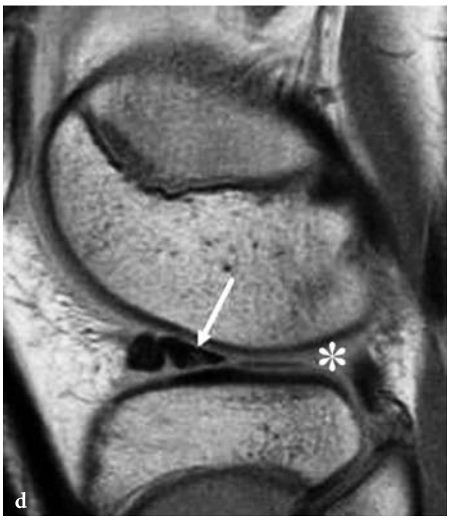

Fig. 16.8a–d. Direct signs of meniscal tear. **a** Thirty-three-year-old marathon runner with pain at the medial knee joint. Sagittal PD-WI demonstrates equivocal grade 3 signal intersecting the inferior articular surface of the meniscus, representing oblique meniscal tear. **b** Twenty-two-year-old gymnast after acute knee dislocation. Coronal fat suppressed PD-WI displays abnormal morphology of the medial meniscus with inferomedial displacement of meniscal fragment deep in relation to medial collateral ligament and adjacent to tibial plateau. **c,d** Fifteen-year-old male with sudden extension deficit of his right knee while playing football. Coronal fat suppressed PD-WI (**c**) displays medially displaced lateral meniscal fragment (*arrow*). On sagittal PD-WI (**d**), the posterior horn of the lateral meniscus is missing (*), and seen just behind the slightly anteriorly displaced anterior horn of the meniscus (*arrow*) ('flipped meniscus'). Arthroscopically, lateral meniscal tear with subsequent anterior luxation of the posterior horn was seen

The "*indirect*" signs (Costa et al. 2004) associated with meniscal tears on MRI include:

1. Abnormal superior popliteomeniscal fascicle and posterior pericapsular edema: lateral meniscal tear, most commonly posterior horn.
2. Posterior bone bruise of the medial tibial plateau: peripheral tears of the posterior horn of the medial meniscus or tears of the posterior root ligament of the medial meniscus. Tears of this ligament can be associated with ganglioncysts at the posterior aspect of the tibia as well.
3. Extrusion (>3 mm) of the medial meniscus: degeneration, complex or large radial tear, tear involving the meniscal root.

Meniscal tears can be classified into two primary tear planes: vertical and horizontal (Fig. 16.9). Vertical tears are often of a traumatic origin and occur in younger individuals, whereas horizontal tears are usually secondary to meniscal (mucoid) degeneration and occur at later age.

Vertical tears are further subdivided into radial (perpendicular to the surface of the meniscus) and longitudinal (parallel to the long axis of the meniscus) varieties. An oblique vertical ("flap") tear is the most common meniscal tear type and demonstrates both radial and longitudinal components, as it courses obliquely across the meniscus, resulting in a flap of unstable meniscus. They most commonly affect the posterior horn and are seen as predominantly horizontal on sagittal MR images originating along the inferior surface at the free edge.

Radial tears are relatively uncommon meniscal tears and most commonly occur at the junction of

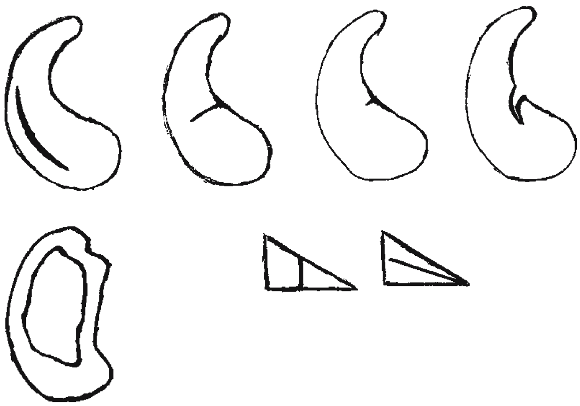

Fig. 16.9. Classification of meniscal tears (*left to right*): peripheral, longitudinal tear; large and small radial tear; oblique parrot-beak tear; bucket-handle tear; vertical tear; horizontal tear

the anterior horn and body of the lateral meniscus and at the meniscotibial attachment of the posterior horn of the medial meniscus. They are often seen as blunting of the free edge on coronal (MR) images. On sagittal images, the only evidence of a radial tear may be increased signal intensity on one or two peripheral sections (Figs. 16.10 and 16.11).

A bucket-handle tear is an important and not infrequent type of meniscal injury, occurring in about 10% of meniscal tears in most series. It typically consists of a vertical or oblique tear in the posterior horn that extends longitudinally through the body segment and anterior horn, usually occurring acutely with a sudden impact splitting the meniscus longitudinally. Coronal and sagittal MR images demonstrate blunting of the meniscus donor with the remaining meniscus being smaller than normal. The inner meniscal fragment is often displaced in the intercondylar notch, creating a "handle". Reported MRI signs for bucket-handle tears include absent bow tie sign, the double PCL sign, the disproportional posterior horn sign, the anterior flipped fragment sign and double anterior horn sign (Aydingôz et al. 2003) (Fig. 16.12).

Horizontal tears extend through the meniscus along a plane parallel to the tibial plateau, dividing the meniscus in inferior and superior segments. A horizontal cleavage tear is the most common type of tear to be associated with a meniscal cyst (Fig. 16.13). These cysts occur as a result of fluid extruding through the tear by a ball valve effect, and collecting either in the meniscus (intrameniscal cyst) or at the meniscocapsular junction (parameniscal cyst). These cysts tend to recur after resection if the underlying meniscal cyst is not repaired. With a horizontal tear, a portion of the meniscus may flip into the adjacent synovial gutter along the margin of the joint. These fragments may be missed easily at arthroscopy, when they are not identified on MRI.

Complex meniscal tears display combinations of vertical and horizontal tear patterns.

a

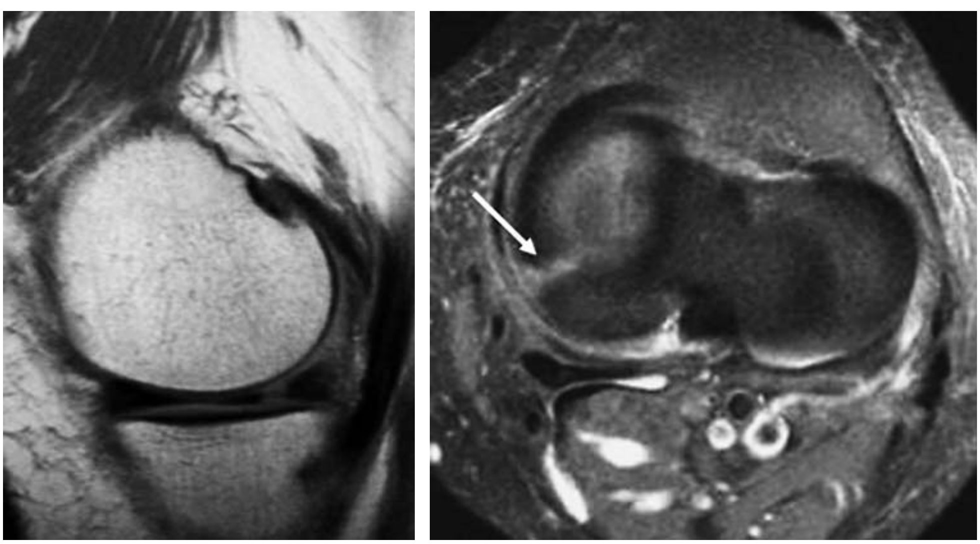

b

Fig. 16.10a,b. Radial tear. Thirty-five-year-old female jogger with pain at the medial joint line for some weeks. **a** Sagittal PD-WI demonstrates vertical oriented grade 3 signal in the posterior horn of the medial meniscus. **b** Axial fat suppressed PD-WI shows radially oriented tear (*arrow*) at the junction of the body and posterior horn of the medial meniscus

a b c

Fig. 16.11a–c. Radial tear. Twenty-nine-year-old man after clipping injury while playing football. CT arthrography with axial (**a**), coronal (**b**) and sagittal (**c**) reformatted images. Axial image displays radially oriented tear at the junction of the body and anterior horn of the lateral meniscus. Both coronal and sagittal images demonstrate blunting of the free inner edge of the meniscus, typically seen in radial meniscal tear

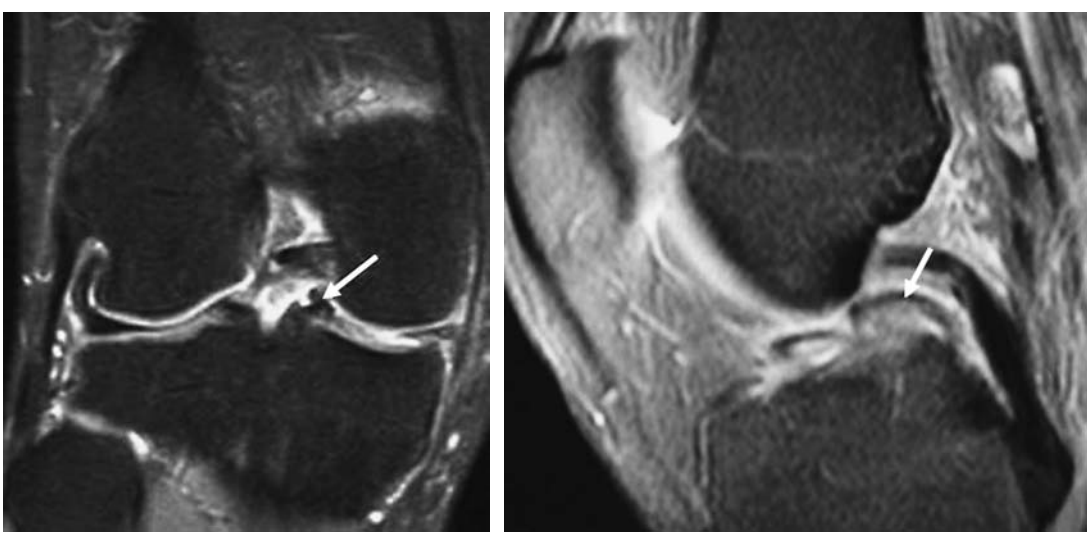

a b

Fig. 16.12a,b. Bucket-handle tear of the medial meniscus. Twenty-eight-year-old male track athlete felt sudden knee pain after twisting injury. **a** Coronal fat suppressed PD-WI displays abnormal morphology and grade 3 signal in the medial meniscus with internally displaced meniscal fragment (*arrow*). **b** Sagittal fat suppressed PD-WI demonstrates the meniscal fragment (*arrow*) in front of the PCL (‘double PCL sign’)

a b

Fig. 16.13a,b. Meniscal cyst. Coronal fat suppressed PD-WI (**a**) and sagittal PD-WI (**b**) display large horizontal tear in the lateral meniscus with parameniscal cyst, extending laterally and posteriorly

Meniscocapsular separation is a subtype of meniscal tear, occurring most commonly along the medial meniscus, but the lateral meniscus may be affected also. Typically, the posterior meniscal horn is separated from the capsule with displacement of the posterior meniscal margin from the posterior tibial border by more than 8–10 mm.

16.3.2.4
MR Accuracy and Limitations

With improved technology, the accuracy of MRI for detecting meniscal injury ranges is now considered to be approximately 95% or better, and it has been shown that the level of experience of the image reader is the most important factor in obtaining the highest level of accuracy (De Smet et al. 1994).

However, MR findings do not always agree with surgical findings. In a study by De Smet et al. (1994), the various causes of incorrect MR diagnoses were analyzed. Of the 83 original diagnostic errors made in the MR evaluation of 800 menisci (accuracy 90%), 33 (40%) were unavoidable errors, 32 (39%) were due to equivocal MR findings and 18 (21%) were interpretation errors.

Unavoidable false positive results may be obtained when dealing with a healing or healed meniscal tear. A healing tear (e.g., after meniscal repair) may be seen as hyperintense signal intensity in meniscal substance owing to the presence of granulation tissue (Farley et al. 1991). Also, they may be related to incomplete arthroscopic evaluation of the meniscus. Blind spots for the arthroscopist include the anterior horn of each meniscus, the extreme inner portion of the posterior horn of the medial meniscus, and the undersurface of both menisci. Therefore, it is important to describe any tear in these areas clearly, because they may be easily missed during arthroscopy. Confusion between what represents fraying and what represents a tear may be another source of erroneous MR diagnosis.

Unavoidable false negative errors are due to limitations of the MR sequences and imaging planes and do not represent observer errors. Small meniscal tears may not be discernible with current MR imaging techniques because the edges of small tears may be very closely apposed. Radial tears have been reported to be very difficult to visualize on MR images, and these tears account for a large percentage (up to 11% in the lateral meniscus) of meniscal tears missed by MRI (Justice and Quinn 1995; De Smet et al. 1994). Furthermore, if a tear of the ACL is present, meniscal tears are more likely to be missed on MR images. Presumably, the biomechanical forces that result in an ACL tear cause meniscal tears that are difficult to diagnose on MRI, namely in the posterior and peripheral part of the lateral meniscus (De Smet and Graf 1994).

It is not always possible to neatly categorize meniscal signal and determine if it is confined to the substance of the meniscus or extends through the surface (Kelly et al. 1991). MR imaging findings may be equivocal for a tear, leading to both false positive and false negative results. De Smet et al. (1993) found that menisci with signal possibly contacting the surface had the same frequency of tears as menisci without signal contacting the surface. Furthermore, only 55% of medial and 30% of lateral menisci with signal contacting the surface on only one image were torn. Thus, when linear signal closely approximates, but does not convincingly violate an articular surface, it is best to be descriptive rather than overcall a questionable finding. If surface contact is seen on only one image, the diagnosis should be qualified as a possible tear. Menisci with internal signal that only possibly contacts the surface should be considered intact.

Interpretation errors may occur due to normal variants (Fig. 16.14). Radiologists must be aware of numerous pitfalls simulating a meniscal tear, including normal anatomical structures in close proximity to the meniscus (anterior transverse ligament, oblique meniscomeniscal ligament, meniscofemoral liga-

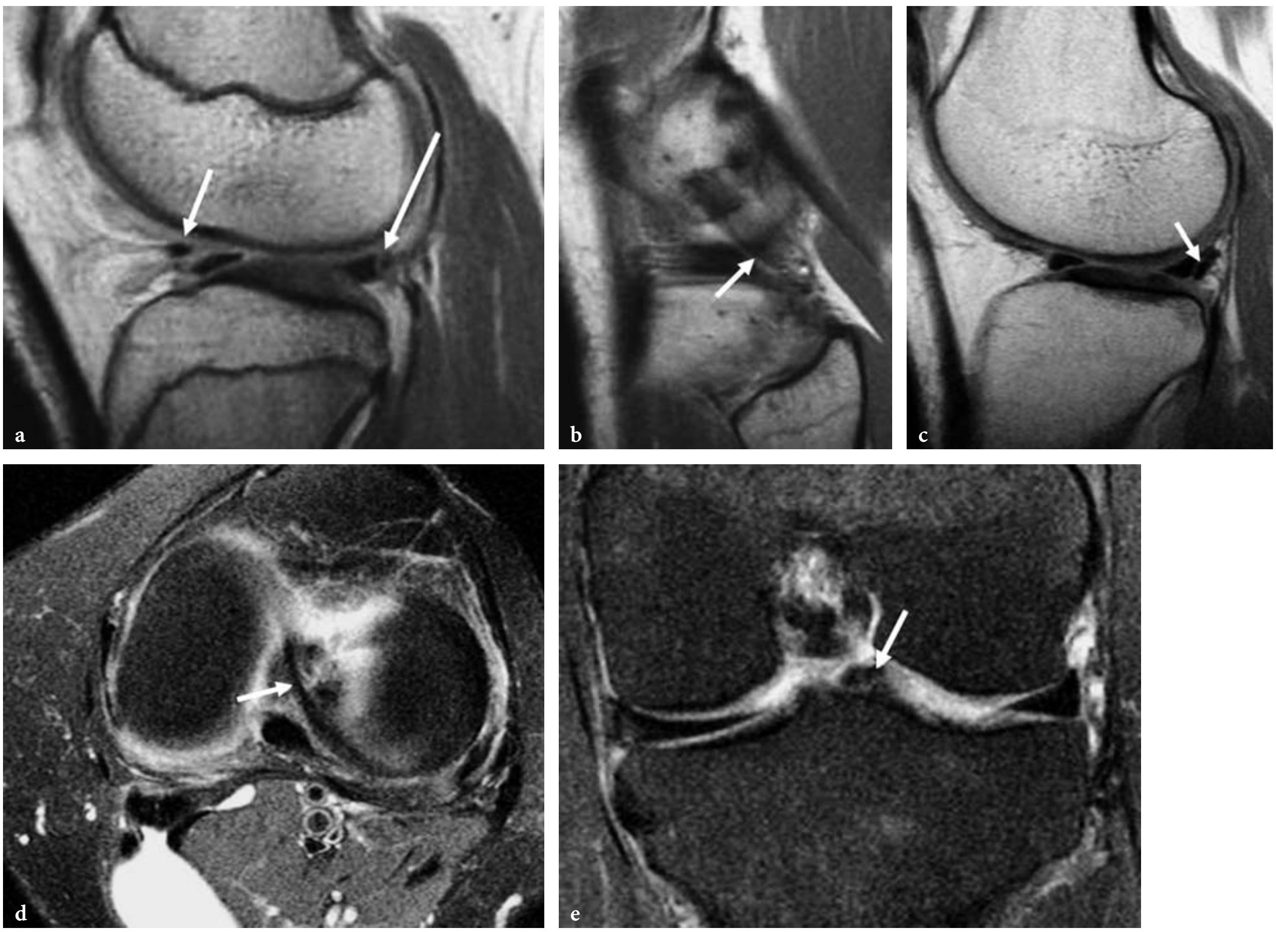

Fig. 16.14a–e. Normal variants simulating a meniscal tear. **a** Sagittal PD-WI demonstrates the anterior transverse meniscal ligament (*small arrow*), mimicking a grade 3 signal as it attaches to the anterior horn of the lateral meniscus. Posteriorly, the normal appearance of the meniscofemoral ligament is shown (*large arrow*), as it arises from the posterior horn of the lateral meniscus, also mimicking a grade 3 signal. **b** Sagittal PD-WI demonstrates the normal appearance of the popliteus tendon (*arrow*) as it traverses posteriorly to the lateral meniscus, mimicking a grade 3 signal. **c** Wrisberg's variant of discoid lateral meniscus. Sagittal PD-WI shows posterior horn of the lateral meniscus unattached to capsule, simulating a vertical meniscal tear. According to Watanabe's classification system (Watanabe and Takeda 1974) for the discoid lateral meniscus, this is referred to as a type 3 discoid meniscus (Wrisberg's variant). This variant may have a normal appearance but there is deficiency of attachment of the posterior-horn meniscotibial ligaments, resulting in instability of the posterior horn. **d,e** Axial fat suppressed PD-WI (d) shows oblique meniscomeniscal ligament (*arrow*). On coronal fat suppressed PD-WI (**e**), a displaced meniscal fragment is simulated (*arrow*)

ment, popliteal tendon, Wrisberg's variant of discoid lateral meniscus), MR artefacts (volume averaging of adjacent bright structures e.g., fat or fluid, truncation and motion-blurring artefacts, magic angle phenomenon) and pathologic conditions (gas within the joint-vacuum phenomenon or iatrogenic, chondrocalcinosis, cartilage defects, meniscal ossicle).

16.3.3 Computed Tomographic Arthrography

Although MRI is the preferred imaging modality for evaluating internal derangement of the knee, computed tomography (CT) has become a powerful imaging tool because of the development of the spiral acquisition mode and the availability of multidetector row technology that enable submillimeter spatial resolution and multiplanar capacity. Multidetector CT arthrography (CTA) of the knee is an accurate and reproducible method for detecting meniscal abnormalities (Vande Berg et al. 2000). Vande Berg et al. found a sensitivity and specificity for the detection of meniscal abnormalities of 98 and 94%, respectively. These values are equivalent to those in most studies with MR imaging (Rubin et al. 1994). Furthermore, CTA proved to be an accurate technique for detection of unstable meniscal tears with a sensitivity and specificity of 97 and 90%, respectively. Poor performance of MR imaging in the recognition of displaced meniscal fragments smaller than one-third of the meniscus has been reported (Wright et al. 1995).

Other potential advantages of CTA are the short examination time as well as the low sensitivity and limited degree of imaging artefacts related to the presence of microscopic metallic debris which may hinder MR imaging studies. Furthermore, CTA of the knee may be useful for evaluation of the postoperative meniscus.

Limitations inherent to the performance of this technique include invasiveness, possible allergic reaction, the use of ionizing radiation and limited value for detection of associated ligamentous and/or soft tissue disorders.

16.4 Postoperative Meniscus

Because meniscal surgery is so common in the young, athletic population, many patients who have undergone meniscal surgery present with recurrent knee injury or pain. For the radiologist, imaging the postoperative meniscus remains a challenge. As in preoperative patients, MR imaging is the most valuable imaging method for postoperative evaluation of the knee (McCauley 2005).

Standard MR imaging protocols are less reliable in imaging postoperative knees than in unoperated knees, especially for the diagnosis of meniscal tears, with accuracies ranging from less than 50% to 80%. Contour abnormalities and diffuse signal changes may be present in both normal postoperative menisci and in recurrent meniscal tears. The basic criteria for identifying a meniscal tear – increased intrameniscal signal on a T1-weighted or proton density-weighted image extending to the meniscal surface – becomes an unreliable predictor in the postoperative knee. A high signal line that reaches the articular surface (grade 3) may represent an area of meniscal healing and may be misinterpreted as a new tear. Furthermore, a partial resection could convert a grade 2 intrameniscal signal into a grade 3 signal, extending to the new surface of the partly resected meniscus (Fig. 16.15). Fluid-intensity signal on a T2-weighted image extending into the meniscus is a stricter criterion for recurrent or residual tear, providing high specificity (92%) but low sensitivity (60%) (Farley et al. 1991).

Fig. 16.15. Normal postoperative meniscus simulating a meniscal tear. When a partial meniscectomy is performed (*dotted lines*), hyperintense intrasubstance (grade 1 or 2) signal intensity can be converted into grade 3 signal intensity, thus simulating a meniscal tear

In an attempt to increase the diagnostic accuracy, MR arthrography (MRA) (with direct injection of the joint with a dilute solution containing gadolinium) has been applied to the postoperative meniscus. The criterion for diagnosing a recurrent or residual tear of the meniscus using MRA is seeing extension of

the gadolinium into the meniscal fragment or into the site of a meniscal repair. Applegate et al. (1993) reported that in the patients in whom a great amount of the meniscus was removed (more than 25%), MR arthrography was significantly more accurate compared to conventional MRI (87% vs 65%), whereas in patients with minimal meniscal resection (less than 25%), the two techniques performed equally well (89% accuracy).

However, a recent study comparing conventional MR imaging with MRA found that the increased accuracy of MRA for detection of retorn menisci was not statistically significant (White et al. 2000). Also, in a study by Sciulli et al. (1999), conventional arthrography, conventional MR, MRA with iodinated contrast material and MRA with gadolinium were compared for the detection of recurrent or residual tear in the postoperative meniscus. The only statistically significant difference was found between conventional arthrography and MRA using gadolinium, with accuracies of 58 and 92%, respectively.

Indirect MRA involves an intravenous injection of a gadolinium solution (0.1 mmol/kg) prior to the MRI. Synovial excretion of contrast medium occurs in the minutes after injection to shorten the relaxation time of the synovial fluid. This technique has the advantage of not requiring direct access to the joint but lacks the perceived advantages of joint distension, which accompany an intra-articular injection. Recently, indirect MRA has been proposed for assessment of the natural healing process after meniscal repair (Hantes et al. 2004).

In conclusion, the design of an imaging strategy for investigating patients with recurrent or residual symptoms following meniscal surgery, depends on several factors, including local radiological expertise, hardware resources, multidisciplinary team activity and clinical case mix. Of utmost importance in the evaluation of the postoperative meniscus, is the availability of the preoperative images if possible and the operative report with details of the extent of resection.

In general, most patients do not need to undergo MR arthrography and conventional MRI should be considered as the first line investigation (Magee et al. 2003) (Fig. 16.16). We look for unequivocal sites of fluid-intensity signal within the meniscal remnant, displaced fragments or tears in a new location, as the only reliable criteria for a recurrent or residual tear. Standard criteria can be used to interpret areas of the menisci known to be separated from the site of prior surgery. Investigation with MRA (or CTA) could then be considered if conventional MRI is normal (no severe degenerative arthrosis, avascular necrosis, chondral injuries, native joint fluid extending into a meniscus, or a tear in a new area), if the clinical suspicion of recurrent tear is high, or if conventional MRI is inconclusive. In particular, MRA may be useful

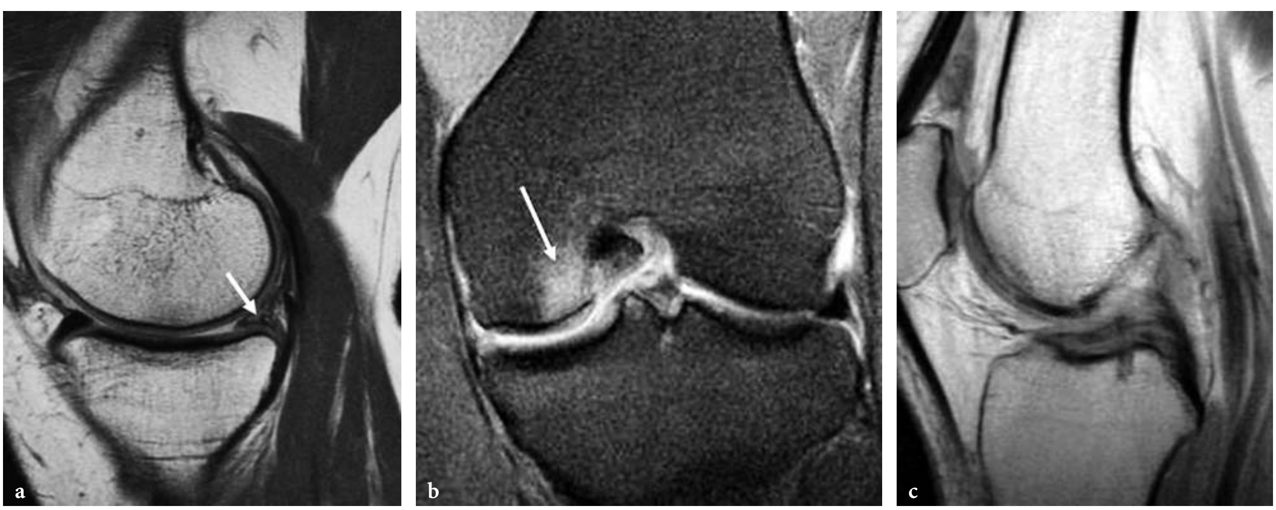

Fig. 16.16a–c. Postoperative meniscus-standard MRI. Forty-four-year-old woman received partial medial meniscectomy for bucket-handle meniscal tear after ski trauma 6 months ago. Actually, she presents with knee pain after twisting injury and standard MRI is performed. **a,b** Sagittal PD-WI (**a**) and coronal fat suppressed PD-WI (**b**) show abnormal morphology and increased signal intensity of the medial meniscus due to prior partial meniscectomy. There is no direct sign of recurrent nor residual meniscal tear. However, extensive bone bruise (*arrow*) in the medial femoral condyle is depicted on the coronal fat suppressed PD-WI. **c** Sagittal PD-WI shows rupture of the ACL. No further examinations are necessary

when there is prior knowledge of significant meniscal resection (more than 25%) or meniscal repair with new symptoms in the same area as the initial symptoms. Furthermore, MR arthrography is of additional value in assessing the articular cartilage, deteriorating more rapidly after meniscectomy.

16.5 Therapeutic Management in Athletes

When faced with a meniscal tear, the orthopaedic surgeon has three options: (1) leave the tear alone, (2) attempt a primary meniscal repair, or (3) perform a partial or complete meniscectomy. For optimal treatment planning, the overall clinical situation must be evaluated.

In older or less-active patients with minor symptoms, a more conservative approach is often employed. The mere presence of a meniscal tear in the degenerative knee is not an indication for arthroscopy. One recent study demonstrated that meniscal tears were a very common magnetic resonance imaging finding in asymptomatic patients and that there was no difference in pain or function between osteo-arthritic patients with or without meniscal tears (Miller 2004). However, in athletes, non-operative treatment is usually inadequate for a patient with high physical demands associated with sport, as the reduction in activity necessitated by the symptoms is not acceptable (Ludman et al. 1999).

Meniscal tear location, extent and stability are essential criteria for deciding whether to resect, repair, or leave alone a meniscal lesion (Weis et al. 1989).

Although MRI provides valuable information by displaying the location and extent of the tear, it is often impossible to determine with certainty whether or not a tear is stable using MRI (unless a displaced fragment is present). Meniscal tear stability is best determined with direct depiction and palpation at arthroscopy (Dandy 1990). Following arthroscopic probing, only those parts that are found to be unstable (displacement of any portion of the meniscus more than 3 mm during probing) will be resected. However, on MRI, tears that are considered stable include (1) a partial-thickness tear (less than half the height of the meniscus), (2) a full-thickness oblique or vertical tear measuring less than 7 to 10 mm in length, and (3) a radial tear measuring less than 5 mm (Matava et al. 1999).

Based on MR images, it is important to classify the location of the tear relative to the blood supply of the meniscus. This allows repair potential of the lesion to be predicted. A red-red tear is located at the meniscal periphery within the vascularised zone or represents capsular detachment. It has the best prognosis for healing, as the blood supply persists in this region (Fig. 16.17). The red-white tear has no blood supply from the inner surface of the lesion.

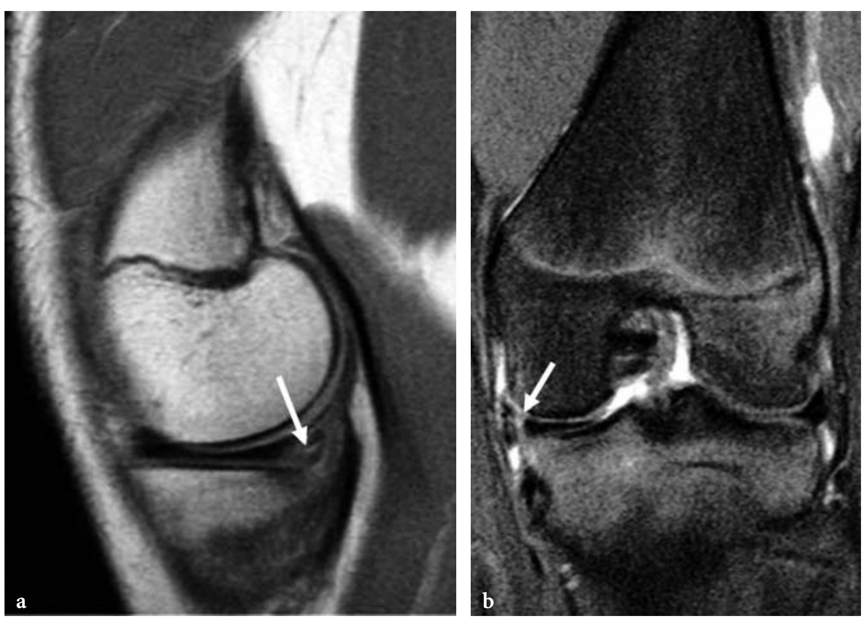

Fig. 16.17a,b. Meniscocapsular injury. Thirteen-year-old female patient sustained acute knee injury while playing tennis. **a,b** Sagittal PD-WI (**a**) and coronal fat suppressed PD-WI (**b**) display hyperintense grade 3 signal at the meniscocapsular junction of the posterior horn of the medial meniscus, consistent with vertical meniscal tear. As the blood supply persists in this region, it has the best prognosis for healing, and therefore, therapeutic management will be conservative

The remaining vascularity is usually sufficient for the healing process. A white-white tear is located in the avascular zone and therefore has no potential to heal. A red-red and red-white tear may spontaneously heal or may be repaired. White-white tears need to be resected.

The treatment goal is to preserve as much functional meniscal tissue as possible to lessen the probability of developing osteoarthritis, while addressing the clinical symptoms caused by meniscal tears. The stabilizing effect and vascularization of the peripheral third of the meniscus is the basis for attempts to preserve this tissue in partial meniscectomies.

Meniscal allograft transplantation is a relatively new concept but the indications are not well defined yet. The role of MRI in patients who have undergone meniscal transplantation still requires clarification.

16.6 Specific Sports and Overuse Trauma of the Meniscus

16.6.1 Injury Mechanisms in Sports Injury

Sports-related meniscal tears may result from excessive application of force to a normal meniscus (in the young athlete) or normal forces acting on a degenerative meniscus (in older patients). Meniscal injury, particularly sports-related injuries, usually involve damage due to twisting motions, which are common in sports, with a varus or valgus force directed to a flexed knee. Contact with another player typically does not occur, nor does lunging or landing awkwardly. A single "wrong" step is sufficient.

The most common traumatic mechanism, accounting for nearly half of all injuries, combines valgus force directed to a flexed knee with the tibia in exorotation (Hayes et al. 2000). Therefore, compression with impaction injury usually occurs in the lateral compartment, whereas tension with distraction injury occurs in the medial compartment. Thus, the medial meniscus is at risk for peripheral avulsion injury at the capsular attachment site resulting in peripheral meniscal tear (and/or meniscocapsular injury) whereas the lateral meniscus gets entrapped by compressive force, splays and splits (because of its more circular shape and decreased radius of curvature) the free margin resulting in a radial tear.

In contact sports, tackles are often directed towards the lateral side of the knee, resulting in the same injury mechanism and type of (meniscal) lesions.

Injury to the medial meniscus is about five times more common than injury to the lateral meniscus. Compared to the lateral meniscus, the medial meniscus is relatively immobile because of its firm attachment to the medial capsule along its peripheral border. The lateral meniscus, loosely applied to the joint capsule, moves freely with the condyle and usually can escape entrapment (Muller 1983).

The trauma-related medial meniscal tear typically demonstrates a vertical orientation extending across the full-thickness of the meniscus. It may redirect itself obliquely towards the free margin of the meniscus, creating a flap configuration.

Radial tears are rare in the medial meniscus and appear to follow more severe forms of athletic trauma (Kidron and Thein 2002). Kidron and Thein described the presence of a small radial root tear in the posterior horn of the medial meniscus in 11 of the 1270 operated knees (0.86%). Each of these 11 patients, all active in demanding sports, including handball, judo and gymnastics, had a history of acute flexion injury and medial joint line pain. Arthroscopic trimming of the edges of the tear revealed a developing cleavage plane tear extending to the body of the meniscus, resulting in partial meniscectomy.

Moreover, according to a study by Magee et al. (2004), the prevalence of meniscal radial tears may be increased in the postoperative knee due to the altered hoop mechanism of the meniscus and decreased ability to transmit loads. These authors found a prevalence of meniscal radial tears of 32% in the postoperative knee as opposed to a reported prevalence of 14% in the non-operated knee.

There are significant regional differences in sports-related meniscal injuries depending upon the popularity of specific sports. In a study by Baker et al. (1985), meniscectomies performed in Syracuse, New York from 1973 to 1982 were reviewed. Medial vs lateral meniscus injury was 81 vs 19%. Football had a 75% predominance of medial meniscectomy; basketball, 75%; wrestling, 55%; skiing, 78%; and baseball, 90%. These data indicate that there are differences in the ratio of medial vs lateral meniscal disruption associated with specific sports activities. Medial meniscal injuries were consistently more common in all sports categories, except wrestling, where the frequency of lateral meniscal tear is nearly equal to that of a medial meniscal tear.

16.6.2
Symptomatic and Asymptomatic Meniscal Lesions in Athletes

Asymptomatic or "silent" grade 3 intrameniscal signal abnormalities have been described in both athletes and less active patients (Ludman et al. 1999). The incidence of asymptomatic meniscal tears increases with age, with 5.6 to 13% of those less than 45 years old and 36% of those more than 45 years old (Greis et al. 2002). Some studies have suggested that athletic groups, including American football players and marathon runners, show an increased incidence of meniscal abnormalities (Shellock et al. 1991). In a study by Ludman et al. (1999), the overall incidence of grade 3 changes (13%) in gymnasts was not significantly different from the incidence in the controls. However, when compared with the control group, the group of gymnasts had a significantly different distribution of grade 3 intrameniscal changes, preferentially involving the lateral meniscus (evenly divided between the anterior and posterior horn), whereas in the control group, grade 3 changes were mostly found in the medial meniscus (only posterior horn). The reason why the lateral meniscus of gymnasts is preferentially affected is unclear. Nevertheless, knowledge of these MR appearances is important when evaluating the lateral menisci within this group of athletes to prevent unnecessary treatment or intervention. This is particularly important when the imaging findings do not closely correlate with the site of symptoms.

On the other hand, symptomatic grade 2 intrameniscal signal has been described in athletes (Biedert 1993). In 35 of 43 patients (77.7%) with clinical features of a possible meniscus lesion, a pure intrasubstance tear with linear grade 2 signal was identified on MRI. This type of lesion in the posterior horn represents a frequent cause of false negative result on arthroscopy. All patients were free of symptoms after conservative treatment or partial meniscectomy. In this study, the highest rates of intrasubstance tears were found in soccer, running and ice hockey.

Although not specifically described in any sports branch, a potential source for false positive interpretation for meniscal tear in the MR evaluation of the posttraumatic knee, is the so-called "*meniscal contusion*". Cothran et al. (2001) described focal signal abnormalities in the knees of six patients who had a history of acute knee trauma, associated with tears of the ACL and bone contusions. This signal reached the articular surface of the meniscus, but did not meet criteria for a meniscal tear or degeneration. The meniscus gets trapped between, the femur and tibia during a traumatic event. The adjacent bone contusion should alert one to the possible presence of a contusion rather than a meniscal tear.

Meniscocapsular tears are a well known entity but may be more difficult to diagnose on MR images than meniscal tear. They are most commonly seen along the medial meniscus, which is more tightly adherent to the joint capsule. Small avulsed corners of the medial meniscus may be difficult to identify unless a directed search is made for them.

Recently, George et al. (2000) have found that anterolateral meniscocapsular separations of the lateral aspect of the knee were frequently missed on MRI reporting in a group of athletes presenting with lateral joint line pain suggestive of meniscal injury. During arthroscopy, in all patients meniscocapsular separation was confirmed and no meniscal tears were found. Meniscocapsular tears can also occur along the posterolateral corner of the joint, with disruption of the meniscopopliteal fascicles.

Another entity, recently described in severe acute (sports) injury of the knee by Bikkina et al. (2005), is the so-called "*floating meniscus*", corresponding to a meniscal avulsion or detachment from the tibial plateau with an associated disruption of the meniscotibial coronary ligaments, which attach the meniscus to the tibia, allowing fluid to encompass the meniscus. It is usually seen as a sequela of high-impact (sports) injury or trauma. The presence of a "floating meniscus" on MRI is often associated with significant ligamentous injury without evidence of a tear within the substance of the meniscus. Alerting the surgeon to the presence of a meniscal avulsion facilitates appropriate surgical planning with meniscal reattachment to the tibial plateau.

16.6.3
Musculoskeletal Tumors Around the Knee in Athletes

Musculoskeletal tumors, both benign and malignant, are much less common in young athletes than sports-related lesions. However, they frequently occur in the same age group and have a predilection for the same joint. In addition, the clinical presentation of a musculoskeletal tumor may mimic that of a sports-related injury. At oncologic musculoskeletal centers, it is not uncommon to see

patients with a knee tumor that had been previously treated as an athletic injury. In the study by Muscolo et al. (2003), 12 of 14 patients with final diagnosis of a malignant tumor about the knee were initially treated for a meniscal lesion. These authors found that initial poor-quality radiographs and an unquestioned original diagnosis despite persistent symptoms seemed to be the most frequent causes of an erroneous diagnosis. Prior treatment with an invasive diagnostic or therapeutic procedure for a traumatic condition might influence the final treatment, either by increasing the time required to make the final diagnosis of the tumor or by contaminating surrounding tissues. Hence, the original identified tumor stage, the prognosis, and the surgical approach required to treat the tumor may be altered.

The authors conclude that although MR imaging prior to the arthroscopy would have led to the final diagnosis earlier, the indications for MRI under these circumstances have been controversial (Rangger et al. 1996).

16.7 Conclusion

Meniscal injuries are very common among professional and amateur athletes and are a major cause of functional impairment of the knee. For athletes, unnecessary treatment or intervention may be as damaging to a competitive future as failure to diagnose a clinically significant injury. Therefore, rapid and accurate evaluation of possible meniscal injuries is crucial in these patients.

For detection of meniscal pathology, MRI is an excellent diagnostic imaging tool, with accuracy of as high as 95%, compared to arthroscopy, remaining the gold standard. Furthermore, MRI proved useful, on the basis of its high negative predictive value, to avoid unnecessary arthroscopy and hospitalization, morbidity, and waste of limited financial and manpower resources.

However, radiologists must be aware of numerous pitfalls simulating a meniscal tear. Furthermore, MRI pictures contain many details with an uncertain clinical relevance, delineating the need to correlate MRI with clinical findings in order to plan treatment optimally.

Things to Remember

1. Meniscal tears are the most common cause of knee pain and instability in athletes.
2. Symptoms and clinical findings are usually non-specific and must be regarded as of little value in making the correct diagnosis.
3. MRI has replaced other imaging techniques for diagnosis of meniscal tears. MR criteria for classifying meniscal tears have been clearly described. In addition to diagnosing meniscal tears, the radiologist should describe the features of each meniscal tear that may affect treatment.
4. As the long term protective effect of the menisci on the joint surfaces has been well documented, meniscal preservation should be the goal of treatment. Stability, location and type of meniscal tear are essential in deciding whether to repair, resect or leave alone a meniscal lesion. Allograft replacement is an evolving technique and the role of MRI in patients who have undergone meniscal transplantation still requires clarification.

References

Applegate GR, Flannigan BD, Tolin BS et al. (1993) MR diagnosis of recurrent tears in the knee: value of intra-articular contrast material. AJR Am J Roentgenol 161:821

Aydingöz Ü, Firat AK, Atay ÖA et al. (2003) MR imaging of meniscal bucket-handle tears: a review of signs and their relation to arthroscopic classification. Eur Radiol 13:618–625

Baker BE, Peckham AC, Pupparo F et al. (1985) Review of meniscal injury and associated sports. Am J Sports Med 13:1–4

Biedert RM (1993) Intrasubstance meniscal tears. Arch Orthop Trauma Surg 112:142–147

Bikkina RS, Tujo CA, Schraner AB et al. (2005) The "floating" meniscus: MRI in knee trauma and implications for surgery. AJR Am J Roentgenol 184:200–204

Costa CR, Morrison WB, Carrino JA (2004) Medial meniscus extrusion on knee MRI: is extent associated with severity of degeneration or type of tear? AJR Am J Roentgenol 183:17–23

Cothran RL, Major NM, Helms CA et al. (2001) MR imaging of meniscal contusion in the knee. AJR Am J Roentgenol 177:1189–1192

Dandy DJ (1990) The arthroscopic anatomy of symptomatic meniscal lesions. J Bone Joint Surg Br 72:628–633

De Smet AA, Asinger DA, Johnson RL (2001) Abnormal superior popliteomeniscal fascicle and posterior pericapsular edema: Indirect MR imaging signs of a lateral meniscal tear. AJR Am J Roentgenol 176:63–66

De Smet AA, Graf BK (1994) Meniscal tears missed on MR imaging: relationship to meniscal tear patterns and anterior cruciate ligament tear. AJR Am J Roentgenol 162:905–911

De Smet AA, Norris MA, Yandow DR et al. (1993) MR diagnosis of meniscal tears of the knee: Importance of high signal in the meniscus that extends to the surface. AJR Am J Roentgenol 161:101–107

De Smet AA, Tuite MJ, Norris MA et al. (1994) MR diagnosis of meniscal tears: analysis of causes of errors. AJR Am J Roentgenol 163:1419–1423

Elvenes J, Jerome CP, Reikeras O et al. (2000) Magnetic resonance imaging as a screening procedure to avoid arthroscopy for meniscal tears. Arch Orthop Trauma Surg 120:14–16

Farley TE, Howell SM, Love KF et al. (1991) Meniscal tears: MR and arthrographic findings after arthroscopic repair. Radiology 180:517–522

George J, Saw KY, Ramlan AA et al. (2000) Radiological classification of meniscocapsular tears of the anterolateral portion of the lateral meniscus in the knee. Australas Radiol 44:19–22

Greis PE, Bardana DD, Holmstrom MC et al. (2002) Meniscal injury: basic science and evaluation. J Am Acad Orthop Surg 10:168–176

Hantes ME, Zachos VC, Zibis AH et al. (2004) Evaluation of meniscal repair with serial magnetic resonance imaging: a comparative study between conventional MRI and indirect MR arthrography. Eur J Radiol 50:231–237

Hayes CW, Brigido MK, Jamadar DA et al. (2000) Mechanism-based pattern approach to classification of complex injuries of the knee depicted at MR imaging. Radiographics 20:S121–S134

Justice WW, Quinn SF (1995) Error patterns in the MR imaging evaluation of menisci of the knee. Radiology 196:617–621

Karachalios T, Hantes M, Zibis AH et al. (2005) Diagnostic accuracy of a new clinical test (the Thessaly test) for early detection of meniscal tears. J Bone Joint Surg 87:955–962

Kelly MA, Flock TJ, Kimmel JA et al. (1991) MR imaging of the knee: clarification of its role. Arthroscopy 7:78–85

Kidron A, Thein R (2002) Radial tears associated with cleavage tears of the medial meniscus in athletes. Arthroscopy 3:254–256

Ludman CN, Hough DO, Cooper TG et al. (1999) Silent meniscal abnormalities in athletes: magnetic resonance imaging of asymptomatic competitive gymnasts. Br J Sports Med 33:414–416

Magee T, Shapiro M, Rodriguez J et al. (2003) MR arthrography of postoperative knee: for which patients is it useful? Radiology 229:159–163

Magee T, Shapiro M, Williams D (2004) Prevalence of meniscal radial tears of the knee revealed by MRI after surgery. AJR Am J Roentgenol 182:931–936

Matava MJ, Eck K, Totty W et al. (1999) Magnetic resonance imaging as a tool to predict meniscal reparability. Am J Sports Med 27:436–443

McCauley TR (2005) MR imaging evaluation of the postoperative knee. Radiology 234:53–61

Miller MD (2004) What's new in sports medicine? J Bone Joint Surg (Am) 86:653–661

Muller W (1983) The knee. Springer, New York

Muscolo DL, Ayerza MA, Makino A et al. (2003) Tumors about the knee misdiagnosed as athletic injuries. J Bone Joint Surg 85:1209–1214

Rangger C, Klestil T, Kathrein A et al. (1996) Influence of magnetic resonance imaging on indications for arthroscopy of the knee. Clin Orthop 330:133–142

Rath E, Richmond JC (2000) The menisci: basic science and advances in treatment. Br J Sports Med 34:252–257

Rubin DA, Kneeland JB, Listerud J et al. (1994) MR diagnosis of meniscal tears of the knee: value of fast spin-echo vs conventional spin-echo pulse sequences. AJR Am J Roentgenol 162:1131

Sciulli RL, Boutin RD, Brown RR (1999) Evaluation of the postoperative meniscus of the knee: a study comparing conventional arthrography, conventional MR imaging, MR arthrography with iodinated contrast material, and MR arthrography with gadolinium-based contrast material. Skeletal Radiol 28:508–514

Shellock FG, Deutsch AL, Mink JH et al. (1991) Do asymptomatic marathon runners have an increased prevalence of meniscal abnormalities? An MR study of the knee in 23 volunteers. AJR Am J Roentgenol 157:1239

Shoemaker SC, Markolf KL (1986) The role of the meniscus in the anterior-posterior stability of the loaded anterior cruciate deficient knee: effects of partial versus total excision. J Bone Joint Surg Am 68:71–79

Stoller DW, Martin C, Crues JV III et al. (1987) Meniscal tears: pathological correlation with MR imaging. Radiology 163:452

Tarhan NC, Chung CB, Mohana-Borges AV et al. (2004) Meniscal tears: role of axial MRI alone and in combination with other imaging planes. AJR Am J Roentgenol 183:9–15

Vande Berg BC, Lecouvet FE, Poilvache P et al. (2000) Dual-detector spiral CT arthrography of the knee: accuracy for detection of meniscal abnormalities and unstable meniscal tears. Radiology 216:851–857

Voloshin AS, Wosk J (1983) Shock absorption of meniscectomized and painful knees: a comparative in-vivo study. J Biomed Eng 5:157–161

Watanabe M, Takeda S (1974) Arthroscopy of the knee joint. In: Helfet J (ed) Disorders of the knee. JB Lippincot, Philadelphia, pp 145–159

Weiss CB, Lundberg M, Hamberg P et al. (1989) Non-operative treatment of meniscal tears. J Bone Joint Surg Am 71:811–822

White LM, Schweitzer ME, Weishaupt D et al. (2000) Prospective evaluation of conventional MR imaging, indirect MR arthrography, and direct MR arthrography in the diagnosis of recurrent meniscal tears. Radiology 217:575

Wright DH, De Smet AA, Norris M (1995) Bucket-handle tears of the medial and lateral menisci of the knee: value of MR imaging in detecting displaced fragments. AJR Am J Roentgenol 165:621–625

Knee: Ligaments

17

Eugene G. McNally

CONTENTS

Box 17.1. Plain Radiography/CT

- Plain radiographs have little role in most sporting injuries
- They are indicated if there has been a significant impact injury
- Occasionally positive findings can be demonstrated in anterior cruciate ligament disruption., with depression of the lateral femoral notch, tibial translation and the Segond fracture
- Lipohaemarthrosis implies a fracture in most cases, however occasionally significant synovial disruption can cause this finding
- CT is generally required to categorise fractures of the tibia plateau

Box 17.2. Ultrasound

- Ultrasound plays a subsidiary role to magnetic resonance imaging in many knee injuries. If the patient's symptoms are located in the anterior joint, and are focal, then ultrasound can reliably assess the quadriceps and patellar tendons
- The collateral ligaments are also easy to see using ultrasound, however injuries to these structures are frequently associated with internal derangement and consequently MRI is necessary to demonstrate the full spectrum of injury

Box 17.3. MRI

- Magnetic resonance imaging is indicated early in the diagnosis and management of athletes with internal derangement of the knee
- In the acutely locked knee, MRI can distinguish between mechanical and nonmechanical causes of locking. Nonmechanical causes are present in between 40 and 50% of patients, and are usually due to a significant injury to the medial collateral ligament
- Mechanical causes include bucket handle tears of the meniscal way, loose bodies and impinging anterior cruciate ligament stumps

E. G. McNally, MD
Consultant Musculoskeletal Radiologist, Dept. of Radiology, Nuffield Orthopaedic Centre, NHS Trust, Windmill Road, Headington, Oxford OX3 7LD, UK

17.1 Introduction

This chapter will be divided into two main parts, the intra-articular ligaments and extra-articular ligaments of the knee. This division is important as the extra-articular ligaments are not visible on routine arthroscopic procedures and consequently MRI plays a most important role in their evaluation.

17.2 Intra-articular Ligaments

The principle intra-articular ligaments are the anterior cruciate and posterior cruciate ligaments. Minor ligaments including the anterior intermeniscal ligaments, the posterior intermeniscal ligament, the meniscofemoral ligament, the oblique intermeniscal ligament and the infrapatellar plica.

17.2.1 The Anterior Cruciate

17.2.1.1 Anatomy

The anterior cruciate ligament (ACL) runs from a semicircular origin on the medial aspect of the lateral femoral condyle, in a spiral course forwards and laterally to a fan shaped insertion on the anterior tibial eminence. In its proximal portion it runs parallel to the intercondylar roof. It is composed of a number of collagen fibre bundles which are organised into two principle bundles. The largest of these, the anteromedial bundle, comprises densely packed fibres compared with the more loosely packed posterolateral bundle. The anteromedial band becomes taut in flexion, when most of the ligament is relaxed. In extension, the larger, posterolateral portion is under tension (Remer et al. 1992). The attachment sites are like other entheses, with a transitional zone of fibrous and mineralized cartilage. The ligament is enclosed in a fibro connective tissue sheath which also contains a little fluid. The size of the ACL averages 4 cm long and 1 cm thick, but differs between the sexes, being slightly smaller in women. The femoral notch is also correspondingly smaller and these findings may account for the differences between the sexes in the incidence of ACL injury (Charlton et al. 2002). Neurovascular supply to the ACL is from the lateral geniculate artery and tibial nerve branches respectively.

17.2.1.2 Imaging

On most sequences the anterior cruciate ligament is easily identified as a structure of low signal intensity (Fig. 17.1). The anteromedial bundle is best depicted on sagittal sections, where the taut ACL shows as a hypointense line which can be traced from origin to close to the insertion on the tibia. In the insertional area, the fibres of the anteromedial bundle spread out and may therefore become poorly defined as the space between them is filled with fluid, fat or connective tissue. This apparent loss of conspicuity of the ligament should not be misinterpreted as an insertional tear. The posterolateral bundle is more poorly defined but can be identified as a number of strands separated by fluid and connective tissue. A number of variants in the normal appearance can be identified. Occasionally linear confluence of fluid can be seen separating the fibre bundles (Fig. 17.2). This is particularly evident on gradient echo. In children the lower third of the ligament in particular can be

Fig. 17.1. Normal ACL. Sagittal fat suppressed proton density MR image. Note the hypointense line representing the anteromedial bundle (*arrow*). The fibres spread out as they approach the tibial insertion (*arrowhead*)

Fig. 17.2. Normal ACL. Sagittal fat suppressed proton density MR image showing prominent fluid lines between fibres (*arrow*)

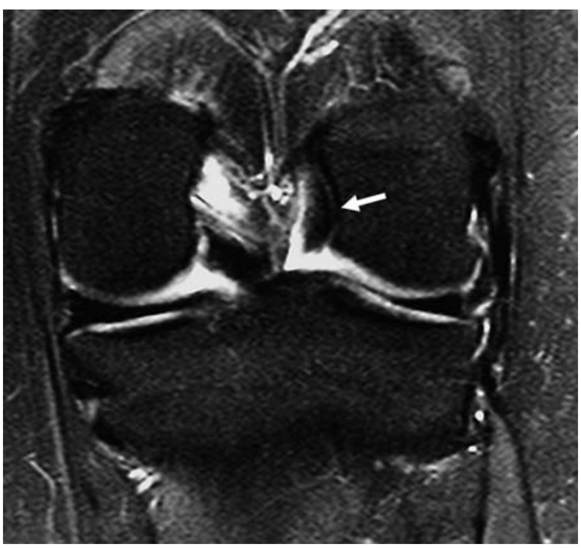

Fig. 17.3. Normal ACL. Coronal fat suppressed proton density MR image demonstrating the origin of the ACL from the medial aspect of the lateral condyle (*arrow*)

poorly defined. Indeed in very young children the anteromedial bundle in its entirety may be poorly demarcated making interpretation of anterior cruciate ligament rupture more difficult. Fortunately, in children it is a rare injury and when it occurs it is usually an avulsion injury from the tibial insertion.

A minimum slice thickness of 4 mm is recommended to ensure that the ligament is properly seen. Orientation of images along the axis of the ACL can be helpful. The anterolateral margin of the lateral femoral condyle can be used as a guide. In practice, with 3- to 4-mm slices on modern imaging equipment, angulation is rarely necessary, though is useful to show the anterior cruciate in a single slice. Sagittal images can be supported by coronal and axial sections (Fig. 17.3). These can be particularly helpful in providing alternative visualisation of the femoral origin which can sometimes be difficult to depict on sagittal images.

17.2.1.3
Injuries to the Anterior Cruciate

Sports injuries account for a high proportion of injuries to the ACL. The injury can occur by a variety of mechanisms but most frequently occurs with tibial internal rotation and abduction. It is an especially common skiing injury, where two main mechanisms cause ACL rupture, valgus-external rotation and flexion-internal rotation. The latter is more common in women and older skiers (Jarvinen et al. 1994). Valgus results in distraction of the medial joint compartment and impaction of the lateral femoral condyle with the lateral tibia plateau. There is a 6% five-year incidence of ACL rupture in professional soccer players (Pereira et al. 2003), 4% of Australian rules football (Gabbe and Finch 2001) and 2% of American footballers in the NFL (Bradley et al. 2002). The rate is likely to be higher in semi professional and amateur players.

Typically the patient will describe an instantaneous moment of injury, where indeed an audible “pop” may be heard. This is followed by slow onset haemarthrosis occurring 2–3 h after the event. The delay is due to a slow drip from the investing blood vessels. Signs of ACL rupture are divided into primary (those that directly depict the tear) and secondary signs. Subsequent sections will describe the primary imaging findings in complete ACL rupture, changes that might suggest partial rupture, secondary signs of ACL rupture as well as their usefulness and associated injuries.

17.2.1.3.1
Primary Signs of ACL Rupture

The principle finding in acute anterior cruciate ligament rupture on sagittal orientated MR images is failure to identify the normal hypointense low signal line of the anteromedial bundle (Fig. 17.4). After injury, the ligament fibres are grossly disrupted and separated by haemorrhage and edema such that it is often difficult to identify whether the injury involves the proximal, distal or midsubstance of the ligament. Less commonly the anterior cruciate ligament may displace anteriorly within the notch and present as an inability to fully extend the knee. This locked knee presentation may mimic a bucket handle tear of the meniscus. Huang et al. (2002) have described he appearance of the entrapped ACL stump as being of two types. The more common Type 1 stump appeared as a nodular mass located in the anterior recess of the joint. Type 2 stumps had a tongue like fold of ACL displacing out of the intercondylar notch into the anterior joint recess. Most often, it is often difficult to identify a displaced anterior cruciate ligament stump as the cause of impingement and should be considered in cases of knee locking where a displaced meniscal tear is not identified. The differential diagnosis on the locked knee in the absence of a displaced bucket handle tear also includes injury to other ligaments, particularly a tear of the medial collateral ligament, leading to muscle spasm and pseudo locking. Osteochondral fragment impingement should also be considered particularly if there is a suspicion of reduced patellar dislocation. Care should be taken not to confuse a prominent oblique intermeniscal ligament for a torn anterior cruciate ligament.

In more chronic stages, the torn anterior cruciate ligament can undergo complete atrophy such that no remnant of the ligament is visible. In other cases, as the edema and haemorrhage settle the torn ligament may reappear, having fallen to the floor of the intercondylar groove (Fig. 17. 5).

Fig. 17.4. Acute ACL rupture. Sagittal fat suppressed proton density MR image. The ACL is torn proximally (*arrow*) and assumes a lax wavy configuration (*arrowhead*)

Fig. 17.5. Chronic ACL rupture. Sagittal fat suppressed proton density MR image. The torn ACL has a horizontal configuration along the floor of the joint (*arrow*)

17.2.1.3.2
Secondary Signs

The primary signs described above carry strong predictive values for ACL rupture. When the primary signs of non-visualisation of fibre bundles or focal disruption and intrinsic edema are also applied to coronal and axial images, the diagnosis can usually be established (Fig. 17.6). A variety of secondary signs of anterior cruciate ligament disruption have been

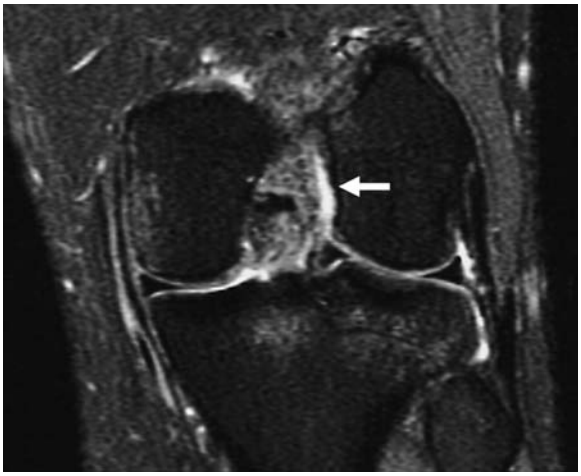

Fig. 17.6. ACL rupture. Coronal fat suppressed proton density MR image. There is a bare area at the femoral origin of the ACL (*arrow*) compare with (Fig. 17.3)

described. In the majority of cases, the primary signs have a reliability such that the secondary signs are rarely if ever of practical value. They may however be helpful in differentiating a partial or low-grade tear from a complete or high grade injury. Secondary signs of anterior cruciate ligament rupture can be divided into three groups 1) those that involve a bony injury, 2) those reflecting soft tissue injury and 3) those that reflect anterior tibial translation.

Secondary Signs: Bone Injury

Three separate bony injuries are associated with ACL rupture. The most common of these is microfracture of the posterior and lateral margin of the tibial plateau (Fig. 17.7). Indeed if this typical pattern of microfracture is identified, the patient should be regarded as having a torn anterior cruciate ligament until this can be firmly proven otherwise. It should be remembered that microfracture is more usually encountered in the acute phase following injury, although the finding can persist for many months. Posterolateral tibial microfracture may be associated with lateral femoral condylar microfracture in a proportion of patients. In a series reported by Kaplan et al. (1992) occult fractures were isolated in 43% of ACL ruptures and were present in combination with the lateral femoral condyle microfracture in 46%. Less common patterns were fractures in the posterior aspect of the medial tibial plateau in 7% and fractures involving all three areas in 2% (Kaplan et al. 1992). In a study of 32 patients, Murphy et al. found this pattern of posterolateral microfracture in 94% and an associated 'kissing' femoral lesion in 91% (Murphy et al. 1992). Differences in the nature of the injury therefore can cause differing presentations. Occasionally this bone injury associated with ACL rupture can been seen on the plain radiograph (Stallenberg et al. 1993).

Another common pattern is a compression injury to the anterior aspect of the lateral femoral condyle, which causes deepening of the femoral notch and injury to the overlying articular cartilage. The compression fracture is easily seen in fat suppressed MR images (Fig. 17.8). There is also a plain radiographic correlate to this injury, deepening of the femoral notch by more than 1.5 mm on a lateral plain film is strongly associated with ACL rupture (Cobby et al. 1992).

Less common are bony injuries to the posteromedial tibia (Chan KK et al. 1999) with avulsion of the central slip of semimembranosis from the infra glenoid tubercle. Whether this is a true avulsion due to external rotation (Yao and Lee 1989) or impaction as a result of anterior subluxation of the medial tibia

Fig. 17.7. Secondary bone bruise associated with ACL rupture. Coronal fat suppressed proton density MR image. Typical location of tibial microfracture posterolaterally (*arrow*). There is also bone bruise at the posteromedial corner (*arrowhead*): see text for explanation

Fig. 17.8. Secondary bone bruise associated with ACL rupture. Sagittal fat suppressed proton density MR image. Lateral condylar microfracture (*arrow*)

during varus and external rotation (Vanek 1994) is debated. The latter has been shown to occur experimentally, but the tell tale impaction injury that might be expected in the medial femoral condyle is not always present.

The Segond fracture (Fig. 17.9) is an avulsion fracture of the anterolateral margin of the proximal tibial plateau, originally described by a French surgeon Paul Ferdinand Segond (Segond 1879). This is a tiny avulsion flake vertically orientated on the posterolateral aspect of the tibia at the site of attachment of the lateral capsular ligament. The Segond fracture results from internal rotation and varus stress on the ligament resulting in avulsion. Although uncommon, there is a very high association with ACL rupture.

Secondary Signs: Soft Tissue

In the acute phase of injury, haemorrhage and edema result in non-visualisation of the ligament, the typical primary sign. In more chronic injuries, the torn ligament reappears as the acute haemorrhage and edema settles. In many cases it lies in a clearly abnormal position along the floor of the joint, in others it can reattach to the femur or PCL and simulate a normal ligament. In these cases, evaluation of the ACL or Blumensaats angle can help diagnose a tear.

ACL Angle

The ACL angle is the angle formed by the intersection of the anterior aspect of the distal portion of the ACL and the most anterior aspect of the intercondylar eminence on a mid-sagittal MRI image. The normal angle lies between 53 and 56° (Gentili et al. 1994; Murao et al. 1998; Mellado et al. 2004). An angle of less than 45° is regarded as abnormal and indicative of a torn ACL. Sensitivity and specificity increase with decreasing angle, reaching 100% at angles less than 25° (Mellado et al. 2004).

Blumensaats Angle

The Blumensaats angle is formed by the anterior aspect of the distal portion of the ACL and the intercondylar roof. By convention angles with proximal vortices are considered negative and those with distal vortices positive. As the ACL usually parallels Blumensaats line, the angle is normally zero or up to 8° negative (Gentili et al. 1994; Lee K et al. 1999; Mellado et al. 2004). An angle over 21° positive is strongly associated with ACL rupture.

Secondary Signs: Anterior Tibial Translation

An intact anterior cruciate ligament prevents forward displacement of the tibia with respect to the femur. When disrupted, tibial translation is free to

Fig. 19.9. Segond fracture. Plain radiograph demonstrating a vertically oriented avulsion flake fracture at the lateral proximal tibia

occur, though it is not seen in all patients. It is less likely to occur in sporting injuries, where there is good muscle tone, particularly when the posterior portions of the menisci remains intact. In these cases, the meniscus abuts the posterior aspect of the femoral condyle and prevents anterior translation. When the tibia translates anteriorly the configuration of other structures changes, and it is these changes that are used as secondary signs. Signs of anterior tibial translation include the PCL line sign, the PCL angle sign, the PCL curvature ratio, the femoral line sign, straight FCL sign and the lateral condylar tangent.

The PCL Line Sign

On sagittal images, the posterior cruciate ligament assumes a sigmoid appearance caused by forward movement of its tibial insertion with respect to the femoral insertion. This is readily apparent on visual inspection, but several measures of this PCL laxity have been described. A line drawn connecting two points outlining a linear region in the distal portion of the PCL when traced proximally should intersect the medullary cavity within 5 cm of its distal aspect (Schweitzer et al. 1992). The sign is positive when the proximally extended line does not intersect the medullary cavity of the femur (Fig. 17.10). The reason for this becomes obvious when the line is drawn along the buckled PCL.

Fig. 17.10. Anterior tibial translation as secondary sign of ACL rupture. Sagittal fat suppressed proton density MR image. A line drawn along the posterior margin of the PCL does not intersect femoral medulla within 5 cm

The PCL Angle Sign

As the PCL buckles during anterior tibial translation, the angle between the proximal and distal portion becomes more acute. Under normal circumstances the angle is greater than 115° and usually greater than 125. This angle becomes more acute when the tibia has translated anteriorly (Fig. 17.11). Maximum angles between 96 and 111° have been described in ACL rupture. The variation in these findings probably reflecting the variation in anterior tibial translation that will be present in the study populations (Gentili et al. 1994; McCauley et al. 1994; Lee K et al. 1999).

Fig. 17.11. Anterior tibial translation as secondary sign of ACL rupture. Sagittal fat suppressed proton density MR image. The angle between the proximal and distal limbs of the PCL become more acute when there is tibial translation

Lateral Condyle Tangent

A further useful method of assessing for anterior tibial translation is to measure it directly. A tangent is drawn at the most posterior point of the lateral femoral condyle to form the baseline from which the tibial translation will be measured (Chan WP et al. 1994). The section midway between the cortex adjacent to the posterior cruciate ligament

and the most lateral section containing the femoral condyle is used. Under normal circumstances the posterior margin of the tibial plateau passes within 5 mm of this line (Fig. 17.12). A distance of greater than 5 mm separating the posterior margin of the tibial plateau from this line indicates anterior tibial translation.

Fig. 17.12. Anterior tibial translation as secondary sign of ACL rupture. Sagittal fat suppressed proton density MR image. A line drawn tangential to the lateral femoral condyle passes more than 5 mm. from the posterior tibial margin

Posterior Femoral Line

The sign is positive when a line drawn at 45° from the posterosuperior corner of the Blumensaats line, fails to intersect the flat portion of the proximal tibial surface or within 5 mm of its posterior margin (Robertson et al. 1994).

Straight LCL

The lateral collateral ligament runs in an oblique coronal plane from its insertion on the lateral femoral condyle to the head of the fibula. On orthogonal coronal slices, the course of the ligament has to be traced to a series of adjacent slices, reflecting its oblique course. As the tibia translates anteriorly, the ligament is brought into a true coronal plane and can therefore be visualised on a single coronal slice.

PCL Curvature

The bowstringing that occurs as the PCL buckles has also been quantified by Siwinski (Siwinski and Ziemianski 1998) and Tung (Tung et al. 1993). The longest perpendicular is dropped from the PCL to a line drawn from the origin to insertion (the string of the bow). The ratio of the perpendicular to the 'string' is calculated. The more the PCL is buckled, the larger this ratio becomes and values over 0.39 have a high specificity for ACL rupture.

Other signs that have been described include: the posterior synovial bulge sign irregular anterior margin of the ACL, rupture of the iliotibial band, severe buckling of the patella tendon, shearing injury of Hoffa's fat pad and posterior displacement of lateral meniscus(Lee JK et al. 1988; Weber et al. 1991; Remer et al. 1992; Schweitzer et al. 1993; Robertson et al. 1994).

17.2.1.3.3
Partial ACL Rupture

In the majority of cases the presence of an intact anteromedial bundle confirms an intact anterior cruciate ligament and its absence is a reliable sign of rupture. The diagnosis of partial anterior cruciate ligament rupture can be more problematic. The reported signs are neither as sensitive nor as specific as those indicating complete rupture. Focal areas of loss of signal, other than close to the insertion, kinks, buckles or loss of parallelism between the ligament and the intercondylar roof should all be regarded with suspicion.

In a study of 13 patients with arthroscopically proven partial ACL tear and using criteria which included abnormal intrasubstance signal, bowing of the ACL, or non-visualisation of the ACL on one MR imaging sequence with visualization of intact fibres on other, in the absence of findings of complete ACL tear, the sensitivity of MR ranged from 0.40 to 0.75, and the specificity ranged from 0.62 to 0.89 (Umans et al. 1995). Lawrance et al. (1996) in a retrospective review proposed four features which helped to differentiate partial ACL tears from either complete ACL fears or normal ligaments. These were the appearance of some intact fibres, thinning of the ligament, a wavy or curved ligament and the presence of an inhomogeneous mass posterolateral to the ACL (Lawrance et al. 1996). These have not been tested prospectively.

In the presence of such findings, it is important to seek the secondary signs, both those of bony injury and anterior tibial translation. If secondary signs are

present they are likely to indicate a high-grade tear. In the absence of secondary signs the diagnosis is more circumspect. Clinical correlation, particularly the presence of an anterior draw sign can be helpful in identifying a significant ACL injury. Many clinicians regard a partial anterior cruciate ligament with less clinical concern if the knee is stable clinically. It is therefore more helpful for the radiologist to attempt to differentiate stable from unstable tears, rather than partial from normal/complete tears. Signs of anterior tibial translation as outlined above are likely to be indicators of an unstable tear. Roychowdhury et al. (1997) used axial images to try to differentiate stable from unstable knees. Stable ACLs were described as elliptical, attenuated or showing areas of increased intrasubstance signal intensity. Unstable ligaments showed an isolated ACL bundle, nonvisualisation of the ligament or a cloudlike mass in place of the ACL. The latter are more typical of primary signs. Despite these difficulties, a combination of clinical and MRI findings are usually sufficient to allow the correct choice of management.

17.2.1.4 Associated Injuries

Rupture of the anterior cruciate ligament is commonly associated with injuries to other structures of the knee. The associated bony contusions have been outlined above, the pattern and prevalence of associated soft tissue injuries varies, dependent on the nature of the injury (e.g., type of sport) and the age of the patient. Particular care should be taken to exclude an associated meniscal tear, which will be present in up to 70% of cases. Overall lateral meniscal tears are more common, Duncan et al. (1995) found a significantly greater preponderance of lateral meniscal tears in patients undergoing ACL reconstruction following alpine skiing injuries, where the lateral meniscus was affected in 83% of cases. Conversely, in children Prince et al. (2005) found meniscal tears occurring in 37% of patients with ACL rupture, two-thirds of which were medial. Meniscal tear patterns that are typically associated with ACL rupture include a vertical tear of the meniscal periphery and a radial tear involving the posterior portion or meniscal attachment. Particular attention should therefore be paid to the posterior thirds of the menisci especially the lateral (De Smet and Graf 1994).

From the nature of the injury anterior cruciate ligament ruptures are also associated with valgus sprain, hence tears of the medial collateral ligament are not infrequently associated. The combination of anterior cruciate ligament rupture, medial meniscal tear and medial collateral ligament injury is sometimes referred to as the “O’Donoghues” or “Sorry” triad. A tetrad has also been described, with the additional finding of trabecular microfracture. Although well known amongst radiologists, the triad is relatively uncommon. Shelbourne divided patients with ACL rupture and MCL tear according to the grade of MCL injury. Patients with Grade 2 MCL injury had more medial meniscus tears than Grade 3 or completely rupture MCL. Lateral meniscal tears were more common in both groups, and in the Grade 2 MCL group, medial meniscal injuries were always associated with lateral meniscal injury (Shelbourne and Nitz 1991). The MCL was injured in 22% in Prince’s paediatric study group (Prince et al. 2005).

Injuries to the posterolateral corner are well recognised in anterior cruciate ligament injury though there is disagreement on both their incidence and importance. It has been suggested that failure to identify a lax posterolateral corner is the commonest cause of anterior cruciate ligament graft failure, though studies to support this are lacking. Others argue, that only patients who re-present with graft failure undergo detailed assessment of their posterolateral corner and the prevalence of posterolateral deficient knees in successful ACL reconstructed patients remains unknown.

When the radiologist encounters an anterior cruciate ligament rupture, a careful checklist to look for a vertical tear, particularly of the medial meniscus, a radial tear, particularly of the posterior portion of the lateral meniscus and the posterolateral corner should be undertaken.

17.2.1.5 Ganglion Cyst of the Cruciate Ligament

The ability of MRI to depict the internal anatomy of the knee with great detail has led to increased recognition of intra-articular ganglionic cysts (Vanhoenacker 2003; McCarthy and McNally 2004). These are most commonly associated with Hoffa’s fat pad, where they may arise from the intermeniscal ligament. Ganglion cysts are also recognised as arising from the cruciate ligaments. Bui-Mansfield identified cruciate ganglia in 1.3% of a retrospective review of over 1700 knee MRI (Bui Mansfield and Youngberg 1997). The majority were not associated with any other internal derangement. Pain was described as the most common complaint, worse

on activity and sport, but medial joint line tenderness was also described. One quarter gave a history of trauma. Only five (20%) of the patients in this group underwent arthroscopic debridement; four had improved symptoms. On this basis, it is difficult to apply a pattern of symptoms to ACL ganglia or to comment on aetiology, though improved symptoms have been described in other studies following arthroscopic or CT aspiration (Nokes et al. 1994).

ACL ganglia typically have two patterns. One is where the ganglion is interspaced between the fibres of the ACL, distending its sheath with posterior bulging (Fig. 17.13). The fibres of the ACL are easily seen within the sheath, though their course may be deviated by the mucinous material. The second pattern is more cyst like, where the ganglion extends from the ACL sheath, most commonly near its femoral attachment (Fig. 17.14).

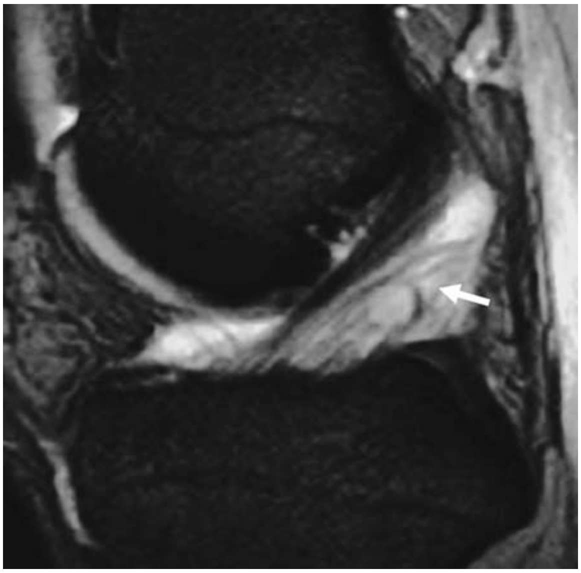

Fig. 17.13. ACL ganglion. Sagittal fat suppressed proton density MR image. The fibres of the ACL are distended and separated by ganglionic material (*arrow*)

Fig. 17.14. ACL ganglion. Sagittal fat suppressed proton density MR image. The ganglioncyst is protruding from the proximal sheath close to the femoral origin (*arrow*)

17.2.2 Posterior Cruciate Ligament

17.2.2.1 Anatomy

The function of the anterior cruciate ligament is balanced by its counterpart, the posterior cruciate ligament (PCL). The PCL courses from the lateral aspect of the medial femoral condyle to its insertion in a depression in the posterior aspect of the intra-articular tibia, approximately 1 cm below the articular surface. The PCL is between 32 and 38 mm in length from origin to insertion and thicker and stronger than the ACL. Its main function is to prevent posterior translation of the tibia. Like the ACL, the PCL made up of spirally arranged collagen fibre bundles. Functionally there are two fibre bundles, an anterolateral (AL) and posteromedial (PM) bundle, named for the anatomical location of the femoral insertion to the tibial insertion (Girgis et al. 1975; Vanhoenacker et al. 2001; Wind et al. 2004). Like the ACL, the two main bundles are taut at different stages in the flexion/extension cycle. The AL bundle tightens in knee flexion and loosens in knee extension. The PM bundle tightens in knee extension and is lax in knee flexion (Girgis et al. 1975). The PCL is also intracapsular but extrasynovial. It appears darker and more uniform than the ACL due to the presence of a tighter stronger investing sheath (Fig. 17.15). The anterolateral and posteromedial bundles are less well

Fig. 17.15. Normal PCL. Sagittal fat suppressed proton density MR image. Note the slight heterogeneity at the femoral insertion which may relate to magic angle (*arrow*)

separated and may be difficult to make out on routine MR sequences. It takes considerably more force to rupture the posterior cruciate ligaments that it does the anterior. It has a more abundant blood supply than ACL.

17.2.2.2 Imaging

Once again sagittal images are the mainstay for diagnosis. Spin echo provide the most homogenous depiction. T2 weighted or proton density images, preferably with fat saturation, are best. Internal signal changes seen only on T1 weighted images are non specific and may not indicate a tear (Grover et al. 1990). Some variation in signal can be encountered in the proximal third especially on gradient echo sequences. A variety of explanations have been offered for this most likely it represents a form of magic angle phenomenon. A number of apparent focal thickenings may be identified in the region of the middle third of the ligament. This is usually due to section through prominent meniscofemoral ligaments which will be discussed later in this section.

17.2.2.3 Posterior Cruciate Ligament Injury

The force required to disrupt the PCL is larger than the ACL, consequently knee injuries resulting in PCL tears are most often in combination with other ligamentous injuries. The incidence of these combined injuries varies between 80 and 95% of PCL injuries, which themselves vary from 1% to 44% of all acute knee injuries (Shelbourne et al. 1999). Of all patients with knee haemarthrosis, 37% have an associated PCL injury (Fanelli 1993). Injuries occur more frequently in contact sports and those involving high-contact forces. Not all are symptomatic, Parolie found a 2% incidence of PCL injury among asymptomatic college football players at the NFL predraft examinations (Parolie and Bergfeld 1986). The mechanism of PCL injury in the athlete is most commonly a fall on the flexed knee with a plantar flexed foot and hyperflexion of the knee (Wind et al. 2004). Dashboard injuries account for another high proportion of PCL injuries, where the flexed knee is impacted and the tibia forced posteriorly. When this force is combined with a varus or rotational component, the lateral or posterolateral structures may also be injured. Hyperextension injuries also occur, these are associated with a higher incidence of avulsion injuries.

MRI plays an important role in the assessment of PCL injuries. This is because not all are apparent on clinical examination, even under general anaesthesia (Grover et al. 1990) and at arthroscopy the PCL can be difficult to identify in the presence of an intact ACL (Grover et al. 1990) or meniscofemoral ligament. Furthermore, untreated lesions may predispose to early onset osteoarthritis (Cross and Powell 1984) and extensor mechanism failure.

Signs of a complete PCL tear include non-visualisation of the ligament with or without an haemorrhagic or edematous mass (Fig. 17.16). Discrete tears are identified more commonly than with ACL rupture. This is thought to be due to the tighter synovial sheath within which the ligament is invested. Tears are most commonly intrasubstance (Grover et al. 1990; Sonin et al. 1994; Mair et al. 2004). The incidence of distal vs proximal injuries is more variable reported. In Sonins group of 71 patients, 27% were proximal and only 3% distal. In contrast, Grover found distal avulsions three times more common than proximal, though the number of patients was much smaller in this study group (Grover et al. 1990). In a more recent study of 35 high grade PCL tears, Mair also

Fig. 17.16. Gross disruption of the PCL (*arrow*) following anterior impact injury with tibial microfracture (*open arrow*) and haemarthrosis (*arrowhead*) on a sagittal gradient echo image. The microfracture is dark due to susceptibility artefact

found tibial avulsions to be more common than femoral (Mair et al. 2004). The criteria for partial tear is less well defined, Sonin suggests that the presence of abnormal signal intensity within the substance of the PCL or a combination of intact and disrupted as signs of a partial tear (Sonin et al. 1995).

PCL injuries are isolated in about a quarter of cases (Sonin et al. 1994) with associated meniscal tears in 25–50%, medial slightly more than lateral and ligamentous injuries in 40%, most commonly ACL in a quarter and MCL in a fifth. Posterolateral corner injuries are present in approximately half of PCL injuries, but two-thirds of these will be minor with edema around the capsule, no discernable structural abnormality and a stable knee to examination (Mair et al. 2004).

The incidence of bony injury has also been variously reported, with more recent studies identifying a higher incidence, possibly reflecting improved detection. Sonin identified microfracture in 35% (Sonin et al. 1994), whereas the incidence in Mairs group was 83% (Mair et al. 2004). Of these 29 patients with microfracture, 16 were in the lateral tibial plateau, 10 lateral femoral condyle, 14 medial tibial plateau, 5 medial femoral condyle, and 4 patella. Patients with medial bone bruises were more likely to have posterolateral ligamentous injuries and patients with lateral bone bruises were more likely to have MCL injuries.

17.2.3 Minor Intracapsular Ligaments

There is a large number of minor ligaments that lie within the joint. Although the function of these ligaments is incompletely understood, from a radiological perspective disruption rarely imparts clinically significant instability. Their impact on imaging therefore is mainly that they mimic other pathology when enlarged or prominent and can thus lead to difficulties in interpretation.

17.2.3.1 Intermeniscal Ligaments

There are three intermeniscal ligaments, anterior, posterior and oblique. The anterior ligament runs between the two anterior meniscal horns. Also called the transverse geniculate ligament or anterior transverse ligament, it is 33 mm long and its average midsubstance width is 3.3 mm. (Nelson and LaPrade 2000) (Fig. 17.17). Whilst the attachments were most commonly to the substance of the menisci themselves, some variation is seen and in some cases the ligament attaches to the capsule

Fig. 17.17. The anterior intermeniscal ligament. Sagittal fat suppressed proton density MR image. The ligament is darker and more rounded (*arrow*) than the adjacent anterior horn of the lateral meniscus. It can be followed on serial sagittal images

anterior to the meniscus (Nelson and LaPrade 2000). On MRI, a cord like structure representing the anterior intermeniscal ligament can be identified on most studies. The ligament is generally round or oval shaped and can be quite prominent. The ligaments attaches to the anterior portion of the menisci some distance external to the tip of the horn (Fig. 17.18). As a consequence, a small slither of fluid can gather between the ligament and the meniscus. When the ligament is prominent this can mimic a meniscal tear. The anterior intermeniscal ligament runs at the posterior tip of Hoffa's fat pad, either through the fat or just below it. Hoffa's ganglia which are multiloculated fluid filled structures are most commonly found in this location, indeed the ganglia may arise from degenerative or possibly post traumatic changes to the anterior intermeniscal ligament.

There is also a posterior intermeniscal ligament although this is less prominent than the anterior and is less commonly visualised in its entirety. A further ligament runs in the transverse plane from the posterior horn of the lateral meniscus to the anterior horn of the medial meniscus. This is called the oblique intermeniscal ligament (Fig. 17.19). It separates the posterior cruciate ligament from the anterior cruciate ligament. When it is prominent it can give the impression of additional tissue lying within the notch (Sanders et al. 1999). It therefore

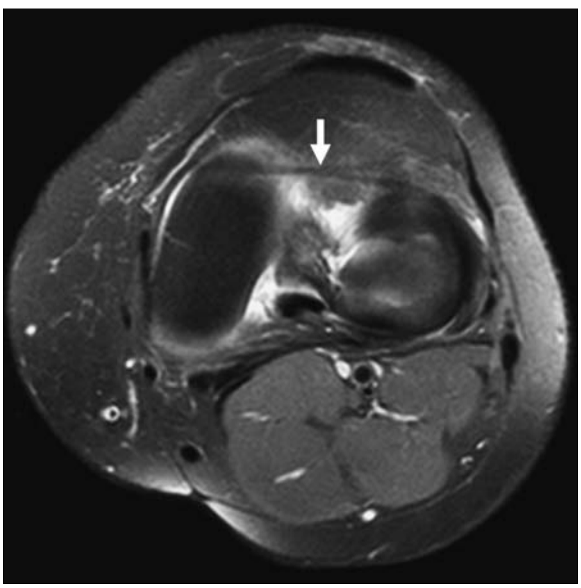

Fig. 17.18. The anterior intermeniscal ligament. Axial fat suppressed proton density MR image. The ligament attaches external to the tips of the anterior horns (*arrow*)

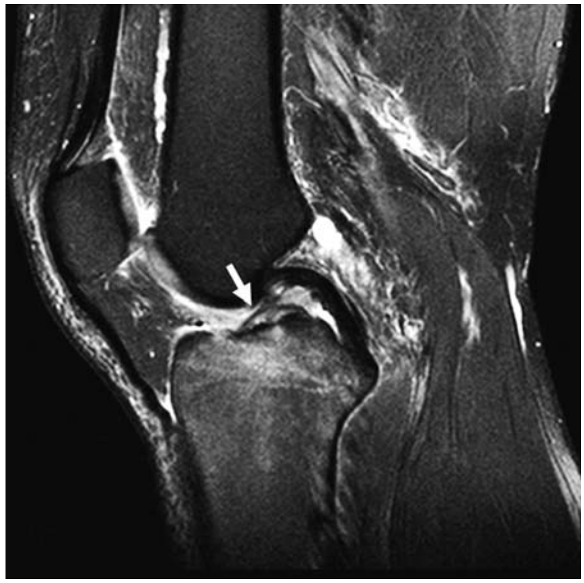

Fig. 17.19. A prominent oblique intermeniscal ligament. Sagittal fat suppressed proton density MR image. The ligament (*arrow*) can mimic a torn ACL, displaced meniscal fragment or an osteochondral loose body lying in the notch

appears on the differential diagnosis of tissue within the notch which includes rupture of the anterior cruciate ligament with the torn ligament lying along the floor of the notch, a displaced meniscal fragment or an osteochondral loose body. Usually these can easily be differentiated. The intact anterior cruciate ligament should be readily apparent, no microfracture or fluid blood levels are apparent to suggest an osteochondral fragment and the anatomical location of the oblique intermeniscal ligament should provide useful clues. Once the diagnosis is considered, the structure can be traced on the workstation or sequential images between the two meniscal horns.

17.2.3.2 The Meniscofemoral Ligament

Close to the attachment of the posterior intermeniscal ligament to the lateral meniscus is a further ligament which runs superiorly and obliquely to the lateral aspect of the medial femoral condyle. The meniscofemoral ligament (MFL) is a prominent intra-articular structure. It has two components either one of which can be dominant. One component runs posterior to the posterior cruciate ligament when it is given the name "ligament of Wrisberg". A second component runs anterior to the PCL whence it is called the "ligament of Hum-

phrey" (Vanhoenacker et al. 2001). There is considerable variation in the size of the MFL. Care must be taken not to mistake an often separated bunch of PCL fibres, which has been termed the oblique PCL (Fig. 17.20), from the MFL (Gupte et al. 2002). They are believed to play a role in protecting the lateral menisci from femorotibial compression by it forward when the knee is flexed (Heller and Langman 1964).

One or other of the MFL will be visualised on over 80% of MR examinations (Grover et al. 1990; Lee BY et al. 2000). Like the intermeniscal ligaments, the principal impact of the MFL is to mimic a tear of the posterior horn of the lateral meniscus. Fluid can gather between a prominent MFL and the meniscus simulating a tear (Fig. 17.21). This is more obvious when the MFL is enlarged. In these cases, it should be appreciated that the posterior horn of the lateral meniscus is approximately the same size as the anterior horn. Were the ligament a tear, this normal morphological rule would be broken. As for the intermeniscal ligaments, tracing the ligament medially to its insertion also confirms its true nature.

Fig. 17.21. Pseudotear of the meniscus due to MFL. Sagittal fat suppressed proton density MR image. MFL attachment to the posterior third of lateral meniscus simulating a tear

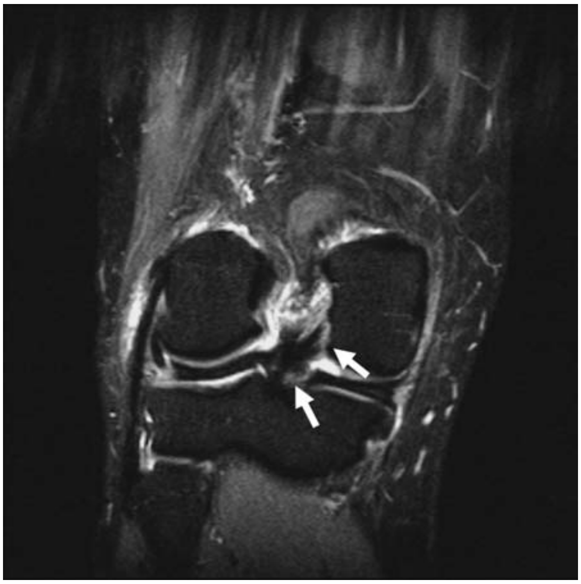

Fig. 17.20. The false MFL or oblique PCL. Coronal fat suppressed proton density MR image. This ligamentous structure (*arrows*) does not arise from the lateral meniscus and in fact is a bundle of PCL fibres rather that another intra-articular ligament

17.2.3.3 Miscellaneous Intra-articular Minor Ligaments

A number of other rarer variants on meniscofemoral attachments have been described. The infrapatellar plica or ligamentum mucosum runs an arcuate course from its posterior femoral attachment just anterior to the ACL, anteriorly and inferiorly to the posteroinferior tip of Hoffa's fat pad, before turning superiorly to approach the lower pole of the patella. When prominent, this ligament has been reported to be misinterpreted as the ACL resulting in a false negative diagnosis for ACL rupture. Anderson identified the rare anterior meniscofemoral ligament (Anderson et al. 2004) whose course matches the posterior portion of infrapatellar plica. A normal infrapatellar plica was found to co-exist with the anterior meniscofemoral ligament in all cases and the attachment of the latter into the medial meniscus was clearly shown to be separate from the infrapatellar plica. An anterior meniscofemoral ligament running from the lateral meniscus to the condylar notch has also been described (Wan and Felle 1995).

17.3 Extra-articular Ligaments

The stability of the knee joint to valgus or varus strain is preserved by the presence of strong ligaments on the medial and lateral aspect of the joint.

17.3.1 The Lateral Stabilisers

On the lateral side ligamentous stability is maintained by two separate ligamentous components. Anteriorly the iliotibial band and posteriorly the fibular collateral ligament/biceps/popliteus complex.

17.3.1.1 The IlioTibial Band

The iliotibial band or tract (ITB) is a condensation of fibrous tissue which extends from the tensor fascia lata at the hip along the entire length of the lateral aspect of the thigh to insert on Gerdy's tubercle on the anterolateral aspect of the tibia. It passes close to the lateral femoral condyle separated from it by a little connective tissue and fat and two layers of synovium lining of the knee joint. In this position, it can impinge against the lateral femoral condyle resulting in iliotibial tract friction syndrome which is also referred to as "runner's knee". Although classically associated with runners, step aerobics and cycling are other reported sporting associations (Holmes et al. 1993). Clinically this presents as an area of tenderness overlying the tract two to three centimetres above the knee joint. Radiologically it is best appreciated on coronal fat suppressed images. Signs include changes within the ligament itself which becomes thickened, and changes within the surrounding soft tissues. The immediate medial and lateral relationship of the iliotibial tract is fat. Consequently increased signal within the fat surrounding the iliotibial band at the level of the lateral femoral condyle should be regarded as a sign of this condition (Fig. 17.22). Care should be taken in ensuring that high signal changes are differentiated from normal joint fluid or knee effusion. According to some authors, frictional bursa formation may occur between the iliotibial tract and the anterolateral aspect of the tibia (Simoens et al. 2002). Treatment by corticosteroid injection has been reported to be effective (Gunter et al. 2004) and modification of training or adjustment to cycling equipment. Rupture of the iliotibial band can occur but is uncommon (Fig. 17.23). These are most commonly seen at the level of the knee joint rather than where friction syndrome occurs.

Fig. 17.22. Iliotibial band friction syndrome (runner knee). Coronal fat suppressed proton density MR image. Increased signal within the fat deep to the ITB (*arrow*)

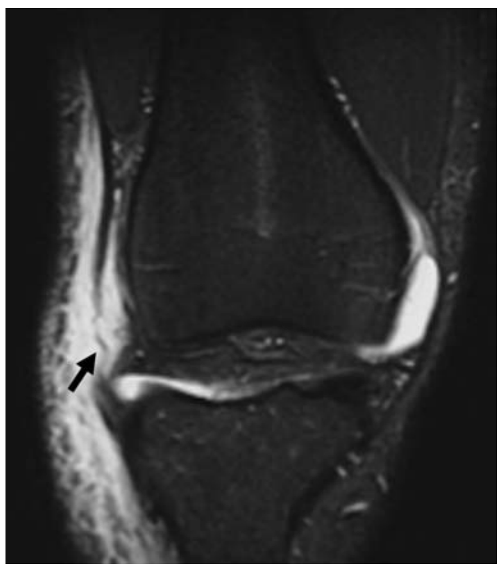

Fig. 17.23. Iliotibial band rupture. Coronal fat suppressed proton density MR image demonstrating rupture of the ITB close to its insertion (*arrow*)

17.3.1.2 Posterolateral Corner

More posteriorly the posterolateral corner is supported by the biceps femoris tendon, the fibular collateral ligament and the popliteus complex as well as a number of other smaller ligamentous structures which are little more than condensations of the posterolateral capsule (LaPrade et al. 2000). The biceps femoris tendon arises from the ischial tuberosity and descends in the posterolateral compartment to insert on the fibular head. The fibular collateral ligament averages 67 mm in length and 3.4 mm in thickness. Its femoral attachment is 3 mm posterior to the ridge of the lateral femoral condyle (Meister et al. 2000) above and a little anterior to the popliteus tendon. It inserts on a V shaped bony depression that extends to the distal one-third of the lateral aspect of the fibular with some fibres extending along the peroneus longus fascia (LaPrade et al. 2003). The insertion can be either on its own or as a conjoint tendon with the biceps tendon. If they are separated, the insertion of the fibular collateral ligament is more anterior and medial than biceps femoris. The popliteus muscle runs from its "origin" on the dorsal aspect of the proximal tibia to insert into the popliteus fossa on the lateral femoral condyle. The final component of the posterolateral corner is the posterior capsule with specifically named ligamentous condensations. These minor ligaments can be divided into the long and short ligaments. The long ligament is the fabellofibular ligament if a fabella is present and an arcuate ligament if it is not. The short ligament is the fibulopopliteal ligament. These ligaments are variously identified on MR imaging (De Maeseneer et al. 2001). Coronal oblique imaging orientated to the posterior limb of the posterior cruciate is said to improve visualisation but this still remains less than 50% of cases. Non-visualisation therefore is difficult to interpret and tears of these specific ligaments are difficult to identify on MRI. Coronal images have also been advocated for visualising the fabellofibular ligament (Recondo et al. 2000).

Injuries to the posterolateral corner are most commonly caused by a combination of rotation and varus stress. They are less common than medial collateral ligament injuries but are more disabling. They are associated with full thickness ruptures of the anterior cruciate ligament when, on occasion, the clinical signs of cruciate rupture can mask the presence of posterolateral instability. It has been said that an overlooked posterolateral corner injury is the commonest cause of anterior cruciate ligament graft failure, but not all authors agree.

17.3.1.3 Fibular Collateral Ligament Injury

Tears of the fibular collateral ligament and most commonly mid-substance (Fig. 17.24) or fibular avulsions (Fig. 17.25) though more proximal tears can also occur. They are usually combined with other lateral injuries though isolated injuries have been reported (Shahane et al. 1999). Lesions of the fibular collateral ligament are divided into sprains, partial tears or complete tears. Like the iliotibial tract, the external anatomical relationship of the collateral ligaments is fat. Consequently, the most subtle change of injury is fluid within subcutaneous fat abutting the ligament. Injuries are therefore best appreciated on coronal orientated images with fat suppression. The presence of edema surrounding the ligament with an otherwise normal ligament is termed a Grade 1 injury or sprain. These are largely treated conservatively. When the ligament itself becomes disorganised but remains continuous from origin to insertion a partial tear or Grade 2 injury is diagnosed. Complete interruption of the normal low signal constitutes a complete rupture. Occasionally avulsion fractures can occur and these can be proximal or distal. A further clue to the presence of a lateral ligament injury is microfracture in the medial femoral condyle. This occurs during varus strain with impaction of the tibial plateau against the medial femoral condyle.

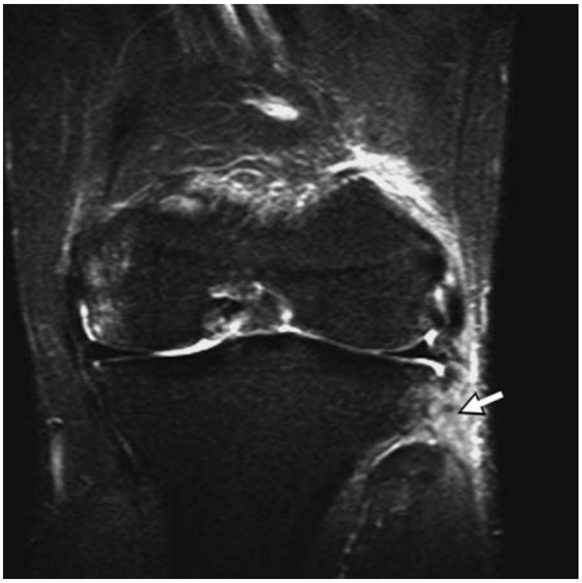

Fig. 17.24. Rupture of the FCL (*arrow*) on coronal STIR image

Fig. 17.25. Avulsion of the FCL from its distal insertion (*arrow*) on a coronal fat suppressed proton density MR image

17.3.1.4
Biceps Femoris Injuries

Biceps femoris injuries are less common than FCL injuries. Most often they are seen as overuse tendinopathy with thickening of the tendon just proximal to its insertion, but when the injury is more acute a tendon tear can occur. This is most commonly an avulsion fracture. Like avulsion injuries elsewhere, the degree of microfracture associated with them is less than is normally expected for fracture. The posterolateral corner is no exception and avulsion of the biceps femoris tendon can be difficult to appreciate if not specifically sought. Tracing the cortical margin of the fibula is a helpful way of assessing this (Fig. 17.26). An interruption due to avulsion of a small component of the cortex is a clue to rupture and is termed the arcuate sign (Huang et al. 2003). Occasionally biceps femoris injuries can occur in conjunction with injuries to the ilio-tibial tract due to shared fibres (Terry and LaPrade 1996a,b). Other biceps injuries include subluxation (Bach and Minihane 2001), when the long tendon is displaced over the fibular head during knee extension from a flexed position. There may be an association with a prominent fibular head or anomalous insertions of the tendon. Subluxation may also occur in the asymptomatic population (Bach and Minihane 2001).

17.3.1.5
Popliteus Complex Injuries

The popliteus complex includes a muscular origin from the tibia, a fibular origin referred to as the popliteofibular ligament, the tendinous insertion into the popliteus fossa, superior and inferior popliteomeniscal ligaments which form the popliteal hiatus and soft-tissue attachments to the lateral meniscus and posterior tibia (Shahane et al. 1999). The complex is important in preventing external rotation. The popliteofibular ligament is a frequently identified structure measuring 47 mm long and 9 mm^2 in cross-section which acts as a sling centered at the musculotendinous junction (LaPrade et al. 2003). Two divisions, anterior and posterior, are described. Its contribution to posterolateral stability is debated (Maynard et al. 1996; Shahane et al. 1999; Sugita and Amis 2001; LaPrade et al. 2003).

Injuries to the popliteus muscle tendon complex also occur during posterolateral corner strain. The commonest site is at the musculotendinous junction (Fig. 17.27) but tendon tears or avulsions are also reported. An acute haemarthrosis, lateral or posterolateral tenderness and pain on resisted internal tibial rotation have been described as clinical signs (Guha

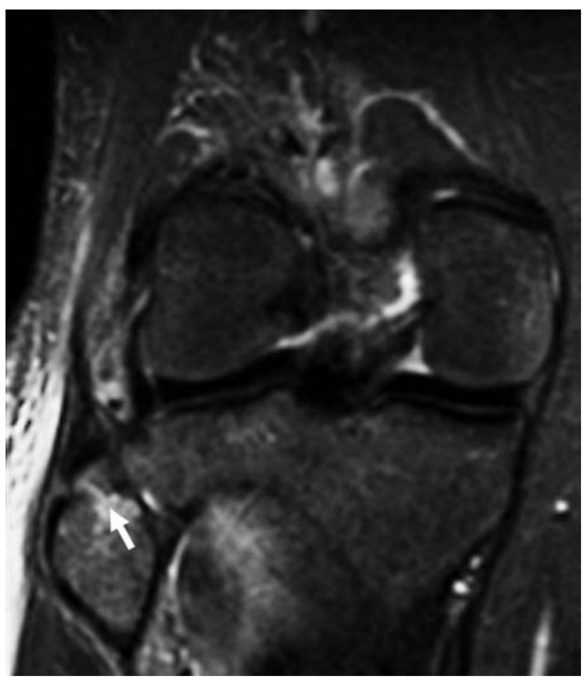

Fig. 17.26. Avulsion fracture of biceps insertion. Coronal fat suppressed proton density MR image showing loss of cortical continuity (*arrow*)

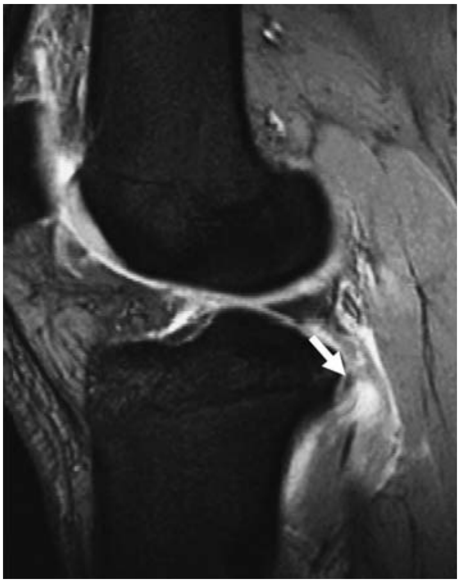

Fig. 17.27. Popliteus tear. Sagittal fat suppressed proton density MR image revealing a high signal at the musculotendinous junction (*arrow*)

et al. 2003). Anatomically, the muscle can be difficult to depict due to the oblique course it follows from origin on the posterior margin of the tibia to insertion in the popliteus fossa. Both sagittal and coronal images should therefore be perused for increased signal particularly at the musculotendinous junction. Acute findings include edema at the musculotendinous junction or avulsion of the tendon insertion in the popliteus fossa. Chronic injuries have been described with late onset muscle atrophy. Popliteus tendon snapping is a differential diagnosis on iliotibial friction and snapping and may be bilateral (Cooper 1999; McAllister and Parker 1999). The tendon subluxes from its groove, proximal to the lateral meniscus. This area cannot be appreciated at arthroscopy. The dynamic capabilities of US offer a distinct advantage over MRI in depicting this entity.

17.3.1.6
Capsule and Capsular Ligaments

Tears of the individual small ligaments of the posterolateral corner are difficult to appreciate. More usefully in the authors view is to determine whether there is a significant capsular disruption by identifying abnormal fluid in the popliteal fossa (Fig. 17.28). This indicates that there is a significant ligament disruption though it is often difficult to determine precisely which ligament has been torn. The presence of fluid in the popliteal fossa is an important finding to transmit to the referring clinician particularly if the patient is to undergo arthroscopy for associated internal derangement. In the presence of an unsealed capsular leak then fluid flowing into the knee during arthroscopy can fill the posterior calf and precipitate compartment syndrome. Chronic injuries to these structures are less easy to appreciate on both clinical and imaging. Popliteomeniscal ligament tears in college wrestlers have been described (LaPrade and Konowalchuk 2005). Increased lateral meniscal motion on flexion may be a clue (Staubli and Birrer 1990) though the imaging appearances have not been described.

17.3.1.7
Lateral Compartment Ganglia

Just as ganglia have been described in relation to the intra-articular ligaments there are also ganglia that have been associated with the lateral ligament complex involving both the iliotibial tract (Simoens et al. 2002) and fibular collateral ligament. A more common cause of an apparent ganglion or synovial cyst posterolaterally is a synovial out-pouching from the proximal tibiofibular joint.

17.3.2
The Medial Stabilisers

The medial knee is stabilised by the deep static components of the medial collateral ligament (MCL) and the dynamic posteromedial pes anserine ten-

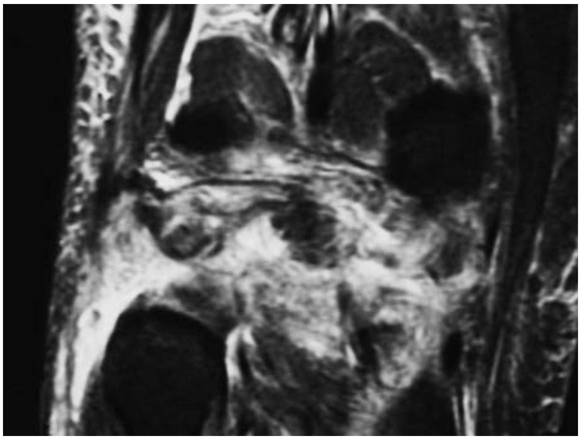

Fig. 17.28. Posterior capsule tear. Coronal fat suppressed proton density MR image. The popliteal fossa is filled with fluid indicative of a tear of the posterior capsule

dons. Anteriorly the medial retinaculum and fibres of the vastus medialis obliquus provide additional support.

17.3.2.1 The Medial Collateral Ligament

The medial collateral ligament is made up of a number of layers. The strongest, outermost layer is the dominant structure and comprises two portions. The anterior is a strong low signal ligament that extends from approximately 5 cm above the knee joint from the medial femoral condyle to insert 7 cm below the knee joint in a broad elongated insertion. Beneath the superficial MCL are the deep fibres which comprise two separate components, the meniscal femoral ligament and the meniscal tibial ligament. These are separated from the outer or superficial fibres by potential space generally only filled with connective tissue but which may fill with a bursa termed "the tibial collateral ligament bursa" (Fig. 17.29). The posterior, oblique portion of this ligament arises from the adductor tubercle, posterior to the medial epicondyle. Its insertion has three components, a tibial insertion close to the margin of the articular surface with a strong attachment to the medial meniscus, a capsular insertion and an insertion reinforcing the semimembranosus tendon. Because of the separate origin, it is often referred to as a separate ligament the postero oblique ligament (POL). Other authors define three layers of the medial stabilisers: layer 1 is the most superficial and is represented by the deep fascia and forms the medial retinaculum by combining with some fibres from layer 2. Layer 2 is the superficial MCL and POL and layer 3 is represented by the capsule proper but includes the deep layer of the MCL.

Fig. 17.29. Tibial collateral bursa. Coronal fat suppressed proton density MR image. Fluid fills the TCL bursa separating the superficial fibres of the MCL (*arrow*) and the deep fibres (*arrowhead*)

Fig. 17.30. Grade 1 MCL injury. Coronal fat suppressed proton density MR image. Note edema medial to an intact ligament. Other evidence of valgus strain is an impaction injury to the lateral femoral condyle (*arrowhead*)

Just like the lateral collateral ligament the immediate external relationship of the MCL is subcutaneous fat. Consequently injuries to the collateral ligaments are best appreciated on coronal fat suppressed images. For simple MCL injury, there is a good correlation between clinical and MRI staging. A Stage 1 injury clinically has medial sided pain, some laxity but with a firm end-point. The MRI findings under these circumstances are generally limited to edema around the ligament (Fig. 17.30). A Grade 2 injury has a valgus laxity with a soft but definable end-point. Under these circumstances the ligament shows internal structural changes, often it is multi-layered giving an onion skin appearance (Fig. 17.31). This is also associated with edema surrounding the ligament in the acute stages. A Stage 3 lesion where there is valgus laxity without a defined end-point is correlated with complete rupture on MRI (Fig. 17.32). Femoral insertion injuries are commonest but midsubstance and distal tears also occur. Most medial collateral liga-

Fig. 17.31. Grade 2 MCL injury. Coronal fat suppressed proton density MR image, showing an 'onion skin' configuration to the ligament (*arrow*) and edema medial to the ligament

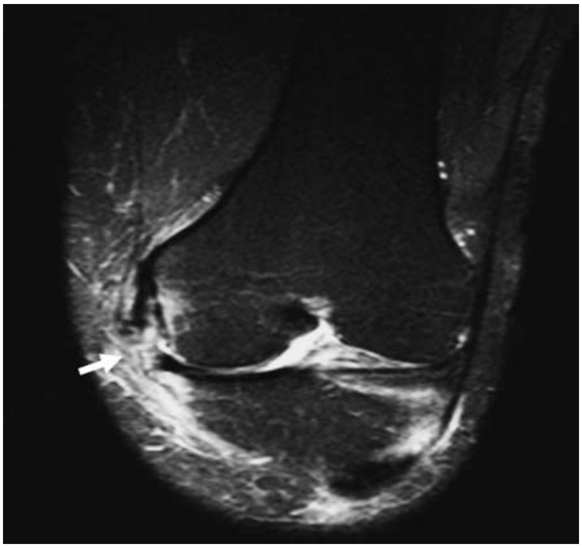

Fig. 17.32. Complete rupture of the MCL. Coronal fat suppressed proton density MR image. The tear is located in its midsubstance (*arrow*)

ment injuries resolve with conservative treatment, in some cases without the patient being particularly aware that they have been torn. Repair leaves only a thickened ligament which may persist for many years. Occasionally ossification can occur adjacent to the ligament termed the "Pellegrini-Stieda" lesion.

17.3.2.2
The Posteromedial Knee

The dynamic stabilisers posteromedial to the MCL comprise the three pes anserine tendons semimembranosus, semitendinosus and gracilis and their ligamentous condensations and bursae. The semimembranosus tendon is the key structure which has a complex of five insertions. The direct insertion is augmented by two additional anterior aponeuroses and two posterior. The anterior two are the pars reflexa inferiorly and an expansion to the POL superiorly. The posterior expansions are the oblique popliteal ligament superiorly and the popliteus aponeurosis inferiorly (Sims and Jacobson 2004). The relationships of these stabilisers to the medial meniscus are important in determining the combination of injuries and their pattern that may follow sporting trauma. Sims and Jacobson (2004) have divided these into simple valgus injury with MCL tear and anteromedial rotatory instability (AMRI), which they describe as an abnormal opening of the medial joint space in abduction at 30° of knee

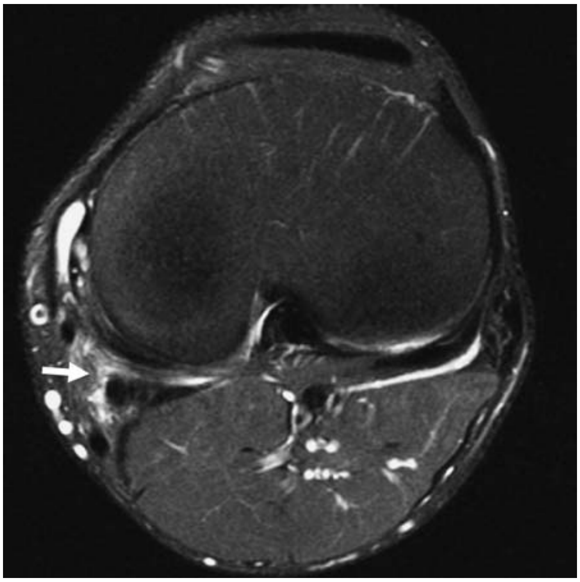

Fig. 17.33. Posteromedial corner lesion. Axial fat suppressed proton density MR image. Edema around the semimembranosus insertion associated with ACL rupture (*arrow*)

flexion, with a simultaneous anteromedial rotatory subluxation of the medial tibial condyle on the central axis of the intact posterior cruciate ligament.

When MCL injuries are detected, a careful study of the posteromedial structures is warranted, as in a small proportion tears of the semimembranosus tendon and associated insertions may be found (Fig. 17.33). As yet, a detailed description of the MRI findings of injuries to these smaller structures has yet to be defined. Chronic overuse semimembranosus tendinopathy is more common that acute injury and will described elsewhere.

17.3.2.3 Medial Compartment Ganglia

As with ligaments elsewhere, ganglion cysts can occasionally be associated with the medial collateral ligament. These need to be distinguished from the tibial collateral ligament bursa, the semimembranosus bursa and the pes anserine bursa (McCarthy and McNally 2003). The semimembranosus bursa and pes anserine bursa are distinguished by the presence of a central tendon. The two bursae themselves are distinguished by their position, with the semimembranosus bursa lying superior to the pes anserine bursa. The tibial collateral ligament bursa lies deep to the superficial MCL and superficial to the meniscofemoral and meniscotibial ligaments.

17.4 Conclusion

MRI plays a key role in the assessment of suspected ligamentous disruption of the knee. The anterior cruciate ligament is one of the most important stabilising structures of the knee, and is frequently injured in contact sports and skiing. Successful rehabilitation of the sports related anterior cruciate ligament injury is dependent on accurate diagnosis, leading to appropriate surgical stabilisation. In the presence of anterior cruciate ligament injury, assessment of associated meniscal and posterolateral corner injury are also vital. Disruptions of the posterior cruciate ligament are less common but also important for stable knee function. Most injuries to the collateral ligaments can be treated conservatively, though acute disruptions of the medial collateral ligament can lead to a fixed flexion 'locked' knee mimicking a bucket handle tear.

Things to Remember

1. The anterior cruciate ligament should be identified on all MR examinations as a line of low signal intensity.

2. In the presence of a tear of the anterior cruciate ligament, it is important to search for meniscal disruption and to carefully scrutinise the posterolateral corner.

3. The immediate external relationship of the collateral ligaments is subcutaneous fat. Coronal orientated fat saturated images most efficient in assessing injury to these structures

References

Anderson AF, Awh MH, Anderson CN (2004) The anterior meniscofemoral ligament of the medial meniscus: case series. Am J Sports Med 32:1035–1040

Bach BR Jr, Minihane K (2001) Subluxating biceps femoris tendon: an unusual case of lateral knee pain in a soccer athlete: a case report. Am J Sports Med 29:93–95

Bradley JP, Rytel MJ, Klimkiewicz JJ, Powell JW (2002) Anterior cruciate ligament injuries in the National Football League: epidemiology and current treatment trends among team physicians. Arthroscopy 18:502

Bui Mansfield LT, Youngberg RA (1997) Intraarticular ganglia of the knee: prevalence, presentation, etiology, and management. AJR Am J Roentgenol 168:123–127

Chan KK, Resnick D, Goodwin Det al. (1999) Posteromedial tibial plateau injury including avulsion fracture of the semimembranous tendon insertion site: ancillary sign of anterior cruciate ligament tear at MR imaging. Radiology 211:754–758

Chan WP, Peterfy C, Fritz RC et al. (1994) MR diagnosis of complete tears of the anterior cruciate ligament of the knee: importance of anterior subluxation of the tibia. Am J Roentgenol 162:355–360

Charlton WPH, St. John TA, Ciccotti MG et al. (2002) Differences in femoral notch anatomy between men and women. A magnetic resonance imaging study. Am J Sports Med 30:329

Cobby MJ, Schweitzer ME, Resnick D (1992) The deep lateral femoral notch: an indirect sign of a torn anterior cruciate ligament. Radiology 184:855–858

Cooper DE (1999) Snapping popliteus tendon syndrome: a cause of mechanical knee popping in athletes. Am J Sports Med 27:671–674

Cross MJ, Powell JF (1984) Long-term followup of posterior cruciate ligament rupture: a study of 116 cases. Am J Sports Med 12:292–297

De Maeseneer M, Shahabpour M, Vanderdood K et al. (2001) Posterolateral supporting structures of the knee: findings on anatomic dissection, anatomic slices and MR images. Eur Radiol 11:2170–2177

De Smet AA, Graf BK (1994) Meniscal tears missed on MR imaging: relationship to meniscal tear patterns and anterior cruciate ligament tears. Am. J. Roentgenol 162:905–911

Fanelli GC (1993) Posterior cruciate ligament injuries in trauma patients. Arthroscopy 9:291–294

Gabbe B, Finch C (2001) A profile of Autralian football injuries presenting to sports medicine clinics. J Sci Med Sport 4:386

Gentili A, Seeger LL, Yao L et al. (1994) Anterior cruciate ligament tear: Indirect signs at MR imaging. Radiology 193:835–840

Girgis FG, Marshall JL, Monajem A (1975) The cruciate ligaments of the knee joint. Anatomical, functional and experimental analysis. Clin Orthop Relat Res 216–231

Grover JS, Bassett LW, Gross ML et al. (1990) Posterior cruciate ligament: MR imaging. Radiology 174:527–530

Guha AR, Gorgees KA, Walker DI (2003) Popliteus tendon rupture: a case report and review of the literature. Br J Sports Med 37:358–360

Gunter P, Schwellnus MP, Fuller PJ (2004) Local corticosteroid injection in iliotibial band friction syndrome in runners: a randomised controlled trial * Commentary. Br J Sports Med 38:269–272

Gupte CM, Smith A, McDermott ID et al. (2002) Meniscofemoral ligaments revisited: anatomical study, age correlation and clinical implications. J Bone Joint Surg Br 84B:846–851

Heller L, Langman J (1964) The menisco-femoral ligaments of the human knee. J Bone Joint Surg Br 46:307–313

Holmes JC, Pruitt AL, Whalen NJ (1993) Iliotibial band syndrome in cyclists. Am J Sports Med 21:419–424

Huang G-S, Lee C-H, Chan WP et al. (2002) Acute anterior cruciate ligament stump entrapment in anterior cruciate ligament tears: MR imaging appearance. Radiology 225:537–540

Huang G-S, Yu JS, Munshi M, Chan WP et al. (2003) Avulsion fracture of the head of the fibula (the „arcuate" sign): MR imaging findings predictive of injuries to the posterolateral ligaments and posterior cruciate ligament. Am J Roentgenol 180:381–387

Jarvinen M, Natri A, Laurila S et al. (1994) Mechanisms of anterior cruciate ligament ruptures in skiing. Knee Surg Sports Traumatol Arthrosc 2:224–228

Kaplan PA, Walker CW, Kilcoyne RF et al. (1992) Occult fracture patterns of the knee associated with anterior cruciate ligament tears: assessment with MR imaging. Radiology 183:835–838

LaPrade RF, Konowalchuk BK (2005) Popliteomeniscal Fascicle Tears Causing Symptomatic Lateral Compartment Knee Pain: Diagnosis by the Figure-4 Test and Treatment by Open Repair. Am J Sports Med 33:1231–1236

LaPrade RF, Gilbert TJ, Bollom TS et al. (2000) The magnetic resonance imaging appearance of individual structures of the posterolateral knee. A prospective study of normal knees and knees with surgically verified grade III injuries. Am J Sports Med 28:191–199

LaPrade RF, Ly TV, Wentorf FA et al. (2003) The posterolateral attachments of the knee: a qualitative and quantitative morphologic analysis of the fibular collateral ligament, popliteus tendon, popliteofibular ligament, and lateral gastrocnemius tendon. Am J Sports Med 31:854–860

Lawrance JA, Ostlere SJ, Dodd CA (1996) MRI diagnosis of partial tears of the anterior cruciate ligament. Injury 27:153–155

Lee BY, Jee WH, Kim JM et al. (2000) Incidence and significance of demonstrating the meniscofemoral ligament on MRI. Br J Radiol 73:271–274

Lee JK, Yao L, Phelps CT et al. (1988) Anterior cruciate ligament tears: MR imaging compared with arthroscopy and clinical tests. Radiology 166:861–864

Lee K, Siegel MJ, Lau DM et al. (1999) Anterior cruciate ligament tears: MR imaging-based diagnosis in a pediatric population. Radiology 213:697–704

Mair SD, Schlegel TF, Gill TJ et al. (2004) Incidence and location of bone bruises after acute posterior cruciate ligament injury. Am J Sports Med 32:1681–1687

Maynard MJ, Deng X, Wickiewicz TL et al. (1996) The popliteofibular ligament. Rediscovery of a key element in posterolateral stability. Am J Sports Med 24:311–316

McAllister DR, Parker RD (1999) Bilateral subluxating popliteus tendons: a case report. Am J Sports Med 27:376–379

McCarthy CL, McNally EG (2004) The MRI appearance of cystic lesions around the knee. Skeletal Radiol 33:187–209

McCauley TR, Moses M, Kier R et al. (1994) MR diagnosis of tears of anterior cruciate ligament of the knee: importance of ancillary findings. Am J Roentgenol 162:115–119

Meister BR, Michael SP, Moyer RA et al. (2000) Anatomy and kinematics of the lateral collateral ligament of the knee. Am J Sports Med 28:869–878

Mellado JM, Calmet J, Olona M et al. (2004) Magnetic resonance imaging of anterior cruciate ligament tears: reevaluation of quantitative parameters and imaging findings including a simplified method for measuring the anterior cruciate ligament angle. Knee Surg Sports Traumatol Arthrosc 12:217–224

Murao H, Morishita S, Nakajima M et al. (1998) Magnetic resonance imaging of anterior cruciate ligament (ACL) tears: diagnostic value of ACL-tibial plateau angle. J Orthop Sci 3:10–17

Murphy BJ, Smith RL, Uribe JW et al. (1992) Bone signal abnormalities in the posterolateral tibia and lateral femoral condyle in complete tears of the anterior cruciate ligament: a specific sign? Radiology 182:221–224

Nelson EW, LaPrade RF (2000) The anterior intermeniscal ligament of the knee: an anatomic study. Am J Sports Med 28:74–76

Nokes SR, Koonce TW, Montanez J (1994) Ganglion cysts of the cruciate ligaments of the knee: recognition on MR images and CT-guided aspiration. AJR Am J Roentgenol 162:1503

Parolie JM, Bergfeld JA (1986) Long-term results of nonoperative treatment of isolated posterior cruciate ligament injuries in the athlete. Am J Sports Med 14:35–38

Pereira MT, Nanni G, Roi GS (2003) Epidemiology of anterior cruciate ligament injuries in professional football players [Epidemiologia de las lesiones del ligamento cruzado anterior en el futbolista profesional]. Archiv Med Deporte 20:299

Prince JS, Laor T, Bean JA (2005) MRI of anterior cruciate ligament injuries and associated findings in the pediatric knee: changes with skeletal maturation. Am J Roentgenol 185:756–762

Recondo JA, Salvador E, Villanua JA et al. (2000) Lateral stabilizing structures of the knee: functional anatomy and injuries assessed with MR imaging. Radiographics 20:91S–102

Remer EM, Fitzgerald SW, Friedman H et al. (1992) Anterior cruciate ligament injury: MR imaging diagnosis and patterns of injury. Radiographics 12:901–915

Robertson PL, Schweitzer ME, Bartolozzi AR et al. (1994) Anterior cruciate ligament tears: evaluation of multiple signs with MR imaging. Radiology 193:829–834
Sanders TG, Linares RC, Lawhorn KW et al. (1999) Oblique meniscomeniscal ligament: another potential pitfall for a meniscal tear - anatomic description and appearance at MR imaging in three cases. Radiology 213:213–216
Schweitzer ME, Cervilla V, Kursunoglu-Brahme S et al. (1992) The PCL line: an indirect sign of anterior cruciate ligament injury. Clin Imaging 16:43
Schweitzer ME, Mitchell DG, Ehrlich SM (1993) The patellar tendon: thickening, internal signal buckling, and other MR variants. Skeletal Radiol 22:411–416
Segond P (1879) Recherches cliniques et expérimentales sur les épanchements sanguins du genou par entorse. Prog Med 7:297
Shahane SA, Ibbotson C, Strachan R et al. (1999) The popliteofibular ligament: an anatomical study of the posterolateral corner of the knee. J Bone Joint Surg Br 81–B:636–642
Shelbourne KD, Nitz PA (1991) The O'Donoghue triad revisited. Combined knee injuries involving anterior cruciate and medial collateral ligament tears. Am J Sports Med 19:474–477
Shelbourne KD, Davis TJ, Patel DV (1999) The natural history of acute, isolated, nonoperatively treated posterior cruciate ligament injuries: a prospective study. Am J Sports Med 27:276–283
Simoens WA, Vanhoenacker FM, Willemen D et al. (2002) Iliotibial band friction syndrome. JBR-BTR 85:152–153
Sims WF, Jacobson KE (2004) The posteromedial corner of the knee: medial-sided injury patterns revisited. Am J Sports Med 32:337–345
Siwinski D, Ziemianski A (1998) Value of posterior cruciate ligament index in the diagnosis of anterior cruciate ligament injuries. Arch Orthop Trauma Surg 118:116–118
Sonin AH, Fitzgerald SW, Friedman H et al. (1994) Posterior cruciate ligament injury: MR imaging diagnosis and patterns of injury. Radiology 190:455–458
Sonin AH, Fitzgerald SW, Hoff FL et al. (1995) MR imaging of the posterior cruciate ligament: normal, abnormal, and associated injury patterns. Radiographics 15:551–561
Stallenberg B, Gevenois PA, Sintzoff SA Jr et al. (1993) Fracture of the posterior aspect of the lateral tibial plateau: radiographic sign of anterior cruciate ligament tear. Radiology 187:821–825
Staubli HU, Birrer S (1990) The popliteus tendon and its fascicles at the popliteal hiatus: gross anatomy and functional arthroscopic evaluation with and without anterior cruciate ligament deficiency. Arthroscopy 6:209–220
Sugita T, Amis AA (2001) Anatomic and biomechanical study of the lateral collateral and popliteofibular ligaments. Am J Sports Med 29:466–472
Terry GC, LaPrade RF (1996a) The biceps femoris muscle complex at the knee. Its anatomy and injury patterns associated with acute anterolateral-anteromedial rotatory instability. Am J Sports Med 24:2–8
Terry GC, LaPrade RF (1996b) The posterolateral aspect of the knee. Anatomy and surgical approach. Am J Sports Med 24:732–739
Tung GA, Davis LM, Wiggins ME et al. (1993) Tears of the anterior cruciate ligament: primary and secondary signs at MR imaging [see comments]. Radiology 188:661–667
Umans H, Wimpfheimer O, Haramati N et al. (1995) Diagnosis of partial tears of the anterior cruciate ligament of the knee: value of MR imaging. Am J Roentgenol 165:893–897
Vanek J (1994) Posteromedial fracture of the tibial plateau is not an avulsion injury. A case report and experimental study. J Bone Joint Surg Br 76:290–292
Vanhoenacker FM, Vanhoenacker P, Crevits I et al. (2001) MR imaging anatomy of the knee. JBR-BTR 84:10–15
Vanhoenacker FM, Van de Perre S, De Vuyst D et al. (2003) Cystic lesions around the knee. JBR-BTR 86:302–304
Wan AC, Felle P (1995) The menisco-femoral ligaments. Clin Anat 8:323–326
Weber WN, Neumann CH, Barakos JA et al. (1991) Lateral tibial rim (Segond) fractures: MR imaging characteristics. Radiology 180:731–734
Wind WM Jr, Bergfeld JA, Parker RD (2004) Evaluation and treatment of posterior cruciate ligament injuries: revisited. Am J Sports Med 32:1765–1775
Yao L, Lee JK (1989) Avulsion of the posteromedial tibial plateau by the semimembranosus tendon: diagnosis with MR imaging. Radiology 172:513–514

Imaging of Anterior Knee Pain and Maltracking

18

Simon Ostlere

Contents

Box 18.1. CT

- High radiation dose
- Poor soft issue contrast
- Not indicated in the assessment of anterior knee pain except in exceptional circumstances

Box 18.2. Radiography

- Indicated in acute trauma
- Has a lower sensitivity for almost all pathologies when compared to MR
- Not routinely indicated in anterior knee pain in the athlete
- Occasionally useful as second line investigation to clarify an abnormality seen on MR

Box 18.3. Ultrasound

- Excellent tool for assessing the superficial soft tissues
- Quick, easy and cheap
- Patient friendly
- Dynamic and Doppler imaging useful
- Direct interaction with patient often helpful

Box 18.4. MRI

- Excellent tool for assessing joint, bones and soft tissues
- Sensitive and specific for most conditions causing anterior knee pain
- Expensive and not very patient friendly
- First line test for assessment of all pathologies of the patellofemoral joint

S. Ostlere, FRCR
Department of Radiology, Nuffield Orthopaedic Centre, NHS Trust, Windmill Road, Headington, Oxford OX3 7LD, UK

18.1 Introduction

Symptoms related to the anterior knee are common in the athlete. There are a number of specific conditions of the patellar tendon, patellofemoral joint and Hoffa's fat pad but in many cases of retropatellar pain there is no identifiable cause which has led to the use of the term 'patellofemoral pain syndrome'. Acute injuries of the extensor mechanism account for a minority of cases. Imaging is useful in acute injuries and in a minority of those non-acute cases. In most cases of non specific patellofemoral pain, no imaging is required unless there has been a poor response to standard conservative treatment.

18.2 Acute Trauma to the Extensor Mechanism

The most common acute injury to the anterior knee is patellar dislocation. More unusual injuries include patellar tendon rupture and direct trauma may result in patellar fractures or haemorrhage into the prepatellar bursa. Fractures are rare in the athlete. Patellar fractures are due to a direct blow. In children avulsion fractures of the inferior patella and tibial tubercle may occur.

18.2.1 Acute Dislocation

Acute patellar dislocation may be associated with underlying patellofemoral dysplasia (see below) but in most cases the anatomy is normal. Dislocation usually occurs following a twisting injury to the knee. Typically the patient experiences acute pain and the knee immediately swells. Examination of the knee is difficult in the acute setting and the diagnosis is often not suspected prior to imaging. MRI is an excellent tool for the assessment of the acutely injured knee, as it will demonstrate a surgical lesion and lead to rapid implementation of appropriate treatment. Patellar dislocation can be readily diagnosed on MRI as the signs are specific. At the time of injury the patellar initially subluxes laterally until the medial retinaculum ruptures. The patella then dislocates and its medial aspect impacts against the anterolateral aspect of the lateral femoral condyle. This often results in an osteochondral fragment originating from the medial patellar facet. The typical MR signs are therefore rupture of the medial retinaculum, subcortical edema/haemorrhage in the anterolateral aspect of the lateral femoral condyle with a corresponding 'kissing' lesion in the medial aspect of the patella, with or without an osteochondral fracture (Fig. 18.1). Sometimes the medial retinaculum remains intact (Kirsch et al. 1993).

18.2.2 Patellar Tendon Rupture

Patellar tendon rupture is rare. Predisposing factors are patellar tendinosis, previous steroid injections, previous ACL repair with patellar graft and certain chronic medical disorders. The patient complains of sudden pain and inability to extend the knee. The tear usually occurs close to the tendon's origin at the inferior pole of the patella. Early surgical repair is indicated so it is important to make a timely diagnosis. Ultrasound is the easiest and quickest method to make the diagnosis and determine the site and extent of the tear although MRI provides similar information (Fig. 18.2) (Matava 1996).

18.2.3 Prepatellar Bursa

Prepatellar bursitis is a common condition in the general population, particularly in occupations requiring kneeling. In the athlete the commonest problem is an acute haemorrhagic bursitis resulting from a direct blow. The diagnosis is usually obvious on clinical inspection and can be easily confirmed on ultrasound or MR (Fig. 18.3) (Larson and Osternig 1974).

18.2.4 Fractures

Fractures are an uncommon cause of anterior knee pain. In the adult patellar fractures may occur secondary to a direct blow. In the child, the patellar sleeve avulsion fracture is a rare but important lesion in which the unossified inferior pole plus a small amount of bone is avulsed along with a sleeve of retropatellar articular cartilage and periosteum (Hunt

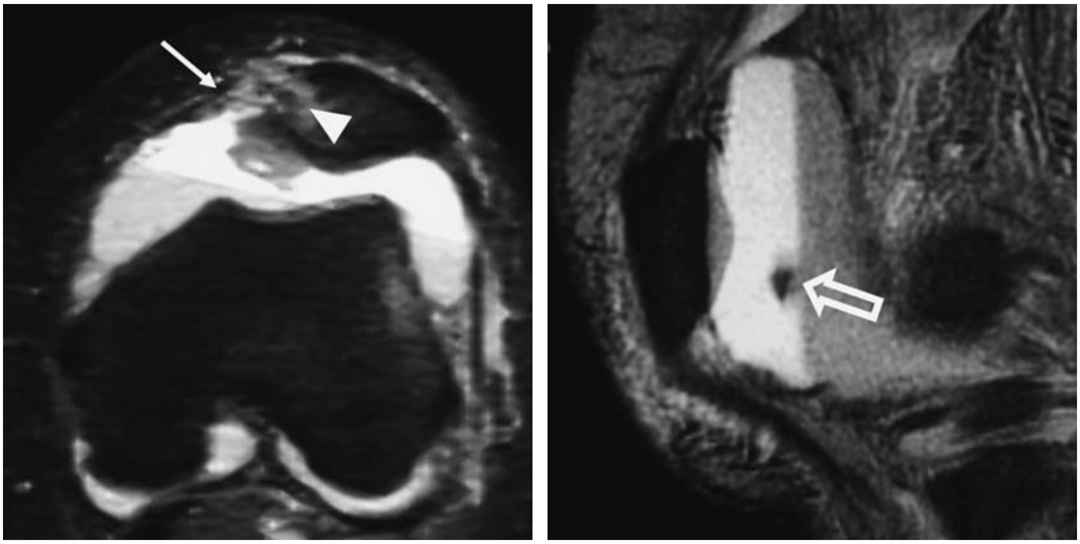

a b

Fig. 18.1a,b. Acute patellar dislocation. **a** Proton density fat suppression axial; **b** Sagittal T2 gradient echo MR image showing. tear of the medial retinaculum (*arrow*), high signal in the anterolateral aspect of the lateral femoral condyle and medial aspect of the patella (*arrowhead*) and patellar osteochondral fracture floating on fluid/fluid level (*open arrow*)

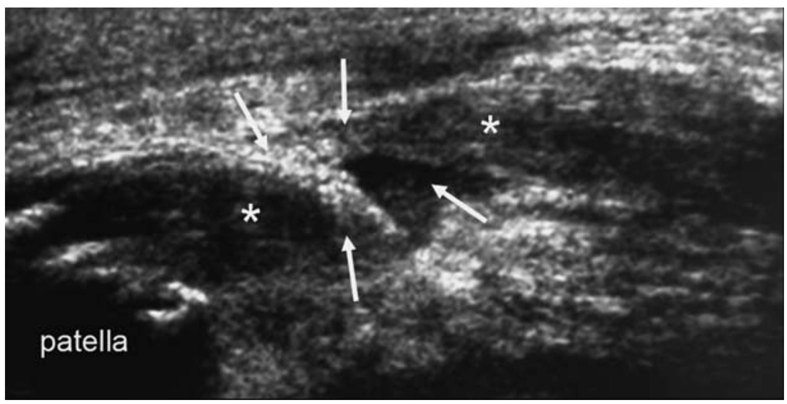

Fig. 18.2. Patellar rupture. Sagittal ultrasound shows a defect in the proximal portion of the tendon (*arrows*). The asterisk marks the free ends of the tendon

Fig. 18.3. Pre patellar bursa. Sagittal proton density fat suppressed MR image showing high signal in the prepatellar bursa following trauma (*arrow*)

Fig. 18.4. Avulsion fracture of the tibial tubercle. The fragment has rotated nearly 180°

and Somashekar 2005). This fracture requires fixation. Another rare fracture is avulsion of the unfused tibial tubercle (Fig. 18.4).

18.3 Anterior Knee Pain Without Acute Trauma

Anterior knee pain is common complaint in the athlete and general population. In most cases symptoms are due to pathology of patellar tendon, patellofemoral joint or Hoffa's fat pad. Most patients do not require any imaging. In certain circumstances imaging will help to make a diagnosis, assess the degree of abnormality or guide therapy. MRI and ultrasound are the most useful techniques in investigating anterior knee pain. Plain films have a limited role and are not required in most cases. Ultrasound is the easiest method of investigating suspected patellar tendon pathology. MRI is used for suspected patellofemoral problems and when the symptoms are non specific.

18.3.1 Disorders of the Patellar Tendon

The patellar tendon is vulnerable to overuse type injuries. In the adolescent the commonest condition is Osgood Schlatter's disease which is a traction injury at the tibial tubercle. The condition is more common in males and is associated with running sports. A tender bony swelling at the tibial tubercle is found on clinical inspection. Imaging is rarely required and is usually requested to reassure the patient or their parents that there is no sinister pathology. Plain films will show fragmentation of the tibial tubercle, accompanied by some soft tissue swelling representing thickened tendon and fluid in the deep infrapatellar bursa. Ultrasound is often preferred as it does not involve ionizing radiation and will demonstrate the soft tissue component to better effect (Fig. 18.5) (Blankstein et al. 2001). Sinding-Larsen Johansson syndrome is a similar traction type injury that occurs at the proximal end of the tendon. Plain film shows fragmentation of the inferior pole of the patella. The appearances on ultrasound and MR are similar to Osgood Schlatter's disease with fragmentation of the inferior pole of the patella and widening of the adjacent tendon with edema and hypervascularity (Fig. 18.6). These two conditions have a good prognosis and resolve with conservative management. In contrast, the condition termed jumper's knee (patellar tendinosis) can be much more troublesome. This condition occurs in the adolescent and young adults and can become chronic. The pathology is degeneration of the proximal tendon directly adjacent to the

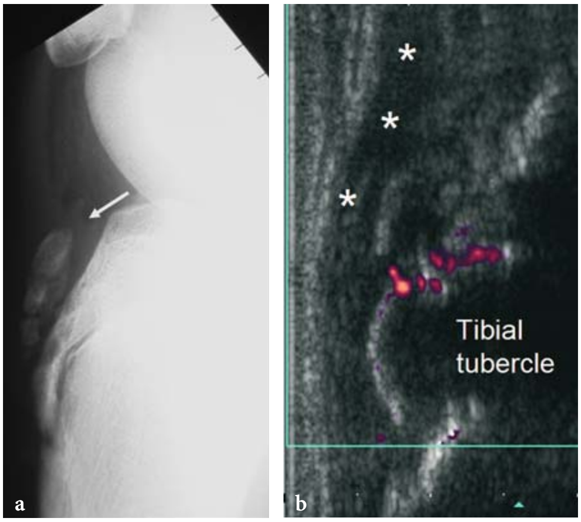

Fig. 18.5a,b. Osgood Schlatter's disease. **a**) plain film; **b**) ultrasound showing fragmentation of the tibial tubercle. An infrapatellar effusion can be seen on the radiograph (*arrow*). On ultrasound the distal end of the tendon is seen to be widened and hypoechoic. There is hypervascularity around the bony fragments. Asterisks mark the tendon

inferior pole of the patella. The probable mechanism of injury is impingement of the tendon by the inferior pole of the patella. The abnormality is typically confined to the deep surface of the central portion of the tendon. The diagnosis and management is usually based solely on clinical evaluation. When imaging is indicated ultrasound is the technique of choice. A focal swelling of the tendon with hypervascularity is seen adjacent to the inferior pole of the patella (Terslev et al. 2001). Calcification is not uncommon. On MRI the abnormal portion of the tendon returns increased signal on all sequences (Fig. 18.7). Imag-

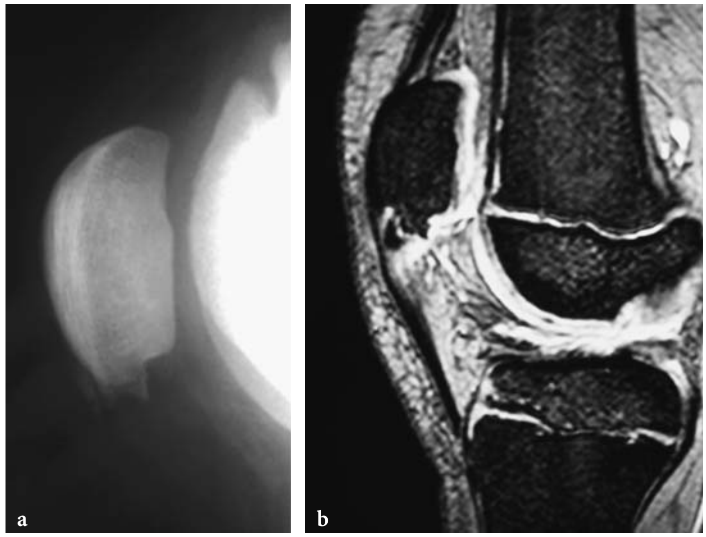

Fig. 18.6a,b. Sinding-Larsen Johansson syndrome **a** plain film; **b** T2 gradient echo sagittal image showing fragmentation of the inferior pole of the patella. On MRI there is bony fragmentation and high signal in the adjacent tendon

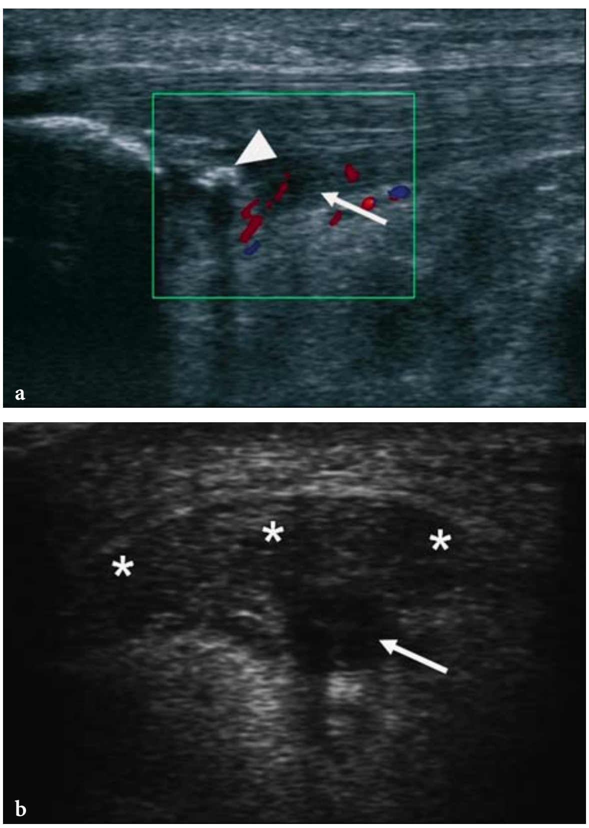

Fig. 18.7a–c. Patellar tendinosis: **a** sagittal; **b** axial ultrasound showing a focal hypervascular mass in the deep portion of the proximal end of the patellar tendon (*arrows*). There is some calcification (*arrowhead*). Asterisk mark the tendon; **c** sagittal proton density fat suppressed MR image in a different case showing typical focal high signal deep to the tendon near its origin (*open arrow*)

ing evidence of patellar tendinosis in asymptomatic athletes is a risk factor for developing symptoms in the future (Fredberg and Bolvig 2002; Gisslen and Alfredson 2005).

A common finding on MRI is impingement of the lateral aspect of the patellar tendon on the anterolateral articular margin of the lateral femoral condyle. Some minor high signal may be detected in the fat that is interposed between the tendon and the condyle. Although this entity may be seen in patients with anterior or anterolateral pain (Chung et al. 2001), it is so common a finding on routine MRI that its significance is open to question (Fig. 18.8).

Fig. 18.8. Patellar tendon 'impingement'. Sagittal T2 gradient echo MRI demonstrating impingement of the most lateral aspect of the proximal patellar tendon on the lateral femoral condyle. There is high signal seen deep to the tendon at the site of impingement (*arrow*)

18.3.2 Iliotibial Band Friction Syndrome

Iliotibial band friction syndrome is a common condition seen in runners and is due to impingement of the band against the lateral aspect of the lateral femoral condyle. The clinical picture is typical with focal lateral pain on running. Imaging is not required in the classical case. On T2 weighted MRI ill-defined or fluid like high signal is seen in the space between the iliotibial band and the lateral condyle. The band itself usually appears normal (Fig. 18.9) (Muhle et al. 1999).

18.3.3 Synovial Plica

Impingement of the medial patellar plica between the patella and the medial condyle has been implicated as a cause of anterior knee pain. The patient may experience pain, clicking and pseudolocking and tenderness over the medial plica. Visualization of the normal plica on MRI is very common in patients with an effusion. In medial patellar plica syndrome the plica is seen to be thickened. This is best appreciated on the axial images. In the absence of fluid the thickened plica may appear as a low signal intensity mass in the medial recess (Jee et al. 1998) (Fig. 18.10).

18.3.4 Hoffa's Fat Pad

Hoffa's fat pad lies deep to the patellar tendon and has an apex pointing toward the ACL insertion. Cysts, neoplasms and inflammatory conditions are sometimes seen in the fat pad (Saddik et al. 2004). The

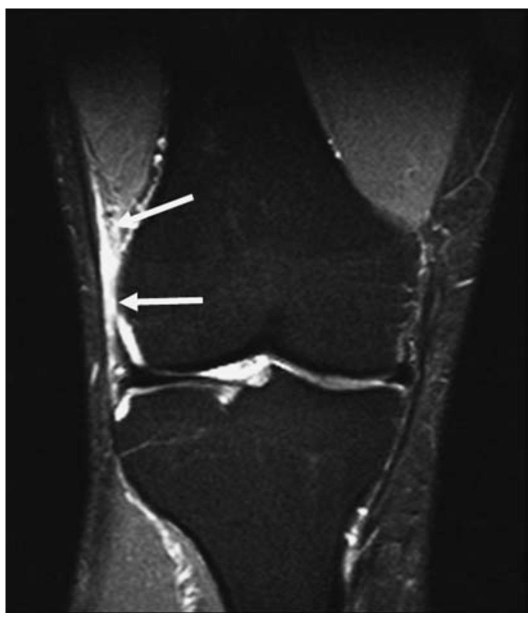

Fig. 18.9. Iliotibial band syndrome. Coronal proton density fat suppressed MRI showing high signal deep to the iliotibial band (*arrows*)

Fig. 18.10. Medial patellar plica. Axial MRI showing low signal mass in the medial synovial recess. In this case there is an associated bony spur seen at the site of impingement

Fig. 18.11. Infrapatellar plica. Sagittal proton density fat suppressed MR image demonstrating a normal infrapatellar plica (*arrows*)

concept of Hoffa's fat pad impingement syndrome is controversial but edema is sometimes seen in the pad without any obvious explanation. The normal infrapatellar plica can be frequently identified on MRI as it runs through the fat pad and attaches to the inferior pole of the patella (Fig. 18.11). Occasionally high signal is seen surrounding the plica on MRI (Cothran et al. 2003). Whether this abnormality itself is related to symptoms is open to question. The most common lesion found in the fat pad is a ganglion (Fig. 18.12). Ganglia are usually found on MRI but US is useful to confirm their cystic nature. Ultrasound guided aspiration and injection of steroid may be beneficial. The commonest solid tumours are the nodular form of pigmented villonodular synovitis (PVNS) and synovial osteochondromatosis. Nodular PVNS contains haemosiderin and fibrosis which is seen as low signal intensity on T2 weighted images (Fig. 18.13). Synovial osteochondromatosis is usually calcified to a varying degree but otherwise imaging features are non-specific (Fig. 18.14) (Helpert et al. 2004).

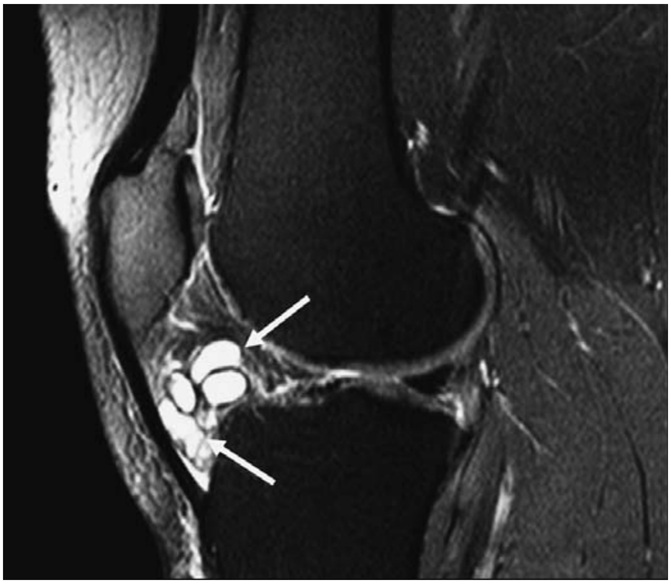

Fig. 18.12. Hoffa's fat pad ganglion. Sagittal proton density fat suppressed MR image showing lobulated cystic mass (*arrows*)

Fig. 18.13a,b. Nodular PVNS: **a** axial T1; **b** coronal proton density fat suppressed T2 weighted MR image shows a well defined mass (*arrows*) in Hoffa's fat pad which contains some low signal intensity on the fat suppression images representing haemosiderin and fibrosis

Fig. 18.14. Synovial osteochondromatosis. Sagittal proton density fat suppressed MR image showing a well defined high signal mass (*arrows*) containing low signal foci representing calcification

18.3.5 Patellofemoral Joint

Definable conditions of the patellofemoral joint that cause anterior knee pain are chondromalacia, osteochondritis dissecans, and patellar maltracking. 'Patellofemoral pain syndrome' is a term is usually reserved for cases of retropatellar knee pain without an identifiable cause.

18.3.5.1 Patellofemoral Pain Syndrome

The underlying pathology may be chondromalacia or clinically occult patellar malalignment. The term merely describes a clinical picture and is not a true syndrome. This entity is common in athletes and non-athletes alike. The condition is much more common in females. Imaging is rarely required as achieving a more specific diagnosis does not usually alter management. Most patients have normal imaging including normal patellofemoral anatomy. A proportion of patients will have demonstrable chondromalacia of the retropatellar cartilage and some will have anatomical abnormality predisposing to maltracking of the patella. Imaging is indicated if symptoms are atypical or persistent, mainly to rule out treatable pathology such as osteochondritis dissicans. If maltracking is suspected and surgery is being considered then MRI is useful to document any dysplasia. Dynamic imaging is useful to detect and quantify maltracking. Imaging is not indicated for suspected chondromalacia although macroscopic lesions may be reliably seen on good quality MRI (Fig. 18.15).

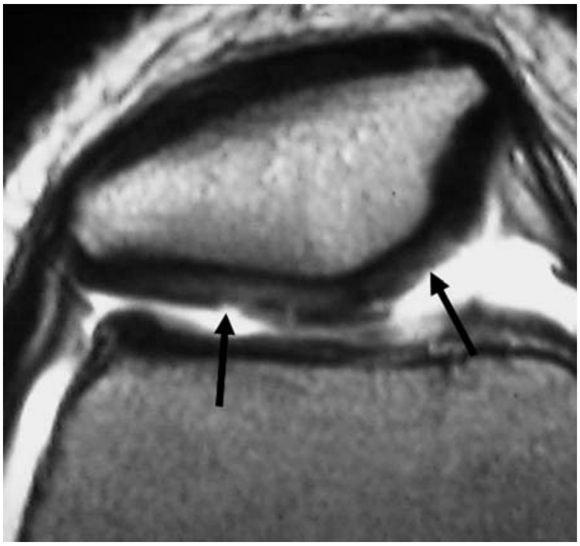

Fig. 18.15. Chondromalacia. Axial T2 fat suppressed MR image showing small defects in the articular cartilage (*arrows*)

18.3.5.2
Bipartite Patella

Bipartite patella is a normal variant where there is a small separate ossification at the superolateral aspect of the patella. Bipartite patellar can be easily identified on plain films and MRI. Symptomatic case are very rare but is persistent localized pain following injury has been reported (Iossifidis and Brueton 1995). On MRI, edema either side of the divide between the accessory ossification and the main body of the patella may be encountered (Vanhoenacker et al. 2002) (Fig. 18.16).

18.3.5.3
Osteochondritis Dissecans

Osteochondritis dissecans is a disease of childhood and adolescence. It is more common in the athletic individuals and is due to repetitive loading on the articular surface. In the knee, the lateral aspect of the medial femoral condyle, the weight bearing portion of the lateral femoral condyle, the patella and the trochlear groove are typical sites (Peters and McLean 2000). The patient may present with anterior pain when the lesion involves the patellofemoral joint or the anterior aspects of the femoral condyles. Osteochondritis dissecans can usually be identified on plain films but MRI is more sensitive. Radiographically osteochondritis dissecans is seen as a subchondral lucency which may contain a density representing the osteonecrotic fragment. Intra-articular loose bodies may also be seen. On MRI the defect may be seen to be filled with fibrocartilage or to contain the necrotic fragment (Fig. 18.17). The generally accepted criteria for diagnosing an unstable lesion is high signal lying deep to the fragment and breach of the articular cartilage (De Smet et al. 1997). Accurate staging of osteochondritis dissecans usually requires arthroscopy. Normal irregularity of the posterior aspect of the medial femoral condyle in children may simulate osteochondritis dissecans (Gebarski and Hernandez 2005).

18.3.5.4
Patellar Maltracking

Patients with maltracking may present with non-specific retropatellar pain or symptoms of patellofemoral joint instability including dislocation. Imaging is useful in suspected acute patellar dislocation (see above) and in patients with chronic patellofemoral instability who are being considered for surgery.

Patients with chronic instability usually suffer from some degree of patellofemoral dysplasia with one or more of the following adverse anatomical features: a high riding patellar (patella alta); a flat trochlear groove; a laterally positioned tibial tubercle. The relative importance of each of these measurements depends on the surgical options available. The most popular operation for maltracking is medial or anteromedial transfer of the tibial tubercle (Bellemans et al. 1997). Refashioning the trochlear groove (trochleoplasty) is not universally favoured but has its

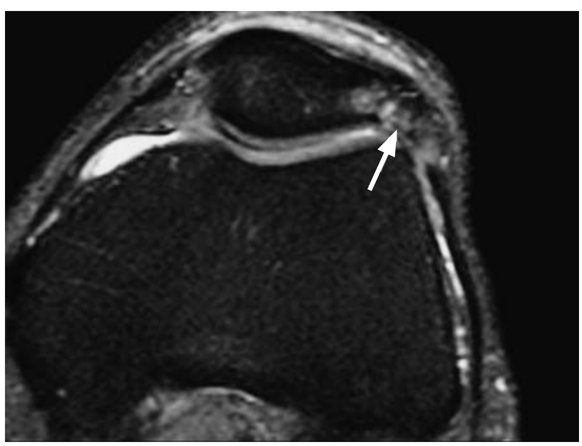

Fig. 18.16. Bipartite patella. Axial fat suppressed MR image showing bipartite patella (*arrow*) with edema either side of the division between the two ossicles

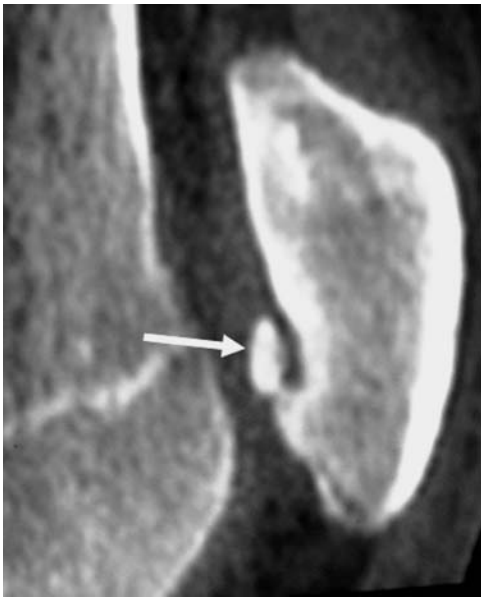
a


b


c

Fig. 18.17a–c. Osteochondritis dissecans of the patellofemoral joint: **a** sagittal reconstruction CT; **b** axial T1 MR image showing a focus of necrotic bone in an articular defect (*arrows*); **c** Sagittal T2 gradient echo MR image showing similar lesion of the trochlear groove

advocates (Verdonk et al. 2005). Popularity of lateral retinaculum release alone has waned in light of evidence questioning the effectiveness of the operation in maltracking without tibial tubercle transfer (Panni et al. 2005). MRI will identify and quantify the anatomical abnormalities. The degree of patellar alta is assessed on sagittal images by calculating the ratio of the maximum length of the patella by the minimum length of the posterior surface of the patellar tendon. This ratio should be under 1.3–1.5 (Fig. 18.18) (Miller et al. 1996; Shabshin et al. 2004). The trochlear groove is best assessed on the axial scans. The groove may be shallow, flat or even convex in its most proximal part (Fig. 18.19). The relative position of the tibial tubercle is clinically estimated by measuring the Q angle, that is, the angle between a line drawn from the anterosuperior iliac spine to the centre of the patella and a line drawn from the centre of the patella to the tibial tubercle. This is a difficult angle to estimate on MRI because of the double obliquity of the tendon. A more realistic method is to measure the tibial tubercle-trochlear groove (TT-TG) distance which approximates the Q angle. This is the distance between the position of the trochlear groove and the

Fig. 18.18. Patellar alta. Sagittal proton density fat suppressed MR image demonstrating a high riding patella

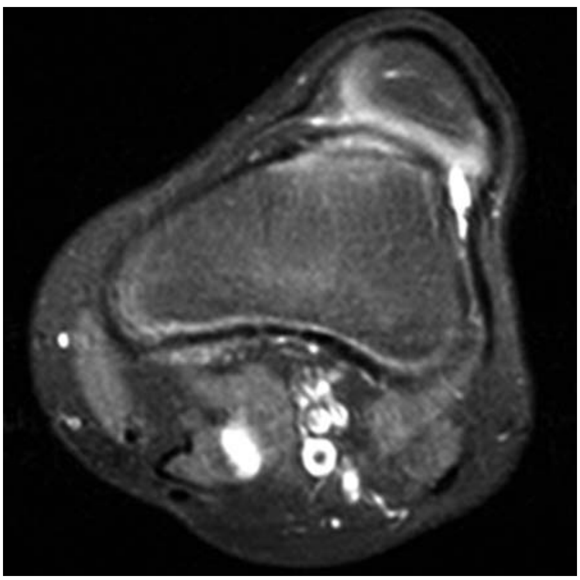

Fig. 18.19. Patellofemoral dysplasia. Axial proton density fat suppressed MR image through the proximal part of a dysplastic convex trochlear 'groove'

tibial tubercle in the sagittal plane. In practice two slices are selected on an axial scans, one at the level of the trochlear groove and one at the level of the attachment of the patellar tendon at the tubercle. The two slices are superimposed. A baseline is drawn along the back of the femoral condyles. Two lines are drawn perpendicular to this baseline, one through the tibial tubercle and one through the deepest point of the trochlear groove. The TT-TG is the distance between these two lines (Fig. 18.20). The upper limit of normal is about 1.7–1.8 cm. In almost all cases – with a value above 2 cm – maltracking can be demonstrated on dynamic imaging (Dejour et al. 1994; McNally et al. 2000). Patients with high TT-TG distance are likely to benefit from tibial tubercle medialisation.

In patients with suspected chronic instability it may also be helpful to document whether or not a patient is indeed maltracking. In some cases this may be obvious on clinical examination but often imaging is required, particularly in obese patients and those with relatively minor degrees of maltracking. Lateral subluxation may be demonstrated on skyline radiographs but this is an insensitive test as maltracking

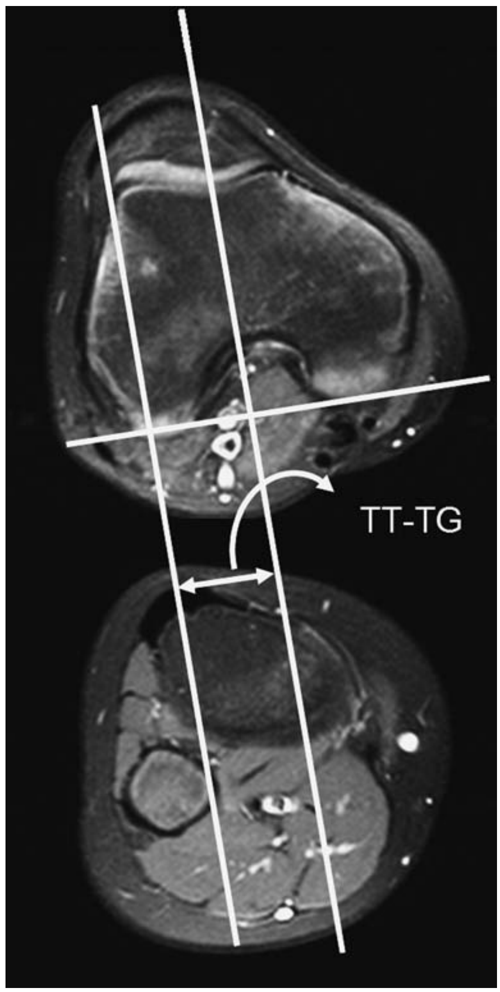

Fig. 18.20. Laterally positioned tibial tubercle. The TT-TG distance is 2.1 cm, which is above the normal range

is maximal from 30° of flexion to full extension. CT or MRI has the advantage of being able to provide axial images of the knee within this range of flexion. The two main methods are pseudodynamic and true dynamic imaging. In the former, static axial sections are obtained through the patella with the knee in various degrees of flexion. The images are then compiled into a cine loop which can be viewed on the monitor. The disadvantage of this method is that it a poor simulation of patellar movement during active knee extension. Dynamic imaging acquires data while the knee is actually moving. One method is to acquire multiple rapid axial images through the patella as the knee is slowly extended. We use a deflatable beach ball jammed between the shins and the roof of the magnet to help control the rate of extension. A continually repeated series of around five axial images and one sagittal image are obtained through the patella during extension. For each series the slice through the centre of the patella is selected and a cine loop created (Fig. 18.21). The sagittal slices can also be compiled into a cine loop to document the range of excursion achieved by the patient. Interpreting the cine loop is subjective. We divide the cases into three grades. Grade one, which represents the mildest form of maltracking is common in the asymptomatic population, whereas grade three is almost always associated with symptoms (O'Donnell et al. 2005).

18.3.5.5 Lateral Patellar Compression Syndrome

In this condition there is little subluxation but abnormal pressure on the lateral facet, supposedly due to a tight lateral retinaculum. The diagnosis is usually clinical but tilting of the patella without subluxation may be seen on dynamic imaging. Patients may respond to lateral retinaculum release (Panni et al. 2005).

18.4 Conclusion

Most cases of anterior knee pain originate from the patellar tendon, Hoffa's fat pad or the patellofemoral joint. Most cases do not require imaging. Acute traumatic pain requires plain films to exclude fracture supplemented by MRI if patella dislocation is considered a possibility. Soft tissue overuse injuries of the patellar tendon are best assessed by ultrasound. MRI is the technique of choice for assessing the patellofemoral joint and abnormalities of Hoffa's fat pad. Plain films are of limited value in the assessment of chronic anterior knee pain.

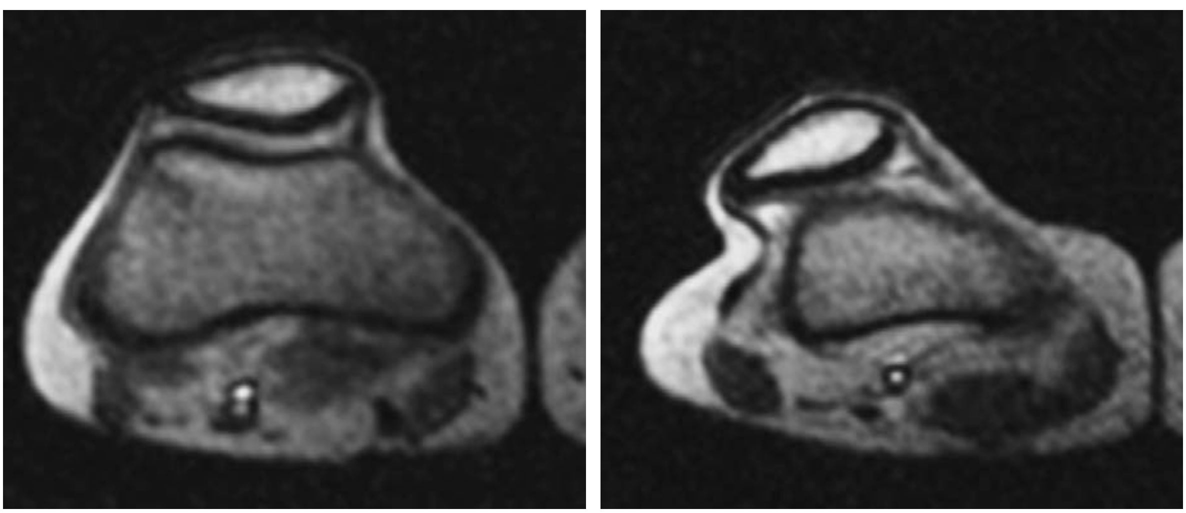

a b

Fig. 18.21a,b. Patellar maltracking. Axial images with one second acquisition time in: **a** 30° of flexion; **b** full extension. There is lateral subluxation and tilt of the patella in extension

Things to Remember

1. The triad of MRI findings found in patellar dislocation is specific for this injury.
2. Ultrasound is an excellent method of assessing the patellar tendon and other superficial soft tissue injuries. No other imaging is required in the vast majority of cases.
3. 'Patellofemoral pain syndrome' merely describes a symptomatic state. Imaging is usually not required.
4. Patellofemoral dysplasia, a complex disorder involving the position of the patella and the tibial tubercle and the shape of the trochlear groove, is best assessed by MRI.
5. True dynamic imaging is possible with MRI to demonstrate maltracking.

References

Bellemans J, Cauwenberghs F, Witvrouw E et al. (1997) Anteromedial tibial tubercle transfer in patients with chronic anterior knee pain and a subluxation-type patellar malalignment. Am J Sports Med 25:375–381

Blankstein A, Cohen I, Heim M et al. (2001) Ultrasonography as a diagnostic modality in Osgood-Schlatter disease. A clinical study and review of the literature. Arch Orthop Trauma Surg 121:536–539

Chung CB, Skaf A, Roger B et al. (2001) Patellar tendon-lateral femoral condyle friction syndrome: MR imaging in 42 patients. Skeletal Radiol 30:694–697

Cothran RL, McGuire PM, Helms CA et al. (2003) MR imaging of infrapatellar plica injury. AJR Am J Roentgenol 180:1443–1447

De Smet AA, Ilahi OA, Graf BK (1997) Untreated osteochondritis dissecans of the femoral condyles: prediction of patient outcome using radiographic and MR findings. Skeletal Radiol 26:463–467

Dejour H, Walch G, Nove-Josserand L et al. (1994) Factors of patellar instability: an anatomic radiographic study. Knee Surg Sports Traumatol Arthrosc 2:19–26

Fredberg U, Bolvig L (2002) Significance of ultrasonographically detected asymptomatic tendinosis in the patellar and achilles tendons of elite soccer players: a longitudinal study. Am J Sports Med 30:488–491

Gebarski K, Hernandez RJ (2005) Stage-I osteochondritis dissecans versus normal variants of ossification in the knee in children. Pediatr Radiol 35:880–886

Gisslen K, Alfredson H (2005) Neovascularisation and pain in jumper's knee: a prospective clinical and sonographic study in elite junior volleyball players. Br J Sports Med 39:423–428

Helpert C, Davies AM, Evans N et al. (2004) Differential diagnosis of tumours and tumour-like lesions of the infrapatellar (Hoffa's) fat pad: pictorial review with an emphasis on MR imaging. Eur Radiol 14:2337–2346

Hunt DM, Somashekar N (2005) A review of sleeve fractures of the patella in children. Knee 12:3–7

Iossifidis A, Brueton RN (1995) Painful bipartite patella following injury. Injury 26:175–176

Jee WH, Choe BY, Kim JM et al. (1998) The plica syndrome: diagnostic value of MRI with arthroscopic correlation. J Comput Assist Tomogr 22:814–818

Kirsch MD, Fitzgerald SW, Friedman H et al. (1993) Transient lateral patellar dislocation: diagnosis with MR imaging. AJR Am J Roentgenol 161:109–113

Larson RL, Osternig LR (1974) Traumatic bursitis and artificial turf. J Sports Med 2:183–188

Matava MJ (1996) Patellar tendon ruptures. J Am Acad Orthop Surg 4:287–296

McNally EG, Ostlere SJ, Pal C et al. (2000) Assessment of patellar maltracking using combined static and dynamic MRI. Eur Radiol 10:1051–1055

Miller TT, Staron RB, Feldman F (1996) Patellar height on sagittal MR imaging of the knee. AJR Am J Roentgenol 167:339–341

Muhle C, Ahn JM, Yeh L et al. (1999) Iliotibial band friction syndrome: MR imaging findings in 16 patients and MR arthrographic study of six cadaveric knees. Radiology 212:103–110

O'Donnell P, Johnstone C, Watson M et al. (2005) Evaluation of patellar tracking in symptomatic and asymptomatic individuals by magnetic resonance imaging. Skeletal Radiol 34:130–135

Panni AS, Tartarone M, Patricola A et al. (2005) Long-term results of lateral retinacular release. Arthroscopy 21:526–531

Peters TA, McLean ID (2000) Osteochondritis dissecans of the patellofemoral joint. Am J Sports Med 28:63–67

Saddik D, McNally EG, Richardson M (2004) MRI of Hoffa's fat pad. Skeletal Radiol 33:433–444

Shabshin N, Schweitzer ME, Morrison WB et al. (2004) MRI criteria for patella alta and baja. Skeletal Radiol 33:445–450

Terslev L, Qvistgaard E, Torp-Pedersen S et al. (2001) Ultrasound and power Doppler findings in jumper's knee - preliminary observations. Eur J Ultrasound 13:183–189

Vanhoenacker FM, Bernaerts A, Van de Perre S et al. (2002) MRI of painful bipartite patella. JBR-BTR 85:219

Verdonk R, Jansegers E, Stuyts B (2005) Trochleoplasty in dysplastic knee trochlea. Knee Surg Sports Traumatol Arthrosc 13:529–533

Injuries of the Ligaments and Tendons in the Ankle and Foot

19

David J. Wilson

CONTENTS

Box 19.1. CT

- High radiation dose
- Poor soft tissue contrast
- Not indicated in the assessment of ligament injuries

Box 19.2. Radiography

- Not indicated in ligament injuries

Box 19.3. Ultrasound

- Excellent tool for assessing the superficial soft tissues
- Allows stress testing of ligaments
- Quick, easy and cheap
- Patient friendly
- Dynamic and Doppler imaging useful
- Direct interaction with patient often helpful

Box 19.4. MRI

- Excellent tool for assessing joint, bones and soft tissues
- Sensitive and specific for most ligament injuries
- Expensive and not very patient friendly
- Shows associated bone disease
- Easier to interpret than US for the inexperienced
- May not show dynamic instability

D. J. Wilson, MD, FRCP, FRCR
Senior Clinical Lecturer University of Oxford, Consultant Radiologist, Department of Radiology, Nuffield Orthopaedic Centre and John Radcliffe Hospital, NHS Trust, Windmill Road, Headington, Oxford OX3 7LD, UK

19.1 Introduction

Acute injuries to the ankle and foot present a substantial portion of cases of sporting injuries. Running, twisting and turning activities all present the athlete with continued risk of an injury which might range from a simple ankle sprain to a career threatening injury. To place imaging in its proper context one must understand that the vast majority of injuries to the ankle are dealt with by the athlete alone and resolve spontaneously. Only the minority of all are presented to a clinical team and of these an even smaller minority require any form of investigation or decisive management.

The issues that we must address is first how this triage process occurs to ensure that those with relatively minor injuries are not over investigated, but also to establish need for investigation in those who may dismiss their injuries as trivial when early intervention might prevent medium to long-term disablement.

Changes in the availability, quality and understanding of the imaging appearances of tendon ligament injuries have made a substantial impact on any management of sporting trauma. On many occasions a substantial increase in information has not yet been met by a significant alteration in clinical practice. It may be that as time goes by our increased knowledge of the nature and type of injury will allow us to divide patients into those who require newer and novel forms of treatment from those who are unlikely to benefit (Bencardino et al. 1999; Lazarus 1999; Schlegel et al. 1999; Bleakney and White 2005). In this chapter I will not only deal with the current state-of-the-art knowledge but also address the potential of imaging to act as a tool for the clinical investigator looking towards novel forms of management.

The vast majority of soft tissue injuries will settle spontaneously with rest, elevation, analgesia and treatment with ice packs and indeed many minor injuries require no active management. Initial management will include plain films to exclude fracture when there is bone tenderness. If the individual's occupation or sporting career do not depend on early use of the injured limb then it is often reasonable to treat conservatively. However, there will be occasions where the high performance athlete and those whose occupation depends on early activity, may warrant more complex investigation to determine the extent and nature of the injury and the safety of early mobilisation.

A prerequisite for understanding traumatic ankle pathology is a thorough knowledge of the anatomy of the ankle ligaments. This is summarized in Figures 19.1 and 19.2.

Fig. 19.1. Ligaments of the lateral side of the ankle

Fig. 19.2. Ligaments of the medial side of the ankle

19.2 Mechanisms of Ankle Injury

The most common injury to the ankle is due to an inversion stress. The majority of these events will lead to tearing of the anterior lateral soft tissue structures including the talofibular and tibiofibular ligaments. Severe injuries and those injuries occurring in the older age group with less resilient bones may fracture.

Eversion injuries are much less common. However, the same rules apply and the imaging assessment is very similar.

Direct axial loading injuries typically from a fall from a height or descending from a jump are more likely to cause compression fractures in the tibia, talus and the calcaneus. This chain of bones may take the whole body weight. Paradoxically falls of less than 30–40 cm in height may produce much greater stress on this complex than a fall where the individual has time to react to the sensation of descent by contracting muscles in the lower limb. We will all have experienced the shock of impact that occurs when we mistakenly think that we have reached the bottom of the staircase and then take an additional step. The descent of a step is insufficient height for the nerve conduction to occur from labyrinth to cerebral cortex and downward to the motor pathways. The clinician may mistakenly imagine that a descent from a modest height will not lead to an injury.

Repetitive strain most commonly causes stress injuries in the forefoot and particularly the second metatarsal. In this chapter we will discuss the investigation and assessment of patients with potential stress injury. Tears of the Achilles tendon are in many circumstances a form of stress injury. Whilst an acute hyperextension force may lead to a tear in the tendon, it is far more common that the force involved is relatively minor. The previous minor injuries and repetitive strain seem to predispose this ligament to partial and full thickness tears. In this area imaging has made a significant impact in management protocols (Linklater 2004). Unfortunately not all clinical centres have taken advantage of these changes and clinical teams should study this advancing area in detail.

19.3 Inversion Injuries of the Ankle

The nature of the damage in an inversion injury will depend on the velocity of the impact, the weight of the individual, the age of the patient and weaknesses generated by previous injuries. If there are elements of rotation to the inversion, this may affect different parts of the ligamentous and bony complex. In simple terms an inversion injury initially leads to stretching and minor intra substance tears of the lateral and anterior lateral ligamentous structures (Fig. 19.1). In younger patients the ligaments then start to fail. The talofibular ligament being the first and most common to rupture; this is a relatively thin structure and susceptible to minor inversion injuries. The anterior tibiofibular ligament which has two discrete segments and arguably three components may tear partially or completely. Only in the more severe injuries does calcaneofibular ligament tear. This ligament is three to five times thicker than the anterior lateral ligamentous structures and its rupture very commonly leads to long-term instability. It is much more likely that a surgeon would consider repair of injuries to this ligament, both in the sporting and the non-sporting individuals.

The distal fibula is prone to fracture. If there is a rotatory element to the injury, spiral fractures may occur or if there is simply pure inversion, avulsion of the tip of fibula may result. The incidence of fractures increases with age. There is a good evidence of clinical examination with a careful palpation will adequately exclude bony injury and obviate the need for examination by plain film. Should there be doubt or suspicion then plain radiographs will normally be more than sufficient to identify and classify the type of fracture. Depending on the nature of the fracture assumptions may be made about the integrity or damage to ligamentous structures.

The peroneus brevis tendon inserts onto the proximal part of the fifth metatarsal. Severe inversion injuries may lead to injuries of this tendon or, perhaps more commonly, avulsion fractures of the proximal fifth metatarsal. Clinical suspicion of this injury should be raised when there point tenderness. The first investigation should be a plain radiograph.

Direct imaging of the ligamentous structures is best achieved with either ultrasound or MRI (Figs. 19.3 and 19.4).

19.3.1 Ultrasound

Ultrasound has a very high line pair resolution when compared to MR, provided that it is used for superficial structures. Around the foot and ankle all the ligaments and tendons are superficial and therefore very well visualised in fine detail with high resolution ultrasound. The signs of ligamentous injury on ultrasound are failure to identify the normal structures, thickening of the normal ligament, adjacent haemorrhage and edema, synovial or soft tissue hyper-

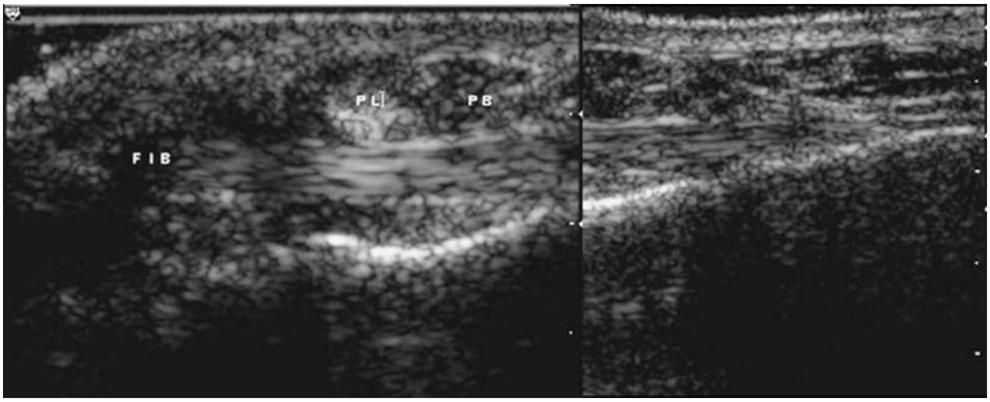

Fig. 19.3. Normal calcaneo-fibular ligament on a composite ultrasound image

Fig. 19.4. Normal calcaneo-fibular ligament. Axial FSE T2-weighted MR image of the calcaneo-fibular ligament, the foot is held in an equinus position

trophy (Fig. 19.5). In the repair stages granulation tissue and reactive synovitis may lead to new blood vessels which can be identified on power Doppler imaging. Because the anatomy of the lateral ligamentous structures is complex, imaging in multiple planes will be necessary. A clear understanding of the normal location of the ligaments is essential to interpret the significance of their absence. Comparison should be made with the normal and unaffected limb to be certain that a ligament is truly absent. Dynamic stressing of the ligament by either passive or active inversion of the foot and ankle increases the sensitivity of ultrasound in detecting injuries of the ligaments. Paradoxical motion is when one bone moves away from the other in a location where it should be tethered. In an acute injury, the pressure involved should be very mild and should not cause the patient significant discomfort. Even minor degrees of movement are often sufficient to confirm a full tear of the ligament. In the case of chronic instability where the local pain has settled, the stress applied may be more vigorous, however it is recommended that the movements involved again are small, as careful observation of relatively mild motion is usually more sensitive than dramatic degrees of stress. Soft tissue edema and synovitis are demonstrated by alteration in the tissue contour with thickening of the tissue planes. Soft tissue edema is reflected by a reduction in the echo pattern (hypo-echogenicity) and scar tissue which will be seen as a more reflective material. Synovial tissue within the mortise joint or anterolateral gutter may hypertrophy particularly in chronic ankle strain. This may lead to a mass effect in the anterolateral gutter (Fig. 19.6). This so-called synovitic lesion may in turn impinge against the adjacent bony structures and cause significant dysfunction ("anterolateral impingement syndrome"). This is typically seen in professional footballers and those whose activity leads to rapid turning and kicking motions (Linklater 2004; Robinson and White 2005). This area is difficult to examine by imaging as the synovitic mass may sit deep within the anterolateral gutter. It has a similar appearance on MRI to adjacent soft tissues (Fig. 19.6). The accuracy of MRI in detecting lesions that are clearly identified at subsequent arthroscopy is, however, poor. Recently it

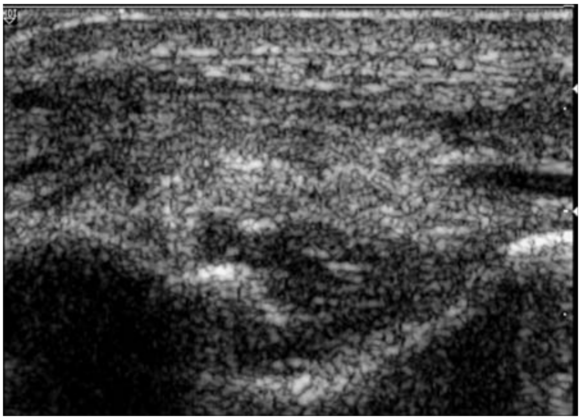

Fig. 19.5. Ruptured talo-fibular ligament. Axial ultrasound. There should be a band of echogenic fibres running horizontally across the image, the examiner must know where to find this structure to be sure that it is absent

has been demonstrated that ultrasound examination with the addition of a dynamic compression of the fibular against the tibia is a more accurate technique in detecting synovitic lesions (Fig. 19.6). The lesion is seen as a mushroom shaped object which emerges from the anterolateral gutter on a compression of the two bones. There is a high correlation between this appearance and arthroscopic findings.

Repetitive injury to joints may also be associated with pigmented villonodular synovitis (PVNS). This is a benign but locally aggressive tumour of a single joint that is seen more commonly in those who have been athletically active. It should be considered in those with a destructive monarthropathy and when MRI shows signal distortion that suggests hemosiderin deposition (Fig. 19.7) in a joint (Saxena and Fullem 2004).

a

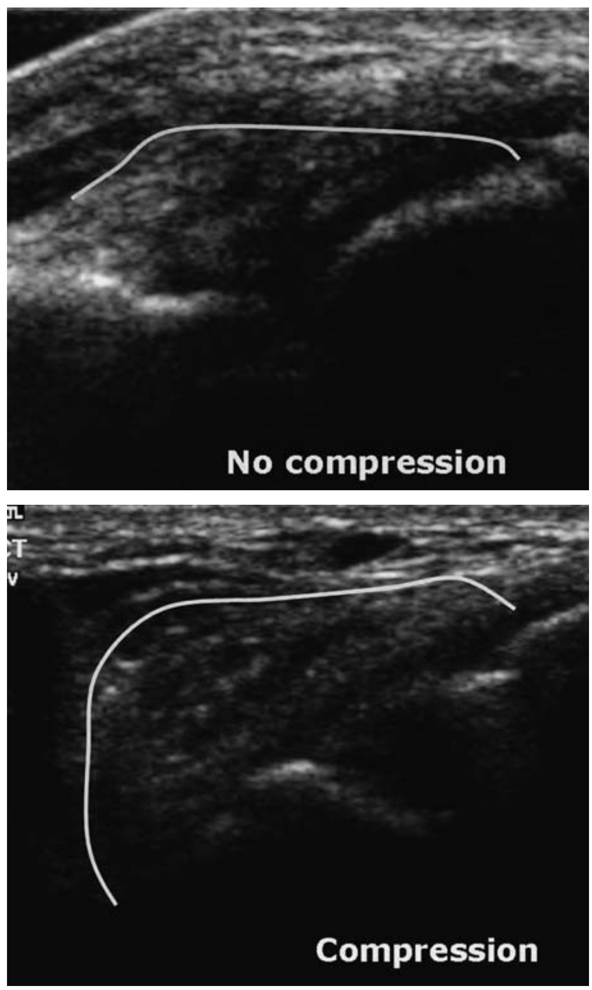

b

c

Fig. 19.6a–c. Anterolateral gutter pain and swelling are symptoms of a synovitic lesion (anterolateral impingement syndrome). This axial MRI (**a**) shows a low signal mass adjacent to some joint fluid and absence of the anterior talo-fibular ligament. Ultrasound examination shows a bulging mass and no ligament (**b**). When the tibia is pressed towards the fibula this mass pushes out in an anterior direction (**c**)

Fig. 19.7. PVNS. Sagittal gradient T2* MR image shows low signal intensity areas with blooming artefact (due to hemosiderin deposition) at the tibiotalar joint, subtalar joint and along the course of the flexor hallucis longus tendon (image courtesy of F. Vanhoenacker)

19.3.2
MRI

This is commonly used in the assessment of the lateral ligamentous structure (Van De Perre et al. 2004). T1 weighted images are particularly useful at demonstrating the normal anatomy. Ligaments will appear black against the adjacent fat which will be white. In case of injury, T2 weighted images will show edema in the soft tissues and if fat suppression is used then this can easily be differentiated from fatty structures. Therefore T2 weighted images with fat suppression, or perhaps more sensitively, Fast STIR images should be employed (Morrison 2003; Narvaez et al. 2003a, b).

Because the anatomy of the lateral complex is variable, the choice of imaging planes is difficult (Zoga and Schweitzer 2003). True axial images are particularly useful for looking at both the anterior and posterior tibiofibular ligaments. The anterior talofibular ligament will also be seen on most axial images although arguably an oblique axial running along the plane of this ligament may be more precise. Much more difficult is the calcaneofibular ligament (Figs. 19.4 and 19.8). This is unfortunate as it is the most structurally important and therefore where we would like to image most accurately. The calcaneofibular ligament runs in oblique plane from the calcaneus running anteriorly and superiorly to the fibula. The angle varies with individuals and the shape of the hind foot. It is very difficult to judge the inclination of the best imaging plane to produce a true axial of this ligament. It is common that axial images will show the ligament on multiple slices and it is difficult to follow its integrity even with MIP reconstructions. Alternative strategies are to place the foot in an equinus position, which elevates the calcaneus, making the calcaneofibular ligament a more horizontal structure (Figs. 19.4). In this position a true axial is more likely to show the calcaneofibular ligament in its full length but this may be a difficult position for the patient to achieve and hold, particularly if the ankle is painful. Therefore it may be easier to examine the foot

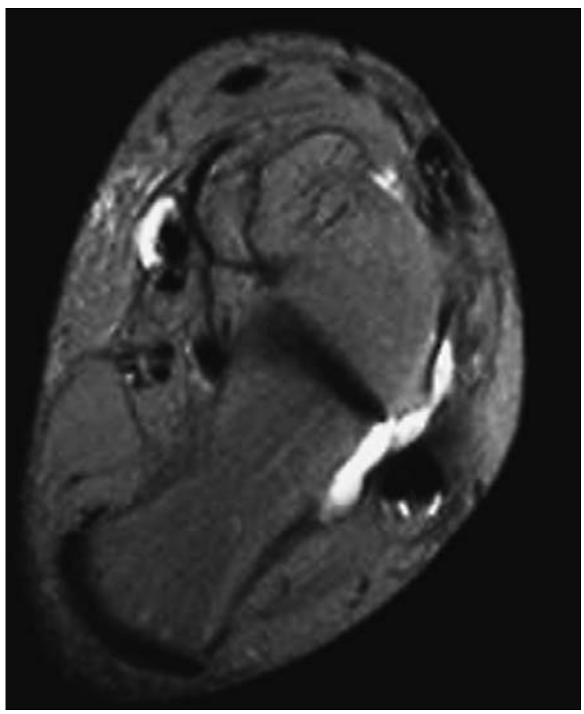

Fig. 19.8. Complete rupture of the calcaneo-fibular ligament. Axial FSE T2-weighted MR image shows fluid from the joint filling the space where the ligament should be

in a neutral position and incline the imaging plane with the anterior margin more cranial. The difficulty is how to assess the degree of angulation that would be required for an individual. Careful palpation of the ankle and judgement of the imaging plane by the examining technician or radiographer may assist. True 3D volume imaging of this region has an advantage that reconstructions can be made in different planes. However, 3D volume is most effectively achieved using gradient echo imaging and the contrast between the ligament and the adjacent structure is not as effective as it is on spin echo imaging. Therefore 3D volume images are more difficult to interpret.

19.4 Eversion Injuries of the Ankle

The first structure to fail in an eversion injury is the medial collateral complex (Fig. 19.2). This is a deltoid (triangular) shape. Whilst it may be anatomically described as being divided into the tibiotalar and tibiocalcaneal components, dissection is more likely to show a continuous sheet of ligaments. Avulsion injuries of the medial malleolus are a common accompaniment and these will be associated with point bony tenderness. Impaction of the everted hind foot against the fibula may cause fractures of lateral structures or diastasis of the tibia from the fibula with rupture of the intra-osseous membrane and the anterior and posterior tibiofibular ligament. When fractures and complex injuries of this type occur it may be useful to assess the functional stability with the patient under a general anaesthetic using stress radiographs. In the setting of an acute injury stress views are not indicated as pain inhibition will prevent abnormal motion and this type of examination would be exceptionally painful. Direct imaging of the medial collateral complex may be performed with either ultrasound or magnetic resonance imaging.

19.4.1 Ultrasound

Ultrasound examination has the advantage that it is fast and easy to perform, although experience is required for correct interpretation. The ligament should be examined in all its sub-components including the anterior, middle and posterior portion. Sprains and tears may affect part, or all, of the ligament. A clear understanding of the anatomy is important as the operator should be able to reliably find the normal medial collateral complex in order that its absence can be definitely detected. Absence of the ligament itself is the primary sign of a rupture. Loss of clarity, thickening, adjacent edema and haematoma are supplementary signs. Perhaps most useful is to perform dynamic stress. Even in the relatively acute injury, very mild degrees of stress will show alterations in the dynamics of the collateral ligament. The bones will move in a paradoxical direction with no tethering. Comparison can be made with the normal unaffected side to assess the normal degree of ligamentous laxity in individual patients. When examining with dynamic stress it should never be necessary to cause discomfort; however in a more acutely injured ankle a degree of stress applied is very mild. Power Doppler imaging allows the examination of the soft tissues for vessel injection which is an indication of a repair process.

19.4.2 MRI

Magnetic resonance imaging is best achieved using a combination of T1- and T2-weighted images. Ideally the T2-weighted images should be with either spectral fat suppression or a Fast STIR sequence. For the medial collateral complex a true coronal plane is ideal. The signs of ligamentous injury are absence of the normal ligaments, edema, thickening and associated haematoma. MRI has the additional advantage that it will show edema in the bone at the site of the insertion of the ligament if there has been an insertion strain (Trappeniers et al. 2003). Avulsion injuries may be surprisingly difficult to detect on MRI. They are identified as edema in the fragments of bone and low signal lines at the fracture site. Care must be taken in analysing the image and reference made to plain radiographs. When there is doubt and other investigations are not available it may be appropriate to perform plain radiographs and/or CT examination. The importance of detecting bony avulsion is that they are often much pure easier to repair surgically and is clinically difficult to differentiate avulsion from ligamentous injury.

19.5 Foot Injuries

19.5.1 Spring Ligament Tears

MRI is really the only practical way of detecting spring ligament tears. It will also allow diagnosis of concomitant injury or other ligaments as these are common. Surgical repair is possible and effective (Fig. 19.9). A gap in the ligament, edema, irregularity, changes in calibre and associated tendinosis of the posterior tibial tendon are all signs associate with surgically proven tears (Balen and Helms 2001; Toye et al. 2005).

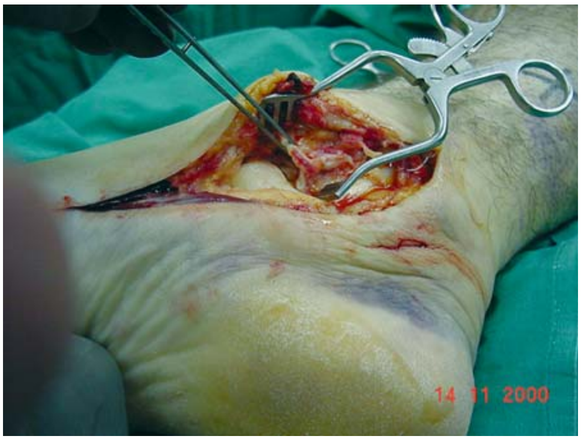

Fig. 19.9. Ruptures of the spring ligament may be repaired by surgery (image courtesy of Mr R. Sharp FRCS)

19.5.2 Plantar Fascia Injuries

Most patients with symptoms that arise from the plantar fascia have chronic insertion pain at the medial aspect of its calcaneal insertion. Tenderness and swelling in this region are fairly specific clinical signs. US and MRI (Fig. 19.10) are useful as they show thickening (>4 mm depth is abnormal), edema and insertional enthesites (Theodorou et al. 2002; Sabir et al. 2005). US guided injection of local anaesthetic and steroid may be and effective therapy. There are advocates of shock wave therapy, "dry needling" and autologous blood injection; currently there is little scientific evidence to indicate the best method (Kane et al. 2001; Zhu et al. 2005). Acute tears are uncommon and appear as defects in continuity on MR or US (Saxena and Fullem 2004).

19.5.3 Turf Toe

This is a condition that principally affects American Football and Australian Rules football players. It results from the use of light footwear, hard surfaces and a hyperextension injury. The injuries that result are rupture of the plantar plate to the first metatarsophalangeal joint associated with separation and sometimes fractures of the sesamoid bones (Ashman et al. 2001; Mullen and O'Malley 2004). MR will show edema and discontinuity in the fascia on sagit-

Fig. 19.10a,b. Plantar fascia rupture. **a** Sagittal T2 FSE fat suppressed MR images of the hind foot of an elite triple jumper who sustained an acute injury of the plantar fascia. **b** Note the edema at the calcaneal insertion and the disruption of continuity best seen on the coronal image

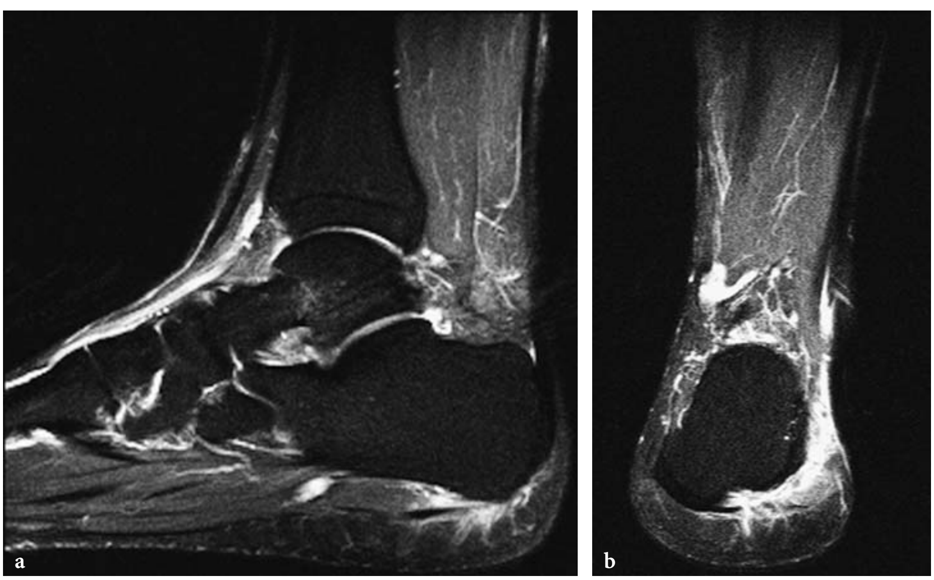

tal images. Fractures of the sesamoids as less obvious on MRI and careful examination of the plain films (Fig. 19.11). or CT may be required. US will show any fracture and may also demonstrate dynamic opening of the gap (Fig. 19.12).

Fig. 19.11. On a lateral radiograph separation of the sesamoid in a sagittal direction demonstrates that there has been a soft tissue plantar plate rupture (image courtesy Mr R. Sharp FRCS)

Fig. 19.12. Athletes with Turf Toe present with pain and swelling over the plantar aspect of the first MTP joint *(cross sign* on the plantar aspect of the foot)

19.6 Stress Injuries

Stress fractures will be dealt with elsewhere in Chap. 7 of this book. Stress injuries to ligaments and tendons occur due to repetitive loading (Sijbrandij et al. 2002; Chambers 2003; Wilder and Sethi 2004). It is argued that it is more likely in the athlete who does not warm up or stretch in advance of exercise. It certainly is much more common as age advances and the strength and integrity of the ligaments and tendons diminishes. It can be argued that the majority of cases of chronic tendinosis are simply results of multiple small injuries to the tendon which leads to partial and incomplete repair. This leads to thickening and enlargement of the tendon with pain, a moderate level of paratenonisis and new vessel growth into the tendon as part of the repair process. Overuse of tendons may lead to inflammatory changes in the synovium that lines the sheaths where the tendons run around corners, particularly under the malleoli and, to a lesser extent, in the anterior part of the ankle. Here the disease is in the tendon sheath itself and the term tenosynovitis is reasonably used.

There is some confusion of terminology. For the purposes of this discussion we use the term tendinosis to indicate a chronic abnormality of the tendon substance itself. Paratenonitis means edema and swelling in the soft tissues adjacent to the tendon, this being discreet from abnormalities of the synovial sheath seen where tendons make acute angles around a joint. Tenosynovitis is swelling and abnormality of the synovium within the tendon sheath, which is often associated with increased quantities of fluid in that sheath. In itself it does not necessarily indicate a disease of the tendon proper. However, tenosynovitis may be seen in association with tendinosis.

Degeneration within the tendon and mucoid change is part of the process of tendinosis. This may be subdivided into chronic thickening, vessel injection (Fig. 19.13), internal splits and tears and eventually complete tendon rupture.

Plain radiographs have little role in the assessment of tendon disease, with the exception of avulsion injuries of a tendon insertion. The two common injuries that of this type that may occur around the ankle are avulsion of the proximal pole of the fifth metatarsal due to the peroneus brevis tendon avulsion and avulsion of the posterior superior aspect of the calcaneus by the Achilles tendon.

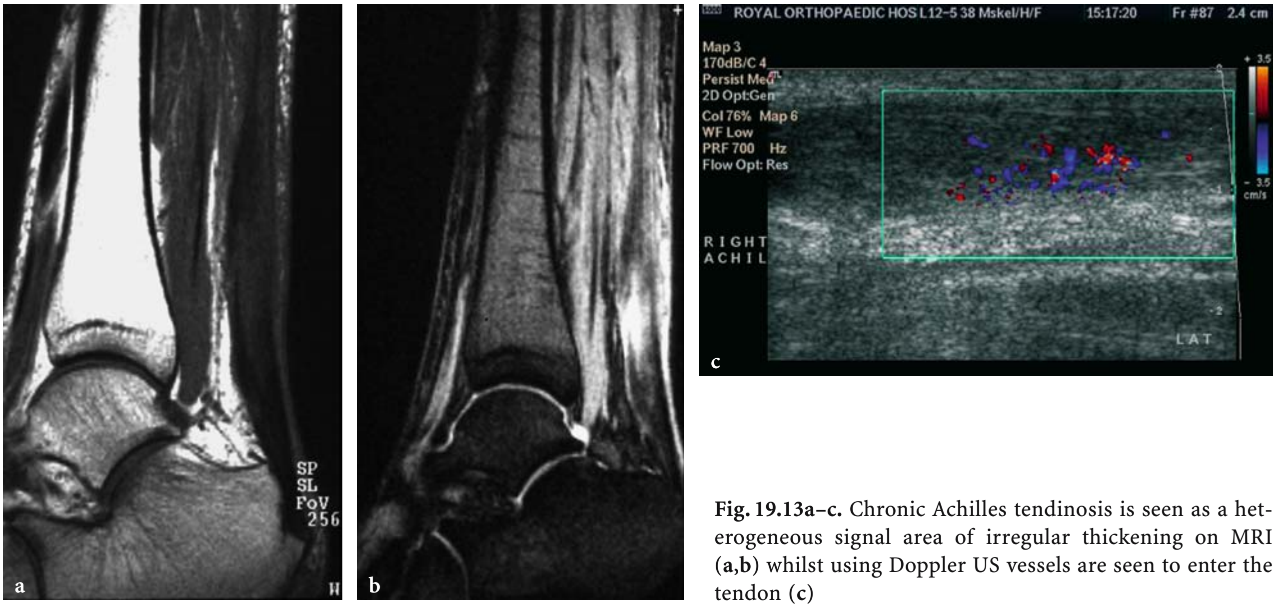

Fig. 19.13a–c. Chronic Achilles tendinosis is seen as a heterogeneous signal area of irregular thickening on MRI (**a**,**b**) whilst using Doppler US vessels are seen to enter the tendon (**c**)

19.6.1 Ultrasound

Ultrasound is probably the best method of initially assessing tendons. The tendon should be examined in a longitudinal and axial plane. Where the tendons run around corners it will be necessary to rotate the probe so that it follows the tendon. In the first instance this is often easiest to image in a plane axial to the tendon, reserving a sagittal image until the examiner has a clear idea of the route of the tendon in the patient being examined. Ultrasound is extremely effective at demonstrating fluid around the tendon and in differentiating synovial thickening from free fluid. Blood vessel injection is easily demonstrated using Power Doppler. Power Doppler is more effective than conventional Colour Doppler imaging at demonstrating the low flow rate in vessels that grow into tendons and synovium.

Examination of tendons using ultrasound must include a dynamic assessment. Moving the tendon actively (muscle contraction) or passively (the examiner moves the limb) may give different information as these actions apply force to different ends of the tendon. When the tendon is more of a supporting structure (for example tibialis posterior), loading strain may be applied by standing or pressing on the limb to pull on the tendon. Dynamic examination should be performed routinely. Movement will differentiate between full and partial thickness tears. Partial tears may open under load when they are difficult to identify on static imaging but they will not separate or show paradoxical movement of the tendon ends.

Longitudinal and internal splits within tendons may only be visible on the axial view and may be difficult to assess on sagittal planes (Figs. 19.14 and 19.15). Impingement of tendons against bony spurs and osteophytes may only be demonstrated on dynamic imaging. In general the amount of fluid in the tendon sheath should not exceed the size of the tendon itself. Therefore the cross sectional diameter of the fluid should be less than the diameter of the tendon. The exception to this rule is flexor hallucis longus. In a significant proportion of the normal population (around 50%) there is a communication between the mortise joint and the flexor longus tendon sheath. This means that small quantities of fluid within the joint may extrude into the flexor hallucis tendon and give the impression that there is a disease of the tendon. The amount of fluid in the tendon sheath may exceed the size of the tendon itself by many times. In these cases care should be taken to examine the tendon in detail to look for tendinosis. The presence of fluid around the flexor hallucis longus tendon as a result of communication with the mortise joint suggests that there is a joint disease.

There should be no blood vessels identifiable within normal tendons. The presence of neovascularity is a specific sign of disease and attempted repair.

Full rupture of a tendon presents with pain and disability. There are many occasions from which these

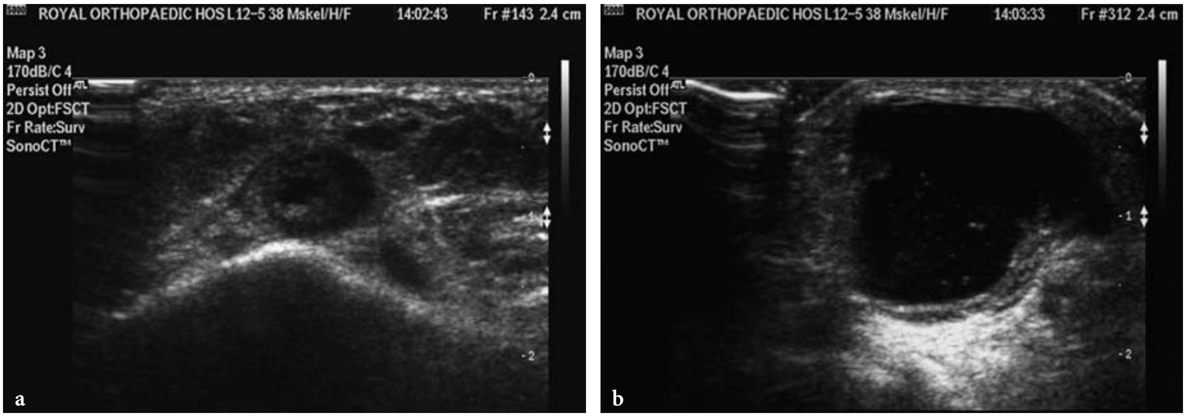

Fig. 19.14a–c. Longitudinal splitting of the peroneus brevis tendon. Using ultrasound a longitudinal split in the peroneus brevis tendon is seen as a dark (hypoechoic) area. In this case the central split (**a**) extends into a ganglion adjacent to the tendon (**b**). Both are seen well on the sagittal view (**c**)

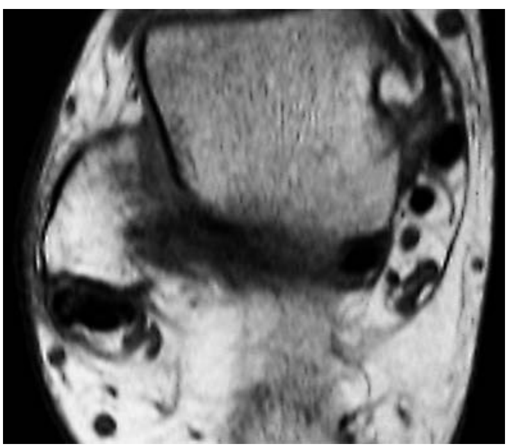

Fig. 19.15. A split of the peroneus brevis allows the longus tendon to enter the defect and is seen a three oval low signal areas on axial MRI

tears are difficult to diagnose clinically. In particular, injury to the tibialis posterior tendon may present with confusing clinical features.

Identification of a full rupture of a tendon is best achieved with ultrasound and a dynamic stress (Fig. 19.16). This is particularly true of the Achilles tendon where the clinical team will be deciding whether to treat the patient conservatively with immobilisation in an equinus position or by surgical procedure (Bleakney and White 2005). In the patient with an acute Achilles injury the clinical questions are firstly whether the injury is to the tendon or the musculotendinous junction. Injuries to the muscular tendonous junction are much more likely to settle spontaneously. Having determined that the injury is in the tendon proper, locating the tear with respect to a fixed anatomical point is important. Surgical repair of tendon ruptures is now commonly performed through small incisions which need to be precisely localised by imaging. The imager should find the rupture and identify its location from a fixed reference point. In the case of the Achilles tendon it is best to choose the posterior superior aspect of the calcaneus, as this is one that can be palpated clinically. Reference should then be made to the position of the tear with relationship to this bony landmark when the patient's foot is in a defined position, for example a true neutral position. If the patient is shortly to undergo surgery it is reasonable to mark

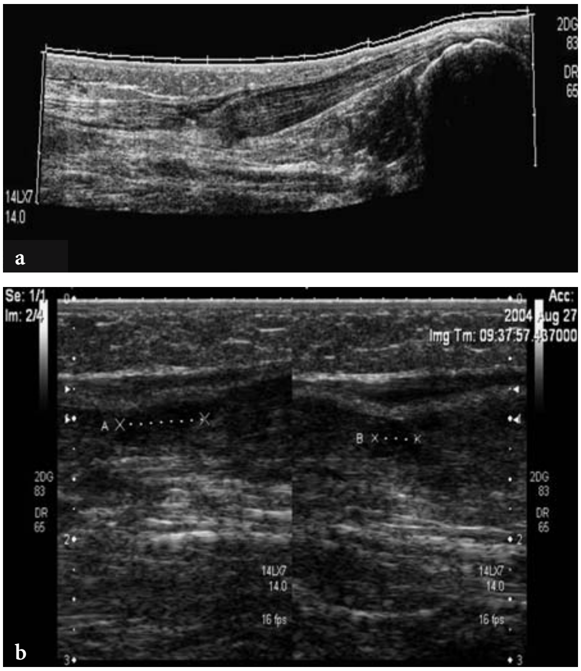

Fig. 19.16a,b. Tear in the mid portion of the Achilles tendon on ultrasound with extended field of view shows (**a**). Dynamic stress achieved by moving the toes up and down by about one centimetre shows the gap open and close confirming that this is a full thickness tear (**b**)

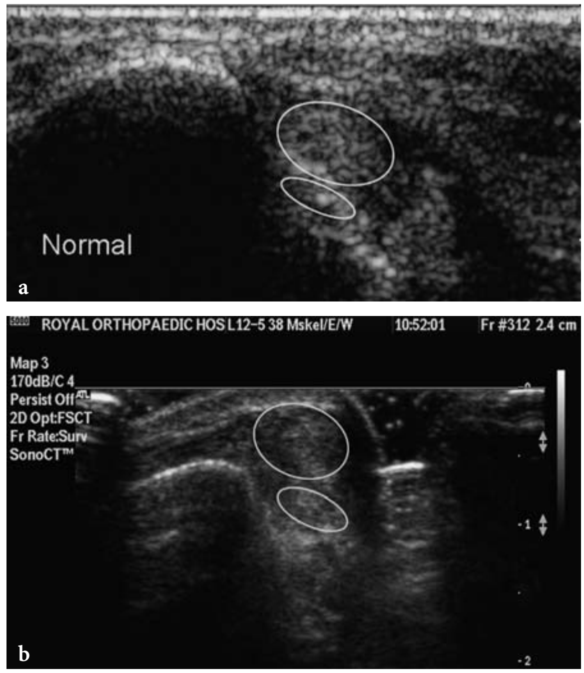

Fig. 19.17a,b. The peroneal tendons lie beneath the distal fibular and appear as two round structures on this axial ultrasound image (**a**). In (**b**) both tendons are seen to sublux into a position superficial to the tip of the fibula. The retinaculum is therefore deficient

the tears on the skin with an indelible marker, again indicating the position the joint was in at the time this marking took place.

At corners tendons are held by retinaculae which are fibrous pulleys. These structures guide the tendon movement and prevent bow stringing. The retinaculae are very thin and difficult to image but injury may be implied. Movement of the tendon away from its normal position and subluxation in varied positions are the specific sign. US (Fig. 19.17) is arguably more effective in this type of case and MRI has a significant error rate (Saxena and Fullem 2004).

Chronic tendinosis probably represents multiple small partial tears and incomplete or unfinished repair. Focal thickening, heterogeneity, loss of a clear tendon margin and vascular ingrowth are all imaging features (Fig. 19.13). However athlete with particular training regimes may show focal changes in tendons and edema in bones as part of the response to the loads imposed on the tendon. These changes are asymptomatic and symmetric (Lohman et al. 2001; Magnusson and Kjaer 2003).

19.6.2 MRI

Axial and sagittal images are the most useful. Axial planes are the most effective at assessing the tendon integrity as these can be performed serially throughout the length of the potentially injured area. Where a tendon runs around a corner, for example the peroneal tendons or the tibialis posterior and the flexor digitorum longus tendons, then the axial images will need to be supplemented by a coronal view to show a true axial of the tendon through the majority of its length. Sagittal images are more difficult to achieve as tendons tend to course in oblique routes and may traverse several slices. 3D volume imaging may be useful but there can be problems in the contrast between the tendon and the adjacent structures as 3D imaging is most commonly achieved using gradient echo sequences. Tenosynovitis will be seen as edema around the tendon seen as high signal on T2 weighted images. Using conventional MRI it is not possible to differentiate the synovial thickening from free fluid. If intravenous Gadolinium DTPA is

given, the increased signal that occurs within most areas of synovitis will assist. However some forms of synovitis have a relatively low flow particularly if they are chronic and there may be continued difficulty in making this differentiation. Note that ultrasound is not limited by these circumstances and does not require contrast agents to differentiate fluid from synovitis. Hence, ultrasound may be a very useful supplement to an MRI examination. Internal degeneration within tendons may be seen as increasing on T1-weighted images due to mucoid change. Internal splits and tears are seen as lines on T1-weighted images and/or edema within the tendon. MRI is a little less sensitive to this diagnosis when compared to ultrasound. Full thickness tears and retraction are relatively easy to identify on MRI, but partial tears, or tears without retraction may be difficult to assess (Fig. 19.18). When there is doubt dynamic imaging should be performed and this is best achieved by a supplementary ultrasound examination. MRI and CT have both been used to image dynamically but this is a more complex and cumbersome method (Renard et al. 2003).

Fig. 19.18. Torn Achilles tendon on a sagittal fat suppressed proton density MR image. The defect is shown but it is uncertain whether there are any residual intact fibres as the tendon ends are not very far apart

19.7 Variations of Normal

Around the ankle and hind foot there are a number of common variants. Some of the normal variations in alignment of tendons and ligaments have been described above. Additional muscles have been described, peroneus tertius, peroneus quartus and accessory soleus (Fig. 19.19) being the most common.

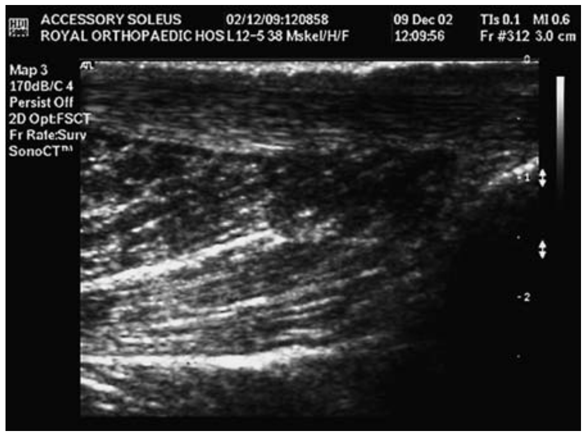

Fig. 19.19. An accessory soleus muscle appears as a very low insertion of the soleus onto the anterior surface of the Achilles tendon

The hallmarks of an accessory muscle are that it is usually bilateral (but not always), the muscle will have a pennate or fibrillar structure on ultrasound and it will contract normally. Some so-called accessory or additional muscles are simply variations in the structure of a normal muscle. It may be argued, for example, that the accessory soleus is simply a very low insertion of the normal soleus belly. The plantaris muscle and tendon is a common variant. It arises from a small muscle belly in the medial side of the proximal calf next to or within the medial head of gastrocnemius. The plantaris tendon runs parallel to the Achilles tendon. It may insert in the calcaneus, but equally it may insert at any point along the Achilles tendon. In patients who not have an identifiable separate plantaris tendon, it is likely that the muscle belly and tendon are embryologically part of the Achilles. This may produce a dent or bump on the Achilles tendon surface. The plantaris tendon is very useful when tendon transfers and transplants are being considered. Pre-operative identification of the plantaris

may be achieved either using ultrasound examination or MRI.

There are rare occasions when accessory muscles may become injured or painful. In these circumstances it may be difficult to differentiate these from soft tissue masses or a tumour. In these circumstances comparison with the normal side is especially useful.

19.8 Image Guided Injections

Injection of a local anaesthetic against topical steroid is a common means of treating chronic injuries in and around the ankle. There are a number of hazards. Unguided injections may penetrate the tendon and cause further damage. The adjacent neurovascular structures may be damaged. Numbing and temporary anaesthesia of a tendon or ligament may allow the patient to perform actions which produce excess loading and lead to rupture of the tendon or ligament. This is a particularly serious risk in those tendons which are weight bearing which includes the majority of those in and around the ankle. Local anaesthetic and steroid injections should only be given to tendons in and around the ankle when careful consideration has been given to the risk of rupture. It is wise to perform initial imaging to ensure that the disease is not within the tendon itself (tendonosis). In those patients where there are partial tears, longitudinal splits, mucoid degeneration or thickening of the tendon considerable care should be taken before considering injection of that region. It is relatively safe to inject patients who have pure tenosynovitis and a normal tendon. On the other hand if a ligament or tendon is fully ruptured, then there is unlikely to be any worsening due to an injection procedure. If consideration is being made to giving injections in patients with tendon abnormalities, then the patient should be carefully consented for the risk of rupture. A surgeon who would be involved in a repair should be consulted and consideration should be given to immobilising the limb for one or two weeks in a lightweight splint. Certainly the patient should be non-weight bearing for several days after the injection if a splint is not provided. Image guidance using ultrasound is the most effective method of placing needles in a location that does not damage adjacent structures. The needle should be introduced as close to 90° to the incident ultrasound beam as possible, as this gives the best visualisation of the needle track (Fig. 19.20). The needle tip can be followed and the injectate observed as it flows into the target tissue.

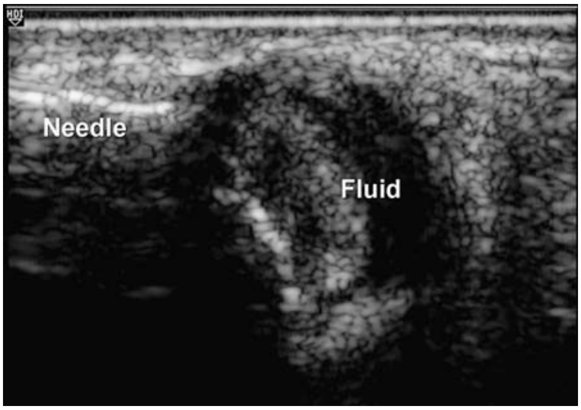

Fig. 19.20. Ultrasound guided intervention. Ultrasound is the ideal means of guiding needles into tendon sheaths. A needle is introduced at almost 90° to the ultrasound beam and moved up to the tibialis posterior tendon sheath

19.8.1 Treatment of Neovascularity

It has been suggested that either dry needling of areas of neovascularity and tendinosis or alternatively the direct injection of autologous blood (drawn from the patient by venesection) will accelerate healing. As yet there are no randomised control trials to assess this technique and it must at present be regarded as experimental. Other authors have suggested the injection of sclerosing agents at the base of the neovascularity; similarly this is an experimental procedure.

19.9 Conclusion

Ultrasound and MRI now provide us with tools to assess and quantify the nature of tendon and ligament disease around the ankle. They are playing an increasing role in prognosis, management and treatment for those patients with ankle injuries.

Things to Remember

1. The initial investigation of sports related ankle trauma should be a standard radiograph in order to exclude fractures, such as a distal fibula fracture or a fracture at the base of the fifth metatarsal. Moreover, avulsion fractures are very difficult to detect on MRI.

2. A major advantage of ultrasound is its ability to perform a dynamic stressing of the ankle ligaments. This allows detection of anterolateral impingement syndrome of the ankle much more accurately than on static MRI.

3. As the anatomy of the lateral ankle ligaments is complex, the choice of MR imaging planes may be difficult. To evaluate the calcaneofibular ligament, the patient may be placed in equinus position. Alternatively, 3D gradient echo technique with subsequent reconstruction along with the plane of the ligament may be required.

4. MRI has the advantage that it will demonstrate associated bone marrow edema.

5. MRI is the only practical way to detect spring ligament tears.

References

Ashman CJ, Klecker RJ, Yu JS (2001) Forefoot pain involving the metatarsal region: differential diagnosis with MR imaging. Radiographics 21:1425–1440

Balen PF, Helms CA (2001) Association of posterior tibial tendon injury with spring ligament injury, sinus tarsi abnormality, and plantar fasciitis on MR imaging. AJR Am J Roentgenol 176:1137–1143

Bencardino J, Rosenberg ZS, Delfaut E (1999) MR imaging in sports injuries of the foot and ankle. Magn Reson Imaging Clin N Am 7:131–49, ix

Bleakney RR, White LM (2005) Imaging of the Achilles tendon. Foot Ankle Clin 10:239–254

Chambers HG (2003) Ankle and foot disorders in skeletally immature athletes. Orthop Clin North Am 34:445–459

Kane D, Greaney T, Shanahan M et al. (2001) The role of ultrasonography in the diagnosis and management of idiopathic plantar fasciitis. Rheumatology (Oxford) 40:1002–1008

Lazarus ML (1999) Imaging of the foot and ankle in the injured athlete. Med Sci Sports Exercise 31:S412–20

Linklater J (2004) Ligamentous, chondral, and osteochondral ankle injuries in athletes. Semin Musculoskelet Radiol 8:81–98

Lohman M, Kivisaari A, Vehmas T et al. (2001) MRI abnormalities of foot and ankle in asymptomatic, physically active individuals. Skeletal Radiol 30:61–66

Magnusson SP, Kjaer M (2003) Region-specific differences in Achilles tendon cross-sectional area in runners and non-runners. Eur J Appl Physiol 90:549–553

Morrison WB (2003) Magnetic resonance imaging of sports injuries of the ankle. Top Magn Reson Imaging 14:179–197

Mullen JE, O'Malley MJ (2004) Sprains–residual instability of subtalar, Lisfranc joints, and turf toe. Clin Sports Med 23:97–121

Narvaez JA, Cerezal L, Narvaez J et al. (2003a) MRI of sports-related injuries of the foot and ankle: part 1. Curr Probl Diagn Radiol 32:139–155

Narvaez JA, Cerezal L, Narvaez J et al. (2003b) MRI of sports-related injuries of the foot and ankle: part 2. Curr Probl Diagn Radiol 32:177–193

Renard M, Simonet J, Bencteux P et al. (2003) Intermittent dislocation of the flexor hallucis longus tendon. Skeletal Radiol 32:78–81

Robinson P, White LM (2005) The biomechanics and imaging of soccer injuries. Semin Musculoskelet Radiol 9:397–420

Sabir N, Demirlenk S, Yagci B et al. (2005) Clinical utility of sonography in diagnosing plantar fasciitis. J Ultrasound Med 24:1041–1048

Saxena A, Fullem B (2004). Plantar fascia ruptures in athletes. Am J Sports Med 32:662–665

Schlegel TF, Boublik M, Ho CP et al. (1999) Role of MR imaging in the management of injuries in professional football players. Magn Reson Imaging Clin N Am 7:175–190, ix

Sijbrandij ES, van Gils AP, de Lange EE et al. (2002) Overuse and sports-related injuries of the ankle and hind foot: MR imaging findings. Eur J Radiol 43:45–56

Theodorou DJ, Theodorou SJ, Resnick D et al. (2002) MR imaging of abnormalities of the plantar fascia. Semin Musculoskelet Radiol 6:105–118

Toye LR, Helms CA, Hoffman BD et al. (2005) MRI of spring ligament tears. AJR Am J Roentgenol 184:1475–1480

Trappeniers L, De Maeseneer M, De Ridder F et al. (2003) Can bone marrow edema be seen on STIR images of the ankle and foot after 1 week of running? Eur J Radiol 47:25–28

Van de Perre S, Vanhoenacker FM, De Vuyst D et al. (2004) Imaging anatomy of the ankle. JBR-BTR 87:310–314

Wilder RP, Sethi S (2004) Overuse injuries: tendinopathies, stress fractures, compartment syndrome, and shin splints. Clin Sports Med 23(1):55–81, vi.

Zhu F, Johnson JE, Hirose CB et al. (2005) Chronic plantar fasciitis: acute changes in the heel after extracorporeal high-energy shock wave therapy–observations at MR imaging. Radiology 234:206–210

Zoga AC, Schweitzer ME (2003) Imaging sports injuries of the foot and ankle. Magn Reson Imaging Clin North Am 11:295–310

Ankle and Foot: Osteochondral Injuries

20

Mario Maas, Milko C. de Jonge, and Ronald A. W. Verhagen

CONTENTS

Box 20.1. Standard radiography

- Used for initial survey and to define additional pathology
- AP view helpful, lateral not in detecting OCL
- When negative, OCL is not ruled out
- Additional AP view with 4 cm heelrise may be beneficial

M. Maas, MD, PhD
M. de Jonge, MD
Department of Radiology, Academic Medical Center, PO Box 22660, Suite C1-210, 1105 AZ Amsterdam, The Netherlands
R. A. W. Verhagen, MD, PhD
Ziekenhuis Hilversum, Department of Orthopedics Surgery & Traumatology, P.O. Box 10016, 1201 DA Hilversum, The Netherlands

Box 20.2. MRI

- Very powerful in detecting OCL
- Bone marrow edema detection is important, yet hampering adequate true lesion demarcation
- All three imaging planes must be used to rule out or to detect concomitant lesions

Box 20.3. MDCT

- Axial high resolution (0.5/0.6 mm) acquisition with coronal and sagittal MPR
- Is as powerful as MRI in the diagnostic workup of a patient with chronic ankle pain
- Enables exact delineation of the OCL
- Provides surgeon with adequate information on location and especially the extent of the OCL

20.1 The Ankle

20.1.1 Osteochondral Injuries

20.1.1.1 Introduction: Specific Anatomy and Incidence

The anatomy of the ankle will not be described in detail. In order to understand better the occurrence and location of osteochondral injuries of the ankle we thought it would be wise to discuss the cartilaginous anatomy briefly.

Since the sports related biomechanics of osteochondral injuries of the ankle is closely related to the sports in which ligamentous ankle injuries and ankle sprains occur, the reader is advised to read the chapter by D. Wilson (Chap. 19).

20.1.1.1.1 Cartilage Anatomy

Osteochondral injuries in the ankle most often occur in the tibiotalar joint most frequently in the talar dome. It is interesting to know that the talus is covered with cartilage not only on top of the talar dome, but also on the medial and lateral facets facing the medial malleolus and the fibula. In a recent cadaver study Sugimoto et al. (2005) examined the thickness of the cartilage at the talar surface. Specific interest was paid to those regions where osteochondral injuries predominantly occur (Sugimoto et al. 2005). In 29 cadaver ankles (22 male) a coronal pie-wedge shaped section of the mid talar dome was obtained, with 2 mm width and 5 mm depth. With the use of radiographs (high resonance X-ray analyzer) measurements were obtained at nine areas in each specimen. The average cartilage thickness of the total area was 1.35 mm (±0.22) in males and 1.11 mm (±0.28) in females. The difference was considered statistically significant between the sexes ($p=0.025$). The mean thickest area was found in the medial talar corner (1.56 mm in males, 1.42 mm in females). The thinnest cartilage was found in the lateral fibular surface (1.00 mm in males, 0.86 mm in females). The fact that only a small sample was measured, a great variation between the samples was found and only one cross section was measured, are study limitations. Compared to the knee, where the cartilage is much thicker, the cartilage in the ankle is thin. This is thought to be due to the fact that the ankle joint is a congruent joint, compared to the knee.

20.1.1.1.2 Incidence

Osteochondral injuries very often are described as sequellae of inversion sprains. Inversion sprains of the ankle are common injuries at all levels of sports worldwide. Approximately 25% of the sprains occur in soccer, 40% in basketball and 23% in athletics (Bergfeld 2005). In 2002, in the Netherlands, 78,000 patients presented at hospital emergency departments with ankle injuries, 59% of which were treated for an inversion sprain (Consumer Safety Institute 2004). In more than 40% of cases the injuries were sports-related. Although most patients go on to an uncomplicated recovery, those who continue to have pain in the ankle and hind-foot can present as a diagnostic problem. The athletes present themselves with chronic ankle pain (Verhagen et al. 1995).

20.1.1.2 Bone Bruise

With the introduction of fat suppressed MR imaging the radiological diagnosis of a bone bruise is introduced in the field of sports medicine. A bone bruise (bone contusion) usually happens during an inversion injury of the ankle. The impaction and rotation forces that occur cause microfractures in the trabecular bone, hyperemia and hemorrhage (Sijbrandij et al. 2002; Rosenberg et al. 2000). While standard radiography will not detect these lesions, the MRI image consists of ill-defined reticular areas of low signal on T1-weighted and high signal on fat suppressed (TSTIR, fat sat T2-weighted) sequences. There usually is a broad based contact with the articular surface, with an intact cortical surface. On Multi Detector Computed Tomography (MDCT) this might show as areas of increased sclerosis, also broad based with the articular surface. The clinical manifestation of these lesions is often non-specific and the clinical significance in the ankle is yet unknown; the clinical consequences of bone bruise around the knee is recently reported (Vincken et al. 2006). The clinical history is essential, because when bone marrow edema is an isolated finding it can be caused by various pathologies such as ischemia, (migrating) osteoporosis, infection or high level of mechanical stress. It is known that in high performing athletes this edema without clinical significance is a frequent encountered phenomenon and should be interpreted with clinical correlation. The appearance of bone bruise on MRI can persist for quite some time. Although there is literature stating that it will persist for 6–12 weeks, in the authors experience in high performing athletes it will persist even longer, since athletes will not stay inactive when there is no physical limitation (Horton and Timins 1997; Morrison 2003).

It is debatable whether bone bruise is a precursor of the development of a talar osteochondral defect (Martinek et al. 1998). It has however become increasingly known that repetitive stress can also be causing and maintain the presence of these lesions

and when continued may lead to the development of a complete osteochondral lesion (Rosenberg et al. 2000). The location of bone bruises at sides where osteochondral talar lesion most frequently occur supports this theory. Reporting such a bone bruise as a precursor of a talar osteochondral lesion by the radiologist may be beneficially for patient management and is therefore advised.

20.1.1.3 Osteochondral Lesion (OCL)

20.1.1.3.1 Background, Definition and Etiology

In 1738 the famous anatomist Alexander Monro I was the first to describe the presence of cartilaginous bodies in the joint in his Medical Essays and Observations, six volumes (1732–1744) (Monro 1738). König described free bodies in the joint and coined the term osteochondritis dissecans in 1888, and Kappis was the first to describe the osteochondral lesion of the talus in 1922 (König 1888; Kappis 1922; Bohndorf 1998; Linz et al. 2001). A lot of aliases appeared in the literature, (such as osteochondral fracture, talar dome fracture and flake fracture) of which osteochondritis dissecans (OCD) probably is the most common designation (Barnes and Ferkel 2003; Stroud and Marks 2000; Linz et al. 2001; Bohndorf 1998). The accepted term to use nowadays is the osteochondral lesion of the talus (OCL), which is defined as the separation of a fragment of articular cartilage, with or without subchondral bone (Bohndorf 1998; Berndt and Harty 1959; Alexander and Lichtman 1980).

The incidence of an OCL after an ankle sprain is probably underestimated because these lesions often remain undetected, not clinically significant or are misdiagnosed as other ankle pathology (Barnes and Ferkel 2003; Benthien et al. 2002). The incidence has been reported to be as high as 6.5% after ankle sprains (Flick and Gould 1985; Verhagen et al. 1995; Benthien et al. 2002). Concomitant pathology in the ankle frequently occurs, with anterior impingement, synovitis and adhesive capsulitis being the most frequent pathology (Benthien et al. 2002). Bilateral lesions occur in 10–25% of cases, suggesting underlying patient susceptibility: etiology is thought to be ossification defects, vascular anomalies and endocrine abnormalities (Verhagen et al. 2003; Bohndorf 1998; Benthien et al. 2002).

An OCL is usually located in the anterolateral or posteromedial aspect of the talar dome. In a recent meta-analysis of over 600 lesions, it was demonstrated that 56% were located medially and 44% located laterally (Tol et al. 2000). Histologically the medial and lateral lesions are identical, but morphologically they differ. The lateral lesions are shallow and more wafer shaped, indicating a shear mechanism of injury (Stroud and Marks 2000; Canale and Belding 1980; Berndt and Harty 1959). The experiments of Berndt and Harty showed a forcible inversion and dorsiflexion with impaction of the talus to the fibula to be the cause of this lesion (Berndt and Harty 1959; Linz et al. 2001). It is thought that all lateral lesions are of a posttraumatic nature (Benthien et al. 2002; Flick and Gould 1985; Tol et al. 2000; Stone 1996).

In contrast, medial lesions are located over the posteromedial surface of the talar dome. They generally are deep, cup shaped, and located posterior, indicating a mechanism of torsion impact (Davis and Alexander 1990; Berndt and Harty 1959). Literature reports only 60% of medial lesions to be posttraumatic from origin (Flick and Gould 1985; Tol et al. 2000; Benthien et al. 2002).

Although initial symptoms may be absent, in chronic cases most patients present with intermittent pain located deep in the ankle joint which increases on weight bearing. On physical examination signs are often lacking. A discrete limitation of range of motion with some synovitis may be present. Local tenderness on palpation with recognition is absent in most cases. Since the OCL is described as an associated injury in patients with chronic lateral ankle instability, a high index of suspicion in this latter patient group may help in detecting the OCL as cause of ankle pain (DiGiovanni et al. 2000).

Since there are no specific pathognomonic signs or symptoms, it is of key importance that the examining physician and radiologist are aware of the fact that an osteochondral lesion could be present: history of flexion inversion injury, exercise related deep ankle pain, sensations of clicking and catching and persistent swelling will raise the suspicion-index (Thompson and Loomer 1984).

20.1.1.3.2
Diagnostic Imaging
Standard Radiography

Standard antero-posterior radiography of the ankle, which is weight-bearing mortise an AP view (20° of endorotation), enables clear delineation of the tibiotalar joint, including a good view of the medial and lateral facets. The talar dome is clearly defined (Fig. 20.1). The weight-bearing lateral view is very useful for detecting accompanying pathology (bony impingement, loose fragment, os trigonum) but will not aid in detecting an OCL. It should be noted that with a normal mortise AP view an OCL is not excluded (Fig. 20.2).

Additional Views

Additional views of value can be AP mortise in plantar flexion. The weight-bearing plantar flexion view is easily accomplished with 4 cm heel rise, which enables a better delineation of the posterior aspect of the talus. Thus the posteromedial located OCL might be better visible (Fig. 20.3).

Although in our experience the adding of this view is beneficial in selected cases, as is shown in Figs. 20.3 and 20.4, a recently performed study could not confirm the potential value of heelrise views in a studied population of patients with chronic ankle pain (Verhagen et al. 2005). The true extent of the lesion is the most important information necessary for surgical planning. This information will not be provided with the heel rise view.

Fig. 20.1. Osteochondral lesion (OCL) AP radiograph. Standard radiograph weight-bearing Mortise view. OCL is suggested at the medial talar dome (*arrow*)

a

b

Fig. 20.2a,b. Cystic OCL, with a negative standard radiography and positive coronal MPR of MDCT. AP Mortise view (**a**) and MDCT with coronal MPR (**b**). No abnormalities are seen on the AP standard radiography. On MDCT the cystic OCL is clearly seen as a hypodense lesion surrounded by sclerosis

Fig. 20.3. Value of heelrise view: AP 4 cm mortise heelrise view. The same patient as in Fig. 20.1, in which heelrise view tangentiates the posterior medially located OCL (*arrow*)

MRI

MRI enables cartilage imaging as well as surrounding bone and soft tissue. When imaging the ankle attention should be focused on coil choice and slice thickness. In the authors opinion it is advisable to image only one ankle using a surface coil. Slice thickness can be three-four mm in three anatomical planes; angulation is not necessary. For detecting an OCL, the MRI protocol is tailored to detect bone marrow edema, cartilage defects and effusion of the joint. However since concomitant ankle pathology frequently is present, this should be taken into account in defining the definite MRI protocol in patients with chronic ankle pain. In our opinion all three anatomical imaging planes are helpful. Sagittal TSTIR and T1-weighted, axial FSE short TE (PD or T1-weighted), coronal fat suppressed T2-weighted and a 3D Gradient T2* sequences with isotropic voxels enabling MPR would be sufficient (Morrison 2003). Cartilage lesions nowadays may be best evaluated using high-resolution FSE intermediate sequences with long echo trains and adding fat saturation (Manaster et al. 2005). The normal cartilage will appear intermediate, whereas a defect will show a heterogeneous or high signal intensity.

Hallmarks for detection of an OCL are edema (high signal intensity) on fat suppressed T2-weighted MR images or TSTIR, low signal on short TE MR images and a high signal intensity within the intermediate cartilage as sign of a defect (Fig. 20.4).

Although the detection of bone marrow edema is a very powerful feature of MR imaging, it also can have its disadvantage. From a surgical point of view it can obscure the true extent of the lesion, making the OCL

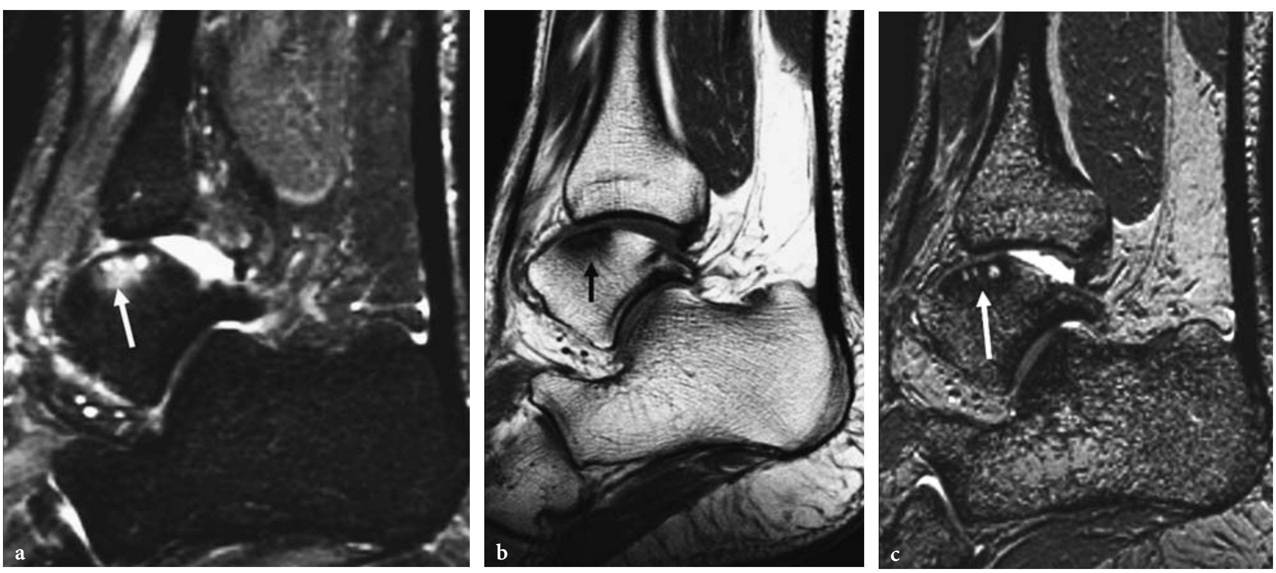

Fig. 20.4a–c. OCL appearance on various MR sequences. Sagittal TSTIR (**a**), sagittal T1-weighted SE (**b**), sagittal Dess 3D (**c**). On TSTIR the edema surrounding the cystic lesions is seen (*arrow*). The true extent of the lesion is not clearly delineated. On the T1 weighted MR image a clearly defined hypointense region is seen, without differentiation between cysts and edema (*arrow*). On the Dess 3D sequence the cystic changes within the lesion are hyperintense, whereas the sclerosis is hypointense (*arrow*)

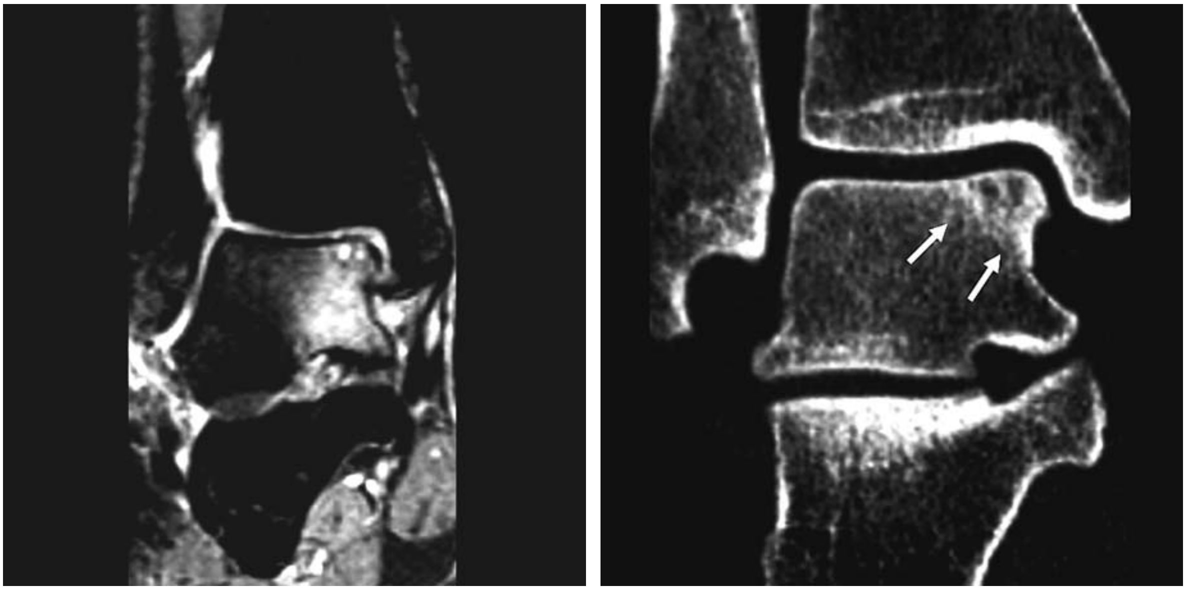

a b

Fig. 20.5a,b. Extent of an OCL. Coronal TSTIR (**a**) and coronal reformatted MDCT (**b**). On the TSTIR images a cystic lesion is seen, however the surrounding edema masks the true extent of the lesion making it difficult for the surgeon to decide whether ankle arthroscopy is sufficient, or whether osteotomy is necessary. The MDCT clearly defines the extent of the OCL

larger in size than truly is the case. This is unhelpful since the planning of the surgical procedure will be hampered. Questions that the surgeon will have and that imaging needs to answer are: "Can this lesion be operated through anterior ankle arthroscopy?", "is a posterior arthroscopy preferable?" or "should a medial malleolus osteotomy be performed?" or "is an arthrotomy indicated?" or "is the subtalar joint involved?". In our daily practice, working in a tertiary referral center for ankle pathology, the use of multidetector helical CT (MDCT) with Multi Planar Reformatting (MPR) is of great value in answering these questions (Fig. 20.5).

Multi Detector Computed Tomography (MDCT)

CT scanning is described as a successful tool, superior to standard radiography in detecting OCLs. Furthermore, it is known to describe the true extent and healing of fragments (Zinman et al. 1988; Stone 1996).

The introduction of multidetector helical CT (MDCT) enables the acquisition of very thin slices (0.5 mm) in a 3D data set. Multiplanar Reformatting (MPR) of this data creates sagittal and coronal plane images, easy to use and interpret, also by non-radiologists. We have been fortunate to gain experience in using MDCT in patients with chronic ankle pain since the mid-1990s. In a recent study it was shown that MDCT with MPR performed as good as diagnostic arthroscopy in detecting or excluding OCLs. Furthermore no statistical significant difference was found between MRI and MDCT in this study (Verhagen et al. 2005). Helical CT gave more certainty than MRI that an OCL was present, where MRI was more certain in a negative test result.

In order to emphasize the gaining role of MDCT in diagnosing OCL, various appearances of arthroscopically proven OCLs are shown (Fig. 20.6). There is a wide spectrum of aspects of OCL on MDCT, ranging from a clear defect in the talar surface, with or without fragments within (Fig. 20.6), a small defect on the lateral fibular surface (Fig. 20.7), to a subtle disturbance of normal bony architecture of the talar bone (Fig. 20.8).

Arthrography Combined with Cross-Sectional Imaging

MR arthrography, both direct and indirect, is described valuable in assessing osteochondral lesions in the ankle (Morrison 2003). It is thought to increase the depiction of unstable lesions; when gadolinium extends under the osteochondral lesion, it is classified as unstable (Morrison 2003; DeSmet et al. 1996). In this way a differentiation can be made between a true unstable lesion and a stable lesion. The MRI protocol needs adjustment, with inclusion of fat suppressed T1-weighted SE MR images (Morrison 2003).

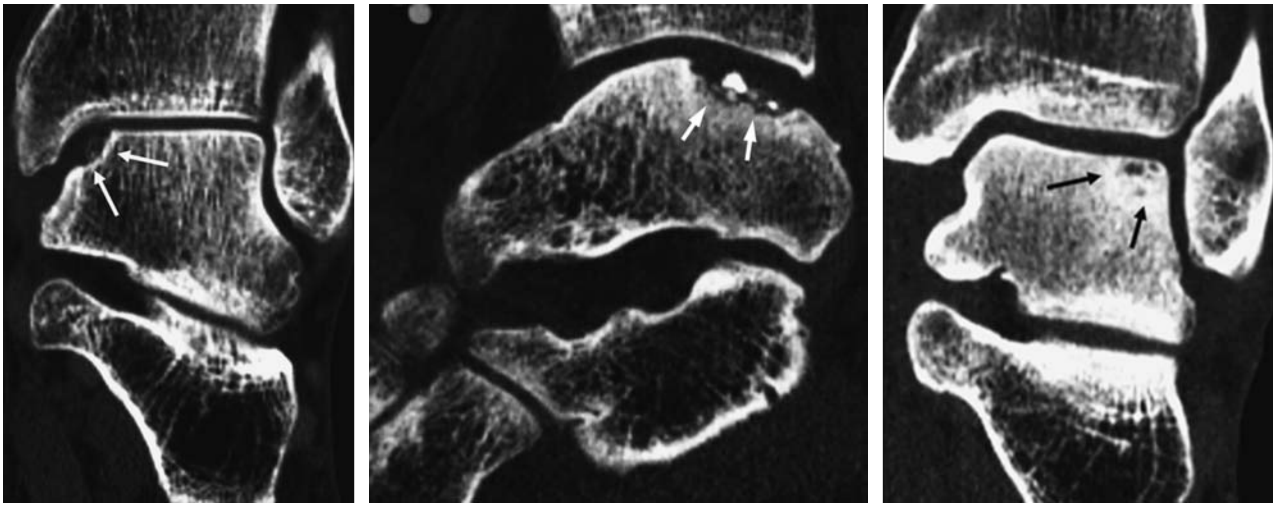

Fig. 20.6a–c. Various appearances of OCL on MDCT. Coronal (**a**), sagittal (**b**) 2-mm MPR of MDCT dataset of the left ankle. A huge defect at the posteromedial part of the talus is seen (*white arrows*), while standard radiography was negative. A large osteochondral lesion is seen with multiple fragments within the defect (*arrows*) (**b**). A multicystic OCL, with a sclerotic border is seen on the lateral talar dome in another patient (*black arrows*) (**c**)

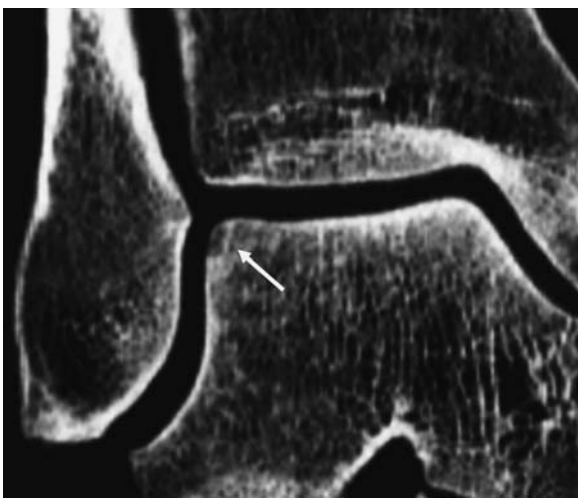

Fig. 20.7. Subtle OCL of the talus. Coronal 2-mm MPR. A very small osteochondral lesion is seen in the lateral talar surface with disrupted architecture (*arrow*)

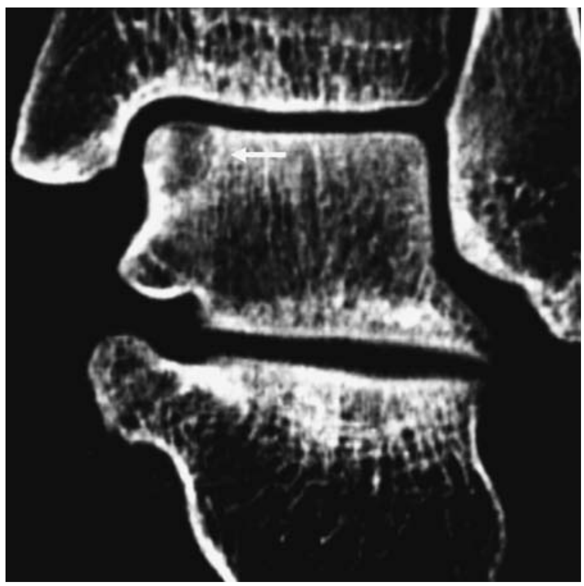

Fig. 20.8. Subtle appearance of a talar OCL. Coronal MPR. The talar bony structure is disturbed in the posteromedial part (*white arrow*)

There have been no reports on the accuracy of CT arthrography for detection of osteochondral lesions in the ankle. However, case reports and small studies suggest that CT arthrography may be a useful tool for assessing the stability or prognosis of osteochondral lesion (Heire 1988; Davies 1989).

More recently it was shown that CT arthrography was superior to MRI, in evaluating cartilage lesions (MR arthrography), or cartilage thickness in the ankle (Schmid et al. 2003; El-Kouhry et al. 2004). The authors however do not have experience with this technique; the results of the study comparing MDCT, MRI and arthroscopy do not make

it necessary to make MRI an invasive technique in patients with an OCL of the ankle (Verhagen et al. 2005).

20.1.1.3.3
Staging

Classification systems are described based on the various techniques described earlier. A short summary is provided.

Radiographic

The classification described by Berndt and Harty (1959) is still the still most frequently used. Stage I lesions are small areas of compressed subchondral bone (7%), stage II lesions are partially detached yet stable (25%), stage III lesions are completely detached but nondisplaced, located in the fragment bed (40%) and stage IV are displaced osteochondral fragments (28%) (Berndt and Harty 1959; Benthien et al. 2002).

MRI

One of the earliest MR based grading of OCLs in the talus was made in the late 1980s (Anderson et al. 1989). Stage I is bone marrow edema, nowadays called bone bruise, stage IIa shows a subchondral cyst, stage IIb incomplete separation of the fragments, stage III complete separation without dislocation, with dislocation in stage IV (Anderson et al. 1989; Josten and Rose 1999). The MRI criteria for instability of the fragment as defined by DeSmet et al. (1990), including high signal intensity on T2-weighted, fluid passing through the subchondral bone or a fluid-filled cyst located deep to the lesion correlated with arthroscopy (Manaster et al. 2005).

Computed Tomography

Using single slice CT Ferkel proposed a CT-based classification of OCD lesions (Ferkel 1992; Ferkel and Scranton 1993; Linz et al. 2001; Benthien et al. 2002). Stage I lesion shows a subchondral cyst with an intact articular surface. Stage IIA shows communication between the cyst and the joint at the talar dome. A stage IIB lesion communicates with an overlying non-displaced fragment. A stage III lesion has a radiolucency around a non-displaced fragment and stage IV shows an unstable displaced fragment.

Arthroscopy

Various classification systems are described, which are not all generally accepted. The most widely accepted staging classification is from Ferkel; it shows grade A being smooth, intact cartilage which is soft and ballotable, stage B has got a rough surface, stage C shows fibrillation or fissures, in stage D a cartilage flap is present. Stage E shows a loose undisplaced fragment, with displacement of the fragment in stage F (Ferkel and Scranton 1993; Bohndorf 1998; Barnes and Ferkel 2003). However a good reproducibility study on arthroscopic staging is lacking.

Discussion on Staging

An interesting observation concerning radiological staging was described in a recent review (Verhagen et al. 2003). It was observed that the radiological classification used varied, widely and that only a minority of authors had based their decision for selection of treatment on staging according to Berndt and Harty. It was concluded that preoperative staging is of minor importance, and that intraoperative staging might be more appropriate. Not the staging of the lesion, but the clinical situation is the important feature. This is important for clinical practice. Radiologists are advised to check with their orthopedic surgeons whether a radiological classification of the OCL is mandatory in preoperative planning. In this way the radiological strategy can be tailored to the need of the surgeon.

20.1.1.3.4
Treatment

Treatment options can be divided into operative or non-operative options. Non-operative options such as immobilization with casting for six to eight weeks in early stages were described as being successful (Pettine and Morrey 1987). Recent ISAKOS consensus stated that asymptomatic or minor symptomatic patients can be treated conservatively, consisting of rest, ice, temporarily reduced weight bearing and in some cases orthosis (Van Dijk 2005). Open surgical procedures also have shown to produce good results in the era prior to arthroscopy (Berndt and Harty 1959; Flick and Gould 1985). However nowadays the most widely accepted therapy in case of any talar OCL is arthroscopic excision, curettage (debridement) and drilling. Many authors reported favorable results (Benthien et al. 2002; Barnes and Ferkel 2003). A recent systematic review, in which the effectiveness of

various treatment options was evaluated, confirmed these results (Verhagen et al. 2003).

A newer operation technique, not included in previous mentioned systematic review is cartilage transplantation with mosaicplasty. It has been shown successful in a large cohort (Hangody et al. 2001). However it should be reserved for those patients that do not respond to first choice treatment of excision, curettage and drilling (Hangody 2004)

20.1.1.3.5 Pitfalls

The presence of kissing lesions, both in talus and tibia, is a well known entity (Sijbrandij et al. 2000; Morrison 2003). It should not be mistaken for osteoarthritis, especially when other signs of osteoarthritis (increased sclerosis, joint space narrowing and bone formation) are lacking.

When using MRI bone marrow edema is seen on both sides of the joint, while no focal pathology may be visible on T1-weighted images. MDCT may aid in correctly diagnosing the kissing lesions; this will guide arthroscopic intervention (Fig. 20.9).

Postoperative evaluation of an OCL is difficult. The anatomical situation has totally changed and without adequate information concerning prior arthroscopy and current clinical situation of the patient the reading radiologist can be misguided (Fig 20.10).

Although arthroscopy is extremely accurate in detection talar OCLs, it seems less powerful in detecting the accompanying tibial lesions (Verhagen et al. 2005). It was stated that "satisfaction of search" may be the mechanism being responsible for this: the treating orthopedic surgeon is comfortable with the idea that the cause has been treated (i.e. the talar OCL), and fails to inspect the tibial plafond systematically (Verhagen et al. 2005). This phenomenon is known from (osteo)-radiological studies and the sports radiologist dealing with OCL in the ankle should be aware of this phenomenon (Samuel et al. 1995; Ashman et al. 2000). Stressing the presence of lesions in both tibia and talar articular surface in the radiological report is advised.

20.1.2 Osseous Injury

In any sports an unexpected movement may cause acute osseous injury. The trauma mechanism will easily explain the fracture extension. The more fre-

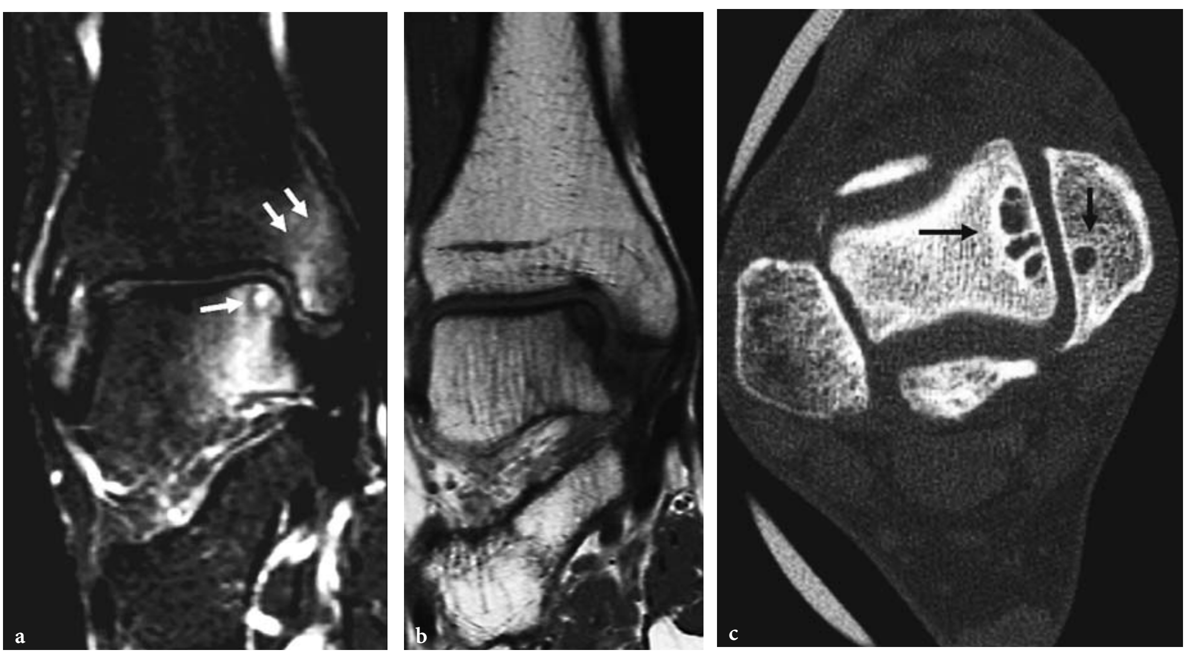

Fig. 20.9a–c. Kissing OCL. Coronal TSTIR 3-mm MR image (**a**), T1-weighted spin echo (**b**) and axial 0.6-mm MDCT (**c**). On TSTIR edema is seen in the medial talus. In the cranial talar surface a separate cystic lesion is seen (*arrow*). More subtle bone marrow edema can be seen in the medial malleolus (*double arrows*). The T1-weighted MR image clearly defines the talar OCL. No clear lesion in the medial malleolus is seen (**b**). The axial 0.6-mm CT clearly defines the kissing lesions in both talus and medial malleolus (*arrows*). A preserved joint space width is seen, therefore no osteoarthritis is diagnosed

quent encountered fractures in the ankle are beyond the scope of this chapter. However a specific sports related fracture is discussed below.

20.1.2.1 Snowboarder's Fracture

A well-documented sports related fracture is the fracture of the lateral process of the talus. In a prospective study of foot and ankle injuries in snowboarders a very high incidence of these fractures was found (Kirkpatrick et al. 1998). It should be noted that many of these fractures are not visible on standard radiography. When MRI is performed, usually in a later stage, when the patient is complaining of chronic lateral ankle pain, bone marrow edema is seen. However it may still be hard to diagnose the fracture. MDCT will aid in diagnosing this lesion and can help the surgeon to tailor therapy (Fig. 20.11).

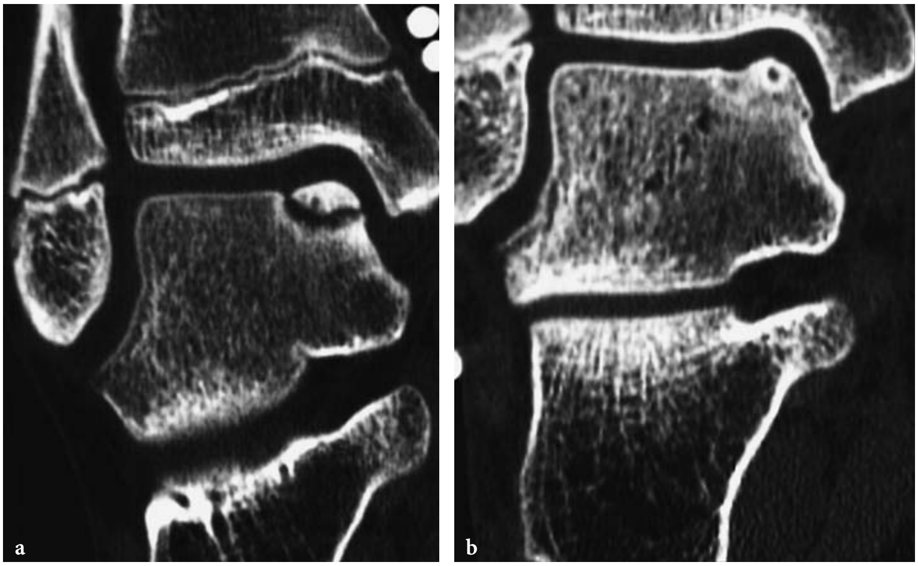

Fig. 20.10a,b. Post operative pitfall. Pre operative (**a**) and post operative (**b**) images of an OCL. Coronal MPR MDCT. The osteochondral defect is clearly seen with a large fragment (**a**). Two year postoperative (**b**), the OCL has healed. Although no normal anatomy is achieved, the patient is without any complaints, so this must be regarded as a normal postoperative situation

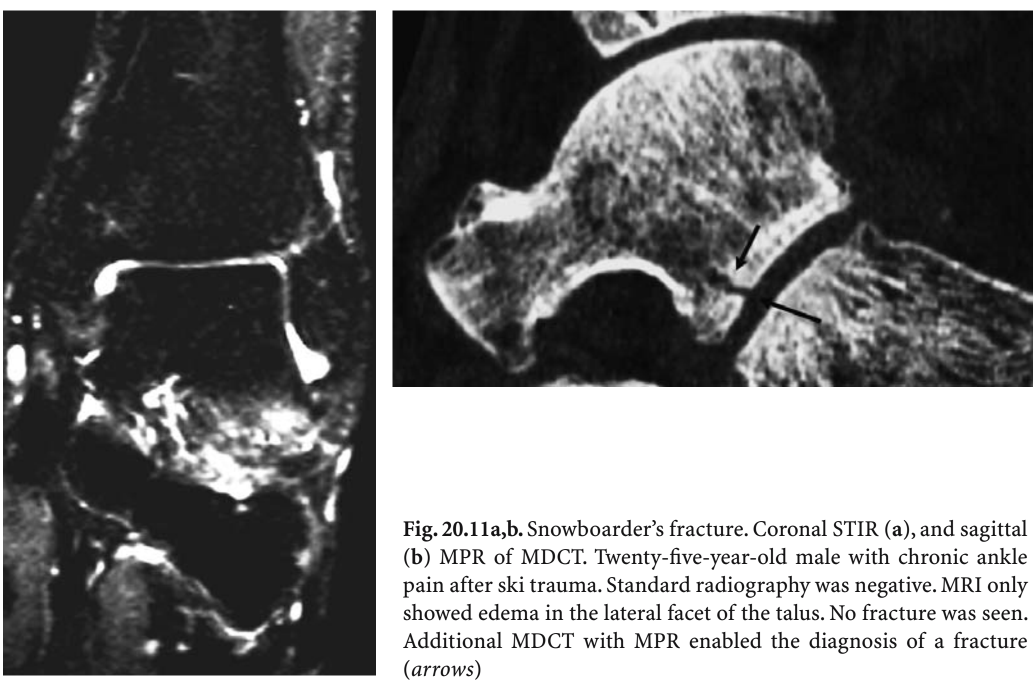

a b

Fig. 20.11a,b. Snowboarder's fracture. Coronal STIR (**a**), and sagittal (**b**) MPR of MDCT. Twenty-five-year-old male with chronic ankle pain after ski trauma. Standard radiography was negative. MRI only showed edema in the lateral facet of the talus. No fracture was seen. Additional MDCT with MPR enabled the diagnosis of a fracture (*arrows*)

20.2 The Foot

20.2.1 Osteochondral Injury

Osteochondral lesions of the foot can occur in the toes, especially in the first toe. Although there is not much literature on the subject, in our experience this is not an uncommon encountered phenomenon. It has been described in adolescent soccer players and elite ballet dancers and is characterized by pain, swelling and tenderness at the interphalangeal joint (Van Dijk et al. 1995; Kinoshita et al. 1998). Radiographic appearance is similar to the OCL in the ankle. Therapy can also be arthroscopic curettage and drilling.

20.2.2 Sports Specific Acute Foot Injury

20.2.2.1 Turf Toe

Originally described in 1976 is the hyper extension injury of the first metatarsophalangeal joint, occurring on a surface of artificial turf, hence turf toe and resulting in partial or complete disruption of the fibrocartilaginous plantar plate (Bowers and Martin 1976; Allen et al. 2004; Ashman et al. 2001). This entity is described in detail in Chap. 19.

20.2.2.2 Skimboarder's Toe

More recently an injury of the dorsal aspect of the first metatarsophalangeal joint is described as a skimboarder's toe (Donnely 2005). In this beachside sport a hyperdorsal flexion of the MTP joint causes injury to the extensor muscle, and the extensor expansion. On MRI a soft tissue swelling with edema is seen. The dorsal aspect of the extensor expansion is disrupted, while the plantar plate is intact. Bone marrow edema or joint effusion can accompany the lesion.

20.2.3 Overuse Injury of the Foot

20.2.3.1 Navicular Stress Fracture

Stress fractures of the navicular bone are familiar lesions in athletes (Pećina and Bojanić 2004). They most often occur in explosive athletic activities, involving jumping, sprinting and hurdling. Chronic stress usually produces sagittal fractures of the navicular bone. The patients usually complain of a vague pain on the dorsum of the foot. On physical examination a localized painful point may be found on the proximal dorsal border. The navicular stress fracture will generally not be detected by plain radiology. As a rule of thumb, standard radiography is not sensitive enough to detect these stress fractures. When there is a high clinical suspicion, further modalities can be used. Bone marrow edema is the key finding in diagnosing stress fractures with MRI. A linear hypointense configuration on T1-weighted MR sequences should be present when diagnosing a true fracture. The use of high resolution MDCT with 0.6-mm axial source images and MPR in any given plane aids in making a final diagnosis. In order to detect navicular stress fracture the axial plane will be adequate (Fig. 20.12).

20.2.3.2 Sesamoid Overuse Injury

Stress related injury to the sesamoid bones, also known as sesamoiditis, is a common problem in athletes, who require maximum dorsiflexion of the great toe. Athletes at risk are joggers, sprinters, figure skaters, ballet dancers, basketball players, football players and tennis players (Linz et al. 2001). It is a painful condition increased with weight bearing under the first metatarsal head, usually in the region of the medial rather than the lateral sesamoid.

Sesamoiditis on imaging can be seen as a broad spectrum: A true stress fracture of the sesamoid bone may be seen. However this has to be differentiated from bipartite sesamoids, which can occur in up to 75% of patients. Other findings, include bone marrow edema without a fracture line, reactive soft tissue edema, and tendinosis of the flexor hallucis tendon. Synovitis and bursitis are frequently associated. Some authors state that when edema is seen on TSTIR or fat suppressed T2-

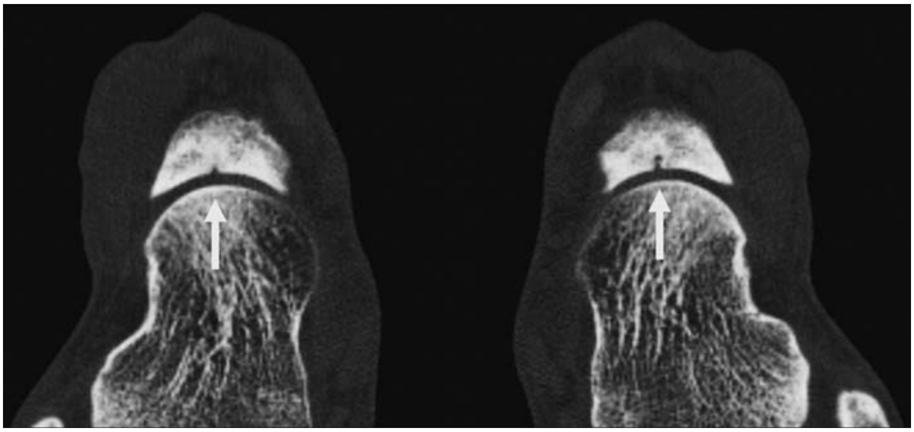

Fig. 20.12. Navicular stress overuse injury. MDCT of both ankles. Long distance runner with complaints of vague pain in both midfoots. Bilateral navicular bones show fracture lines, without history of an acute trauma

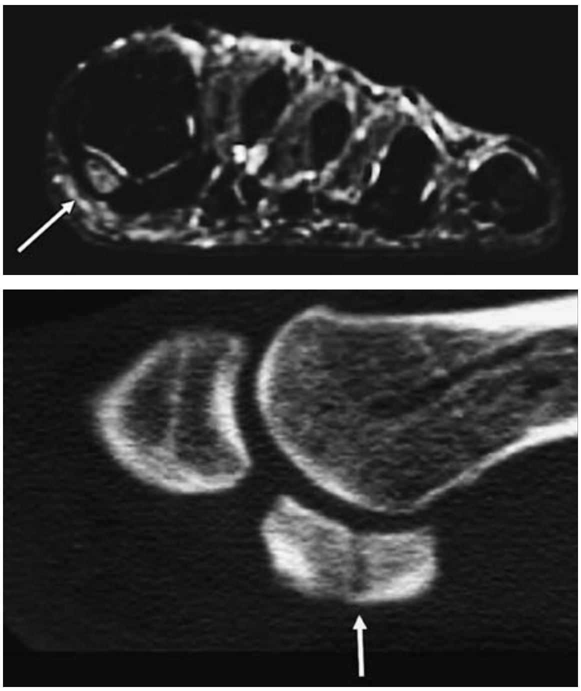

Fig. 20.13a,b. Sesamoiditis . Coronal TSTIR (**a**) and sagittal MPR (**b**) of the MDCT. On TSTIR edema in the medial sesamoid with accompanying soft tissue edema is seen (*arrow*). The sagittal MPR shows a fracture line suggesting a stress related lesion (*arrow*)

weighted MR images with absence of abnormalities on T1-weighted MR images, this is favorable for sesamoiditis. We have experience that MDCT can be helpful in these cases (Fig. 20.13).

Things to Remember

1. Think about an osteochondral lesion of the ankle in a patient with chronic ankle pain.
2. Standard radiography can detect but will not exclude this lesion.
3. The most important feature of the osteochondral defect of the talus is the exact location and extent. This is the surgical question that radiology needs to answer.
4. Both MRI and MDCT with MPR will detect the OCL.

References

Alexander AH, Lichtman DM (1980) Surgical treatment of transchondral talar dome fractures (osteochondritis dissecans). Long-term follow up. J Bone Joint Surg Am 62A:645–652

Allen LR, Flemming D, Sanders TG (2004) Turf Toe: ligamentous injury of the first metatarsophalangeal joint. Mil Med 169:19–24

Anderson IF, Crichton KJ, Grattan-Smith T et al. (1989) Osteochondral fractures of the dome of the talus. J Bone Joint Surg Am 71A:1143–1152

Ashman CJ, Yu JS, Wolfman D (2000) Satisfaction of search in osteoradiology. Am J Roentgenol 175:541–544

Ashman CJ, Klecker RJ, Yu JS (2001) Forefoot pain involving the metatarsal region: differential diagnosis with MR imaging. Radiographics 21:1425–1440

Barnes CJ, Ferkel RD (2003) Arthroscopic debridement and drilling of osteochondral lesions of the talus. Foot Ankle Clin N Am 8:243–257

Benthien RA, Sullivan RJ, Aronow MS (2002) Adolescent osteochondral lesions of the talus. Ankle arthroscopy in pediatric patients. Foot Ankle Clin 7:651–667

Bergfeld J (2005) Epidemiology of ankle instabilities. In: Chan KM, Karlsson J (eds)Isakos-Fims World Consensus Conference on ankle instability,. pp 8–9

Berndt AL, Harty M (1959) Transchondral fractures (osteochondritis dissecans) of the talus. J Bone Joint Surg 41A:988–1020

Bohndorf K (1998) Osteochondritis (osteochondrosis) dissecans – a review and new MRI classification. Eur Radiol 8:103–12

Bowers KD, Martin RB (1976) A shoe-surface related football injury. Med Sci Sports 8:81–83

Canale S, Belding RH (1980) Osteochondral lesions of the talus. J Bone Joint Surg 62A:97–102

Consumer Safety Institute (2004) The Dutch Injury Surveillance System: Ankle injuries. Personal communication

Davis AW, Alexander IJ (1990) Problematic fractures and dislocations in the foot and ankle of athletes. Clin Sports Med 9:163–181

DeSmet AA, Fisher DR, Burnstein MI et al. (1990) Value of MR imaging in staging osteochondral lesions of the talus (osteochondritis dissecans): results in 14 patients. AJR Am J Roentgenol 154:555–558

DiGiovanni BF, Fraga CJ, Cohen BE et al. (2000) Associated injuries found in chronic lateral ankle instability. Foot Ankle Int 21:809–815

Donnely LF, Betts JB, Fricke BL (2005) Skimboarder's Toe: findings on high-field MRI. AJR Am J Roentgenol 184(5):1481–1485

El-Khoury GY, Alliman KJ, Lundberg HJ et al. (2004) Cartilage thickness in cadaveric ankles: measurement with double-contrast multi-detector row CT arthrography versus MR imaging. Radiology 233:768–773

Ferkel RD (1992) Arthroscopy of the foot and ankle. In: Mann RA, Coughlin MJ (eds) Surgery of the foot and ankle. St Louis CV Mosby, pp 1277–1310

Ferkel RD, Scranton PE (1993) Arthroscopy of the ankle and foot. J Bone Joint Surg 75:1233–1242

Flick AB, Gould N (1985) Osteochondritis dissecans of the talus (transchondral fractures of the talus): review of the literature and new surgical approach for medial dome lesions. Foot Ankle Int 5:165–85

Hangody L (2004) Personal communication

Hangody L, Kish G, Modis L et al. (2001) Mosaicplasty for the treatment of osteochondritis dissecans of the talus: Two to seven year results in 36 patients Foot Ankle Int 22(7):552–558

Heare MM, Gillespy T, Bittar ES (1988) Direct coronal computed tomography arthrography of osteochondritis dissecans of the talus. Skeletal Radiol 17:187–189

Horton MG, Timins ME (1997) MR imaging of injuries to the small joints. Radiol Clin North Am 35:671–700

Josten C, Rose T (1999) Akute und chronische osteochondrale läsionen am talus. Orthopäde 28:500–508

Kappis M (1922) Weitere beiträge zur traumatich-mechanischen entstehung der "spontanen" knorpelablösungen. Dtsch Z Chir 171:13–29

Kinoshita M, Okuda R, Morikawa J et al. (1998) Osteochondral lesions of the proximal phalanx of the great toe: a report of two cases. Foot Ankle Int 19:252–254

Kirkpatrick DP, Hunter RE, Janes PC et al. (1998) The snowboarder's foot and ankle. Am J Sports Med 26:271–277

König F (1888) Über freie Körper in den Gelenken. Dtsch Z Chir 27:90–109

Linz JC, Conti SF, Stone DA (2001) Foot and ankle injuries. In: Fu and Stone (eds) Sports injuries, 2nd edn. Lippincott Williams & Wilkins Philadelphia, pp 1135–1163

Manaster BJ, Johnson T, Narahari U (2005) Imaging of cartilage in athletes. Clin Sports Med 24:13–37

Martinek V, Öttl G, Imhoff AB (1998) Chondrale und osteochondrale läsionen am oberen sprunggelenk. Der Unfallchirurg 101:468–475

Monro A (1738) Part of the cartilage of the joint separated and ossified. Medical Essays Observ 4:19 (http://www.sofarthro.com/ANNALES/ANNALES_1998, http://www.whonamedit.com/doctor.cfm/940.html)

Morrison WB (2003) Magnetic resonance imaging of sports injuries of the ankle. Top Magn Reson Imaging 14(2):179–198

Orava S, Karpakka J, Taimela S et al. (1995) Stress fractures of the medial malleolus. J Bone Joint Surg Am 77A:362–365

Pećina MM, Bojanić I (2004) Stress fractures. Overuse injuries of the musculoskeletal system, 2nd edn, Chap. 12. CRC Press, Boca Raton, pp 315–349

Pettine KA, Morrey BF (1987) Osteochondral fractures of the talus. J Bone Joint Surgery 69(B)1:89–92

Pritsch M, Horohovski H, Farine I (1986) Arthroscopic treatment of osteochondral lesions of the talus. J Bone Joint Surg Am 68:862–865

Rosenberg ZS, Beltran J, Bencardino JT (2000) MR imaging of the ankle and foot. Radiographics. Oct 20 Spec No:S153–79

Samuel S, Kundel HL, Nodine CF et al. (1995) Mechanism of satisfaction of search: eye position recordings in the reading of chest radiographs. Radiology 194:895–902

Schills JP, Andrish JT, Piraino DW et al. (1992) Medial malleolus stress fractures in seven patients: review of the clinical and imaging features. Radiology 185:219–221

Schmid MR, Pfirrmann CW, Hodler J et al. (2003) Cartilage lesions in the ankle joint: comparison of MR arthrography and CT arthrography. Skeletal Radiol 32:259–265

Sijbrandij ES, van Gils APG, Louwerens JW et al. (2000) Posttraumatic subchondral bone contusions and fractures of the talotibial joint: occurrence of "kissing" lesions. AJR Am J Roentgenol 175:1007–1010

Sijbrandij ES, van Gils APG, de Lange EE (2002) Overuse and sports related injuries of the ankle and hind foot: MR imaging findings. Eur J Radiol 43:45–56

Stone JW (1996) Osteochondral lesions of the talar dome. J Am Ac Orthop Surg 4:63–73

Stroud CS, Marks RM (2000) Imaging of osteochondral lesions of the talus. Foot Ankle Clin N Am 5:119–133

Sugimoto K, Takakura Y, Tohno Y et al. (2005) Cartilage thickness of the talar dome. Arthroscopy 21:401–404

Thompson JP, Loomer RL (1984) Osteochondral lesions of the talus in a sports medicine clinic. Am J Sports Med 12:460–463

Tol JL, Struijs PA, Bossuyt PM et al. (2000) Treatment strategies in osteochondral defects of the talar dome: a systematic review. Foot Ankle Int 21:119–126

Van Dijk CN (2005) Osteochondral defect. In: Chan KM, Karlsson J (eds) ISAKOS-FIMS World Consensus Conference on ankle instability, pp 68–69

Van Dijk CN, Lim LS, Poortman A et al. (1995) Degenerative joint disease in female ballet dancers. Am J Sports Med 23:295–300

Verhagen RA, de Keizer G, van Dijk CN (1995) Long-term follow-up of inversion trauma of the ankle. Arch Orthop Trauma Surg 114:92–96

Verhagen RA, Struijs PA, Bossuyt PP et al. (2003) Systematic review of treatment strategies for osteochondral defects of the talar dome. Foot Ankle Clin 8:233–242

Verhagen RA, Maas M, Dijkgraaf MG et al. (2005) Prospective study on diagnostic strategies in osteochondral lesions of the talus: is MRI superior to helical CT? J Bone Joint Surg 87-B:41–46

Vincken PW, Ter Braak BP, van Erkel AR et al. (2006) Clinical consequences of bone bruise around the knee. Eur Radiol 16(1):97–107

Zinman C, Wolfson N, Reis ND (1988) Osteochondritis dissecans of the dome of the talus. Computed tomography scanning in diagnosis and follow-up. J Bone Joint Surg 70(A):1017–1019

Acute and Overuse Lesions of the Leg and Calf

21

Philip Robinson

CONTENTS

21.1 Introduction

The lower limb is the focus for marked biomechanical stresses during all athletic activity (Dvorak and Junge 2000). This region is the most frequently injured area in the majority of sports with audits in soccer demonstrating 87% of all injuries occurring here, in particular the thigh (23%), ankle (17%), knee (17%), leg (12%) and groin (10%) (Hawkins et al. 2001). Among acute injuries muscular strain (37%) and ligamentous sprain (19%) of the knee and ankle are the most frequent.

This chapter will discuss the biomechanics and role of imaging in the management of several lower limb injuries highlighting specific acute and chronic osseous, muscle and tendon injuries commonly encountered in athletes. Injuries relating to the pelvis, knee, ankle and foot will not be discussed in detail as these areas are covered in their specific chapters.

21.2 Acute Osseous Injury

Biomechanically cortex provides the majority of a bone's strength for force absorption (Nordin and Frankel 2001a). The trabecular bone and marrow contribute relatively little to overall strength, but do determine the bone's cross-sectional area influencing the distribution of applied forces, important for resisting chronic stress explaining the subsequent distribution of injuries particularly seen in the tibia.

P. Robinson, FRCR
Consultant Musculoskeletal Radiologist, Dept. of Radiology, Musculoskeletal Centre, Chapel Allerton Hospital, Leeds Teaching Hospitals, Leeds LS7 4SA, UK

Box 21.1. Acute osseous injury

- Radiographs – sufficient in majority of cases
- CT – to define complex fracture patterns prior to treatment
- MRI – for suspected radiographically occult injuries

Box 21.2. Chronic osseous stress

- MRI most useful for defining severity of cortical and bone marrow changes
- Radiographs – usually negative but performed initially
- CT – can be helpful in ruling out a cortical fracture
- Isotope bone scanning – sensitive but lacks spatial resolution compared to MRI

Box 21.3. Acute lower limb muscle injury

- Ultrasound – accurate, fast and dynamic. Particularly useful in differentiating large grade 2 from grade 3 injuries. Can be negative in very low grade injury
- MRI – accurate and useful in athletes with large muscle bulk or diffuse symptoms

Box 21.4. Complications of muscle injury

- Ultrasound – particularly useful in diagnosing early myositis ossificans, muscle hernias and adherence of scar tissue
- MRI – particularly useful in defining subtle atrophic changes

Acute trauma in the context of sporting injuries frequently results in soft tissue injury, however in contact sports acute fractures can occur on tackling or player collision (Chomiak et al. 2000; Fuller et al. 2004; Hawkins et al. 2001). Unlike general non-sporting trauma, acute fractures of the femur and hip are rare but injuries of the tibia, fibula, ankle and foot are more frequent.

While concomitant injuries and local muscle imbalance are important for the development of chronic osseous stress, in acute injury the forces applied are usually sudden and excessive leading to acute structural failure (fracture) not dependent on concomitant injuries (Nordin and Frankel 2001a). The rate of application is also important, as forces applied at a high rate induce increased bone stiffness resulting in shattering if the bone's strength limit is exceeded. As bone fails the energy producing the fracture is dissipated into the soft tissues resulting in significant associated injury due to the high energies involved (Nordin and Frankel 2001a).

The forces applied to the tibia and fibula can be direct, torsional or bending which influence the subsequent fracture configuration. The majority of fractures of the tibia and fibula usually have an oblique orientation in the mid to distal shaft resulting from the lateral or medial oblique forces produced from a direct blow during a fall, tackling or from falling players. (Figs. 21.1–21.3) (Fuller et al. 2004; Giza et al. 2003). This particular fracture pattern is sometimes termed 'footballer's fracture' (Boden et al. 1999).

Fig. 21.1a,b. Professional footballer with acute severe leg pain after tackle. AP (**a**) and lateral (**b**) radiographs, both showing a transverse oblique fracture through the distal diaphysis of the tibia and fibula with comminution at the distal fracture margin. The player went on to have plate fixation

Fig. 21.2a–d. Professional footballer with tender fibula after tackle. Lateral (**a**) and AP (**b**) radiographs of the leg and ankle, both showing a possible linear lucency (*arrows*) on the lateral view only. **c** Coronal T2-weighted fat suppressed MR image shows bone marrow edema with an oblique low signal fracture line (*arrows*) and extensive soft tissue edema (*arrowheads*). **d** Corresponding axial T2-weighted fat suppressed MR image shows edema (*asterisk*) within the fibula. There is further soft tissue edema at the point of impact (*arrows*) as well as tracking along the intraosseous membrane and tibia (*arrowheads*)

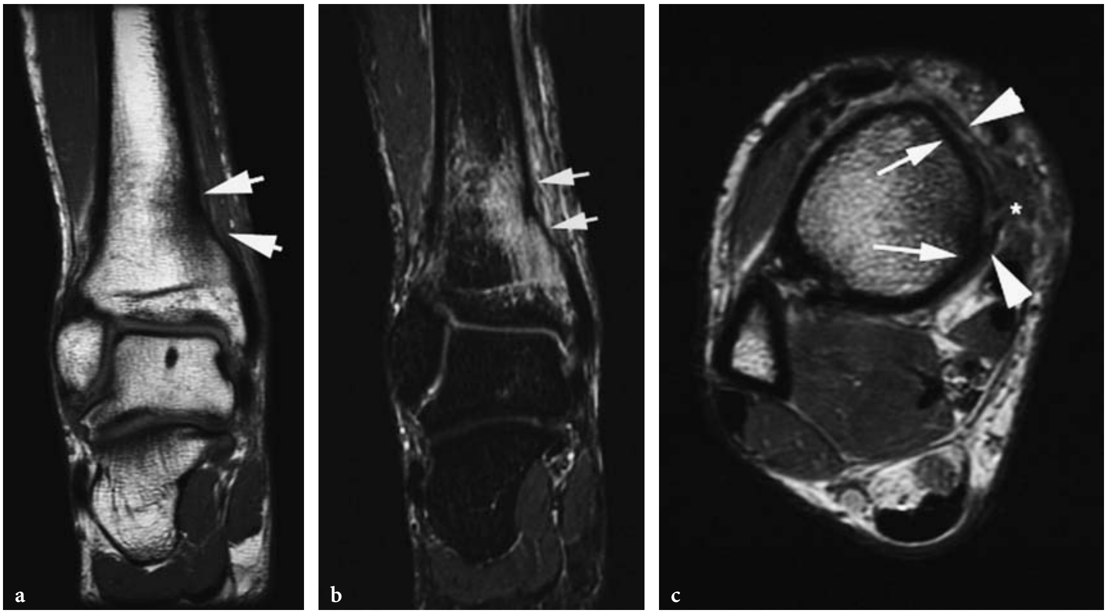

Fig. 21.3a–c. Professional footballer with severe lower leg pain after stamping, radiographs showed some cortical irregularity. Coronal (**a**) T1-weighted and (**b**) T2-weighted fat suppressed MR images show depression of the distal medial tibial cortex (*arrows*) with associated bone marrow edema. **c** Corresponding axial T1-weighted MR image shows the main cortex (*arrows*) with periosteal haematoma and elevation (*arrowheads*). Note the defect in the elevated periosteum with haematoma (*asterisk*) extruding

21.2.1
Imaging Strategy and Management

For fractures of the tibia and fibula, radiographs are usually sufficient to confirm the diagnosis and fracture configuration (Figs. 21.1 and 21.4). MR imaging can be used to confirm fractures when radiographs are negative and an undisplaced fracture rather than just soft tissue contusion is suspected (Fig. 21.2). MR imaging demonstrates soft tissue edema in the area of impact but also allows evaluation of the cortical and trabecular bone for edema and low signal fractures lines. Cortical abnormalities include buckling or increased thickness with high T2-weighted signal due to periosteal haematoma (Fig. 21.3).

Treatment for tibia and fibula fractures can be conservative with casting, but if the injury is high velocity resulting in bone comminution and soft tissue disruption internal fixation and soft tissue reconstruction will be required. In these cases CT examination can be useful to define the exact fracture configuration and extent for surgical treatment. Despite the soft tissue damage subsequent reconstruction (primary or grafting) does not require MR or ultrasound imaging unless there are specific vascular complications (Box 12.1).

The recovery time for these injuries will depend on the fracture position and severity of associated injuries. Fracture of the tibia and fibula can be career ending for athletes involved in contact sports (Chomiak et al. 2000). One series of 31 soccer players reported a full return to sport taking a mean of 18–40 weeks with the longer duration occurring when the tibia alone or both tibia and fibula were involved (Boden et al. 1999). Non-union is the most significant complication and if appearances are indeterminate on radiographs ultrasound can be used to give a more accurate assessment of callous formation (Fig. 21.4). If non-union is confirmed internal fixation or revision and bone grafting may be required (Fig. 21.5).

Fig. 21.5. Professional footballer with acute left leg injury during tackle. AP radiograph shows an oblique fracture through the distal diaphysis of the tibia and fibula treated with intramedullary nail and plate, respectively

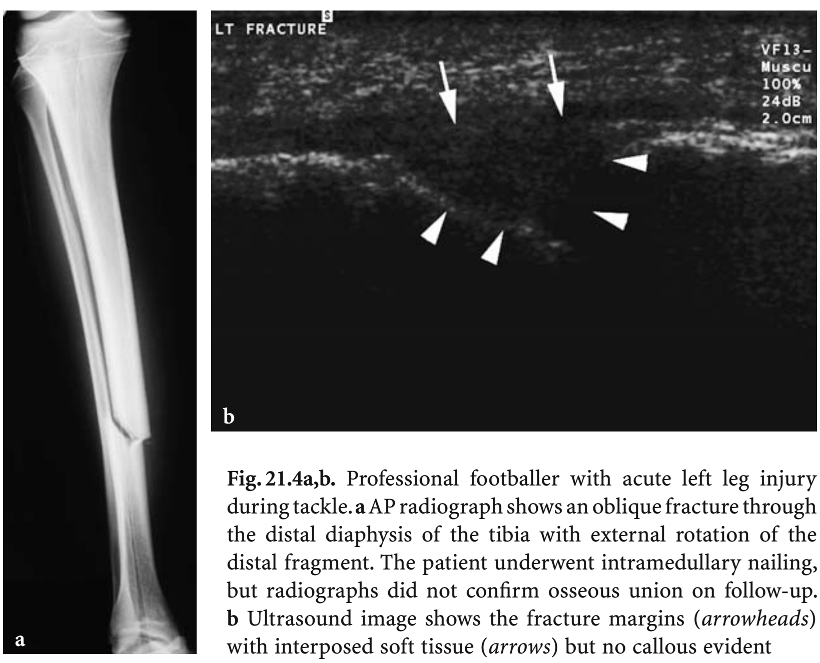

Fig. 21.4a,b. Professional footballer with acute left leg injury during tackle. **a** AP radiograph shows an oblique fracture through the distal diaphysis of the tibia with external rotation of the distal fragment. The patient underwent intramedullary nailing, but radiographs did not confirm osseous union on follow-up. **b** Ultrasound image shows the fracture margins (*arrowheads*) with interposed soft tissue (*arrows*) but no callous evident

21.3 Chronic Exertional Leg Pain

The commonest causes of chronic exertional athletic leg pain include medial tibial stress syndrome, stress fracture, chronic exertional compartment syndrome, popliteal artery entrapment syndrome and nerve entrapment. Several series have found slightly different incidences for each type of injury but together these processes are the most frequently occurring in athletes (Edwards et al. 2005; Kaufman et al. 2000).

21.3.1 Chronic Osseous Stress Response and Injury

Overuse injuries occur when the ability for cortical bone to remodel and compensate is exceeded by chronic excessive forces not individually reaching acute overload (Anderson et al. 1997; Nordin and Frankel 2001a). Causes of increased stress normally relate to a sustained increase in training and more commonly present in athletes who are female, have suffered prior osseous injury, have concomitant lower limb injuries (e.g. muscle strain) and, especially in the lower leg, if there is ankle pronation (Anderson et al. 1997; Batt et al. 1998; Fredericson et al. 1995).

Studies of military recruits have shown stress injuries and fractures most commonly affect the tibia (50%), foot (40%) and femur (10%) (Kaufman et al. 2000; Yates and White 2004). In the femur, stress reactions most frequently occur in the femoral neck and are important to detect early as the consequences for osteonecrosis or complete fracture are serious.

21.3.1.1 Tibia and Fibula

In the tibia the fracture position can vary according to sporting activity with runners experiencing mid to distal 1/3, dancers mid 1/3 and jumping athletes (e.g. tennis, basketball and volleyball) proximal 1/3 injuries (Batt et al. 1998). The mid and distal diaphysis of the tibia is thought to be the most vulnerable region as this is the narrowest cross-sectional area of the bone and has relatively little surrounding musculature to dissipate applied forces. In the tibia compressive forces concentrate medially and fractures can present here or be part of medial tibial stress syndrome (MTSS, see below) (Anderson et al. 1997; Batt et al. 1998; Fredericson et al. 1995). Fractures that develop on the anterolateral tibia occur as a result of tensile forces and subsequently have a higher risk of non-union, especially if the orientation is longitudinal and not perpendicular to the cortex (Edwards et al. 2005; Fredericson et al. 1995; Green et al. 1985).

Symptoms are usually of insidious onset, occurring on exertion, and are a differential diagnosis for chronic exercise induced pain. However if allowed to progress pain can be present at rest or on weight bearing (Fig. 21.6) (Edwards et al. 2005; Fredericson et al. 1995). Clinical findings can include localised tenderness and indirect pain produced by tibial percussion (Batt et al. 1998; Yates and White 2004). This latter finding is thought to correlate well with severer clinical and imaging extent (Fredericson et al. 1995).

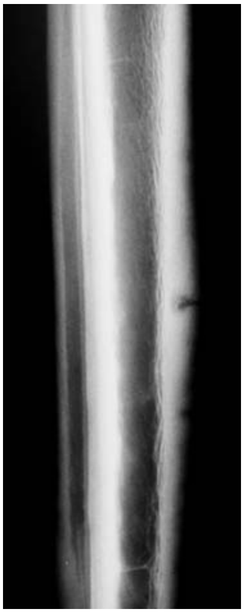

Fig. 21.6. Female marathon runner presenting at major games with continuous anterior tibial pain. Lateral radiograph of the tibia shows anterior cortical thickening and multiple stress fractures. The athlete had to withdraw from competition

21.3.1.2 Medial Tibial Stress Syndrome (MTSS)

This is an overuse syndrome in running and jumping athletes which is defined as involving the posteromedial tibial periosteum (Batt et al. 1998; Yates and White 2004). There has been previous controversy concerning the aetiology of this condition with initial theories suggesting a chronic periosteal traction injury from adjacent muscles (Anderson et al. 1997; Batt et al. 1998; Fredericson et al. 1995; Yates and

White 2004). However the osseous changes are usually distal to the main muscle origins and it is now thought to be the beginning of the spectrum of osseous stress reaction of the tibia (Fig. 21.7). This condition is interchangeable with posterior 'shin splints' (Fig. 21.8) and some clinicians define both terms as lower leg exertional pain not due to a compartment syndrome, fracture or muscle hernia (Batt et al. 1998; Edwards et al. 2005).

Compressive stresses are concentrated on the concave aspect of the posteromedial tibial cortex stimulating osteoblastic and osteoclastic activity as the bone remodels (Anderson et al. 1997; Batt et al. 1998; Fredericson et al. 1995; Yates and White 2004). As with other osseous stress reactions as the repetitive loading continues trabecular failure can occur potentially resulting in cortical fracture.

As this syndrome is recognized, the reported incidence in susceptible groups is increasing. Previous studies describe an incidence of 6.4%–13% for all stress injuries but a recent series of military recruits reported an incidence of 35% (Batt et al. 1998; Kaufman et al. 2000; Yates and White 2004). As in other osseous stress injuries the development of this condition is increased in athletes that are female, have a pronated foot or have injury elsewhere within the lower limb kinetic chain (Batt et al. 1998; Yates and White 2004). It is bilateral in over 70% of cases which presumably relates to running and jumping (e.g., basketball and tennis) being the most common underlying mechanisms of injury. The area of diaphysis affected can vary depending on sporting activity but the majority of injuries involve the mid and distal diaphyseal region where the cross-sectional area is smallest (Anderson et al. 1997; Batt et al. 1998; Fredericson et al. 1995; Yates and White 2004). Clinical findings include localised posteromedial tibial tenderness which is unaffected by ankle or knee movement (Batt et al. 1998; Edwards et al. 2005).

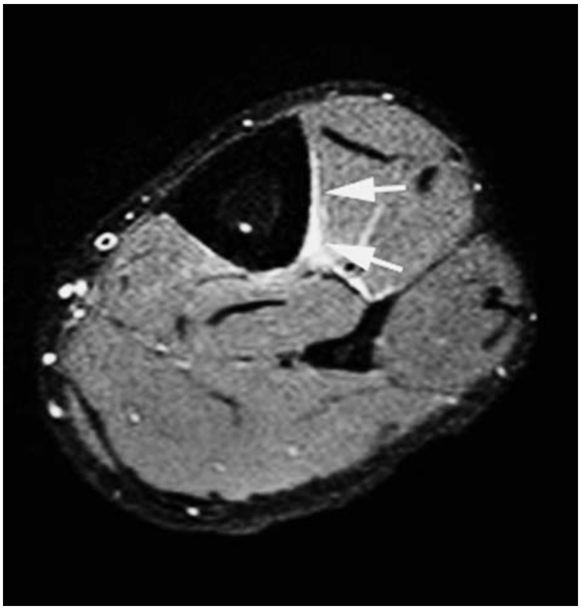

Fig. 21.8. Running athlete with clinical diagnosis of anterior shin splints. Axial T2-weighted fat suppressed MR image shows marked anterolateral periosteal edema of the tibia with no associated intracortical or bone marrow change

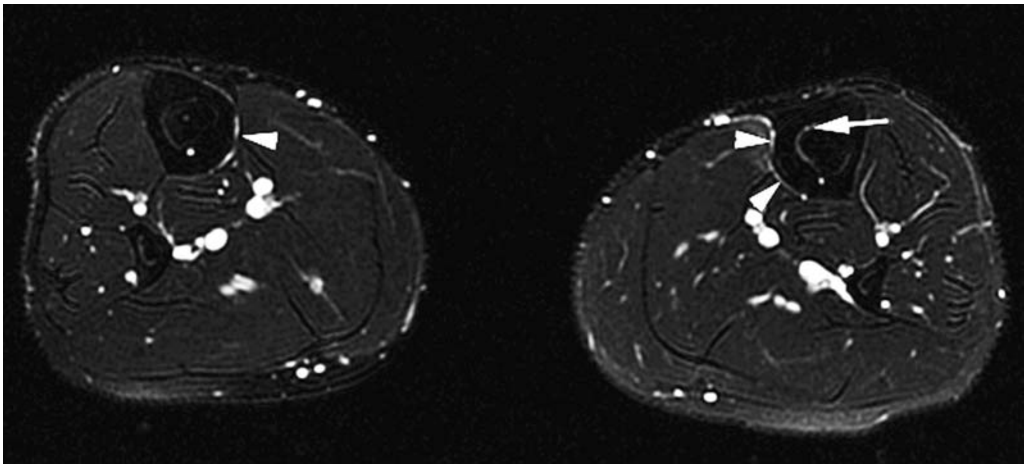

Fig. 21.7. Male running athlete with left sided posteromedial tibial pain. Axial T2-weighted fat suppressed MR image of both legs shows bilateral posteromedial periosteal edema (*arrowheads*) slightly more extensive on the left with associated bone marrow edema (*arrow*)

21.3.1.3 Imaging and Management of Osseous Stress Reaction

In athletes it is especially important to make an early diagnosis and determine the extent of osseous damage to give prognostic information (Ohta-Fukushima et al. 2002). Radiographs are insensitive and can be negative in up to 85% of cases but are usually performed initially to exclude a complete fracture (Fig. 21.6) (Anderson et al. 1997; Batt et al. 1998; Fredericson et al. 1995; Gaeta et al. 2005; Ohta-Fukushima et al. 2002). MR imaging has been repeatedly shown to be an accurate, sensitive and specific technique compared to CT and isotope scanning (Anderson et al. 1997; Batt et al. 1998; Fredericson et al. 1995; Gaeta et al. 2005; Milgrom et al. 1984) (Box 21.2).

T2-weighted (fat suppressed) MR sequences are most sensitive for detecting periosteal, cortical and bone marrow edema (Figs. 21.8–21.10) (Anderson et al. 1997; Batt et al. 1998; Gaeta et al. 2005). Isotope bone scans show increased activity but lack spatial resolution (Fig. 21.11) and can be negative if osteoblastic activity is markedly reduced (Milgrom et al. 1984).

The MR classification and the management of osseous stress reaction are summarized in Table 21.1. Further discussion is beyond the scope of this chapter (see Chaps. 7 and 28, respectively).

21.3.2 Chronic Exertional Compartment Syndrome

Compartment syndrome is defined as increased interstitial pressure within an anatomically confined compartment that interferes with neurovascular function. Normal pressures within a muscle compartment are between 0 and 4 mmHg and can peak above 60 mmHg on exercise but quickly dissipate on cessation. However if this pressure is sustained above 15 mmHg blood flow is compromised and muscle ischaemia can occur (Zabetakis 1986).

Chronic exertional compartment syndrome commonly affects the anterior and deep posterior calf lower leg musculature (Martens et al. 1984; Peterson and Renstrom 1986; Zabetakis 1986). It is thought that chronic traction on the muscle fascia alters its compliance and subsequent ability to accommodate volume change on exercise (Nicholas and Hershman 1986; Peterson and Renstrom 1986). Potentially any athlete can be affected but it particularly common in distance runners, cyclists

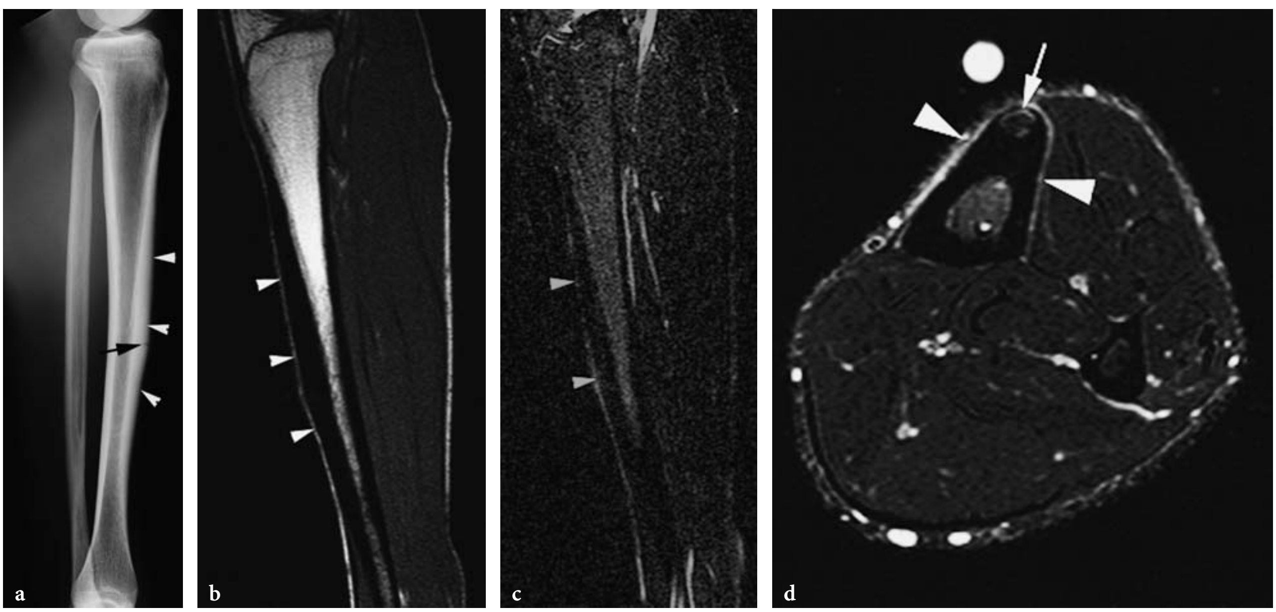

Fig. 21.9a–d. Male running athlete with exertional anterior tibial pain. **a** Lateral radiograph shows anterior cortical thickening (*arrowheads*) with a linear lucency (*black arrow*) consistent with stress reaction and possibly early fracture. **b,c** Corresponding sagittal (**b**) T1- and T2- (**c**) weighted fat suppressed MR images show cortical thickening (*arrowheads*) but little corresponding edema. **d** Axial T2-weighted fat suppressed MR image shows periosteal (*arrowheads*) and intra-cortical edema (*arrow*) with no definite fracture

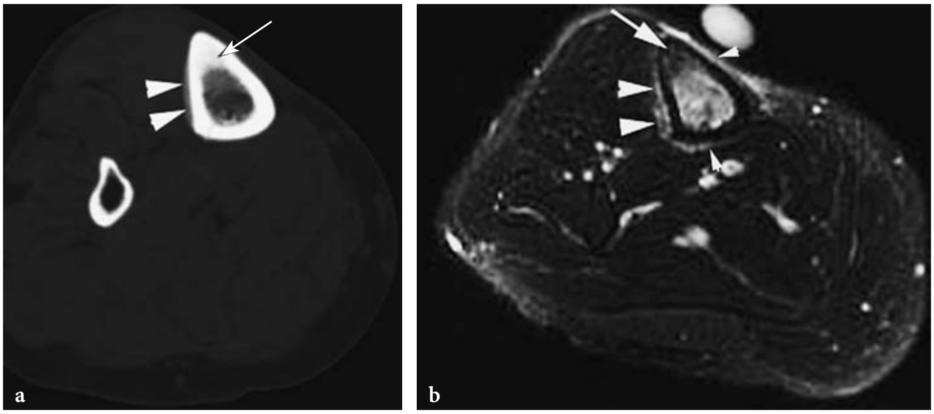

Fig. 21.10a,b. Running athlete with weight bearing tibial pain. **a** Axial CT scan shows lateral tibial periosteal reaction (*white arrowheads*) with some resorption in the anterior cortex (*arrow*). No fracture seen. **b** Corresponding axial T2-weighted fat suppressed MR image shows the lateral periosteal edema (*large arrowheads*), but also shows edema posteriorly and medially (*small arrowheads*). There is both intracortical (*arrow*) and bone marrow edema seen; however no fracture is present

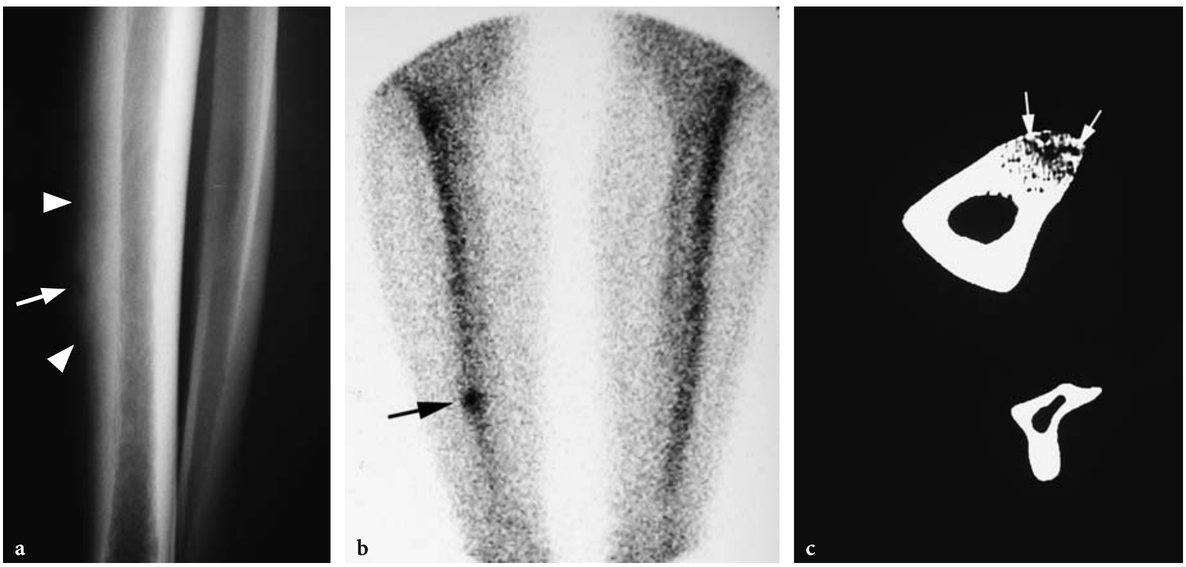

Fig. 21.11a–c. Running athlete with tibial pain. **a** Lateral radiograph shows diffuse anterior cortical thickening (*arrowheads*) with an ill-defined lucency in the superficial cortex (*arrow*). **b** Isotope bone scan image shows increased uptake (*arrow*) in the region. **c** Corresponding axial CT shows diffuse resorption through the anterior cortex but also a linear fracture (*arrows*)

Table 21.1. Summary of MR imaging classification and potential relationship with return to weight-bearing for osseous stress injuries (Fredericson et al. 1995)

MR Grade	Grade 1	Grade 2	Grade 3	Grade 4
Periosteal and adjacent soft tissue edema	-	+	+	+
Bone marrow edema	-	-	+	+
Cortical Fracture	-	-	-	+
Typical time to weightbearing (weeks)	2–3	3–6	6–9	12+ (including 6 weeks in cast)

and cross-country skiers. The athlete usually presents with crescendo pain and paraesthesia after exercise which eases on ceasing activity and unlike popliteal artery syndrome is not posture dependant (Martens et al. 1984; Nicholas and Hershman 1986). There may also be muscle swelling and it is important to rule out an underlying muscle hernia. The diagnosis can sometimes be made with history alone but compartmental pressure measurements may be necessary. Pressure pre exercise of greater than 15 mmHg, or post exercise pressure greater than 30 mmHg at 1 min, or greater than 20 mmHg at 5 min confirm the diagnosis (Pedowitz et al. 1990).

21.3.2.1 Imaging

Appearances on imaging can be nonspecific and are not always reliable in confirming the diagnosis (Edwards et al. 2005).

On ultrasound the muscle can appear echogenic with relative sparing of periseptal areas which are still receiving sufficient blood flow from the adjacent fascia (Van Holsbeeck and Introcasco 2001). Studies evaluating muscle cross sectional area on ultrasound both before and after exercise describe two different patterns in symptomatic patients. In one group the muscle compartment cannot expand with a relatively rigid fascia compared to normal subjects (where muscle volume can increase by 10%–15%). In the other symptomatic group, although the muscle compartment does expand during exercise, there is a slow reduction in volume post exercise compared to normal subjects (Van Holsbeeck and Introcasco 2001).

Post exercise MR imaging can show edema in the clinically affected muscles confirming the diagnosis (Fig. 21.12). However, like ultrasound, this technique is not completely sensitive or specific with edema being found in asymptomatic athletes and normal muscle appearances occurring in athletes with objective clinical features (Fig. 21.13) (Fleckenstein et al. 1988; Shellock et al. 1991).

The initial treatment of chronic exertional compartment syndrome includes training modifications and assessment for orthotics, however if symptoms persist fasciotomy of the muscle compartment is performed. Morbidity can potentially result if there is subsequent muscle herniation or scarring (Van Holsbeeck and Introcasco 2001).

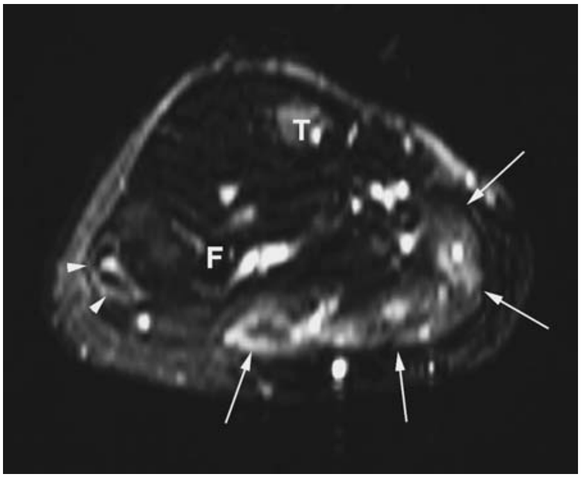

Fig. 21.13. Running athlete with chronic exertional right leg pain, clinically related to soleus. Axial T2-weighted fat suppressed MR image post exercise shows soleus edema (*arrows*). Note asymptomatic peroneus muscle edema (*arrowheads*)

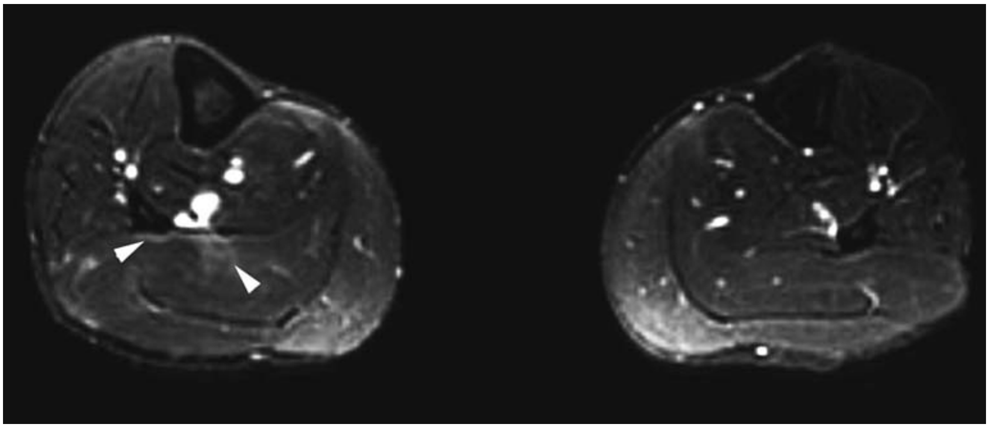

Fig. 21.12. Running athlete with chronic exertional right leg pain. Axial T2-weighted fat suppressed MR image post exercise shows persisting soleus edema (*arrowheads*). The athlete underwent fasciotomy

21.3.3 Popliteal Artery Entrapment Syndrome

Popliteal artery entrapment is an uncommon cause of chronic exertional calf pain which can occur during exercise or on particular postural changes (Atilla et al. 1998; Elias et al. 2003). The condition is usually precipitated in young male athletes by a change in muscle bulk due to adolescent growth or increased training (Atilla et al. 1998; Collins et al. 1989; Edwards et al. 2005). This most commonly occurs in sports which involve high intensity repetitive plantar and dorsiflexion such as soccer, basketball and running. Repeated knee flexion causing microtrauma and intimal fibrosis of the artery resulting in this condition has been described in a skier (Toorop et al. 2004).

Symptoms occur due to muscle ischaemia from compression of the popliteal artery (and occasionally vein) at the level of the medial head of gastrocnemius (MHG). The MHG can be normal with compression resulting from muscle hypertrophy, however more frequently there is also a congenital anomalous origin or fibrous slip. Causes of the condition can be classified into six types (Fig. 21.14); medial deviation of popliteal artery and normal MHG (type 1), aber-

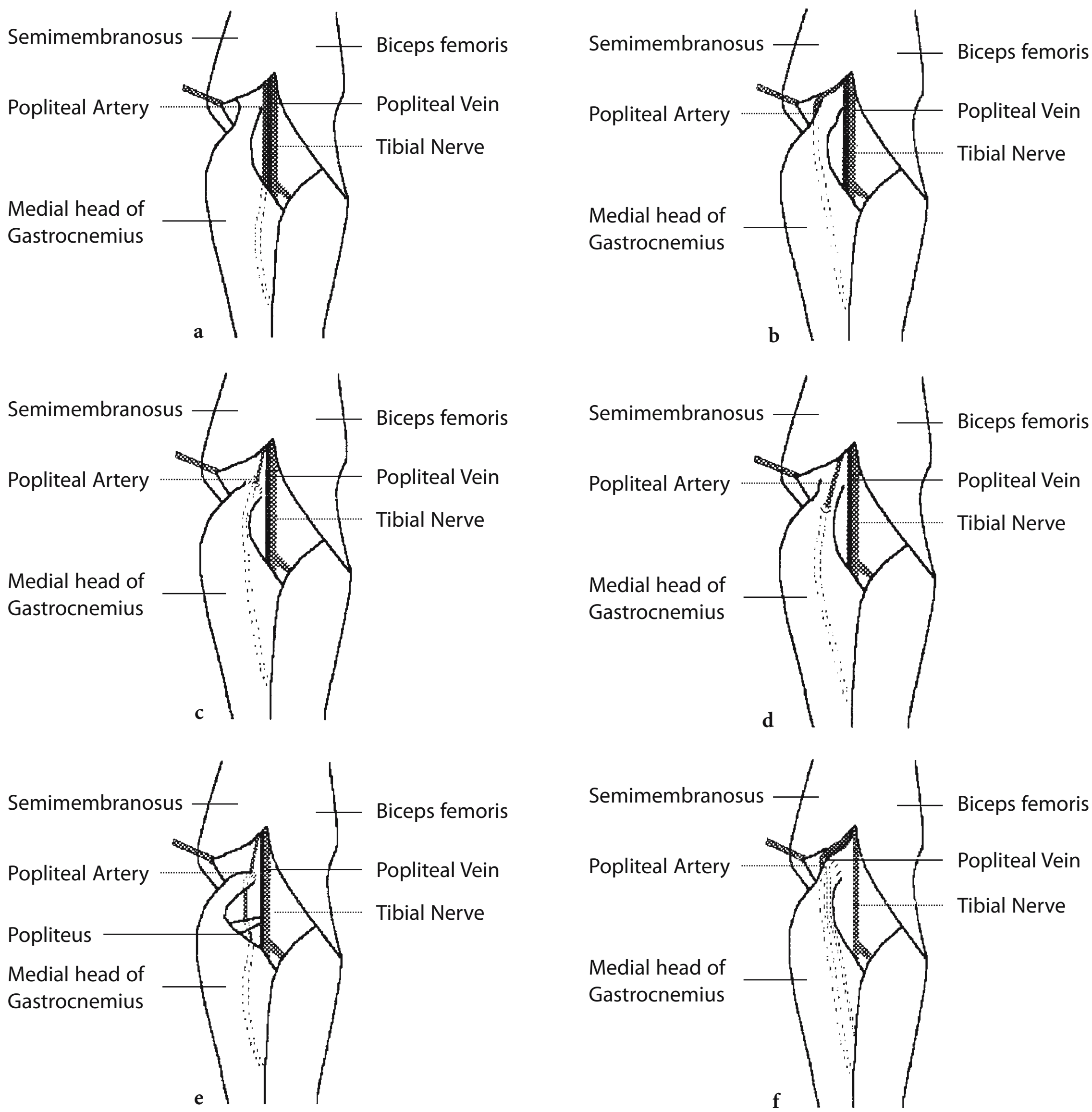

Fig. 21.14a–f. Aberrant course of popliteal vessel(s) indicated by dotted line. (**a**) normal. (**b**) type 1. (**c**) type 2. (**d**) type 3. (**e**) type 4. (**f**) type 5. See text for full description of types

rant origin of MHG from intercondylar notch compressing the artery (type 2), slip of MHG compressing the popliteal artery (type 3), the popliteal artery passing deep to popliteus muscle or fibrous band in the popliteal fossa (type 4), any entrapment also resulting involvement of the popliteal vein (type 5) and compression of a normal artery by a normal but hypertrophied MHG (type 6) (Collins et al. 1989; Rich et al. 1979).

The diagnosis is clinical with complete loss or a decrease in ankle pulses between dorsiflexion and plantarflexion associated with calf and foot pain. The underlying abnormality can be bilateral in up to 67% but does not always result in bilateral symptoms (Chernoff et al. 1995; Collins et al. 1989).

21.3.3.1
Imaging and Management

The diagnosis, extent and severity of compression can be confirmed by imaging using a combination of ultrasound, MR imaging (angiography) or conventional arteriography. Ultrasound is typically the first technique used and can depict change in vessel calibre and distal flow showing systolic peaks and dampening during dynamic manoeuvres (Fig. 21.15a,b). The artery may be medially deviated by muscle but this is present in less than 25% of cases. MR imaging is nearly always then performed as it allows complete non-invasive investigation of muscular anatomy while time of flight angiography can depict vessel compres-

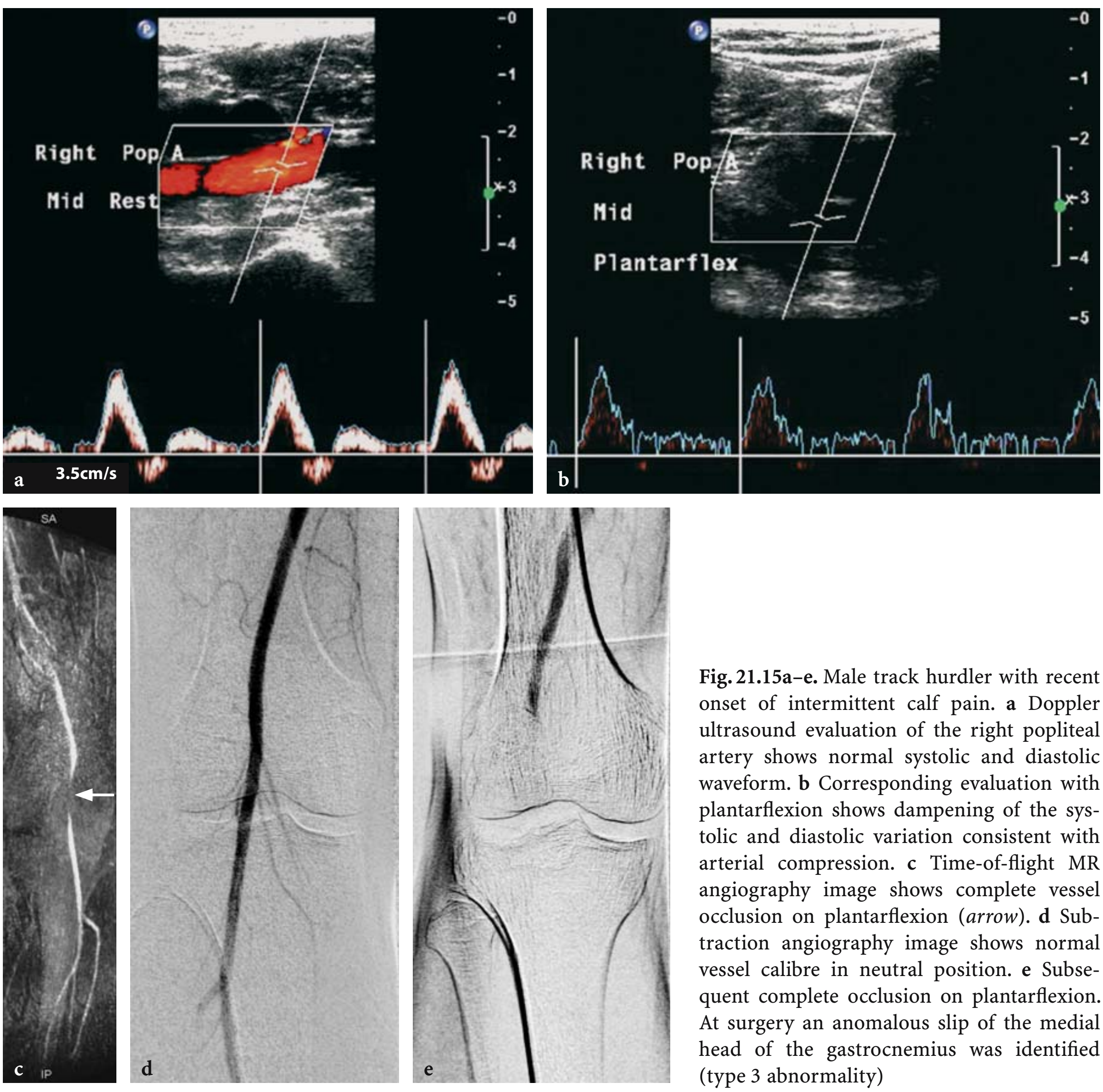

Fig. 21.15a–e. Male track hurdler with recent onset of intermittent calf pain. **a** Doppler ultrasound evaluation of the right popliteal artery shows normal systolic and diastolic waveform. **b** Corresponding evaluation with plantarflexion shows dampening of the systolic and diastolic variation consistent with arterial compression. **c** Time-of-flight MR angiography image shows complete vessel occlusion on plantarflexion (*arrow*). **d** Subtraction angiography image shows normal vessel calibre in neutral position. **e** Subsequent complete occlusion on plantarflexion. At surgery an anomalous slip of the medial head of the gastrocnemius was identified (type 3 abnormality)

sion in different foot positions (Fig. 21.15c) (Atilla et al. 1998). Subsequent complications such as adventitial disease or post-stenotic aneurysms can also be demonstrated by MR imaging although this is rare in true athletic induced pain. If MR imaging features are equivocal angiography may be required to more accurately define the degree of compression (Fig. 21.15d,e) (Atilla et al. 1998; Edwards et al. 2005).

Treatment in athletes usually requires surgical release of the MHG and anomalous slips as modification of activity to limit symptoms is not an acceptable option.

21.3.4 Nerve Compression

In the lower limb this most commonly involves the common or superficial peroneal nerves. This is usually thought to be due to fascial thickening, scarring (see later) or less commonly because of an adjacent bony abnormality or ganglion (Nicholas and Hershman 1986). Superficial peroneal injury can occur through trauma and is seen in dancers, football players and runners. Common peroneal nerve injury is associated with repetitive inversion and eversion which can occur in cycling or running.

A ganglion of the proximal tibiofibular joint can result in direct compression of the common peroneal nerve (Fig. 21.16a,b) or actually extend into and along the nerve sheath (Fig. 21.16c) (Ilahi et al. 2003; Miskovsky et al. 2004; Spinner et al. 2000).

Occasionally compression can be secondary to braces used in treatment of other leg and knee injuries. Imaging is rarely necessary except to exclude clinically suspected extrinsic causes of nerve irritation. Nerve conduction studies can confirm the diagnosis with alteration of braces or surgical release in resistant cases (Edwards et al. 2005).

21.4 Acute Lower Limb Muscle Injury

Muscle and tendon injury occur at zones of anatomical or functional transition as these sites generate the greatest concentrations of intrinsic forces (Garrett et al. 1987; Nordin and Frankel 2001b). These are the commonest injuries in all sporting activities because the lower limb is essential for athletic movement.

21.4.1 Biomechanical Basis of Acute Lower Limb Muscle Injury

Lower limb muscles experience a wide range of physiological movement in play (and training) and must be

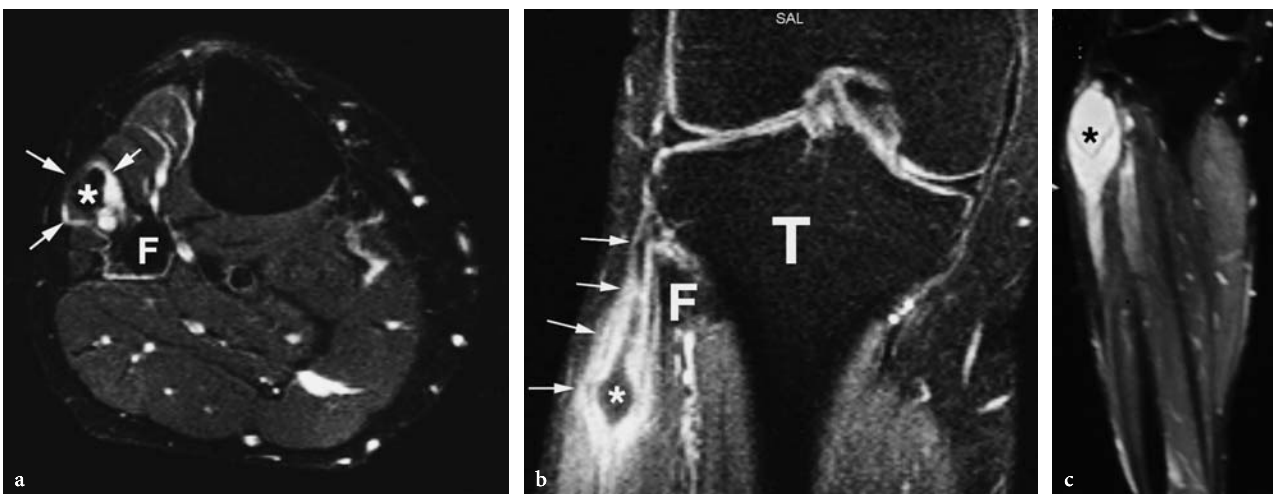

Fig. 21.16a–c. Two runners with lateral calf pain on exertion. **a** Axial T2-weighted fat suppressed MR image shows a ganglion (*arrows*) extending into the peroneus muscles adjacent to the fibula (*F*). Note low signal fibrous tissue (*asterisk*) within the ganglion. **b** Coronal T1-weighted fat suppressed post IV gadolinium MR image shows low signal fluid (*asterisk*) and the enhancing ganglion wall (*arrows*) tracking to the tibiofibular joint (*T*, tibia; *F*, fibula). **c** Coronal T2-weighted fat suppressed MR image in a different runner shows a high signal and enlarged common peroneal nerve (*asterisk*). At surgery this was found to be a neural cyst originating from the tibiofibular joint

able to maintain significant stamina while undergoing repetitive explosive activity. Studies have shown acute muscle injury, especially of the lower limb, accounts for more than 37% of all athletic injuries with the hamstrings most commonly affected followed by rectus femoris and gastrocnemius in decreasing frequency (Hawkins et al. 2001; Noonan and Garrett 1992; Speer et al. 1993). These muscles are more susceptible because they contain a high proportion of type 2 fibres, span two joints and arise from more than one head generating complex intrinsic forces while modulating hip and knee movement on sprinting, running and jumping (Novacheck 1998b).

21.4.2 Imaging of Acute Lower Limb Muscle Injury

In experienced hands and with modern equipment, MR imaging and ultrasound are both accurate techniques for the evaluation of lower limb muscle strain (Connell et al. 2004; Cross et al. 2004; Robinson 2004; Steinbach et al. 1998; Van Holsbeeck and Introcasco 2001). However, the large muscle bulk often present in athletes means that the depth of resolution and field of view offered by ultrasound can be limiting especially in the pelvis and proximal thigh (Box 21.3).

21.4.3 Hamstring Injuries

This muscle group is particularly susceptible to strain with injury occurring during running and sprinting as the muscles eccentrically contract decelerating knee extension (De Smet and Best 2000; Garrett 1988; Garrett et al. 1984; Mink 1992; Nicholas and Hershman 1986; Shellock et al. 1991; Slavotinek et al. 2000; Speer et al. 1993; Taylor et al. 1993). The three muscles (semimembranosus, semitendinosus, and biceps femoris) cross two joints (hip and knee) and have the largest proportion of T2 fibres in the body. A number of clinical and imaging studies have confirmed that biceps femoris is the most commonly injured muscle accounting for over 80% of all injuries (alone or in combination) with partial tears commoner than complete tears (De Smet and Best 2000; Slavotinek et al. 2000; Speer et al. 1993). In comparison to the other muscles within the group it has two heads proximally (long and short), which mechanically reduces the elasticity of the muscle making it more susceptible to acute injury (Fig. 21.17). The proximal or distal myotendinous area can be injured with almost equal incidence and strains can appear intramuscular as histologically the tendons extend throughout a large proportion of the main muscle (Fig. 21.18) (Garrett et al. 1984). Acute injuries are more frequent in older players, those with previous hamstring injuries, higher level players and with fatigue (Woods et al. 2004).

Semimembranosus and semitendinosus are rarely affected on their own although isolated semitendinosus tears can occur in particular running and jumping athletes (Fig. 21.19) (De Smet and Best 2000). This is thought to be secondary to sudden forced hip flexion with knee extension which is required to hurdle or perform the long jump.

Several studies have evaluated specific imaging factors for hamstring injury and subsequent time to recovery. They have found that increased cross-sectional area, biceps femoris tears, longer injury length and sparing of the myotendinous junction may indicate an increased recovery time (Connell et al. 2004; Croisier et al. 2002; Gibbs et al. 2004; Pomeranz and Heidt 1993; Slavotinek et al. 2000, 2002).

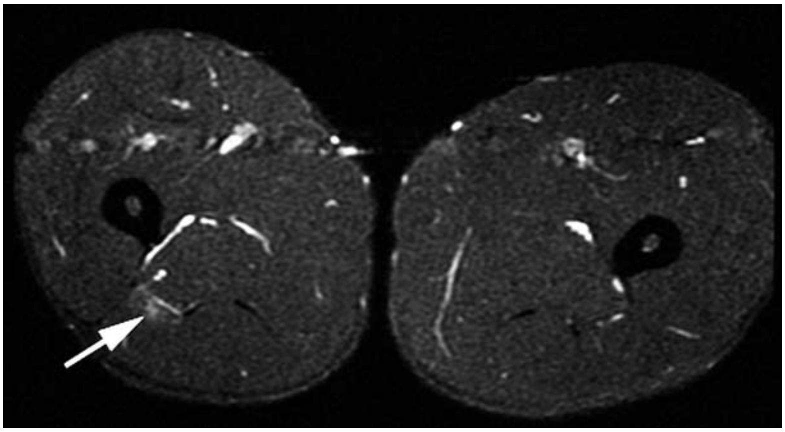

Fig. 21.17. Professional footballer with acute onset thigh pain. Axial T2-weighted fat suppressed MR image shows minor area of edema (*arrow*) within the long head of biceps femoris (grade 1 injury)

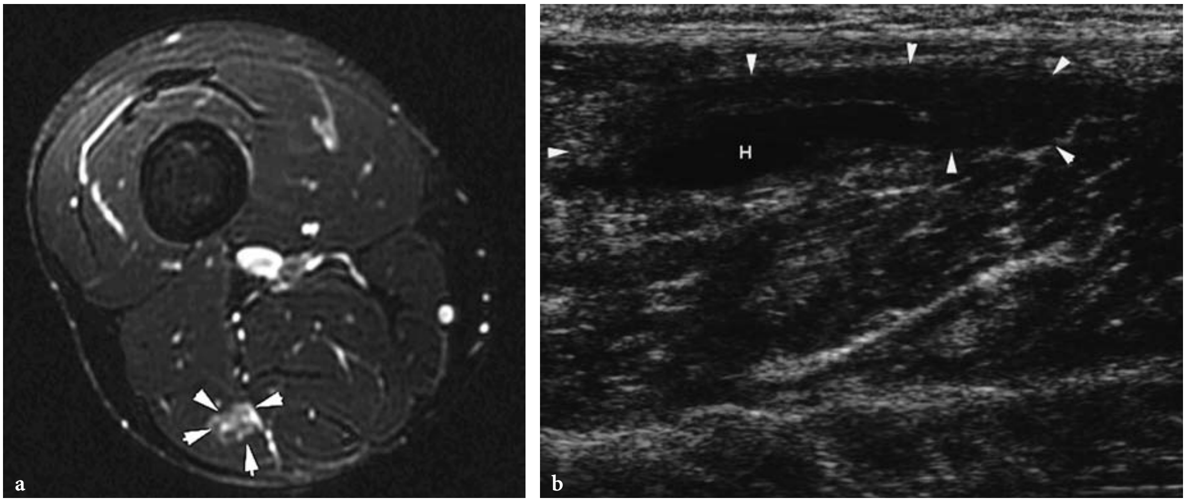

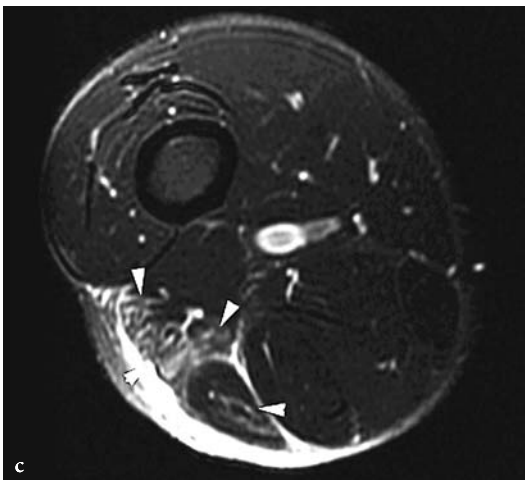

Fig. 21.18a–c. Professional footballer with recurrent hamstring injuries. **a** Axial T2-weighted fat suppressed MR image from 2002 shows an acute grade 2 injury involving the long head of biceps femoris (*small arrowheads*). **b** Corresponding longitudinal ultrasound image 1 week later shows a hypoechoic haematoma (*H*) with an area (*arrowheads*) occupying 10%–20% of the muscle diameter (grade 2 injury). **c** Axial T2-weighted fat suppressed MR image from new injury in 2005 shows marked edema involving the myotendinous junction of the short and long heads (*arrowheads*) of biceps femoris

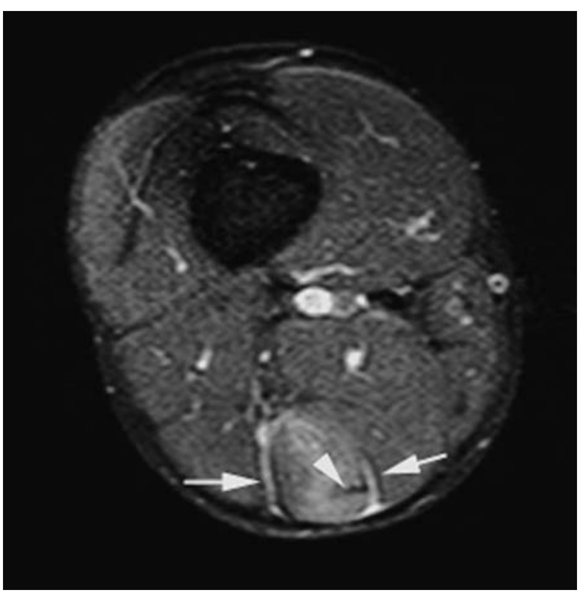

Fig. 21.19. Male athletics hurdler with acute leg pain. Axial T2-weighted fat suppressed MR image shows perifascial edema and fluid (*arrows*) as well as muscle edema within semitendinosus surrounding the low signal tendon (*arrowhead*) (grade 2 injury)

21.4.4 Quadriceps

Rectus femoris is the most commonly injured muscle within the quadriceps group (Garrett 1988, 1990; Noonan and Garrett 1999; Peterson and Renstrom 1986; Speer et al. 1993; Taylor et al. 1993). The rectus femoris differs from the other group muscles in that it spans the hip and the knee joints as well as originating from two heads (straight and reflected). There are two main patterns of injury

described with the commonest type involving strain of the distal myotendon when the muscle belly strips away from the under surface of the distal tendon (Fig. 21.20) (Hasselman et al. 1995; Hughes et al. 1995; Speer et al. 1993). This injury classically occurs with running or kicking as the muscle eccentrically contracts while decelerating knee flexion.

The second pattern of injury described is an apparent mid substance tear. Imaging and cadaver studies have shown this to be a failure at another transition zone involving the myotendinous junctions of the reflected and straight heads (Figs. 21.21 and 21.22) (Cross et al. 2004; Hasselman et al. 1995). The proximal rectus femoris has complex muscle architecture with the reflected head arising from a wide origin over the superior acetabulum. The tendon, although adjacent to the direct head actually remains separate and spirals into the muscle

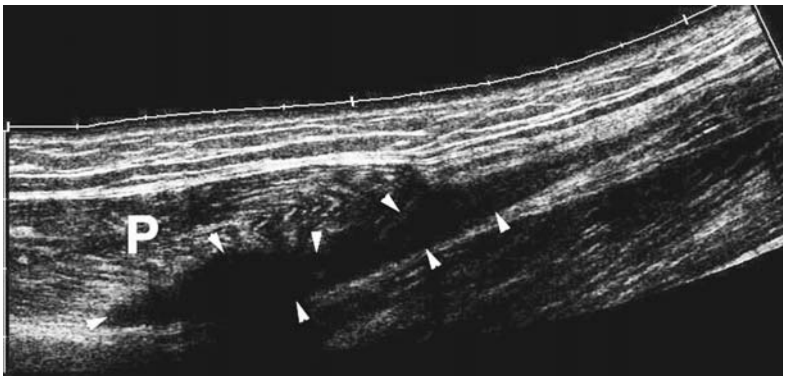

Fig. 21.20. Professional footballer with acute distal thigh pain. Longitudinal extended field of view ultrasound image shows a large hypoechoic haematoma (*arrowheads*) separating the retracted proximal rectus femoris muscle (*P*) from the distal tendon consistent with a grade 3 tear

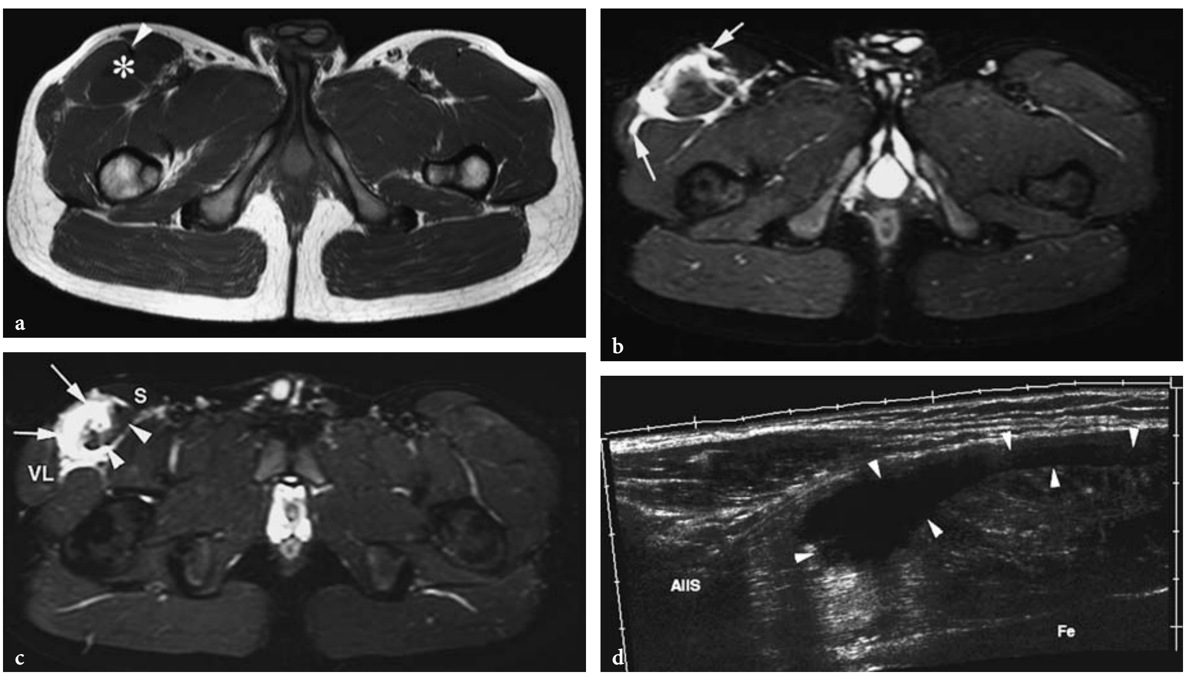

Fig. 21.21a–d. Professional footballer with severe acute proximal thigh pain. **a,b** Axial T1- (**a**) and T2- (**b**) weighted fat suppressed MR images show a swollen and edematous proximal right rectus femoris (*asterisk*), extensive perifascial fluid (*arrows*) and intact low signal tendon (*arrowhead*). **c** Axial T2-weighted fat suppressed MR image above the level of the previous images shows more extensive muscle edema and fluid (*arrows*) extending towards vastus lateralis (*VL*) and overlying sartorius (*S*). A small remnant of muscle is seen intact (*arrowheads*). **d** Longitudinal extended field of view ultrasound image confirms grade 2 injury (*arrowheads*) just distal to the origin from the anterior inferior iliac spine (*AIIS*). The muscle deep to the area and adjacent to the femur (*Fe*) appears intact (*arrows*)

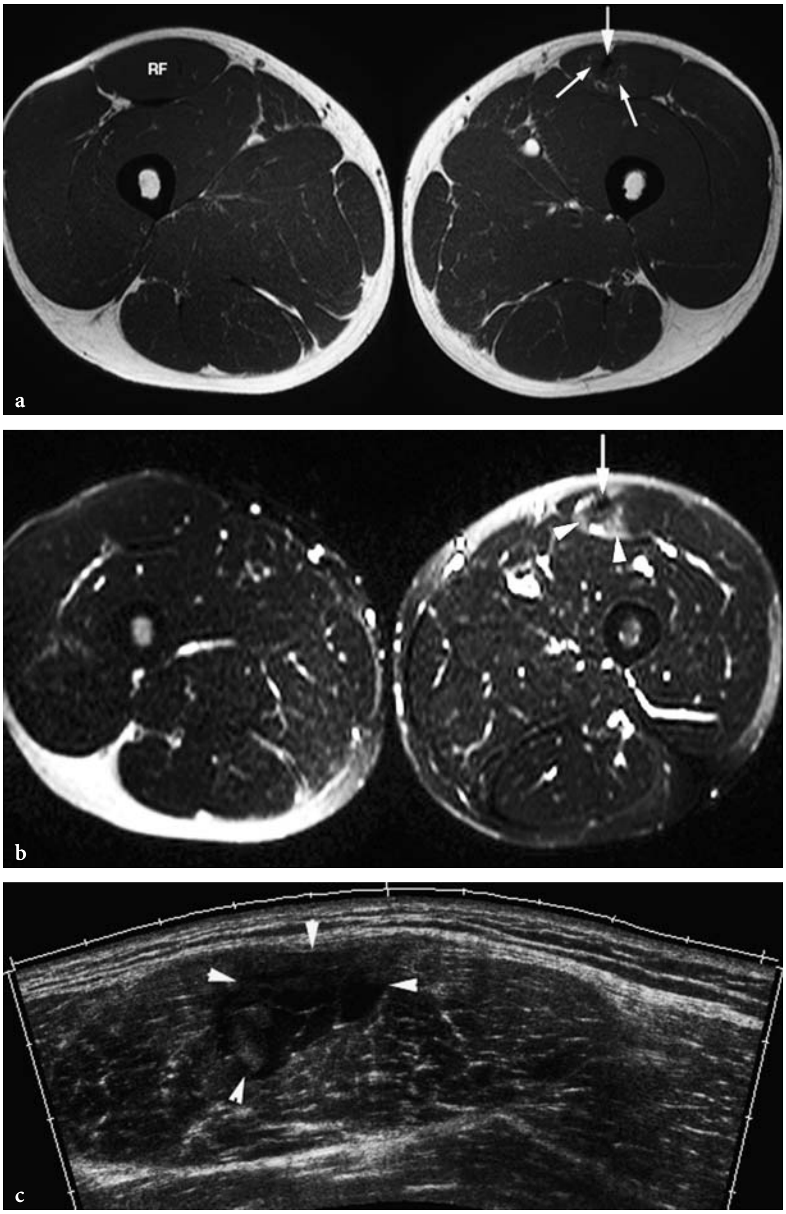

Fig. 21.22a–c. Professional footballer with acute distal thigh pain with minor injury 3 months earlier. **a,b** Axial T1- (**a**) and T2- (**b**) weighted fat suppressed MR images of both thighs shows normal muscle bulk of the right rectus femoris (*RF*). There is edema (*arrowheads*) within the muscles surrounding the left thickened rectus femoris tendon (*large arrow*). The T1-weighted image shows the reduced muscle bulk and fatty infiltration (*small arrows*) indicating atrophy secondary to the previous injury. **c** Transverse extended field of view ultrasound image shows mixed echogenicity haematoma (*arrowheads*) within the superficial aspect of the muscle but the atrophy is not as easily detected

belly extending over a considerable length of the visible muscle (Hasselman et al. 1995; Hughes et al. 1995; Speer et al. 1993). This explains why, although clinically and radiologically the tear can appear to be within the main muscle belly, it is still a myotendinous tear (Figs. 21.21 and 21.22). The mechanism of injury for this less common proximal strain is similar to the distal strain however there is an increased incidence in kicking when the hip is extended and the knee is forced into flexion. Clinically this injury presents with pain over the proximal and mid third of the thigh (Hasselman et al. 1995).

21.4.5 Calf

The gastrocnemius-soleus muscles eccentrically contract to modulate dorsiflexion at the ankle during normal gait and heel strike. However in sprinting the foot initially strikes the ground with the distal first and second rays and not the heel resulting in more forceful ankle dorsiflexion (Lees and Nolan 1998; Novacheck 1998a; Sammarco and Hockenbury 2001). This muscle complex also concentrically contracts on push off for sprinting, jumping and cutting-in.

Aponeurosis distraction is a specific type of injury which occurs at the margin of two synergistic muscles. The muscles most frequently involved are the medial head of gastrocnemius and soleus or, less commonly, semimembranosus and semitendinosus (Bianchi et al. 1998). When this involves the medial head of gastrocnemius it is known as "tennis leg" (Bianchi et al. 1998; Mink 1992). This injury typically occurs during forced dorsiflexion of the ankle with the knee in extension causing powerful eccentric loading of the gastrocnemius and soleus muscles. Although in the past there has been debate over whether the plantaris muscle is primarily involved (Helms et al. 1995), larger reviews of this condition have subsequently shown little or no involvement of plantaris with the gastrocnemius the primary site of injury (Fig. 21.23) (Bianchi et al. 1998; Delgado et al. 2002; Speer et al. 1993). The aponeurosis between the two muscles is a potentially weak area as the soleus consists mainly of T1 fibres and is relatively inelastic compared to the gastrocnemius which also spans two joints and consists of T2 fibres (Bianchi et al. 1998; Mink 1992). The Achilles tendon itself is usually uninjured.

Ultrasound or MR imaging can demonstrate muscle fibre disruption adjacent to the aponeurosis and the presence of perifascial fluid and haematoma (most commonly a grade two injury) (Fig. 21.23) (Bianchi et al. 1998; Delgado et al. 2002). These injuries respond well to conservative treatment although scarring can occur in the region of the aponeurosis (Fig. 21.24) (Bianchi et al. 1998).

21.4.6 Delayed Onset Muscle Soreness

Delayed onset muscle soreness (DOMS) develops when specific muscle groups undergo unaccustomed strenuous exercise (Armstrong 1984; Newham et al. 1983; Zabetakis 1986). This usually occurs in recreational athletes who sporadically participate in sport, however this can also occur in professional

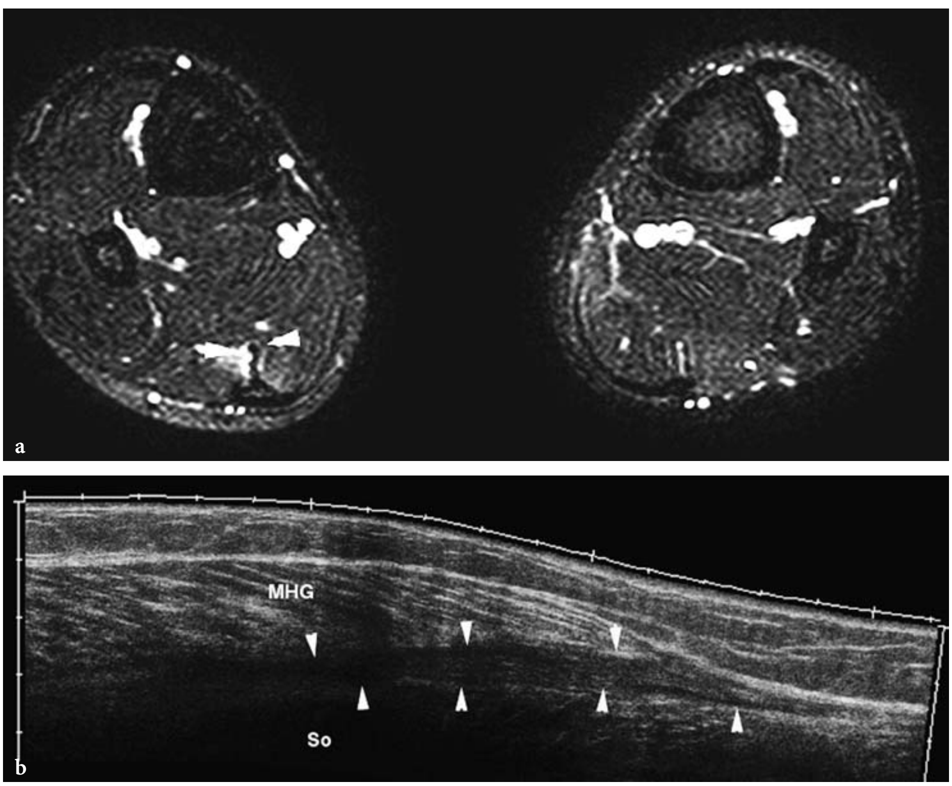

Fig. 21.23a,b. Ballet dancer with acute calf pain. **a** Axial T2-weighted fat suppressed MR image of both calves shows right sided edema (*small arrow*) adjacent to the myotendinous junction of the gastrocnemius and soleus (*arrowheads*). **b** Longitudinal extended field of view ultrasound image shows extensive hypoechoic haematoma (*arrowheads*) between the medial head of the gastrocnemius (*MHG*) and soleus (*So*)

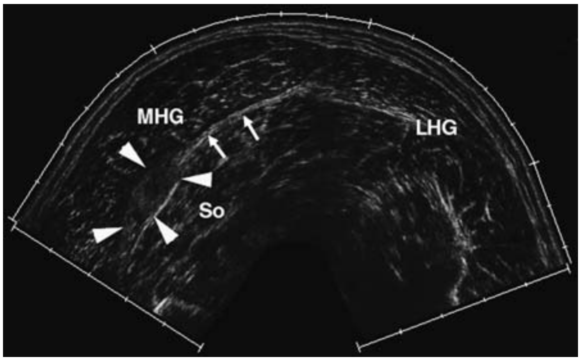

Fig. 21.24. Professional ballet dancer with previous calf pain and persisting swelling but relatively little symptoms. Transverse extended field-of-view ultrasound image shows a normal appearing lateral head of gastrocnemius (*LHG*) but hyperechoic nodular thickening (*arrowheads*) between the medial head of gastrocnemius (*MHG*) and soleus (*So*). This is consistent with scar tissue and adjacent fascia appears of more normal thickness (*arrows*)

athletes when training is intensified after injury. It is thought to occur because of microscopic disruption of muscle fibrils, particularly at the myotendinous junction where there are also large concentrations of pain receptors (Armstrong 1984).

Clinically diffuse lower limb muscle pain develops 12–24 h after activity and is exacerbated by eccentric contraction (Newham et al. 1983; Noonan and Garrett 1999; Zabetakis 1986). This helps to differentiate clinically DOMS from a muscle tear or strain, which usually causes immediate focal pain and is exacerbated by concentric contraction. Additionally DOMS usually resolves within seven days without any specific treatment (Mink 1992; Peterson and Renstrom 1986).

Imaging is rarely necessary in the majority of cases (Fornage 2000) but can be useful in excluding other causes of severe pain if the clinical history is not clear. MR imaging can show edema in multiple muscles, but this is not a specific or sensitive finding with the abnormality persisting up to 82 days after clinical resolution (Marcantonio and Cho 2000; Steinbach et al. 1998). Ultrasound is usually normal but its main role is for excluding a significant muscle strain or tear, which allows appropriate rehabilitation to continue.

21.4.7 Muscle Contusion

Muscle contusion occurs secondary to direct trauma causing muscle fibre disruption and haematoma. This usually results from muscle being compressed against bone but can also occur when superficial muscle is compressed against a contracted underlying muscle (Jarvinen et al. 2005). Muscle contusion is commonly seen in contact sports ("dead leg") with the quadriceps the most affected muscle group. It is a clinical diagnosis obtained from patient history, but on examination, compared to a severe muscle tear, muscle function is relatively normal given the degree of pain (Armstrong 1984; Jackson and Feagin 1973; Jarvinen et al. 2005; Stauber 1988; Zarins and Ciullo 1983).

21.4.7.1 Imaging

In a similar manner to muscle strain MR imaging or ultrasound can be used to evaluate the muscle and underlying periosteum although MR imaging is preferable if an associated bone injury is suspected. The difficulty for either imaging modality is defining if there is muscle distraction especially if the clinical history is unclear.

On ultrasound an acute contusion (0–48 h) appears ill defined with irregular margins and marked echo-

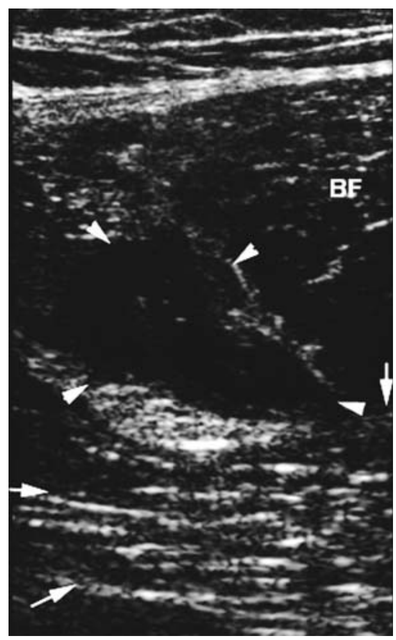

Fig. 21.25. Rugby player with thigh pain, 1 week after tackle. Transverse ultrasound image of the posterior thigh shows hypoechoic haematoma (*arrowheads*) predominately involving semitendinosus extending into the adjacent biceps femoris (*BF*) with the deeper lying muscle appearing echogenic (*arrows*)

genic swelling of the fascicles and entire muscle (Fig. 21.25) (Aspelin et al. 1992). MR imaging also demonstrates edema and mixed intrinsic signal as the blood products develop. In comparison to muscle strain contusion is characterized by the haematoma crossing aponeurotic boundaries representing the demarcation of the impact (Robinson 2004; Van Holsbeeck and Introcasco 2001).

In severe clinical cases dynamic ultrasound imaging confirms that a complete tear is not present and documents the extent of muscle damage. At 48–72 h ultrasound appearances become better defined with the haematoma appearing hypoechoic and a clearer echogenic margin which expands centrally as the muscle repairs (Robinson 2004; Van Holsbeeck and Introcasco 2001). MR imaging also demonstrates these changes although the degree of adjacent muscle and soft tissue edema can persist for some time.

In the following weeks the contusion can be monitored for regeneration of muscle (see Chap. 3), scar tissue or more rarely myositis ossificans (see complications and Chap. 29) (Garrett 1988; Zarins and Ciullo 1983). However, in sporting injuries, the majority of contusions heal with normal muscle regeneration and chronic complications are relatively rare (Jarvinen et al. 2005; Peterson and Renstrom 1986).

21.5 Complications of Lower Limb Muscle Injury

21.5.1 Fibrous Scarring

Scar tissue can restrict muscle function resulting in reduced contractile strength increasing the risk of re-injury at the junction of the muscle and scar (Fig. 21.26) (Jarvinen et al. 2005; Speer et al. 1993; Taylor et al. 1993). Scar tissue, especially after hamstring tears, can also involve adjacent nervous tissue and cause referred symptoms which produce significant pain on sprinting or sudden movement (Fig. 21.26).

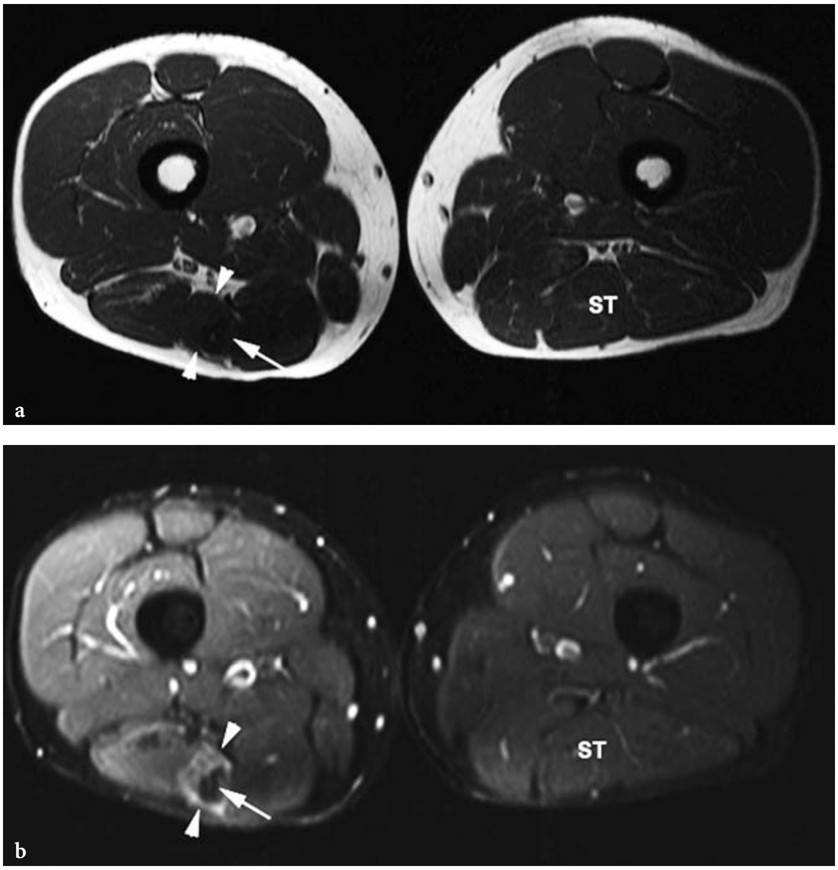

Fig. 21.26a,b. Professional footballer with previous hamstring injury complaining of recurrent pain. Axial T1- (**a**) and T2- (**b**) weighted fat suppressed MR images show normal left semitendinosus (*ST*). There is reduced muscle bulk on the right, thickened (scarred) low signal tendon (*arrow*) and edema (*arrowheads*) within the remaining muscle indicating a retear

MR imaging usually defines scar tissue as a low signal soft tissue thickening either paralleling the tendon (Fig. 21.26) or with a more amorphous appearance at the muscle periphery (Fig. 21.27). Ultrasound detects fibrotic scarring as an echogenic focus but dynamic stressing can assess the relative inelasticity of this tissue and any adherence to adjacent structures which is why I find this technique most useful for initial evaluation in athletes (Fig. 21.27) (Box 21.4).

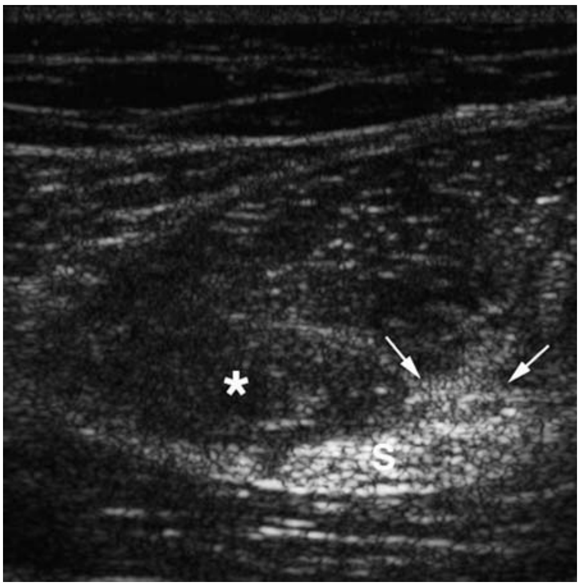

Fig. 21.27. Professional football player with previous hamstring tear and leg pain on sprinting. Transverse ultrasound image shows peripheral echogenic scar tissue (*arrows*) of semitendinosus adherent to the sciatic nerve (*S*) with some loss of the normal muscle echotexture (*asterisk*) due to previous injury

21.5.2 Myositis Ossificans

Myositis ossificans is a rare complication of muscle injury and usually develops after injuries associated with a large haematoma or contusion.

Clinically the development of myositis ossificans should be suspected when the degree of pain and soft tissue swelling persists and is out of proportion to the original injury (Peterson and Renstrom 1986). The commonest muscle group involved by this condition is the quadriceps as this area is most commonly affected by muscle contusion.

Prior to the development of calcification or ossification ultrasound appearances are similar to an organising haematoma (see contusion before). However an advantage of ultrasound is that it can demonstrate the relatively well defined peripheral margins and borders with adjacent soft tissues (Bodley et al. 1993; Peck and Metreweli 1988). MR imaging performed at this stage can show an extremely heterogeneous appearance with surrounding edema that can sometimes be misinterpreted as an aggressive process (Fig. 21.28) (De Smet et al. 1992; Shirkhoda et al. 1995). Ultrasound can also demonstrate peripheral calcification and ossification, as early as 2–3 weeks, before it is clearly evident on plain film or MR imaging (Fig. 21.29) (Bodley et al. 1993; Peck and Metreweli 1988).

21.5.3 Muscle Atrophy/Hypertrophy

On MR imaging muscle atrophy shows decreased muscle bulk and increased T1-weighted signal due to fat deposition between the muscle fibres. These features are not uncommonly seen in muscles which retear (Figs. 21.22 and 21.26). On ultrasound the muscle echotexture is increased due to fat deposition with additional loss of fascial plane definition.

21.5.4 Muscle Hernia

A muscle hernia is defined as protrusion of muscular tissue through a defect in the containing epimysium (fascia) (Miniaci and Rorabeck 1987). This commonly occurs in the anterior and lateral muscle groups of the lower leg (especially tibialis anterior) (Fig. 21.30) but is also recognised with rectus femoris and the hamstrings (Bianchi et al. 1995). It is thought that the fascia overlying tibialis anterior has an area of potential weakness due to penetrating branches of the peroneal nerve and associated vasculature (Nicholas and Hershman 1986).

The hernia usually presents as a mass which may only appear after exercise or on standing (Bianchi et al. 1995). The hernia may be painful on exertion and the clinical differential diagnosis includes an incompetent perforating vein or chronic exertional compartment syndrome.

Ultrasound can accurately identify the normal thick echogenic muscle fascia with any defect seen as

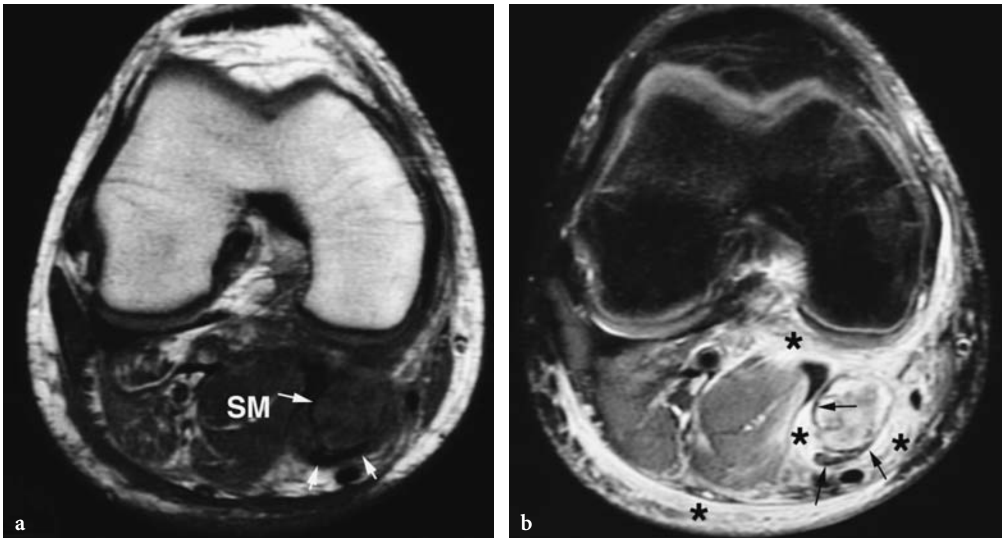

Fig. 21.28a,b. Young athlete with thigh pain. Axial T1- (**a**) and T2- (**b**) weighted fat suppressed MR images show semimembranosus (*SM*) with adjacent haematoma and low signal linear areas (*arrows*) peripherally. Note extensive edema extending throughout distal thigh and subcutaneous fat (*asterisks*). Radiographs confirmed myositis ossificans

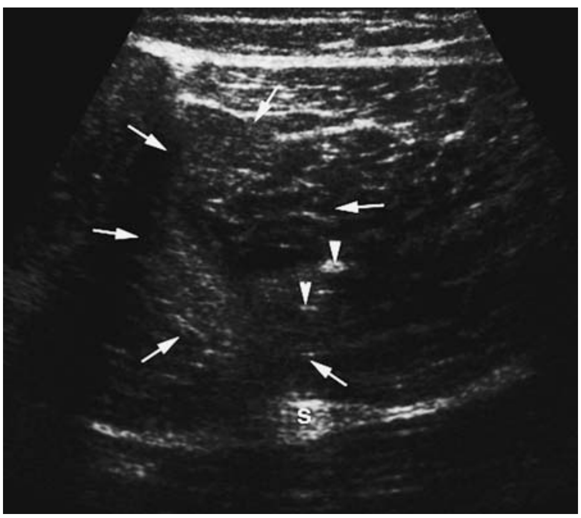

Fig. 21.29. Same player as in Figure 21.25, 5 weeks later, complaining of persisting pain and swelling. Transverse ultrasound image shows ill-defined muscle attenuation consisting with the previous haematoma (*arrows*). There are a number of areas of small echogenic foci (*arrowheads*) consistent with early ossification

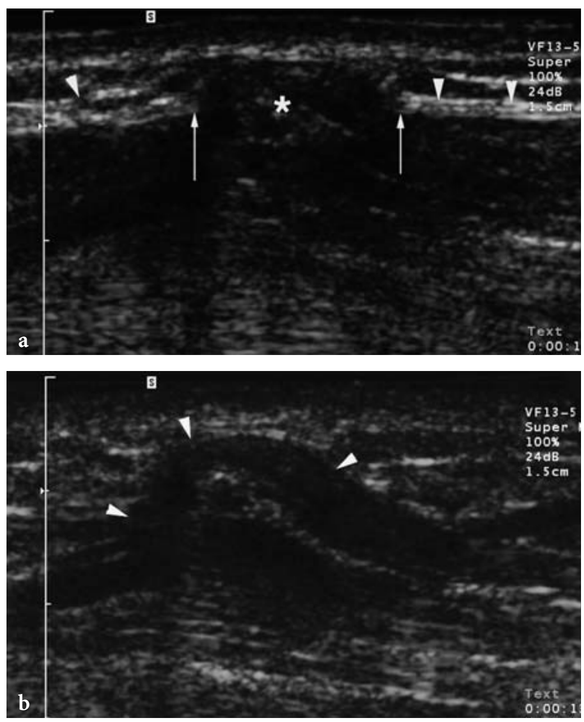

Fig. 21.30a,b. Professional footballer with intermittent anterior leg lump. **a** Longitudinal ultrasound image at rest show a small muscle hernia (*asterisk*) protruding through a defect (*arrows*) in the deep echogenic fascia (*arrowheads*). **b** Post exercise the hernia (*arrowheads*) has become swollen and more hypoechoic

a hypoechoic gap (Fig. 21.30) (Bianchi et al. 1995). Dynamic manoeuvres (using a gel stand-off) can be performed to reproduce the muscle hernia if it is currently reduced. On acute herniation the muscle may appear hyperechoic due to compression of the fascial planes within it. However, if chronic it may appear hypoechoic and ill-defined due to a degree of edema (Bianchi et al. 1995). MR imaging can demonstrate a hernia if present at rest but may be relatively ineffective in demonstrating small or exertional lesions (Bianchi et al. 1995; Steinbach et al. 1998).

21.6 Lower Limb Tendon Injury

Acute catastrophic tears of normal lower limb tendons are extremely rare in athletes and overuse injuries are more common (Hawkins et al. 2001). Decreased activity of the tendon, overuse (training errors), injury elsewhere in the kinetic chain and increasing age can alter the tendon's matrix and collagen composition and subsequently its line of action (Kainberger et al. 2001; Novacheck 1998b; Teitz et al. 1997; Towers et al. 2003). Initially this alteration in tendon function may not be evident clinically or radiologically but begins a cycle which leads to further injury as greater forces are required to produce the same tendon deformity. Chronic injury also develops at sites predetermined by the anatomical structure and biomechanical function of the tendon (Novacheck 1998b; Teitz et al. 1997). Areas of mechanical friction are important in the development of chronic damage and can occur at the greater trochanter (tensor fascia lata), lateral femoral condyle (iliotibial band) and iliopectineal eminence (iliopsoas tendon). Osseous spurs, retinaculum injuries or impingement syndromes can also result in chronically increased stresses in adjacent tendons (Bencardino et al. 2001; Shetty et al. 2002).

21.6.1 Imaging Tendon Injury

Tendinopathy, tears and paratenon inflammation can be accurately assessed by MR imaging and ultrasound and appearances are discussed in Chap. 5 (Bencardino et al. 2001; Van Holsbeeck and Introcasco 2001).

21.6.2 Iliotibial Band Injury

Iliotibial band injury will be discussed in detail in Chap. 17 on ligaments and tendons of the knee.

21.6.3 Distal Hamstring Tendons

Primary tendinopathy and acute rupture of the distal hamstring tendons are rare. Acute injury is possible and semimembranosus can be injured during knee trauma by its involvement with the posterior oblique component of the medial collateral ligament (Beltran et al. 2003). We also have experience in a subgroup of soccer and rugby athletes who have developed subacute distal semitendinosus tendon injury. The injury seems to be initiated when the player is tackled while eccentrically stretching. This results in acute medial popliteal fossa pain and tenderness which is relatively mild and does not initially inhibit training and playing. However chronic pain can develop after 6–8 weeks resulting in a reduction in sprint speed, probably due to adhesive scarring. MR and ultrasound imaging performed at this stage usually shows minor paratendon edema but also a longitudinal split just distal to the myotendinous junction (Fig. 21.31). Operative dehiscence of scar tissue with tenotomy seems to be beneficial in this patient group (Schilders et al. 2006).

21.7 Conclusion

Imaging injuries in high level athletes is a complex but rewarding process as the diagnosis can markedly influence treatment and performance. There are a number of imaging techniques available for evaluating lower limb osseous and soft tissue injuries but choice can be limited by local availability and radiologist preference. The radiologist's role in assessing injury is to grade the severity and extent of injury so appropriate treatment can be implemented. It is ideal if the radiologist is confident with multiple imaging techniques and can then offer more flexibility for solving such problems.

In acute osseous injuries radiographs are usually sufficient to confirm or exclude immediate severe

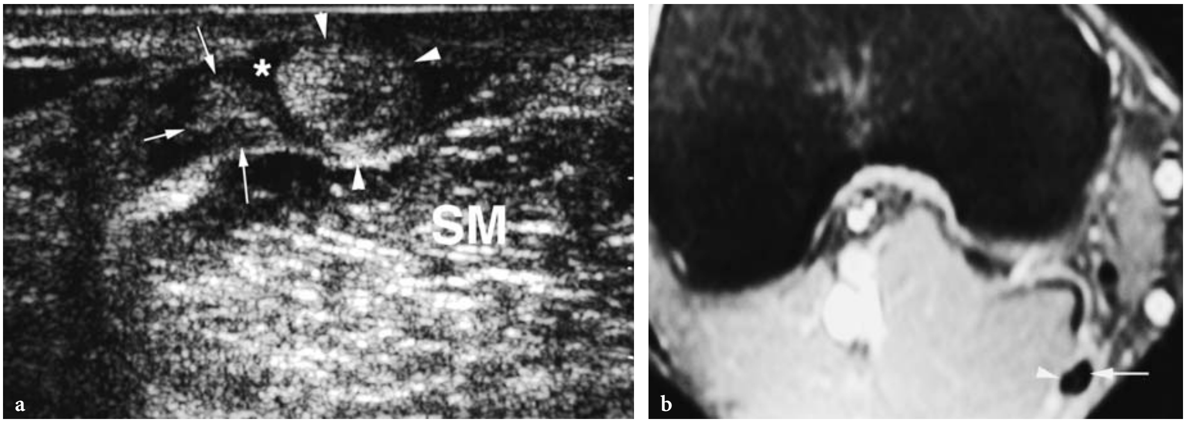

Fig. 21.31a,b. Professional rugby player with persisting posteromedial thigh tenderness. **a** Transverse ultrasound image shows longitudinal split of the semitendinosus tendon into two components (*arrowheads* and *arrows*) with some edematous tissue (*asterisk*) separating the components. Note semimembranosus (*SM*). **b** Corresponding axial T2-weighted MR image shows splitting of the semitendinosus tendon into medial (*arrow*) and lateral (*arrowhead*) components with minor surrounding edema

injury. For indeterminate cases and chronic osseous injuries MR imaging is the most effective and accurate imaging tool available. In soft tissue injuries ultrasound and MR imaging are both accurate and effective techniques that compliment each other in specific areas. Ultrasound can be used for initial assessment of the majority of acute and chronic soft tissue injuries; however MR imaging is required when symptoms are diffuse or in athletes with a larger muscle bulk in the thigh and pelvis.

Acknowledgements.
The author would like to thank Drs P Bearcroft, AJ Grainger, AA Nicholson, PJ O'Connor, CA Speed and M Stone for contributing images to this chapter.

Things to Remember

1. The lower limb is essential for all athletic movement and is the most commonly injured area for all sporting activities.
2. Radiographs are the first line imaging investigation for evaluating acute osseous injury but MR imaging is a sensitive technique for acute complications and overuse injuries.
3. MR imaging and ultrasound are both accurate techniques for assessing acute and chronic soft tissue injuries as well as subsequent complications:
   a) Ultrasound provides a rapid and dynamic assessment
   b) MR imaging is sensitive for very low grade injuries and also maintains its field of view in athletes with large muscle bulk or diffuse symptoms

References

Anderson MW, Ugalde V, Batt M et al. (1997) Shin splints: MR appearance in a preliminary study. Radiology 204:177–180
Armstrong RB (1984) Mechanisms of exercise-induced delayed onset muscular soreness: a brief review. Med Sci Sports Exerc 16:529–538
Aspelin P, Ekberg O, Thorsson O et al. (1992) Ultrasound examination of soft tissue injury of the lower limb in athletes. Am J Sports Med 20:601–603
Atilla S, Ilgit ET, Akpek S et al. (1998) MR imaging and MR angiography in popliteal artery entrapment syndrome. Eur Radiol 8:1025–1029

Batt ME, Ugalde V, Anderson MW et al. (1998) A prospective controlled study of diagnostic imaging for acute shin splints. Med Sci Sports Exerc 30:1564–1571

Beltran J, Matityahu A, Hwang K et al. (2003) The distal semimembranosus complex: normal MR anatomy, variants, biomechanics and pathology. Skeletal Radiol 32:435–445

Bencardino JT, Rosenberg ZS, Serrano LF (2001) MR imaging of tendon abnormalities of the foot and ankle. Magn Reson Imaging Clin N Am 9:475–492, x

Bianchi S, Abdelwahab IF, Mazzola CG et al. (1995) Sonographic examination of muscle herniation. J Ultrasound Med 14:357–360

Bianchi S, Martinoli C, Abdelwahab IF et al. (1998) Sonographic evaluation of tears of the gastrocnemius medial head ("tennis leg"). J Ultrasound Med 17:157–162

Boden BP, Lohnes JH, Nunley JA et al. (1999) Tibia and fibula fractures in soccer players. Knee Surg Sports Traumatol Arthrosc 7:262–266

Bodley R, Jamous A, Short D (1993) Ultrasound in the early diagnosis of heterotopic ossification in patients with spinal injuries. Paraplegia 31:500–506

Chernoff DM, Walker AT, Khorasani R et al. (1995) Asymptomatic functional popliteal artery entrapment: demonstration at MR imaging. Radiology 195:176–180

Chomiak J, Junge A, Peterson L et al. (2000) Severe injuries in football players. Influencing factors. Am J Sports Med 28:S58–S68

Collins PS, McDonald PT, Lim RC (1989) Popliteal artery entrapment: an evolving syndrome. J Vasc Surg 10:484–489; discussion 489–490

Connell DA, Schneider-Kolsky ME, Hoving JL et al. (2004) Longitudinal study comparing sonographic and MRI assessments of acute and healing hamstring injuries. AJR Am J Roentgenol 183:975–984

Croisier JL, Forthomme B, Namurois MH et al. (2002) Hamstring muscle strain recurrence and strength performance disorders. Am J Sports Med 30:199–203

Cross TM, Gibbs N, Houang MT et al. (2004) Acute quadriceps muscle strains: magnetic resonance imaging features and prognosis. Am J Sports Med 32:710–719

De Smet AA, Best TM (2000) MR imaging of the distribution and location of acute hamstring injuries in athletes. AJR Am J Roentgenol 174:393–399

De Smet AA, Norris MA, Fisher DR (1992) Magnetic resonance imaging of myositis ossificans: analysis of seven cases. Skeletal Radiol 21:503–507

Delgado GJ, Chung CB, Lektrakul N et al. (2002) Tennis leg: clinical US study of 141 patients and anatomic investigation of four cadavers with MR imaging and US. Radiology 224:112–119

Dvorak J, Junge A (2000) Football injuries and physical symptoms. A review of the literature. Am J Sports Med 28: S3–S9

Edwards PH Jr, Wright ML, Hartman JF (2005) A practical approach for the differential diagnosis of chronic leg pain in the athlete. Am J Sports Med 33:1241–1249

Elias DA, White LM, Rubenstein JD et al. (2003) Clinical evaluation and MR imaging features of popliteal artery entrapment and cystic adventitial disease. AJR Am J Roentgenol 180:627–632

Fleckenstein JL, Canby RC, Parkey RW et al. (1988) Acute effects of exercise on MR imaging of skeletal muscle in normal volunteers. AJR Am J Roentgenol 151:231–237

Fornage BD (2000) The case for ultrasound of muscles and tendons. Semin Musculoskelet Radiol 4:375–391

Fredericson M, Bergman AG, Hoffman KL et al. (1995) Tibial stress reaction in runners. Correlation of clinical symptoms and scintigraphy with a new magnetic resonance imaging grading system. Am J Sports Med 23:472–481

Fuller CW, Smith GL, Junge A et al. (2004) The influence of tackle parameters on the propensity for injury in international football. Am J Sports Med 32:43S–53S

Gaeta M, Minutoli F, Scribano E et al. (2005) CT and MR imaging findings in athletes with early tibial stress injuries: comparison with bone scintigraphy findings and emphasis on cortical abnormalities. Radiology 235:553–561

Garrett WE Jr (1988) Injuries to the muscle-tendon unit. Instr Course Lect 37:275–282

Garrett WE Jr (1990) Muscle strain injuries: clinical and basic aspects. Med Sci Sports Exerc 22:436–443

Garrett WE Jr, Califf JC, Bassett FH III (1984) Histochemical correlates of hamstring injuries. Am J Sports Med 12:98–103

Garrett WE Jr, Safran MR, Seaber AV et al. (1987) Biomechanical comparison of stimulated and nonstimulated skeletal muscle pulled to failure. Am J Sports Med 15:448–454

Gibbs NJ, Cross TM, Cameron M et al. (2004) The accuracy of MRI in predicting recovery and recurrence of acute grade one hamstring muscle strains within the same season in Australian Rules football players. J Sci Med Sport 7:248–258

Giza E, Fuller C, Junge A et al. (2003) Mechanisms of foot and ankle injuries in soccer. Am J Sports Med 31:550–554

Green NE, Rogers RA, Lipscomb AB (1985) Nonunions of stress fractures of the tibia. Am J Sports Med 13:171–176

Hasselman CT, Best TM, Hughes CT, Martinez S, Garrett WE Jr (1995) An explanation for various rectus femoris strain injuries using previously undescribed muscle architecture. Am J Sports Med 23:493–499

Hawkins RD, Hulse MA, Wilkinson C et al. (2001) The association football medical research programme: an audit of injuries in professional football. Br J Sports Med 35:43–47

Helms CA, Fritz RC, Garvin GJ (1995) Plantaris muscle injury: evaluation with MR imaging. Radiology 195:201–203

Hughes Ct, Hasselman CT, Best TM et al. (1995) Incomplete, intrasubstance strain injuries of the rectus femoris muscle. Am J Sports Med 23:500–506

Ilahi OA, Younas SA, Labbe MR et al. (2003) Prevalence of ganglion cysts originating from the proximal tibiofibular joint: A magnetic resonance imaging study. Arthroscopy 19:150–153

Jackson DW, Feagin JA (1973) Quadriceps contusions in young athletes. Relation of severity of injury to treatment and prognosis. J Bone Joint Surg Am 55:95–105

Jarvinen TA, Jarvinen TL, Kaariainen M et al. (2005) Muscle injuries: biology and treatment. Am J Sports Med 33:745–764

Kainberger F, Ulreich N, Huber W et al. (2001) Tendon overuse syndrome: imaging diagnosis. Wien Med Wochenschr 151:509–512

Kaufman KR, Brodine S, Shaffer R (2000) Military training-related injuries: surveillance, research, and prevention. Am J Prev Med 18:54–63

Lees A, Nolan L (1998) The biomechanics of soccer: a review. J Sports Sci 16:211–234

Marcantonio DR, Cho GJ (2000) Focus on muscle in orthopedic MRI. Semin Musculoskelet Radiol 4:421–434
Martens MA, Backaert M, Vermaut G et al. (1984) Chronic leg pain in athletes due to a recurrent compartment syndrome. Am J Sports Med 12:148–151
Milgrom C, Chisin R, Giladi M et al. (1984) Negative bone scans in impending tibial stress fractures. A report of three cases. Am J Sports Med 12:488–491
Miniaci A, Rorabeck CH (1987) Tibialis anterior muscle hernia: a rationale for treatment. Can J Surg 30:79–80
Mink JH (1992) Muscle injuries. In: Deutsch A, Mink JH, Kerr R (eds) MRI of the foot and ankle, 1st edn. Raven Press, New York, pp 281–312
Miskovsky S, Kaeding C, Weis L (2004) Proximal tibiofibular joint ganglion cysts: excision, recurrence, and joint arthrodesis. Am J Sports Med 32:1022–1028
Newham DJ, Mills KR, Quigley BM et al. (1983) Pain and fatigue after concentric and eccentric muscle contractions. Clin Sci (Lond) 64:55–62
Nicholas J, Hershman E (1986) The lower extremity and spine in sports medicine. Mosby, St Louis
Noonan TJ, Garrett WE Jr (1992) Injuries at the myotendinous junction. Clin Sports Med 11:783–806
Noonan TJ, Garrett WE Jr (1999) Muscle strain injury: diagnosis and treatment. J Am Acad Orthop Surg 7:262–269
Nordin M, Frankel VH (2001a) Biomechanics of bone. In: Nordin M, Frankel VH (eds) Basic biomechanics of the musculoskeletal system, 3rd edn. Lippincott Williams and Wilkins, Philadelphia, pp 26–58
Nordin M, Frankel VH (2001b) Biomechanics of skeletal muscle. In: Nordin M, Frankel VH (eds) Basic biomechanics of the musculoskeletal system, 3rd edn. Lippincott Williams and Wilkins, Philadelphia, pp 149–174
Novacheck TF (1998a) The biomechanics of running. Gait Posture 7:77–95
Novacheck TF (1998b) Running injuries: a biomechanical approach. Instr Course Lect 47:397–406
Ohta-Fukushima M, Mutoh Y, Takasugi S et al. (2002) Characteristics of stress fractures in young athletes under 20 years. J Sports Med Phys Fitness 42:198–206
Peck RJ, Metreweli C (1988) Early myositis ossificans: a new echographic sign. Clin Radiol 39:586–588
Pedowitz RA, Hargens AR, Mubarak SJ et al. (1990) Modified criteria for the objective diagnosis of chronic compartment syndrome of the leg. Am J Sports Med 18:35–40
Peterson L, Renstrom P (1986) Sports injuries. Year Book Medical, Chicago
Pomeranz SJ, Heidt RS Jr (1993) MR imaging in the prognostication of hamstring injury. Work in progress. Radiology 189:897–900
Rich NM, Collins GJ Jr, McDonald PT et al. (1979) Popliteal vascular entrapment. Its increasing interest. Arch Surg 114:1377–1384
Robinson P (2004) Ultrasound of muscle injury. In: McNally E (ed) Practical musculoskeletal ultrasound. Churchill Livingston, London
Sammarco GJ, Hockenbury RT (2001) Biomechanics of the foot and ankle. In: Nordin M, Frankel VH (eds) Basic biomechanics of the musculoskeletal system, 3rd edn. Lippincott Williams and Wilkins, Philadelphia, pp 222–255
Schilders E, Bismil Q, Sidhom S et al. (2006) Partial rupture of the distal semitendinosus tendon treated by tenotomy – a previously undescribed entity. Knee 13:45–47
Shellock FG, Fukunaga T, Mink JH et al. (1991) Exertional muscle injury: evaluation of concentric versus eccentric actions with serial MR imaging. Radiology 179:659–664
Shetty M, Fessell DP, Femino JE et al. (2002) Sonography of ankle tendon impingement with surgical correlation. AJR Am J Roentgenol 179:949–953
Shirkhoda A, Armin AR, Bis KG et al. (1995) MR imaging of myositis ossificans: variable patterns at different stages. J Magn Reson Imaging 5:287–292
Slavotinek JP, Verrall GM, Fon GT (2000) Hamstring injuries in footballers: The prevalence and prognostic value of MRI findings. Radiology 217:191
Slavotinek JP, Verrall GM, Fon GT (2002) Hamstring injury in athletes: using MR imaging measurements to compare extent of muscle injury with amount of time lost from competition. AJR Am J Roentgenol 179:1621–1628
Speer KP, Lohnes J, Garrett WE Jr (1993) Radiographic imaging of muscle strain injury. Am J Sports Med 21:89–95; discussion 96
Spinner RJ, Atkinson JL, Harper CM Jr et al. (2000) Recurrent intraneural ganglion cyst of the tibial nerve. Case report. J Neurosurg 92:334–337
Stauber W (1988) Eccentric action of muscles: physiology, injury, and adaption. In: Stauber W (ed) Exercise and sports sciences reviews. Franklin Institute, Philadelphia, pp 158–185
Steinbach L, Fleckenstein J, Mink J (1998) MR imaging of muscle injuries. Semin Musculoskeletal Radiol 1:128–141
Taylor DC, Dalton JD Jr, Seaber AV et al. (1993) Experimental muscle strain injury. Early functional and structural deficits and the increased risk for reinjury. Am J Sports Med 21:190–194
Teitz CC, Garrett WE Jr, Miniaci A et al. (1997) Tendon problems in athletic individuals. Instr Course Lect 46:569–582
Toorop R, Poniewierski J, Gielen J et al. (2004) Popliteal artery entrapment syndrome. Jbr-Btr 87:154–155
Towers JD, Russ EV, Golla SK (2003) Biomechanics of tendons and tendon failure. Semin Musculoskelet Radiol 7:59–65
Van Holsbeeck M, Introcasco J (2001) Musculoskeletal ultrasound, 2nd edn. Mosby, St Louis, Miss
Woods C, Hawkins RD, Maltby S, Hulse M, Thomas A, Hodson A (2004) The Football Association Medical Research Programme: an audit of injuries in professional football–analysis of hamstring injuries. Br J Sports Med 38:36–41
Yates B, White S (2004) The incidence and risk factors in the development of medial tibial stress syndrome among naval recruits. Am J Sports Med 32:772–780
Zabetakis P (1986) Muscle soreness and rhabdomyolysis. In: Nicholas J, Hershman E (eds) In: The lower extremity and spine in sports medicine. Mosby, St Louis, pp 59–81
Zarins B, Ciullo JV (1983) Acute muscle and tendon injuries in athletes. Clin Sports Med 2:167–182

The Spine in Sports Injuries: Cervical Spine

22

Paul M. Parizel, Jan L. Gielen, and Filip M. Vanhoenacker

CONTENTS

22.1 Introduction

Injuries to the spine are commonly associated with all kinds of sports activities, both contact and non-contact sports, and at all levels of competition ranging from the high school level to the professional level (Tall and DeVault 1993). The spectrum of potential spinal injuries is wide; some resolve on their own, others might require conservative therapy, and still others might require surgical intervention. Sports injuries involving the cervical spine include intervertebral disc lesions, acute cervical sprain/strain,

P. M. Parizel, MD, PhD, Professor of Radiology
J. L. Gielen, MD, PhD, Associate Professor
F. M. Vanhoenacker, MD, PhD
Department of Radiology, University Hospital Antwerpen, Wilrijkstraat 10, 2650 Edegem, Belgium

Box 22.1. Plain radiographs

- Remain useful in mild cervical spine trauma
- Underestimate fractures, especially near the cervico-thoracic junction
- Flexion-extension views are useful to show instability

Box 22.2. CT

- Preferred technique in more severe trauma (fracture-dislocation)
- Very fast (MDCT requires only seconds to scan the cervical spine)
- Provides limited soft tissue contrast

Box 22.3. Myelography and CT myelography

- Have been largely supplanted by non-invasive cross-sectional imaging techniques
- Remain useful in the diagnosis of nerve root and brachial plexus avulsion

Box 22.4. MR

- Method of choice for assessing spinal cord, ligaments, muscles and soft tissues
- Fat-suppressed sequences are sensitive to bone marrow edema

nerve root and brachial plexus injuries, transient (or in rare cases permanent) quadriplegia, unstable injuries with and without fracture dislocation.

In the media covering sports events, tragic cervical spine injuries of well-known professional athletes are often brought to national attention. These catastrophic cervical spine injuries most commonly occur in collision sports or motorized sports and can lead to devastating consequences for the athlete (Banerjee et al. 2004). Fortunately, these serious injuries are rare in sports. An elaborate review of epidemiologic studies, involving all types of sports activities at all levels of competition, reveals that the overwhelming majority of sports injuries related to the spine are soft-tissue injuries (sprains and strains) and are self-limiting (Tall and DeVault 1993). It is relatively rare for athletic injuries to the spine to result in significant neurologic compromise. However, in cases with neurologic symptoms, the cervical spine is most commonly involved.

Accurate and timely radiological examination of the cervical spine in athletes is therefore essential to establish a correct diagnosis and to prevent further injury.

22.2 Anatomical Considerations

Before proceeding with the radiological examination of the spine, we shall present a brief reminder of cervical spine anatomy. The cervical spine consists of seven vertebrae, numbered from C1 to C7. Cervical vertebrae are the smallest of the true vertebrae, and can be readily distinguished from those of the thoracic or lumbar regions by the presence of a foramen in each transverse process. They are ring-shaped with the vertebral body anteriorly, the pedicles laterally, and the laminae and spinous process posteriorly. The first cervical vertebra, C1 or also known as the atlas because it supports the globe of the head, does not possess a vertebral body, but has two lateral masses, which articulate with the occipital condyles. The second cervical vertebra, C2 or also known as the axis because it forms the pivot on which the first vertebra rotates, has a vertical toothlike projection called the dens or odontoid process, on which the atlas (C1) pivots. Embryologically, the odontoid process can be thought of as representing the vertebral body of C1, and articulates with the anterior arch of C1. With the notable exception of C1–C2, the cervical vertebrae articulate with one another anteriorly via the intervertebral disc and two uncovertebral joints. Laterally, they articulate via the facet joints (also known as zygoapophyseal joints).

The successive openings in the articulated ring-shaped vertebrae, which are stacked upon one another, enclose the spinal canal (also known as vertebral or neural canal). On cross section, the spinal canal presents an isosceles triangular shape, with the base of the triangle anteriorly (formed by the posterior wall of the vertebral bodies and intervertebral discs), and the sides posterior and lateral (formed by the lamina on either side). The angle between the laminae (interlaminar angle) determines to a large extent the anteroposterior diameter of the spinal canal.

The spinal canal contains the spinal cord, nerve roots, blood vessels, and meninges. At each intervertebral disc level, cervical spinal nerves originate from the spinal cord as the anterior (motor) and posterior (sensory) rootlets. Posterior and anterior rootlets join to form a spinal nerve, which lies within the intervertebral foramen. The posterior rootlet has a nerve root ganglion at the inner portion of the intervertebral foramen. The spinal nerve divides into a posterior and anterior ramus at the outlet of the intervertebral foramen. In the cervical spine, the spinal nerves exit the intervertebral foramen above the same-numbered cervical vertebra (e.g. the seventh spinal nerve exits at the C6–C7 level). Though there are only seven cervical vertebrae, there are eight spinal nerves on either side. The eighth cervical nerve exits between the C7 and T1 segment.

The cervical intervertebral disc constitutes a separate anatomic and functional entity, and is distinctly different from the lumbar intervertebral disc (Mercer and Bogduk 1999). The anulus fibrosus of the cervical intervertebral disc does not consist of concentric laminae of collagen fibers, as in the lumbar discs. Rather, the anulus forms a crescent-shaped mass of collagen, which is thickest anteriorly and tapers laterally toward the uncinate processes. Posteriorly, the anulus is merely a thin layer of paramedian vertically oriented fibers. The anterior longitudinal ligament (ALL) covers the front of the disc, and the posterior longitudinal ligament (PLL) reinforces the deficient posterior anulus fibrosus with longitudinal and alar fibers. In this way, the cervical anulus fibrosus is likened to a crescentic anterior interosseous ligament, rather than a ring of fibers surrounding the nucleus pulposus (Mercer and Bogduk 1999).

22.3 Biomechanics of the Cervical Spine

The cervical spine is the most mobile of all the segments of the vertebral column. It allows an extensive range of motion in flexion and extension, which is mainly due to the upwardly oriented inclination of the superior articular surfaces. In *flexion* (forward movement), the anterior longitudinal ligament (ALL) is relaxed, while the posterior longitudinal ligament (PLL), the ligamenta flava, and the inter- and supraspinous ligaments are stretched. During flexion, the intervertebral discs are compressed anteriorly, the interspaces between the laminæ are widened, and the inferior articular processes glide upward, upon the superior articular processes of the subjacent vertebræ. Flexion of the cervical spine is arrested just beyond the point where the cervical convexity is straightened. In *extension* (backward movement), the opposite motions occur. Extension can be carried farther than flexion and is limited by stretching of the anterior longitudinal ligament (ALL), and by the approximation of the spinous processes. In the cervical spine *lateral flexion and rotation* always occur as combined movements. The upward and medial inclinations of the superior articular facet joint surfaces convey a rotary movement during lateral flexion, while pure rotation is prevented by their slight medial slope. During lateral flexion, the sides of the intervertebral discs are compressed, and the extent of motion is limited by the resistance offered by the surrounding ligaments.

In sports-related injuries, the most common mechanism of cervical spine trauma is neck flexion with axial loading (Torg et al. 1987). Neck flexion causes the physiological cervical lordosis to disappear. The axial loading of the head is thus dissipated through a straight spine (Torg et al. 1987).

Examples of axial loading injuries to the cervical spine are found in a variety of sports, such as:

- American football (Fig. 22.1) (player striking opponent with the crown of his helmet) or rugby (Fig. 22.2) (during the scrum phase of the game)
- Ice hockey (player striking his head on the board while doing a push or check)
- Diving in shallow water (Figs. 22.3–22.4) (head striking the ground)
- Gymnastics (Fig. 22.5) (athlete accidentally landing head down while performing a somersault on a trampoline) (Torg 1987).

The spectrum of cervical spine injury is related to the mechanism, the force involved, and the point of application of the force (Tall and DeVault 1993). Axial loading injuries of the cervical spine include vertebral fractures (Figs. 22.2 and 22.3), cervical disc herniations (Fig. 22.1), ligament rupture, facet fracture, and dislocations (Figs. 22.5 and 22.6). Neurologic deficits tend to be greater in athletes with spinal stenosis (Fig. 22.7), either developmental, or acquired through degenerative disease (Torg et al. 1997). Moreover, the biochemistry and biomechanics of the intervertebral disc and spine are age related. Thus, the adolescent and older athlete may have different concerns with regards to diagnosis, treatment, and prognosis after injury to the spine.

Recent studies have indicated that there also is a gender differential regarding injuries of the cervical spine (Kelley 2000). Cervical strain injuries are more prevalent in female athletes than male athletes. For cervical disc injury and cervical disc herniation, the male to female incidence is approximately equal. With increasing participation of women in contact sports that cause major structural injury, a greater incidence of these injuries may be seen in women.

The radiologist examining an athlete with cervical spine trauma, should recognize and understand the mechanism of injury (Pavlov and Torg 1987).

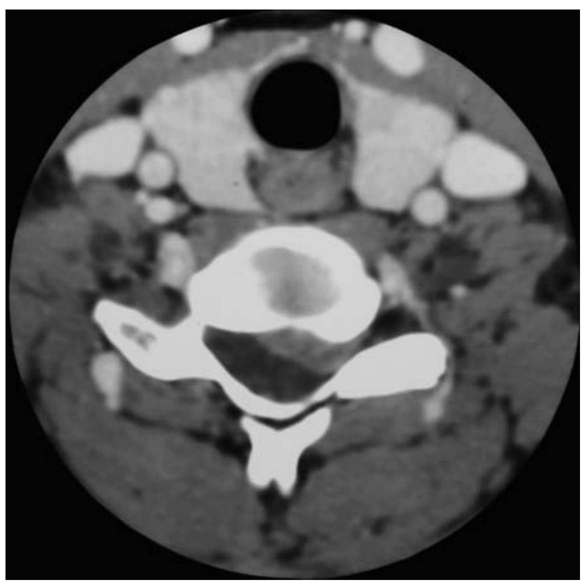

Fig. 22.1. Acute cervical disc herniation in a 32-year-old man who was injured during a football game. Contrast-enhanced CT scan of the cervical spine. At C5–C6, there is a disc herniation extending into the left lateral recess and into the intervertebral foramen. Note the asymmetric deformation of the dural sac and impingement on the left C6 nerve root

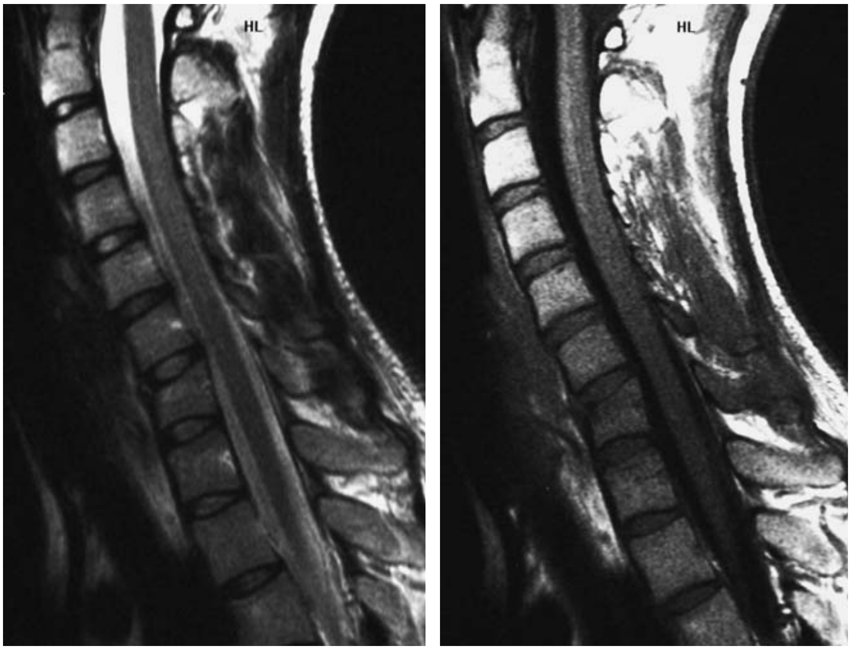

a b

Fig. 22.2a,b. Hyperflexion injury with simple anterior wedge fracture of C7 in a 23-year-old rugby player. MRI scan with sagittal T2-weighted (**a**) and sagittal T1-weighted (**b**) images. The antero-superior corner of the vertebral body C7 is depressed, and there is band of bone marrow edema subjacent to the upper endplate. The posterior wall is not displaced, the diameter of the spinal canal remains normal, and there is no medullary contusion

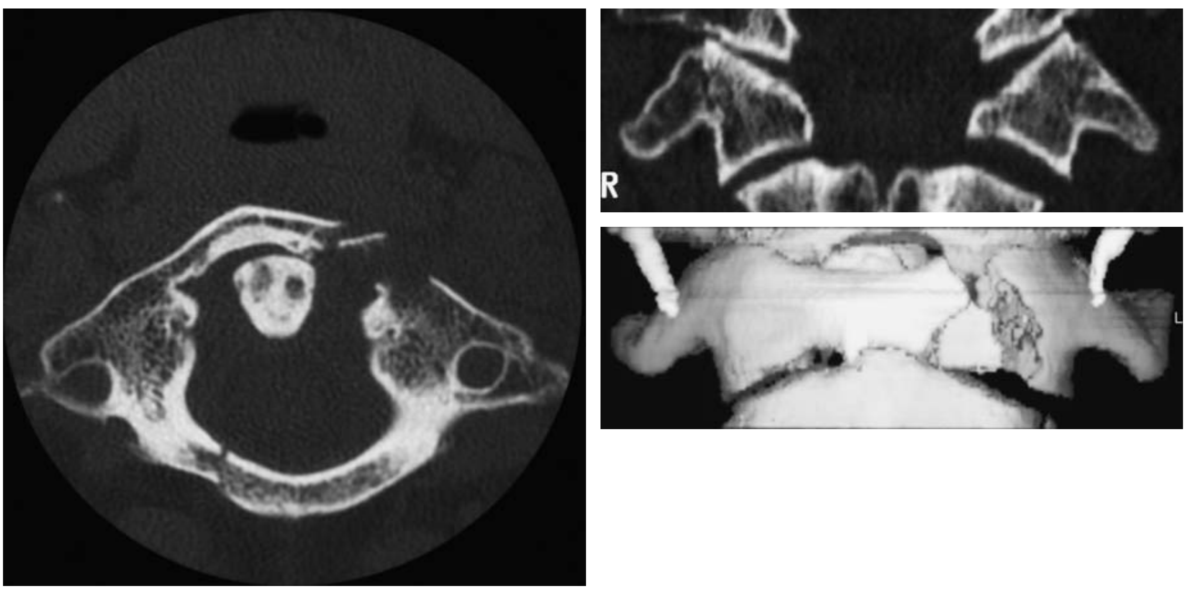

a b c

Fig. 22.3a–c. Jefferson fracture of C1 in a 26-year-old man patient who was injured in a diving accident. Non-contrast axial CT scan (**a**) with coronal (**b**) and three-dimensional reformatted images (**c**). There is a comminuted fracture of the anterior arch and a linear fracture of posterior arch (**a**). The coronal reformatted image shows lateral displacement of the lateral masses of C1 with respect to the superior articular surfaces of C2 (**b**). The 3-D volume rendered image confirms the comminuted fracture in the anterior arch of C1 (**c**)

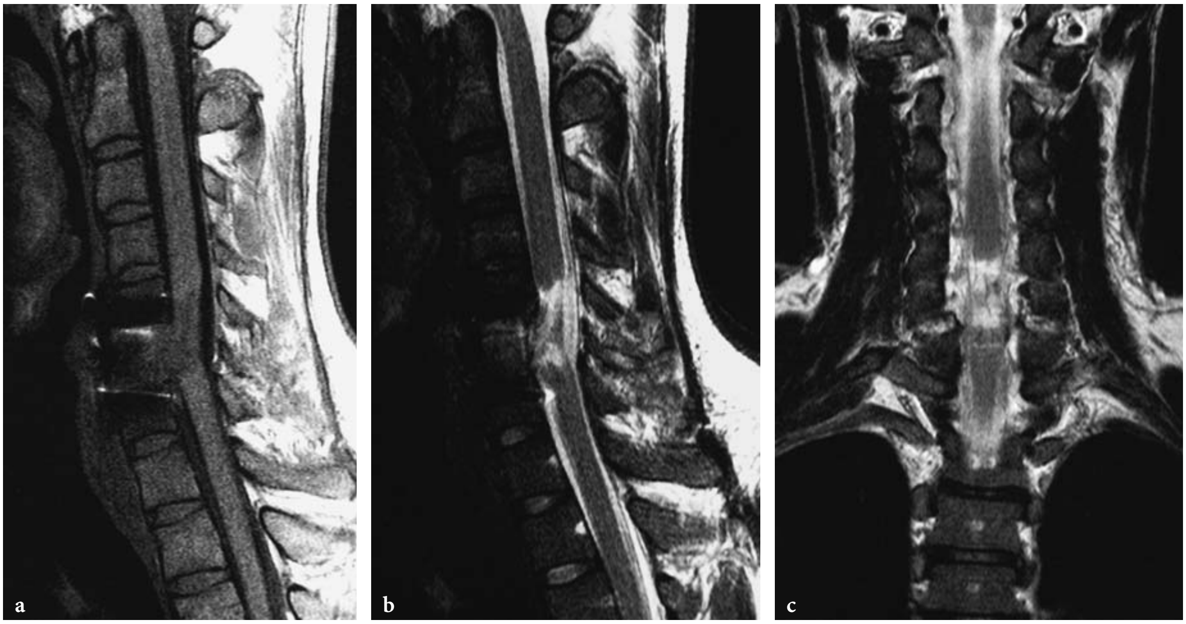

Fig. 22.4a–c. Catastrophic neck injury (diving accident) with contusion and partial transsection of the spinal cord in a 23-year-old man. MRI examination with sagittal T1-weighted (**a**), sagittal T2-weighted (**b**) and coronal T2-weighted (**c**) scans. The study was obtained after anterior fixation at C5–C6–C7 with titanium plate. Despite the magnetic susceptibility artifacts caused by the instrumentation, the spinal cord contusion is clearly identified as a focal intramedullary high intensity abnormality on the T2-weighted scans

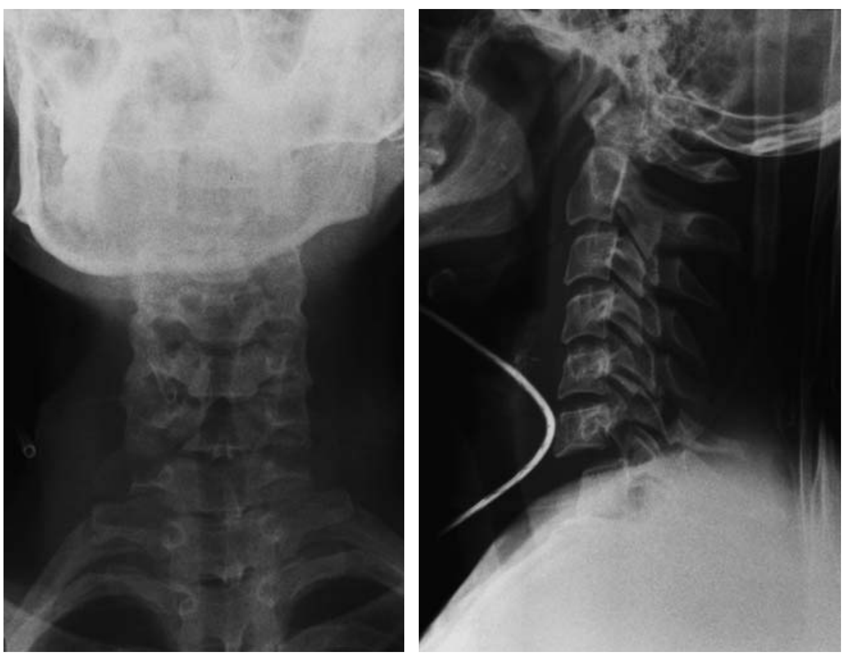

a b

Fig. 22.5a,b. Distracted hyperflexion injury in a young gymnast with anterior subluxation at C6–C7. Plain radiographs of the cervical spine in AP (**a**) and cross-table lateral (**b**) projection. The marked anterior displacement of C6 indicates disruption of all ligamentous structures and interfacetal dislocation. This finding is only visible on the lateral view. The cervicothoracic prevertebral soft tissue shadow is widened, indicating the presence of a hematoma secondary to the injury

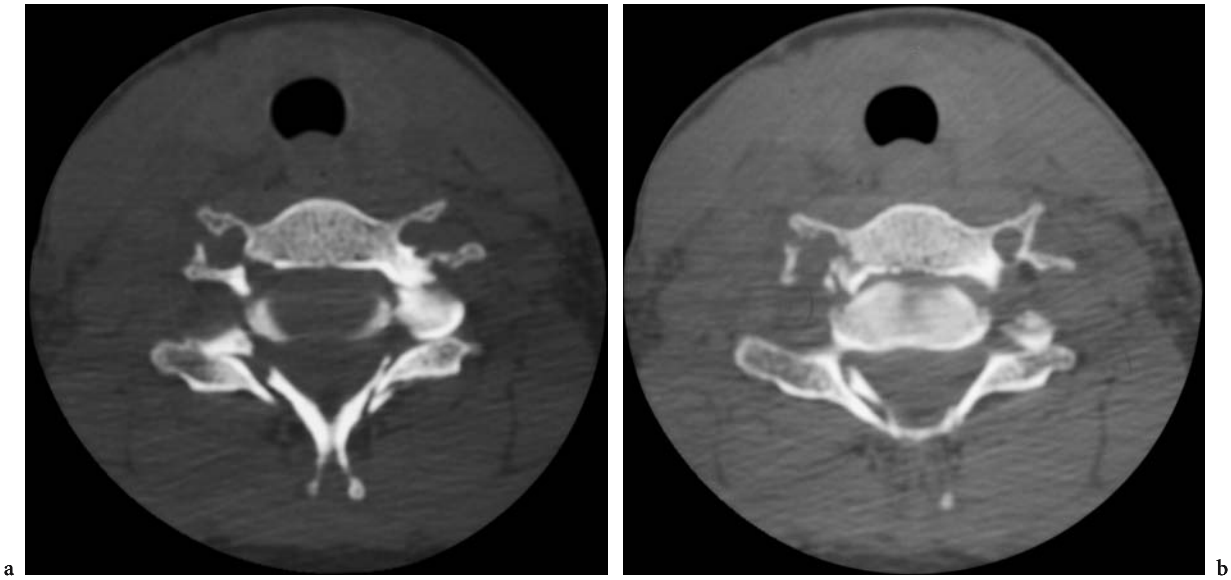

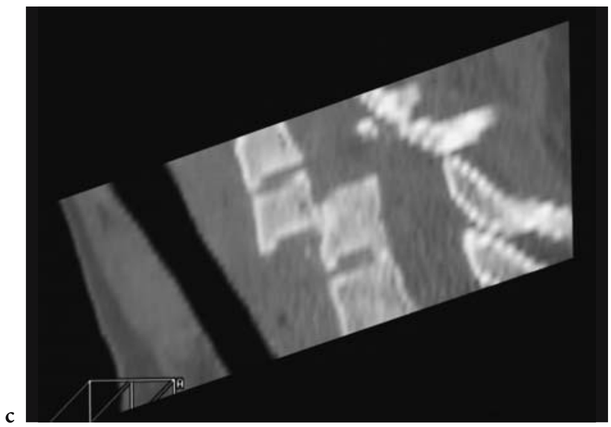

Fig. 22.6a–c. Bilateral interfacetal dislocation with anterior translation of C6 with regard to C7 in a 34-year-old woman following a catastrophic skiing injury. Non-contrast CT scans with axial images (**a**,**b**) and mid-sagittal reformatted image (**c**) show anterior displacement of C6 on C7 with marked step-like deformation of the spinal canal

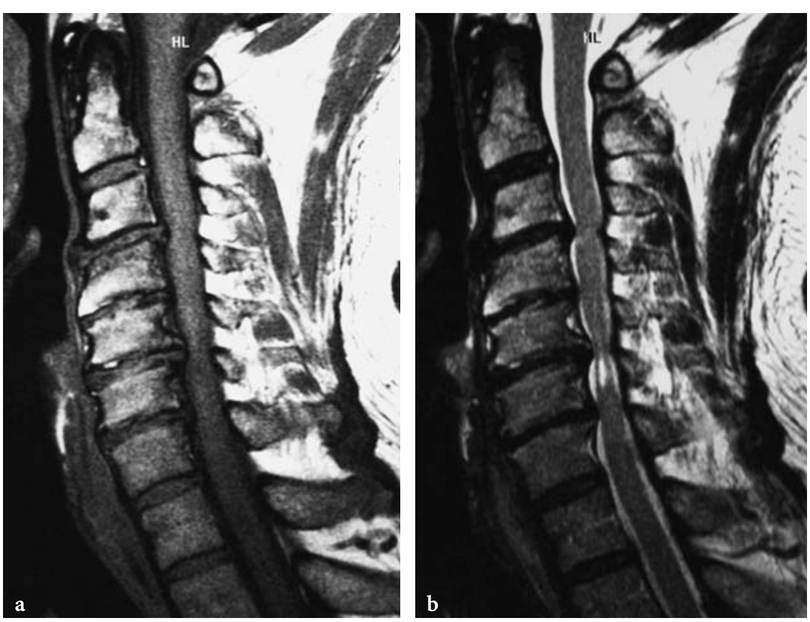

Fig. 22.7a,b. Cord contusion secondary to spinal stenosis in a 49-year-old recreational tennis player, who complained of neck pain and paresthesias in both arms after a collision with another player. MRI examination with sagittal T1-weighted (**a**) and sagittal T2-weighted images (**b**). Sagittal images show severe narrowing of the spinal canal due to chronic disc herniations and posterior osteophytes. There is a focal intramedullary area of increased signal intensity indicating cord contusion

Accurate radiological evaluation of the cervical spine must be performed immediately following the possibility of injury and in such a manner as not to compromise the neurologic status of the patient. Subtle radiographic findings indicating ligamentous injuries must be recognized in order to prevent cervical spine instability. Occult fractures are often difficult to diagnose on plain films. Therefore, in many trauma centers, computed tomography (CT) is increasingly being used to detect fractures.

22.4 Radiological Examination

The radiological investigation of the cervical spine must be guided by the clinical presentation. Three major issues should be addressed (Mintz 2004):

- Stability of the cervical spine is essential element in sports. Instability of the cervical spine indicates damage to one or several of structural elements including the intervertebral disc, the ligaments, the osseous structures (vertebral bodies, facet joints) and the facet joint capsule. Instability should be suspected when there is lack of alignment of the vertebral bodies or facet joints, which may reflect subluxation (White and Panjabi 1987).
- Impingement can be defined as encroachment on either the spinal cord (through narrowing of the spinal canal) or the nerve roots (through narrowing of the intervertebral foramina).
- The term impairment indicates loss of function, ranging from pain to paraplegia. Impairment can be due to structural causes (e.g. disc herniation, fracture-luxation, ligament injury) or to mild functional causes.

The purpose of the radiological investigation in the injured athlete is to document lesions that must be treated, such as disc disease or instability. Pain in itself is not an indication for imaging (for example, most acute burner or stinger injuries do not require imaging, see section 22.7) (Mintz 2004). On the other hand, when the athlete shows signs or symptoms of instability or neurological deficit, imaging studies are required to document potentially serious lesions.

In most cases, the radiological examination of the cervical spine in sports injuries starts with plain radiographs, including frontal, lateral and odontoid projections. Additional views should be added as needed, in order to decrease the incidence of missed fractures. When instability due to ligamentous injury is suspected, flexion and extension views should be obtained; this can only be done when a fracture has been ruled out.

In more severe sports injuries, the use of computed tomography (CT) is required. Since the 1980s it has been shown that CT can document cervical spine fractures that are difficult or impossible to see on plain radiographs (Mace 1985). With new generation multi-row detector CT (MDCT) scanners, it only takes a few seconds to examine the entire cervical spine, from the clivus to the upper thoracic segments. The volumetric MDCT dataset can be used to make multiplanar reformations in axial, sagittal and coronal planes. The cervico-thoracic junction, which is often difficult to assess on plain radiographs to overprojection of the shoulders, is well depicted on CT. Moreover, CT is now the first choice modality to demonstrate osseous causes of instability such as fractures of the vertebral bodies, the posterior elements (facet joints, laminae and pedicles), and the odontoid. The less time-consuming CT examination, with sagittal and coronal reconstructions, has replaced conventional tomography for the detection of odontoid fractures and provides equivalent or greater diagnostic accuracy (Weisskopf et al. 2001).

The most important limitations of MDCT in assessing the cervical spine are its relative inability to demonstrate damage to the neural elements (spinal cord, cervical nerve roots) and to the ligaments (transverse, alar, facet joint capsule, supraspinous, anterior and posterior longitudinal ligament). This is where magnetic resonance imaging (MRI) becomes useful, because of its intrinsically higher soft tissue contrast resolution. In an in vitro model with cadaver spine specimens, it has been shown that MRI reliably and directly allows assessment of spinal ligament tears of various types (White and Panjabi 1987; Emery et al. 1989; Kliewer et al. 1993). The foundation of any cervical spine MRI protocol consists of sagittal and axial T1- and T2-weighted scans. For sagittal scans, we use turbo spin echo (TSE) sequences with flow compensation to eliminate artifacts from CSF pulsations. Excellent T2-weighted contrast, with bright CSF signal can be obtained through the use of Restore (Siemens) or Drive (Philips) sequences which add a supplementary 90° pulse at the end of the TSE pulse train. For axial images with bright CSF, T2- or T2*-weighted sequences can be used; it is important to use thin section (3 mm or less slice thickness) contiguous axial images, to prevent miss-

ing a facet, pedicle or soft-tissue injury (Mintz 2004). Gradient echo T2*-weighted scans provide excellent myelographic contrast, but are less sensitive for the detection of intramedullary lesions such as edema or contusion. Gradient echo images can be degraded by susceptibility ("blooming") artifacts; this can be avoided through the use of 3D gradient echo scans with thinner slices. Fat suppression techniques, either with spectral fat saturation or inversion recovery, are important to demonstrate osseous and soft tissue injuries. In addition to the sagittal and axial imaging planes, a coronal sequence with intermediate to long TE is useful to show muscle injury (Mintz 2004). Diffusion-weighted imaging, with optional diffusion tensor fiber tracking techniques, is under study for the spinal cord.

22.5 Cervical Disc Herniation

Traumatic sports injuries of the cervical spine can occur at the level of the disc, resulting in disc herniation, disc degeneration, and ultimately developmental stenosis. Acute disc pathology is the most common cause of sports-induced impingement syndromes. It can cause a variety of neurological complications including paraplegia, neuralgia and spasticity of the lower extremities due to compression of the spinal nerve roots and/or of the spinal cord. For example, acute traumatic herniation of a cervical intervertebral disk may lead to spinal cord injury. In one reported case, the injury was sustained during a "tug-of-war" game, and the patient also suffered a brachial plexus injury in addition to a ruptured spleen (Lin et al. 2003).

The radiological examination should focus on the detection of narrowing of the intervertebral foramina and spinal canal. Recent disc herniations tend to have a higher signal intensity on T2- or T2*-weighted images, whereas osteophytes present a low signal intensity. T2-weighted MR images are the method of choice to demonstrate abnormal intramedullary signal intensity due to extrinsic compression by an intervertebral disc. On MRI it can be difficult to distinguish between a disc herniation ("soft" disc) and an osteophyte ("hard" disc).

The association between participation in several specific sports, and herniated lumbar or cervical intervertebral discs has been examined in a case-controlled multicenter epidemiologic study (Mundt et al. 1993). The authors analyzed 287 patients with lumbar disc herniation and 63 patients with cervical disc herniation, each matched by sex, source of care, and decade of age to one control who was free of disc herniation and other conditions of the back or neck. Specific sports considered were baseball or softball, golf, bowling, swimming, diving, jogging, aerobics, and racquet sports. The authors found that most sports are *not* associated with an increased risk of herniation, and may in fact be protective. Relative risk estimates for the association between individual sports and lumbar or cervical herniation were generally less than or close to 1.0. There was, however, a weak positive association between bowling and herniation at both the lumbar and cervical regions of the spine. Use of weight lifting equipment was not associated with herniated lumbar or cervical disc, but a possible association was indicated between use of free weights and risk of cervical herniation (relative risk, 1.87; 95% confidence interval, 0.74 to 4.74). Cervical disc herniation occurring in close association with playing football (soccer) has also been reported (Fig. 22.1) (Tysvaer 1985).

22.6 Impingement Syndromes and Spinal Stenosis

Neurological symptoms indicating a cervical spinal cord lesion, which occur after a spine injury from contact sports, require a precise work up to detect cervical spinal stenosis. In these instances, advanced imaging techniques such as CT and MRI more accurately identify true spinal stenosis than radiographic bone measurements alone can provide (Cantu 1998).

The presence of a narrow cervical spinal canal constitutes a significant risk factor for the development of traumatic neck injuries (including sports-related injuries) even without a fracture or dislocation (Epstein et al. 1980). In a study of 39,377 athletes, a decreased antero-posterior diameter of the spinal canal was found to be a predisposing factor to the occurrence of cervical spinal cord neurapraxia with transient quadriplegia (Torg and Pavlov 1987). This distinct clinical syndrome is characterized by sensory changes (including burning pain, numbness, tingling, and loss of sensation) as well as motor changes (ranging from weakness to complete paraly-

sis) (Torg et al. 1986). Neuropraxia of the cervical spinal cord with transient quadriplegia is caused by spinal cord compression during forced hyperextension or hyperflexion, in athletes with diminution of the anteroposterior diameter of the spinal canal. In one study, there was a statistically significant spinal stenosis ($p<0.0001$) in patients having suffered cervical neuropraxia and transient quadriplegia, as compared with the control subjects (Torg et al. 1986). If on plain radiographs of the cervical spine, the sagittal diameter of the spinal canal is <12.5 mm (corrected for magnification), MRI of the cervical spine is recommended.

Computed tomography (CT) provides an excellent way of studying the sagittal and transverse diameters of the cervical spinal canal. The sagittal diameter of the spinal canal of some individuals may be inherently smaller than normal, and that this reduced size may be a predisposing risk factor to spinal cord injury (Matsura et al. 1989).

The definition of cervical spinal stenosis should not be made on measurements of the diameter of the bony canal alone but should be made instead on imaging studies that document the relative size of the neural tissue relative to the size of the spinal canal. The functional reserve of the spinal canal is defined as the amount of CSF surrounding the spinal cord. MRI is excellent for demonstrating this parameter. "Functional" cervical spinal stenosis, defined as a loss of CSF around the spinal cord, and/or in more extreme cases deformation of the cervical spinal cord, should be the criteria for defining cervical spinal stenosis.

Patients can become quadriplegic after a minor trauma to the spine, even without suffering a spinal fracture dislocation (Fig. 22.7). Predisposing factors are marked developmental stenosis of the spinal canal, with superimposed degenerative changes (e.g. disc herniation, osteophytic spurs, calcification of posterior longitudinal ligament) (Firooznia et al. 1985). It appears that the spinal cord can tolerate slowly increasing mechanical pressure for many years and conform to the shape of the spinal canal without causing any neurological symptoms. However, when the spinal stenosis is severe, any additional pressure, for example, swelling and edema from trauma, may cause a neurologic catastrophe. Therefore, patients with severe cervical spinal stenosis have been advised to discontinue participation in contact sports (Ladd and Scranton 1986). This recommendation has been recently revised such that stenosis of the cervical spine in itself does not constitute a absolute contra-indication to participation in contact sports (Mintz 2004; Cantu 1998; Torg et al. 2002). According to currently accepted guidelines, an episode of neuropraxia with cervical spine stenosis is a relative contra-indication to participation in contact sports; instability, or abnormal intramedullary signal intensity on MRI are absolute contra-indications (Torg et al. 2002).

In cases of fracture-dislocation, one study in a group of 98 patients (45 without neurologic deficits, 39 with incomplete quadriplegia, and 14 with complete quadriplegia) concluded that small diameter canals were correlated significantly with neurologic injury, while large diameter canals allowed protection from neurologic injury in cervical fracture dislocation (Eismont et al. 1984).

22.7 Burners and Stingers

The most common cervical injury in players of contact sports is a transient loss of function (weakness) with burning pain, numbness or tingling irradiating down one arm following a collision (Weinstein 1998). The phenomenon is known as a "stinger" or "burner" injury. These lesions are often underdiagnosed or inadequately assessed (Weinstein 1998). Symptoms usually resolve within a few minutes; however, recurrences are common and can lead to permanent neurologic deficits (Feinberg 2000). The most commonly affected muscle groups in terms of motor weakness are shoulder abductors, elbow flexors, external humeral rotators, and wrist and finger extensors. Function gradually returns from the proximal muscle groups to the distal muscle groups. Though the burner or stinger syndrome is one of the most common injuries in American football, it can occur in other sports such as wrestling, ice hockey, basketball, boxing, and weightlifting (Feinberg 2000). Prospective studies performed at Tulane University have shown a 7.7% incidence of stingers in a group of college football players (Castro et al. 1997). In high-school football players experiencing significant neck pain during the season, the incidence of radiologic evidence of neck injuries was as high as 32% and was related to years of experience. In the preseason examination, half the players who volunteered a history of significant neck pain had abnormal X-ray films (Albright et al. 1976).

The stinger or burner syndrome most likely represents an upper cervical root injury. The pathogenesis can be twofold (Albright et al. 1976):

- Stretching or distraction injury to the upper cords of the brachial plexus due to forced depression of the ipsilateral shoulder, with movement of the head to the side opposite the painful arm.
- Compression and rotation of the cervical spine toward the painful arm. This causes tethering of the cervical nerves between the vertebral arteries and the distal foramina at each cervical level. These dentate ligament attachments become taut and stretch the cervical nerve roots as they leave the spine.

The severity of the injury correlates with the underlying pathophysiology. *Neuropraxia* refers to a selective demyelination of the nerve sheath, and it is the most benign form of injury. *Axonotmesis* is a disruption of the axon and the myelin sheath, but the epineurium remains intact. The most severe injury is a *neurotmesis* or a compete disruption of the endoneurium. This injury is associated with the most unfavorable prognosis.

Because stinger or burner injuries are usually self-limited, the most important treatment obligation is to rule out an unstable cervical injury. The clinical assessment should focus on determining the full pain-free neck range of motion. If neck motion is decreased or painful, a radiological investigation should be performed to rule out fracture/dislocation. If the symptoms persist for three to four weeks following injury, an electromyogram should be obtained to evaluate upper trunk function. The differential diagnosis of stinger and burner injuries includes: acute cervical disk herniation, foraminal stenosis, and extradural intraspinal mass lesion.

22.8 Catastrophic Athletic Cervical Spine Injuries

Contact and collision sports, such as rugby, American football or ice hockey, expose the athlete to a wide array of potential injuries, including serious injuries to cervical spine (Wilson et al. 2006). This is equally true for motorized sports involving high speeds. The outcome of athletic neck injuries ranges from complete recovery to death, depending on the degree of spinal cord damage sustained (Quarrie et al. 2002). Potentially catastrophic athletic cervical spine injuries have been reported to occur in as many as 10–15% of all American football players (Torg et al. 1979). In one study, the American National Football Head and Neck Injury Registry has documented 1129 injuries that involved hospitalization for more than 72 h, surgical intervention, fracture-dislocation, permanent paralysis, or death (Torg et al. 1979). Of this group of injuries, 550 were fracture-dislocations of the cervical spine, of which 176 were associated with permanent quadriplegia. The introduction of a protective helmet-face mask system in American football has decreased the incidence of head injuries associated with intracranial hemorrhage, and injuries associated with death. Conversely, cervical spine injuries with fracture-dislocation and with permanent quadriplegia have increased.

In a more recent study analyzing epidemiological and medical data from 1977 through 1998, 118 athletes died as a direct result of participation in American football, with 200 football players received a permanent cervical cord injury, and 66 sustained a permanent cerebral injury (Cantu and Mueller 2000). The most commonly reported mechanism of injury has been hyperflexion of the cervical spine, resulting in fracture dislocation of C4–C5 or C5–C6 (Quarrie et al. 2002). The axial loading mechanism of spinal cord injury was identified in 27% of tackling injuries (Cantu and Mueller 2000). Most cervical injuries occurred to defensive players during the act of tackling.

22.9 Nerve Root and Plexus Avulsion

A severe type of brachial plexus lesion is the brachial plexus avulsion, which is an uncommon but serious injury associated with contact sports (Williams and Hoeper 2004), and motorized sports, especially motorcycle racing. The term refers to complete or incomplete avulsion of one or more cervical nerve roots from the spinal cord. Traumatic brachial plexus avulsion is usually associated with a dural tear, through which CSF leakage occurs to form a pseudomeningocele. Traditionally cervical myelography, followed by CT myelography, has been the gold standard for demonstration of these lesions, showing both complete and incomplete traction injuries (Volle et al. 1992). The combination of CT and CT myelography can dif-

ferentiate pre- from post-ganglionic lesions, and this information is essential for deciding whether exploration of the plexus or a motor substitution operation is indicated (Volle et al. 1992). Moreover, CT has the added advantage of being able to rule out an associated fracture of the spinal column. Conventional MRI scanning of the cervical spine is useful to reveal traumatic pseudomeningoceles or additional lesions, such as intramedullary or extradural haematomas, but root avulsions are difficult to depict (Vielvoye and Hoffmann 1993). With the use of high resolution, thin-section slices (Fig. 22.8), the sensitivity for detection of cervical nerve root avulsion was the same (92.9%) with MRI as myelography/CT myelography (Doi et al. 2002). Using overlapping coronal-oblique slices, the roots of the brachial plexus can be adequately assessed in order to decide whether to proceed with exploration, nerve repair, primary reconstruction, or other imaging modalities. Alternatively, MR myelography provides excellent accuracy for detection of damaged nerve roots or root sleeves (Nakamura et al. 1997). MR myelography is non-invasive, relatively quick, requires no contrast medium, provides imaging in multiple projections, and is comparable in diagnostic ability to the more invasive, time-consuming techniques of conventional myelography and CTM.

22.10 Differential Diagnosis

Finally, as a word of caution, it should be remembered that injuries are not the only cause of neck pain in the athlete. Disorders simulating athletic injury include, among others, tumors and inflammatory connective tissue disease (Harvey and Tanner 1991). As the number of middle-aged or elderly recreational athletes increases steadily, we should keep in mind that these athletes can also have tumors, infection, rheumatologic disorders, and other non-traumatic etiologies of pain (Tall and DeVault 1993). For these conditions, radiological examination should be guided by an adequate and precise clinical work-up.

a  b

Fig. 22.8a,b. Left brachial plexus nerve root avulsion with formation of a pseudomeningocele filled with cerebrospinal fluid. The patient is a 29-year-old man who was injured in a cross-country motorcycle racing accident. Coronal thin section turbo spin echo T2-weighted MRI scans (**a**,**b**) reveal a CSF-filled pseudomeningocele extending to the apex of the left lung

Things to Remember

1. Cervical spine injuries occur in many sports. Most lesions are benign and resolve spontaneously; serious injuries are mostly associated with contact sports and motorized sports.

2. In sports-related injuries, the most common mechanism of cervical spine trauma is neck flexion with axial loading.

3. Cervical strain injuries are more prevalent in female athletes than male athletes. For cervical disc injury and cervical disc herniation, the male to female incidence is approximately equal.

4. Pain in itself is not an indication for imaging; conversely imaging studies are required when there are signs or symptoms of instability or neurological deficit.

5. Plain radiographs of the cervical spine with flexion-extension views remain useful in mild injuries to assess instability. However, plain radiographs underestimate fractures.

6. In more severe cervical spine trauma, CT scanning is the method of choice to detect traumatic bone lesions.

7. MRI is the preferred technique to demonstrate soft tissue injuries, e.g. medullary contusion, ligament disruption, muscle injury, as well as bone marrow contusion.

8. Severe sports-related injuries of the cervical spine can occur in athletes with spinal canal stenosis (developmental and or acquired degenerative changes). Imaging studies must take into account the relative diameter of the spinal canal.

9. Nerve root and brachial plexus avulsion is an unusual but severe type of sports injury. It can be investigated with myelography and CT myelography or with MRI.

References

Albright JP, Moses JM, Feldick HG et al. (1976) Nonfatal cervical spine injuries in interscholastic football. JAMA 236:1243–1245

Banerjee R, Palumbo MA, Fadale PD (2004) Catastrophic cervical spine injuries in the collision sport athlete, part 1: epidemiology, functional anatomy, and diagnosis. Am J Sports Med 32:1077–1087

Cantu RC (1998) The cervical spinal stenosis controversy. Clin Sports Med; 17:121–126

Cantu RC, Mueller FO (2000) Catastrophic football injuries: 1977–1998. Neurosurgery 47:673–675

Castro FP Jr, Ricciardi J, Brunet ME et al. (1997) Stingers, the Torg ratio, and the cervical spine. Am J Sports Med 25:603–608

Doi K, Otsuka K, Okamoto Y et al. (2002) Cervical nerve root avulsion in brachial plexus injuries: magnetic resonance imaging classification and comparison with myelography and computerized tomography myelography. J Neurosurg 96:277–284

Eismont FJ, Clifford S, Goldberg M et al. (1984) Cervical sagittal spinal canal size in spine injury. Spine 9:663–666

Emery SE, Pathria MN, Wilber RG et al. (1989) Magnetic resonance imaging of posttraumatic spinal ligament injury. J Spinal Disord 2:229–233

Epstein N, Epstein JA, Benjamin V et al. (1980) Traumatic myelopathy in patients with cervical spinal stenosis without fracture or dislocation: methods of diagnosis, management, and prognosis. Spine 5:489–496

Feinberg JH (2000) Burners and stingers. Phys Med Rehabil Clin N Am 11:771–784

Firooznia H, Ahn JH, Rafii M et al. (1985) Sudden quadriplegia after a minor trauma. The role of preexisting spinal stenosis. Surg Neurol 23:165–168

Harvey J, Tanner S (1991) Low back pain in young athletes. A practical approach. Sports Med 12:394–406

Kelley LA (2000) In neck to neck competition are women more fragile? Clin Orthop Relat Res 372:123–130

Kliewer MA, Gray L, Paver J et al. (1993) Acute spinal ligament disruption: MR imaging with anatomic correlation. J Magn Reson Imaging 3:855–861

Ladd AL, Scranton PE (1986) Congenital cervical stenosis presenting as transient quadriplegia in athletes. Report of two cases. J Bone Joint Surg 68A:1371–1374

Lin PH, Chiu FY, Hsiao NC et al. (2003) Injuries during a massive tug-of-war game. J Chin Med Assoc 66:436–439

Mace SE (1985) Emergency evaluation of cervical spine injuries: CT versus plain radiographs. Ann Emerg Med 14:973–975

Matsuura P, Waters RL, Adkins RH et al. (1989) Comparison of computerized tomography parameters of the cervical spine in normal control subjects and spinal cord-injured patients. J Bone Joint Surg 71A:183–188

Mercer S, Bogduk N (1999) The ligaments and annulus fibrosus of human adult cervical intervertebral discs. Spine 24:619–626

Mintz DN (2004) Magnetic resonance imaging of sports inju-

ries to the cervical spine. Semin Musculoskelet Radiol 8:99–110
Mundt DJ, Kelsey JL, Golden AL et al. (1993) An epidemiologic study of sports and weight lifting as possible risk factors for herniated lumbar and cervical discs. The Northeast Collaborative Group on Low Back Pain. Am J Sports Med 21:854–860
Nakamura T, Yabe Y, Horiuchi Y et al. (1997) Magnetic resonance myelography in brachial plexus injury. J Bone Joint Surg 79B:764–769
Pavlov H, Torg JS (1987) Roentgen examination of cervical spine injuries in the athlete. Clin Sports Med 6:751–766
Quarrie KL, Cantu RC, Chalmers DJ (2002) Rugby union injuries to the cervical spine and spinal cord. Sports Med 32:633–653
Tall RL, DeVault W (1993) Spinal injury in sport: epidemiologic considerations Clin Sports Med 12:441–448
Torg JS (1987) Trampoline-induced quadriplegia Clin Sports Med 6:73–85
Torg JS, Pavlov H (1987) Cervical spinal stenosis with cord neurapraxia and transient quadriplegia. Clin Sports Med 6:115–133
Torg JS, Truex R Jr, Quedenfeld TC et al. (1979) The national football head and neck injury registry. Report and conclusions 1978. JAMA 241:1477–1479
Torg JS, Pavlov H, Genuario SE et al. (1986) Neurapraxia of the cervical spinal cord with transient quadriplegia. J Bone Joint Surg 68A:1354–1370
Torg JS, Sennett B, Vegso JJ (1987) Spinal injury at the level of the third and fourth cervical vertebrae resulting from the axial loading mechanism: an analysis and classification. Clin Sports Med 6:159–183
Torg JS, Corcoran TA, Thibault LE et al. (1997) Cervical cord neurapraxia: classification, pathomechanics, morbidity, and management guidelines. J Neurosurg 87:843–850
Torg JS, Guille JT, Jaffe S (2002) Injuries to the cervical spine in American football players. J Bone Joint Surg 84A:112–122
Tysvaer AT (1985) Cervical disc herniation in a football player. Br J Sports Med 19:43–44
Vielvoye GJ, Hoffmann CF (1993) Neuroradiological investigations in cervical root avulsion. Clin Neurol Neurosurg 95 Suppl:S36–38
Volle E, Assheuer J, Hedde JP et al. (1992) Radicular avulsion resulting from spinal injury: assessment of diagnostic modalities. Neuroradiology 34:235–240
Weinstein SM (1998) Assessment and rehabilitation of the athlete with a „stinger“. A model for the management of noncatastrophic athletic cervical spine injury. Clin Sports Med 17:127–135
Weisskopf M, Reindl R, Schroder R et al. (2001) CT scans versus conventional tomography in acute fractures of the odontoid process. Eur Spine J 10:250–256
White AA III, Panjabi MM (1987) Update on the evaluation of instability of the lower cervical spine. Instr Course Lect 36:513–520
Williams J, Hoeper E (2004) Brachial plexus injury in a male football player. Curr Sports Med Rep 3:125–127
Wilson JB, Zarzour R, Moorman CT III (2006) Spinal injuries in contact sports. Curr Sports Med Rep 5:50–55

The Spine in Sports Injuries: Thoracic and Lumbar Spine

23

Franz Kainberger

CONTENTS

Box 23.1. Plain radiography

- Primary investigation
- Enables documentation of segmental abnormalities of flexion and extension

Box 23.2. Computed tomography

- Should be performed after severe acute traumatic events
- Enables multiplanar reformations in three planes and 3D volume reconstructions

Box 23.3. MR Imaging

- Should be performed in case of neurological deficit
- Evaluation of disc disease and spinal cord
- Evaluation of rupture of joints/ligaments
- Evaluation of bone and soft tissue edema

23.1 Introduction

Spinal manifestations of sports injuries or of overuse at the spine mainly result from activities in certain trend sports with high deceleration or from monotonous-repetitive movement patterns. An involvement of the spine has been reported in 10%–15% of sports injuries (Tall and DeVault 1993). For many forms of sports-associated overuse, especially those located at the vertebral arches, childhood and adolescence form more than 60% of the "vulnerable phases" of life, whereas degenerative disc disease is more commonly observed in adults and has been reported to occur in only 10% in earlier decades (Micheli and Wood 1995). Among the various forms of sports injury and overuse certain relationships exist as "structures of weakness" within a kinetic chain may be prone to earlier or more severe degeneration than others.

The imaging modalities used for documenting sports injuries include conventional radiography,

F. Kainberger, MD, PhD
Professor of Radiology, Medical University of Vienna, AKH, Waehringer Gürtel 18–20, 1090 Vienna, Austria

computed tomography (CT) with multiplanar reformations, and magnetic resonance imaging (MRI). Bone scintigraphy with 99m-Tc-Diphosphonates has been advocated especially for detecting stress reactions but is of limited value with respect to the continuous improvements of the spatial resolution gained with CT and MRI. Ultrasound has been described for measuring the width of spondylolytic clefts and the thickness of spinal muscles but has not been established in clinical routine (Hides et al. 1995). In the context of biomechanical concepts of trend sports the indications for imaging, the techniques of investigation and the interpretation of normal and abnormal findings will be reviewed.

23.2 Indications

As a general recommendation based on European referral criteria and the American College of Radiology appropriateness criteria, conventional radiographs should be used as primary investigations. They are, with the exception of congenital disorders and of spinal myelopathy or serious neurological disorders, classified as "indicated" or "indicated under specific circumstances" (Armstrong et al. 2001). Similar recommendations exist for spinal trauma in which multiplanar CT may be advocated as an alternative. An important advantage of projection radiography is its potential to document segmental abnormalities of flexion and extension. Such direct information about malalignment may be as well appreciated with dedicated low-field MR units.

Specific aspects in sports medicine that should be mentioned in the referral with respect to a dedicated treatment plan include:

- The symptoms and signs of the biomechanical "kinetic chain" associated with the type of trauma or overuse (Kainberger et al. 2006; Lennard and Crabtree 2005).
- Red flags, i.e. signs of severe trauma that may be associated with a neurologic deficit. They should be differentiated from less severe and more commonly observed signs of pain and movement disorders due to self-limiting muscle strains.
- The urgency of "return to play", whether the patient is a professional athlete or is involved in recreational sporting activities (Eck and Riley 2004).

These general, as well as specific, recommendations are also true for back pain in children which is most commonly observed at the lumbar segment in conjunction with sports.

23.2.1 Trauma

Fractures mainly result from compression or from a hyperflexion-hyperextension movement pattern with high deceleration, acceleration, or an abrupt change of the direction of movement. With increasing frequency they are associated with trend sports with high speed or jumping movements like motor sports or kite surfing. A typical location is at the thoraco-lumbar junction.

After acute traumatic events, CT should be performed with multiplanar reformations in three planes. Three-dimensional volume reconstructions are helpful for documenting complex rotational malalignment but its interpretation is associated with a flat learning curve, so that specific experience is needed in using this technique (Schroder et al. 2003). MRI is especially indicated if neural structures seem to be involved which may be caused by a haematoma or by direct violation. MRI is further helpful

Fig. 23.1. A 17-year-old dancer with lumbar disk protrusion at L4/5 on a sagittal TSE T2-weighted MR image

for documenting a rupture of joints or ligaments, or a disk protrusion or prolapse that in the adolescent athlete may result from abrupt rotational or hyperflexion movements (Fig. 23.1).

Late sequels of macro- or microtrauma are degeneration of disks or facet joints and may be documented with conventional radiograms, CT, or MRI (Fig. 23.2).

Fig. 23.2. A 59-year-old former female high jumper with extensive lumbar hyperlordosis treated with posterior lumbar spinal fusion and associated with a thoracolumbar wedge vertebra and a single Schmorl's node. Sagittal TSE T2-weighted MR image

23.2.2 Overuse

Stress reactions of the bone most commonly manifest at the caudal lumbar spine and are associated with track-and-field athletics, dancing and various activities associated with lumbar hyperextension. Conventional radiographs which include views in two plains and a lateral view of the lumbo-sacral junction should be exposed. They are generally more reliable than oblique views which, especially in case of an associated scoliosis, may be difficult to be interpreted (Amato et al. 1984). A CT with multiplanar reconstructions may be added in equivocal cases. MRI should be performed for assessing the width of the spinal canal and for an associated degenerative disc disease.

Sacral stress fractures are less commonly observed and result from excessive transmission of load from the spine to the lower extremities due to jogging, basket ball, volley ball, or aerobics (White et al. 2003). MRI is the modality of choice in these cases whilst the diagnosis may be missed with conventional radiographs.

Overuse of the sacroiliac joints in the athlete is often associated with asymmetric load on the pelvic ring and imaging, especially MRI, should be performed to document bone marrow or soft tissue edema as being important foot prints of stress or trauma (Brolinson et al. 2003). Hypertrophy of the piriformis muscle with or without additional muscle fibers originating from the anterior sacral surface may be associated with sciatic nerve entrapment and cross-sectional imaging may have the potential to clarify its clinical appearance (McCrory and Bell 1999).

23.2.3 Osteoporosis

A decreased bone mineral density has been described in young gymnasts or in ballet dancers with or without secondary amenorrhoea (Kaufman et al. 2002). A bone densitometry should be performed in any case of an unclear stress fracture, especially in young active women, as high intensity training may be regarded as a significant risk factor for developing osteoporosis (Braam et al. 2003). Positive effects of sporting activities on bone density, on the other hand, have been reported for short-term high-performance activities such as sprint, tennis, fencing as well as weight lifting or heavy athletics (Felsenberg and Gowin 1998; Sabo et al. 1996; Seidl et al. 1993).

23.3 Image Interpretation

The image analysis has to be focussed on the distribution, the characteristics and the differential diagnosis of so-called footprints of kinetic chains. The spinal kinetic chains associated with sports are caused by effects of high kinetic energies in cases with acute trauma and by effects from monotonous repetitive

forces (rowing), asymmetric forces (golf, cricket), or various and less standardized movement patterns (gymnastics).

23.3.1 Imaging Findings

23.3.1.1 Trauma

Osseous lesions occur, in contrast to injuries of the cervical spine, less commonly and with less severity observed at the thoracolumbar spine as it has been described in detail for pole-vaulters (Boden et al. 2001). Reports include compression fractures, mainly in contact sports, cycling or skiing, and flexion-distraction injuries in gymnasts (Katz and Scerpella 2003). The facet-lamina fractures (posterior column fractures) of the thoracic spine and the facet posterior fractures of the lumbar spine are typical fracture types that are associated with sports. The concept of the functional reserve of spinal capacity, originally developed by Burrows, may be applied on the thoracolumbar spine respectively (Prasad et al. 2003).

Physeal injuries are referred to the vertebral growth plate. Slipped vertebral ring apophysis may occur in childhood if the apophysis together with the adjacent disk that is tightly fixed by the annulus fibers is displaced posteriorly into the spinal canal. It is a rare entity which usually results from lifting heavy weights.

Spinal cord injury without radiographic abnormality (SCIWORA) is an entity described for children whose spinal structures are of less stiffness than in adulthood. In a metaanalysis it was shown that, in 13%, SCIWORA was associated with sports injuries and 26% occurred at the thoracic spine whereas it was virtually never observed at the lumbar spine (Launay et al. 2005). The prognosis can be improved if the syndrome is diagnosed early and adding MRI to the diagnostic workup may show neural and extraneural injuries.

Muscle strains may be detected rarely with MRI (Bennett et al. 2006).

23.3.1.2 Congenital and Developmental Disorders

Variants and congenital diseases occur especially at the lumbo-sacral junction and have, as intrinsic risk factors for overuse syndromes and degenerative diseases, to be assessed radiologically. An incomplete fusion of the vertebral arch at the level of S1 may be associated with a spondylolysis of L5. From the three patterns of incomplete fusion (type I with a wide cleft, type II with small contact between the divided branches and type III with overlapping borders), types II and III are regarded as parts of retarded spinal development and are typically observed together with a spondylolysis of L5 (Fig. 23.3) (Niethard et al. 1997).

In the radiological assessment of scoliosis with respect to sports the Cobb angle should be measured to differentiate more severe forms (higher than 20°) in which axial load should be prohibited from less severe forms (Hochmuth et al. 2002).

23.3.1.3 Stress Reactions of the Bone and the Discovertebral Junction

Spondylolysis and apophyseal damage form, together with scoliosis, a characteristic triad of overuse of the thoracic and the lumbar spine. Accelerated growth (growth spurt) during adolescence is regarded as an important trigger mechanism in its development (Seitsalo et al. 1991).

23.3.1.4 Osseous Stress Reactions

Spondylolysis manifests typically at the age of 6 years and is in more than 90% located at the fifth lumbar vertebra, less commonly at the fourth or at other segments. Sometimes, two or more segments of the lumbar spine may be involved. A reduced resistance of the interarticular portion of the vertebral arch and increase stress due to hyperlordosis are regarded as main causative factors. Therefore, spondylolysis is defined as a stress fracture and many concepts about its etiology and its treatment base on this definition (Standaert and Herring 2000). According to Vialle et al. (2005), radiologic signs support the concept that a global dystrophic pattern of the lumbosacral junction is an underlying cause of severe spondylolisthesis with increased shear stresses. Spondylolysis seems to be, despite asymptomatic forms have been observed in rare cases, the most common cause of back pain in athletes and occurs with higher frequency than in the general population in which it is occurs in about 10% (Rossi and Dragoni 1990; Soler and Calderon 2000). There is a racial preponderance with a prevalence of 5%–7% in Europe-

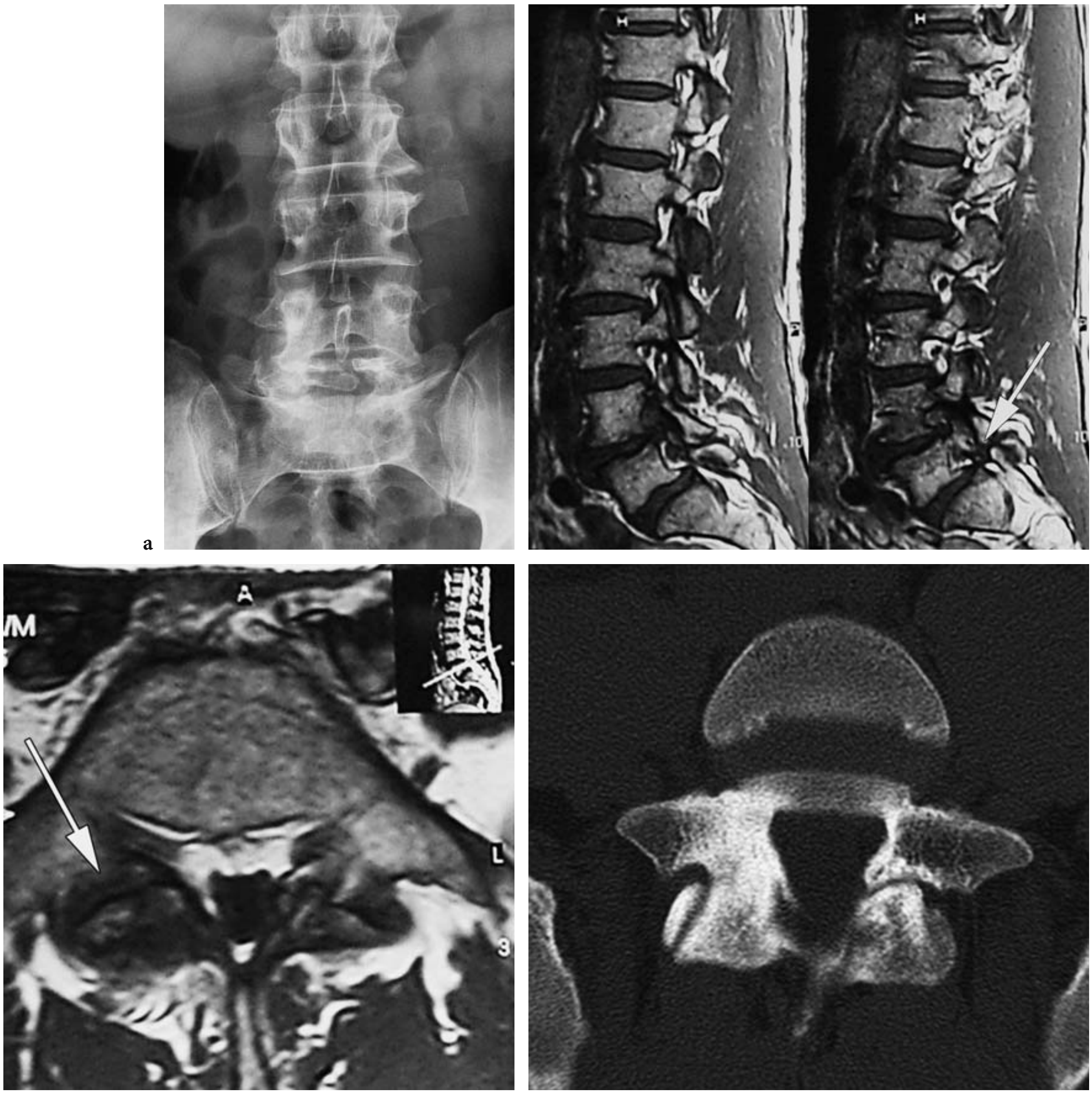

Fig. 23.3a–d. Former gymnast with incomplete fusion of vertebral arches of L5 and S1 on a plain radiograph (type III) (**a**) and interruption of pars interarticularis of L5 (*arrow*) (**b**), whereas the pars of L4 is elongated but intact (sagittal TSE T1-weighted MR image). **c** "Double facet joint" sign on right side on an axial TSE T1-weighted MR image (*arrow*). **d** Axial oblique CT scan in another gymnast with unilateral spondylolysis on the left side and associated sclerosis at the contralateral right pedicle L5 (case courtesy of F.M. Vanhoenacker)

ans, 9% in Bantus, 7%–10% in Japanese, and up to 50% in Eskimos (Engelhardt et al. 1997). Typical movement patterns for the development of spondylolysis have been described (Table 23.1) (Bono 2004). Spondylolysis results from a low stress-resistance of the pars interarticularis of the vertebral arch on one side, and from high stress applied to this structure on the other side. Low stress-resistance is mainly due to an elongation and thinning of the pars and is exaggerated by a prominent lordosis of the lumbar spine. Such lordosis especially develops at between 6 and 8 years and is associated with a physiological flexion of the hip joints. Radiological evidence of a lumbosacral transitional vertebra, a congenital cleft of the posterior arch of the S1 segment (spina bifida occulta), or of zygoapophyseal joint anomaly is strongly associated with spondylolysis of L5 (Standaert and Herring 2000). A spina bifida occulta has been described to occur between 13% and 58% concomitant with spondylolysis (Niethard et al. 1997). Spondy-

Table 23.1. Common forms of applied forces leading to spondylolysis. [Modified from Junghanns (1986)]

Applied force	Type of activity
Repetitive hyperextension manœuvres	Gymnastics, wrestling, diving, throwing sports, basketball, volleyball, pole vaulting, certain swimming styles (butterfly), high diving
Strong muscle forces	Body building, wrestling, hockey
Repeated monotonous exercises	Rowing
Rotational motion creating unilateral defects	Throwing sports, golf
High and various degrees of movement	Football, track and field athletics, dancing, figure skating

lolysis also occurs in patients with Marfan's syndrome and Ehlers-Danlos syndrome; in the latter disorder it may be severe. Osteogenesis imperfecta and osteopetrosis are other forms of systemic diseases related to spondylolysis. Repeated microfractures are mainly related to hyperextension movements, thus amplifying the lordotic state. Muscle strength and tension may influence the development of spondylolysis by shortening or tightness of the hamstring muscles of the thigh with increased tension on the posterior vertebral arches of the lower lumbar spine. Weakening of the spinal and the anterior abdominal wall muscles is a precursor in the development of spondylolysis, too, whereas strengthening parts of these muscles should have a preventive effect.

In the later course of spondylolysis, fibrous or bony callus formation at the pars defect site may develop. Bony outgrowths, facet joint arthrosis, or instability may lead to nerve root impingement with leg pain, numbness, or weakness.

A cleft of the vertebral arch detected on oblique views ("Scotty dog" or "LaChapel's dog") is a direct sign of spondylolysis. More sensitive imaging techniques for the diagnosis may be a lateral view of the lumbo-sacral junction, multiplanar CT, and MRI. Flexion and extension views are helpful to document signs of hypermobility. These findings and a cleft of more than 3 mm width are indicators of a late phase of spondylolysis with a poorer prognosis than during the early phase (Engelhardt et al. 1997). During anteflexion, a complex gliding mechanism may be observed fluoroscopically: the vertebra, partially fixed at the facet joints, moves with a sudden jump in a retrolisthetic position. With such abnormal movement the increased stress on the facet joints and the spinal nerves in the adjacent intervertebral foramina may be explained. On axial CT or MR images, the spondylolytic clefts adjacent to the facet joint spaces may appear as the "double facet joint" or "incomplete ring" sign (Fig. 23.3). In the case of unilateral spondylolysis, reactive sclerosis may develop at the contralateral pedicle (Fig. 23.3). On MR images, bone marrow edema within the vertebral arch or a bony sclerosis may be observed in 40% and MR imaging may be used as a reliable modality for the diagnosis of juvenile spondylolysis (Fig. 23.3) (Campbell et al. 2005; Ulmer et al. 1997). Stäbler et al. (2000) have described the importance of a type I-reaction (T1-weighted hypointense and T2-weighted hyperintense) of such changes for the early diagnosis. The degree of destruction of the interarticular portion may be graded as follows: 0, normal; I, intact with bone marrow edema (stress reaction); II, sclerosis or low signal with intact cortex; III, indeterminate; IVa, cortical discontinuity on one side of pars; iVb, complete discontinuity of pars (Campbell et al. 2005). Sherif and Mahfouz (2004) mentioned the interposition of fatty tissue between the dural sac and the spinous process of L5 as a helpful indirect sign of spondylolysis.

An isthmic spondylolisthesis may develop in 4% of spondylolysis (Danielson et al. 1991). It is a forward movement of the body of one of the lumbar vertebrae on the vertebra below it, whereas the posterior joints and the neural arches are aligned with the posterior elements of the inferior vertebral body. Spondyloptosis is a fully dislocated vertebral body. Spondylolisthesis occurs in the preadolescent and is found in up to 50% of athletes with persistent back pain. Symptoms may not occur until later in life. In a longitudinal study by Fredrickson et al. (1984), three-quarters of all individuals with spondylolysis had an identifiable pars defect on plain films by age 6, and approximately 75% of these patients had evidence of a slip at that time. Further progression of the slip in adulthood is rare (Floman 2000).

An early gliding of more than 20% is the only predictor for spondylolisthesis that has been described (Seitsalo et al. 1991). Muschik et al. (1996) observed a progression of this entity especially during growth

spurt. Meyerding's grading into four stages oriented on the sagittal diameter of the subjacent vertebra has been generally accepted (Meyerding 1932). On axial CT or MR images, an oval elongation of the spinal canal and a stenosis of the intervertebral foramina with atrophied perineural fat are associated findings.

Other forms of spinal stress fractures are rare and may be observed at the cervical spine. At the chest, such fractures generally occur at the ribs rather than at the thoracic spine (Karlson 2004). The ribs of the lower chest may be injured in golfers or rowers, whereas fractures of the first rib may occur in weight-lifters, throwers or rucksack-carrying hikers.

23.3.1.5 Discovertebral Overuse

Apophyseal damage or microfractures of the vertebral endplates are typical findings in weight lifters, wrestlers and track and field athletes and are part of Scheuermann's disease. It is also observed in professional down-hill skiers (Ogon et al. 2001). There is a clear genetic predisposition for developing Scheuermann's disease, but observations in adolescents with high athletic activity underline the aspect of overuse in its etiology especially in the "atypical" or "traumatic" subtype which is located at the thoracolumbar junction (Alexander 1977).

With respect to the different types of endplate reactions that may or may not be associated with Scheuermann's disease, there is general agreement that Schmorl's nodes, especially their chronic forms, are not indicators of athletic injury, whereas anterior lesions are related to sports and may be associated with back pain (Ogon et al. 2001).

These anterior lesions (Fig. 23.4), the limbus vertebrae (LV) or slipped vertebral apophysis, are a disorder with cartilaginous node formation due to intraosseous disk penetration at the border of the rim apophysis. During flexion, the anterior part of the disk is pressed under the superior nonfused endplate. It typically occurs during the second decade of life after the rim apophysis has formed (7–9 years) and before its fusion with the vertebral body. The abnormality is typically observed in athletic adolescents (Ross et al. 2004).

The degree of thoracic kyphosis is increased in adolescent gymnasts but, in contrast to heavy workers, does not reach the pathologic ranges that are associated with Scheuermann's disease (Hochmuth et al. 2002).

23.3.1.6 Degenerative Joint and Disk Disease

Degeneration, despite its higher frequency in the later decades of life, may be observed in young athletes

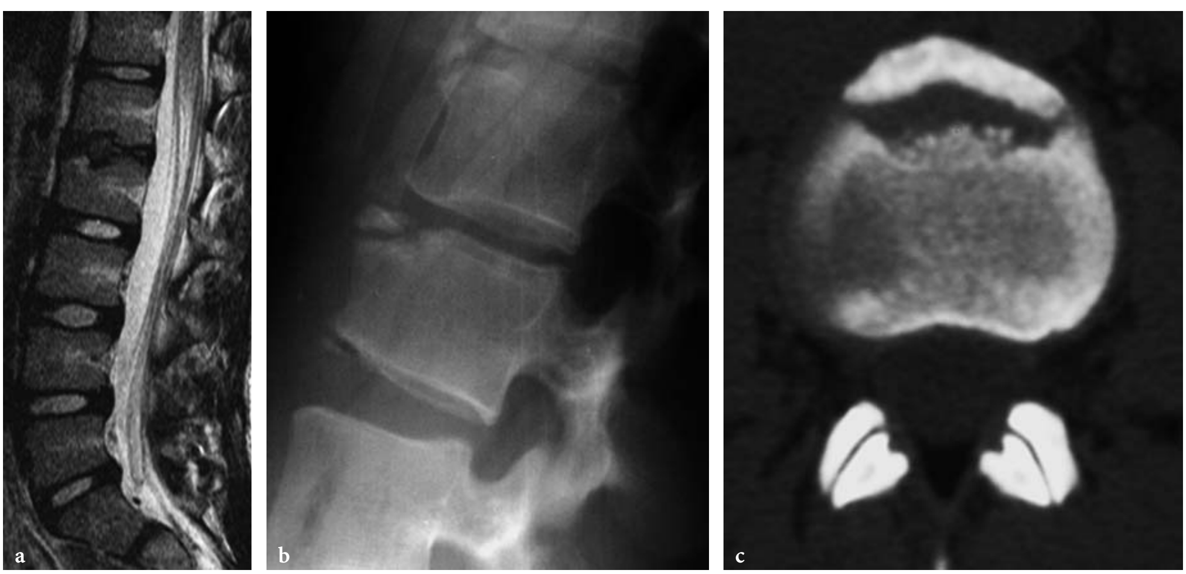

Fig. 23.4a–c. Limbus vertebrae in two different patients. **a** Sagittal TSE T2-weighted MR image shows the defect on anterior ring apophysis in a 14-year-old gymnast. **b,c** Conventional radiograph (**b**) and CT scan (**c**) in another gymnast showing separation of the rim apophyses at multiple levels (case courtesy of F.M. Vanhoenacker)

– especially gymnasts and wrestlers – and occurs rather in the nucleus than in the annulus (Sward 1992). In the same way as with Scheuermann's disease, a genetic influence has been proposed for the development of disk degeneration in children. Abnormal segmental movement patterns in the forms of hyper- or hypomobility or of instability may be best documented on flexion and extension views.

23.3.2 Differential Diagnosis

Back pain in athletes not resulting from sporting activities may be due to diseases commonly occurring in adolescents and young adults, especially rheumatic diseases, tumours or unexpected trauma. Their first clinical manifestation may, however, be in conjunction with sporting activities and characteristic imaging findings can be a hallmark of the correct diagnosis.

Inflammatory back pain is a typical symptom of seronegative spondylarthropathies (ankylosing spondylitis, psoriatic arthropathy, Reiter's disease and other reactive arthritides). Bone marrow edema, sclerosis or erosions may be observed at the sacroiliac joints or in the form of anterior spondylitis at the thoraco-lumbar junction.

Osteoid osteoma is typically located at the pedicle roots of the lumbar spine with a characteristic calcified nidus within an osteolysis. CT is the modality of choice for its detection, whereas MRI may be difficult to be interpreted because of the various tissue contrast of the nidus. Bone scintigraphy is helpful especially if performed with single photon emission computed tomography (SPECT). Primary malignant bone tumours (osteosarcoma, chondrosarcoma, chondroma) or malignant bone marrow diseases are generally rare and present with osteolysis and typical calcification patterns.

The battered child-syndrome has to be considered in any case of unclear trauma, especially if manifestations do not match with patterns of kinetic chains of if they are observed asynchronically. Apophyseal injuries at the thoracic or lumbar spine have been described to be associated with this entity (Levin et al. 2003).

Congenital vertebral clefts at the lumbar spine are in most cases observed as median interruptions of the vertebral arch, and less commonly as paraspinal, retroisthmic or retrosomatic forms. They have to be differentiated from spondylolysis vera.

23.4 Conclusion

The biomechanics of all major types of sports with spinal involvement along with the typical movement patterns is the basis for the diagnosis and treatment of pain, restricted motion or other associated findings (Lennard and Crabtree 2005). Cross-sectional imaging modalities and attempts to document the spinal kinematics are promising techniques to document normal as well as abnormal states and movement patterns. Imaging interpretation should therefore be based on "footprint" patterns of kinetic chains associated with certain athletic activities.

Things to Remember

1. The spine is involved in 10%–15% of sports injuries.
2. Overuse trauma of the vertebral arches is mainly seen in childhood and adolescence, whereas degenerative disc disease is most commonly seen in older athletes.
3. Overuse trauma is most commonly seen at the lumbar spine in sports activities associated with lumbar hyperextension. Spondylosis, apophyseal damage and scoliosis form a typical triad of overuse of the thoracic and lumbar spine.
4. Congenital and developmental disorders are risk factors for overuse syndromes and degenerative diseases of the spine.
5. A limbus vertebrae occurs typically in athletic adolescents.

References

Alexander C (1977) Scheuermann's disease: a traumatic spondylodystrophy? Skeletal Radiol 1:209–221

Amato M, Totty WG, Gilula LA (1984) Spondylolysis of the lumbar spine: demonstration of defects and laminal fragmentation. Radiology 153:627–629

Armstrong P, Ringertz H, Bischof Delaloye A (2001) Referral guidelines for imaging. European Commission Directorate-General for the Environment, Luxembourg, pp 44–58

Bennett DL, Nassar L, Delano MC (2006) Lumbar spine MRI in the elite-level female gymnast with low back pain. Skeletal Radiol 35:503-509

Boden BP, Pasquina P, Johnson J et al. (2001) Catastrophic injuries in pole-vaulters. Am J Sports Med 29:50–54

Bono CM (2004) Low-back pain in athletes. J Bone Joint Surg Am 86A:382–396

Braam LA, Knapen MH, Geusens P et al. (2003) Factors affecting bone loss in female endurance athletes: a two-year follow-up study. Am J Sports Med 31:889–895

Brolinson PG, Kozar AJ, Cibor G (2003) Sacroiliac joint dysfunction in athletes. Curr Sports Med Rep 2:47–56

Campbell RS, Grainger AJ, Hide IG, Papastefanou S, Greenough CG (2005) Juvenile spondylolysis: a comparative analysis of CT, SPECT and MRI. Skeletal Radiol 34:63–73

Danielson BI, Frennered AK, Irstam LK (1991) Radiologic progression of isthmic lumbar spondylolisthesis in young patients. Spine 16:422–425

Eck JC, Riley LH III (2004) Return to play after lumbar spine conditions and surgeries. Clin Sports Med 23:367–379, viii

Engelhardt M, Reuter I, Freiwald J et al. (1997) Spondylolysis and spondylolisthesis and sports. Orthopäde 26:755–759

Felsenberg D, Gowin W (1998) Bone densitometry: applications in sports-medicine. Eur J Radiol 28:150–154

Floman Y (2000) Progression of lumbosacral isthmic spondylolisthesis in adults. Spine 25:342–347

Fredrickson BE, Baker D, McHolick WJ et al. (1984) The natural history of spondylolysis and spondylolisthesis. J Bone Joint Surg Am 66:699–707

Hides JA, Richardson CA, Jull GA (1995) Magnetic resonance imaging and ultrasonography of the lumbar multifidus muscle. Comparison of two different modalities. Spine 20:54–58

Hochmuth K, Mack MG, Kurth AA et al. (2002) Sports-related injuries of the spine. Radiologe 42:823–832

Junghanns H (1986) Die Wirbelsäule unter den Einflüssen des täglichen Lebens, der Freizeit, des Sports. Thieme, Stuttgart, p 35

Kainberger F, Weidekamm CM, Trieb K (2006) Sports injury of the spine: imaging diagnosis. Rontgenpraxis 56:47-57

Karlson KA (2004) Thoracic region pain in athletes. Curr Sports Med Rep 3:53–57

Katz DA, Scerpella TA (2003) Anterior and middle column thoracolumbar spine injuries in young female gymnasts. Report of seven cases and review of the literature. Am J Sports Med 31:611–616

Kaufman BA, Warren MP, Dominguez JE et al. (2002) Bone density and amenorrhea in ballet dancers are related to a decreased resting metabolic rate and lower leptin levels. J Clin Endocrinol Metab 87:2777–2783

Launay F, Leet AI, Sponseller PD (2005) Pediatric spinal cord injury without radiographic abnormality: a meta-analysis. Clin Orthop Relat Res:166–170

Lennard T, Crabtree H (2005) Spine in sports. Elsevier Mosby, Philadelphia, pp 57–220

Levin TL, Berdon WE, Cassell I et al. (2003) Thoracolumbar fracture with listhesis – an uncommon manifestation of child abuse. Pediatr Radiol 33:305–310

McCrory P, Bell S (1999) Nerve entrapment syndromes as a cause of pain in the hip, groin and buttock. Sports Med 27:261–274

Meyerding H (1932) Spondylolisthesis. Surg Gynec Obstet 54:371–377

Micheli LJ, Wood R (1995) Back pain in young athletes. Significant differences from adults in causes and patterns. Arch Pediatr Adolesc Med 149:15–18

Muschik M, Hahnel H, Robinson PN et al. (1996) Competitive sports and the progression of spondylolisthesis. J Pediatr Orthop 16:364–369

Niethard FU, Pfeil J, Weber M (1997) Etiology and pathogenesis of spondylolytic spondylolisthesis. Orthopäde 26:750–754

Ogon M, Riedl-Huter C, Sterzinger W et al. (2001) Radiologic abnormalities and low back pain in elite skiers. Clin Orthop Relat Res 390:151–162

Prasad SS, O'Malley M, Caplan M et al. (2003) MRI measurements of the cervical spine and their correlation to Pavlov's ratio. Spine 28:1263–1268

Ross J, Brant-Zawadzki M, Moore K et al. (2004) Diagnostic imaging: spine. Amirsys, Salt Lake City, pp I, 1:82–85

Rossi F, Dragoni S (1990) Lumbar spondylolysis: occurrence in competitive athletes. Updated achievements in a series of 390 cases. J Sports Med Phys Fitness 30:450–452

Sabo D, Bernd L, Pfeil J et al. (1996) Bone quality in the lumbar spine in high-performance athletes. Eur Spine J 5:258–263

Schroder RJ, Albus M, Kandziora F et al. (2003) Diagnostic value of three-dimensional reconstruction in CT of traumatic spinal fractures. Rofo 175:1500–1507

Seidl G, Kainberger F, Haber P et al. (1993) Systematisches Krafttraining in der Postmenopause: begleitende densitometrische Kontrolle mittels DXA. Radiologe 33:452–456

Seitsalo S, Osterman K, Hyvarinen H et al. (1991) Progression of spondylolisthesis in children and adolescents. A long-term follow-up of 272 patients. Spine 16:417–421

Sherif H, Mahfouz AE (2004) Epidural fat interposition between dura mater and spinous process: a new sign for the diagnosis of spondylolysis on MR imaging of the lumbar spine. Eur Radiol 14:970–973

Soler T, Calderon C (2000) The prevalence of spondylolysis in the Spanish elite athlete. Am J Sports Med 28:57–62

Stäbler A, Paulus R, Steinborn M et al. (2000) Spondylolysis in the developmental stage: diagnostic contribution of MRI. Rofo 172:33–37

Standaert CJ, Herring SA (2000) Spondylolysis: a critical review. Br J Sports Med 34:415–422

Sward L (1992) The thoracolumbar spine in young elite athletes. Current concepts on the effects of physical training. Sports Med 13:357–364

Tall RL, DeVault W (1993) Spinal injury in sport: epidemiologic considerations. Clin Sports Med 12:441–448

Ulmer JL, Mathews VP, Elster AD et al. (1997) MR imaging of lumbar spondylolysis: the importance of ancillary observations. AJR Am J Roentgenol 169:233–239

Vialle R, Schmit P, Dauzac C et al. (2005) Radiological assessment of lumbosacral dystrophic changes in high-grade spondylolisthesis. Skeletal Radiol 34:528–535

White JH, Hague C, Nicolaou S et al. (2003) Imaging of sacral fractures. Clin Radiol 58:914–921

Maxillofacial Injuries in Sports

Anja Bernaerts, Philippe Ehlinger, and Karen Chapelle

CONTENTS

24.1 Introduction

Trauma due to sports can have a significant impact on unprotected sites of the body such as the maxillofacial region. The commonest sports related maxillofacial injuries are soft tissue lacerations followed by dentoalveolar fractures and minor facial bone fractures (Hill et al. 1998; Tuli et al. 2002). The most frequently recorded maxillofacial bone fractures involve the mandible, the zygomatic and nasal bone (Maladiere et al. 2001).

According to different reports, sports-related facial fractures account for 4%–18% of all sports injuries and 6%–33% of all facial bone fractures (Bayliss and Bedi 1996; Carroll et al. 1995; Mourouzis and Koumoura 2005). This variation in occurrence may reflect the geographic differences in the level of participation in sports activities and the type of popular sports. Which sport is responsible for the majority of injuries varies above all according to the popularity that each sporting activity has in a particular country (Cerulli et al. 2002; Flanders and Bhat 1995; Lim et al. 1993; Tanaka et al. 1996). The majority of facial fractures in Western countries today occur during team sports, such as soccer, basketball and rugby (Cerulli et al. 2002; Maladiere et al. 2001; Mourouzis and Koumoura 2005). Fractures of the maxillofacial region are more frequent in males and between the ages of 20 and 30 years, most likely reflecting the high levels of physical activity in this sex and age group (Mourouzis and Koumoura 2005). Sports are also a primary cause of maxillofacial fractures in the paediatric population, probably because of the learning stages of sports ability and the ignorance of the consequences of taking greater risks (Gassner et al. 2004). A recent study has shown that 26% of paediatric facial fractures were caused by bicycle accidents (Iida and Matsuya 2002).

Various sports committees have adopted specific guidelines for the prevention of dental and craniomaxillofacial injuries. Sports such as hockey and American football have adopted full facial and cranial protective headgear. Evolution of these protective devices has significantly reduced many types of head and neck injuries in these sports (Greenberg and Haug 2005). Nevertheless, there are an increasing number of people who are engaged in sporting activities and new, high-velocity vehicular and high

A. Bernaerts, MD
Department of Radiology, Sint-Augustinus Hospital, Oosterveldlaan 24, 2610 Wilrijk, Belgium
P. Ehlinger, MD
Department of Oral and Maxillofacial Surgery, Sint-Augustinus Hospital, Oosterveldlaan 24, 2610 Wilrijk, Belgium
K. Chapelle, MD
Department of Oral and Maxillofacial Surgery, Sint-Maarten Hospital, Rooienberg 25, 2570 Duffel, Belgium

Box 24.1. Panoramic radiograph

- Easy interpretation
- Isolated trauma of the mandibula
  - Dentoalveolar injuries
  - Mandibular fractures
- Screening in all patients with maxillofacial fracture

Box 24.2. Conventional radiographs (Waters view; Caldwell view; lateral view and submentovertex view)

- Difficult interpretation
- Solitary, low-impact, fractures
- Nasal trauma

Box 24.3. Computed tomography (CT) with 2D and 3D reformations

- High accuracy
- Midface trauma
- Complex fractures
  - Multiplicity of fragments
  - Degree of dislocation and rotation
  - Skull base involvement
  - Cribriform plate, lacrimal duct, optic canal, superior orbital fissure or infraorbital canal involvement
- Further characterization and classification of solitary fractures
- Posttraumatic osteomyelitis

altitude activities are introduced. Moreover, amateur athletes often do not use any protective clothing or equipment in sports in which the use of protective gear is recommended.

24.2 Correlation Between Injury Type and Injury Mechanism Among Sports

There have been few studies that have been directed toward the biomechanics of maxillofacial injuries associated with sports. Perhaps the difficulty of engaging in such a study is the large variety of sports activities that are available today, ranging from those with minimal interpersonal contact to those with high-energy contact. In addition, comparative analysis of these studies is hampered by varied selection criteria and the use of retrospective non-consecutive data.

24.2.1 Dentoalveolar Fractures

In dentoalveolar fractures, a high-velocity trauma, such as a baseball that takes a bad hop and strikes the maxillary incisors, is more likely to cause a tooth fracture, whereas a low velocity trauma is expected to cause a displacement injury (e.g., an avulsion). Children with a type 2 malocclusion (so-called retrognathism or overbite) in particular will be prone to sports-related dentoalveolar injuries of the upper incisors.

Another mechanism, indirect trauma, occurs when the mandible whiplashes into collision with the maxilla. This trauma can occur from a blow to the chin, such as an uppercut in boxing, a football tackle, or a hockey stick. The concussion is capable of shattering posterior teeth.

Enamel infraction can be caused by acute or chronic trauma such as grinding or clenching (e.g., weightlifting) (Kurtz et al. 2005).

24.2.2 Facial Bone Fractures

Sporting activities can be grouped into different categories in order to understand better the injury mechanism in sports related facial bone fractures:

- Team sports: soccer, rugby, basketball, football, handball
- Vehicular sports: bicycling, mountainbiking,

Box 24.4. Magnetic resonance (MR) imaging

- Cranial nerve palsy
  - Nerve compression due to haematoma
  - Nerve transsection
  - Axonal injury
- Traumatic damage to the temporomandibular joint disc
- Brain concussion
- Posttraumatic meningocele
- Posttraumatic meningitis
  - Inflammatory collections
  - Abscess formation
- Posttraumatic ischemic necrosis of the condylar head of the mandible

horse-riding, skiing, snowboarding, ice-hockey, in-line skating

- Sports with small balls: tennis, baseball, cricket, golf
- Combat sports: boxing, karate, Kung-fu, wrestling
- Individual sports: swimming, diving, gymnastics, body-building etc.

In team sports the main type of impact in facial bone fractures appears to be a collision with another player that takes place mainly when the ball is played with the forehead. At this instant there can be an elbow-head impact or a head-head impact. An analysis of the anatomic distribution of facial fractures sustained during team sports showed that the mandible, followed by the zygomatic region, is most commonly affected (Maladiere et al. 2001; Mourouzis and Koumoura 2005). Football players do not encounter orofacial injuries as often as other athletes because faceguards and mouth protectors are now mandatory (Flanders and Bhat 1995; Sane 1988). This might also explain the relative low incidence of facial injuries reported in contact sports such as boxing (Hill et al. 1998).

In vehicular, non-car, sports, a fall to the ground is the most commonly reported type of impact. Fractures of the mandible and zygoma are most prominent in vehicular sports as well, but, unlike team sports, the frontal sinus and central midface are commonly affected too (Gassner et al. 1999a; Maladiere et al. 2001). Generally, mountainbikers sustain more severe maxillofacial injuries in comparison with bicyclists. The dominant fracture site in bicyclists is the zygoma, whereas mountainbikers encounter more serious midface fractures such as Le Fort I, II, and III fractures (Gassner et al. 1999b). In horse-riding, being kicked by the horse is correlated with more severe injuries (Fig. 24.1) (Ueeck et al. 2004).

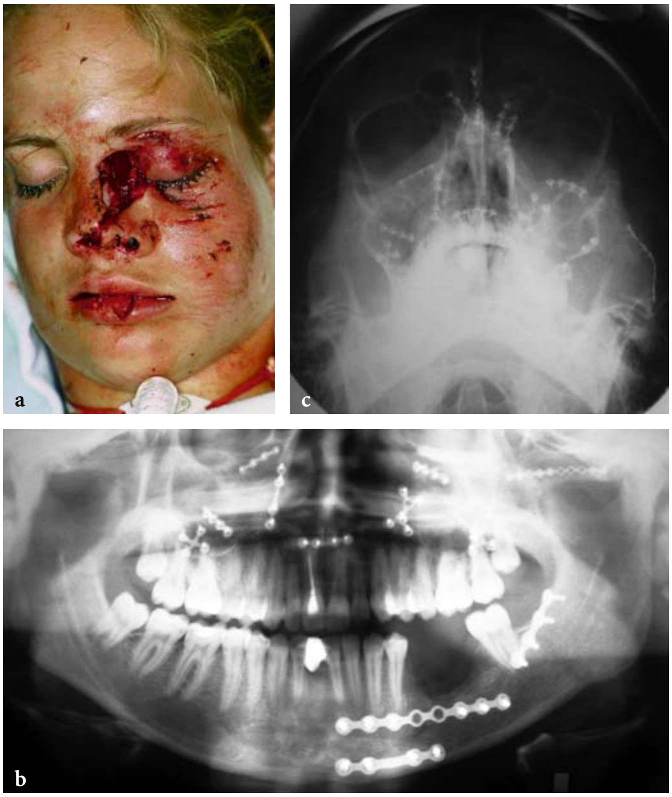

Fig. 24.1a–c. Horsewoman with a complex maxillofacial injury after being kicked in the face. A clinical photograph immediately following injury shows severe soft-tissue lacerations (**a**). A postoperative panoramic radiograph (**b**) and Waters view (**c**) after reduction and internal fixation demonstrate the involvement of the mandible, maxilla, nose and zygoma. [Reprinted with permission from Raghoebar et al. (2005)]

A missile type of injury to the head caused by the ball or other implement is most mentioned in sports with small balls such as baseball (Bak and Doerr 2004; Delilbasi et al. 2004; Maladiere et al. 2001). Contact with the racquet, the bat or club also is a common cause of injury in this category (Lim et al. 1993).

Sport diving carries inherent risk to the maxillofacial region in its own way. Atypical facial pain and temporomandibular joint dysfunction may result from repeated use of the mouthpiece of the regulator. The mechanical effects from changes in ambient pressure may cause paranasal sinus barotraumas, cranial nerve injury, and barodontalgia (Brandt 2004).

24.3 Imaging Strategy

The diagnosis of facial fractures is usually accomplished by a combination of clinical and imaging examinations. Often, deformity of the facial skeleton is initially concealed by overlying edema, haemorrhage, and soft tissue injury. Therefore, the clinician is primarily concerned with the detection of malocclusion, abnormal mobility, and crepitation as signs of fractures. Any evidence of a palpable step-off at the orbital rim, diplopia, hypertelorism, midfacial elongation, cerebrospinal fluid rhinorrhea, or flattening of the cheek further helps the clinician identify the type of fracture present. However, only after imaging studies can the fracture be completely identified and characterized (Greenberg and Haug 2005).

24.3.1 Plain Radiography

The panoramic radiograph is still a highly cost-effective and accurate method for the determination of the presence of mandibular and dentoalveolar fractures (Fig. 24.2). In addition, it is used as an initial survey film in all maxillofacial fractures to spot associated lesions such as dentoalveolar fractures or inflammatory lesions of the jaws which could complicate the postoperative course (Box 24.1). In case of dental trauma, supplementary intraoral periapical films always are required to obtain adequate image detail (Fig. 24.3) (White and Pharoah 2000).

When trauma of the viscerocranium occurs as an isolated injury due to a blow or fall, like in sports injuries, it can be investigated by conventional radiographs first. A basic facial series consists of three or four films: a Waters view (PA view with cephalad angulation), a Caldwell view (PA view), a lateral view, and occasionally a submentovertex view (Fig. 24.4b–e). A Waters view allows recognition of interruption of the zygomaticoalveolar arch and of the orbital floor and lateral wall, while a Caldwell view permits delineation of the lamina papyracea, zygomaticofrontal suture, floor of the nasal cavity and maxillary sinus. Delineation of zygomatic arch fractures is best performed by a submento-vertex view. Nasal and anterior nasal spine fractures and posterior displacement of the midface are recognized on a lateral film. A focussed lateral, Waters and superior-inferior view may be requested for documentation of a nasal fracture (Fig. 24.5a) (Box 24.2) (Schuknecht and Graetz 2005; Som and Brandwein 2003).

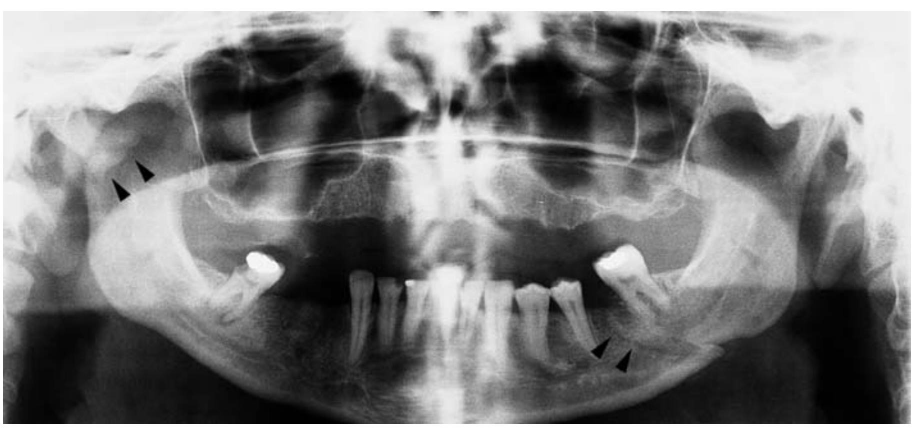

Fig. 24.2. Panoramic radiograph demonstrating an oblique fracture of the left mandibular body and an extracapsular fracture of the right condylar process (*arrowheads*)

Fig. 24.3. Periapical radiograph shows a transverse root fracture of the left primary central maxillary incisor with some distraction of the fragments (*arrowheads*)

Fig. 24.4a–e. Three-dimensional (3D) surface shaded CT reconstruction (**a**) of a trimalar (zygomatic) fracture in a young male soccer player after being struck in the face by an opponent's knee. Radiographic evaluation after osteosynthesis includes a Waters view (**b**), a Caldwell view (**c**), a lateral (**d**) and submento-vertex view (**e**). The latter view best delineates the zygomatic arch (*arrowheads*)

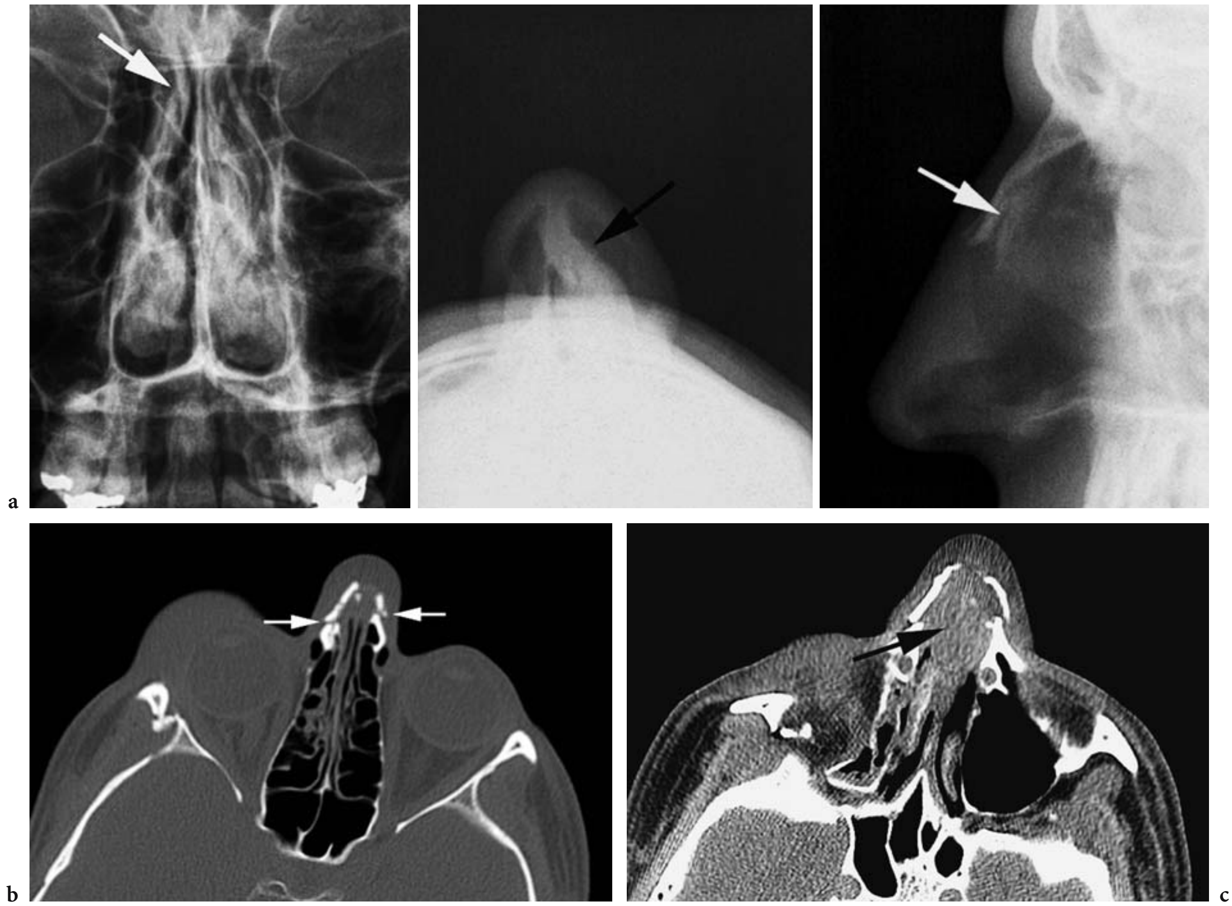

Fig. 24.5a–c. A 25-year-old male soccer player who sustained a complex nasal fracture after being kicked in the face by an opponent's foot. Radiographic evaluation of the nasal bone including a frontal, superior-inferior and lateral view (**a**) confirms a fracture of the nasal bone (*white arrows*). A deviation of the cartilaginous portion of the nasal septum is noted (*black arrow*). Axial CT scans viewed at "bone" (**b**) and "soft-tissue" (**c**) window settings show comminuted fractures of both nasal bones and right frontal process of the maxilla (*white arrows*). Also note the presence of a septal haematoma (*black arrow*) and an associated displaced fracture at the right zygomaticosphenoid suture

24.3.2 Computed Tomography

The traditional strong role of conventional images in patients with facial bone fractures, however, is currently decreasing. Spiral multislice computed tomography (CT) is progressively replacing the panoramic radiograph and conventional radiographs for maxillofacial trauma, and is increasingly being performed in addition to conventional films to detail and classify trauma to the mandible as well. Metal artefacts from tooth fillings however may degrade bone visualisation. CT is the imaging technique of choice to display the multiplicity of fragments, the degree of dislocation and rotation, or skull base involvement (Fig. 24.5b,c). CT is also particularly important to recognize potential, cribriform plate, lacrimal duct, optic canal (optic nerve), superior orbital fissure (cranial nerve III–VI) or infraorbital canal (infraorbital nerve) involvement. Maxillofacial trauma with suspicion of osseous involvement requires thin collimation of slices (0.75–1 mm) to detail the location and course of fracture lines. The data set provides high-resolution two-dimensional (2D) multiplanar reconstructions (MPR) with contiguous 2-mm slices in the axial and coronal plane displayed in high resolution bone window (window width, 3200 HU; center level, 700) and in soft tissue settings (window width, 300 HU; center level, 100). Additional sagittal reconstructions are reserved for central midface and mandibular condylar fractures. Three-dimensional (3D) surface shaded CT reconstructions add the third dimension at one glance and are particularly help-

ful for treatment in case of multiple fragments and/or severe fragment dislocation (Fig. 24.4a) (Box 24.3) (Reuben et al. 2005; Schuknecht and Graetz 2005; Som and Brandwein 2003; Turner et al. 2004).

24.3.3 Magnetic Resonance Imaging

Magnetic resonance (MR) imaging does not visualize the bone directly and therefore small yet unstable nondisplaced facial fractures may not be seen. Nevertheless, supplementary MR examinations are required when cranial nerve palsy occurs in order to recognize neural compression. MR imaging is more sensitive to detect nerve compression due to haematoma, nerve transsection, or axonal injury. MR imaging also is the most sensitive technique to evaluate traumatic damage to the temporomandibular joint disc (Fig. 24.6) (Box 24.4).

Early and late complications of trauma related to the orbit, anterior cranial fossa, or lateral skull base due to infection, brain concussion, or herniation require CT to visualize the osseous prerequisites of complications, and MR to define the adjacent brain and soft tissue involvement. MR is more sensitive to display dural defects, recognize inflammatory collections following meningitis, or distinguish brain concussion from abscess formation. In patients with suspicion of posttraumatic osteomyelitis, CT is superior to MR, as it provides additional information with respect to a likely incomplete stability of the osteosynthesis, the degree of callus formation, or the presence of sequestra as sequela of osteomyelitis. MR imaging, however, is more sensitive to detect early osteomyelitis or ischemic necrosis of the condylar head of the mandible (Reuben et al. 2005; Schuknecht and Graetz 2005; Som and Brandwein 2003; Turner et al. 2004).

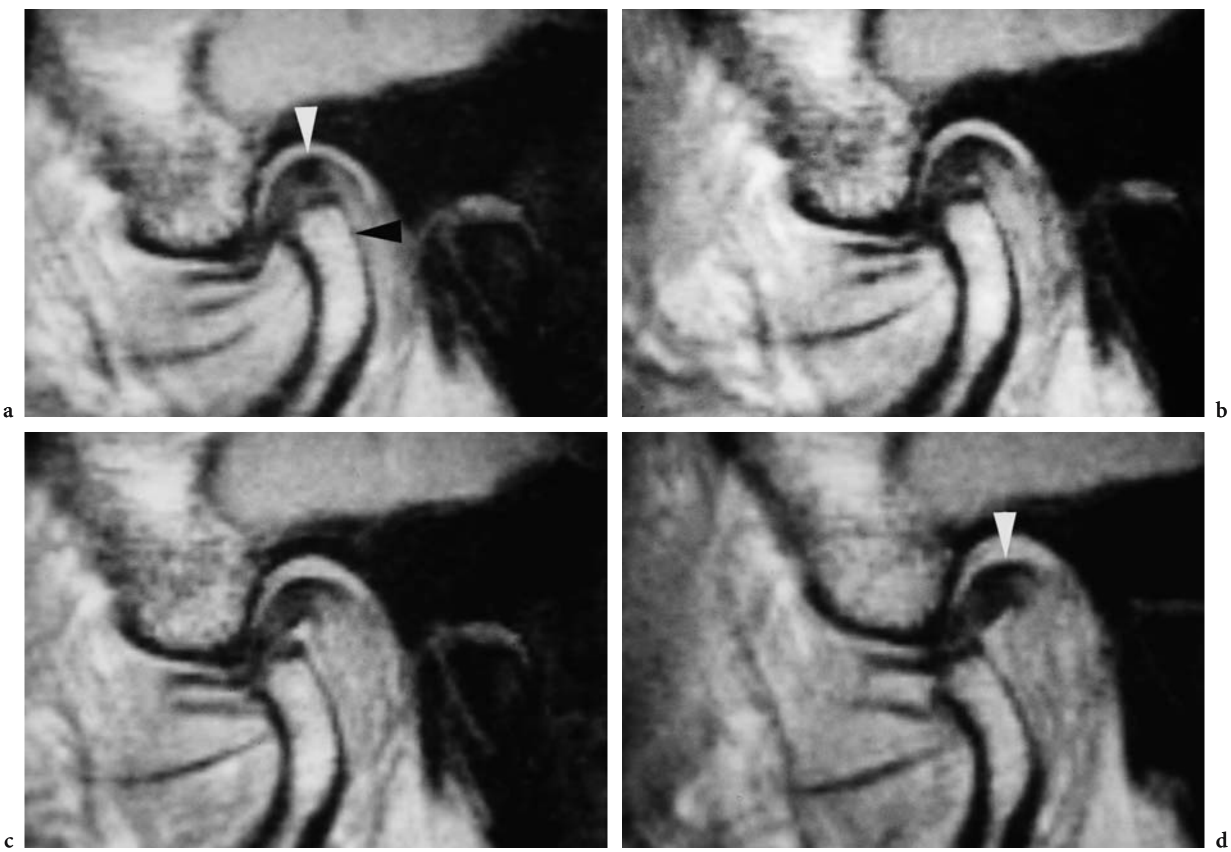

Fig. 24.6a–d. Posttraumatic disk adhesion demonstrated by T1-weighted MR images. Closed-mouth image (**a**) shows a normal position of the disk (*white arrowhead*) and the condyle (*black arrowhead*) relative to the glenoid fossa. Upon opening of the mouth (**b**–**d**), the condyle moves inferior to the articular eminence; however the disk (*white arrowhead*) remains stuck in the glenoid fossa. Courtesy of Dr. J. Casselman

24.4 Specific Sports-Related Maxillofacial Injuries

24.4.1 Soft-Tissue Injuries

Soft-tissue injuries are by far the most common maxillofacial injuries associated with sports (Hill et al. 1998). Soft-tissue injuries may be classified as abrasions, lacerations, cuts, haematomas and burns.

Ocular soft tissue injuries also are frequently seen in sports related trauma, mainly in racquet sports (squash, tennis, and badminton) and soccer (Barr et al. 2000). Problems such as hyphema (bleeding in the anterior chamber), retinal tears, lens dislocation, penetrating globe injury, optic nerve compression, superior orbital fissure syndrome (cranial nerve III to VI paralysis) and retrobulbar hematoma should be cautiously thought about (Greenberg and Haug 2005).

Radiologic examination should be carefully considered in each patient to spot underlying fractures.

24.4.2 Dentoalveolar Injuries

Dental injuries range from minor enamel fragments, to complete crown-root fractures, or complete tooth avulsion. When the dental fracture involves the alveolar bone, whether in the maxilla or the mandible, these injuries are classified as dentoalveolar fractures.

These types of injuries are common in sports and are highly preventable with the use of mouthguards (Greenberg and Haug 2005). Children have a disadvantage with regard to dentition. When the tooth germ lies in the fracture, the tooth can fall during healing or have delayed development and deformity that does not manifest clinically until the permanent tooth erupts (Som and Brandwein 2003).

Crown fractures are very common. They can involve only the enamel (infraction) or can in addition involve the dentine (uncomplicated fracture) and pulp (complicated fracture) (Fig. 24.7). Dental root fractures (Fig. 24.3) and crown-root fractures are less common. The term “concussion” indicates a crushing injury to the vascular structures at the tooth apex and to the periodontal ligament, resulting in inflammatory edema. The radiographic appearance of a dental concussion is widening of the periodontal ligament space (radiolucency between the cementum of the root and the lamina dura of the bony socket).

Fig. 24.7. Spot view of a panoramic radiograph demonstrating a crown fracture of the right lateral maxillary incisor (tooth 12)

Luxation of teeth is dislocation of the articulation (represented by the periodontal ligament) of the tooth. Traumatic forces, depending on their nature and orientation, can cause intrusive luxation (displacement of teeth into the alveolar bone), extrusive luxation (partial displacement of teeth out of the sockets), or lateral displacement (movement of teeth other than axial displacement). In intrusive and lateral luxation, comminution or fracture of the supporting alveolar bone accompanies dislocation of the tooth. Radiographic examination of luxated teeth may demonstrate the direction of the displacement by the widening and/or obliteration of the periodontal ligament space and shows associated fractures of the alveolar bone (Fig. 24.8).

Avulsion is the complete displacement of the tooth from its socket. The maxillary incisors are the most frequently avulsed teeth. Avulsion is not an uncommon occurrence in sports (Kurtz et al. 2005; White and Pharoah 2000).

24.4.3 Mandibular Fractures

There is a variety of causes for mandibular fractures predominated by assaults and motor vehicle collisions, with sports as a smaller aetiology (2%–6%) (Greenberg and Haug 2005). However, according to the investigations of Emshoff et al. (1997) sports are increasingly implicated in the causes of mandibular fractures. His study showed sporting activities to be

Fig. 24.8. Oblique view of the mandible demonstrating a vertical fracture of the mandibular body. There is a concomitant extrusive luxation of the right canine. Note the widening of the periodontal ligament space that is accentuated at the apical region (*white arrow*)

the main causative factor of mandibular fractures, accounting for 31.5%. The difference may be attributable to the extensive sports facilities and tourism industry in the studied region (Innsbruck).

Mandibular fractures can be categorized based on anatomic location: (para)-symphyseal, body, angle, and ascending ramus (Figs. 24.2 and 24.8). Fractures affecting the ramus mandibulae are subdivided into those directed to the coronoid or condylar process. Condylar fractures may be intracapsular or extracapsular in location. In extracapsular fractures, the fracture line is below the insertion of the lateral pterygoid muscle. Displacement is usually in an anteromedial direction (Schuknecht and Graetz 2005). In sports-related mandibular fractures, the subcondylar region is most commonly affected (Emshoff et al. 1997).

24.4.4 Central Midface Fractures

Central midface fractures are classified into fractures of the nose and nasoethmoid complex, isolated maxillary fractures and Le Fort I, II and III types of fractures, (Som and Brandwein 2003).

Nasal fractures are the most common sports related facial fractures with sports accounting for up to 27% of all nasal fractures (Greenberg and Haug 2005). There is, however, a large discrepancy of prevalence amongst papers. Nose fractures can be treated by other specialities (ENT and plastic surgeons) than maxillofacial surgeons in some hospitals and therefore might be underestimated in some studies (Frenguelli et al. 1991; Maladiere et al. 2001). The majority of nasal bone fractures involve the thinner, distal third of the nasal bones. A lateral blow to the nose usually causes a simple cartilage depression or fracture of only the ipsilateral nasal bone. On the other hand, a frontal nasal blow usually fractures both nasal bones at their lower ends, and the septum is also displaced and fractured. With a greater force, the entire nasal pyramid, including the frontal processes of the maxillae, may become detached (Fig. 24.5) (Som and Brandwein 2003).

Nasoethmoid fractures are most often caused by a blow over the bridge of the nose resulting in posterior displacement of the nasal bone and frontal process of the maxilla with telescope-like deformation and foreshortening of the anterior ethmoid. The lacrimal bone and cribriform plate are frequently involved (Schuknecht and Graetz 2005; Som and Brandwein 2003).

Isolated maxillary fractures, other than alveolar fractures, can result from a blow directly over the anterior maxillary wall. The fractures involve the anterior and lateral antral walls and extend toward the pyramid aperture and down into the maxillary alveolus (Fig. 24.9) (Som and Brandwein 2003).

Complex midface fractures are typically referred to in the context of Le Fort's early anatomic studies. Although visualization of injury to the struts and buttresses of the face is required for repair of these fractures with restoration of the 3D stability and symmetry of the face, the Le Fort classification still appears to be a succinct way of summarizing and communicating the major planes of certain fractures. The greatest frequency of Le Fort types of fractures results from assaults and motor-vehicle collisions, with sports accounting for 5%–8% of such fractures (Greenberg and Haug 2005).

Common to all Le Fort fractures is fracture of the pterygoid processes. In addition, each Le Fort fracture has a unique component (Fig. 24.10) (Rhea and Novelline 2005). The Le Fort I fracture runs horizontally above maxillary alveolar process and is the only one that involves the anterolateral margin of the nasal fossa just above the maxillary alveolar process.

Fig. 24.9. Axial CT scan in bone window setting of an isolated maxillary fracture involving the left anterior antral wall (*arrow*) in a 19-year-old woman after falling from her bicycle. Note the presence of a haemorrhage within the right antrum with an air-fluid level

Fig. 24.11. Three-dimensional (3D) surface shaded CT reconstruction of a left hemi-Le Fort II fracture caused by a skiing accident (*black arrow*). This type of Le Fort fracture is the only one that involves the orbital rim

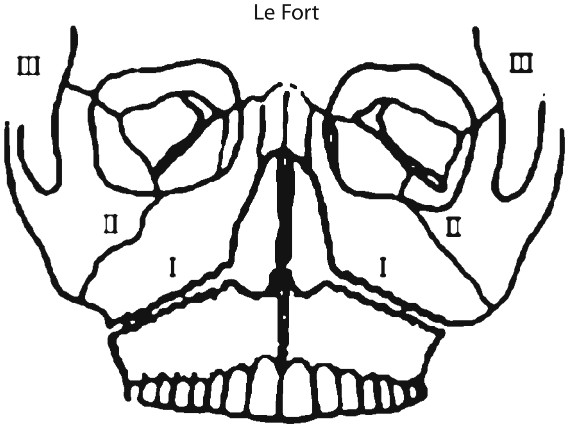

Fig. 24.10. Drawing in frontal projection showing Le Fort I, II, and III types of fractures. [Modified from Rhea and Novelline (2005)]

The Le Fort II fracture is pyramidal in shape with teeth at base of pyramid and nasofrontal suture at apex of pyramid. This type of fracture is the only one that involves the inferior orbital rim. Posterior and lateral walls of maxillary sinus are broken (Fig. 24.11). The Le Fort III fracture separates bones of face from the rest of the skull. The fracture crosses the nasomaxillary suture, the lamina papyracea medially, and the superior orbital fissure and courses laterally to involve the sphenozygomatic and frontozygomatic suture. The Le Fort III fracture is the only one that involves the zygomatic arch.

24.4.5 Lateral Midface Fractures

Lateral midface fractures consist of zygomatic fractures (trimalar, or tripod), zygomatic arch fractures, zygomaticomaxillary fractures, zygomaticomandibular fractures and fractures of the floor of the orbit (blow-out fractures) (Som and Brandwein 2003). Sports injuries account for 4%–11% of all zygomatic fractures (Greenberg and Haug 2005).

In a so-called trimalar or tripod fracture, the fracture line extends from the lateral orbital wall (zygomaticofrontal suture and the zygomaticosphenoid suture) to the inferior orbital fissure, then across the orbital floor near the orbital canal, down the anterior maxilla near the zygomaticomaxillary suture, and up the posterior maxillary wall back to the inferior orbital fissure. There is also a fracture through the weakest part of the zygomatic arch, which is about 1.5 cm dorsal to the zygomaticotemporal suture (Figs. 24.4 and 24.12).

When there is an isolated fracture of the zygomatic arch, there are usually at least three discrete fracture lines, creating two fracture segments. These pieces are displaced medially and downwards, reflecting the direction of the impact force (Fig. 24.13).

Zygomaticomaxillary fractures differ from trimalar fractures in that the former fractures involve the

a
b
c

Fig. 24.12a–c. Axial CT images through the orbit (**a**), the zygomatic arch (**b**), and the maxilla (**c**) show a left trimalar fracture sustained during a bicycling accident due to a fall. The left frontosphenoid fracture is minimally displaced (*arrow* in **a**). The zygomatic arch is also fractured in two places (*arrows* in **b**). The most caudal image shows the complex fracture near the zygomaticomaxillary suture (*arrow* in **c**) with involvement of the orbital floor, the orbital canal, and anterior and posterior maxillary wall. There is orbital and subcutaneous emphysema, and haemorrhage is present in the left antrum. Also note the presence of a prolapsed fracture segment in the antrum

Fig. 24.13. Spot view of a submentovertical view shows a depressed fracture of the left zygomatic arch sustained during an elbow-head impact in a soccer game. [Reprinted with permission from Raghoebar et al. (2005)]

orbital floor, extend down the anterior maxilla (often more medially than in a typical trimalar fracture), run to the premolar region, and then extend across the palate to the maxillary tuberosity and lower pterygoid plates.

Zygomaticomandibular fractures differ from zygomatic fractures only by the additional fracture of the mandibular condyle, coronoid process, or both (Som and Brandwein 2003).

One-third of orbital blow-out fractures are sustained during sports. Soccer is most commonly involved (Jones 1994). A blow to the orbit by an object that is too large to enter the orbit (baseball, fist, etc.) may cause a blow-out fracture resulting in fracture of the orbital floor and – by definition – leaving the inferior orbital rim intact. Herniation of orbital fat, inferior rectus muscle and inferior oblique muscle can occur (Fig. 24.14). Additionally, or rarely alternatively, the medial orbital wall may be displaced into the ethmoid resulting in the so-called "medial blow-out fracture" with potential herniation of the medial rectus muscle. Supraorbital roof fractures are uncommon (Schuknecht and Graetz 2005; Som and Brandwein 2003).

a b

Fig. 24.14a,b. A Waters view (**a**) and coronal CT image (**b**) of a blow out fracture. A completely displaced piece of bone, a trapdoor fracture (*arrow*), can be identified as can the typical "teardrop" herniation of orbital contents

24.4.6 Frontal Sinus Fractures

Frontal fractures are less common than other fractures of the craniomaxillofacial skeleton because of their greater thickness and biomechanical advantages. Sports injuries account for 3%–5% of all fractures (Greenberg and Haug 2005).

Frontal bone fractures are classified according to the involvement of the supraorbital rim, anterior wall, posterior wall, or sinus floor (Fig. 24.15) (Som and Brandwein 2003).

24.5 Conclusions

In conclusion, the majority of sports-related craniomaxillofacial injuries are of a minor nature including soft tissue lacerations followed by dentoalveolar fractures and minor facial bone fractures. The most frequently recorded maxillofacial bone fractures involve the mandible, the zygomatic and nasal bone and occur during team sports, such as soccer and rugby, as a consequence of an impact against another player. Dentoalveolar fractures always require intraoral periapical films to obtain adequate image detail. CT is the modality of choice for the most complete evaluation of the facial skeleton and facial soft tissues.

Things to Remember

1. The majority of sports-related craniomaxillofacial injuries are of a minor nature including soft tissue lacerations followed by dentoalveolar fractures and minor facial bone fractures respectively.
2. The most frequently recorded facial fractures in sports include nasal, mandibular, and zygomatic fractures.
3. The majority of facial fractures occur during team sports, such as soccer and rugby, and as a consequence of an impact against another player.
4. In vehicular sports, a fall to the ground is the most commonly reported type of impact and the frontal sinus and central midface are commonly affected.
5. Dentoalveolar fractures always require intraoral periapical films to obtain adequate image detail. CT is the modality of choice for the most complete evaluation of the facial skeleton and facial soft tissues.

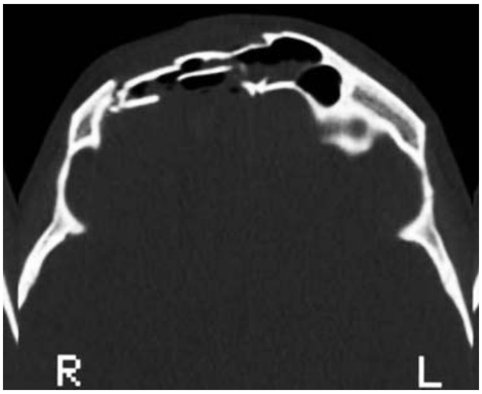

a

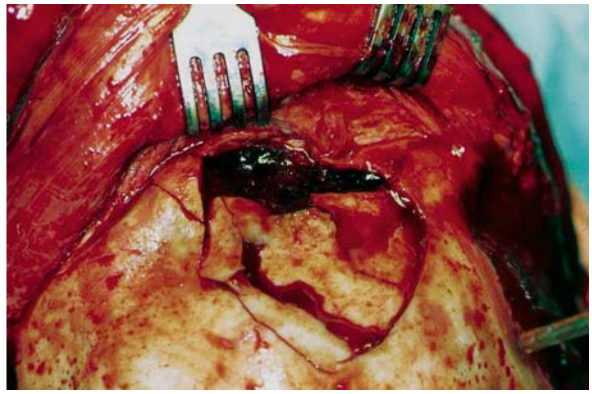

b

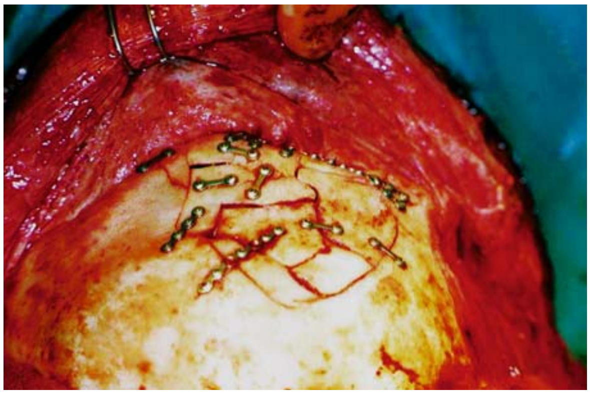

c

d

Fig. 24.15a–d. Young male soccer player who sustained a frontal sinus fracture in a heading duel. A preoperative axial CT scan (**a**) shows a depressed comminuted fracture of both the anterior and posterior frontal sinus tables. Peroperative photographs before (**b**) and after (**c**) repositioning and osteosynthesis show the impact site. Postoperative lateral view (**d**) shows an anatomic alignment of the fracture fragments. [Reprinted with permission from Raghoebar et al. (2005)]

References

Bak MJ, Doerr TD (2004) Craniomaxillofacial fractures during recreational baseball and softball. J Oral Maxillofac Surg 62(10):1209–1212

Barr A, Baines PS, Desai P et al. (2000) Ocular sports injuries: the current picture. Br J Sports Med 34(6):456–458

Bayliss T, Bedi R (1996) Oral, maxillofacial and general injuries in gymnasts. Injury 27(5):353–354

Brandt MT (2004) Oral and maxillofacial aspects of diving medicine. Mil Med 169(2):137–141

Carroll SM, Jawad MA, West M et al. (1995) One hundred and ten sports related facial fractures. Br J Sports Med 29(3):194–195

Cerulli G, Carboni A, Mercurio A et al. (2002) Soccer-related craniomaxillofacial injuries. J Craniofac Surg 13(5):627–630

Delilbasi C, Yamazawa M, Nomura K et al. (2004) Maxillofacial fractures sustained during sports played with a ball. Oral Surg Oral Med Oral Pathol Oral Radiol Endod 97(1):23–27

Emshoff R, Schoning H, Rothler G et al. (1997) Trends in the incidence and cause of sport-related mandibular fractures: a retrospective analysis. J Oral Maxillofac Surg 55(6):585–592

Flanders RA, Bhat M (1995) The incidence of orofacial injuries in sports: a pilot study in Illinois. J Am Dent Assoc 126(4):491–496

Frenguelli A, Ruscito P, Bicciolo G et al. (1991) Head and neck trauma in sporting activities. Review of 208 cases. J Craniomaxillofac Surg 19(4):178–181

Gassner R, Hackl W, Tuli T et al. (1999a) Facial injuries in skiing. A retrospective study of 549 cases. Sports Med 27(2):127–134

Gassner R, Tuli T, Emshoff R et al. (1999b) Mountainbiking – a dangerous sport: comparison with bicycling on oral and maxillofacial trauma. Int J Oral Maxillofac Surg 28(3):188–191

Gassner R, Tuli T, Hachl O et al. (2004) Craniomaxillofacial trauma in children: a review of 3,385 cases with 6,060 injuries in 10 years. J Oral Maxillofac Surg 62(4):399–407

Greenberg AM, Haug RH (2005) Craniofacial injuries. In: Scuderi GR, McCann PD (eds) Sports medicine: a comprehensive approach, 2nd edn. Mosby, Philadelphia, pp 132–151

Hill CM, Burford K, Martin A et al. (1998) A one-year review of maxillofacial sports injuries treated at an accident and emergency department. Br J Oral Maxillofac Surg 36(1):44–47

Iida S, Matsuya T (2002) Paediatric maxillofacial fractures: their aetiological characters and fracture patterns. J Craniomaxillofac Surg 30(4):237–241

Jones NP (1994) Orbital blowout fractures in sport. Br J Sports Med 28(4):272–275

Kurtz MD, Camp JH, Andreasen JO (2005) Dental injuries. In: Scuderi GR, McCann PD (eds) Sports medicine: a comprehensive approach, 2nd edn. Mosby, Philadelphia, pp 152–178

Lim LH, Moore MH, Trott JA et al. (1993) Sports-related facial fractures: a review of 137 patients. Aust N Z J Surg 63(10):784–789

Maladiere E, Bado F, Meningaud JP et al. (2001) Aetiology and incidence of facial fractures sustained during sports: a prospective study of 140 patients. Int J Oral Maxillofac Surg 30(4):291–295

Mourouzis C, Koumoura F (2005) Sports-related maxillofacial fractures: a retrospective study of 125 patients. Int J Oral Maxillofac Surg 34(6):635–638

Raghoebar GM, Bos RR, Vissink A (2005) Sports and orofacial injuries. Ned Tijdschr Tandheelkd 112(4):141–146

Reuben AD, Watt-Smith SR, Dobson D et al. (2005) A comparative study of evaluation of radiographs, CT and 3D reformatted CT in facial trauma: what is the role of 3D? Br J Radiol 78(927):198–201

Rhea JT, Novelline RA (2005) How to simplify the CT diagnosis of Le Fort fractures. AJR Am J Roentgenol 184(5):1700–1705

Sane J (1988) Comparison of maxillofacial and dental injuries in four contact team sports: American football, bandy, basketball, and handball. Am J Sports Med 16(6):647–651

Schuknecht B, Graetz K (2005) Radiologic assessment of maxillofacial, mandibular, and skull base trauma. Eur Radiol 15(3):560–568

Som PM, Brandwein MS (2003) Facial fractures and postoperative findings. In: Som PM, Curtin HD (eds) Head and neck imaging, 4th edn. Mosby, St. Louis, pp 374–438

Tanaka N, Hayashi S, Amagasa T et al. (1996) Maxillofacial fractures sustained during sports. J Oral Maxillofac Surg 54(6):715–719

Tuli T, Hachl O, Hohlrieder M et al. (2002) Dentofacial trauma in sport accidents. Gen Dent 50(3):274–279

Turner BG, Rhea JT, Thrall JH et al. (2004) Trends in the use of CT and radiography in the evaluation of facial trauma, 1992–2002: implications for current costs. AJR Am J Roentgenol 183(3):751–754

Ueeck BA, Dierks EJ, Homer LD et al. (2004) Patterns of maxillofacial injuries related to interaction with horses. J Oral Maxillofac Surg 62(6):693–696

White S, Pharoah M (2000) Trauma to teeth and facial structures. In: White S, Pharoah M (eds) Oral radiology: principles and interpretation, 4th edn. Mosby, St. Louis, pp 566–587

Thoracic and Abdominal Wall Injuries in Sports

25

Jan L. Gielen, Filip M. Vanhoenacker, and Pieter Van Dyck

CONTENTS

25.1 Introduction

Specific imaging literature on abdominal and thoracic wall injuries is relatively uncommon compared to the overall incidence in sports medicine. This is because the clinical diagnosis is usually straightforward and imaging is only needed to exclude anatomical variants (scapulothoracic crepitus) and concomitant lesions (rib fractures, handle bar trauma of the abdomen). However, radiological grading and follow up of musculo-tendinous unit (MTU) strains may be significant in athletes. Moreover, radiological diagnosis is relevant in specific circumstances. Rectus abdominis sheath haematoma has to be excluded in cases of muscular strain as it does not self-tamponade. Clinical diagnosis of groin lesions is difficult and therefore radiological procedures may be of additional help in the diagnosis of sports hernia and groin disruption.

A thorough knowledge of the anatomy and biomechanics of the thoracic and abdominal wall is a prerequisite for understanding the pathological conditions of this area. The anatomy and biomechanics of the thoracic and abdominal wall is summarized in Figure 25.1 and Tables 25.1 and 25.2, respectively.

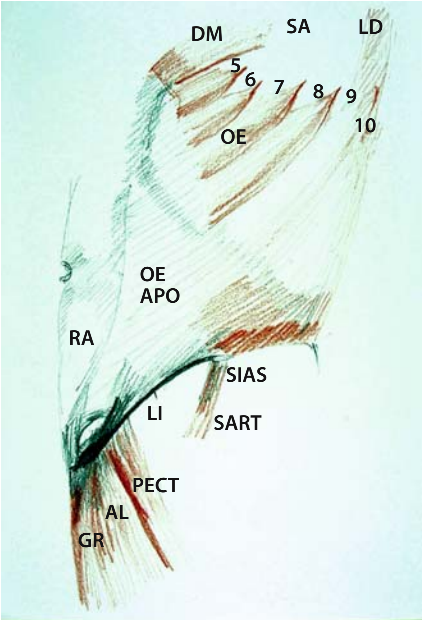

Fig. 25.1. Superficial muscles of the groin and abdominal wall: *AL*, adductor longus muscle; *GR*, gracilis muscle; *LI*, ligamentum inguinale; *LD*, lattisimus dorsi; *OE*, obliquus externus abdominis muscle; *APO*, aponeurosis, external inguinal ring; *PECT*, pectineus muscle; *PM*, pectoralis major; *RA*, rectus abdominis muscle; *SART*, sartorius muscle; *SIAS*, spina iliaca anterior superior

J. L. Gielen, MD, PhD
Associate Professor, Department of Radiology, University Hospital Antwerp, Wilrijkstraat 10, 2650 Edegem, Belgium
F. M. Vanhoenacker, MD, PhD
P. Van Dyck, MD
Department of Radiology, University Hospital Antwerp, Wilrijkstraat, 10, 2650 Edegem, Belgium

Box 25.1. Radiographs

- Chest series and rib series – sufficient in majority of cases of rib injury, exclude pneumothorax, visceral laceration

Box 25.2. Scintigraphy

- Sensitive but non-specific in chronic osseous stress of the ribs

Box 25.3. Ultrasound

- Detection of occult rib fracture and chondral injury
- Acute muscle strain – accurate, fast and dynamic. Particularly useful in grading. Can be negative in grade 1 injury
- Probably useful in the detection of sports hernia
- Evaluation of abdominal wall injury and (rectus sheath) haematoma
- Endofibrosis of the iliac arteries: greyscale and power Doppler demonstrate tapering – Doppler only useful after exercise

Box 25.4. MRI

- Chronic groin disruption and sports hernia – probably useful in defining subtle atrophic changes and "osteitis"
- Accurate and useful in athletes with large muscle bulk

Box 25.5. CT

- Handlebar injury – evaluation of visceral injury

Box 25.6. Angiography, MR angiography, CT angiography

- Endofibrosis– specific diagnosis

25.2 Rib Cage and Thoracic Wall

Rib and sternum injuries are relatively rare in athletes. Rib fractures can be divided into two main categories: traumatic fractures and stress fractures.

25.2.1 Rib Fractures and Chondral Lesions

Rib fractures are the most common injury of the chest wall. Mostly, they occur at the middle and lower ribs with blunt trauma. Lateral rib fracture or injury to the costochondral junction is caused by a direct force to a small area most often coming from an anterior direction. Compression of the entire thorax results in fractures of multiple ribs.

Fractures of the first four ribs or the last two ribs, multiple fractures and flail segments have a less benign cause than other rib fractures, as they may result in injury to surrounding structures. In lower left or right rib fractures associated splenic or hepatic trauma is reported in up to 20% and 10%, respectively. Ultrasound is an excellent tool to detect occult fracture. The term "Flail chest" is used if three or more ribs are fractured in two or more locations provoking paradoxical motion during respiration.

Rib fractures also may be caused by violent muscle contractions. First rib and floating rib fractures are uniquely athletic fractures; caused by a sudden vigorous contraction in different directions of pull (Miles and Barret 1991; Coris and Higgins 2005). Fractures of the first rib have been reported in basketball players.

Fracture diagnosis is generally straightforward on standard radiographs (chest series and rib series). The differential diagnosis includes severe rib contusion, costochondral separations, muscle strains and pneumothorax. The focal pain area points to the fracture site (Fig. 25.2).

Furthermore, chondral lesions and costochondral separations may be dynamically examined with ultrasound (Fig. 25.2). By using ultrasonographic palpation to detect the pain at the region of interest (ROI) the accuracy of the technique is improved. Examination of the painful ROI is performed during inspiration, expiration and pain provoking manipulations. A short video sequence can be used to capture the intermittent step off at a costochondral separation or the snapping movement at the region of interchondral friction.

Table 25.1. Relevant anatomy of the thoracic and abdominal wall

Muscle	Origin	Insertion	Comment
M. obliquus externus abdominis	Eight lower ribs (cartilages)	Outer lip of iliac crest Anterior superior crystal iliaca Aponeurosis -Symphysis pubis -Inguinal ligament	Interdigitate with serratus anterior Outer layer of abdominal wall
M. obliquus internus abdominis	Lateral two-third of inguinal ligament Anterior two-third of the crista iliaca Thoracolumbar fascia	Lower three or four ribs Rectus abdominis Linea alba	Middle layer of abdominal wall
M. transversus abdominis	Lateral third of inguinal ligament Anterior two-third of the crista iliaca Twelfth rib Lower six costal cartilages	Aponeurosis toward obliquus internus abdominis Crista and pecten ossis pubis (conjoined tendon)	Innermost layer of abdominal wall
M. rectus abdominis	Crista pubis, pecten ossis pubis Front of pubis	Fifth through seventh costal cartilages	Interconnection: linea alba Intersected with tendinous intersections
M. latissimus dorsi	Spina vertebra Th 6-12 Thoracolumbar fascia -spinae vertebra L1-L6 -spinae vertebra sacrum Crista iliaca posterior lip Three or four lower ribs	Sulcus intertubercularis of humerus (common insertion with teres major tendon)	
M. serratus anterior	Upper eight or nine (ten) ribs	Medial border of the scapula	Frequent variations at the origin

Table 25.2. Biomechanics of the thoracoabdominal wall

Muscle	Bilateral actions	Unilateral actions	Strains
Iliopsoas muscle	Forward bending of trunk	Hip flexion	Resisted hip flexion Soccer
Obliquus externus abdominis	Aids in expiration Forward bending of trunk	Contra-lateral bending	Twisting motions Tennis, football, hockey Groin disruption
Obliquus internus abdominis	Retains abdominal viscera in position Bending trunk forward	Ipsilateral bending	Twisting motions Tennis Groin disruption
Transversus abdominis	Retains abdominal viscera in position		
Rectus abdominis	Retain abdominal viscera in position Forward bending of trunk		Groin disruption
Serratus anterior		Pulls scapula anterior, reaching and pushing movements	Swimming, baseball pitcher (rare)
Latissimus dorsi	Violent expiratory movements (coughing, sneezing)	Adduction, extension, medial rotation of the ipsilateral humerus	Throwing sports (rare)

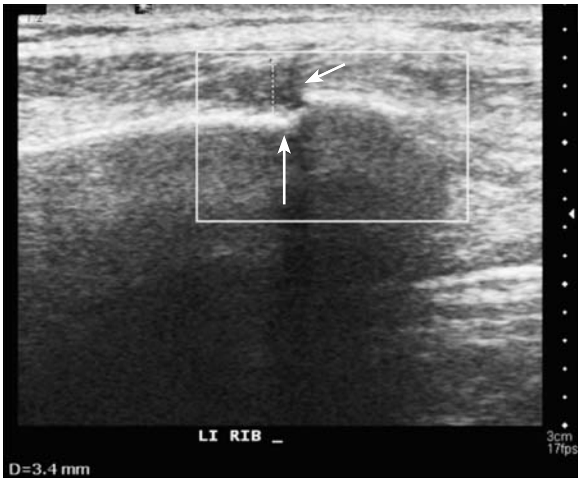

Fig. 25.2. Rib fracture in a male patient with local pain at the anterior part of the left second rib. Chest and rib radiographs show no rib abnormality. Ultrasound examination and palpation along the long axis of the rib. Cortical interruption at the point of tenderness with discrete step off (*arrow*) and small haematoma (*arrowhead*)

25.2.2 Stress Fractures of the Ribs

Stress fractures of the rib have been reported in throwing, golf, rowing, canoeing, and swimming (Iwamoto and Takeda 2003) and occasionally in soccer (Matsumoto et al. 2003), kickboxing (Sakellaridis et al. 2004) and baseball players (Curran and Kelly 1966; Gurtler et al. 1985). In soccer, fractures are located at the first rib, whereas the lower ribs are involved in golfers and rowers. Fractures at the antero- to posterolateral aspects of ribs 5 through 9 were most often associated with long-distance training and heavy load per stroke. Clinically, patients present with difficulty in abducting the arm (Gaffney 1997). A mechanism involving pull of the serratus anterior and external oblique muscles on the rib has been proposed as the cause of repetitive bending of the rib, leading to stress fracture. A modified technique using less reach, pull-through, and layback should decrease the forces transmitted to the rib by these muscles, and decrease the risk for stress fractures (Karlson 1998).

Avulsion fractures of the floating ribs may also result from the opposing pulls of the latissimus dorsi, the internal obliques, and the serratus posterior inferior muscles (Tullos et al. 1972). Diagnosis is confidently made by bone scintigraphy.

25.2.3 Injuries to the Sternum

Injuries of the sternum in athletes are rare. Most sternal injuries occur in automobile racing. Fowler 1957 reported three mechanisms of trauma: direct, indirect and muscular. Direct injuries occur when a helmet, steering wheel or elbow (basketball players) strikes the sternum directly producing an inward displacement of the lower portion of the sternum. Indirect injury results from flexion compression injury of the cervicothoracic spine leading to posterior displacement of the cranial part of the sternum with manubriosternal dislocation due to direct strike of the chin to the manubrium. This has been reported in a football player.

Barbaix (1996) and Keating (1987) reported stress fractures of the sternum in a golfer and a wrestler, respectively.

25.2.4 Injuries to the Pectoralis Major

Pectoralis major injuries are rare, typically occurring in active individuals participating in manual labour or sports. Diagnosis can usually be made based on a patient's history and physical examination. However, ultrasound and magnetic resonance imaging are helpful for diagnosis and pre-operative planning. Specific treatment options should be based on the severity of the injury and the patient's individual needs. In recent studies, operative repair of pectoralis major rupture has been shown to restore normal chest-wall muscle contours and pre-operative strength (even in competitive athletes) (Dodds and Wolfe 2002; Neitzschman and Wilson 1999).

25.2.5 Scapulothoracic Crepitus and Bursitis

Symptomatic scapulothoracic crepitus is also known as the snapping scapula, the washboard syndrome or the scapulothoracic syndrome. This is due to repetitive friction of the scapula against the thoracic wall. A gentle friction (*froissement)* was described as physiologic but grating (*frottement)* and loud snapping (*craquement)* is definitively pathologic. Symptomatic scapulothoracic bursitis affects the superomedial and the inferior angle of the scapula. Predisposing anatomic conditions include osteochondroma or malunion of rib of scapula, hooked superomedial angle

of the scapula. A common cause of scapulothoracic crepitus in athletes involves abnormalities in congruence of the scapulothoracic articulation (i.e. scoliosis and thoracic kyphosis) (Hellstrom et al. 1990; Wojtys et al. 2000). In scapula infra coracoid dyskinesis syndrome – frequently seen in throwing athletes – the scapula assumes a protracted and depressed position, with the inferior angle deviating laterally and leading to scapulothoracic crepitus (Kuhn 2003). Athletes who participate in sports that require repetitive overhead activity are also commonly affected. Repetitive motion may irritate soft tissues until a chronic inflamed adventitious bursitis and inflammation develops. The bursa then undergoes scarring and fibrosis, with crepitus and pain to follow. MRI will occasionally demonstrate increased signal and even fluid collections in an inflamed bursa on T2-weighted MR images. This finding is highly specific for bursitis, but in case of fibrosis, there may be absence of high signal changes. Ultrasound may detect these fibrotic adventitious bursae by revealing a volume increase in comparison with the normal side (Fig. 25.3) (Huang et al. 2005). Radiographs with tangential views of the lateral scapula, computed tomography (CT), or magnetic resonance imaging (MRI) may be helpful in identifying predisposing anatomic disease.

25.3 Abdominal Wall

25.3.1 Introduction

Sports injuries to the hip and groin region have been noted in 5%–9% of high school athletes (Morelli

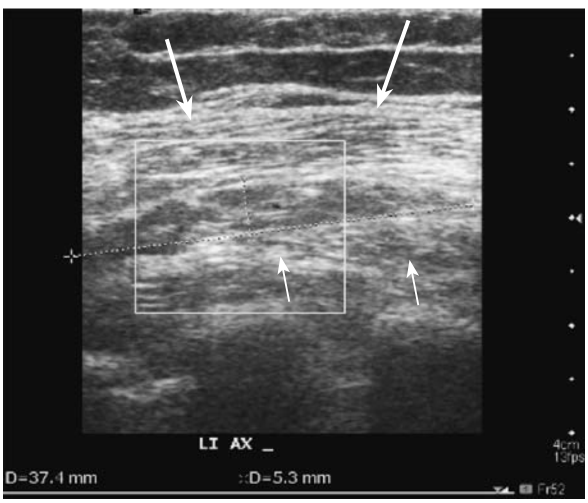

a

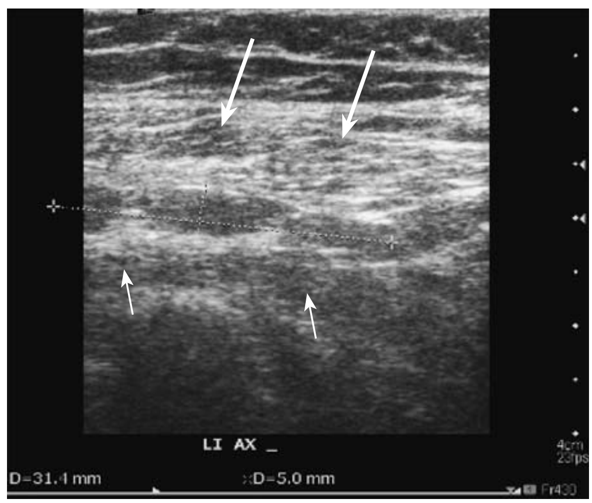

b

c

Fig. 25.3a–c. Scapulothoracic crepitus in a 25-year-old female with pain and snapping during left shoulder abduction-elevation at the level of the angulus inferior of the scapula. Patient with hyperkyphosis of the thoracic spine. Ultrasound axial (**a**) and sagittal (**b**, cranial, *left*) imaging plane at the painful region of the latero-inferior margin of the left and right scapula respectively. Thickening of the tissue in between m. serratus anterior (*arrows*), m. latissimus dorsi (*small arrows*) and adjacent to the angulus inferior of the scapula at the left side. Aspect of adventitious bursa with non-homogeneous low reflective tissue, that is slightly compressible and demonstrates no vascularization on power Doppler technique. Comparison with right side (**c**), asymmetry with smaller volume of the interposed tissue. Within 4 weeks after ultrasound guided loco-regional corticosteroid infiltration, there is gradual reduction of pain and snapping

and Weaver 2005). These injuries occur most commonly in athletes participating in sports involving side-to-side cutting, quick accelerations and decelerations, and sudden directional changes.

Injuries about the abdominal wall fall into three basic categories: abdominal wall muscle and tendon injuries, acute and chronic groin disruption, and nerve compression injuries. The muscle groups that are susceptible to strain injury are the internal and external obliques, the rectus abdominis, adductor and obturator muscle groups, gracilis, pectineus, rectus femoris and the iliopsoas. This chapter will focus on trauma of the abdominal wall and iliopsoas and groin disruption. The other groin lesions are studied in Chap. 15.

25.3.2 Abdominal Wall Muscle Strains

Most commonly, there is a typical history of a sudden violent contraction of the muscle against resistance with the muscle maximally stretched. Nearly all muscle strains occur just adjacent to the musculotendinous junction (Garret et al. 1993). In the abdominal region most muscles have short tendons or muscular origins and insertions, and therefore muscle strain is often found near its origin or insertion (except for rectus abdominis).

Injury to the oblique muscles of the abdomen will occur during twisting motions of the trunk. Lacroix et al. 1998 reported on operative findings of varying degrees of tearing of the external oblique aponeurosis and external oblique muscle associated with ilioinguinal nerve entrapment in 11 elite ice hockey players. In this study, preoperative physical examination and imaging findings (scintigraphy, US, CT, MRI), the preoperative findings were consistently negative. Despite the lack of specific literature on the subject, it is our personal experience that state of the art ultrasound and MR imaging techniques are valuable methods for diagnosis, grading and follow up of abdominal muscle strains.

25.3.2.1 Side Strain and Hip Pointer

Side strain tears are rarely a diagnostic dilemma for clinicians. The study by Connell et al. (2003) showed that side strain is caused by an acute tear of the internal oblique musculature where it originates on the under surface of the 9th, 10th, or, most commonly, the 11th rib or costal cartilages. Movements associated with bowling (cricket), rowing, swimming, and golf cause lengthening of the muscle, and superimposed eccentric contraction, making it vulnerable to rupture. MRI can depict the site of a muscle tear, characterize the severity of injury, and monitor healing. Sagittal oblique muscle images are most useful for assessing the degree of muscle injury (Fig. 25.4). Stripping of the periosteum occurs as the muscular attachment is avulsed from the osseous or cartilaginous origin. This may result in excessive haemorrhage even though the muscle tear may be of low grade. The presence of a haematoma often aids in the identification of the site of muscle injury. The MR signal characteristics of haemorrhage varies with different sequences and is time dependent. Follow-up MRI may be useful for monitoring healing and scar formation in patients who fail to respond to treatment.

Sometimes fibres inserting on the anterior portion of the iliac crest may be disrupted, resulting in a so-called hip pointer. Patients present with local tenderness along the injured muscle and iliac crest. Pain is aggravated by passive stretching of the muscles due to contra-lateral bending and activation of the muscle by twisting and flexing the abdomen.

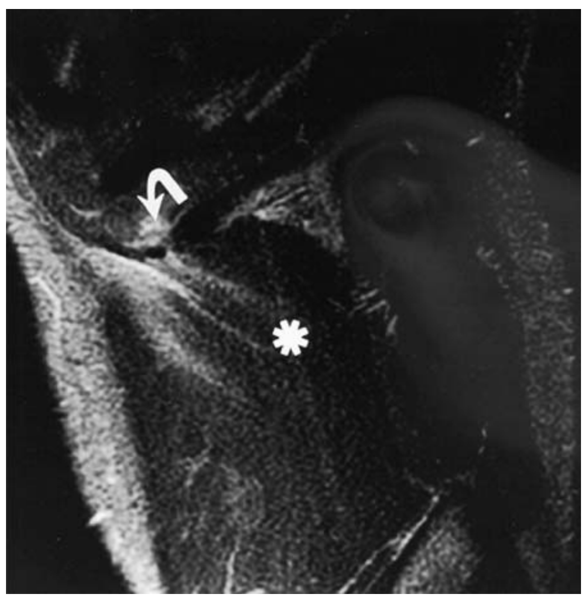

Fig. 25.4. Side strain in a 23-year-old male javelin thrower with point tenderness and pain during competition. Sagittal oblique STIR MR image (5300/38; inversion time, 120 ms) shows high signal at the origin a m obliquus internus at the under surface of tenth rib (*arrow*). Haematoma tracks along muscle fibres of m obliquus internus abdominis (*asterisk*). [Reprinted with permission from Conell et al. (2003)]

25.3.2.2
Rectus Abdominis Lesions

Similar problems result from strain of the rectus abdominus muscle. This paragraph discusses the strains of the rectus abdominis muscle located at different levels near its tendinous intersections. The lesions at the insertion are discussed in the paragraphs on acute groin disruption and sports hernia. It is, however, not uncommon to have injury to several muscle groups of the abdomen at the same time.

Johnson (2006) acknowledges the importance of rectus sheath haematoma in cases of muscular tear or contusion from damage of the superior or inferior epigastric arteries or their branches. Rectus sheath haematoma is not always self limiting and can cause hypovolemic shock with associated mortality. Ultrasound is a very valuable tool for evaluation of the possible haematoma.

25.3.2.3
Iliopsoas Injury

Iliopsoas injuries occur during forceful resisted hip flexion. Clinically, the athlete will feel a sharp pain in the groin region that may radiate into the lower abdomen. Passive external rotation and hip extension and resisted hip flexion will be painful. In adolescents, an avulsion fracture of the lesser tuberosity may occur, whereas adults will present with an injury to the musculotendinous junction. Therefore radiographs are sufficient for diagnosis in adolescents, whereas in adults, MRI is needed for a reliable diagnosis (Shin et al. 1996).

25.3.2.4
Acute Groin Disruption

Literature on acute groin disruption does not exist. Our personal experience includes two cases of acute groin disruption that occurred in skiing (alpine skiing and water-skiing with right and left lesions, respectively). The patients experienced hyperextension of the spine-abdomen and abduction-extension of the hip while making a slip and fall. Both patients were diagnosed on ultrasound and MRI (Fig. 25.5). In both patients ipsilateral strain with edema was found at the external oblique aponeurosis, rectus abdominis conjoined tendon and inguinal ligament with haematoma and strain grade 2 or 3 at the origin of the gracilis, adductor longus and pectineus and dehiscence of these structures at the pubis. There is no interruption of the superficial muscle fascia that covers the inferior abdominal wall musculature and the adductor region. This finding favours the common adductor origin or CAO concept (see Chap. 15 for more in-depth discussion) and confirms the hypothetic mechanism of injury with the pubic bone as pivot point. A similar pivot shift mechanism may be found in chronic groin overuse.

25.3.2.5
Chronic Groin Disruption (Sports Hernia)

Sports hernia refers to a condition of chronic groin pain caused by a weakness of the posterior inguinal wall *without* a clinically obvious hernia (Taylor et al. 1991). Westin 1997; Renstroem 1997 and Renstrom 1992 believe that sports hernias may be the most common cause of chronic groin pain in athletes. By definition, none of the patients have evidence of a preoperative hernia, although some patients are found to have occult hernias at the time of surgery (Fishman and Zybert 1992). Because of the insidious onset and non-specific nature of the symptoms, there is often a prolonged course before diagnosis. In one study, the average duration of symptoms was 20 months, with a range of 6 weeks to 5 years (Hackney 1993).

Our findings in acute groin disruption suggest that sports hernia is only part of a spectrum of lesions described as groin disruption. The term groin disruption was first coined in 1980 when three professional soccer players with chronic, apparently career-ending groin pain, underwent surgical exploration and repair and were then able to return to competitive sport. The posterior wall abnormalities found in groin disruption are more varied than those associated with sports hernias. They may include tears of the external oblique aponeurosis, tears of the conjoined tendon or dehiscence of the conjoined and inguinal ligament, again without any evidence of a *true* hernia (Meyers et al. 2000a,b; Gilmore 1998). Clinical complaints of loose feeling of the inguinal floor are common. There is also groin pain on exertion but uncommon with Valsalva's manoeuvre, coughing and sneezing.

25.3.2.5.1
Mechanism of Injury in Chronic Groin Disruption and Sports Hernia

Most patients describe a hyper extension injury in association with hyper abduction of the thigh. The pivot point seems to be the anterior pelvis and pubic symphysis. The location of pain suggests that the injury involves both the rectus abdominis and adduc-

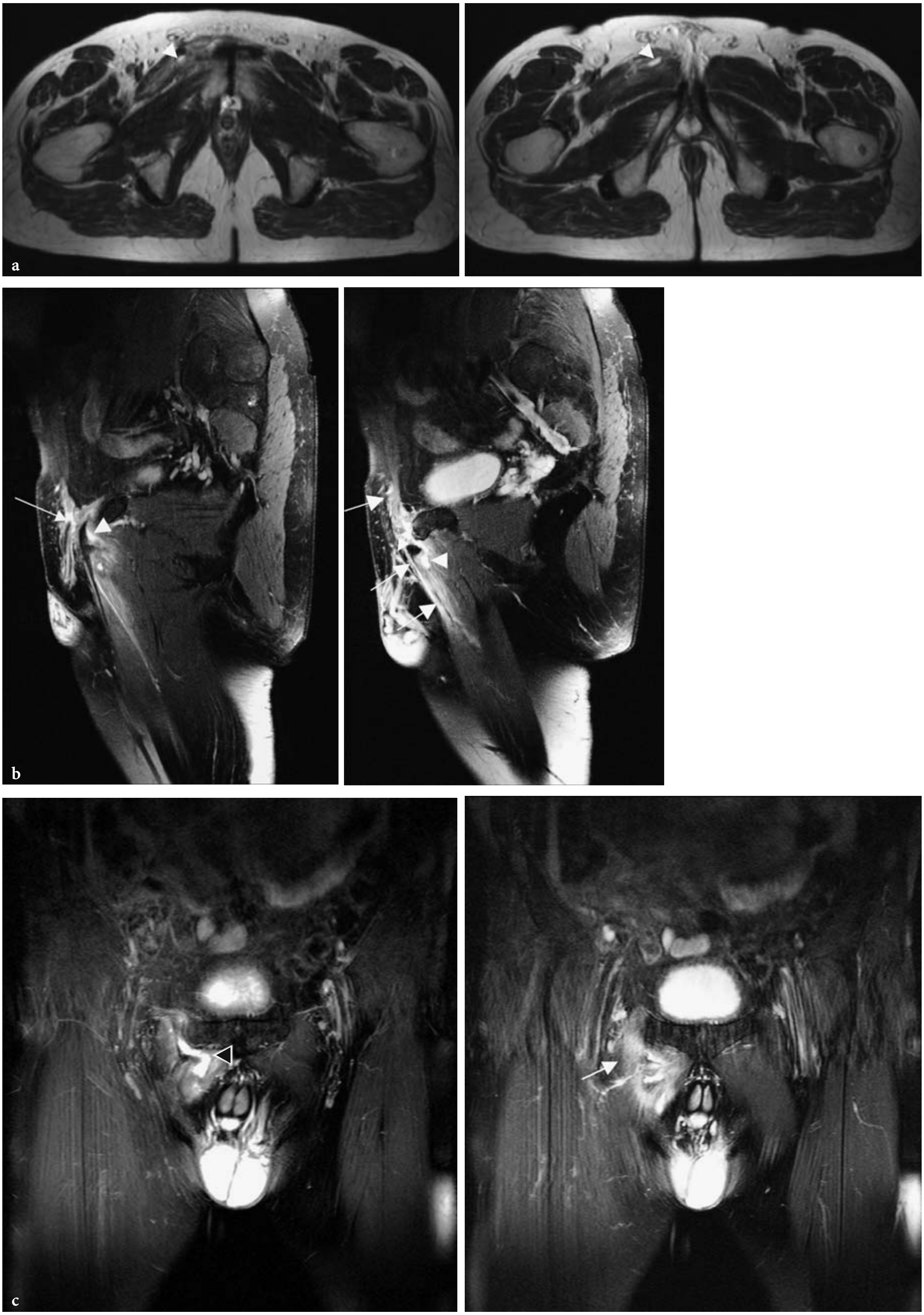
a
b
c

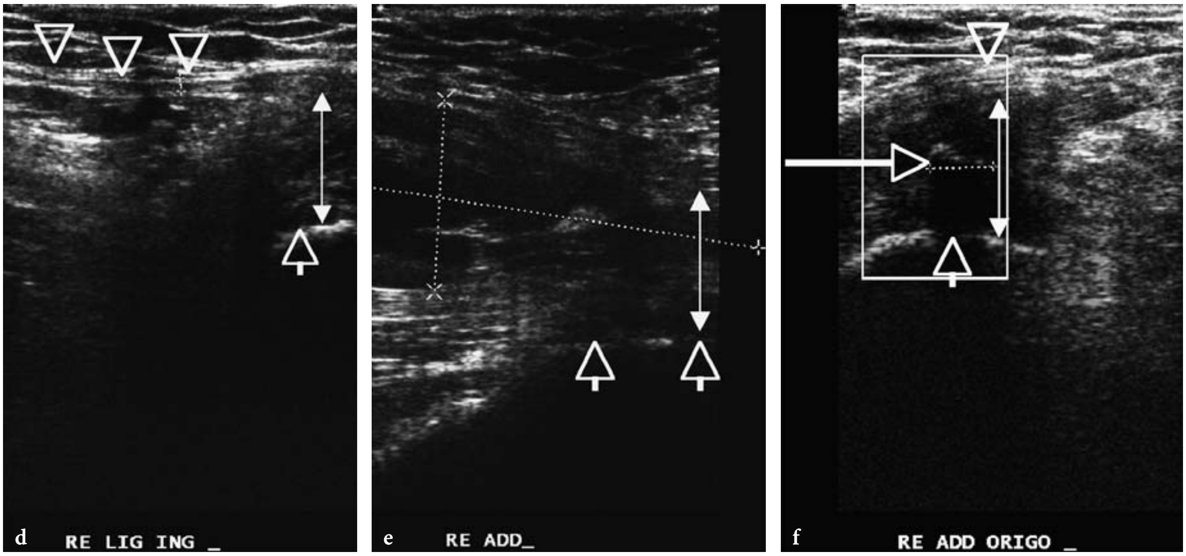

Fig. 25.5a–f. Acute groin disruption in a 49-year-old-male alpine skier after resisted hyper-abduction extension of the right hip and extension of the abdomen. Acute pain and swelling at the right groin. **a** Axial TSE T2-weighted MR image, cranial and caudal part of pubis respectively. **b** Sagittal TSE T2-weighted fat suppressed MR image (intermediary TE), lateral and paramedian through the right pubic bone respectively. **c** Coronal TSE T2-weighted fat suppressed MR image (intermediary TE), anterior and midsection through the pubic bone respectively. High SI haematoma (*arrowheads*) at the right adductor longus, gracilis and rectus abdominis muscle separating the pubic bone and the muscles, surrounded by edema. Note edema at the pectineus origin (*small arrow*), the inguinal canal (*arrow*) the external obliquus muscle aponeurosis (superficial) and the conjoined tendon (deep). Dehiscence of the rectus abdominis, adductor tendon complex and inguinal ligament-conjoined tendon-obliquus externus abdominis aponeurosis from the pubic bone is obvious through widening of the distance between the tendon and the bone with interposition of high SI haematoma and edema (*double-sided arrow*). Continuity of the rectus abdominis and adductor longus in front of the pubic bone at the level of the dehiscence (*large arrows*). **d** Oblique axial ultrasound view along the axis of the ligamentum inguinale up to the pubic bone. **e** Sagittal ultrasound view at the level of the m. rectus abdominis up to the pubic bone. **f** Sagittal ultrasound view at the level of the pubic bone at the adductor origin. Dehiscence of the ligamentum inguinale (*arrowheads*), adductor complex from the pubic bone (*small arrow*) with small avulsion fracture fragment (*large arrow*). Dehiscence distance (*double sided arrow*). Thickening of the m. rectus abdominis with non-homogeneous reflectivity and disruption of its layered architecture at the distal musculotendinous junction (region within *dotted crossing lines*)

tor longus muscles and the inguinal canal near the insertion of the rectus muscle on the pubis (Williams and Foster 1995). The location of the pain during further progression of the process in these athletes suggests a redistribution of forces around the pivot apparatus and a subsequent involvement of obliquus externus abdominis, ligamentum inguinale, gracilis, adductor brevis, perineal regions, and eventually the opposite side during extremes of exercise (Ingoldby 1997; Meyers et al. 2000a,b). These ligaments and tendons not only insert or originate on the pubic bone but there may also be anatomical continuity of infra- and suprapubic tendons and ligaments in front of the pubic bone explaining simultaneous supra- and infrapubic involvement. (Figs. 25.6 and 25.9e) This particular anatomical continuity with involvement of supra- and infrapubic structures is demonstrated in two patients involved in ski traumas with acute groin disruption (Fig. 25.5). Bilateral involvement is also explained by anatomical continuity of left and right sided structures in front of the pubic bone.

25.3.2.5.2 Clinical Presentation

Athletes with a sports hernia will typically complain of an insidious onset of gradually worsening groin pain that he or she may attribute to repeated adductor strain. However, this pain is felt "deeper", slightly more proximal, and may be more intense. Kicking tends to increase the symptoms, as will endurance running. The pain tends to be diffuse with radiation along the inguinal ligament, the perineum, the rectus muscles, adductor muscles, and sometimes to the opposite side. Testicular pain is a component in about 30% of male cases. A history of increased pain during manoeuvres that cause increased intraabdominal pressure such as coughing, sneezing, or during bowel movements can assist in the diagnosis (Lynch 2000; Morelli 2001).

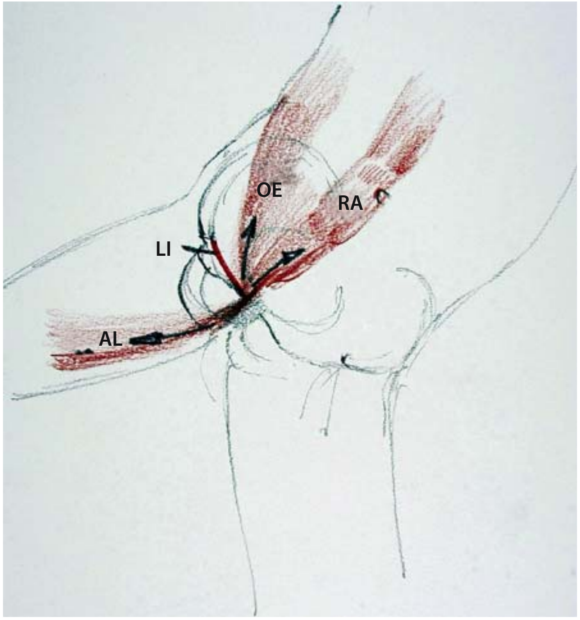

Fig. 25.6. Mechanism of injury in sports hernia and groin disruption, supra and infrapubic tendon complex of the conjoined tendon (m. rectus abdominis, m obliquus externus, internus abdominis, ligamentum inguinale) and mm. adductor longus, gracilis, respectively. Continuity of tendon and superficial muscle fascia (epimysium) of the muscles above and below the pubic bone. The pubic bone acts as central point of attachment and pivot point in hip extension-abduction and abdomino-lumbar extension. Detachment and strain of these structures in resisted extension-abduction. *AL*, adductor longus muscle; *OE*, external oblique muscle; *LI*, ligamentum inguinale; *RA*, rectus abdominis muscle

25.3.2.5.3
Physical Examination

The most specific physical findings are tenderness and enlargement of the external ring of the inguinal canal and tenderness of the posterior wall of the inguinal canal. Sometimes a bulge can be felt with increased intra-abdominal pressure from coughing. Pain will be exacerbated during coughing.

25.3.2.5.4
Imaging of Chronic Groin Disruption and Sports Hernia

In case of obvious clinical signs and symptoms, the diagnosis of a hernia is straightforward. Unfortunately, this is usually not the case for sports hernias. In these athletes with continued groin pain, despite adequate rest and no obvious hernia, herniography may be of great value. Smedberg et al. (1990) have shown that herniography is accurate in disclosing nonpalpable hernias (Figs. 25.7 and 25.8). Herniography is performed by injecting contrast medium under fluoroscopic control into the peritoneal cavity under local anaesthesia (Smedberg et al. 1985). After injection of the dye, the patient should be placed in the reverse Trendelenburg position to allow pooling of contrast in the inferior peritoneal cavity along the inguinal canal. The athlete is the asked to perform a Valsalva manoeuvre. Radiographs of the lower pelvis are performed in this position to detect bulging through the canal and into the scrotum. Few complications have been reported with herniography (Ekberg 1983). Puncture of the intestine with the small needle can occur, but as long as no aspiration occurs at that time, further problems are rare. Peritonitis from contact with the contrast medium has been reported, but this is uncommon with the new water-soluble contrasts. Herniography is contra-indicated in patients with incarcerated hernias, and a history of previous abdominal surgery or bowel obstruction. Incarcerated or irreducible hernias may give false-negative results because the contrast will be unable to leak through the defect.

Ultrasound is a valuable non-invasive technique to study the inguinal and femoral canal and its contents. It is performed dynamically during rest and valsalva testing as well as in decubitus dorsalis and prone position. If the ultrasonographer is familiar with the specific anatomy of this region, a good discrimination between femoral and inguinal hernia is possible. Also, direct and non-direct inguinal hernia are discriminated.

In our opinion, and also in concordance with the findings of Orchard et al. (1998), sports hernia refers on ultrasound to a condition of bulging at the site of the external inguinal ring through sprain of the posterior inguinal wall at this level. Most often this bulging is only present during valsalva test and is spontaneously reduced at rest. A frank hernia with recognition of a hernia sac is usually not found in sports hernia (Fig. 25.9a–e).

MRI findings may assist the surgeon in decision making, because MRI can often indicate the location of injury. The MRI findings may be a mild relative enlargement of the rectus abdominis fascia and a bulbous enlargement of the external opening of the ipsilateral inguinal canal. Other common MRI findings include asymmetry, distinct edema and irregularity of the rectus abdominis, atrophic changes, small pubic avulsions fractures and edema, or disruption of the pectineus muscle. Albers et al. (2001) used the term primary abdominal musculofascial abnormality (PAMA) to describe the spectrum of abnormalities in groin disruption on MRI. These findings are summarised in Table 25.3. Increased signal within

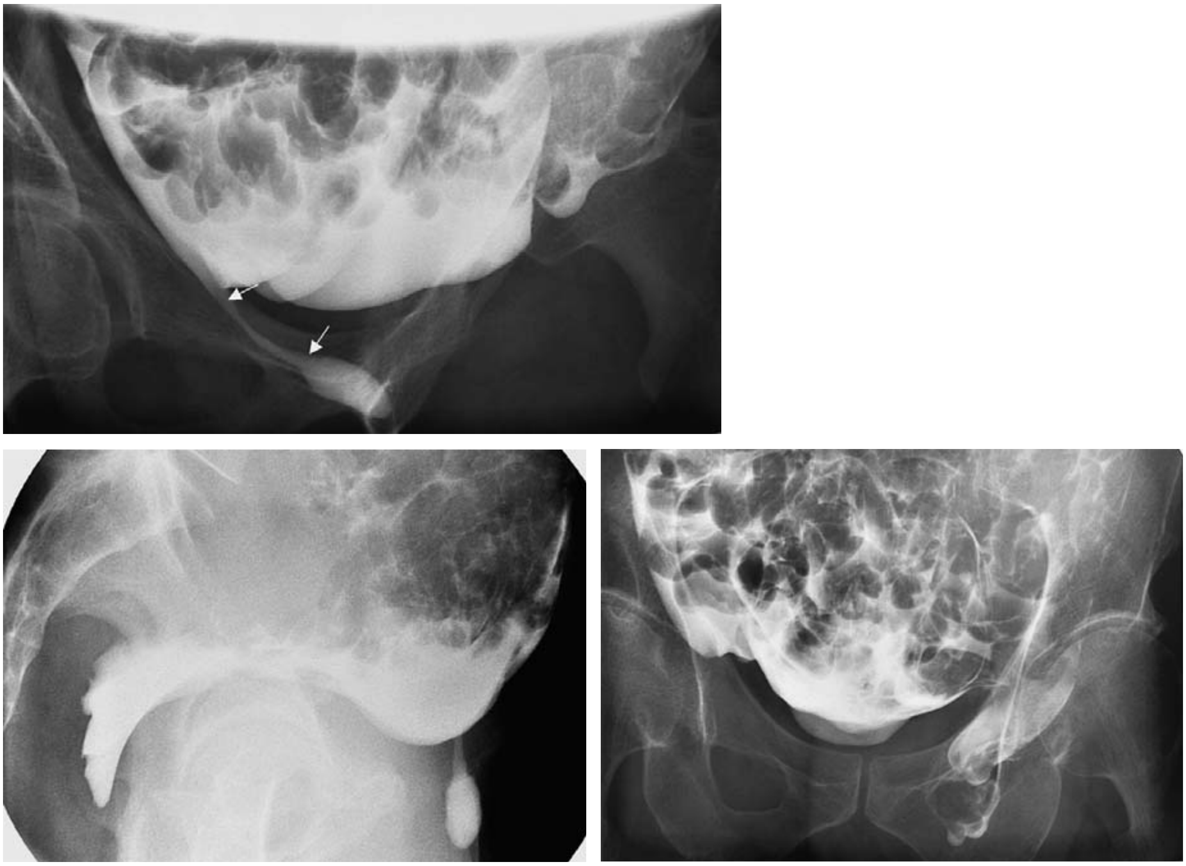

a

b

c

Fig. 25.7a–c. Inguinal hernia in a 45-year-old male. Radiograph of the abdomen after herniography, AP (**a**) and lateral (**b**) view in prone position. Peritoneal contrast is visualized below the lining of the inguinal ligament at the right side without small intestine at the herniation sac: non-occupied inguinal hernia. Narrowing of the herniation sac at the level of the gate that is located at the inguinal canal (*arrows*). **c** A 53-year-old male. Radiograph of the abdomen after herniography, AP view in prone position. Peritoneal contrast is visualized below the lining of the inguinal ligament at the left side with small intestine at the herniation sac: occupied inguinal hernia. (Courtesy of R. Salgado, MD, Department of Radiology, University of Antwerp, Belgium)

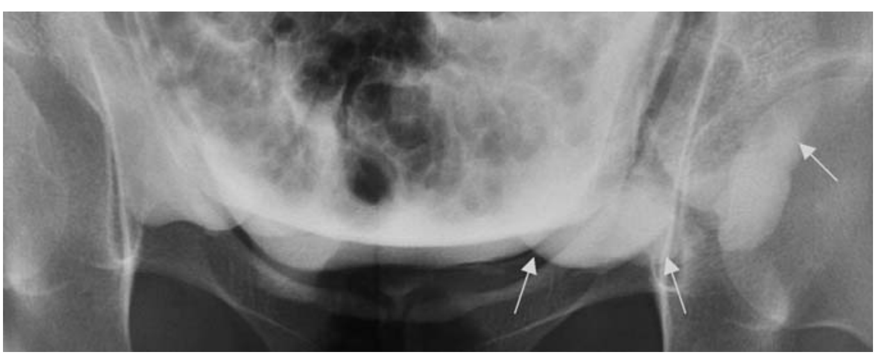

Fig. 25.8. Sports hernia, herniography. Broad based bulging in prone position at the left external inguinal ring. (Courtesy of R. Salgado, MD, Department of Radiology, University of Antwerp, Belgium)

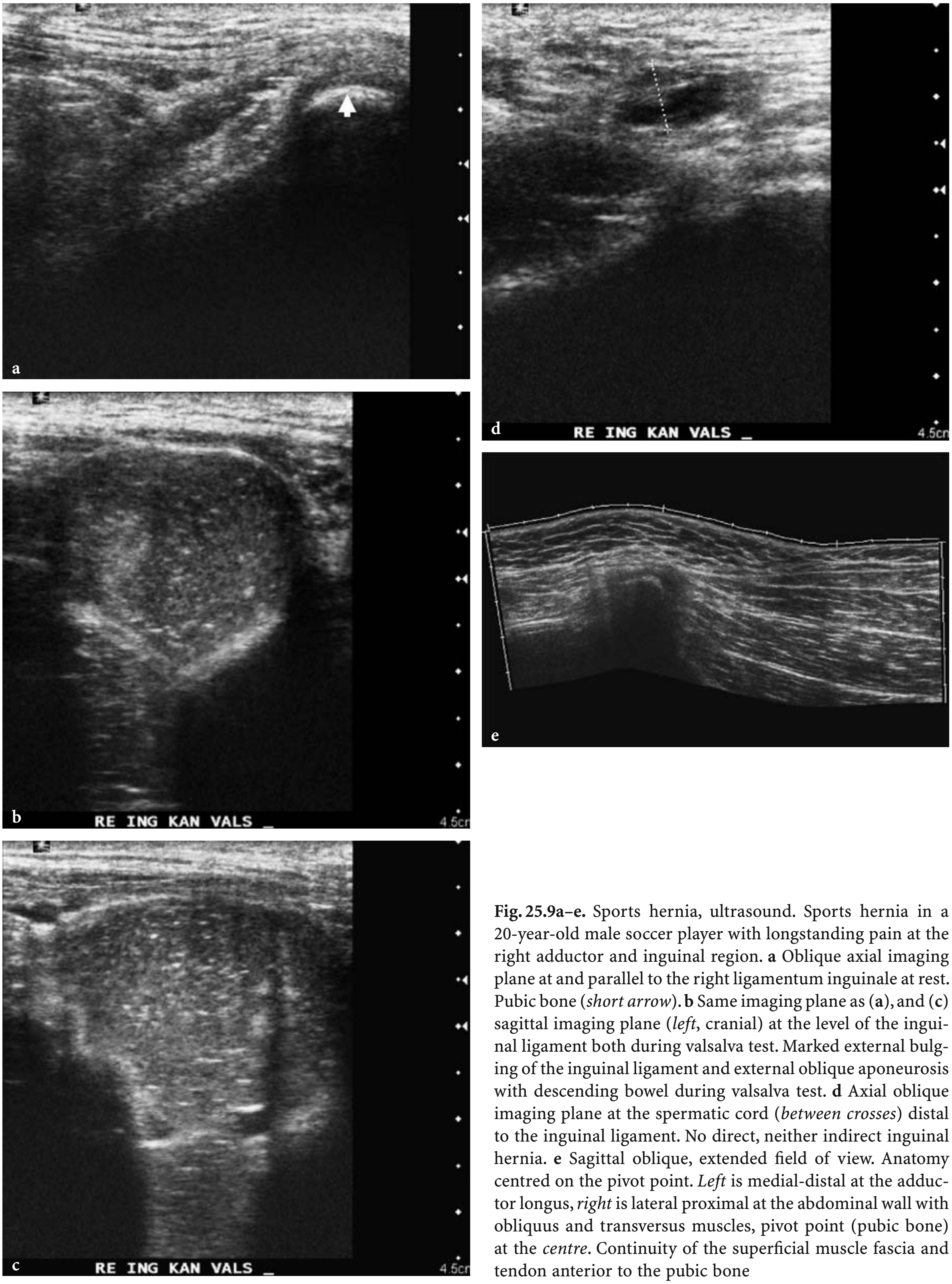

Fig. 25.9a–e. Sports hernia, ultrasound. Sports hernia in a 20-year-old male soccer player with longstanding pain at the right adductor and inguinal region. **a** Oblique axial imaging plane at and parallel to the right ligamentum inguinale at rest. Pubic bone (*short arrow*). **b** Same imaging plane as (**a**), and (**c**) sagittal imaging plane (*left*, cranial) at the level of the inguinal ligament both during valsalva test. Marked external bulging of the inguinal ligament and external oblique aponeurosis with descending bowel during valsalva test. **d** Axial oblique imaging plane at the spermatic cord (*between crosses*) distal to the inguinal ligament. No direct, neither indirect inguinal hernia. **e** Sagittal oblique, extended field of view. Anatomy centred on the pivot point. *Left* is medial-distal at the adductor longus, *right* is lateral proximal at the abdominal wall with obliquus and transversus muscles, pivot point (pubic bone) at the *centre*. Continuity of the superficial muscle fascia and tendon anterior to the pubic bone

Table 25.3. MRI findings in primarily abdominal musculofascial abnormality (PAMA) (Albers et al. 2001). Of 30 surgically confirmed cases, 13 had unilateral and 17 bilateral groin pain. T1-weighted, T2-weighted and STIR MR images in the axial and coronal planes were obtained on a 1.5-T system

Location	Number	MRI abnormality
Pubic bone	21 (70%)	Bone marrow edema, one or both sides
	19	Cortical irregularity
	9 (30%)	Fluid in the symphysis pubis
Rectus abdominis musculotendinous complex	6 (20%)	Edema
Adductor muscles	18 (60%)	Edema
	11 (37%)	Atrophy, size asymmetry or insertional signal increase
Pectineus muscle	6 (20%)	Edema
Abdominal wall musculofascial layer	27 (90%)	Edema
	17 (57%)	Bulge of the musculofascial layers
Abdominal wall conjoined tendon	28 (93%)	Bulging and/or signal increase on T1-weighted MR images

one or more of the groin muscles likely represents edema and/or haemorrhage form sprain, partial or complete tear, or avulsion injury in the acute setting. (see Sect. 25.3.2.4). In the more chronic setting, it likely reflects edema from chronic stress with or without tenosynovitis or tendinopathy. Bone marrow edema signal within pubic bones is never an isolated finding; it should alert the radiologist to search for other musculotendinous and musculofascial abnormalities.

25.3.3 Traumatic Abdominal Wall Injury and Hernia in Children

Handlebar injuries are a significant cause of both blunt abdominal trauma and lacerations to the contact area. The infrequent finding of external bruising in the presence of major organ damage suggests that, although the velocity at impact may be relatively low, the small cross-sectional area of the end of the handlebar is a major factor contributing to organ damage. The high proportion of lacerations observed in this type of trauma result from the sharp metallic end of the handlebar cutting through the soft rubber handle (Clarnette and Beasley 1997). Erez et al. (2001) reported on children who presented with abdominal injuries caused by bicycle handlebars. In 12 of the 76 children, there was an imprint of the handlebar edge on the hypochonder. The most common injuries were isolated ruptures of spleen or liver, traumatic pancreatitis or transsection of the pancreas, renal contusions, duodenal haematoma and bowel perforation. Mesenteric haematoma is relatively uncommon (Chao and Kong 1999). In addition, there may be urethral injuries and lacerations involving the abdominal wall and inguino-scrotal region. CT is most helpful in evaluating children who have sustained blunt abdominal trauma and is usually regarded as the method of choice for diagnosing mesenteric and abdominal wall lesions (Strouse et al. 1999; Mitchiner 1990).

Handlebar hernia is a rare, traumatic, abdominal wall hernia caused by high-velocity direct trauma. There are only 21 reported cases of handlebar hernias (Goliath et al. 2004). It involves disruption of the abdominal wall muscles, with bowel loop herniated through the defect in the abdominal wall, and may have major or even lethal complications. All layers of the abdominal wall may be disrupted by a fall when bicycling, although skin and intra-abdominal organs may be completely intact. Computed tomography demonstrates subcutaneous intestinal loops protruding through the rent (Chen et al. 2005; Holmes et al. 2002; Perez et al. 1998; Linuma et al. 2005).

25.4 Endofibrosis of the Iliac Arteries

Arterial endofibrosis is an arterial disease discovered in the 1980s that is specific to endurance athletes. The location at the external iliac artery is most frequent

and found in cyclists. It is characterized by thickening of the intima and/or adventitia, a result of smooth muscle hyperplasia with only mild collagen or elastin deposition, and/or hypertrophy of the media. There is no inflammation and only rarely calcification of the media. Mural thrombus is found in less than half of cases (Kral et al. 2002). There is intermittent exercise induced claudication with lower limb and thigh pain during near-maximal exercise (Feugier and Chevalier 2004; Chevalier et al. 1986). A post exercise asymmetric measurement of ankle systolic pressure lower at the symptomatic side, and positive ankle to arm systolic pressure index is highly suggestive. Systolic pressure is mostly symmetric with normal ankle to arm index at rest. Angiographic examination (conventional arteriography, CT arteriography or MR arteriography) demonstrates tapering of the arterial lumen with elongation of the artery (Fig. 25.10) (Hindryckx et al. 1996). An acute claudication with complete obstruction due to thrombus is rare. Grayscale ultrasound findings included parietal thickening and increased echogenicity of the arterial wall with straightness of the abnormal segment. There is a mild narrowing of the involved arterial diameter (Abraham et al. 1993). Abraham et al. 1997 demonstrated normal velocity profiles at rest in 80% of the Doppler ultrasound examinations. Power Doppler appears to be an effective technique to visualize and scale kinks and intravascular lesions (Schep et al. 2001). Conservative treatment mainly consists of advise to change sports activity. Surgical mobilization of the iliac arteries for functional lesions, and vascular reconstructions in case of intravascular lesions are possible. Percutaneous transluminal angioplasty and intravascular stent are contra-indicated because of high risks for dissection and reactive intimal hyperplasia, respectively (Schep et al. 1999).

25.5 Conclusions

Abdominal and thoracic wall lesions often are self evident. Imaging interest is merely confirmation of diagnosis or grading.

Several diagnoses must be considered in patients with groin pain, including musculoskeletal and more severe visceral problems (Renstrom 1992). These other possible diagnoses emphasize the importance of a detailed careful history, physical examination and obtaining the appropriate imaging tests.

Things to Remember

1. Prompt radiological investigation is needed in cases of suspicion of abdominal visceral trauma, pneumothorax and rectus sheath hematoma.
2. The pivot mechanism at the pelvis and pubic bone explains superior and inferior located lesions in groin disruption.
3. Groin disruption demonstrates strain (acute) and hypotrophy (chronic) at the involved musculotendinous components and may present as myofascial bulging and bone marrow edema (osteitis pubis). Ultrasound and MRI are useful in acute and chronic groin disruption, respectively.
4. Sports hernia is probably a minor form of (chronic) groin disruption. It should be investigated first by dynamic ultrasound and second by herniography.
5. The presence of external bruising in handlebar injury is a poor indicator of underlying damage.

Fig. 25.10a–d. Endofibrosis of the external iliac artery. Endofibrosis in a 33-year-old professional cyclist with a longstanding history of claudication-like pain at the right thigh and calf especially during maximum exertion. Post exertion hydrostatic pressure is 105 mmHg at the right calf, 165 mmHg at the left calf and 150 mmHg at the right arm. No difference in hydrostatic pressure between both calves is present at rest. **a** Subtraction angiography of the iliac arteries, two right oblique views. Mild regular narrowing of the lumen, *tapering*, of the right arteria iliaca externa at the area between arrows. A 20% area reduction of the artery is obvious. The low grade stenosis only produces symptoms at maximum exertion. [Image (**a**) courtesy of G. Vanderstraeten, Department of Physiotherapy, University of Ghent, Belgium; images (**b**,**c**) reprinted with permission from Hindryckx et al. (1996)]. **d** Kinking of the artery during extreme flexion of the hip. Reduced wall elasticity at the endofibrosis area produces kinking with high grade stenosis during extreme flexion of the hip. [Reprinted with permission from Von Lanz and Wachsmuth (1972)]

▷▷

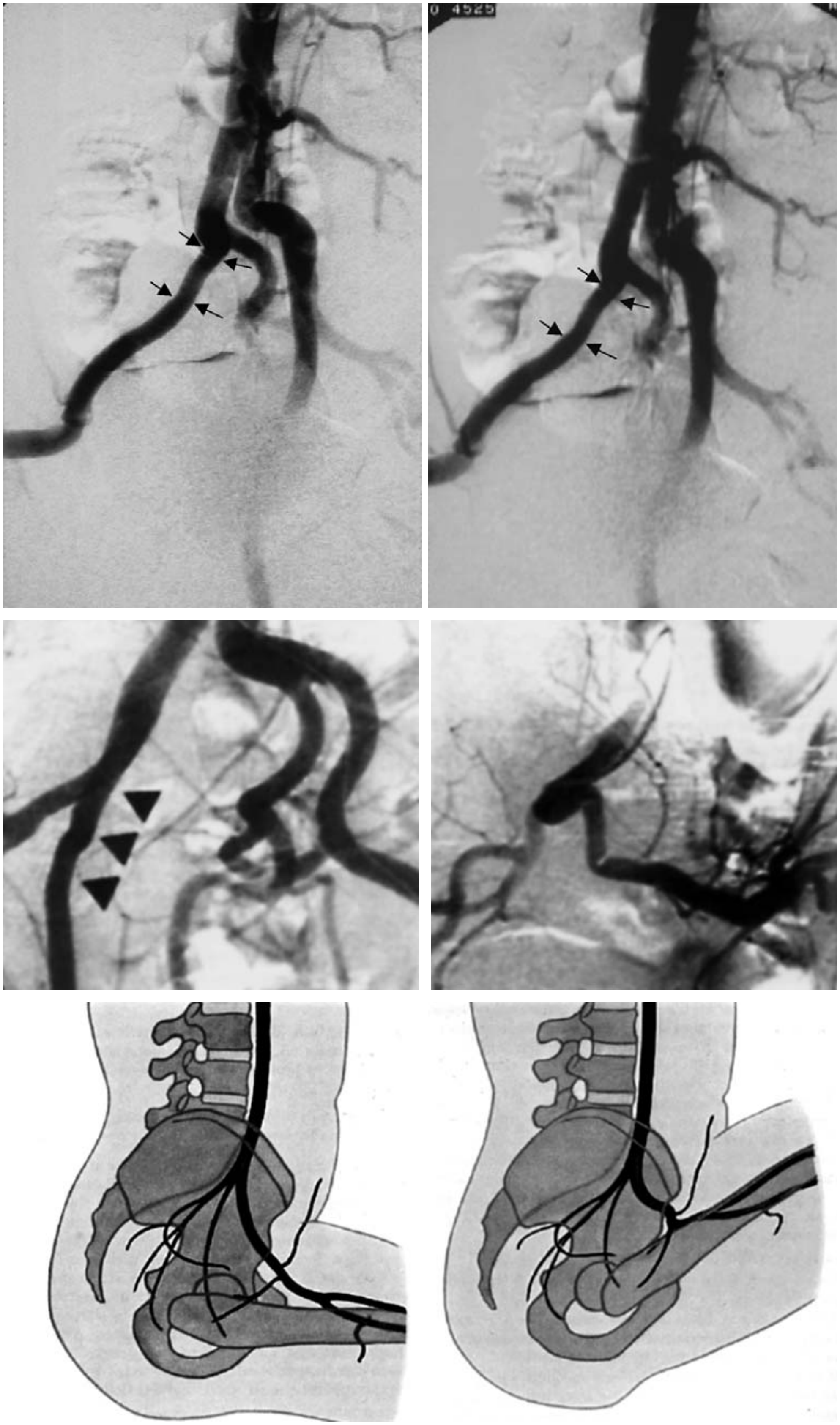

a b c d

References

Abraham P, Leftheriotis G, Bourre Y et al. (1993) Echography of external iliac artery endofibrosis in cyclists. Am J Sports Med 21:861–863

Abraham P, Chevalier JM, Leftheriotis G et al. (1997) Lower extremity arterial disease in sports. Am J Sports Med 25:581–584

Albers SL, Spritzer CE, Garrett WE Jr et al. (2001) MR findings in athletes with pubalgia. Skeletal Radiol 30:270–277

Barbaix E (1996) Stress fracture of the sternum in a golf player. Int J Sports Med 17:304–305

Chao HC, Kong MS (1999) Sonographic diagnosis of mesenteric hematoma. J Clin Ultrasound 27:284–286

Chen HY, Sheu MH, Tseng LM (2005) Bicycle-handlebar hernia: a rare traumatic abdominal wall hernia. J Chin Med Assoc 68:283–285

Chevalier JM, Enon B, Walder J et al. (1986) Endofibrosis of the external iliac artery in bicycle racers: an unrecongnized pathological state. Ann Vasc Surg 1:297–303

Clarnette TD, Beasley SW (1997) Handlebar injuries in children: patterns and prevention. Aust N Z J Surg 67:338–339

Connell DA, Jhamb A, James T (2003) Side strain: a tear of internal oblique musculature. Am J Roentgenol 181:1511–1517

Coris EE, Higgins HW II (2005) First rib stress fractures in throwing athletes. Am J Sports Med 33:1400–1404

Curran J, Kelly D (1966) Stress fracture of the first rib. Am J Orthop 8:16–18

Dodds SD, Wolfe SW (2002) Injuries to the pectoralis major. Sports Med 32:945–952

Ekberg O (1983) Complication after herniography in adults. Am J Roentgenol 140:491–495

Erez I, Lazar L, Gutermacher M et al. (2001) Abdominal injuries caused by bicycle handlebars. Eur J Surg 167:331–333

Feugier P, Chevalier JM (2004) Endofibrosis of the iliac arteries: an underestimated problem. Acta Chir Belg 104:635–640

Fishman LM, Zybert PA (1992) Electrophysiologic evidence of piriformis syndrome. Arch Phys Med Rehabil 84:213

Fowler AW (1957) Flexion-compression injury of the sternum. J Bone Joint Surg Br 39:487–497

Gaffney KM (1997) Avulsion injury of the serratus anterior: a case history. Clin J Sport Med 7:134–136

Garret W, Safran M, Seaber A et al. (1993) Biomechanical comparison of stimulated and nonstimulated skeletal muscle pulled to failure. Am J Sports Med 21:89–96

Gilmore J (1998) Groin pain in the soccer athlete: fact, fiction, and treatment. Clin Sports Med 17:787–793,vii

Goliath J, Mittal V, McDonough J (2004) Traumatic handlebar hernia: a rare abdominal wall hernia. J Pediatr Surg 39: e20–22

Gurtler R, Pavlov H, Torg J (1985) Stress fractures of the ipsilateral first rib in a pitcher. Am J Sports Med 13:277–279

Hackney R (1993) The sports hernia. Br J Sports Med 27:58–61

Hellstrom M, Jacobsson B, Sward L et al. (1990) Radiologic abnormalities of the thoracolumbar spine in athletes. Acta Radiol 31:127–132

Hindryckx C, Rousseaux M, Vanderstraeten G et al. (1996) Endofibrosis of the external iliac artery: a cyclists' syndrome? A case report a. Eur J Phys Med Rehab 6:126–127

Holmes J, Hall R, Schaller R (2002) Thoracic handlebar hernia: presentation and management. J Trauma 52:165–166

Huang CC, Ko SF, NG SH et al. (2005) Scapulothoracic bursitis of the chest wall: sonographic features with pathologic correlation. J Ultrasound Med 24(10):1437–1440

Ingoldby CJH (1997) Laparoscopic and conventional repair of groin disruption in sportsmen. Br J Surg 84:213

Iwamoto J, Takeda T (2003) Stress fractures in athletes: review of 196 cases. J Orthop Sci 8(3):273–278

Johnson R (2006) Abdominal wall injuries: rectus abdominis strains, oblique strains, rectus sheath hematoma. Curr Sports Med Rep. 5:99–103

Karlson D (1998) Rib stress fractures in elite rowers. A case series and proposed mechanism. Am J Sports Med 26:516–519

Keating T (1987) Stress fracture of the sternum in the wrestler. Am J Sports Med 15:92–93

Kral CA, Han DC, Edwards WD et al. (2002) Obstructive external iliac arteriopathy in avid bicyclists: new and variable histopathologic features in women. J Vasc Surg 36:565–570

Kuhn JE (2003) Scapulothoracic crepitus and bursitis in athletes. In: Delee JC, Drez D, Miller MD (eds) Orthopedic sports medicine. Principles and practice, 2nd edn. Saunders, Philadelphia, pp 1006–1014

Lacroix VJ, Kinnear DG, Mulder DS et al. (1998) Lower abdominal pain syndrome in national hockey league players: a report of 11 cases. Clin J Sport Med 8:5–9

Linuma Y, Yamazaki Y, Hirose Y et al. (2005) A case of a traumatic abdominal wall hernia that could not be identified until exploratory laparoscopy was performed. Pediatr Surg Int 21:54–57

Lynch SA, Renström PA (2000) Pelvis, abdominal wall, and adductors. In: Garett WE, Peer K, Kirkendall DT (eds) Principles and practice of orthopedic sports medicine. Lippincott Williams and Wilkins, Philadelphia, pp 215–222

Matsumoto T, Fujita K, Fujioka H et al. (2003) Stress fracture of the first rib in a soccer player: a rare etiology of shoulder pain. J Shoulder Elbow Surg 12:197–199

Meyers WC, Foley DP, Garret WE et al. (2000a) Management of severe lower abdominal or inguinal pain in high-performance athletes. Am J Sports Med 28:2–8

Meyers WC, Ricciardi R, Busconi BD et al. (2000b) Athletic pubalgia and groin pain. In: Garret WE, Speer KP, Kirkendall DT (eds) Principles and practice of orthopaedic sports medicine. Lippincot Williams and Wilkins, pp 223–230

Miles JW, Barrett GR (1991) Rib fractures in athletes. Sports Med 12:66–69

Mitchiner JC (1990) Handlebar hernia: diagnosis by abdominal computed tomography. Ann Emerg Med 19:812–813

Morelli V, Smith V (2001) Groin injuries in athletes. Am Fam Physician 64:1405-1415

Morelli V, Weaver V (2005) Groin injuries and groin pain in athletes: part 1. Prim Care 32:163–183

Neitzschman HR, Wilson S (1999) Radiology case of the month. Tearing pain and swelling in the left chest wall. Grade III muscle strain of the pectoralis major and minor. J La State Med Soc 51:19–20

Orchard JW, Read JW, Neophyton J et al. (1998) Groin pain associated with ultrasound finding of inguinal canal posterior wall deficiency in Australian rules footballers. Br J Sports Med 32:134–139

Perez V, McDonald A, Ghani A et al. (1998) Handlebar hernia: a rare traumatic abdominal wall hernia. J Trauma 44:568–570

Renstroem AF (1997) Groin injuries: a true challenge in orthopaedic sports medicine. Sports Med Arthroscopy Rev 5:247–251

Renstrom AF (1992) Tendon and muscle injuries in the groin area. Clin Sports Med 11:815

Sakellaridis T, Stamatelopoulos A, Andrianopoulos E et al. (2004) Isolated first rib fracture in athletes. Br J Sports Med 38:e5

Schep G, Bender MH, Kaandorp D et al. (1999) Flow limitations in the iliac arteries in endurance athletes. Current knowledge and directions for the future. Int J Sports Med 20:421–428

Schep G, Bender MH, Schmikli SL et al. (2001) Color Doppler used to detect kinking and intravascular lesions in the iliac arteries in endurance athletes with claudication. Eur J Ultrasound 14:129–140

Shin AY, Morin WD, Gorman JD et al. (1996) The superiority of magnetic resonance imaging in differentiating the cause of hip pain in endurance athletes. Am J Sports Med 24:168–176

Smedberg S, Broome A, Elmer O et al. (1985) Herniography in the diagnosis of obscure groin pain. Acta Chir Scand 151:663–667

Smedberg S, Broome A, Elmer O et al. (1990) Herniography in primary inguinal and femoral hernia: an analysis of 283 operated cases. Contemp Surg:36–48

Strouse PJ, Close BJ, Marshall KW et al. (1999) CT of bowel and mesenteric trauma in children. Radiographics 19:1237–1250

Taylor DC, Meyers WC, Moylan JA et al. (1991) Abdominal musculature abnormalities as a cause of groin pain in athletes. Inguinal hernias and pubalgia. Am J Sports Med 19:239–242

Toorop R, Poniewierski J, Gielen J et al. (2004) Popliteal artery entrapment syndrome. JBR-BTR 87:154–155

Tullos HS, Erwin WD, Woods GW et al. (1972) Unusual lesions of the pitching arm. Clin Orthop 88:169–182

Von Lanz T, Wachsmuth W (1972) Praktische Anatomie. Springer Berlin

Westin N (1997) Groin pain in athletes from Southern Sweden. Sports Med Arthroscopy Rev 5:280–284

Williams P, Foster ME (1995) Gilmore's groin – or is it? Br J Sports Med 29:206

Wojtys EM, Ashton-Miller JA, Huston LJ et al. (2000) The association between athletic training time and the sagittal curvature of the immature spine. Am J Sports Med 28:490–498

Special Considerations in the Immature Skeleton

26

A. Mark Davies and Suzanne E. Anderson

CONTENTS

26.1 Introduction

It is well recognized that physical activity, sporting or otherwise, is required for the healthy development of the growing child into adulthood. While important, the pervasive influence of sport can affect all aspects of our culture including fashion, life-styles, and institutional and even national identity (Hyndman 1996). The result can be that the growing skeleton, more susceptible to trauma than the healthy mature skeleton, is exposed to forces well above that which evolution intended or allowed for. Injury is defined as the response in bone and the soft tissues to applied kinetic energy. The mode of injury can be classified into three groups. The first occurs as a result of a direct blow. This form of injury in the context of sport can be minimised by the use of protective

Box 26.1. Standard radiography

- Initial imaging modality for diagnosis of fractures, Salter-Harris fractures or apophyseal avulsion fracture
- Knowledge of age-related anatomy of the patients and normal variants is mandatory for correct interpretation
- Systematic contralateral views should be discouraged
- Some type of stress fractures, particular in complex anatomical areas (e.g., sacrum) may be very difficult to detect on standard radiographs

Box 26.2. Other (cross sectional) imaging techniques

- MRI may be useful for early detection of stress fractures or reactions, assessment of internal derangement of joints and for staging of osteochondrosis dissecans
- US is mainly used for overuse trauma of the tendons (e.g., patellar tendon)
- SPECT is very sensitive to detect subtle spondylolysis, whereas multi-detector CT is the imaging technique for direct visualisation of the fracture line and for assessment of healing in spondylolysis

A. M. Davies, MD
Consultant Radiologist, The MRI Centre, Royal Orthopaedic Hospital, Birmingham B31 2AP, UK
S. Anderson, MD
Institut of Diagnostic, Interventional and Pediatric Radiology, University Hospital, Inselspital, Freiburg Strasse, 3010 Bern, Switzerland

clothing/equipment. The second occurs as a result of an indirect blow or force such as a fall onto the wrist leading to an injury to the elbow or shoulder. The third group is chronic repetitive injuries otherwise known as overuse injuries. The mode of injury may be identical be it applied to a child or an adult. How the kinetic energy is dissipated in the tissues and the trauma manifested can be very different depending on age. A fall onto an outstretched hand (FOOSH) in an adolescent typically causes a Salter-Harris Type 2 fracture/separation of the distal radial growth plate. In the young adult an identical injury may cause a fracture of the scaphoid. Whereas in the older individual, particularly the postmenopausal woman, a Colles fracture would be the anticipated result. This is because the physis (growth plate), at the time of the adolescent growth spurt, is up to four times weaker than the adjacent bones, ligaments and tendons (Harsha 1957). It is therefore important to stress that the child should not be viewed as a mini-adult. Injuries sustained in the pursuit of sporting excellence depend on the type of sport. There can, therefore, be major geographical differences in the incidence of specific injuries. For example, cases of Little Leaguer's shoulder and elbow are well recognized in adolescent baseball pitchers in North America and are uncommon in the rest of the world. Whereas adolescent cricketers, with a different bowling action, are susceptible to spondylolysis defects. Cricket is played in the United Kingdom and it's former colonies but rarely elsewhere.

Many of the acute bony injuries seen in the paediatric population are covered in the preceding chapters. A number of overuse injuries, if unrecognized, may simulate a tumour. These conditions are the subject matter of Chap. 8. This chapter will give a brief mention of variations of skeletal development that may mimic the effects of trauma and concentrate predominantly on overuse injuries as seen at different anatomical sites in the paediatric skeleton.

26.2 Normal Variants Simulating Traumatic Lesions

Normal skeletal development tends to follow a well-ordered pattern. Within this pattern there are numerous minor variations that fall within the spectrum of normal. The extent of these variations is no better illustrated than in Keat's authoritative atlas (Keats and Anderson 2001). All too often growth plates and accessory ossification centres may be misinterpreted as fractures. The prudent radiologist will not only have an appropriate atlas to hand when reporting radiographs but also knowledge of the approximate age and normal sequence of appearance of the epiphyses. This is particularly important in the elbow with no less than six separate ossification centres appearing between at a few months and 10–13 years of age. A problematic example is the acute avulsion of the medial epicondyle that can become trapped between the trochlea and the ulna. The trochlea ossification centre tends to appear after the medial epicondyle. Therefore, if the "trochlea" is visible in the absence of a medial epicondyle this type of injury has to be seriously considered (Fig. 26.1). In the past some have advocated obtaining comparison views of the controlateral joint to help confirm/exclude injury. While this has some merit the practise should not be encouraged as it necessitates irradiating an entirely normal structure.

The distinction between a normal variant and a developmental abnormality, be it trauma-related or not, may in some instances be blurred. The avulsive cortical irregularity of the posteromedial distal femur, otherwise known as a periosteal desmoid or cortical irregularity syndrome, is frequently attrib-

Fig. 26.1a,b. AP radiographs of the elbow in two 5-year-old children. **a** Normal appearances with visible medial epicondyle and absent trochlea. **b** Acute avulsion and displacement of the medial epicondyle simulating the trochlea ossification centre (arrow)

uted to mechanical stresses applied to the insertion of the adductor magnus or the origin of the medial head of the gastrocnemius muscle (Fig. 26.2) (Bufkin 1971; Barnes and Gwinn 1974; Resnick and Greenway 1982; Pennes et al. 1984). Bone scintigraphy tends to show normal skeletal activity that is somewhat atypical for a trauma-related abnormality of bone (Dunham et al. 1980; Burrows et al. 1982; Craigen et al. 1994). Whatever the precise aetiology the important thing to note is that the process is self-limiting and of no immediate clinical consequence. A number of the heterogeneous group of conditions known as the osteochondroses also fall into this category of self-limiting. These include osteochondritis of the calcaneal apophysis (Sever's disease) (Lokiec and Weintroub 1998), the tarsal navicular (Kohler's disease) (Borges et al. 1995) and the ischiopubic synchondrosis (Van Neck's disease) (Brower 1983). These conditions need to be distinguished from the other articular osteochondroses (e.g., Freiberg's infraction and Kienbock's disease) and the nonarticular osteochondroses (e.g., Osgood-Schlatter disease and Sinding-Larsen-Johanson disease) (Fig. 26.3) in which trauma is considered a significant contributory factor. Occasionally osteomyelitis, particularly subacute, may present in the child with little or no abnormality detected on routine blood tests such that it may be mistaken for an overuse injury.

Fig. 26.2. Avulsive cortical irregularity otherwise known as a periosteal desmoid. Oblique radiograph of the knee in an adolescent male showing irregularity of the cortex of the posteromedial aspect of the distal femoral metaphysis

Fig. 26.3. Traumatic osteochondritis (Sinding-Larsen-Johansen disease). Lateral radiograph of the knee in an adolescent male showing fragmentation of the lower pole of the patella

26.3 Upper Limb

26.3.1 Shoulder

The classic overuse injury seen in the paediatric age group is the Little Leaguer's shoulder first described over 50 years ago (Dotter 1953). It has been variously referred to in the literature as proximal humeral epiphyseolysis (Barnett 1985), osteochondrosis of the proximal humeral epiphysis (Adams 1966; Tullos and King 1972), stress fracture of the proximal humeral epiphyseal plate (Ireland and Andrews 1988) and rotational stress fracture of the proximal humeral epiphyseal plate (Cahill et al. 1974; Tullos and Fain 1974). It is thought to be an overuse injury due to repetitive rotational stress applied to the proximal humeral growth plate (physis) (Carson and Gasser 1998) and is best considered as a form of Salter-Harris Type 1 stress fracture through the growth plate (Fleming et al. 2004). Baseball pitchers are the most commonly affected athletes with an average age of 14 years with a range from 13 to 16 years old (Carson and Gasser 1998). Cases have also been reported in an adolescent badminton player (Boyd and Batt 1997) and a gymnast (Daldorg and Bryan 1994). Typically patients present with shoulder pain aggravated by throwing and tenderness over the lateral aspect of the shoulder. Radiographic changes include widening of the

proximal humeral growth plate with irregularity and sclerosis of the metaphyseal margin and fragmentation/cystic change laterally (Adams 1966; Barnett 1985; Lipscomb 1975; Fleming et al. 2004). The MR imaging findings in Little Leaguer's shoulder have been recently reported with asymmetric physeal widening and edema (Fig. 26.4) (Hatem et al. 2006; Song et al. 2006).

Acute avulsion injuries that may occur around the shoulder girdle include the following: avulsion of the coracoid apophysis due to pull of the coracoclavicular ligament usually in association with acromioclavicular separation (Benton and Nelson 1971); avulsion of the acromial apophysis due to pull of the deltoid muscle (Rask and Steinberg 1978); avulsion of the infraglenoid tubercle at the site of origin of the long head of triceps muscle (Heyes-Moore and Stoker 1982); avulsions of the greater and lesser tuberosities are uncommon in children; isolated avulsion of the lesser tuberosity has been reported in children participating in American football, hockey, volleyball, wrestling, skateboarding and baseball (Klasson et al. 1993; Paschal et al. 1995; Ogawa and Takahashi 1997; Sugalski et al. 2004). Rotator cuff tears, in the absence of avulsions, are rare in children (Battaglia et al. 2003) and may involve the subscapularis tendon more commonly than seen in the over 40-years-of age group (Tarkin et al. 2005).

Fatigue-type stress fractures of the humeral diaphysis usually occur secondary to athletic throwing injuries due to repeated muscular torque (Allen 1984) and have been termed "ball-thrower's fractures" (Callaghan et al. 2004). They have even been described with the throwing of hand grenades but mercifully this is not a childhood activity (Chao et al. 1971; Kaplan et al. 1998). One of the authors (AMD) has seen a similar injury in an elite adolescent tennis player due to excessive serving practise (Fig. 26.5). Keats coined the term tug lesion to describe new bone formation at muscle insertions suggesting they are due to muscular forces. These may be seen in the humerus at the insertion of the deltoid and latissimus dorsi muscles but are of no clinical significance (Keats 1990).

26.3.2 Elbow

The elbow is the focus of loading in many sports and is particularly susceptible to both acute and chronic injuries prior to skeletal fusion. Arguably, it also the site of the greatest spectrum of skeletal development which can make distinction of normal variants from pathology problematic (Fig. 26.1) (Silberstein et al. 1979, 1981, 1982a,b; McCarthy and Ogden 1982). Imaging should always start with the conventional radiograph (Sofka and Potter 2002). However, because of the incidence of transphyseal fractures and avulsion injuries both ultrasound and MR imaging can be useful in assessing elbow injuries in the child (Beltran and Rosenberg 1997; Fritz 1999; Markowitz et al. 1992; May et al. 2000). The principal traumatic abnormal forces experienced in the elbow joint are medial torsion, lateral compression and extension stress (Slocum 1968; Gore et al. 1980).

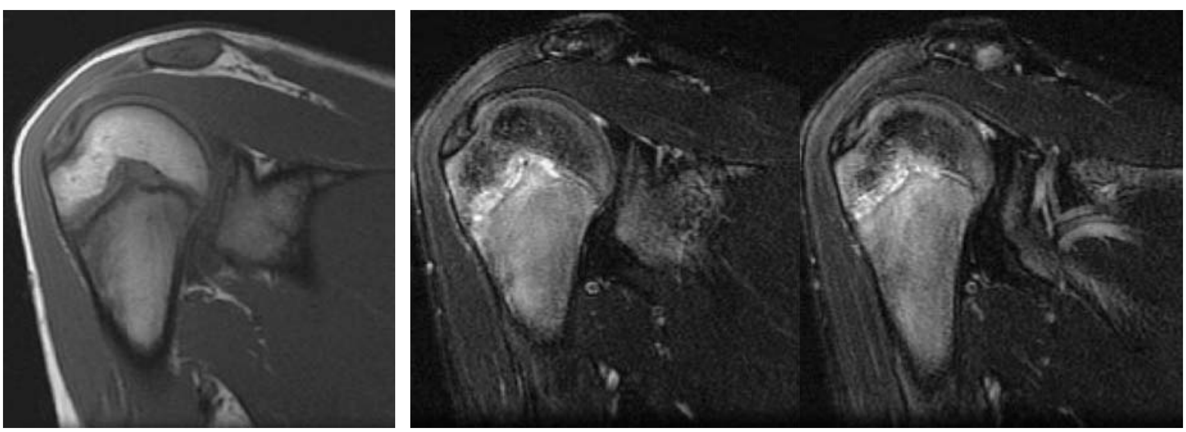
a b

Fig. 26.4a,b. Little Leaguer's shoulder. Coronal oblique T1-weighted (**a**) and fat-suppressed T2-weighted (**b**) MR images showing widening of the growth plate with surrounding edema indicating a stress injury. [Reproduced from Song et al. (2006) with permission]

Fig. 26.5. Stress fracture in a 12-year-old elite male tennis player with 3 months aching in the dominant upper arm. He sustained a fracture of the humerus while practising serving. The presence of minor periosteal reaction preceding the injury indicates the presence of a stress fracture

An acute medial torsion injury can result in an avulsion of the medial epicondylar apophysis. Chronic medial torsion injuries are typically associated with sports requiring a repetitive vigorous throwing action. A classic example is the chronic avulsion or traction apophysitis of the medial epicondyle seen in baseball pitchers, part of a spectrum of injuries known as Little Leaguer's elbow (Adams 1965; Pappas 1982). Similar overuse injuries may be seen in those practising racquet sports (Gore et al. 1980; Priest et al. 1974) as well as gymnasts (Goldberg 1980). Radiographic changes comprise fragmentation or widening of the medial epicondyle apophysis (Hang et al. 2004). Overuse prolongs epiphyseal closure and the medial epicondyle may remain unfused throughout life (Pappas 1982). On MR imaging there are variable signal changes depending on the degree of sclerosis and edema which, in turn, relates to the chronicity of the lesion (Fig. 26.6). Edema and defects may also be seen in the related medial collateral ligament complex.

Lateral compression causes forced impaction of the radial head into the capitellum. In full elbow extension the forces act on the anterior aspect of the radial head causing anterior depression (Ellman 1975). If the excess shear forces continue a chronic Salter Harris Type IV stress fracture may extend to involve the proximal radial metaphysis (Fig. 26.7) (Chan et al. 1991). In the initial stages of ossification of the capitellum, usually before 11 years of age, avascular necrosis (Panner's disease) may occur. At a slightly older age subchondral fractures occur which may progress to post-traumatic subarticular osteonecrosis (osteochondritis dissecans) of the capitellum with or without loose body formation (Fig. 26.8). This is recognized in gymnasts (Priest and Weise 1981; Singer and Roy 1984; Jackson et al. 1989; Chan et al. 1991) as well as sports involving repetitive throwing (Pappas 1982), the use of a racquet (Gore et al. 1980) and in BMX-bicycle riding where up to 40% of the weight of the rider is borne by the arms (Fixsen and Maffulli 1989). MR imaging can be helpful in distinguishing stable from unstable lesions. Unstable lesions are surrounded by

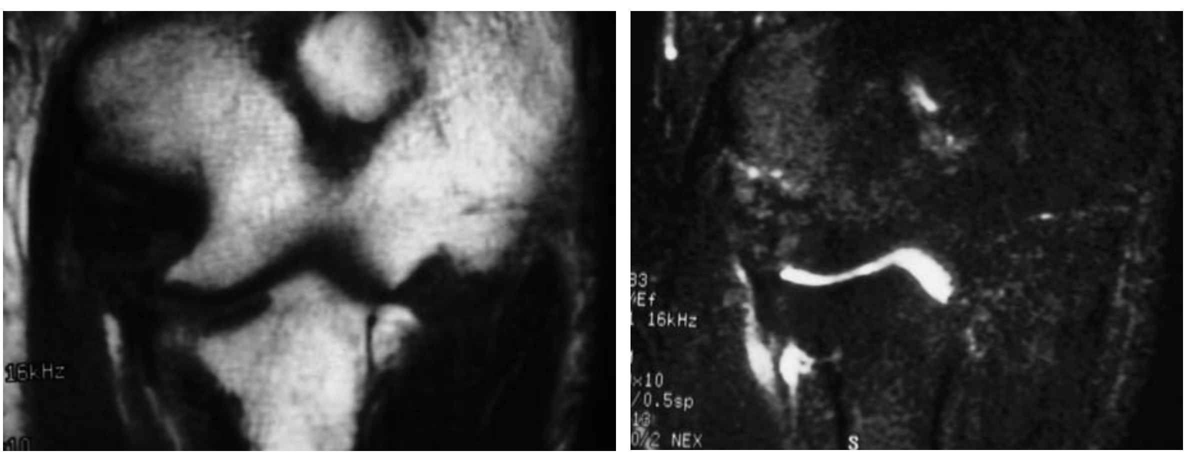

a b

Fig. 26.6a,b. Little Leaguer's elbow in a 16-year-old baseball player. Coronal T1-weighted (**a**) and coronal T2-weighted (**b**) fat-suppressed MR images showing a partial tear in a chronically thickened medial collateral ligament with early degenerative joint disease

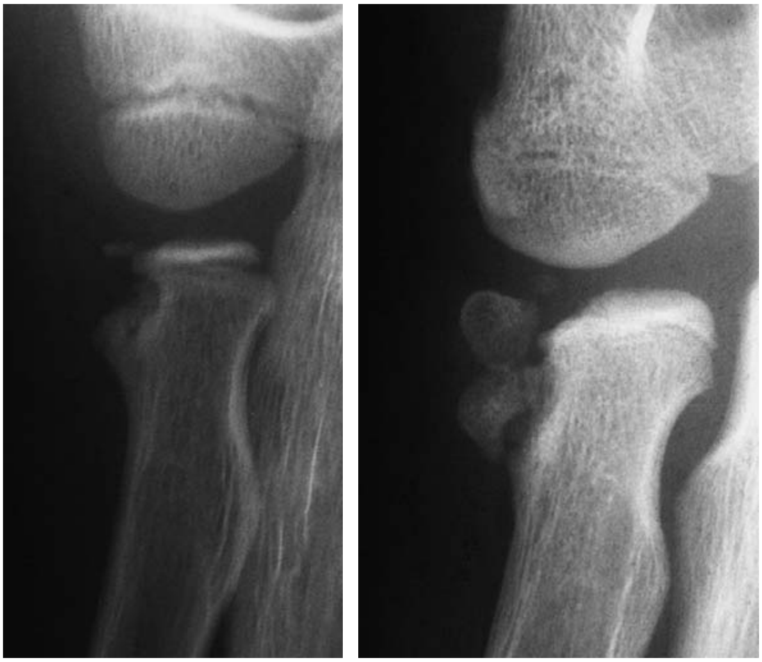

Fig. 26.7a,b. Salter Type IV stress fracture of the radial metaphysis. Over-rotated AP radiographs of the elbow in a child gymnast showing (**a**) a lateral epiphyseal cleft with a prominent underlying metaphyseal defect. At 2 years later (**b**) the radial head is dysplastic with disordered ossification laterally

a rim of high signal intensity on T2-weighted images (Kijowski and De Smet 2005).

Explosive extension of the elbow by the triceps muscle exerts both traction and shearing forces on the olecranon. Acute avulsions of the olecranon apophysis are well recognized. With chronic trauma a Salter Type I stress fracture may develop through the physis resulting in widening and irregularity of the growth plate (Fig. 26.9). This has been reported in gymnasts, baseball pitchers, divers and hockey players (Torg and Moyer 1977; Hunter and O'Connor 1980; Danielsson et al. 1983; Wilkerson and Johns 1990; Chan et al. 1991).

Fig. 26.8. Post-traumatic subarticular osteonecrosis of the capitellum in a 17-year-old male gymnast. AP radiograph of the elbow showing subchondral cyst and loose body formation

26.3.3 Wrist and Hand

Acute injuries of the distal forearm bones in the young child are typically of the torus or greenstick varieties. In adolescence the Salter Harris Type II fracture-separation of the distal radial growth plate predominates. In the adolescent gymnast chronic wrist pain is a frequent complaint and can be associated with a Salter Type I stress fracture of the distal radial growth plate. The radiographic findings are widening and irregularity of the growth plate with normal appearances of the distal ulnar growth plate (Fig. 26.10) (Read 1981; Roy et al. 1985; Fliegel 1986; Carter et al. 1988). MR imaging will show similar appearances (Liebling et al. 1995) but is not necessary to establish the diagnosis. The condition, known as Gymnast Wrist may be subclinical (Auberge et al. 1984) and is often self-limiting (Carter et al. 1988). There is some controversy as to whether this form

Fig. 26.9. Chronic Salter Type I stress fracture in a female adolescent gymnast. Lateral radiograph of the elbow showing widening and irregularity of the olecranon growth plate

Fig. 26.10. Chronic Salter Type I stress fracture in an adolescent male gymnast. PA radiograph of the wrist showing widening and irregularity of the distal radial growth plate

of injury, if longstanding, results in relative positive ulnar variance in adulthood (De Smet L et al. 1994; DiFiori et al. 2002). Carpal injuries are fairly uncommon preskeletal fusion. Stress fractures may rarely affect the scaphoid (Matzkin and Singer 2000). Acute fractures and dislocations are relatively common in the hand at all ages.

26.4 Spine

Adolescent idiopathic scoliosis is one of the commonest childhood deformities more frequent in girls than boys. The overall prevalence is less than 3% but a much higher incidence of up to 25% has been reported in athletes, particularly dancers (Warren et al. 1986). Increased frequency of scoliosis has also been reported in many other sports including swimmers (Becker 1986), javelin throwers (Gussbacher and Rompe 1983), tennis and volleyball players (Hellstrom et al. 1990; Omey et al. 2000). It is thought that the scoliosis is due to excessive lateral torque forces developed in certain activities such as serving and throwing (Omey et al. 2000).

The ring apophysis of the vertebral body is susceptible to axial compressive loading in the adolescent in sports such as gymnastics and water ski-jumping (Horne et al. 1987; Sward et al. 1990). Injuries to the apophysis most often occur anteriorly but can arise posteriorly (Fig. 26.11) (Gundry and Fritts 1999).

Fig. 26.11. Adolescent gymnast with multiple level juvenile vertebral osteochondrosis due to chronic axial compressive loading

If multiple levels are involved then Scheuermann-like changes are seen with Schmorl's nodes, vertebral endplate irregularities, disc space narrowing, minor anterior body wedging and disc dehydration on T2-weighted MR images (Sward et al. 1991).

Spondylolysis, considered to be a stress fracture through the pars interarticularis, is a relatively common cause of low back pain in adolescent athletes and dancers (Micheli 1979, 1983, 1985; Soler and Calderon 2000; Rassi et al. 2005). There is a progression from a pre-fracture stress reaction through the pars interarticularis, to fracture that may be unilateral or more frequently bilateral (spondylolysis), to vertebral displacement (spondylolisthesis) (Jackson et al. 1981). Repetitive load-bearing flexion and extension is considered the major risk factor predisposing to the development of spondylolysis (Letts et al. 1986). It may be seen in almost any sport associated with high levels of mobility and loading. The incidence in gymnasts can be as high as 32% and divers 63% (Omey et al. 2000). A lateral radiograph of the lumbar spine will demonstrate the fracture if it is relatively well established and show any slip. Oblique radiographs will reveal more subtle fractures. A standard bone scan will identify most cases but single photon emission computed tomography (SPECT) is more sensitive to subtle fractures and pre-fracture stress reactions (Collier et al. 1985; Bellah et al. 1991). Thin section CT with the plane of the image viewed perpendicular to the pars, or multislice CT with parasagittal reconstructions, will allow for direct visualization of the fracture and can be helpful in assessing healing. MR imaging can be useful in the detection of acute and pre-fracture stress reactions owing to its ability to detect focal reactive bone marrow edema (Ulmer et al. 1995; Gundry and Fritts 1999). Rarely, apophysitis of the spinous processes in gymnasts may clinically mimic spondylolysis (Mannor and Lindenfield 2000). Localization of this particular condition abnormality can be readily made with lateral SPECT images.

Fatigue-type stress fractures of the sacrum are uncommon and tend to affect running athletes such as cross-country and marathon runners (Johnson et al. 2001). The fractures are more common in the female athlete but have also been reported in the male (Featherstone 1999; Shah and Stewart 2002). These fractures are notoriously difficult to detect on radiographs and some other form of imaging – be it CT, MR imaging or bone scintigraphy – is usually required (Fig. 26.12). In the female athlete the identification of a sacral stress fracture should prompt inquiry into the dietary habits of the individual as a concurrent eating disorder might indicate that this was indeed an insufficiency-type stress fracture (Bono 2004).

26.5 Pelvis

The pelvic ring is a strong structure such that most acute bony fractures in a sporting context are as a result of major falls, e.g. horseriding. The growth of the bony pelvis is contributed to by multiple apophyses that serve as the origin/insertion of a number of major muscle groups (see Table 26.1).

a  b

Fig. 26.12a,b. Stress fracture of the sacrum in an adolescent female cross-country runner. Radiographs of the sacrum were normal. **a** CT showing a linear band of sclerosis in the left sacral ala. **b** Axial T2-weighted fat suppressed MR image showing the fracture as a dark line with surrounding marrow edema

Table 26.1. Avulsion of pelvic apophyses – muscles and sporting activities involved

Apophysis	Muscle(s)	Sport
Iliac crest	Abdominal	Running Jumping Figure skating
Anterior-superior iliac spine	Sartorius/tensor fascia lata	American football Baseball Running Cycling
Anterior-superior iliac spine	Rectus femoris	Soccer Field hockey Running
Ischium	Hamstrings	Gymnastics Baseball Figure skating Ice hockey Hurdling American football
Pubis	Adductors	Running American football Soccer

Preskeletal fusion, acute or chronic loading applied by these muscles can cause an avulsion injury. In the acute injury a small linear fragment of the avulsed apophysis can be identified in the adjacent soft tissues. If there is avulsion of the whole apophysis, with preservation of the blood supply, then it can continue to grow to form a large piece of mature bone within the soft tissues. This is well recognized with ischial injuries (Fig. 26.13). In a large series of acute pelvic avulsion injuries the mean age was 13.8 years and the sites involved were ischial apophysis (54%), anterior-inferior iliac spine (22%) and anterior-superior iliac spine (19%) (Fig. 26.14) (Rossi and Dragoni 2001). These injuries can be multiple (Sundar and Carty 1994). In the chronic injury there can be a spectrum of radiographic appearances that depend on the severity of the trauma and the degree of repair. The changes can vary from subtle irregularity of the bone surface through to marked irregular new bone formation (Vanhoenacker et al. 2005). It is the latter entity that can readily be mistaken for a malignant tumour of bone (see Chap. 8).

26.6 Lower Limb

Fatigue-type stress fractures of the lower limb including the femoral neck, distal femoral diaphysis, proximal tibial diaphysis, distal fibular diaphysis and the metatarsals (March fracture) are well recognized in adolescent athletes, particularly runners. The imaging features and differential diagnosis are covered in Chaps. 7 and 8.

a  b

Fig. 26.13a,b. Chronic ischial avulsion in an adolescent male athlete. **a** AP radiograph showing irregularity of the ischial cortex with overgrowth of the avulsed apophysis in the adjacent soft tissues. **b** CT showing the deformity of the ischium and new bone formation

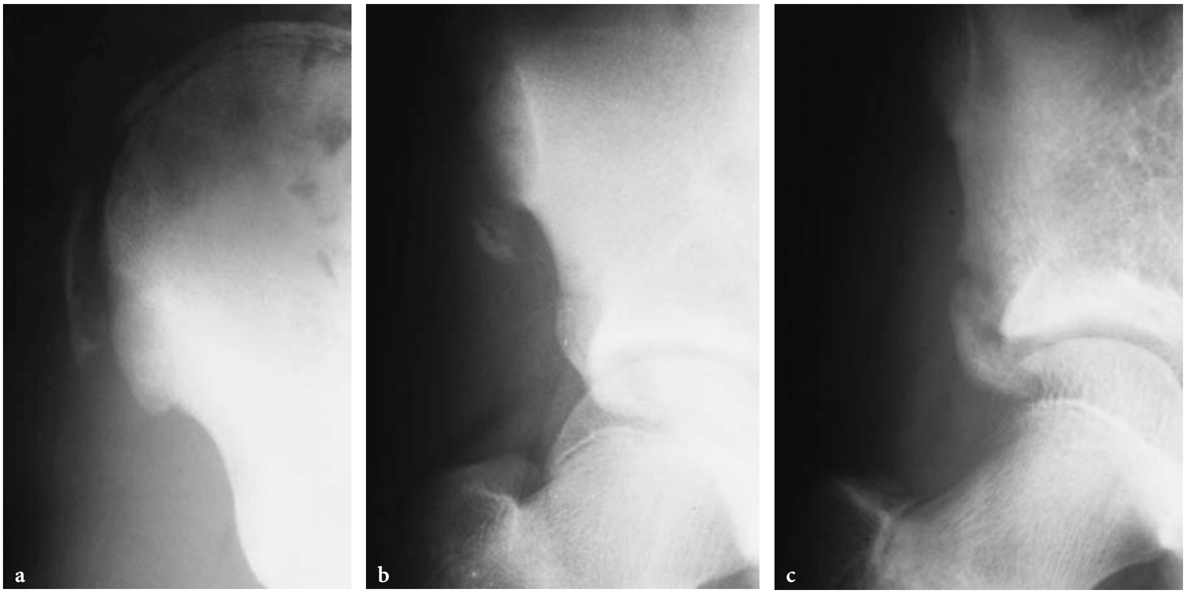

Fig. 26.14a–c. AP radiographs in children of acute avulsion injuries of the (**a**) iliac apophysis, (**b**) anterior superior iliac spine, and (**c**) anterior inferior iliac spine

26.6.1 Proximal Femur

Fatigue-type stress fractures of the femoral neck are four times more common than elsewhere in the femur (see Chap. 7).

Thigh splints has been reported occasionally in a skeletally immature boy (Van de Perre et al. 2003).

Acute avulsion of the lesser trochanteric apophysis, due to pull-off of the iliopsoas tendon, is most commonly seen in adolescent athletes (Fig. 26.15) (Theologis et al. 1997). It should be distinguished from cases in the middle-aged and elderly where avulsion of the lesser trochanter is typically associated with malignant marrow infiltration.

26.6.2 Knee

The commonest acute avulsion around the knee in children and adolescents is at the site of the origin of the anterior cruciate ligament from the anterior tibial spine. Avulsion of the insertion of the posterior cruciate ligament and origin of the medial collateral ligament are much less frequent (Fig. 26.16). As stated above (see Sect. 26.2), the avulsive cortical irregularity of the posteromedial distal femur, otherwise

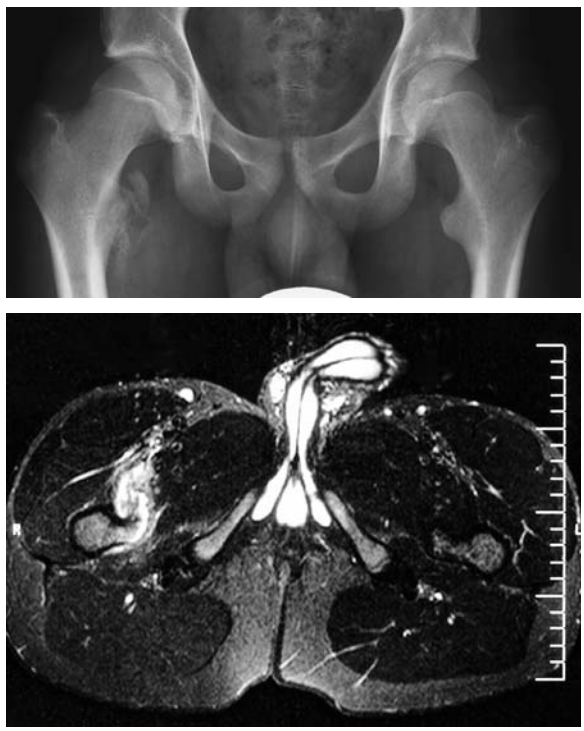

Fig. 26.15a,b. Young girl with avulsion of the right lesser trochanter imaged 2 weeks after acute injury. **a** AP radiograph showing new bone formation around the avulsion simulating a bone forming tumour. **b** Axial T2-weighted fat suppressed MR image showing an irregular "mass" adjacent to the lesser trochanter with surrounding edema

Fig. 26.16. Acute avulsion fracture of the insertion of the posterior cruciate ligament. Lateral radiograph of the knee in an adolescent male showing a bony fragment at the posterior aspect of the tibia

Fig. 26.17. Osteochondrosis dissecans of the knee. Sagittal proton density MR arthrographic image in a 17-year-old male with chronic knee symptoms. There is extensive osteochondrosis dissecans of the medial femoral condyle with an adherent bony fragment and a full thickness cartilage defect posteriorly

known as a periosteal desmoid or cortical irregularity syndrome, may be a normal variant or a self-limiting traumatic lesion (Fig. 26.2). The presence of marrow edema in the adjacent bone on MR imaging should not be considered indicative of infection or malignancy (Posch and Puckett 1998).

Stress fractures through the growth plates of the distal femur and proximal tibia, analogous to the Little Leaguer's shoulder and gymnast's wrist, are documented but rare (Godshall and Hansen 1981; Liebling et al. 1995).

Trauma is considered to be an important factor in the development of osteochondrosis dissecans of the distal femur as it is more common in athletes than in those who do not participate in sports (Schenk and Goodnight 1996). It is also much more common in males than females and typically affects the inner aspect of the medial femoral condyle. The abnormality may be unilateral or bilateral and on radiographs the osteochondral fragment may remain attached to the host bone or form a loose body in the joint. MR imaging has superceded other imaging techniques in assessing the stability and extent of the lesion (Fig. 26.17) (De Smet AA et al. 1996). A lesion is considered unstable if one or more of the following MR criteria is present: (1) high signal intensity fluid/granulation line deep to the lesion; (2) cyst more than 5 mm in width beneath the lesion; (3) focal cartilage defect; (4) fluid passing through an articular cartilage defect (De Smet AA et al. 1996).

Congenital intra-articular abnormalities which may predispose to problems in the immature knee include congenital absence of the anterior cruciate ligament (Gabos et al. 2005) and discoid menisci. Discoid menisci are more common laterally, may be bilateral and can be associated with tears, meniscal cysts and premature degenerative joint disease (Rohren et al. 2001).

Chronic repetitive trauma can cause pain, tenderness, soft tissue swelling and bony fragmentation at the origin of the patellar tendon from the inferior pole of the patella (Sinding-Larsen-Johansson disease, aka "jumper's knee") (Fig. 26.3) and at its insertion into the tibial tubercle (Osgood-Schlatter disease) commonest in adolescent athletes. If required, the clinical diagnosis of both conditions can be confirmed with ultrasound or MR imaging (Hirano et al. 2002). Arguably, the role of imaging in this situation is to exclude other occult pathology. Care should be taken not to over-diagnose minor signal change within the patellar tendon as indicative of chronic trauma without evidence of swelling and edema as it may be artefactual due to the magic angle phenomenon.

"Shin splints" refers to activity-related lower leg pain thought to be related to traction periostitis of the calf muscles along the posteromedial tibia. MR imaging may show juxtacortical and marrow edema as well as subtle cortical changes (Anderson et al. 1997). It forms part of the spectrum of stress-related pathology affecting the tibial diaphysis with the fatigue-type stress fracture the most severe manifestation. If in doubt MR imaging can be used to distinguish between shin splints and a stress fracture (Aoki et al. 2004).

26.6.3 Ankle and Foot

The foot and ankle are the most commonly injured and imaged parts of the musculoskeletal system affecting athletes of all ages (Dunfee et al. 2002). Ankle injuries account for over one quarter of all sports-related injuries in school-aged children (Backx et al. 1989). Acute Salter-Harris fractures of the distal tibia are associated with premature fusion of the growth plate in approximately one third of cases (Barmada et al. 2003). Fatigue-type stress fractures around the ankle and foot pre-skeletal fusion tend to involve the navicular (Coris et al. 2003), distal fibula and uncommonly the medial malleolus (Shabat et al. 2002). Torsional or inversion stress injuries in adolescent athletes may lead to osteochondral defects/osteochondrosis dissecans of the talar dome (Fig. 26.18). The average age at presentation is approximately 13 years and the medial dome of the talus is the most commonly affected (Letts et al. 2003a; Vanhoenacker et al. 2002). Both CT and MR imaging can be used to confirm the diagnosis and for surgical planning.

Ankle sprains are one of the commonest sports-related injuries in adolescence (see also Chap. 20 for further discussion. Most will improve with non-operative management. Imaging of the ligaments and tendons, be it with MR imaging or ultrasound, is best reserved for those cases where surgical intervention is being considered. These include persistent chronic lateral ankle instability (Letts et al. 2003b) and posterior tibial tendon dysfunction (McCormack et al. 2003).

Ballet dancers are particularly prone to foot and ankle pain. The causes can be classified into four groups: impingement syndromes, tendon, ligament and osseous pathologies (Hillier et al. 2004). Posterior impingement is a particular problem because of forced plantar flexion in the en pointe position and is aggravated by the presence of an os trigonum or prominent lateral talar tubercle.

Fig. 26.18. AP radiograph of the ankle of an adolescent girl following an acute injury. There is a fracture of the lateral talar dome which has flipped through 180° and a tiny avulsion injury from the tip of the lateral malleolus

Things to Remember

1. How trauma is manifested in the skeleton depends on the age of the individual.
2. The nature of the sport will determine the pattern of injuries sustained.
3. In the adolescent the growth plate (physis) is particularly susceptible to trauma.
4. The differential diagnosis of chronic overuse injuries in the immature skeleton includes normal variants, osteomyelitis and primary bone tumours.

References

Adams JE (1965) Injury to the throwing arm. A study of traumatic changes in the elbow joints of boy baseball players. Calif Med 102:127–132

Adams JE (1966) Little League shoulder: osteochondrosis of the proximal humeral epiphysis in boy baseball pitchers. Calif Med 105:22–25

Allen ME (1984) Stress fracture of the humerus: a case report. Am J Sports Med 12:244–245

Anderson MW, Ugalde V, Batt M, Gacayan J (1997) Shin splints: MR appearance in a preliminary study. Radiology 204:177–180

Aoki Y, Yasuda K, Tohyama H (2004) MR imaging in stress fractures and shin splints. Clin Orthop 421:260–267

Auberge T, Zenny JC, Duvallet A et al. (1984) Etude de la maturation osseuse et des lesions ostéo-articulaires des sportifs de haut niveau, J Radiol 65:555–561

Backx FJ, Erich WB, Kemper AB et al. (1989) Sports injuries in school-aged children: an epidemiological study. Am J Sports Med 17:234–240

Barmada A, Gaynor T, Mubarak SJ (2003) Premature physeal closure following distal tibial physeal fractures: a new radiographic predictor. J Pediatr Orthop 23:733–739

Barnes GR, Gwinn JL (1974) Distal irregularities of the femur simulating malignancy. AJR Am J Roentgenol 122:180–185

Barnett LS (1985) Little league shoulder syndrome: proximal humeral epiphyseolysis in adolescent baseball pitchers: case report. J Bone Joint Surg Am 67A:495–496

Battaglia TC, Barr MA, Diduch DR (2003) Rotator cuff tear in a 13-year-old baseball player. Am J Sports Med 31:779–782

Becker TJ (1986) Scoliosis in swimmers. Clin Sports Med 5:149–158

Bellah RD, Summerville DA, Treves ST, Micheli LJ (1991) Low back pain in adolescent athletes: detection of stress injury to the pars interarticularis with SPECT. Radiology 180:509–512

Beltran J, Rosenberg ZS (1997) MR imaging of pediatric elbow fractures. MRI Clin North Am 5:567–578

Benton J, Nelson C (1971) Avulsion of the coracoid process in an athlete. J Bone Joint Surg Am 53A:356–358

Bono CM (2004) Current concepts review: low-back pain in athletes. J Bone Joint Surg Am 86A:382–396

Borges JLP, Guille JT, Bowen JR (1995) Kohler's disease of the tarsal navicular. J Pediatr Orthop 15:956–968

Boyd KT, Batt ME (1997) Stress fracture of the proximal humeral epiphysis in an elite junior badminton player. Br J Sports Med 31:252–253

Brower AC (1983) The osteochondroses. Orthop Clin North Am 14:99–117

Bufkin WJ (1971) The avulsive cortical irregularity. AJR Am J Roentgenol 112:487–492

Burrows PE, Greenberg ID, Reed MH (1982) The distal femoral defect: technetium-99m pyrophophate bone scan results. J Can Assoc Radiol 33:91–93

Cahill BR, Tullos HS, Fain RH (1974) Little League shoulder: lesions of the proximal humeral epiphyseal plate. J Sports Med 2:150–151

Callaghan EB, Bennett DL, El-Khoury GY et al. (2004) Ballthrower's fracture of the humerus. Skeletal Radiol 33:355–358

Carson WG Jr, Gasser SI (1998) Little Leaguer's shoulder: a report of 23 cases. Am J Sports Med 26:575–580

Carter SR, Aldridge MJ, Fitzgerald R et al. (1988) Stress changes of the wrist in adolescent gymnasts. Br J Radiol 61:109–112

Chan D, Aldridge MJ, Maffulli N et al. (1991) Chronic stress injuries of the elbow in young gymnasts. Br J Radiol 64:1113–1118

Chao SL, Miller M, Teng SW (1971) A mechanism of spiral fracture of the humerus: a report of 259 cases following the throwing of hand grenades. J Trauma 11:602–605

Collier BD, Johnson RP, Carrera GF (1985) Painful spondylolysis or spondylolisthesis studied by radiography and single photon emission computed tomography. Radiology 154:207–211

Coris EE, Kaeding CC, Marymont JV (2003) Tarsal navicular stress fractures in athletes. Orthopedics 26:733–737

Craigen MAC, Bennet GC, MacKenzie JR et al. (1994) Symptomatic cortical irregularities of the distal femur simulating malignancy. J Bone Joint Surg Br 76B:814–817

Daldorg PG, Bryan WJ (1994) Salter-Harris type 1 injury in a gymnast. A slipped capital humeral epiphysis? Orthop Rev 23:538–541

Danielsson LG, Hedlund ST, Henricson AS (1983) Apophysitis of the olecranon: a report of four cases. Acta Orthop Scand 54:777–778

De Smet AA, Ilahi OA, Graf BK (1996) Reassessment of the MR criteria for stability of osteochondritis dissecans in the knee and ankle. Skeletal Radiol 25:159–163

De Smet L, Claessens A, Lefevre J et al. (1994) Gymnast wrist: an epidemiological survey of ulnar variance and stress changes of the radial physis in elite female gymnasts. Am J Sports Med 22:846–850

DiFiori JP, Puffer JC, Aish B et al. (2002) Wrist pain, distal radial physeal injury, and ulnar variance in young gymnasts: does a relationship exist? Am J Sports Med 30:879–885

Dotter WE (1953) Little Leaguer's shoulder. Guthrie Clin Bull 23:68

Dunfee WR Dalinka MK, Kneeland JB (2002) Imaging athletic injuries to the ankle and foot. Radiol Clin N Am 40:289–312

Dunham WK, Marcus NW, Enneking WF et al. (1980) Developmental defects of the distal femoral metaphysis. J Bone Joint Surg Am 62A:801–806

Ellman H (1975) Anterior angulation deformity of the radial head: an unusual lesion occurring in juvenile baseball players. J Bone Joint Surg Am 57A:776–778

Featherstone T (1999) Magnetic resonance imaging in the diagnosis of sacral stress fracture. Br J Sports Med 33:276–277

Fixsen JA, Maffulli N (1989) Bilateral intra-articular loose bodies of the elbow in an adolescent BMX player. Injury 20:363–364

Fleming JL, Hollingsworth CL, Squire DL et al. (2004) Little Leaguer's shoulder. Skeletal Radiol 33:352–354

Fliegel CP (1986) Stress related widening of the radial growth plate in adsolescents. Ann Radiol 29:374–376

Fritz RC (1999) MR imaging of sports injuries of the elbow. Magn Reson Imaging Clin N Am 7:51–72

Gabos PG, El Rassi G, Pahys J (2005) Knee reconstruction in syndromes with congenital absence of the anterior cruciate ligament. J Pediatr Orthop 25:210–214

Godshall RW, Hansen CA (1981) Stress fractures through the distal femoral epiphysis in athletes. Am J Sports Med 9:114–116

Goldberg MJ (1980) Gymnastic injuries. Orthop Clin N Am 11:717–726

Gore RM, Rogers LF, Bowerman J, Suker J, Compere CL (1980) Osseous manifestations of elbow stress associated with sports activity. AJR Am J Roentgenol 134:971–977

Gundry CR, Fritts HM (1999) MR imaging of the spine in sports injuries. Magn Reson Imaging Clin N Am 7:85–103

Gussbacher A, Rompe G (1983) Die dynamische und statische beanspruchung der Wirbelsaule und ihre moglichen auswirkungen bei verschiedenen sportaten. Schweiz Z Sportmed 31:119–124

Hang DW, Chao CM, Hang YS (2004) A clinical and roentgenographic study of Little League elbow. Am J Sports Med 32:79–84

Harsha WN (1957) Effects of trauma upon epiphyses. Clin Orthop 10:140–147

Hatem SF, Recht MP, Profitt B (2006) MRI of Little Leaguer's shoulder. Skeletal Radiol 35:103–106

Hellstrom M, Jacobsson B, Sward L et al. (1990) Radiological abnormalities of the thoraco-lumbar spine in athletes. Acta Radiol 31:127–132

Heyes-Moore GH, Stoker DJ (1982) Avulsion fractures of the scapula. Skeletal Radiol 9:27–32

Hillier JC, Peace K, Hulme A et al. (2004) MRI features of foot and ankle injuries in ballet dancers: pictorial review. Br J Radiol 77:532–537

Hirano A, Fukubayashi T, Ishii T et al. (2002) MR imaging of Osgood-Schlatter disease: the course of the disease. Skeletal Radiol 31:334–342

Horne J, Cockshott WP, Shannon HS (1987) Spinal column damage from water ski jumping. Skeletal Radiol 16:612–616

Hunter LY, O'Connor GA (1980) Traction apophysitis of the olecranon: a case report. Am J Sports Med 8:51–52

Hyndman JC (1996) The growing athlete. In: Harries M, Williams C, Stanish WD, Micheli LJ (eds). Oxford textbook of sports medicine. Oxford University Press, Oxford, pp 620–633

Ireland ML, Andrews JR (1988) Shoulder and elbow injuries in the young athlete. Clin Sports Med 7:473–494

Jackson DW, Wiltse LL, Dingeman RD (1981) Stress reactions involving the pars interarticularis in young athletes. Am J Sports Med 9:304–312

Jackson SW, Silvino N, Reiman P (1989) Osteochondrosis in the female gymnasts elbow. Arthroscopy 5:129–136

Johnson AW, Weiss CB Jr, Stento K et al. (2001) Stress fractures of the sacrum. An atypical cause of low back pain in the female athlete. Am J Sports Med 29:498–508

Kaplan H, Kiral A, Kuskucu M et al. (1998) Report of eight cases of humeral fractures following the throwing of hand grenades. Arch Orthop Trauma Surg 117:50–52

Keats TE (1990) Radiology of musculoskeletal stress injury. Year Book Medical Publishers, Chicago, p 13

Keats TE, Anderson MW (2001) Atlas of normal roentgen variants that may simulate disease, 7th edn. Mosby, St Louis, pp 154–901

Kijowski R, De Smet A (2005) MRI findings in osteochondritis dissecans of the capitellum with surgical correlation. AJR Am J Roentgenol 185:1453–1459

Klasson SC, Vande Schilden JL, Park JP (1993) Late effect of isolated avulsion fractures of the lesser tubercle of the humerus in children: report of two cases. J Bone Joint Surg Am 75A:1691–1694

Letts M, Smallman T, Afanasiev R et al. (1986) Fracture of the pars interarticularis in adolescent athletes: a clinical-biomechanical analysis. J Pediatr Orthop 6:40–46

Letts M, Davidson D, Ahmer A (2003a) Osteochondritis dissecans of the talus in children. J Pediatr Orthop 23:617–625

Letts M, Davidson D, Mukhtar I (2003b) Sugical management of chronic lateral ankle instability in adolescents J Pediatric Orthop 23:392–397

Liebling MS, Berdon WE, Ruzal-Shapiro C et al. (1995) Gymnast's wrist (pseudorickets growth plate abnormality) in adolescent athletes: findings on plain films and MR imaging. AJR Am J Roentgenol 164:157–159

Lipscomb AB (1975) Baseball pitching injuries in young athletes. J Sports Med 3:25–34

Lokiec F, Weintroub S (1998) Calcaneal osteochondritis: a new overuse injury. J Pediatr Orthop 17:243–245

Mannor DA, Lindenfield TN (2000) Spinal process apophysitis mimics spondylolysis. Am J Sports Med 28:257–260

Markowitz RI, Davidson RS, Harty MP et al. (1992) Sonography of the elbow in infants and children. AJR Am J Roentgenol 159:829–833

Matzkin E, Singer DI (2000) Scaphoid stress fracture in a 13-year-old gymnast: a case report. J Hand Surg Am 25A:710–713

May DA, Disler DG, Jones EA et al. (2000) Using sonography to diagnose an unossified medial epicondyle avulsion in a child. AJR Am J Roentgenol 174:1115–1117

McCarthy SM, Ogden JA (1982) Radiology of postnatal skeletal development: VI. Elbow joint, proximal radius and ulna. Skeletal Radiol 9:17–26

McCormack AP, Varner KE, Marymont JV (2003) Surgical treatment for posterior tibial tendonitis in young competitive athletes. Foot Ankle Int 24:535–538

Micheli LJ (1979) Low back pain in the adolescent: differential diagnosis. Am J Sports Med 7:362–364

Micheli LJ (1983) Back injuries in dancers. Clin Sports Med 2:473–484

Micheli LJ (1985) Back injuries in gymnastics. Clin Sports Med 4:85–93

Ogawa K, Takahashi M (1997) Long-term outcome of isolated lesser tuberosity fractures of the humerus. J Trauma 42:955–959

Omey ML, Micheli LJ, Gerbino PG (2000) Idiopathic scoliosis and spondylolysis in the female athlete. Clin Orthop 372:74–84

Pappas AM (1982) Elbow problems associated with baseball during childhood and adolescence. Clin Orthop 164:30–41

Paschal SO, Hutton KS, Weatherall PT (1995) Isolated avulsion fracture of the lesser tuberosity of the humerus in adolescents: a report of two cases. J Bone Joint Surg Am 77A:1427–1430

Pennes DR, Braunstein EM, Glazer GM (1984) Computed tomography of cortical desmoid. Skeletal Radiol 12:40–42

Posch TJ, Puckett ML (1998) Marrow MR signal abnormality associated with bilateral avulsive cortical irregularities in a gymnast. Skeletal Radiol 27:511–514

Priest JD, Weise DJ (1981) Elbow injury in women's gymnastics. Am J Sports Med 9:288–295

Priest JD, Jones HH, Nagel DA (1974) Elbow injuries in highly skilled tennis players. J Sports Med 2:137–149

Rask MR, Steinberg LH (1978) Fracture of the acromion caused by muscle forces: a case report. J Bone Joint Surg Am 60A:1146–1147

Rassi GE, Takemitsu M, Woratanarat P et al. (2005) Lumbar spondylolysis in pediatric and adolescent soccer players. Am J Sports Med 33:1688–1693

Read MTF (1981) Stress fractures of the distal radius in adolescent gymnasts. Br J Sports Med 15:272–276

Resnick D, Greenway G (1982) Distal femoral cortical defects, irregularities and excavations. Radiology 143:345–354

Rohren EM, Kosarek FJ, Helms CA (2001) Discoid lateral meniscus and the frequency of meniscal tears. Skeletal Radiol 30:316–320

Rossi F, Dragoni S (2001) Acute avulsion fractures of the pelvis in adolescent competitive athletes: prevalence, location and sports distribution of 203 cases collected. Skeletal Radiol 30:127–131

Roy S, Caine D, Singer KM (1985) Stress changes of the distal radial epiphysis in young gymnasts. Am J Sports Med 13:301–308

Schenk RC, Goodnight JM (1996) Current concepts review: osteochondritis dissecans. J Bone Joint Surg Am 78A:439–456

Shabat S, Sampson KB, Mann G et al. (2002) Stress fractures of the medial malleolus: review of the literature and report of a 15-year-old elite gymnast. Foot Ankle Int 23:647–650

Shah MK, Stewart GW (2002) Sacral stress fractures: an unusual cause of low back pain in an athlete. Spine 27:E104–108

Silberstein MJ, Brodeur AE, Graviss ER (1979) Some vagaries of the capitellum. J Bone Joint Surg Am 61A:244–247

Silberstein MJ, Brodeur AE, Graviss ER et al. (1981) Some vagaries of the olecranon. J Bone Joint Surg Am 63A:722–725

Silberstein MJ, Brodeur AE, Graviss ER (1982a) Some vagaries of the lateral epicondyle. J Bone Joint Surg Am 64A:444–448

Silberstein MJ, Brodeur AE, Graviss ER (1982b) Some vagaries of the radial head and neck. J Bone Joint Surg Am 64A:1153–1157

Singer KM, Roy SP (1984) Osteochondrosis of the humeral capitellum. Am J Sports Med 12:351–360

Slocum DB (1968) Classification of elbow injuries from baseball pitchers. Texas Med 64:48–53

Sofka CM, Potter HG (2002) Imaging of elbow injuries in the child and adult athlete. Radiol Clin N Am 40:251–265

Soler T, Calderon C (2000) The prevalence of spondylolysis in the Spanish elite athlete. Am J Sports Med 28:57–62

Song JC, Lazarus ML, Song AP (2006) MRI findings in Little Leaguer's shoulder. Skeletal Radiol 35:107–109

Sugalski MT, Hyman JE, Ahmad CS (2004) Avulsion fracture of the lesser tuberosity in an adolescent baseball pitcher: a case report. Am J Sports Med 32:793–796

Sundar M, Carty H (1994) Avulsion fractures of the pelvis in children: a report of 32 fractures and their outcome. Skeletal Radiol 23:85–90

Sward L, Hellstrom M, Jacobsson B et al. (1990) Acute injury of the vertebral ring apophysis and intervertebral disc in adolescent gymnasts. Spine 15:144–146

Sward L, Hellstrom M, Jaconsson B et al. (1991) Disc degeneration and associated abnormalities of the spine in elite gymnasts: a MR imaging study. Spine 16:437–443

Tarkin IS, Morganti CM, Zillmer DA et al. (2005) Rotator cuff tears in adolescent athletes. Am J Sports Med 33:596–601

Theologis TN, Epps H, Latz K et al. (1997) Isolated fractures of the lesser trochanter in children. Injury 28:363–364

Torg JS, Moyer RA (1977) Non-union of a stress fracture through the olecranon epiphyseal plate observed in an adolescent baseball pitcher: a case report. J Bone Joint Surg Am 59A:264–265

Tullos HS, Fain RH (1974) Little League shoulder: rotational stress fracture of the proximal epiphysis. J Sports Med 2:152

Tullos HS, King JW (1972) Lesions of the pitching arm in adolescents. JAMA 220:264–271

Ulmer JL, Elster AD, Mathews VP et al. (1995) Lumbar spondylolysis: reactive changes seen in adjacent pedicles on MR images. AJR Am J Roentgenol 164:429–433

Van de Perre S, Vanhoenacker F, De Schepper AM (2003) Thigh splints in a skeletally immature boy. Rofo Forschr Geb Rontgenstr Neuen Bildgeb Verfahr 175(11):1582–1584

Vanhoenacker FM, Bernaerts A, Gielen J et al. (2002) Trauma of the pediatric ankle and foot. JBR-BTR 85:212–218

Vanhoenacker FM, Snoeckx A, Gielen JL et al. (2005) Imaging of muscle injuries in children and adolescents. Vlaams Tijdschrift Sportgeneeskunde en Wetenschappen101:39–41

Warren MP, Brooks-Gunn J, Hamilton LH, Warren LF, Hamilton WG (1986) Scoliosis and fractures in young ballet dancers. Relation to delayed menarche and secondary amenorrhea. N Engl J Med 314:1348–1353

Wilkerson RD, Johns JC (1990) Nonunion of an olecranon stress fracture in an adolescent gymnast. Am J Sports Med 18:432–434

The Aging Athlete

27

Eva Llopis and Mario Padrón

CONTENTS

27.1 Introduction

Our society has become fitness oriented; participation in sports has increased over recent decades. The benefits of exercises are extensive and many of physiological consequences of aging may be mitigated or reversed by regular exercise. The greatest threat to the health of the aging athlete is not the aging process itself but rather inactivity (Menard and Stanish 1989).

E. Llopis, MD
Hospital de la Ribera, C/Carretera de Corbera km1, 46600 Alzira, Valencia, Spain
M. Padrón, MD
Clínica Cemtro, C/Ventisquero de la Condesa nº42, 28035 Madrid, Spain

Box 27.1. Radiography

- Late stage imaging method for osteoarthrosis and not always correlation with pain
- Limited value in internal joint disease
- Not indicated for muscle, tendon disease
- Late imaging method for stress fractures, radiological pattern (linear sclerosis perpendicular to the major trabecular lines) and specific location (pubic rami, femoral neck, metatarsal bones) are the clues to the diagnosis. May be normal, inability to show sacral fractures

Box 27.2. Ultrasound

- Imaging guided percutaneous technique
- Excellent tool for assessing the superficial soft tissues, muscles and tendons
- Quick, cheap and available, but operator-dependent

Box 27.3. CT

- High radiation
- Indicated for stress fractures specially in sacrum
- Indicated in acute trauma

Box 27.4. MRI

- Excellent tool for assessing cartilage and joint, beware of asymptomatic findings with aging
- Early diagnosis for stress fractures
- Excellent tool for tendon and muscle evaluation

Aging athletes can be divided into those that wish to remain active as they age, weekend warriors and some of those who have never before exercised and practiced sports. Injuries may result from acute trauma (“macrotrauma”), insidious overuse injuries (“microtrauma”) or from a combination of these two mechanisms, although older athletes experience a lower incidence of acute traumatic injuries (Armsey and Hosey 2004; Chen et al. 2005). The risk of lesions are from their current programme and past indiscretions (Menard and Stanish 1989). Injuries of master-level practitioners reflect the impact of tissue aging (degenerative disease), repetitive joint stresses (chronic overuse injuries) or the long-term effects of athletic injuries (Bert and Gasser 2002; Wolf and Amendola 2005).

The aim of this chapter is to provide an overview of the different specific injuries that aging athletes can sustain, to help to differentiate “normal” from pathological aging, to identify radiological findings that are clearly associated with symptoms or disability and to provide some guidelines to help the practitioner respond more effectively to each individual patient (Table 27.1).

27.2 Impact of Osteoarthritis in Sport Activities: Risk and Consequences

Osteoarthritis is the progressive loss of normal cartilage structure and function, and involves all the joint tissues, bone, capsule, synovium and the cartilage (Wolf and Amendola 2005). The content and type of mucopolysaccharides in cartilage change in response to aging. This leads to a change in water content of the articular cartilage matrix, thus predisposing the cartilage to injury. There are multiple risk factors for osteoarthritis (OA), so determining whether an athlete’s OA is due to participation in sports or other factors is difficult. The joints that are particularly susceptible to OA in the general population are those involved in load bearing and a history of high sports participation increases the risk of osteoarthritis. The type of sport is an important factor in the subsequent risk of OA, with high-impact sports being more detrimental. Top athletes that competed in endurance (running, cross-country skiing), team (soccer, basketball, hockey) or power sports (boxing, wrestling, weightlifting) demonstrate an increase in hip and knee OA, with higher rates in team and power athletes (Fig. 27.1). For some sports such as running there is some controversy as to the role of exercise and the risk of OA; some authors found an increase in hip and knee OA in professional runners, but these data have not been confirmed by others. Among the throwing sports MRI revealed increased numbers of rotator cuff tears and acromio-clavicular OA in the dominant arm compared with the non-dominant limb. In addition, those athletes also displayed radiographic evidence of elbow OA. Increased hand OA has been found in rock climbers.

Chronic tendinosis is related to microtrauma to the tendons, and is therefore more frequent in the adult athlete population. Rotator cuff tendinosis, medial epicondylitis or wrist tendon tendinosis are common in golfers. Achilles tendinosis is the most common injury in joggers. Lateral epicondylitis is more common in middle age racquetball players (Chung and Kim 2003; Potter et al. 2004).

Furthermore, the effects of changes due to OA on different joints in the body have different implications for participants in different sports. Degenerative changes to any of lower extremity joints will be poorly-tolerated by those participating in running, cutting or pivoting sports, such as basketball, football, soccer, tennis and so on. OA in the shoulder, elbow, wrist or hands are likely to be well tolerated unless their sport involves some overhead activity. Overhead athletes such as tennis players, baseball players or swimmers would be far less tolerant to OA changes involving the upper extremity especially in the dominant arm.

The number of master female athletes has also increased. The majority of injuries sustained by female athletes are due to participation in the sport rather than their sex, but there are anatomic, hormonal, and functional differences between the sexes which must be considered (Ireland and Ott 2004).

Imaging of early cartilage damage evaluation is important for treatment options, focal disease have a different therapeutic approach than diffuse cartilage disease. MRI is a useful tool for the evaluation of subtle OA on cartilage-specific sequence due to its high soft tissue contrast. Although radiographs are a late stage imaging method and only provide an indirect evaluation, plain films remain the most widely available and least expensive imaging method. Joint space narrowing, subchondral sclerosis, subchondral cysts and osteophytes are classical OA imaging features. The absence of statistical correlation between the severity of the joint degeneration and the high prevalence of

Table 27.1. Radiological musculoskeletal manifestation of normal aging vs pathologic aging

	Normal aging	Pathologic aging
Bone	Decrease bone density	Stress insufficiency fractures Bone marrow edema
Articular cartilage	Chondromalacia	Osteochondral lesions
Meniscus and fibrocartilage	Knee Intrasubstance degeneration Meniscus horizontal tears	Knee Radial, vertical, complex or displaced meniscal tears
	Wrist Triangular fibrocartilage tear type II	Wrist Ulnar site attachment tears Bone marrow edema and osteochondral associated injuries
Ligament and tendons	Mucoid degeneration of major ligaments, ACL, PCL Mild increased intratendon signal, peritendonitis	Total disruption of fibers Thicker tendon Tears
Muscle	Muscle weakness Musculotendinous unit loss of flexibility	Acute muscular strains or tears Musculotendinous unit rupture


a b

Fig. 27.1a,b. Knee osteoarthritis in 50-year-old soccer player. AP (**a**) and lateral standard radiograph (**b**), Joint space narrowing especially at the medial femorotibial and patellofemoral compartments, subchondral sclerosis and osteophyte formation

asymptomatic imaging findings makes a diagnostic dilemma in determining the cause of the pain.

MR imaging has found an association between patient pain and bone marrow edema. Bone marrow edema is defined on MRI as ill-defined hyperintensities on STIR images and on fat suppressed T2-weighted MR images (see Chap. 6). This "edema" on histopathological examination shows fibrosis, areas of osteonecrosis, bony remodelling and only little edema. Therefore, some authors have suggested using the term "ill-defined signal intensity abnormality" or "edema-like MRI abnormality". More specific con-

comitant abnormalities must be ruled out, such as trabecular fracture demonstrated as a well-defined hypointense line within a high signal area (Fig. 27.2). Long-term consequences of bone marrow edema have yet to be determined (Zanetti et al. 2000; Felson et al. 2003; Felson 2004).

27.3 Long-Term Joint Injuries

Joint injury during sports activities is frequent, and can be secondary to a single acute trauma or secondary to repetitive loads and microtrauma during sport participation. A history of joint injury increases the incidence rate of joint OA but does not affect the rate of progression of OA. Recently the tissue homeostasis theory as a model that maintains knee function is introduced. The range of loads that a joint can accept, transfer and dissipate without failure is represented by an area that can be termed the envelope function. The envelope of function for a given injured joint can vary significantly and reduces with aging. Loading outside of this threshold induces a loss of tissue homeostasis, resulting in injury (Bartz and Laudicina 2005).

Long-term consequences of the most frequent associated sport injuries will be reviewed in this chapter.

27.3.1 Lower Extremity: Knee

Knee injuries are frequent and associated with contact and non-contact sports, often related to a twisting or pivoting episode and repetitive athletic activity loading.

27.3.1.1 Knee: ACL

ACL injury has a drastic effect on an athlete's ability to perform sports; however there is little consensus on the long-term consequences of isolated ACL tears and the effectiveness of ACL reconstruction on preventing long-term sequelae after an isolated injury. Both surgical and conservative treatment may result in cartilage degeneration and osteoarthritis. The rates of radiological degenerative changes in ACL deficient knee vary between 13% and 65%. Even in older patients over the age of 50, there is growing evidence that ACL can be reliably reconstructed allowing patients to return to sport activity (Fig. 27.2) (O'Neill et al. 2002; Blyth et al. 2003).

Areas of occult bone lesions in the lateral femoral condyle and in the posterolateral corner of the medial plateau are frequently seen on MRI in acute ACL injuries secondary to compressive forces (see Chap. 6). However, the most common cartilage lesion in ACL chronic deficient knee were located in the articular surface of the medial femoral condyle, especially associated with bucked-handle meniscal rupture, while it is infrequent to find lateral femoral condyle cartilage lesion. It is probably due to bone bruise healing in the lateral compartment and persistent rotational instability loading the medial compartment. The presence of a medial femoral condyle osteophyte adjacent to the anterior tibial spine is a radiographic indirect sign of chronic ACL deficiency (Maffulli et al. 2003).

Degenerative changes can occur to the cruciate ligaments with aging. Intrasubstance ganglia, mucoid degeneration and intraosseous ganglia at the femoral or tibial ACL attachment may be part of a degenerative aging process. MRI finding are fairly specific and should not be mistaken for a tear. MRI of mucoid degeneration shows a mass-like ligament with homogeneous marked increase signal intensity on T2WI without fibers disruption. McIntyre et al. (2001) concluded 'mucoid degeneration of the ACL must be suspected when an apparently thickened, ill-defined ligament with increased signal intensity, "celery stick appearance", with absence of discontinuity is identified in a patient with a clinically intact ligament'. Clinical significance has to be determined, although pain and restriction to flexion have been reported; those patients respond well to arthroscopic release and notchplasty (McIntyre et al. 2001; Bergin et al. 2004; Narvekar and Gajjar 2004).

27.3.1.2 Knee: PCL

The natural history and treatment options for PCL rupture is still a matter of debate. PCL injuries may not be benign in the long term. Chronic PCL tears demonstrate a variable progression of articular degeneration and late arthrosis. PCL has a unique feature – it may heal after injury. MRI studies have shown that chronic PCL injuries that develop a con-

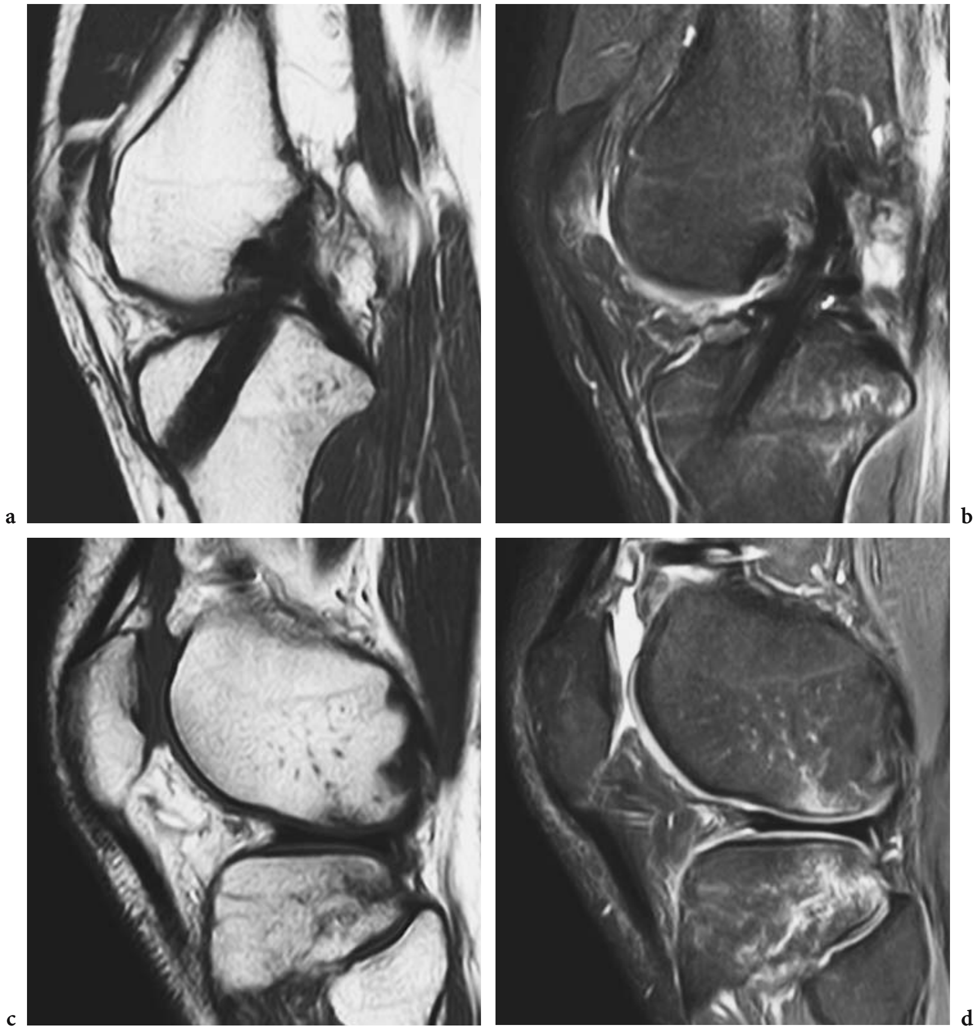

Fig. 27.2a–d. Trabecular fracture in a 39-year-old man soccer player after a twisting knee motion. Previous history included ACL graft reconstruction. Sagittal FSE T1 weighted MR images (**a**,**c**) and sagittal SE proton density fat suppressed MR images (**b**,**d**). The course, signal intensity and morphology of the ACL graft is normal. More lateral images – however – show bone marrow edema at the posterolateral tibial plateau and in the subchondral area of the lateral femoral condyle surrounding two hypointense linear foci , indicative of trabecular fractures (*black arrow*)

tinuous low signal intensity pattern on MRI were less unstable. Prognostic factors such as combined injuries predict long term outcome as well as appropriate treatment. PCL tears without associated intra-articular injury, significant posterior tibial displacement or multidirectional instability were more likely to remain symptom free, while combined instabilities were more likely to result in a decreasingly functional knee (Bartz and Laudicina 2005; Shelbourne and Muthukaruppan 2005).

The overall incidence of degenerative articular cartilage lesions has been 67.4%, the majority being within the medial femoral condyle. Posterior tibial translation secondary to PCL deficiency alters the kinematics of the knee and results in anterior shifted tibiofemoral contact and increased postero-lateral corner stress during knee loading. This unloads the posterior horn of the medial meniscus and leads to increased joint pressure in the anterior medial compartment. The more posterolateral structures are involved, the more rotational shift is present, increasing the loads acting on the medial compartment (Strobel MJ et al. 2003; Logan et al. 2004; Bartz and Laudicina 2005).

27.3.1.3
Knee: Meniscus Tears

Athletic activity loads the lateral compartment, especially the anterior horn of the lateral meniscus. Among asymptomatic aging athletes over the age of 50, MRI shows a significant number of lateral meniscal anterior horn lesions. Therefore, meniscal tears must be only treated if they are considered to be responsible for the patient's discomfort and it is important to identify those MRI features associated with patient's symptoms. Horizontal or oblique meniscal tears on MRI are frequently encountered in both asymptomatic and symptomatic knees and do not always correlate with the patient's symptoms. Radial, vertical, complex or displaced meniscal tears are found to be more prevalent in symptomatic knees, especially when they have associated collateral ligament, pericapsular soft tissue strains or bone marrow (Jerosch et al. 1996; Zanetti et al. 2003).

Factors that influence the risk of osteoarthritis after meniscectomy include the compartment involved (lateral meniscectomy is worse than medial), the amount of resection (the more removed the greater the risk), the type of resection (radial resection of even a small portion may destroy the hoop stress function and is probably equivalent to a near total meniscectomy), associated conditions such as ACL or chondral lesions are probably overall even more significant indications of probable degenerative progression, tibio-femoral alignment, body habitus, patient age and activity level.

After meniscectomy there is an alteration in the load-distribution. Medial meniscectomy reduces 50–70% femoral condyle area and a 100% increase in contact stress in the medial compartment. Lateral meniscus meniscectomy has been shown to result in a 40–50% decrease in contact area and a 200–300% increase in contact stress in the lateral compartment (Figs. 27.3 and 27.4) (Klimkiewicz and Shaffer 2002; Bartz and Laudicina 2005).

An unusual complication of postmeniscectomy is osteonecrosis of femoral condyle. Its physiopathology is not yet fully understood. The reduction of weight bearing by approximately 50% leads to an increase in tibiofemoral pressure. Altered mechanical force has been suggested to be an etiological factor (Johnson et al. 2000). In the initial phase MRI appearance of postmeniscectomy osteonecrosis displays a large area of non-specific intramedullary edema. After three months, the edema decreases and the clearly defined central area of necrosis shows high signal intensity on T2-weighted MR images. A subchondral band of low intensity is seen on both pulse sequences, related to a variable portion of impacted and necrotic medullary bone. After this, bone sequestration may occur, loose bodies may develop or it may resolve with residual flattering of the articular surfaces (Faletti et al. 2002).

27.3.1.4
Articular Cartilage Injury

The natural history of acute osteochondral or chondral injury to the knee continues to be an often debated and controversial subject. It is not known at what point articular cartilage injury becomes irreversible and the chondrocytes lose their potential to maintain a balance between matrix synthesis and degradation.

27.3.2
Lower Extremity: Hip

Osteoarthritis of the hip in athletes is typically the result of cumulative overuse, without specific injury in the majority of cases. It is relatively common, second only to osteoarthritis of the knee. Hip and knee OA have been found to be higher in soccer, football, handball, jumping, track and field sports even without a history of injury, with higher prevalence than age-matched controls. It is unclear whether running is a risk factor for hip osteoarthritis. Specific risk factors include high loads, sudden or irregular impact, repetitive flexion and internal rotation movements or pre-existing abnormalities such as hip dysplasia, labral tears or avascular necrosis sequelae. Acute or chronic hip pain presents a diagnostic and therapeutic challenge because of the vague, non-specific symptoms and signs. Symptoms include pain and lack of range of motion, particularly in internal rotation. The athlete may not specifically complain of pain per se, but rather discomfort or stiffness, usually when starting or after being sedentary (Koh and Dietz 2005; L'Hermette et al. 2006).

Despite the fact that excessive loading to the hip promotes osteoarthritis, it was not until recently that femoroacetabular impingement was associated with the early development of degenerative disease. Femoroacetabular impingement is a condition of abnormal contact between the proximal femur and the acetabulum that may result in lesions of the labrum and cartilage which may progress to osteoarthritis. Hip

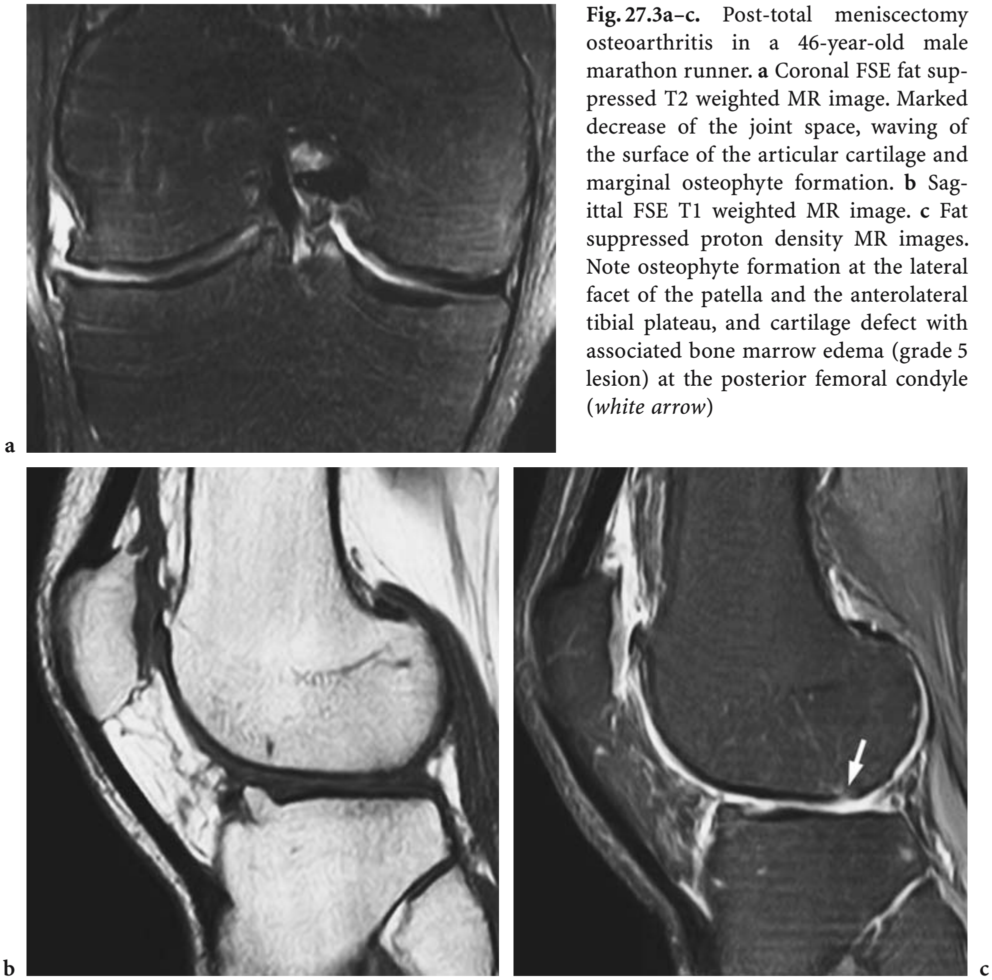

Fig. 27.3a–c. Post-total meniscectomy osteoarthritis in a 46-year-old male marathon runner. **a** Coronal FSE fat suppressed T2 weighted MR image. Marked decrease of the joint space, waving of the surface of the articular cartilage and marginal osteophyte formation. **b** Sagittal FSE T1 weighted MR image. **c** Fat suppressed proton density MR images. Note osteophyte formation at the lateral facet of the patella and the anterolateral tibial plateau, and cartilage defect with associated bone marrow edema (grade 5 lesion) at the posterior femoral condyle (*white arrow*)

arthroscopy is becoming popular and early treatment can alleviate pain and improve function in athletes with OA.

Radiographic features of adult hip dysplasia range from subtle acetabular dysplasia to complex sequelae of development dysplasia. MRI is an accurate method for the diagnosis of hip diseases. MR-arthrography is usually performed to assess the acetabular labrum, although its greater accuracy is questioned by some authors. MRI findings include abnormal head-neck or acetabular morphology, juxta-articular cyst formation at the anterosuperior femoral neck, cyst of the acetabular rim, paralabral cyst with or without bone marrow edema and labral tears (Fig. 27.5) (Delaunay et al. 1997; Kassarjian et al. 2005; Leunig et al. 2005; Lebrun et al. 2005)

However, the labrum is subject to continuous weight-bearing stresses and with age there is an increase in the incidence of asymptomatic tears diagnosed by MRI, so imaging findings must be correlated with patient symptoms. The labrum undergoes changes in signal intensity and shape with aging. The shape tends to change from triangular to round and irregular. High signal intensity reflects normal tissue degeneration and may even communicate with the articular surface (Lecouvet et al. 1996; Abe et al. 2000; Mintz et al. 2005). The response to an intra-articular injection of anaesthetic is a reliable indicator of intra-articular abnormality (Byrd and Jones 2004).

27.3.3 Lower Extremity: Ankle

Osteoarthritis of the ankle is more common in professional football, baseball, soccer players and ballet dancers but not significantly so in high jumpers. Ankle OA can often be asymptomatic (Koh and Dietz 2005).

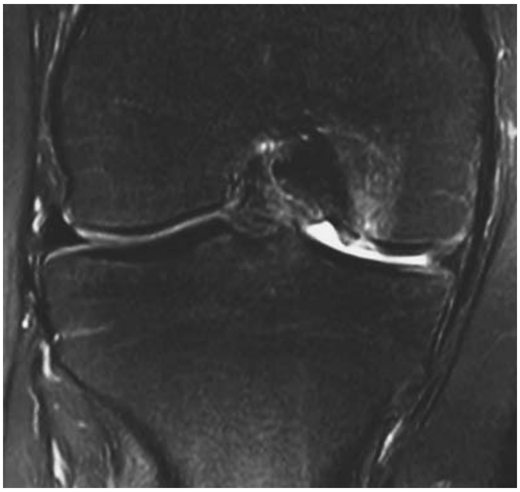

a

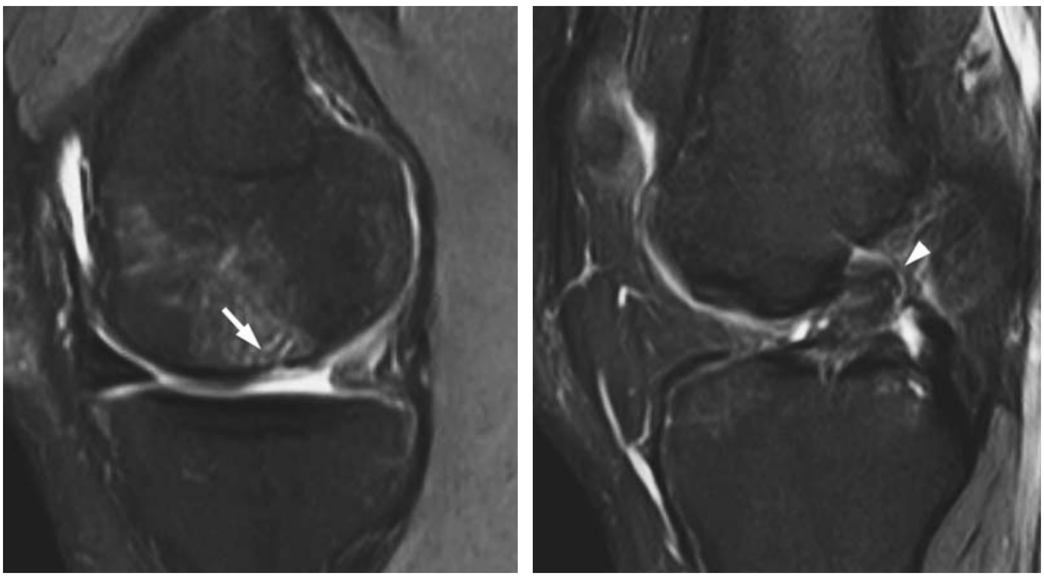

b c

Fig. 27.4a–c. Post-partial meniscectomy changes, meniscal retear, ACL rupture and grade 5 cartilage lesion in a 35-year-old basket player. **a** Coronal FSE fat suppressed T2 weighted MR image. **b,c** Sagittal SE fat suppressed proton density MR images. Morphologic changes (blunting and truncation) and increased intrameniscal signal intensity of the posterior horn of the medial meniscus. The retear was confirmed at arthroscopy. A focal cartilage defect with subchondral bone marrow edema is seen at the medial femoral condyle (*long arrow*). Complete proximal ACL rupture is seen at the level of the intercondylar notch (*arrowhead*)

Osteoarthritis of the ankle is characterized by the formation of impinging bone spurs, loose bodies, and joint space narrowing. This is typically seen in former professional soccer players: known as the Soccers`Ankle Impingement syndromes are painful conditions caused by the friction of joint tissues; they can be classified as anterolateral, anterior, antero-medial, postero-medial and posterior. Anterior impingement resulting from repetitive dorsiflexion appears typically in soccer players, whereas posterior impingement is more typical in ballet dancers. MR imaging is useful in assessing the distribution of the spurs and osteophytes and detecting bone marrow edema, synovitis and cartilage lesions (Fig. 27.6) (Bureau et al. 2000; Cerezal et al. 2003).

27.3.4
Upper Extremity: Shoulder

Shoulder pain is a prevalent musculoskeletal symptom, accounting for 16% of all musculoskeletal complaints, the peak age is 45–64 years (Andrews 2005). Shoulder range of motion decreases with aging for all motions except internal rotation. Among the athletic population such as professional baseball players, tennis players have increased shoulder external rotation and decreased internal rotation in the dominant arm (Barnes et al. 2001). Athletes who trained with heavy weights have a higher risk of degenerative changes in the dominant arm (Schmitt et al. 2001). Chronic shoulder pain may result from one of several categories of intra-articular and extra-articular

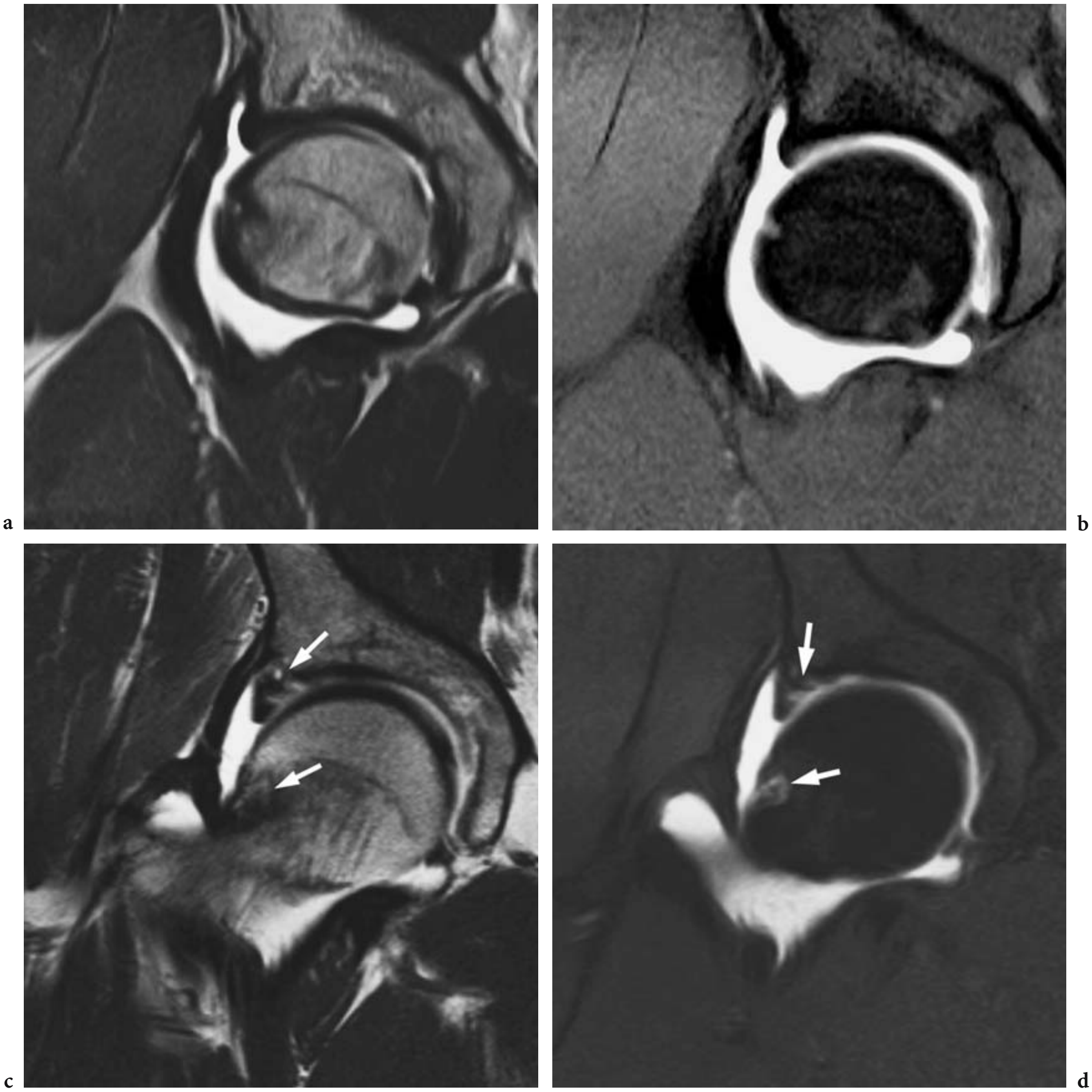

Fig. 27.5a–d. Femoroacetabular Hip Impingement. **a,c** Coronal proton density direct MR arthrogram. **b,d** Fat suppressed T1 weighted direct MR arthrogram. Note a superior labral tear, thickened iliofemoral ligament and bone marrow edema surrounding a cystic lesion in the femoral head-neck junction (*white arrow*)

entities, imaging-guided selective injection of local anaesthetic into the subacromial space or acromioclavicular joint helps to localize the origin of the symptoms (Strobel MJ et al. 2003).

Glenohumeral osteoarthritis includes labrum degeneration, cartilage defects, loose bodies, adhesive capsulitis and osteophytes. A prior shoulder dislocation increased the risk of subsequent shoulder osteoarthritis by 10–20 times that of an uninjured shoulder. However, how quickly and which patients with instability will worsen in time is unclear and it has not yet been determined whether surgical treatment has an impact on the progression of the degenerative disease (Brophy and Marx 2005).

During repetitive shoulder motion, the rotator cuff can impinge on the coracoacromial arch. Rotator cuff tendinosis represents a combination of mechanical attrition, progression of incompletely healed microtears and age-related hypovascularity of the supraspinatus tendon and is vulnerable to tearing while playing throwing sports. The cuff tears tend to occur in the anterior supraspinatus tendon

a b c d e

Fig. 27.6a–e. Ankle Osteoarthritis. **a** Standard radiograph. **b** Axial FSE T1 weighted MR image. **c** Axial STIR image. **d** Sagittal FSE T1 weighted MR image. **e** Sagittal STIR image. Note anterior tibio-talar spur formation with thickening of the anterior capsule (*white arrow*), a prominent posterior lateral talar process (*double white arrow*) with adjacent bone marrow edema and cyst formation, and joint effusion

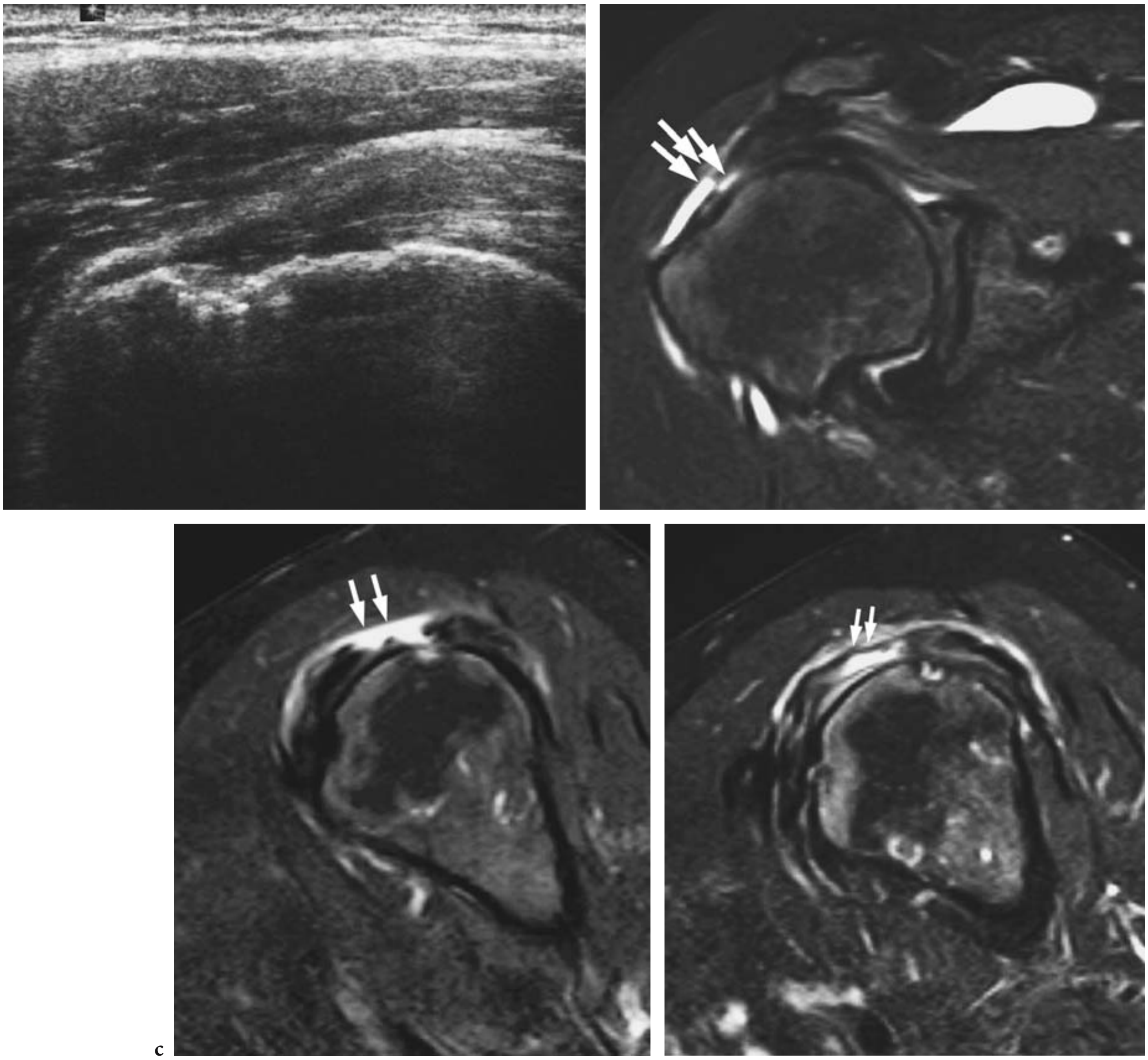

Fig. 27.7a–d. Full-thickness supraspinatus tear. **a** Ultrasound showing a fluid filled gap within the supraspinatus with extension into the subacromial bursa. **b,c** Coronal and sagittal FSE fat suppressed T2 weighted MR image (**b**) show a full thickness supraspinatus tear with fluid extending into the subacromial bursa (*arrows*). **d** The oblique sagittal FSE proton density MR image shows the full-thickness tear extension to the musculotendinous junction

(Fig. 27.7). Another typical injury is the rim rent type tear just at the insertion onto the greater tuberosity (Tuite 2003; Chen et al. 2005).

Acromio-clavicular osteoarthritis manifests as capsular hypertrophy and osteophyte formation. The narrowing of the subacromial space by inferior projecting osteophyte has been associated with subacromial impingement and the development of rotator cuff pathology. Radiological acromio-clavicular osteoarthrosis is a constant finding in patients over 50 years old. MR imaging shows subchondral cyst formation, osteophytes and joint effusion, but bone marrow edema in the distal clavicle and acromion and capsular hypertrophy are the only MRI characteristics associated with clinical findings (Ernberg and Potter 2003; Strobel MJ et al. 2003).

27.3.5 Upper Extremity: Elbow

Long-term osteoarthritis changes secondary to repetitive overuse are seen in many throwing athletes. Posterior olecranon osteophytes, osteophytes in the

olecranon fossa, coronoid osteophytes, loose bodies and chondromalacia may be found.

Chronic stress applied to the elbow is the most frequent injury in athletes. Although these entities have been termed "epicondylitis", tendon changes present fibroblastic proliferation with focal hyaline degeneration rather than inflammation, therefore the term tendinosis is recommended (see Chap. 5).

In throwing sports high valgus stresses are placed on the medial aspect of the elbow, and involve the pronator teres, flexor carpi radialis, and palmaris longus. Lateral "epicondylitis" is the most common problem in the athlete's elbow, many of the cases occurring in non-tennis players, but any sport with overhead arm motion will over-use the extensor muscle. The excessive use of the wrist extensor musculature is associated with lateral "epicondylitis" (Fig. 27.8) (Chung et al. 2004). This is described in detail in Chap. 12.

27.3.6 Upper Extremity: Wrist and Hands

Primary osteoarthritis of the wrist is rare. Radiocarpal osteoarthritis is usually secondary to structural changes that are often precipitated by trauma. Traumatic injuries to the wrist are common in the athletic population. Alterations of biomechanics of the carpal bones of the proximal row can lead to the development of radiocarpal osteoarthritis (Koh and Dietz 2005). Racquet sports aggravate pisotriquetral inflammation secondary to repetitive wrist flexion and direct compression on the joint.

Ulnar-sided pain may be caused by a broad spectrum of disorders, mainly secondary to posttraumatic and overuse syndromes. MRI allows detection of abnormal bones, triangular fibrocartilage tears, bone marrow edema, cartilage lesions, and extensor carpi ulnaris tendinosis (Fig. 27.9). However determin-

a b c

Fig. 27.8a–c. Chronic elbow common extensor tendinosis and intrasubstance tear in a 48-year-old female golf player. **a** Coronal FSE T1 weighted MR image. **b** STIR image. The high intensity area corresponds to a partial tear within the substance of the common extensor tendon. **c** Sagittal ultrasound depicts an intrasubstance tear (*double white arrow*) and a tiny hyperechogenic focus at the tendon insertion related to enthesopathy (*white arrow*). Note that the radial collateral ligament is normal

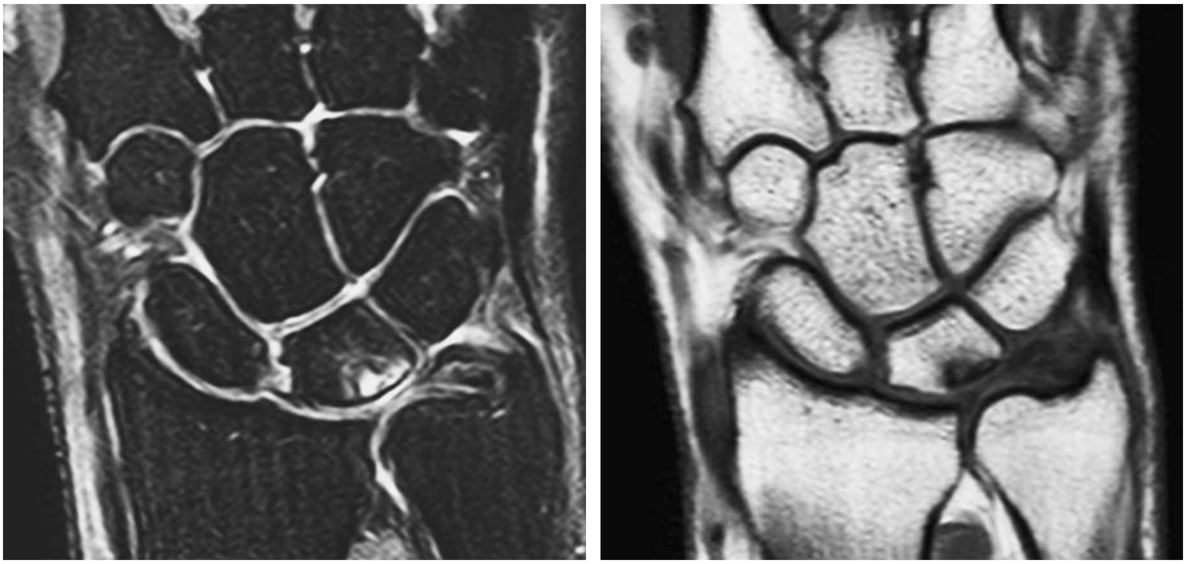

a b

Fig. 27.9a,b. Ulnar impaction syndrome in a 41-year-old paddle player with 1 year complaints of ulnar-sided pain. **a** Coronal fat suppressed FSE proton density MR image. **b** Coronal FSE T1 weighted MR image. There is a central defect within the triangular fibrocartilage, thinning of the lunate cartilage and secondary subchondral cystic lesions

ing the clinical relevance is difficult due high rates of finding in asymptomatic patients (Zanetti et al. 2000b; Cerezal et al. 2004; Zlatkin and Rosner 2004).

27.4 Muscle, Ligament, Tendon

Skeletal muscle becomes weaker and smaller and flexibility decreases as we age, losing the ability to withstand stresses. The slowing of speed and decrease in strength in master athletes is consistent with a loss of type II (fast-twitch) muscle fibers. Chronic endurance training can delay the age of significant decline in peak torque and change in muscle morphology characteristics of the leg. Several cross sectional studies demonstrated significantly greater muscle mass, architecture, and function in strength-trained master athletes compared with sedentary control participants of similar age. However, the increased incidence of muscle injuries in older athlete compared to other adults, and slower repair rates makes training and early diagnosis essential (Morley 2000; Hawkins et al. 2003; Tarpenning et al. 2004).

Among aging athletes muscular strains are frequent, especially in the myotendinous junction. Participation in endurance sports (long distance running) results in muscle fatigue and predisposes to injury (Chen et al. 2005; Close et al. 2005).

Repetitive loading and cumulative microtrauma to tendons lead to tendinosis. Overuse tendon injuries are more common in veteran athletes than in younger athletes. Chronic tendon abnormalities can be found in the midsubstance of the tendon, the insertion site on the bone, and the tenosynovium surrounding the tendon. Different types can also coexist within one tendon (Puddu et al. 1976; Maffulli et al. 1998; Alfredson 2005). Tendinosis affecting the insertion site into the bone or enthesis is a common type, in particular, supraspinatus, common wrist extensor, quadriceps, or patellar tendon (Almekinders et al. 2003).

Mid-substance locations of most common types are Achilles or patellar tendinosis (Fig. 27.10). Although the etiology is not entirely clear, degenerative changes are found in most ruptured tendons, suggesting that there is a pre-rupture phase and even a predisposition to rupture (Maffulli and Wong 2003). The onset of symptoms is related to a partial rupture or series of microruptures in the area of degeneration. Middle-aged men who suddenly increase their activity after a long period of inactivity seem to be most

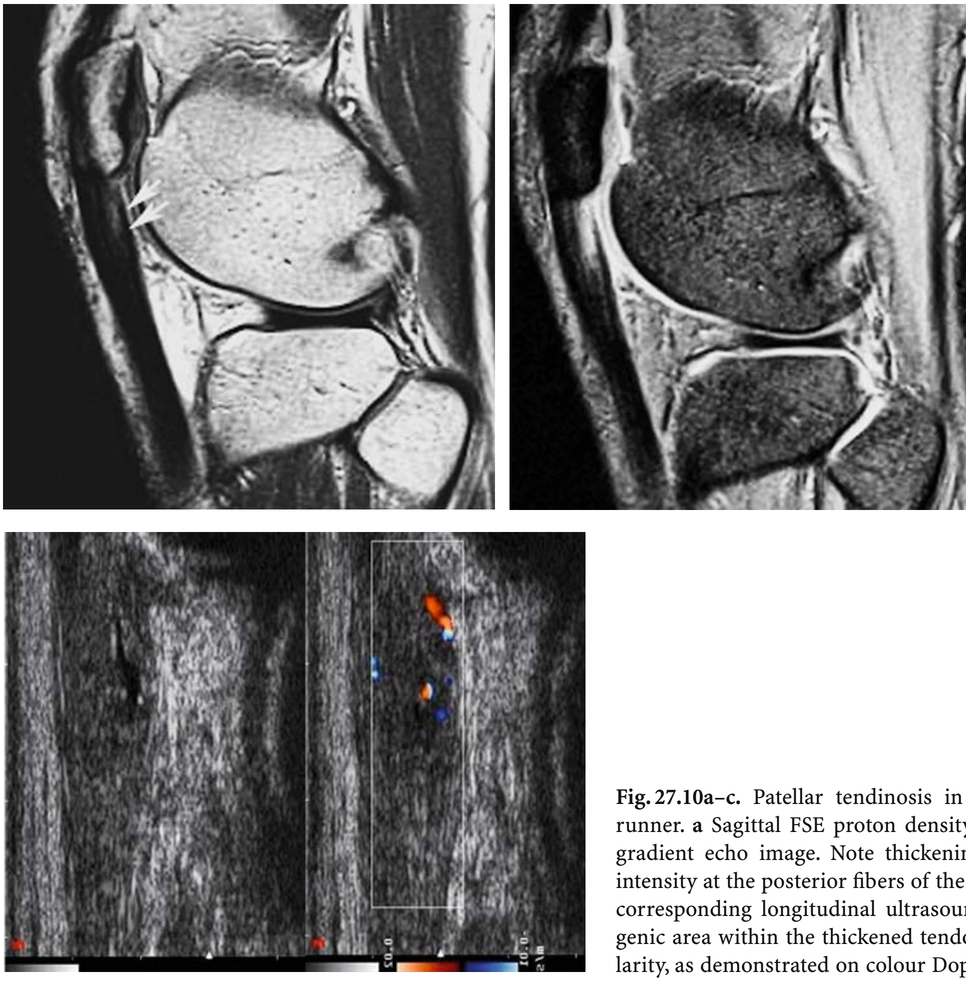

a b c

Fig. 27.10a–c. Patellar tendinosis in a 37-year-old cycling runner. **a** Sagittal FSE proton density MR image. **b** Sagittal gradient echo image. Note thickening and increase signal intensity at the posterior fibers of the tendon (*arrows*). **c** The corresponding longitudinal ultrasound shows a hypoechogenic area within the thickened tendon related to neovascularity, as demonstrated on colour Doppler examination

susceptible to developing micro- or partial ruptures within an area of pre-existing tendinosis. In runners the most common cause of Achilles tendon injuries is training errors, increase in training mileage, change of terrain or an increase in interval training.

Ultrasound is less expensive but examiner-dependent. Undetectable tendon at the site of injury, tendon retraction, and posterior acoustic shadowing at the ends of a torn tendon are characteristics that can be used to aid diagnosis of a full thickness tear (Fig. 27.11). Tendon thickening and areas of high signal intensity on MRI can be seen in asymptomatic and symptomatic patients, so clinical relevance has to be confirmed (Haims et al. 2000; Schepsis et al. 2002).

The role of US or MRI during the tendon healing process is limited. Tendon imaging abnormalities may persist even when patients have functionally recovered; thus they should not be used as a guide to whether or not a patient is fit to return to sport (Moller et al. 2002; Khan et al. 2003).

27.5 Bone Health

There is age-related loss of bone density, increasing bone fragility in men and women (Chen et al. 2005). Weight-bearing physical activity has beneficial effects on bone health across the age spectrum. Exercise and weight-bearing activity have been known to prevent the decline in bone density seen in aging and thus reduce the risk of osteoporotic fractures. However, bone mass density response to training protocols is still a controversial issue. Only sports involving large ground reaction force loading, as in jumping

a c b

Fig. 27.11a–c. Full thickness tear of the Achilles tendon in a 40-year-old tennis teacher. **a** Longitudinal extended field of view ultrasound image shows a full thickness tear (*white arrows*). **b,c** Corresponding sagittal FSE T2 weighted MR image and STIR image show a complete Achilles tendon rupture 3–4 cm from its insertion at the calcaneus (*black arrow*)

and landing, or large dynamic muscle joint reaction forces produce the greatest osteogenic stimulus. Non-impact sports even if performed vigorously do not provide an osteogenic stimulus (Bemben et al. 2000; Nichols et al. 2003; Kohrt et al. 2004).

There is currently no strong evidence that even vigorous physical activity attenuates the menopausal-related loss of bone mineral in woman. Early postmenopause is a critical time for loss of muscular strength and bone mass in woman. Moreover, female athletes involved in intensive training since childhood are at especially high risk for developing osteoporosis because many experienced delayed menarche, oligomenorrhea, or secondary amenorrhea related to their training and diet. Thus, osteoporosis treatment may be indicated even in female master athletes (Ireland and Ott 2004; Kohrt et al. 2004).

Preserving muscle quality and quantity and improving balance reduces the risk of falls and fractures, but insufficiency stress fractures incidence increases with aging, therefore moderation is critical to injury avoidance (Hill 2001). Stress fractures represent the response of normal or abnormal bone to repetitive cyclic loading. The cause of stress fractures changes with aging; fatigue stress fractures are more frequently encountered in young athletes, while older athletes develop insufficiency stress fractures. In younger athletes coordination of muscle action is impaired due to fatigue, but muscle strength and rapid forceful muscle contraction remains, therefore postfatigue impact loading is increased. On the other hand, the loss of muscle strength and endurance with age prevents forceful muscle contraction following fatigue. This may be the cause of the difference in fatigue stress fractures rates between younger and older individuals (Fyhrie et al. 1998). However the normal decrease of bone mineral density increases the risk of fracture.

Clinical symptoms are non-specific and therefore diagnosis is not suspected in many cases. Radiologists must be aware of stress insufficiency fractures, particularly when a patient over 50 starts a new training regimen. The location, distribution and associated findings are the clues for the diagnosis. MRI is an excellent tool for diagnosis (see Chap. 7). Characteristic imaging findings may allow accurate diagnosis, avoid inappropriate studies and the start of early treatment (Daffner and Pavlov 1992; Peh et al. 1996; Hosono et al. 1997; Chowchuen and Resnick 1998; Chen et al. 2005).

27.6 Sports after Total Joint Replacement

The implant designs and surgical advances in joint replacement have allowed patients to return to functional activities. Today it is not uncommon for patients to remain athletically active after total joint replacement. Most patients pursue lower intensity and lower impact activities (golf, walking, swimming, etc.). However, an increasing number of master athletes performing intermediate intensity and impact sports (skiing, tennis, running) are seen and have higher injury rates. High impact loading sports, such as football, soccer or basketball, are not recommended due to the probability of injury. Sports participation increases the risk of traumatic complications, such as dislocation, implant failure, or periprosthetic fracture (Chen et al. 2005; Clifford and Mallon 2005).

27.7 Conclusions

Gaining the benefits of participation in athletics while minimizing the risk of injuries requires understanding of the relationship between sports participation and injury, and the relationship between injury and joint degeneration. It is essential for radiologist to differentiate radiological age-related changes from pathological injuries. Knowledge of the spectrum of injuries in the aging athlete will allow correct diagnosis and early return to athletic activity.

Things to Remember

1. The risk of development of osteoarthritis depends on the load bearing and impact distribution; therefore higher loading sports increase hip and knee osteoarthritis whether throwing and overhead sports predispose to degenerative changes at the upper limb.

2. Due to the high prevalence of degenerative changes in asymptomatic patients, radiological findings must be carefully correlated with clinical presentation, trying to differentiate "normal changes" from pathological aging.

3. Older athletes experience a lower incidence of acute traumatic injuries, and commonly their injuries are related to overuse and repetitive microtrauma. Tendinosis of the rotator cuff, elbow, wrist tendons, Achilles or patellar tendons are more frequent among aging athletes.

4. High impact loading results in cartilage microtrauma and degeneration of the weight-bearing joints. Previous injury or injury may exacerbate this effect.

References

Abe I, Harada Y, Oinuma K et al. (2000) Acetabular labrum: abnormal findings at MR imaging in asymptomatic hips. Radiology 216:576–581

Alfredson H (2005) Conservative management of Achilles tendinopathy: new ideas. Foot Ankle Clin 10:321–329

Almekinders LC, Weinhold PS, Maffulli N (2003) Compression etiology in tendinopathy. Clin Sports Med 22:703–710

Andrews JR (2005) Diagnosis and treatment of chronic painful shoulder: review of nonsurgical interventions. Arthroscopy 21:333–747

Armsey TD, Hosey RG (2004) Medical aspects of sports: epidemiology of injuries, preparticipation physical examination, and drugs in sports. Clin Sports Med 23:255–279

Barnes CJ, Van Steyn SJ, Fischer RA (2001) The effects of age, sex, and shoulder dominance on range of motion of the shoulder. J Shoulder Elbow Surg 10:242–246

Bartz RL, Laudicina L (2005) Osteoarthritis after sports knee injuries. Clin Sports Med 24:9–45

Bemben DA, Fetters NL, Bemben MG et al. (2000) Musculoskeletal responses to high- and low-intensity resistance training in early postmenopausal women. Med Sci Sports Exerc 32:1949–1957

Bergin D, Morrison WB, Carino J et al. (2004) Anterior cruciate ligament ganglia and mucoid degeneration: coexistence and clinical correlation. AJR Am J Roentgenol 182:1283–1287
Bert JM, Gasser SI (2002) Approach to the osteoarthritic knee in the aging athlete: debridement to osteotomy. Arthroscopy 18:107–110
Blyth MJ, Gosal HS, Peake WM et al. (2003) Anterior cruciate ligament reconstruction in patients over the age of 50 years: 2- to 8-year follow-up. Knee Surg Sports Traumatol Arthrosc 11:204–211
Brophy RH, Marx RG (2005) Osteoarthritis following shoulder instability. Clin Sports Med 24:47–56
Bureau NJ, Cardinal E, Hobden R et al. (2000) Posterior ankle impingement syndrome: MR imaging findings in seven patients. Radiology 215:497–503
Byrd JW, Jones KS (2004) Diagnostic accuracy of clinical assessment, magnetic resonance imaging, magnetic resonance arthrography, and intra-articular injection in hip arthroscopy patients. Am J Sports Med 32:1668–1674
Cerezal L, Abascal F, Canga A et al. (2003) MR imaging of ankle impingement syndromes. AJR Am J Roentgenol 181:551–559
Cerezal L, del Pinal F, Abascal F (2004) MR imaging findings in ulnar-sided wrist impaction syndromes. Magn Reson Imaging Clin N Am 12:281–299
Chen AL, Mears SC, Hawkins RJ (2005) Orthopaedic care of the aging athlete. J Am Acad Orthop Surg 13:407–416
Chowchuen P, Resnick D (1998) Stress fractures of the metatarsal heads. Skeletal Radiol 27:22–25
Chung CB, Kim HJ (2003) Sports injuries of the elbow. Magn Reson Imaging Clin N Am 11:239–253
Chung CB, Chew FS, Steinbach L (2004) MR imaging of tendon abnormalities of the elbow. Magn Reson Imaging Clin N Am 12:233–245
Clifford PE , Mallon WJ (2005) Sports after total joint replacement. Clin Sports Med 24:175–186
Close GL, Kayani A, Vasilaki A et al. (2005) Skeletal muscle damage with exercise and aging. Sports Med 35:413–427
Daffner RH, Pavlov H (1992) Stress fractures: current concepts. AJR Am J Roentgenol 159:245–252
Delaunay S, Dussault RG, Kaplan PA et al. (1997) Radiographic measurements of dysplastic adult hips. Skeletal Radiol 26(2):75–81
Ernberg LA, Potter HG (2003) Radiographic evaluation of the acromioclavicular and sternoclavicular joints. Clin Sports Med 22:255–275
Faletti C, Robba T, de Petro P (2002) Postmeniscectomy osteonecrosis. Arthroscopy 18:91–94
Felson DT (2004) An update on the pathogenesis and epidemiology of osteoarthritis. Radiol Clin North Am 42:1–9
Felson DT, McLaughlin S, Goggins J et al. (2003) Bone marrow edema and its relation to progression of knee osteoarthritis. Ann Intern Med 139:330–336
Fyhrie DP, Milgrom C, Hoshaw SJ et al. (1998) Effect of fatiguing exercise on longitudinal bone strain as related to stress fracture in humans. Ann Biomed Eng 26(4):660–665
Haims AH, Schweitzer ME, Patel RS et al. (2000) MR imaging of the Achilles tendon: overlap of findings in symptomatic and asymptomatic individuals. Skeletal Radiol 29:640–645
Hawkins SA, Wiswell RA, Marcell TJ (2003) Exercise and the master athlete–a model of successful aging? J Gerontol A Biol Sci Med Sci 58:1009–1011
Hill C (2001) Caring for the aging athlete. Geriatr Nurs 22:43–45
Hosono M, Kobayashi H, Fujimoto R et al. (1997) MR appearance of parasymphseal insufficiency fractures of the os pubis. Skeletal Radiol 26:525–528
Ireland ML, Ott SM (2004) Special concerns of the female athlete. Clin Sports Med 23:281–298
Jerosch J, Castro WH, Assheuer J (1996) Age-related magnetic resonance imaging morphology of the menisci in asymptomatic individuals. Arch Orthop Trauma Surg 115:199–202
Johnson TC, Evans JA, Gilley JA et al. (2000) Osteonecrosis of the knee after arthroscopic surgery for meniscal tears and chondral lesions. Arthroscopy 16:254–261
Kassarjian A, Yoon LS, Belzile E et al. (2005) Triad of MR arthrographic findings in patients with cam-type femoroacetabular impingement. Radiology 236:588–592
Khan KM, Forster BB, Robinson J et al. (2003) Are ultrasound and magnetic resonance imaging of value in assessment of Achilles tendon disorders? A two year prospective study. Br J Sports Med 37:149–153
Klimkiewicz JJ, Shaffer B (2002) Meniscal surgery 2002 update: indications and techniques for resection, repair, regeneration, and replacement. Arthroscopy 18:14–25
Koh J, Dietz J (2005) Osteoarthritis in other joints (hip, elbow, foot, ankle, toes, wrist) after sports injuries. Clin Sports Med 24:57–70
Kohrt WM, Bloomfield SA, Little KD et al. (2004) American College of Sports Medicine Position Stand: physical activity and bone health. Med Sci Sports Exerc 36:1985–1996
Lebrun C, Vanhoenacker FM, Willemen D (2005) Anterior femoro-acetabular impingement of the CAM type. Radiol Doc 2:15
Lecouvet FE, Vande Berg BC, Malghem J et al. (1996) MR imaging of the acetabular labrum: variations in 200 asymptomatic hips. AJR Am J Roentgenol 167:1025–1028
Leunig M, Beck M, Kalhor M et al. (2005) Fibrocystic changes at anterosuperior femoral neck: prevalence in hips with femoroacetabular impingement. Radiology 236(1):237–46
L'Hermette M, Polle G, Tourny-Chollet C et al. (2006) Hip passive range of motion and frequency of radiographic hip osteoarthritis in former elite handball players. Br J Sports Med 40(1):45–49
Logan M, Williams A, Lavelle J et al. (2004) The effect of posterior cruciate ligament deficiency on knee kinematics. Am J Sports Med 32:1915–1922
Maffulli N, Wong J (2003) Rupture of the Achilles and patellar tendons. Clin Sports Med 22:761–776
Maffulli N, Khan KM, Puddu G (1998) Overuse tendon conditions: time to change a confusing terminology. Arthroscopy 14:840–843
Maffulli N, Binfield PM, King JB (2003) Articular cartilage lesions in the symptomatic anterior cruciate ligament-deficient knee. Arthroscopy 19:685–690
McIntyre J, Moelleken S, Tirman P (2001) Mucoid degeneration of the anterior cruciate ligament mistaken for ligamentous tears. Skeletal Radiol 30:312–315
Menard D, Stanish WD (1989) The aging athlete. Am J Sports Med 17:187–196
Mintz DN, Hooper T, Connell D et al. (2005) Magnetic resonance imaging of the hip: detection of labral and chondral abnormalities using noncontrast imaging. Arthroscopy 21:385–393

Moller M, Kalebo P, Tidebrant G et al. (2002) The ultrasonographic appearance of the ruptured Achilles tendon during healing: a longitudinal evaluation of surgical and nonsurgical treatment, with comparisons to MRI appearance. Knee Surg Sports Traumatol Arthrosc 10:49–56

Morley JE (2000) The aging athlete. J Gerontol A Biol Sci Med Sci 55(11):627–629

Narvekar A, Gajjar S (2004) Mucoid degeneration of the anterior cruciate ligament. Arthroscopy 20:141–146

Nichols JF, Palmer JE, Levy SS (2003) Low bone mineral density in highly trained male master cyclists. Osteoporos Int 14:644–649

O'Neill PJ, Cosgarea AJ, Freedman JA et al. (2002) Arthroscopic proficiency: a survey of orthopaedic sports medicine fellowship directors and orthopaedic surgery department chairs. Arthroscopy 18:795–800

Peh WC, Khong PL, Yin Y et al. (1996) Imaging of pelvic insufficiency fractures. Radiographics 16:335–348

Potter HG, Ho ST, Altchek DW (2004) Magnetic resonance imaging of the elbow. Semin Musculoskelet Radiol 8:5–16

Puddu G, Ippolito E, Postacchini F (1976) A classification of Achilles tendon disease. Am J Sports Med 4:145–150

Schepsis AA, Jones H, Haas AL (2002) Achilles tendon disorders in athletes. Am J Sports Med 30:287–305

Schmitt H, Hansmann HJ, Brocai DR et al. (2001) Long term changes of the throwing arm of former elite javelin throwers. Int J Sports Med 22:275–279

Shelbourne KD, Muthukaruppan Y (2005) Subjective results of nonoperatively treated, acute, isolated posterior cruciate ligament injuries. Arthroscopy 21:457–461

Strobel K, Pfirrmann CW, Zanetti M et al. (2003) MRI features of the acromioclavicular joint that predict pain relief from intraarticular injection. AJR Am J Roentgenol 181:755–760

Strobel MJ,Weiler A, Schulz MS et al. (2003) Arthroscopic evaluation of articular cartilage lesions in posterior-cruciate-ligament-deficient knees. Arthroscopy 19:262–268

Tarpenning KM, Hamilton-Wessler M, Wiswell RA et al. (2004) Endurance training delays age of decline in leg strength and muscle morphology. Med Sci Sports Exerc 36:74–78

Tuite MJ (2003) MR imaging of sports injuries to the rotator cuff. Magn Reson Imaging Clin N Am 11:207–219

Wolf BR, Amendola A (2005) Impact of osteoarthritis on sports careers. Clin Sports Med 24:187–198

Zanetti M, Bruder E, Romero J et al. (2000a) Bone marrow edema pattern in osteoarthritic knees: correlation between MR imaging and histologic findings. Radiology 215:835–840

Zanetti M, Linkous MD, Gilula LA et al. (2000b) Characteristics of triangular fibrocartilage defects in symptomatic and contralateral asymptomatic wrists. Radiology 216:840–845

Zanetti M, Pfirrmann CW, Schmid MR et al. (2003) Patients with suspected meniscal tears: prevalence of abnormalities seen on MRI of 100 symptomatic and 100 contralateral asymptomatic knees. AJR Am J Roentgenol 181:635–641

Zlatkin MB, Rosner J (2004) MR imaging of ligaments and triangular fibrocartilage complex of the wrist. Magn Reson Imaging Clin N Am 12:301–331

Monitoring of Sports Injury Repair

Natural History and Monitoring of Fractures and Microfractures

28

Apostolos H. Karantanas

Contents

Box 28.1. Plain radiographs

- Initial imaging for fractures and avulsions
- Two views are needed for long bones
- Evaluation of fracture healing
- Exclusion of pre-existing osseous lesion in young athletes

Box 28.2. MRI

- Good for soft tissues and bone marrow
- Diagnosis and grading of stress injuries and osteochondral fractures
- Monitoring physeal injuries and scaphoid occult fractures

28.1 Introduction

Over the last three decades there has been an increasing number of people participating in recreational or organized sporting activities. Sports injuries represent 4–9% of attendances of Accident and Emergency departments. The annual health care expenditures in the US has been estimated to be $680 million (Burt and Overpeck 2001). Musculoskeletal injuries are common both in elite athletes of highly competitive sports and among recreational or "weekend" athletes. Delay in diagnosis could lead to improper treatment and development of complications. Imaging with plain radiographs, computed tomography (CT), magnetic resonance imaging (MRI) and scintigraphy, provide valuable information which allows for an early diagnosis (Overdecê and Palmer 2004). The requests for MRI in patients with sports-related injuries are increasing (Livstone et al. 2002). Ultrasonography is a reliable diagnostic modality for imaging sports-related injuries, with wide availability and relative low cost, more efficient though for soft tissues rather than osseous structures (Torriani and Kattapuram 2003; Sofka 2004). Each modality has

A. H. Karantanas, MD, PhD
Associate Professor, Department of Radiology, University Hospital, Stavrakia, Heraklion 711 10, Crete, Greece

advantages and limitations in imaging fractures and microfractures in athletes. Knowledge of the natural history of sports-related fractures and microfractures will aid in understanding the significance of imaging. Monitoring of the above injuries is meaningful only when the imaging diagnosis will alter patient's management.

28.2 Fractures

28.2.1 Osseous Fractures

A fracture is defined as a disruption in the continuity of cortical bone. Sports-related fractures occur in children older than 10 years and in young adults participating in highly competitive sports. Different kinds of athletic activities are often associated with fractures at specific locations, i.e. scaphoid in football, hook of the hamate in golf and baseball, lateral process of the talus in snowboard, tibia in children in skiing, vertebral transverse process in football and hockey, proximal fibula (Maisonneuve's fracture) following twisting injuries in any sport, maxillofacial in football, forearm and ankle in skateboarding and distal radius in football and skiing. The occurrence of a fracture may influence the athlete's future further career. Lawson et al. (1995) reported that only 72.5% of athletes with distal radial fracture returned to their previous level of competition.

The main clinical concerns with regard to a fractured bone refer to normal or abnormal healing, complete or incomplete healing, and timing for its safe use with regard to specific sport and level of activity. In general, fractures of the long bones in athletes correlate to the type of sport activity and heal in the same way as in every healthy subject. In the young injured athlete, the interpreter of plain films should always exclude a preexisting lesion which might predispose to a pathologic fracture.

28.2.1.1 Natural History

Bone healing occurs in three stages: (1) inflammatory, (2) reparative, and (3) remodelling of the bone to normal or near normal shape (Crues and Dumont 1975; Frost 1989a,b). These phases comprise respectively 10%, 40% and 70% of the fracture union period, significantly overlapping each other. The inflammatory phase peaks at two to three weeks after injury and is defined radiographically by a loss of fracture line definition due to the locally increased osteoclastic activity (Islam et al. 2000). The reparative phase consists of vascular dilatation, neovascular proliferation and collagen production. The remodelling phase is characterized by periosteal and endosteal calcium deposition and the growth of new osteoid tissue. Remodeling in the growing skeleton is able to correct deformities if a) the fracture is close to the end of a long bone, b) the deformity parallels the movement plane of the nearest joint or c) two or more years of growth remain in the injured patient. Remodeling is not able to correct a) intraarticular fractures with displacement, b) significantly displaced or rotated diaphyseal fractures, and c) displaced fractures with growth plate involvement at right angles.

Growth plate injuries with associated epiphyseal or metaphyseal fractures, have been classified by Salter and Harris (1963). This radiographic classification highly correlates with the morbidity of these injuries. For type II Salter-Harris fractures, return to sports is possible in 12 weeks, whereas for types III and IV, sports-related loading of the lower extremity joints is sustained for at least 6 months (Stanitski 1998a).

Scaphoid fractures are frequently encountered in sports. Approximately 10% of scaphoid fractures fail to heal and become nonunions requiring internal fixation with bone grafting. Healing with cast lasts more than 12 weeks. In cases of displacement or angulation, fixation is the preferred treatment.

Lumbar transverse process fractures are diagnosed with CT and usually represent isolated injuries necessitating only a few weeks' disability, with a low risk of long-term sequelae.

28.2.1.2 Monitoring

The question of return to full athletic activities should be individualized (i.e. type of fracture, age, specific sport activity) and decision should be based on clinical criteria. For instance, for clinical union of a clavicular fracture in an adult, a period of 3–4 weeks is required, whereas for a femoral shaft fracture that period would extend to 12–14 weeks (Heppenstall 1980).

Plain radiographs are able to demonstrate the normal healing process of the long bone fractures resulting from sports injuries (Figs. 28.1–28.3). Early

radiological signs of repair include blurring of the apposing fracture surfaces, widening of the fracture line and peripheral callus formation. In a fracture less than five to seven days old the well defined fracture line is seen. In a fracture between two and three weeks old, callus formation close to but separate from the cortex is noted. By three to four weeks the separated osseous surfaces start to bridge and the fracture line is not well defined. In most patients, a widened fracture gap corresponds to bone resorption and is obvious radiographically at three to six weeks (Fig. 28.2). A fracture with marginal sclerosis and callus still separable from cortex is probably between 3 and 11 weeks old. A fracture with periosteal new bone inseparable from the cortex is usually older than six weeks (Heppenstall 1980). A partial or whole bridge at the fracture site is expected radiographically at about ten weeks or more after injury where the callus reaches its peak (Islam et al. 2000). The remodelling stage lasts from three months to two years and is faster in children (Chapman 1992). Radiological criteria for fracture healing include demonstration of solid callus and trabecular bone bridging the fracture site. Fracture union is established a) radiologically when there is continuous external bridging callus across the fracture line seen in two orthogonal radiographic projections and b) clinically when there is no pain or motion at the fractured bones (Heppenstall 1980).

Plain radiographs cannot be considered as a valid imaging investigation for detecting occult fractures of the scaphoid (Low and Raby 2005). Avascular necrosis is a common complication of these fractures. Delayed diagnosis may contribute to such a complication (Fig. 28.4).

Physeal fractures, particularly Salter-Harris IV and V, have increased risk for growth arrest and poor prognosis. MRI is the method of choice for demonstrating the physeal bar (Fig. 28.5). If no deformity is depicted at a two-year follow-up, growth arrest is rather unlikely.

28.2.2 Avulsion Fractures

Avulsion fractures following sports are more common in adolescents than in adults, because of the inherent weakness of the growing skeleton apophysis (Zarins and Cuillo 1983). Usually there is a definite history of injury. There are cases though where the athlete does not disclose a history of a single traumatic event. Therefore, radiographic findings without the appropriate history might be confusing and lead to further imaging, biopsy and an incorrect clinical diagnosis (Brandser et al. 1995). Patients with acute injuries present with severe pain and loss of function (el-Khoury et al. 1997). Chronic avulsion injuries result from repetitive microtrauma or overuse and usually occur during organized sports activities (Micheli and Fehlandt 1992). Multiple avulsions may be seen in different stages of healing. Cheerleaders, sprinters and gymnasts as well as football, baseball and

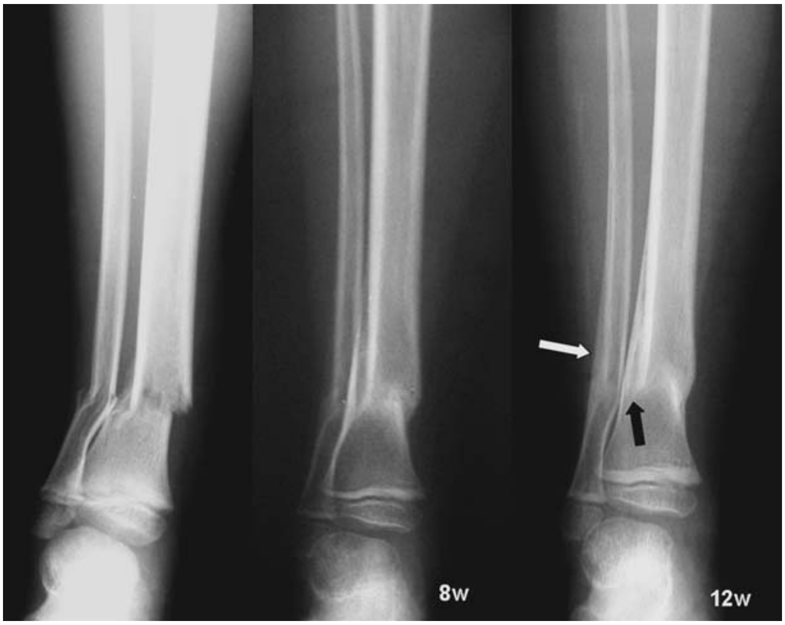

Fig. 28.1. Male seven-year-old with slightly displaced fracture of the distal tibia and fibula during skiing (*left*). In eight weeks after casting, periosteal reaction is obvious and early bridging of the fracture sites with diminished definition of the fracture line (*middle*). Complete bridging of the fracture sites occurs at 12 weeks with mature callus formation (*arrows*, *right*)

Fig. 28.2a–c. Fracture of the proximal radial metaphysis after fall during tennis playing, treated conservatively with casting. **a** The fracture is demonstrated as a lucent thin line without any displacement (*arrow*) extending to the growth plate (Salter-Harris II lesion). **b** In a four week period, the fracture line looks widened (*black arrow*) and callus formation separate from the cortex has developed (*white arrow*). **c** Eight weeks after fracture, there is still some discontinuity of the cortex (*arrow*) but both the callus and the fracture line are not seen, in keeping with healing

Fig. 28.3a–c. Fracture of the fifth metacarpal diaphysis during karate. **a** The fracture is horizontal involving the cortex bilaterally and is associated with displacement and angulation (*arrow*). **b** Ten weeks after external fixation, there is neither remarkable periosteal reaction nor fracture bridging (*arrow*). **c** Sixteen weeks postoperatively, the fracture has completely healed (*arrow*) and the fixation was removed

Fig. 28.4. Scaphoid fracture in a 23-year-old male secondary to ball contact during a basketball competitive game 40 days ago. Persistent pain during training and rest forced the patient to seek medical care. MDCT reveals a fracture of the scaphoid waist (*thin arrow*) without any periostic reaction. The proximal pole of the scaphoid is hyperdense compared to surrounding bones (*thick arrow*) suggesting non-union and early avascular necrosis. A "cyst" like change is obvious in the non-union site

Fig. 28.5. Ten-year-old girl with a previous Salter-Harris fracture (III in tibia and I in fibula) during waterskiing 18 months ago. The postoperative plain film (*left*) shows focal sclerosis and growth plate deformity (*black arrow*). The coronal 2D multi-echo gradient echo MR image (*right*) shows directly the bone bar as a low-signal intensity zone replacing the cartilage (*white arrow*)

track athletes are especially prone to avulsion injuries (Tehranzadeh 1987; Brandser et al. 1995).

Avulsion fractures are diagnosed with plain radiographs in the context of a reliable and informative history. Avulsions in the healing process may demonstrate radiographic characteristics of an aggressive lesion. Chronic avulsion injuries may frequently show bone formation (Fig. 28.6). MRI is generally not required for the evaluation of avulsion per se, as its main usefulness is the evaluation of associated muscular, tendinous and ligamentous disorders.

28.2.2.1
Natural History

Avulsion injuries of the greater tuberosity of the humerus are rare lesions and occur in high energy contact sports such as rugby. These may be occult on initial radiographs and detected at MRI (Zanetti et al. 1999) (Fig. 28.7). An anterior dislocation of the shoulder may be an associated injury. Clinical examination alone is not able to distinguish these injuries from rotator cuff tears. Incomplete avulsion injuries

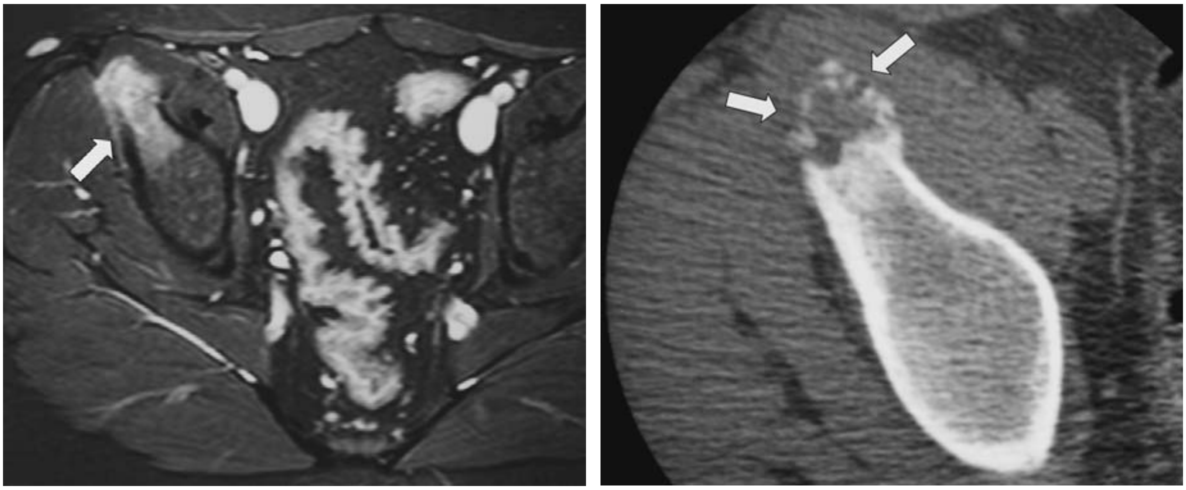

Fig. 28.6a,b. Male 12-year-old participating in organized football activities (junior's football academy) with pain during the last 3 months over the right anterior and lower pelvis. There was no history of contact or other injury. **a** Contrast-enhanced fat-suppressed T1 weighted MR image, demonstrates diffuse bone marrow enhancement. There is also periosteal enhancement (*arrow*). **b** The CT image shows the typical fragmentation of the ossifying subacute avulsion injury of the anterior inferior iliac spine (*arrows*)

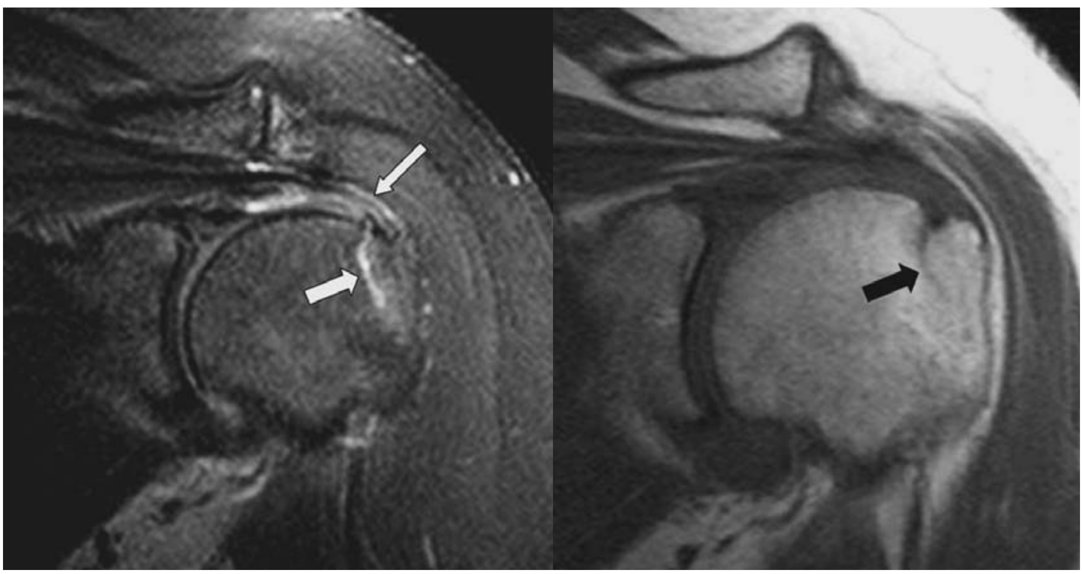

Fig. 28.7. Occult avulsion injury of the greater tuberosity. Oblique coronal fat suppressed T2 weighted MR image (*left*) shows the fracture line (*thick arrow*) with partial healing caudally. There is also a partial tear of the supraspinatus tendon (*thin arrow*). The oblique coronal T2 weighted MR image (*right*) shows the fracture line (*black arrow*) and normal marrow in the most caudal part of the lesion

can result either from a single traumatic event or from overuse activity (Fig. 28.8). Imaging is important since rotator cuff tears require surgical treatment whereas non-displaced avulsion fractures can heal by immobilization alone. Avulsion injuries of the lesser tuberosity of the humerus are rare and occur during wrestling and similar sports. The avulsed fragment may be obvious on plain radiographs or may be erroneously diagnosed as calcific tendinitis secondary to impingement (Fig. 28.9). MRI depicts the associated subchondral marrow changes and allows an accurate diagnosis.

The most common site of avulsion injuries in the pelvis is the ischial tuberosity where the hamstring muscles insert. The above injury is observed in runners or dancers (Metzmaker and Pappas 1985).

Fig. 28.8. A weekend warrior, 56-year-old male, presenting with pain after playing golf for 6 h. Oblique fat-suppressed T2 weighted MR image shows acute avulsion injury of the greater tuberosity (*arrow*)

If the radiologically obvious fragment is displaced more than 2 cm, fibrous union with associated disability may occur. Avulsion injuries of the anterior superior iliac spine occur in sprinters and usually heal without any sequelae after rest. Avulsion injuries of the anterior inferior iliac spine are less common. Athletes with the latter injuries may fully start their activities in about five to six weeks. Avulsion injuries in the symphysis pubis and inferior pubic ramus usually result from chronic overuse and are rarely acute following contact sports. These injuries are not obvious on plain radiographs because osseous fragments are not usually seen. MRI can be diagnostic as it demonstrates bone marrow changes in fat suppressed images in the pubic bones, but it does not have any impact on treatment. The chronic form of this injury may simulate infection or Ewing sarcoma. Avulsion of the greater trochanter of the femur can be minimally displaced and thus plain radiographs may be negative.

Avulsion injuries around the knee include the Segond’s fracture, fibular head avulsion, Gerdy’ s

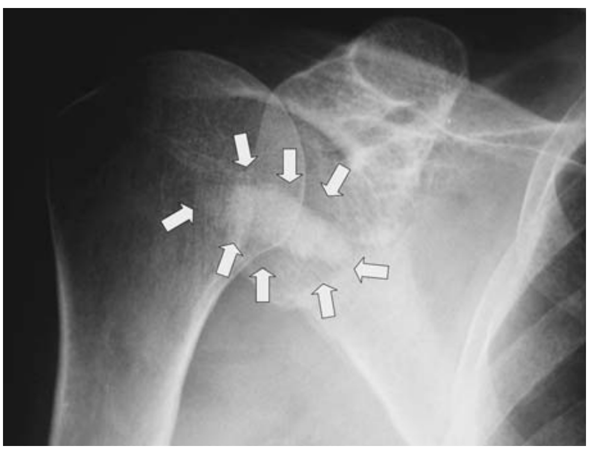

a

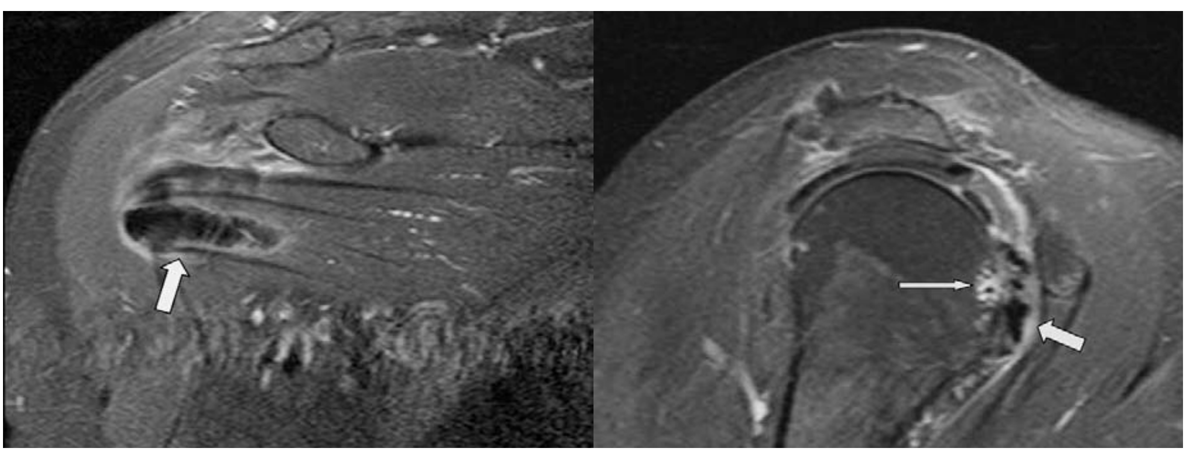

b

Fig. 28.9a,b. Chronic avulsion injury of the lesser tuberosity in a 32-year-old wrestler. **a** The plain radiograph shows extensive calcification of subscapularis tendon (*arrows*). **b** Contrast enhanced fat suppressed T1 weighted MR images in oblique coronal (*left*) and sagittal (*right*) planes, demonstrate calcification of the subscapularis tendon (*thick arrows*) as well as subchondral marrow edema (*thin arrow*)

tubercle avulsion, avulsion of the tibial eminence and avulsion of the posterior cruciate ligament at the tibial insertion. Osgood-Schlatter disease represents a chronic avulsion injury resulting from repetitive microtrauma at the insertion site of the patellar tendon (see Chap. 18). Sports related to this disorder include tennis, soccer and jumping. Acute avulsion injuries of the tibial tubercle are rare and commonly occur in athletes, usually in basketball often superimposed on a pre-existing Osgood-Schlatter (Fig. 28.10). In this case, the fracture pattern determines return to sports ranging from two to six months (Stanitski 1998b).

28.2.2.2 Monitoring

Plain radiographs are generally sufficient for the diagnosis and follow-up of avulsion injuries. MRI is not recommended because it may demonstrate extensive soft tissue and bone marrow edema, misinterpreted as an aggressive lesion. When symptoms persist despite treatment, follow up radiographs are required for assessing possible significant displacement.

Subacute injuries may have an aggressive radiographic appearance due to coexistence of mixed lytic and sclerotic areas. Chronic or old inactive injuries may be associated with an osseous mass, simulating a neoplastic or infectious process. In case of equivocal plain radiographic findings or when the injury is not in the acute phase, CT might provide the correct diagnosis (Fig. 28.6b).

28.2.3 Osteochondral Fractures and Focal Osseous Indentations

Osteochondral fractures are intraarticular fractures involving both the articular cartilage and the bone. These fractures may be acute or chronic. The latter, also known as osteochondritis dissecans, can be caused by repetitive microinjuries. Osteochondritis dissecans is demonstrated on plain radiographs as an oval radiolucency of the articular surface, which may contain a central bony fragment. About 70% of acute osteochondral fractures will be diagnosed correctly by plain radiography (Pettine and Morrey 1987) and most of them with CT (Anderson et al. 1989). However, MRI is the method of choice for assessing these injuries since it can better depict the articular cartilage as well as the subchondral bone (Bohndorf 1999).

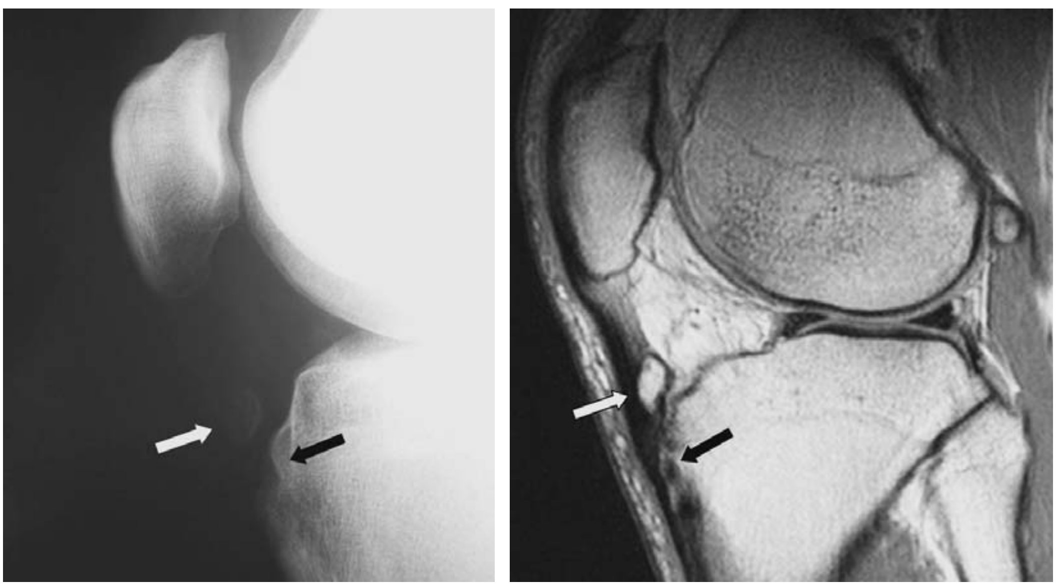

a b

Fig. 28.10a,b. Old avulsion injury of the tibial tubercle in a 21-year-old patient with persistent anterior knee pain, a known Osgood-Schlatter from adolescence and a history of sudden pain after landing during basketball 5 years ago. **a** The lateral radiograph demonstrates the avulsed fragment (*white arrow*) and the healed Osgood-Schlatter disease (*black arrow*). **b** The sagittal PD-TSE MR image shows to better advantage the fragment (*white arrow*), the patella baja and the healed Osgood-Schlatter disease (*black arrow*)

28.2.3.1
Natural History

Acute osteochondral fractures are commonly found at the knee, associated with anterior cruciate ligament ruptures (Rosen et al. 1991) (Fig. 28.11), and at the talar dome, associated with ankle sprains (Shea and Manoli 1993; Stone 1996). Osteochondral lesions of the talus are often missed initially because many athletes with "ankle sprains" are not treated by specialists. The most widely accepted classification applied in both radiology and arthroscopy practice is the one suggested by Berndt and Harty (1959). This staging schema, though, is limited by the inability to predict prognosis and guide treatment. Lesions with flattening on clinical presentation are considered clinically stable, whereas lesions with fragments are unstable (Takahara et al. 2000). MRI is useful in demonstrating instability of the lesion by depicting fluid signal and/or cystic changes at its deep margin (De Smet et al. 1996). MR arthrography can be useful when development of granulation tissue in the deep surface may simulate fluid and may lead to an erroneous diagnosis of an unstable lesion. On conventional MRI the presence of fatty marrow and contrast enhancement suggests viability of the fragment (Linklater 2004). Activity of the lesion with potential further progression and displacement is suggested by the presence of surrounding bone marrow edema the extent of which correlates closely to the degree of clinical symptoms (Morrison 2003) (Fig. 28.12). Stable osteochondral lesions in patients with open physes are usually treated with rest and splinting, whereas unstable lesions are treated surgically. The surgical options include drilling, fixation or debridement of the fragment and performance of autologous osteochondral transfer, autologous chondrocyte implantation or osteochondral allografting (Peterson et al. 2000; Rubin et al. 2000).

Extraarticular focal osseous indentations commonly occur in shoulder instability and dislocations. The Hill-Sachs impaction injury is located in the superolateral aspect of the humeral head. This defect is a compression fracture occurring during anterior dislocation after impaction of the humeral head over the anteroinferior glenoid rim. The presence of subchondral bone marrow edema suggests that the lesion is acute or subacute. Increasing size of this defect in follow-up imaging, suggests that the patient sustains recurrent dislocations. A "reverse" Hill-Sachs defect, results from posterior dislocation. In overhead athletes such as throwers, swimmers and tennis players, an internal (posterosuperior) impingement syndrome may occur (Giaroli et al. 2005). This entity is characterized by supraspinatus tendinopathy resulting from repetitive contact with the posterosuperior labrum between the supra- and infraspinatus tendon interval. A common finding in these athletes is a focal indentation in the cortex of the posterior greater tuberosity (Fig. 28.13) with or without focal bone marrow "edema" like and degenerative cystic changes (Nakagawa et al. 2001). It has been suggested in a limited number of

a 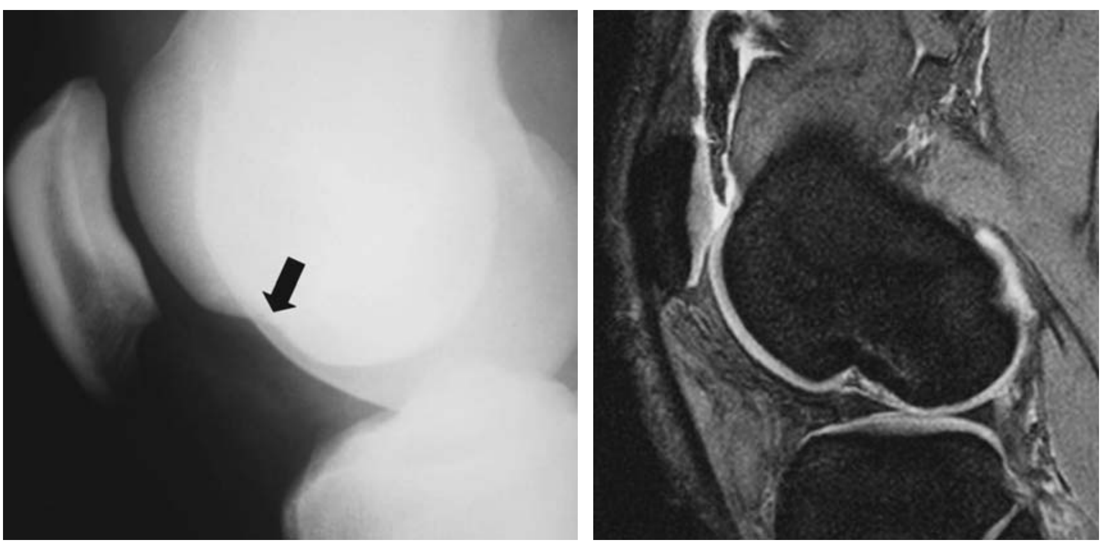 b

Fig. 28.11a,b. A 22-year-old male with twisting injury of the knee and anterior cruciate ligament tear during basketball. **a** The plain radiograph shows the impacted osteochondral injury (*arrow*). **b** The 2D multi-echo gradient echo MR image in the sagittal plane shows to better advantage the disruption of the articular cartilage over the impacted injury

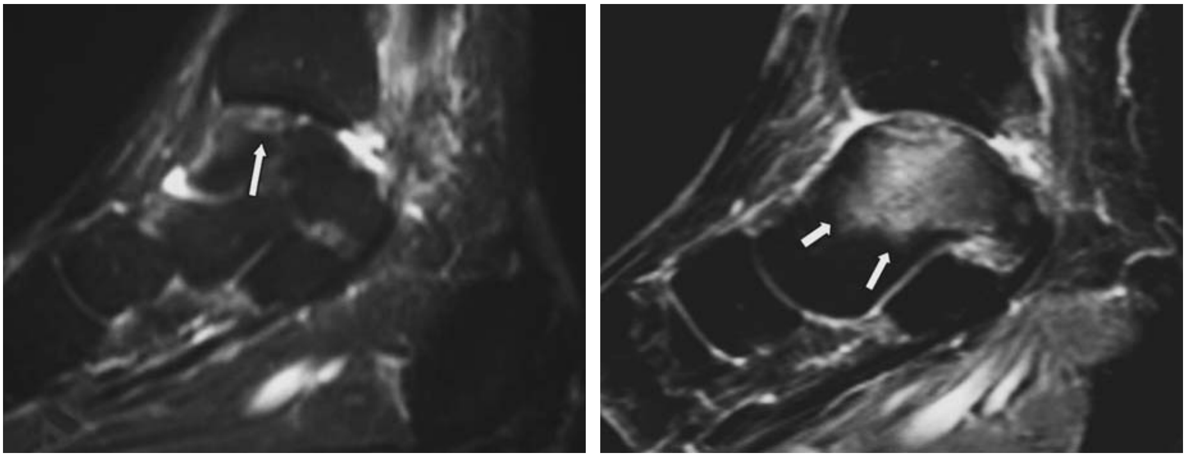

a b

Fig. 28.12a,b. Active osteochondral lesion in a 46-year-old weekend athlete. **a** The fat suppressed MR image in the sagittal plane shows an osteochondral lesion in the talar dome (*arrow*). **b** Eight months later, the symptoms deteriorated despite conservative treatment and MR image shows diffuse bone marrow edema in keeping with activity of the lesion (*arrows*)

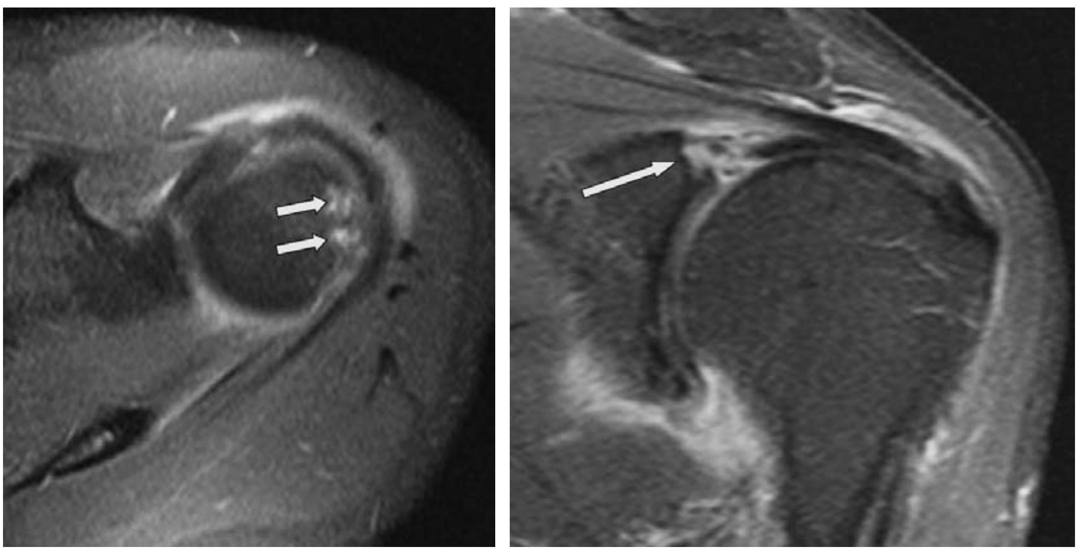

a b

Fig. 28.13a,b. Indirect MR arthrogram in a 30-year-old tennis player with posterosuperior impingement. **a** The axial fat suppressed T1 weighted SE MR image shows a focal notch with small cysts in the posterolateral greater tuberosity (*arrows*). **b** The oblique coronal fat suppressed T1 weighted SE MR image shows disruption of the superior labrum (*arrow*)

patients, that these bony cystlike changes disappear, presumably due to improved mechanics, after a successful surgical treatment (Giaroli et al. 2005).

28.2.3.2
Monitoring

All patients with persistent symptoms 6 to 12 weeks after an ankle sprain should undergo CT or MRI to exclude a possible osteochondral lesion of the talus. Patients with a stable osteochondral lesion and persisting symptoms beyond three months of treatment, may require MRI to determine if the stage of the lesion has changed. Patients with symptoms beyond six months should undergo arthroscopy. MRI is the method of choice for the assessment of the progress of osteochondral lesions and the response to treatment. Unstable fragments will usually progress and become a loose body. Postoperative assessment of healing and incorporation can be evaluated with contrast enhanced MRI (see also Chap. 20) (Sanders et al. 2001). Osseous indentations do not require mon-

itoring with imaging as they do not influence the therapeutic management.

28.3 Microfractures

Before the advent of MRI, microfractures referred to the osseous injuries in the pediatric population not associated with a fracture line in plain radiographs. These injuries, also known as incomplete linear fractures, include *bowing fractures* which usually heal without any periostitis, *greenstick* and *torus* fractures. Scintigraphy was able to demonstrate increased uptake of the injured bone. The application of musculoskeletal MRI allowed depiction of various similar disorders in adults. These include the spectrum of *stress fractures and reactions*, *bone bruise*, *acute occult fractures* and *physeal microfractures*.

28.3.1 Stress Fractures and Reactions

Stress fractures and reactions result from repetitive stress to an otherwise normal bone and represent a variety of osseous and associated soft tissue injuries (Anderson and Greenspan 1996). They are common injuries caused by prolonged activities such as marching or running (Jones et al. 1989; Daffner and Pavlov 1992; Anderson and Greenspan 1996) and are usually encountered in the lower extremities, especially tibia, femoral neck and metatarsals (Coady and Micheli 1997). The importance of early diagnosis of a stress lesion has been highlighted by Ohta-Fukushima et al. (2002) who showed that athletes with an early diagnosis of stress injury return to their sport within 10.4 weeks as opposed to 18.4 weeks in those with a diagnosis later than 3 weeks after the onset of symptoms. Close correlation between imaging and clinical findings is important since MRI is so sensitive that it can show marrow edema-like changes even in asymptomatic runners (Lazzarini et al. 1997; Bergman et al. 2004).

Shin splints, or *medial tibial stress syndrome*, and *thigh splints* or *adductor insertion avulsion syndrome* are terms representing an early form of the stress injuries spectrum (Stress fractures are described in detail in Chap. 7) (Fredericson et al. 1995; Anderson et al. 1997, 2001; Hwang et al. 2005).

28.3.1.1 Natural History and Monitoring

Plain radiographs are not a sensitive method for depicting early stress injuries (Matheson et al. 1987). Stress fractures are demonstrated radiologically two to four weeks after the onset of pain, as a sclerotic line perpendicular to the long axis of the trabeculae. Depending upon the duration of symptoms, a periosteal reaction may be present. Indeed, periostitis may be the only radiological manifestation of the underlying injury. Follow-up radiographs demonstrate the evolution and healing of the injury thus eliminating the need for a biopsy in cases that the clinical history is not helpful and an aggressive lesion is suspected. Multi-detector CT with its multiplanar capability and bone algorithm reconstructions is able to detect the fracture lucent line or the periosteal reaction in specific anatomic locations such as the tibia (Fig. 28.14), sacrum, spine, and tarsal navicular. Bone scintigraphy has been used as the gold standard for assessing stress injuries (Anderson and Greenspan 1996). The low specificity though of this imaging modality together with the radiation risk and lack of anatomic detail, limits its role in the management of stress injuries. In addition, follow-up which is important in elite athletes, is further limited by the fact that uptake may be present for several months (Anderson and Greenspan 1996).

MRI applying STIR and T2 weighted fat suppressed sequences has emerged as the imaging technique of choice, providing excellent sensitivity and specificity together with superb anatomical detail (Fredericson et al. 1995; Arendt and Griffiths 1997; Yao et al. 1998). MRI findings precede by weeks those of plain radiographs also demonstrating associated soft tissue injuries. MRI is better than scintigraphy at depicting early stress injuries, possibly due to absence of significant osteoblastic response at this stage and lacks ionizing radiation which is of consideration when applied to young athletes and in follow-up studies (Deutch et al. 1997; Gaeta et al. 2005).

Bone marrow changes may be present on MRI of asymptomatic athletes undertaking intensive physical activity. These stress reactions reflect high training load and resolve or continue as asymptomatic changes on imaging regardless of continuation of intensive physical training (Kiuru et al. 2005). Bergman et al. (2004) have shown that tibial stress reactions detected on MRI in asymptomatic runners are not associated with future symptomatic tibial stress injuries. Therefore, these findings are not clini-

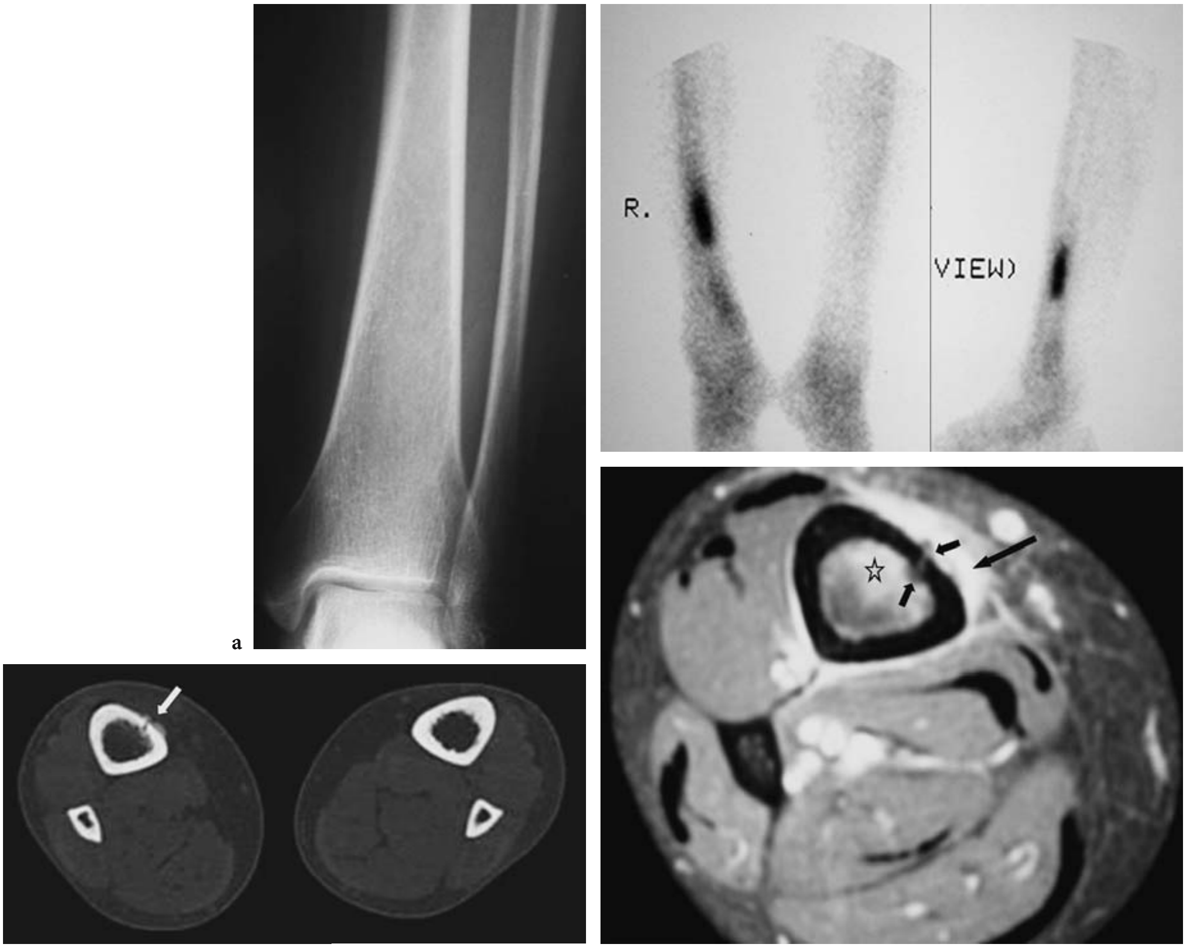

Fig. 28.14a–d. Stress fracture in a runner. **a** The plain film is normal. **b** Scintigraphy reveals increased uptake in the tibia. **c** CT shows the lucent fracture line and the callus formation in the anterior cortex (*arrow*). **d** Contrast-enhanced fat suppressed SE T1 weighted MR image shows the soft-tissue enhancement (*long arrow*), the periosteal and endosteal new bone formation at the fracture site (*small arrows*) and bone marrow edema (*asterisk*)

cally important and there is no need for unnecessary rest or modification of the training program.

Symptomatic patients with stress injuries present with localized pain in the end rather than at the onset of the athletic activity. Patients' complaints tend to occur following increase or change in sports activity. The pain is typically relieved at rest and can recur with the onset of the activity. With increased severity of the injury, the pain may persist at rest. A suggested two- to three-week period of rest or decrease in training may be curative. No follow-up imaging in *shin splint* and *thigh splint* syndromes is needed.

Patients with sacral stress fractures recover quickly with rest and return to sports within 4–6 weeks. Stress fractures of the pubic rami heal successfully after six to ten weeks of rest. Femoral neck stress fractures need to be diagnosed early because of their tendency for a frank complete fracture with displacement, particularly when located laterally (Spitz and Newberg 2003). A high degree of clinical suspicion for its presence should be followed by a prompt MRI examination. Most fractures, however, occur medially where the risk for displacement is lower. Most patients with femoral shaft stress fractures are able to resume full sport activity by 12 weeks.

Spondylolysis is considered a non-united stress fracture of the pars interarticularis in children and young adult athletes. Athletes with asymptomatic spondylolysis require no treatment or follow-up imaging. For symptomatic patients with acute spondylolysis, treatment consists of restriction of sports activity varying from six weeks to six months that should generally continue until the athlete becomes asymptomatic. The treatment is different in patients

with a bilateral pars defect, due to the risk of spondylolisthesis. In athletes with stress-induced spondylolysis, fat suppressed MRI and scintigraphy can demonstrate if this lesion is active and therefore responsible for the symptoms. Most athletes become asymptomatic and develop no long-term sequelae although only 30–50% of stress fractures demonstrate radiologically bony healing.

Fredericson et al. (1995) classified stress injuries in four grades according to MRI findings. Patients with grade I injuries return to controlled athletic activities within two to three weeks, patients with grade II injuries within four to six weeks, and patients with grade III in six to nine weeks. Patients with grade IV injuries, on the other hand, should be treated with a cast for six weeks and restrain from impact activities for another six weeks. The presence of a medullary line or a cortical abnormality in keeping with grade IV was shown by Yao et al. (1998) to correlate with a longer period of recovery. In pediatric stress fractures, there is often extensive periosteal reaction and bone marrow changes which might lead to an erroneous diagnosis of a neoplastic process (Horev et al. 1990; Anderson and Greenspan 1996) (Fig. 28.15). In these cases, MRI can be applied for the diagnosis with direct evaluation of bone marrow edema and for the evaluation of the healing process due to its inherent lack of radiation (Fig. 28.16). CT should be only used when no fracture line is demonstrated with plain radiographs and MRI.

Low risk stress fractures are considered those located at the posterior or medial aspect of the tibia, fibula and lateral malleolus. Treatment consists of a rest period of two to eight weeks with limited weightbearing progressing gradually to full athletic activities.

High risk stress fractures are considered those located at the femoral neck, anterior midtibia, medial malleolus, tarsal navicular, talus, fifth metatarsal, base of second metatarsal, patella, and great toe sesamoids. High risk fractures may require longer recovery period and often surgical intervention.

28.3.2 Acute Subchondral Injury-Bone Bruise

Bone bruise and *bone contusion* are synonymous terms to describe the occult injury of the trabecular bone resulting in haemorrhage, edema and infarction (Rangger et al. 1998; Bohndorf 1999; Ryu et al. 2000; Mandalia et al. 2005). MRI is very sensitive in detecting bone bruises (Mink and Deutch

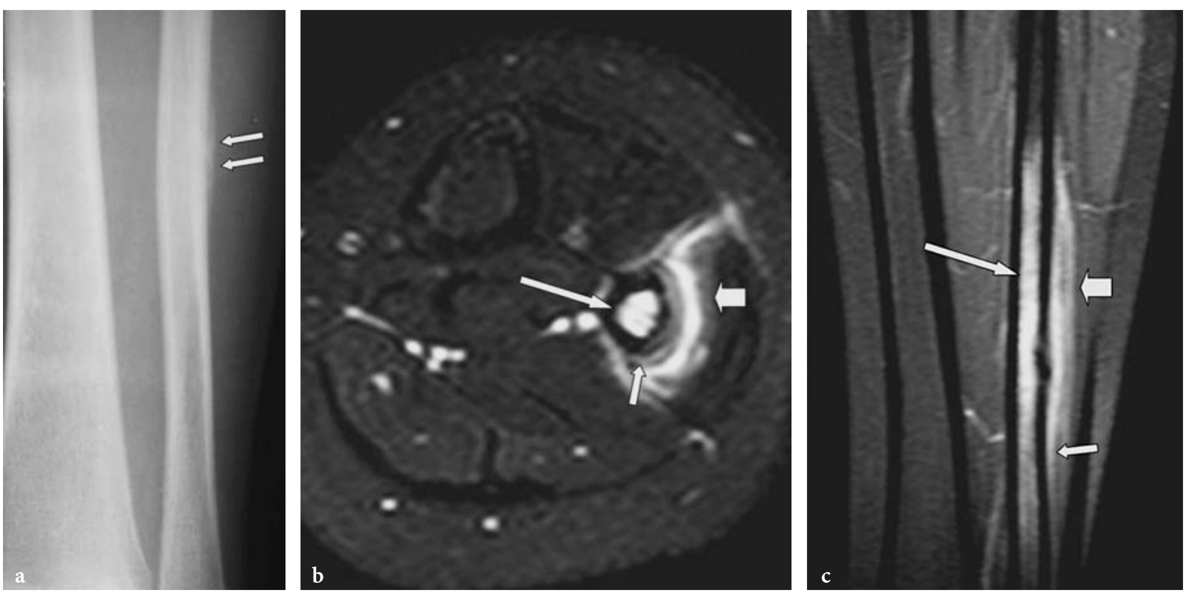

Fig. 28.15a–c. A seven-year-old girl with calf pain but no history of trauma or sports activity and a biopsy proven stress fracture of the fibula. **a** The plain film shows a periosteal new bone formation (*arrows*). **b** The axial fat suppressed T2 weighted MR image shows the soft tissue changes (*thick arrow*), the periosteal new bone formation (*arrow*) and the bone marrow changes (*long white arrow*). **c** Contrast-enhanced fat suppressed SE T1 weighted MR image in the coronal plane shows extensive soft tissue enhancement (*thick arrow*), subperiosteal enhancement (*arrow*) and bone marrow changes (*long arrow*)

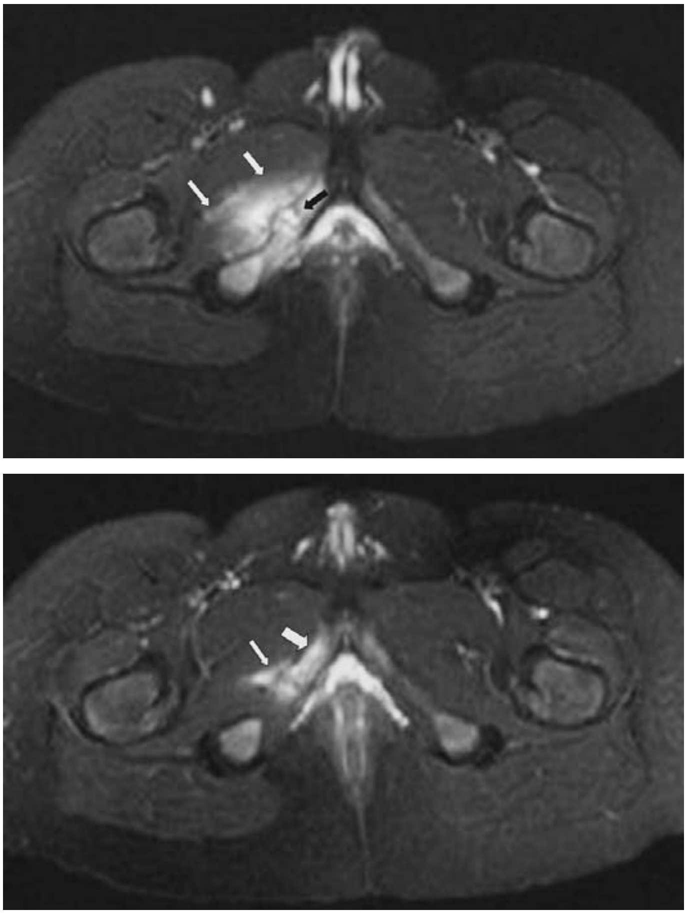

a

b

Fig. 28.16a,b. A 14-year-old male with a stress fracture of the pubic bone. **a** The fat-suppressed T2 weighted MR image one week after the onset of symptoms, shows the stress fracture (*black arrow*) and the muscular strain (*white arrows*). **b** A repeat MR imaging examination one month later shows resolution of the muscular strain (*thin arrow*) and of the fracture line with residual bone marrow edema (*arrow*)

1989; Kapelov et al. 1993) and understanding the mechanism and severity of injury (Sanders et al. 2000).

28.3.2.1
Natural History and Monitoring

There might be an increase with MRI in volume of the bone bruise within a few weeks following injury (Davies et al. 2004). Various studies have addressed the rate and degree of resolution of the bruised bone, mainly after knee injuries (Ariyoshi et al. 1997; Bretlau et al. 2002; Davies et al. 2004). It appears that in most patients there is a significant decrease or complete resolution of the lesion within 12–18 weeks (Vanhoenacker et al. 2005) (Fig. 28.17); however patients with persisting MRI abnormalities for up to two years have been reported. Athletes with isolated bone bruises appear to return to previous sports activities within three months on average (Wright et al. 2004).

Bone bruises might indicate an overlying osteochondral injury. This should be particularly suspected when the pattern of resolution on follow-up studies occurs towards the articular surface (Davies et al. 2004). Long term cartilage degeneration might occur even without imaging findings of acute chondral injury during the acute phase. This may be due either to microinjury of the chondrocytes or to inadequate weight bearing protection during resolution which might induce increased load to the articular cartilage.

28.3.3
Acute Occult Fractures

Acute occult fractures are defined as those not detected by plain radiographs. They may be seen on MRI as fracture lines either associated with bone bruises or without any bone marrow changes (Fig. 28.18). Usually they are detected with MRI in the subacute

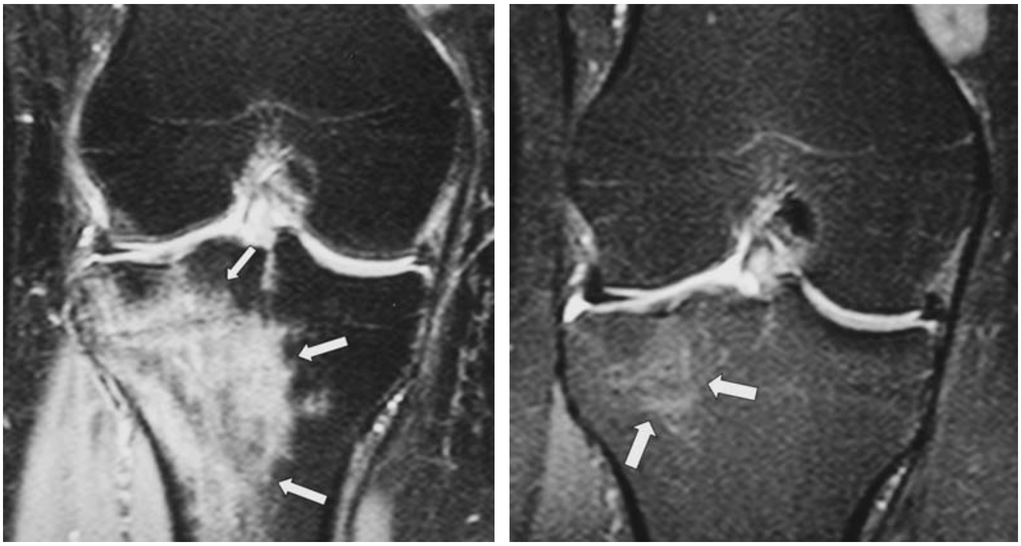

Fig. 28.17a,b. Resolution pattern of bone bruise. Coronal fat suppressed TSE T2 weighted MR image of the right knee immediately after a contact injury and three months later. **a** Extensive impaction bone marrow edema at the proximal tibia (*arrows*). **b** There is centripetal resolution of the marrow edema, with some residual lesion at the centre of the original lesion (*arrows*) (Images courtesy of F. Vanhoenacker)

stage, due to persistent symptoms. Common sites for occult fractures include proximal tibia, distal femur, talar neck, scaphoid, anterior calcaneal process and lateral talar process, also known as snowboarder's fracture. In one study, it was found that in patients with presumed scaphoid fracture and normal radiographs, scintigraphy was able to demonstrate abnormal uptake in 45% and CT depicted a fracture in 27.4% of the cases (Groves et al. 2005).

28.3.3.1
Natural History and Monitoring

The true incidence of long bones occult fractures can not be estimated, as these injuries are not detected with plain radiographs. Most of these injuries will resolve after six to eight weeks and therefore no radiological monitoring is required. Non-union is unlikely since no major cortical disruption occurs.

Acute scaphoid fractures are of particular interest because in up to 65% of cases they remain radiographically occult immediately after injury, and disrupted blood supply may result in proximal pole osteonecrosis. In addition, these fractures may not be painful enough to demand medical care and therefore late diagnoses with non union and/or osteonecrosis are common (Fig. 28.4). Focal radiolucent areas may develop at the site of previous

Fig. 28.18. A 15-year-old football player with a normal radiograph after injury (not shown). The sagittal fat suppressed PD MR image, shows the fracture line extending from the physis to the posterior cortex (*arrow*). There is also post-traumatic edema surrounding the patellar tendon

microfractures (Rennie and Finlay 2003). Occult fractures are best appreciated with MRI (Rosner et al. 2004). Early use of MRI may prove to be cost-effective if early confirmation of the presence of a scaphoid fracture would affect treatment and the patient's returning to sports activities. Gadolinium-enhanced MRI is the method of choice for the preoperative assessment of the vascular status and healing potential of a given fracture as well as for postoperative assessment of graft viability (Cerezal et al. 2000; Dailiana et al. 2004).

28.3.4 Physeal Microfractures

Growth plate or physis in the growing skeleton represents a thin layer of cartilage located between the metaphysis and epiphysis or apophysis. Most of the physeal injuries occur during sports activities, more commonly in males with a median age of 13 years. The most frequently injured bones are the distal femur, radius, tibia, ulna, fibula and proximal humerus.

Fig. 28.19. A ten-year-old male with a water skiing injury. The coronal fat suppressed T2 weighted MR image shows bone bruise in the tibial metaphysis and epiphysis and a physeal injury demonstrated with high signal intensity without any widening of the physis (*arrows*). There are also soft tissue edematous and hemorrhagic changes

Before the advent of MRI, the growth plate was indirectly evaluated on plain radiographs, seen as a radiolucent line. Acute injury of the growth plate was diagnosed when there was decreased or increased width of the physis with or without displacement of the surrounding fractured osseous structures. Acute physeal injuries without osseous changes (types I and V Salter-Harris) commonly occur in children and may be obvious exclusively with MRI (Fig. 28.19). An injured growth plate can be associated with a subperiosteal haematoma up to the diaphysis where the bony attachment of the periosteum is not firm enough (Fig. 28.20).

28.3.4.1 Natural History

Repair of growth plate injury occurs quickly if there is no cartilage cell layer or vascular supply disruption and normal growth occurs in three weeks. Good prognosis is the rule for most of the physeal fractures. About 15% of all physeal fractures lead to growth arrest with a bony bridge formation across the physis. This may cause limb shortening or angular deformity depending upon several factors (Oeppen and Jaramillo 2003). Growth arrest results from vascular compromise in the epiphyseal site and is much more common at the distal ends of long bones and in the lower extremities. Patients close to skeletal maturity are less likely to develop deformity. A fracture parallel to the physis is at greater risk for growth arrest, especially when the juxtaepiphyseal layer, which includes the germinal zone, rather than the juxtametaphyseal layer is involved. For types I Salter-Harris fractures, return to sports is possible within 12 weeks (Stanitski 1998a).

Chronic physeal stress injuries are commonly found in young gymnasts, involving the distal radius and ulna bilaterally where the surrounding structures are stronger than the physis. Repetitive stress from overuse causes shearing microfractures locally. Chronic physeal injuries have also been described in skateboarders and adolescent runners with involvement of the distal femoral, proximal tibial and distal fibular sites. Plain radiographs may show widened physis along with sclerosis and rarely lucent metaphyseal changes. Cessation of the sports activity allows for a full recovery in six months. Undiagnosed chronic physeal injuries of the distal radius may cause premature fusion and ulnar positive variance in adulthood.

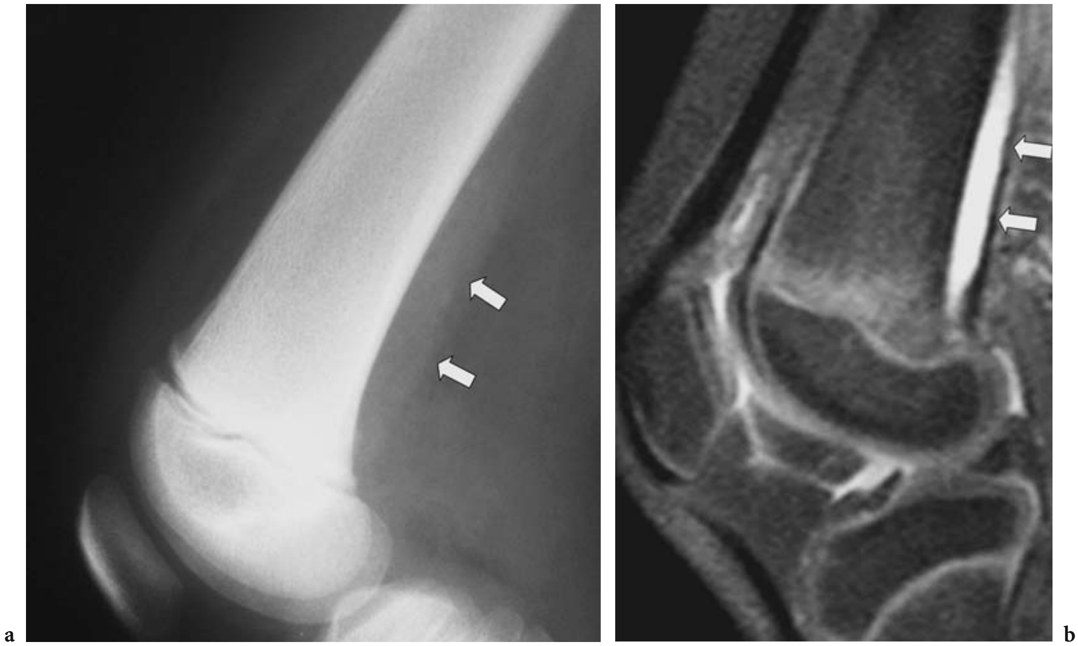

Fig. 28.20a,b. A nine-year-old girl with a skiing injury. **a** The lateral plain film shows a soft tissue opacity posterior to the femoral metadiaphysis (*arrows*). **b** The sagittal fat suppressed PD MR image shows that the opacity represents a subperiosteal hematoma (*arrows*), presumably secondary to an occult physeal fracture. There is also a shearing injury of the Hoffa's fat pad

28.3.4.2 Monitoring

MRI can be used to depict an acute physeal fracture in very young children with unossified epiphyses but as a rule it is not routinely performed in acute physeal injuries. Radiological follow-up is essential in order to assess normal growth and guide surgical management in cases of suspected growth disturbance. Even the most benign type I Salter-Harris injuries may produce growth arrest. Comparative radiographs of both sides at quarterly intervals for a year should be performed. Most growth arrests are evident by two years after a severe physeal injury. When a bony bridge is suspected on the plain radiographs, MRI can assess the central or peripheral location as well as the physeal area involved. Gradient echo 3D with fat suppression sequences can be applied to demonstrate the bony bridge as a low signal intensity structure surrounded by the hyperintense physeal cartilage and to calculate the area with its multiplanar capabilities. Bony bridges involving less than 50% of the physeal area are associated with resumption of growth if resected (Peterson 1984).

28.4 Conclusions

Evaluation of sports-related fractures and microfractures is heavily dependent on imaging. With increased participation of children and adults in organized or recreational sports activities, radiologists are frequently asked to assist in the diagnosis and management of these patients. Plain radiographs are important in depicting and monitoring osseous fractures, avulsion injuries and osteochondral lesions. MRI is extremely valuable for assessing, grading and monitoring healing of osteochondral lesions and microfractures in the context of both acute trauma and stress injury.

Things to Remember

1. Evaluation of sports-related fractures and microfractures is heavily dependent on imaging.
2. Plain radiographs are important in depicting and monitoring osseous fractures and avulsion injuries.
3. CT can depict most of the osteochondral fractures and is able to differentiate subacute avulsion injury and stress fracture from a malignant lesion.
4. MRI is extremely valuable for assessing and grading the osteochondral lesions and microfractures.
5. Monitoring of the healing process of microfractures is better performed with MRI

References

Anderson IF, Crichton KJ, Grattan-Smith T et al. (1989) Osteochondral fractures of the dome of the talus. J Bone Joint Surg Am 71:1143–1152

Ánderson MW, Greenspan A (1996) Stress fractures. Radiology 199:1–12

Anderson MW, Ugalde V, Batt M et al. (1997) Shin splints: MR appearance in a preliminary study. Radiology 204:177–180

Anderson MW, Kaplan PA, Dussault RG (2001) Adductor insertion avulsion syndrome (thigh splints): spectrum of MR imaging features. AJR Am J Roentgenol 177:673–675

Arendt EA, Griffiths HJ (1997) The use of MR imaging in the assessment and clinical management of stress reactions of bone in high-performance athletes. Clin Sports Med 16:291–306

Ariyoshi M, Nagata K, Sato K et al. (1997) Hemarthrosis of the knee and bone contusion. Kurume Med J 44:135–139

Bergman AG, Fredericson M, Ho C et al. (2004) Asymptomatic tibial stress reactions: MRI detection and clinical follow-up in distance runners. AJR Am J Roentgenol 183:635–638

Berndt AL, Harty M (1959) Transchondral fractures (osteochondritis dissecans) of the talus. J Bone Joint Surg 41:988–1020

Bohndorf K (1999) Imaging of acute injuries of the articular surfaces (chondral, osteochondral and subchondral fractures). Skelet Radiol 28:545–560

Brandser EA, el-Khoury GY, Kathol MH (1995) Adolescent hamstring avulsions that simulate tumors. Emerg Radiol 2:273–278

Bretlau T, Tuxoe J, Larsen L et al. (2002) Bone bruise in the acutely injured knee. Knee Surg Sports Traumatol Arthrosc 10:96–101

Burt CW, Overpeck MD (2001) Emergency visits for sports related injuries. Ann Emerg Med 37:301–308

Cerezal L, Abascal F, Canga A et al. (2000) Usefulness of gadolinium-enhanced MR imaging in the evaluation of the vascularity of scaphoid nonunions. AJR Am J Roentgenol 174:141–149

Chapman S (1992) The radiological dating of injuries. Arch Dis Child 67:1063–1065

Coady C, Micheli L (1997) Stress fractures in the padiatric athlete. Clin Sports Med 16:225–238

Crues RL, Dumont J (1975) Fracture healing. Can J Surg 18:403–413

Daffner R, Pavlov H (1992) Stress fractures: current concepts. AJR Am J Roentgenol 159:245–252

Dailiana ZH, Zachos V, Varitimidis S et al. (2004) Scaphoid nonunions treated with vascularised bone grafts: MRI assessment. Eur J Radiol 50:217–224

Davies NH, Niall D, King LJ et al. (2004) Magnetic resonance imaging of bone bruising in the acutely injured knee-short-term outcome. Clin Radiol 59:439–445

De Smet AA, Ilahi OA, Graf BK (1996) Reassessment of the MR criteria for stability of osteochondritis dissecans in the knee and ankle. Skelet Radiol 25:159–163

Deutsch AL, Coel MN, Mink JH (1997) Imaging of stress injuries to bone: radiography, scintigraphy, and MR imaging. Clin Sports Med 16:275–290

el-Khoury GY, Daniel WW, Kathol MH (1997) Acute and chronic avulsive injuries. Radiol Clin North Am 35:747–766

Fredericson M, Bergman G, Hoffman KL et al. (1995) Tibial stress reaction in runners: correlation of clinical symptoms and scintigraphy with a new MRI grading system. Am J Sports Med 23:472–481

Frost HM (1989a) Biology of fracture healing: an overview for clinicians. Part I. Clin Orthop Relat Res 248:283–293

Frost HM (1989b) Biology of fracture healing: an overview for clinicians. Part II. Clin Orthop Relat Res 248:294–309

Gaeta M, Minutoli F, Scribano E et al. (2005) CT and MR imaging findings in athletes with early tibial stress injuries: comparison with bone scintigraphy findings and emphasis on cortical abnormalities. Radiology 235:553–561

Giaroli EL, Major NM, Higgins LD (2005) MRI of internal impingement of the shoulder. AJR Am J Roentgenol 185:925–929

Groves AM, Cheow H, Balan K et al. (2005) 16-MDCT in the detection of occult wrist fractures: a Comparison with skeletal scintigraphy AJR Am J Roentgenol 184:1470–1474

Heppenstall RB (1980) Fracture healing. In: Heppenstall RB (ed) Fracture treatment and healing. Saunders, Philadelphia, pp 35–64

Horev G, Koreneich L, Ziv N et al. (1990) The enigma of stress fractures in the pediatric age: clarification or confusion through the new imaging modalities. Pediatr Radiol 20:469–471

Hwang B, Fredericson M, Chung CB et al. (2005) MRI findings of femoral diaphyseal stress injuries in athletes. AJR Am J Roentgenol 185:166–173

Islam O, Soboleski D, Symons S et al. (2000) Development and duration of radiographic signs of bone healing in Children. AJR Am J Roentgenol 175:75–78

Jones BH, Harris JM, Vinh TN et al. (1989) Exercise-induced stress fractures and stress reactions of bone. Epidemiology, etiology, and classification. Exerc Sport Sci Rev 17:379–422
Kapelov SR, Teresi LM, Bradley WG et al. (1993) Bone contusions of the knee: increased lesion detection with fast spin-echo MR imaging with spectroscopic fat saturation. Radiology 189:901–904
Kiuru MJ, Niva M, Reponen A et al. (2005) Bone stress injuries in asymptomatic elite recruits: a clinical and MRI study. Am J Sports Med 33:272–276
Lawson GM, Hajducka C, McQueen MM (1995) Sports fractures of the distal radius-epidemiology and outcome. Injury 26:33–36
Lazzarini KM, Troiano RN, Smith RC (1997) Can running cause the appearance of marrow edema on MR images of the foot and ankle? Radiology 202:540–542
Linklater J (2004) Ligamentous, chondral, and osteochondral ankle injuries in athletes. Semin Musculoskelet Radiol 8:81–98
Livstone BJ, Parker L, Levin DC (2002) Trends in the utilization of MR angiography and body MR imaging in the US medicare population: 1993–1998. Radiology 222:615–618
Low G, Raby N (2005) Can follow-up radiography for acute scaphoid fracture still be considered a valid examination? Clin Radiol 60:1106–1110
Mandalia V, Fogg AJ, Chari R et al. (2005) Bone bruising of the knee. Clin Radiol 60:627–636
Matheson GO, Clement DB, McKenzie DC et al. (1987) Stress fractures in athletes; a study of 320 cases. Am J Sports Med 15:46–58
Metzmaker JN, Pappas AM (1985) Avulsion fractures of the pelvis. Am J Sports Med 13:349–358
Micheli LJ, Fehlandt AF Jr (1992) Overuse injuries to tendons and apophyses in children and adolescents. Clin Sports Med 11:713–726
Mink JH, Deutsch AL (1989) Occult cartilage and bone injuries of the knee: detection, classification and assessment with MR imaging. Radiology 170:823–829
Morrison WB (2003) MRI of sports injuries of the ankle. Top Magn Reson Imaging 14:179–197
Nakagawa S, Yoneda M, Hyashida K et al. (2001) Greater tuberosity notch: an important indicator of articular-side partial rotator cuff tears in the shoulders of throwing athletes. Am J Sports Med 29:762–770
Oeppen RS, Jaramillo D (2003) Sports injuries in the young athlete. Top Magn Reson Imaging 14:199–208
Ohta-Fukushima M, Mutoh Y, Takasugi S et al. (2002) Characteristics of stress fractures in young athletes under 20 years. J Sports Med Phys Fitness 42:198–206
Overdeck KH, Palmer WE (2004) Imaging of hip and groin injuries in athletes. Semin Musculoskel Radiol 8:41–55
Peterson HA (1984) Partial growth plate arrest and its treatment. J Pediatr Orthop 4:246–258
Peterson L, Minas T, Brittberg M et al. (2000) Two- to 9-year outcome after autologous chondrocyte transplantation of the knee. Clin Orthop 374:212–234
Pettine KA, Morrey B (1987) Osteochondral fractures of the talus. A long term follow-up. J Bone Joint Surg Br 69:89–92
Rangger C, Kathrein A, Freund MC et al. (1998) Bone bruise of the knee: histology and cryosections in 5 cases. Acta Orthop Scand 69:291–294
Rennie WJ, Finlay DB (2003) Posttraumatic cystlike defects of the scaphoid: late sign of occult microfracture and useful indicator of delayed union. AJR Am J Roentgenol 180:655–658
Rosen M, Jackson D, Berger P (1991) Occult osseous lesions documented by magnetic resonance imaging associated with anterior cruciate ligament ruptures. Arthrosopy 7:45–51
Rosner JL, Zlatkin MB, Clifford P et al. (2004) Imaging of athletic wrist and hand injuries. Semin Musculoskelet Radiol 8:57–79
Rubin DA, Harner CD, Costello JM (2000) Treatable chondral injuries in the knee: frequency of associated focal subchondral edema. AJR Am J Roentgenol 174:1099–1106
Ryu KM, Jin W, Ko YT et al. (2000) Bone bruises: MR characteristics and histological correlation in the young pig. Clin Imaging 24:371–380
Salter RB, Harris R (1963) Injuries involving the epiphyseal plate. J Bone Joint Surg 45A:587–622
Sanders TG, Medynski MA, Feller JF et al. (2000) Bone contusion pattern of the knee at MR imaging: footprint of the mechanism of injury. RadioGraphics 20:S135–151
Sanders TG, Mentzer KD, Miller M et al. (2001) Autogenous osteochondral "plug" transfer for the treatment of focal chondral defects: postoperative MR appearance with clinical correlation. Skeletal Radiol 30:570–578
Shea MP, Manoli A II (1993) Osteochondral lesions of the talar dome. Foot Ankle 14:48–55
Sofka CM (2004) Ultrasound in sports medicine. Semin Musculoskel Radiol 8:17–27
Spitz D, Newberg A (2003) Imaging of stress fractures in the athlete. Magn Reson Imaging Clin N Am 11:323–339
Stanitski CL (1998a) Epiphyseal fractures about knee. Oper Techn Sports Med 6:234–242
Stanitski CL (1998b) Acute tibial tubercle avulsion fractures. Oper Techn Sports Med 6:243–246
Stone JW (1996) Osteochondral lesions of the talar dome. J Am Acad Orthop Surg 4:63–73
Takahara M, Ogino T, Takagi M et al. (2000) Natural progression of osteochondritis dissecans of the humeral capitellum: initial observations. Radiology 216:207–212
Tehranzadeh J (1987) The spectrum of avulsion and avulsion-like injuries of the musculoskeletal system. RadioGraphics 7:945–974
Torriani M, Kattapuram SV (2003) Musculoskeletal ultrasound: an alternative imaging modality for sports-related injuries. Top Magn Reson Imaging 14:103–111
Vanhoenacker FM, Snoeckx A, Vandaele L et al. (2005) Bone marrow changes in sports injuries. JBR-BTR 88:332–335
Wright RW, Phaneuf MA, Limbird TJ et al. (2000) Clinical outcome of isolated subcortical trabecular fractures (bone bruise) detected on magnetic resonance imaging in knees. Am J Sports Med 28:663–667
Yao L, Johnson C, Gentili A et al. (1998) Stress injuries of bone: analysis of MR imaging staging criteria. Acad Radiol 5:34–40
Zanetti M, Weishaupt D, Jost B et al. (1999) MR imaging for traumatic tears of the rotator cuff: high prevalence of greater tuberosity fractures and subscapularis tendon tears. AJR Am J Roentgenol 172:463–467
Zarins B, Cuillo JV (1983) Acute muscle and tendon injuries in athletes. Clin Sports Med 2:167-182

Monitoring of Muscle, Tendon and Ligament Repair

29

John Slavotinek

CONTENTS

J. Slavotinek, MBBS, FRANZCR
Division of Medical Imaging, Flinders Medical Centre and Flinders University, Flinders Drive, Adelaide, South Australia 5042, Australia

29.1 Normal Healing Response to Muscle Injury

Muscle injury is widely believed to be one of the commonest injuries encountered in the context of sporting activity. Although muscle injury may arise following laceration, direct trauma or more commonly, strain injury, muscle healing usually follows a common pattern. Stages of repair following injury may be considered in three phases as below (Jarvinen et al. 2005).

29.1.1 Early/Destruction Phase

Shortly after injury, the gap between the ends of ruptured muscle fibres becomes filled with haematoma and ruptured muscle fibres undergo necrosis, usually limited by myofibril contraction bands. An inflammatory response begins to develop shortly after injury and inflammatory cells enter the haematoma (Nikolaou et al. 1987).

29.1.2 Intermediate or Repair Phase

In the repair phase, necrotic tissue undergoes phagocytosis, capillary ingrowth occurs and fibroblasts synthesize components of the extracellular matrix, including fibronectin, a protein believed responsible for much of the elasticity of early granulation tissue. Macrophages responsible for phagocytic activity leave the basement membrane intact and this acts as scaffolding for reconstitution of the myofibril. This process fails if the region of muscle damage is too large, there being a higher propensity for scar formation with more extensive muscle injury. Type III collagen formation begins before muscle fibre regeneration (Best et al. 2001) and is followed a few days later by the onset of type I collagen production. The latter leads to improved tensile strength of scar tissue.

29.1.3 Late or Remodelling Phase

During the remodelling phase, contraction and reorganisation of scar tissue occur, regenerated myofibrils mature, the injured portion of muscle becomes revascularised, intramuscular nerves regenerate and muscle functional capacity returns.

Box 29.1. Ultrasound technique for assesment of muscle

- High frequency transducer
- Transverse and longitudinal imaging
- Transducer orientation perpendicular to muscle
- Comparison with other side
- Palpation with transducer

29.2 Imaging of Normal Muscle Healing

Assessment of muscle healing is dependent upon the capacity to adequately demonstrate pathological processes within muscle and observe the manner in which they alter with time. Given that imaging studies cannot demonstrate the ultrastructural changes outlined above (Sect. 29.1), assessment of muscle healing is directed toward monitoring regression of imaging findings observed after acute injury and demonstration of complications.

Computed tomography (Garrett et al. 1989; Speer et al. 1993) has been used to demonstrate muscle injury but ultrasound, and particularly MRI are the most appropriate imaging techniques with which to monitor muscle injury. It should be noted that much of the information regarding prognosis and follow-up of muscle injury has been derived from studies of hamstring muscle strain injury and these form the basis of current knowledge.

29.2.1 Ultrasound

Appropriate technique is important if muscle pathology is to be demonstrated and assessed accurately (Box 29.1). During ultrasound studies, high frequency transducers (10–17 MHz) should be utilised for superficial structures and lower frequency transducers are employed if deeper musculature is to be assessed. Scans should be performed in transverse and longitudinal planes and care should be taken to ensure that transducer orientation is perpendicular to muscle fibres because non-orthogonal orientation may result in a hypoechoic appearance of muscle. Comparison with the opposite side is often useful and colour Doppler may be used to assess vascularity. The transducer may be employed as a gentle aid to palpation in order to localise the region of maximal tenderness and the most probable site of abnormality. Extended field of view provides a sense of perspective, particularly for clinicians who are less familiar with ultrasound images.

Shortly after injury, ultrasound of low grade acute muscle strain injury typically reveals no abnormality or a region of increased echogenicity. The latter has been reported in up to 50% of cases of Grade I injury (Takebayashi et al. 1995). In the context of mild injury, ultrasound will occasionally demonstrate abnormality not detected by MRI. If injury is more severe, hypoechoic regions indicative of fluid adjacent muscle fibrils or adjacent the epimysium may also be observed. Such fluid may reside either within or outside the epimysium depending upon whether the epimysium itself is torn. Linear fluid adjacent the epimysium or interposed between muscle bellies is present in approximately 50% of cases. Separation of muscle fibrils from the myotendinous junction or epimysium may be observed and if substantial, muscle retraction may be present. A focal intramuscular fluid collection or haematoma may be demonstrated and this typically has a surrounding echogenic halo. Relative to MRI, ultrasound is less able to demonstrate fluid or haematoma adjacent the musculotendinous junction or between muscle fibrils, particularly if the injury is deeply situated.

At follow-up, findings observed during normal healing depend upon the nature of the original injury. Healing of a minor or grade I strain should be manifest as loss of increased echogenicity and return of normal muscle architecture and echotexture. During healing, grade II tears should show an increase in echogenicity of the margins of the tear and the defect gradually fills with echogenic material over time (Fig. 29.1). Resolution or significant decrease in the quantity of fluid and decrease in size of any haematoma are also expected findings. In gen-

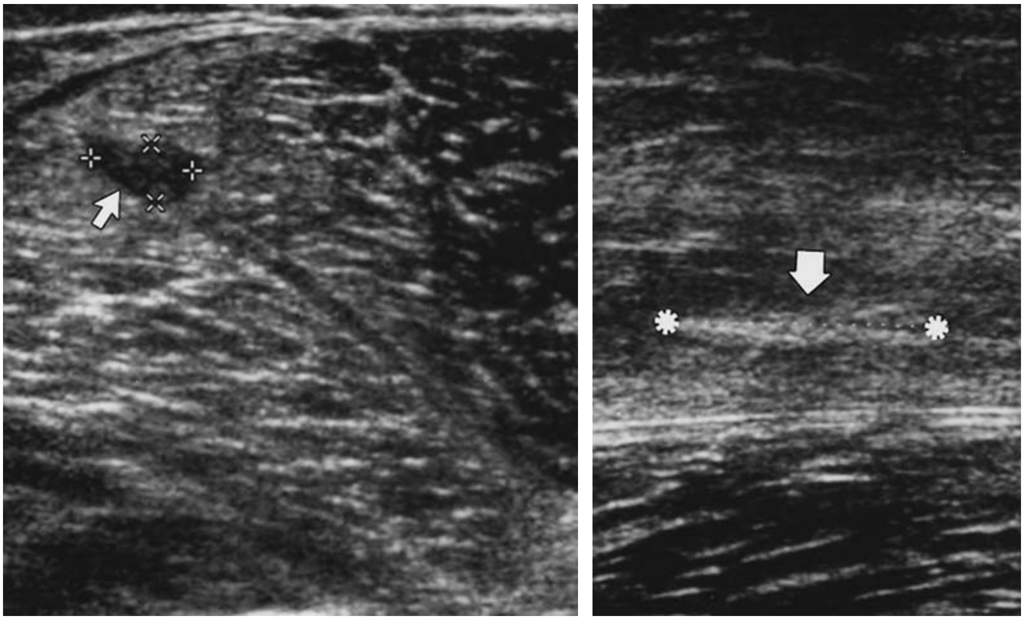

a b

Fig. 29.1a,b. Epimysial strain involving the periphery of the long head of biceps femoris in a 24-year-old Australian Rules footballer. Transverse ultrasound image obtained shortly after injury (**a**) demonstrates focal low echogenicity region (cursors) corresponding to the muscle tear (*arrow*). Longitudinal sonogram at six weeks after injury (**b**) reveals a linear band of increased echogenicity (*asterisks*) corresponding to the site of epimysial injury (*arrow*). (Reprinted with permission, Connell et al. 2004)

eral, ultrasound is less suited for monitoring of healing of muscle injury than MRI due to its lower soft tissue contrast. Evidence of complications such as scar formation or development of an intramuscular cyst should be sought. The significance of the former lies in the fact that extent of scar is believed to relate to likelihood of recurrent injury.

29.2.2 Magnetic Resonance Imaging

With regard to technique, MR images are acquired in transverse and longitudinal (sagittal or coronal) planes with fat suppressed proton density or T2-weighted images being most sensitive to muscle pathology (Box 29.2). Prior to scanning, a vitamin E capsule may be affixed to the skin to indicate the site of maximal tenderness. In the athlete with little adipose tissue, anatomical localisation may be assisted by visualisation of small quantities of fat that delineate muscles on non fat suppressed T1-weighted or proton density images. These images should be obtained at the same slice position as fat suppressed proton density or T2-weighted images. When reviewing follow-up examinations, comparison with imaging performed at the time of initial injury is important. At this time, measurements of the extent of muscle injury may also be used to assess progress of healing.

Box 29.2. MRI technique for assesment of muscle

- FS PD or T2 images most sensitive
- Longitudinal (sagittal or coronal) and axial planes
- Comparison with previous imaging
- Measurement of injury extent
- MRI preferred method to assess healing

Appearances of acute muscle injury have been considered previously in Chap. 3. Once an acute muscle injury has been diagnosed, imaging may be used to provide prognostic information based upon initial imaging of the acute injury and to assess the state of healing during follow-up scans.

29.2.2.1 Prognostic Information

Based upon images acquired shortly after injury, an association has been shown between athlete recov-

ery time and parameters of the extent of muscle injury (Slavotinek et al. 2002; Connell et al. 2004). Such parameters include the estimated volume of muscle injury, percentage cross sectional area of abnormal muscle and the cranio-caudal length of muscle abnormality adjacent the musculotendinous junction. Although all three parameters are associated with rehabilitation time, probably the strongest association is with the longitudinal extent of injury adjacent the musculotendinous junction. These associations (and hence prognostic information) relate to the number of muscle units disrupted at the time of injury and therefore the severity of injury. In particular, the longitudinal extent of injury along the musculotendinous junction is more closely associated with the number of muscle fibres separated from the musculotendinous junction (Fig. 29.2). These substantial muscle injuries often heal with residual macroscopic scar tissue and this is apparent as low signal intensity on T1 and T2 images (Fig. 29.3). The above studies of acute injury have prompted greater clinical interest in use of imaging to plan athlete rehabilitation but an algorithm for integration of clinical and imaging information remains to be established.

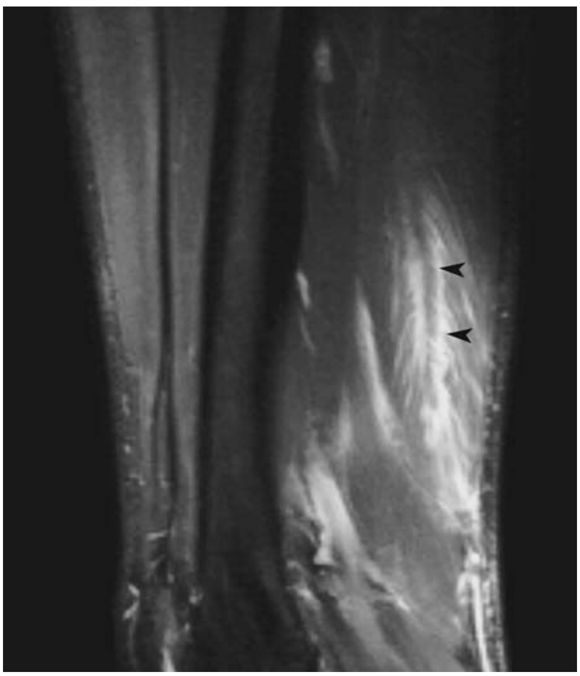

Fig. 29.2. Sagittal inversion recovery T2-weighted image illustrates hyperintense fluid among muscle fasciculi and adjacent the intramuscular tendon (*black arrowheads*) resulting in a featherlike appearance. The longitudinal extent of injury is considerable and despite lengthy rehabilitation this athlete was unable to return to the same level of competition. (Reprinted with permission, Slavotinek et al. 2002)

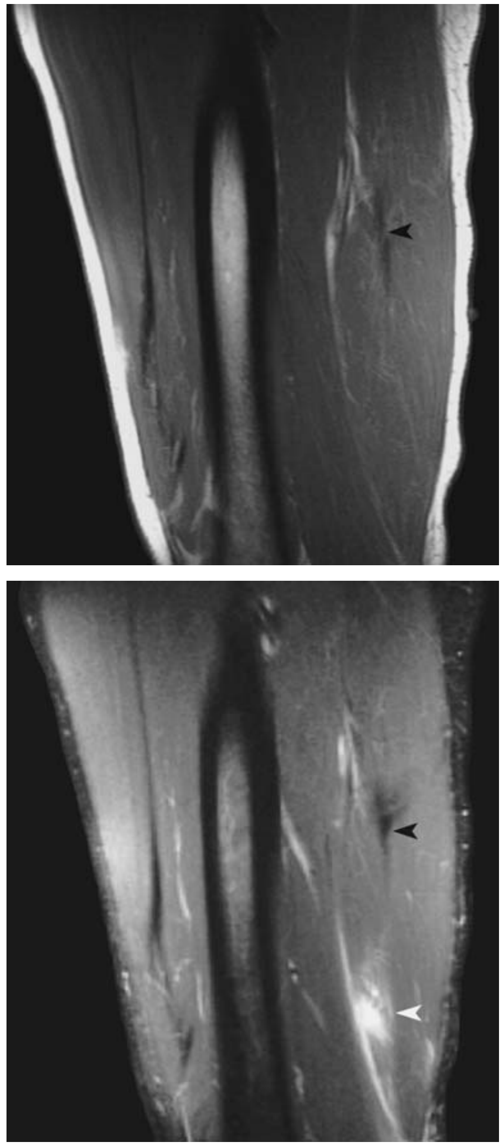

a

b

Fig. 29.3a,b. Sagittal T1-weighted (**a**) and inversion recovery T2-weighted (**b**) images in an athlete with recurrent hamstring muscle strain demonstrating a region of hypointensity (*black arrowhead*) due to scar and/or haemosiderin at the site of past injury. The T2-weighted image demonstrates hyperintensity at the site of recent recurrent injury (*white arrowhead*)

29.2.2.2
MRI of Muscle Healing

During the repair or healing phase of muscle injury there is gradual resolution of fluid between muscle fascicles, in relation to the epimysium and increased T2 signal within muscle slowly reduces in extent and intensity. At follow-up, the degree to which high

signal intensity has resolved is variable but in many instances, particularly when the initial injury is more severe, abnormality on MRI has not resolved at six weeks (Fig. 29.4). This persistent increased T2 signal is in keeping with the fact that healing continues beyond the time normally elapsed before athletes return to competition. Observations regarding resolution of muscle injury are largely derived from studies using follow-up MRI shortly before athletes with hamstring injury return to competition. These studies have measured the extent of muscle injury using parameters such as the percentage cross sectional area of abnormal muscle, approximate volume of muscle injury and the longitudinal extent of injury. Persistence of abnormality at follow-up has been confirmed but little is known about evolution of the above parameters of injury with time. In a small unpublished series, the approximate volume of muscle injury reduced by 38–100% when athletes underwent follow-up MRI shortly before successfully returning to competition. The percentage cross sectional area of abnormal muscle was less useful exhibiting reduction of 28–100%. This preliminary data indicates a wide range of healing response and suggests that a reduction of at least 30–50% in the volume of muscle abnormality on MRI studies obtained just before return to competition is most unlikely to be associated with recurrent injury. Thus far, there is no information to indicate the expected degree of resolution of the cranio-caudal extent of injury adjacent the musculotendinous junction. Although preliminary data are encouraging, a clear relationship between the above parameters at follow-up and subsequent recurrent injury has not been established.

29.2.3 Monitoring of Muscle Injury

There is no clinical or imaging gold standard as to when return to sport should occur after a muscle strain injury. Typical clinical criteria for return to sport include return of full range of motion, strength and capacity to undertake functional activities. It is widely believed that healing of hamstring muscle injury takes weeks to months, yet athletes typically return to competition before healing is complete. In keeping with this, there is increased risk of recurrent injury for at least five weeks after the individual returns to sport (Orchard and Best 2002) and imaging studies often demonstrate residual muscle abnormality for six weeks or more following injury. Given that imaging abnormality may persist beyond the time an athlete returns to competition, complete resolution of imaging findings cannot be applied uniformly to direct management decisions regarding return to sport.

There is evidence that information gathered by ultrasound and MRI shortly after initial injury can to some extent predict the convalescence interval. Athletes with no abnormality on imaging studies return to sport within one to two weeks almost without exception. In cases of Grade I injury both ultrasound and MRI usually show resolution of abnormality at

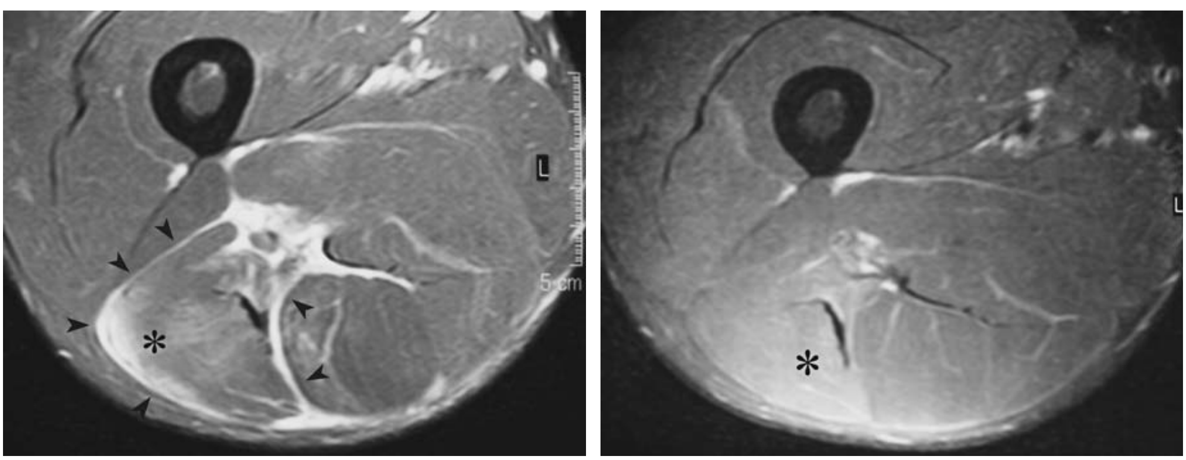

a b

Fig. 29.4a,b. Axial inversion recovery T2-weighted images following hamstring muscle strain injury. The initial scan (**a**) demonstrates extensive T2 hyperintensity within the long head of biceps femoris (*asterisk*) and to a lesser extent there is involvement of semitendinosus. There is abundant fluid signal intensity between muscle bellies adjacent the epimysium (*black arrowheads*) and also surrounding the sciatic nerve. Some 42 days later the follow-up scan (**b**) reveals resolution of fluid, there being persisting extensive but less intense muscle hyperintensity (*asterisk*) within the long head of biceps femoris

follow-up and typically such injuries require no more than one to two weeks rehabilitation. Clinical management is quite successful in this setting and monitoring of healing is probably not warranted unless there is reason for concern regarding the athlete's progress. In this situation recurrent injury is most unlikely (Gibbs et al. 2004).

Although a similar argument may be presented with respect to imaging of Grade II injuries during convalescence, the risk of recurrent injury is higher and there is a greater role for follow-up imaging. It is at present unresolved whether scans should be performed to monitor healing at approximately three weeks after injury or a few days before the athlete is due to return to competition. Having said this, demonstration of significant partial resolution of muscle abnormality and fluid is encouraging, whereas static appearances should raise concern regarding the need for longer rehabilitation. Specifically, if separation or retraction of muscle fibres at the site of the tear persists this should also give rise to concern. Progression of muscle abnormality may also be observed if training is too aggressive or is instituted too soon and this imaging finding should also alter the approach to management.

Comparison of ultrasound and MR imaging indicates that shortly after injury sensitivity for muscle damage is approximately equal but that ultrasound demonstrates residual abnormality less frequently than MRI (24% vs 36% at six weeks) during follow-up (Connell et al. 2004). This is probably due to the superior sensitivity of MRI to muscle edema. Both ultrasound and MRI normally reveal resolution of linear fluid adjacent the epimysium at follow-up. Given that ultrasound is less sensitive for intrinsic muscle pathology than MRI and that fluid usually resolves by the time of follow-up, ultrasound is in general considered to be less appropriate than MRI for monitoring of healing (Box 29.3). It is important to recognize that many aspects of imaging remain to be explored (e.g., does follow-up imaging improve long term outcome of athletes) and some aspects of ultrasound (e.g., colour Doppler imaging) have not been fully assessed for their utility.

Box 29.3. Comparison of ultrasound and MRI for monitoring of muscle healing

- Similar sensitivity for acute muscle injury
- Ultrasound underestimates residual injury at follow-up
- Measurement of injury extent easier with MRI
- MRI preferred method to assess healing

29.3 Complications of Muscle Healing

Imaging studies used to monitor healing may demonstrate inadequate progress of healing as discussed above but a number of complications should also be sought on follow-up imaging studies. These complications may induce diverse clinical manifestations including delay in healing when present during rehabilitation (haematoma), increased risk of recurrence (scar), reflect sequela of longstanding injury (atrophy), and even simulate soft tissue tumour (myositis ossificans).

29.3.1 Scar

Severe muscle injury may lead to significant scar formation. If follow up is performed at six weeks or later, a scar may be apparent as reduced T1 and T2 signal intensity on MRI. On ultrasound scar appears as an irregular hyperechoic region that may extend to the epimysium (Lee and Healy 2004). Such injuries may result in reduced strength and altered capacity of the muscle to elongate with associated loss of athletic performance and increased risk of recurrent injury.

29.3.2 Chronic Haematoma

This is particularly likely to be seen in tennis leg, a tear involving the aponeurosis between the soleus and gastrocnemius muscles. Intramuscular haematoma may decrease in size over time but is less likely to resolve spontaneously than extramuscular haematoma. Intramuscular haematoma is therefore more likely to result in delayed return to sporting activity and in many instances aspiration of such fluid collections is required in order to assist progress of healing. At ultrasound small collections of blood may resolve slowly over many weeks, the fluid becoming echogenic peripherally with later progression of

increased echogenicity centrally (Peetrons 2002). Intramuscular cysts are also a recognized complication and these may be simple or septate.

29.3.3 Recurrent Injury

There is a relatively high recurrence rate of hamstring injury in sports that require sprinting or jumping such as Australian Rules football and the cumulative risk in this sport has been reported at levels as high as 30% (Orchard and Best 2002). Recurrent muscle injury is more likely in those of older age, with greater extent of injury and with past history of muscle injury. Imaging appearances of recurrent injury are similar to those of other muscle strain injuries and the recurrence may occur close to the site of injury or at a distance within the same muscle group. Experimental studies (Jarvinen 1976; Kaariainen et al. 1998) suggest that, although healing is far from complete, scar tissue achieves equal or greater strength compared to normal muscle at approximately ten days post injury. At this time recurrent injury is therefore more likely to occur at the junction between scar tissue and normal muscle, or within muscle elsewhere rather than within scar tissue itself (Fig. 29.3).

29.3.4 Myositis Ossificans

Muscle injury may result in significant haemorrhage and subsequent myositis ossificans, a non-neoplastic condition in which heterotopic bone is formed. This benign condition follows trauma in approximately 60–75% of cases, most commonly affects adolescents and young adults and typically involves the quadriceps and brachialis muscles (Parikh et al. 2002). Clinical presentation with pain and a palpable mass may result in clinical suspicion of soft tissue tumour and an understanding of imaging appearances is therefore important in order to avoid unnecessary biopsy. This lesion evolves in well recognized fashion and at pathology eventually manifests distinctly different zones in its central, intermediate and peripheral portions. For the first two weeks the lesion essentially represents a haematoma but by four weeks, distinct histological zones are becoming apparent. Centrally there are immature proliferating fibroblast-like cells with haemorrhage and muscle necrosis, in the intermediate zone there are osteoblasts, immature osteoid and woven/fibre bone, and at the periphery mature osteoid and lamellar bone formation are present.

The key to diagnosis lies in demonstrating imaging findings that recapitulate the zonal phenomenon observed at pathology. Correct diagnosis is important because different zones are not apparent in the early phase of myositis ossificans and if the centre of the lesion is biopsied, the pathologist may erroneously diagnose a soft tissue sarcoma. Typically, low density material is present centrally and a more mature calcified or ossified peripheral region is evident. For diagnosis, CT and ultrasound are preferred to MR imaging because the latter may not detect peripheral calcification or ossification, a hallmark of this condition. In the earliest stages of ossification ultrasound shows sheet-like calcification manifest as peripheral increased echogenicity. The centre of the lesion is hypoechoic and these findings may establish the diagnosis (Peck and Metreweli 1988). The peripheral zone becomes more echogenic as ossification develops and internal visualisation is lost. As the peripheral calcification becomes macroscopic it becomes demonstrable by CT and later plain X-ray (Fig. 29.5). At six to eight weeks ossification is present and should be detected by all forms of imaging. When the lesion is fully mature bone marrow is present centrally.

Magnetic resonance images demonstrate a lesion isointense or hypointense to muscle with T2 hyperintensity centrally. There may be quite extensive peripheral edema on T2-weighted images, a less common finding in the context of soft tissue tumour. In the early stages of myositis ossificans the lesion may enhance. Peripheral hypointensity suggests ossification (Fig. 29.6) and implies the diagnosis but this may not be observed at MRI. For this reason MRI is less likely to establish existence of zonal phenomenon by demonstration of peripheral calcification, extensive edema may make margins of the lesion harder to show and MRI appearances may therefore resemble a soft tissue sarcoma (Wang et al. 2003).

29.3.5 Muscle Atrophy

Fatty atrophy of muscle with a decrease in muscle mass and power is associated with complete muscle or tendon tear of chronic nature. In this setting retraction and disuse lead to atrophy and fatty replacement of muscle. At MRI, signal intensity in keeping with fat

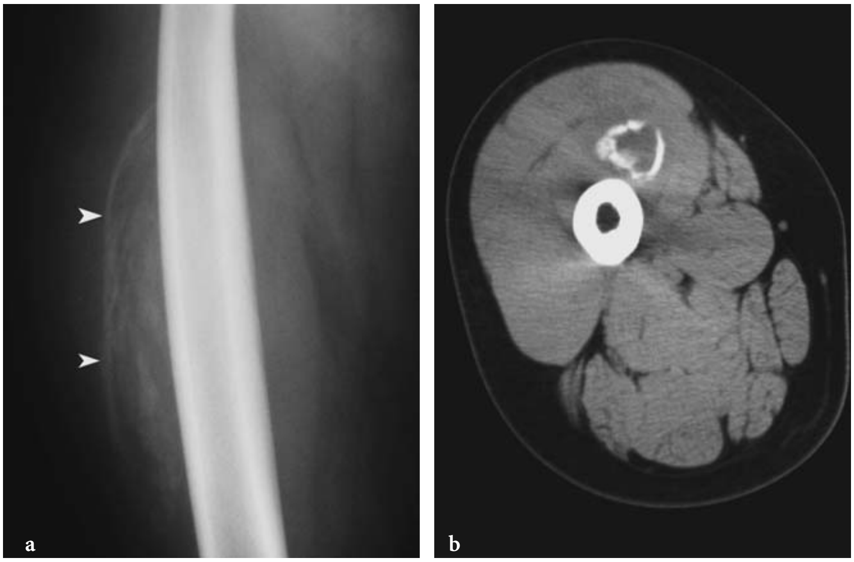

Fig. 29.5a,b. Lateral plain X-ray (**a**) demonstrating curvilinear calcification (*white arrowheads*) in the anterior thigh musculature. The calcification encloses a lower density region in keeping with myositis ossificans. Axial CT image of the thigh (**b**) confirms peripheral disposition of calcification and central low attenuation typical of this condition

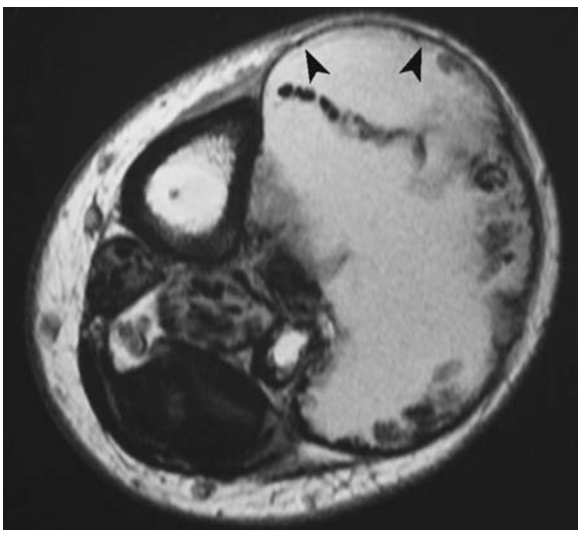

Fig. 29.6. T1-weighted transverse image of a 50-year-old male investigated for a mass situated at the anterolateral aspect of the left lower limb. Peripheral hypointensity (*black arrowheads*) indicates calcification and the diagnosis of myositis ossificans. Central hyperintensity is due to blood products derived from the haematoma

is observed within muscle and fat suppression techniques may be used if there is any doubt. Ultrasound reveals increased echogenicity of muscle of diffuse nature and is moderately accurate for detection of muscle atrophy (Strobel et al. 2005). If utilised, CT demonstrates material of fatty attenuation. All imaging techniques show reduction in muscle bulk. The finding of muscle atrophy is relevant because it is unlikely to reverse following surgical repair.

29.3.6 Muscle Hernia

Muscle hernias are usually observed in the lower leg particularly in relation to the tibialis anterior muscle of the anterior compartment. Other sites of muscle herniation are less common but include flexor muscles of the forearm. Muscle injury with an associated tear of the epimysium and/or muscle fascia may be responsible but weakness of the fascia where vessels perforate has also been implicated. If appropriate emphasis is placed upon technical aspects of the examination, ultrasound has a clear advantage over MRI for the diagnosis of muscle hernia (Beggs 2003). In general, MRI will detect hernias if they are present at rest but the dynamic capacity of ultrasound and its ability to direct visualisation to a small field of view at the site of palpable abnormality represent significant advantages (Box 29.4).

Attention to technique during ultrasound examination is important because supine positioning with the patient at rest may result in a false nega-

Box 29.4. Muscle hernia – ultrasound technique

- Upright position
- Muscle contraction
- Light transducer pressure
- Optimise for near field at level of fascia

tive examination. With few exceptions, muscle hernias are more prominent when the patient is upright and muscle contraction is occurring at the time of scanning. Gain should be optimised to demonstrate the near field at the level of the fascia. The degree of transducer pressure during scanning is also important as subtle muscle herniation may be effaced by transducer pressure.

Signs of muscle herniation include focal thinning or indistinctness of the fascia, mild elevation of the fascia and visualisation of hypoechoic herniated muscle. With contraction, the hernia typically increases in size and overhang of the fascia may be present (Fig. 29.7). Reassurance is sufficient in the large majority of patients unless there is persistent significant pain. Surgical closure of any fascial defect should occur only after consideration of the potential for a compartment syndrome.

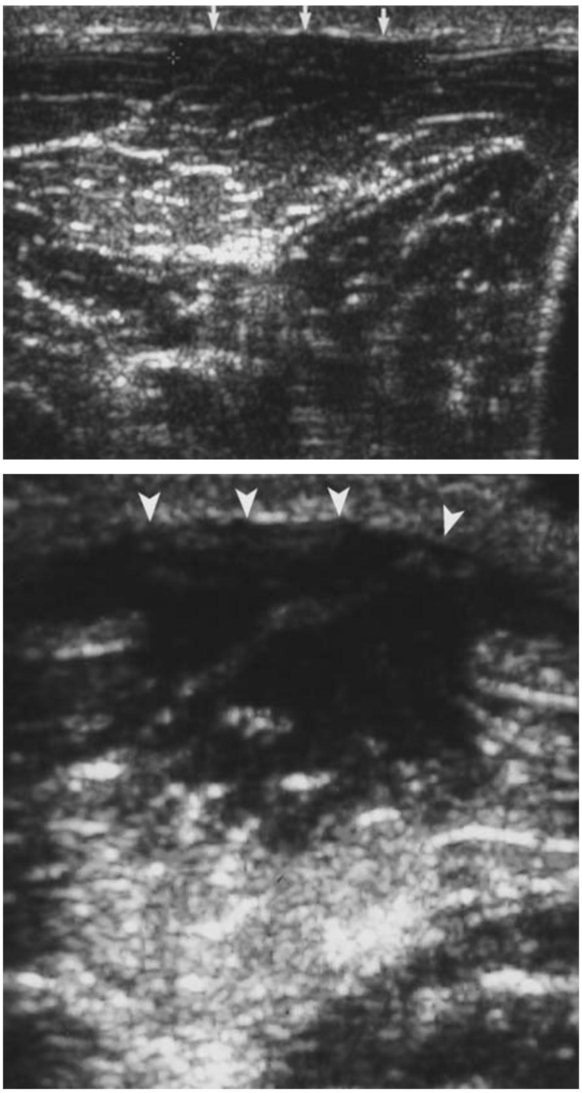
a
b

Fig. 29.7a,b. Twenty-seven-year-old male with tibialis anterior hernia presenting as painless swelling. The transverse ultrasound image (**a**) shows well-defined margins of the fascial defect that is marked by calipers. White arrows indicate the muscle hernia extending through the fascial defect. The hernia (*white arrowheads*) becomes larger and more hypoechoic during muscle contraction (**b**). (Reprinted with permission, Beggs 2003)

29.4 Normal Response to Tendon and Ligament Injury

Normal tendon comprises predominantly extracellular matrix (80%) but also contains cellular elements (20%) such as tenocytes. Extracellular matrix composition is largely collagen (95% type I and 5% type III) but water and elastin are also present. Following tendon rupture, tenocyte hyperplasia occurs, there is ingrowth of small blood vessels, a transient inflammatory reaction ensues and collagen degeneration is present (Cetti et al. 2003). Fibroblast infiltration of the tendon is also important in achieving adequate healing response. If there is adequate proximity of the ends of ruptured tendons, connective tissue develops between tendon ends. Tenocytes and other cells within this connective tissue deposit collagen fibres that undergo a remodelling process and develop orientation closely related to that of the tendon. Despite the above process, in the long term the tendon is unlikely to reconstitute itself completely and regions of scar and degeneration (mucoid, fibrillary and eosinophilic) have been well documented at histology (Kjellin et al. 1991).

It has been shown that tenocytes within injured tendons or within tendons with pre-existing tendinopathy produce greater quantities of type III collagen than tenocytes within normal tendons. Type III collagen has greater elasticity but inferior strength (Maffulli et al. 2000). Repeated episodes of minor or microtrauma with associated deposition of weaker type III collagen during the healing response may therefore eventually result in sufficient tendon weakening and tendon rupture. Others (Cook et al. 2004) have also suggested that mechanical load may induce changes in tenocytes as a primary event with resultant production of increased ground substance, separation of collagen fibres, hypoxia and neovascularization. The latter may be related to tendon pain.

29.5 Imaging of Normal Tendon and Ligament Healing

29.5.1 Tendon Injury

Ultrasound (Box 29.5) and MRI are frequently employed to diagnose tendon and ligament injury but are less commonly used to assess the state of healing of these structures. The time course of tendon appearances during healing has been documented at relatively few sites but the Achilles tendon has been serially examined with ultrasound 6, 12 and 24 months after complete rupture in the context of a randomised controlled trial (Moller et al. 2002). Although edema and defects within the tendon were common in the first 6 months of healing, these were less frequent after 12 months. Both ultrasound and MRI observed tendon thickening (fusiform or generalised) and heterogeneity of tendon appearance 12 months after tendon rupture but edema of the peritenon was uncommon. Patients undergoing conservative treatment had similar findings to those that were randomised to surgery with the exception that the latter were more likely to have alteration in tendon glide or motion. There was limited correlation between tendon appearances and patient outcome as measured by muscle strength and range of motion at one year follow-up.

Box 29.5. Ultrasound technique during assessment of tendons and ligaments

- Longitudinal and transverse scans
- High frequency transducer
- Dynamic assessment
- Best for superficial structures

Evolution of the healing response of the Achilles tendon has also been monitored by MRI (Box 29.6). Core biopsies were used to induce small regions of iatrogenic injury within the Achilles tendon (Shalabi et al. 2004) and serial MRI examinations were used to assess healing. At one week, tendon volume and signal intensity were increased but by three months signal intensity changes begin to regress and in treated patients such changes had decreased at one year. After surgical repair following full thickness Achilles tendon rupture (Karjalainen et al. 1997) abnormal T2 signal intensity persists for at least three months but should decrease or completely regress at six months. It seems likely the high T2 signal observed relates to the healing response but it is difficult to distinguish between healing and new tendon pathology such as a recurrent tear at less than six months following surgery.

Box 29.6. MRI technique during assessment of tendon healing

- Longitudinal and transverse scans
- T1 and FS PD or T2 images
- Coil selection and positioning are key
- Beware magic angle artefact

29.5.2 Ligament Injury

When managed conservatively, ligament injury is usually monitored clinically with there being little need for imaging during routine follow-up. On occasion follow-up imaging may be requested and an understanding of appearances during ligament healing is therefore required. The choice of imaging modality partially depends upon the structure to be imaged, the cruciate ligaments of the knee being best assessed by MRI. Integrity of superficial ligaments such as the anterior talofibular ligament of the ankle may also be assessed by ultrasound. During ultrasound examination ligament integrity may also be confirmed by application of stress in real time.

Studies have documented that ligaments such as the anterior cruciate ligament (ACL) frequently heal successfully following conservative management (Ihara et al. 1996). After three months mobilization in a knee brace, at follow-up MRI 42% of individuals had a well defined normal-sized straight low signal intensity structure and 32% had similar appearances but with small regions of intraligamentous high signal intensity. The remaining 26% exhibited a significant structural deficit in the ligament at MRI in the form of either a fine band (8%) or a non-discernable low signal intensity region (18%). At arthroscopic assessment 78% of patients had a continuous taut ACL with varying decrease in thickness and this corresponds

well with the 74% with intact structure demonstrated at MRI.

Posterior cruciate ligament (PCL) tears frequently regain continuity at six month MRI follow-up, there being no association between the location of the tear within the PCL and ligament integrity (Shelbourne et al. 1999). The majority of posterior cruciate ligaments (79%) exhibit altered morphology at follow-up in the form of thickening, elongation, lobulation, thinning and/or contour alteration. In many instances there is persisting loss of clarity of fat planes adjacent the ligament. In the same study, when combined with a PCL tear, MCL healing was also successful. In this sense, multiple ligament injury was not associated with worse outcome as assessed by MRI but functional and other patient outcome data were not recorded. Given that healing has been shown after PCL injury and conservative management, MRI may have a role as an assessment tool in that setting.

In summary, during the healing process both MRI and ultrasound typically show generalised or fusiform thickening of the relevant ligament or tendon. There may be heterogeneity of echotexture (ultrasound) or signal intensity (MRI) and defects may be observed within the tendon or ligament substance, particularly shortly after injury. Tendon defects are manifest as increased signal intensity on proton density or T2-weighted images. It should be noted that such defects (3–5 mm) may be present within the asymptomatic Achilles tendon and unless they are large they are unlikely to be significant. Adjacent edema and loss of clarity of fat planes is also common. Apposition of tendon and ligament ends should be confirmed during follow-up imaging studies and the dynamic capacity of ultrasound may be used to confirm that proximity of tendon or ligament components is maintained during motion or stress. In contradistinction, if there is significant separation between tendon or ligament ends healing is unlikely to be successful. Blood or synovial fluid interposed between tendon or ligament components also reduces the probability of successful healing because vascularisation and access of fibroblasts are limited in this situation.

29.6 Complications of Tendon and Ligament Healing

29.6.1 Recurrent Injury

Injured tendons with pre-existing tendon tears or tendinopathy produce type III collagen during the normal healing process. As indicated above (see Sect. 29.4), the tendon is weakened by this process and recurrent tendon tear or tendon rupture may follow relatively minor trauma. The supraspinatus and Achilles tendons are both sites of chronic tendinopathy and this is a well recognized antecedent of tendon rupture (Fig. 29.8).

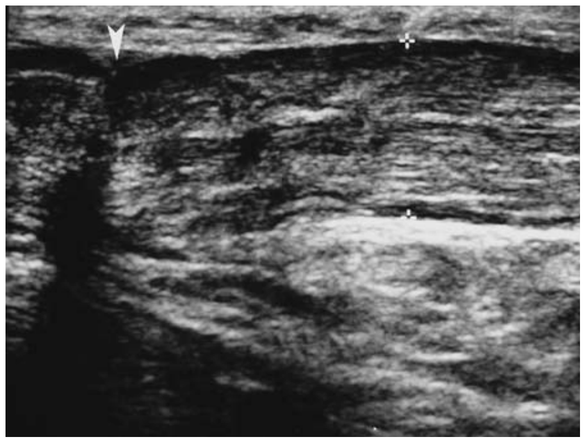

Fig. 29.8. Longitudinal ultrasound image of a 46-year-old former triathlete demonstrating an Achilles tendon tear (*white arrowhead*) and associated hypoechoic fluid in small quantities. The tendon more distally (calipers) is thickened (10 mm as opposed to 7 mm on opposite side) and exhibits heterogeneous echotexture in keeping with pre-existing tendon degeneration

29.6.2 Muscle Atrophy

If tendon healing fails, particularly after full thickness tendon tear, muscle atrophy follows. As indicated in Sect. 29.3, imaging findings include low attenuation at CT, increased echogenicity at ultrasound and fat signal intensity at MRI. Fatty replacement does not reverse after surgical repair and is a negative prognostic factor with respect to functional outcome.

29.6.3
Tendon/Ligament Malposition

Healing of tendon or ligament injury may be complicated by failure to heal, particularly if there is separation of ligament ends and interposition of fluid or other tissue. In the context of fluid at the site of complete rupture, imaging findings are straightforward with there being hypoechoic fluid between tendon or ligament ends at ultrasound. In this setting MRI demonstrates signal intensity in keeping with fluid. If healing is incomplete and this is combined with continued activity and tendon degeneration, attrition of the tendon may develop. This appearance has been well documented in the case of type 2 tears of the tibialis posterior tendon.

Ligament displacement may occur and this is exemplified by the Stener lesion in which the ulnar collateral ligament of the thumb comes to lie superficial to the adductor aponeurosis and/or adductor pollicis muscle. Similarly, although the ACL may heal with normal orientation it may also become displaced. If adjacent the PCL, fibrosis between the ACL and PCL may occur with the ACL superficially resembling a normal ligament.

29.6.4
Degenerative Change

If ligament or tendon healing fails there may be loss of stability of the joint, abnormal motion of joint components, premature chondral loss and eventually premature degenerative joint disease.

29.6.5
Post Traumatic Synovitis and Impingement Syndromes

Post traumatic synovitis may follow ligament or tendon injury and is a recognised cause of ongoing pain following injury. Imaging demonstrates synovial thickening and fluid within the tendon sheath. At MRI intermediate signal intensity synovial tissue is best visualised on proton density FSE images. Tendon injury and associated post traumatic synovitis may lead to synechiae within the tendon sheath and alteration or loss of tendon motion (e.g., trigger finger).

Synovial proliferation and associated fibrosis may induce a variety of impingement syndromes that have been described at many different sites. Synovial thickening, effacement of fat and hypointense fibrosis are best visualised on MRI, the diagnosis being more straightforward if joint fluid is present. Erosion of adjacent bone and low signal intensity loose bodies may also be present. Figure 29.9 illustrates anterolateral impingement of the ankle following a tear of the anterior talofibular ligament.

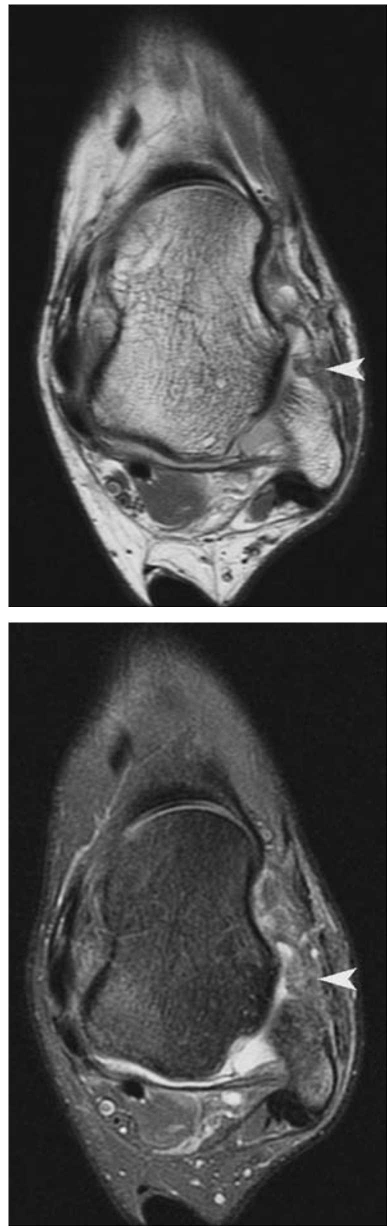

a

b

Fig. 29.9a,b. Axial proton density (**a**) and fat suppressed proton density (**b**) images of a patient with anterolateral impingement of the ankle. Both images demonstrate intermediate signal intensity material due to synovial proliferation and fibrosis (*white arrowhead*) within the anterolateral gutter. (Images courtesy of Dr. Shaun Fowler, Dr Jones and Partners)

29.7 Conclusion

Appearances of acute muscle, tendon and ligament injury are well documented but thus far imaging has had a limited role in assessment of such injuries during healing. In this context ultrasound and MRI have been largely used to detect complications when clinical progress is unsatisfactory. Normal healing appearances have been documented at sites such as the Achilles tendon, hamstring musculature and cruciate ligaments and in many cases abnormalities persist for some time. Given that abnormality is present for weeks following muscle injury and months following tendon and ligament injury, follow-up imaging shortly after injury may be difficult to interpret and as yet, a clear relationship between imaging findings and clinical outcome has not been shown. At present, there are few specific criteria that may be used to distinguish normal from inadequate healing but persisting separation of muscle, tendon or ligament components is a reliable indicator of inadequate healing. Absence of regression of fluid at the site of injury or an increase in the extent of abnormality at follow-up may also be used to indicate an inadequate healing response. Algorithms integrating imaging findings into clinical management are not yet available and the ultimate role of follow-up imaging will depend upon its capacity to alter management and predict adverse outcomes.

Things to Remember

1. Ultrasound may be used to assess structural integrity of superficially placed tendons and ligaments but overall, MRI is the preferred imaging modality for assessing repair of muscle, ligament and tendon injury.
2. Baseline imaging and appropriate technique are essential when ultrasound or MRI is employed to assess healing of muscles, tendons or ligaments.
3. Persistent separation of muscle, tendon or ligament components is the most reliable indicator of unsuccessful repair but persistence of abnormal signal intensity may be used in combination with an understanding of the way that appearances during normal healing evolve.

References

Beggs I (2003) Sonography of muscle hernias. AJR Am J Roentgenol 180:395–399

Best TM, Shehadeh S, Leverson G et al. (2001) Analysis of changes in mRNA levels of myoblast- and fibroblast-derived gene products in healing skeletal muscle using quantitative reverse transcription-polymerase chain reaction. J Orthop Res 19:565–572

Cetti R, Junge J, Vyberg M (2003) Spontaneous rupture of the Achilles tendon is preceded by widespread and bilateral tendon damage and ipsilateral inflammation: a clinical and histopathologic study of 60 patients. Acta Orthop Scand 74:78–84

Connell DA, Schneider-Kolsky ME, Hoving JL et al. (2004) Longitudinal study comparing sonographic and MRI assessments of acute and healing hamstring injuries. AJR Am J Roentgenol 183:975–984

Cook JL, Feller JA, Bonar SF et al. (2004) Abnormal tenocyte morphology is more prevalent than collagen disruption in asymptomatic athletes' patellar tendons. J Orthop Res 22:334–338

Garrett WE, Rich FR, Nikolaou PK et al. (1989) Computed tomography of hamstring muscle strains. Med Sci Sports Exerc 21:506–514

Gibbs NJ, Cross TM, Cameron M et al. (2004) The accuracy of MRI in predicting recovery and recurrence of acute grade one hamstring muscle strains within the same season in Australian Rules footballers. J Sci Med Sport 7:248–258

Ihara H, Miwa M, Deya K et al. (1996) MRI of anterior cruciate ligament healing. J Comput Assist Tomogr 20:317–321

Jarvinen M (1976) Healing of a crush injury in rat striated muscle, 4: effect of early mobilization and immobilization on tensile properties of gastrocnemius muscle. Acta Chir Scand 142:47–56

Jarvinen TAH, Jarvinen TLN, Kaariainen M et al. (2005) Muscle injuries: biology and treatment. Am J Sports Med 33:745–764

Kaariainen M, Kaariainen J, Jarvinen TLN et al. (1998) Correlation between biochemical and structural changes during the regeneration of skeletal muscle after laceration injury. J Orthop Res 16:197–206

Karjalainen PT, Aronen HJ, Pihlajamaki HK et al. (1997) Magnetic resonance imaging during healing of surgically repaired Achilles tendon ruptures. Am J Sports Med 25:164–171

Kjellin I, Ho CP, Cervilla V et al. (1991) Alterations in the supraspinatus tendon at MR imaging: Correlation with histopathologic findings in cadavers. Radiology 181:837–841

Lee JC, Healy J (2004) Sonography of lower limb muscle injury. AJR Am J Roentgenol 182:341–351

Maffulli N, Ewen SWB, Waterston SW et al. (2000) Tenocytes from ruptured and tendinopathic Achilles tendons produce greater quantities of type III collagen than tenocytes from normal Achilles tendons. Am J Sports Med 28:499–505

Moller M, Kalebo P, Tidebrant G et al. (2002) The ultrasonographic appearance of the ruptured Achilles tendon during healing: a longitudinal evaluation of surgical and nonsurgical treatment with comparisons to MRI appearance. Knee Surg Traumatol Arthrosc 10:49–56

Nikolaou PK, MacDonald BL, Glisson RR et al. (1987) Biomechanical and histological evaluation of muscle after controlled strain injury. Am J Sports Med 15:9–14

Orchard J, Best TM (2002) The management of muscle strain injuries: an early return versus the risk of recurrence. Clin J Sport Med 12:3–5

Parikh J, Hyare H, Saifuddin A (2002) The imaging features of post-traumatic myositis ossificans, with emphasis on MRI. Clin Radiol 57:1058–1066

Peck RJ, Metreweli C (1988) Early myositis ossificans: a new echographic sign. Clin Radiol 39:586–588

Peetrons P (2002) Ultrasound of muscles. Eur Radiol 12:35–43

Shalabi A, Svensson L, Kristoffersen-Wiberg M et al. (2004) Tendon injury and repair after core biopsies in chronic Achilles tendinosis evaluated by serial magnetic resonance imaging. Br J Sports Med 38:606–612

Shelbourne KD, Jennings RW, Vahey TN (1999) Magnetic resonance imaging of posterior cruciate ligament injuries: assessment of healing. Am J Knee Surg 12:209–213

Slavotinek JP, Verrall GM, Fon GT (2002) Hamstring Injury in athletes: using MR imaging measurements to compare extent of muscle injury with amount of time lost from competition. AJR Am J Roentgenol 179:1621–1628

Speer KP, Lohnes J, Garrett WE (1993) Radiographic imaging of muscle strain injury. Am J Sports Med 21:89–95

Strobel K, Hodler J, Meyer DC et al. (2005) Fatty atrophy of supraspinatus and infraspinatus muscles: accuracy of US. Radiology 237:584–589

Takebayashi S, Takasawa H, Banzai Y et al. (1995) Sonographic findings in muscle strain injury: clinical and MR imaging correlation. J Ultrasound Med 14:899–905

Wang XL, Malghem J, Parizel PM et al. (2003) Myositis ossificans circumscripta. JBR-BTR 86:278–285

Addendum

Sport-Specific Injuries

30

Olympia Papakonstantinou, Alexis D. Kelekis, Nikolaos L. Kelekis, and Dimitrios A. Kelekis

CONTENTS

Most frequent musculoskeletal injuries based on the experience during the Summer Olympic Games 2004

30.1 Introduction

The purpose of this chapter is to give an overview of the relative frequency of musculoskeletal sports injuries, documented by imaging studies in a population of elite athletes. The information within this chapter is derived from our experience during the summer Olympic Games, held in Athens 2004. The games brought together approximately 11,000 athletes from all over the world. Medical care to athletes, members of national missions and workforce was provided at a multidisciplinary clinic, the Polyclinic, which was located in the Olympic Village. Polyclinic Services were linked to the Greek National System Health Service System, which provided free access to emergency services offered by dedicated Olympic Hospitals. The Radiology Department of the Polyclinic was installed and mostly staffed by the 2nd Department of Radiology of the University of Athens. Volunteer radiologists and technologists from all over the country were recruited whereas Hellenic Armed Forces provided additional medical and paramedical personnel in order to insure access to all imaging facilities for athletes residing in the Olympic Village on a 24 h basis. The equipment of the Radiology Department comprised standard radiography (including digital fluoroscopy), ultrasound, multidetector CT and MR imaging. Additionally, Picture Archiving and Communication System was available. From 29th of July to 30th of August 2004, approximately 1500 imaging studies were performed in the Olympic Polyclinic, involving approximately 800 athletes, providing a wide spectrum of injuries suffered by elite athletes in a wide variety of sporting activities. The majority of the requests for imaging concerned suspicion of stress fractures, muscle injuries, knee and ankle injuries in athletes during competition or training. The 2004 Olympic records, deriving from the archives of Olympic Polyclinic, were reviewed for sports related injuries by competing athletes, and are summarized in Table 30.1.

Some additional comments on the most frequent injuries will be provided in the next paragraphs.

O. Papakonstantinou,
Lecturer of Radiology, 2nd Radiology Department, University of Athens, Rimini 1, 12462, Athens, Greece
A. D. Kelekis, MD, PhD
Lecturer of Interventional and Musculoskeletal Radiology, 2nd Radiology Department, University of Athens, Rimini 1, 12462, Athens, Greece
N. L. Kelekis, MD, PhD
Associate Professor of Radiology, 2nd Radiology Department, University of Athens, Rimini 1, 12462, Athens, Greece
D. A. Kelekis, MD, PhD
Professor of Radiology, Research Department of Imaging and Interventional Radiology, University of Athens, Eugenidion Hospital, Papadiamantopoulou 20, 11528, Athens, Greece

Table 30.1. Most common injuries in Olympics 2004

Fractures, stress fractures and stress reactions
Muscle strains
Ligamentous and meniscal injuries of the knee
Achilles tendinosis
Plantar fasciitis
Tears of plantar fascia and plantar plate
Injuries to lateral ligamentous complex of the ankle
Rotator cuff tendinosis and tears
Labral tears in shoulder
Disk hernia and spondylolysis of the lumbar spine

30.2 Stress Fractures

Stress fractures and stress reactions accounted for more than 10% of injuries. Stress fractures were located most commonly at the anterior tibial surface. Stress fractures of the navicular bone, metatarsals, malleoli, calcaneum, ischium, carpal bones and pars interarticularis of lumbar vertebrae were also recorded. Sport activities that most commonly caused stress fractures or reactions were running for superior tibia and femur, gymnastics for anterior tibia and ischium, team sports requiring jumping and running such as basketball and handball for metatarsals and navicular bone and, finally, weight-lifting and diving for lumbar vertebrae. Patients presented with pain that was relieved with rest and restarted after activity, whereas in more severe injuries the patients suffered even in rest.

Standard radiographs were quite sensitive for visualization of cortical stress fractures in tibia. Cortical stress fractures were typically seen in gymnasts, at the anterior aspect of the tibia. Occasionally, multiple and bilateral stress fractures were seen (Fig. 30.1).

The most frequent stress fracture of cancellous bone involved the navicular bone, seen in four athletes (two basketball, one handball player and one long jumper).

In contradistinction to cortical stress fractures, these fractures could not be visualized on radiographs and may be missed as they may present with non specific signs and insidious onset. In these cases, additional CT or MRI was required for the diagnosis (Figs. 30.2 and 30.3). Navicular stress fractures could be demon-

Fig. 30.1. Multiple cortical stress fractures of the tibia in a 25-year-old female gymnast with chronic bilateral lower leg pain. Lateral radiograph of the left leg demonstrates horizontal lucent lines in the cortex of anterior tibia (*arrows*), with adjacent cortical sclerosis

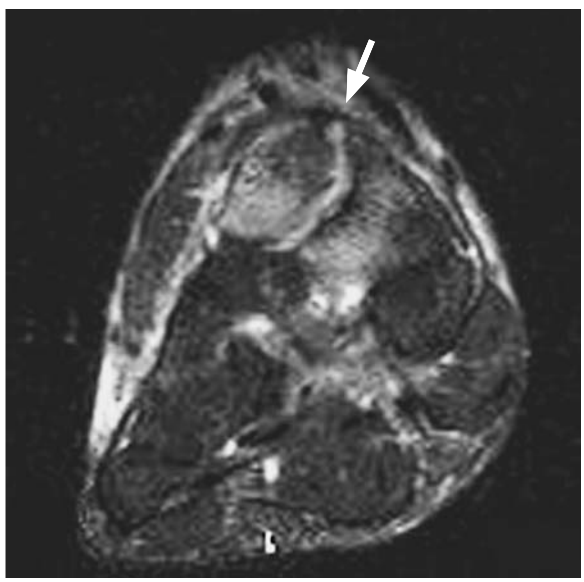

Fig. 30.2. Non-united stress fracture of the navicular bone in a 33-year-old basketball player presenting with non-specific ankle pain. A coronal STIR image shows a linear area of high signal at the fracture site with surrounding bone marrow edema. The fracture has a typical sagittal orientation

Fig. 30.3a,b. Stress fracture at the capitate in a 33-year-old cyclist with wrist injury. Reformatted CT images in the coronal (**a**) and sagittal plane (**b**) revealing a stress fracture at the middle aspect of the capitate (*arrow*)

strated on coronal and axial MR images as complete or incomplete fractures in the medial third of the bone (Fig. 30.2), which is considered to be relative avascular and more prone to the shearing forces oriented in the sagittal plane (Ting et al. 1988; Vanhoenacker et al. 2004). Multidetector CT, however, was more accurate to demonstrate the precise extent of the fracture line, due to due to its multiplanar reconstruction capabilities in the sagittal and coronal plane (Fig. 30.3).

MR imaging could additionally reveal early osseous stress injuries and thus modified training of the athletes (Arendt and Griffith 1997).

Stress injuries were categorized according to the classification proposed by Fredericson et al. (1995) into four grades, which are discussed in more detail in Chap. 7. Stress reactions grades 2 and 3 were more frequently seen than complete stress fractures.

30.3 Muscle Injuries

Muscle injury was the most common indication for ultrasound and the third most common indication for MR imaging (after knee and ankle injury). Muscle injuries have been categorized in muscle strains, contusions and avulsions (Nguyen et al. 2000; Boutin et al. 2003; De Smet et al. 1993). Muscle strains were the most frequent muscle injuries (n=28), whereas muscle contusions (n=2) and avulsions (n=2) were rare. Muscle strains occurred more frequently in runners (n=15), followed by volleyball and tennis players (n=7), in whom a powerful muscle contraction was combined with simultaneous forced lengthening of the myotendinous unit (De Smet et al. 1993), and involved more frequently muscles that crossed two joints such as rectus femoris (n=5), gastrocnemius (n=6) and hamstrings (n=21). Another mechanism of injury included eccentric contraction of muscle crossing one joint (Boutin and Newmann 2003), such as adductor muscles injuries (seen in two runners and four judo players) or pectoralis major injury in a weight-lifter.

Grading of muscle strains was done by using the grade 3 classification system (see Chap. 3). Approximately 70% of muscle injuries comprised mild strains. US was more sensitive than MR in subtle muscle strains including muscle elongation and subtle perifascial edema (Figs. 30.4 and 30.5) whereas MR provided more accurate estimation of the extent of severe muscle injury (Figs. 30.6 and 30.7). Furthermore, MR could reveal associated bone injury (if any)

a

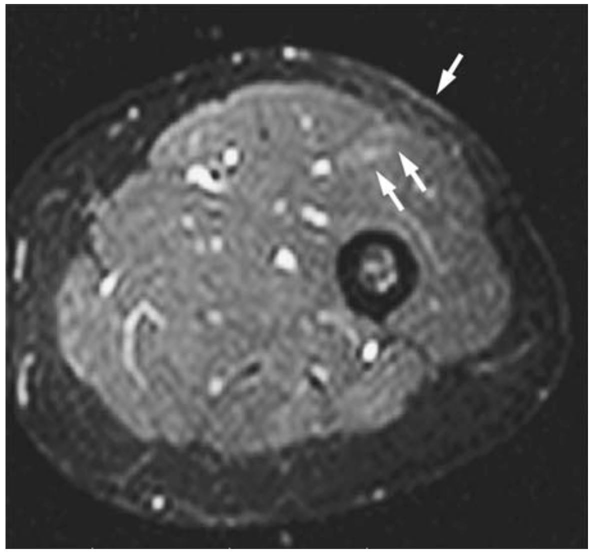

b

Fig. 30.4a,b. Mild muscle injury in a 22-year-old elite tennis player who presented with acute calf pain during competition. **a** Ultrasound of the right calf demonstrates subtle subfascial hyperechogenicity adjacent to the vastus lateralis muscle. **b** On a transverse STIR MR image, a barely seen hyperintensity with indistinct margins is shown at the vastus lateralis muscle and adjacent subcutaneous fat

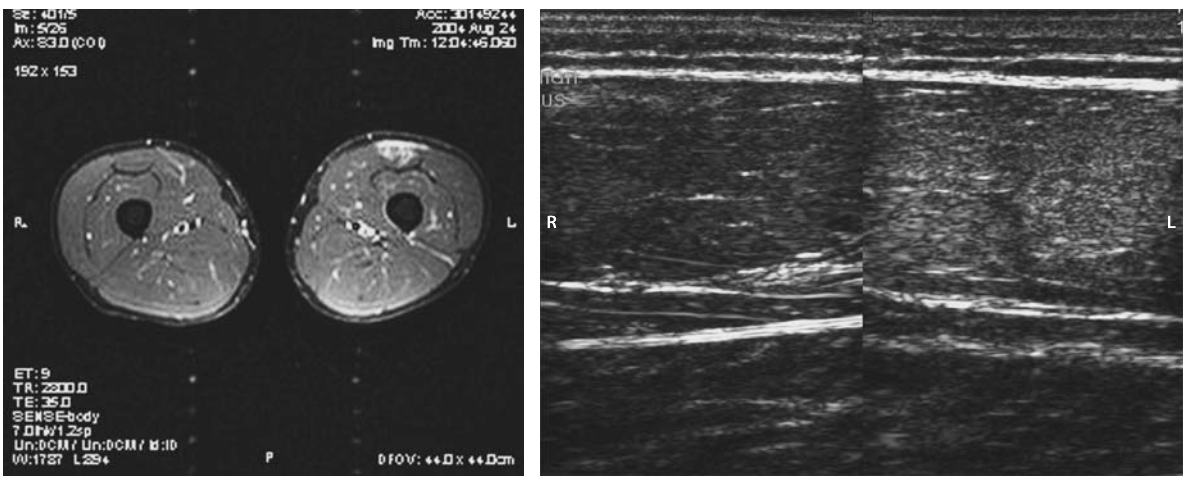

a b

Fig. 30.5a,b. An axial STIR image shows a grade 1 strain of the left rectus femoris muscle in a 23 year-old hockey player. A feathery pattern is seen on MRI **a**), whereas a diffuse hypoechogenicity is seen on US **b**), without disruption of muscle fibers

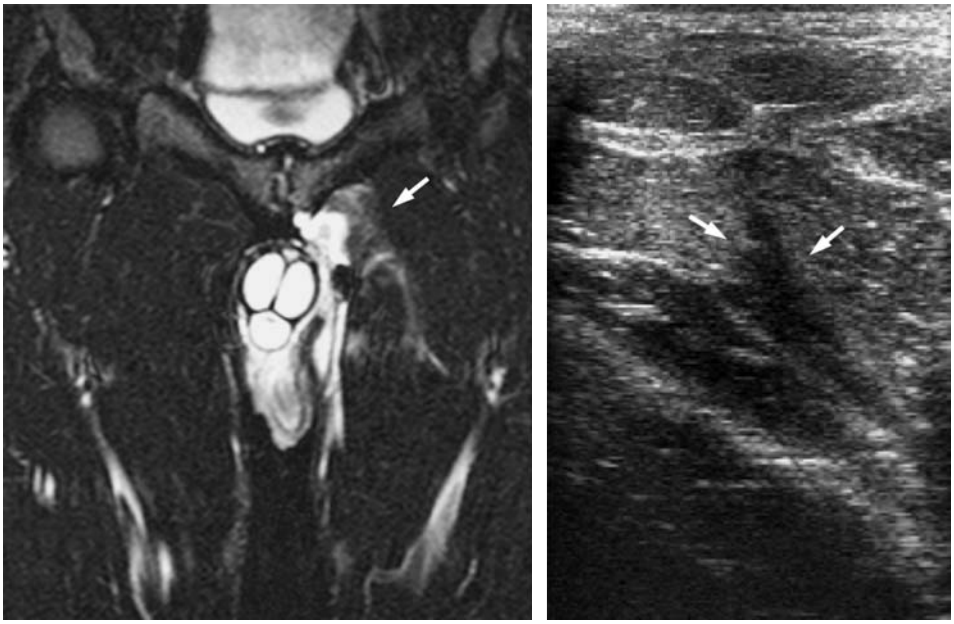

a b

Fig. 30.6a,b. Third degree strain in a 21-year-old judo player presenting with acute pain at the symphysis pubis. A coronal T2-weighted MR image shows complete rupture of the left adductor longus muscle with distal retraction (**a**). Corresponding longitudinal ultrasound image (**b**) of the same patient, demonstrates retraction of the proximal muscle belly and hypoechoic fluid extending along the fascia

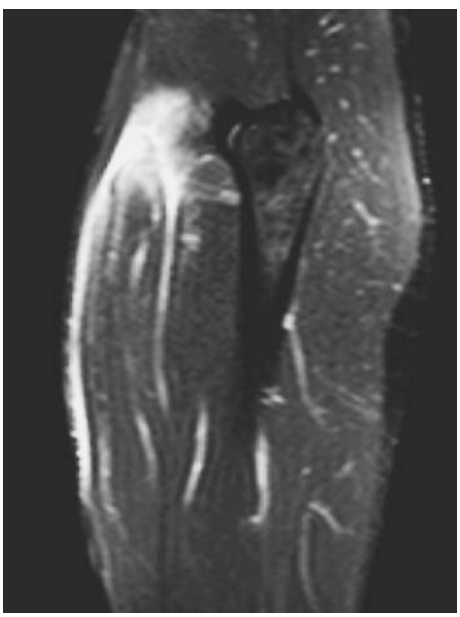

a

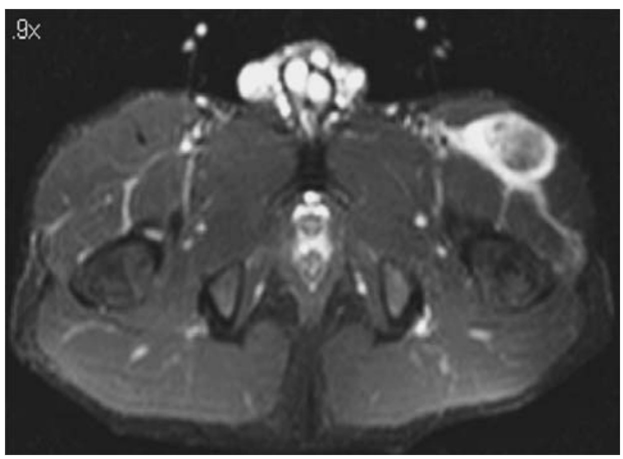

b

Fig. 30.7a,b. Rupture of the rectus femoris muscle in a 29-year-old runner who presented with a palpable mass at the anterior thigh. A sagittal STIR image (**a**) shows rupture of the rectus femoris muscle with distal retraction of the tendon and hematoma extending along the proximal muscle belly (**b**)

that might be missed on clinical examination. Partial tears were shown as discrete round or stellate lesions with high signal on T2-weighted MR images and were characterized by partial disruption of muscle fibers, low grade, if less than one-third of muscle fibers was torn, and high grade if more than two-thirds were torn (Boutin et al. 2003). Some degree of laxity and attenuation of the tendon occasionally accompanied the muscle injury due to diminished strength of the injured muscle (De Smet et al. 1993; Boutin and Newmann 2003). The signal of the hematomas is expected to modify in regard to the age of the hematoma; however the hematomas depicted in this study population were in the acute stage and, thus, disposed the signal intensities of fluid on T1- and T2-weighted images. Both in mild and moderate muscle injuries there were perifascial fluid and edema adjacent to the injured muscle. A severe injury of the rectus femoris muscle created a pseudotumor appearance (Temple at al. 1998) that was seen as an indiscrete, rather inhomogenous mass like lesion at the site of musculotendinous junction (Fig. 30.7). In that case, clinical examination usually reveals a palpable mass at the site of disruption of rectus femoris muscle. Of the six cases of complete muscle tear, seen in our series, three involved the adductor longus, one the rectus femoris and one the adductor gracilis.

Muscle contusions were rare and were caused by direct blunt trauma to muscles, as seen in the rectus abdominis muscle of a tennis player hit by the tennis ball. Hematoma formation in and around the muscle coexisted. Blunt trauma results in interstitial edema and hemorrhage, that is more extensive compared to

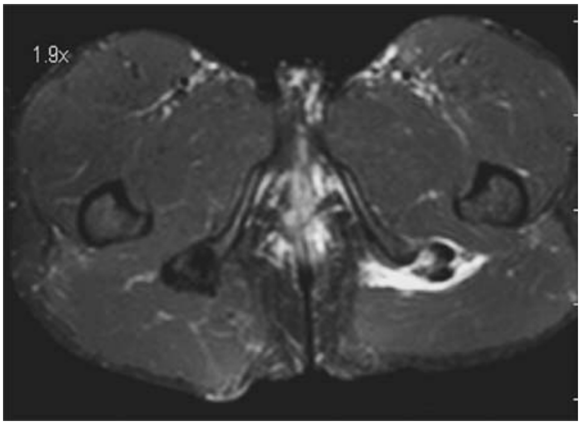

Fig. 30.8. Avulsion of the left hamstring tendons from the ischial tuberosity, in a 39-year-old long distance runner. Axial STIR image demonstrating edema and hemorrhage surrounding the avulsed fragment

strains however the recovery is faster (Coulouris and Connell 2003).

Muscle avulsions were not common in our study population as they usually occur in skeletally immature patients (see Chap. 26). One case of avulsion of the hamstring tendon from ischial tuberosity was recorded in a runner (Fig. 30.8) and another avulsion of the triceps tendon from the olecranon in a weightlifter. The hamstring tendons are the most frequently injures tendons in jumping and running. In our series, the myotendinous junction or the muscle belly was the most frequent location of tendon injury, which is in line with the literature (Coulouris and Connell 2003). Indeed, avulsion of the hamstrings from their insertion site at the posterolateral ischial tuberosity is considered a rare acute injury.

30.4 Spondylolysis and Other Sports Related Lesions of the Spine

Stress fracture of the pars interarticularis is due to repetitive hyperextension of the spine putting stress on the posterior bony elements (Commandre et al. 1988). Initially, a stress reaction in the pars is incited that leads to real stress fracture (Rossi 1988). Such injuries were observed in two weight-lifters, one gymnast and one diver (Fig. 30.9). All patients presented with low back pain that could be confused clinically with disk disease or strain of the back muscles. In our series, CT with axial and sagittal reformatted images was more sensitive in visualization of subtle cortical defects and in the follow-up of healing of stress fractures, whereas MR imaging was more sensitive for the initial diagnosis of stress reactions by demonstrating bone marrow edema (Gundry and Fritts 1999). Other lesions causing low back pain included disk bulging, protrusion or extrusion and decreased disk height. Annular tears were also not uncommon and aggravated low back pain.

30.5 Knee Injuries

MRI of the knee was the most frequently requested MR study which comprised 25% of requested MR

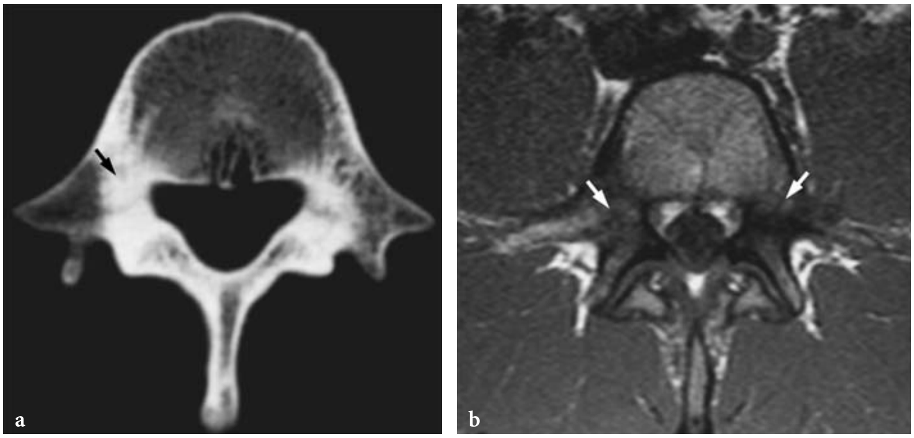


Fig. 30.9a–c. Stress fractures at the pars interarticularis in a 25-year-old diver with low back pain. CT revealed lucent fracture lines with adjacent sclerosis (**a**). The fractures are hypointense on axial T1-weighted MR images (**b**) as well on sagittal STIR images surrounded by hyperintense bone marrow edema (**c**)

imaging studies. Meniscal tears and ligamentous injuries were found in 33 and 28 studies respectively. The most common ligamentous injury was a complete tear of the anterior cruciate ligament (ACL) in 17 athletes, followed by a partial tear or sprain of the medial collateral ligament (MCL) in 13 and lateral collateral ligament (LCL) in 7 athletes, with concomitant popliteus injury in 3 of them. Complex ligamentous injuries, comprising injury of two ligaments and accompanied by at least one meniscal tear, were found in ten athletes of volleyball, basketball and fighting sports such as judo and tae-kwo-do. Complex ligamentous injuries usually included an injury to anterior cruciate ligament (ACL), medial collateral ligament (MCL) along with tears of the medial or lateral meniscus or both, comprising an 'unhappy triad" or "tetrad", respectively. In fighting sports, simultaneous injuries to both the lateral and medial supporting structures were not uncommon, implying involvement of more than one mechanisms of injury and recurrent injuries. Numerous mechanisms of injury can be associated with ACL tears (Hayes et al. 2000; Sanders et al. 2000; Recondo et al. 2000), including a valgus and external rotation force or a varus and internal rotation force on a fixed tibia in fighting sports, rapid change of direction or sudden contraction of the quadriceps tendon in basketball or handball. In all cases, there were concomitant bone bruises on the posterolateral tibial plateau and lateral femoral condyle, due to anterior translocation of the tibia and impaction between lateral posterior tibia and femur, whereas more subtle bone marrow edema was often seen at the posteromedial tibial plateau and at the femoral site of attachment of medial collateral ligament due to traction forces (Chan et al. 1999). Displaced meniscal tears were observed in 8 of 33 meniscal injuries and were in most cases associated with ligamentous injuries (Fig. 30.10). Rupture of the ACL graft was seen in three athletes (Fig. 30.11); in one of them there was anterior placement of the tibial or femoral tunnel (Papakonstantinou et al. 2000), whereas degenerative changes were uncommon in athletes with an old ACL injury. Avulsion fractures around the knee joint were rare. Only a subtle Segond avulsion fracture that accompanied ACL and lateral meniscus tear was seen in a judo athlete.

On the other hand, overuse injuries involving the extensor mechanism were much more frequent in jumpers and volley ball players. They included chondromalacia patellae in six cases and a spectrum of patellar overuse injury in seven athletes, ranging from patellar tendinosis, demonstrated as signal increase in the proximal end of patellar tendon (jumper's knee) (Khan et al. 1996) to severe cystic degeneration (Fig. 30.12).

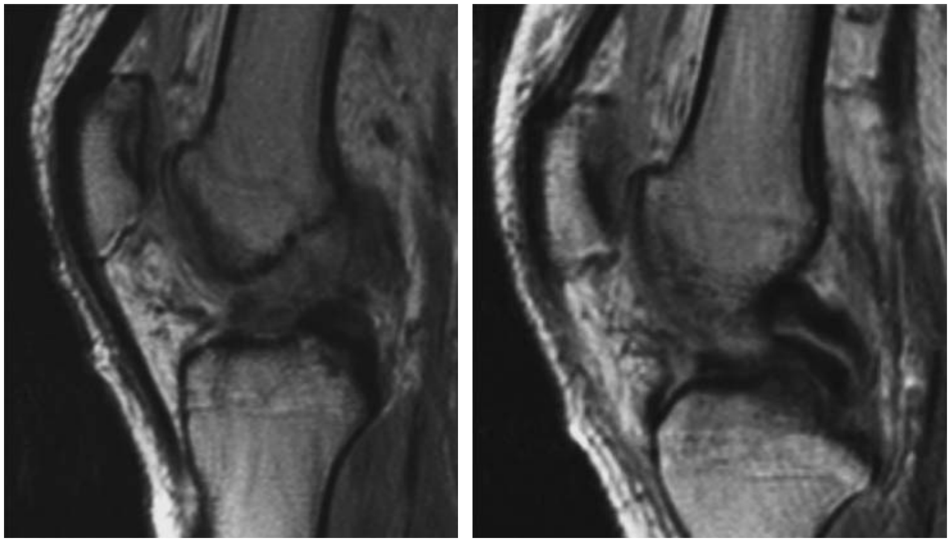

a b

c

Fig. 30.10a–c. A 29-year-old female judo player with clinical suspicion of ACL tear and acute blocking of the knee. A sagittal proton density weighted MR image (**a**) displays acute tear of the ACL whereas on a adjacent sagittal proton density weighted MR image (**b**) the double PCL sign indicative of a bucket handle tear of the posterior horn of medial meniscus is seen. On a coronal T2* MR image (**c**) a partial tear of the LCL (*arrow*) is also seen along with absence of the posterior horn of medial meniscus

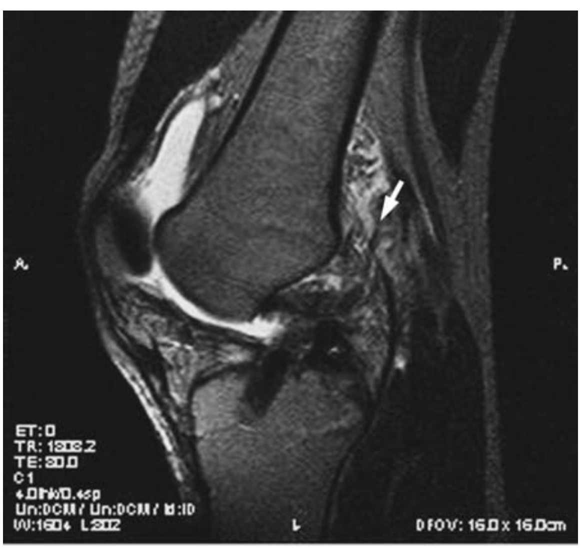

Fig. 30.11. Recurrent injury in a 27-year-old handball player with an ACL graft from patellar tendon, although the tibial tunnel was appropriately positioned. A sagittal T2 weighted MR image shows complete disruption of an ACL graft at its femoral attachment, along with tearing of the posterior capsule (*arrow*)

Fig. 30.12. A 25-year-old, male, volleyball player with anterior knee pain. A sagittal proton density weighted MR image shows extensive mucoid degeneration of patellar tendon (*arrow*), along with avulsion of the tibial tuberosity (*arrowhead*)

30.6 Ankle Injuries

Injuries to the ankle joint and foot were the most common injuries during the Olympics. Radiographs of the foot and ankle were the most frequently requested imaging examination, whereas MRI of the ankle was the second most requested MR examination. A variety of injuries involved the ankle joint the most frequent being overuse injuries to the Achilles tendon (n=11), injuries to the anterior talofibular (n=9) including chronic tears with anterolateral impingement, syndesmotic sprain (n=4), plantar fasciitis (n=9) with tear of the plantar fascia (n=4) and finally osseous injuries including stress fractures or stress reactions of the navicular bone (n=5), metatarsals (n=3), fibula (n=2) and calcaneum (n=1). Osseous impingement (Miller et al. 1995) caused either by bony excrescences, osteophytes at the talonavicular joint or accessory ossicles, such as the os trigonum posteriorly or accessory navicular bone (Bernaerts et al. 2004) were not infrequent, occasionally leading to tendinopathy of adjacent tendons or bone and syndesmotic injury.

Achilles tendon was evaluated initially with US. An additional MR examination was only performed if associated injuries to other structures were suspected and if a larger FOV was needed (Zoga and Schweitzer 2003). Interstitial tendinonis with partial tear and paratenonitis was frequent in athletes involved in jumping and running, whereas insertional tendinosis, with paratenonitis and retrocalcaneal bursitis was common in runners (Bencardino et al. 1999; Dunfee et al. 2002).

Lateral ankle sprains, associated with inversion and plantar flexion and occasionally axial loading, were seen in athletes of all sport categories, more frequently in basketball, soccer, handball and runners. Chronic or acute injuries to the anterior talofibular ligament were common, leading to instability and osteochondral injuries at the posteromedial or the midlateral talar dome, whereas tibiofibular syndesmotic injuries were less frequent. Chronic injuries of the lateral ligamentous structures were seen as absence, attenuation or thickening and laxity of the ligaments (Fig. 30.13) and were usually associated with scarring of the capsule, resulting in the so called meniscoid lesion (Robinson and White 2002; Jordan et al. 2000). This hypointense lesion occupied the anterolateral gutter of the joint and provoked anterolateral impingement and chronic pain during dorsiflexion of the foot.

Heel pain was a frequent clinical indication for ankle MRI and plantar fasciitis was the most common cause of heel pain, observed in nine patients. Although it is basically a clinical diagnosis, MR imaging was used to evaluate the extent of injury whereas radiographs were useful to exclude other causes of heel pain. MR imaging clearly depicted increased intrasubstance signal in acute plantar fasciitis, whereas thickening of the plantar fascia with perifascial edema indicated chronic fasciitis. A calcaneal spur at the insertion of the plantar fascia along with bone marrow edema of the calcaneum were frequent ancillary findings. Tears of plantar fascia were seen in two athletes, as partial or complete disruption of the fascia respectively.

Metatarsal stress fracture and/or plantar plate rupture causing metatarsalgia were seen in handball player (Fig. 30.14) and runners. The plantar plate is a fibrocartilagenous structure contiguous with the anterior and plantar aspect of the joint capsule of the metatarsophalangeal joints, providing resistance to dorsiflexion (Mohana-Borges et al. 2003; Umans and Elsinger 2001). Springing forward a plantar flexed foot on a hard surface (handball) or in runners accelerating from the starting blocks (Zoga and

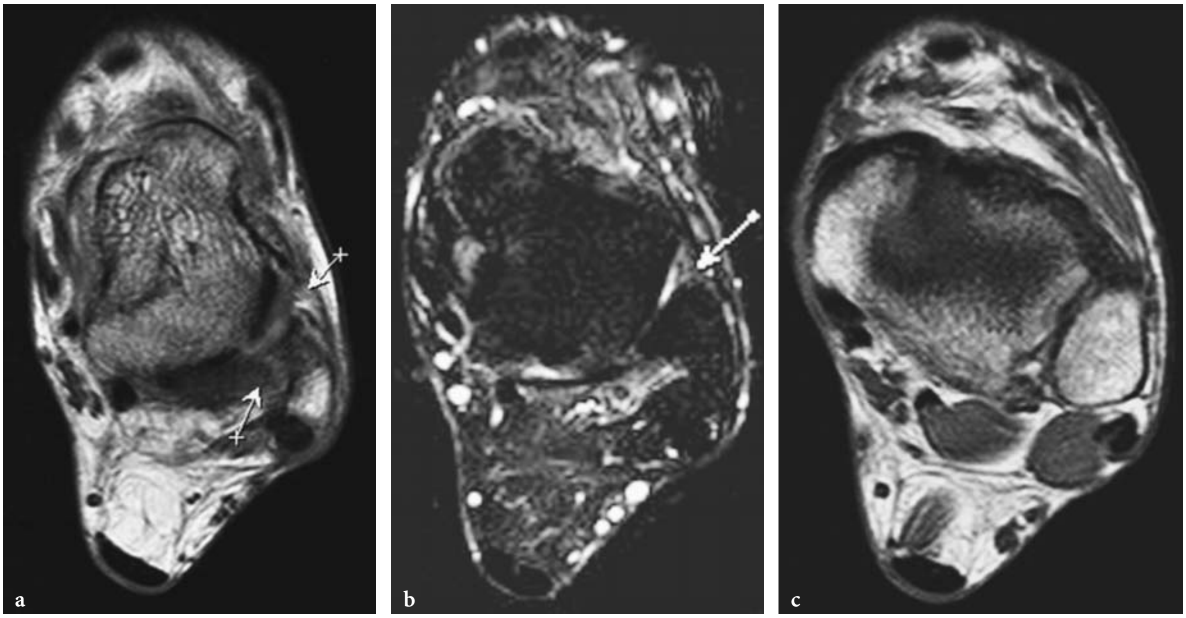

Fig. 30.13a–d. A 30-year-old female basketball player disposed extensive low signal in the lateral gutter that displays low signal on an axial T1-weighted MR image (**a**), and on an axial STIR image (**b**) (*arrow*). It extends anteriorly and posteriorly in (**a**). The anterior talofibular ligament is torn in (**a**). There is concomitant chronic injury of the anterior tibiofibular ligament that is thickened (**c**) and an osteochondral injury at the midlateral talar dome (**d**)

Schweitzer 2003), may generate dorsiflexion forces at the metatarsophalangeal joints resulting in rupture of the plantar fascia or stress fracture of the metatarsals or both.

Stress fractures or stress reactions, as described above, were not uncommon, and were seen in seven athletes (three basketball players, two jumpers and two gymnasts) (Fig. 30.2). Foci of bone marrow edema in multiple tarsal bones and malleoli without associated ligamentous injuries were occasionally seen in gymnasts and runners who presented with ankle pain (Schweitzer and White 1996). Gymnasts were frequently very young and thus skeletally immature and subject to injuries of epiphyseal plates, which appeared widened and irregular (Fig. 30.15).

30.7 Shoulder Injuries

Shoulder injuries are typically associated with throwing sports (Altcheck and Hobbs 2001; Sherbondy and McFarland 2004); however in our study group apart from throwing athletes, such as two javelin throwers, injuries to the shoulder were recorded in athletes involved in a variety of sports including boxing, judo, handball, basketball, softball, swimming, sailing, weightlifting and gymnastics. Lesions suggesting rotator cuff impingement or instability were found in 22 of the MR studies of the shoulder, whereas both impingement and instability were diag-

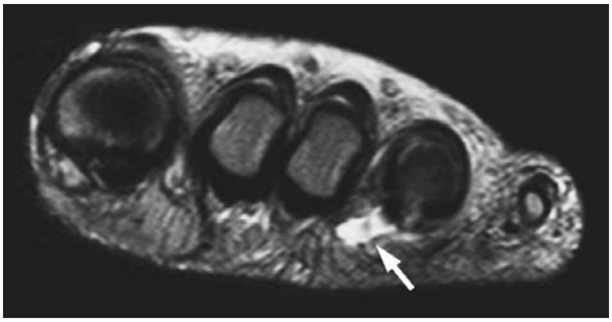

a

b

Fig. 30.14a,b. A 25-year-old, male, handball player with forefoot pain. A short axis T2-weighted MR image shows rupture of the plantar plate with adjacent fluid collection, after acute dorsiflexion on a hard surface (**a**). A long axis STIR image reveals a barely visible stress fracture (*arrow*) at the base of the fifth metatarsal (**b**)

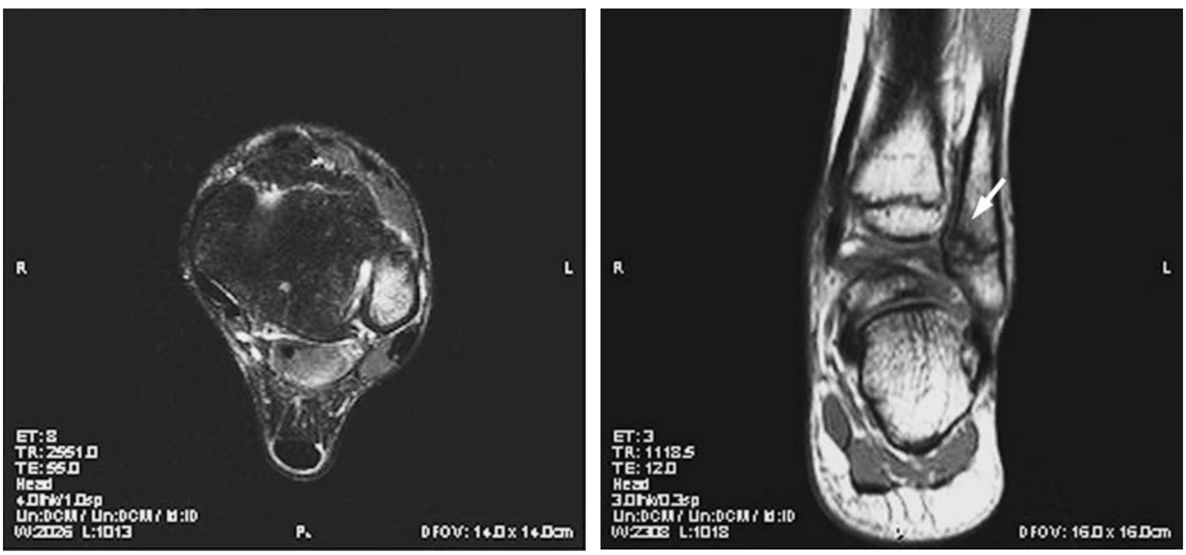

a b

Fig. 30.15a,b. Salter-Harris I injury in a 15-year-old female gymnast with chronic left ankle pain. STIR images (**a**) display increased marrow signal of the fibula. Note widening of the epiphyseal plate of the distal fibula (*arrow* in **b**). Note also strain of the flexor hallucis longus muscle and scattered foci of bone marrow edema through the ankle joint in (**a**)

nosed in 6 out of those 22 (28%). Superior labrum anterior to posterior lesions (SLAP) were visualized in 3/22 (14%); however the true incidence of the above mentioned lesions may be underestimated since MR arthrography which is the method of choice, was not performed due to constraints regarding the application of invasive procedures and contrast media.

In case of suspected or known isolated injury of the supraspinatus tendon, US was the first examination performed. It was also used for follow up to evaluate the healing procedure (Fig. 30.16).

Imaging features of instability comprised injuries to the anterior inferior capsulolabral complex including injury to the inferior glenohumeral ligament

Fig. 30.16. Ultrasound examination of the rotator cuff, showing a chronic partial rupture of the supraspinatus tendon (*arrow*)

(IGHL), detachment of the anterior inferior labrum with tear of the anterior periosteum (Bankart lesion) with associated compression fracture of the posterolateral aspect of the humeral head (Hill-Sachs lesion) and in one athlete, additional avulsion of the IGHL from the humeral head (Fig. 30.17).

Posterosuperior internal impingement syndrome was seen in three athletes involved in boxing, handball and in one gymnast in whom there were concomitant signs of instability (Fig. 30.17). Occult fractures of the greater tuberosity were seen in two cases of contact injuries in young athletes, due to an excessive tensile strength of the cuff compared to the resistant forces of bone (Zanetti et al. 1999).

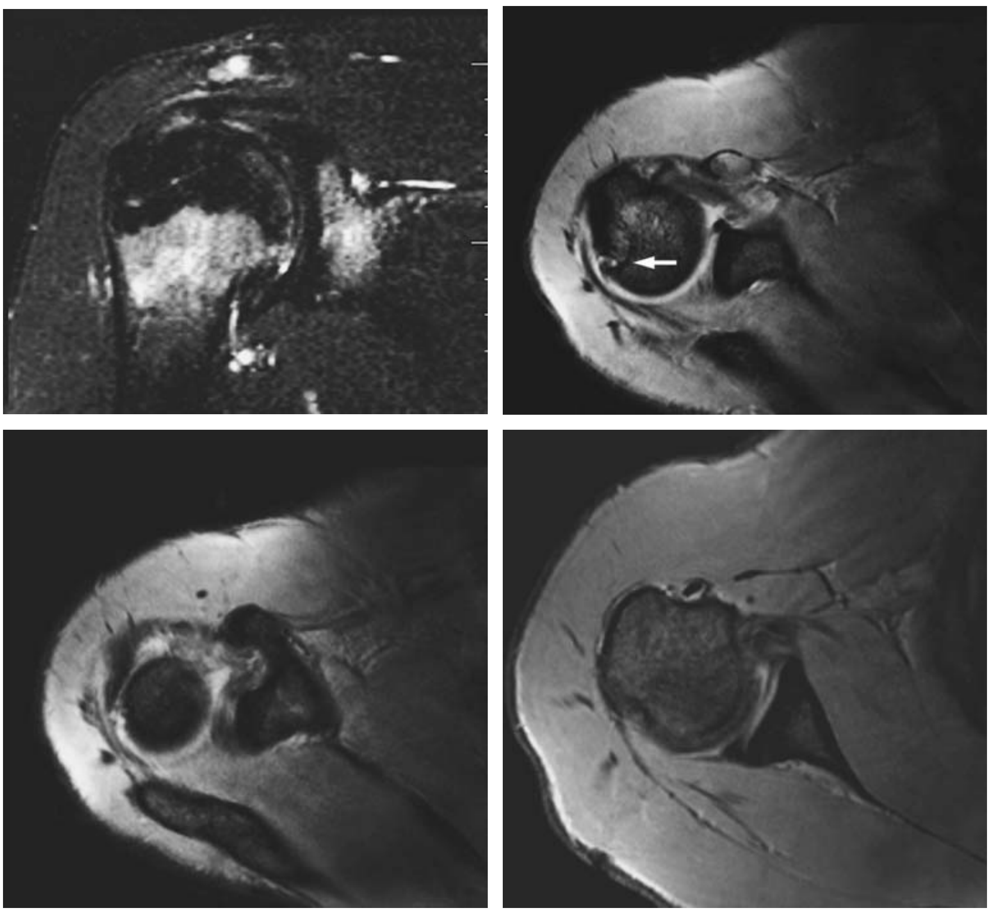

a b c d

Fig. 30.17a–d. A 23-year-old male gymnast with right shoulder pain. There is an undersurface tear of the posterior part of the supraspinatus and the superior part of the infraspinatus tendons shown on coronal STIR images (**a**). An axial T2-GRE MR image shows a tear of the superior – posterior labrum and an impaction fracture at the posterolateral aspect of humeral head (**b**). A cyst on the insertion of cuff on the humeral head which also seen (*arrow*). A more cranial section (**c**) displays thickening and waviness of the rotator interval structures along with tear of superior labrum extending anteriorly to posteriorly (SLAP), whereas a more caudal section (**d**) shows injury to the inferior glenohumeral ligament (IGHL) which is avulsed from the humeral head and a Bankart lesion medially

30.8 Conclusion

During the Summer Olympics in 2004 the most frequent musculoskeletal injuries consisted of muscle strains, mainly of biceps femoris, gastrocnemius, adductors and rectus femoris, stress fractures (located mainly in the tibia, navicular bone and metatarsals) and knee injuries including isolated meniscal tears, ACL ruptures followed by more complex ligamentous injuries. Subtle muscle strains could be depicted by ultrasound whereas MRI was more accurate in identifying the extent of a more severe injury. The most common injuries at the ankle joint were lateral ligamentous injuries often combined with impingement, tendinosis of the Achilles tendon and plantar fasciitis, or tears, and stress fractures of the navicular bone and metatarsals. At the shoulder, rotator cuff tears and/or instability lesions were most frequent. Lower back complaints were frequent and stress injuries of the pars interarticularis were not uncommon.

Things to Remember

1. Although ankle and foot lesions were the most frequent sports injuries, MR examination of the knee was the most frequent requested MR examination, followed by MRI of the ankle and foot.
2. Stress fractures/reactions comprise 10% of sports injuries.
3. Muscle injuries were the most frequent indication for ultrasound.
4. Shoulder injuries were not exclusively seen in throwing sports, but in a variety of athletes.

References

Altchek DW, Hobbs WR (2001) Evaluation and management of shoulder instability in the elite overhead thrower. Orthop Clin N Am 3:423–430

Arendt EA, Griffiths HJ (1997) The use of MR imaging in the assessment and clinical management of stress reactions of bone in high-performance athletes. Clin Sports Med 16:291–306

Bencardino J, Rosenberg ZS, Delfault E (1999) MR imaging in sports injuries of the foot and ankle. Magn Reson Imaging Clin N Am 7:131–148

Bernaerts A, Vanhoenacker FM, Van de Perre S et al. (2004) Accessory navicular bone: not such a normal variant. JBR-BTR 87:250–252

Boutin RD, Newmann JS (2003) MR imaging of sports-related hip disorders. Magn Reson Imaging Clin N Am 11:255–281

Boutin RD, Fritz RC, Steinbach LS (2003) Imaging of sports-related muscle injuries. Magn Reson Imaging Clin N Am 11:341–371

Chan KK, Resnick D, Goodwin D et al. (1999) Posteromedial tibial plateau injury including avulsion fracture of the semimembranous tendon insertion site: ancillary sign of anterior cruciate ligament tear at MR imaging. Radiology 211:754–758

Commandre FA, Taillan B, Gagnerie F et al. (1988) Spondylolysis and spondylolisthesis in young athletes: 28 cases. J Sports Med Phys Fitness 28:104–107

Coulouris G, Connell D (2003) Evaluation of hamstring muscle complex following acute injury. Skelet Radiol 32:582–589

De Smet AA, Fisher DR, Heiner JP et al. (1993) Magnetic resonance findings in skeletal muscle tears. Skelet Radiol 22:479–484

Dunfee WR, Dalinka MK, Kneeland JB (2002) Imaging of athletic injuries to the ankle and foot. Radiol Clin N Am 40:289–312

Fredericson M, Bergman G, Hoffman KL et al. (1995) Tibial stress reaction in runners: correlation of clinical symptoms and scintigraphy with a new magnetic resonance imaging grading system. Am J Sports Med 23:472–481

Gundry CR, Fritts HM (1999) MR imaging of the spine in sport injuries. Magn Reson Imaging Clin N Am 7:85–103

Hayes CW, Brigido MKI, Jamadar DA et al. (2000) Mechanism-based pattern approach to classification of complex injuries of the knee depicted at MR imaging. Radiographics 20:S121–S134

Jordan LK, Helms CA, Cooperman AE et al. (2000) Magnetic resonance imaging findings in anterolateral impingement of the ankle. Skelet Radiol 29:34–39

Khan KM, Bonar F, Desmond PM et al. (1996) Patellar tendinosis (jumpers knee): findings at histopathologic examination, US and MR imaging. Victorian Institute of Sport Tendon Study Group. Radiology 200:821–827

Miller TT, Staron RB, Feldman F et al. (1995) The symptomatic accessory tarsal navicular bone: assessment with MR imaging. Radiology 195:849–853

Mohana-Borges AV, Theumann NH, Pfirmann CW et al. (2003) Lesser metatarsophalageal joints: standard MR imaging, MR arthrography, and MR bursography- initial results in 48 cadaveric joints. Radiology 227:175–182

Nguyen B, Brandser E, Rubin DA (2000) Pains, strains and fasciculations: lower extremity muscle disorders. Magn Reson Imaging Clin N Am 8:391–408

Papakonstantinou O, Chung C, Chanchairujira K et al. (2003) Complications of anterior cruciate ligament reconstruction: MR imaging. Eur Radiol 13:1106–1117

Recondo JA, Salvador E, Villanua JA et al. (2000) Lateral stabilizing structures of the knee: functional anatomy and injuries assessed with MR imaging. Radiographics 20: S91–S102

Robinson P, White LM (2002) Soft tissue and osseous impingement syndromes of the ankle: Role of imaging in diagnosis and management. Radiographics 22:1457–1471

Rossi F (1998) Spondylolysis, spondylolisthesis and sports. J Sports Med Phys Fitness 18:317–340

Sanders TG, Medynski MA, Feller JF et al. (2000) Bone contusion patterns of the knee at MR imaging: footprint of the mechanism of injury. Radiographics 20:S135–151

Schweitzer ME, White LM (1996) Does altered biomechanics cause marrow edema? Radiology 198:851–853

Sherbondy PS, McFarland EG (2004) Shoulder instability in the athlete. Phys Med Rehabil Clin N Am 4:729–743

Temple HT, Kuklo TR, Sweet DE et al. (1998) Rectus femoris muscle tear appearing as a pseudotumor. Am J Sports Med 26:544–548

Ting AM, King W, Yocum L et al. (1988) Stress fractures of the tarsal navicular in long distance runners. Clin Sports Med 7:89–101

Umans HR, Elsinger E (2001) The plantar plate of the lesser metatarsophalangeal joints: potential of injury and role of MR imaging. Magn Reson Imaging Clin N Am 9:659–669

Vanhoenacker FM, Van de Perre S, De Praeter G et al. (2004) Proceedings of the SRBR-KBVR Osteoarticular section meeting of October 18, 2003 in Antwerp – part two: imaging of foot anomalies. JBR-BTR 87:305–309

Zanetti M, Weishaupt D, Jost B et al. (1999) MR imaging for traumatic tears of the rotator cuff: high prevalence of greater tuberosity fractures and subscapularis tendon tears. Am J Roentgenol 172:463–467

Zoga AC, Schweitzer ME (2003) Imaging of sports injuries of the foot and ankle. Magn Reson Imaging Clin N Am 11:295–310

Subject Index

A

B

H

I

J

K

L

N

O

P

Q

R

S

T

U

V

W

Z

List of Contributors

Gina Allen, DCH, MRCP, FRCR
The Royal Orthopaedic Hospital
NHS Trust
Bristol Road South
Northfield, Birmingham, B31 2AP
UK

Suzanne E. Anderson, PhD
Institut of Diagnostic, Interventional and
Pediatric Radiology
University Hospital
Inselspital
Freiburgstrasse
3010 Bern
Switzerland

Javier Beltran, MD, FACR
Professor, Department of Radiology
Maimonides Medical Center
4802 Tenth Avenue
Brooklyn, NY 11219
USA

Anja Bernaerts, MD
Department of Radiology
Sint-Augustinus Hospital
Oosterveldlaan, 24
2610 Wilrijk
Belgium

Peter Brys, MD
Department of Radiology
University Hospitals Leuven
Herestraat 49
3000 Leuven
Belgium

Karen Chapelle, MD
Department of Oral and Maxillofacial Surgery
Sint-Maarten Hospital
Rooienberg 25
2570 Duffel
Belgium

A. Mark Davies, MD
Consultant Radiologist
The MRI Centre
Royal Orthopaedic Hospital NHS Trust
Birmingham B31 2AP
UK

Milko de Jonge, MD
Department of Radiology
Academic Medical Center
PO Box 22660, Suite G1-239
1100 DD Amsterdam
The Netherlands

Michel De Maeseneer, MD, PhD
Division of Radiologic Sciences
Wake Forest University Hospital
Medical Center Boulevard
Winston-Salem, NC 27157
USA

Annick Demeyere, MD
Department of Radiology
Imelda Hospital
Imeldalaan, 9
2820 Bonheiden
Belgium

Farhad Ebrahim, MD
University of Michigan Hospitals
Ann Arbor, MI
USA

Philippe Ehlinger, MD
Department of Oral and Maxillofacial Surgery
Sint-Augustinus Hospital
Oosterveldlaan, 24
2610 Wilrijk
Belgium

Diana G. Franssen-Franken, MD
Department of Radiology
Onze Lieve Vrouwe Gasthuis
PO Box 95500
1090 HM Amsterdam
The Netherlands

Howard R. Galloway, BMBS, FRANZCR
Clinical Associate Professor
Department of Radiology
Australian National University
The Canberra Hospital
Yamba Drive
Garran, ACT 2605
Australia

Eric Geusens, MD
Department of Radiology
University Hospitals Leuven
Herestraat 49
3000 Leuven
Belgium

Wim Geyskens, MD
Algemeen Ziekenhuis Maria Middelares
Hospitaalstraat 17
9100 Sint-Niklaas
Belgium

Wayne Gibbon, MD, PhD
Professor of Radiology
18th Seventh Ave., St. Lucia
Brisbane Q 4067
Australia

Jan L. Gielen, MD, PhD
Associate Professor
Department of Radiology
University Hospital Antwerp
Wilrijkstraat 10
2650 Edegem
Belgium

Wouter C. J. Huysse, MD
Ghent University
De Pintelaan, 185
9000 Gent
Belgium

Franz Kainberger, MD, PhD
Professor of Radiology,
Medical University of Vienna, AKH
Währinger Gürtel 18-20
1090 Wien
Austria

Apostolos Karantanas, MD, PhD
Associate Professor, Department of Radiology
University Hospital
Stavrakia
Heraklion 711 10, Crete
Greece

Alexis Kelekis, MD, PhD
Lecturer of Interventional and
Musculoskeletal Radiology
2nd Radiology Department
University of Athens
Rimini 1
12462, Athens
Greece

Dimitrios Kelekis, MD, PhD
Professor of Radiology, Research Department of
Imaging and Interventional Radiology
University of Athens
Eugenidion Hospital
Papadiamantopoulou 20
11528, Athens
Greece

Nikolaos L. Kelekis, MD, PhD
Associate Professor of Radiology
2nd Radiology Department
University of Athens
Rimini 1
12462, Athens
Greece

Eva Llopis, MD
Hospital de la Ribera
C/Carretera de Corbera km1
46600 Alzira
Valencia
Spain

Mario Maas, MD, PhD
Department of Radiology
Academic Medical Centre
PO Box 22660, Suite C1-210
1105 AZ Amsterdam
The Netherlands

Eugene G. McNally, MD
Consultant Musculoskeletal Radiologist
Department of Radiology
Nuffield Orthopaedic Centre
NHS Trust
Windmill Road
Headington, Oxford OX3 7LD
UK

Simon Ostlere, FRCR
Department of Radiology
Nuffield Orthopaedic Centre
NHS Trust
Windmill Road
Headington, Oxford OX3 7LD
UK

Mario Padron, MD
Clinica Cemtro
C/Ventisquero de la Condesa 42
28035 Madrid
Spain

Olympia Papakonstantinou, MD
Lecturer of Radiology
2nd Radiology Department
University of Athens
Rimini 1
12462 Athens
Greece

Paul M. Parizel, MD, PhD
Professor of Radiology
Department of Radiology
University Hospital Antwerpen
Wilrijkstraat 10
2650 Edegem
Belgium

Wilfred C. G. Peh, MD, MBBS, FRCPE, FRCPG, FRCR
Clinical Professor and Senior Consultant Radiologist
Singapore Health Services
7 Hospital Drive, # 02-09
Singapore 169611
Republic of Singapore

Babette M. Pluim, MD, PhD
KNLTB, Box 1617
3800 BP Amersfoort
The Netherlands

Philip Robinson, FRCR
Consultant Musculoskeletal Radiologist
Department of Radiology
Musculoskeletal Centre
Chapel Allerton Hospital
Leeds Teaching Hospitals
Leeds, LS7 4SA
UK

Ernest Schilders, MD
18th seventh Ave., St. Lucia
Brisbane Q 4067
Australia

John Slavotinek, MBBS, FRANZCR
Division of Medical Imaging
Flinders Medical Centre and
Flinders University
Flinders Drive
Adelaide
South Australia, 5042
Australia

Augustinus Suhardja, MD
Department of Radiology
Maimonides Medical Center
4802 Tenth Avenue
Brooklyn, NY 11219
USA

Anja Van der Stappen, MD
Department of Radiology
University Hospital Antwerp
Wilrijkstraat 10
2650 Edegem
Belgium
and
Department of Radiology, Institut J. Bordet
Waterloolaan 121, 1000 Brussels
Belgium

Henk-Jan Van der Woude, MD, PhD
Department of Radiology
Onze Lieve Vrouwe Gasthuis
PO Box 95500
1090 HM Amsterdam
The Netherlands

Pieter Van Dyck, MD
Department of Radiology
University Hospital Antwerp
Wilrijkstraat, 10
2650 Edegem
Belgium

Filip M. Vanhoenacker, MD, PhD
Department of Radiology
University Hospital Antwerp
Wilrijkstraat 10
2650 Edegem
Belgium
and
Department of Radiology
AZ St-Maarten Duffel/Mechelen
Belgium

Ronald A.W. Verhagen, MD, PhD
Ziekenhuis Hilversum
Department of Orthopedics Surgery & Traumatology
P.O. Box 10016
1201 DA Hilversum
The Netherlands

Koenraad L. Verstraete, MD, PhD
Professor of Radiology
Department of Radiology
Ghent University
De Pintelaan, 185
9000 Gent
Belgium

W. Jaap Willems, MD
Department of Orthopaedic Surgery
Onze Lieve Vrouwe Gasthuis
PO Box 95500
1090 HM Amsterdam
The Netherlands

David J. Wilson, MD, FRCP, FRCR
Senior Clinical Lecturer University of Oxford
Consultant Radiologist
Department of Radiology
Nuffield Orthopaedic Centre and
John Radcliffe Hospital
NHS Trust
Windmill Road
Headington, Oxford OX3 7LD
UK

Medical Radiology Diagnostic Imaging and Radiation Oncology

Titles in the series already published

Diagnostic Imaging

Innovations in Diagnostic Imaging
Edited by J. H. Anderson

Radiology of the Upper Urinary Tract
Edited by E. K. Lang

The Thymus - Diagnostic Imaging, Functions, and Pathologic Anatomy
Edited by E. Walter, E. Willich, and W. R. Webb

Interventional Neuroradiology
Edited by A. Valavanis

Radiology of the Pancreas
Edited by A. L. Baert, co-edited by G. Delorme

Radiology of the Lower Urinary Tract
Edited by E. K. Lang

Magnetic Resonance Angiography
Edited by I. P. Arlart, G. M. Bongartz, and G. Marchal

Contrast-Enhanced MRI of the Breast
S. Heywang-Köbrunner and R. Beck

Spiral CT of the Chest
Edited by M. Rémy-Jardin and J. Rémy

Radiological Diagnosis of Breast Diseases
Edited by M. Friedrich and E.A. Sickles

Radiology of the Trauma
Edited by M. Heller and A. Fink

Biliary Tract Radiology
Edited by P. Rossi, co-edited by M. Brezi

Radiological Imaging of Sports Injuries
Edited by C. Masciocchi

Modern Imaging of the Alimentary Tube
Edited by A. R. Margulis

Diagnosis and Therapy of Spinal Tumors
Edited by P. R. Algra, J. Valk, and J. J. Heimans

Interventional Magnetic Resonance Imaging
Edited by J. F. Debatin and G. Adam

Abdominal and Pelvic MRI
Edited by A. Heuck and M. Reiser

Orthopedic Imaging
Techniques and Applications
Edited by A. M. Davies and H. Pettersson

Radiology of the Female Pelvic Organs
Edited by E. K.Lang

Magnetic Resonance of the Heart and Great Vessels
Clinical Applications
Edited by J. Bogaert, A.J. Duerinckx, and F. E. Rademakers

Modern Head and Neck Imaging
Edited by S. K. Mukherji and J. A. Castelijns

Radiological Imaging of Endocrine Diseases
Edited by J. N. Bruneton in collaboration with B. Padovani and M.-Y. Mourou

Trends in Contrast Media
Edited by H. S. Thomsen, R. N. Muller, and R. F. Mattrey

Functional MRI
Edited by C. T. W. Moonen and P. A. Bandettini

Radiology of the Pancreas
2nd Revised Edition
Edited by A. L. Baert. Co-edited by G. Delorme and L. Van Hoe

Emergency Pediatric Radiology
Edited by H. Carty

Spiral CT of the Abdomen
Edited by F. Terrier, M. Grossholz, and C. D. Becker

Liver Malignancies
Diagnostic and Interventional Radiology
Edited by C. Bartolozzi and R. Lencioni

Medical Imaging of the Spleen
Edited by A. M. De Schepper and F. Vanhoenacker

Radiology of Peripheral Vascular Diseases
Edited by E. Zeitler

Diagnostic Nuclear Medicine
Edited by C. Schiepers

Radiology of Blunt Trauma of the Chest
P. Schnyder and M. Wintermark

Portal Hypertension
Diagnostic Imaging-Guided Therapy
Edited by P. Rossi
Co-edited by P. Ricci and L. Broglia

Recent Advances in Diagnostic Neuroradiology
Edited by Ph. Demaerel

Virtual Endoscopy and Related 3D Techniques
Edited by P. Rogalla, J. Terwisscha Van Scheltinga, and B. Hamm

Multislice CT
Edited by M. F. Reiser, M. Takahashi, M. Modic, and R. Bruening

Pediatric Uroradiology
Edited by R. Fotter

Transfontanellar Doppler Imaging in Neonates
A. Couture and C. Veyrac

Radiology of AIDS
A Practical Approach
Edited by J.W.A.J. Reeders and P.C. Goodman

CT of the Peritoneum
Armando Rossi and Giorgio Rossi

Magnetic Resonance Angiography
2nd Revised Edition
Edited by I. P. Arlart, G. M. Bongratz, and G. Marchal

Pediatric Chest Imaging
Edited by Javier Lucaya and Janet L. Strife

Applications of Sonography in Head and Neck Pathology
Edited by J. N. Bruneton in collaboration with C. Raffaelli and O. Dassonville

Imaging of the Larynx
Edited by R. Hermans

3D Image Processing
Techniques and Clinical Applications
Edited by D. Caramella and C. Bartolozzi

Imaging of Orbital and Visual Pathway Pathology
Edited by W. S. Müller-Forell

Pediatric ENT Radiology
Edited by S. J. King and A. E. Boothroyd

Radiological Imaging of the Small Intestine
Edited by N. C. Gourtsoyiannis

Imaging of the Knee
Techniques and Applications
Edited by A. M. Davies and V. N. Cassar-Pullicino

Perinatal Imaging
From Ultrasound to MR Imaging
Edited by Fred E. Avni

Radiological Imaging of the Neonatal Chest
Edited by V. Donoghue

Diagnostic and Interventional Radiology in Liver Transplantation
Edited by E. Bücheler, V. Nicolas, C. E. Broelsch, X. Rogiers, and G. Krupski

Radiology of Osteoporosis
Edited by S. Grampp

Imaging Pelvic Floor Disorders
Edited by C. I. Bartram and J. O. L. DeLancey
Associate Editors: S. Halligan, F. M. Kelvin, and J. Stoker

Imaging of the Pancreas
Cystic and Rare Tumors
Edited by C. Procacci and A. J. Megibow

High Resolution Sonography of the Peripheral Nervous System
Edited by S. Peer and G. Bodner

Imaging of the Foot and Ankle
Techniques and Applications
Edited by A. M. Davies, R. W. Whitehouse, and J. P. R. Jenkins

Radiology Imaging of the Ureter
Edited by F. Joffre, Ph. Otal, and M. Soulie

Imaging of the Shoulder
Techniques and Applications
Edited by A. M. Davies and J. Hodler

Radiology of the Petrous Bone
Edited by M. Lemmerling and S. S. Kollias

Interventional Radiology in Cancer
Edited by A. Adam, R. F. Dondelinger, and P. R. Mueller

Duplex and Color Doppler Imaging of the Venous System
Edited by G. H. Mostbeck

Multidetector-Row CT of the Thorax
Edited by U. J. Schoepf

Functional Imaging of the Chest
Edited by H.-U. Kauczor

Radiology of the Pharynx and the Esophagus
Edited by O. Ekberg

Radiological Imaging in Hematological Malignancies
Edited by A. Guermazi

Imaging and Intervention in Abdominal Trauma
Edited by R. F. Dondelinger

Multislice CT
2nd Revised Edition
Edited by M. F. Reiser, M. Takahashi, M. Modic, and C. R. Becker

Intracranial Vascular Malformations and Aneurysms
From Diagnostic Work-Up to Endovascular Therapy
Edited by M. Forsting

Radiology and Imaging of the Colon
Edited by A. H. Chapman

Coronary Radiology
Edited by M. Oudkerk

Dynamic Contrast-Enhanced Magnetic Resonance Imaging in Oncology
Edited by A. Jackson, D. L. Buckley, and G. J. M. Parker

Imaging in Treatment Planning for Sinonasal Diseases
Edited by R. Maroldi and P. Nicolai

Clinical Cardiac MRI
With Interactive CD-ROM
Edited by J. Bogaert, S. Dymarkowski, and A. M. Taylor

Focal Liver Lesions
Detection, Characterization, Ablation
Edited by R. Lencioni, D. Cioni, and C. Bartolozzi

Multidetector-Row CT Angiography
Edited by C. Catalano and R. Passariello

Paediatric Musculoskeletal Diseases
With an Emphasis on Ultrasound
Edited by D. Wilson

Contrast Media in Ultrasonography
Basic Principles and Clinical Applications
Edited by Emilio Quaia

MR Imaging in White Matter Diseases of the Brain and Spinal Cord
Edited by M. Filippi, N. De Stefano, V. Dousset, and J. C. McGowan

Diagnostic Nuclear Medicine
2nd Revised Edition
Edited by C. Schiepers

Imaging of the Kidney Cancer
Edited by A. Guermazi

Magnetic Resonance Imaging in Ischemic Stroke
Edited by R. von Kummer and T. Back

Imaging of the Hip & Bony Pelvis
Techniques and Applications
Edited by A. M. Davies, K. J. Johnson, and R. W. Whitehouse

Imaging of Occupational and Environmental Disorders of the Chest
Edited by P. A. Gevenois and P. De Vuyst

Contrast Media
Safety Issues and ESUR Guidelines
Edited by H. S. Thomsen

Virtual Colonoscopy
A Practical Guide
Edited by P. Lefere and S. Gryspeerdt

Vascular Embolotherapy
A Comprehensive Approach
Volume 1
Edited by J. Golzarian. Co-edited by S. Sun and M. J. Sharafuddin

Vascular Embolotherapy
A Comprehensive Approach
Volume 2
Edited by J. Golzarian. Co-edited by S. Sun and M. J. Sharafuddin

Head and Neck Cancer Imaging
Edited by R. Hermans

Vascular Interventional Radiology
Current Evidence in Endovascular Surgery
Edited by M. G. Cowling

Ultrasound of the Gastrointestinal Tract
Edited by G. Maconi and G. Bianchi Porro

Imaging of Orthopedic Sports Injuries
Edited by F. M. Vanhoenacker, M. Maas, J. L. M. A. Gielen

Parallel Imaging in Clinical MR Applications
Edited by S. O. Schoenberg, O. Dietrich, and F. M. Reiser

MR and CT of the Female Pelvis
Edited by B. Hamm and R. Forstner

Ultrasound of the Musculoskeletal System
S. Bianchi and C. Martinoli

Radiology of the Stomach and Duodenum
Edited by A. H. Freeman and E. Sala

Medical Radiology Diagnostic Imaging and Radiation Oncology

Titles in the series already published

Radiation Oncology

Lung Cancer
Edited by C.W. Scarantino

Innovations in Radiation Oncology
Edited by H. R. Withers and L. J. Peters

Radiation Therapy of Head and Neck Cancer
Edited by G. E. Laramore

Gastrointestinal Cancer – Radiation Therapy
Edited by R.R. Dobelbower, Jr.

Radiation Exposure and Occupational Risks
Edited by E. Scherer, C. Streffer, and K.-R. Trott

Radiation Therapy of Benign Diseases
A Clinical Guide
S. E. Order and S. S. Donaldson

Interventional Radiation Therapy Techniques – Brachytherapy
Edited by R. Sauer

Radiopathology of Organs and Tissues
Edited by E. Scherer, C. Streffer, and K.-R. Trott

Concomitant Continuous Infusion Chemotherapy and Radiation
Edited by M. Rotman and C. J. Rosenthal

Intraoperative Radiotherapy – Clinical Experiences and Results
Edited by F. A. Calvo, M. Santos, and L.W. Brady

Radiotherapy of Intraocular and Orbital Tumors
Edited by W. E. Alberti and R. H. Sagerman

Interstitial and Intracavitary Thermoradiotherapy
Edited by M. H. Seegenschmiedt and R. Sauer

Non-Disseminated Breast Cancer
Controversial Issues in Management
Edited by G. H. Fletcher and S.H. Levitt

Current Topics in Clinical Radiobiology of Tumors
Edited by H.-P. Beck-Bornholdt

Practical Approaches to Cancer Invasion and Metastases
A Compendium of Radiation Oncologists' Responses to 40 Histories
Edited by A. R. Kagan with the Assistance of R. J. Steckel

Radiation Therapy in Pediatric Oncology
Edited by J. R. Cassady

Radiation Therapy Physics
Edited by A. R. Smith

Late Sequelae in Oncology
Edited by J. Dunst and R. Sauer

Mediastinal Tumors. Update 1995
Edited by D. E. Wood and C. R. Thomas, Jr.

Thermoradiotherapy and Thermochemotherapy
Volume 1:
Biology, Physiology, and Physics
Volume 2:
Clinical Applications
Edited by M.H. Seegenschmiedt, P. Fessenden, and C.C. Vernon

Carcinoma of the Prostate
Innovations in Management
Edited by Z. Petrovich, L. Baert, and L.W. Brady

Radiation Oncology of Gynecological Cancers
Edited by H.W. Vahrson

Carcinoma of the Bladder
Innovations in Management
Edited by Z. Petrovich, L. Baert, and L.W. Brady

Blood Perfusion and Microenvironment of Human Tumors
Implications for Clinical Radiooncology
Edited by M. Molls and P. Vaupel

Radiation Therapy of Benign Diseases
A Clinical Guide
2nd Revised Edition
S. E. Order and S. S. Donaldson

Carcinoma of the Kidney and Testis, and Rare Urologic Malignancies
Innovations in Management
Edited by Z. Petrovich, L. Baert, and L.W. Brady

Progress and Perspectives in the Treatment of Lung Cancer
Edited by P. Van Houtte, J. Klastersky, and P. Rocmans

Combined Modality Therapy of Central Nervous System Tumors
Edited by Z. Petrovich, L. W. Brady, M. L. Apuzzo, and M. Bamberg

Age-Related Macular Degeneration
Current Treatment Concepts
Edited by W. A. Alberti, G. Richard, and R. H. Sagerman

Radiotherapy of Intraocular and Orbital Tumors
2nd Revised Edition
Edited by R. H. Sagerman, and W. E. Alberti

Modification of Radiation Response
Cytokines, Growth Factors, and Other Biolgical Targets
Edited by C. Nieder, L. Milas, and K. K. Ang

Radiation Oncology for Cure and Palliation
R. G. Parker, N. A. Janjan, and M. T. Selch

Clinical Target Volumes in Conformal and Intensity Modulated Radiation Therapy
A Clinical Guide to Cancer Treatment
Edited by V. Grégoire, P. Scalliet, and K. K. Ang

Advances in Radiation Oncology in Lung Cancer
Edited by Branislav Jeremić

New Technologies in Radiation Oncology
Edited by W. Schlegel, T. Bortfeld, and A.-L. Grosu

Technical Basis of Radiation Therapy
4th Revised Edition
Edited by S. H. Levitt, J. A. Purdy, C. A. Perez, and S. Vijayakumar

Springer

Printing and Binding: Stürtz GmbH, Würzburg